Advances in Intelligent and Soft Computing 134

Editor-in-Chief: J. Kacprzyk

Advances in Intelligent and Soft Computing

Editor-in-Chief

Prof. Janusz Kacprzyk
Systems Research Institute
Polish Academy of Sciences
ul. Newelska 6
01-447 Warsaw
Poland
E-mail: kacprzyk@ibspan.waw.pl

Further volumes of this series can be found on our homepage: springer.com

Vol. 118. A. Kapczynski, E. Tkacz, and M. Rostanski (Eds.)
Internet - Technical Developments and Applications 2, 2011
ISBN 978-3-642-25354-6

Vol. 119. Tianbiao Zhang (Ed.)
Future Computer, Communication, Control and Automation, 2011
ISBN 978-3-642-25537-3

Vol. 120. Nicolas Loménie, Daniel Racoceanu, and Alexandre Gouaillard (Eds.)
Advances in Bio-Imaging: From Physics to Signal Understanding Issues, 2011
ISBN 978-3-642-25546-5

Vol. 121. Tomasz Traczyk and Mariusz Kaleta (Eds.)
Modeling Multi-commodity Trade: Information Exchange Methods, 2011
ISBN 978-3-642-25648-6

Vol. 122. Yinglin Wang and Tianrui Li (Eds.)
Foundations of Intelligent Systems, 2011
ISBN 978-3-642-25663-9

Vol. 123. Yinglin Wang and Tianrui Li (Eds.)
Knowledge Engineering and Management, 2011
ISBN 978-3-642-25660-8

Vol. 124. Yinglin Wang and Tianrui Li (Eds.)
Practical Applications of Intelligent Systems, 2011
ISBN 978-3-642-25657-8

Vol. 125. Tianbiao Zhang (Ed.)
Mechanical Engineering and Technology, 2012
ISBN 978-3-642-27328-5

Vol. 126. Khine Soe Thaung (Ed.)
Advanced Information Technology in Education, 2012
ISBN 978-3-642-25907-4

Vol. 127. Tianbiao Zhang (Ed.)
Instrumentation, Measurement, Circuits and Systems, 2012
ISBN 978-3-642-27333-9

Vol. 128. David Jin and Sally Lin (Eds.)
Advances in Multimedia, Software Engineering and Computing Vol.1, 2011
ISBN 978-3-642-25988-3

Vol. 129. David Jin and Sally Lin (Eds.)
Advances in Multimedia, Software Engineering and Computing Vol.2, 2011
ISBN 978-3-642-25985-2

Vol. 130. Kusum Deep, Atulya Nagar, Millie Pant, and Jagdish Chand Bansal (Eds.)
Proceedings of the International Conference on Soft Computing for Problem Solving (SocProS 2011) December 20–22, 2011, 2012
ISBN 978-81-322-0486-2

Vol. 131. Kusum Deep, Atulya Nagar, Millie Pant, and Jagdish Chand Bansal (Eds.)
Proceedings of the International Conference on Soft Computing for Problem Solving (SocProS 2011) December 20–22, 2011, 2012
ISBN 978-81-322-0490-9

Vol. 132. Suresh Chandra Satapathy, P.S. Avadhani, and Ajith Abraham (Eds.)
Proceedings of the International Conference on Information Systems Design and Intelligent Applications 2012 (India 2012) held in Visakhapatnam, India, January 2012, 2012
ISBN 978-3-642-27442-8

Vol. 133. Sabo Sambath and Egui Zhu (Eds.)
Frontiers in Computer Education, 2012
ISBN 978-3-642-27551-7

Vol. 134. Egui Zhu and Sabo Sambath (Eds.)
Information Technology and Agricultural Engineering, 2012
ISBN 978-3-642-27536-4

Egui Zhu and Sabo Sambath (Eds.)

Information Technology and Agricultural Engineering

Springer

Editors
Prof. Egui Zhu
South China Normal University
Guangzhou
P.R. China

Prof. Sabo Sambath
South China Normal University
Guangzhou
P.R. China

ISSN 1867-5662
e-ISSN 1867-5670
ISBN 978-3-642-27536-4
e-ISBN 978-3-642-27537-1
DOI 10.1007/978-3-642-27537-1
Springer Heidelberg New York Dordrecht London

Library of Congress Control Number: 2012930482

© Springer-Verlag Berlin Heidelberg 2012
This work is subject to copyright. All rights are reserved by the Publisher, whether the whole or part of the material is concerned, specifically the rights of translation, reprinting, reuse of illustrations, recitation, broadcasting, reproduction on microfilms or in any other physical way, and transmission or information storage and retrieval, electronic adaptation, computer software, or by similar or dissimilar methodology now known or hereafter developed. Exempted from this legal reservation are brief excerpts in connection with reviews or scholarly analysis or material supplied specifically for the purpose of being entered and executed on a computer system, for exclusive use by the purchaser of the work. Duplication of this publication or parts thereof is permitted only under the provisions of the Copyright Law of the Publisher's location, in its current version, and permission for use must always be obtained from Springer. Permissions for use may be obtained through RightsLink at the Copyright Clearance Center. Violations are liable to prosecution under the respective Copyright Law.
The use of general descriptive names, registered names, trademarks, service marks, etc. in this publication does not imply, even in the absence of a specific statement, that such names are exempt from the relevant protective laws and regulations and therefore free for general use.
While the advice and information in this book are believed to be true and accurate at the date of publication, neither the authors nor the editors nor the publisher can accept any legal responsibility for any errors or omissions that may be made. The publisher makes no warranty, express or implied, with respect to the material contained herein.

Printed on acid-free paper

Springer is part of Springer Science+Business Media (www.springer.com)

ICITAE 2011 Preface

Ladies and Gentlemen, I am delighted to announce 2011 International Conference on Information Technology and Agricultural Engineering (ICITAE 2011) is to be held in Sanya, China, December 1–2, 2011.

Information technology (IT) is the acquisition, processing, storage and dissemination of vocal, pictorial, textual and numerical information by a microelectronics-based combination of computing and telecommunications. The term in its modern sense first appeared in a 1958 article published in the Harvard Business Review, in which authors Leavitt and Whisler commented that the new technology does not yet have a single established name. We shall call it information technology (IT).. Some of the modern and emerging fields of Information technology are next generation web technologies, bioinformatics, cloud computing, global information systems, large scale knowledgebases, etc.

IT is the area of managing technology and spans wide variety of areas that include but are not limited to things such as processes, computer software, information systems, computer hardware, programming languages, and data constructs. In short, anything that renders data, information or perceived knowledge in any visual format whatsoever, via any multimedia distribution mechanism, is considered part of the IT domain. IT provides businesses with four sets of core services to help execute the business strategy: business process automation, providing information, connecting with customers, and productivity tools.

IT professionals perform a variety of functions (IT Disciplines/Competencies) that ranges from installing applications to designing complex computer networks and information databases. A few of the duties that IT professionals perform may include data management, networking, engineering computer hardware, database and software design, as well as management and administration of entire systems. Information technology is starting to spread further than the conventional personal computer and network technologies, and more into integrations of other technologies such as the use of cell phones, televisions, automobiles, and more, which is increasing the demand for such jobs.

Agricultural engineering is the engineering discipline that applies engineering science and technology to agricultural production and processing. Agricultural engineering combines the disciplines of animal biology, plant biology, and mechanical, civil, electrical and chemical engineering principles with a knowledge of agricultural principles.

Agricultural Engineers may perform tasks as planning, supervising and managing the building of dairy effluent schemes, irrigation, drainage, flood and water control systems, perform environmental impact assessments, agricultural product processing and interpret research results and implement relevant practices. A large percentage of

agricultural engineers work in academia or for government agencies such as the United States Department of Agriculture or state agricultural extension services. Some are consultants, employed by private engineering firms, while others work in industry, for manufacturers of agricultural machinery, equipment, processing technology, and structures for housing livestock and storing crops. Agricultural engineers work in production, sales, management, research and development, or applied science.

ICITAE 2011 is to bring together researchers working in many different areas of Information Technology and Agricultural Engineering to foster international collaborations and exchange of new ideas.

The proceeding presents a selection of 117 papers from over 365 submissions from universities and industries all over the world based on their quality and relevancy to the conference. All the papers have been peer reviewed by the selected experts. These papers represent the latest development in the field of materials manufacturing technology, spanning from the fundamentals to new technologies and applications. Specially, these papers cover the topics of Information Technology and Agricultural Engineering.

I believe that this book provides a greatly valuable reference for researchers in the field of Information Technology and Agricultural Engineering who wish to further understand the underlying mechanisms and create innovative and practical techniques, systems and processes. It should also be particularly useful for engineers in information technology and agriculture who are responsible for the efficient and effective operations.

I wish to express my highly appreciation to all the members of ICITAE 2011 Organizing Committee, Academic Committee and Program Committee as well as the referees, staff and volunteers for their tremendous efforts and dedications. Without their hard work and excellent jobs, it was impossible to lead the success of ICITAE 2011 and this book.

Egui Zhu
Sabo Sambath

Contents

Optimum Condition for 2, 6-DNT–Microbe Degrading Using Uniform Design 1
Yubin Ji, Changru Xu, Wenlan Li, Xingjie Zhu, Jinyu Zhou

Effects of Juglone on ROS Production and Mitochondrial Transmembrane Potential in SGC-7901 Cells 7
Yubin Ji, Zhongyuan Qu, Xiang Zou, Chenfeng Ji

The Study about the Degradation of Nitrobenzene by Domesticated Activated Sludge and the Initial Validation of Toxicology before and after the Degradation 15
Yubin Ji, Zhongyuan Qu, Wenlan Li, Changru Xu, Xingjie Zhu

Study on the Screening for Chloronitrobenzene: Degrading Bacteria and Degradation of Chloronitrobenzene 23
Yubin Ji, Zhongyuan Qu, Wenlan Li, Changru Xu, Xingjie Zhu

Identification and Characterization of *Lactobacillus* Planetarium TH1 31
Hua Tian, Xue-gang Luo, Zhao Han, Ran Hao, Nan Wang, Yong Jiang, Tong-Cun Zhang

Broth Recycling in Liquid Cultivation of Nostoc Flagelliforme Cells 39
Yujie Dai, Feng Zhang, Guoliang Wang, Yonghong Chang, Shiru Jia

Express Transmissible Gastroenteritis Virus Spike Gene B and C Antigen Sites in Multiple Expression Systems 49
Tian-fei Yu, Shu-li Shao, Xing-jun Xu, Jian-wei Lv, Ming Li

Prediction of TGEV Spike Protein Secondary Structure and B Cell Epitopes 57
Tian-fei Yu, Shu-li Shao, Xing-jun Xu, Jian-wei Lv, Ming Li

Total Paeony Glycoside Inhibits Tumor Growth and Induces Apoptosis in K562 Cells and in S180 Tumor-Bearing Mice 61
Huiyu Xu, Yanmin Wu, Xiaoqing Luo, Hui Wang, Zhiwei Chen, Meng Zhang, Danyang Liu

A BP Neural Network Activation Function Used in Exchange Rate Forecasting 69
Xu Chun-Dong, Liao Wei, Zhou Mu-Gui, Liu Jin-Gao

Studying the Ecological Value of "Green Core" in Changsha-Zhuzhou-Xiangtan Area 77
Liu Sihua

Protective Effect of G on UVC-Induced DNA Damage in Mouse Lymphocytes in Vitro 85
CuiLin Cheng, ZhenYu Wang, HaiTian Zhao, Lei Yao

SOC Content and Its Spatial Distribution Characteristics in Urban Forest Ecosystems of Changsha in China 95
Xiao Ying, Liu Sihua

Components from Callus Cultures of *Sonchus Oleraceus* L. and Their Cytotoxicity in Vitro 107
Ming Zhao, Yunpeng Zhao, Fenglan Xing, Liming Bai

Protoplast Formation and Regeneration of *Rhodococcus* sp. BX2 113
Liping Feng, Chunyan Li, Chunhong Xu, Minghua Xiong, Junbo Pan, Xiaosong Cheng

Hyperglycemia and Advanced Glycation Eend-Products Prevent Cognate Differentiation of Human Adipose-Derived Stromal Cells into Bone In Vitro 121
Li Dong Song, Li Shu Qiang, Cai Bo, Wang Ping, Feng Wei, Liu Jian Guo

Expression Abnormality of Myostatin in Malformed Chicken Embryos 129
Chaolai Man

Artificial Intelligence Based Optimization of the Extracting Process of Protein from DDGS Using Alkali Method 135
Yuan Dong, Hongxi Shi, Xin Chen, Cong Liu, Lingyan Liu, Nan Zhao, Yingkun Cheng, Yibo Zhang, Feng Lin, Lirong Teng

Chloroplast-Targeted Expression of Human sTRAIL Protein in Transgenic Tobacco 143
Dan Wang, Xue-Liang Bai, Qing Liu, Ye-Rong Zhu, Yan-Ling Bai, Yong Wang

Comparative Study in Functional Morphology of Antennary Gland of Pacific White Shrimp, Litopenaeus Vannamei, Reared under Various Salinity Condition 151
Xugang He, Guangfu Hu, Guangtao Lu

Association of PS1 Gene Polymorphisms with Alzheimer's Disease in Chinese Population: A Meta-analysis of Case-Control Studies 161
Yaodong Zhang, Yong Xu, Hongwei Nei

Effects of Traditional Chinese Drug on Postoperative Immunoregulation in Breast Cancer Patients 167
Guo-Yong Shan, Jun Yun, Ling Wang

The Research Progress of Bioinformatics-Led Design of Single-Chain Antibody Molecules 175
Guo-Yong Shan, Jian-Hua Zhang

The Design of Ecological Restoration Projects in the River Network Area in Southern Jiangsu Province: Chen Xiangbang Ecological Restoration Demonstration Project 183
Zhang Wenyi, Tan Fangyuan, Liu Mingyuan, Han Youfa, Chen Rong

Antimicrobial Properties of *Xylaria Coprinicola* Accompaning the Growth of *Coprinus Comatus* in China 191
Du Ai-ling, Cao Zhi-min

Growth Inhibition of *Karenia mikimitoi* by Extracts from *Gracilaria lemaneiformis* Using Five Solvents 199
Yingying Sun, Jing Zhang, Shenzhen Xu, Wenhao Li, Changhai Wang

Antialgal Substances from *Isochrysis Galbana* and Its Effects on the Growth of *Isochrysis Galbana* and Six Species of Feed Microalgae 211
Yingying Sun, Shenzhen Xu, Wenhao Li, Jing Zhang, Changhai Wang

Effect of Peanut Roots Intercropped with Rice on Excretion of Nitrogenous Compounds at Different Growth Stages 225
Bo Wang, Shuqi Wang

In Vitro* Antibacterial Effect of Chinese Herbal Medicine against *Aeromonas hydrophila 233
Zhenxia Su, Hui Xiao, Liehuan Chen

Isolate and Characterize ACC Deaminase-Containing Plant Growth-Promoting Rhizobacteria 241
Guo Changhong, Liu Jiali, Lv Yueping

Effects of *aadA* Transplastomic Tobacco on Soil Microbe Number 249
Guo Changhong, Lv Yueping, Yu Jianping, Liu Jiali, Liu Qingguo

Analysis of Crosses between CS-1E Addition Line and CS- 2C Addition Line 255
Guo Changhong, Liu Chunying, Xu Guohui, Su Wenyue

Isolation and Characteristion of Formaldehyde-Degrading Bacteria from Furniture Factory 261
Guo Changhong, Song Lili, Song Ge, Yu Diansi, Dong Rui

Nucleotide Substitution Pattern in Mitochondrial Cytochrome b Pseudogenes of Ten Species in Galliformes 269
Jing Sun, Zeqing Feng, Yiping Liu

Limited Genetic Diversity of Chinese Muscovy Duck (Cairina moschata) Revealed by Partial Sequences of Mitochondrial DNA Cytochrome *b* Gene 279
Jing Sun, Jing Huang, Xiaoling Zhao, Hang Zhong, Qing Zhu, Yiping Liu

Status and Prospect of Crop Rotation of Procambarus Clarkii and Mid-season Rice in China 283
Luojun Gong, Xinya Shu, Congyi Zhang, Bangxi Xiong, Lansong Yang, Qianhong Gu, Jie Chen

Analysis of Codon Usage Bias in Interferon Alpha Gene of the Giant Panda (Ailuropoda Melanoleuca) 293
Yue Yi, Chengdong Wang, Zhiwen Xu, Desheng Li, Ling Zhu, Fengqin Li, Xinqiao Qi, Wanzhu Guo

Effects of Amniotic Membrane Extraction on Rabbit Corneas with Herpes Simplex Keratitis 307
Nan Hu, Ling Yang, Huaijin Guan

Effects of Acetic Acid on Germination and Growth of Turions of *Potamogeton crispus* and Fragments of *Elodea nuttallii* 315
Zuo Jin-Cheng, Liang Wei, Xu Dong, He Feng, Zhou Qiaohong, Wu Zhen-Bin

Efficacy of *Xanthium sibiricum* Fruit Extract on *Lasioderma serricorne* (Coleoptera: Anobiidae) 323
Jian-Hua Lü, Xin-Hong Su

Study on the Meitauza Production from Okara by *Actinomucor Elegans* and *Zymomonas Mobilis* 329
Xilin Xu, Hongwei Liu, Yanliang Zhou

An Evaluation Method of Marine Water Quality Based on Cloud-Model Chart Representation Theory and Its Role in Tourism of Coastal Cities 337
Wang Lu, Wang Yueru, Li Xin

The Qualitative Analysis of Generalized Kolmogorov Biological Population Model with Harvesting Rate 345
Zhang Jian

Adaptive Ideal Image Reconstruction for Bacteria Colony Detection 353
Anan Liu, Zheren Liu, Limin Song, Dong Han

Predicting SOC Concentrations in a Subtropical Mixed Secondary Forest Using Hemispherical Photography 361
Zhi-yao Su, Yu-duan Ou, Dan-dan Xie

Regulation of Resveratrol Prodution by Precursors and Elicitors in Cell Culture of 'Pinot Noir' 371
Zhen Zhang, Sheng Li, Shaoying Ma, Wei Li, Delong Yang, Yuan Liu

Salinization Resistance Transgenic Soybean Reduced Bacterial Diversity in Rhizosphere 377
Zheng Wang, Zhihua Liu, Hongyan Wang

Analysis on Quality Characters Diversity of Wheat Landraces from Yangtze River Valley 385
Wei Zheng, Dongfa Sun, Feng Pan

Effects of Cold Stress on Porcine Fibroblasts HSP90 mRNA Expression 397
Zhongqiu Li, Jianzhang Ma, Chunlong Liu, Hong Ma, Zhenhua Guo, Bo Fu, Liang Wang, Jinyan Sun, Fugang Peng, Di Liu

Experimental Study on Acidic Fibroblast Growth Factor Composited by Partially Deproteinised Bone in Repair of Early-Stage Avascular Necrosis of the Femoral Head in Rabbits 405
Zhu Xiao-qi, Guo Hao, Ge Bao-feng, Zhu Xiao-qi

Insecticidal Activity of Extract from *Cynanchi Auriculati* against Agricultural Pests 419
Minli Yang, Xiaomei Ma, Fengxia Hao

Insecticidal, Antifeedant and Growth-Inhibition Activities of Different Extracts from *Pedicularis Spicata* against *Plutella Xylostella* 425
Minli Yang, Rui Liang, Fengxia Hao

Cloning, Characterization and Expression Analysis of a Cytosolic Ascorbate Peroxidase Gene from *Grimmia Pilifera* 433
Xiao Hong Song, Wei Sha, Zhong Min Jin, Yan Fu Zhang

Isolation and Characterization of Sunflower Protein Isolates and Sunflower Globulins 441
Jian Ren, Xiao-Hong Sun, Guo-Ping Lin, Xi-Qun Zheng, Xiao-Lan Liu

The Inhibitory Effects of Bamboo Vinegar against Bacteria and Fungi 451
Ting Jin, Yuxue Wu, Qiang Wang

Cloning and Sequence Analysis of Donkey Growth Hormone Gene 459
Zhu Wen-jin, Su Yong-mei, Guan Xue-min, Wu Jian-hua, Zhao Yuan-yuan

The Roles of Timosaponin in Inhibiting Adherence of Fungus and Enhancing Function of Phagocyte 465
Lianlan Ma, Zhichun Liu, Xiaoyun Wu, Wenping Zhang

Genetic Polymorphisms of the Second Intron of GH Genes in Chinese Donkeys 471
Xuemin Guan, Yanfang Liu, Yongmei Shu, Wenjin Zhu

Degradation of Soybean Stalk Lignin with White-Rot Fungus and SEM Characterization of Surface Structure 479
Xu Wei

Response Surface Methodology Used for Statistical Optimization of Fermentation Media of *Cordyceps Militaris* 485
Dongxue Liang, Na Zhang, Yaowen Zhang, Tinglan Zhang, Li Lü, Zhenzuo Wang, Lirong Teng

Detection Class I Integron of Multidrug Resistace Pathogenic *Salmonella* from Chicken 493
Qiuyue Wang, Yanying Zhang, Qiumei Shi, Wei Yao, Cuizhen Chen, Guangping Gao, Donglin Zhang, Hai Fang

Ecological Genetics of Himalayan Snowcock *(Tetaogallus himalayensis)* 501
Luzhang Ruan, Huaxing Luo, Naifa Liu, Lixun Zhang, Longying Wen

Isolation, Identification and Significance of Cryptococcus Neoformans and Candida Albicans from Faecal Specimen of Pigeon 507
Zhichun Liu, Lianlan Ma, Youtian Zhong, Xiaoli Wang, Shuixiang Xie

Indole Alkaloids from South China Sea Marine Sponge *Callyspongia* sp. ... 513
Bin Wang, Riming Huang, Yonghong Liu

Development of IgY-Based Sandwich Enzyme-Linked Immunosorbent Assay for the Detection of *Vibrio parahaemolyticus* 517
Qingping Zhong, Yuqing Dong, Li Wang, Binbin He

Subcellular Localization of Melon (*Cucumis melo* L.) Glutamine Synthetases 525
Deng Yang-wu, Yu Shui-jing, Zhang Ping, Zhang Yi-dong, Huang Dan-feng

Magnolia Ethanol Extract on Growth of Tumor in Tumor Mice S180 535
Lin Yuan, Xianju Huang, Jiaqiang Sun

Stability of Anthocyanin in Wild Blueberry Fruit and Its Degradation Kinetics 539
Na Zhang, Qingqi Guo, Yongqiang Ma

A Preliminary Study on Activity Mechanism and Identification of an Extract of Pharbitis Purpurea Seeds against Tetranychus Cinnabarinus . . . 547
Juan Du, Lei Zhao, Lan-qing Ma, Yu-bo Liu, Guang-lu Shi, You-nian Wang, Bao-sheng Tong

The Effects of Lupeol from the Petroleum Ether Extract of Inula Britanica on the Biological and Enzyme Activity of Tetranychus Cinnabarinus 557
Lan-qing Ma, Dan-dan Duan, You-nian Wang, Jun Cheng, Yu-bo Liu, Guang-lu Shi

The Isolation and Identification of the Acaricidal Principal Extracted from Mentha Piperita 565
Jian-ju Ren, Lan-qing Ma, Yu-bo Liu, Guang-lu Shi, You-nian Wang

Effects of Mentha Piperita Extracts on Activities of Several Enzymes of Tetranychus Cinnabarinus 577
Jian-ju Ren, Guang-lu Shi, Lan-qing Ma, Yu-bo Liu, You-nian Wang

Analysis of Acaricidal Activities and Enzymatic Activities of Polygonum Aviculare Extracts against Tetranychus Cinnabarinus 589
Jun Cheng, You-nian Wang, Lan-qing Ma, Yu-bo Liu, Guang-lu Shi

Acaricidal Activity of Stigmasterol from Inula Britannica against Tetranychus Cinnabarinus 599
Jun Cheng, Dan-dan Duan, You-nian Wang, Lan-qing Ma, Yu-bo Liu, Guang-lu Shi

Insecticidal Activity of *Juglans regia* Extracts against *Tetranychus cinnabarinus* and Their Effects on Relative Enzymes Activity in *Tetranychus Cinnabarinus* 611
You-nian Wang, Hai-xiang Wang, Yu-bo Liu, Guang-lu Shi

Acaricidal Activity of the Oleic Acid Methyl Ester from Pharbitis Purpurea Seeds against Tetranychus Cinnabarinus 621
Juan Du, Lei Zhao, Lan-qing Ma, Yu-bo Liu, Guang-lu Shi, You-nian Wang, Bao-sheng Tong

Studies on Action Mechanism of Acrocidal Activity of Extracts of Pharbitis Purpurea Seeds against Tetranychus Cinnabarinus 629
Yan-Wang, Guang-lu Shi, Lan-qin Ma, Yu-bo Liu, You-nian Wang

Componential Analysis and Acaricidal Activities of Stellera Chamaejasme Extracts by Supercritical Fluid Extraction 643
Wei Liang, Jun Cheng, Lan-qing Ma, Yu-bo Liu, Guang-lu Shi, You-nian Wang

Antifungal Activity of Extracts by Supercritical Carbon Dioxide Extraction from Roots of Stellera chamaejasme L. and Analysis of Their Constituents Using GC-MS 653
Xue-na Bai, Jun Cheng, Wei Liang, Lan-qing Ma, Yu-bo Liu, Guang-lu Shi, Younian Wang

Isolation and Identification of the Acaricidal Components Extracted from Stellera chamaejasme 663
Wei Liang, Jun Cheng, Chun-ya Bu, Yong-sheng Jin, Lan-qing Ma, Yu-bo Liu, Guang-lu Shi, You-nian Wang

Effects of Inula britannica Extracts on Biological Activities against Tetranychus cinnabarinus and Several Enzyme Systems in Tetranychus cinnabarinus 673
Lan-qing Ma, Dan-dan Duan, You-nian Wang, Yu-bo Liu, Guang-lu Shi

Antifungal Activity of Extracts of *Stellera chamaejasme* against *Botrytis cinerea* 683
Lei Zhao, You-nian Wang, Juan Du, Chun-ya Bu, Lan-qing Ma, Yu-bo Liu, Guang-lu Shi

Inhibitory Effect and Antifunal Mechanism of Umbelliferone on Plant Pathogenic Fungi 693
Xue-na Bai, Wei Liang, Jun Cheng, Lan-qing Ma, Yu-bo Liu, Guang-lu Shi, You-nian Wang, Ji-cheng Gu

Acaricidal Activity of Ethyl Palmitate against Tetranychus cinnabarinus . . . 703
Chun-ya Bu, Dan-dan Duan, You-nian Wang, Lan-qing Ma, Yu-bo Liu, Guang-lu Shi

Acaricidal Activity of Lupeol from Inula britanica against Tetranychus cinnabarinus (Acari: Tetranychidae) 713
You-nian Wang, Dan-dan Duan, Jun Cheng, Yu-bo Liu, Guang-lu Shi, Bao-sheng Tong

Effects of Stigmasterol to Activities of Several Enzymes of Tetranychus cinnabarinus 721
Dan-dan Duan, Chun-ya Bu, Jun Cheng, Lan-qing Ma, Yu-bo Liu, You-nian Wang, Guang-lu Shi

Acaricidal Activities of the Polygonum Aviculare Extracts against Tetranychus cinnabarinus and Its Affection to the Enzyme Activities 731
Yong-sheng Jin, Qing Li, Jun Cheng, Lan-qing Ma, Yu-bo Liu, You-nian Wang, Guang-lu Shi

Identification of Acarcidal Compounds in Inula japonica Extracts against Tetranychus cinnabarinus 739
Dan-dan Duan, Chun-ya Bu, Lan-qing Ma, Yu-bo Liu, You-nian Wang, Guang-lu Shi

Characterization of Synonymous Codon Usage in the Newly Identified Duck Plague Virus UL16 Gene 747
Qin He, Mingshu Wang, Anchun Cheng, Dekang Zhu, Xiaoyue Chen, Renyong Jia, Qihui Luo, Yi Zhou, Zhengli Chen

Microbe Distribution and Dynamic Characters of Oil Degradation in the Contaminated Soils 763
Luqing Jiang, Xilai Zheng, Lei Chen

Iteratively Predict Protein Functions From Protein- Protein Interactions . . . 771
Xiaoxiao Chia, Jingyu Hou

Integration of Multiple Methods to Identify Major Wild Bird Species around Qinghai Lake 779
Li Jian, Zhang RuiYing, Wan SunHua, Cao WenBin, Zhu ChaoDong, Lei FuMin, Yan BaoPing

Downregulation of IL-15 and IL-18 in Chicken Embryo Fibroblasts in Response to Virulent or Lentogenic Newcastle Disease Virus Infection 789
Yuanping Wang, Wenquan Liu, Mingxing Tian, Yan Lin, Fangfang Zhao, Min Shi, Sanjie Cao, Xintian Wen, Yong Huang

Changes in Phenotypic Traits for Key Inbred Lines of Chinese Maize 801
Ying-Hong Liu, Yubi Huang, Mengliang Tian, Junjie Zhang

Association of EphrinB2 Gene Polymorphism with Litter Size in Pigs 811
Yanfeng Fu, Guiying Wang, Jinluan Fu, Aiguo Wang

Efficient Water-Saving Irrigation Solution for Direct Seeding Rice under No-Tillage after Cultivating Wheat 819
Zhengguo Sun, Chengming Sun, Yizhao Chen, Jianlong Li, Hongcheng Zhang

Molecular Cloning of Arabidopsis thaliana HsfA2 Gene and Agrobacterium-Mediated Genetic Transformation of Chrysanthemum Morifolium Ramat 827
Lingli Zhao, Huitang Pan, Ming Sun, Qixiang Zhang

Isolation, Characterization and Sequence Analysis of Resistance Gene Analogs (RGAs) in Plants Related to Huanglongbing (HLB) 835
Liu Tingting, Yin Youping, Lin Yayu, Wang Zhongkang

Chromosomal Heterozygosity of Knob-Associated Sequences in Maize Inbred Line Zi330 843
Fei Yang, Yanho Xu

Quantum Yields in Photolyses of Mammalian Carboxy-Hemoglobin Studied by Pulsed Laser Pump-Probe Technique 849
Jin-yu Zhao, Min Qu, Jia-huang Li, Zheng Zhang, Shu-yi Zhang, Yue-tao Yang, Zi-chun Hua

Last Instar Larval Morphology of Three Species of Catocalinae (Lepidoptera: Noctuidae) from China 857
Piao Mei-hua, Fan Le-hui, Zheng Ying-cha

3D Observation and Preliminary Quantitative Analysis of Germinal Vesicle Oocytes in Aging and Pubertal Mice 863
Ning Tian, Lu Zhang, Jing-gao Zheng, Die-yan Chen, Ying Li, Wan-yun Ma

Species Sensitivity Distribution for Arsenic Toxicity on Plant Based on Soil Culture Data: Implications for Benchmarks of Soil Risk Assessments 871
Bai-ye Sun, Xiao-ru Pan, Feng Zhou

SA and PEG-Induced Priming for Water Stress Tolerance in Rice Seedling 881
Xuemei Li, Lihong Zhang

Exogenous Treatment with Salicylic Acid Attenuates Ultraviolet-B Radiation Stress in Soybean Seedlings 889
Lihong Zhang, Xuemei Li

Effect of Cold-Active Protease Treatments on Bigeye Tuna (Thunnus Obesus) Meat during Chilled Storage 895
Wang Quan-fu, Hou Yan-hua, Yan Pei-sheng

Application Efficacy of Biological Seed Coating Agent from Combination of PGPR on Cotton in the Field 903
Zhansheng Wu, Lixia Yao, Imdad Kaleem, Chun Li

Arsenite Exposure Induces Oxidative Stresses in the Nematode Caenorhabditis Elegans 911
Shunchang Wang, Zhizhong Geng, Yan Yu, Jinhua Guo

RNA3 of a Cucumber Mosaic Virus Strain Infecting Musa Basjoo Based on the Molecular Characterization of Its 5' UTR 919
Zuodong Qin, Leilei Jin, Fangjiao Xu, Jingwei Zhang, Pingkai Ouyang, Jishuang Chen

Analysis of Flavonoids and Phenolic Acids of Aqueous Extracts in Leaves of Apocynum venetum L. 925
Xiao-ying Yin, Jian-jiang Fu, Hua-sheng Yang, Hong-ning Liu, Yong-ming Luo

Effect of Glomus Mosseae Inoculation on Growth and Reproduction of Rice 935
Wang Li, Ma Fang, Zhang Shujuan, Zhang Xue

Distinctness Determination of DUS Test on Some Quantitative Characteristics of Rice 943
Yanfang Liu, Xiaohong Yang, Jianhua Zhang, Junjiao Guan, Jiangmin Wang, Hui Zhang

Effect of Different Wet Oxidation Pretreatment Conditions on Ethanol Fermentation from Corn Stover 953
Zhang Qiang, Anne Belinda Thomsen

Polysaccharides from Acanthopanacis Senticosi: Isolation, Purification, Antioxidant and Immunological Activities in Vitro 959
Chen Ruizhan, Yang Simin, Dong Hang, Liu Zhiqiang

Effects of Trehalose, Glycerin and NaCl on the Growth and Freeze-Drying of Lactobacillus Acidophilus 967
Chen He, Ji Zhe, Wang Lei, Shu Guowei

Microbial Changes and Fresh-Keeping of Fresh Noodles under Refrigerated Condition 973
Shuncheng Ren, Ruiping Ma, Ning Wang

Effects of Functional Protein from Milk on Osteoclasts of Rats 981
Jie Sun, Guoyou Yin

Author Index 987

Optimum Condition for 2, 6-DNT –Microbe Degrading Using Uniform Design

Yubin Ji[1], Changru Xu[1], Wenlan Li[1], Xingjie Zhu[2], and Jinyu Zhou[2]

[1] Institute of Materia Medica and Postdoctoral Programme Harbin University Commerce
Harbin, China
[2] Engineering Reseach Center of Natural Anticancer Drugs, Ministry of Education
Harbin, China
wudi1270@yahoo.cn

Abstract. The GC-ECD was used in this study. The optimization of preparation was performed by U9(94)uniform design method，With the rate of 2，6-DNT -degrading result as investigative indexes, the influences of of ratio the concentration of substrate and PH,The speed of shaker and Temperature. the result were screened by Uniform Design to found the optimum condition of degrading . Result the optimum condition for 2, 6-DNT -degrading as fllowing: The concentration of substrate is 135mg/L, pH=7.3, Temperature is 29℃, speed of shaker is 129 rpm/min. The result show：It is scientific and feasible to screen the experimental condition of for 2, 6-DNT - degrading by using the uniform design and regression.

Keywords: Uniform design, COD, Degradation, Domestication.

1 Introduction

Dinitrotoluene (DNT) is a nitro-aromatic organic pollutant, which has a certain chemical activity. it is broken down by heated, potential application of DNT and its derivatives have been of interest in the past few years in a broad range of weapon industry and the production of military and civilian goods. it is mutagenic and suspected carcinogenic, having toxic effects on both animals and human beings, on the human central nervous system, especially(1). It is a potential hazard to human health. the 2,4-DNT and 2,6-DNT are common in the municipal sludge and groundwater. It is hard to degradable (2-3), they can cause the pollution of soil and crops and the impact on the growth, development and reproduction of the aquatic life(4). When the concentration is up to 10mg/L, they can cause the death of fish and aquatic organisms (5). And the synergy of binary mixtures makes toxicity much stronger, which brings a serious damage to the aquaticecosystem. it is classified as a member of the "excellent control of pollutants" by the United States National Environmental Protection Agency (USEPA)(6) .Therefore, it is necessary to find a degradation method that is economical and does not cause secondary pollution.

Biodegradation is a phenomenon that biological organisms turn to simpler compounds through a series of biochemical reactions .by the help of enzymes; sometimes they can completely turn to inorganic. In most aerobic and anaerobic environments, a lot of recalcitrant compounds can be degraded effectively through the

E. Zhu and S. Sambath (Eds.): Information Tech. and Agricultural Eng., AISC 134, pp. 1–6.
springerlink.com © Springer-Verlag Berlin Heidelberg 2012

metabolic activities of the environmental microbe. Microbial degradation becomes a principal degradation method of environmental pollutants, because of the advantages such as the low price, easy to control, the simple condition, not any secondary pollution and so on. In this study 2,6-DNT-degrading activity sludge was gained from the domestication of the strain; multi-factor multi-level Uniform Design was also invited to gain the.

2 Materials and Methods

2.1 Experimental Strain

Bacteria come from the activated sludge in the aeration tank of Harbin Sewage Treatment Plant.

2.2 Instruments and Reagents

Inorganic salt medium: MnSO4.7H2O 0.28mg; FeSO4.7H2O 0.3mg; MgSO4.7H2O 0.06mg; CaCl2 1mg; CuSO4 0.05mg; ZnSO4 0.05mg; H3BO3 0.05mg; distilled water 1000mL. Test reagent: 2,6-Dinitrotoluene standard (AccuStandard); 2,6-Dinitrotoluene analytically pure (MERCK); chromatography pure benzene (Tianjin Chemical Reagent Research Institute), analytically pure ethanol (Tianjin Tianxin Fine Chemicals Development Center), distilled water.

Instrument: HDL turbulence incubator HZQ-F16 (vibration mode: maneuver); Aikele Analytical Balance (ALC-110.4); Angilent6890 gas chromatography-electron capture detector instrument (United States); DPS statistical software (Beijing Zhongnongbosi Science and Technology Development Corporation).

2.3 Methods

1) Domestication and Ex-cultivation of Degradation Bacteria

Add 50 mL inorganic salt medium into a 250mL-conical beaker, and then add some 2,6-DNT(the concentration is up to the following experimental conditions). Shake it then it becomes the domestication medium. Take 1mL of the supernatant of activated sludge into it and cultivated in the incubator shaker at 30℃, 130r/min. Take 50mg/L as the initial concentration, 5d as a cycle to domesticate it. And during this period increase the concentration of 2,6-Dinitrotoluene gradually as 50,70,90,110,130,150, 170mg/L. After the domestication, add 100 mL inorganic salt medium into a 500mL-conical beaker and then add a small amount of beef extract. Take it for high-pressure sterilization. After the sterilization, take 10mL domesticated bacilli into the 500mL-conical beaker to expand the training and achieve the logarithmic growth phase (6).

2) Analytical Methods

Sample Treatment: Extract the 2mL-degradated fluid twice through 2mL chromatography with Benzene and combine the extractions. Dry it over through the anhydrous sodium sulfate column and filter under the use of microporous membrane.

GC-ECD Determination Conditions: capillary column HP-5MS (30m×0.25mm×0.25μm); 63Ni electron capture detector; carrier gas flow rate

0.8mL/min, inlet temperature: 230℃; temperature 300℃; column temperature 165℃; split injection, split ratio 50:1; injection volume 0.2μL.

3) Factors Affecting Degradation

Conditions affect the degradation are mainly: PH value, temperature, oxygen demand (shaker speed), the substrate concentration. Selected ranges for the major factors are as shown in Table 1(7).

Carry out the uniform experimental design to the data by the use of DPS software. Add 100mL domesticated medium into the conical flask, and then add 4mL domesticated bacilli. The degradation time is 5d. Sample respectively at 24,48,72,96,120h, and each for 1mL.Calculate the degradation rate, half-life, degradation rate constant, and verify the optimal conditions through screening.

Table 1. Factors in the table

NO	Substrate concentration (mg/L)	PH Valve	Temperature (℃)	Shaker Speed (r/min)
1	15	5	5	100
2	30	5.5	10	110
3	45	6	15	120
4	60	6.5	20	130
5	75	7	25	140
6	90	7.5	30	150
7	105	8	35	160
8	120	8.5	40	170
9	135	9	45	180

3 Results and Analysis

3.1 Drawing of the Standard Curve and the Linear Range

Weigh 10 mg of 2,6-Dinitrotoluene standard accurately into 100mL-flask, adding benzene to the scale in order to gain the 100mg/L standard solution. Dilute it to a series of concentrations as 30,60,90,120,150,180,210,240,270,300μg/L 2,6-Dinitrotoluene standard solution. Detect with GC-ECD. Take peak area (AUS) as the vertical axis, the concentration (C) as the abscissa, and then the standard curve is Y = 275353X + 600000, R = 0.9997. It shows that 2,6-DNT has a good linear relationship within the concentration scope of 30 ~ 300μg/L.

3.2 Result Analysis on the Degradation Conditions by Uniform Design Analysis

Gain the 9 units testing conditions by using U9 (94) uniform design method for optimal degradation conditions(8). And after the 5d-degradation, degradation rates under different conditions can be know. The equation is fitted to a kinetic equation, and the degradation rate constants and half-life are shown in Table 2.

The optimization equation is obtained through the quadratic polynomial regression of the four factors and the degradation rate in Table 2 by the use of DPS software: Y=197.9294712-22.929928813X1-0.7058404862X3+1.4521173438X1X1+0.0028964509323X3X3-0.0008412500401X4X4-0.0005513381186X1X2+0.04325027929X1X4, significance level p=0.0492, statistical value F=244.1291, correlation coefficient R=0.9997, adjusted correlation coefficient Ra=0.9977. Goodness of fit shows a good equation, and factors are significant. The above data indicate that the optimal degradation conditions based on the degradation rate, half-life and degradation rate constant were: PH value 7.2749, temperature 28.5388℃, speed 128.9894r/min, substrate concentration 135mg/L.

Table 2. U9 (94) Uniform design, degradation rate and half-life（n=3）

NO	Initial concentration(mg/L)	PH	Temperature (℃)	Shaker Speed (r/min)	Degradation rate (%)	Degradation rate Constant	half-life (d)
1	30	5.5	40	120	61.05	0.943	0.73
2	90	7	45	160	60.13	0.920	0.75
3	105	6.5	25	100	75.42	1.403	0.494
4	75	9	15	110	59.5	0.904	0.77
5	45	8.5	30	180	67.45	1.122	0.62
6	60	5	20	150	55.37	0.807	0.86
7	120	6	10	170	60.68	0.933	0.74
8	135	8	35	130	85.21	1.794	0.39
9	15	7.5	5	140	45.49	0.607	1.14

3.3 Compliance Test

In the optimizing conditions (PH value 7.3, temperature 29℃, speed 129r/min, substrate concentration 135mg/L), the verification experiment is carried out. Take 4mL domesticated activated sludge into 100mL medium. Set three parallel sample groups. Placed them in the constant temperature shaker incubator cultured for 120h.

Sample for 1mL respectively at 2,4,10,24,36,48,72,96,120h, accompanying supplement. After the sample extraction, dry it through anhydrous sodium sulfate and then filter it through the membrane, dilute it to the linear range of standard curve, detect it with GC-ECD and calculate the concentration of 2,6-DNT with the one point external standard method. Under these conditions, the degradation rate of 2,6-DNT was 96.5%, the degradation half-life was 0.38d, and the degradation rate constant was 1.821. The degradation curve is shown in Figure 1. The verification results were similar to the predicted one through the uniform design experiment, which indicated that the degradation conditions of this experiment was accurate and feasibe.

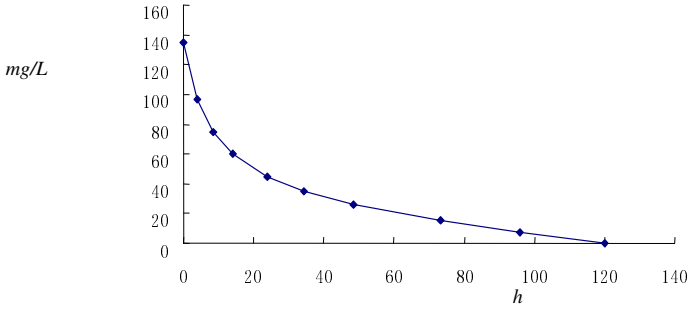

Fig. 1. 2,6-DNT degradation curve

4 Conclusion

- Domesticate the activated sludge comes from the aeration tank of Harbin Sewage Treatment Plant, taking 2,6-DNT as the sole carbon and nitrogen source, and gradually increasing its concentration. Therefore, the activated sludge has a much stronger degradation ability to 2, 6-DNT the degradation rate of which can reaches 96.5% in 5d.
- The uniform design is a multi-factor experimental design method which can reduce the reduce the number of experiments, make a quantitative prediction of the optimum conditions and results . In this study, with the uniform design, the ultimate optimizing conditions for the degradation of 2,6-DNT were: PH value 7.5, temperature 29℃, speed 129r/min, substrate concentration 135mg/L. In this degradation condition, the degradation rate of 2,6-DNT was 96.5%, the degradation half-life was 0.38d, and the degradation rate constant was 1.821.

References

1. Xu, Y., Zhao, J.: Study on the Treatment of Dye Intermediate Wastewater. Journal of Hehai University 29(4), 99–103 (2001); Clerk Maxwell, J.: A Treatise on Electricity and Magnetism, 3rd edn., vol. 2, pp. 68–73. Clarendon, Oxford (1892)
2. Liang, L., et al.: The Effects of Trinitrotoluene on Rhesus Monkey Peripheral Blood Lymphocytes Sister Chromatid Exchange. China Tropical Medicine 5(5), 1146–1147 (2005)

3. Peng, K., et al.: Sub-acute Toxicity and Accumulation Toxicity and Mutagenic Effects of Triphenyl Bismuth. Industrial Hygiene Occupational Diseases 31(1), 35–38 (2005)
4. Sheng, L., et al.: Studies on the Microbial Degradation of Nitrobenzene Compounds. Journal of Applied Ecology 18(7), 1654–1660 (2007)
5. Xu, Y., Qin, N., Liu, X., et al.: Chromium Pollution and the Ecological Effects. Environmental Science and Technology 25(Suppl.), 8–9, 28 (2002)
6. Turchi, C.S., Ollis, D.: F1 Photocatalytic degradation of organi cwatercontaminants: mechanisms involving hydroxyl radical attack. J. Catalysis 122(1), 178–192 (1990)
7. Strandberg, G.W., Lewis, S.N.: The Solubilization of Coal byan Extracellular Product from Streptomyees Setonii 75Vi2 Ind. Microbiol. 1, 371–376 (1987)
8. Zhang, C., Li, W., Nan, L., et al.: Optimization on the Extraction Process of Total Glycosides from Ba Zhen Tang with Uniform Design. Harbin University of Commerce Sinica 2(25), 135–139 (2009)

Effects of Juglone on ROS Production and Mitochondrial Transmembrane Potential in SGC-7901 Cells

Yubin Ji[1], Zhongyuan Qu[1], Xiang Zou[2], and Chenfeng Ji[2]

[1] Institute of Materia Medica and Postdoctoral Programme, Harbin University of Commerce
Harbin, China
[2] Engineering Reseach Center of Natural Anticancer Drugs, Ministry of Education
Harbin, China
Smilejcf001@sina.com, jichenfeng@hrbcu.edu.cn

Abstract. To investigate the effects of juglone on ROS production and mitochondrial transmembrane potential ($\Delta\Psi_m$) in SGC-7901 cells in vitro, further to elucidate the apoptosis mechanism. The apoptosis morphological changes of SGC-7901 cells were observed using fluorescence microscope. The level of ROS and $\Delta\Psi_m$ of cells were detected by FCM. The change of $[Ca^{2+}]_i$ in cells stained with Fluo-3/AM was observed by LCSM. Hoechst 33258 staining assay showed thick granulated fluorescence in condensed nuclei and cytoplasm, and the number of apoptotic bodies was increased with increasing of juglone concentration. The level of ROS at the dose of 5, 10, 15 and 20μM of juglone was 34.83±1.45%, 42.43±1.36%, 53.73±1.38% and 68.67±1.33%, respectively, which were significantly higher than that in control group (P<0.01). The concentration of Ca^{2+} in cells exposed to juglone for 24 h was increased significantly in a dose dependent manner compared with control group (P<0.01). $\Delta\Psi_m$ of treatment groups was 85.53±1.82%, 53.57±2.48%, 46.33±1.46%, 36.43±2.64%, respectively, which were significantly lower than that in control group (P<0.01).Therefore, juglone can increase intracellular level of ROS and concentration of Ca^{2+}, decrease $\Delta\Psi_m$ and induce the cells apoptosis.

Keywords: Juglone, ROS, Mitochondrial transmembrane potential, Human gastric carcinoma SGC-7901.

1 Introduction

Juglone, one of naturally occurring naphthoquinone found in *Juglands mandshurica*, *J. nigra*, *J.regia* and *J. cinerea*, has been documented to be an antitumor active composition. According to the reference, juglone could inhibit intestinal carcinogenesis induced by azoxymethane in rats and might be a promising chemopreventive agent to human intestinal neoplasia [1]. Juglone was also proved as a potent cytotoxic agent against tumor cell lines. Juglone could inhibit growth of HCT-15 cells derived from human colon carcinoma and block S phase in cell cycle

E. Zhu and S. Sambath (Eds.): Information Tech. and Agricultural Eng., AISC 134, pp. 7–14.
springerlink.com © Springer-Verlag Berlin Heidelberg 2012

mainly revealed by flow cytometric histograms [2]. Human leukemia (HL-60) cells and doxorubicin-resistant human leukemia (HL-60R) cells were equally sensitive to juglone [3]. Our previous studies suggested juglone could inhibit the growth and induce apoptosis of human gastric cancer cell line SGC-7901. However, the extract mechanism of apoptosis inducing effect of juglone remains vague. In the present study, the mechanisms of juglone-induced apoptosis on SGC-7901 cells were preliminarily investigated.

2 Materials

2.1 Drug and Reagent

Juglone with a purity of 98.5% was prepared by Center of Research and Development on Life Sciences and Environmental Sciences of Harbin University of Commerce; HCPT was purchased from Harbin Shengtai Pharmaceutical Co., Ltd. RPMI 1640 culture medium (Invitrogen Corporation); fetal bovine serum (Hangzhou Sijiqing Biological Engineering Materials Co.,Ltd); pancreatin (Gibco); Hoechst 33258 (Sigma); Reactive Oxygen Species Assay Kit (Beyotime Institute of Biotechnology); Fluo-3/AM(Molecular Probes Inc,USA) ; Rhodamine 123 (Sigma).

2.2 Apparatuses

CO_2 incubator (CO-150, NBS, US); superclean bench (DL-CJ-1N, Beijing Donglian Har Instrument Manufacture Co.,Ltd.); inverted microscope (CKX 41, Olympus, Japan); fluorescence microscope (DMI3000B, Leica, Germany); laser confocal scanning microscope (SP2, Leica, Germany); flow cytometry (EPICS XL-MCL, Beckman Coulter, US); micromixer (TL-2000MM III, Jiangyan Medical Equipments Co., Ltd., Jiangsu); centrifuge (TDL80-2B, shanghai anting scientific instrument factory); Whatman filter (3 mm, Watson Biotechnologies, Inc.).

2.3 Tumor Cell Lines

Human gastric cancer SGC-7901 cells were purchased from the Institute for Cancer Research, Heilongjiang Cancer Hospital.

3 Methods

3.1 Cell Incubation

SGC-7901 cell culture was incubated in RPMI 1640 medium containing 10% fetal bovine serum with CO_2 and at 37℃, and transfer of culture was performed once every 2-3 days.

3.2 Observation of Morphological Changes of SGC-7901 Cells Using Fluorescence Microscope

Apoptotic morphology of SGC-7901 cells treated with juglone was observed by using fluorescence microscope with Hoechst 33258 labeling method. SGC-7901 cells of the phase of logarithmic growth were digested with 0.25% pancreatin, diluted with RPMI-1640 culture medium containing 10% fetal bovine serum and the cell concentration was adjusted to 3×10^5 cells/mL. Cells were plated at 1mL /well in 6-well plates and incubated at 37℃ with 5% CO_2. Juglone and HCPT (positive control drug) were initially dissolved in ethanol and then diluted with the medium and the final ethanol content was no more than 2%. After the cells had been incubated for 24 h, juglone was added to the wells, 1 mL per well, at the final concentration of 5, 10, 15 and 20μM respectively. HCPT, was also added to the wells, 1mL per well, at the final concentration of 60μM. In control group, the same volume of the medium was added to the wells. After further incubated for 48 h, the supernatant was removed and the cells were washed with PBS once. Then the fixation fluid (methanol: acetic acid, 3:1) was added to 6-well plates at 800 μL/well at 4℃. After 60 min the fixation fluid was removed and the cells were washed with PBS once. Then the cells were fluorescence stained with Hoechst 33258 at 37℃, avoiding light, for 30min and then observed under fluorescence-microscope.

3.3 Determination of Generation of ROS in SGC-7901 Cells Using FCM

Levels of ROS in control and juglone treated cells was determined by staining the cells with DCFDA. DCFDA is cell permeable and is cleaved by nonspecific esterases and oxidized by peroxides produced in the cells to form fluorescent DCF. The intensity of DCF fluorescence is proportional to the amount of peroxide produced in the cells (Rakhee *et al.*, 2008). Briefly, SGC-7901 cells were plated at in 6-well plates (3×10^5 cells /well) and allowed to attach overnight. After treatment of cells with juglone or medium for 24 h, cells were further incubated with 10 μM DCFDA at 37℃ for 20min. In positive control group, 3×10^5 cells labelled by DCFH-DA were treated with 1 μL Rosup for 20min.Subsequently, cells were removed, washed and re-suspended in PBS, filtrate with 300 apertures and analyzed for DCF fluorescence by FCM. Approximately 10,000 cells were evaluated for each sample.

3.4 Detectation of the Change of the Concentration of Calcium in SGC-7901 Cells Using LCSM

The change of the concentration of calcium in SGC-7901 cells were detected by using a LCSM with Fluo-3 AM labeling method. SGC-7901 cells were plated at in 6-well plates (3×105 cells /well) and allowed to attach overnight. After treated with ethanol, juglone or HCPT for 24 h, cells were collected, re-suspended with PBS and the cell

concentration was adjusted to 2×105 cells/mL. The cell suspension was centrifuged at 1500 rpm for 10 min and the supernatant was removed. Then the cells were fluorescence stained with Fluo-3/AM at 37℃, avoiding light, for 60min. Stained cells were centrifuged and the supernatant was removed. Then the cells was re-suspended with 400 μL of PBS and observed by LCSM.

3.5 Detection of Juglone-Induced Change in Mitochondrial Transmembrane Potential ($\Delta\Psi_m$) in the Cells Using FCM

Rhodamine 123 was used to evaluate perturbations in mitochondrial transmembrane potential. SGC-7901 cells were plated at in 6-well plates (3×10^5 cells/well) and allowed to attach overnight. After treatment of cells with juglone, HCPT or medium for 24 h, cells were collected to 10 mL centrifuge tube and re-suspended in 500 μL PBS, and then 500μL 20 μg/mL of Rhodamine 123 was gently added to the tube, so that the final concentration was 10μg/mL. The cells were then incubated for 30 min in the dark. Cells were centrifuged at 1 500 rpm for 5 min and removed supernatant, gently rinsed one times with PBS and then re-suspended in 800 μL PBS. After filtration (300 apertures), the suspension was analyzed by FCM.

3.6 Statistical Analysis

All values are expressed as $\bar{x}\pm s$, and all statistical analysis was performed by analysis of variance (ANOVA). A P value less than 0.05 was considered as statistically significant.

4 Results

4.1 Effect of Juglone on the Morphology of SGC-7901 Cells

SGC-7901 cells were stained with Hoechst 33258 and then observed by fluorescence microscope. As shown in Fig. 1, homogeneous fluorescence of the cells was seen in control group and thick granulated fluorescence in condensed nuclei and cytoplasm of SGC-7901 cells treated with juglone for 48 h, and the number of apoptotic bodies increased with increasing of juglone concentration. Apoptotic bodies could also be seen in positive control group.

4.2 Effects of Juglone on Generation of ROS in SGC-7901 Cells

The results showed that the level of ROS at the dose of 5, 10, 15 and 20μM of juglone was 34.83±1.45%, 42.43±1.36%, 53.73±1.38% and 68.67±1.33 %, respectively, which were significantly higher than that in control group (P<0.01). The level of ROS of positive group was 72.53±1.27 %% (Fig. 2).

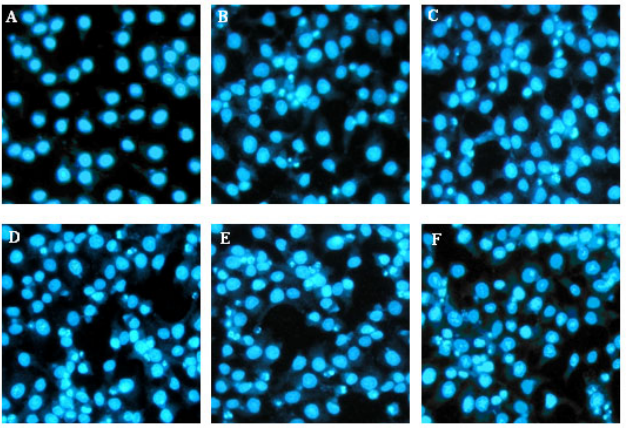

Fig. 1. Effect of juglone on the morphology of SGC-7901 cells
A. Control B. Juglone (5 μM) C. Juglone (10 μM) D. Juglone (15μM) E. Juglone (20μM) F. HCPT (60μM)

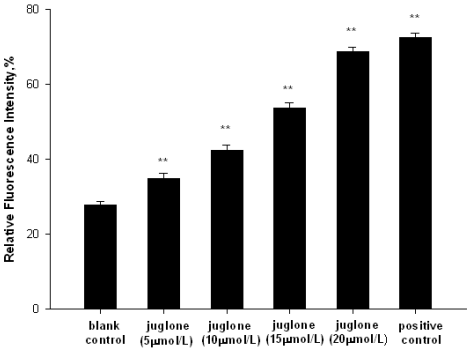

Fig. 2. Effect of Juglone on generation of ROS of SGC-7901 cells
A. Control B. Juglone (5 μM) C. Juglone (10 μM) D. Juglone (15μM) E. Juglone (20μM) F. HCPT (60μM)

4.3 Change of the Concentration of Calcium in SGC-7901 Cells Induced by Juglone

SGC-7901 cells were double stained with Fluo-3/AM, and change of $[Ca^{2+}]_I$ in the cells were observed by LCSM. The results showed that the concentration of Ca^{2+}in the cells exposed to juglone for 24 h was increased significantly in a dose dependent manner compared with control group(P<0.01) (Table 1).

Table 1. Effects of juglone on $[ca^{2+}]_i$ in sgc-7901 cells ($\bar{x}$±s, n=20)

	Concentration (μM)	Variation of $[Ca^{2+}]_i$ (fluorescent Intensity)		
		Test 1	Test 2	Test 3
	—	32.08±3.86	31.74±3.82	32.18±3.87
	5	66.22±3.97**	66.55±3.99**	64.26±3.86**
	10	80.63±4.25**	80.91±4.26**	78.11±4.12**
	15	90.74±4.89**	89.28±4.90**	91.10±4.92**
	20	103.86±4.98**	100.33±4.73**	104.48±5.00**
HCPT	60	97.83±6.10**	98.27±6.13**	94.82±5.91**

**Compared with control $P<0.01$

4.4 Mitochondrial Transmembrane Potential ($\Delta\Psi_m$) Changes in SGC-7901 Cells Induced by Juglone

From Fig. 3 it can be seen that juglone could decrease the mitochondrial transmembrane potential in SGC-7901 cells. There was a negative correlation between the $\Delta\Psi_m$ and the concentration of juglone.

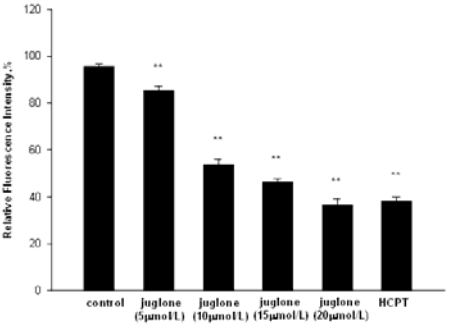

Fig. 3. Effect of Juglone on mitochondrial transmembrane potential of SGC-7901 cells by FCM A. Control B. Juglone (5 μM) C. Juglone (10 μM) D. Juglone (15μM) E. Juglone (20μM) F. HCPT (60μM)

5 Discussion

Many Quinones, such as adriamycin, Mitoxantrone, Carboquone and shikonin have been applied as anticancer drugs. The biological effects of Quinones are largely caused by the formation of reactive oxygen species through redox activation and the covalent modification of free thiols to form thioethers [4]. In our previous study, the results suggested juglone (5-hydroxy-1,4-naphthoquinone) was a strong cytotoxic agent which was in accordancewith that reported in literature. Its cytotoxicity is based on the high reactivity with oxygen and it is frequently applied as a free radical enhancer [5]. Juglone were found to undergo rapid single-electron reduction to semiquinone radicals and the relevant enzymes are microsomal NADPH-cytochrome P450 reductase, microsomal NADH-cytochrome b_5 reductase and mitochondria1 NADH-ubiquinone oxidoreductase [6]. The semiquinone radicals rapidly reduce molecular oxygen to form the superoxide anion radical ($O_{2\cdot}^{-}$) and thereby regenerate the quinone. Subsequent enzymatic or spontaneous dismutation of $O_{2\cdot}^{-}$ yields hydrogen peroxide (H_2O_2), which can enter into further reactions to form the hydroxyl radical (OH·) [7]. So we conjecture that ROS production by redox-cycling quinones may be involved in juglone-induced apoptosis. In this study, the results showed that after exposed to juglone for 24h, the level of ROS of the cells was increased in a concentration- dependent manner in each group, which were significantly higher than that in control group ($P<0.01$). ROS are the known mediators of intracellular signaling cascades. Excessive production of ROS nevertheless leads to oxidative stress, loss of cell function, and ultimately apoptosis or necrosis [8, 9]. ROS can induce lipid peroxidation or cross linking of thiol groups in proteins, both of which can result in opening of the mitochondrial permeability transition pore (PTP) [10].

Ca^{2+} also plays an important role during the process of apoptosis. Intracellular Ca^{2+}concentration increasing leads to mitochondrial calcium overload. Excessive Ca^{2+} within mitochondria can induce apoptosis by opening the mitochondrial PTP. Our results showed that the concentration of Ca^{2+}in the cells exposed to juglone for 24 h was increased significantly in a dose dependent manner compared with control group($P<0.01$).

The opening of mitochondrial PTP can lead to the release of cytochrome C and other pro-apoptotic molecules from the intermembrane space. Once cytochrome c is released into the cytosol, it forms an apoptosome with Apaf-1 and procaspase-9. This causes the activation of caspase-9, which further activates caspase-3 and perform the final steps in the apoptosis process [11, 12]. Mitochondrial PTP opening causes a series of apoptosis-related events. PT channels are a kind of channels with high electric conductivity. The lowering or even disappearance of membrane potential would suggest that PT channels are open. Our results indicated that juglone could decrease the mitochondrial transmembrane potential in SGC-7901 cells. There was a negative correlation between the mitochondrial transmembrane potential and the concentration of juglone.

Taken together, our results demonstrate that juglone can induce apoptosis in SGC-7901 cells through generation of ROS, increasing $[Ca^{2+}]_i$ in the cells, promotion the opening of mitochondrial PTP and then induce apoptosis of SGC-7901 cells. However, to elucidate how the mitochondrial PT channels are opened and which proteins and genes are involved in this process, further research is needed.

Acknowledgements. This work was supported by Supported by National Natural Science Foundation of China (No. 30600816) and the Research Fund for the Doctoral Program of Higher Education of China (No. 20060240001).

References

1. Sugie, S., Okamoto, K., Rahman, K.M., et al.: Inhibitory effects of plumbagin and juglone on azoxymethane-induced intestinal carcinogenesis in rats. Cancer Letters 127, 177–183 (1998)
2. Kamei, H., Koide, T., Kojima, T., et al.: Inhibition of cell growth in culture by quinones. Cancer Biotherapy and Radiopharmaceuticals 13, 185–188 (1998)
3. Segura-Aguilar, J., Jonsson, K., Tidefelt, U., et al.: The cytotoxic effects of 5-OH-1,4-naphthoquinone and 5,8-diOH-1,4-naphthoquinone on doxorubicin-resistant human leukemia cells (HL-60). Leukemia Research 16, 631–637 (1992)
4. Bolton, J.L., Trush, M.A., Penning, T.M., et al.: Role of quinones in toxicology. Chemical Research in Toxicology 13, 135–160 (2000)
5. Bhuyan, K.C., Bhuyan, D.K., Podos, S.M.: Free radical enhancer xenobiotic is an inducer of cataract in rabbit. Free Radical Research Communications 12-13, 609–620 (1991)
6. Monks, T.J., Hanzli, R.P.K., Cohen, G.M., et al.: Quinone chemistry and toxicity. Toxicol. Appl. Fharmacol. 112, 2–16 (1992)
7. Babich, H., Stern, A.: In vitro cytotoxicities of 1,4-naphthoquinone and hydroxylated 1,4-naphthoquinones to replicating cells. Journal of Applied Toxicology 13, 353–358 (1993)
8. Ito, K., Nakazato, T., Yamato, K., et al.: Induction of apoptosis in leukemic cells by homovanillic acid derivative capsaicin through oxidative stress implication of phosphorylation of p53 at Ser-15 residue by reactive oxygen species. Cancer Research 64, 1071–1078 (2004)
9. Das, R., Roy, A., Dutta, N., et al.: Reactive oxygen species and imbalance of calcium homeostasis contributes to curcumin induced programmed cell death in Leishmania donovani. Apoptosis 13, 867–882 (2008)
10. Kroemer, G., Dallaporta, B., Resche Rigon, M.: The mitochondrial death/life regulator in apoptosis and necrosis. Annual Review of Physiology 60, 619–642 (1998)
11. Li, P., Nijhawan, D., Budihardjo, I., et al.: Cytochrome c and dATP-dependent formation of Apaf-1/caspase-9 complex initiates an apoptotic protease cascade. Cell 91, 479–489 (1997)
12. Launay, S., Hermine, O., Fontenay, M., et al.: Vital functions for lethal caspases. Oncogene 24, 5137–5148 (2005)

The Study about the Degradation of Nitrobenzene by Domesticated Activated Sludge and the Initial Validation of Toxicology before and after the Degradation

Yubin Ji[1], Zhongyuan Qu[1], Wenlan Li[1], Changru Xu[2], and Xingjie Zhu[2]

[1] Institute of Materia Medical and Postdoctoral Programme, Harbin University of Commerce
Harbin, China
[2] Engineering Research Center of Natural Anticancer Drugs, Ministry of Education
Harbin, China
happyzhouming@yahoo.com.cn

Abstract. In this paper, the domestication of the activated sludge by which nitrobenzene can be degraded in a relatively poor nutrition is studied. The ability of activated sludge degradation of nitrobenzene is studied by degradation kinetics. The toxicology validation about the effect of activated sludge degradation of nitrobenzene is preliminarily explored. The results show that: The nitrobenzene could be the sole carbon and nitrogen source in the domestication of the activated sludge; The degradation process is in line with the feature of first order kinetics; When nitrobenzene of 130mg/L ,85mg/L and 40mg/L is degraded, the kinetic equations are : lnC = -0.0112t + 4.5767, lnC= -0.0116t + 4.5075 and lnC = -0.0098t + 4.514, the half-life t1/2 are 61.88h, 59.74h and 70.71h, the degradation rate constant K (h^{-1}) are 0.0112,0.0116 and 0.0098; MTT assay can be used to initially study the changes of cytotoxicity before and after the biodegradation of nitrobenzene polluted water samples; The activated sludge domesticated in this experiment is preliminarily verified that it can significantly reduce the toxicity of nitrobenzene polluted water sample.

Keyword: Nitrobenzene, Biodegradation, Toxicology validation, Activated sludge.

1 Introduction

Nitrobenzene, also be known as the dense patch oil, is colorless or slightly yellow oil with almond-flavored liquid. Mainly used for making aniline, benzidine, azobenzene, and so on. Nitrobenzene have toxic, absorbing large quantities of steam or contamination from high concentration of it on skin can cause acute poisoning, make hemoglobin oxidated or complex, the color of blood will turn to dark brown, and cause headaches, nausea and vomiting. Chemical properties of nitrobenzene make it be more stable in the water, and be slightly soluble in water. The density of nitrobenzene is greater than water. When being discharged into water, nitrobenzene would deposit on the bottom for a long time as water pollution [1].

E. Zhu and S. Sambath (Eds.): Information Tech. and Agricultural Eng., AISC 134, pp. 15–22.
springerlink.com © Springer-Verlag Berlin Heidelberg 2012

Traditional degradation methods of nitrobenzene are low efficiency and easy to cause secondary pollution. Full domesticated activated sludge can be efficiently and securely on the biological degradation of nitrobenzene in water, but aniline and other higher toxic compounds often be produced after degradation, and activated sludge usually be influenced by the nutrition conditions. A kind of activated sludge by which nitrobenzene can be degraded in a relatively poor nutrition is domesticated and the toxicology validation about the effect of activated sludge degradation of nitrobenzene preliminarily explored.

2 Materials

2.1 Chemicals

Fetal calf serum (FCS) (Hyclone); RPMI 1640 (Gibco); Trypsin(Gibco); Dimethyl sulfoxide (DMSO) (Beijing Soledad Lite-On Technology Co., Ltd.); MTT (Sigma); Nitrobenzene (Tianjin Guangfu Fine Institute of Chemistry); Beef extract (Beijing obo Star Bio-Technology Co., Ltd.); Peptone (Beijing obo Star Bio-Technology Co., Ltd.); Sodium chloride (Tianjin Tianxin Fine Chemicals R&D Center); Potassium dihydrogen phosphate (Tianjin Chemreagent Chemical Reagents Development Center); Dipotassium hydrogen phosphate (Tianjin Tianxin Fine Chemicals R & D Center); Sodium hydroxide (Tianjin Tianxin Fine Chemicals R & D Center); Hydrochloric acid (Tianjin Tianxin Fine Chemicals R&D Center). Benzene (HPLC pure, Tianjin Chemical Reagent Research Institute).

Trace Element Solution: $MnSO_4.H_2O$ 0.28g, $FeSO_4.7H_2O$ 0.3g, $MgSO_4.7H_2O$ 0.06g, $CaCl_2$ 1g, $CuSO_4$ 0.05g, $ZnSO_4$ 0.05g, H_3BO_3 0.05g, add them to distilled water of 1000mL.

2.2 Equipment

Agilent 6890N gas chromatograph (Agilent Technologies, Inc.); SANYO MC0175-type CO2 incubator (NAPCO); OLYMPUS inverted microscope, Olympus Corporation, Japan; GILSON pipette (France); 96-well culture plates (Orange Scientific); WELLSCAN MK3 type micro plate reader (United States Bio-Rad company); Clean Bench (Sujing Group); Constant temperature shaker (hadonglian); 752 spectrophotometer (Shanghai Spectrum Instruments Co., Ltd.); high-pressure Autoclave (SANYO); High-speed centrifuge (Shanghai Anting Scientific Instrument Factory).

2.3 Tumor Cell Lines

The HepG2 cells are provided by the Institute of Medical, Harbin University of Commerce.

2.4 Activated Sludge Source

Harbin City Wastewater Treatment Plant.

2.5 Medium Preparation

1) Domestication medium
Take sodium chloride 5g, dipotassium hydrogen phosphate 4g, potassium dihydrogen phosphate 1.5g, 1ml by adding trace elements in 1000ml distilled water, adjust the ph value to 7.0,120 ℃ sterilization 20min, prior to use aseptic technique by adding a certain amount of nitrobenzene.

2) Enrichment medium
Add sodium chloride 5g, beef extract 5g, peptone 10g to distilled water of 1000mL, adjusting the ph value to 7.0, sterilizes at 120℃ for 20 minutes.

3 Methods

3.1 The Domestication of Activated Sludge

Add activated sludge for 5g to enrichment medium of 100mL, set the constant temperature shaker to 30℃, 140r/min, and culture for 24h.

Centrifuge medium at 3000r/min for 20min, remove supernatant, add nitrobenzene to domestication medium of 100ml, make the concentration of nitrobenzene to 10mg/L, and set the constant temperature shaker to 30℃, 140r/min, and culture for 3d.

Centrifuge medium at 3000r/min for 20min, remove supernatant, add the same concentration of nitrobenzene as previous step to enrichment medium of 100mL, and set the constant temperature shaker to 30℃, 140r/min, and culture for 24h. Centrifuge the culture medium at 3000r/min for 20min, remove supernatant, then add nitrobenzene to domestication medium of 100mL, make the concentration of nitrobenzene to 20mg/L, set the constant temperature shaker to 30℃, 140r/min, and culture for 3d.

Repeat the steps above in medium containing 40mg/L, 60mg /L, 80mg /L, 100mg/L, 120mg/L, 130mg/L, 140mg/L, 150mg/L of nitrobenzene, separate the final culture medium according to the conditions above after domestication, use the domestication medium without nitrobenzene to wash bacteria centrifuge for one time then continue separate by centrifuge after washing.

3.2 Degradation

1) Draw the activated sludge growth curve to find the slow growth stage of activated sludge
The isolated bacteria will be added as the measure as 5% of the whole volume to enrichment medium of 100mL, culture in the shaker at 30 ℃ and 140r/min, respectively, sample 1ml at 0,4,8,12,24,28,36,48,60,72h, using spectrophotometer to measure all samples at wavelength of 600nm, make the sampling time as X-axis, OD values as the Y-axis ,draw the activated sludge growth curve.

2) Activated Sludge Degradation of nitrobenzene experiment
Take activated sludge in slow growth period, add it as the measure as 5% of the whole volume to domestication mediums of 100mL which contain nitrobenzene of 130mg/L,

85mg/L and 40mg/L, set the constant temperature shaker to 37℃, 130r/min, set up the control experiments without bacteria, respectively, sampling 1mL at 4, 8,12,24,36,48,72, and 96h, prepare the samples and use the gas chromatograph to measure the concentration of nitrobenzene[2].

3) Analysis Method

Sample treatment method: Adding 3mL of benzene in the sample bottle, oscillating for 1min, extracting for two times then combine the extract, preserve them at 4℃ for the test.

Gas chromatography conditions: Column: HP-5 column (30m×0.25mm×0.25μm); Mobile phase: high-purity nitrogen gas (N_2, 99.99%); Flow rate of carrier gas: 0.8mL/min; Sample volume: 1μL; Split ratio: 50:1; Column temperature: 120℃; Injection port temperature: 260℃; electron capture detector temperature: 240℃ [3, 4].

4) MTT assay

HepG2 human hepatoma cells and human gastric cancer cell SGC-7901 was cultured with the RPMI1640 culture medium which containing 10% volume fraction of fetal bovine serum. Set incubator to 37℃, 5% of the CO_2. Using the cells in logarithmic growth phase for the experiment [5].

Take the cells in logarithmic growth phase, use complete culture medium to adjust cell concentration to 5×10^4/L, then put the cells into 96-well plate, as 100μL each hole, set humidified incubator to 37℃, 5% of the CO_2, culture for 24 h.

Put the nitrobenzene samples that before and after be depredated to 96-well plate as 100μL each hole, make the concentrations of the respectively 1, 1/2, 1/4 times initial concentration of the samples; Blank control group: plus RPMI1640 medium for 100μL; set three flat-shaped holes for each concentration. Set incubator as 37℃ and 5% humidified CO2, then culture for 72h.

Use quickly flap method to discard the supernatant, add MTT test solution ($0.5g \cdot L^{-1}$) 100μL to each well, continue to foster the supernatant discarded after 4h, then add DMSO to each hole for 200μL, dissolved it using the micro-oscillator, measure the absorbance values of each hole by using the micro plate reader in detective wavelength of 570nm. Calculate the cell viability, cell growth inhibition rate.

$$\text{Cell viability}(\%) = \frac{\text{OD values of cells in the experimental group}}{\text{OD value of control cells}} \times 100$$

$$\text{Cell growth inhibition rate}\ (\%) = 1 - \text{Cell viability}(\%)$$

4 Results

4.1 Growth Curves of Activated Sludge

The growth curve of activated sludge which be got from the experiment shows as Figure 1.

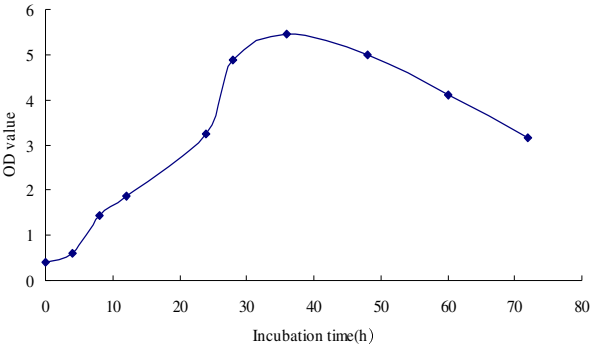

Fig. 1. The grows curve of activated sludge

The activated sludge in slow growth period has both strong oxidation and adsorption capacity of organic matter, and also has a good settling characteristic. From the growth curve, we can see that the activated sludge that be cultured for 28 ~ 36h is in the slow growth period, which consistent with the requirement of experiment.

4.2 Nitrobenzene Standard Curve and Linear Range

Dissolve the nitrobenzene standard in benzene; respectively prepare six different concentrations of nitrobenzene standard solutions as 1.2, 2.16, 3.12, 4.08, 5.04 and 6.0mg/L. After testing them by gas chromatography methods, make the nitrobenzene concentration (C) as the value of abscissa, the integral area (AUS) as the longitudinal coordinates, then we got the standard curve: y = 1E+07x + 2E+06, r=0.9983. The results showed that the nitrobenzene of 1.2-6.0mg/L have good linearity.

4.3 Determination of the Recovery Rate of Nitrobenzene

Take the sterilized culture mediums with different concentrations of nitrobenzene, make them be extracted and determined according to experimental method, then we got the nitrobenzene extraction percent recovery is (86.65 ± 2.20)% (n = 5).

4.4 The Kinetics Analysis to Nitrobenzene Degradation

In order to understand the dynamics property of degradation, the test studied degradation rates of nitrobenzene which initial concentration are 130mg/L, 85mg/L and 40mg/L in a under the conditions of inoculating a certain amount of activated sludge. Measured results shown in Figure 2, Table 1.

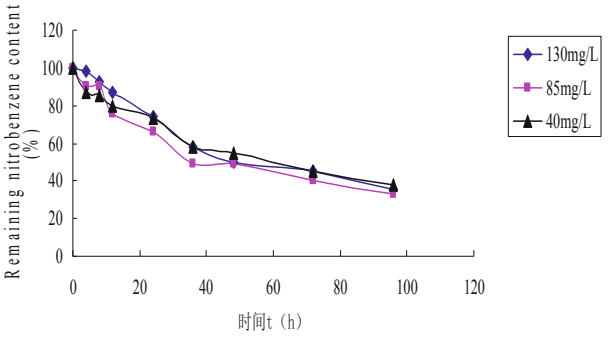

Fig. 2. Growth curve of nitrobenzene

Table 1. Degradation kinetics of nitrobenzene

The initial concentration of nitrobenzene /mg·L^{-1}	Kinetic equation	Half-life $t_{1/2}$/h	Degradation rate constant K/h^{-1}	Correlation r
130	lnC = -0.0112t + 4.5767	61.88	0.0112	0.9812
85	lnC = -0.0116t + 4.514	59.74	0.0116	0.9686
40	lnC = -0.0098t + 4.5075	70.71	0.0098	0.9844

Figure2 shows that the activated sludge can use nitrobenzene as the sole carbon and nitrogen sources and in that way, the nitrobenzene could be depredated. Table 1 show that the degradation process is in line with the feature of first order kinetics. When nitrobenzene of 130mg/L, 85mg/L and 40mg/L is degraded, the kinetic equations are: lnC = -0.0112t + 4.5767, lnC= -0.0116t + 4.5075 and lnC = -0.0098t + 4.514.

4.5 MTT Assay Results

MTT results are shown in table 2.

Table 2. The inhibitory effect of nitrobenzene on HepG2 cell($x\pm s$, n=3)

Content	The number of parallel samples	OD value	inhibition rate （%）
Control	3	1.168±0.022	-
Before degradation			
1	3	0.670±0.028	42.620±2.379
1/2	3	0.742±0.066	36.453±5.616
1/4	3	0.866±0.006	25.807±8.018
After degradation			
1	3	0.919±0.093	21.297±7.935*
1/2	3	1.021±0.032	12.590±2.735**
1/4	3	1.043±0.064	10.650±5.450*

**P<0.01 vs. control * P<0.05 vs. control

MTT assay detected the changes of cytotoxicity before and after the biodegradation of nitrobenzene polluted water samples, the result is shown in the table. Nitrobenzene acting on HepG-2 cells for 72h, then we can see that cell growth was inhibited to varying degrees, the growth inhibition rate reduced when the nitrobenzene concentration is decreased, it is statistically significant when be compared with the control group and the various concentrations of nitrobenzene before degradation.(P <0.05 or P <0.01).

5 Conclusions

The domestication of the activated sludge by which nitrobenzene can be degraded in a relatively poor nutrition, and the degradation process is in line with the feature of first order kinetics.

MTT assay is able to initially study the changes of cytotoxicity before and after the biodegradation of nitrobenzene polluted water samples, so this method can be used to study the degradation effect of the activated sludge method, the degradation conditions and the way of domestication.

After the initial identification of MTT assay, the activated sludge domesticated in this experiment is preliminarily verified that it can significantly reduce the toxicity of nitrobenzene polluted water sample.

References

1. Zhang, L., Xu, J.B.: The Toxicity of Nitrotoluenes to Guppy. Ecology and Environment 13(1), 31–33 (2004)
2. Li, W.-L., Yang, Y., Ji, Y.-B., Yu, L., Fan, Q.: Study on Biodegradation of Butyl benzyl Phthalate by Acclimated Activated Sludge. Environmental Sciences 26(4), 156–159 (2005)

3. Luo, K., Wang, Y., Sun, X., Sun, Z.: The detection of the nitrobenzene pollution in water of Songhua River by gas chromatography. Chinese Health Care 15(11), 117–118 (2007)
4. Liu, Y., Wu, Y.: Determination of nitrobenzene compounds in water by gas chromatography-mass spectrometry (GC/MS). Heilongjiang Science and Technology of Water Conservancy 36(1), 73–74 (2008)
5. Bu, S.-H., Fang, L., Tian, H.-P.: MTT assay in vitro tumor sensitivity experiment factor. Beijing Medicine 24(5), 349 (2002)

Study on the Screening for Chloronitrobenzene: Degrading Bacteria and Degradation of Chloronitrobenzene

Yubin Ji[1], Zhongyuan Qu[1], Wenlan Li[1], Changru Xu[2], and Xingjie Zhu[2]

[1] Institute of Materia Medical and Postdoctoral Programme, Harbin University of Commerce Harbin, China
[2] Engineering Research Center of Natural Anticancer Drugs Ministry of Education Harbin, China
jyb@hrbcu.edu.cn, chnzhxj@163.com

Abstract. With sewage plant aeration tank activated sludge as mixed bacteria source, Nitrobenzene concentration gradient of the chlorine used to increase the aerobic bacterial degradation of oscillating bottle method of domestication and enrichment culture. Separation and purification out of one can right-chloronitrobenzene as the sole carbon, nitrogen and energy of bacteria。 Through physiological and biochemical reactions characteristic morphology and 16S rDNA sequence analysis, to determine the strain is Bacillus subtilis.The degradation kinetics analysis showed that the degradation of single strain 4CNB kinetic characteristics consistent with features.

Keywords: Chloro-nitrobenzene, Uniform design, Bacillus subtilis.

1 Introduction

Chloronitrobenzene are a class of chlorine-containing nitro-aromatic compounds and widely used as dyes, pesticides, pharmaceutical intermediates production, According to incomplete statistics, the country's right-chloronitrobenzene (4CNB, 4 - chloro-nitrophenyl) total production is about 120,000 tons in 2000th(1). wastewater in the process of chloro-nitrobenzene production, for containing chlorinated nitrobenzene, nitro-phenol, chlorobenzene, sulfuric acid, nitric acid and other pollutants, especially for the chlorinated nitrobenzene toxic and refractory, result in serious water discharge exceeded. Once poured into the soil and groundwater will be difficult to repair environmental damage(2). Due to the toxicity of chlorinated nitrobenzene toxicity including blood, spleen toxicity, liver toxicity, immunotoxicity, and also result in kidney damage, damage to the nervous system, etc.(3、4) even the mutations and cancer. Therefore, the EC had list chloronitrobenzene as a pernicious and difficult to degrade in the environment of organic pollutants.(5) In this study, 4CNB pollution of the environment for the purpose of repair, the multi-source mixing domesticated bacteria, enrichment, separation and purification of a strain able to 4CNB as the sole carbon and nitrogen source of the bacterial strain, to be identified as Bacillus subtilis, and also the degradation characteristics of bacteria have been studied. The 4CNB predominant strains of the environment to provide bioremediation for the degradation of 4CNB provide the scientific theoretical approach.

E. Zhu and S. Sambath (Eds.): Information Tech. and Agricultural Eng., AISC 134, pp. 23–29.
springerlink.com © Springer-Verlag Berlin Heidelberg 2012

2 Materials and Methods

2.1 Experimental Strain

Activated sludge, provide from Harbin Wenchang Wastewater Treatment Plant.

2.2 Instruments and Reagents

Experimental Instruments: HDL turbulence incubator model is HZQ-F19(Harbin East Union Electronics Co., Ltd.), Angilent6890 Gas chromatography - electron capture detector(Angilent Co., Ltd.) DPS statistical software (Beijing Boshi Technology Development Corporation)

Experimental reagents: Chloro-nitrobenzene(J & K Chemical Technology Co., Ltd., Standard sample, purity 100%); Benzene(Tianjin Chemical Reagent Research Institute, Chromatography pure)

Inorganic salt medium: Na2HPO4 14.3g/L、KH2PO4 3g/L、MgSO4.7H2O 0.06mg/L、FeSO4.7H2O 0.3 mg/L、MnSO4.7H2O 0.28mg/L、CaCl2 1mg/L、CuSO4 0.05mg/L、ZnSO4 0.05mg/L、H3BO3 0.01mg/L、NaOH(PH adjusted to 7.0), Medium (MSB) composed of Na2HPO4 1g/L, KH2PO4 0.5g/L,MgSO4·7H2O 0.03g, trace element solution, 5mL,(6) pH 7.0. Solid medium by adding 15g / L agar.

2.3 Analysis Method

Sample treatment: 4CNB the solution obtained after degradation of the sample bottle by adding 10mL in 10mL of benzene chromatographic eluent oscillation extraction 3 times, combined extract, using GC-ECD was determined 4CNB content.

GC-ECD determination conditions(7): HP-5 (30m×0.25mm×0.25μm) capillary, Column temperature 135℃ ; injection volume: 0.2μL; Split ratio：50:1; Injection temperature; 230℃; Carrier gas flow rate: 0.8mL/min; 63Ni electron capture detector; Detector temperature 300 ℃.

2.4 Strain Enrichment, Separation and Purification

Sludge sample volume of 10% of the access to vaccination in the inorganic medium at 30 ℃, 130rpm shaking the bed shaking culture for about one week, Sampling measurement of the chlorine content of nitrobenzene, pending on the chlorine concentration of nitrobenzene is reduced, then 1% of the amount transferred to the new access medium to cultivate a week or so, so repeated 3 times. and then crossed on agar plates separated until they have a pure, single colony（8、9）.

2.5 Strain Identification

1) Degradation of physiological and biochemical characteristics of bacteria analyzed in accordance with conventional methods of identification（10、11）
2）DNA extracted using CTAB / NaCl method（12）
3) 16S rDNA sequence analysis

Used in the PCR reaction amplification of 16S rDNA primers for a pair of universal primers (9), positival primer Pf：5′-AGAGTTTGAT CCTGGCTCAG-3′; reverse primer Pr: 5′-AAGGAGGTGATCCAGCCGCA-3′。PCR reaction system(50μL): 10×buffer 5μL、25mmol/L MgCl2 3μL 、10mmol/L dNTP 4μL、20μmolPL primer per 1μL、Template DNA 4μL、ddH2O 31μL、Taq DNA enzyme 1μL。PCR reaction conditions: 94℃3min; 94℃1min, 56℃2min, 72℃3min, 29 cycles; 72℃10min.

4) DNA quality inspection

Electrophoresis buffer prepared with 0.7% (m / v) agarose melted in the microwave oven,add 4μl ethidium bromide, cool to 50℃, pour into the irrigation system has been sealed gel platform, plug in the sample comb, DNA10μl and 2μl spotting buffer full mixing, pour into the point-like hole. make λDNA / Hind Ⅲ Marker as molecular marker, 38V constant-voltage electrophoresis, 150min later, turn off the power, gel imaging device on the camera.

5) Sequencing and the establishment of phylogenetic trees

PCR product purification and sequencing by Dalian Bao Bio-Technology Co., Ltd. Completed, make measured in the NCBI database for sequence similarity search, select the sequence in which a higher similarity to neighbor-joining phylogenetic tree, the procedure is MEGA4.

2.6 Single Strain(4CNB) of Biodegradation Test

Already sterile solution of inorganic salt solution by adding 4CNB, 4CNB as the only carbon, 4CNB concentrations: 60 mg/L, 100mg/L, 140mg/L, each concentration do at least three parallel samples by adding a single strain, get into the constant temperature oscillator 30 ℃ incubator, and set up the control without inoculum tests,after 4 、8、12、24、36、48、72 和96 hr take 1mL sample.and then fill full. Samples were prepared according to sample treatment solution, precision draw a certain amount of sample solution into the gas chromatograph to measure the content of 4CNB.

3 Experimental Results and Discussion

3.1 Standard Curve and Linear Range of Drawing

4CNB dissolved in benzene chromatographic preparation of pure: 0.025、0.05、0.1 、0.2、0.4、0.6、0.8、0.9mg/L, standard solutions of different concentrations of 4CNB, Autosampler 0.2μL injected into gas chromatography to analysis, the concentration of chloro nitrobenzene (C) as the abscissa, integral area (AUS) value of longitudinal coordinates, Standard curve: Y=73924X+3000000, R=0.9991， the results show that 4CNB at 25 ~ 900μg/L within the linear relationship.

3.2 Identification of Efficient Strains of Decomposition 4CNB

1) Morphological identification
PDA on the surface of opaque colonies, orange colonies, Columnar, no branching, Spore surface folds, nearly spherical. The results shown in Figure 1, Figure 2.

Fig. 1. Morphological characteristics of strain 4CNB

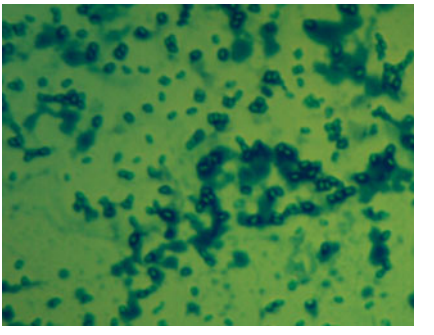

Fig. 2. Morphological characteristics of strain 4CNB

2) After DNA extraction and amplification quality inspection
DNA extraction and amplified genomic gel electrophoresis images, The results shown in Figure 3, Figure 4.

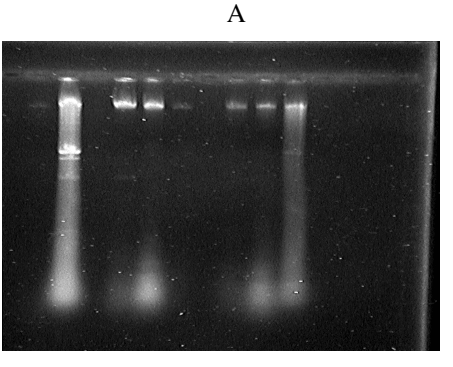

Fig. 3. Electrophoresis patterns of strain genome

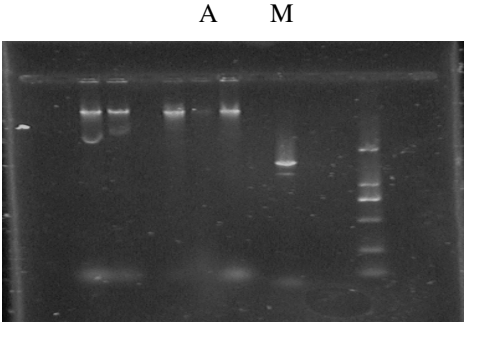

Fig. 4. PCR products of gel electrophoresis patterns of genome

3) 2.2.3 Reconstruction of phylogenetic trees
Make measured in the NCBI database for sequence similarity search (BLAST), Select one already published, the high sequence similarity with the strain A sequence in order to neighbor-joining phylogenetic tree.,the procedures is MEGA4, analysis repeated 1,000 times. The results shown in Figure 5.

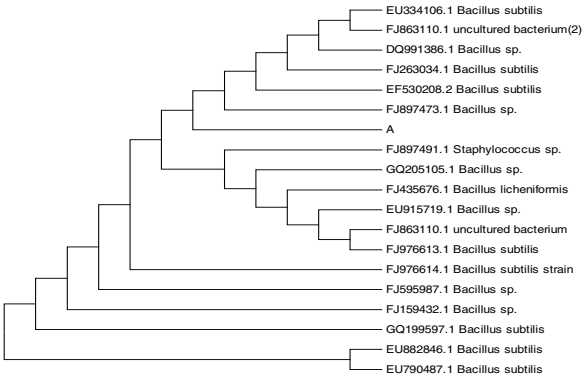

Fig. 5. Strain A based on rDNA-ITS sequence phylogenetic tree reconstruction

4) 2.2.4 Identification results

Using universal primer pairs of strains obtained gene DNA amplification of the ITS fragment size 549bp fragment of the PCR amplified products were sequenced, Conserved sequence of the strain on the NCBI Web site homologous comparison, discover that Bacillus subtilis (Bacillus subtilis) to a high degree of similarity, similarity is aboat 100%. Shows that both has a special closed kinship. Access to GenBank accession number is GQ899186.

3.3 Degradation Analysis of the Single Strain of 4CNB

In order to understand the kinetics of the single strain of the nature degradation 4CNB, In a certain amount of the single strain conditions, the study of the initial concentration of the single strain of 60,100,140 mg/L of 4CNB degradation rate, the determination of the results shown in Figure 6.

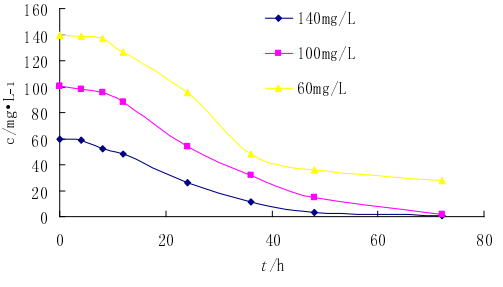

Fig. 6. The single strain of different concentrations of the degradation of 4CNB

Figure 6 The results show that 4CNB can be rapidly degraded, the initial concentration of 100mg/L while in 2days the degradation rate of 90% or more, and

was completely degraded within 3days, the results also shows a single strain of living a highly efficient degradation is a highly efficient right-chloronitrobenzene degradation of bacteria. 4CNB by different concentrations of the initial rate of degradation can be show that the degradation rate decreases with increasing concentration 4CNB, indicating high concentrations of 4CNB inhibit its biological degradation, and as 4CNB initial concentration increases.

4 Results and Discussion

4.1 Select the strain of efficient degradation 4CNB, the strainis is Bacillus subtilis after identified, and get GenBank accession number is the GQ899186.

4.2 The degradation of the single strains 4CNB- a highly efficient degradation, the degradation rate decreases with increasing concentration of 4CNB, indicating high concentrations of 4CNB inhibit its biological degradation, and as 4CNB initial concentration increases.

References

1. Wu, J., Shen, X., Zhou, G.: Study on the isolation and identification of Comamonas sp. CNB1's degradation characteristics. Journal of Microbiology 2(44), 8–11 (2004)
2. Liu, L., Wu, J., Ma, Y., Wang, S.-Y., Zhao, G.-P., Liu, S.-J.: A Novel Deaminase Involved in Chloronitrobenzene and Nitrobenzene Degradation with Comamonas sp. Strain CNB-1. Journal of Bacteriology, 2677–2682 (April 2007)
3. Lessner, D.J., Johnson, G.R., Parales, R.E., Spain, J.C., Gibson, D.T.: Molecular Characterization and Substrate Specificity of Nitrobenzene Dioxygenase from Comamonas sp. Strain JS765. Applied and Environmental Microbiology, 634–641 (February 2002)
4. Lin, R.-J., Wu, B.-N., Lo, Y.-C., An, L.-M., Dai, Z.-K., Lin, Y.-T., Tang, C.-S., Chen, I.-J.: A Xanthine-Based Epithelium-Dependent Airway Relaxant KMUP-3 (7-[2-[4-(4-Nitrobenzene)piperazinyl]ethyl]-1,3-dimethylxanthine) Increases Respiratory Performance and Protects against Tumor Necrosis Factor-a-Induced Tracheal Contraction, Involving Nitric Oxide Release and Expression of cGMP and Protein Kinase G, JPET. The Journal of Pharmacology and Experimental Therapeutics 316, 709–717 (2006)
5. He, Z.-Q., Spain, J.C.: A Novel 2-Aminomuconate Deaminase in the Nitrobenzene Degradation Pathway of Pseudomonas pseudoalcaligenes JS45. Journal of Bacteriology, 2502–2505 (May 1998)
6. Kaminski, U., Janke, D., Prauser, H., et al.: Degradation of aniline and monochloroanilines by Rhodococcus sp. An117 and a pseudomonad:a comparative study. Allg. Mikrobio. 23, 235–246 (1983)
7. Sheng, J., Xie, L., Di, G.: Study on the liquid-liquid extraction - gas chromatography and its degradation products of nitrobenzene influencing factors. Water Purification Technology 3(26), 69–72 (2007)
8. Zhang, J., Wang, Z., Su, T.: Chlorobenzene degrading bacteria screening mechanism and degradation conditions. Journal of Liaoning University of Petroleum and Chemical Engineering Technology 3, 37–39 (2005)

9. Study on the acclimated activated sludge degrade environmental hormone butylbenzyl phthalate ester. Environmental Science 25(1), 7–13 (2004)
10. The classification section of microbiology-Chinese academy of bacteria. The Commonly Identification of Bacteria. Science press (1978)
11. Dong, X., Cai, M.-Y.: The manual of identification common bacterial systems. Science press (2001)
12. Wang, G., Fang, H.: Plant genetic engineering, pp. 742–744. Science press (2002)

Identification and Characterization of *Lactobacillus* Planetarium TH1

Hua Tian[1,*], Xue-gang Luo[1,*], Zhao Han[1], Ran Hao[1], Nan Wang[1], Yong Jiang[1], and Tong-Cun Zhang[3,4,**]

[1] Key Laboratory of Industrial Microbiology, Ministry of Education, Tianjin, China
[2] Tianjin Key Laboratory of Marine Resources and Chemistry, Tianjin University of Science and Technology, 300457, Tianjin, China
[3] School of Medicine, Wuhan University of Science and Technology, Wuhan, China
[4] Tianjin Key Laboratory of Industrial Microbiology, Tianjin, China
tony@tust.edu.cn, xuegangluo@yahoo.com.cn

Abstract. *Lactobacillus plantarum* (*L. plantarum*) is a flexible and versatile microorganism that inhabits a variety of environmental niches, and some strains are marketed as probiotics. In this study, a strain TH1 which was isolated from silage in our former works was classified as *L. plantarum* by 16S rDNA sequence analysis and phylogenetic tree. Then its potential abilities of bile tolerance, nitrate reduction and anti-hypertension were investigated. The results showed that *L. plantarum* TH1 had capacity to resistance to bile salt, directly deoxygenate nitrate to nitrogen or ammonia rather then nitrite, and produce ACE inhibitory components in fermented milk. These works indicated that this novel lactobacillus strain might be considered as candidates for probiotics strains using in the food or drug system to improve the health of patients suffering from hypertension or other chronic disease.

Keywords: L. plantarum, Identification, probiotics, bile salt resistance, Nitrate reduction, ACE inhibitory.

1 Introduction

The use of probiotics in general clinical practice is not far away. Probiotics are applied to balance disturbed intestinal microflora and related dysfunctions of the gastrointestinal tract (GI tract) [1]. Accumulating evidence showed that probiotics were valuable in current clinical applications such as treatment of acute rotavirus diarrhoea, lactose maldigestion, constipation, colonic disorders and side-effects of pelvic radiotherapy, and more recently, food allergy including milk hypersensitivity [2,3].

Many *Lactobacillus* strains have been promoted as good probiotics for human usage, among them, *L. plantarum* is a flexible and versatile species that is encountered in a large variety of environmental niches, including some dairy

[*] The first two authors contributed equally to the project.
[**] Corresponding author.

E. Zhu and S. Sambath (Eds.): Information Tech. and Agricultural Eng., AISC 134, pp. 31–37.
springerlink.com © Springer-Verlag Berlin Heidelberg 2012

products, pickled vegetables or plants, fish products and silage. Some strains of *L. plantarum* are also found as natural commensals in the gastrointestinal tract [4]. Previous studies had shown that many *L. plantarum* could inhibit the growth of pathogens by compete the limiting nutrients to regulate the composition of intestinal microflora and to form a biological barrier. They could decrease the levels of serum cholesterol, reduce the incidence of cardiovascular disease, and exhibited good effect on cute liver damage caused by intestinal metastases outside the intestinal tract.

In this study, a *L. plantarum* isolated from silage in our former works was identified by 16S rDNA sequence analysis and phylogenetic tree, and then its ability of bile tolerance, nitrate reduction and lower blood pressure were investigated.

2 Materials and Methods

2.1 Bacterial Strains Identification by 16S rDNA Sequence Analysis

Strain TH1 isolated from silage in our former works was grown in MRS broth for 12h at 37°C. One milliliter of culture was harvested by centrifugation and the genomic DNA was extracted by the genomic DNA extraction kit.

The 16S ribosomal DNA was amplified by polymerase chain reaction (PCR) using the genomic DNA as a template and the following primer pairs 5′-AGAGTTTGATCCTGGCTAG -3′ (forward) and 5′- GGCTACCTTGTTACGACTT -3′ (reverse). PCR was performed at 94°C for 5 min, then 30 cycles at 94°C for 45 s, at 56°C for 45 s, and at 72°C for 1.5 min; extension was carried out at 72°C for 10 min.

After PCR amplification, 10 μL sample of each reaction mixture was analyzed by electrophoresis on a 1.0% agarose gel at 120 V for 45 min, and DNA was visualized with ethidium bromide under UV light. The PCR-amplified fragments were purified using the PCR purification kit and sequenced.

To construct the phylogenetic tree, the obtained 16S rDNA sequence was used for similarity search in the NCBI BLAST databases (http://www.ncbi.nlm.nih.gov/BLAST) [5]. Multiple sequence alignments were performed using the CLUSTAL X program [6]. Phylogenetic analysis was performed using the MEGA3.1 program package. The unrooted phylogenetic tree was constructed by the neighbour-joining method using the Jukes-Cantor correction for multiple substitutions according to the one-parameter model [7]. Bootstrapping was performed using 500 iterations. Phylogenetic trees were generated based on the 16S rRNA gene sequences of TH1.

2.2 Bile Salts Tolerance Assay

Stationary phase culture inoculums (1%) were added to MRS broth supplemented with bile salt at a concentration of 0.1%, 0.2%, 0.3%, respectively, and then anaerobic incubated at 37°C. The growth curves were generated by measurement of the OD620 for 20 h at intervals of 2 hours.

2.3 Nitrate Reduction Test

This test was used to assay for the presence of enzymes capable of reducing nitrate to nitrite to nitrogen gas: NO_3 (nitrate) —> NO_2 (nitrite) —> N_2 (nitrogen gas) or NH_3

(ammonia). In brief, *L. plantarum TH1* was incubated in trypticase nitrate broth for 48 hours at 37°C. Three drops of Nitrate solution A(2% starch) and 5 drops of Nitrate solution B(6mol/L HCl) reagents were added and then followed with the adding of 2 drop of Nitrate solution C(5% KI). If the medium turned blue, it showed that nitrate had been reduced to nitrite. If there was no color change, a small amount of zinc dust should be added. If there was still no color change, it showed that nitrate had been completely reduced to nitrogen gas. If a blue color was produced, it meaned that nitrate was still present and had not been reduced at all (nitrate could react with zinc dust to produce the blue color).

2.4 Determination of ACE-Inhibitory Activity [8]

Angiotensin-converting-enzyme (ACE) - inhibitory activity was assayed using the modified method of Roy et al [9]. Briefly, 100 μL of HHL buffer (5 mM HHL in 0.1 M sodium borate buffer containing 0.3 M NaCl, pH 8.3) was mixed with 100 μL of inhibitory solution for 5 min at 37°C. The reaction was initiated by adding 150μL of ACE (0.05 units/mL), and the mixture was incubated for 1 h at 37°C. The reaction was stopped by adding 250 μL of 1 M HCl, and the reaction mixture was mixed with 1.4 mL of ethyl acetate. Solvents were removed from the test fractions by evaporation. Fractions were redissolved in 1 mL of distilled water, and the absorbance was measured at 228 nm. The sample test value was recorded as S. The value of water tested as control was recorded as C. The value of ACE solution without reaction with any sample was recorded as A. The inhibition rate was calculated as follows: ACE inhibition rate (%) = (A-S) / (A-C) × 100.

3 Results

3.1 Identification of Strain TH1 by 16S rDNA Sequence Analysis

The gene of 16S rRNA was amplified from the genomic DNA of *strain TH1*. The result showed the length of target fragment was about 1.5 kb (Fig.1).

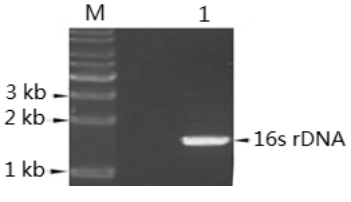

Fig. 1. Agarose gel electrophoretic of PCR products. Lane M: 1 kb marker; lane 1: 16S rDNA of strain TH1.

The obtained 16S rDNA fragment was sequenced and then analyzed by BLAST. Phylogenetic tree was constructed with Clustal X process and Mega 3.1 Software. As shown in Fig 2, the result showed that the strain TH1 has the closest relationship with *L. plantarum*, thus, it was identified as a novel *L. plantarum*.

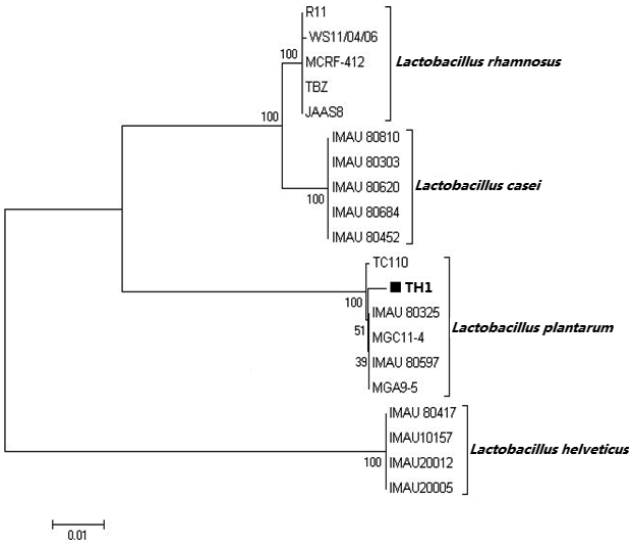

Fig. 2. Phylogenetic relationship of strain TH1 based on maximum-likelihood analysis of 16S rDNA sequence. The numbers were based on bootstrap analysis. The black box represented the strain identified in the present study.

3.2 Bile Salt-Resistant Ability of L. Planetarium TH1

Lactobacillus is detected in large numbers in all regions of the murine and human GI tracts. In order to verify whether this strain can live in the intestinal tract to carry out its function, the bile salt-resistant ability of *L. plant arum* TH1 was detected. As shown in Fig 3, *L. planetarium* TH1 could proliferate well in the medium containing bile salt at the range from 0.1% to 0.3%, and there were no significant difference between the maximum bacterial amounts (proportional to OD620) of the entire tested group and that of control group, suggesting that *L. planetarium* TH1 had capacity of resistant to bile salt.

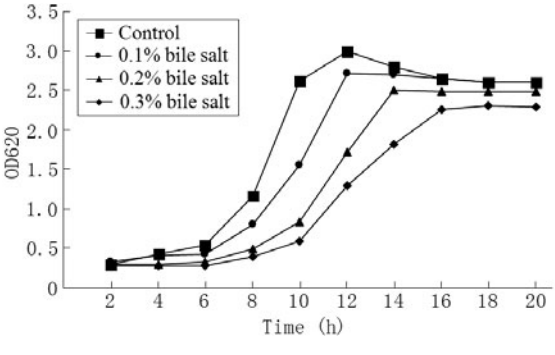

Fig. 3. Growth curves of *L. plantarum* TH1 in MRS broth added with different concentration of bile salts

3.3 Nitrate Reduction Ability of L. Plantarum TH1

To determine the effects of *L. plantarum* TH1 on the nitrate, which commonly existed in the vegetables or plants fermentation of *L. plantarum*, the nitrate reduction test was performed as described in the materials and methods section. As shown in Fig 4, there was no color change in the tube of medium control during the whole examination, while the broth of *L. plantarum* TH1 changed to blue after reacted with the nitrate solutions and returned to clear after contacted with the zinc dust., indicating that *L. plantarum* TH1 could directly reduce nitrate to ammonia or nitrogen and without the production of nitrite.

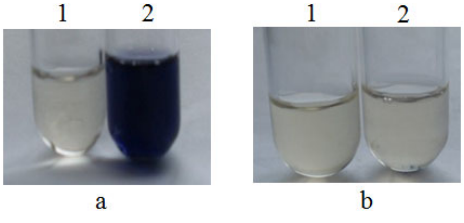

Fig. 4. Detection of the nitrate reduction ability of *L. plantarum* TH1. a1: blank control reacted with nitrate solution A, B and C; b1: the broth of *L. plantarum* TH1 reacted with nitrate solution A, B and C; b1: a1 reacted with zinc dust; b2: a2 reacted with zinc dust.

3.4 ACE-Inhibitory Activities of L. Plantarum TH1 Fermented Milk

Researches had reported that some probiotics fermented milk could produce ACE inhibitorys, which could lower blood pressure in spontaneously hypertensive rats after oral administration. To investigate whether *L. plantarum* TH1 also had such functions, the supernatant of milk fermented by the bacteria was incubated with ACE and its substrate. The ACE inhibiting effect was inversely proportional to the absorbance of the final solution at 228 nm [10]. As shown in Fig 5, *L. plantarum* TH1 fermented milk suppressed the ACE activity, and the calculated inhibition rate reached 32%, implying that it might be used in the prevention and therapy of hypertension.

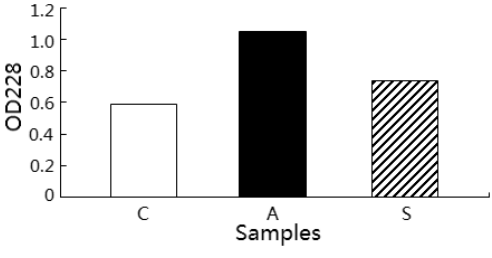

Fig. 5. ACE-inhibitory activities of *L. planetarium* TH1 fermented milk. C: control; A: ACE solution; S: sample solution of *L. planetarium* TH1 fermented milk.

4 Discussion

Nowadays, chronic disease, including of diabetes, cardiovascular diseases (such as hypertension, hyperlipidemia, etc), inflammatory, selfimmune and cancer, has been more and more popular in the world. It has become one of the key issues in the challenge to improve the health of people and the leading cause of mortality in the world [11]. Except the drug therapy, many researches have demonstrated that probiotics might help prevent these chronic disease and optimize health, thereby reducing healthcare costs and improving the quality of life for many patients.

Up to date, *Lactobacilli* and *bifidobacteria* are the mainly type of probiotics used in foods. Although an expanding range of *L. plantarum* has be isolated and showed valuable in health care, it could not be used as probiotics in the food or drug system unless it had the ability to resist the environment in the GI tract. In this study, using the method of 16S rDNA sequence analysis, we identified a novel *L. plantarum* strain named TH1 which was first isolated from silage. It showed that *L. plantarum* TH1 was bile salt-resistant, indicating that it could possess growth advantages in the intestinal tract and therefore might be considered as candidates for Probiotics strains helping the health of consumers *in vivo.*

Furthermore, the present study found that *L. plantarum* TH1 could denitrify the nitrate to produce ammonia or molecular nitrogen while without the production of nitrite, a risk factor for tumorigenesis in the pickle. Thus, it may be very safe to use in the pickle vegetables or other plant fermentation products. In addition, this stain was also shown to be able to produce ACE inhibitory components when it was used to fermented milk. As we known, ACE converts angiotensin I into angiotensin II, which constricts the vascular and increases blood pressure. This result speculated that *L. plantarum* TH1 and its associated products might be used to assist the prevention and therapy of hypertension.

In summary, this study identified a novel *L. plantarum* with engaging probiotics characters. These works might provide a significant foundation for the following study of *L. plantarum* TH1, and contribute to the development of related probiotics products in food or drug system.

Acknowledgments. This study was financially supported by the 863 (Hi-tech research and development program of China) program under contract No. 2008AA10Z336, and the foundation (No. 200911) of Tianjin Key Laboratory of Marine Resources and Chemistry (Tianjin University of Science & Technology), P. R. China.

References

1. Reid, G., Jass, J., Sebulsky, M.T., McCormick, J.K.: Potential Uses of Probiotics in Clinical Practice. Clinical Microbiology Reviews 16(14), 658–672 (2003)
2. Guarino, A., Canani, R.B., Spagnuolo, M.I., Albano, F., Di Benedetto, L.: Oral bacterial therapy reduces the duration of symptoms and of viral excretion in children with mild diarrhea. J. Pediatr. Gastroenterol. 25, 516–519 (1997)

3. Salazar-Lindo, E., Miranda-Langschwager, P., Campos-Sanchez, M., Chea-Woo, E., Sack, R.B.: Lactobacillus casei strain GG in the treatment of infants with acute watery diarrhea: a randomized, double-blind, placebo controlled clinical trial (ISRCTN67363048). BMC Pediatr. 4 (September 2004)
4. Peter, A., Bron, Grangette, C., Mercenier, A., de Vos William, M., Kleerebezem, M.: Identification of Lactobacillus plantarum Genes That Are Induced in the Gastrointestinal Tract of Mice. Journal of Bacteriology 186(17), 5721–5729 (2004)
5. Jones, D.T., Swindells, M.B.: Getting the most from PSI-BLAST. Trends Biochem. Sci. 27, 161–164 (2002)
6. Thompson, J.D., Higgins, D.G., Gibson, T.J.: CLUSTAL W: improving the sensitivity of progressive multiple sequence alignment through sequence weighting, position-specific gap penalties and weight matrix choice. Nucleic Acids Res. 22, 4673–4680 (1994)
7. Hagopian, R., Davidson, J.R., Datta, R.S., Samad, B., Jarvis, G.R., Slander: MO-JS: a webserver for simultaneous protein multiple sequence alignment and hylogenetic tree construction. Nucleic Acids Res. 1, 29–34 (2010)
8. Raza, S., Graham, S.M., Allen, S.J., Sultana, S., Cuevas, L., Hart, C.A.: Lactobacillus GG promotes recovery from acute nonbloody diarrhea in Pakistan. Pediatr. Infect. Dis. 14, 107–111 (1995)
9. Kalliomäki, M., Salminen, S., Arvilommi, H., Kero, P., Koskinen, P., Isolauri, E.: Probiotics in primary prevention of atopic disease: a randomized placebo-controlled tria. Lancet 357, 1076–1079 (2001)
10. Pailin, T., Kang, D.H., Schmidt, K., Fung, D.Y.C.: Detection of extracellular bound proteinase in EPS-producing lactic acid bacteria cultures on skim milk agar. Lett. Appl. Microbio. 33, 45–49 (2001)
11. Grangette, C., Müller-Alouf, H., Geoffroy, M., Goudercourt, D., Turneer, M., Mercenier, A.: Protection against tetanus toxin after intragastric administration of two recombinant lactic acid bacteria: impact of strain viability and in vivo persistence, vol. 20, pp. 3304–3309 (September 2002)

Broth Recycling in Liquid Cultivation of Nostoc Flagelliforme Cells*

Yujie Dai, Feng Zhang, Guoliang Wang, Yonghong Chang, and Shiru Jia

Key Laboratory of Industrial Microbiology, Ministry of Education
Tianjin University of Science and Technology
Tianjin 300457, China
yjdai@126.com

Abstract. Broth recycling is a favorable way to make the most of nutrients in culture medium and to minimize the discharge of waste water from the fermentation process. In this study, the recycling of the effluent broth after the collection of *Nostoc flagelliforme* cells and polysaccharides was examined in consecutive batch fermentations with and without new nutrient elements supplemented. *Nostoc flagelliforme* cells grew well in consecutive batch fermentations with broth recycling for three cycles and there are no significant differences in cell growth rate and polysaccharide's accumulation when nutrient elements equivalent to 50% of the BG-11 culture medium were supplemented into the recycling broth after each cycle of cultivation. However, the cell growth rate and the polysaccharide's accumulation decreased distinctly and chlorisis of cells took place in the 3rd run of the consecutive batch fermentations without new nutrient elements supplemented. On the latter occasion, the content of inorganic nutrients in fermentation broth after three cycles of fermentation decreased to a considerable low extent, thus the influence of discharging fermentation broth on environment can be minimized. As a conclusion, the broth recycling is a promising method for improving the utilization efficiency of culture medium and lowering the waste water discharge.

Keywords: Broth recycling, Nostoc flagelliforme cells, Liquid cultivation, Consecutive batch fermentations.

1 Introduction

Fermentation is a water-intensive process discharging large amounts of effluent broth [1]. Waste water treatment or dewatering of large amounts of effluent broth is costly and needs a high-capacity treatment facility or high energy-consumption processing. It is desirable to minimize the discharge of waste water from the fermentation process. On the other hand, there are many valuable components in the effluent broth, which can be reused. For these reasons, recycling of process effluent can be environmentally and economically beneficial. However, not many attempts at the reuse of effluent broth in fermentations have been studied.

* This work is supported by National High-Tech Research and Development Plan of China #2008AA10Z326 to Y Dai and National Natural Science Foundation of China #20776112 to S Jia.

E. Zhu and S. Sambath (Eds.): Information Tech. and Agricultural Eng., AISC 134, pp. 39–48.
springerlink.com © Springer-Verlag Berlin Heidelberg 2012

In a fermentation producing intracellular penicillin amylase, Babul and Panda found that recycling of 40% to 60% of spent broth could be continued for three subsequent batches without inhibiting biosynthesis of product [2]. Ye et al. developed a cross-flow filtration coupled to an anion-exchange resin column technology to achieve biomass recycle and broth reuse for lactic acid fermentation [3]. The effluent was recycled accompanied by being diluted with fresh medium and supplementing some glucose and nutrients. There was no significant decrease seen in fermentation performance in three consecutive biomass recycle fermentations. Converti et al. examined an in situ ethanol recovery and complete recycling of the spent broth during continuous fermentation by *Saccharomyces cerevisiae* to produce ethanol in a lab-scale process, and found that fermentable polysaccharides and ions reached inhibitory levels eventually [4]. The inhibition can be overcome by installing enzymatic hydrolysis and ion removal stages in the process. Hsiao et al. investigated a strategy of recycling a large fraction of broth effluent to the subsequent fermentation for L-lysine production [5]. This was done on a lab scale process with *Corynebacterium glutamicum* ATCC 21253 as the L-lysine-producing organism. Broth effluent from the fermentation in a defined medium was able to replace 75% of the water for the subsequent batch. This recycle ratio was maintained for three sequential batches without affecting cell mass and L-lysine production.

These studies mentioned above showed that the recycling of fermentation broth (or coupled with separation and purification process) is a desirable measure for improving process economics or a desirable measure for improving process economics or reducing the quantity of pollutants discharged.

Nostoc flagelliforme is a terrestrial filamentous cyanobacterium that is distributed in some arid and semi-arid areas. It is favored by Chinese and East-Asia people as food for more than 2,000 years, and its herbal value was recognized more than 400 years ago [6]. Recently, some components having anti-tumor and anti-viral effects have been reported [7,8]. However, *N. flagelliforme* grows very slowly in the natural environment. Its annual growth rate is less than 6% [9]. Increased market demands have resulted in excessive exploitation of this species, which, in turn, has caused the endangered status of this species and deterioration of the environment [6]. Therefore, artificial culture of *N. flagelliforme* is needed to meet market demands and to conserve this endangered species. Cultivation of free cells in liquid medium has been performed [10-12]. Yu et al. compared the growth characteristics of the cyanobacterium *N. flagelliforme* in photoautotrophic, mixotrophic and heterotrophic cultivation and it was found that the growth rate of the *N. flagelliforme* in liquid suspension culture is much quicker than that in natural state [12]. The specific growth rate of *N. flagelliforme* cells in photoautotrophic mode reaches 0.138 day^{-1} under 60 μmol photon m^{-2} s^{-1} of light intensity. The highest biomass, 1.67 g L^{-1} cell concentration was obtained under 7 days mixotrophic culture. Some studies on the accumulation and separation of the polysaccharides from the culture broth have been done in our laboratory [8,13]. The scale-up cultivation of *N. flagelliforme* cells in a 20-L photo-bioreactor was also conducted. These studies showed that the liquid suspension culture is a promising method which can be potentially used for the scale-up production of *N. flagelliforme* cells and polysaccharides. After *N. flagelliforme* cells and polysaccharides are collected, there are many nutrient metals such as Fe, Mg, Cu, Zn, B, Mo, etc. in the effluent broth; however, the effluent broth is usually

discarded. Considering the cost of the cultivation of *N. flagelliforme* cells and the environmental protection, these nutrient metals should be recycled. In this study, the broth reuse for the next batch of cultivation of *N. flagelliforme* cells was conducted and some influencing factors are analyzed.

2 Materials and Methods

2.1 Cultivation of N. Flagella for Me with Broth Recycling

The axenic cells of *N. flagelliforme* used for this study were same as those reported previously [12]. The culture medium was BG-11 with 2.0 g L^{-1} $NaNO_3$ and 1.0 g L^{-1} K_2HPO_4 added as extra N, P and K sources. The *N. flagelliforme* cells pre-cultured in 500 ml flasks (with 150 ml of culture medium) under continuous illumination of 40 μmol photon m^{-2} s^{-1} on a rotary shaker (140 rpm) at 25°C for 10 days were used as inoculum. It was then inoculated (10%, v/v) to a 20 L photo-bioreactor (Shanghai Baoxing Bioengineering Equipment Co., Ltd., China) with 15 L culture medium. Then the cultivation of *N. flagelliforme* cells was conducted at 25°C and 8.0 of pH for 14 days. The aeration rate was set to 0.8 vvm, and the agitation rate was maintained at 150 rpm, which had been determined previously to be appropriate for *N. flagelliforme* cell growth [10]. Continuous illumination was provided using 3 fluorescent lamps set into the bioreactor, generating an average light intensity of 60 μmol photon m^{-2} s^{-1}. After that, the fermentation broth was transferred to a 20 L plastic barrel and precipitated for 20 min. the supernatant was filtered with a Büchner funnel (20 cm in diameter) under vacuum pumping. The sediment was centrifuged with a refrigerated centrifuge (Himac CR21G, Japan) for 10 min with 4,000×g at 4°C. The cells were collected and the supernatant was also filtered as previously stated. All the filtrate was concentrated to 1.0-1.5 g L^{-1} polysacchrides using ultra-filtration equipment (UEIP-503 MOTIANMO Group of Tianjin Polytechnic University, China) for the collection of polysaccharides and the effluent was analyzed and used for the next batch of cultivation.

2.2 Determination of the Dry Cell Weights of N. Flagelliforme

The biomass was determined by weighing the dry cells obtained from the subsequent procedure: 50 ml of the fermentation broth was centrifuged in a 100 ml centrifuge tube at 4,000×g for 10 min. The supernatant was removed and the tube (pre-weighted) with the sediment was dried at 80°C until the weight was constant.

2.3 Calculation of Specific Growth Rate

Specific growth rate (μ, day^{-1}) was obtained from the linear range of the slope of growth curve. $\mu = (\ln x_2 - \ln x_1)\ (t_2 - t_1)^{-1}$, where x_2 is the cell concentration at experimental time t_2, and x_1 the cell concentration at time t_1.

2.4 Determination of Polysaccharide and Chlorophyll-a Contents

Polysaccharide content was determined by the phenol-sulfuric acid method [13]. Chlorophyll-a in the cell was extracted and determined according to the method reported by Hall and Rao [14].

2.5 Elemental Analysis of the Fermentation Broth

Elemental contents of Na, K, Mg, Ca, Mn, Zn, Mo, Cu, Co, Fe and B in the fermentation broth were determined by atomic absorption spectroscopy using the atomic absorption spectrophotometer (Shimadzu AA-6800, Kyoto, Japan).

2.6 Determination of PO_4^{3-} and NO_3^-

PO_4^{3-} was determined with molybdenum blue method [15]. NO_3^- was determined by the salicylic-sulfuric acid methods [16]. Each sample (50 ml of fermentation broth) was filtered through a cellulose nitrate filter (0.45 μm). An aliquot of 200μl filtrate was taken and 800 μl of the mixture having 5% salicylic acid in sulphonic acid was added into a 50 ml volumetric flask. The mixture was being shaken for 20 min and 30 ml 1.5 M of NaOH was slowly added. Samples were cooled to room temperature and spectrophotometer readings were performed at 410 nm. The nitrate content was calculated using calibration standards containing 0, 1, 2.5, 5, 7.5 and 10 mM KNO_3.

2.7 Morphology Observation of N. Flagelliforme Cells

Morphology observation of *N. flagelliforme* cells was conducted using a microscope with a camera (OLYMPUS CX 40, *Hamamatsu*, Japan).

3 Results and Discussion

3.1 Changes of the Nutrient Elements in the Fermentation Broth of Different Recycling Numbers

The broth recycling was conducted as follows: When the first run of cultivation was ended, *N. flagelliforme* cells and polysacchrides were collected and the effluent broth

Table 1. Nutrient element contents in the permeated liquid from the ultrafiltra-tion equipment for different broth recycling numbers

Elements	n[a]			
	0	1	2	3
Na^+	541.300	275.188	90.424	26.247
K^+	448.960	166.786	51.643	19.732
Mg^{2+}	7.390	2.980	1.261	0.835
Ca^{2+}	9.797	2.673	1.129	0.553
Mn^{2+}	505.000	24.364	17.064	6.413
Zn^{2+}	50.390	39.035	9.132	1.453
Fe^{2+}	964.070	101.94	24.737	18.313
Mo^{7+}	158.500	58.824	56.660	51.445
Co^{2+}	2.476	4.078	2.201	1.579
Cu^{2+}	20.000	5.671	1.305	0.110
B^{3+}	500.072	271.163	49.662	1.779

[a] Concentration: Na^+, K^+, Mg^{2+}, Ca^{2+} (mg L^{-1}); Mn^{2+}, Zn^{2+}, Fe^{2+}, Mo^{7+}, Co^{2+}, Cu^{2+}, B^{3+} (μg L^{-1})

was sterilized and then inoculated for the next run of cultivation. The concentration changes of the main non-metal elements, N and P, in the fermentation procedure were monitored every two days and are shown in Fig. 1 and 2. The contents of other non-metal and metal-ions in the effluent broth of each run are listed in Table 1. It can be seen that the $c_{NO_3^-}$ and $c_{PO_4^{3-}}$ in the culture medium decreased with the cultivation time. For the first run of cultivation (the first run was the control and the fastest because *N. flagelliforme* cells grew fastest with the recycling number n = 0, the culture medium is initial BG-11 without recycling broth), the decline of $c_{NO_3^-}$ and $c_{PO_4^{3-}}$ were adequate nutrients, however, with the increase of the recycling numbers, the nutrient elements became more scarce and the growth rate of the *N. flagelliforme* cells got slower. Especially for NO_3^-, Co^{2+}, Zn^{2+} and Cu^{2+}, they are nearly exhausted after 3 runs of recycling cultivation.

3.2 Effect of Broth Recycling on the Growth of N. Flagelliforme Cells

The biomass profiles for each run of fermentation are shown in Fig. 3. The biomass in each run of fermentation increased with the cultivation time. However, the total biomass of each run decreased with the recycling numbers. This is due to the reduction of the nutrient elements in the fermentation broth. For the first run of the cultivation (n = 0), *N. flagelliforme* cells grew well and were all in the logarithmic phase for the 14 days of cultivation. For the second run of cultivation (n = 1), the biomass and the growth rate become slower than the first run (the average growth rates of the first and second runs are 107.1 mg L^{-1} d^{-1} and 85.0 mg L^{-1} d^{-1}, respectively. After 12 days of cultivation, the cell growth got to the stationary phase. For the third run, the cell growth rate decreased significantly (the average growth rate is only 35 mg L^{-1} d^{-1}) because of the serious scarce of the nutrient elements (Fig. 3 and Table 1). From the 7th day of the cultivation, chlorisis took place and on the 10th day the cell growth came to the stationary phase.

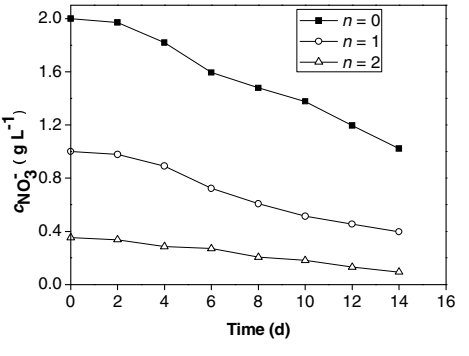

Fig. 1. $c_{NO_3^-}$ changes during the fermentation of *N. flagelliforme* cells with different broth recycling numbers

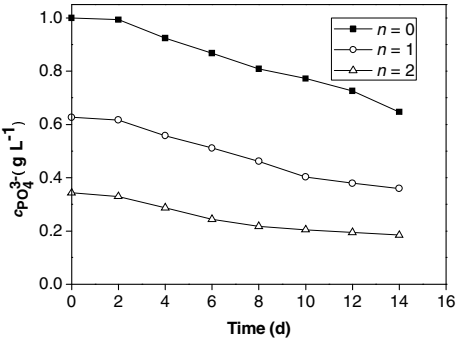

Fig. 2. $c_{PO_4^{3-}}$ changes during the fermentation of *N. flagelliforme* cells with different recycling numbers

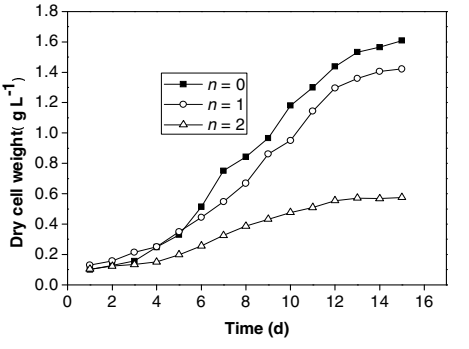

Fig. 3. Biomass changes during the fermentation of *N. flagelliforme* cells with different recycling numbers

3.3 Effect of Broth Recycling on the Production of Extracellular Polysaccharides

The changes of extracellular polysaccharide concentration in the fermentation broth are shown in Fig. 4. For each run of fermentation, the concentration of the polysaccharide increased with the cultivation time. At the end of the fermentation, the polysaccharide concentration of 2nd run is the highest. The polysaccharide concentrations of 1st, 2nd and 3rd runs are 120.43 mg L^{-1}, 158.75 mg L^{-1} and 79.42 mg L^{-1}, respectively. The reason for this phenomenon may be the nitrogen starvation. For the first run of cultivation, there are plenty of macroelements (such as N, P, K, etc.) and trace elements nutrient (such as Cu, Zn, Mn, etc.), which favors to the growth of *N. flagelliforme* cells and the biomass increased rapidly. For the 2nd run, most of the elements could basically fulfil the necessity of *N. flagelliforme* cells for normal physiological activities, however, some elements such as N were inadequate.

The syntheses of proteins and nucleic acids were inhibited, which facilitated the accumulation of the polysaccharides though the cell growth rate decreased to some extent. For the 3rd run of cultivation, the normal physiological activities of *N. flagelliforme* cells are inhibited significantly because of the extremely scarce of the necessary elementssuch as N, P, K, Cu, Zn and Mn, etc. The growth of *N. flagelliforme* cells and the synthesis of the polysaccharide simultaneously decreased and the concentration of polysaccharide was the lowest.

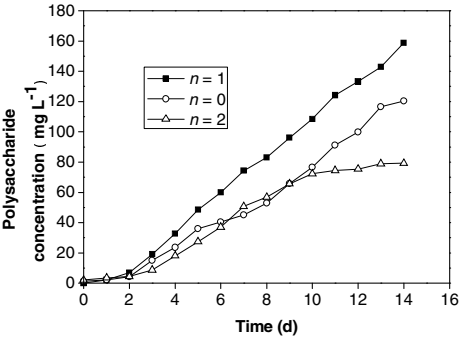

Fig. 4. Polysaccharide concentration changes during the fermentation of *N. flagelliforme* cells with different recycling numbers

3.4 Effect of Broth Recycling on the Morphology and the Color of N. flagelliforme Cells

Fig. 5 shows the morphology and color changes of *N. flagelliforme* cells in the different runs of cultivation. It can be seen that the cells are all in the normal shape for the three runs of cultivation. Chlorophyll-a is one of the important substances for the photosynthesis of the plants. For the 1st and 2nd runs, the nutrients can meet the necessity of the growth of *N. flagelliforme* cells. Chlorophyll-a can be formed normally and the cells are green. The content changes of chlorophyll-a with the fermentation are depicted in Fig. 6. It can be seen that the content of chlorophyll-a increase with the cultivation time. After the 1st and 2nd runs of cultivation, the contents of chlorophyll-a are all very high compared with the third run. They reached 9.744 μg ml^{-1} and 8.145 μg ml^{-1} respectively, which are 3.96 times and 3.31 times higher than the third run. Because the significant scarce of the important nutrient elements such as N and P in the fermentation broth, the synthesis of chlorophyll-awas held-up and the *N. flagelliforme* cells became yellow (Fig. 5c).

3.5 Recycling with Supplementation of BG-11 Culture Medium

Table 1 indicates that the residual contents of Mn and Fe in fermentation broth are much lower than those of the otherelements after 1st run of fermentation. It is supposed that they are not totally consumed by the growth of *N. flagelliforme* cells.

It may be due to low solubilities of these elements at high pH of 9-10. Mn^{2+} and Fe^{2+} in the culture medium may be precipitated according to the following reactions:

$$2Mn^{2+} + O_2 + 4OH^- = MnO_2 \downarrow + 2H_2O \quad (1)$$

$$4Fe^{2+} + O_2 + 8OH^- + 2H_2O = 4Fe(OH)_3 \downarrow \quad (2)$$

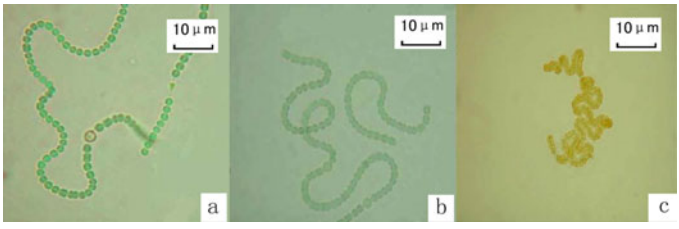

Fig. 5. The morphology and color changes of *N. flagelliforme* cells in the different runs of cultivation (a, b, and c are 1st, 2nd, and 3rd of runs of cultivation, respectively)

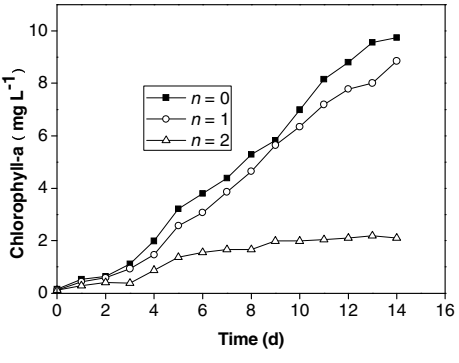

Fig. 6. Chlorophyll-a changes during the fermentation of *N. flagelliforme* cells with different recycling numbers

Most of other element consumption ratios (R_{ec}, the ratio of concentration of a element after cultivation to the initial concentration in the broth) after the first run are nearly in the range of 0.3-0.5, therefore, a consecutive batch cultivation of *N. flagelliforme* cells was conducted for three cycles with supplementing an equivalent to 50% of the BG-11 culture medium into the recycling broth after each run of cultivation. Fig. 7 and 8 show the changes of biomass and polysaccharides with the fermentation time respectively. All the polysaccharide and biomass productions have no significant differences for three cycles of fermentation and chlorisis doesn't take place, which means the fermentation broth can be recycled for the liquid cultivation of *N. flagelliforme* cells for three cycles. The recycle of the fermentation broth not only saves the nutrient and water resources, but also reduces the influences on environment.

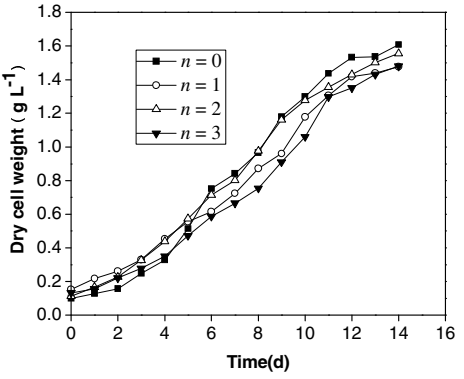

Fig. 7. Biomass changes in the broth recycling fermentation of *N. flagelliforme* cells with recycling with supplementation of BG-11 culture medium

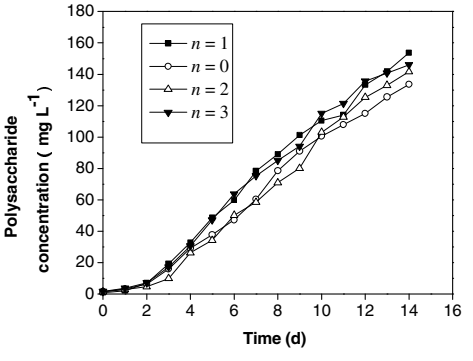

Fig. 8. Polysaccharide concentration changes in the broth recycling fermentation of *N. flagelliforme* cells with recycling with supplementation of BG-11 culture medium

4 Conclusion

It was found that there are large quantities of nutrient elements left in the broth after the liquid fermentation of *N. flagelliforme* cells is finished. They can be reused for the next batch of fermentation. It was proved from this study that most of the nutrient elements in the fermentation broth can be reduced to considerable low concentrations using consecutive batch broth recycling fermentation without any new nutrient elements supplemented. When an equivalent to 50% of the BG-11 culture medium was supplemented into the recycling broth after each cycle of cultivation, *N. flagelliforme* cells can grow well in recycled broth and the fermentation can be continued for three cycles. As a conclusion, the broth recycling is a promising method for improving the utilization efficiency of culture medium and lowering the waste water discharge.

References

1. Hsiao, T., Glatz, C., Glatz, B.: Broth recycle in a yeast fermentation. Biotechnol. Bioeng. 44(10), 1228–1234 (1994)
2. Babu, P.S.R., Panda, T.: Effect of recycling of fermentation broth for the production of penicillin amidase. Proc. Biochem. 26(1), 7–14 (1991)
3. Ye, K., Jin, S., Shimizu, K.: Cell recycle and broth reuse fermentation with cross-flow filtration and ion-exchange resin. J. Chem. Tech. Biotechnol. 66(3), 223–226 (1996)
4. Converti, A., et al.: In-situ ethanol recovery and substrate recycling during continuous alcohol fermentation. Bioproc. Eng. 7(1-2), 3–10 (1991)
5. Hsiao, T.-Y., Glatz, C.E.: Water Reuse in the L-Lysine Fermentation Process. Biotechnology and Bioengineering 49(3), 341–347 (1996)
6. Gao, K.: Chinese studies on edible blue-green alga, Nostoc flagelliforme: a review. J. Appl. Phycol. 10(1), 37–49 (1998)
7. Kanekiyo, K., et al.: Isolation of an antiviral polysaccharide, Nostoflan, from a terrestrial cyanobacterium, Nostoc flagelliforme. J. Nat. Prod. 68(7), 1037–1041 (2005)
8. Jia, S., Yu, H., Lin, Y., Dai, Y.: Characterization of extracellular polysaccharides from Nostoc flagelliforme cells in liquid suspension culture. Biotechnol. Biotechnol. Eng. 12(3), 271–275 (2007)
9. Dai, Z.: Review of Nostoc flagelliforme research. J. Ningxia Univ. (Nat. Sci.) 13(1), 71–76 (1992)
10. Liu, X., Chen, F.: Cell differentiation and colony alteration of an edible terrestrial cyanobacterium Nostoc flagelliforme, in liquid suspension cultures. Folia Microbiol. 48(5), 619–626 (2003)
11. Bi, Y., Hu, Z.: Influence of temperature, nutrients and light intensity on the growth of Nostoc flagelliforme. Chin. J. Proc. Eng. 6(3), 245–249 (2004)
12. Su, J., Jia, S., Chen, X., Yu, H.: Morphology, cell growth, and polysaccharide production of Nostoc flagelliforme in liquid suspension culture at different agitation rates. J. Appl. Phycol. 20(3), 213–217 (2008)
13. Yu, H., Jia, S., Dai, Y.: Accumulation of Exopolysaccharides in Liquid Suspension Culture of Nostoc flagelliforme Cells. Appl. Biochem. Biotechnol. 160(2), 552–560 (2010)
14. Hall, D., Rao, K.: Photosynthesis, 5th edn., p. 43. The Press Syndicate of Cambridge, Springfield (1994)
15. Murphy, J., Riley, J.: A modified single solution method for the determination of phosphate in natural waters. Anal. Chim. Acta 27, 31–36 (1962)
16. Cataldo, D.A., Maroon, M., Schrader, L.E.: Rapid colorimetric determination of nitrate in plant tissue by nitration of salicylic acid. Commun. Soil Sci. Plant Anal. 6(1), 71–80 (1975)

Express Transmissible Gastroenteritis Virus Spike Gene B and C Antigen Sites in Multiple Expression Systems*

Tian-fei Yu, Shu-li Shao, Xing-jun Xu, Jian-wei Lv, and Ming Li

College of Life Science and Agriculture Forestry University of Qiqihar
Qiqihar, Heilongjiang Province, China
{yutianfei2001,shshl32}@163.com, fiona001lee@yahoo.cn

Abstract. In order to illuminate the antigenicity of porcine transmissible gastroenteritis virus (TGEV) spike protein B and C antigen sites, the truncated spike gene including B and C antigen sites of Chinese isolate TH-98 was expressed respectively in *E.coli*, *baculovirus* and *pichia pastoris* expression systems. Dot enzyme-linked immunosorbent assays (Dot-ELISA) based on these three recombinant proteins were developed preliminarily. Ten sera obtained correspondingly from ten piglets two months old which showed up clinical symptom were used for examination. The study indicates that the assays are rapid, reliable and sensitive and it has the potential for use as serological methods for TGEV diagnosis.

Keywords: Transmissible gastroenteritis virus, Spike protein, Expression, Dot-ELISA.

1 Introduction

Transmissible gastroenteritis (TGE) is a highly contagious viral disease of swine characterized by vomiting, diarrhea, and dehydration. Its causative agent is transmissible gastroenteritis virus (TGEV), considered the principal etiologic agent responsible for dramatic outbreaks of diarrhea and high mortality of newborn pigs, in which mortality approaches 100% [1-2]. Porcine respiratory coronavirus (PRCV) is believed to be a mutant of TGEV, as it has been shown to be genetically related to TGEV but has a selective tropism for respiratory tissue with very little to no replication in the intestinal tissue of infected swine [3]. TGEV and PRCV share high homology in genome and can generate the full cross-reaction neutralizing antibody [4-6], so it is difficult to discriminate TGE in clinical diagnosis with traditional serological methods.

* This work is supported by National High-Tech Research and Development Plan of China #2008AA10Z326 to Y Dai and National Natural Science Foundation of China #20776112 to S Jia.

E. Zhu and S. Sambath (Eds.): Information Tech. and Agricultural Eng., AISC 134, pp. 49–56.
springerlink.com © Springer-Verlag Berlin Heidelberg 2012

The truncated spike gene including B and C antigen sites which is absent in PRCV was expressed in *E.coli*, *baculovirus* and *pichia pastoris* in this research. Dot-ELISA assays based on these three recombinant proteins were developed to detect TGEV antibodies and could avoid antibody cross-reaction from PRCV theoretically.

2 Materials and Methods

2.1 Viruses and Cells

TGEV strain named TH-98 was isolated from a suburb of Harbin, Heilongjiang province, P.R. China, and Swine testicle (ST) cell line was grown as monolayer in Dulbecco's modified Eagle medium (DMEM) (GIBCO, USA) containing 10% fetal calf serum (GIBCO, USA) and 5% CO_2 in air. Viruses were harvested by three cycles of freezing and thawing, cellular debris was removed by low speed centrifugation at $1.0\times l0^4$g (HITACHI CR22E, Japan) at 4℃ for 25 min, and virions in supernatant were pelleted by centrifugation at 1.0×10^5g at 4℃ for 1.5 h (HITACHI CR22E, Japan).

2.2 Oligonucleotide Primers

All the three pairs of primers were prepared according to the sequence of TGEV strain TH98 from a data base, GenBank (Accession no.AF494337). PGu/PGl contained *EcoR Ⅰ* or *Sal Ⅰ* restriction enzyme site respectively, PHu/PHl contained *Pst Ⅰ* or *Sal Ⅰ* restriction enzyme site respectively, and PYu/PYl contained *EcoR Ⅰ* or *Not Ⅰ* restriction enzyme site respectively. All the primers contained artifical start codon or termination codon (Table. 1).

Table 1. Nucleotide sequence of PCR primers for amplification of each expression system

Expression system	Sequence(5′-3′)	Primer annealing temperature (℃)
E.coli	PGu: CCCgAATTCATgACCTTCCTTCTAAACTAT PGl : CCggTCgACTTATAACCTgCACTCACTAC from 115nt to 472nt of spike gene.	55
Baculovirus	PHu: ggCTgCAgTATgTgTTCTAAATTgAC PHl: CggTCgACACgATTATACggTAC-3′ from 61nt to 741nt of spike gene	53.5
pichia pastoris	PYu: GTAGAATTCATGTGTTCTAAATTGACT′ PYl: TTTGCGGCCGCTTAACCATTTTTATTATTA from 61nt to 744nt of spike gene	56

2.3 RNA Isolation and Reverse Transcription-Polymerase Chain Reaction

RNA was extracted as described by Yin et al [7], meanwhile the ST cell RNA was also extracted as the negative control. Extracted RNA 4μl was added into the below components: 5×reverse transcription buffer 1μl, dNTP mixture (2.5 mM) 4μl, RNase inhibitor 0.5μl, primer PYl 5μl, AMV reverse transcriptase 2μl (10 U), sterile water 3.5μl, gently mixed in an Eppendorf tube and incubated at room temperature for 10 min, then transferred to a water incubator at 42℃ for l h prior to stored at -20℃ until use in PCR. PCR amplification was performed using PE2400 PCR equipment (USA). PCR was in 100μl volumes, using 10μl of 10×buffer (50 mM KC1, 100 mM Tris-Cl pH8.3, 15 mM $MgCl_2$, 0.1% gelate, 16μl dNTP mixture (10mM), 1μl cDNA, 5μl of primers and lμl ExTaq polymerase (0.5u Takara, Dalian, China). For the PCR the mixture was submitted to 30 cycles of amplification involving heating at 95℃ for 30s, 55℃ (*E.coli* expression), 53.5℃ (*baculovirus* expression), 56℃ (*pichia pastoris* expression) for 30s, and 72℃ for 60s, there was then a final extension time of 10min at 72℃. A 2μl aliquot of PCR product was visualized by agarose gel electrophoresis (2% agarose, 100 Vs for 20 min, 0.8μg/ ml ethidium bromide included in gel) and subsequent U.V transillumination. The purified PCR product was named ts, tg or ty respectively.

2.4 Expression Plasmids Construction

The amplified S gene (ts) DNA was digested with *EcoR Ⅰ*, *Sal Ⅰ* and the resulting fragment was inserted into the *EcoR Ⅰ*, *Sal Ⅰ* sites of the vector pGEX-6P-1 (Pharmacia Biotech, Inc., USA) to place the cDNA under the control of the tac promoter. The amplified S gene (tg) DNA was digested with *Pst Ⅰ*, *Sal Ⅰ* and the resulting fragment was inserted into the *Pst Ⅰ*, *Sal Ⅰ* sites of the transfer vector pBlueBacHis2A (Invitrogen Co., USA) to place the cDNA under the control of the polyhedrin promoter. The amplified S (ty) gene DNA was digested with *EcoR Ⅰ*, *Not Ⅰ* and the resulting fragment was inserted into the *EcoR Ⅰ*, *Not Ⅰ* sites of the transfer vector pPIC9K (Invitrogen Co., USA). The three recombinant vectors were sequenced by Sangon bio-company, Shanghai, China.

2.5 Expression of B and C Antigen Sites in *E.coli*, *Baculovirus* and *Pichia Pastoris*

Expression of B and C antigen sites in *E.coli* and recombinant proteins purification was followed the procedures offered by the description of *Glutathione S-transferase (GST) Gene Fusion System* (amersham pharmacia biotech, third edition, revision 2).

Expression of B and C antigen sites in baculovirus and pichia pastoris were followed Manual of Bac-N-Blue Transfection and Manual of Expression Guide and Methods for Expression of Recombinant Proteins in Pichia pastoris (Invitrogen Co., USA).

Twelve percent SDS polyacrylamide gel was used to analyze the three recombinant proteins. After electrophoresis, one of the gels was stained with Coomassie Brilliant Blue R250 to visualize the protein bands. The proteins of the other gel were transferred onto the NC membrane for the Western blot analysis. The diluted protein samples were spotted on the NC membrane for the Dot-ELISA. The membrane was blocked with 5% non-fat dried milk powder in PBS with 0.05%Tween20 (blocking solution). The membrane was probed with the TGEV immunized rabbit serum, in blocking solution (1:100). A peroxidase conjugated sheep anti-rabbit IgG (Promega, USA) was used as the secondary antibody (1:1000) and the signal was detected with H_2O_2 and 4-Chlor-1-naphthol as a chromogenic substrate.

3 Results

3.1 Expression of B and C Antigen Sites in *E.coli*

IPTG induced the *E.coli* BL21 (DE_3) pLysS transformed with the pGEX-6P-ts plasmid to express the recombinant fusion protein of about 40KD (Fig. 1. Ⅰ illustrate). This was consistent with the expected molecular mass of the fusion protein of pGEX-6P-ts which consisted of the GST (26KD) and S gene B and C antigen sites subunit (14KD).

3.2 Expression of B and C Antigen Sites in *Baculovirus* Expression System

Two different MOIs, 5 and 10 were tested. Seed two 6-well plates with 10^6 cells in each well. The final volume in each well should be 1-1.5 ml. The harvest (post infection) was, 24 hours, 48 hours, 72 hours, and 96 hours. As shown in Fig. 1. Ⅱ illustrate and Fig. 1. Ⅲ illustrate, recombinant baculovirus expressed 33 KD protein corresponded to the molecular weight of TG of TGEV at 24 hours post-infection and the protein was accumulated in high amount till 96 hours post-infection. No specific band was detected in the culture medium by Coomassie brilliant blue staining.

Sf9 cells were inoculated recombinant virus with MOIs, 5. Infected cells were harvested after 96h. The cell sediments were resuspended in PBS (PH7.4). After interruptible ultrasonic treatment, the lysate and supernatant were analyzed by SDS-PAGE. The result showed that recombinant protein was soluble bulk in supernatant (The result was not given).

3.3 Expression of B and C Antigen Sites in *Pichia Pastoris*

The recombinant B and C antigen sites protein expressed into the yeast culture supernatant was identified on the bases of its molecular weight. Numerous bands were observed in the 14-116 KD molecular mass range. A sharp band was observed at molecular masses of approximately 40 KD by SDS-PAGE. The recombinant protein is the major protein component observed in the culture supernatant (Fig. 1. Ⅳ illustrate).

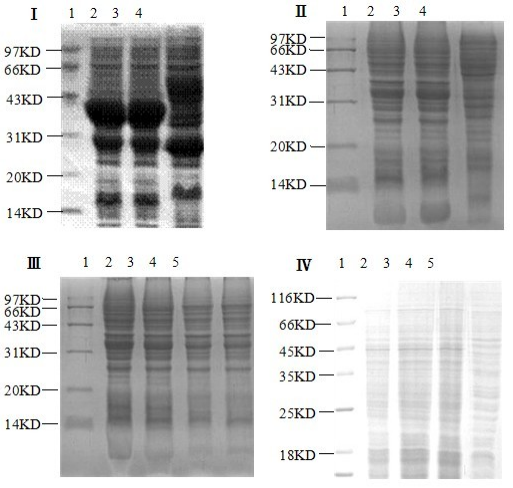

Fig. 1. SDS-PAGE analysis of expressed B and C antigen sites recombinant proteins. Ⅰ. Expression of B and C antigen sites in E.coli. The vector or recombinant plasmid transformed E. coli was cultured in LB medium and induced with IPTG. Lane1: Protein molecular marker; Lane2 and Lane3: pGEX-6P-ts with IPTG induction for 4h; Lane4: pGEX-6P-1 with IPTG induction for 4h. Ⅱ. Expression of B and C antigen sites in baculovirus expression system. Lane1: Protein molecular marker; Lane2: The sediment of Sf9 cell infected by recombinant baculovirus with MOIs, 10; Lane3: The sediment of Sf9 cell infected by recombinant baculovirus with MOIs, 5; Lane4: Uninfected Sf9 cells control. Ⅲ. Sediments of Sf9 cell infected by recombinant baculovirus in different times. Lane1: Protein molecular marker; Lane2~Lane5: The sediments of Sf9 cell infected by recombinant baculovirus with MOIs, 5 after 96h, 72h, 48h and 24h. Ⅳ. Expression of B and C antigen sites in pichia pastoris. Lane1 was the protein molecular mass range. Samples were taken 24 h (Lane2), 48 h (Lane3) and 72 h (Lane4) after induction with methanol. Culture supernatant (20μl) from each time-point was analyzed by SDS-PAGE. Lane5 was the GS115 cells supernatant transformed with pPIC9K plasmids.

3.4 The Antigenicity of the Recombinant Proteins

The antigenicity of the three recombinant proteins was analyzed by Dot-ELISA assay. When the amount of spotting is 750ng, the recombinant protein expressed in prokaryotic system shows the positive reaction in contrast with GST (Fig. 2. Ⅰ illustrate).

When the amount of spotting is 100ng, the ultrasonic lysis supernatant of Sf9 cell infected by recombinant baculovirus show the positive reaction in contrast with ultrasonic lysis supernatant of Sf9 cell (Fig. 2. Ⅱ illustrate).

When the amount of spotting is 50ng, the recombinant B and C antigen sites protein expressed into the yeast culture supernatant show the positive reaction in contrast with the GS115 cells transformed with pPIC9K plasmids (Fig. 2. Ⅲ illustrate).

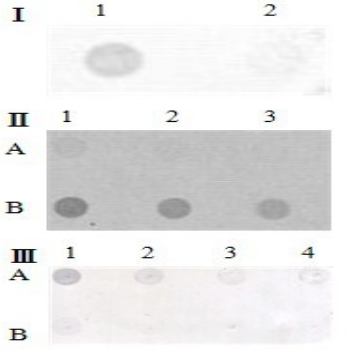

Fig. 2. The antigenicity of the recombinant proteins by Dot-ELISA assays. Ⅰ. Analysis of the antigenicity of recombinant protein expressed in prokaryotic system. Lane1. Purified recombinant protein (750ng); Lane2. Purified GST protein (750ng). Ⅱ. Analysis of the antigenicity of recombinant protein expressed in baculovirus system. Dots A_1 (1000ng), A_2 (100ng), A_3 (10ng) were ultrasonic lysis supernatant of Sf9 cell; Dots B_1 (1000ng), B_2 (100ng), B_3 (10ng) were ultrasonic lysis supernatant of Sf9 cell infected by recombinant baculovirus. Ⅲ. Analysis of the antigenicity of recombinant protein expressed in *pichia pastoris* expression system. Dots A_1 (100ng), A_2 (50ng), A_3 (25ng), A_4 (12.5ng) were the positive yeast culture supernatant; Dots B_1 (100ng), B_2 (50ng), B_3 (25ng), B_4 (12.5ng) were the GS115 cells supernatant transformed with pPIC9K plasmids.

3.5 Detection of Transmissible Gastroenteritis Virus Antibody by Dot-ELISA

Ten field sera obtained from ten piglets about two months old which showed typical signs of epizootic TGE used for examination and the ten corresponding sera were positive detected by Dot-ELISA (Fig. 3).

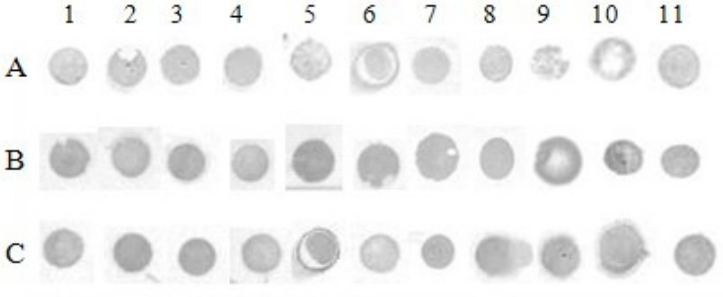

Fig. 3. Detection of transmissible gastroenteritis virus antibody by Dot-ELISA. The coating antigen in A, B, C rows were the recombinant protein expressed in *E.coli*, *baculovirus* and *pichia pastoris* respectively. The 11th column was the positive TGEV antibody control.

4 Discussion and Conclusion

The spike protein of TGEV has been shown to contain four major antigenic sites (A, B, C, and D). Site A is the main inducer of neutralizing antibodies and has been previously subdivided into the three subsites Aa, Ab, and Ac. Site A contains the residues 538, 591, and 543, which are essential in the formation of subsites Aa, Ab, and Ac, respectively. The peptide 537-MKSGYGQPIA-547 represents, at least partially, subsite Ac which is highly conserved among coronaviruses. This site is relevant for diagnosis and could be of interest for protection. Other residues contribute to site B (residues 97 and 144), site C (residues 50 and 51), and site D (residue 385). Site C can be represented by the peptide 48-P-P/S-N-S-D/E-52 but is not exposed on the surface of native virus [8]. Site B is dependent on intracellular glycosylation and is complex and conformation-dependent. This site is formed by at least three epitopes. Although site B is conformation dependent, MAbs specific for this site can bind TGEV spike protein by immunoblotting providing that the samples were not treated with 2-mercaptoethanol. Most probably, renaturation of spike protein occurs during the blotting of the protein to nitrocellulose paper [8]. Site C is linear and continuous. It is recognized by MAbs in Western blot analysis after treatment of the virus with 2.5% SDS and 5% 2-mercaptoethanol; It is represented by synthetic nonapeptides derived from TGEV spike protein [9]; It is present in recombinant products expressed in bacteria, which do not reconstitute the native spike protein [10]; and it is formed in the absence of glycosylation [8]. In addition, because binding and sequencing studies indicate that site C is not present in the respiratory variants of TGEV, this peptide could be useful to discriminate serum from TGEV or PRCV infected animals. The purified recombinant protein expressed in prokaryotic system in this research, can be recognized specially by polyclonal antibody according to the research of Yang et al [10].

Although, the three recombinant proteins shared the same antigen sites, the quantity of amino acids of the former exceed the latter (the recombinant protein expressed in eucaryotae has 227 amino acids, the recombinant protein expressed in prokaryosyte has 119 amino acids). If this difference has an effect on antigenicity between them or how deeply effect on antigenicity need more experiment to identify.

Recently, some new ways to detection TGEV were developed, such as real-time RT-PCR [11-12], but these ways need expensive equipment and reagent. It seems to unsuitable applied in open country, especially in the third world countries. So we developed the simple ways to detecting antibody induced by TGEV, and the results seem more reliable. The study indicates that the assay reported above is rapid, reliable and sensitive and it has the potential for use as serological method for TGEV diagnosis.

References

1. Schwegmann-Wessels, C., Herrler, G.: Transmissible gastroenteritis virus infection: a vanishing spectre. Dtsch Tierarztl Wochenschr 113(4), 157–159 (2006)
2. Eleouet, J.-F., et al.: Complete sequence (20 kilobases) of the polyprotein-encoding gene 1 of transmissible gastroenteritis virus. Virology 206(2), 817–822 (1995)

3. Pensaert, M., Callebaut, P., Vergote, J.: Isolation of a porcine respiratory, non-enteric coronavirus related to transmissible gastroenteritis. Vet Q 8(3), 257–261 (1986)
4. Simkins, R.-A., Weilnau, P.-A., Bias, J., Saif, L.-J.: Antigenic variation among transmissible gastroenteritis virus (TGEV) and porcine respiratory coronavirus strains detected with monoclonal antibodies to the S protein of TGEV. Am. J. Vet. Res. 53(7), 1253–1258 (1992)
5. Paton, D., Ibata, G., Sands, J., McGoldrick, A.: Detection transmissible gastroenteritis virus by RT-PCR and differentiation from porcine respiratory coronavirus. J. Virol. Methods 66(2), 303–309 (1997)
6. Kwon, H.-M., Saif, L.-J., Jackwood, D.-J.: Field isolates of transmissible gastroenteritis virus differ at the molecular level from the miller and purdue virulent and attenuated strains and from porcine respiratory coronavirus. J. Vet. Med. Sci. 60(5), 589–597 (1998)
7. Yin, J.-C., Ren, X.-F., Li, Y.-J.: Molecular cloning and phylogenetic analysis of ORF7 region of Chinese isolate TH-98 from transmissible gastroenteritis virus. Virus Genes 30(3), 395–401 (2005)
8. Gebauer, F., et al.: Residues involved in the antigenic sites of transmissible gastroenteritis virus S glycoprotein. Virology 183(1), 225–238 (1991)
9. Correa, I., et al.: Localization of antigenic sites of the E2 glycoprotein of transmissible gastroenteritis coronavirus. J. Gen. Virol. 71(2), 271–279 (1990)
10. Yang, L.-L., Guo, F.-S., Sun, S.-F., Wu, B., Chen, H.-C.: Comparsion of antigenicity between expressed proteins of the fragment including S gene whole antigenic sites and the deleted fragment in porcine respiratory coronavirus of transmissible gastroeritis virus. Chinese Journal of Virology 21(5), 384–389 (2005)
11. Chen, R., et al.: Development of a novel real-time RT-PCR assay with LUX primer for the detection of swine transmissible gastroenteritis virus. J. Virol. Methods 122(1), 57–61 (2004)
12. Vemulapalli, R., Gulani, J., Santrich, C.: A real-time TaqMan RT-PCR assay with an internal amplification control for rapid detection of transmissible gastroenteritis virus in swine fecal samples. J. Virol. Methods 162(1-2), 231–235 (2009)

Prediction of TGEV Spike Protein Secondary Structure and B Cell Epitopes*

Tian-fei Yu[1], Shu-li Shao[1], Xing-jun Xu[1], Jian-wei Lv[1], and Ming Li[2]

[1] College of Life Science and Agriculture Forestry University of Qiqihar Qiqihar, Heilongjiang Province, China
[2] College of Computer and Control Engineering, University of Qiqihar, Qiqihar, Heilongjiang Province, China
{yutianfei2001,shshl32}@163.com, fiona001lee@yahoo.cn

Abstract. The spike gene of TGEV TH98 strain was translated into amino sequence by Editseq. The secondary structure and B cell epitope of spike protein of TGEV TH98 strain were predicted by Protean. Combining the results according to these methods, the spike protein of TGEV TH98 strain has complicated secondary structure. There are several epitopes of the B-cells in spike protein, including 43-56aa, 97-104aa, 117-128aa, 132-173aa, 238-257aa, 391-398aa, 535-706aa, 779-799aa, 918-987aa, 1165-1200aa, 1257-1266aa and 1430-1446aa.

Keywords: Lasergene, TGEV, Spike protein, Secondary structure, Epitope.

1 Introduction

Lasergene was exploited by DNASTAR, Inc. It was committed to providing innovative and easy to use desktop software tools for today's life researchers. The modules of Lasergene were: SeqBuilder, visualization and sequence editing Video; SeqMan Pro, sequence assembly and SNP discovery Video; MegAlign, sequence alignment; PrimerSelect, oligo primer design; Protean, protein structure analysis & prediction; GeneQuest, gene finding; EditSeq, utility for importing unusual file types. The Data Manager enables data integration between the Lasergene modules so that edits, additions and deletions made to a sequence in one module will synchronize and automatically update when opened in most other modules. Bioinformatics researchers paid close attention to the software from the day of its exploitation. It has been widely used in these days.

Transmissible gastroenteritis (TGE) is a highly contagious viral disease of swine characterized by vomiting, diarrhea, and dehydration. Its causative agent is transmissible gastroenteritis virus (TGEV), considered the principal etiologic agent responsible for dramatic outbreaks of diarrhea and high mortality of newborn pigs, in which mortality approaches 100% [1].

* This work is supported by National High-Tech Research and Development Plan of China #2008AA10Z326 to Y Dai and National Natural Science Foundation of China #20776112 to S Jia.

E. Zhu and S. Sambath (Eds.): Information Tech. and Agricultural Eng., AISC 134, pp. 57–60.
springerlink.com © Springer-Verlag Berlin Heidelberg 2012

TGEV spike protein is a major viral antigen and plays a crucial role in the induction of neutralizing antibodies. Its binding to the cellular receptor porcine aminopeptidase N (pAPN) is required or the initial stage of infection. Therefore, the spike protein of TGEV is a good target for vaccine design and antigen detection [2-6].

In this research, the secondary structure and B cell epitopes of spike protein were predicted by Protean. The work settled the foundation for diagnose of TGEV and functional analysis of related protein.

2 Materials and Methods

2.1 Prediction of Secondary Structure

Nucleotide sequence of TGEV TH98 spike gene (GenBank number: AF494337) was translated into amino acid sequence by EditSeq, one module of Lasergene. The Gamier-Robson method, Chou-Fasman method and Karplus-Schulz method were used to predict the secondary structure of spike protein.

2.2 Prediction of B Cell Epitopes

The hydrophilicity and surface probability of spike protein were analyzed by Kyte-Doolittle method and Emini method. Antigenic index was showed by Jameson-Wolf method. Finally, synthetic conclusion was got to evaluate the potential epitopes of spike protein.

3 Results

3.1 Prediction of Secondary Structure

Alpha helical structure appeared at 312-316aa, 890-902aa, 910-914aa, 1094-1099aa, 1141-1145aa, 1173-1177aa, 1347-1352aa, 1440-1444aa according to Gamier-Robson method and Chou-Fasman method. Beta folds were well-distributed according to these methods. Among the beta fold units there are several turn regions.

3.2 Hydrophilicity of Spike Protein

The hydrophobicity of spike protein was analyzed by Kyte-Doolittle method. The results showed there were many hydrophilicity plots, 19-32aa, 45-51aa, 67-76aa, 87-105aa, 119-125aa, 136-172aa, 194-205aa, 236-247aa, 325-335aa, 347-354aa, 391-402aa, 481-490aa, 538-546aa, 554-568aa, 587-596aa, 613-621aa, 640-651aa, 668-674aa, 683-693aa, 699-705aa, 765-796aa, 819-829aa, 862-874aa, 918-935aa, 946-959aa, 973-987aa, 1082-1091aa, 1134-1146aa, 1164-1198aa, 1236-1243aa, 1256-1277aa, 1306-1326aa, 1342-1358aa, 1378-1389aa, 1429-1444aa. These regions could be potential epitopes.

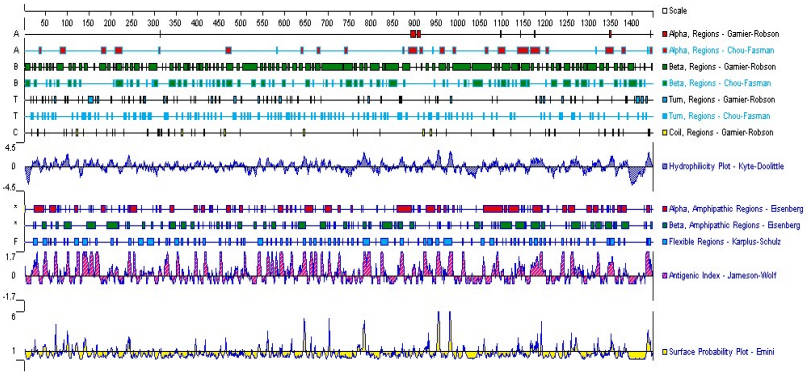
Scale
Alpha, Regions - Garnier-Robson
Alpha, Regions - Chou-Fasman
Beta, Regions - Garnier-Robson
Beta, Regions - Chou-Fasman
Turn, Regions - Garnier-Robson
Turn, Regions - Chou-Fasman
Coil, Regions - Garnier-Robson
Hydrophilicity Plot - Kyte-Doolittle
Alpha, Amphipathic Regions - Eisenberg
Beta, Amphipathic Regions - Eisenberg
Flexible Regions - Karplus-Schulz
Antigenic Index - Jameson-Wolf
Surface Probability Plot - Emini

Fig. 1. Prediction of TGEV spike protein secondary structure and B cell epitopes by Lasergene

3.3 Surface Probability of Spike Protein

The surface probability plots of spike protein appeared at 43-50aa, 97-103aa, 117-124aa, 136-145aa, 234-243aa, 557-563aa, 641-647aa, 765-786aa, 949-958aa, 975-985aa, 1163-1192aa, 1257-1273aa, 1347-1356aa, 1432-1441aa. The probability of other regions was low.

3.4 Coil Regions of Spike Protein

There were a lot of coil regions in TGEV TH98 spike protein. These coil regions distributed evenly. The extents of coil regions in N terminal were wider.

3.5 Prediction of B Cell Epitopes

According to Jameson-Wolf method and former results, the potential epitopes at 43-56aa, 97-104aa, 117-128aa, 132-173aa, 238-257aa, 391-398aa, 535-706aa, 779-799aa, 918-987aa, 1165-1200aa, 1257-1266aa and 1430-1446aa. Some regions showed antigenicity by Jameson-Wolf method only, but other indexes were lower. Such regions were questionable.

4 Discussion and Conclusion

Viruses are major factors of human infectious diseases. Understanding of the structure-function correlation in viruses is important for the identification of potential anti-viral inhibitors and vaccine targets. In virology research, virus-related databases and bioinformatic analysis tools are essential for discerning relationships within complex datasets about viruses and host-virus interactions. Bioinformatic analyses on viruses include the identification of open reading frames, gene prediction, homology searching, sequence alignment, and motif and epitope recognition. The predictions of features such as transmembrane domains, glycosylation sites, and protein secondary and tertiary structure are important for analyzing the structure-function relationship of proteins encoded in viral genomes. Biochemical pathway analysis can help elucidate information at the biological systems level [7].

The secondary structure of protein had great influence on epitope. The chemical bond energy of alpha helical and beta fold was high. They could maintain fast higher structure of protein and could not be the epitopes. Meanwhile, the turn and coil regions were noncohesive structure and easily twist. The structures usually hovered over and displayed on the surface of protein. Therefore, antigenic indexes of these domains antigenic index were high [8]. In this research, the N terminal of spike protein had more turns and high indexes of hydrophilicity and surface probability. The characteristics of such regions could be the indexes of potential epitopes. In a word, the potential epitopes of spike protein were at 43-56aa, 97-104aa, 117-128aa, 132-173aa, 238-257aa, 391-398aa, 535-706aa, 779-799aa, 918-987aa, 1165-1200aa, 1257-1266aa and 1430-1446aa. The 43-56aa domains were in coincidence with already definite epitope [9].

Because all the theories of predictable methods were based on protein primary structure, the intermolecular force was neglected. The prediction of conformational epitopes was not suitable by these methods. Up to now, there were no better effective ways to predict conformational epitopes. Even the predicted epitopes presented on the surface of protein actually, but, these epitopes could be barricaded in posse by the tertiary structure.

References

1. Schwegmann-Wessels, C., Herrler, G.: Transmissible gastroenteritis virus infection: a vanishing spectre. Dtsch Tierarztl Wochenschr 113(4), 157–159 (2006)
2. Ballesteros, M.-L., Sanshes, C., Enjuanes, L.: Two amino changes at the N-terminal of TGEV spike protein result in the loss of enteric tropism. Virology 227(2), 378–388 (1997)
3. Izeta, A., et al.: The spike protein of transmissible gastroenteritis coronavirus controls the tropism of pseudorecombinant virions engineered using synthetic minigenomes. Adv. Exp. Med. Biol. 440, 207–214 (1998)
4. Sanchez, C.-M., et al.: Targeted recombination demonstrates that the spike gene of transmissible gastroenteritis coronavirus is a determinant of its enteric tropism and virulence. J. Virol. 73(9), 7607–7618 (1999)
5. Krempl, C., et al.: Characterization of the sialic acid binding activity of transmissible Gastroenteritis coronavirus by analysis of haemagglutination-deficient mutants 81(2), 489–496 (2000)
6. Schwegmann-Wessels, C., Zimmer, G., Schroder, B., Breves, G., Herrler, G.: Binding of transmissible gastroenteritis coronavirus to brush border membrane sialoglycoproteins. J. Virol. 77(21), 11846–11848 (2003)
7. Persson, B.: Bioinformatics in protein analysis. EXS 88, 215–231 (2000)
8. Poland, G.-A., Ovsyannikova, I.-G., Johnson, K.-L., Naylor, S.: The role of massspectrometry in vaccine development. Vaccine 19(17-19), 2692–2700 (2001)
9. Gebauer, F., et al.: Residues involved in the antigenic sites of transmissible gastroenteritis virus S glycoprotein. Virology 183(1), 225–238 (1991)

Total Paeony Glycoside Inhibits Tumor Growth and Induces Apoptosis in K562 Cells and in S180 Tumor-Bearing Mice*

Huiyu Xu[1], Yanmin Wu[1], Xiaoqing Luo[1],
Hui Wang[1], Zhiwei Chen[2,**], Meng Zhang[2], and Danyang Liu[2]

[1] Department of Immunology University of Qiqihar Medical Qiqihar, Heilongjiang Province, China
[2] Department of Histology and Embryology, University of Qiqihar Medical, Qiqihar, Heilongjiang Province, China
xhymy2005@163.com, czwzp@sina.com

Abstract. Total paeony glycoside (TPG) studies on anti-tumor are very little. In this study, It also showed cytotoxic effects against five tumor cell lines and inhibits grow of tumor-bearing mice by establishing a model of mouse sarcoma S180. K562 cells treated with TPG showed typical morphological appearance of apoptosis. The activation of caspase-9 and caspase-3, but not caspase-8, was also demonstrated that the apoptotic signaling triggered by TPG was mediated through the intrinsic mitochondria dependent pathway. The expressions of Bcl-2, Bax and Bcl-xL, which were revealed by western blot when K562 cells were treated with TPG. Meanwhile the cell cycle also showed special change with the appearance of G1 peak and increase of S cells. TPG could prolong survival time and change the expression of Bcl-2. TPG has anticancer activity and may contribute to the clinical application in cancer prevention and treatment.

Keywords: TPG, Apoptosis, Mitochondria, S180, K562.

1 Introduction

Radix Paeoniae Rubra is one of the Chinese peonies. It is commonly used in clearing heat and cooling blood, analgesic action. The extract from Paeoniae Radix can improve blood flow through its endothelium dependent vasodilator action on aorta and inhibitory effects on thrombosis and platelet aggregation[1]. Recent studies have determined that TPG has significant biological and pharmacological activities[2], which exhibit inherently immunoregulator and potent antitumor activity. The inhibitory effect of tumor cell growth on Paeoniae Radix may be due to activation of immunological action against the tumor[3]. The study of the anticancer effects in vivo and in vitro and identification of drug targets would provide a rationale for clinical development of this agent as a therapeutic drug in cancer therapy.

* This work is partially supported by Heilongjiang Education Department Project Grant No.D2007-109 to Zhiwei Chen , No.D2007-108 to Huiyu Xu and the Natural Science Foundation of Heilongjiang Province Grant No.11531434 to Huiyu Xu.
** Corresponding author.

E. Zhu and S. Sambath (Eds.): Information Tech. and Agricultural Eng., AISC 134, pp. 61–68.
springerlink.com © Springer-Verlag Berlin Heidelberg 2012

2 Materials and Methods

2.1 Preparation of TPG

TPG was purchased from Xian aojing Science and technology development Company, LTD. lot number: 060417, purity: 99%. The final storage concentration was 200 mg/ml and the concentration used in the experiment was based on the dry weight of the extract (50μg/ml).

2.2 Tumor Cell Lines and Culture

Human cell line of Hela (cervical carcinoma), A549 (lung carcinoma), Bel-7402 (hepatoma) and HCT-8 (colon carcinoma) were provided by institute of medical university medicaments.

2.3 Flow Cytometric Analysis of Apoptosis

Cells were fixed by 70% ethanol at 20℃for at least 12h. After two washes with phosphate-buffered solution (PBS), the cells were incubated in RNase A/PBS (100 Ag/ml) at 37℃ for 30min. Intracellular DNA was labelled with PI (100 Ag/ml) and analyzed with a FACS Calibur fluorescence-activated cell sorter (FACS) using.

2.4 Western Blot

Cytoplasm proteins were isolated from 120 mg of frozen hippocampus tissues using Cytoplasmic Protein Extraction kit, and protein concentrations were determined using the BCA Protein Assay kit according to the protocol provided by the manufacturer. The electrophoretic mobility of the proteins in this study was determined by SDS polyacrylamide gel electrophoresis using 12.5% (Bcl-xL and Bax), and 15% (Bcl-2) polyacrylamide gels. The membrane was then incubated overnight at 4 °C.

2.5 RNA Isolation and Real-Time Polymerase Chain Reaction

Total RNA was extracted from 100 mg of frozen hippocampus tissues using RNAiso Reagent kit, and cDNA was synthesized with SYBR ExScriptTM reverse transcription (RT)-PCR kit according to the protocol provided by manufacturer. All of mRNA fold change relative to glyceraldehyde phosphate dehydrogenase (GAPDH) was calculated with the comparative Ct method of $2^{-\Delta\Delta Ct}$) .The following primers were used: 5'-gca ccg tca agg ctg aga ac- 3' (sense) and 5' –tgg tga aga cgc cag tgg a-3'(anti-sense) for the GAPDH gene; 5'-cag cat tag gga cag gaa tgg a-3' (sense) 5'-tgc tct act gtg cag tca tgt g-3' (anti-sense) for the caspase-8 gene; 5'-ccc ata gat gat cga gga cat cca-3' (sense) and 5'-aca act ttg ctg ctt gcc tgt tag-3' (anti-sense) for the caspase-9 gene; 5'-aag gca gag cca tgg acc ac -3' (sense) and 5'-ctg gca gca tca tcc aca cat ac-3' (anti-sense) for the caspase-3 gene. The levels of mRNA were expressed as -fold changes after normalization with GAPDH. All tests were done in triplicate to ensure reproducibility.

2.6 In Vivo Mouse Experiments

This study was approved by the Animal Care and Use Committee of Qiqihar Medical University. A total of 40 pathogen-free adult male kunming mice (weight range: 18 to 22g) were employed in the study. In these experiments, the mice were randomly divided into four groups with 10 mice per group, including control group, CTX therapy group, TPG therapy group and CTX + TPG combined therapy group. Mice of the control group were administered tap water; CTX therapy group were administered tap water and intraperitoneally injected of CTX (30mg/kg) every day; TPG therapy group were administered TPG (6 mg/ml) solution from drinking water; CTX + TPG combined therapy group were intraperitoneally injected of CTX (30mg/kg) ever day at the same time provided with TPG(6mg/ml) ad libitum. Drug administration was started from 1 week before transplantation of tumor cells and continued until the end of the experiment. Mice were sacrificed 1 week after transplantation. Tumor suppressor rate = (control group of mean tumor weighs - other groups of mean tumor weighs) / control group of mean tumor weighs×100%.

2.7 Immunohistochemistry Analysis

Tumor tissue sections (5mm in thickness) were incubated at 4 °C overnight with primary antibody(Bcl-xL antibody and Bcl-2 antibody Santa Cruz Biotechnology, Santa Cruz, CA, U.S.A, ; Bax antibody Cell Signaling Technology Inc., Beverly, MA, U.S.A.), in concentrations of 1:100 (Bax), 1:200 (Bcl-2) and 1:150 (Bcl-xL).

2.8 Statistical Analysis

One-way analysis of variance (ANOVA) was performed to determine the significance between groups. P value of less than 0.05 ($P<0.05$) was considered as statistically significant.

3 Results

3.1 TPG Suppresses the Growth of Tumor Cells Lines in Vitro

The morphologic changes of four tumor cell lines were observed with an inverted microscope. The cultured cells (Hela, A549, Bel-7402 and HCT-8) displayed monolayer growth well. Five tumor cell lines in logarithmic growth time were selected for experiment. Five cell lines were incubated with the different drug concentrations of TPG (0, 50, 100, 200, 300 and 400μg/ml) for 24 h. The inhibitory rates of five tumor cell lines were determined in triplicate by MTT assay. Each point represents the mean of the data from three independent experiments, bars represent the standard deviation. TPG was not specific to the inhibitory growth of five tumor cell lines. IC50 value Concentration of a compound at which it inhibits a particular phenomenon by 50%. Five cell lines of IC50 value were very different after calculation. They were observed respectively about 60.45±3.87, 111.02±4.89, 135.09±6.37, 175.22±5.44, 193.55±7.48. The drug sensitivity proved human chronic myelogenous leukemia (K562)>human cervix carcinoma (Hela)>lung cancer

(A549)>hepatoma (Bel-7402)>colon carcinoma (HCT-8). IC50 value indicated that K562 was as low as about 60μg/ml which was the most sensitive to treat with TPG among other tumor cell lines . K562 cells were treated with the different drug concentration of TPG (0, 25, 50, 75, 100, 150, 200 and 400μg/kg) for the different times (24, 48 and 72 hours) in triplicate by MTT assay. The data revealed a significant dose-effect and time-effect correlation of cytotoxicity of TPG.

3.2 TPG Induces Apoptosis in K562 Cells

Morphologic alteration is an important characteristic of apoptosis. The representative morphological changes of K562 cells exposed to TPG (50μg/ml) for the different time (0, 12, 24 and 48 hours). K562 cells appeared normal and the nuclei were round and homogeneous with the untreated control. When the time of treatment with TPG was prolonged, the cells exhibited decrease in the number of cells and the death of more quantity of cells under light microscopy. Wright–Giemsa staining distinctly showed the formation of apoptotic bodies. The typical characteristics of apoptosis were cytoplasmic edema and nuclei condensed, the fragmented chromatin arranged against the nuclear membrane under light microscopy. K562 cells were treated with TPG (50μg/ml for 0, 12, 24, and 48 h). The percentages of G1, S and G2/M cells were evaluated by PI staining and flow cytometric analysis. The representative cell cycle profile was shown when K562 cells were treated with TPG for 48 h. When the time treatment with TPG (50μg/ml) was prolonged, the experimental groups of the apoptotic rates (APO) (20.66% and 46.29%) were higher than that in the untreated control group of APO (5.15%). Along with the extending of time, the experimental group of TPG for 48 h appeared typical apoptosis peak. Meanwhile the cell cycle also showed special change with the appearance of G1 peak and increase of G0/G1cells. Furthermore, we performed phosphatidylserine externalization (annexinV binding) and cell membrane integrity (PI staining) binding assay to detect the redistribution of phosphatidylserine, which is a hallmark for early apoptotic cells. The dual parametric dot plots combining annexin V-FITC and PI fluorescence show the viable cell population in the lower left quadrant (annexin V-PI-), the early apoptotic cells in the lower right quadrant (annexin V+ PI-), and the late apoptotic cells in the upper right quadrant (annexin V+ PI+).In untreated K562 cells, 3.1% of cells were annexinV+/PI-, whereas 4.3% of cells were annexin V-/PI-. The treatment of TPG (50μg/ml) for 48 h increased the annexin V+/PI- cells to 19.7% and the annexin V+ PI+ cells to 41.18%.

3.3 TPG Induces the Activation of Caspase-3 and 9, But Not Caspase-8 in the Apoptotic Process

Caspases were activated in the cell death response induced by TPG. TPG (50μg/ml) induced dramatic increases of caspase-3 and 9 activities in K562 cells in a time-dependent manner by real-time PCR. They were approximately two fold compared to the control group when cells were treated for 48 h. A time-dependent activating process accompanied by Caspase-3. Caspase-9 was activated as early as 12 h after treatment with TPG. In contrast, negligible caspase-8 activity was observed by TPG from 0 to 48 h, suggesting no involvement of caspase-8 in the apoptotic process.

TPG induces the transient elevation of Ca^{2+} concentration

When the time was prolonged treatment with TPG (50μg/ml), the intracellular Ca^{2+} level rapidly enhanced. The fluorescence intensity of Fluo-3 reached to a maximum when K562 cells were treated with TPG (50μg/ml) for 48 h. The elevation of Ca^{2+} concentration is an important initial step for induced apoptosis.

3.4 TPG Induces Loss of MMP and Release of Cytochrome c into Cytosol

The loss of MMP (Rh123 uptake) was analyzed by flow cytometry. The percentage of M1 reflected the reduction of ($\triangle\Psi$m). The fluorescence intensity of Rh123 shifted, demonstrating the efficiency of TPG in depolarizing mitochondria. Time course analysis confirmed that TPG induced a fast and sustained decline in MMP. when K562 cells were treated with TPG (50μg/ml) for 48 h, MMP ($\triangle\Psi$m) appeared two peak and decrease the fluorescence intensity of Rh123. The cytosolic cytochrome c level was showed by western blotting following an exposure to TPG (50μg/ml for 0, 12, 24, 36 and 48 h). The experiment group of TPG (50μg/ml for 48 h) were higher than that in the control group of TPG for the cytosolic cytochrome c level ($p<0.05$). TPG induced mitochondrial dysfunction, resulting in the release of cytochrome c and subsequent activation of caspase cascade, indicating that the intrinsic mitochondria-dependent pathway was involved in the apoptotic process.

3.5 Expression of Anti-apoptotic Bcl-2, Bcl-xL, and Pro-apoptotic Bax by TPG

The Bcl-2 family of proteins plays a key role in the apoptotic process by western blotting. When normalized to the intracellular β-actin serving as the control .the anti-apoptotic Bcl-2 and Bcl-xL level of the experiment group of TPG (50μg/ml for 36 and 48 h) were significantly reduced as compared with that in the control group of TPG (50μg/ml for 0 h) ($p<0.05$). When the time was prolonged treatment with TPG (50μg/ml), of special interest was markedly increased the expression of the pro-apoptotic Bax level compared with that in the control group of TPG (50μg/ml for 0 h) ($p<0.05$).

3.6 Effects of Oral Administration of TPG in the S180 Tumor Mice

The different treatment groups of the inhibitory rates were respectively about 63.54%, 44.12% and 56.28% compared with the control group ($p<0.05$). Tab.3 investigated the effect on the weight of the mice with sarcoma S180 by different groups which were calculated the mean data of 25.39g, 19.36g, 25.87g, 24.64g. The weight of the tumor-bearing mice in CTX therapy group was the lightest among other groups ($p< 0.05$). We observed that the S180 tumor mice in CTX therapy group had bad psychosis and appetite. The mice weight of TPG therapy group was the same as the mice weight of control group so that it was statistically insignificant ($p>0.05$). Tab. 4 showed that the survival rates of different groups were -25.62%, 25.07%, 20.67% respectively. The survival rate of the CTX+TPG therapy group was higher than CTX therapy group ($p<0.05$). TPG prolonged life-span that could lower the toxicity of CTX.

3.7 Apoptosis in S180 Tissues Detected by Morphological Observation

We made tumor tissue into isolating single cells to detect cell cycle by flow cytometry. The TPG therapy group and the CTX+TPG therapy group of cell cycle appeared special change with the apperance of G1 peak and increase of S+G2/M cells. The CTX+TPG therapy group of apoptotic rate (27.57%) was greater value than the control group of apoptotic rate (1.25%). Morphological changes of the apoptosis in tumor tissue were observed by HE staining through light microscope and transmission electron microscopy. HE staining showed that tumor cell of control group was dense, giant, size different, hyperchromatic nuclei and rare interstitial lymphocytic infiltrates. In contrast, the tumor cell of TPG therapy group was homogeneous that it's ultrastructure was no significant difference with normal cell. Cell morphology was studied by transmission electron microscope which showed that nuclear DNA of apoptotic cells displayed nucleus pycnosis and distortion, chromatin condensation, margination and Fracture.

3.8 Expression of Bcl-2 Family Proteins in Tumor Tissue

Immunohistochemical staining of Bax, Bcl-2 and Bcl-xL showed the expression of proteins in tumor tissues. The staining of Bax of the TPG therapy group, its staining intensity become stronger gradually than the control group ($p<0.01$), indicating high cell proliferation activity. Staining intensity of Bcl-2 and Bcl-xL was significantly weaker in tumors-bearing mice treated with TPG (6mg/ml) compared with the control group ($p< 0.01$) .The result revealed that TPG could down-regulate the expression of Bcl-2 and Bcl-xL protein meanwhile up-regulate the expression of Bax protein.

4 Discussion

Natural products have been used in traditional and folk medicine for therapeutic purposes. Traditional Chinese medicine of TPG which display high levels of chemopreventive and antitumor activities, a kind of Paeoninacaeae with distinct structures, have been reported to have remarkable biological and pharmacological activities, such as apoptosis induction, host-mediated antitumor activity, activating blood and eliminating stasis[4]. TPG was employed in this study and its mechanism to induce apoptosis in vitro and in vivo. The results demonstrated that TPG initiated a series of events leading to apoptotic cell death in vitro, such as mitochondrial dysfunction, caspase activation. Caspases are the central executioners of apoptosis. In this study, caspase-3 was activated when cytochrome c was released into cytosol following the collapse of MMP. It was the decisive point during the commitment stage of apoptosis. The low activity of caspase-8 in K562 cells demonstrated that the death-receptor pathway was not activated. On the other hand, the processing of caspase-9, as well as the cytosolic accumulation of cytochrome c, confirmed that the mitochondria-dependent (intrinsic) pathway contributed to the TPG-induced apoptosis. Mitochondrial homeostasis plays a pivotal role in regulating apoptosis.

Pro-apoptotic signals can trigger the mitochondria to release caspase-activating proteins into cytosol. TPG induced a fast and sustained collapse of MMP ($\triangle\Psi m$), which reflected the perturbation of the inner membrane. It appeared in the cells that still lacked obvious morphological signs of apoptosis. The decline of MMP was temporally correlated with the opening of the permeability transition pore, leading to the release of caspase-activating proteins. Because mitochondrial dysfunction was prevalent in the early stages of TPG treatment, it should be directly responsible for the apoptotic cell death observed. Moreover, we believe that a threshold of mitochondrial destruction needs to be reached before a cell die. To investigate the effects of TPG on expression of anti-apoptotic Bcl-2 and Bcl-xL, pro-apoptosis Bax.We determined these proteins by Western blotting in K562 cells. Bcl-2 and Bcl-xL have been previously shown to exert their inhibitory effects on apoptosis by blocking the release of cytochrome c and decline of mitochondrial MMP. TPG decreased their expression levels in the process of K562 cell death, in conjunction with the impairment of their anti-apoptotic roles. It is found that the level of pro-apoptotic Bax increases during apoptosis. The cleaved Bax might favorably insert into the inner membrane and form an ion channel, leading to the release of cytochrome c. TPG induced a transient elevation of cytoplasmic. The concentration of Ca^{2+} before caspase-3 activation was suggested that the Ca^{2+} homeostasis plays an important role in the apoptotic process. K562 cells were arrested the cell cycle at G0/G1 phase. In conclusion, TPG, some compounds of monoterpenoid, causes fast mitochondrial dysfunction and induces apoptosis in human CML K562 cells through the intrinsic pathway.

In vivo, the experiments of the S180 tumor mice with TPG (6 mg/ml) or cooperated with CTX inhibited S180 tumor growth in mouse[5]. The weight of tumor-bearing mice and survival time may be showed the suppressive effect of CTX toxicity by TPG.K562 cells were arrested the cell cycle at G0/G1 phase. Instead, S180 cells were arrested the cell cycle at G2/M phase. The most probable reason was that S180 tumor tissue had many cellular debris and necrotic tissue to interrupt the results of animal experimentation. TPG may serve as a novel promising compound in cancer therapy. In a word, the present study will open interesting perspectives in the research of toxicology and pharmacology for the compounds of monoterpenoid.

Acknowledgements. We are grateful to Prof. Iianzhao Niu and Prof. Jifeng Wang for their support of the paper. We gratefully acknowledge the excellent support from all the members in Prof. Niu's laboratory.

References

1. Lee, S.M.Y., Li, M.L.Y., Chung, Y., et al.: Paeoniae Radix, a Chinese herbal extract, inhibit hepatoma cells growth by inducing apoptosis in a p53 independent pathway. Life Sciences 71(19), 2267–2277 (2002)
2. Dou, Z.H., Luo, L., Lu, D., et al.: Purification of Total Paeony Glycoside by Macroporous Resin with Double Indices of Albiflorin and Paeoniflorin. Journal of Chinese Medicinal Materials 32(8), 1282–1284 (2009)
3. Liu, C., Wang, J., Yang, J.: Study on activating blood and eliminating stasis of total paeony glycoside (TPG). Zhong Yao Cai 23(9), 557–560 (2000)

4. Chen, L.C., Chou, M.H., Lin, M.F., et al.: Effects of Paeoniae Radix, a traditional Chinese medicine, Journal of Clinical Pharmacy and Therapeutics on the pharmacokinetics of phenytoin. Journal of Clinical Pharmacy and Therapeutics 26(4), 271–278 (2001)
5. Feng, C., Liu, M., Shi, X., et al.: Pharmacokinetic properties of paeoniflorin, albiflorin and oxypaeoniflorin after oral gavage of extracts of Radix Paeoniae Rubra and Radix Paeoniae Alba in rats. Journal of Ethno Pharmacology 130(2), 407–413 (2010)

A BP Neural Network Activation Function Used in Exchange Rate Forecasting

Xu Chun-Dong[1], Liao Wei[2], Zhou Mu-Gui[3], and Liu Jin-Gao[2]

[1] College of Information Science and Technology, Jiang Xi University of Science and Technology, Ganzhou341000
[2] Department of Information Science and Technology, East China Normal University, Shanghai China
[3] College of Mechanical and Electrical Control Engineering Jiangxi University of Science and Technology
191365470@qq.com, {liaowei54,vsgoster}@126.com, mujia6179@sina.com

Abstract. Traditional BP algorithm has defects of local minima and slow convergence. Based on application for exchange rate forecasting, this paper gives an improved BP neural network activation function. Then propose a new activation function after by analyze influence factor of the exchange rate and design structure of forecasting of the improved BP model. Take simulation forecast for a sample data of the RMB exchange rate. The results show that the improved BP neural network not only has accelerated in the training speed, also has a significant improvement in forecasting performance compare to the traditional BP neural network.

Keywords: BP Neural Network, Activation function, exchange rate, forecast.

1 Introduction

The accurate forecasting of the field of exchange rate and share price is the necessary condition for market competition. Exchange rate is a nonlinear and open system which comply with dissipative structure [1], so the traditional forecasting methods is unequal to economical index forecasting. Neural network has nonlinear mapping, adaptive learning and robustness tolerance, which can describe nonlinear dynamic process accurately [2]. The neural network has many advantages that the traditional modeling method didn't has, it has a small requirement for experimental knowledge of the model object, generally, it is unnecessary to know the parameter, structure and dynamic characteristic of the model object before modeling, but gives input and output data of the object, the mapping relationship of the input and output can be gained by network learning. So, this offered a new thought to forecasting research of variation trend of the exchange rate. A lot of ascertained problems had been tested for BP algorithm, generally, it has a good effect, and used in pattern recognition, function fitting, system identification and forecast [4] [5].

E. Zhu and S. Sambath (Eds.): Information Tech. and Agricultural Eng., AISC 134,, pp. 69–76.
springerlink.com © Springer-Verlag Berlin Heidelberg 2012

2 Design of Model Structure

The exchange rate forecasting is estimation for the relationship of the input and output of exchange rate system based on given training sample, and make it can has a accurate forecasting for unknown output as far as possible. This paper have designed the structure of forecasting of BP model, and researched how the activation function influence the model accuracy, and analyzed detailed process of the improved BP algorithm.

2.1 Selection of BP Model Layer

This paper use the increase of the exchange rate of RMB to dollar in 2005~2007 and the related input factor, such as dollar, yen, euro and KRW as training sample, take training and test for different number of hidden layer, through comparison, the more number of the hidden layer, the smaller training error of the BP model. Integrated view, the mimesis accuracy of the third layer is better than the forth layer [6].

2.2 Selection of the Number of Hidden Layer

For the network, the number of hidden layer has direct influence to mapping level of complex problem [7]. This paper has take four steps to determine the model of neural network. (1) In the beginning, use fewer hidden layer. (2) Train and test the network repeatedly. (3) Increase the number of the hidden layer slowly. (4) Take comparative analysis for the results of the training and test of each program, which can gain satisfied hidden layer number.

2.3 Selection of Learning Rate

The variation of weight in each cycle training was determined by learning rate. According to the BP model feature, the learning rate lr has determined the variation of weight in each cycle training. Take comparison for three layer BP network with different learning rate lr, where, $lr \le 0.2$, Training is smoothly and convergence, and the fitting and forecast is good. Where, $lr = 0.4$, it is divergence. So the scope of lr is 0.01~0.02.

2.4 Selection of Activation Function

The activation function of neuron is a main reason for the slow convergence of the traditional BP algorithm. In BP network, besides the node of input layer, the input of all nodes will through the activation function $f(x)$ before output. Different activation function can reflect different correspondence for the sample of input and output. The operating range and range of sensitivity should be considered in the selection of activation function. The range of sensitivity is the area near origin of coordinates, it has been reflected in diagram of derived function. This curve was expected as a wide and steep curve, which can convenient for increase its convergence speed. The classic BP algorithm, it adopt sigmoid function is: $f(x) = 1/(1+e^{-\beta x})$ (generally $\beta = 1$), and its dynamic scope of output is $(0,1)$.

After derivation, which can obtain: $f(x)' = df(x)/dx = f(x)(1-f(x))$, and derivative is in scope $(0,0.25)$. In many applications, the error correction signal can only in this scope and its maximum is 0.25, so, in this time the convergence speed is not fast enough. When the value of the sigmoid function is close to 0 or 1, the value of the function doesn't has a good sensitivity for the change of independent variable, in this time, if the variation of weight is very small, which don't has influence to the output of neural network, and has a little influence that from the subsequent sample learning, thereby, the convergence speed of the network has been influenced, this situation as "platform".

3 Improvement of Activation Function

In order to speed the convergence speed, solve the so-called "platform" problem, this paper given a new activation function, it has a good effect and has clear physical significance. As follow:

$$f(x) = \frac{(1+\lambda x)^2}{(1+\lambda x)^2 + (1-\lambda x)^2} \tag{1}$$

$-\frac{1}{\lambda} < x < \frac{1}{\lambda}$ (λ is a small positive)

In reference [8], it given a activation function as model of fuzzy optimum theory. $f(x) = \frac{1}{1+(x^{-1}-1)^2}$, $0 < x < 1$. Because the activation function is a unipolarity activation function, and $0 < x < 1$ is limited, so, it has a great limitation for its application. For this, this paper has taken translation for it, introduce parameter λ to enlarge the scope of independent variation, obtained formula (1) by a lot of mathematical computation.

$$\frac{df(x)}{dx} = \frac{\lambda(1-\lambda^2 x^2)}{(1+\lambda^2 x^2)^2} \tag{2}$$

Because $-\frac{1}{\lambda} < x < \frac{1}{\lambda}$, $\frac{df(x)}{dx} > 0$, $f(x)$ is a monotone-increasing function of x , in addition:

$$\frac{d^2 f(x)}{dx^2} = \frac{2\lambda^3 x(\lambda^2 x^2 - 3)}{(\lambda^2 x^2 + 1)^3} \tag{3}$$

So, if $x = 0$, $\frac{d^2 f(x)}{dx^2} = 0$; if $0 < x < 1/\lambda$, $\frac{d^2 f(x)}{dx^2} < 0$; formula (1) is a convex function in $[0,1/\lambda]$; if $-1/\lambda < x < 0$, $\frac{d^2 f(x)}{dx^2} > 0$, formula (1) is a concave

function in $[1/\lambda,0]$. So, $x=0$ is the unique inflexion of the formula in $[-1/\lambda,1/\lambda]$. The formula (1) is a monotonous and differentiable bounded function, according the requirement of the BP algorithm to activation function, formula (1) can reflect the nonlinearity of the BP neural network. Because in the both sides of the domain is -1 and 1, this activation function is bipolar, and can used into the activation function of the neural network.

4 Analysis of Forecast Example for Influencing Factor of Exchange Rate Forecast

4.1 Data Selection and Preprocessing

Observe the superiority of the new activation function by use the actual RMB exchange rate as an example.

The data selection includes training sample selection, retraining sample selection and forecast data selection [9]. Data capture is the selection of related data form original exchange rate database based on unit of time. Show in table 1.

Table 1. Data segment of training set

Number of data set	Data date	Data volume
1	2005.7-2007.7	479
2	2007.7-2008.7	103

Through analysis for traditional BP network, the transfer function of the middle layer is tansig-purelin composite function, network use traingdx as the training function, this function use gradient degressive algorithm to learning, and learning rate is self-adapting.

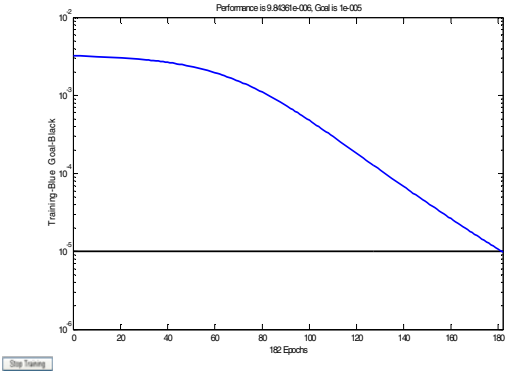

Fig. 1. Curve of training error (traditional BP network)

The carve of training error is shown in Figure 1.

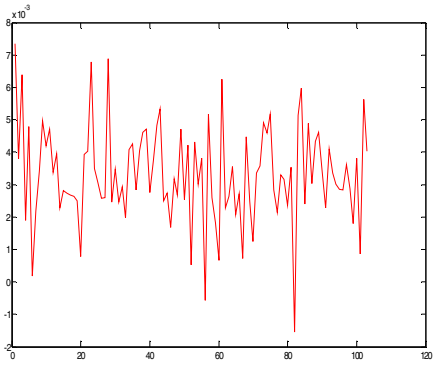

Fig. 2. The curve of forecasting error

The Network to meet the requirements of the target by trained 182 times. After training, the forecasting error of traditional BP neural network is shown in Figure 2.

Because the structure of network is very complex, and a number of neuron, the training time and learning rate must be enlarged. The training parameter was set in table 2.

Table 2. Parameter training

Training time	Training objectives
1000	0.0001

The Network to meet the requirements of the target by trained 181 times. The results is shown in figure 3.

Compared figure 1 with Figure 3, the training speed of the improved BP network has obvious advance.

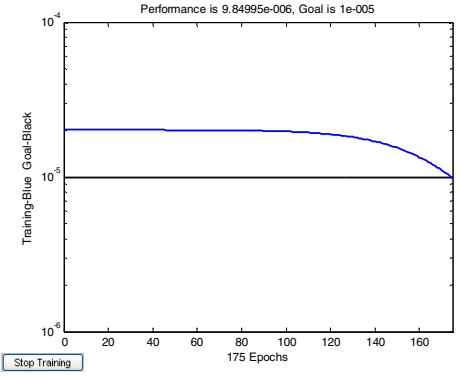

Fig. 3. Curve of training error (improved BP network)

After network training, it should take test before its application. The test data is the 103 days exchange rate data between 2008.1~2008.7. The test that is use emulation function to obtain the network output, computes whether the error between output and actual measure value reached the requirement and standard.

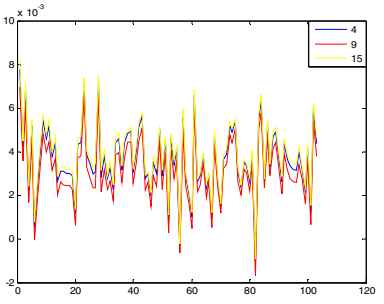

Fig. 4. Curve of forecasting error comparison (improve BP network)

Take the error of the three states (the number of neuron is 4, 9, 15) for comparison, and shown in figure 4, when the number of the middle layer neuron is 9, the network forecasting error is minimum, namely the forecasting performance is best.

Obviously, if add the number of the middle number layer neuron, even if it can make forecasting more precision, but can not explain certainly improve the performance of the neural network.

4.2 Analytic Comparison of the Forecasting Performance

Input the test data to the network, compared computing results with actual results, compute the forecasting performance of network. Network forecasting performance index include: MAPE (mean absolute percentage error), MAE (mean absolute error) and RMSE (root mean square error).

This paper use the above index to compare the fitting precision between forecast value and actual value, is computational formula is:

$$MAPE = \frac{1}{n}\sum_{t\in P}\left|\frac{(x_t - \hat{x}_t)}{x_t}\right| \tag{4}$$

$$MAE = \frac{1}{n}\sum_{t\in P}(x_t - \hat{x}_t) \tag{5}$$

$$RMSE = \sqrt{\frac{\sum_{t\in P}(\hat{x}_t - x_t)^2}{n}} \tag{6}$$

In these formulas, P is the test sample set, $\hat{x}_t$ is the forecast exchange rate value, x_t is the actual exchange rate value.

Through program in MATLAB software, compute these above indexes [11].

Table 3. Comparison of forecasting performance

	Traditional BP	Improved BP(4)	Improved BP(9)	Improved BP(15)
MAPE	1.6887	0.6208	0.6115	0.6116
MAE	0.3581	0.0266	0.0221	0.0357
RMSE	0.0034	0.0033	0.0015	0.0034

The table 3 has shown the index value of the forecasting exchange rate error of the traditional neural network and improved MP neural network.

Through comparison of the training speed and the table 3, use improved BP algorithm to forecast exchange rate will gain a satisfied result. Compared to traditional BP neural network, for the three forecasting index MAPE, MAE and RMSE, forecasting performance has obvious improvement.

5 Conclusion

BP network is a new method for analysis and process of exchange rate forecasting, it has a remarkable function in economy, but itself convergence speed is slow. Increase the convergence speed by research the activation function of the BP network, this paper proposed a new activation function by the selection of the BP network model structure. Results show: the improved BP neural network algorithm has a satisfied training speed compare to the traditional BP network in research of exchange rate forecasting, for the MAPE, MAE and RMSE, the forecasting performance has obvious improvement, which proved the validity of the BP algorithm especially the new activation function.

Acknowledgment. The research has been supported by the National Natural Science Foundation of China (11062002), Project of Jiangxi Province Educational Science and Technology Program (GJJ10156).

References

1. Tang, G., Xu, J.: Modern exchange theory and model research. China financial press, Beijing (2003)
2. Wei, L., Feng, X., Xu, C.: Research for exchange rate forecast model of RBF neural network. Application and Engineering of Computer 45(24) (2009)
3. Chi, X., Liang, O.: Neural network method and comparison of exchange rate. Finance Forum 5, 47–53 (2008)
4. Xiang, X.: Several improvement of BP algorithm 19(7), 148–150 (2000)

5. Li, Z., Wang, C.: Research for learning algorithm of neural network. System Engineering and Electronics 19(5) (1997)
6. Wei, L.: Research for exchange rate forecasting technique based on genetic programming and neural network. East china normal university, Shanghai (2010)
7. Rigler, A.K., Iruine, J.M., Vogl, T.P.: Rescaling of variables in back propagation learning. Neural Networks 4(2), 225–229 (1991)
8. Walczak, S.: An Empirical Analysis of Data Requirements for Financial Forecasting with Neural Networks. Management Information Systems 17(4), 203–222 (2001)
9. Li, X.: Research of exchange rate forecasting based on neural network. Nanjing university of aeronautics astronautics, Nanjing (2005)
10. Jin, F., Fan, J.: Application research and theory of neural network. Southwest jiaotong university press, Cheng du (2000)
11. Lou, S., Shi, Y.: Analysis system and design of neural network based on MATLAB, pp. 9–154. Xi'an electronic science and technology university press, Xi'an (1998)

Studying the Ecological Value of "Green Core" in Changsha-Zhuzhou-Xiangtan Area

Liu Sihua

Department of Tourism
Central South University of Forest & Technology
Changsha, Hunan Province, China
sihual@sina.com

Abstract. The papers try to discuss the actuality and ecological valuation of"green core" in Changsha-Zhuzhou-Xiangtan area(CZT)."Green core" exerts main ecological valuation in increaseing the heterogeneity of landscape,accommodateing entironment, protecting the biodiversity,developing ecotourism,and promotes the course of CZT area.And the more important thing is how to protect the green core，not to exploiture and building.

Keywords: Green Core, Changsha-Zhuzhou-Xiangtan area, ecological value.

"Green core" is new phenomena appears in the urban planning in recent years, which is a relatively large range delineated in urban planning (from tens to hundreds of sq. miles sq. miles range) as the city's ecological dependency. This idea originated in the 19th century, British sociologist Howard's "garden city" theory, in his book "Garden Cities of Tomorrow," , pointed out that the Garden City in size shall meet the requirements of social life, but not too much large, it should be around green space[1].At present, the Green Core study is rarely, mainly green core of the city as a part of urban green space, focusing on city green core planning and design and position .Luo Zhi figured out that the Green Core should be located in the ecological, cultural, efficiency and harmony. Two most crucial question of the development of the Green Core is "three rural issues" as well as the intensity of development and construction issues.[2] Lu Xiao-ming et al focus on the green core of cultural values manifest.[3]The ecological value of the Green Core is equivalent to the ecological value of the urban green space , and as the development of urban group , it is has become a new urban development model to plan the green core in urban group. Urban Agglomeration green core is the differences in scale, size, making their ecological value is also differ from traditional the ecological value of green space, an urban agglomeration in the green core. Except the features and functions for being eco-green possess cleaning up the environment, conserving water, adjusting climate, ecological oxygen bar and absorb carbon dioxide, the maintenance of ecological diversity, and pleasant features and functions, there is a different from the ordinary sense of the ecological value of urban green space system, this article as the CZT "green core", for example, make an research on the urban agglomeration in the green core of the ecological value.

E. Zhu and S. Sambath (Eds.): Information Tech. and Agricultural Eng., AISC 134, pp. 77–84.
springerlink.com © Springer-Verlag Berlin Heidelberg 2012

1 The Study Area Overview

Changsha,Zhuzhou and Xiangtan City, located on the east side of Hunan Province, with in the Xiangjiang River, the three cities was "品"-shaped distribution, the two place is about 45 km apart, of the total land area of 28,106 square kilometers, the core of the total land area was approximately 4500^2 . Hunan provincial government in 1997 decided that the three cities as the integration of construction, the three cities into a single edge combination of the overall advantages, making it becomes Central South region of the high-tech industries of Hunan, as well as gathering areas, a modern city network groups, to stimulate economic development in Hunan.

Changsha-Zhuzhou-Xiangtan area(CZT) is the first time carried out by a joint group of the practice of inner cities ,in its development, the provincial government take full account of recent developments in the urban group and long-term development of development space. In 2005, the Coordination Group CZT integration "compiled by CZT regional planning", made a reservation three downtown of about 200 square kilometers of area as the integration of the three cities "green core." The formation of CZT for the core and the central node of the radial urban layout, with three vertical and two horizontal that is a main folder twice two auxiliary green core of "Ran-shaped structure" support our cities and towns throughout the region for development."Green Core" to the junction of Changsha and Zhao Mountain as the center, mainly including the south of town planning CZT formed a delegation, Zhao Shan - yijiawan organizing groups and long-term Mu-Yun Lu formed a delegation, as well as the town, Jiuhua town, the White Horse town, the town vault, horn Tangxiang other regional scope, about 200km2. Here the vegetation cover was high, biodiversity-rich, including Skyline Ridge National Forest Park, Tai Wai Mountain Forest Park, Akira Green Mountain Forest Park and other large nature reserve. Existing residents, most of them are agricultural production. In the urban agglomeration development process, the green core on the one hand, you can play pool city group, give full play to the advantages of various cities.

To enhance the whole competitiveness of the role; the other hand, the "Green Core" also played a role in isolation, avoiding "the pie" type of urban development patterns appear in the CZT integration process. Thus, although the green core of in the three cities marginal areas, but its own development advantages are obvious.

1.1 The Location Advantage

CZT's "green core" is different from the settings in the city's "green core", which is set in the middle of an urban agglomeration, which belonged to a different city. The Green Core area is located at the junction of the three cities CZT land, with basically the same distance from the three cities. Between the three cities to facilitate it from becoming a transit point, but also can serve as a link the three cities.

1.2 Resources Advantage

The Green Core area is rich in cultural, natural resources. On human resources, Zhao Shan was a history mountains , the preservation of the rich cultural resources, such as the famous one of Xiaoxiang Eight Sights "Mountain City, Seiran" Zhaoshan

Mountain is located. Natural resources, particularly rich, in the Green Zone take Akira Mountain as the center, including large tracts of green space system within Skyline Ridge National Forest Park, Shiyan Hu Scenic Area, Zhuzhou Lotus Forest Park and Xiangtan Fahuashang Forest Park, In the building processing of the ecological economy, as long as the "scientific outlook on development as guidance……scientific use of 'green core' ecological resources and landscape resources, to establish a rational ecological structure and Tourism Industry to achieve social, economic and environmental sustainability co-ordination development. "[2]

1.3 Transportation Advantage

The Green Core area is CZT three cities must pass Road through China Unicom, water, land and air gathered in a variety of transport modes. The existing Changtan highway, on the Swiss highway, 107 State Road, Beijing-Guangzhou Railway, the Xiangjiang waterway all through the core place, but also includes Datuo airport which is located in south of Changsha, the traffic is very convenient.

2 The Ecological Value of Green Core

2.1 Improve Heterogeneity of the Landscape

Landscape heterogeneity is one of the important properties of the landscape, but also the core of landscape ecology, landscape or its properties is the degree of variation. [4] landscape heterogeneity, including heterogeneity of the landscape, landscape features and heterogeneity of landscape dynamic , the heterogeneity was large , the high density, stability was great. [5] landscape heterogeneity to human habitation of the eco-system has a long-term stability and the necessary flexibility to withstand interference.

Urban agglomeration of several of the development is not simply merged into one single city, but to maintain their respective characteristics, under the premise, achieving rapid economic development. In its construction, people tend to have such a misunderstanding, regards as the city's development as a group of urban assimilation, even involuntarily regards as the city's development group is to merge together several cities to build a mega-city. In such a psychology, the urban agglomeration development, particularly in urban agglomerations was tangled in its development, several cities in plaque constantly extending to the center and eventually the entire city will become a big group of construction plaque, not only there is no speak to features, and all the landscape tend to signal. That is not use of the stability of urban agglomerations. Anti-jamming ability was weak,the entire city is vulnerable to the effects of external interference to lose stability.

It take CZT urban construction land as a cluster of several heterogeneous plaques embedded in the substrate into the green, avoiding a number of urban landscape towards a single CZT three cities was shaped "品"structure ordered, Changsha face to south; Zhuzhou, Xiangtan northward trend of development will be easy to take the three cities together into one, as a whole. That is, three large construction plaque aggregate into a large building plaques, tend to the same landscape. Not only the urban landscape is monotonous, and the three cities a number of unique features will

also be weakened and become a simple city big peices. Green Core is under the man-made interference, improve the landscape heterogeneity of urban agglomeration. In the landscape pattern, the Changsha, Zhuzhou, Xiangtan City and its three large green area outside existing quarantine zone: Xiangjiang River Scenic Belt, Yuelu Mountain Scenic Area, Black Forest Park Mi-feng, Tai Wai Mountain Forest Park, Shaoshan, Hua-Ming House Landscape with the existing city roads, rivers-body system with built CZT good, green mesh pattern of base from the center of the green core of this green network to enhance the integrity and robustness. Landscape pattern of this network is the best urban landscape ecosystem landscape pattern, it will CZT urban construction land as a cluster of several heterogeneous plaques embedded in the substrate into the green, avoiding several cities landscapes into a single.

2.2 Adjust the Urban Ecological Environmental Quality

Urbanization effects on the ecological environment mainly by the changing of the land cover types and the type of urban spatial expansion , such as change agricultural land into industrial, commercial or residential areas, etc., which is the most important factor cause the ecological environmental change, In particular, the unlimited expansion of industrial land, reducing the area of urban green space, their emissions of various pollutants, sulfur dioxide, soot, industrial wastewater and so on which aggravate the extent of urban environmental pollution.

A good ecological environment is a necessary condition for quality of life, as a developing urban agglomeration, CZT three cities emissions in the atmosphere a year to 30,000 tons of sulfur dioxide smoke 18,000 tons, 15,000 tons of industrial waste water, solid waste 10 million cubic meters these pollutants join into the natural circulation system of CZT city group, so that make the ecological environment of CZT three cities have been heavily polluted. Coupled with the unique topography of the environment in Hunan Province, surrounded mountains on three sides, only the north is open. Direction was southwest to northeast tilt of the Kei-shaped. This terrain directly impact on climate is the summer monsoon to the north can not be blowing into, the weather was anomaly hot and stuffy; while in winter the cold to the south can be directly blowing into from south of the gap, the weather was anomaly cold .With the continuous development of industrial production, which is another terrain to bring the biggest impact is the decline in air quality index. As the entire central area with poor ventilation, easy to form a calm wind, and industrial production emitted a large number of pollutant gases in the air is not proliferation, dilution, this harmful gases in the air, condensation will form a fog or haze, this gas can be direct harm for people's health, in particular the haze, its pollution levels more than the fog.

In recent years Changsha City, there is an increasing trend which the number of days in winter formed the fog,the appearance of haze likely to have increased greatly. According to statistics, Changsha, haze-year the number of days have emerged to meet or exceed the historical maximum situation. This gives the quality of the urban environment an alarm. Once you connect the three cities, three different pollution groups will be linked together, with the air quality in the city group will be further reduced. During the urban agglomeration which distribution appeared as gobbets, the "green core" will be possible separated contamination by a large heterogeneous plaques for three, giving a spread of pollutants in natural space, just like the "lung" of

urban agglomeration, has played a allow the breathing function to increase the self-purification capacity of the atmosphere, reducing the health threat for the natural world and people own.

2.3 The Conservation of Biological Diversity and Animal Habitat

Biological diversity refers to a general features for a region, a national and variety of global organisms (animals, plants and micro-organisms) Organic combination [6].

Biodiversity conservation and use is one of the goals to achieve harmonious development between man and nature ,is also an important indicator of eco-city construction, to establish a consummate and relatively stable urban ecosystem must not lose sight of conservation and use of biodiversity.[7] With the continuing deterioration of urban ecological environment, human increasingly pay attention to urban ecological environment, but also have realized the importance of the city's biodiversity conservation and building, urban levels of biodiversity has become an important element and indicators to a city's ecological environment construction [8] .The Green Core area coverage rate of forests was high ,biological resources are rich. Being plant-building, botanical garden construction is an important measure for biodiversity conservation. Hunan Forest Botanical Garden are covered an area of 2100 acres, has planted more than 1100 kinds introduction contains forest plants, has set up the sky Ridge National Forest Park in Hunan Province, wildlife resource and breeding center for the subtropical region's largest rare and endangered plants ex-situ conservation areas, preservation of rare and Endangered Plants was 118 species of 95 genera in 54 families. Abundant plant species coverage and provide a habitat for a variety of animals, all kinds of wildlife were habitats here, such as rabbits, pheasants, as well as thrush, azaleas and other animals and birds. Established in 1992, Hunan Province wildlife rescue center.

Ambulance and domesticated the red-crowned cranes, deer, Cabot's Tragopan and a number of rare animals. With the further improvement of the ecological environment, the Green Core area will be in the protection of biological diversity and animal habitat has played a more important role.

2.4 Increase the Ecological and Economic Benefits

Green core can't only improve the city's ecological environment, but also create considerable economic benefits. The marginal effect of the landscape done by the expert simulation results show that in an ideal state, along with the natural landscape and ecological urban green area ratio was decreasing, the corresponding expansion of artificial landscape area can bring economic benefits dropped, the resulting the loss of environmental benefits tends to infinity.[9] In other words, the economic benefits of a city building land will not be an infinite increase because of the constant expansion , but will quickly reduce, and pay more because of the loss of environmental benefits.

However, in the traditional urban development, people neglect of the urban economic and environmental correlation between profit and loss, trying to continuously expand the city's building land area in order to maximize the economic benefits of the Town. Development of modern cities, our urban built-up areas a considerable number of green area ratio of less than 20%. These cities are access to

double the economic benefits, while losses may be several times or several times the environmental benefits. Set aside by government planning the green core of the city, particularly in urban cluster of building land has played the role of a certain limit .To avoid construction sites by the unlimited expansion of environmental benefits resulting from losses due to offset more economic benefits.

With the development of urbanization, such an economic-effective of green ground has gradually revealed. Building green ground can bring economic effective this point of view has been accepted by an increasing number of operators. Development of market economy also contributed to significant indirect benefits of green ground appear. The city's business and real estate boom, large public green space near the real estate appreciation, business prosperity, the Government also derive out more tax revenue. Thus, domestic and foreign experts have proposed the new theory "green economic chain" ,consider that regards green ground as the main improvement of the ecological environment, at the same time improving the urban environment for economic development, so that a vibrant economy; through effective management tools and ways can change environmental advantages into economic advantages, drive the around regional commercial, real estate, tourism and exhibition industry, as well as the rapid development of tertiary industry; the use of high-quality environment to improve the city's visibility, lead the entire city's tangible and intangible value-added is conducive to attracting foreign investment; to form the surrounding area capacity of gathered and radiation and advanced regional economic development .The construction of economic chain of green , will further demonstrate the city green can bring immense ecological and economic benefits, play an important role in forming a fast-track of coordinated development of economy and environment, as well as the realization of economic, social, and environmental sustainability.[10]

2.5 Promote Eco-tourism Development

Eco-tourism is based on knowledge, novelty and fun as the psychological basis, in order to appreciate, study, protecting natural resources for the purpose of tourism activities. Held in China in 1995, eco-tourism seminar, which defined eco-tourism as the point of view under the guidance of the ecology and theory to enjoy and protect the natural and cultural heritage, which is a special form of special tourism with ecological science, ecological science color,[11] develop eco-tourism, on the one hand can contribute to the Green Core region's economic development and improve people's living standards; the other hand, it can enhance the public's ecological and environmental awareness as well as literacy; reduce the impact and pressure in the area of traditional tourism to the travel environment and resources; to achieve a dual purpose for eco-tourism and natural environment protection and construction; has enormous social, economic and environmental benefits to communities.[12] Relative terms, due to the involvement of the forest has a good performance, people can enjoy the fine spring day in the forest, enjoy entertainment, people harmony along with nature, More potential of development of eco-tourism .

The Green Core area of CZT ups and downs, valleys, grasslands, lakes and other natural landscapes show itself, where lush vegetation is a natural oxygen bar. Provided with a local secondary forest, pine forest, torch pine, fir, cedar forest, Elaeocarpus forest, camphor forest, mulberry trees, shrubs, and other forest stands.

There can opened up a variety of unique plant growing areas, such as the cherry blossom park, Guihua Garden, Tea Garden, Bamboo Yuen, magnolia garden, an azalea garden, plum and flowers Bonsai Garden. There are varieties of rare tropical plants such as yew, the Millennium Ginkgo tree, Metasequoia, and various celestial wonders phenomena such as " screen afterglow", "TuoLing Danxia", "Mountain City, Ching-lan," and so on , natural resources was rich .

In addition, the Green Core area is also rich in cultural landscape resources.Zhaoshan Hill is a historical famous hill, many celebrities had lived and stay here, such as the Spring and Autumn Period, the famous moralist Laozi, Tang Dynasty poet Du Fu, Mi Pei during the Northern Song, Northern Song Dynasty the famous Anti-Jin Liu Qi , modern Jianhu Woman Qiu Jin, as well as with the founding Marshal Peng de-huai.Zhao Shan formed a deep bond. It is said that when the Northern Song Dynasty, the famous landscape painters Mi Pei ascend Zhaoshan hill attract by the hill's landscape and have been painting a picture "Mountain City, Chinglan" and title poem.[13]Then Zhao Shan famous in the world. The rich natural and cultural landscape so that tourists enjoy the beauty at the same time, but also stimulate a love of nature, protection of wild flora and fauna and the enthusiasm of ecological environment , then enhance the awareness of protection nature and sense of responsibility. And can enhance their knowledge of history and culture of ancient civilizations, and thereby stimulate love of the motherland.

3 Conclusion

To sum up, the green core plays an important role in the urban agglomeration of landscape heterogeneity, biological conservation, the ecological environment, eco-efficiency and eco-tourism. As the Green Core area is located urban fringe, at present, should play the ecological functions of green core in the urban CZT, the most important is not how to build, but rather focus on the protection of green core of the ecological environment to the ecosystem with a stable self-recovery capability. To form a short, medium and long-term planning programs, and not just immediate benefit, blind to develop and construct. It would undermine the ecological environment of green core and prevent its ecological functions into full play. As for the future development, should be carried out under the protection of the premise. Focus on long-term interests of the play for the ecological functions of the Green Core effective, made the green core onto a sustainable development path.

References

1. Zhang, J.W.: The problems in the urban green space constrution, take ningbo for example, vol. 6, p. 4. Najin Forestry University (2006)
2. Lou, W.Z., Li, J., Li, H.Q.: Research on "green core" of urban planning—taking the plan of "green core"in Leshan. Huazhong Architecture, 132–135 (2007)
3. Lu, X.M.: Green core–cultural garden. Landscape Design, 54–55 (2003)
4. Li, C.L., Qi, L.J.: Study of heterogeneity for urban landscape. Wuhan Urban Construction Institute 21(1), 84–86 (2004)

5. Zhang, L.Y., Zhou, Y.Z., Wen, Z.Y.: Landscape ecological consideration on construction of eco-city. Ecologic Science 24(3), 274–278 (2005)
6. Zhang, Y.J., Qiao, H.T.: The ecological value of greenery patches in the city. Qingdao Institute of Architecture and Engineering 25(2), 66–70 (2004)
7. He, S.-A.N., Xia, B.: Botanical garden and biodiversity protection and utilization in cities. Plant Resources & Environment 8(4), 47–51 (1999)
8. Zhou, X.Y.: Abrief analysis on ecotourist development and ecoenvironmental protection in Lushan. Yunnan Geographic Environment Research 17(1), 69–71 (2005)
9. Zong, Y.G.: Method of marginal utility analysis applied in ecological valuation on urban landscape. Urban Environment & Urban Ecology 11(4), 52–54 (1998)
10. Wu, R.W.: On strategy of urban biodiversity. Urban Planning Forum (1), 18–20 (1999)
11. Xiao, D.N., Li, X.-Z.: Landscape Ecology. Science Publicshing Company (2003)
12. Hu, Y.H., Wang, L.Q.: The analysis for the comprehensive benefit of shanghai urban open spaces. Chinese Landscape Architecture 18(4), 27–29 (2002)
13. Zuo, J.Q.: Tourism resource and exploiting conceive of Zhaoshan. Central South Forest Inventory and Planning 20(2), 41–43 (2001)

Protective Effect of G on UVC-Induced DNA Damage in Mouse Lymphocytes in Vitro

CuiLin Cheng, ZhenYu Wang*, HaiTian Zhao, and Lei Yao

School of food science and Engineering
Harbin Institute of Technology
Harbin, Heilongjiang Province, China
wzy219001@yahoo.com.cn, ccuilin@hit.edu.cn

Abstract. UV irradiation induces lipid and protein peroxidation in mammalian cells. In the present study, we report the protective effect of G on UVC-induced lipid and protein peroxidation using lecithin and BSA in vitro model.Treatment of lipid or protein solution with G before 30 minutes of irradiation inhibited UVC induced peroxidation. And the anti-peroxidation had a dose-effect relationship with the concentration of G. Moreover, the protective effect of G on DNA damage in rat spleen lymphocytes induced by UVC was evaluated using single cell electrophoresis (comet assay). G caused DNA repair when compared with the control group. When lymphocytes in the medium added G were irradiated by UVC and incubated for 30min, the DNA damage decrease at the concentration 6.1uM and 390uM, while repair decreased at a concentration of 3.05mM and 50mM. This result was accorded with MTT assay. Thus, G could reduce UVC-induced damage at low concentration of less than 390uM, and there is a dose-effect relationship. The result provides research basis to develop new anti-radiation products.

Keyword: spleen lymphocytes, sodium guanylate, anti-peroxidation, anti-radiation.

1 Introduction

Lymphocytes participate in cell immunization and body fluid immunization as main constitution of distinctive immunization in organism and have high sensibility to irradiation, which can reflect the abnormal of immunity and blood system when body suffers irradiation. Therefore, these cells are commonly used as a test system to detect chromosome aberrations, DNA repair and mutations. M. Holmberg studied the effect of deoxynucleosides on repair of DNA breaks in UVC-irradiated human lymphocytes [1].

All live maintaining on earth are connected with sunlight directly or indirectly. Solar spectrum contains UV zone 200nm ～ infrared zone 1800nm. The ultraviolet sector of the solar spectrum is commonly divided into four regions, UVA (320-400nm), UVB (280-320nm), UVC (200-280nm) and vacuum ultraviolet (10-200nm). However, UVC radiation in solar radiation is a great less, it has intense biological effect. DNA damage has been identified as an important step in UV carcinogenesis.

* Corresponding author.

E. Zhu and S. Sambath (Eds.): Information Tech. and Agricultural Eng., AISC 134, pp. 85–93.
springerlink.com © Springer-Verlag Berlin Heidelberg 2012

Solar radiation induces acute and chronic reactions in human and animal skin [2]. The incidence of skin cancer is increasing in most western countries and there is strong evidence that this trend is due to increased exposure of the population to UV radiation [3]. UV radiation also reduces body immunity and decrease the resistance to disease. Squires and Johnson studied the kinetic parameters of incision in UVC-irradiated human fibroblastes by using repair inhibitors [4]. Collins accumulated breaks in UVC-irradiated mammalian cells with the aid of the repair inhibitor cytosine-1-β-D-arabinofuranoside and aphidicolin [5].

It is well known that nucleotides is important constitution of DNA, and involved in the DNA metabolism. Some researches have reported the effect of exogenous nucleotides to body. Wang L.F. investigated the supplementation of exogenous nucleotides can accelerate the repair of damaged DNA in mouse thymocytes in vitro [6]. Chen X. G. reported nucleotides mixture promoted migration of IEC-6 after wounded by a TGFβ-independent way [7]. Liu Y. showed that mixed nucleotides could be used to cure acute and chronic hepatitis and its effect might be acted through immune system [8]. Based on our primary experiments, we studied the protective effect of sodium guanylate (G) on UVC-induced DNA damage in rat spleen lymphocytes to assess another effect-anti-radiation.

2 Materials and Methods

2.1 Experimental Animal

ICR mice from Harbin Veterinary Research Institute, (CAAS, license number: SCXK (HEI) 2006－009), aged 7-8 weeks and weighed (20±3)g, were used in the experiment.

2.2 Spleen Lymphocytes Preparation

The rats were killed by dislocation and sterilized in 75% ethanol for 10 min. It is anatomized to take out spleen. Spleen was minced with scissors and passed through a stainless steel mesh. Spleen cells were collected and centrifuged at 1000 rpm for 8 min. Sediment was treated by red blood cell break solution for 3-5 min. lymphocytes were harvested and washed twice with PBS. Final single cell suspensions ($1\sim5\times10^7$ cells ml^{-1}) were prepared in RPMI 1640 medium supplemented with L-glutamine (2 mM), penicillin (100 units ml^{-1}), streptomycin (100 μg ml^{-1}), 10% fetal bovine serum.

2.3 Determination of Resistance to Lipid Peroxides Induced by UV

Referred to Duh PD [9] with some modification, the principle of the method is the spectrophotometric measurement of the color generated by the reaction of thiobarbituric acid with liposome liquid system. The mixed solution system, with 1ml of 10 mg ml^{-1} lecithin (dissolved in 10 mM pH7.4 PBS) and 1ml different concentrations of G, was UVC-irradiated with the dose intension of 120 μW cm^{-2} for 30 min after 30 min of placement at 37℃. Then 2 ml TCA－TBA－HCl mixed

solution (15%TCA, 0.4%TBA, 2%HCl) was added into the solution, and boiled for 15 min. After cooling in ice water, the tubes were centrifuged at 1000 g for 10 min,the absorbance of the supernatant was measured at 535 nm using a spectrophotometer (Shimadzu UV-2100, Japan). Liposome was replaced by ddH_2O as the blank reference. Index of resistance (IR) was indicated resistant ability to lipid peroxides and expressed as follows:

$$IR = (OD_n - OD_s) / OD_n \times 100\%$$

Where OD_n was the absorbance of control (the sample solution was replaced by ddH_2O). OD_s was the absorbance of the sample reaction solution.

2.4 Determination of Resistance to Protein Peroxides Induced by UV

According to Lenz [10] with a little modification, reaction solution, with 1ml 24 mg ml^{-1} BSA (Bovine Serum Albumin) (dissolved in 20 mM pH 7.4 PBS) and 200 μl of different concentration of G, was UVC-irradiated with the dose intension of 120 μW cm^{-2} for 30 min after 30 min of placement at 37℃. Then1ml 20 mM 2,4-dinitrophenylhydrazine (dissolved in 2 M HCl) and 1ml cooling trichloroacetic acid (TDA) (20%) was added into the mixed system . It was centrifuged at 3000 g for 10min after oscillation. The sediment was washed with 2 ml ethanol－ethyl acetate (1:1,V/V) for twice and then dissolved in 5 ml guanidine hydrochloride (6 M, pH 6.5). The absorbance of the protein solution was measured using a spectrophotometer (Shimadzu UV-2100, Japan) at 370 nm. BSA was replaced by ddH_2O as the blank reference. Index of resistance (IR) was indicated resistant ability to protein peroxides and expressed as follows:

$$IR = (OD_n - OD_s) / OD_n \times 100\%$$

Where OD_n was the absorbance of control (the sample solution was replaced by ddH_2O). OD_s was the absorbance of the sample reaction solution.

2.5 UVB Irradiation Procedures

Spleen cell suspensions without G or with different concentrations of G were plated in 96-well microtiter plates, and incubated at 37℃ in a humidified incubator with 5% CO_2 for 30 min, and then was UVC-irradiated with the dose intension of 120 μW cm^{-2} for 40 s. Cell samples were collected for next MTT assay and comet assay.

2.6 MTT Assay

Referred to Fiona M. Young [11] with some modification, MTT assay was carried out in 96-well round-bottom plate. MTT was dissolved in PBS (10 mM, pH 7.4) with 5 mg ml^{-1} final concentration. 100 μl of cell suspension and 20 μl MTT was added into each well, and then incubated for 4 h. After incubated with DMSO for 1 h, the absorbance of each well was determined by using an automatic plate reader (Model 550 with Microplate Manager Software; Biorad) with a 570 nm test wavelength and a reference wavelength of 655 nm.

2.7 SCGE Assay

According to relative research method [12], slides were cleansed in ethanol and double-distilled water and dried. About 100 μl of 1% normal agarose prepared in double-distilled water was layered on each slide, covered with a cover-slip and put at 4℃ for solidification. The same dose of cells were collected and mixed with 1% low melting agarose at 37℃ in a ratio 1:1. From this mixture, 100 μl were laid on top of the first gel and covered with a cover-slip as before. Once the upper layer solidified, the cover-slips were gently removed and slides were carefully immersed in prepared cold lysis solution (2.5 mM NaCl, 100 mM Na_2EDTA, 10 mM Tris, add 1% Triton X-100, 10% DMSO, 1% N-Lauroyl Sarcosine Sodium before use) for 1h at 4℃ in dark place. After Slides were removed from the lysis solution, immerse them in an electrophoresis buffer (0.3 M NaOH, 1 mM Na_2EDTA, pH 13) for 20 min to unwind DNA, and then carried out electrophoresis at 20 V, 200 mA for 20 min. After electrophoresis, the slides were washed twice with neutralization buffer (0.4 M Tris, pH 7.5) and stained with 50 μl of 200 μg ml^{-1} EB solution for 2 min. Slides gel were washed twice with double-distilled water. Examination of slides was viewed under a fluorescence microscope (Olympas) equipped with a 365 nm excitation filter and 435 nm barrier filter at 200×magnification and imaged with a networking digital camera (Computer Optics, Germany).

2.8 Statistical Analysis

Statistical analysis of data was carried out by the Statistical Analyses System software package (SPSS 11.0).

3 Results

3.1 Resistant to Lipid Peroxides Induced by UV

G showed the resistance to lipid peroxides induced by UV (Fig. 1). With the increase of G concentration from 15.26 μM to 125 mM, the anti-radiation effect was more obvious, and this relationship is nonlinear. Moreover, the effect of G is not better than VC (a recognized antioxidant), but the difference between them is not significant.

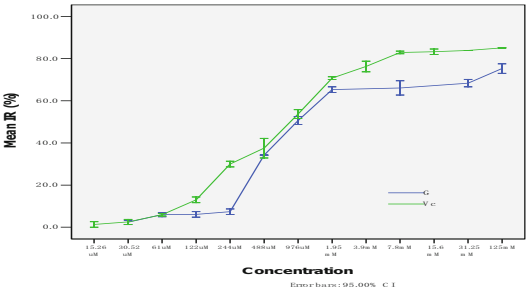

Fig. 1. Resistant effect of different concentrations of G to lipid peroxides induced by UV

3.2 Resistant to Protein Peroxides Induced by UV

G showed the resistance to protein peroxides induced by UV (Fig. 2). With the increase of G concentration from 325 μM to 83 mM, the anti-radiation effect was more obvious, and this relationship is nonlinear as lipid anti-peroxides. Moreover, the effect of G is better than VC (a recognized antioxidant), and the difference between them is significant, which expressed as a potential antioxidant for further application.

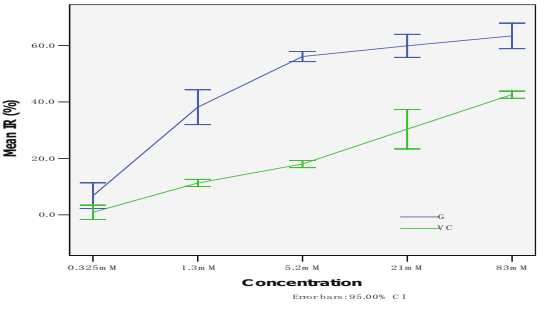

Fig. 2. Resistant effect of different concentrations of G to protein peroxides induced by UV

3.3 Resistant to Killing of Spleen Lymphocytes Induced by UV Radiation

We assessed the resistant effect as follows:

$$IR=(OD_{G\text{-}treated}-OD_{irradiated})/(OD_{non\text{-}irradiated}-OD_{irradiated})\times 100\%$$

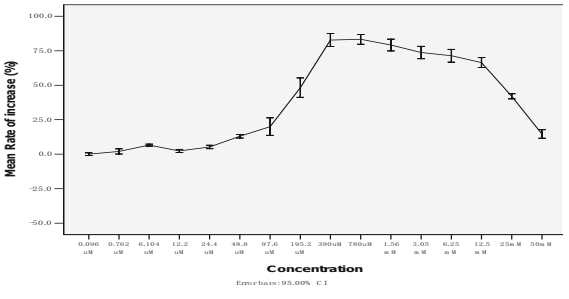

Fig. 3. Resistant effects of different concentrations of G to killing of spleen lymphocytes induced by UV

UV-radiation induced the killing of spleen lymphocytes, and the number of active cells reduced remarkably (Fig. 3). The addition of G in culture medium can reduce the killing at 0.096 μM～600 μM. With the increase of G concentration, the anti-killing effect was stronger and there is a nice dose-effect relationship. But when more than 800 uM, G showed accelerated killing rather than anti-killing effect. However, protective effect against UV radiation could not recover lymphocytes to normal degree.

3.4 Comet Assay/Single Cell Gel Electrophoresis (SCGE)

Based above experimental results, we chose 4 concentrations of G to treat cell suspensions (6.104 μM, 390 μM, 3.05 mM and 50 mM). After incubated for 90 min, the cell samples were taken for comet assay. Results were showed as follows:

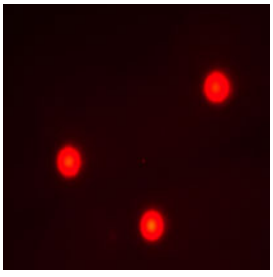

non-radiated

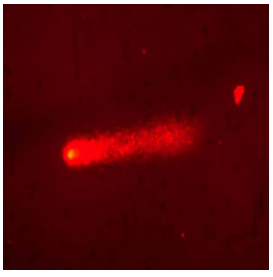

UVC-radiated

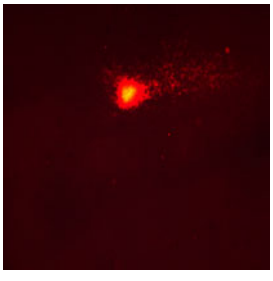

UVC-irradiated plus G (6.104 μM)

UVC-irradiated plus G (390 μM)

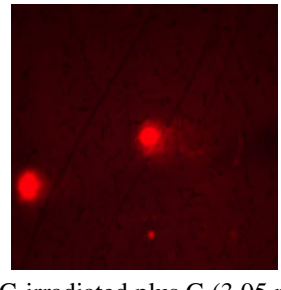

UVC-irradiated plus G (3.05 mM)

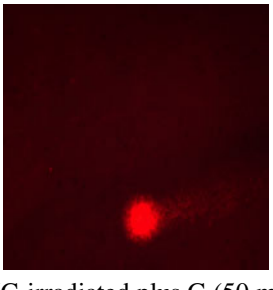

UVC-irradiated plus G (50 mM)

Fig. 4. Protective effects of 4 different concentrations of G to DNA damage induced by UVC

From Fig. 4, UVC radiation induced DNA damage in lymphocytes with large comet tail length compared with non-irradiated group. The spleen lymphocytes in culture medium with addition of G showed less effusion of DNA compared with UVC-irradiated group, which indicated that G can improve the DNA damage induced by UVC radiation. When 390 μM of G was added in culture medium, the degree of DNA damage is the lowest. When more than 390 μM of G was added, DNA damage began to aggravate, which illustrated high concentration of G had some certain

cytotoxicity to lymphocytes. This protective effect of G on DNA damage changed with concentration was consistent with the result in MTT assay.

4 Discussion

With the aggravation of environmental pollution in recent years, more and more researchers are interested in UV radiation. Number of studies using UVC radiation (254 nm) has been conducted to demonstrate the effect of UV on DNA [13], since UVC is close to the maximum absorption spectrum of DNA to initiate photochemical reactions. UV exposure can lead to oxidation of proteins and membrane lipids, which are considered to be important initial steps with respect to photoaging and photocarcinogenesis [14]. People begin to investigate active components to anti-UV radiation for protecting DNA damage. N. Rajendra Prasad reported the protective effect of ferulic acid (FA; 3-methoxy-4-hydroxycinnamic acid), a dietary antioxidant, on UV-B–induced oxidative stress and lipid peroxidation using normal human lymphocytes [15]. Treatment of human lymphocytes with FA before 30 min of irradiation inhibited UV-B–induced lipid peroxidation. Ferulic acid also inhibited UV-B–induced depletion of antioxidant defense components, such as GSH peroxidase, catalase, superoxide dismutase, and GSH. The addition of the combination dAdo dGuo dThd or addition of the combination dAdo dThd to culture medium of human lymphocytes can efficiently reduces the yield of transient DNA breaks during a repair period of 3h after the UVC irradiation [1]. When WEHT and lymphocytes were irradiated by UV-C and then incubated for 35 min, the DNA damage decreased with an increase of the concentration of WEHT since WEHT contains high amounts of flavonoids and phenoic compounds [16].

Detection of DNA damage and repair has often been studies in bulk experiments. In these techniques, single cell techniques haves gained interest since the individuality of a cell within a population could be considered [17,18]. Here, we have investigated the degree of DNA damage and repairment using the comet assay. In different treated spleen lymphocytes, the damage or repairment was reflected as an increase in comet tail lengths. Single cell gel electrophoresis (SCGE) or comet assay is a highly sensitive and rapid method to investigate the response of single cells to DNA damaging agents. Its use has increased significantly in the past few years [19,20]. Most of the reports using the single cell gel assay as a method for determining DNA damage have been designed for cell studies in vitro. SCGE has been applied to investigate UV radiation induced DNA strand breaks and KNA repair mostly in lymphocytes from peripheral blood. Army Tuck determined the different response to UVC irradiation between healthy and CLL cells by comet analysis [21]. Claudia Bock detected the cold repair of UVA damages in human lymphoblast cell by comet assay [22]. Maarit H. Myllyperkio studied the kinetics of UVC irradiation-induced DNA single-strand breaks (SSBs) generated during the excision repair of damaged DNA using the alkaline comet assay [23]. Nagarajan Rajendra Prasad examined the photoprotective effect of caffeic acid in the UVB irradiated human blood lymphocytes by comet assay [15].

Some reports has testified a significant increase of DNA migration was seen as soon as 20 min after UV exposure, reaching the peak within 80～90 min [3].

Afterwards, a rapid decline was observed, approaching the basal level at 180～240 min [12]. In this study, we detected the DNA damage at 1.5 h after UV radiation.

The major macromolecular in cell include lipid, protein and DNA. We assess anti-radiation effect of G with these matters. From the results, G could resist UV-induced damage with possible reason that G had an absorption maximum at 200 and 279.5 nm which is the absorption spectrum of UVC. Therefore, the G may have a filtering effect on UVC irradiation and may inhibit DNA damage in spleen lymphocytes induced by UVC irradiation. The potent inhibition of G on UV-induced oxidative DNA damage suggested that G has potential role in the chemoprevention of photooxidation. By intaking UV, G protected protein and DNA against damage induced by more UV energy.

5 Conclusion

G has protective effect on lipid peroxidation and protein peroxidation induced by UVC irradiation in vitro. And G also can reduce DNA damage and death induced by UVC irradiation in mouse spleen lymphocytes.

Acknowledgments. We acknowledge technical support by Bioengineering Lab of Harbin Institute of Technology (HIT). Thanks are also given to Prof. Wang for his valuable suggestions.

References

1. Holmberg, M.: The effect of deoxynucleosides on repair of DNA breaks in UVC-irradiated human lymphocytes. Mutation Research 218, 33–39 (1989)
2. Ichihashi, M., Ueda, M., Budiyanto, A., et al.: UV-induced skin damage. Toxicology 189, 21–39 (2003)
3. Henriksen, E.K., Moan, J., Kaalhus, O., et al.: Induction and repair of, DNA damage in UV-irradiated human lymphocytes. Spectral differences and repair kinetics. Journal of Photochemistry and Photobiology B: Biology 32, 39–48 (1996)
4. Squires, S., Johnson, R.T.: Kinetic analysis of UV-induced incision discriminates between fibroblastes from different xeroderma pigmentosum complementation groups, XPA heterozygotes and normal individuals. Mutat. Res. 193, 181–192 (1988)
5. Collins: Estimates of the rate of ligation during excision repair of ultraviolet-damaged DNA inmammalian cells. Biochim. Biophys. Acta 908, 103–106 (1987)
6. Fang, W.L., Wei, L.G., Ping, D.Q.: Effect of exogenous nucleotides on repair of damaged DNA in mouse thymocytes. J. Fourth Mil. Med. Univ. 28(7), 613–615 (2007)
7. Chen, X.-G., Ang, R.-S., Deng, M.-X., et al.: Effects of Exogenous Nucleotides on the Proliferation and Migration of Intestinal Epithelial Cells. Journal of Sichuan University of Science and Technology Supplementary issue, 81–85 (2003)
8. Liu, Y., Song, Y., Yan, T.-H., et al.: Effects of mixed nucleotide on acute Hepatic injury and immunoregulation in mice. Journal of China Pharmaceutical University 32(6), 444–447 (2001)
9. Duh, P.D., Du, P.C., Yen, G.C.: Action of methanolic extract of mung bean hulls as inhibitors of lipid peroxidatio and non-lipid oxidative damage. Food Chem. Toxicol. 37(11), 1055–1061 (1999)

10. Lenz, A.G., Costabel, U., Shaltiel, S., et al.: Determination of carbonyl groups in oxidatively modified proteins by reduction with tritiated sodium borohydride. Anal. Biochem. 177(2), 419–425 (1989)
11. Young, F.M.: Modification of MTT assay conditions to examine the cytotoxic effects of amitraz on the human lymphoblastoid cell line, WIL2NS. Toxicology in Vitro 19, 1051–1059 (2005)
12. Cipollini, M., He, J., Rossi, P., et al.: Can individual repair kinetics of UVC-induced DNA damage in human lymphocytes be assessed through the comet assay? Mutation Research 601, 150–161 (2006)
13. Mitchell, D.L., Jen, J., Cleaver, J.E.: Relative induction of cyclobutane dimmers and cytosine photohydrates in DNA irradiated in vitro and in vivo with ultraviolet-C and ultraviolet-B light. Photochem. Photobiol. 54, 741–746 (1991)
14. Muller, L., Kasper, P., Kersten, B., et al.: Photochemical genotoxicity and photochemical carcinogenesis: two sides of a coin? Toxicol. Lett. 102, 383–387 (1998)
15. Rajendra Prasad, N., Ramachandran, S., Pugalendi, K.V., et al.: Ferulic acid inhibits UV-B–nduced oxidative stress in human lymphocytes. Nutrition Research 27, 559–564 (2007)
16. Yen, G.C., Hung, Y.L., Hsieh, C.L.: Protective effect of extracts of Mesona rocumbens Hemsl. on DNA damage in human lymphocytes exposed to hydrogen peroxide and UV irradiation. Food and Chemical Toxicology 38, 747–754 (2000)
17. Ostling, Johanson, K.J.: Microelectrophoretic study of radiation-induced DNA damages in individual mammalian cells. Biochem. Biophys. Res. 123(1), 291–298 (1984)
18. Singh, N.P., Banner, D.B., Tice, R.R., et al.: Abundant alkali-sensitive sites in DNA of human and mouse sperm. Exp. Cell Res. 184, 461–470 (1989)
19. Singh, N.P., McCoy, T., Tice, R.R., et al.: A simple technique for quantitation of low levels of DNA damage in individual cells. Exp. Cell Res. 175, 184–191 (1988)
20. Olive, P.L., Wlodek, D., Durand, R.E., et al.: Factors influencing DNA migration from individual cells subjected to gel electrophoresis. Exp. Cell Res. 198, 259–267 (1992)
21. Tuck, A., Smith, S., Larcom, L.: Chromic lymphocytic leukemia lymphocytes lack the capacity to repair UVC-induced lesions. Mutation Research 459, 73–80 (2000)
22. Bock, C., Dittmar, H., Gemeinhardt, H., et al.: Comet assay detects cold repair of UV-A damages in a human B-lymphoblast cell line. Mutation Research 408, 111–120 (1998)
23. Myllyperkio, M.H., Koski, T.R.A., Vilpo, L.M., et al.: Kinetics of excision repair of UV-induced DNA damage, measured using the comet assay. Mutation Research 448, 1–9 (2000)

SOC Content and Its Spatial Distribution Characteristics in Urban Forest Ecosystems of Changsha in China

Xiao Ying and Liu Sihua

Department of Tourism Central South University of Forest &Technology
Changsha, Hunan Province, China
{seaskyxiao,sihual}@sina.com

Abstract. Biomass and soil organic carbon (SOC) contents in urban forest (Pinups masoning Lamb, Cinnamomum camphor Persil, Cunninghame lancelets Hook, Liquidambar Formosans Hance) in Changsha were estimated. The results were as follows: there were significant differences in the biomass between conifer forest and broadleaf forest. Significant differences in SOC content were found between conifer forest and broadleaf forest. The depth is from 0 to 60cm. Most of the SOC of four forest ecosystems was in the upper 15cm of soil profile.

Keywords: Forest ecosystem, Biomass, Soil organic carbon.

1 Introduction

There are around 1400-1500 Gt carbon stored in the soil stated by the form of organic is the terrestrial vegetation carbon pools (500-600 Gt) 2-3 times is the global atmospheric carbon pool (750 Gt) 2 times more [1] . Every year the soil respiration released CO^2 into the atmosphere is more than 10 times CO^2 which released from fossil fuel combustion [2].As the huge storage capacity of the soil organic carbon storage even if the soil carbon storage and soil respiration occurring small changes can significantly affect the concentration of CO^2 in the atmosphere, thereby affecting composition, structure and function of the distribution of terrestrial ecosystems. Forest ecosystems as the main body of the terrestrial biosphere, not only in itself to maintain a large number of carbon pool (about global vegetation carbon pools 86% or more), but also to maintain a huge database of soil carbon (about the world's soil carbon pool to 73%) [3]. And thus the carbon balance of forest ecosystems in the global carbon cycle is extremely important components and plays an irreplaceable role in the global carbon balance. With the forest ecosystem carbon storage reflects the capacity of the ecosystem carbon retention, due to under the different ecological conditions, the different factors of control of soil organic carbon(SOC) cycle, that led to soil organic carbon has a high spatial variability, so accurate estimates the global soil carbon pool is more difficult to overcome of difficulties of the regional studies for the regional differences resulted by precise estimates of the global soil carbon pool amount and improve the collection of regional estimates obtained , through the world's soil organic carbon storage estimates are useful exploration [4].

SOC and its vertical distribution have become an ecologist concern. Jobbágy and Jackson [5] use three global soil database obtain the relationship during the soil organic carbon content, climate and the texture, and verify the hypothesis that the type

E. Zhu and S. Sambath (Eds.): Information Tech. and Agricultural Eng., AISC 134,, pp. 95–106.
springerlink.com © Springer-Verlag Berlin Heidelberg 2012

of vegetation vertical distribution of soil organic carbon is controlling factor. The results showed that with the increase in soil depth, SOC content between climate, gradually weakened, but not with the relationship between the texture gradually increase; scrub, grassland and forest 0~20 cm soil organic carbon, respectively accounted for 33% , 42% and 50% of the total , of which the distribution of organic carbon in the deepest was bush, followed by grassland, forest was most shallow.

Up to now, the domestic scholars in the vegetation carbon pool [6~9] and the soil carbon pool [10~13] have done a lot of work, but for the study of the vertical distribution of soil organic carbon [14~15] was very little. Changsha is rich in forest resources, an accurate estimate of the size of its SOC content, to understand their carbon content of the vertical distribution of the carbon cycle of forest research has important scientific significance. In this paper, finishing biomass and the measured SOC data, four kinds of forest ecosystem researched in Changsha. Discussed the differences between SOC and their vertical distribution characteristics of four forest types(*Cunninghame lancelets Hook, Pinups masoning Lamb, Cinnamomum camphor and Liquidambar Formosans Hance*).

2 Materials and Methods

2.1 Study Area Overview

Test in the southern suburbs of Changsha City, located in the Hunan National Forest Park. That is, longitude 113 ° 01 '~ 113 ° 02', north latitude 28 ° 06 '~ 28 ° 07', the core area of about 4356 hm2, elevation 46 ~ 114 m, gradient of 5~ 25 ℃ Local annual average temperature of 17.2 ℃, January coldest, an average of 4.7℃, extreme minimum temperature of 11.3℃; July hottest, with an average temperature of 29.4℃, extreme maximum temperature of 40.6℃; frost-free period is 270 ~ 300d, sunshine for several years were 1677.1h; plenty of rainfall, the annual average rainfall is 1422mm. belongs to the typical subtropical humid monsoon climate. Whose formation is mainly of Quaternary alluvial Pleistocene reticulate red clay and gravel, is a typical red soil hilly area, the park niche are many over 2200 kinds of plant species, vegetation, secondary forest dominated by hand.

From the beginning of December 2006, in Forest Tianjilin National horizon choose the same or similar age of *Cunninghamia lanceolata Hook, Pinus massoniana Lamb, Cinnamomum camphora* and *Liquidambar formosana Hance* 4 types forest communities for the study, in January 2007 to investigate four kinds of forest communities in the basic situation is shown in Table 1.Four kinds of main components of forest communities are as follows: fir community dominated *Cunninghamia lanceolata*, *Sassafeas tsumu Hemsl* undergrowth vegetation, *Symplocos caudata Wall. Ex A. DC.*, *Clerodendron cyrtophyllum Turcz* and *Cinnamomum camphora,* herbaceous plants have *Nephrolepis auriculata Trimen, Lophantherum. gracile Brengn* and *Phytolacca. acinosa Roxb.; Liquidambar communities* dominated by *Liquidambar formosana, Schima superba Gardn . Et Champ., Castanopsis sclerophylla Schott, Symplocos caudata Wall. ex A. DC., Clerodendron cyrtophyllum Turcz* and *Cinnamomum camphora,* herbaceous plants there are *Miscanthus floridulus Warb*, *Lophantherum. gracile Brengn and Phytolacca. acinosa Roxb; Pinus massoniana* community to *Pinus massoniana*

Table 1. Description of 4 types of forest communities

Forest type	Year (a)	Number per hm2(plant)	DBH (cm)	Tree Height (m)	High of ranch (m)	Crown density
Cunninghamia lanceolata	18	1102	16.26	12.47	5.26	0.8
Liquidambar formosana	21	1146	12.46	12.83	5.27	0.9
Pinus massoniana	33	690	18.65	13.57	7.83	0.7
Cinnamomum camphora	31	775	17.47	12.6	4.0	0.7

mainly. Undergrowth vegetation are *Cinnamomum camphora, Clerodendron cyrtophyllum Turcz, Symplocos caudata Wall. ex A. DC.*and *Cyclobalanopsis glauca Oerst.;* herbs have *Miscanthus floridulus Warb, Nephrolepis auriculata Trimen, Lophantherum. gracile Brengn* and *Phytolacca. acinosa Roxb*; *Cinnamomum camphora community-based Cinnamomum camphora, Quercus fabri Hance, Paulowwnia tomaentosa Steud, Castanopsis sclerophylla Schott*, *Symplocos caudata Wall. Ex A. DC, Aphananthe aspera Planch* and *Cudrania tricuspidata Bur*., herbaceous plants a *Lophantherum. gracile Brengn, Oxalis. comiculata L.*, *Paederia scandens Merr.* and *Phytolacca. acinosa Roxb*.

2.2 Data Processing

Biomass

For different forest types of biomass sources of data, mainly based on the collection and collation of Fang Jing-yun, the study of forest biomass and productivity in the study conducted by Hunan Provincial Forest Resources Monitoring Center, as well as the forest resource inventory data in the various forest types of area, growing stock etc. to estimate the underlying data. Pairs of different types of information and data collected and analyzed, to obtain major forest types of biomass.

Soil organic carbon content and carbon density measurement

In January 2008, since the TianJiLing National Forest Park (*Cunninghamia lanceolata, Cinnamomum camphora.Liquidam barformosana and Pinus massoniana*) our kinds of forest communities, each choose three fixed radius 15 m circular plots, a total of 12, during each plot the separated by 100 m or more. Surveys occur within each sample plot species and their height, cover, and recorded its diameter at breast height and so on. Selected in each plot 5~6 points, each point of digging a soil profile,

using hierarchical ring knife (0~15,15~30,30~45,45~60 cm) collected for the determination of bulk density of the soil samples collected at the same time layered organic carbon in soil samples for analysis.

The soil under conditions of 105 ℃ drying samples to constant weight, and to determine bulk density and in which> 2 mm of the gravel content; for the determination of organic carbon concentrations of air-dried soil samples, cross to the sample after the pick of them > 2 mm of the gravel, and make it all passed the 2 mm soil sieve, and then pick one of the root system to the last ball mill Retsch S100 used crushed, and make it all passed the 100 mesh soil sieve. External heating oxidation method using potassium dichromate measured the concentration of soil organic matter [16].

Soil organic carbon density refers to per unit area a certain depth of soil in the storage of SOC, soil carbon density has become the evaluation and measurement for soil organic carbon storage in an extremely important indicator. Taking into account the soil organic carbon density changes with depth in the vertical (Jobbágy & Jackson, 2000), using a layered approach calculated for each section of the organic carbon content (kg cm^{-2}). First, the calculation of the organic carbon density of each layer ($g \cdot cm^{-3}$) (Equation 1), in this based on the organic carbon content and depth of a function and calculate the cross-section of the organic carbon content (type 2).

$$SOCDi = 0.58 \times \rho i \times Mi \times (1\text{-}Ci) / 10 \quad (1)$$

Type in 0.58 for Bemmelen factor (the concentration of the organic matter into organic carbon concentration), ρi said that the first i-layer soil bulk density ($g \cdot cm^{-3}$), Mi said the organic matter content (%), Ci said the> 2 mm of the gravel content (%), SOCDi for the first i-layer soil organic carbon density ($g \cdot cm^{-3}$).

$$SOCC=\sum_{i=1}^{n} 0.58\times T_i\times \rho_i\times M_i\times(1\text{-}C_i)/10 \quad (2)$$

Where, for the section layer, 0.58 for Bemmelen factor (organic matter content will be converted to organic carbon content), Ti said that the first i-layer soil thickness (cm), ρi that soil bulk density ($g \cdot m^{-3}$), Mi said organic matter content (%); Ci said> 2mm gravel content (%), SOCC soil organic carbon content ($kg \cdot m^{-2}$) [17]

Vertical distribution of soil organic carbon

The establishment of soil carbon content and function of the depth for the projected carbon content of soil at different depths. In order to quantify soil organic carbon in the vertical distribution of the soil profile is divided into 0~15cm,15~30cm,30~45cm,45~60cm 4 level, and calculated separately for each level of soil organic carbon. Meanwhile, the use of 0~15cm of soil organic carbon, respectively of their total (60cm) to represent the roots than the composition and vertical distribution of soil organic carbon, that is, a proportion of 0~15cm higher, meaning that the more shallow distribution of soil organic carbon ; the other hand deeper. Analysis software and mapping tools were used SPSS14.0 and Excel2003.

3 Results and Analysis

3.1 Different Types of Soil Organic Carbon Content of Forest

On the four kinds of forest ecosystems， we measured biomass, SOC content (0~60cm), fine root biomass and determination of the amount of litter (see Table 2). As can be seen from Table 2, the amount of litter returned to: *Pinus massoniana* > *Cinnamomum camphora* > *Liquidambar formosana* > *Cunninghamia lanceolata,* the difference between significance level reached the 1%. Four kinds of biomass during the forest communities was Liquidambar *formosana* > *Cinnamomum camphora* > *Cunninghamia lanceolata* > *Pinus massoniana* , *Liquidambar formosana* 36.52 (3.753) t/hm^2, *Cinnamomum camphora*16.28 (16.28) t/hm^2, *Cunninghamia lanceolata* 84.35 (4.43) t/hm^2, and *Pinus massoniana* 127.27 (6.234) t/hm^2, During the different forest ecosystems, a significant difference in tree biomass, the biomass of Liquidambar formosana more than *Pinus massoniana* reached 7.8 times. Four kinds of forest ecosystems, the average biomass was 66.105t/hm2, was lower than the national average of forest biomass (82.68t/hm^2) [18] the calculation of Fang Jin-yun. The reason of this article only related to the biomass of tree layer biomass, and Fang Jin-yun, a calculation of the average biomass of the national forest including the ground biomass and below-ground biomass,; second, article was concerned only with four kinds of biomass of forest tree layer, on average, There are some differences between the levels with the national average. Combination of measured data, Liquidambar formosana and *Cinnamomum camphora* ecosystems show a high level of soil organic carbon, while *Cinnamomum camphora* and *Cinnamomum camphora* have shown a lower soil organic carbon levels, which can intuitively be seen from Table 2. *Liquidambar formosana* (36.6t·hm^2) > *Cinnamomum camphora* (27.56 t /hm^2)> *Pinus massoniana* (18.05t/hm^2)> *Cunninghamia lanceolata* (14. 73 t/hm^2), the largest *Liquidambar formosana* and the smallest *Cunninghamia lanceolata* the difference reached 2.48 times, while the *Pinus massoniana* and *Cinnamomum camphora* in soil organic carbon content there are also significant differences. Fine root biomass (0~30cm) with the highest was *Liquidambar formosana*, *Liquidambar formosana* (120.89g/m) > *Pinus massoniana*(109.63g/m) > *Cunninghamia lanceolata*(76.99g/m) > *Cinnamomum camphora*(37.19g / m).

In order to explain the different types of forest soil organic carbon content of the spatial variation, we have been carried out correlation analysis by soil organic carbon content and soil moisture, fine root biomass,C/N and PH value. Found that there were no positively correlated between soc content and soil moisture, fine root biomass, C/N and PH value. However, Figure 2 shows the soil moisture could explain *Pinus massoniana* forest ecosystems, soil organic carbon content of 59% of variation, fitting equation: $y = 14.215-0.766x$, $R^2 = 0.586$, $p = 0.004$. This means that water conditions may have contributed to spatial differences of SOC content of *Pinus massoniana* forest ecosystems. Soil moisture content can only be explained, however, *Cinnamomum camphora* and *Cunninghamia lanceolata*, forest ecosystems, soil organic carbon content variation of 30% and 32%, and Liquidambar soil carbon content of 34%, indicating that moisture conditions are not the decisive factor for *Liquidambar formosana, Cinnamomum camphora and Cunninghamia lanceolata* communities in SOC content. May be related to topography, tree species itself, or other factors.

Table 2. Biomass, SOC content, fine root biomass, total litter, PH value and C/N for soil under different forests

Item	*Cunninghamia lanceolata*	*Cinnamomum camphora*	*Pinus massoniana*	*Liquidambar formosana*
Biomass(t/hm2)	36.52 (3.74)	84.35 (4.43)	16.28 (1.43)	127.27 (6.23)
SOC(t/hm2)	14.73 (6.77)	27.56 (6.31)	18.05 (10.159)	36.6 (15.38)
Fine root biomass (g/m)	76.99 (10.25)	37.19 (7.14)	109.63 (15.38)	120.89 (14.76)
Total litter (g/m2)	575.1 (51.5)	1003.4 (20.9)	1157.5 (145.1)	931.5 (104.8)
PH value	3.55 (0.091)	3.85 (0.179)	3.7 (0.151)	3.67 (0.092)
C/N	11.83 (1.491)	12.57 (1.24)	12.76 (1.521)	12.82 (1.132)

3.2 Under Different Forest Types of the Vertical Distribution of Soil Organic Carbon

Of soil organic carbon content is not only an important parameter for the statistics of soil organic carbon storage, but also reflects an important indicator of soil properties [19]. Figure 2 shows the four kinds of forest types (*Cunninghamia lanceolata, Pinus massoniana, Cinnamomum camphora, Liquidambar formosana*) of the ratio of vertical distribution of soil organic carbon. As can be seen, Changsha urban forest ecosystem in 0~60cm of soil organic carbon content in surface layer (0~15cm) allocated the largest proportion, with the decline in soil depth, soil organic carbon content is gradually reduced, for 0~15cm 33% , 15~30cm26%, 30~45cm23% and 45~60cm18%. Note that 0 ~15cm was the SOC of Changsha forest ecosystems in the main distribution area.

We have made an correlation analysis for four kinds of forest ecosystems in the vertical distribution of carbon storage (Figure 3), we found four kinds of forest ecosystem carbon content in 0 ~ 60cm with depth increases, the relevance of *Cunninghamia lanceolata* and *Pinus massonianaare* was more significant, *Cunninghamia lanceolata* fitting equation: y=6.891-0.936x,R2=0.877,P=0.018;Pinus massoniana are fitting equation: y=8.101-0.831x, R2=0.691,P=0.049. *Liquidambar formosana* and *Cinnamomum camphora* ecosystems, soil carbon content in the vertical distribution of the performance of the correlation is not obvious. *Liquidambar formosan*a fitting equation: R^2= 0.005,P=0.057; *Cinnamomum camphora* fitting equation: R^2 = 0. 489,p=0.012;

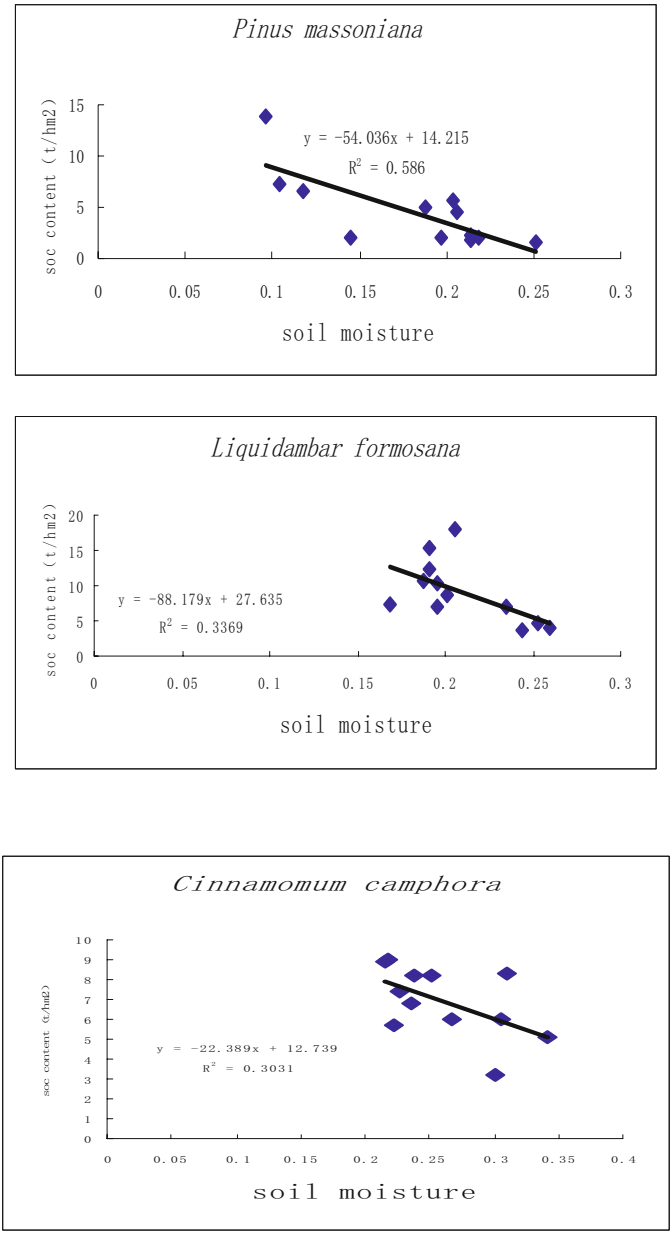

Fig. 1. Relation between soil organic content and soil moisture

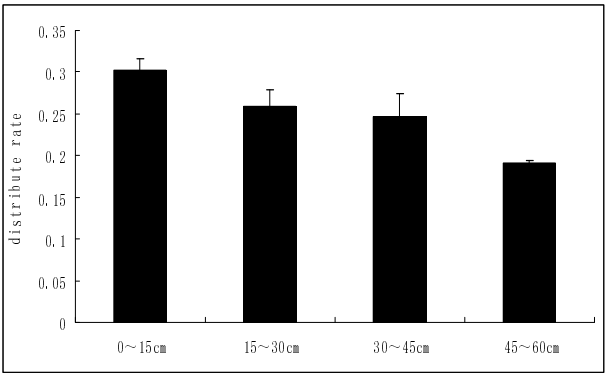

Fig. 2. Vertical distribution of forest ecosystems

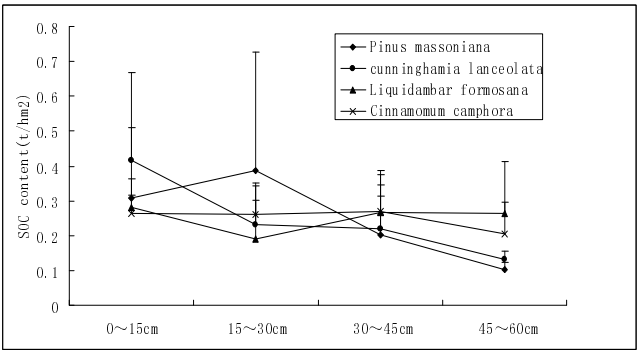

Fig. 3. SOC content of different forest ecosystems in vertical

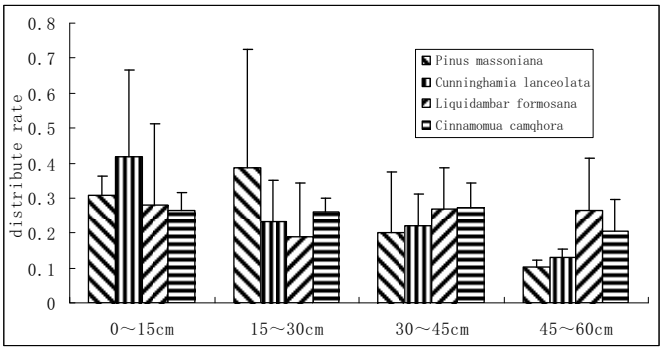

Fig. 4. Vertical distribute rate of SOC content with different forest ecosystems

Figure 4 provide the four kinds of forest ecosystems in the levels of the distribution ratio , from Figure 4 can be seen, four kinds of forest ecosystems in the vertical structure of the carbon content of a certain difference in the ratio, 0 ~ 15cm of soil carbon content in the allocation of ratio as follows: *Cunninghamia lanceolata* (42%)> *Liquidambar formosana* (37%)> *Pinus massoniana* (31%) >*Cinnamomum camphora* (26%); 15 ~ 30cm of soil carbon content in the distribution of the largest percentage was *Cinnamomum camphora*, respectively, as follows: *Pinus massoniana* (39%)>*Cinnamomum camphora*(26%) *Cunninghamia lanceolata* (23%) > *Liquidambar formosana*(20%); 30 ~ 45cm of soil in the *Pinus massoniana* soil carbon content at least, for *Cinnamomum camphora* (27%) > *Cunninghamia lanceolata* (22%) > *Liquidambar formosan*a(21%)>*Pinus massoniana* (20%); 45 ~ 60cm soil, *Liquidambar formosana* distribution of soil carbon content in the largest proportion, 22% of *Liquidambar formosana*, *Pinus massoniana* 10%, *Cinnamomum camphora* 21% and *Cunninghamia lanceolat*a 13%. In the Coefficient of variation, the *Cinnamomum camphora* was most stable at 0.029, followed by *Liquidambar formosan* for the 0.078, *Pinus massoniana* and *Cunninghamia lanceolata* have shown greater variability, respectively, 0.124 and 0.12. *Liquidambar formosan* soil carbon content in the soil profiles showed surface soil organic carbon content and lower carbon content of the significant difference may be related to *Liquidambar formosan* ecosystem litter decomposition and plant root death. *Pinus massoniana* 0~15cm of soil carbon content was significantly lower than 15 ~ 30cm of soil carbon content, indicating pine forest ecosystems in the surface litter was not a major source of soil organic carbon, while the death of roots and soil could lead to 15 ~ 30cm of soil organic main reason for the increase of carbon.

4 Discussion and Conclusion

4.1 The Distribution Characteristics of Soil Organic Carbon Content and Its Affecting Factors

Soil is a non-uniform three-dimensional structure presents a complex mosaic in space. And with the climate terrestrial vegetation and biology occur a complex interaction, so that the density has great room for SOC. Soil organic carbon comes mainly from animals, plants, microorganisms and their remnants excreta, secretions, some decomposition products, and soil humus. In a particular ecosystem forest plants developed root systems, the impact on the soil depth was far more than other land types, and protect the integrity of forest litter, there is no human damage, the soil in the animals, micro-organisms types and quantities was rich, SOC is the equilibrium value that these organic sources of carbon in the process of decomposition and the formation of the dynamic.

In this study, SOC content in forest ecosystems of Changsha, fluctuations in the 14 ~ 37t/hm^2 between soil organic carbon content increased with soil depth decreases, which is consistent with previous findings. [20 ~ 21] Wang Xiao-ke and other forest vegetation in China reported an average carbon content of 38.4 ~ 49.45 t/hm^2 [22], between the four forest types in this study, soil organic carbon content in an overall average of 24.23t/hm^2 (9.88), and Wang Xiao-ke, etc. reported a larger difference between the range of variation, and LI Ke-rang, WANG Shao-qiang and other

reported changes in the range of soil organic carbon (10.03 ~ 21.27kg/m2) [10,12,13,20] between the There is also a big gap. Throughout the current study reported that SOC density and its variation is very great. The main reason for this variation has two sides, namely the soil carbon storage by vegetation type, climate (temperature and precipitation), parent rock, soil physical and chemical biological properties (soil structure, texture, temperature) and so the combined effect. Differences in these factors will inevitably affect the soil carbon formation and decomposition process. [23]

Second, the research methods of non-uniform leading to soil carbon pool estimate uncertainty. Comes mainly from differences in research methods, soil classification, sampling the quantity and quality, profile analysis, soil parameter estimation, soil thickness estimates, the researchers used different sources of information, soil survey data measured the number and so on. [24] Therefore, using a large number of measured data, a unified methodology is to reduce the uncertainties in the carbon balance of an extremely important step. Hunan, four kinds of average carbon density of the forest (25.31t/hm^2) and China compared with some studies estimate there is a big gap, especially the low estimate of conifers, which are many reasons for this, also shows how to strengthen stand management and rational ecological planning and improvement of stand structure, mainly in the future of Hunan Province to improve carbon storage in forest ecosystems have a great significance to the potential of space.

4.2 Under Different Vegetation Types of Soil Carbon Content of Urban Forests

Vegetation and soil are closely related, plants not only absorb from the soil of its growth and development of the essential nutrition, and its own organic residues is an important source of soil organic matter. In Changsha, the four major types of vegetation of forest soil organic carbon content in the distribution shown in Table 2, different vegetation, soil organic carbon content in the order as follows: *Liquidambar formosana>Pinus massoniana >Cinnamomum camphora>Cunninghamia lanceolata.* 0 ~ 60cm of soil organic carbon content in a larger concentration range of 14 ~ 35t/hm2 between how different vegetation types on soil organic carbon contribution is different. Xu Qiu-fang et al [25] studies have shown that soil organic carbon content of evergreen broad-leaved forest and above the *Cunninghamia lanceolata* and *Liquidambar formosana* forest. The results of this study also show that Liquidambar formosana and *Cinnamomum camphora* tree forest soil organic carbon content was significantly higher than the *Cunninghamia lanceolata* and *Pinus massoniana* forest. However, In Changsha, *Cunninghamia lanceolata* and *Pinus massoniana* are the most important forest types, planting area accounts for an absolute advantage, makes the final total amount of biomass and carbon storage of *Cunninghamia lanceolata* and *Pinus massoniana* forest on to become the most important forest Changsha carbon storage systems.

The sources of different forest ecosystems, organic carbon (surface litter and root exudates and fine root turnover generated by debris) in the quantity and quality differences are affecting soil organic carbon in the soil and the distribution of one of the key factors. Different vegetation composition of the soil surface can form a specific climate, affecting litter decomposition rates, and thus to some extent control the decomposition rate of soil organic carbon. [26] These are caused by forest

ecosystems in the same ecosystem and between the various layers within the possible reasons for differences between the SOC. [27] In this study, The surface soil organic carbon pool of soil organic carbon pools in Changsha accounted for 33%. In recent years, soil organic carbon pool in China conducted by statistical research [28], indicating that soil organic carbon pool in China was 50Pg, where the surface soil organic carbon pool was 20Pg, surface soil organic carbon pools accounted for 40%. The surface ratio of soil organic carbon pool in Changsha closed to the national average.

References

1. Schlesinger, W.H.: Evidence from chronosequence studies for a low carbon-storage potential of soil. Nature 348, 232–234 (1990)
2. Raich, J.W., Potter, C.S.: Global patterns of carbon dioxide emissions from soils. Global Biochemical Cycles 9, 23–26 (1995)
3. Post, W.M., Emanuel, W.R.: Soil carbon pools and world life zones. Nature 289, 156–159 (1982)
4. Bemoux, M., Conceicao Santana Carvalho, M., Volkoff, B., et al.: Braizil's soil carbon stock. Soil Sci. Soc. Am. J. 66, 888–896 (2002)
5. JobbÀgy, E.G., Jackson, R.B.: The vertical distribution of soil organic carbon and its relation to climate and vegetation. Ecological Applications 10, 423–436 (2000)
6. Piao, S.L., Fang, J.Y., He, J.S., Xiao, Y.: Spatial distribution of grassland biomass in China. Acta Phytoecologica Sinica 28, 491–498 (2004) (in Chinese)
7. Zhou, G.S., Wang, Y.H., Jiang, Y.L., Yang, Z.Y.: Estimating biomass and net primary production from forest inventory data—a case study of Chinese Larix forests. Forest Ecology and Management 169, 149–157 (2002) (in Chinese)
8. Luo, T.X., Li, W.H., Zhu, H.Z.: Estimated biomass and productivity of natural vegetation on the Tibetan Plateau. Ecological Applications 12, 980–997 (2002) (in Chinese)
9. [9] Fang, J.Y., Chen, A.P., Peng, C.H., Zhao, S.Q.: Changes in forest biomass carbon density in China between 1949 and 1998. Science 292, 2320–2322 (2001) (in Chinese)
10. Li, K.R., Wang, S.Q., Cao, M.K.: Vegetation and soil carbon density in China. Science in China, Series D 33, 72–80 (2003) (in Chinese)
11. Wang, S.Q., Liu, J.Y., Yu, G.R.: Error analysis of estimating terrestrial soil organic carbon density in China. Chinese Journal of Applied Ecology 14, 797–802 (2003) (in Chinese)
12. Wang, S.Q., Zhou, C.H.: Estimating soil carbon reservoir of terrestrial ecosystem in China. Geographical Research 18, 349–356 (1999) (in Chinese)
13. Wang, S.Q., Zhou, C.H., Li, K.R., Zhu, S.L.: Analysis on spatial distribution characteristics of soil organic carbon reservoir in China. Acta Geographica Sinica 55, 533–544 (2000) (in Chinese)
14. Anwar, M., Yang, Y.H., Guo, Z.D., Fang, J.Y.: Carbon contents and its vertical distribution in Alpine grasslands in Bayinbulak, middle stretch of the Tianshan moutains of Xinjiang. Acta Phytoecologica Sinica 30(4), 545–552 (2006) (in Chinese)
15. Wang, S.Q., Huang, M., Shao, X.M., Mickler, R.A., Li, K.R.: Vertical distribution of soil organic carbon in China. Environmental Management 33(Suppl.) (2004) (in Chinese), doi:2004,10.1007/s00267-003-9130-5
16. Bao, S.D., Jiang, R.F., Yang, C.G.: Soil and Agricultural Chemistry Analysis. China Agriculture Pres (2001) (in Chinese)

17. Wu, H.B., Guo, Z.T., Peng, C.H.: Distribution Storage of soil organic carbon in China. Global Biogeochemical Cycles 17 (2001) (in Chinese), doi:10.1029/2001GB110844
18. Fang, J.Y., Liu, G.H., Xu, S.L.: Soil carbon pool in China and its global significance. Journal of Environmental Sciences 8, 249–254 (1996)
19. Jin, F., Yang, H., Cai, Z.C.: Calculation of density and reserve of organic carbon in soils. Acta Pedologica Sinica 8, 522–528 (2001) (in Chinese)
20. Wang, S.Q., Zhou, C.H., Liu, J.Y.: Simulation analysis of terrestial carbon cycle balance model in Northeast China. Acta Geographica Sinica 56(4), 390–400 (2001) (in Chinese)
21. Li, Z., Sun, B., Lin, X.X.: Density of soil organic carbon and the factors controlling its turnover in east China. Scientia Geographica Sinica 21(4), 301–307 (2001) (in Chinese)
22. Wang, X.K., Feng, Z.W., Ouyang, Z.Y.: Vegetation carbon storage and density of forest ecosystems in China. Chinese Journal of Allpied Ecology 12(1), 13–16 (2001) (in Chinese)
23. Harden, J.W., Fries, T.L., Huntington, T.G.: Mississippi basin carbon project-uplands oil database for site sinYazoobasin. Northwestern Mississippi, U.S. Geological Survey (1999)
24. Rozhkov, V.A., Betal, W.V.: Soil carbon estimates and soil carbon map for Russia. II ASA Workpaper, 1–44, WR96-60 (1996)
25. Xu, Q.F., Jiang, P.K.: Study on active organic carbon of soils under different types of vegetation. Journal of Soil and Water Conservation 18(6), 84–87 (2004) (in Chinese)
26. Zhou, L., Li, B.G., Zhou, G.S.: Advances in controlling factors of soil organic carbon. Advances in Earth Science 20(1), 99–105 (2005) (in Chinese)
27. Lavado, R.S., Sierra, J.O., Hashimoto, P.N.: Impact of grazing on soil nutrients in a Pampean grassland. Journal of Range Management 49(5), 452–457 (1996)
28. Pan, G.X., Li, L.Q., Wu, L.S.: Storage and sequestration potential of topsoil organic carbon in China's paddy soils. Global Change Biology 10, 79–92 (2003) (in Chinese)

Components from Callus Cultures of *Sonchus Oleraceus* L. and Their Cytotoxicity In Vitro

Ming Zhao, Yunpeng Zhao, Fenglan Xing, and Liming Bai

College of Chemistry and Chemical Engineering, Qiqihar University,
Qiqihar 161006, P.R. China
qqhrzhaoming@163.com, bailiming7@hotmail.com

Abstract. A stable and fast-growing callus culture of *Sonchus oleraceus* L. was established. Two known triterpenes were isolated from Callus Cultures of *Sonchus oleraceus* cultivated on a modified MS medium with 2.0 mg/L NNA. The compounds were identified by analyses of the spectroscopic data the compounds were identified to be the combinations of betulinic acid (1) and oleanolic acid (2). Cytotoxic activations of 1 and 2 were evaluated against three cell lines, WI-38, VA-13 and HepG2. Compound 1 showed strong activity.

Keywords: Callus cultures, Triterpenes, Cytotoxicity in Vitro.

1 Introduction

Sonchus oleraceus L. (Compositae), known as Nogeshi, is a biennial plant that grows in various places in Japan and China. This plant is called Kucai in China and is a traditional Chinese medicine (TCM) used for the treatment of bronchitis, pneumonia, pharyngitis, dysentery, and poisonous indigestion based on its antifebrile, antidota [1], and anglesic effects [2]. Studies on this plant and other species of this genus revealed the presence of triterpenes and sesquiterpene lactones such as guaianolides, eudesmanolides, germacranolides, and their glycosides [3-5]. To date, many studies showed that some triterpenes and sesquiterpene lactones in this plant and other species of this genus exhibit significant biological activities such as anticancer and anti-inflammatory activity [6, 7]. These substances have been extracted from pure natural plants. However, the approach in these studies involves large-scale crop cultivation which is difficult to culture and lead to either a long cultivation period or a low metabolite yield. However, plant cell culture provides an alternative approach which is controllable and under reproducible conditions, independent of geographical and climatic factors. From an engineering perspective, we have great interest to the process of producing these substances using the approach which is involved with plant cell cultures of this plant. In this paper, we investigated the effects of culture conditions on the secondary metabolites and production of useful natural products in the callus culture of *Sonchus oleraceus* L. In the following sections, the structure of two triterpenes and their inhibitory activity in Vitro are elucidated, which was isolated from the above mentioned callus culture.

E. Zhu and S. Sambath (Eds.): Information Tech. and Agricultural Eng., AISC 134, pp. 107–112.
springerlink.com © Springer-Verlag Berlin Heidelberg 2012

2 Materials and Methods

2.1 General Experimental Procedures

Melting points were determined with a Yanagimoto micro-melting point apparatus and are uncorrected. Optical rotations were measured using a Horiba SEPA-200 polarimeter. IR spectra were recorded in $CHCl_3$ on a Hitachi 270-30 spectrometer. UV spectra were performed with JASCO V-500 UV/vis spectrophotometer. 1H NMR (499.87MHz) and ^{13}C NMR (125.70 MHz) spectra were recorded on a Varian UNITY-PS 500 spectrometer. HREIMS spectra were obtained using a JEOL JMS HX-110 spectrometer. Normal phase (taking the mixtures of ethyl acetate and hexane as the eluents) semi-preparative HPLC were performed on a Hitachi L-6200 HPLC instrument with an Inertsil Prep-sil stainless steel column (250 mm x 10 mm i.d.) and a YRU-883 RI/UV bi-detector; the flow rate for HPLC was 5 mL/min, unless otherwise stated. Silica gel (230-300 mesh) was employed for column chromatography, analytical TLC plates (silica gel 60 F_{254}, Merck) were visualized at UV_{254}.

2.2 Plant Material

The young stems of *Sonchus oleraceus* L were collected from the campus of Niigata University, in March 2003 and used as explants for CR-B in the experiments. The plant was identified by Dr. K.Yonekura, Department of Biology, Faculty of Science, Tohoku University, Sendai, Japan. The stems were stripped of needles, washed with distilled H_2O, immersed for 3 min in 70% EtOH, and surface sterilized by immersion in saturated calcium hypochlorite solution for 15 min. After sterilization, the stems were rinsed three times with sterile distilled water and aseptically dissected into explants 5-8 mm in length.

2.3 Induction and Culture Conditions

MS medium supplemented with 30 g/L sucrose was used with either 2.0 mg/L NNA for CR-A or 5.0 mg/L NNA for CR-B (all medium components were purchased from Wako Pure Chemicals, Co., Ltd., Osaka, Japan). After the PH of the medium was adjusted to 5.8 with 0.1 M sodium hydroxide, 9 g/L agar was added. The medium were autoclaved at 120 ℃ for 15 min [8]. The explants were placed on the solidified nutrient media and incubated in darkness at 25 ℃ for 29 days. Then the initiated calluses (CR-A and CR-B) were sub-cultured continuously every 30 days under the same conditions (MS medium, 30 g sucrose, NAA 2.0 mg/mL). The callus lines of CR-A and CR-B were continuously sub-cultured 12 times and 11 times, respectively. During this period, we compared the color degree and growing rate of CR-A and CR-B from fourth to ninth subcultures.

2.4 Isolation of Production of Secondary Metabolite

The calluses of the eighth and ninth cultures of CR-A were used for the experiment, the production of secondary metabolite. The fresh callus that harvested for analysis

was filtered. The wet solid callus (1776.05 g) was obtained. The former was freeze-dried and gave 114.3 g of dry callus. Then the dry callus was extracted with hexane (4×2000 mL), EtOH (4×2000 mL), and methanol (4×2000 mL), successively and 825.2 mg of the EtOH extract was obtained after the supernatant was filtered and evaporated. The EtOH extract was separated into five fractions (F1-F5) by flash column chromatography using a gradient elution from hexane-EtOH (9:1) to MeOH. F3 (148.0 mg) was further separated into four fractions (F3-1-F3-4) by flash column chromatography using a gradient elution from hexane-EtOH (7:3) to MeOH. F3-2 (80.2 mg) was separated by normal-phase HPLC [hexane-EtOH (7:3), flow rate 9 mL/min] to afforded a mixture (56.4 mg), which was purified using normal-phase HPLC [hexane-EtOH (93:7)] to afforded compound 1 (14.6 mg) and compound 2 (30.1 mg).

3 Results and Discussion

3.1 The Comparison of Growth Rate and Color Degree of Callus Cultures

The growth rate and color degree of CR-A and CR-B were compared from fourth culture to ninth culture (Fig. 1 and Fig. 2).

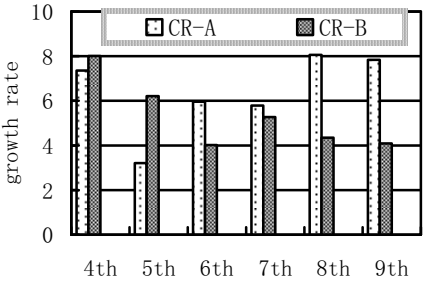

Fig. 1. Growth rate of each callus cultures

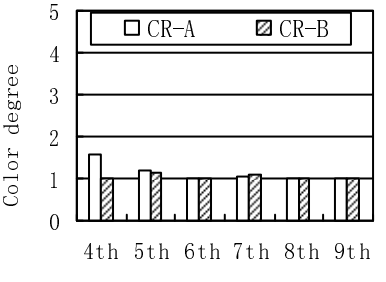

Fig. 2. Color degree of each callus cultures

The relationship between the color degree of callus and their growth rate was examined in the fifth culture (Fig. 3).

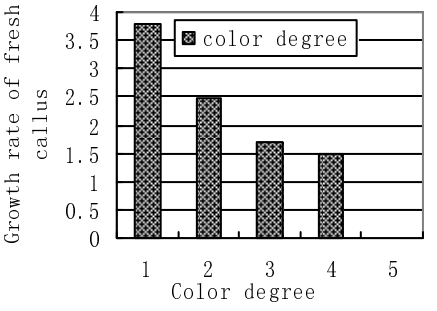

Fig. 3. Effect of Color degree on callus growth

The growth rate of the callus with lower color degree is larger than that of the callus with higher color degree. The growth rate of the callus with color degree 1 is 2.5 times faster than that of the callus with color degree 4. The effective production by callus culture is expected in the calluses of color degree. Generally, the callus cultures with good growth conditions were selected for continuous subculture. That means the callus with color degree (the color of callus cultures was evaluated in five degree: 1 colorless to 5 dark brown) < 3 and growth rate (the growth rate of callus cultures was calculated by the formula: growth rate = final weight of fresh callus/initial weight of fresh callus in a period of subculture) > 2 had the ability to grow continuously through subculture.

3.2 Identification and Compounds

By analysis of the products of the callus cultures with good growth conditions, two known compounds, 1 and 2, were isolated. Base on its chemical and physical data, the structures of the compounds were identified. Betulinic acid (1) Colorless needles ($CHC1_3$-MeOH); mp 275–278°C. IR (KBr) ν_{max} 3450, 3075, 2942, 2896, 1689, 1452, 1388; EI-MS m/z: 456 [M^+]. ^{1}H-NMR (500 MHz, $CDCl_3$) δ 0.93 (3H, s, H-23), 0.73 (3H, s, H-24), 0.86 (3H, s, H-25), 0.92 (3H, s, H-26), 0.97 (3H, s, H-27), 1.71 (3H, s, H-30), 3.01 (1H, ddd, J=11.1, 11.1, 5.4 Hz, H-19), 3.15 (1H, dd, J=10.1, 4.7 Hz, H-3).^{13}C-NMR (125 MHz, $CDCl_3$) δ 38.6 (C-1, t), 27.4 (C-1, t), 77.8 (C-3, d), 38.9 (C-4, s), 55.3 (C-5, d), 18.2 (C-6, t), 34.4 (C-7, t), 40.7 (C-8, s), 50.4 (C-9, d), 37.1 (C-10, s), 20.8 (C-11, t), 25.6 (C-12, t), 38.5 (C-13, d), 42.6 (C-14, s), 30.1(C-15, t), 32.3 (C-16, t), 56.3 (C-17, s), 47.1 (C-18, d), 49.2(C-19, d), 150.5 (C-20, s), 29.7 (C-21, t), 37.1 (C-22, t), 28.2 (C-23, q), 15.4 (C-24, q), 16.1 (C-25, q), 16.2 (C-26, q), 14.5 (C-27, q), 178.5 (C-28, s), 19.3 (C-29, q), 109.7 (C-30, t). These MS, IR and NMR spectral data were identical with those of betulinic acid [9].

Oleanolc acid (2) White amorphous powder; mp 287-289°C. IR (KBr) ν_{max} 3422, 3075, 2943, 2896, 1696, 1463, 1387; EI-MS m/z: 456[M^+]. $[a]_D^{20}$=+80.5°(c 0.59, CHCl3). ^{1}H-NMR (500 MHz, $CDCl_3$) δ 0.77 (3H, s, H-23), 0.91 (3H, s, H-24), 1.00

(3H, s, H-25), 0.75 (3H, s, H-26), 1.13 (3H, s, H-27), 0.91 (3H, s, H-29), 0.96 (3H, s, H-30), 2.91 (1H, dd, J=4.1, 4.1 Hz, H-18), 3.19 (1H, dd, J=10.2, 5.3 Hz, H-3), 5.19 (1H, m, H-12). ^{13}C-NMR (125 MHz, $CDCl_3$) δ 38.4 (C-1, t), 27.2 (C-1, t), 77.8 (C-3, d), 38.9 (C-4, s), 38.4 (C-4, s), 54.7 (C-5, d), 18.0 (C-6, t), 31.9 (C-7, t), 38.9 (C-8, s), 47.3(C-9, d), 36.5 (C-10, s), 23.1 (C-11, t), 121.6 (C-12, d), 143.1 (C-13, s), 41.2 (C-14, s), 28.1 (C-15, t), 22.7 (C-16, t), 46.5 (C-17, s), 40.8 (C-18, d), 45.1 (C-19, t), 30.1 (C-20, s), 33.4(C-21, t), 32.7(C-22, t), 30.3 (C-23, q), 16.8 (C-24, q), 15.2 (C-25, q), 17.9 (C-26, q), 26.6 (C-27, q), 182.1 (C-28, s), 32.2 (C-29, q), 23.1 (C-30, q). These MS, IR and NMR spectral data were identical with those of Oleanolc acid [10, 11].

3.3 Cytotoxicity Assays

Cytotoxic activities of compounds 1 and 2 were evaluated against three cell lines, WI-38, VA-13, and HepG2 cells (Table 1). Experimental details were described in previous papers [12, 13].

Compound **1** showed significant cell growth inhibitory activity against the normal cell model, WI-38 cells. As well, it also showed moderate cell growth inhibitory activity against the malignant lung tumor model, VA-13 cells. Compound 2 showed weak cell growth inhibitory activities against VA-13 cells. Furthermore, Compounds **1** showed moderate cell growth inhibitory activities to human liver cancer model, HepG2.

Table 1. Cell growth inhibitory activities of compounds against wi-38, va-13, and hepg2 cells

	IC_{50} (M)[a]		
compound	WI-38	VA-13	HepG2
1	1.3	11.6	21
2	14.5	123	165
taxol	0.04	0.005	8.1
ADM[b]	0.70	0.40	1.3

[a] IC_{50} represents the mean of duplicate determination.

[b] adriamycin.

Finally, the compounds with a lupane skeleton such as **1** showed stronger activity than the corresponding oleanane (**2**), which possesses the same functional groups at the corresponding positions.

Acknowledgment. This work was supported by the Overseas Scholars Foundation of Heilongjiang Province Education Department, China (No. 1153h23).

References

1. Jiangsu New Medical College. Dictionary of Chinese Herbal Drugs, p. 1286. Shanghai Science and Technology Press, Shanghai (1986)
2. Feng, X.-Z., Xu, S.-X., Yao, J.-P., Sha, Y., Li, W.: Studies on chemical constituents of Ixeris soncjifolia. Chinese Traditional and Herbal Drugs 32(2), 97–99 (2002)

3. Yang, X.-W., Zou, L., Wu, Q., Fu, D.-X.: Studies on chemical constituents from whole plants of crossostephium Chinese. China Journal of Chinese Materia Medica 33(8), 905–908 (2008)
4. Zhang, S., Wang, J., Deng, Q., Ando, M.: New triterpenes from siyekucai (Ixeris chinenseis). Chinese Chemical Letter 17(2), 195–197 (2006)
5. Zhang, S., Wang, J., Ando, M.: Three new guaianolides from siyekucai (Ixeris chinenseis). Journal of Natural Products 65(12), 1927–1929 (2002)
6. Fu, L., Zhang, S., Li, N., Wang, J., Zhao, M., Ando, M.: Three new triterpenes from nerium oleander and biological activity of the isolated compounds. Journal of Natural Products 68(1), 198–206 (2005)
7. Zhang, S., Zhao, M., Bai, L., Hasegawa, T., Ando, M.: Bioactive guaianolides from siyekucai (Ixeris chinensis). Journal of Natural Products 69(10), 1425–1428 (2006)
8. Bai, J., et al.: Taxoids and abietanes from callus cultures of taxus cuspidate. Journal of Natural Products 68, 497–501 (2005)
9. Siddiqui, S., et al.: A new pentacyclic triterpene from the leaves of Nerium oleander. Journal of Natural Products 51, 229–233 (1988)
10. Yu, Z.-B., Wu, X., Ye, Y.-H., Zhou, Y.-W.: Chemical Constituents of Glechoma longituba. Nat. Prod. Res. Dev. 20, 262–264 (2008)
11. Zhang, Q.-G., et al.: Studies on the chemical constituents of Ampelopsis humuliflia var, heterophylla (Thunb.) K. Koch. Journal of TCM 26, 636–637 (2003)
12. Wu, J., et al.: Bioactive tetrahydrofuran lignans from peperomia dindygulensis. Journal of Natural Products 68, 1656–1660 (2005)
13. Li, N., et al.: Bioactive dibenzoylbutyrolactone and dibenzoylbutanediol lignanes from peperomia duclouxi. Journal of Natural Products 69, 234–239 (2006)

Protoplast Formation and Regeneration of *Rhodococcus* sp. BX2

Liping Feng[1], Chunyan Li[1,*], Chunhong Xu[1], Minghua Xiong[1], Junbo Pan[1], and Xiaosong Cheng[2]

[1] Department College of Resource & Environment Northeast Agricultural University Harbin 150030, China
[2] College of First Clinical Medicine, Harbin Medical University, Harbin 150030, China
chunyanli@neau.edu.cn, xiaosongcheng0911@163.com

Abstract. In order to construct a multi-functional genetic strain which could both degrade bensulfuron-meghyl and butachlor efficiently by protoplast fusion of *Rhodococcus* sp. BX2 and *Acinetobacter* sp. LYC-1, conditions for protoplast formation and cell wall regeneration of *Rhodococcus* sp. BX2 were investigated. Protoplasts from *Rhodococcus* sp. BX2 were obtained by treatment with the combination of 0.5% glycine preprocessing culture solution at 35℃for 6 h and 6 mg·mL^{-1} lysozyme incubating bacterial suspension at 35℃ for 3 h. Consequently protoplast formation rate was up to 91%. The best medium for protoplast regeneration was RNB containing 1.5% polyvinylpyrrolidone; the regeneration rate of protoplasts was 14.83 %.

Keywords: Rhodococcus sp. BX2, protoplast, formation, regeneration.

1 Introduction

Bensulfuron-methyl and butachlor are both super-effective herbicide, which were widely used to control weed in paddy field. However, they have given rise to much public concern about their residues and harmful effects, along with extensive and long term application in paddy field. Degrading residuale Bensulfuron-methyl and butachlor by microorganism has been a research hotspot in recent years [1-7]. *Rhodococcus* sp. BX2 capable of degrading Bensulfuron-methyl efficiently and *Acinetobacter* sp. LYC-1 capable of degrading butachlor efficiently were screened in our lab and we attempt to construct a multi-functional genetic strain with protoplast fusion of *Rhodococcus* sp. BX2 and *Acinetobacter* sp. LYC-1, which may degrade Bensulfuron-methyl and butachlor. The information regarding the construction of multi-functional genetic strain by protoplast fusion capable of degrading Bensulfuron-methyl and butachlor hasn't been presented.

Since the 80s of 20th century, protoplast fusion technology has been widely used for industrial microbial breeding as an important means [8,9,10]. Recent reports have described the use of protoplast fusion to breed an efficient-degrading strain for methamidophos, DDVP and parathion with native bacterium GH-1 and white rot

* Corresponding author. Professor.

E. Zhu and S. Sambath (Eds.): Information Tech. and Agricultural Eng., AISC 134, pp. 113–120.
springerlink.com © Springer-Verlag Berlin Heidelberg 2012

fungi [11] and to construct fusant Xhhh for pharmaceutical wastewater treatment with fungus P. *Chrysosporium*, yeast S. *Cerevisiae* and native bacterium *Bacillus* sp. [12]. The key factors in the use of this technique are protoplast formation and cell wall regeneration. As a Gram-positive bacteria, cell wall digestion of *Rhodococcus* sp. BX2 was insufficient. Therefore, in order to construct an multi-functional genetic strain of *Rhodococcus* sp. BX2 and *Acinetobacter* sp. LYC-1 successfully by protoplast fusion, the detailed conditions of protoplast formation and cell wall regeneration of *Rhodococcus* sp. BX2 were studied in this paper.

2 Materials and Methods

2.1 Bacterial Strain

A gram-positive bacteria *Rhodococcus* sp. BX2 capable of degrading bensulfuron-meghyl efficiently was used in this study. It was isolated and purified from the sewage sludge samples collected from the activated sludge tank of a bensulfuron-meghyl plant by classical enrichment techniques.

2.2 Medium

LBSG medium ($g \cdot L^{-1}$): beef extract 3, peptone 10, glycine 5, NaCl 5, pH 7.2.

NB medium ($g \cdot L^{-1}$): beef extract 5, pepone 10, yeast extract 5, glucose 2, NaCl 5, agar 18, pH 7.2.

RNB medium was used with NB medium supplementing 0.5 moL sucrose, 0.02 moL $MgCl_2 \cdot 6H_2O$, and 1.5% polyvinylpyrrolidone(PVP-30). Semisolid RNB reduced agar to 0.6%.

R_2YE medium ($g \cdot L^{-1}$): sucrose 103, glucose10, peptone 4, yeast extract powder 4, tryptone 2, casein hydrolysate 1, K_2SO_4 0.25, $MgCl_2 \cdot 6H_2O$ 10.12, agar 18, pH 7.2.

HNM medium ($g \cdot L^{-1}$): beef extract 1.5, peptone 5, sucrose 200, NaCl 5.0, $MgSO_4 \cdot 7H_2O$ 0.2, K_2HPO_4 1.0, KH_2PO_4 1.0, NH_4NO_3 1.0, $FeCl_3$ 0.5, agar 18, pH 7.2.

SMM hypertonic buffer containing 0.5 moL sucrose, 0.02 moL $MgCl_2 \cdot 6H_2O$, 0.02 moL maleic, pH 7.2.

All medium used were sealed and autoclaved at 121℃ for 30 min.

Lysozyme was dissolved with SMM and sterilized by filtration.

2.3 Determination of Rhodococcus sp. BX2 Growth Curve

Rhodococcus sp. BX2 were grown in 250 ml triangular flasks containing 100 ml of bacterium culture solution with 0.5% glycine. Cultures were incubated at 35℃ , 165 $r \cdot min^{-1}$ on a rotary shaker and were detected every 2 h by ultraviolet spectrophotometer, OD_{600} read of which were used as the indicator for *Rhodococcus* sp.BX2 growth.

2.4 Protoplast Formation of Rhodococcus sp. BX2

Protoplast formation were performed as previously described for strains of *Rhodococcus erythropolis* by Z.Etemadifar[13] and M.E.Vogt singe[14], with some

substantial modifications. The cells were grown to mid-exponential phase in 100 ml bacterium culture solution containing 0.5% glycine, collected by centrifugation, washed two times with distilled water, suspended in SMM buffer, adjusted to OD_{600}=1.5. Then lysozyme dissolved in SMM was added to a final concentration of 6 $mg \cdot mL^{-1}$. After 3 h with gentle shaking at 35°C, samples with gram stain was inspected under a microscope, and main protoplast suspensions were centrifuged and usually suspended in 3 ml SMM. The rate of protoplast production was determined by dividing the number of protoplasts formed by the initial cell number [15, 16].

$$\text{Formation rate } (\%) = (A - B)/A \times 100\ \%$$

A——the initial cell number appeared on the NB solid medium that bacterium without lysozyme were serially diluted in the sterile water.

B——the cell number appeared on the NB solid medium that protoplast suspensions were serially diluted in the sterile water.

C——the cell number appeared on the regeneration medium that protoplast suspensions were serially diluted in the SMM buffer.

In order to obtain the optimum conditions, glycine concentration of 0, 0.1%, 0.3%, 0.5%, 0.7% and 0.9% were tested, respectively. Tests to determine the effect of lysozyme concentration were first examined at four levels:2,4,6,8 $mg \cdot mL^{-1}$. These were followed by tests of 4 different time levels from 1 to 4 h and 6 different temperature levels: 25, 28,32,35,37,40℃.

2.5 Protoplast Regeneration of Rhodococcus sp. BX2(Double Layers Culture Method)

The protoplasts suspensions were serially diluted in the SMM buffer to a final concentration of 10^{-5}, 10^{-6}. A 100 μL volume of the suspension was transferred to coagulated regeneration medium plates, followed by pouring semisolid regeneration medium which was premelted and maintained in a 45°C water bath and immediately being mixed. After cold at room temperature, the protoplast-containing medium plates were incubated at 35°C for 2 to 3 days. The rate of regeneration was estimated by dividing the number of colonies that protoplast regenerated by the number of protoplasts formed.

$$\text{Regeneration rate } (\%) = (C - B)/(A - B) \times 100\ \%$$

3 Results and Discussion

3.1 The Choice of Cell Age

The growth curve of strain *Rhodococcus* sp. BX2 accorded with the classical "S" curve as shown in Fig.1. Growth curve proved that the time of mid-exponential phase of *Rhodococcus* sp. BX2 was about 14--18 h. The age of the bacteria is an important factor in protoplasts release. Generally, lesser age cells had the bad resistance to environmental factors and regeneration of its protoplast is difficult, while larger age cells went against releasing protoplast. Only in mid-exponential phase, peptidoglycan in the cell wall was the lowest, the cells were most sensitive to lysozyme and were used for releasing protoplast efficiently [17]. Therefore, the cells at 16 h were chose as sample of preparing protoplast.

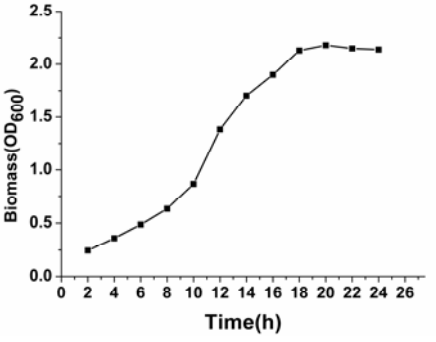

Fig. 1. Growth curve of *Rhodococcus* sp. BX2

3.2 Effects of Glycine Concentration on Protoplast Formation and Regeneration of Strain Rhodococcus sp. BX2

Protoplast formation and regeneration of strain *Rhodococcus* sp.BX2 were remarkably effected by different glycine concentrations as shown in Table 1. Since *Rhodococcus* sp.BX2 is a Gram-positive bacteria, cell wall digestion was insufficient when the cells were treated with lysozyme alone. Therefore, in initial-exponential phase experiments, glycine was added to cultures for pretreatment at 35℃ for 6 h. It has been reported by several authors that the addition of amino acids, DL-threonine or glycine to the culture media makes the cells lysis more sensitive [18,19]. The results indicated that the formation and regeneration of protoplast were both maximum when glycine concentration was 0.5%.

Table 1. The effects of glycine concentration on protoplast formation and regeneration

glycine%(g·mL^{-1})	Formation rate rate	Regeneration rate
0	0.59	0.083
0.1	0.64	0.091
0.3	0.72	0.122
0.5	0.85	0.134
0.7	0.61	0.117
0.9	0.55	0.079

3.3 Effects of Lysozyme on Protoplast Formation and Regeneration of Strain Rhodococcus sp. BX2

1) Effects of lysozyme concentration on protoplast formation and regeneration
Lysozyme dissolved in SMM was added to a final concentration of 2 to 8 mg·mL^{-1}, and the cells were checked periodically for the formation of protoplasts by measuring the level of expansion of the lysozyme concentration, through observing the aggregation of protoplasts under an optical microscope. The results showed that increasing the concentration of lysozyme may improve the protoplasting as shown in Fig.2. At low lysozyme concentrations, the protoplasts formation and regeneration

rate were both minimum; Whereas at high concentrations, the bacteria lysed yielding large numbers of protoplasts, but they bursted and resulted in the low regeneration rate. Therefore, among the concentrations of lysozyme tested, 6 mg·mL^{-1} was optimal for the formation and regeneration of protoplast. Although, this lysozyme concentration was much larger than that of other bacteria(0.5-2.0 mg·mL^{-1})[20,21,22], and that of *Rhodococcus* sp. (more than 5 mg·mL^{-1})used by Z.Etemadifar [13] and M.E.Vogt singe [14].

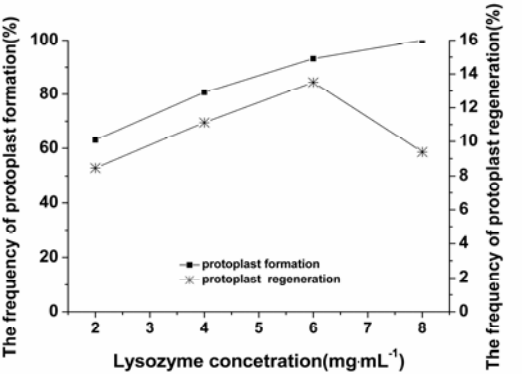

Fig. 2. Effects of lysozyme concentration on protoplast formulation and regeneration of *Rhodococcus* sp. BX2

2) Effects of enzymolysis time on the protoplast formation and regeneration

The duration of enzymolysis time on *Rhodococcus* sp.BX2 for the formation and regeneration of protoplasts was optimized. It was determined when the percentage of protoplasts was approximately 60-70%. The results (Fig.3) indicated that the optimal enzymolysis time was 3 h. Along with increasing enzymolysis time, protoplast formation of *Rhodococcus* sp. BX2 was increased gradually but regeneration gradually decreased among 1, 2, 3 and 4 h.

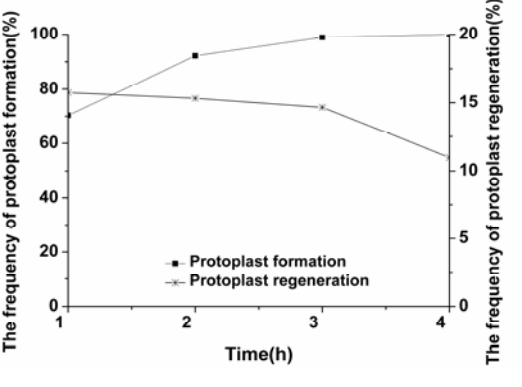

Fig. 3. Effects of enzymolysis time on protoplast formulation and regeneration of *Rhodococcus* sp. BX2

3) Effects of enzymolysis temperature on the protoplast formation and regeneration
According to the principle of enzyme reaction kinetics, the enzymatic reaction speeds were affected directly by enzymolysis temperature. At the conditions of 25, 30, 35, 37 and 40°C for 3 h, protoplasts formation and regeneration were compared. Along with increasing enzymolysis temperature, protoplast formation and regeneration of *Rhodococcus* sp. BX2 were first increased and then decreased. Therefore, the optimal enzymolysis temperature was 35°C, formation and regeneration rate were up to 92% and 15.14%, respectively. Although protoplast release was faster at 37°C than 35°C, bursting of protoplasts occurred during later state of incubation at 37 °C but not at 35 °C.

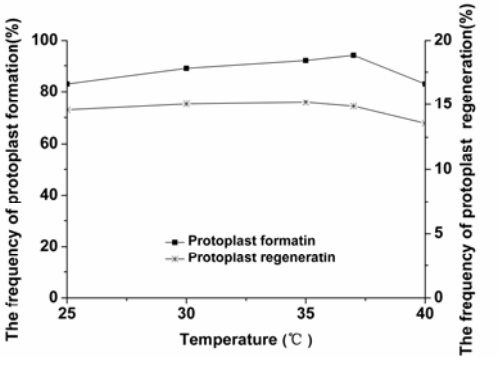

Fig. 4. Effects of enzymolysis temperature on protoplast formulation and regeneration of *Rhodococcus* sp. BX2

3.4 The Choice of Regeneration Medium

Influence of regeneration medium on protoplast regeneration was investigated through double layers culture method as shown in Table 2. Since PVP had the characteristics of stabilizing cells and stimulating cell's regeneration, the best results were achieved by spreading protoplasts on RNB plates containing 1.5% PVP. Under the condition of 6 $mg \cdot mL^{-1}$, 35℃ and 3 h, regeneration rate of *Rhodococcus* sp. BX2 was reached to 14.83% on RNB plates, which didn't exceeded the range of 0.1-50% reported by Peberdy [23].

Table 2. Effects of different regeneration media

Regeneration medium	Regeneration effect of BX2
R_2YE	+
HNM	++
RNB	+++

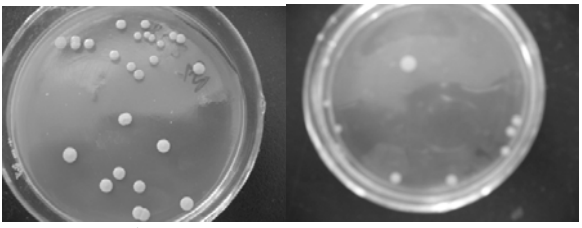

A. B.

Fig. 5. The colony of *Rhodococcus* sp. BX2 (A) and its protoplast regeneration (B) on LB

4 Conclusion

The protoplasts of *Rhodococcus* sp. BX2 were obtained by treatment with the combination of 0.5% glycine preprocessing culture solution at 35℃for 6 h and 6 mg·mL^{-1}lysozyme incubating bacterial suspension at 35℃for 3 h, and the protoplast formation rate was up to 91%. The regeneration rate of protoplasts was 14.83% on RNB medium containing 1.5% polyvinylpyrrolidone. This study provided the foundation to construct an excellent multi-functional genetic strain of *Rhodococcus* sp. BX2 and *Acinetobacter* sp. LYC-1 by protoplast fusion, which may solve the problem of environmental pollution of bensulfuron-meghyl and butachlor.

Acknowledgment. This work was supported by Science and Technology Research Project of Heilongjiang Education Bureau (No.11541015); Postdoctoral Science & Research Foundation of Heilongjiang（No. LBH-Q09158）; The National Key Technology R&D Program of China (No. 2007BAD87B03); Innovative Team Foundation of Northeast Agricultural University (CXT003-1-3) in China.

References

1. Deng, J.B.: Summary of sulfonylurea herbicides. World Pesticides 25(3), 24–32 (2003)
2. Xiao, Y.S., Tan, L., Chen, G.H.: Microbial Degradation of the Sulfonylurea Herbicides. Agrochemicals Research and Application 11(3), 15–19 (2007)
3. Ghamry, M., Xu, J.M., Huang, C.Y., Gan, J.: Microbial Response to Bensulfuron-Methyl Treatment in Soil. Journal of Agric. Food Chem. 50(1), 136–139 (2002)
4. Min, H., Ye, Y.F., Chen, Z.Y.: Effects of butachlor on microbial populations and enzyme activities in Paddy soil. Journal of Environ. Sei. Health B 36(5), 581–595 (2001)
5. Xia, H.Y., Zhu, Q.H.: Research progress on Butachlor degradation by microorganism. China Plant Protection 29(7), 12–14 (2009)
6. Chen, Y.L., Chen, J.S.: Degradation and dissipation of the herbicide butachlor in paddy field. Journal of Nippon Noyaku Gakaishi 4(4), 431–438 (1979)
7. Chen, Y.L., Wu, T.C.: Degradation of butachlor herbicide by soil microbes. Journal of Nippon Noyaku Gakaishi 3(4), 411–417 (1978)
8. Okamoto, T., Fujita, Y., IRie, R.: Protoplast Formation and Regeneration of Streptococcus lactis Cells. Agric. Biol. Chem. 47(2), 259–263 (1983)

9. Schaeffer, P., Cami, B., Hotchkiss, R.D.: Fusion of bacterial protoplasts. Proc. Natl. Acad. Sci. USA 73(6), 2151–2155 (1976)
10. Finnerty, W.R.: The biology and genetics of the genus Rhodococcus. Ann. Rev. Microbiol. 46, 193–218 (1992)
11. Shen, Q.Y., Liu, L., Shen, Q.Y.: Breed of phenol-degrading microorganism with protoplast fusion. Techniques and Equipment for Enviromental Pollution Control 4(4), 39–44 (2003)
12. Zhang, X.X., Jia, H.Y., Wua, B.: Genetic analysis of protoplast fusant Xhhh constructed for pharmaceutical wastewater treatment. Bioresource Technology 100, 1910–1914 (2009)
13. Etemadifar, Z.: Enhanced desulfurization activity in protoplast transformed rhodococcus erythropolis. Amenrican-Eurasian J. Agric. & Environ. Sci. 3(2), 285–291 (2008)
14. Vogt, M.E.: Construction of an Escherichia coli-Rhodococcus shuttle vector and plasmid transformation in Rhodococcus spp. Journal of Bacterlogy 170(2), 638–645 (1988)
15. Liu, T.H., Lin, M.J., Ko, W.H.: Factors affecting protoplast formation by Rhizoctonia solani. J. New Biotechnology 27, 64–69 (2010)
16. Schaeffer, P.B., Hothkiss, R.D.: Fusion of bacterial protoplasts. Proc. Natl. Acad. Sci. USA 3(6), 2151–2155 (1976)
17. Chassy, B.M., Giuffride, A.: Appl. Environ. Microbiol. 39, 153 (1980)
18. Liao, J.S., Guo, Y., Zhuang, G.: Protoplast preparation and fusion of bacteria degrading PVA. Journal of South China University of Technology (Natural Science Edition) 32(5), 74–79 (2004)
19. Balts, R.H., Gen, J.: Microbiol. 10, 93 (1978)
20. Foder, K., Alfoldi, L.: Proc. Natl. Acad. Sci. U.S.A 73, 2147 (1976)
21. Ochi, K., Hitchcock, M.J.M., Katz, E., Bacteriol, J.: 139, 984 (1979)
22. Kaneko, H., Sakaguchi, K.: Agric. Biol. Chem. 43, 1007 (1979)
23. Ulhoa, C.J., Peberdy, J.F.: Regulation of chitinase synthesis in Trichoderma harzianum. Journal of General Microbiology 137, 2163–2169 (1991)

Hyperglycemia and Advanced Glycation End-Products Prevent Cognate Differentiation of Human Adipose- Derived Stromal Cells into Bone In Vitro

Li Dong Song[1], Li Shu Qiang [1], Cai Bo[2], Wang Ping[1], Feng Wei[1], and Liu Jian Guo[1]

[1] Department of Orthopedics, The First Hospital of Jilin University, Changchun, 130021, China
[2] Special Diagnosis Department, No.208 People's Liberation Army Hospital, Changchun, 130062, China
jgliu.2005@yahoo.com.cn

Abstract. Objective to explore the effects of Hyperglycemia and AGEs on human ADSCs' osteogenesis ability. Methods Human adipose derived stromal cells were isolated and induce to the bone formation; 27.5 mmol/L high glucose concentration and 100μg/ml AGEs were used to simulate the diabetic environment. There were four groups in the present study, 6 specimen in each group. Through immunofluorescence detection and observation of calcification in each group, the different change in CNI secretion and osteogeniesis ability were statistically analyzed. Results Hyperglycemia and AGEs prevented ADSCs cognate differentiation into bone. On 21d, the CNI amount in combination group was 2.76 time lower than the normal group, and the average calcification nodes was (4.10±1.24).There were significant difference in these two groups ($P<0.01$) Conclusion Hyperglycemia and AGEs had a deleterious effect on ADSCs' osteogenesis ability.

Keyword: Hyperglycemia, Advanced glycation end-products Adipose-derived stroma cells.

1 Introduction

AGEs are formed non-enzymatically by reducing sugars interacting with the amino groups of proteins to initiate a complex series of rearrangements and dehydrations, ultimately producing a class of irreversibly cross-linked and fluorescent moieties[1]. The formation and accumulation of AGEs in response to the hyperglycemic state is a characteristic feature of tissues in the elderly population and, more so, in patients with diabetes mellitus. As such, AGEs have been strongly implicated in the pathogenesis of age-related and diabetic complications. It has been reported that AGEs are involved in musculoskeletal diseases such as osteoarthritis (OA), the most common chronic disabling disorder for aged people[2]. The current findings suggest that AGEs may play a role in the pathogenesis of Diabetic Osteopenia, as well as that of various bone and joint disorders in non-diabetic patients; however, the details of such deleterious mechanisms remain to be completely understood.

Zuk [3]. first isolated and cultured ADSCs in 2001 and originally termed them Processed Liposuction. ADSCs are multipotent cells present in various tissues during

E. Zhu and S. Sambath (Eds.): Information Tech. and Agricultural Eng., AISC 134,, pp. 121–127.
springerlink.com © Springer-Verlag Berlin Heidelberg 2012

human development and are able to be isolated from adult fat tissue and differentiated into bone, cartilage, muscle, and adipose tissues. In injured adults, ADSCs can be used in the formation, remodeling, and repair of musculoskeletal tissues, suggesting the potential for therapeutic approaches using ADSCs in orthopedic and regenerative medicine.

During bone formation, pre-osteoblasts, osteoblasts, and osteocytes all originate from mesenchymal stem cells (MSCs). Defects in the number and proliferation potential of MSCs have been suggested to underlie age-related defects in osteoblast number and function. It has also been reported that AGEs influence osteoblasts development through specific receptors, including the AGE receptor (RAGE) [4]. These findings suggest that AGEs have the ability to regulate proliferation and differentiation of musculoskeletal lineage cells, but no studies have been published investigating whether AGEs and HG directly affect the function of ADSCs in bone repair. Thus, we studied the effects of AGEs on the osteogenic abilities of ADSCs using cultured human ADSCs in vitro.

2 Materials and Methods

2.1 Cell Culture Conditions for Human ADSCs

Adult human ADSCs were isolated from the fat tissue of liposuction patients after obtaining informed consent (The First Hospital of Jilin University, Changchun city, Jilin Province, China). The cells were cultured at 37°C in a humidified 5% CO_2–95% air mixture and were maintained at a sub-confluent density. Cells within five generation were used in this study. Cell proliferation rates were observed by drafting a cell growth curve. Stem cell-specific protein, $CD_{44,}$ was detected by immunofluorescence using a confocal microscope (Fluview1000; Olympus, Japan).

2.2 Preparation of AGEs

AGEs were prepared as described previously [5].Briefly, 50 mg/ml of BSA (Sigma-Aldrich, Wisconsin, USA) was incubated for 12 weeks under sterile conditions with D-glucose (Shanghai Fine-Chemical Co, Ltd, Shanghai, China). Unincorporated sugars were removed by dialysis against 0.2M PBS (pH 7.4). Non-glycated BSA was incubated under the same conditions except in the absence of D-glucose and used as a negative control. Preparations were tested for endotoxin contamination using an Endospecy ES-20S system (Seikagaku Co., Tokyo, Japan), and found to be endotoxin- free. Spectrophotometer detection (370nm/440nm) of AGEs in the experimental and control groups were 24.7 and 3.1, respectively.

2.3 Osteogenic Differentiation Medium

Osteogenic differentiation was induced with a commercially available osteogenic differentiation medium (Bio-Whittaker, MD, USA) containing 0.1μM dexamethasone, 0.05mM ascorbic acid 2-phosphate, and 10nM β-glycerophosphate.

2.4 Group Division

Cells were divided among four groups, with *six specimens in each*: Group A (control): ADSCs + 5.5mmol/L cell culture medium + osteogenic differentiation medium (ODM); Group B (HG): ADSCs + 27.5mmol/L HG + ODM; Group C (AGEs): ADSCs + AGEs (100μg/ml) + 5.5mmol/L + ODM; Group D (Combination): ADSCs + HG + AGEs + ODM.

2.5 CNI Immunofluorescence Microscopy

ADSCs were grown on the Laboratory-Tekchamber (NUNC Denmark, purchased from Bio Dee Biotech Company, Beijing, China). At the end of the culture period, the cells were fixed with 4% Para formaldehyde in PBS (pH 7.4) for 30 minutes. The fixed cells were rinsed with PBS three times for 15 minutes each. The cells were then treated with 0.1% Triton X-100 for 15 minutes. The cells were incubated with a 1:200 dilution of polyclonal antibody for CNI (Santa Cruz, from Boster Biological Engineering Co., Ltd., Wuhan, China) for one hour, followed by incubation with a 1:400 dilution of Alexa Fluor 555-conjugated secondary antibodies (After counterstaining with 5μg/ml of propidium iodide (Sigma- Aldrich), the specimens were observed under a fluorescence confocal microscope (FluoView™ FV1000; Olympus, Japan). Fluorescent quantitation of CNI was calculated in different groups by the FV1000 scan program. Negative control staining, in which a primary antibody was omitted, was performed and analyzed for comparison purposes.

2.6 Osteogenic Differentiation of ADSCs

Osteogenic differentiation was induced with a commercially available osteogenic differentiation medium (Bio-Whittaker). ADSCs were seeded at 1×10^3 cells/mL and were cultured up to four weeks with replacement of the fresh osteogenesis induction medium every four days. For the detection of osteogenic differentiation, bone nodule formation was examined under a phase-contrast microscope (TS 100; Nikon, Japan) after chinalizarin staining as previously described [6]. The number of the calcified nodes was counted five times under a different vision scope and the average number was compared within each group.

2.7 Statistical Analysis

Data from different experimental groups were processed using SPSSv12.0 statistical software (IL, USA) and, when appropriate, by using Scheffe's test for multiple comparisons. All data have been expressed as mean ± SD. A level of $p<0.05$ was considered as statistically significant.

3 Results

3.1 ADSCs Culture and Identification

Most isolated ADSCs adhered to the wall of the culture bottle within 48 hours. Fiber-like cells growing in the shapes of long streaks appeared after 72 hours. These cells

showed a clone-like growth within 10 days after being started in culture. Stem cell-specific CD_{44} protein was positive in the test cells.

3.2 CNI Immunofluorescence Microscopy

CNI is the specific early stage biochemical marker for ADSC differentiation into bone. The results of CNI fluorescent quantitation revealed positive CNI expression in the cytoplasm of ADSCs and directly under the cell membrane (Table 1). Green fluorescence appeared to be strongest in the control group (A) and lowest in the combination group (D). The AGEs group (C) had a lower quantitation of fluorescence than did the HG group (D). All groups were statistically different (p<0.01). The fluorescent quantitation scan showed the magnitude of CNI in the AGEs+HG treated group was 2.76 times lower than in the control group.

3.3 ADSCs Osteogenic Differentiation

Under osteogenic stimulation, bone nodule formation was observed in the control culture, while very little was observed in AGE and HG treated cells. Chinalizarin staining revealed a large mass of calcium deposition in accordance with the bone nodule formation in the control (Fig.1). However, loss of mineralization was observed in AGE and HG treated cells (Fig.2). The average number of calcification nodes counted under the microscope in the different groups on different days has been shown in (Table 2.) The combination group (D) presented the least node formation compared with the other groups (p<0.01), which suggested that AGEs with HG had the strongest inhibition effects on the osteogenesis of ADSCs.

Table 1. CNI expression in response to AGE and HG exposure for 21 days（Mean±SD）

	A	B	C	D
Fluorescent Quantitation	124.1±25.11	88.3±17.62	68.2±11.70△	44.9±13.53*

Note: * D vs. other groups p<0.01; △ C vs. B p<0.01

Table 2. Number of calcification nodes formed in response to AGE and HG treatments (Mean±SD)

Group \ Day	14	21	28
A	11.55±1.29	21.05±1.32	26.4±1.17
B	6.70±1.52	12.75±1.22	13.3±1.69
C	4.45±1.27	7.70±1.16	12.15±1.33
D	0	4.10±1.24*	5.55±1.46*

Note: * D vs other groups p<0.01

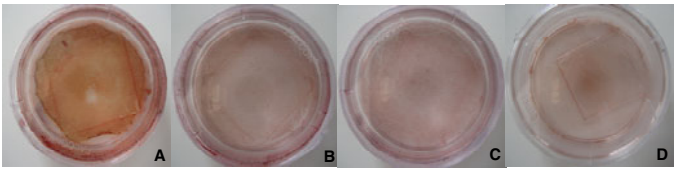

Fig. 1. Calcium deposition in ADSCs under high glucose and AGEs condition (21d) as revealed by chinalizarin staining

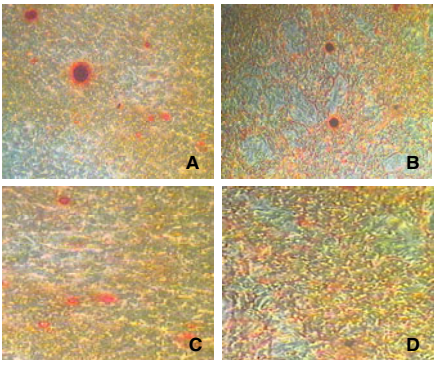

Fig. 2. ADSCs chinalizarin stain results (day 21) (×40 on phase contrast microscope)

4 Discussion

Hyperglycemia is the initial factor which induces many chronic complications of diabetic patients. Long-term hyperglycemia can cause molecular structure changes in stable, long-lived proteins to produce a class of irreversibly cross- linked and fluorescent moieties, known as advanced glycation end-products. The formation and accumulation of AGEs through hyperglycemia are characteristic features of tissues in the elderly, especially in those individuals suffering from diabetes mellitus.

There has been little information about the influence of AGEs and HG on the differentiation process of ADSCs. The present study reports that AGE and HG interfered with the differentiation of ADSCs into osteocytes. It has been previously shown that AGEs and/or HG inhibit cell growth in several different cell lines. In particular, AGE and HG inhibited proliferation of cultured bovine retinal pericytes, in addition to promoting apoptosis, through the down regulation of the expression ratio of bcl-2/bax [7]. In rat Schwann cells, reduced cell replication and induction of apoptosis by AGE have been observed, suggesting that AGEs may play a role in the onset and progression of diabetic neuropathy [8]. On the other hand, AGEs have the ability to promote proliferation of cells under specific conditions. In bovine retinal endothelial cells, AGEs enhanced reactive oxygen species generation, protein kinase C activation, and vascular endothelial cell growth factor expression, implicating AGEs in the excess vascular formation in diabetic retinopathy [9]. Furthermore, it has

been reported that low concentrations (<1μM) of AGEs were able to stimulate mesangial cell proliferation, whereas higher concentrations (>10μM) reduced the proliferation of the same. In osteoblastic cell lines, AGE-collagen has been reported to have the opposite effect on proliferation and the number of surviving cells, which is dependent on the stage of osteoblastic differentiation.

In this study, we observed that relatively higher doses of extra cellular AGEs and HG (100μg/ml and 27.5mmol/L, respectively) prevented ADSC differentiation into bone. The presence of HG and AGEs inhibited the osteogenic differentiation of ADSCs. In this suppression process, AGEs suppression ability was stronger than that of high glucose and weaker than that of the AGE and HG combination group. The bimodal effects of AGEs presumably vary according to the source of AGEs, the type of cells, and culture conditions. Therefore, further study will be needed to clarify the details of the mechanism of AGE and HG mediated growth control of MSCs, particularly studies which can model the *in vivo* microenvironment for specific developmental or disease processes.

Several specific signaling processes have been identified as contributing to osteogenesis, such as MAP kinase and Notch. signaling. Bone-specific gene expression is known to be influenced by specific transcriptional factors, such as osteocalcin gene regulation by Runx2/Cbfa1. Further studies would be needed to determine exactly how AGEs and HG influence the differentiation of ADSCs through specific intracellular signaling pathways.

5 Conclusions

AGEs and HG lead to the loss of ADSC mass *in vitro* and may similarly contribute to the delay of tissue repair *in vivo* by inhibiting the maturation of calcification. AGEs alone had a stronger effect than HG on ADSCs osteogenesis, but had a weaker effect than when in combination with HG. Fluorescent quantitation scan revealed the magnitude of CNI in AGEs+HG treated group was 2.76 times lower than in the control group. AGEs+HG also reduced the number of ADSC calcification nodes. Further study will be needed to clarify the detailed mechanism of the deleterious effect of AGEs and HG on ADSCs.

References

1. Christopher, J.: Trabecular microfracture and the influence of pyridinium and non-enzymatic glycation mediated collagen cross-links. J. Bone 37(6), 825–832 (2005)
2. Valcour, U.: Non-enzymatic Glycation of Bone Collagen Modifies Osteoclastic Activity and Differentiation. Journal of Biological Chemistry 282(8), 5691–5703 (2007)
3. Zuk, P.A., Zhu, M., Mizuno, H., et al.: Multilineage cells form human adipose tissue: implications for cell-based therapies. Tissue Eng. 7, 211–228 (2001)
4. Hong, L., Peptan, I.A., Colpan, A., et al.: Adipose tissue engineering by human adipose-derived stroma cells. Cells Tissues Organs 183(3), 133–140 (2006)
5. Santana, R.B., Xu, L.: A role for advanced glycation end products in diminished bone healing in type 1 diabetes. Diabetes 52(6), 1502–1510 (2003)

6. Geoffroy, K., Wiernsperger, N., Lagarde, M., et al.: Bimodal effect of advanced glycation end production on mesangial cell proliferation if mediated by neutral ceramidase regulation and endogenous sphingolipids. J. Biol. Chem. 279, 34343–34352 (2004)
7. Chen, B.H., Jiang, D.Y., et al.: Advanced glycation end- products induce apoptosis involving the signaling pathways of oxidative stress in bovine retinal pericytes. Life Sci. 79(11), 1040–1048 (2006)
8. Shinichiro, K., Seiya, K., Yamagishi, S.-I., et al.: Advanced glycation end-products attenuate human mesenchymal stem cells and prevent cognate differentiation into adipose tissue, cartilage and bone. Journal of Bone and Mineral Research 20(9), 1647–1658 (2005)
9. Mamputu, J.C., Renier: Advanced glycation end products increase, through a protein kinase C-dependent pathway, vascular endothelial growth factor expression in retinal endothelialcells. Inhibitory effect of gliclazide. J. Diabetes Complications 16, 284–293 (2000)

Expression Abnormality of Myostatin in Malformed Chicken Embryos*

Chaolai Man

College of Life Science and Technology
Harbin Normal University
Harbin, Heilongjiang province, China
manchaolai@126.com

Abstract. Myostatin is a potent growth and differentiation factor involved in skeletal muscle tissue formation in vertebrates. However, recent studies in chicken embryos suggest that the myostatin is expressed even before the establishment of myogenic lineage,and the functions of myostatin are not limited to skeletal muscle, because of its ubiquitous expression in chicken. No studies have thus far been definitively reported the expression patterns of myostatin in malformed chicken embryos. The present experiment was designed to study myostatin mRNA expression and distribution pattern in normal and malformed chicken embryos (HH26) using whole-mount in situ hybridization. The expression and distribution patterns of myostatin in the two kinds of developing chicken embryos were compared. The results showed that myostatin mRNA expression and distribution patterns in normal chicken embryos were symmetry and orderliness. However, myostatin expression in malformed chicken embryos was disorderly and unsystematic. In conclusion, we found for the first time that there existed different myostatin expression and distribution patterns between normal and malformed chicken embryos, and the results may be useful in further studying myostatin functions.

Keywords: Myostatin, Chicken, Malformed Embryo, Whole-mount in Situ Hybridization.

1 Introduction

Myostatin (GDF-8) belongs to the TGF-βsuperfamily and is a potent growth and differentiation factor involved in skeletal muscle formation in vertebrates [1,2]. At early embryonic stages, myostatin is restricted to the myotome compartment of the developing somites, and myostatin has been proposed to play an essential role in skeletal muscle growth and development [3,4]. Myostatin inhibits the myoblast proliferation by preventing the progression of myoblasts from G1 to S phase of the cell cycle[5].

It is believed in avian species that myostatin is expressed only in muscle [6,7]. Recently, it was reported that in ovo administration of anti-myostatin antibody resulted

* This work is supported by foundation for Young Scholars of Harbin Normal University #KGB200806.

E. Zhu and S. Sambath (Eds.): Information Tech. and Agricultural Eng., AISC 134, pp. 129–134.
springerlink.com © Springer-Verlag Berlin Heidelberg 2012

in not only increasing muscle mass but also increasing some tissues [8]. In chicken, the developmental pattern of myostatin mRNA abundance coincides roughly with the progression of muscle fiber formation [2,9]. However, recent studies identified that the role of myostatin may not be restricted to muscle growth regulation. Myostatin might be involved in the organogenesis and embryogenesis, as the ubiquitous expression of myostatin was noticed in chicken embryonic tissues [2,10-14].

Indeed, myostatin may play significant roles in early development and myogenesis. There are very few cases of malformed embryos during development, but the malformed embryos may provide us with many valuable clues to analyzing some genes functions. Study on the expression changes of myostatin gene in malformed embryos will provide significant reference values for further studing myostatin functions in developing embryos. However, few studies have been reported to define the roles of myostatin during the embryonic embryogenesis in birds. Here we investigated expression of myostatin in normal and malformed chicken embryos by whole-mount in situ hybridization. An interesting differences in myostatin gene expression pattern between normal and malformed embryos were observed.

2 Materials and Methods

2.1 Chicken Embryos

All experiments were performed using layer chicken embryos (Hy-line Layer). Fertilized chicken eggs were purchased from a local supplier (Yuanda Poultry Farm, Harbin, China) and incubated with intermittent rocking at 37–38°C under a relative humidity of 60–70%. Embryos were staged according to Hamburger and Hamilton (1951).

2.2 Synthesis of Chicken Myostatin cDNA and cRNAs

Total RNA was isolated from the whole embryos at the fifth day of incubation (stage HH26) using TRIZOL (Invitrogen, USA) according to the instruction manual. One microgram of the prepared RNA was subjected to reverse transcription for 60 min at 37 °C in 20 mL of 1×M-MLV reaction buffer, 300 ng oligo (dT) 17-20, 20U RNA guard, 200U M-MLV reverse transcriptase (Invitrogen, USA), 0.5 mM each of dNTPs (TaKaRa Biotechnology. Dalian, China). The PCR reaction was performed in 10 μl of 1×PCR buffer, 0.2 mM each of dNTP, 0.25U TaKaRa Taq, 0.2 μM each of the synthetic primer sets and 0.1 μL of the RT reaction. Specific PCR primer sets of chicken GDF-8 (GenBank Accession No. AF346599) gene were designed from the known cDNA sequences as follows: 5′-ATGCAAAAGCTAGCAGTCTATG-3′ (GDF-8: sense) (1-22), 5′-TCATGAGCACCCGCAACGATCT-3′ (GDF-8: antisense) (1107-1128). After an initial denaturation step (95 °C for 10 min), the amplification was performed in 30 cycles under a thermal profile of denaturation (95 °C for 45 s), annealing (for 45 s), and extension reaction (72 °C for 1 min). The myostatin PCR product was subcloned into pGEM-T Easy Vector (Promega, USA) and sequenced, respectively. Their antisense and sense cRNA probes were synthesized using PCR amplified templates containing full length the sequence of myostatin and RNA

polymerase promoter sequence. Digoxigenin (DIG)-labeled antisense and sense cRNA probes were prepared with T7 or SP6 RNA polymerase using a DIG RNA Labeling Mix kit (Roche Diagnostics, Mannheim, Germany).

2.3 Whole-Mount in Situ Hybridization

Chicken embryos at HH26 were fixed in 4% paraformaldehyde overnight. The samples were dehydrated with ethanol, rehydrated, washed with PBS containing 0.1% Tween 20, and digested in 10μg/mL proteinase K at 37°C for 20 min.The samples were fixed in PBS containing 0.1% Tween 20, 0.2% glutaraldehyde and 4% paraformaldehyde, and washed with PBS containing 0.1% Tween 20. Prehybridization was performed in 5×SSC containing 50% formamide, 50 mg/mL yeast RNA, 1% SDS, and 50 mg/mL heparin at 65 °C for 1 h with gentle shaking. cRNA probes were hybridized at a final concentration of 1μg/mL at 65 °C overnight. The samples were serially washed at 70°C with the post-hybridization solutions, i.e., 5×SSC containing 50%formamide and 1% SDS,5×SSC containing 50% formamide, 1% SDS and 0.1% Tween 20, 5×SSC containing 0.1% Tween 20, and 2×SSC containing 50% formamide and 1% SDS. The samples were treated for 90 min with 1.5% blocking reagent (Sheep serum),and then incubated with anti-DIG antibody conjugated with alkaline phosphatase at 4 °C overnight. The samples were serially washed with 100 mM Tris-HCl (pH7.5) containing 150 mM NaCl and 0.1% Tween 20, 100mM Tris-HCl (pH9.5) containing 100mM NaCl, 50mM $MgCl_2$ and 1% Tween 20, and 100 mM Tris-HCl (pH9.5) containing 100mM NaCl, 50mM $MgCl_2$, 1% Tween 20 and 5% polyvinylalcohol. A subsequent enzyme-catalyzed color reaction with BCIP/NBT produced an insoluble blue precipitate. After color development, the samples were washed with PBT and ethanol.

3 Results

3.1 Expression of GDF-8 in Normal Chicken Embryos

Fifteen normal embryos were collected from chicken embryos at HH26 (Ham-burger and Hamilton, 1951), and subjected to whole-mount in situ hybridization for myostatin. Strong expression of myostatin was detected in brain,eyes and heart (Fig.1A and B). Additionally, faint expression was also found in somites,limb buds and tail bud. In summary, at HH26, Myostatin was mainly expressed in brain, eyes, heart, somites, limb buds and tail bud.

3.2 Expression of GDF-8 in Malformed Chicken Embryos

Fifteen malformed chicken embryos were gathered from 600 embryos at HH26. These malformed embryos appearances were basically different and each has its specific features. The malformed embryos, compared with normal embryos, showed thin trunk, small head, small eyes or no eyes, and twin embryos which have a single head with two bodies or one trunk with two heads, etc. (Fig.2 A, B and C). All the malformed embryos had heartbeats and blood circle. Expression of myostatin was detected by whole-mount in situ hybridisation in malformed chicken embryos, and the

results of myostatin expression pattern was different from that of normal chicken embryos. Strong expression of myostatin in some tissues (brain and eyes) of normal embryos changed into faint expression in some malformed chicken embryos (Fig.2 A, B and C). However, faint expression of myostatin in some tissues (limb buds) of normal embryos turned into strong expression in some malformed chicken embryos (Fig.2 A). Moreover, different malformed embryos showed diversity of myostatin expression patterns (Fig.2 A, B and C). In a word, strong or faint of myostatin expression distributions in malformed chicken embryos were different from that of normal embryos, and did not exist any rules.

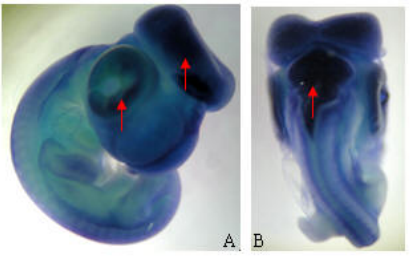

Fig. 1. The results of whole-mount in situ hybrization from chicken embryos at HH26. A/B: The different photos of the same embryo. Arrows show the sections which have strong hybridization signals.

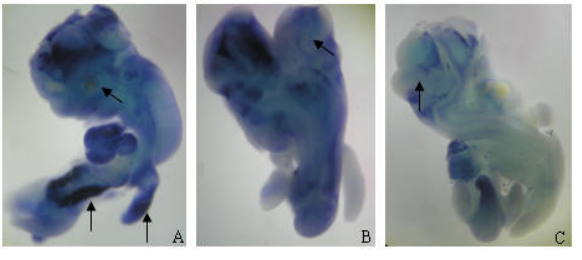

Fig. 2. The results of whole-mount in situ hybridization from malformed chicken embryos at HH26. A, B, C: The results of whole-mount in situ hybridization from malformed embryos.Arrows partially show sections with abnormal myostatin expression in malformed embryos.

3.3 Difference of Myostatin Expression between Normal and Malformed Chicken Embryos

Whole-mount in situ hybridization on normal chicken embryos was performed to identify the patterns of myostatin expression. As shown in Fig.1, myostatin positive hybridization signals were mainly distributed on brain, eyes, beak part, heart, trunk, limb bud and tail bud, which showed that some symmetry and orderliness existed in expression distribution of myostatin in normal embryos. However, expression distribution of myostatin in malformed embryos presented disorderly and unsystematic contrast to normal embryos.

4 Discussion

Myostatin is a highly conserved, potent growth and differentiation regulator of skeletal muscle in many species, from teleost fishes to humans, although its mechanisms of action are incompletely understood [15]. In mice,myostatin is expressed in the myotome and developing skeletal muscles as early as 9.5 days post coitus [3]. In chicken, the skeletal muscle is also a principle source of myostatin [6,7]. Myostatin was expressed even before the establishment of myogenic lineage [13,16]. Moreover, there are some reports that myostatin is expressed in another organs and tissues other than skeletal muscles in chicken [10,12,13]. In the present study, we clearly show that there existed expression of myostatin in brain and eyes using whole-mount in situ hybridization. These results are basically consistent with the myostatin expression reported by earlier workers [10,12,13], although there existed myostatin expression diversity in different chicken breeds [13]. The ubiquitous expression of myostatin is found in oviparous species including chicken and fish. In mammals, deletion or mutation of myostatin gene causes an increase in muscle mass during embryogenesis. Conversely, in bird, the embryonic growth may be limited in the space of the eggs under the myostatin action [10]. Myostatin maybe have some functions in target tissues as an endocrine factor as well as an autocrine factor. However, the relationship between the embryonic development and myostatin action needs to be investigated in future.

Interestingly, our results show that there are differences of myostatin expression and distribution between malformed and normal embryos. That is, strong or faint signals of myostatin expression and distribution in malformed chicken embryos are different from that of normal embryos. If the abnormal myostatin expression induces the results of malformed embryos development, which show myostatin may play very important roles on normal embryo development and body form. Inversely, If some other reasons lead to the change or abnormity of myostatin expression, then embryos maybe realize malformed development partially through the abnormal myostatin expression.

We provide the first information that there exist differences of myostatin expression and distribution between malformed chicken embryos and normal chicken embryos. Of course, only one stage embryos (HH26) was examined, and we do not yet fully confirm whether the malformed embryos development is related to abnormal myostatin expression. Additional data on other stages, different breed such as broiler, and validation on the difference tissues in normal and malformed embryos will be studied in the subsequent research.

Acknowledgment. I thank Prof. Qiong Wu (Developmental Biology Lab, Harbin Institute of Technology, Harbin, China) for providing the excellent technical assistance.

References

1. Lee, S., McPherron, A.: Regulation of myostatin activity and muscle growth. Proc. Natl. Acad. Sci. USA 98(16), 9306–9311 (2001)
2. Castelhano-Barbosa, E., Gabriel, J., Alvares, L., et al.: Temporal and spatial expression of the myostatin gene during chicken embryo development. Growth Dev. Aging. 69(1), 3–12 (2005)

3. McPherron, Lawler, A., Lee, S.: Regulation of skeletal muscle in mice by a new TGF-beta superfamily member. Nature 387(6628), 83–90 (1997)
4. Sharma, M., Kambadur, R., Matthews, K., et al.: Myostatin, a transforming growth factor-beta superfamily member, is expressed in heart muscle and is upregulated in cardiomyocytes after infarct. Journal of Cellular Physiology 180(1), 1–9 (1999)
5. Bass, J., Oldham, J., Sharma, M., et al.: Growth factors controlling muscle development. Domestic Animal Endocrinology 17(2-3), 191–197 (1999)
6. Kocamis, H., Kirkpatrick-Keller, D., Richter, et al.: The ontogeny of myostatin, follistatin and activin-B mRNA expression during chicken embryonic development. Growth Dev. Aging 63(4), 143–150 (1999)
7. Mott, Ivarie, R.: Expression of myostatin is not altered in lines of poultry exhibiting myofiber hyper-and hypoplasia. Poult. Sci. 81(6), 799–804 (2002)
8. Kim, Y., Bobbili, N., Paek, K., et al.: Production of a monoclonal anti-myostatin antibody and the effects of in ovo administration of the antibody on posthatch broiler growth and muscle mass. Poult. Sci. 85(6), 1062–1071 (2006)
9. Kocamis, H., Gahr, S., Richter, J., et al.: Myostatin and TGF-beta2 gene expression patterns in response to in ovo administration of rhIGF-I during chicken embryonic development. Growth Development and Aging 66(1), 3–10 (2002)
10. Kaiyu, K., Sato, F., Aramaki, S., et al.: Ubiquitous expression of myostatin in chicken embryonic tissues: Its high expression in testis and ovary. Comp. Biochem. Physiol. A Mol. Integr. Physiol. 148(3), 550–555 (2007)
11. Manceau, M., Gros, J., Savage, K., et al.: Myostatin promotes the terminal differentiation of embryonic muscle progenitors. Genes Dev. 22(5), 668–681 (2008)
12. Sundaresan, N., Saxena, V., Singh, R., et al.: Expression profile of myostatin mRNA during the embryonic organogenesis of domestic chicken (Gallus gallus domesticus). Res. Vet. Sci. 85(1), 86–91 (2008)
13. Saxena, V., Sundaresan, N., Malik, F., et al.: Temporal expression of transforming growth factor-β2 and myostatin mRNA during embryonic myogenesis in Indian broilers. Research in Veterinary Science 82(1), 50–53 (2007)
14. Amthor, H., Huang, R., McKinnell, I., et al.: The regulation and action of myostatin as a negative regulator of muscle development during avian embryogenesis. Dev. Biol. 251(2), 241–257 (2002)
15. Morissette, M., Cook, S., Foo, S., et al.: Myostatin regulates cardiomyocyte growth through modulation of Akt signaling. Circulation Research 99(2), 15–24 (2006)
16. Kocamis, H., McFarland, D., Killefer, J.: Temporal expression of growth factor genes during myogenesis of satellite cells derived from the biceps femoris and pectoralis major muscles of the chicken. Journal of Cellular Physiology 186(1), 146–152 (2001)

Artificial Intelligence Based Optimization of the Extracting Process of Protein from DDGS Using Alkali Method*

Yuan Dong[1], Hongxi Shi[1], Xin Chen[1], Cong Liu[1], Lingyan Liu[1], Nan Zhao[1], Yingkun Cheng[1], Yibo Zhang[1], Feng Lin[1,**], and Lirong Teng[1,2,**]

[1] College of Life Science, Jilin University, Changchun 130012, China
[2] College of Life Science, Zhuhai College of Jilin University, Changchun 130012, China
yuandong09@mails.jlu.edu.cn,
{linfeng,tenglr}@jlu.edu.cn

Abstract. DDGS is the major coproduct generated from the fermentation of grain, but it is high in protein and an inexpensive source of protein. To optimize the extracting process of protein from DDGS, two different artificial intelligence techniques namely artificial neural network(ANN) and genetic algorithm(GA) have been developed using the three influential process variables as model inputs and the extraction rate of protein as the model output. The correlation coefficient for the ANN model were 0.98664. The input parameters of ANN model were subsequently optimized using the GA. The ANN-GA model predicted a maximum extraction rate of 0.424 g/2 g DDGS which gave a 15.46% increase of extraction rate over the statistical optimization. It was in good agreement with the actual experiment under the optimum conditions.

Keywords: Artificial intelligence (AI), Artificial neural network (ANN), Genetic algorithm (GA), DDGS, Protein Extraction.

1 Introduction

Corn is used worldwide as both animal feed and human food, but its major use is animal feed. However, due to the increasing prices and demands for biofuels such as ethanol and biodiesel, increasing amounts are being required as sources for fuel production, which will led to the increasing productions of DDGS, the major coproducts generated from the fermentation of grain [1]. DDGS is the residue left after starch is converted to ethanol. It is rich in proteins (～30-40% on average) [2] and is primarily sold as an animal feed replacement for whole corn [3]. Furthermore, as a potential source of protein, it has been used for many bioindustrial applications such as adhesives and resins. However, there are limited uses of DDGS in food and feed applications and about one-tenth of the DDGS produced is being waste.

* This work is supported by foundation for Young Scholars of Harbin Normal University #KGB200806.
** Corresponding authors.

E. Zhu and S. Sambath (Eds.): Information Tech. and Agricultural Eng., AISC 134, pp. 135–141.
springerlink.com © Springer-Verlag Berlin Heidelberg 2012

Several methods have been investigated for extracting protein from maize-based DDGS [4-6], and statistical techniques like response surface methodology(RSM) are also increasingly being used in the extracting process [7]. The development of accurate models for a biological system on a chemical and physical basis is still a critical challenge, mainly due to the complex and highly nonlinear nature of the extraction conditions [8]. It has been improved that genetic algorithm(GA) based Artificial neural networks *(ANN)* is a algorithm which is good at mimicking and modeling different aspects of biological information in food science and biochemical engineering and has a well established tradition [9]. Also the predictive accuracy of ANN models is superior to RSM model using the same experiment design [10].

A genetic algorithm is implemented as a computerized search and non-linear optimization procedure that uses the principles of natural genetics and natural selection [11]. It mimics the biological evolution process known as "Survival of the fittest"; improved solutions evolve from previous generations until reaching to a near optimal solution [12].

In this paper, the extraction rate of protein from DDGS was optimized by following steps: (i) an ANN model has been developed using the influential process variables as model inputs and the extraction rate of protein as the model output, (ii) the input space of the ANN model is optimized using the GA formalism with a view of maximizing the extraction rate, and (iii) the actual experiment is carried out to evaluate the feasibility of the model.

2 Materials and Methods

2.1 Materials

DDGS was supplied by Jilin Fuel Alcohol Company Ltd, China. The DDGS had about 39.32% protein and was yellow in color. It was milled to a particle size of 80 mesh when used.

2.2 Methods

2.2.1 The Extraction of Protein Form DDGS

2 g DDGS was presoaked in 30 volumes of sodium hydroxide for 1.5 h at 120 rpm in an orbital shaker. The solution was heated to the desired temperature in about 10 min and held at various alkali concentration, solid-liquid ratio and time. After this extraction, the solution was centrifuged at 4000 rpm for 10 min to separate the solution from the other components in DDGS. The pH of the solution was adjusted to 4.0 using 20% (v/v) hydrochloric acid or 20% (w/w) aqueous sodium hydroxide after the centrifugation. Finally, the solution was centrifuged at 9000 rpm for 10 min to obtain the crude protein.

2.2.2 ANN-Based Modeling of Protein Extraction

An artificial neural network is a superior and more accurate modeling technique as compared to RSM as it represents the nonlinearity in a much better way [13]. In this

study, a feed-forward ANN with three layers, namely the input layer(extraction condition), the hidden layer and the output layer(the dry weight of the crude protein) was employed to fit the experimental data of the protein extraction.

The data of RSM were randomly separated to three sets: calibration set、test set and prediction set. Calibration set was used for established ANN model. Test set and prediction set were used for checking the generalization and the predictive capability of ANN model, respectively. As the number of hidden nodes greatly affected the capabilities of the ANN model, a criterion named the degree of approximation (Da) was employed to select the suitable number of hidden nodes, as defined in the following (1):

$$D_a = \frac{c}{\frac{n_c}{n} \times MSE_c + \frac{n_t}{n} \times MSE_t + \left| MSE_c - MSE_t \right|} \tag{1}$$

MSE_c is the mean-square-errors (MSE) of calibration set;

MSE_t is the mean-square-errors (MSE) of validation set;

n_c is the number of calibration set;

n_t is the number of validation set;

n was the sum number of calibration set and validation set;

c was a constant number (in present work c was 0.02) by which Da was adjusted to get a good chart.

Once a capable ANN model with good prediction accuracy was developed, a genetic algorithm can be used to optimize its input space.

SAS Version 9.0 TS (SAS Institute Inc., Cary, nc, USA) was used for designing the experiments, Matlab version 7.10.0.499 (R2010a) (The Mathworks, Inc., USA) was used for establishing the ANN model and implementing GA.

3 Results and Discussion

3.1 The Results of RSM Design Experiments

The extraction rate of the protein had been optimized previously using statistical method. We optimized the extraction rate using RSM. Each extraction condition was previously using statistical method. We optimized the rate using RSM. Each extraction condition was tested at three levels (-1, 0, 1) (table 1). The Experimental design and the dry weight were shown in Table 2, a second-order polynomial was established to identify the relationship between the extraction rate and three extraction factors. The maximum extraction rate by RSM model was 0.367 g/2 g DDGS.

3.2 ANN-Based Modeling of Protein Extraction

Two of the 15 runs in the RSM design experiments were randomly chosen and used as prediction set and the test set, respectively. The other experimental data were used as calibration set. A three layers feed back artificial neural network (ANN) model was established. The suitable number of hidden nodes of ANN model was selected depend

on Da, and the results were shown in Fig. 1. According to (1), it was bvious that the larger Da was, the more ANN models approached the experimental data. As can be seen, Da achieved the maximum value when there were 12 hidden nodes; so the number of hidden nodes was set to 12.

The determination coefficient (R^2) of the optimized ANN.

Table 1. Variables and their levels used in rsm

Independent	Variable levels		
	-1	0	1
Alkali Concentration(mol/L)	0.45	0.55	0.65
Time (h)	1	2	3
Solid-Liquid Ratio	1:20	1:30	1:40

Table 2. Experimental design and results of rsm

Run	X_1*	X_2*	X_3*	Dry Weight
1	-1	-1	0	0.236
2	-1	1	0	0.259
3	1	-1	0	0.245
4	1	1	0	0.325
5	0	-1	-1	0.163
6	0	-1	1	0.291
7	0	1	-1	0.262
8	0	1	1	0.329
9	-1	0	-1	0.221
10	1	0	-1	0.262
11	-1	0	1	0.262
12	1	0	1	0.363
13	0	0	0	0.319
14	0	0	0	0.339
15	0	0	0	0.357

*X_1, X_2 and X_3 represent the Alkali Concentration, Time and Solid-Liquid Ratio, respectively.

model was 0.98664, indicating that the fitting of the ANN was acceptable. The root mean square error of calibration set ($RMSE_C$) was 0.011328, the root mean square error of test set($RMSE_T$) was 0.00852, and the root mean square error of prediction set ($RMSE_P$) was 0.008593. These indicated that the ANN model had good generalization and the predictive capability.

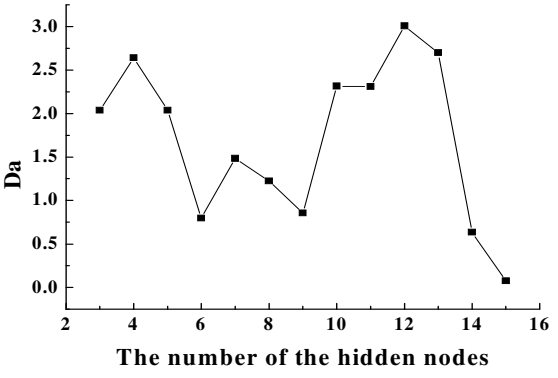

Fig. 1. The effect of the number of hidden nodes

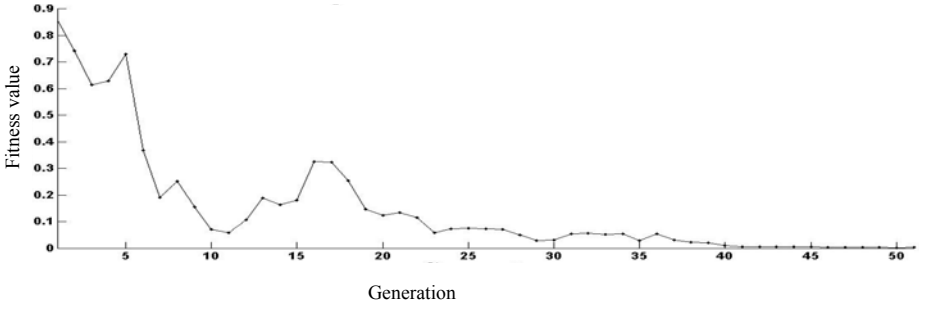

Fig. 2. The effect of the number of generation on fitness

3.3 GA-ANN Model

After the ANN model was established, GA was employed to search for the optimum extraction condition in the regions.The parameters of GA were:population type as test double vector, population size as 20, the initial population as given randomly, selection function as stochastic uniform, elite count as 2, crossover fraction as 0.8, crossover function as scattered, migration fraction as 0.2, penalty factor as 100 and number of generation over which GA evolved as 51.

The variation of the fitness depending on the increasing generation. The number of the generation was shown in Fig. 2. As can be seen, when the number of generation was 40, the fitness reached the lowest levels; when the number of generation continued to increase, the fitness stayed at the lowest level. The coded values of the optimum extraction conditions obtained by GA were: X_1=0.48744; X_2=-0.15080 and X_3=0.70136 and the corresponding experimental values were: x_1=0.60 mol/L, x_2=1.86 h and x_3=1:37. The expected extraction rate at the optimum conditions was 0.424 g/2 g DDGS. The validation experiments with these optimum conditions were implemented in triplicate and the average extraction rate was 0.433 g/2 g DDGS. The relative error between expected value and experimental value was 2.18%, which

indicating that the predictive accuracy of the ANN employed to search for the optimum extraction condition in model was better than that of the quadratic regression model.

4 Conclusions

It had been demonstrated that integrating RSM and ANN-GA modeling method were valuable tools in optimizing extraction rate of protein from DDGS. RSM was a statistical tool to design experiment and identify interactions. While artificial neural network was a superior and more accurate modeling technique as compared to RSM as it represented the nonlinearity in a much better way.

The data obtained from RSM were used and processed using ANN–GA for further enhancing the extraction rate of protein. The results showed that the training of an artificial neural network with the experimental data was quite successful. The ANN–GA predicted optimized extraction rate of 0.424 g/2 g DDGS was about 15.46% higher than that of predicted by RSM model. The relative error between the predictive value and experimental value was 2.18%, which indicated that the proposed method was an effective way and could be used for modeling and optimization of other bioprocess systems.

Acknowledgments. We sincerely acknowledge the Central Lab Of General Biology in JiLin University for their financial support and directions to carry out this research work.

References

1. Severinghaus, J.: Where will all the DDGS go? Iowa Farm Bur. Int. Trade Analyst 4, 1–2 (2006)
2. Corredor, D.Y., Bean, S.R., Schober, T., Wang, D.: Effect of decorticating sorghum on ethanol production and composition of DDGS. Cereal Chem. 83, 17–21 (2006)
3. Kansas Ethanol-Clean Fuel from Kansas Farms. DDGS, valuable ethanol co-product/valued livestock feed, `http://www.ksgrains.com/ethanol/ddgs.html` (accessed May 2009)
4. Wolf, W.J., Lawton, J.L.: Isolation and characterization of zein from corn distillers' grains and related fractions. Cereal Chem. 74, 530–536 (1997)
5. Xu, W., Reddy, N., Yang, Y.: An acidic method of zein extraction from DDGS. Agric. Food Chem. 55, 6279–6284 (2007)
6. Cookman, D.J., Glatz, C.E.: Extraction of protein from distiller's grain. Bioresour. Technol. 100, 2012–2017 (2009)
7. Almeida, J.S.: Predictive non-linear modeling of complex data by artificial neural networks. Curr. Opin. Biotechnol. 13, 72–76 (2002)
8. Davis, L.: Handbook of genetic algorithms. Van Nostrand Reinhold, NY (1991)
9. Venkatasubramanian, V., Sundaram, A.: Genetic algorithms: introduction and applications. Encyclopedia of Computational Chemistry, 1115–1127 (1998)
10. Anderson-Cook, C.M., Borrir, C.M., Montgomery, D.C.: Response surface design evaluation and comparison. Journal Statistical Planning and Inference 139, 629–641 (2009)

11. Mellit, A., Kalogirou, S.A., Drif, M.: Application of neural networks and genetic algorithms for sizing of photovoltaic systems. Renewable Energy 35, 2881–2893 (2010)
12. Russell, S., Norvig, P.: Artificial Intelligence A Modem Approach, 2nd edn. Local Search Algorithms and Optimization Problems-Genetic algorithms, pp. 116–119. Prentice Hall (2003)
13. Zhang, Y., Teng, L., Quan, Y., Tian, H., Dong, Y., Meng, Q., Lu, J., Lin, F., Zheng, X.: Artificial Intelligence Based Optimization of Fermentation Medium for β-Glucosidase Production from Newly Isolated Strain Tolypocladium Cylindrosporum. In: Li, K., Jia, L., Sun, X., Fei, M., Irwin, G.W. (eds.) LSMS 2010 and ICSEE 2010. LNCS, vol. 6330, pp. 325–332. Springer, Heidelberg (2010)

Chloroplast-Targeted Expression of Human sTRAIL Protein in Transgenic Tobacco*

Dan Wang, Xue-Liang Bai, Qing Liu, Ye-Rong Zhu,
Yan-Ling Bai, and Yong Wang

College of Life Sciences Nankai University Tianjin, China 300071
wangyong@nankai.edu.cn, wangdan_2006@yahoo.cn

Abstract. This study was aimed to express the soluble extracellular domain of tumor necrosis factor (TNF)-related apoptosis-inducing ligand (sTRAIL), an important potential agent for cancer therapy, in transgenic tobacco. Transformation vectors were constructed either for targeting the protein into chloroplasts (*35S:tp-strail*) or for accumulating it in the cytosol (*35S:strail*). After *Agrobacterium*-mediated transformation of wild type tobacco with vector *35S:tp-strail* or vector *35S:strail*, 8 and 3 transgenic lines were obtained, respectively. The transcription of the recombinant gene encoding sTRAIL was analyzed by RT-PCR. And the expressed sTRAIL in transgenic tobacco plants was detected by both Western blot and ELISA analysis. The results showed that *strail* gene was transcribed in all transgenic lines for both untargeted and targeted expression. However, sTRAIL protein accumulation was only detected in transgenic lines transformed with vector *35S:tp-strail*. Our preliminary results showed the sTRAIL expressed and accumulated in chloroplast of transgenic tobacco was biologically active. This is, to our knowledge, the first report of an active sTRAIL expressed in higher plant.

Keywords: Chloroplast targeting, sTRAIL, RBCS transit peptide, Transgenic tobacco.

1 Introduction

Tumor necrosis factor (TNF)-related apoptosis-inducing ligand (TRAIL) was discovered by Wiley and his colleague in 1995 [1]. It is capable of inducing apoptosis in tumor cells but not in normal cells [2]. It is a type II transmembrane protein with the carboxylic terminal forming an extracellular domain. When this domain is expressed solely, it is soluble and has the same physiological function as the whole length protein. Therefore, this soluble part of TRAIL, abbreviated to sTRAIL, is regarded as a potential pharmaceutical agent in cancer therapy, and the production of sTRAIL by recombinant biotechnique has been investigated in many systems [3, 4, 5].

* This work is supported by the Foundation of the Application Base and Frontier Technology Research Project of Tianjin to Yong Wang (Grant No. 08JCZDJC20800).

E. Zhu and S. Sambath (Eds.): Information Tech. and Agricultural Eng., AISC 134, pp. 143–149.
springerlink.com © Springer-Verlag Berlin Heidelberg 2012

Plants have been used to develop efficient bioreactors to produce pharmaceutical proteins. It has been estimated that production of pharmaceutical proteins by plant bioreactor will be much less expensive compared with other systems. Proteins accumulated in plants are also easy for storage and transport, and most importantly without the danger of contamination by human pathogens [6]. Chloroplasts are important organelles of plants. They are considered to be an efficient factory for foreign protein production because of their abundance in plant cells. Moreover, heterologous proteins expression in chloroplast can be protected from degradation of protease in cytosol. One efficient way for targeting foreign proteins into chloroplast is that a chloroplast transit peptide is fused to the N-terminal of foreign protein, which should be cleaved off by stromal processing peptidase in stroma. The chloroplast transit peptide of small subunit of ribulose-1, 5-bisphosphate carboxylase (Rubisco) gene from *Pisum sativum* has been successfully used in plants to target foreign proteins to chloroplasts [7, 8].

In this study, sTRAIL protein was expressed and targeted into the chloroplasts of transgenic tobacco plants by using the transit peptide of *rbcS* gene from *Pisum sativum*. In comparison we also obtained transgenic tobacco lines that were transformed with a construct without the cTP sequence.

2 Materials and Methods

2.1 Construction of Transformation Vectors

Plasmid harbouring the *strail* gene was provided by Prof. Dexian Zheng (Chinese Academy of Medical Sciences & Peking Union Medical College, China). sTRAIL encoding sequence was amplified by PCR with a pair of primers P1F: 5'-GGGGTACCATGGTGAGAGAAAGAGGTC-3' and P1R: 5'-CGGGATCCTTAG CCAACTAAAAAGGCCC-3', in which restriction sites *Kpn* I and *Bam*H I were underlined. The amplified product was then cloned into pPGN plasmid to generate the *35S:strail* expression vector.

Total DNA was extracted from *Pisum sativum* with CTAB method as described in Doyle and Doyle [9]. *rbcS* cTP encoding sequence (*ctp*) was amplified by PCR with primers PtpF: 5'- GGGGTACCATGGCTTCTATGATATCCTC-3' and PtpR:5'-CGGAATTC GTCGACGCACTTTACTCTTC CACCAT-3'. The 171bp fragment was then cloned into pMD-19 T-vector for sequencing. The correct *ctp* was digested with *Kpn* I and *Eco*R I restriction enzymes and inserted into pBluescript SK+ vector. The *ctp* fragment plus restriction sites of *Sal* I, *Eco*R I, *Pst* I, *Sma* I, *Bam*H I, *Spe* I and *Xba* I was cleaved out from *Kpn*I and *Xba* I sites, and then cloned into the pPGN vector to generate a universal vector pPGN-TP.

The sTRAIL encoding sequence was amplified by PCR with P2F: 5'-ACGCGTCGACGTCATGGTGAGAGAAAGA GGTC-3' and P2R: 5'-CGGGATCCCGTTAGCCAACTAA AAAGGCCC-3', in which the restriction sites *Sal* I and *Bam*H I were underlined, and then cloned into the corresponding sites of pPGN-TP, to generate the *35S:tp-strail* expression vector.

2.2 Agrobacterium Mediated Transformation

Two vectors generated in this experiment were transformed into *Agrobacterium tumefaciens* LBA4404 by electroporation, respectively. Tobacco plants of *Petite Havana* were grown in sterile conditions, cultured in 16 h photoperiod at 25℃, on MS medium containing 3% (w/v) sucrose and 0.8% (w/v) agar. Young leaves were cut into small squares, about 5mm×5mm, and infected with *Agrobacterium* containing *35S:strail* or *35S:tp-strail* constructs for 10-15min. After co-cultivation at 25℃ in dark, infected explants were transferred to selection medium, RMOP containing 250mg/L kanamycin and 300mg/L cefotaxime. Regenerated shoots were transferred to MS medium containing 250 mg/L kanamycin and 300 mg/L cefotaxime for rooting.

2.3 PCR Analysis

Total DNA was extracted from transformed tobacco lines and wild type tobacco with CTAB buffer as the method described previously. Primers specific to *strail* gene were used for detecting foreign gene insertion.

2.4 RT-PCR Analysis

Total RNA was extracted with TRNzol extraction buffer (TIANGEN Biotech., Beijing, China) following the protocol. RNA samples were then treated with DNase I (Takara, Dalian, China), to digest traces of genomic DNA. cDNA reversely transcribed by M-MLV(Promega) was used as template in RT-PCR analysis. The same primers as those for transgene insertion detection were used. Total RNA sample was used as template in PCR for DNA contamination detection.

2.5 Western Blot Analysis

100 mg leaves from transformed and untransformed tobacco were used for protein extraction. Total soluble protein was extracted using the method described in Oey, et al [10].

40 μg total soluble protein (TSP) per sample was used for western blot analysis. Proteins were separated on 15% SDS-containing polyacrylamide gels for 30 min at 100 V, and then 3 h at 150 V. Separated proteins were transferred to a methanol-treated PVDF membrane (Millipore) by electro blotting at 100 mA for 1 h. Blocking was performed by incubation of the membrane in 5% (w/v) milk in TBST buffer for 1 h at room temperature. Then the membrane was incubated in TBST solution containing a 1:1000 dilution of commercially available rabbit anti-TRAIL polyclonal antibodies (Sigma) for 2h at room temperature. The membrane was washed with TBST buffer for four times, 15min each, and incubated in 1:5000 TBST dilutions of alkaline phosphatase-conjugated goat anti-rabbit IgG (Santa Cruz Biotechnology) for 1 h. After washing the membrane again as the method above, the incubation with Pro-light HRP lighting substrate (TIANGEN Biotech., Beijing, China) was performed and fluorescence signal was explored to X-ray films (FUJIFILM).

2.6 ELISA

Samples for ELISA analysis were prepared as described previously [11]. Total soluble proteins were diluted with extraction buffer and quantified by a commercially available enzyme-linked immunosorbent assay kit (R & D system) according to the manufacturer's protocol.

2.7 Test of Apoptosis in Tumor Cells

Human cervical cancer HeLa cells were maintained in Dulbecco's modified Eagle's medium (DMEM) supplemented with 10% fetal bovine serum, 4mM glutamine, 100U/ml penicillin, and 100 μg/ml streptomycin, and incubated at 37 ℃ in a humidified atmosphere of 5% CO_2. After 8h of cultivation, crude protein extracts from transgenic line and wild type tobacco were added into cell cultures, respectively. The concentration of sTRAIL from transgenic line in cell culture was about 0.2 μg/ml. After 48h of treatment, cells were observed by using an optical microscope.

3 Results

3.1 Construction of the Two Vectors

Two transformation vectors were constructed as shown in Fig.1A: *35S:strail* for untargeted and *35S:tp-strail* for chloroplast targeted expression. 35S promoter was used to regulate gene expression. Both expression constructs were linked to a expression cassette carrying the coding region of neomycin phosphotransferase Ⅱ (NPT Ⅱ), which confers the kanamycin resistant to transgenic plants. Fig. 1B shows the results of *Kpn* I/*Xba* I digestion. The fragment cleaved from *35S:tp-strail* construct was larger than that from the *35S:strail* construct.

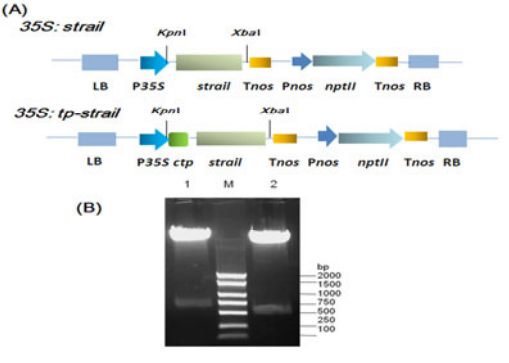

Fig. 1. Vector construction (A) Scheme of *35S:strail* and *35S:tp-strail* constructs. (B) Restriction analysis of vector construction with *Kpn* I/*Xba* I. Lane 1: Plasmid of *35S:tp-strail*; Lane 2: Plasmid of *35S: strail;* Lane M: Marker DGL 2kb.

3.2 The Presence of Foreign Gene

PCR was used for testing foreign gene insertion, by which 8 in 13 of *35S:tp-trail* and 3 in 9 of *35S:strail* independent resistant lines were confirmed (Fig.2).

3.3 Transcription of Strail Gene

3 independent lines T2, T3, T5 of *35S:tp-strail* and 3 independent lines L1, L3, L4 of *35S:strail* were used for transcription analysis by RT-PCR. Total RNA sample was used as template of PCR to prove that the contaminated DNA in it had been degraded completely (data not show). Results showed that *strail* gene was transcribed in all the selected lines (Fig.3).

3.4 Expression of sTRAIL Protein

Western blot was performed to test the expression of sTRAIL protein in transgenic tobacco plants. As shown in Fig. 4, *35S:tp-strail* transformed lines T2 and T3 accumulated sTRAIL protein to a detectable level, but no distinguishable protein accumulation was detected in *35S:strail* transformed lines. The accumulation of sTRAIL protein in T2 line was confirmed by ELISA analysis (data not shown). Our preliminary results also showed that sTRAIL protein expressed in T2 line had biological activity in inducing apoptosis in tumour cells.

4 Discussion

The high potential application in cancer therapy of sTRAIL has inspired us to express it in transgenic tobacco. Our results showed that a biologically active sTRAIL protein could be successfully expressed and accumulated by chloroplast targeting and that the chloroplast-targeted expression system is superior to non-targeted expression. The latter conclusion has been proved by several reports before [8, 12, 13].

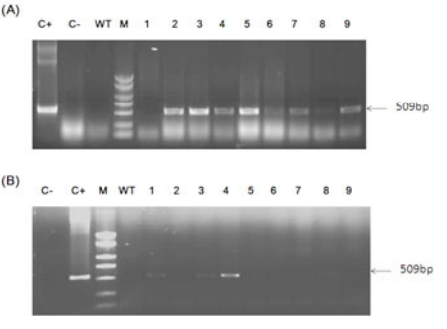

Fig. 2. PCR analysis of foreign gene presence (A) and (B) PCR detection of *35S:tp-stail* and *35S:strail* insertion, respectively. Lane C+:Positive control using plasmid as template; Lane C-:Negative control using water as template; Lane WT: Wild type tobacco; Lane 1-9: transgenic lines 1-9; Lane M: Marker DGL2k.

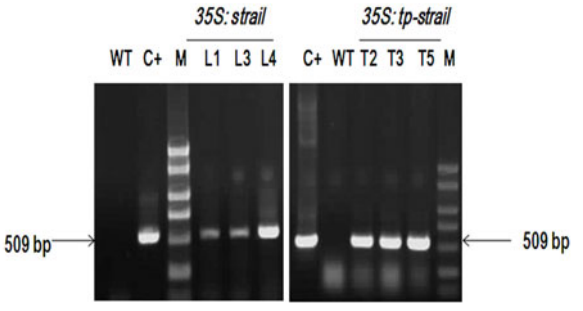

Fig. 3. RT-PCR analysis of *strail* transcription Lane C+:Positive control using plasmid as template; Lane WT: Wild type tobacco; Lane M: Marker DGL2k.

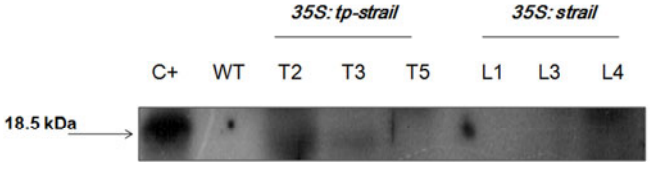

Fig. 4. Western Blott analysis of sTRAIL protein Lane C+: Positive control with 0.5 μg standard protein; Lane WT: Wild type tobacco.

However, the highest level of sTRAIL in our transgenic plants was estimated to be lower than 0.3% of the total soluble protein. This is too low for commercial application and therefore, should be improved in the future.

Recently, it was reported that a 5% TSP level of hyperthermostable endoglucanase Cel5A in tobacco was achieved, by which the 80-amino acids-N-terminal of Rubisco small subunit from *Arabidopsis thaliana* was used [13]. This strategy could be tested for sTRAIL expression in the future.

Acknowledgment. We would like to thank Dr. Yu-Shan Zhu for assistance in performing the apoptosis bioassay.

References

1. Wiley, S.R., et al.: Identification and characterization of a new member of the TNF family that induces apoptosis. Immunity 3(6), 673–682 (1995)
2. Ashkenazi, A., et al.: Safety and antitumor activity of recombinant soluble Apo2 ligand. J. Clin. Invest 104(2), 155–162 (1999)
3. Lin, Z.H., Lei, H.Z., Cao, P.: Expression, purification, and in vitro refolding of soluble tumor necrosis factor-related apoptosis-inducing ligand (TRAIL). Protein Expres. Purif. 51(2), 276–282 (2007)
4. Xu, H., Lai, X.T., Ye, K., Ma, H.W., Hong, K.: Expression of a DNA fragment encoding the active domain of human TNF related apoptosis inducing ligand in pichia pastoris. Sheng Wu Gong Cheng Xue Bao 19(2), 163–167 (2003) (in Chinese)

5. Walczak, H., et al.: Tumoricidal activity of tumor necrosis factor-related apoptosis-inducing ligand in vivo. Nat. Med. 5(2), 157–163 (1999)
6. Daniell, H.: Production of biopharmaceuticals and vaccines in plants via the chloroplast genome. Biotechno. J. 1(10), 1071–1079 (2006)
7. Van Breusegem, F., et al.: Processing of a chimeric protein in chloroplasts is different in transgenic maize and tobacco plants. Plant Mol. Biol. 38(3), 491–496 (1998)
8. Kim, E.H., et al.: Chloroplast-targeted expression of synthetic cry1Ac in transgenic rice as an alternative strategy for increased pest protection. Planta 230(2), 397–405 (2009)
9. Doyle, J.J., Doyle, J.L.: Isolation of plant DNA from fresh tissue. Focus 12, 13–15 (1990)
10. Oey, M., Lohse, M., Kreikemeyer, B., Bock, R.: Exhaustion of the chloroplast protein synthesis capacity by massive expression of a highly stable protein antibiotic. Plant J. 57(3), 436–445 (2009)
11. Youm, J.W., et al.: High-level expression of a humanβ-site APP cleaving enzyme in transgenic tobacco chloroplasts and its immunogenicity in mice. Transgenic Res. 19(6), 1099–1108 (2010)
12. Hood, E.E., et al.: Subcellular targeting is a key condition for high-level accumulation of cellulase protein in transgenic maize seed. Plant Biotechnol. J. 5(6), 709–719 (2007)
13. Kimm, S., Lee, D.S., Choi, I.S., Ahn, S.J., Kim, Y.H., Bae, H.J.: Arabidopsis thaliana Rubisco small subunit transit peptide increases the accumulation of Thermotoga maritime endoglucanase Cel5A in chloroplasts of transgenic tobacco plants. Transgenic Res. 19(3), 489–497 (2010)

Comparative Study in Functional Morphology of Antennary Gland of Pacific White Shrimp, Litopenaeus Vannamei, Reared under Various Salinity Condition

Xugang He*, Guangfu Hu, and Guangtao Lu

Fisheries College Huazhong Agriculture University Wuhan, Hubei Province, China
xgh@mail.hzau.edu.cn

Abstract. The microstructure of antennary gland of Pacific white shrimp was observed and the effect of salinity on this microstructure was studied. The results show that antennary gland consists of coelomosac, labyrinth and nephridial canal. The coelomosac lies in the center of the antennary gland, and takes up most of the gland. The coelomosac wall is composed of podocytes and basement membrance. The projections of the podocytes are connected with the basement membrance. The labyrinth closes the whole gland, and its columnar cells are possessed of microvilli and basal plasmalmmal invaginations. The nephridial canal cells also have microvilli but shorter, its basal plasmalmmal invaginations is deeper and wider. When the shrimp was cultured with lower salinity, the clearance and the volume of coelomosac its antennary gland are smaller, while the length and density of microvilli on the apical side of labyrinth and nephridial canal is longer, the basal plasmalmmal invaginations is wider.

Keywords: Litopenaeus vannamei, antennary gland, microstructure, salinity.

1 Introduction

The Pacific white shrimp, *Litopenaeus vannamei,* is a euryhaline species capable of tolerating a wide range of environmental salinity (0.5 to 40 ppt) [1, 2]. The ability of *L. vannamei* to tolerate a wide range of salinities has made it a popular species for low salinity culture [3, 4, 5]. Now the culture of *L. vannamei* in inland low salinity waters is currently being practiced in various countries around the world.

As so far, information about metabolism or biochemical composition of white shrimp at different salinities is limited. The physiological responses are believed to be essential to assess the animal performance at different environmental conditions [6, 7, 8, 9].

The antennary gland is the emunctory of the Crustacea, In marine decapods, it is involved in the control of hemolymph volume, the hyporegulation of magnesium and sulfate in the hemolymph, excretion of organic compounds and reabsorption of fluid,

* Corresponding author.

E. Zhu and S. Sambath (Eds.): Information Tech. and Agricultural Eng., AISC 134, pp. 151–159.
springerlink.com © Springer-Verlag Berlin Heidelberg 2012

sugars and amino acids from the primary urine filtrate [10, 11]. The function of the antennal gland in penaeid shrimp has been associated with the differences in the osmolarity and sodium and chloride concentration between hemolymph and urine. As in the majority of stenohaline and euryhaline crustaceans, the urine in penaeid shrimps is isosmotic to the hemolymph [12, 13]. In penaeid shrimps, the urine is hypoionic to the hemolymph with respect to sodium and isoionic to the hemolymph with respect to chloride [12, 13].

A few studies in the morphorlogy of antennal gland have been revealed in some crustacean species [14, 15, 16], but there was no information about that of white shrimp.

The objectives of the present study were to elucidate the structure of white shrimp antennary gland and the histological changes in the antennary gland of *L. vannamei* when acclimated in water with salinity of 2‰, 7‰, 12‰, 17‰ and 30‰, respectively.

2 Materials and Methods

2.1 Materials and Experimental Designs

Juvenile white shrimp, obtained from Wuhan Aquaculture Company, were held in two fiberglass tanks (60×50×50 cm) at a salinity of 10‰ for 5 days. Then, the salinity was adjusted at a rate of 2‰ per day to target values by adding freshwater or artificial seawater. Seawater was prepared by adding artificial sea salt (Reef Crystals) to natural pond water, and filtered through an activated carbon cartridge for at least 3 days before entering the culture system.

After being acclimated from 10‰ to 2.0‰, 7.0‰, 12.0‰, 17.0‰ and 22‰ separately, juvenile shrimp were randomly stocked into 15 tanks (60×50×50 cm) at a density of 60 individuals per tank with triplicates. During the 70-day experiment, shrimp was fed twice per day (10:00am and 18:00pm) with a commercial feed, which contains 41.1% crude protein, 9.6% crude lipid, 12.0% ash, and 10.0% moisture, at a daily rate of 5% wet body weight. Residue feed was siphoned out 2 hours later after feeding. Tank water was circulated by an 8 W pump with a daily retention in the tank. During whole experiment period, the water temperature was fluctuated within 27.9°C to 29.5 °C, dissolved oxygen, 5.63 mg/L to 6.64 mg/L, and total ammonia nitrogen, less than 0.01 mg/L.

2.2 Tissue Preparation for Histological Observation

At the end of experiment, 10 individuals of shrimp were take out from each tank and anaesthetized on ice; the antennary glands were dissected out and fixed in Bouin's solution for 24 h, then dehydrated through a series of increasing concentrations of ethanol, cleared in xylene, infiltrated with liquid paraffin at 58 °C, and finally embedded in paraffin blocks. The blocks were trimmed and sectioned at 5~7μm thick and stained with Harris' Hematoxylin and counter-stained with Eosin (H&E stain).

The sections were viewed and photographed with a Nikon Optiphot compound microscope equipped with planachromatic objective lenses and an HFX-II photomicrographic attachment. The microscope was calibrated with a stage micrometer (100 lines/mm).

3 Results

3.1 The Outline and Cross-Section of Antennary Gland

With the base of the antenna, there is a fabaceous body of a undertone colour, in shape somewhat like one of the fruits of the horsebean, which is known as the antennary gland. The antennary gland consists of the coelomosac, labyrinth and nephridial canal. The open blood sinuses and small arteries are scattered within the antennal gland. The coelomosac lies in the center of the antennary gland, and takes up most of the gland. The labyrinth closes the whole gland, and nephridial canal lies in one side of the gland (see Plate I).

Plate 1：The outline and cross-section of antennary gland (1~4) and Microstructure of coelomosac (5~8)

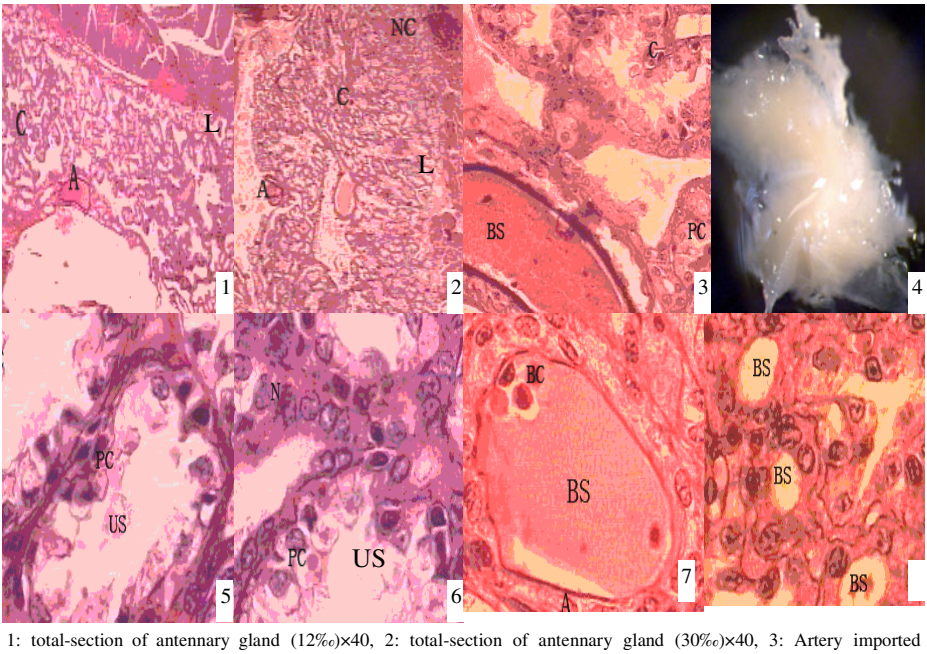

1: total-section of antennary gland (12‰)×40, 2: total-section of antennary gland (30‰)×40, 3: Artery imported antennary gland (30‰)×400, 4: Antennary gland×2.5, 5: Small room in coelomosac (2‰)×1000, 6: Coelomosac (7‰)×1000, 7: Small artery in coelomosac (12‰)×1000, 8: Blood sinuse in coelomosac (17‰)×1000.

A: Artery, BS: Blood spaces, C: Coelomosac, L: labyrinth, NC ： Nephiridial canal, PC: Podocyte, US: Urine spaces, R: small room, N: Nucleus, M:Membrane of coelomosac.

Plate Ⅱ : Microstructure of labyrinth and Nephiridial canal

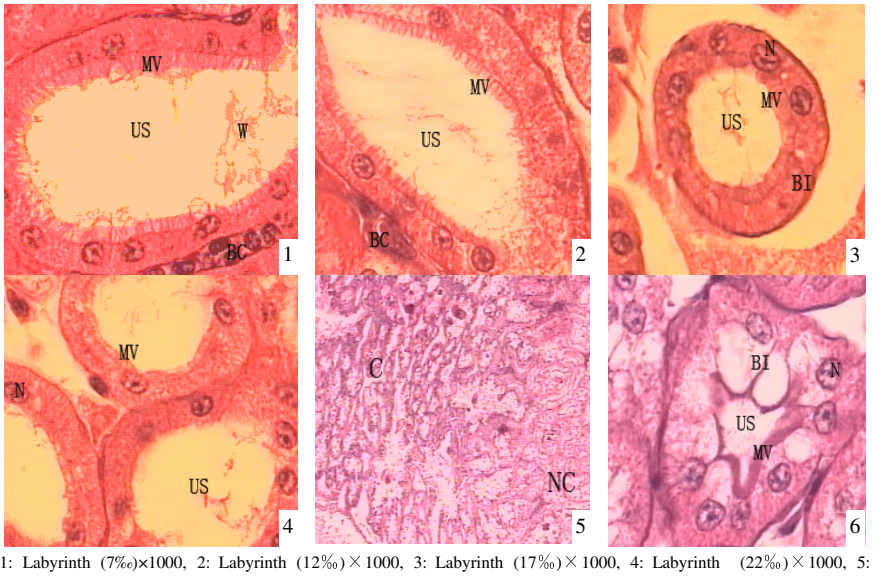

1: Labyrinth (7‰)×1000, 2: Labyrinth (12‰)×1000, 3: Labyrinth (17‰)×1000, 4: Labyrinth (22‰)×1000, 5: Nephiridial canal (22‰)×100, 6: Nephiridial canal (2‰)×1000.

C: Coelomosac, L: labyrinth, US: Urine spaces, N: Nucleus, MV: Micovilli, BI: basal plasmalmmal invaginations, W: Substanse in antrum, BC: Blood cell, NC: Nephiridial canal, BI: basal plasmalmmal invaginations.

Plate Ⅲ: The compare among total-section of antennary gland reared in various salinity condition

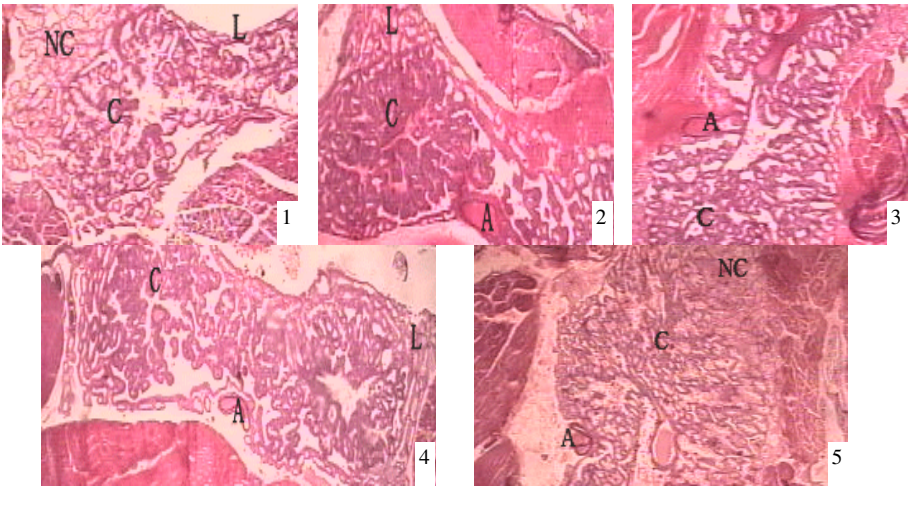

1: total-section of antennary gland (2‰)×40, 2: total-section of antennary gland (7‰)×40, 3: total-section of antennary gland (12‰)×40, 4: total-section of antennary gland (17‰)×40, 5: total-section of antennary gland (30‰)×40.

C: Coelomosac, L:labyrinth, NC:Nephiridial canal, A: Artery.

Plate Ⅳ: The compare among antennary gland reared in various salinity condition

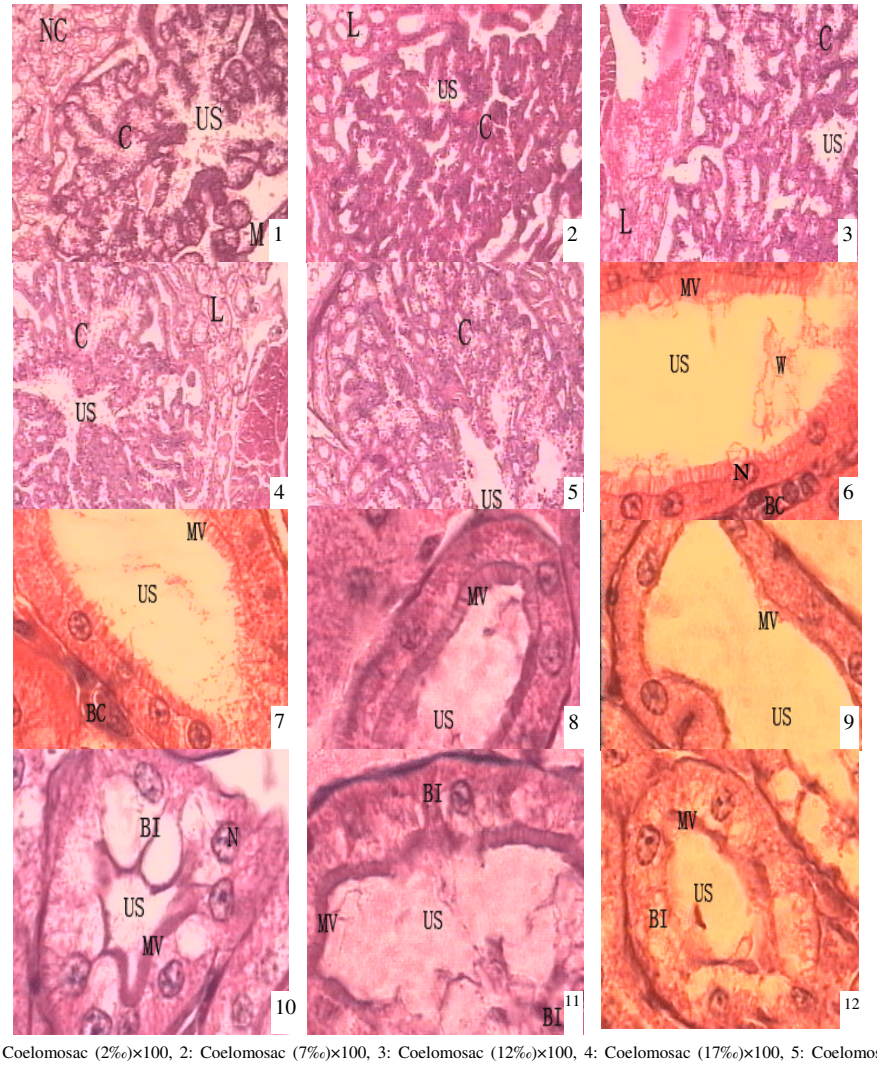

1: Coelomosac (2‰)×100, 2: Coelomosac (7‰)×100, 3: Coelomosac (12‰)×100, 4: Coelomosac (17‰)×100, 5: Coelomosac (22‰)×100, 6: labyrinth (7‰)×1000, 7: labyrinth (12‰)×1000, 8: labyrinth (17‰)×1000, 9: labyrinth (22‰)×1000, 10: Nephiridial canal (2‰)×1000, 11: Nephiridial canal (7‰)×1000, 12: Nephiridial canal (30‰)×1000.

C: Coelomosac, L: labyrinth, NC: Nephiridial canal, US: Urine spaces, BI: basal plasmalmmal invaginations, MV: Micovillus.

3.2 Microstructure of the Antennary Gland

1) Coelomosac: The transverse section of the antennary gland shows that the coelomosac lies in the center of the antennary gland, and takes up most of the gland (see Plate I). The outskirt of coelomosac is smooth, but there are many small gauffers that divide the coelomosac into many small rooms. The coelomosac wall is composed

of podocytes and basement membrance. The projections of the podocytes are connected with the basement membrance. In addition, there are lots of blood sinuses and small arteries that are dispersed in the coelomosac.
2) The labyrinth: The labyrinth located in the outside of coelomosac, and enclose the whole gland.The front side of the tubules of labyrinth connect with the coelomosac. The canal of the labyrinth are compossed of a single layer columnar cells, which have long and regular microvilli on the apical side and basolateral infolding on the base (see Plate Ⅱ).
3) The nephridial canal: The nephridial canal located in the top of antennary gland, it is composed of lots of frizzy canals (see Plate II). The canals are also composed of a single layer cells, but the cells are hypertrophied and irregulaer. The nephridial canal cells also have microvilli and the plasmalemmal invaginations, but microvilli is shorter than that in labyrinth epithelial cell, the plasmalemmal invaginations in the basal and lateral cell membranes of the nephridial canal epicthelial cell are deeper and more considerable than that labyrinth epithelial cell.

3.3 Comparison among Microstructure of Antennary Gland of Shrimp Reared Under Different Salinity Condition

1) The total-section of antennary gland: The comparison among total-section of antennary gland show that there are no obvious differences in the morphology of antennary gland within the shrimp reared in different salinity condition (see Plate III) except that the color of antennary gland is deeper for the shrimp reared in higher salinity .

2) Coelomosac of antennary gland: Silinity has a significant effect on the clearance and volume of coelomosac. When the shrimp was cultured in higher salinity, the clearance and volume of coelomosac of antennary gland increased (see Plate IV).

3) Labyrinth of antennary gland: The volume of the labyrinth in the shrimp reared in low salinity have a higher proportion than that of the shrimp reared in high salinity (see Plate 4). Furthermorel, the plasmalemmal invaginations in the basal and lateral cell membranes of the labyrinth epicthelial cell are deeper and more considerable in shrimp reared in lower salinity than in high salinity.

4) nephiridial canal of antennary gland: The comparison of the nephiridial canal among shrimps reaed in different salinity shows that there is no obviouse difference in the volume of the nephridial canal. But the plasmalemmal invaginations in the basal and lateral cell membranes of the nephridial canal and epicthelial cell are deeper and more considerable in the shrimp reared in lower salinity than that reared in high salinity(see Plate 5).

4 Discussion

Generally speaking, the antennary gland of the crustacean has an analogy to the kidney of the mammal, the coelomosac is similar to the renal corpuscle, the labyrinth is alike to the proximal convoluted tubule, the nephiridial canal is analogous to the

distal convoluted tubule [17]. The blood sinuses and small artries are like to the glomerulus.

4.1 Coelomosac

The coelomosac lies in the center of the antennary gland, and takes up most of the gland. The outskirt of coelomosac is smooth, but there are many small gauffers that divide the coelomosac into many small rooms.

The coelomosca wall is composed of podcytes and basement membrance. The projections of the podocytes are connected with the basement membrane. The blood plasma in the blood sinuses and small arteries is filtered by the basement membrane of the coelomosac then the wall of the small artery into the coelomosac and forms primary urinary. The podocytes play a role in absorbing large molecular matter from the primary urinary, and in intracell digestion and detoxification.

4.2 The Labyrinth

The epithelia of labyrinth have long and regular microvilli on the apical side and basolateral infolding on the base, which greatly promoted to exchange between cell and interstitial substance. The activity of Na^+, K^+-ATPase in the basolateral infolding is higher [18].

It has been suggested that Na^+, K^+-ATPase is of central importance in ion regulation and cellular water balance by aquatic vertebrates and invertebrates, and directly related to their osmoregulation capacity [19]. The activity of Na^+, K^+-ATPase reflected the osmoregulation of crustaceans. The Na^+, K^+-ATPase was positioned to pump sodium ions from the cytosol across the basolateral membrane into the extracellular fluid in exchange for potassium ions moving in the opposite direction (reviewed by Reference [20]).The basolateral Na^+, K^+-ATPase generated an electrochemical gradient for Na^+ from the plasma to the cytoplasm, which drove both Na^+ and Cl^- inward across the basolateral membrane, so the labyrinth plays an important role in maintaining osmotic balance. In addition, the tubules of the labyrinth can reabsorb large molecular matter, water, and abio-ions, and appearcation be active in eliminatling waste.

4.3 The Nephridial Canal

The cells of the nephridial canal are less compact, larger, and cuboidal to columnar in shape. The plasmalemmal invaginations in the basal and lateral cell membranes of the nephridial canal epicthelial cell are deeper and more considerable than that labyrinth epithelial cell. The epithelial cell of the nephridid canal can farther absorb water and abio-ions from the lumen of the nephridial canal. It plays an important role in the formation of highly osmotic urinary.

4.4 The Effect of Culturing Salinity on the Microstructure of Antennary Gland

Because the osmotic pressure in the shrimps that lived in low salinity is greatly different with the osmotic pressure in their environment, while it's almost the same to those shrimps that lived in high salinity. So in shrimps living in low salinity, the

structure related to osmoregulation in canal portion of excretory organ such as microcilli, basolateral infoldings, mitochondria and so on, are more abundant and more developed than those in high shrimps, so do the structures related to excretion. These specified the unity of structure and function in crustaceans. For crustaceans, feature are chiefly the result of long term adaptability to their environment.

The filtration barriers of excretion in developed or less developed crustaceans are consist of podocytes, slit membrane, basal lamina and the pores of endothelia cells. 99 percent of ingredients of blood through these barriers into coelomosac and become the initiative filtrate solution. From this solution, the podocytes reabsorbed, digested and utilized glucose and part of proteins, peptides and amino acids are reabsorbed by podocytes and labyrinth cells, then become formed bodies and secreted into urinary space again and flow with the urine. These nutritions are digested in formed bodies and then reabsorbed and utilized by cells of nephridial canal. At the same time, the labyrinth cells reabsorbed a small part of ions and water through isomostic way from initiative filtrate solution, then the most of ions and water of this solution are reabsorbed by the cells of nephridial canal through active transport. And the cells of nephridial canal secreted H^+ into urine to regulation its pH. At last, the waste of metabolism and hetero-materials such as toxical materials which are invaded into the organisms accidentally are excreted with the urine. Then the role of holding organisms' homeostasis of excretory organs is completed.

Acknowledgment. This study was supported by natural science foundation of Hubei Province, China (Project no. 2006ABA161). The authors are grateful to Jing Chen and Libo Sheng for their help during shrimp culture.

References

1. Menz, Blake, B.F.: Experiments on the growth of Penaeus vannamei. J. Exp. Biol. Ecol. 48, 99–111 (1980)
2. Bray, W.A., Lawrence, A.L., Leung-Trujillo, J.R.: The effect of salinity on growth and survival of Penaeus vannamei, with observations on the interaction of IHHN virus and salinity. Aquaculture 122, 133–146 (1994)
3. McGraw, J.W., Davis, D.A., Teichert-Coddington, D., Rouse, D.B.: Acclimation of Litopenaeus vannamei postlarvae to low salinity: influence of age, salinity endpoint, and rate of salinity reduction. J. World Aquac. Soc. 33, 78–84 (2002)
4. Samocha, T.M., et al.: Review of some recent developments in sustainable shrimp farming practices in Texas, Arizona, and Florida. J. Appl. Aquac. 12, 1–30 (2002)
5. Samocha, T.M., Lawrence, A.L., Pooser, D.: Growth and survival of juvenile Penaeus vannamei in low salinity water in a semi-closed recirculating system. Isr. J. Aquac. 50, 55–59 (1998)
6. Hernández, R.M., Bückle, R.L.F., Palacios, E., Barón, S.B.: Preferential behavior of white shrimp Litopenaeus vannamei (Boone 1931) by progressive temperature–salinity simultaneous interaction. J. Therm. Biol. 31, 565–572 (2006)
7. Allan, E.L., Froneman, P.W., Hodgson, A.N.: Effects of temperature and salinity on the standard metabolic rate (SMR) of the caridean shrimp Palaemon peringueyi. J. Exp. Biol. Ecol. 337, 103–108 (2006)

8. Menezes, S., Soares, A.M.V.M., Guilhermino, L., Peck, M.R.: Biomarker responses of the estuarine brown shrimp Crangon crangon L. to non-toxic stressors: temperature, salinity and handling stress effects. J. Exp. Mar. Biol. Ecol. 335, 114–122 (2006)
9. Cheng, W., Chen, J.C.: Effects of pH, temperature and salinity on immune parameters of the freshwater prawn Macrobrachium rosenbergii. Fish Shellfish Immunol. 10, 387–391 (2000)
10. Riegel, J.A., Cook, M.A.: Recent studies of excretion in Crustacea. In: Wessing, A. (ed.) Excretion. Fortschritte der Zooogie 23, pp. 48–74. Gustav Fisher Verlag, Stuttgart, Germany (1975)
11. Mantel, L.H., Farmer, L.L.: Osmotic and ionic regulation. In: Mantel, L.H. (ed.) The Biology of Crustacea, Internal Anatomy and Physiological Regulation, vol. 5, pp. 54–162. Academic Press, New York (1983)
12. Bursey, Lane, C.: Osmotic regulation in the pink shrimp Penaeus dourarum Burkenroad. Comp. Biochem. Physiol. 39A, 483–493 (1971)
13. Castille, F.L., Lawrence, A.L.: A comparison of the osmotic, sodium, and chloride concentrations between the urine and hemolymph of Penaeus setiferus (L.) and Penaeus stylirostris Stimpson. Comp. Biochem. Physiol. 70A, 525–528 (1981)
14. Ueno, M., Inoue, Y.: The Fine Structure of Podocytes in Crayfish Antennal Glands. Journal of Electron Microscopy 45(5), 95–400 (1996)
15. Peterson, R., Loizzi, R.F.: Ultrastructure of the crayfish kidney coelomosac, labyrinth, nephridial canal. J. Morphology 142, 241–263 (1974)
16. Miyawaki, M., Ukeshima, A.: On the ultrastructure of the antennal gland epithelium of the crayfish Procambarus clarkia. J. Sci. 8, 59–73 (1967)
17. Kirschner, L.B.: Comparative physiology: invertebrate excretory organs. Annual Review of Physiology 29, 169–196 (1967)
18. Peterson, D.R., Loizzi, R.F.: Regional cytology and cytochemistry of the crayfish kidney tubule. J. Morphology 141, 133–146 (1973)
19. Towle, D.W.: Role of Na+, K+-ATPase in ionic regulation by marine and estuarine animals. Biol. Lett. 2, 107–122 (1981)
20. Lucu, Č., Towle, D.W.: Na+, K+-ATPase in gills of aquatic crustacean. Comp. Biochem. Physiol. 135(A), 195–214 (2003)

Association of PS1 Gene Polymorphisms with Alzheimer's Disease in Chinese Population: A Meta-Analysis of Case-Control Studies

Yaodong Zhang, Yong Xu*, and Hongwei Nei

School of Radiation Medicine and Public Health Soochow University Suzhou, Jiangsu Province China
childhealth@suda.edu.cn

Abstract. The aim of our study was to assess the association of PS1 gene polymorphisms with Alzheimer's disease in Chinese population using a meta-analysis. We identified 11 studies and found significant associations with Alzheimer's disease for 1/2 genotype of PS1 gene polymorphism (odds ratio 0.69, 95%confidence interval 0.50–0.94, P=0.02), under dominant and recessive genetic models, associations were also exited. The heterogeneity existed among all studies (P<0.05).The present meta-analysis suggested a significant association of PS1 gene polymorphisms with Alzheimer's disease in Chinese population. The 1/2 genotype of PS1 gene is associated with risk for Alzheimer's disease in the Chinese population.

Keywords: Alzheimer's disease (AD), Presently 1 gene, Polymorphism, Meta analysis.

1 Introduction

Alzheimer's disease (AD) is a common cause of morbidity and mortality in the elderly. The key features of AD brains are neuronal and synapse loss, extracellular plaques composed of Amyloid-β peptides and intrapersonal neurofibrillary tangles consisting of hyperphosphory lated tau protein. Genetic factors are believed to contribute substantially to an individual's risk for developing Alzheimer disease. The APOE4 allele is the only genetic factor that is unequivocally associated with an increased risk of late-onset AD [1, 2]. But it has been estimated to account for less than half of the genetic contribution to AD risk, Beyond this, nearly 1,000 papers have been published claiming or refuting association between Alzheimer disease and literally hundreds of putative risk alleles in other genes [3].

Wragg.et al. [4] firstly described an association with variation in balletic polymorphism of the presenilin 1 gene (PS1 gene in the intron region 3 to exon8.subsequent studies of this polymorphism have shown inconsistent results. In some studies,PS1 allele1 was found to be associated with the risk for AD[5,6].while in other studies, PS1 allele1 was found to have no association with the risk for AD [7,8,].

* Corresponding author.

A. Xie, X. Huang (Eds.): Advances in Computer Science & Education, AISC 140, pp. 161–166.
springerlink.com © Springer-Verlag Berlin Heidelberg 2012

In China, genetic association studies are also widely carried out to evaluate the relationship between these three polymorphisms and Alzheimer disease. Like the same situation in the worldwide populations, the obtained conclusions in Chinese populations are also inconsistent.

Therefore, we performed a meta-analysis with the aim of assessing the association of PS1 gene polymorphism with Alzheimer's disease in Chinese case-control studies.

2 Methods

2.1 Selection of Studies

We conducted a systematic computerized literature search for studies published before 12 August 2010.We searched the Chinese Biomedicine Database, the China National Knowledge Infrastructure plat-form, Pubmed and Medline, using the search terms' Alzheimer's disease', 'PS-1', 'polymorphism', 'China' and 'Chinese', without limiting to specific language. The full texts of the retrieved studies were carefully read to assess if they should be included in the meta-analysis. All of the references cited in the studies were also searched to identify potentially relevant articles.

2.2 Selection Criteria

The data were included in the following meta-analysis if the research papers fulfilled the subsequent two conditions: the association of Alzheimer's disease and PS-11/2, polymorphism was examined in Chinese in dividual; the genotype frequencies were reported in both patients and controls. After that, we re-evaluated the Hardy-Weinberg equilibrium (HWE) for every included study result, and the studies that did not follow HWE were excluded.

2.3 Data Extraction

Two workers examined the retrieved studies to extract…" Instead, try "R.B.G. thanks …" Put sponsor acknowledgments in the unnumbered footnote on the first page.the standard information from independent studies. From each study, the following information was collected: first author, year of publication, distribution of genotypes and alleles in both control and AD groups, average case and control characteristics (age, sex, and sample size).

2.4 Statistical Analysis

The strength of the association between the three gene polymorphisms and AD was evaluated by the odds ratio and the corresponding 95% confidence interval (CI). Based on the individual OR, a pooled OR was estimated, of which the statistical significance was determined using the Z-test. Where there was heterogeneity in studies, a pooled OR was estimated by the random effects model; otherwise, the fixed effects model was used. Funnel plots were used to investigate publication bias. All analyses were performed with Cochrane RevMan software version 5.0 (Cochrane Library, UK).

3 Results

For PS1 1/2 polymorphism, the literature research generated 15 papers, of which 11 articles met the election criteria (Table 1). The summary OR for 11/22 is shown in Table 2 , and the summary OR was 1.77(95%CI, 1.16–2.03), by random effects model (P=0.002), The heterogeneity was significant (I^2=76%).As shown in Table 2.The summary OR for 12/22 was 1.45(95%CI, 0.97–2.17), by random effects model (P=0.07).The summary OR for 1/2 was 1.26(95%CI, 0.99–1.61), by random effects model (P=0.06).The summary OR for dominant model was 1.68(95%CI, 1.08–2.61), by random effects model (P=0.02).The summary OR for recessive model was 0.68(95%CI, 0.58–0.79), by random effects model (P< 0.01).

Table 1. Characteristics of Studies Included in the Analyses and Distribution of Ps-1 Genotypes and Alleles For Cases and Controls

Study	Year	Area	Sample age and sex				genotypes and distribution			alleles	
			group	size	Age	Sex	1/1	1/2	2/2	1	2
Tang GM[9]	1999	Shanghai	AD	123	75.9±8.9	59/64	49	59	15	89	157
			Control	140	71.6±18.5	60/80	40	70	30	130	150
Ma QL[10]	2000	Guangdong	AD	75	81±8	29/46	28	40	7	96	54
			Control	73	78±8	39/34	17	38	18	72	74
Chen HD[11]	2004	Guangdong	AD	66	67.9±6.4	29/37	25	35	6	85	47
			Control	143	68.3±6.0	65/78	33	75	35	141	145
Wu DB[123]	2002	Beijing	AD	135	73.63±8.62	89/46	54	57	24	165	105
			Control	138	69.64±5.43	57/81	63	65	10	191	85
Wu XD[13]	1998	Shanghai	AD	71	76.9±8.8		26	37	8	90	52
			Control	69	68.9±6.0		31	28	10	90	48
Zhu JY[14]	2000	Shandong	AD	32	73`1±6.5		11	17	4	25	39
			Control	32	72.8±6.85		12	18	2	22	42
Ma C[15]	2000	Guangdong	AD	103	83±12.6	41/62	38	47	18	123	83
			Control	98	80.6±9.5	50/48	19	57	22	95	101
Bi JH[16]	1999	Shandong	AD	43	73.2±6.8		18	22	3	56	30
			Control	46	73.4±7.5		23	20	3	63	29
Zhang YD[17]	2004	Jiangsu	AD	144	71.5±7.3	72/72	50	77	17	177	111
			Control	140	71.3±7.6	71/69	25	74	31	144	136
Wu XD[18]	2000	Shanghai	AD	91			39	44	8	122	60
			Control	73			29	34	10	92	54
Jia LF[19]	2006	Hebei	AD	467	75.3±7.3		19	239	32	631	303
			Control	480			124	254	102	503	457
Hu CJ[20]	1998	Taiwan	AD	55	78.2(62-69)		23	25	7	71	39
			Control	93	79.2(67-87)		42	41	10	125	61

Table 2. Meta-analysis of association between PS1 Polymorphism and AD risk

Gene polymorphism	I2 (%)	Model	Pooled OR	OR(95%CI)	Z	P
1/2	75	Random-effects	1.26	0.99~1.61	1.86	0.06
11/22	76	Random-effects	1.77	1.03~3.04	2.05	0.04
12/22	60	Random-effects	1.45	0.97~2.17	1.83	0.07
Recessive	61	Random-effects	0.68	0.58~0.79	5.00	< 0.01
Dominant	70	Random-effects	1.68	1.08~2.61	2.31	0.02

4 Discussion

The present meta-analysis differed from the previous ones by focusing on Chinese population. Furthermore, we included the most extensive studies on the three polymorphisms by inclusion of recently published articles as well as all related articles published both in English and Chinese.

In a meta-analysis [21], including both white and Japanese data sets disclosed a significant association between the PS1 1/1 genotype and late onset Alzheimer's disease. Miguel RMet al. [22] have also conducted a meta-analysis and found that the PS-1 2/2 genotype is a risk factor for late onset Alzheimer disease in the Spanish population, and probably for Europeans. But for Chinese population, only two articles were included, and the number of included participants was limited. In order to confirm whether PS-1 is associated with AD in Chinese population, we did the current analysis including 11 studies with 1745 patients and 1525 controls.

The results indicated that the 1 allele showed borderline statistical significance on AD risk compared to 2 allele on Chinese population, and the meta analysis under other genetic contrasts revealed significant association of PS1 gene to AD in Chinese population .11 genotype of the PS-1 gene was significantly associated with increased risk of Alzheimer's disease in Chinese population.

The positive association of this polymorphism may be attributed to the polymorphism itself as well as linkage disequilibrium between this locus and another active locus in the PS1 gene. We attempted to further figure out possible interaction of the APOE and PS1 genes by conducting additional meta-analysis. Disappointedly, the number of related articles did not reach five articles by which number a meta-analysis can be done.

There are several limitations that should be considered when interpreting our results. Firstly, because of data limitation, we could not further divide studies into subgroups by age. Secondly, due to the lack of original data, we did not perform an evaluation of potential interactions such as gene-gene, gene environment, which might influence the results. Thirdly, publication bias occurred when investigated the effect of PS-1 1/2 on the risk of AD. Only published studies were included in the two meta-analyses, therefore, publication bias may have occurred.

Despite the limitations mentioned above, the present meta-analysis indicates that the 1/2 genotype of PS-1 is associated with susceptibility to AD in the Chinese population. Our present results also suggest that further studies using large numbers of participants, well-matched controls and multi-ethnic groups should be conducted to validate the association.

References

1. Saunders, A.M.: Association of Apo lipoprotein E allele epsilon 4 with late-onset familial and sporadic Alzheimer's disease. Neurology 43, 1467–1472 (1993)
2. Farrer, L.A.: Effects of age, sex, and ethnicity on the association between Apo lipoprotein E genotype and Alzheimer disease, a meta-analysis. J. Am. Med. Assoc. 278, 1349–1356 (1997)
3. Bertram, L.: Alzheimer's disease: one disorder, too many genes? Hum. Mol. Genet. 13, 135–141 (2004)
4. Wagg, M., Hutton, M., Talbot, C.: Genetic association between intron polymorphism in presenilin-1 gene and late-onset Alzheimer's disease. Lancet. 347, 509–512 (1996)
5. Sanchez-Guerra, M., Combarros, O., Infante, J.: Case-control and Meta analysis of low density lipoprotein receptor related protein gene axon 3 polymorphism in Alzheimer's disease. Neurosci. Lett. 316, 17–20 (2001)
6. Tilley Glamorgan, K., Grainger, J.: Evaluation of polymorphism in the Presenilin-1 gene and the butyrycholinesterase gene as risk factors in sporadic Alzheimer's disease. Eur. J. Hum. Genet. 7, 659–663 (1999)
7. Scott, W.K., Gowon, J.H., Roses, A.D.: Presenilin-1 polymorphism and Alzheimer's disease. Lancet. 347, 1186–1187 (1996)
8. Korovaitseva, G.I., Bukina, A., Farrer, L.A.: Presenilin-1 polymorphism in Alzheimer's disease. Lancet. 350, 336–337 (1997)
9. Tang, G.M., Zhang, M.Y., Jiang, S.D.: Association analysis between antichymotrypsin gene, presinilin 1 gene and Alzheimer's disease in China. Chin. J. Nerve Mint Dies 25, 31–33 (1999)
10. Ma, Q.L., Qian, C.Y., Liu, Z.L.: Intronic polymorphism of presenlin-1 gene with Alzheimer disease. Chinese Journal of Neurology 33, 283–285 (2000)
11. Chen, H.D., Liu, X.H., Wang, Y.P.: Association analysis between polymorphism of presinilin 1 gene and Alzheimer's disease. Journal of Modern Clinical Medical Bioengineering 10, 220–223 (2004)
12. Wu, D.B.: Analysis of presenlin-1, ApoE and MTHFR polymorphism or mutations in patients with dementia. The general hospital of Chinese Peoples Liberation Army, Beijing (2002)
13. Wu, X.D., Jiang, S.D., Jin, T.G.: Association analysis of presenilin 1 polymorphism with Alzheimer's disease. Chin. J. Geriatr. 17, 143–145 (1998)
14. Zhu, J.Y., Xu, W., Gao, Y.: Intronic polymorphism of presinilin 1 gene with Alzheimer's disease. Shandong Medical Journal 40, 14–17 (2000)
15. Ma, C., Li, Q., Fang, R.M.: Genetic association among polymorphism in presenilin 1 gene, APoE gene and late onset Alzheimer's disease. Chin. J. Nerv. Ment. Dis. 26, 345–348 (2000)
16. Bi, J.H., Zhang, J.H., Wang, Y.J.: Association between presinilin 1 gene and Alzheimer's disease. Qianwei Medical Journal 16, 37–39 (1999)
17. Zhang, Y.D., Shen, W., Ke, X.Y.: Correlation between intronic polymorphism of presinilin 1 gene and sporadic Alzheimer's disease. Chinese Journal of Rehabilitation 8, 6876–6878 (2004)
18. Wu, X.D., Jiang, S.D., Lin, S.C.: No association between the intronic presenilin 1 polymorphism and Alzheimer's disease in the Chinese Population. American Journal of Medical Genetics 88, 1–3 (2000)

19. Jia, L.F., Zhou, C.K., Love, H.Y.: Association between presenilin 1 intrinsic polymorphism and late onset Alzheimer's disease in the North Chinese population. Brain Research 1116, 201–205 (2006)
20. Hue Chosen Somalia, H.C.: Association of Apo lipoprotein E genotype and intrinsic polymorphism of the presenilin-1gene with Alzheimer's disease in elderly Taiwan, Chinese. Journal of Neurological Sciences 157, 158–161 (1999)
21. Yasuda, M., Hirono, N., Maeda, K.: Case-control study of presenilin-1 intronic polymorphism in sporadic early and, Alzheimer's disease. J. Neurol Neurosurg. Psychiatry 66, 722–726 (1999)
22. Mantas, M.R., Amorín-Díazb, M., Cañizares-Hernández, F.: Association study and meta-analysis of Alzheimer's disease risk and presenilin-1 intronic polymorphism. Brain Research 1170, 119–128 (2007)

Effects of Traditional Chinese Drug on Postoperative Immunoregulation in Breast Cancer Patients*

Guo-Yong Shan[1], Jun Yun[2], and Ling Wang[2]

[1] Radiotherapy Department, Zhengzhou People's Hospital, Zhengzhou, Henan Province, 450003, China
[2] Department of General Surgery, Xijing Hospital, Fourth Military Medical University Xi'an 710033, China
sgy_zzwy@qq.com, yunjun@fmmu.edu.cn

Abstract. Objective: To observe the effects of traditional Chinese drug Yiqiyangjing on the postoperative immune function in breast cancer patients. Method: 136 breast cancer patients who underwent modified radical mastectomy were randomly divided into treatment group and control group. The treatment group received a decoction of traditional Chinese medicine Yiqiyangjing since the 7th preoperative day and the 3rd postoperative day, while the control group received no additional traditional Chinese drug to the basic therapy same as the treatment group. Each immune index was determined on the 7th preoperative day as well as the 1st, 7th and 14th postoperative days respectively. Results: On the 14th postoperative day, immunoglobulin IgA, IgG and IgM of the treatment group were all significantly higher than those of the control group; CD4, CD4/CD8 and IL-2 were also significantly rebounded after 14-day treatment of traditional Chinese drug (P<0.05); and TNF-α was significantly increased after the surgery, and recovered to the preoperative level in the treatment group while remained at a high level in the control group after the 14th postoperative day. Conclusion: The traditional Chinese drug is beneficial to the postoperative recovery of humoral immune function and cellular immune function in breast cancer patients.

Keywords: Traditional Chinese drug, Breast cancer, Immunoregulation.

1 Introduction

As the postoperative survival rate of breast cancer has been continuously increasing, the significance of improving the postoperative quality of life (QOL) of breast cancer patients has caused people's extensive concern. Operation wound and tumor itself inhibit immune function of the body, and influence the key links of prognosis[1].

The therapeutic mode of determination of treatment based in pathogenesis obtained through differentiation of symptoms and signs and general view of Chinese medical science has distinct advantage in improving the QOL of patients with tumor. Traditional Chinese drug Yiqiyangjing was perioperatively administrated in 86 breast

* This work is partially supported by the science and technology plan projects of development and support of Zhengzhou city (No. 0910SGYS33377-1) and the natural sciences plan projects of education department of Henan province (No. 2010A310018).

E. Zhu and S. Sambath (Eds.): Information Tech. and Agricultural Eng., AISC 134, pp. 167–174.
springerlink.com © Springer-Verlag Berlin Heidelberg 2012

cancer patients who underwent surgery between October, 2003 and July, 2008. And here is the report.

2 Clinical Data

2.1 General Data

The patients were of Vascular & Endocrine Surgery of the Fourth Military Medical University between October, 2003 and July, 2008, 136 in all, and all underwent modified radical mastectomy for breast cancer. On the base of the admission numbers, the patients were randomly divided into 2 groups. 86 patients were of treatment group, (49.41±5.25) years old; and at clinical stage: 63 cases were at stage Ⅱ, and 25 were at stage Ⅲ; 42 cases' tumor diameters were <2cm and 28 were 2-5cm; and 51 cases had lymphatic metastasis, and 35 had no lymphatic metastasis. And 50 patients were of control group, and (47.62±7.58) years old; and at clinical stage:43 cases were at stage I, and 7 were at stage Ⅲ; 30 cases' tumor diameters were <2cm and 15 were 2-5cm; and 41 cases had lymphatic metastasis, and 9 had no lymphatic metastasis. The data difference between the two groups was of no statistical significance (P>0.05), but of comparability.

2.2 Diagnosis Criteria

All the cases were confirmed breast cancer by postoperative pathological examination. Karnofsky performance score (KPS) were >70', and the expected survival time were > 6 months. Referring to Criteria of Diagnosis and Therapeutic Effect of TCM Diseases of State Administration of Traditional Chinese Medicine [China], and seen in TCM view, the disease was postoperative insufficiency of pneuma in both spleen and kidney of breast cancer patients, with symptoms of different degrees of tiredness and weakness, lack of qi and no desire to speak, dizziness, poor appetite, pale tongue with whitish and thin slippery coating, and small and weak pulse.

3 Methods

3.1 Therapy

Besides the routine preoperative and postoperative therapeutic drugs, the treatment group received a decoction of traditional Chinese medicine Yiqiyangjing (composition: 25g of Radix Astragali, 15g of Radix Codonopsis, 15g of Rhizoma Atractylodis Macrocephalae, 10g of Poria, 15g of rehmannia dride rhizome, 15g of Radix Rehmanniae Preparata, 15g of Rhizoma Polygonati, 10g of Fructus Ligustri Lucidi and 12g of Pericarpium Citri Reticulatae) since the 7th preoperative day. The patients continued the decoction on the 3rd～14th postoperative days. While the patients of the control group only received routine preoperative and postoperative therapeutic drugs.

3.2 Examination Indexes and the Methods

The venous bloods of the patients of both groups were sampled and each immune index was determined on the 7th preoperative day as well as the 1st, 7th and 14th postoperative

days respectively. The immunoglobulins (IgA, IgG and IgM) concentrations of peripheral blood were assayed by radio immunoassay. T lymphocyte subsets (CD4, CD8 and CD4/CD8) concentrations of peripheral blood were assayed by flow cytometry. Serum cytokine IL-2 concentration and TNF-α concentration were assayed by ELISA kit of USA Sigma Company. Severe complications and the changes of biochemical indicators including blood routine examination result, hepatic and renal functions, and blood sugar were simultaneously observed.

3.3 Statistical Method

The data was recorded on the 7th preoperative day as well as the 1st, 7th and 14th postoperative days respectively, and then comparatively analyzed by SPSS statistical analysis software and in Matlab7.0 software programming environment for effect evaluation.

4 Results

4.1 Comparison of the Assaying Results of Preoperative and Postoperative Immunoglobulins (IgA, IgG and IgM) Concentrations of Peripheral Blood between the Two Groups

As shown in Fig.1, the immunoglobulins (IgA, IgG and IgM) concentrations of peripheral blood of each group on the 1st postoperative day were all somewhat

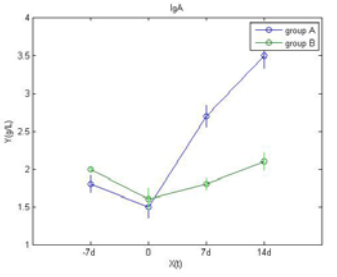

Fig. 1. The difference of immunoglobulins concentrations between the treatment group(A) and the control group(B) in the corresponding period (IgA).

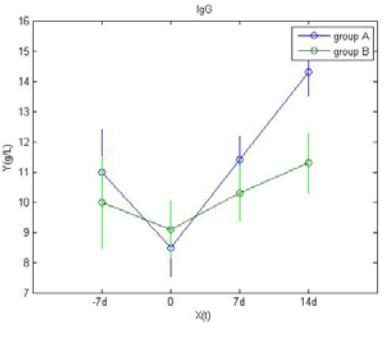

Fig. 2. The difference of immunoglobulins concentrations between the treatment group(A) and the control group(B) in the corresponding period (IgG).

deceased, and after 14-day treatment of traditional Chinese drug, IgA, IgG and IgM concentrations of the treatment group were significantly rebounded, and the difference compared with those of the control group was of statistical significance ($P<0.05$).

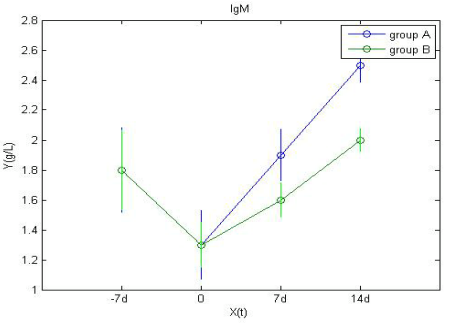

Fig. 3. The difference of immunoglobulins concentrations between the treatment group(A) and the control group(B) in the corresponding period (IgM).

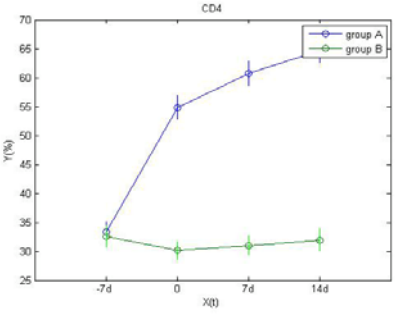

Fig. 4. The difference of T lymphocyte subsets concentrations between the treatment group(A) and the control group(B) in the corresponding period (CD_4).

4.2 Comparison of T lymphocyte Subsets Concentrations of Peripheral Blood between the Two Groups

As shown in Figure 2, after 14-day treatment of traditional Chinese drug, CD_4, CD_8 and CD_4/CD_8 concentrations of the treatment group were significantly rebounded, and compared with those of the control group in the corresponding period, the difference was of statistical significance ($P<0.05$).

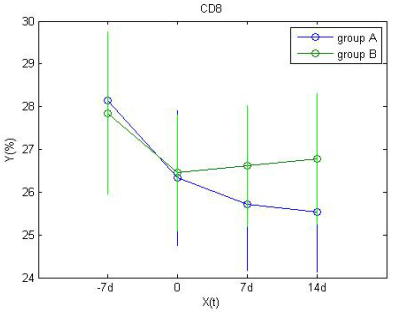

Fig. 5. The difference of T lymphocyte subsets concentrations between the treatment group(A) and the control group(B) in the corresponding period (CD_8).

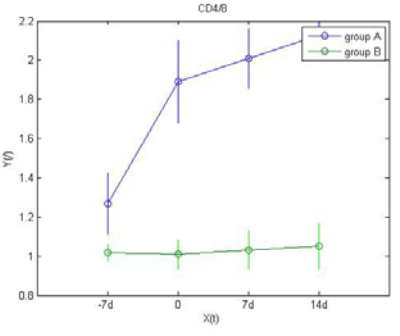

Fig. 6. The difference of T lymphocyte subsets concentrations between the treatment group(A) and the control group(B) in the corresponding period (CD_4/CD_8).

4.3 Comparison of the Changes of Preoperative and Postoperative Concentrations of Serum Cytokine IL-2 and TNF-α between the Two Groups

As shown in Figure 3, after the surgery, IL-2 concentration of the treatment was somewhat increased, while that of the control group was gradually decreased, and the differences of IL-2 concentrations on the 1st and 14th postoperative days between the two groups were of statistical significance ($P<0.05$); And TNF-α was significantly increased after the surgery, and after the 14th postoperative day, TNF-α recovered to the preoperative level in the treatment group while it was still significantly higher than that before the surgery in the control group, and the difference between the two groups was of statistical significance ($P<0.05$).

4.4 Adverse Reaction

During the study, of all the patients, the vital signs were stable, no death or other severe complication occurred, and the differences of the changes of biochemical indicators including blood routine examination result, hepatic and renal functions, and blood sugar were of no statistical significance ($P>0.05$).

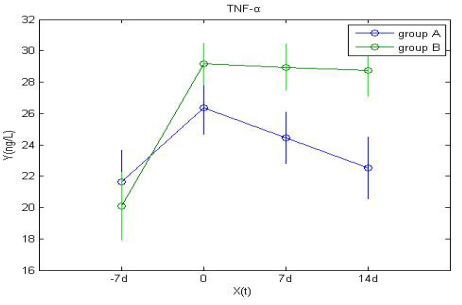

Fig. 7. The difference of preoperative and postoperative concentrations of serum cytokine IL-2 and TNF-α between the treatment group(A) and the control group(B) in the corresponding period (IL-2).

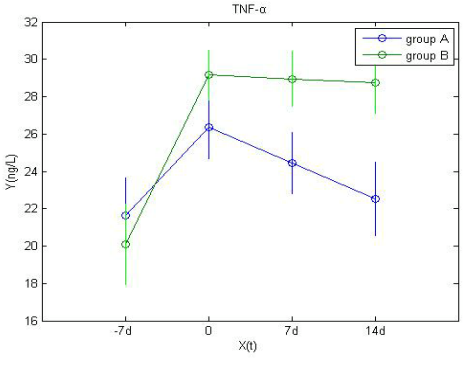

Fig. 8. The difference of preoperative and postoperative concentrations of serum cytokine IL-2 and TNF-α between the treatment group(A) and the control group(B) in the corresponding period (TNF-α).

5 Discussion

In TCM's view, the etiopathogenesis of breast cancer is "insufficiency in liver and kidney, deficiency of QI and blood, deficiency of Chong and Ren Channels, and abnormality of QI-blood circulation"[1]. The so-called "insufficiency in healthy qi" indicates not only absolute sufficiency or insufficiency, but also includes the balance between healthy qi and evil qi; here, "healthy qi" is called immune function in western medicine, and "evil qi" indicates various etiological factors. The onset and development of tumor is related with the immune state of the body, and inhibited cellular immune function is an important factor in the metastasis, relapse, and poor prognosis of tumor. T lymphocyte of the host is the primary functioning cell of the anti-malignancy immune surveillance system of the body. Therefore, immunosupression usually occurs during the development of tumor. Cytokine plays an important role in immunologic process of the body as the synthetic product of immune cells. Its concentration in blood can indirectly reflect the degree of immunologic reaction in postoperative patients[2].

On the base of TCM theory[3,4], breast cancer patients undergo the formation, relapse and metastasis mainly because of insufficiency in spleen and kidney, and the disability of the healthy qi to inhibit the evil qi. Although the tumors have been removed from postoperative patients who are receiving chemotherapy, the damage of the primary disease to the physiological and psychological functions of the body combined with the side effects of the surgery and chemotherapy can make the healthy qi more and more insufficient and the QOL decreased. Actually, breast cancer therapies, including radical surgery, radiotherapy and chemotherapy, are damaging to the body, and the general health of the patient is poor, which make the patient prone to local complications. While TCM in the treatment of breast cancer keeps relieving the primary and secondary symptoms at the same time in mind, entirely regulates yin-yang, qi-blood, viscera, channels and collaterals functions, can arouse the internal defensive function of the body and prevent the relapse and metastasis of the tumor. In recent years, application of traditional Chinese medicine in breast cancer patients has got more and more attentions[5-7].

It has been proved by modern pharmacology that Radix Astragali can exert its effect of supporting the healthy energy by directly or indirectly strengthening adrenal cortex function, can promote anti-tumor activities by increasing the reproductive activity of T cell, and can strengthen the transformation activity of lymphocyte, the immunity of which is low because of cyclophosphamide[8]. Radix Codonopsis[9] contains polysaccharide; polysaccharide is a regulator of biological response, has immunoregulation effect, can provide energy sources for ischemic systole, prevent from adrenal hypertrophy caused by adrenocorticotropic hormone, and also prevent from adrenal atrophy caused by cortical hormone. In addition, Radix Codonopsis and Radix Astragali have good effects of not only strengthening the phagocytosis of reticuloendothelial system but also strengthening the function of reticuloendothelial system, can improve the macrophage and T lymphocyte of the patients, have somewhat inhibitory effect on T suppressor cell, can protect hematopoietic system, decrease chemotherapy toxicity, and improve the immune function of the body. It is revealed by the study results that: Of T cell subsets of the treatment group, after the treatment, CD4 was increased, CD8 was decreased, CD4/CD8 ratio was increased, and IL-2 activity was increased. That manifests TCM Yiqiyangjing can correct the negative influence of T cell percentage and TNF-α of peripheral blood and significantly improve cellular immune function. In the aspect of humoral immunity, IgA, IgG and IgM levels of the control group on the 14th postoperative day were significantly lower than those of the treatment, which illustrates TCM Yiqiyangjing also has somewhat regulation effect on humoral immunity. To sum up, pre- and post-operative administration of TCM Yiqiyangjing in time can somewhat improve the immune function of breast cancer patients, and that is of significance in the following prevention of relapse and metastasis as well as the assurance of radiotherapy, chemotherapy and endocrine therapy conducted as scheduled.

References

1. Yuan, J., Kong, C., Kang, G., et al.: Effects of neoadjuvant chemotherapy combined with shenqifuzheng injection on cell immune function for patients with breast cancer. Lishizhen Medicine and Materia Medica Research 19(5), 1099–1101 (2008)

2. Hu, D., Li, Y., Liu, J.: Influence of herbal medicines with the function of Replenhing Qi and essence on the immune function of patients after mammary cancer operation. Journal of Traditional Chinese Medicine 49(1), 35–37 (2008)
3. Zhang, W., Wang, B., Shi, L.: Application of traditional Chinese medicine in modern breast cancer therapy. Chinese Journal of Integrated Traditional and Western Medicine in Intensive and Critical Care 9(1), 54 (2002)
4. Zhou, Q., Su, S.: Development of empirical study on the interference of traditional Chinese medicine in breast cancer. China Journal of Chinese Materia Medica 32(18), 1947–1950 (2007)
5. Shi, J., Wang, S., Wang, S., et al.: Traditional Chinese drug Erbeimu Capsule in the treatment of advanced breast cancer: in 60 cases. Journal of the Fourth Military Medical University 24(19), 1741 (2003)
6. Wang, J., Wang, C.: Clinical observation on traditional Chinese medicine capsules and plasters in the treatment for breast cancer: in 66 cases. Chinese Magazine of Clinical Medicinal 11(10), 1415 (2005)
7. Wang, X.: On Cassia Tuckahoe Capsule in the treatment of hyperplasia of mammary glands: in 300 cases. Chinese Journal of Misdiagnostics 8(27), 6701 (2008)
8. Liu, S., Fu, Z.: Immunoregulation effect and its clinical application of Radix Astragali. International Journal of Traditional Chinese Medicine 28(4), 203–205 (2006)
9. Leng, Y., Yang, Z., Xiao, Y., et al.: Clinical study on the immunoregulation effect of Huangqi Dangshen Mogu Decoction on post-chemotherapy advanced esophageal carcinoma and gastric cancer. Lishizhen Medicine and Materia Medica Research 19(6), 1474–1477 (2008)

The Research Progress of Bioinformatics-Led Design of Single-Chain Antibody Molecules*

Guo-Yong Shan[1] and Jian-Hua Zhang[2]

[1] Department of Radiation Oncology Zhengzhou People's Hospital
Zhengzhou 450053, China
[2] The Faculty of Biomedical Engineering Zhengzhou University Zhengzhou 450001, China
sgy_zzwy@qq.com, petermails@zzu.edu.cn

Abstract. The development of single-chain antibody (scFv) by recombinant gene expression is an important milestone for cancer gene therapy. Single-chain antibodies are reconstructed for cancer-targeted therapy to provide good penetration into tumor tissue and to improve their pharmacokinetics in vivo, offering a clinically valuable application. However, there may be some variation between the structure and function of the fusion proteins. Analyzing the interaction region between the antibody and the antigen, and the binding sites for molecular conformation, it is clear that the existing antibodies need to be modified, enhancing the biological activity of the antibodies. Based on the view that bio-molecular computer models are closely integrated with biological experiments, a bio-molecular structure–activity relationship model can be established in terms of molecular conformation, physical and chemical properties and the biological activity of single-chain antibodies. On the one hand, the structure–activity relationship is clear for new immune molecules at the gene expression level. On the other hand, a single-chain antibody molecule can be designed and optimized for the cancer-oriented treatment. In this review, we provide the theoretical and experimental basis for the development of single-chain antibodies appropriate for cancer therapy.

Keywords: Single-chain antibody, Fusion genes, Bioinformatics, Structure–activity relationship.

1 Introduction

A single-chain Fv antibody (scFv) is a protein comprising immunoglobulin heavy-and light-chain variable regions, directly or indirectly connected[1,2]. scFvs are ideal tools for constructing single-chain bispecific antibody fusion proteins[3,4]. Bivalent antibodies derived from scFvs using genetic engineering have promising applications clinical settings, as scFvs themselves are therapeutic, and can be used as vectors when combined with a toxin[5,6]. In recent years, there has been some progress in cancer

* This work is partially supported by the science and technology plan projects of development and support of Zhengzhou city (No. 0910SGYS33377-1) and the natural sciences plan projects of education department of Henan province (No. 2010A310018).

E. Zhu and S. Sambath (Eds.): Information Tech. and Agricultural Eng., AISC 134, pp. 175–181.
springerlink.com © Springer-Verlag Berlin Heidelberg 2012

gnosis and treatment using scFvs as carriers. However, the affinity and anti-tumor activity of an scFv can vary compared with that of the individual units.

The development of proteomics has led to an increase in studies on the composition, structure, and function of proteins. In studies on relationships between the structure and activity of fusion proteins, bioinformatics provides a powerful tool. One important aspect of bioinformatics is drug design based on structural simulation of biological molecules. The simulation of spatial structures and molecular drug design, including studies on fusion proteins with various functional domains and inter-peptide linkers, is a current research focus[7-9].

2 The Development of scFv Research

After 20 years of continuous in-depth study, scFvs have become increasingly valued in medicine, biology, immunology, and in many other disciplines. In particular, scFvs can maintain the affinity and specificity of the parental antibodies, allowing the fusion protein to bind to targeted cancer cells for diagnosis[10,11] or treatment of tumors[12-14].

The biological function of a protein derives from the characteristics of the native conformation or structure of the molecules. For fusion proteins to retain the activities of the linked units, the correct, native conformations must be formed. In the construction of single-chain antibodies, the affinity and stability of the fusion proteins within the spatial structure of the fusion protein determines whether the designed molecule has further penetrating power and a reasonable half-life. In recent years, there have been many studies on the design of single-chain antibody molecules[15,16]; however, it is a serious challenge for protein engineering to control the distance and orientation of the units of fusion proteins so that the function of the proteins can be optimized. Thus, it is important to understand how the structure of a protein relates to its function and mechanism of action. With the development of bioinformatics, computer-aided analysis systems have become essentials tool for protein engineering.

At present, homology modeling is widely accepted as a reliable model for predicting the practical structure of proteins from their amino acid sequence. Homology modeling can reliably obtain the three-dimensional structure of a protein for analyzing the relation between its structure and function, and to identify active sites[17]. From the perspective of bioinformatics, homology modeling was adopted[18] to build the three-dimensional structure of a single-chain antibody for hepatocellular carcinoma. The three-dimensional structural information helped us to design a humanized single-chain antibody specific for hepatocellular carcinoma, and to determine the characteristics of the molecule on the epitope of the hepatoma cell.

3 Challenges for Constructing scFv

Using bioinformatics, scientists have predicted and analyzed the spatial structure, and the physical and chemical properties, of antibodies, allowing the simulation of antigen binding sites, and even the design of new types of antibody molecules, to obtain high-affinity, low-antigenicity antibodies for enhancement of clinical applications[19-21]. The spatial structures are mostly analyzed for the antibody bound to the antigen, but it

is also very important, or even critical, that the hydrophobic interactions and electrostatic attractions are taken into account[22]. Thus, when antigen binding sites cannot be accurately predicted, the changes to the hydrophobic interactions and electrostatic attractions, within the context of the spatial structure, should be determined to aid in the identification of antigen–antibody binding sites. By analyzing published data, it is clear that the biological activities of fusion proteins are affected by factors such as structural characteristics, physical and chemical properties, the spatial position and conformation of the units of the fusion protein, and the size and complexity of the linkers.

3.1 The Impact of the Inter-peptide Linker on the scFv

The composition, length, and location of the linker between the heavy chain and light chain variable regions has an impact on the spatial structure, physical and chemical properties, and the biological activity of the fusion protein. Studies[23-25] have shown that it is very important that the flexible and hydrophobic peptide linkers join the functional domains of the protein without disturbing their functions. The use of different linkers will not change the isoelectric point, but the secondary structure of the proteins might be subtly altered. The most important function of a linker is to support and optimize the correct folding of molecules of the fusion proteins[26]. Unfortunately, there are no reliable selection criteria for designing linkers. Most linkers have been designed and selected by intuition, though there has been significant progress in the prediction of the secondary structure from the primary sequences of proteins; however, there is still very limited understanding of the relationship between the sequence and structure of proteins, especially of fusion proteins involving linkers.

By experimental analysis, Shibata *et al.*[27] suggested that linkers should be of sufficient length and good flexibility, to ensure that each unit of the fusion protein has enough freedom of movement and space to display their functions. On the basis of a large number of molecular biological experiments, scholars[28,29]. have reached the consensus that either linker can be too short to allow correct folding of protein antibodies due to intramolecular steric influence; or the linker can be too long to ameliorate the immunogenicity of the antibodies A long linker might also affect the antibody's activity and function. Computer-aided molecular design[30] and three-dimensional molecular modeling[31] are used with selected linkers for constructing molecular models of the spatial structure of single-chain antibodies; the spatial structure with the bound natural epitope is analyzed, which provides a further theoretical basis for the transformation of a single-chain antibody.

3.2 The Iimpact of Other Factors on scFv

The composition, structure and nature of each component of fusion proteins should be taken into account when selecting linkers for different molecules. Studies[32-35] have shown factors that affect the biological activity of the fusion protein include hydrophobic interactions and electrostatic attraction of fusion proteins and the complexity of the linkers. The expression of a fusion protein with an inter-peptide linker can encounter not only problems related to solubility, stability, and the fusion tag[36-37], but also serious degradation of the fusion protein. Many studies[38,39], indicate

that the length of the inter-peptide linker, its amino acid composition, the existence of glycosylation the adaptability of the various units with the inter-peptide linker, and even the codons of the inter-peptide linker, can affect the function and stability of the fusion protein. However, quantitative models have not been established for explaining the relationships between the spatial structures, physical and chemical properties, and the biological activity. Thus, the designed fusion proteins depend mainly on the experience of a "trial" and a "comparative" approach[40], and their optimization becomes problematic.

There are no reasons to believe, however, that a linker suitable for one antibody will be suitable for others, as can be deduced. Indeed, the expression level, solubility, and stability of an scFv depend largely on linker length and sequence, and vary significantly from one linker to another[41]. At present, theoretical research on inter-peptide linkers is still limited for fusion proteins. Although the biological activity and expression of a fusion protein can be improved by optimization of the protein units, we hope to use bioinformatics to analyze and predict the amino acid sequence, secondary structure, and physical and chemical properties of fusion proteins to gain a better understanding of their biological functions. This will allow the production of stable fusion proteins with lower costs in a faster time.

4 Exploring Ways to Solve the Problems

Homology modeling has been successfully applied to the interpretation of the correlation between protein sequences, structures, and functions. In particular, orthologous proteins often have conserved residues, and these residues can be interpreted by the protein 3D modeling. Using the structure model, multiple sequences of orthologous proteins can be compared and interpreted according to the restrictions of natural selection, requirements of protein folding, stability, dynamics and function. In effect, homology modeling can help us determine which functional groups the protein belongs to based on the analyses of critical conserved residues in the active sites and binding sites. Thus, homology modeling plays an important role in computer-aided drug design[42].

In conclusion, studies have highlighted the relationship between an antibody's binding activity and its 3-D conformation[43], which will provide direction for future antibody design and construction of IgM antibodies. Of course, more than one factor affects the biological activity of scFvs. The factors that need to be considered for the comparison of the structure and function of two proteins include the end-to-end distance, the binding sites, and the properties of the linker peptide. Other factors affecting the activity of scFvs will be discovered in future experiments; however, we hope that this review facilitates further research on single-chain antibodies. This review offers a valuable reference for the design of single-chain antibodies in the laboratory. Using the model of molecular quantization, different correlation models can be established that simulate spatial structures for molecular drug design. Combined with bioinformatics and genetic research, this can be used in searching and exploring new agents for gene therapy to combat malignant neoplasms.

References

1. Donaldson, J.M., Kari, C., Fragoso, R.C., Rodeck, U., Williams, J.C.: Design and development of masked therapeutic antibodies to limit off-target effects: Application to anti-EGFR antibodies. Cancer Biol. Ther. 8(22), 2145–2150 (2009)
2. Ohshima, M., Tadakuma, T., Hayashi, H., Inoue, K., Itoh, K.: Generation of a recombinant single-chain variable fragment (scFv) targeting 5-methyl-2'-deoxcytidine. J. Biochem. 147(1), 135–141 (2010)
3. Muller, D., Karle, A., Meissburger, B., Höfig, I., Stork, R., Kontermann, R.E.: Improved pharmacokinetics of recombinant bispecific antibody molecules by fusion to human serum albumin. J. Biol. Chem. 282(17), 12650–12660 (2007)
4. Stone, E., Hirama, T., Tanha, J., Tong-Sevinc, H., Li, S., MacKenzie, C.R., Zhang, J.: The assembly of single domain antibodies into bispecific decavalent molecules. J. Immunol. Methods 318(1-2), 88–94 (2007)
5. Guo, J.Q., Li, Q.M., Zhou, J.Y., Zhang, G.P., Yang, Y.Y., Xing, G.X., Zhao, D., You, S.Y., Zhang, C.Y.: Efficient recovery of the functional IP10-scFv fusion protein from inclusion bodies with an on-column refolding system. Protein Expr. Purif. 45(1), 168–174 (2006)
6. Cao, Y., Marks, J.D., Marks, J.W., Cheung, L.H., Kim, S., Rosenblum, M.G.: Construction and characterization of novel, recombinant immunotoxins targeting the Her2/neu oncogene product: in vitro and in vivo studies. Cancer Res. 69(23), 8987–8995 (2009)
7. Kamphausen, S., Holtge, N., Wirsching, F., Morys-Wortmann, C., Riester, D., Goetz, R., Thürk, M., Schwienhorst, A.: Genetic algorithm for the design of molecules with desired properties. J. Comput. Aided Mol. Des. 16(8-9), 551–567 (2002)
8. Hajduk, P.J., Huth, J.R., Tse, C.: Predicting protein druggability. Drug Discov. Today 10(23-24), 1675–1682 (2005)
9. Jiang, Z., Zhou, Y.: Using bioinformatics for drug target identification from the genome. Am. J. Pharmacogenomics 5(6), 387–396 (2005)
10. Wei, L.H., Olafsen, T., Radu, C., Hildebrandt, I.J., McCoy, M.R., Phelps, M.E., Meares, C., Wu, A.M., Czernin, J., Weber, W.A.: Engineered antibody fragments with infinite affinity as reporter genes for PET imaging. J. Nucl. Med. 49(11), 1828–1835 (2008)
11. Zdobnova, T.A., Dorofeev, S.G., Tananaev, P.N., Vasiliev, R.B., Balandin, T.G., Edelweiss, E.F., Stremovskiy, O.A., Balalaeva, I.V., Turchin, I.V., Lebedenko, E.N., Zlomanov, V.P., Deyev, S.M.: Fluorescent immunolabeling of cancer cells by quantum dots and antibody scFv fragment. J. Biomed. Opt. 14(2), 021004 (2009)
12. Loftus, J.C., Yang, Z., Tran, N.L., Kloss, J., Viso, C., Berens, M.E., Lipinski, C.A.: The Pyk2 FERM domain as a target to inhibit glioma migration. Mol. Cancer Ther. 8(6), 1505–1514 (2009)
13. Nam, C.H., Lobato, M.N., Appert, A., Drynan, L.F., Tanaka, T., Rabbitts, T.H.: An antibody inhibitor of the LMO2-protein complex blocks its normal and tumorigenic functions. Oncogene 27(36), 4962–4968 (2008)
14. Zhu, H., Yang, B., Yang, X., Wang, L., Xu, J., Liao, C., Feng, Q., Tang, H., Hu, L., Chen, Z., Li, Y.: A novel antibody fragment targeting HAb18G/CD147 with cytotoxicity and decreased immunogenicity. Cancer Biol. Ther. 8(11), 1035–1044 (2009)
15. Chang, L., Zhou, C., Xu, M., Liu, J.: Interactions between anti-ErbB2 antibody A21 and the ErbB2 extracellular domain provide a basis for improving A21 affinity. J. Comput. Aided Mol. Des. 24(1), 37–47 (2010)

16. Xu, J., Song, J., Yan, F., Chu, H., Luo, J., Zhao, Y., Cheng, X., Luo, G., Zheng, Q., Wei, J.: Improving GPX activity of selenium-containing human single-chain Fv antibody by site-directed mutation based on the structural analysis. J. Mol. Recognit. 22(4), 293–300 (2009)
17. Tiwari, A., Khanna, N., Acharya, S.K., Sinha, S.: Humanization of high affinity anti-HBs antibody by using human consensus sequence and modification of selected minimal positional template and packing residues. Vaccine 27(17), 2356–2366 (2009)
18. Ye, G., Yang, D.H., Tang, S.H., Zhou, M.D., Ding, S.H., Luo, J.L.: Molecular simulation of a single chain Fv against hepatocellular carcinoma. Chinese Journal of Pathophysiology 23(6), 1246–1248 (2007)
19. Sharma, B.: Structure and mechanism of a transmission blocking vaccine candidate protein Pfs25 from P. falciparum: a molecular modeling and docking study. Silico. Biol. 8(3-4), 193–206 (2008)
20. Wang, Y., Feng, J., Huang, Y., Gu, X., Sun, Y., Li, Y., Shen, B.: The design, construction and function of a new chimeric anti-CD20 antibody. J. Biotechnol. 129(4), 726–731 (2007)
21. Geng, S., Feng, J., Li, Y., Kang, X., Sun, Y., Gu, X., Huang, Y., Chang, H., Shen, B.F.: Human IgG1 Cgamma1 domain is crucial for the bioactivity of the engineered anti-CD20 antibodies. Cell Mol. Immunol. 4(2), 121–125 (2007)
22. Tang, Z.J., Liao, W.J., Yu, B., Zhong, J.X., Zhu, H.F., Yue, Q., Cheng, X., Li, W.H., Shen, G.X.: Modeling of scFv of human antibody against liver cancer. ACTA Biophysica Sinica 21(3), 195–199 (2005)
23. Yan, L.Y., Chen, J.H., Zhang, X.G.: Research Progress in the Linker of Fusion Protein. Biotechnology 18(3), 92–94 (2008)
24. Rea, A.M., Thurston, V., Searle, M.S.: Mechanism of ligand-induced folding of a natively unfolded helixless variant of rabbit I-BABP. Biochemistry 48(31), 7556–7564 (2009)
25. Xi, Y., Yuan, Z., Zhang, H., Guan, H., Kong, F., Liu, N., Liang, F., Cui, J., Guo, S., Sun, Y., Xi, C.: Molecular construction and characterization of a novel exotoxin fusion protein that selectively blocks the B7:CD28 costimulatory signal system. J. Immunother. 29(6), 586–595 (2006)
26. Xue, F., Gu, Z., Feng, J.A.: Linker: a web server to generate peptide sequences with extended conformation. Nucleic Acids Research 32(web server issue), W562–W565 (2004)
27. Shibata, K., Maruyama-Takahashi, K., Yamasaki, M., Hirayama, N.: G-CSF receptor-binding cyclic peptides designed with artificial amino-acid linkers. Biochem. Biophys. Res. Commun. 341(2), 483–488 (2006)
28. Kim, G.B., Wang, Z., Liu, Y.Y., Stavrou, S., Mathias, A., Goodwin, K.J., Thomas, J.M., Neville, D.M.: A fold-back single-chain diabody format enhances the bioactivity of an anti-monkey CD3 recombinant diphtheria toxin-based immunotoxin. Protein Eng. Des. Sel. 20(9), 425–432 (2007)
29. Theisen, D.M., Pongratz, C., Wiegmann, K., Rivero, F., Krut, O., Krönke, M.: Targeting of HIV-1 Tat traffic and function by transduction-competent single chain antibodies. Vaccine 24(16), 3127–3136 (2006)
30. Yang, L.J., Hou, Y.C., Yao, L.B., Su, C.Z.: Analysis of primary structure and modeling of spatial structure of single-chain variable region of antibody against human gastric cancer. World Chinese Journal of Digestology 16(21), 2333–2336 (2008)
31. Arcangeli, C., Cantale, C., Galeffi, P., Gianese, G., Paparcone, R., Rosato, V.: Understanding structural/functional properties of immunoconjugates for cancer therapy by computational approaches. J. Biomol. Struct. Dyn. 26(1), 35–48 (2008)

32. Clark, K.R., Walsh, S.T.: Crystal structure of a 3B3 variant–a broadly neutralizing HIV-1 scFv antibody. Protein Sci. 18(12), 2429–2441 (2009)
33. Koti, M., Farrugia, W., Nagy, E., Ramsland, P.A., Kaushik, A.K.: Construction of single-chain Fv with two possible CDR3H conformations but similar inter-molecular forces that neutralize bovine herpesvirus 1. Mol. Immunol. 47(5), 953–960 (2010)
34. Shen, Z., Yan, H., Zhang, Y., Mernaugh, R.L., Zeng, X.: Engineering peptide linkers for scFv immunosensors. Anal. Chem. 80(6), 1910–1917 (2008)
35. Fisher, A.C., DeLisa, M.P.: Efficient isolation of soluble intracellular single-chain antibodies using the twin-arginine translocation machinery. J. Mol. Biol. 385(1), 299–311 (2009)
36. Asano, R., Ikoma, K., Kawaguchi, H., Ishiyama, Y., Nakanishi, T., Umetsu, M., Hayashi, H., Katayose, Y., Unno, M., Kudo, T., Kumagai, I.: Application of the Fc fusion format to generate tag-free bi-specific diabodies. FEBS J. 277(2), 477–487 (2010)
37. Stork, R., Zettlitz, K.A., Müller, D., Rether, M., Hanisch, F.G., Kontermann, R.E.: N-glycosylation as novel strategy to improve pharmacokinetic properties of bispecific single-chain diabodies. J. Biol. Chem. 283(12), 7804–7812 (2008)
38. Gurkan, C., Ellar, D.J.: Expression in Pichia pastoris and purification of a membrane-acting immunotoxin based on a synthetic gene coding for the Bacillus thuringiensis Cyt2Aa1 toxin. Protein Expr. Purif. 29(1), 103–116 (2003)
39. Olafsen, T., Sirk, S.J., Betting, D.J., Kenanova, V.E., Bauer, K.B., Ladno, W., Raubitschek, A.A., Timmerman, J.M., Wu, A.M.: ImmunoPET imaging of B-cell lymphoma using 124I-anti-CD20 scFv dimers (diabodies). Protein Eng. Des. Sel. (2010), doi: 10.1093/protein/gzp081
40. Schmiedl, A., Zimmermann, J., Scherberich, J.E., Fischer, P., Dübel, S.: Recombinant variants of antibody 138H11 against human gamma-glutamyltransferase for targeting renal cell carcinoma. Hum. Antibodies 15(3), 81–94 (2006)
41. Szantai-Kis, C., Kovesdi, I., Eros, D., Bánhegyi, P., Ullrich, A., Kéri, G., Orfi, L.: Prediction oriented QSAR modelling of EGFR inhibition. Curr. Med. Chem. 13(3), 277–287 (2006)
42. Gu, X., Jia, X.L., Feng, J.N., Shen, B., Huang, Y., Geng, S., Sun, Y., Wang, Y., Li, Y., Long, M.: Molecular Modeling and Affinity Determination of scFv Antibody: Proper Linker Peptide Enhances Its Activity. Annals of Biomedical Engineering (2009), doi: 10.1007/s10439-009-9810-2

The Design of Ecological Restoration Projects in the River Network Area in Southern Jiangsu Province: Chen Xiangbang Ecological Restoration Demonstration Project*

Zhang Wenyi[1,**], Tan Fangyuan[2], Liu Mingyuan[1,**], Han Youfa[1], and Chen Rong[2]

[1] School of Environmental and Safety Engineering, ChangZhou University, Changzhou City, Jiangsu Province, 213164, China
zwy@jpu.edu.cn
[2] Department of Equipment Manufacture Jiangsu Hengliang Centrifuge Manufacturing Co., Ltd, Jintan City, Jiangsu Province, 213200, China
326664395@qq.com

Abstract. The southern Jiangsu Province was located in the fast developing Yangtze River Delta Economic Zone. With the development of agriculture and industries, and the speeding-up of China's urbanization, the problems of water pollution had become more and more serious. Chen Xiangbang Ecological Restoration Project integrated the rural domestic sewage treatment system and river restoration projects. By taking advantage of the on-site terrain conditions and ODBP technology, the riverway could be transformed into a domestic sewage treatment system. Experiments showed that the concentration of CODCr, TN, TP, NH3-N and SS in the effluent had met the first class of B standard of "Discharge standard of pollutants for municipal wastewater treatment plant" (GB-18918-2002).The demonstration project showed that it was very efficient for the rural wastewater treatment of south Jiangsu. It not only saved the investment but also the land resources. For one ton wastewater, the capital construction cost was CNY1876.84, and the treatment cost was only CNY0.085. What's more, the projects do not need professional management. So the Chen Xiangbang Ecological Restoration Projects could widely be used for rural domestic wastewater treatment.

Keywords: Southern Jiangsu Province, Ecological Restoration, River Restoration, Rural Domestic Sewage, Design of Demonstration Projects.

With the deepening of reform and opening up, China's economy had developed rapidly and living standards had steadily increased. However, the problem of rural sewage treatment was still a problem that was not effectively solved. It hampered the construction of the new socialist countryside and the development of rural economy. According to Changzhou Wujin district "Caoqiao river environment comprehensive

* This research was supported by the natural science fund of Jiangsu province (BK200930405, BE201077311) and the natural science fund social development project of Changzhou city(CS20100015, WS201003).
** Corresponding author.

E. Zhu and S. Sambath (Eds.): Information Tech. and Agricultural Eng., AISC 134, pp. 183–190.
springerlink.com © Springer-Verlag Berlin Heidelberg 2012

planning (2008-2020)", Caoqiao river comprehensive environment medium-term target was: the effluent quality reached the target set in the Emissions & Pollution Target of the 11th National Five-year Plan by June 2011.

Bioremediation was a newly developed technology for purification environment with low investment, high efficiency and convenient application. In order to slow down water pollution and restore aquatic ecological functions, the biological measures adopted specific biology (especially microorganisms) to absorb, convert and degrade water pollutants. This process was controlled or spontaneous. The river ecological restoration was just beginning in China, and a lot of meaningful explorations had been done in theory and practice. According to ecological-hydraulic engineering theory, the tasks for ecological restoration of river, one was to improve hydrological conditions, and the other was to improve the characteristic of fluvial geomorphology.

The ecosystem interception project of chen Xiangbang river combined rural domestic sewage treatment project and river ecological restoration project, and the sewage was treated by in-situ ecological treatment.

1 Project Profile

Chen Xiangbang lay in Changzhou city, which was one of the six tributaries of Caoqiao river. This project involved three villages, and they were Lok Street Village, BaiBao lane, a public toilet between AnHe lane and Chen Xiangbang road. The characteristics of this river were: total length of 1240 m, average width of 12 m, water depth of 2.8 m, the highest water level of 5.2 m, the lowest water level for 3.2m, the average design level of 4.2 m, the designed level of 4.2 m, the designed depth of 3.8m, water volume for 25536m^3, total displacement for 840.3m^3/d, surface area about 14480m^2, catchment ditches pond area about 800m^2 , total area about 15280m^2 , cross-strait farmland area about 984 mu, serviced population for 1762 persons.

1.1 Design of Water Quantity

The consumption of water for everyday: 200L/p. d

The quantity of domestic wastewater was 80% of the water consumption, and the total consumption of water was:200L/p.d×80%×1.3×1762p=366.5m^3/d.Agricultural

Table 1. Wastewater Quality of Chen Xiangbang

number	*name*	*Water quality (m^3/d)*	*COD (mg/L)*	*NH_3-N(mg/L)*	*TP (mg/L)*	*SS (mg/L)*	*pH*
1	Sewage (including public toilets excrement)	366.5	400	30	4	250	6 ~ 9
2	Agricultural non-point source water drainage and recharge	372	150	25	5	60	6 ~ 9
3	Initial rainwater drainage	101.8	250	20	3	130	6 ~ 9
4	Total drainage after mixing	840.3	271.2	26.6	4.3	151.3	6 ~ 9

non-point drainage and groundwater recharge were 372m^3/d, and the rainwater into the river was 101.8m^3/d. So the total displacement was 840.3m^3/d, and the designed treatment capability was 840m^3/d.

1.2 Design of Influent Quality

The wastewater quality of Chen Xiangbang was showed in table 1. It based on the related data of rural domestic wastewater for south Jiangsu, and feces discharged into river was also considered.

1.3 Design of Effluent Quantity

According to first class of B standard of **"**Discharge standard of pollutants for municipal wastewater treatment plant**"** (GB 18918-2002), the highest discharged concentration of the main pollutants were showed in table 2.

Table 2. Sewage Discharge Standard（GB 18918-2002 1B）

water quality index	*COD (mg/L)*	*BOD (mg/L)*	*SS (mg/L)*	*NH3-N (mg/L)*	*TP (mg/L)*	*pH*
Concentration	≤60	≤20	≤20	≤8（15）	≤1	6 ~ 9

1.4 Technological Process and Principle

According to the analysis result of Water quality, the summary of wastewater treatment technology and project emissions standards, rural domestic sewage was treated by the combination of in-situ increasing oxygen and dynamic ecological in chen Xiangbang. It was showed in figure 1.

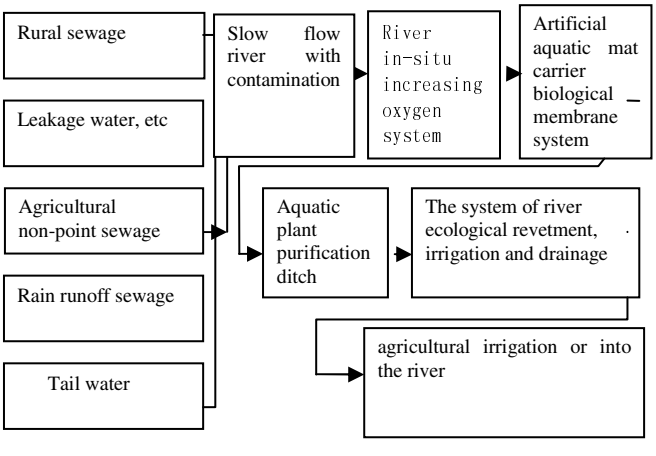
Rural sewage
Leakage water, etc
Agricultural non-point sewage
Rain runoff sewage
Tail water
Slow flow river with contamination
River in-situ increasing oxygen system
Artificial aquatic mat carrier biological membrane system
Aquatic plant purification ditch
The system of river ecological revetment, irrigation and drainage
agricultural irrigation or into the river

Fig. 1. The technological process of wastewater treatment for chen xiangbang

As shown in figure 1, sewage went through the ecological revetment into river. Water quality and quantity were adjusted by hydrolysis, biological adsorption in

aquatic plant purification ditch. The concentration of organic pollutants could be reduced by microbial hydrolysis reaction, and the biodegradability of wastewater was improved. In ordered to remove odour and degradate organic compounds, the wastewater was oxygenated by aeration in section one of in-situ increasing oxygen system. Nitrogen was transformed into ammonia- nitrogen by aquatic plants and biofilm. Ammonia- nitrogen was degraded in section two of insitu increasing oxygen system. At the same time, the river was oxygenated again, and it could restore to original state. In aquatic plants purification ditch, the polluted river was restored by ecological technology, and the sewage from downstream sewage outfall was degraded. In order to remove suspended material and meet emission standard, the river water was deeper purified in ecological revetment. The sediment of artificial aquatic carrier biological membrane system was green ecological fertilizer. The water level of Chen Xiangbang was mainly adjusted by regulating dam. It played the role of agricultural irrigation in the dry season and flood control and drainage in the flood season.

2 Main Structures in the Design

2.1 Aquatic Plant Purification Ditch

Function: intercepting impurity; evening water quality and water quantity; adjusting pH; removal and decomposition of organic pollutants with aerobic/anaerobic hydrolysis; cutting down pollution load; improving the biodegradability of wastewater.

Design parameters: effective volume for 6300m^3; hydraulic retention time for 7.6d; the average width for 14.0m; designed length for 150m; effective depth for 3.0m.

Main construction projects: brick drainage channel; water and soil restoration of the river bank; ecological slop protection; planting zizania latifolia and reed; planting water hyacinth.

2.2 In-situ Increasing Oxygen for 1

Function: intercepting impurity; evening water quality and water quantity; biosorption, filtration, degradation and reoxygenation for sewage.

Design parameters: effective volume for 840m^3; hydraulic retention time for 1d; the average width for 14. 0m; design length for 20m; effective depth for 3 0m.

Main construction projects: iron barriers; underground type steel concrete pouring bottom; stone revetment, etc.

The main equipment: submersible style centrifugal aeration machine (4 sets); artificially stereo aquatic; stainless steel frame.

2.3 Artificial Aquatic Mat Carrier Biological Membrane System

Design parameters: effective volume for 2100 m^3; hydraulic retention time for 2.5d; the average width for14. 0m; design length for50m; effective depth for3 0m.

Main construction projects: brick drainage channel; ecological slop protection; planting zizania latifolia and reed; artificial floating island; planting canna, rushes and other aquatic plants on artificial floating island.

The main equipment: the iron railings; artificially stereo aquatic; stainless steel frame.

2.4 In-situ Increasing Oxygen for 2

Function: intercepting impurity; evening water quality and water quantity; biological adsorption; filtration; degradation and reoxygenation for wastewater.

Main construction projects: iron railings; underground type steel concrete pouring bottom; stone revetment.

Design parameters: effective volume for 840m^3; hydraulic retention time for 1 d; the average width for 14.0m; designed length for 20m; effective depth for 3 0m.

The main equipment: submersible style centrifugal aeration machine (2 sets); artificially stereo aquatic; stainless steel frame.

2.5 Aquatic Plant Purification Ditch

Function: intercepting impurity; evening water quality and water quantity; adjusting pH; decomposing organic pollutant by adsorption and hydrolysis; cutting pollution loading.

Design parameters: effective volume for 4200m^3; hydraulic retention time for 5.0d; the average width for14.0m; design length for100m; effective depth for 3.0m.

Main construction projects: brick drainage channel; water and soil restoration of the river bank; ecological slop protection; planting zizania latifolia and reed; artificial floating island; planting canna, rushes and other aquatic plants on artificial floating island.

The main equipment: iron railings; fixed bracket of artificial floating island.

2.6 Ecological Revetment

Function: intercepting impurity; evening water quality and water quantity; adjusting pH; decomposing organic pollutant by adsorption and hydrolysis; cutting down pollution loading.

Design parameters: effective volume for 9240m^3; hydraulic retention time for 11.1d; the average width for14.0m; design length for 220m; effective depth for 3.0m.

Major construction projects: brick drainage channel; water and soil restoration of the river bank; ecological slop protection; planting zizania latifolia and reed.

G. Regulation dam of water level

Functions: controlling water level; regulating water quantity; agricultural irrigation during the dry season; flood storage in the flood season.

Main parameters: designed width for 22m; crest width for 2.0m; sluices width for 1.0m; height for 2.5; effective height for1.5m.

Main construction project: steel concrete structure dam; sluice.

The main equipment: iron railings; river water; stainless steel fence; steel door for sluice and operation part.

4 Ecological Engineering Technique Characteristics Intercept Demonstration

(1) Slow flow river with contamination was transformed into the artificial wetlands by using the scene topographical condition , and wastewater was treated by wetland ecosystem. So the pipeline network construction of rural sewage was not necessary, and a lot of construction funds were saved. This makes the treatment project of rural sewage possible, and the project could operate for long-term. It provided an efficient processing mode for domestic sewage and agricultural drainage in rural areas of south Jiangsu.

(2) Aquatic plants in the abandoned river could degrade wastewater by biological filtration. Wastewater reoxygenation could be done by improving the contact area of water and air. The abandoned river was transformed into aerated fishponds. So the wastewater could be treated by ecological culture. This method could save land, and reduce the operation cost and engineering investment.

(3) River in-situ increasing oxygen system based on the characteristics of polluted river, and the oxygen was pumped into water. Hence, the process of reoxygenation was improved and the oxygen dissolved level was enhanced. The vitality of aerobic microorganism was strengthened, and the contamination was purified. This system combined aeration oxidation pond and oxidation ditch process with the characteristics of pushing and completely mixing, and it contributed to overcome the short flow and improve the buffering capacity. It was also helpful for oxygen transfer and liquid mixing, and it was a kind of effective treatment method for open water. River aeration reoxygenation adopted fixed blast aeration, that is, the air was introduced to the aeration diffusion system at the bottom of the channel by pipes.

(4) The purification essence of artificial aquatic mat carrier biological membrane system was to change the natural process into a combination of natural and artificial process. Filter material or carrier was packed on the river bed for bacterial growth and biofilm formation. When the polluted river flew through the biofilm, it could contact with zoogloea adhered to the carrier. Owing to the function of bacteria and extracellular polymeric substances, the organism in water was adsorbed or flocculated. This made the surface of zoogloea not only having a large number of active bacteria but also having higher concentration of organic compounds, which was suitable for bacteria reproduction. Because of this favorable condition, the bacteria on the surface of zoogloea grew rapidly and the organic contamination was consumed quickly. The essence of artificial aquatic mat in-situ biological membrane technology was biological contact oxidation. The artificial aquatic mat which had similar characteristics of natural plants was made from new material. Because the aquatic was the foundation of community diversity, many bacteria and fungi attached to the stem and leaf. Moreover, the leaf was extremely flexibility, and could flow by water with small resistance. So the bionic aquatic was made according to these characteristics. Artificial aquatic mat was put in river both improving purification ability and having no effect on the normal function of the river.

(5) The essence of aquatic plants purification ditch was river in-situ remediation technology, including the technology of bioremediation and aquatic plants remediation. Aquatic plants remediation was a new technology, particularly suitable for the treatment of river sewage. Higher aquatic plant grew rapidly, and could effectively absorb and accumulate nutrient in growth period. It played the role of nutrition pump

and nutrition library. Nutrients such as nitrogen and phosphorus could be transfered from water by establishing and maintaining the biomass of aquatic plants, and the capacity of water purification was enhanced. So this newly technology was suitable for the polluted river remediation with slow flow.

(6) The integration system of ecological riverbank, irrigation and drainage was a set of water conservancy facility for the river sewage treatment. Its functions involved water storage of aquaculture, agricultural irrigation, flood control and drainage, ecological revetment, etc. It was composed of water conservancy regulation structures, drainage facilities, etc.

(7) The whole project operation adopted dual control, including industrial control computer and Programmable Logic Controller (PLC). Its many functions were automatic such as facility operation, water quality monitor, process parameters adjustment and so on.

5 Feasibility Analysis of Technical and Economic

Because the terrain was lower, there was no power consumption for wastewater ascension. It needed not any power except the process of river reoxygenation. The whole process was the integration of biological-ecological treatment engineering for removal of carbon, nitrogen, and phosphorus. The parameters of effluent were as follow: 42.2mg/L of COD_{Cr}, 4.3mg/L of TN, 0.2mg/L of TP, 0.8mg/L of NH_3-N, 16mg/L of SS. All these parameters met the first class of B standard of **"**Discharge standard of pollutants for municipal wastewater treatment plant**"** (GB 18918-2002) .Besides the suspended(SS), the other parameters achieved first class of A standard of **"**Discharge standard of pollutants for municipal wastewater treatment plant**"** (GB 18918-2002).This demonstration project has certain reference and the exemplary for the rural domestic sewage treatment of whole south Jiangsu even the south of China.

The capital construction cost was 1059.5CNY/ton wastewater, so the total cost of this project was CNY890000 with the total treatment amount for 840m^3/d. The operation cost of this project was as follows:

(1) The cost of electricity (E_1)
The electrical load of sewage plant was 1.5 kW (the actual operation time was 8 hours for everyday), and the price of electricity was 0.6 CNY/degree. The treatment cost of one ton wastewater was:

$E1=1.5\times0.6\times8\div192=0.038$CNY/$m^3$ wastewater

(2) The cost of labor (E_2)
There was one person (part-time) working for this sewage plant and the wage was CNY150 for every month. The treatment cost for one ton wastewater was:

$E2=150\times1\div(192\times30)=0.026$CNY/$m^3$ wastewater

(3) The cost of daily maintenance (E_3)
The cost was CNY1500 for one year, so the cost for one ton wastewater was:

$E4=1500\div(192\times365)=0.021$CNY /$m^3$ wastewater

The total operation cost for wastewater treatment was:

$E_T= E_1+ E_2+ E_3 =0.085$ CNY/m^3 wastewater

6 Conclusions

The ecological engineering can effectively control main pollution factors of agricultural non-point source pollution. The main effluent quality parameters such as COD_{Cr}, TN, TP, NH_3-N, SS met the first class of B standard of **"**Discharge standard of pollutants for municipal wastewater treatment plant" (GB 18918-2002). Among them, the parameters of COD_{Cr}, TN, TP, and NH_3-N can achieve first class of A standard of **"**Discharge standard of pollutants for municipal wastewater treatment plant" (GB 18918-2002). The combined project of rural domestic sewage treatment and river ecological restoration changed the abandoned river into the domestic sewage treatment site using scene topographical condition. The capital construction cost was CNY 1059.5 /ton sewage, and this could save much money making the rural sewage treatment project possible. The cost of water treatment was CNY 0.085/m^3 after this project was accomplished, so this project could work long-term at low cost. While a perfect drainage and irrigation system was established, and water conservancy function of the river was restored. The demonstration project of ecological interception was technically feasible, low cost and easy to manage, and could provide a sample for the rural domestic sewage treatment of whole south Jiangsu even the south of China.

References

1. Shen, T., Wang, J.: Biochemistry, pp. 45–50. Higher education press, Beijing (1990)
2. Dong, Z.: Rivers and morphological diversity community diversity. Journal of Hydraulic Engineering 11, 1–7 (2003)
3. Dong, Z.: Rivers protection stage of development and thinking. China Water Conservancy 17, 16–18 (2004)
4. Jiang, Z., Du, Y., Wang, B.: Nitrogen phosphorus loss of project performance evaluation of ecological intercept tests. With the Development of Agricultural Environment 6, 47–64 (2009)

Antimicrobial Properties of *Xylaria coprinicola* Accompaning the Growth of *Coprinus Comatus* in China

Du Ai-ling[1] and Cao Zhi-min[2]

[1] Forestry College Henan University of Science and Technology Luoyang, Henan Province, China
[2] College of Plant Protection Northwest A&F University Yangling, Shanxi Province, China
duail@126.com

Abstract. Xylaria coprinicola is a new species that antagonizes cultivation and accompanies the growth of Coprinus comatus in china. The antimicrobial properties of X.coprinicola were studied. The results show that the X.coprinicola culture filtrate shows certain inhibiting effects on the growth of pathomycete and edible fungi. The mycelium growth inhibition rate reaches 62.9% for Fusarium solani and 64.5% for C.comatus. The relative electrical conductivity of the hypha of C.comatus is increased by 180.46% as the concentration of X.coprinicola culture filtrate in medicative medium reaches 40%. Microscopic observation shows that distortion, adhesion, uneven thickness, unclear structure and tenuous and transparent cell protoplasm appear on the hypha of C.comatus.

Keywords: Xylaria coprinicola, Coprinus comatus, Antibiogram, Electrical conductivity.

1 Introduction

Coprinus comatus is a new type of edible mushroom rapidly developed in China in recent years. *Xylaria coprinicola* is a new species that antagonizes cultivation and accompanies the growth of *C.comatus* [1-3].There is no precedent for this *X.coprinicola* infection of many other edible fungi that have been cultivated for a long time and over a large area, and currently there are only reported infection cases on the production beds of *C.comatus* in China. This fungus has a strong tendency to accompany the growth of *C.comatus* and thus does great harm to *C.comatus*. It results in hypha atrophy or death inside the compost of *C.comatus* and thus reduces *C.comatus* harvest by 20%~100%.

Genus *Xylaria* is one of the largest as well as earliest described genera of the family Xylariaceae. More than 100 types *of Xylaria* are found worldwide. Different types of *Xylaria* have different growth habits, while most of them are found on rotten wood and stumpages [4]. From the 1990s onwards, several types of *Xylaria* were found to be inhibitors of bacteria, virus and tumor and can improve immunity. Many active substances were also separated from these *Xylaria* [5-13].

Early studies showed that the hypha culture filtrate of this particular *X.coprinicola* can strongly inhibit the growth of the hypha of *C.comatus*. On the basis of the above discovery, the antibiogram of the *X.coprinicola* fungus culture filtrate was evaluated

E. Zhu and S. Sambath (Eds.): Information Tech. and Agricultural Eng., AISC 134, pp. 191–197.
springerlink.com © Springer-Verlag Berlin Heidelberg 2012

using the plating method in the experiment, and taking *C.comatus* as the test sample, the inhibition mechanism of this *X.coprinicola* was studied preliminary based on the change of electrical conductivity and microscopic features of the hypha of *C.comatus*.

2 Materials and Methods

2.1 Test Materials

2.1.1 Strains to Be Tested

Xylaria coprinicola, *Coprinus comatus*, *Pleurotus ostreatus*, *Lentinus edodes*, *Pholiota adipdsa*, *Botrytis cinerea, Sclerotinia sclerotiorum*, *Alternaria solani*, *Bipolaris maydis* and *Fusarium solani* were provided by Forestry College of Henan University of Science and Technology.

Escherichia coli and *Staphylococcus aureus* were provided by Food & Bioengineering College of Henan University of Science and Technology.

2.1.2 Culture Medium

PD liquid medium: potato 200g, dextrose 20g, water 1000ml.

PDA solid medium: potato 200g, dextrose 20g, agar 20g, water 1000ml.

2.2 Test Methods

2.2.1 Preparation of *X.coprinicola* Culture Filtrate

Inoculate PD liquid medium with solid spawn of *X.coprinicola* and culture statically at 28 ℃ for 30 days, and shake it several times during the incubation period. Then subject the cultures to 45 ℃ for 2 days to inactivate the *X.coprinicola* in the culture solution. Filtrate through four-layer gauze under aseptic conditions and collect the culture filtrate.

2.2.2 Antibiogram Evaluation of *X.coprinicola* Culture Filtrate

Evaluation of bacteriostatic activity: Inoculate the slant culture-medium with test bacteria and culture at a constant temperature of 37 ℃ for 48 hours. Prepare bacteria suspension. Absorb 0.1ml bacteria suspension with micro-pipette and smear on the surface of the plate medium. Place three 0.3 ml oxford cups on the surface of each plate, and fill them with 0.1ml *X.coprinicola* culture filtrate separately. Culture at 28℃ in incubator for 36 hours and measure the diameter of inhibition zone using sterile water as the control group.

Evaluation of the inhibition to the growth of pathomycete and edible fungi: Add aseptic culture filtrate of *X.coprinicola* into sterilized PDA medium to a concentration of 30% to make medicative medium and plate. Each 9cm culture dish contains 15ml of medium. Inoculate test pathomycete or edible fungi on the each plate with a 6 mm fungus colony of the same mass. Taking PDA medium without *X.coprinicola* culture filtrate as the control group. Culture at 25℃ after inoculation. Make three replications in each group. When the mycelium in the control group nearly overgrows the plate, measure the diameter of the colony with criss-cross method, and calculate the inhibition rate against mycelium growth. Cite equations using (1).

$$A = (Dt - Dc) \bullet (Dc - 0.6)^{-1} \quad (1)$$

A: the inhibition rate of mycelium growth(%)
Dt: mycelium diameter in the treatment group
Dc: mycelium diameter in the control group
0.6: diameter of spawn inoculated(cm)

2.2.3 Measurement of Electrical Conductivity

Add inactivated aseptic *X.coprinicola* culture filtrate to PD aseptic liquid medium to concentrations of 0%, 10%, 20%, 30% and 40%.Then transfer the mixed medium to conical flasks, with each 250ml conical flask containing 60ml of liquid. Inoculate each conical flask with five pieces of fungus colony with a diameter of 6mm. Shake at a rate of 100~110 r • min^{-1} and culture for 6 days at 25 ℃.

Take 1g of wet mycelium of *C.comatus* and place it in a test tube. Add 10 ml of water and shake. Place the soak solution statically for 24 hours and shake to make it even and then measure the electrical conductivity of the soak solution. Then put it in boiling water and boil for 10 min. Measure the maximum electrical conductivity of the completely damaged cell membrane after cooled to room temperature. Calculate the relative electrical conductivity. Cite equations using (2).

$$R = Ct \bullet Cc^{-1} \bullet 100\% \quad (2)$$

R: relative electrical conductivity (%)
Ct: electrical conductivity of the treatment group
Cc: maximum electrical conductivity

3 Results and Analysis

3.1 Antibiogram of *X.coprinicola* Culture Filtrate

Please refer to Table 1, 2 and 3 for the inhibiting effects of *X.coprinicola* culture filtrate on pathogenic bacteria, pathogenic fungi and large edible fungi.

Result shows that the diameters of inhibition zone of the culture filtrate of this fungus to the growth of *E. coli* and *S. aureus* were less than 10mm, indicating that the inhibiting effect on the two bacteria is not obvious.

The *X.coprinicola* culture filtrate shows some inhibiting effects on the five plant pathogenic fungi, *F.solani*, *S.sclerotiorum*, *B.maydis, B.cinerea* and *A.solani*. The inhibition rates are all above 50%, with the inhibition rate against *F.solani* hypha growth as high as 62.9%.

The *X.coprinicola* culture filtrate also showes relatively good inhibiting effects on the four large edible fungi, *C. comatus*, *P.adipdsa*, *L.edodes* and *P.ostreatus*. The inhibition rates against all the fungi are above 50% except for that against *P.ostreatus*, which is below 30%. The inhibition rate for the hypha growth of *C. comatus* reaches 64.5%. The results indicate that the metabolite of *X.coprinicola* contains toxin active materials that inhibit the growth of fungi and have a wide antibiogram for the fungi.

Table 1. The inhibiting effects of *X.coprinicola* culture filtrate on the growth of pathogenic bacteria

Pathogenic bacteria	Diameter of inhibition zone(mm)	
	Treatment	Control
Escherichia coli	8.2	0
Staphylococcus aureus	7.5	0

Table 2. The inhibiting effects of *X.coprinicola* culture filtrate on the growth of plant pathogenic fungi

Pathogenic fungi	Mycelium growth diameter(cm)		Inhibition rate (%)
	Treatment	Control	
Fusarium solani	2.6	7.0	62.9
Sclerotinia sclerotiorum	2.8	6.9	59.4
Bipolaris maydis	3.0	7.0	57.1
Botrytis cinerea	3.2	7.0	54.3
Alternaria solani	3.2	6.8	53.0

Table 3. The inhibiting effects of *X.coprinicola* culture filtrate on the hypha growth of four large edible fungi

Edible fungi	Mycelium growth diameter(cm)		Inhibition rate (%)
	Treatment	Control	
Coprinus. comatus	2.2	6.2	64.5
Pholiota adipdsa	2.9	6.4	54.7
Lentinus edodes	3.0	6.1	50.8
Pleurotus ostreatus	5.2	6.9	24.6

The result of this experiment shows that *X.coprinicola* culture filtrate has varying degrees of inhibiting effects on three out of the four tested large edible fungi.

3.2 The Effects of *X.coprinicola* Culture Filtrate on the Cell Membrane Permeability of the Hypha of *C.comatus*

The result of the experiment shows that the relative electrical conductivity of the hypha of *C.comatus* increases with the increase of the concentration of *X.coprinicola* culture filtrate in medium (Table 4). The relative electrical conductivity of the hypha of *C.comatus* is increased by 180.46% as the concentration of *X.coprinicola* culture filtrate in medium reaches 40%.

The result shows that *X.coprinicola* culture filtrate contains toxin active materials, which damage the cell membrane structure of *C.comatus*, resulting in the increase of cell membrane permeability and exudation of materials in the cell.

Table 4. The effects of *X.coprinicola* culture filtrate on the electrical conductivity of the hypha of *C.comatus*

Concentration of *X.coprinicola* culture filtrate	Relative electrical conductivity	Compared with control(±%)
0%	8.7	0.00
10%	14.8	+70.11
20%	17.6	+102.30
30%	20.4	+134.48
40%	24.4	+180.46

3.3 The Effects of *X.coprinicola* Culture Filtrate on the Cultivation and Microscopic Features of the Hypha of *C.comatus*

In the plate containing *X.coprinicola* culture filtrate, the mycelium growth of *C.comatus* appears deformed, uneven and abnormal regiment phenomenon at the late stage of the growth. Microscopic observation shows that distortion, adhesion, uneven thickness, unclear structure and tenuous and transparent cell protoplasm appear on the hypha of *C.comatus* (Figure 1-2).

Fig. 1. Abnormal growth features of the mycelium of *C.comatus* on the medicative medium Left: Control, right: Treatment

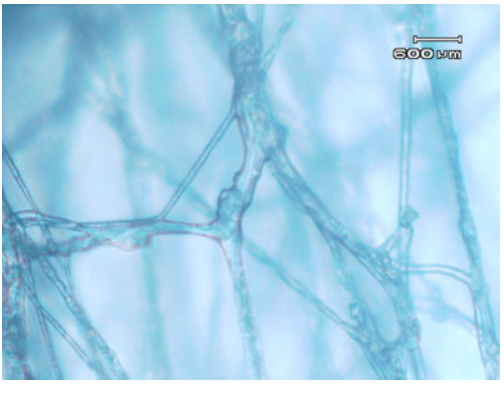

Fig. 2. The malformed mycelium of *C.comatus* on the medicative medium

4 Discussion and Conclusion

The rate and characters of growth of mycelium are the important indexes to evaluate the growth of fungi. The result shows that *X.coprinicola* culture filtrate has certain inhibiting effects on the mycelium growth of tested pathogenic fungi and large edible fungi, with a maximum inhibition rate of 64.5%. Phenomena like distortion, adhesion and abnormal growth appear on the hypha.

The cell membrane is the interface for the exchange of materials between the cell and the environment, as well as the most sensitive part of the cell to environmental stress. Cell membrane permeability is one of the physiological indexes to evaluate the reaction of a plant to environmental stress. Relative electrical conductivity is an important physiological index to measure the extent of damage to cell membranes. The experiment shows that the metabolite of *X.coprinicola* increases the permeability of *C.comatus* cell membrane. The materials in the cell exude so the relative electrical conductivity of the hypha increases, and keeps increasing gradually with the concentration of *X.coprinicola* culture filtrate increasing.

It is also deduced from the experiment that the metabolite of this *X.coprinicola* found on the production beds of *C.comatus* has some kind of toxin active materials, which have a broad-spectrum for the inhibiting effect on fungi.

It is reported that many species of genus *Xylaria* have active materials and it is one of the new hot spots to filter and abstract antifungal drugs from *Xylaria.* Many active materials, like cubensic acid, berteric acid, camenronic acid, globoscinic acid, maldoxin, xylarin (Chem, 1991,1995,1996), cytochalasin (Tetrahedron, 1997), 2,3-didehydrotelfairic anhydride (Annalen, 1996) have been separated from *Xylaria* [14] . Therefore, whether the antifungal materials contained in *X.coprinicola* has similar properties is worth of further study.

References

1. Wang, B.: A new pathogen of Coprinus comatus mushroom—Xylaria furcata. Edible Fungi 19(4), 34 (1997) (in Chinese)
2. Mao, X.-L.: The macrofungi in China, p. 574. Henan Science and Technology Press, Zhengzhou (2000) (in Chinese)
3. Ju, Y.-M., Hsieh, H.-M., He, X.-S.: Xylaria coprinicola, a new species that antagonizes cultivation of Coprinus comatus in China. Mycologia 102 (2010) (in press)
4. Hawksworth, D.L., Kirk, P.M., Sutton, B.C., Pegler, D.N.: Ainsworth & Bisby's. Dictionary of the Fungi, 8th edn., pp. 491–492. C.A.B. International, Wallingford (1995)
5. Wu, X.-Y., Liu, X.-H., Jiang, G.-C., et al.: Xyloketal G, a Novel Metabolite from the Mangrove Fungus Xylaria sp. 2508. Chemistry of Natural Compounds 41(1), 27–29 (2005)
6. Davis, R.A., Watters, D., Healy, P.C.: The isolation and synthesis of 3-chloro-4-hydroxypheny lacetamide produced by a plant-associated microfungus of the genus Xalaria. Tetrahedron Letters 46(6), 919–921 (2005)
7. Lin, Y.-C., Wu, X.-Y., Feng, S., Jiang, G.-C., et al.: A novel N-cinnamoylcyclopeptide containing an allenic ether from the fungus Xylaria sp(strain# 2508) from the South China Sea. Tetrahedron Letters 42(3), 449–451 (2001)

8. Zeng, X.-B., Wang, H.-Y., He, L.-Y.: Medium optimization of carbon and nitrogen sources for the production of eucalyptene A and xyloketal A from Xylaria sp. 2508 using response surface methodology. Process Biochemistry 41(2), 293–298 (2006)
9. Luo, J.-H., Yang, Y.-B., et al.: Effects of Metabolites of Mangrove Fungus Xylaria sp. from South China SeaCoast on the Activity of Acetylcholinesterase in Vitro. Journal of Chinese Medicinal Materials 27(4), 261–264 (2004) (in Chinese)
10. Chen, W.-L., Qian, Y., Meng, W.-F., et al.: A novel marine compound xyloketal B protects against oxidized LDL-induced cell injury in vitro. Biochemical Pharmacology 78(8), 941–950 (2009)
11. Abate, Dawit, Abraham, Wol Rainer, Meyer, Holger: Cytochalasins and phytotoxins from the fungus Xylaria obovata. Phytochemistry 44(8), 1443–1448 (1997)
12. Liu, K.-H., Ding, X.-W., Deng, B.-W., et al.: 10-Hydroxycamptothecin produced by a new endophytic Xylaria sp., M20, from Camptotheca acuminate. Biotechnology Letters 32(5), 689–693 (2010)
13. Liu, X.-L., Dong, M.-S., Chen, X.-H., et al.: Antimicrobial activity of an endophytic Xylaria sp.YX-28 and identification of its antimicrobial compound 7-amino-4-methylcoumarin. Applied Micro-biology and Biotechnology 78(2), 241–247 (2007)
14. Liu, J.-K.: Mycochemistry, pp. 158–161. China science & technology press, Beijing (2004) (in Chinese)

Growth Inhibition of *Karenia mikimitoi* by Extracts from *Gracilaria lemaneiformis* Using Five Solvents*

Yingying Sun[1], Jing Zhang[1], Shenzhen Xu[1], Wenhao Li[1], and Changhai Wang[2]

[1] Jiangsu Key Laboratory of Marine Biotechnology, Huaihai Institute of Technology Lianyungang, Jiangsu Province 222005, China
[2] School of Ocean Yantai University Yantai, Shandong Province, 264005, China
syy-999@163.com, chwang2001@sina.com

Abstract. Effect of extracts with five different organic solvents (methanol, acetone, ethyl acetate, chloroform, and petroleum ether) from Gracilaria lemaneiformis on the growth of Karenia mikimitoi was studied. The methanol extract was further separated by liquid-liquid partition. The results showed the extracts obtained with the five solvents all inhibited growth of K. mikimitoi. Extracts with methanol and acetone had the strongest activity by being lethal to K. mikimitoi at 1.6 g/L, and those extracts caused cavities and ruptures in cells. The extracts with all the five solvents decreased cell mobility and reduced cell sizes of K. mikimitoi, and the strongest activity was achieved by the extract by ethyl acetate. Addition of the five solvent extracts resulted in lower chlorophyll content in the treated algal cells. Contents of protein and polysaccharide were significantly reduced in culture treated with extracts by methanol, acetone and ethyl acetate. The methanol extract was partitioned to petroleum ether phase, ethyl acetate phase, n-butanol phase and distilled water phase by liquid-liquid fractionation. Of the four partitions, the fraction in petroleum ether and ethyl acetate phases had the strongest activity in suppressing microalgal growth.

Keywords: extracts, Gracilaria lemaneiformi, growth inhibition, Karenia mikimitoi.

1 Introduction

The eutrophication problem of coastal waters has become more and more serious in China. In recent years, red tides are occurring more frequently in large scale, causing severe damages. This situation endangers the ecological environment in coastal waters and sustainable development of coastal aquaculture. Many methods have been proposed to resolve this situation, such as using clay minerals [1], quaternary ammonium compounds [2], virus [3], bacteria [4] and others to suppress or kill red tide bloom microalgae. Application of these techniques have achieved some progress

* This work is partially supported by the project of Jiangsu key laboratory of marine biotechnology of Huaihai Institute of Technology # 2008HS017 to Yingying Sun and # 2009HS09 to Changhai Wang.

E. Zhu and S. Sambath (Eds.): Information Tech. and Agricultural Eng., AISC 134, pp. 199–210.
springerlink.com © Springer-Verlag Berlin Heidelberg 2012

in controlling growth of alga, but very limited success in controlling red tide. Therefore, finding highly efficient, safe and simple method for controlling algae has become a frontier and hot research topic in marine water environmental protection.

A new approach is to use marine allelochemicals produced by beneficial algae to control growth of the harmful algal species [5]. Some researches have demonstrated that growth of microalgae is suppressed by chemical compounds produced by many algal species, such as *Corallina pilulifera* [6], *Ulva pertusa* [7], Kelpn (*Laminaria japonica* Aresch) [8], *Laminaria japonica* [9], *Surgassum thunbergii* [10, 11], *Gracilaria tenuistipitata* [12], *Enteromorpha linza*, and *Gelidium amansii* [13], and others. Presently, researches on application of allelochemicals mostly are focused on utilization of fresh tissues, dry powder, water soluble extracts and filtrates of liquid culture of marine algae.

Allelochemical compounds are active against harmful algal species. However, very few cases have been investigated on the activity of dried algal tissues to inhibit growth of microalgae [8, 9, and 14]. We have not found detailed studies on the algal inhibition effect of extracts using various polar solvents.

Karenia mikimitoi distributes widely, recently it is often identified as one major microalgal species in red tide. Red tide has caused tremendous damages in Australia, North European countries, Japan, New Zealand, South America, North Africa and Hong Kong. The hemolytic toxin and ichthyotoxins secreted into the marine water causes cytolytic symptom and destroys fish gill tissue structure. In the contaminated water, fishes cannot breathe normally and will be suffocated to death. Such damages have caused significant loss to fishery industry [15, 16]. In this study we investigated *K mikimitoi*, by measuring cell density and cell sizes, cell morphology, contents of chlorophyll, protein, and polysaccharides of the algal culture when the growth medium were treated by *Gracilaria lemaneiformis* extracts obtained using different polar solvents. The methanol extract was further fractionated by liquid-liquid separation with petroleum ether, ethyl acetate and n-butanol solvents to determine the most active ingredients. The findings from this research will provide theoretical bases for controlling red tide using *G. lemaneiformis.*

2 Materials and Methods

2.1 Materials

Culture stock of *K. mikimitoi* was provided by Ocean University of China. The alga was cultured in f/2 broth, at 20±0.1℃ and light intensity of 40 μmol/ (m^2 s^1) with a 12-h photoperiod.

G. lemaneiformis was collected in the coastal water in Fujian, China. After removal of debris, fresh clean tissues were washed with double distilled water, and surface disinfection was achieved by treating with an antibiotics cocktail followed by 3-4 rinses in sterile water. The middle and long term in *vitro* cultures were propagated in f/2 solution under the same conditions described above.

2.2 Experimental Methodology

2.2.1 Extracts of *G. lemaneiformis* with Five Different Solvents

Dry tissue powder of 250 g was screened by passing through a 0.3 mm-mesh sieve. Each 50 g was placed into one 500 mL flask, and extracted with 400 mL petroleum ether, chloroform, ethyl acetate, acetone and methanol, respectively. The extraction was done under ultrasonic condition at room temperature for 2 h, and the filtrates were evaporated at 40℃ under constant rotation to remove the solvent. The extracts were weighed, and dissolved in 10 mL DMSO. The concentrates were filtered through 0.22 μm sterile organic filter to remove microbes under sterile condition, and stored at 4℃. In the preliminary tests, addition of < 2% DMSO was found to be safe for microalgal culture, therefore this concentration was used in this study.

2.2.2 Evaluation of Algal-Inhibition Ring Treated with the Five Extracts

Agar plates (f/2 containing 2% agar) were overlaid with 30 mm filter paper discs which were soaked in algal culture at the exponential growth stage. After adding a drop of the solvent extracts in the center of the filter paper, the plates were placed at 25℃, light intensity of 60μmol/(m^2 s^1) and a 16:8/d:n photoperiod. Each treatment condition was repeated 3 times. The algal inhibition ring was observed after 24 h, and the diameter of the rings was counted as the mean ±standard error.

2.2.3 Analysis of the Microalgal Liquid Cultures Treated with the Five Solvent Extracts

A 150 mL microalgal culture was composed of f/2 broth and the algal stock cells at exponential growth stage and the extracts from *G. lemaneiformis*. The extract concentration was 0.1, 0.2, 0.4, 0.8 and 1.6 g/L, the control was added with equal volume of DMSO. Each treatment contained three replicates in three flasks. The liquid culture was incubated at 25℃, light intensity of 60 μmol/(m^2 s^1) and a photoperiod of 16:8 (d/n), for 12 d. Every other day, 1 mL liquid was removed from each flask, which was fixed with Lugol's reagents to count cell number.

The cultures in the flasks were replenished with 1 mL of 150 × f/2 broth stock to maintain stable ingredient concentration. Same cultural processes were used in the entire experiment unless indicated otherwise. At the completion of the treatments, contents of chlorophyll, protein and polysaccharide of the micro-algal cells were measured.

2.2.4 Liquid-Liquid Phase Separation of Methanol Extract and Activity Assay of Individual Fractions

Methanol extract has demonstrated the highest algal-inhibition activity; therefore the same extract was further separated to identify the active compounds. Following the procedure described above, 50 g of methanol extract was prepared. The extract was lyophilized under reduced pressure, and then subjected to liquid-liquid phase separation. The powder was dissolved in 90% methanol solution and extracted with petroleum ether for three times. The petroleum ether phase was evaporated under

reduced pressure to obtain petroleum extract. The methanol phase was evaporated at 40℃ and re-dissolved in distilled water, followed by extraction three times with ethyl acetate. The ethyl acetate phase was evaporated under reduced pressure to obtain ethyl acetate extract. Finally, the water phase was extracted with n-butanol for three times. Both n-butanol and water phases were evaporated under reduced pressure to obtain n-butanol and water extracts, respectively. The four types of extracts were dissolved in DMSO, and stored at 4℃.

The microalgal culture (50 mL) contained f/2 broth, algal stock solution at exponential growth stage, and each of the four extracts prepared above to a final concentration of 1.6 g/L. The control was added with equal volume of DMSO in freshly prepared sea water. Each treatment had three replicates and the culture was incubated for 12 d.

2.3 Determination of Physiological Indexes of the Microalgal Cells

2.3.1 Chlorophyll Content

The algal culture was centrifuged at 2000 *g* for 10 min. After removal of supernatant, cell pellets were extracted with 90% acetone at 4℃ for 24 h. After centrifugation, the supernatant was used to measure light absorbance at 630 nm, 645 nm and 665 nm. Chlorophyll content (mg/g cell dry weight) was calculated using an equation in [17].

2.3.2 Protein and Polysaccharides

Algal cell culture (15 mL) was centrifuged at 2000 *g* for 10 min. After removal of supernatant, algal cells were lysed by three cycles of freeze (-20℃) and thaw (room temperature). After addition of 3 mL of PBS buffer followed by vibrant shaking, the mixture was centrifuged for 10 min. The supernatant was used to measure contents of protein and polysaccharides [18], which was expressed as mg/g cell dry weight.

2.4 Cell Growth, Cell Size and Shape of Microalgal Culture

To determine cell density, cell number was counted with a hemocytometer under Olympus optical microscope. Cell size was measured using a reticule and images of the cell shape were taken by photomicrograph at an amplification factor of 10×40.

2.5 Data Analysis

Cell density was used to calculate the algal-inhibition ratio for each of the *G. lemaneiformis* extract using the equation: $I = (1 - N/N_0) \times 100\%$, where N is the cell density of the treated group ($\times 10^4 \cdot mL^{-1}$) and N_0 is the cell density in the untreated control group ($\times 10^4 \cdot mL^{-1}$). EC_{50} values were generated using probability unit method [19].

The dose effect was evaluated using t test. All the experiments were repeated at least three times, and the data were represented as mean±standard error. Statistical analysis was performed using the SPSS11.5 program, the level of significant difference was at $P < 0.05$, and the extremely significant difference at $P < 0.01$.

3 Results

3.1 Effect of G. lemaneiformis Extracts on Suppressing Growth of K. mikimitoi

The five extracts all have demonstrated some algal inhibition effect, and those from methanol and acetone solvents were more effective than the other three extracts (Fig.1).

Fig. 2 also shows that all of the extracts were effective in suppressing algal growth, of which the extracts by methanol and acetone had the highest activity ($P < 0.05$). At concentrations above 0.8 g/L of the two extracts, algal cell growth was strongly reduced resulting in fewer live cells, furthermore cell growth did not recover after termination of the treatments. When the concentration was raised to 1.6 g/L, algal cells started to die, and 100% cell death rate occurred on 2 d and 10 d in the two extract treatments, respectively.

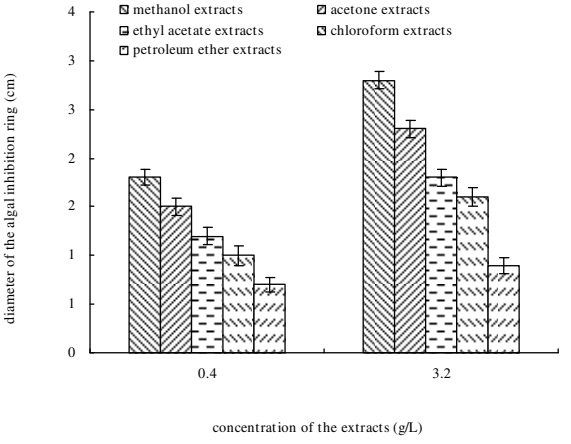

Fig. 1. Diameter of the inhibition ring of *K. mikimitoi* treated with methanol, acetone, ethyl acetate, chloroform and petroleum ether solvent extracts from *G. lemaneiformis* (1d)

For ethyl acetate and chloroform extracts in the 0.8 g/L~1.6 g/L concentration range, the inhibition effect appeared after 4 d of treatment, and continued until the end of the experiment. The algal cells did not resume growth during recovering period

($P < 0.05$). The ethyl petroleum extract also showed some but insignificant ($P > 0.05$) inhibitory effect after 4 d of treatment, moreover the algal inhibition effect diminished significantly over an extended period of culture ($P < 0.05$).

The median effective concentration for each solvent extract (EC_{50}, 12d) was obtained using the method of probability measurement. The EC_{50} value was 0.40 g/L for methanol extract, 0.44 g/L for acetone extract, 0.73 g/L for ethyl ether extract, 0.90 g/L for chloroform extract, and 1.41 g/L for petroleum ether extract. The EC_{50} for methanol extract was the lowest, which corresponds to the best algal inhibition effect.

3.2 Effect G. lemaneiformis Extracts on Cell Morphology and Cell Sizes of K. mikimitoi

Significant differences in the morphology of *K. mikimitoi* cells were identified among the treatments with the five solvent extracts from *G. lemaneiformis* (Fig. 3). After culture for 2 d, the cells treated with methanol and acetone extracts formed large cavities, most of cells ruptured severely, and cell pigments degenerated rapidly. As the culture period extended, the symptoms of empty cavities and cell rupture became worse. The extract by ethyl ester also caused formation of cavities and ruptures of algal cells, and many cells aggregated together. The extracts by chloroform and petroleum ether caused goffers of the algal cells（Fig. 3).

Compared to the control, cell sizes were smaller ($P < 0.05$) in the culture treated with relatively higher concentration of ethyl ether extract. As the cultural period extended, cell shrinkage symptom became more obvious ($P < 0.05$). The other four solvent extracts did not cause obvious changes in sizes of algal cells（$P > 0.05$）(Table 1).

Table 1. Effects of extracts from *G. lemaneiformis* extracted with different solvents on cell sizes of *K. mikimitoi*

Experiments	Length of cells (μm)	Width of cells (μm)
Control	12.13 ± 2.59	11.38 ± 1.06
Methanol extracts (1.6 g/L)	11.38 ± 1.92	11.63 ± 2.97
Acetone extracts (1.6 g/L)	10.50 ± 0.93	10.38 ± 10.92
Ethyl acetate extracts（1.6 g/L)	6.67 ± 1.03	5.67 ± 1.03
Chloroform extracts (1.6 g/L)	11.75 ± 1.58	10.63 ± 0.74
Petroleum ether extracts (1.6 g/L)	10.25 ± 1.03	10.38 ± 0.92

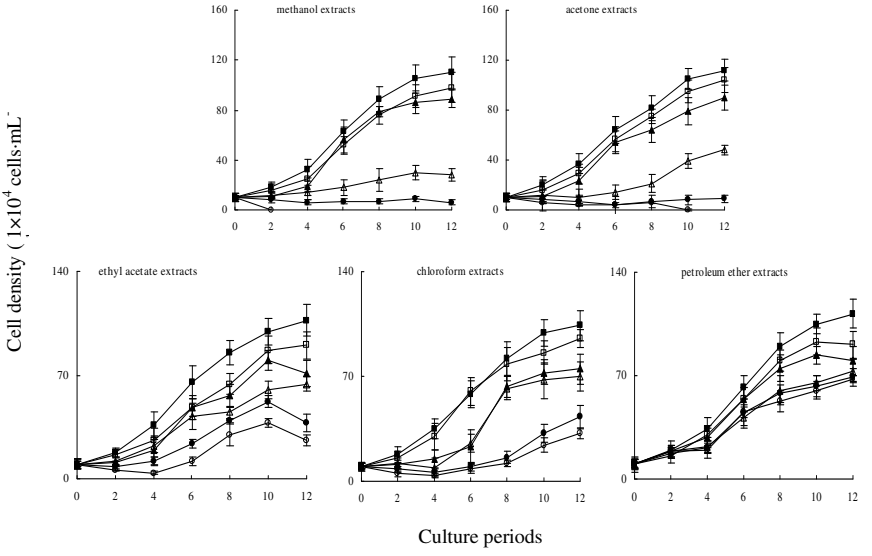

Fig. 2. Effects of *G. lemaneiformis* extracts with different solvents (■ 0, □ 0.1 g/L, ▲ 0.2 g/L, Δ 0.4 g/L, ● 0.8 g/L, ○ 1.6 g/L) on the growth of *K. mikimitoi*

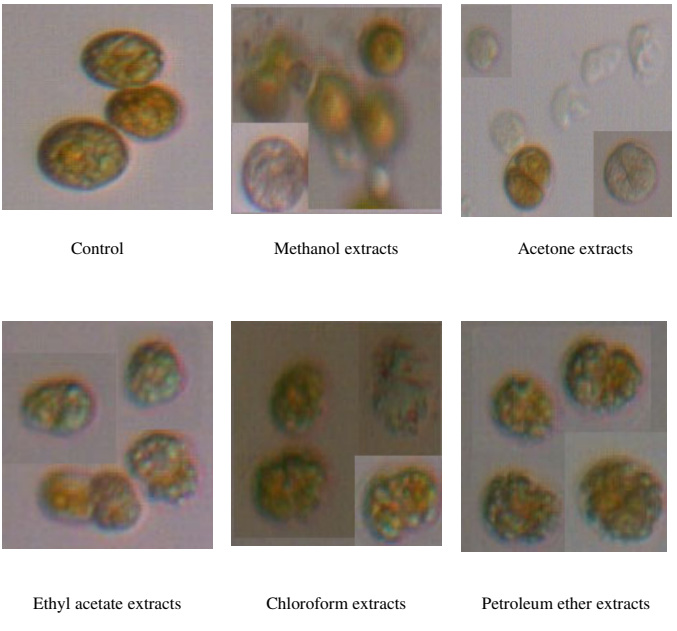

Fig. 3. Effects of extracts with five solvents from *G. lemaneiformis* on morphology of *K. mikimitoi*

3.3 The Effect of G. lemaneiformis Extracts with Different Solvents on Chlorophyll Content, Protein and Polysaccharides of Microalgal Culture

From Fig.4, it can be seen that the five solvent extracts all significantly ($P < 0.05$) inhibited synthesis of chlorophyll in the algal cells, the inhibition effect escalated corresponding to higher extract concentrations. At 1.6 g/L of the extracts with ethyl acetate, chloroform and petroleum ether, chlorophyll content was reduced by 2.3±0.2~2.6±0.2 fold compared to untreated control. At 0.4 g/L and 1.6 g/L of methanol and acetone extracts, the chlorophyll content dropped to 25% of the control.

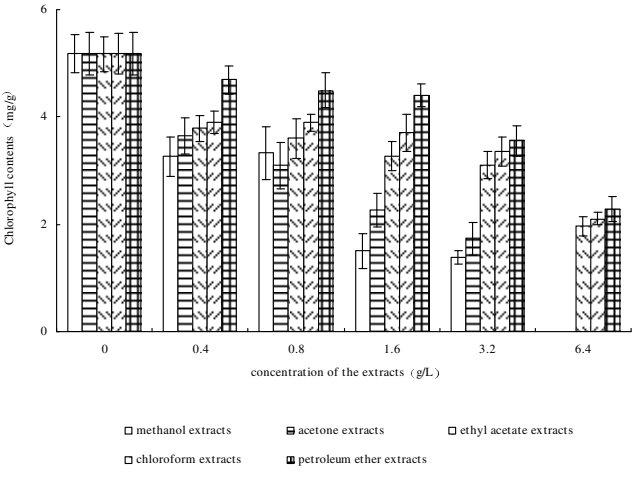

Fig. 4. Effects of extracts with five solvents from *G. lemaneiformis* on chlorophyll content of *K. mikimitoi*

The impact on protein and polysaccharide contents was similar (Fig 5 and 6). Higher concentrations of methanol, acetone and ethyl acetate extracts all significantly ($P < 0.05$) reduced algal cellular protein and polysaccharide contents whereas chloroform and petroleum ether extracts promoted the two parameters ($P > 0.05$).

3.4 Effects of Different Solvent Extracts from G. lemaneiformis on Growth of K. mikimitoi

In the previous experiments, methanol extract has demonstrated very strong algal inhibition activity. Therefore, methanol extracts was further fractionated in petroleum ether, ethyl acetate and 1-butanol solvents, using liquid-liquid separation (Table 2). The results show that the compounds in the petroleum and ethyl acetate phases significantly inhibited ($P < 0.05$) growth of *K. mikimitoi*. On 12 d, the inhibition ratio all exceeded 40%. Therefore, the compounds in petroleum ether and ethyl acetate should be the targets for future separation and purification.

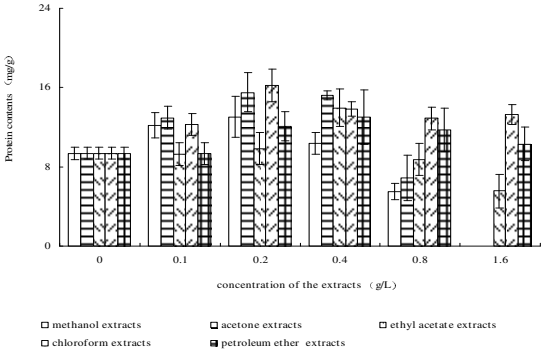

Fig. 5. Effects of extracts with five solvents from *G. lemaneiformis* on protein content of *K. mikimitoi*

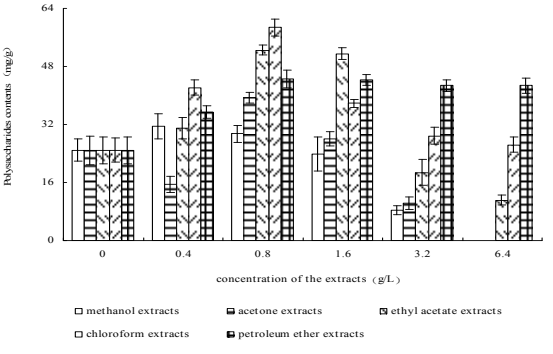

Fig. 6. Effects of extracts with five solvents from *G. lemaneiformis* on polysaccharide content of *K. mikimitoi*

Table 2. Yields of components from liquid-liquid separation of methanol extract and the growth inhibition effect on *K. mikimitoi*

Components	quality (g)	Yield (%)	Growth inhibitory ratio (%)
Petroleum ether phase	21.2	42.4	50.8
ethyl acetate phase	16.6	33.6	41.5
n-butanol phase	4.46	8.92	7.69
Water phase	3.52	7.04	9.23

Note: Data in the table were means of three replicates.

4 Discussions

The inhibition activity of marine algae on microalgae has been reported [6, 7, 20], such as Corallina *pilulifera* against *Cochlodinium polykrikoides*, and *Ulva lactuca* against *Heterosigma akashiwo* and *Alexandrum tamarense*. The results from this study also demonstrated that *G. lemaneiformis* inhibited growth of *K. mikimitoi.*

Moreover, the algal inhibition compounds were extracted with organic solvents (Fig. 1). The data in Fig. 2 show that the five solvent extracts from *G. lemaneiformis* inhibited to various degrees growth of *K. mikimitoi*. Such differences could be caused by the polarity of the solvents by partitioning different amount and species of compounds. Among the five extracts, the one extracted with the more polar solvent had stronger inhibition effect, such as petroleum ether extract < chloroform extract < ethyl acetate extract < acetone extract < methanol extract. According to these results, methanol should be used as the solvent to extract algal inhibition compounds.

Examination of algal cell morphology found that methanol and acetone extracts both led to formation of obvious cavity and severe disruption in the cellular structures, and loss of cell pigments. The ethyl acetate extract treated cells had cavities and ruptures, the cells were aggregated together at later stage of culture. The chloroform and petroleum ether extracts caused the cells to form goffers (Fig. 3). Similar cellular structure alteration was observed in *Microcystis aeruginosa* algal cells that were treated with organic solvent extracts from *Arundo donax* Linn. [21].

We have also found that the extracts with organic solvents significantly reduced mobility of the algal cells. Effect on cell mobility was reported by Nagayama and Jin. It was found that extracts from *Ulva pertusa*, *Laminaria japonica* Aresch, and brown alga *Laminariaceae Bory* reduced cell mobility of *Cochlodinium polykrikoides* and *Alexandrium tamarense* [8, 9].

It was observed that the solvent extract treatments caused the algal cells to shrink and the cell sizes became smaller. Ethyl acetate extract had the most significant effect. It is normally recognized that external environment causes size shrinkage of algal cells through the following three mechanisms. The first one is that algal cells enter programmed cell death [22]. The second one is that the algal cells produce spores to tolerate the unfavorable environment in order to ensure survival of individuals [23]. The third mechanism is cell size changes under the influence of the ion density gradient across cell membranes, the disturbance of ion channel openings leads to alteration in osmotic potential [24]. However, no relevant tests were conducted in this study. Further experiments need to be performed to understand why ethyl acetate extract caused algal cells to become smaller.

The experimental results demonstrated that treatments with different solvent extracts resulted in variation in the morphological characteristics of the algal cells. The reason could be that the five solvents have different degrees of polarity, which could lead to variation in the chemical composition of the partition and consequently different inhibition mechanism on the cells of *K. mikimitoi*. The alga can also activate multiple antagonistic pathways to fight against the external stresses, leading to differential alteration in cell morphology, sizes and mobility.

In this study, we have found that contents of chlorophyll, of protein and polysaccharides changed significantly in the algal cells that were treated with the solvent extracts from *G. lemaneiformis* (Fig 4, 5 and 6). It is possible that the synthetic processes for the associated compounds were affected by the extracts.

In systematic alleloparthy of continental and fresh water ecosystems, allelopathic compounds have demonstrated the activity to reduce chlorophyll content, influence protein synthesis and enzymatic physiological parameters [25, 26]. Whether the

solvent extracts of *G. lemaneiformis* functions in similar mechanism needs to be clarified in future studies.

In the liquid-liquid separation of methanol extract, the compounds in the petroleum ether and ethyl acetate phases both significantly inhibited growth of *K. mikimitoi*. In conclusion, *G. lemaneiformis* has the activity suppressing growth of *K. mikimitoi*. We will continue to identify the associated mechanisms.

Acknowledgment. This work was supported by the project of Jiangsu key laboratory of marine biotechnology of Huaihai Institute of Technology (2008HS017 and 2009HS09).

References

1. Steidinger, K.A.: A re-evaluation of toxic dinoflagellates biology and ecology. Progress Phycology Research 2, 147–188 (1983)
2. Yu, Z.M., Zou, J.Z., Ma, X.N., Li, Q.S.: Chemical methods of controlling red tide. Oceanologia et Limnologia Sinica 24(3), 314–318 (1993)
3. Du, Y.F., Ye, Z.F.: Red tide of Heterosigma akashiwo and its microbial control. Bulletin of Jiangsu Environmental Science 13(4), 35–36 (2000)
4. Tai, V., Lawrence, J.E., Lang, A.S., Chan, A.M., Culley, A.I., Suttle, C.A.: Characterization of HaRNAV, a single-stranded RNA virus causing lysis of Heterosigma akashiwo (Raphidophyceae). Journal of Phycology 39(2), 343–352 (2003)
5. Vyvyan, J.R.: Allelochemicals as leads for new herbicides and agrochemicals. Tetradron 58, 1631–1646 (2002)
6. Jeong, J.H., Jin, H.J., Sohn, C.H., Suh, K.H., Hong, Y.K.: Algicidal activity of the seaweed Corallina pilulifera against red tide microalgae. Journal of Applied Phycology 12(1), 37–43 (2000)
7. Nan, C.R., Zhang, H.Z., Dong, S.L.: Effect of water soluble extracts from Ulva pertusa Kjellm on growth of three three marine red tide algi. Journal of Environmental Sciences 24(4), 702–706 (2004)
8. Nagayama, K., Shibata, T., Fujimoto, K.: Algicidal effect of phlorotannins from the brown alga Ecklonia kurome on red tide microalgae. Aquaculture 218, 601–612 (2003)
9. Jin, Q., Dong, S.L.: Comparative studies on the allelopathic effects of two different strains of U. pertusa on Heterosigma akashiwo and Alexandrium tamarense. Journal of Experimental Marine Biology and Ecology 293, 41–55 (2003)
10. Wang, R.J., Tang, X.X., Feng, L., Xiao, H., Qu, L., Cai, H.J.: Inhibitory effect of Surgassum thunbergii on Heterosigma akashiwo and Skeletonema costatum. Chinese Journal of Applied Ecology 17(12), 2421–2425 (2006)
11. Qu, L., Xiao, H., Wang, R.J., Dong, D., Feng, C., Tang, X.X.: Primary studies on the allelopathic effects of Surgassum thunbergii and Corallina pilulifera on Heterosigam akashiwo. Journal of Ocean University of China 37(4), 621–626 (2007)
12. Liu, T.T., Yang, Y.F., Ye, C.P., Wang, Z.H.: Inhibitory effects of seaweed Gracilaria lemaneiformis on the growth of two red tide microalgal species. Journal of Jinan University (Natural Science) 27(5), 754–759 (2006)
13. Xu, H., Dong, S.L., Jin, Q.: Study on inhibitory effects of nine macroalgae on the growth of Heterosigma akashiwo. Periodical of Ocean University of China 35(3), 475–477 (2005)

14. Jin, Q.: Studies on the antagonistic activity of macro marine algi Ulva Pertusa on red tide microalgi, and isolation and Identification of the antagonistic compounds. Ocean University of China (2005)
15. Wang, C.H., Yi, Y.W., Qi, Y.Z., Xie, L.C., Jiang, T.J.: Histopathological changes in fish gills during Gymnodinium mikimotoi red tide in Guishan Island area, the South China Sea. Acta Oceanologica Sinica 23(1), 133–138 (2001)
16. Yang, Z.B., Hodgkiss, I.J.: Hong kong's worst "red tide": causative factors reflected in a phytoplankton study at Port Shelter station in 1998. Harmful Algae 3, 149–161 (2004)
17. Jensen, A.: Handbook of Physiological Methods, pp. 75–76. Cambridge University Press, New York (1978)
18. Zhang, Z.L., Zai, W.Q.: Experimental Methods of Plant Physiology, pp. 38–42. Higher Education Press, Beijing (2002)
19. Li, F.M., Hu, H.Y.: Isolation and characterization of a novel antialgal allelochemical from Phragmites communis. Applied and Environmental Microbiology 71, 6545–6553 (2005)
20. Keating, K.I.: Blue-green algal inhibition of diatom-growth: transition from mesotrophic to eutrophic community structure. Science 199, 971–973 (1978)
21. Hong, Y., Hu, H.Y., Huang, J.J., Sakoda, K., Sagehashi, M., Li, F.M.: Growth of Microcystis aeruginosa affected by allelochemicals of Arundo donax Linn. Extracted with Different Solvents. Environmental Sciences 29(11), 3143–3147 (2008)
22. Heimlich, G., Bortner, C.D., Cidlowski, J.A.: Apoptosis and cell volume regulation, The importance of ions and ion channels. Cell Volume and Signaling 559, 189–203 (2004)
23. Montechiaro, F., Giordano, M.: Effect of prolonged dark incubation on pigments and photosynthesis of the cave-dwelling cyanobacterium Phormidium autumnale (Oscillatoriales, Cyanobacteria). Phycologia 45, 704–710 (2006)
24. Taylor, A.R., Manison, N.F.H., Fernandez, C., Wood, J., Brownlee, C.: Spatial organization of calcium signaling involved in volume control of the Fucus rhizoid. Plant Cell 8, 2015–2031 (1996)
25. Hu, H.Y., Men, Y.J., Li, F.M.: Research progress on phyto-allelopathic algae control. Ecology and Environment 15(1), 153–157 (2006)
26. Li, F.M., Hu, H.Y.: Mechanism of phyto-allelochemicals and its application for harmful algae control in nature water body. Water Supply and Sewerage 30(2), 1–4 (2004)

Antialgal Substances from *Isochrysis galbana* and Its Effects on the Growth of *Isochrysis galbana* and Six Species of Feed Microalgae*

Yingying Sun[1], Shenzhen Xu[1], Wenhao Li[1], Jing Zhang[1], and Changhai Wang[2]

[1] Jiangsu Key Laboratory of Marine Biotechnology, Huaihai Institute of Technology Lianyungang, Jiangsu Province 222005, China
[2] School of Ocean Yantai University Yantai, Shandong Province, 264005, China
syy-999@163.com, chwang2001@sina.com

Abstract. Antialgal substances produced by Isochrysis galbana affects the growth of other micro-algal cells. In this study, the productions of antialgal substances from Isochrysis galbana and their possible chemical structures were elucidated. The effects of antialgal substances on the growth of Isochrysis galbana and other microalgae (Chaetoceros muelleri, Chaetoceros gracilis, Phaeodactylum tricornutum, Nitzschia closterium, Platymonas elliptica and Dunaliella salina) were studied. The medium for culturing Isochrysis galbana was determined initially and then crude antialgal substances (CEAE) were extracted using ethyl acetate. Subsequently, fractionated using Sephadex G-15 gel filtration chromatography and analyzed by gas chromatography. The contents of the fatty acids were determined by using the normalization method. The results indicated that as Isochrysis galbana culture ages, the concentration of the antialgal substances in the culture medium increases, suggesting that Isochrysis galbana gradually produces antialgal substances from the exponential growth phase to the death phase. The growth inhibitory rates of Isochrysis galbana by CEAE during the three growth phases were 7.17%, 34.2% and 64.1%, respectively. The CEAE showed significant growth inhibition to Isochrysis galbana and the six species of feed microalgae. At the concentration of 21.6 mg/L, the growth inhibitory rate of Isochrysis galbana, Chaetoceros muelleri, Chaetoceros gracilis, Phaeodactylum tricornutum, Nitzschia closterium, Platymonas elliptica and Dunaliella salina by CEAE was 67.2%, 63.3%, 59.6%, 61.1%, 66.2%, 68.3% and 48.5%, respectively. Further investigation found that chlorophyll content significantly decreased in the cells of all tested microalgae, which indicated the chlorophyll synthesis was inhibited by CEAE. The CEAE at 21.6 mg/L, significantly inhibited the protein synthesis in the cells of Isochrysis galbana, Chaetoceros muelleri, Chaetoceros gracilis, Phaeodactylum tricornutum and Nitzschia closterium approximately by 49%. Of the three fractions, F-Ⅰ and F-Ⅱ showed inhibitory activity against the growth of the six species of microalgae, but the inhibition activity of F-Ⅲ was lower. The fatty acids in CEAE, F-Ⅰ and F-Ⅱ were stearic acid (C18:0) and

* This work is partially supported by the project of Jiangsu key laboratory of marine biotechnology of Huaihai Institute of Technology # 2008HS017 to Yingying Sun and research start project # KQ08031 to Yingying Sun.

E. Zhu and S. Sambath (Eds.): Information Tech. and Agricultural Eng., AISC 134, pp. 211–223.
springerlink.com © Springer-Verlag Berlin Heidelberg 2012

oleic acid (C18:1), respectively. Results suggested that stearic acid (C18:0) or oleic acid (C18:1) or the mixture of both stearic acid (C18:0) and oleic acid (C18:1) probably was the substance that could inhibit the growth of the six species of microalgae.

Keywords: Antialgal substances, Inhibitory effect, Isochrysis galbana, Microalgae.

1 Introduction

The inhibitory phenomenon between microalgal cells has been known for at least sixty years. Since 1940, Pratt found that some extracellular metabolites produced by microalgae (e.g. chlorellin from *Chlorella vulgaris*) can control the growth of the cell [1]. Some microalgae, like *Fucus vesiculosus*, *Chlamydomonas reinhardtii* and *Skeletonema costatum* were found to excrete antialgal substances into the medium [2-4]. More recently, microalgae such as *Peridinium bipes*, *Nannochloropsis oculata*, three toxic *Alexandrium* species, *Peridinium polonicum*, *Nitzschia frustulum*, *Scrippesiella trochoidea*, *Prorocentrum donghaiense* and *Haematococcus pluvialis* produced antialgal substances that inhibited either their own growth, or the growth other species, or both [5-9]. Although the allelopathic phenomena has been discovered in these microalgae, most of them only demonstrated the phenomenon of auto-toxicity among red tide microalgae, and few of them demonstrated the phenomenon of allelopathy among marine feed microalgae.

In our previous works, we found a type of antialgal substance produced by *Isochrysis galbana*, which can affect its growth [10]. In order to inspect the allelopathic phenomena between marine microalgae, and to probe the effects on the growth of *Isochrysis galbana* and the six species of feed microalgae (*Chaetoceros muelleri*, *Chaetoceros gracilis*, *Nitzschia closterium*, *Phaeodactylum tricornutum*, *Platymonas elliptica* and *Dunaliella salina*) by antialgal substances, a series of experiments was carried and summarized in this study. Moreover, three fractions of the crude antialgal extracts (CEAE) were obtained and were separated by Sephadex G-15 gel filtration chromatography. The changes in the growth of six species of feed microalgae with and without these fractions were determined and the fatty acid composition of antialgal substances (CEAE) and its isolated fractions was then analyzed by gas chromatography.

2 Materials and Methods

2.1 Algal Species and Culture Conditions

The microalgae *Isochrysis galbana*, *Chaetoceros muelleri*, *Chaetoceros gracilis*, *Nitzschia closterium*, *Phaeodactylum tricornutum*, *Platymonas elliptica*, *Dunaliella salina* was offered by Marine Microalgae Research Center, Ocean University of China and cultured in Erlenmeyer flasks with f/2 medium. Cells were cultured at 23 ℃ and illuminated with fluorescent lamps in a 16/8 dark /light cycle, at an irradiance level of 36 μmol m^{-2} s^{-1}.

2.2 Experimental Methodology

2.2.1 Isochrysis galbana Culture Medium Filtrate Assays

8 L of *Isochrysis galbana* cultures were taken on days 18, 12 and 6 after inoculation, and were centrifuged at 5000 g for 15 min, respectively. The supernatant was filtered through a 0.45 μm Millipore filter membrane. The nutrient concentrations in the filtrates were measured before the enrichment, respectively. The filtrates were added along with the f/2 nutrients. The f/2 medium with sterilized sea water served as the control. The pH of all test media were adjusted to 8.0, and then *Isochrysis galbana* were inoculated into them with an initial cell density of 40×10^4 mL^{-1}. Algal cells were cultured under the same conditions mentioned above for 10 days in 6 L flat plate-organic glass reactors, in which the light-path length was 5.5 cm, containing 4 L of above-motioned test media.

2.2.2 Crude Antialgal Substances (CEAE) Treatment

Isochrysis galbana culture broth of 18 days old was centrifuged at 5000 g for 15 min; the supernatant was filtered through a 0.45 μm membrane filter. The filtrate pH value was adjusted to 2-3 using HCl and extracted three times with ethyl acetate. The crude antialgal substances (CEAE) were evaporated to dryness under reduced pressure at 40 ℃. Then, 1.8, 3.6, 5.4, 10.8, 19.8 and 21.6 mg/L of CEAE were added to the flasks containing 500 mL of f/2 medium, respectively. The pH of all test medium was adjusted to a value of 8.0, and then test microalgae were inoculated into them, respectively. The initial cell density of *Isochrysis galbana*, *Chaetoceros muelleri*, *Chaetoceros gracilis*, *Phaeodactylum tricornutum*, *Nitzschia closterium*, *Platymonas elliptica* and *Dunaliella salina* in the culture medium was $(23\pm3)\times10^4$ cells mL^{-1}, $(63\pm5)\times10^4$ cells mL^{-1}, $(64\pm4)\times10^4$ cells mL^{-1}, $(65\pm3)\times10^4$ cells mL^{-1}, $(93\pm5)\times10^4$ cells mL^{-1}, $(7\pm1)\times10^4$ cells mL^{-1} and $(14\pm3)\times10^4$ cells mL^{-1}, respectively. All tests were carried out in triplicates, and the culture medium without CEAE served as the control. Cultures were incubated for 6 days under the conditions mentioned above.

2.2.3 Initial Purification of CEAE

The CEAE was dissolved in 4 mL of 0.2M NaOH, and then diluted to 10 mL with distilled water. About 5 mL of the solution was loaded onto Sephadex G-15 column (30 mm ID×160 mm) and eluted with distilled water. Five milliliter fractions, were collected and determined by UV absorption at 235 nm, and the growth inhibitory effects of each fraction was detected using the following methods.

Appropriate amounts of samples were evaporated under reduced pressure at 40 ℃, and the residues were added during the logarithmic phase of the six microalgae species, and the changes in the cell densities were monitored. All cultures were incubated for 6 days under the same conditions mentioned above, and the tests were carried out in triplicates, and the culture without the residues was served as control.

2.3 Measurement of Growth

0.1mL cultures medium was sampled every two days and microalgae cells were counted under BX-202B inverted microscope using a haemacytometer.

2.4 Chlorophyll Content Assay

The chlorophyll content was measured on the method based on Jensen [11]. Briefly, samples were collected on glass filters (Whatman GF/F). Then the filtrates were transferred to a 10-mL centrifuge tube with acetone and kept overnight at 4 ℃. The pellets were extracted again until it became colorless. Measurements were performed with a spectrophotometer at what OD_{630}, OD_{645} and OD_{665}, and the equations given by Jensen were used to calculate the chlorophyll concentration.

2.5 Protein Content Assay

Cell suspensions (20 mL) were centrifuged at 5000 *g* for 10 min. The pellets were resuspended in 3 mL potassium phosphate buffer (pH 7.8), sonicated for 3 min, and then centrifuged again at 5000 *g* for 10 min. An aliquot of the extract was used to determine its protein content by using Bradford method utilizing bovine serum albumin as a standard [12].

2.6 Nutrient Concentrations

About 10 mL samples were taken to determine the dissolved nutrient concentrations of ortho-phosphate (PO_4^{3-}), nitrate (NO_3^-), nitrite (NO_2^-) and ammonium (NH_4^+) using an autoanalyzer QuikChem 8000.

2.7 Fatty Acid Analysis

Saponification and fatty acid methylation were carried out according to a method described by Slover and Lanza [13]. Fatty acid methyl esters (FAME) analyses were carried out by gas chromatography (GC) using a chromatograph (Agilent) equipped with a HP-5MS column (30 m×0.32 mm ×0.25 μm) and a flame ionization detector (FID). Nitrogen was used as a carrier gas. Injector and detector were maintained at 250 ℃ whereas oven temperature was raised form 170 to 250 ℃ at 5 ℃ min^{-1}. The FAME compositions were identified and calculated by comparison with standards (Sigma Chem Co).

2.8 Data Analysis

Data were statistically analyzed, using the SPSS 12.0 software package, using one-way ANOVA. Significant differences between two means were determined by Tukey's test at *P*-values < 0.05 were regarded as significant.

Inhibitory rate = (biomass of control − biomass of sample) × 100% / biomass of control.

Determination of EC_{50}: During the period of ethyl acetate extract exposure, the effective concentration of ethyl acetate extract required to reduce population growth by 50% when compared to the growth in the control, is expressed by EC_{50}.

3 Results and Discussion

3.1 Effects of Isochrysis Galbana Culture Medium Filtrate

A typical growth curve of *Isochrysis galbana* as the number of living cells is shown in Fig. 1. Under this experimental condition, the growth process of *Isochrysis galbana* was divided into phases -1~4: ① lag phase (day 0-2), ② exponential phase (days 2-10), ③ stationary phase (days 10-14), ④ death phase (days 14-26). 18, 12 and 6 days belonged to death phase, stationary and exponential phase, respectively.

Isochrysis galbana grew, in all three different medium at phase-2, 3 and 4, with significant differences among them ($P<0.05$) (Fig.2). The culture medium filtrate at phase-2 showed observable growth inhibition to *Isochrysis galbana*, as compared with the control. However, culture medium filtrate at phase-3 and 4 displayed significant inhibition ($P<0.05$) in the growth of *Isochrysis galbana*. The inhibitory rates of *Isochrysis galbana* growth by culture medium filtrate at phases-2, 3 and 4 were 7.17%, 34.2% and 64.1%, respectively in day 10.

Results showed that, as *Isochrysis galbana* culture ages, the concentration of antialgal substances in the external solution increases, which agreed with Hellebust [13] and Imada et al's report [4]. This suggests that the antialgal substances were synthesized, accumulated in the cells, and then releasing slowly into the medium. When a high concentration was accumulated in the culture, the releasing process became stagnant resulted in the accumulation of antialgal substances within the cells themselves. When the concentration of the antialgal substances in the cell reached a lethal level, the cells started dying and the dead cells were rapidly releasing more antialgal substances into the cultural medium, thereby increasing the concentration of the antialgal substances by *Isochrysis galbana* in the culture medium during the death phase (Fig.2).

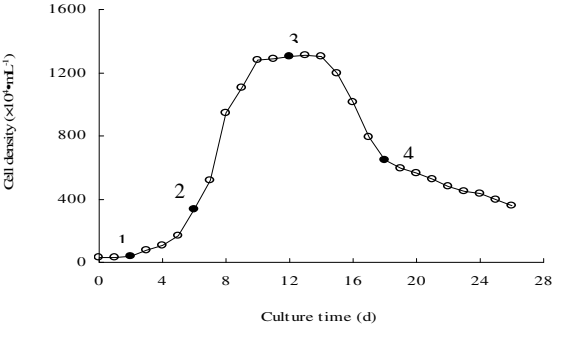

Fig. 1. Typical growth curve of *Isochrysis galbana* The numbers in the figure express the respective growth phase of *Isochrysis galbana* at 2, 6, 12 and 18 day culture, which were subject to confirmation of growth-inhibitor production

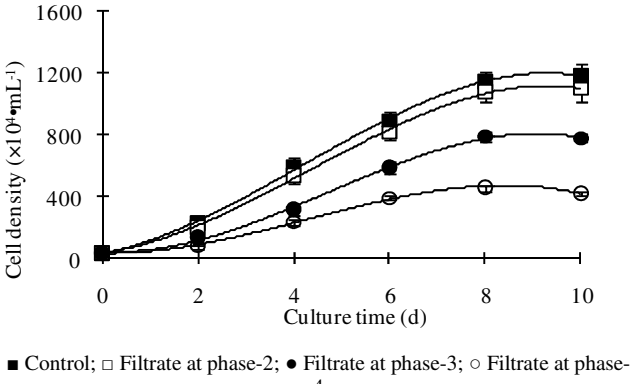

Fig. 2. Effect of the cell-free filtrates from the culture of *Isochrysis galbana* at the three growth phases on growth of *Isochrysis galbana*

3.2 Effects of Different Concentrations of Antialgal Substances Extract (CEAE) on Growth

The CEAE significantly (P<0.05) inhibited the cell growth of all tested microalgae (Fig.3 and 4). When CEAE concentration was at 21.6 mg/L, the inhibitory rate of *Isochrysis galbana*, *Chaetoceros muelleri*, *Chaetoceros gracilis*, *Phaeodactylum tricornutum*, *Nitzschia closterium*, *Platymonas elliptica* and *Dunaliella salina* growth by CEAE were 67.2%, 63.3%, 59.6%, 61.1%, 66.2%, 68.3% and 48.5%, respectively. On the 6th day, the EC_{50} values for *Isochrysis galbana*, *Chaetoceros muelleri*, *Chaetoceros gracilis*, *Phaeodactylum tricornutum*, *Nitzschia closterium*, *Platymonas elliptica* and *Dunaliella salina* growth was 16.1 mg/L, 13.9 mg/L, 15.3 mg/L, 17.2 mg/L, 10.5 mg/L, 11.8 mg/L and 22.1 mg/L, respectively.

In addition, the stimulatory effects of CEAE on the growth of *Isochrysis galbana*, *Platymonas elliptica* and *Dunaliella salina* were also observed, and the cell densities increased significantly at a low CEAE concentration (1.8 mg/L, Fig.3 and Fig.4). Similar phenomenon has been found in plants, Hu and Kong found that a type of allelochemicals, excreted by root of *Arachis hypogaea* before the four-leaf stage, stimulated the seedling growth of rice in low concentration while inhibited at high concentration [14]. Mucciarelli et al. also found that 3, 4-dihydroxybenzoic acid could strongly inhibit the growth of *Nicotiana tabacum* L at high concentration but had stimulation effects at the lowest concentration [15]. However, when the concentration of CEAE was at 21.6 mg/L, the growth of all tested microalgae was inhibited strongly (Fig.3 and Fig.4). The results provided strong support that the allelopathic substance could have played inhibitory role at higher concentrations [16].

3.3 Effects of Different Concentrations of Antialgal Substances (CEAE) on Chlorophyll

A significant (P<0.05) decrease in the chlorophyll contents was observed in all tested microalgae in response to CEAE stress was observed (Fig.5 and Fig.6). When CEAE concentration was 21.6 mg/L, the extracts provided maximum inhibition to chlorophyll of these microalgae. Chlorophyll contents of *Dunaliella salina* decreased by approximately 19.8%, while that of *Isochrysis galbana*, *Chaetoceros muelleri*, *Chaetoceros gracilis*, *Phaeodactylum tricornutum*, *Nitzschia closterium* and *Platymonas elliptica* decreased by 83.9%, 71.7%, 64.4%, 78.8%, 73.3% and 66.8%, respectively.

Based on this study, the chlorophyll syntheses in the cells of all tested microalgae were inhibited by CEAE (Fig.5 and Fig.6). These results were consistent with the speculation by Ervin and Wetzel that aqueous the extractions from aboveground tissues if *Juncus dffusus* retarded *Eleocharis obtuso* seedlings by decreasing the chlorophyll levels [17].

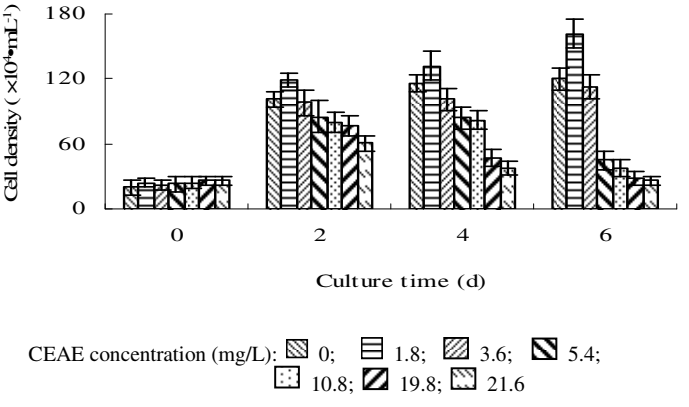

Fig. 3. Effect of CEAE on growth of *Isochrysis galbana*

3.4 Effects of Different Concentrations of Antialgal Substances (CEAE) on Protein

The CEAE significantly affected the accumulation of protein in the cells of *Isochrysis galbana*, *Chaetoceros muelleri*, *Chaetoceros gracilis*, *Phaeodactylum tricornutum* and *Nitzschia closterium.* At CEAE concentration of 21.6 mg/L, the protein contents in the five species of microalgae decreased by approximately 49%. However, the protein levels in the cells of *Dunaliella salina* and *Platymonas elliptica* were increased.

In a study involving allelopathic actions of the alkaloid 12-epihapalindole E and the indolophenanthridinecalothrixin A, isolated respectively from the *Cyanobacterium*

fischerella and *Calothrix* sp., Doan et al. have indicated that both compounds inhibited RNA and protein synthesis, but the levels of such effects strongly depended on the polymerase concentration [18]. Similarly, the effect on the growth, the low CEAE concentration (1.8 mg/L) assayed also made a significant increase in chlorophyll and protein contents of *Isochrysis galbana* cells (Fig.5 and Fig.7). It is an interesting phenomenon, however the mechanism needs further investigation.

3.5 Inhibitory Effect of Fractions Separated by Sephadex G-15 Gel Filtration Chromatography from CEAE on the Growth of the Six Species of Microalgae

Three fractions (F-Ⅰ, F-Ⅱ and F-Ⅲ) were obtained when CEAE was dissolved with 0.2M NaOH and fractionated by gel filtration on Sephadex G-15. Inhibitory rate of six species of microalgae growth by these fractions was shown in Table 1. F-Ⅰ and F-Ⅱ showed the significant (P<0.05) growth inhibition to all six species of microalgae, but the inhibition activity of F-Ⅲ was lower. The inhibitory effect of all test microalgae by F-Ⅰ and F-Ⅱ was approximately 34.5% and 55.4% on day 6, respectively.

3.6 Fatty Acid Analysis of CEAE and Fractions Separated by Sephadex G-15 Gel Filtration Chromatography from CEAE

The fatty acid composition of CEAE and the three fractions (F-Ⅰ~Ⅲ) by gel-filteration on Sephadex G-15 column, were analyzed using gas chromatography. The contents of the fatty acids were determined by the normalization method (Table 2). The results showed that the fatty acids in CEAE, fraction-Ⅰ and fraction-Ⅱ were stearic acid (C18:0) and oleic acid (C18:1), respectively.

Microalgal allelochemicals have not been frequently studied; however they seem to belong to a large array of secondary compounds, with a prevalence of fatty acids in green algae [19]. Pratt and Fong showed that *Chlorella vulgaris* cells produced a growth-inhibiting substance (“chlorellin”), which was a fatty acid mixture [1]. Mccracken et al., following the early report of Proctor confirmed that the green alga *Chlamydomonas reinhardtii* released a mixture of saturated, monounsaturated and polyunsaturated fatty acids, which were active against *Haematococcus pluvialis* [3]. More recently, Chiang et al. reported that the allelochemicals released by *Botryococcus braunii* belonged to a mixture of fatty acids containing α-linolenic, linolenic and palmitic acids [20]. In this paper, we found the same fatty acids in CEAE, F-Ⅰ and F-Ⅱ were stearic acid (C18:0) and oleic acid (C18:1), respectively. In CEAE, fractions F-Ⅰ and F-Ⅱ had significant growth inhibition to all tested microalgae. Therefore, it is suggested that stearic acid (C18:0) or oleic acid (C18:1) or the mixture of both stearic acid (C18:0) and oleic acid (C18:1) could affect the growth of the six species of microalgae.

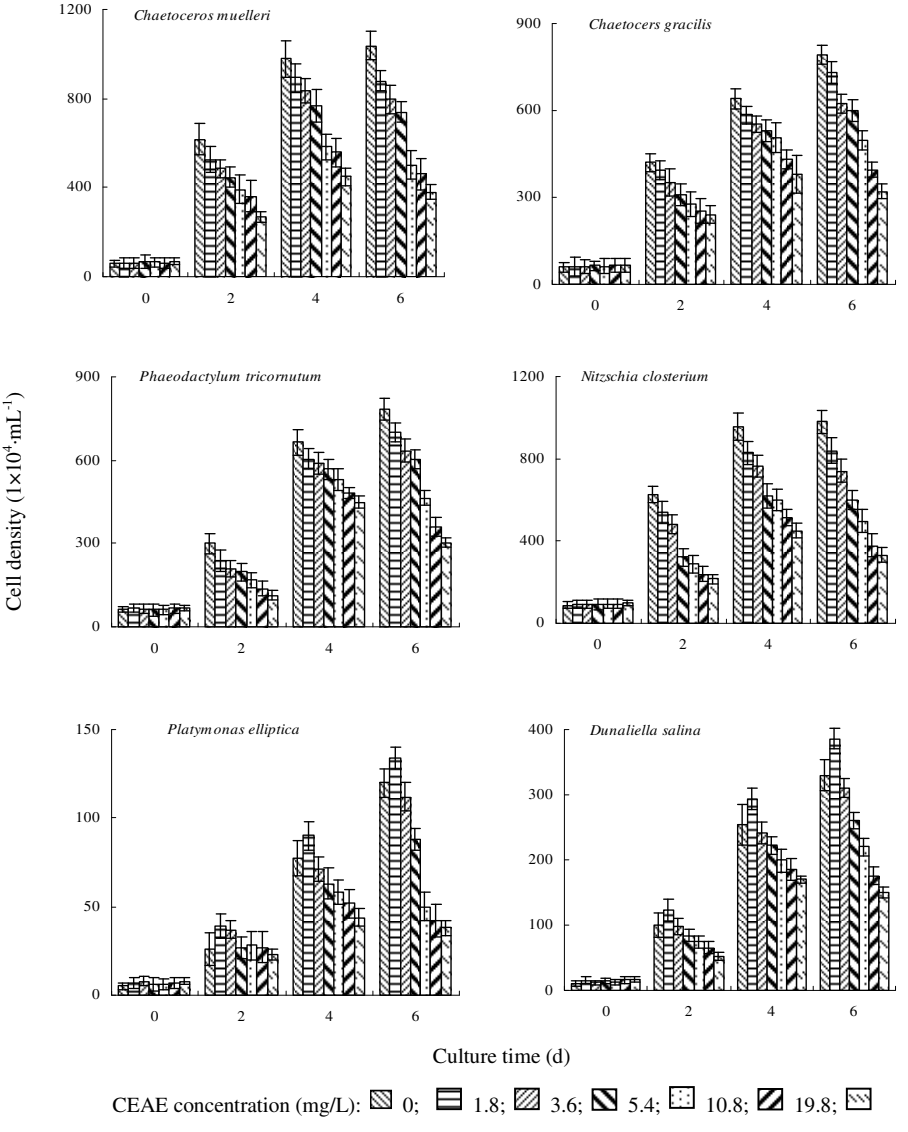

Fig. 4. Effect of CEAE on growth of the six species of feed microalgae

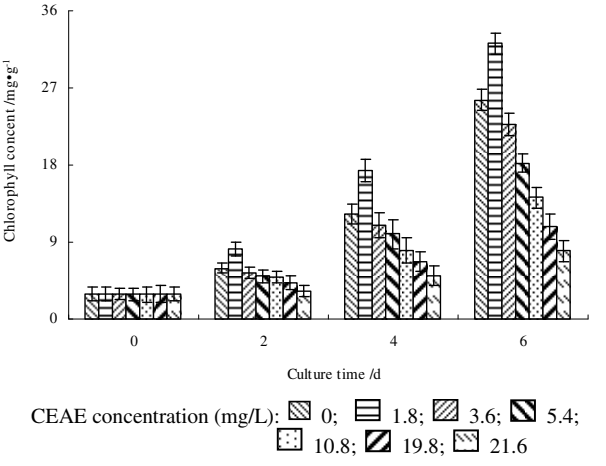

Fig. 5. Effect of CEAE on chlorophyll contents of *Isochrysis galbana*

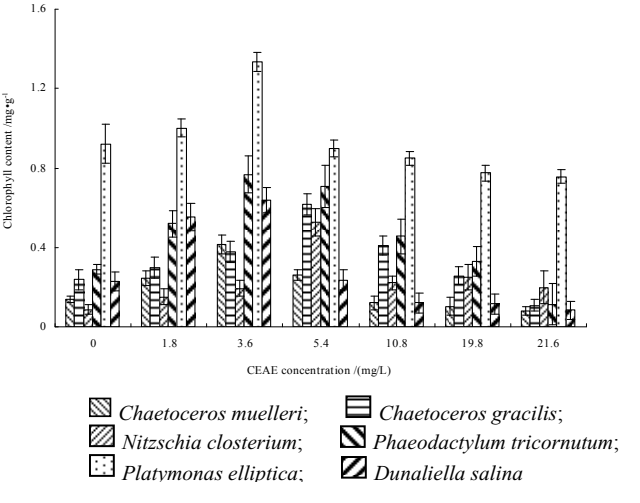

Fig. 6. Effect of CEAE on chlorophyll contents of the six species of feed microalgae

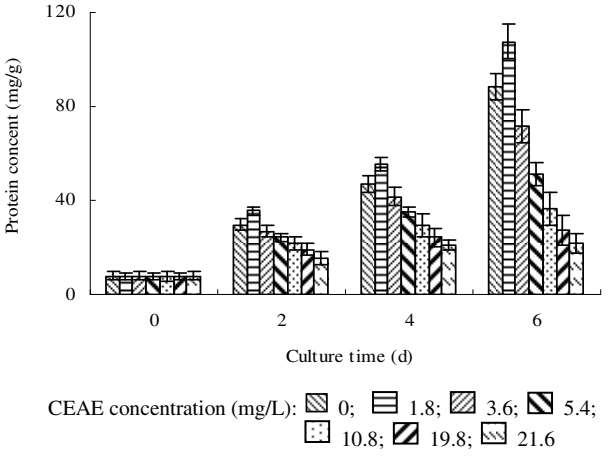

Fig. 7. Effect of CEAE on protein contents of *Isochrysis galbana*

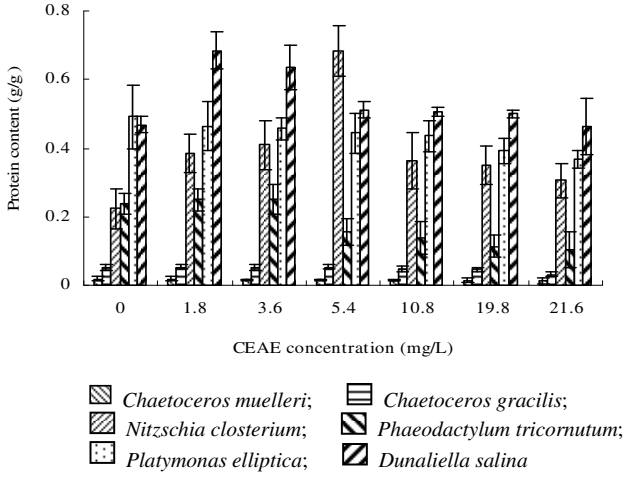

Fig. 8. Effect of CEAE on protein contents of the six species of feed microalgae

4 Conclusion

This study identified that antialgal substances formed by *Isochrysis galbana* strongly inhibited the growth of its cells and also prevented the growth of other microalgae, and affected the synthesis of chlorophyll and protein of seven microalgal species. The results proved again that microalgae can produce toxic substances which could affect the growth of the co-existing species.

Nowadays the algal allelopathy is considered quite a general phenomenon, and the allelopathic phenomena have been recently discovered in some microalgae. However,

until now, only a few allelochemicals from microalgae could be structurally elucidated. In this paper, we considered that stearic acid (C18:0) or oleic acid (C18:1) or the mixture of both fatty acids could be potential antialgal substances.

Acknowledgment. This work was supported by the project of Jiangsu key laboratory of marine biotechnology of Huaihai Institute of Technology (2008HS017 and 2009HS09).

References

1. Pratt, R., Fong, J.: Studies on Chlorella vulgaris ii further evidence that chlorella cells form a growth-inhibiting substance. Americal of Journal Botony 27, 431–436 (1940)
2. Craigie, J.S., McLachlan, J.: Excretion of coloured ultraviolet absorbing substances by marine algae. Can. J. Bot. 42, 23–33 (1964)
3. McCracken, M.D., Middaugh, R.D., Middaugh, R.S.: A chemical characterization of an algal inhibitor obtained from Chlamydomonas. Hydrobiologia 70, 271–276 (1980)
4. Imada, N., Kobayashi, K., Tahara, K., Oshima, Y.: Production of an Autoinhibitor by Skeletonema costatum and its effect on the growth of other phytoplankpyrenoidosa. Nippon Suisan Gakkaishi 57, 2285–2290 (1991)
5. Wu, T.T., Kuo-Huang, L.L., Jensen, L.: Algicidal effect of Peridinium bipes on Microcystis aeruginosa. Current Micobiology 37, 256–261 (1998)
6. Perez, E., Martin, D.E., Padilla, M.: Rate of production of APONINs by Nannochloris oculata. Biomedical Lett. 59, 88–91 (1999)
7. Arzul, G., Seguel, M., Guzman, L., Erard-Le, D.E.: Comparison of allelopathic properties in three toxic Alexandrium species. Journal of Experimental Mainer Biology and Ecology 232, 285–295 (1999)
8. Kearns, K.D., Hunter, M.D.: Green algal extracellular production in cyanobacterium. Environmental Microbiology 2, 291–297 (2000)
9. Sun, Y.N., Yin, M.Y., Liu, J.G.: Auto-signals in Haematococcus pluvialis. Transactions of Oceanology and Limnology 3, 22–28 (2001)
10. Wang, C.H., Sun, Y.Y.: Initial researches on the growth inhibitor in culture of Isochrysis galbana. Mar. Sci. Bull. 25, 29–33 (2006)
11. Jensen, A.: Handbook of Physiological Methods, pp. 45–48. Cambridge University Press, New York (1978)
12. Bradford, M.M.: A rapid and sensitive method for the quantitation of microgram quantities of protein utilizing the principle of protein-dye binding. Analytical Biochemistry 72, 248–254 (1976)
13. Hellebust, J.A.: Extracellular products. In: Stewart, W.D.P. (ed.) Algal Physiology and Biochemistry, p. 755. University of California Press, Oxford (1974)
14. Hu, F., Kong, C.H.: Allelopathic potentials of Arachishypogaea on crops. Journal of South China Agricaltural University 23, 9–12 (2002)
15. Mucciarelli, M., Scannerini, S., Gallino, M., Maffei, M.: Effects of 3,4-dihydroxybenzoic acidon tobacco (Nicotiana tabacum L.) cultured in vitro, Growth regulation in callus and organ cultures. Plant Biosystem 134, 185–192 (2000)
16. Chen, D.H., Liu, Y.D., Song, L.R.: The allelopathy of macrophyte potamogeton pectinatus L on chlorophyta (scenedesmus obliquus) and cyanobacteria (microcystis aeruginosa) and calculation of allelopahtic parameter. Acta Hydrobiologica Sinica 28, 163–168 (2000)

17. Ervin, G.N., Wetzel, R.G.: Allelochemical autotoxicity in the emergent wetland macrophyte Juncus effusus (Juncaceae). American Journal of Botony 87, 853–860 (2000)
18. Doan, N.T., Rickards, R.W., Rothschild, J.M., Smith, G.D.: Allelopathicactions of the alkaloid 12-epi-hapalindoleE isonitrile and calothrixin A from cyanobacteria of the genera Fischerella and Calothrix. Journal of Applied Phycology 12, 409–416 (2000)
19. Ikawa, M.: Algal polyunsaturated fatty acids and effects on plankton ecology and other organisms. UNH Center Freshwater Biol. Res. 6(2), 17–44 (2004)
20. Chiang, I.Z., Huang, W.Y., Wu, J.T.: Allelochemicals of Botryococcus braunii (chlorophyceae). Journal of Phycology 40, 474–480 (2004)

Effect of Peanut Roots Intercropped with Rice on Excretion of Nitrogenous Compounds at Different Growth Stages

Bo Wang[1] and Shuqi Wang[2]

[1] Faculty of Horticulture, Soochow University Suzhou 215123, Jiangsu
[2] China Northeast Institute of Geography and Agriculture Ecology Chinese Academy of Sciences Harbin 150081, Heilongjiang, China
wangb@suda.edu.cn, Wsq-200131@sohu.com

Abstract. Sand-culture and solution-culture experiments were carried out to study the excretion of nitrogenous compounds by peanut roots intercropped with rice cultivated in aerobic soil at different growth stages, i.e., seedling, flowering and pod-filling stage of peanut crop. Considerable amounts of nitrogenous compounds were excreted at all the growth stages, with the highest amount recorded at flowering stage. Maximum nitrogen (including NO_3^-, NH_4^+ and total nitrogen) excretion rate at seedling stage was detected in the 'morning'. The concentrations of NO_3^- and NH_4^+ of rice monocropping, intercropping and peanut monocropping treatments in sand-culture experiment were 1.415, 5.044, 2.140 mg L^{-1} and 0.0482, 0.332, 0.132 mg L^{-1}, respectively, while they were 0.0726, 0.743, 0.181 mg L^{-1} and 1.036, 1.709, 1.736 mg L^{-1}, respectively, in solution culture experiment. However, the maximum excretion of nitrogen was recorded during the 'afternoon' at flowering stage, and it was in the 'evening' at the pod-filling stage. At flowering stage, the total nitrogen concentrations of rice monocropping, intercropping and peanut monocropping treatments were 15.487, 21.530, 10.906 mg L^{-1} in sand-culture experiment, respectively, and they were 4.204, 5.445, 3.813 mg L^{-1}, respectively, in solution-culture experiment. Composition of the nitrogen forms examined as NO_3^-, NH_4^+ and total nitrogen, was found to be changeable during the growth stages, suggesting that the major pathways of excretion are possibly different at different plant ages. Different amounts of nitrogenous compounds were recorded in the two culture experiments and the amounts of nitrogenous compounds in sand-culture were far higher than those in solution-culture experiment, inferring that mechanical resistance of the culture medium could stimulate the excretion of nitrogenous compounds.

Keywords: Growth stage, N-excretion, Rice, Peanut, Intercropping system.

1 Introduction

Rice plants could be cultivated in aerobic soil and reach yields of 7500-8500 kg ha^{-1}, almost similar to those of rice cultivated in waterlogged soil (Liang et al., 1999;

E. Zhu and S. Sambath (Eds.): Information Tech. and Agricultural Eng., AISC 134, pp. 225–232.
springerlink.com © Springer-Verlag Berlin Heidelberg 2012

Shi et al., 2001; Huang et al., 2003). The successful practice of rice cultivation in aerobic condition could not only save more than 100% of irrigating water when compared with waterlogged cultivation (Huang et al., 2003), but also make it possible to intercrop the rice crops with legumes. Peanut is an important economic crop, and often used as component crop in intercropping systems. Rice crops consume almost 30% of the chemical nitrogen fertilizers in China. Therefore, a new intercropping system of peanut with rice crops is of great significance in development of sustainable agriculture in China.

A previous study in this lab has shown an obvious yield advantage and N transferring from peanut to rice plants in a peanut and rice intercropping system (Chu et al., 2004). Exudation of nitrogenous compounds from peanut was one of the potential mechanisms of N release from the component crop. Considerable amounts of nitrogenous compounds were excreted from legume crops during the active growth stages, even if the cereal crops also released a little amount of nitrogenous compounds during the whole growth stages (Shen and Chu, 2004). The amounts of rhizodeposition into soil remain unquantified, largely because of methodological limitations. A large release of nitrogen from actively growing legume root systems has implications for crop cultivation. Nitrogenous compounds released from legume roots into the soil may provide N for neighboring non-N_2-fixing plant roots and for rhizosphere microflora. The quantities of nitrogen released from legume roots can not be easily studied in field or greenhouse experiments. This is because the microbial populations in soil rapidly metabolize and alter water-soluble nitrogenous materials such as amino acids (Alexander, 1977), and nitrogenous compounds may also be bound to mineral lattices, cation exchange complexes and rihzosphere mucigel aggregates (Paul and Schmidt, 1960). Thus, controlled environments and artificial media have been used to determine the nature and mechanisms of nitrogen release from the legume roots. Amino acids, proteins and peptides were identified in leachates from root zones of legume seedlings grown in sterile sand (d' Arcy, 1982; Boulter et al., 1966; Richter et al., 1968; Vancura and Hanzlikova, 1972). To clarify the causes and mechanisms of nitrogen release from legume roots, scientists have compared nitrogen released from plant roots grown in solid versus liquid mediums (d'Arcy, 1982; Ayers and Thornton, 1968; Juo and Stotzky, 1970) and in sterile versus nonsterile conditions (Foster and Rovira, 1976; Hale et al., 1978; Vancura et al., 1977). Mechanisms of nitrogen release from roots may include active or passive release of soluble materials from intact cells, sloughage and decomposition of epidermal cells, release of cell contents via lysis by pathogens, and senescence of nodules and roots.

Fujita et al. (1992) reported that the release of nitrogen compounds was mainly from the decomposition of dead roots and nodules to supply the demand of cereals, and considerable amounts of nitrogenous compounds were released from actively growing legume root systems, however, very little direct evidence has been reported about the relations between root nodules active and nitrogenous compounds released from legume root systems.

Ta et al. (1986) reported that the excreted nitrogenous compounds mostly were formed after nitrogen fixed using ^{15}N methods, and the new fixed nitrogen was the main source of released nitrogenous compounds. The different growing stages were the important factors affecting the quantity and variety of excretions, and Hamlen et al.

(1972) reported that the amounts of carbohydrates released from alfalfa changed with the growing stages.

Although the importance of nitrogen excretion from component plant roots remains controversial, possibly because of the methodological difficulties in experiments, it is still evoked as a possible determinant pathway of nitrogen transference between two component crops. Since the excretion of soluble amino-acids from legume root systems and especially from nodules was documented (e.g. Virtanen, 1937; Wilson, 1937), most studies have invoked the importance of root excretion in nitrogen transfer to grass. These results were based on the uptake of 15N labeled mineral nitrogen, or fixation under 15N atmosphere, but further studies on nitrogen enrichment of the roots in different mediums can not be documented.

In this study, sand-culture and solution-culture experiments were carried out to clarify qualifiedly and quantitatively the excretion of nitrogenous compounds by peanut root systems intercropped with rice cultivated in aerobic soil condition at different time of a day and different growth stages.

2 Materials and Methods

Experiment Ⅰ- Solution- culture experiment

Seeds of rice crop (Teyou 559) and peanut crop (Arachis Hypogaea L. cv.) were surface sterilized with 70% ethanol (15 min) and 1% HClO (1 min), followed by rinsing several times with sterilized water, and germinated on siliceous sand. Seedlings were transferred to 10 L plastic pots filled with a high sandy loam soil collected from Banjing Town, Jiangsu province. Each pot had 6 plants for monoculture of rice or peanut and 3 plants for intercropping of rice and peanut, respectively. The pots containing peanut seedlings were inoculated with a suspension of Rhizobium (ATCC14134，provided by Bacterium Preservation Center, CAAS). Three treatments were designed consisting of 2 monocultures (rice, RR or peanut, PP) and 1 mixture of the both (RP), and each treatment had 4 replicates. Seven days before sampling, the seedlings were transferred to a 5 L containers filled with N-free nutrient solution, during which continuous ventilation using automated timely air pump was done to keep a good aeration of the solutions. The pHs of the nutrient solutions were adjusted to 6.0 every day. The plants were grown in a greenhouse with 20-25℃/25-30℃ night/day. Position of the pots in greenhouse was randomly changed daily.

The solutions were collected at seedling stage (30 days after transplanting), flowering stage (60 days after transplanting) and pod-filling stage (90 days after transplanting) of peanut. The collection was done way as followed: plants were gently removed from the water culture medium and root systems washed gently with distilled water to reduce nitrogen compound contamination from the nutrient solution used for growing the plants. The plants were transferred to distilled water with microorganism inhibitor for starvation culture. At each sampling period, 'Excreted solutions'were collected in the 'morning' (8 am-11 am), during the 'afternoon' (11 am-6 pm) and in the 'evening' (6 pm-8 am). The collected 'excreted solution' was

filtrated with 0.45 μm film to eliminate impurity, and the solution was kept at -15℃. The excreted solution samples were concentrated by lyophilization (SAVANT Super Modulyo).

Experiment Ⅱ- Sand-culture experiment

Seeds of Rice (Teyou 559) and peanut (Arachis Hypogaea L. cv.) were surface sterilized with 70% ethanol (15 min) and 1% HClO (1 min), followed by rinsing several times with sterilized water, and germinated on siliceous sand in an incubator at 25℃. Seedlings were transferred to plastic pots filled with 1.2 L siliceous sand in greenhouse. Pots containing peanut were inoculated with a suspension of Rhizobium (ATCC14134, provided by Bacterium Preservation Center, CAAS). Again, Three treatments were designed consisting of 2 monocultures (rice, RR or peanut, PP) and 1 mixture of the both (RP), and each treatment had 5 replicates. Plants densities of 4 rice or peanut (monoculture) or 2 plants of each species (mixture) per pot were achieved by thinning at two weeks after transplanting. Position of the pots in greenhouse was randomly changed daily. The pots were periodically irrigated with the nutrient solution, of Hoagland and Arnon mixed nutrient solution without nitrogen.

Root solution were collected at seedling stage (30 days after transplanting), flowering stage (60 days after transplanting) and pod-filling stage (90 days after transplanting) of peanut.

Root solutions elution: within the interval of two irrigations, the sands were eluted for three times, the first (8 am-11 am), as 'morning' root excreted solution; the second (11 am-6 pm), as 'afternoon' root excreted solution; and the third (6 pm-8 am) as 'evening' root excreted solution. The sand of each pot was rinsed with 3×200 mL of nutrient solution, from which about 100 mL were collected as sample. The collected 'excreted solution' was filtrated with 0.45 μm film to eliminate impurity, kept at -15℃, and concentrated by lyophilization (SAVANT Super Modulyo). Plants were harvested after the last collection for biomass measurements and nitrogen content of plant.

Measurements and chemical Analysis

Concentrated excreted solution samples were analyzed for total nitrogen by the Kieldahl method, NO_3^- and NH_4^+ by Flow Injection Analysis (Autoanalyzer 3, BRAN+LUBBE GMBH, German).

Statistical analysis

The statistical analyses were done using SPSS11.0 software. Differences amongst were analyzed by ANOVA (GLM-procedure) for a completely randomized factorial design model. Aposteriori compareisons were carried out with Tukey's honest significant differentce (HSD) test at the 0.05 level probability (P = 0.05).

3 Results

NO_3^- and NH_4^+ excretion in rice-peanut associations

At seedling stage, in sand-culture experiment, the highest amounts of NO_3^- and NH_4^+ excreted from root systems emerged in the 'morning' (8 am-11 am), the concentrations

were 1.415, 5.044, 2.140 mg L^{-1} and 0.0482, 0.332, 0.132 mg L^{-1} for rice monocropping, intercropping and peanut monocropping treatment, respectively (Fig. 1) while they were 0.0726, 0.743, 0.181 mg L^{-1} and 1.036, 1.709, 1.736 mg L^{-1} in solution-culture experiment (Fig. 2). The excreted amounts of NO_3^- in sand-culture were much higher than that in solution-culture experiment, but the reverse was true for the NH_4^+ excretion. In the two experiments, the excretion amounts of NO_3^- and NH_4^+ during 'afternoon' and 'evening' were much lower than that during 'morning' at the seedling stage of the peanut. And the excretion in intercropping treatment was larger than that in monocropping treatment, indicating that the intercropping can improve the nitrogen nutrition of both the crops.

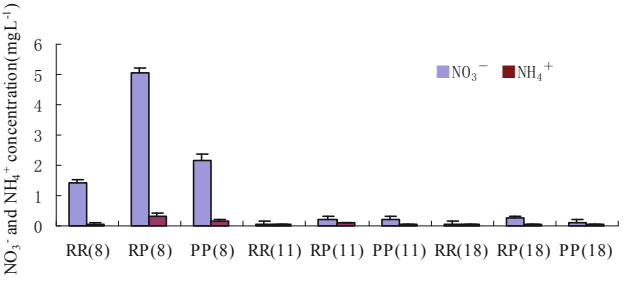

Fig. 1. Variation of NO_3^- and NH_4^+ concentration in sand culture experiment at seedling stage

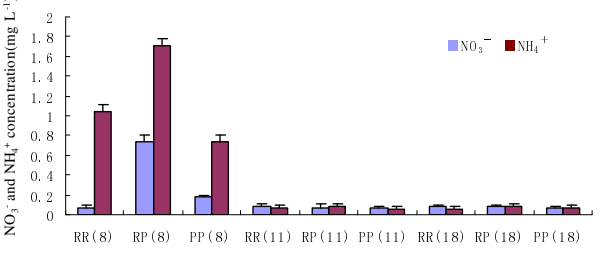

Fig. 2. Variation of NO_3^- and NH_4^+ concentration in solution culture experiment at seedling stage

At flowering stage, the highest excretion occurred during 'afternoon' and there had an apparent excretion peak value, especially for NO_3^-. In sand-culture experiment, the concentrations of NO_3^- and NH_4^+ were 17.338, 25.294, 5.369 mg L^{-1} and 0.162, 0.856, 0.119 mg L^{-1} for rice monocropping, intercropping and peanut monocropping treatment, respectively (Fig. 3). The excretion of NO_3^- was higher than that of NH_4^+ in sand-culture experiment but the NH_4^+ excretion was higher than that of NO_3^- in solution-culture experiment (Fig. 4). In the two experiments, the excretion of NO_3^- and NH_4^+ in intercropping treatment was higher than that in monocropping treatment, showing that intercropping promoted the release of NO_3^- and NH_4^+ from root systems of rice and peanut.

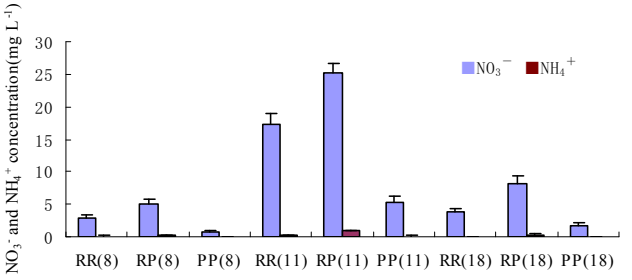

Fig. 3. Variation of NO_3^- and NH_4^+ concentration in sand culture experiment at flowering stage

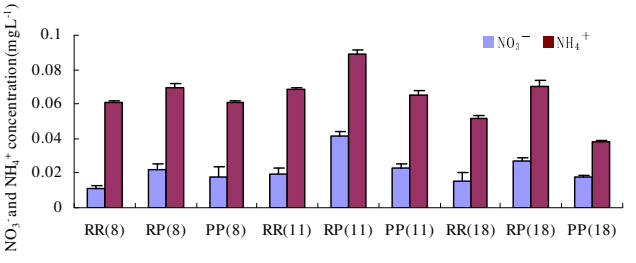

Fig. 4. Variation of NO_3^- and NH_4^+ concentration in solution culture experiment at flowering stage

However, at pod-filling stage, the highest excretion rate appeared during 'evening' (Fig. 5), this is possibly because NO_3^- and NH_4^+ were almost depleted during 'morning' and 'afternoon'. At this stage, the rice plants developed very quickly and the biomass of rice plants were maximum (data not shown). The rice plants took up the nitrogen as much as the medium had during the day but during the evening they absorbed the nitrogen very little (KirKby, 1969), which made the concentration of NO_3^- and NH_4^+ enriched.

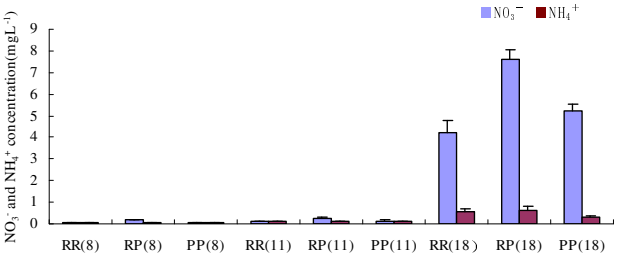

Fig. 5. Variation of NO_3^- and NH_4^+ concentration in sand culture experiment at podding stage

Excretion of total nitrogen in rice and peanut association

At seedling stage, whether in sand-culture or solution-culture experiment, the way of total nitrogen release from rice and peanut root system was that, during 'evening', the concentration of total nitrogen was relatively low whether for intercropping treatment or for monocropping treatment. The total nitrogen, for example, was almost in

depletion for monocropping treatment. The excretion peak of total nitrogen appeared during 'morning'. At different sampling time of the day, the concentration of total nitrogen in intercropping treatment was higher than that in monocropping treatment, showing that intercropping promoted the release of total nitrogen.

At flowering stage, in solution-culture experiment, there was not a big variation for concentration of total nitrogen during different sampling time of the day, whereas the highest excretion rate appeared during afternoon. However, in sand-culture experiment, an excretion peak occurred during 'afternoon', especially for intercropping treatment, the concentration of total nitrogen was much higher than that of monocropping treatment. In the two experiments, the concentration of total nitrogen was 15.487, 21.530, 10.906 mg L^{-1} and 4.204, 5.445, 3.813 mg L^{-1}, respectively, and the excretions were higher at this stage than those at seedling stage.

However, at pod-filling stage, the highest excretion rate of total nitrogen appeared during 'evening'. At this stage, senescence of nodules and roots increased, the total nitrogen in solution maybe from other pathways, such as decomposition of nodules and roots.

Excretion rate of total nitrogen in sand-culture experiment was far higher than that in solution-culture experiment. This showed that mechanical resistance of solid medium stimulated excretion of total nitrogen.

References

1. Alexander, M.: Introduction to Soil Microbiology, 2nd edn., p. 467. John Wiley and Sons, Inc., New York (1977)
2. Ayers, W.A., Thornton, R.H.: Exudation of amino acids by intact and damaged roots of wheat and peas. Plant and Soil 28, 193–207 (1968)
3. Boulter, D., Jeremy, J.J., Wilding, M.: Amino acids liberated into the culture medium by pea seedling roots. Plant and Soil 24, 121–127 (1968)
4. Chu, G.X., Shen, Q.R., Cao, J.L.: N2 fixation and N transfer from peanut to rice cultivated in aerobic soil in an intercropping system and its effects on soil N fertility. Plant and Soil 263, 17–27 (2004)
5. d'Arcy Lameta, A.: Etude des exsudets racinaires de Soja et de Lentille. I. Cinetique d'exsudation des composes phenoliques, des amino acides et des sucres, au cours des premiers jours de la vie des plantules. Plant and Soil 68, 399–403 (1982)
6. Foster, R.C., Rovira, A.D.: Ultrastructure of the wheat rhizosphere. New Phytol. 76, 343–352 (1976)
7. Fujita, K., Ofosu-Budu, K.G., Ogata, S.: Biological nitrogen fixation in mixed legume-cereal cropping systems. Plant and Soil 141, 155–175 (1992)
8. Hale, M.G., Moore, L.D., Griffin, G.J.: Root exudates and exudation. In: Dommergues, Y.R., Krupa, S.V. (eds.) Interactions between Non-pathogenic Soil Microorganisms and Plants, pp. 163–203. Elsevier, Amsterdam (1978)
9. Hamlen, R.A., Lukesic, F.L., Bloom, J.R.: Influence of age and stage of development on the neutral carbohydrate components in root exudates from alfalfa plants grown in a gnotobiotic environment. Can. J. Plant Sci. 52, 633–642 (1972)
10. Huang, X.Y., Xu, Y.C., Shen, Q.R., Zhou, C.L., Yin, J.L.: Dittert K. A study on the water use efficiency by rice plants cultivated in aerobic and waterlogged condition. Journal of Soil and Water Conservation 17(3), 140–143 (2003)

11. Juo, P., Stotzky, G.: Electrophoretic separation of proteins from roots and exudates. Can. J. Bot. 48, 713–718 (1970)
12. Kirkby, E.A.: Ion uptake and ionic balance in plants in relation to the form of nitrogen nutrition. In: Rorison, I.H. (ed.) Ecological Aspects of Mineral Nutrition of Plants, pp. 215–235. Blackwell Scientific Pub., Oxford (1969)
13. Liang, Y.C., Hu, F., Yang, M.C.: Mechanism of high yield and irrigation water use efficiency of rice in plastic film mulched dryland. Scientia Agricultura Sinica 32, 26–32 (1999)
14. Paul, E.A., Schmidt, E.L.: Extraction of free amino acids from soil. Pro. Soil Sci. Am. 24, 195–198 (1960)
15. Richter, M., Wilms, W., Scheffer, F.: Determination of root exudates in a sterile continuous flow culture. Ⅱ. Short-term and long-term variations of exudation intensity. Plant Physiol. 43, 1747–1754 (1968)
16. Shen, Q.R., Chu, G.X.: Bi-directional N transfer in the intercropping system of peanut with rice cultivated in aerobic soil. Biol. Fertil. Soils 40, 81–87 (2004)
17. Shi, Y., Shen, Q.R., Mao, Z.S., Li, W.: Biological response of rice crop cultivated on upland soil condition and the effect of mulching on it. Plant Nutrition and Fertilizer Science 7(3), 271–277 (2001) (in Chinese)
18. Ta, T.C., Macdowall, F.D.H., Faris, M.A.: Excretion of nitrogen assimilated from N2 fixed by nodulated roots of alfalfa (Medicago sativa). Can. J. Bot. 64, 2063–2067 (1986)
19. Vancura, V., Hanzlikova, A.: Root exudates of plants. IV. Differences in chemical composition of seed and seedlings exudates. Plant and Soil 36, 271–282 (1972)
20. Vancura, V., Prikryl, Z., Kalachova, L., Wurst, M.: Some quantitative aspects of root exudation. Ecol. Bull. NFR (Stockholm) 25, 381–386 (1977)
21. Virtanen, A.I., Van Hausen, S., Laine, T.: Investigations on the root nodule bacteria of leguminous plants. XX. Excretion of nitrogen in associated cultures of legumes and non legumes. J. Agric. Sci. 27, 584–610 (1937)
22. Wilson, P.W.: Mixed cropping and the excretion of nitrogen by leguminious plants. Soil Sci. Soc. Am. Proc. 2, 289–297 (1937)

In Vitro Antibacterial Effect of Chinese Herbal Medicine against *Aeromonas hydrophila*[*]

Zhenxia Su[1], Hui Xiao[1], and Liehuan Chen[2]

[1] Department of Marine Science and Technology, HuaiHai Institute of Technology Lianyungang, Jiangsu Province, China
[2] Research and Development Center of Chitins Jiangsu Marine Resources Development Research Institute Lianyungang, Jiangsu Province, China
suzhenxia@sina.com, chitins@126.com

Abstract. In this study, in vitro antibacterial effect of 16 different types of Chinese herbal medicine against Aeromonas hydrophila was evaluated. The boiling method was used to extract the bioactive ingredients from the herbal plants. The agar diffusion method was used to measure the zone of inhibition of gall, coptis, rhubarb, terminalia and other Chinese herbal medicine against Aeromonas hydrophila. The double tube dilution method was used to determine the minimum inhibitory concentration (MIC) and minimum bactericidal concentration (MBC). Our results showed that different types of Chinese herbal medicine had different antibacterial effect against Aeromonas hydrophila. The water extract from gall, coptis, terminalia, rhubarb had stronger antibacterial effect, with their MIC values being 7.81 mg/mL, 15.63mg/mL, 31.25 mg/mL, 62.50 mg/mL, respectively. The MBC values of gall, coptis, terminalia, rhubarb were 15.63 mg/mL, 62.50 mg/mL, 62.50 mg/mL, 125.00 mg/mL, respectively. Next, we mixed gall extract individually with either terminalia, coptis, or rhubarb, and tested the MIC and MBC of the mixed extract. The MIC values of galls+terminalia, galls+coptis, galls+rhubarb were 3.906 mg/mL, 7.813 mg/mL, 15.625 mg/mL, respectively. The MBC values of galls+terminalia, galls+coptis, galls+rhubarb were 3.906 mg/mL, 7.813 mg/mL, 15.625 mg/mL, respectively. The in vitro antibacterial and bactericidal effect of the mixed compound were stronger than the 16 individual Chinese herbal medicine that.

Keywords: Chinese herbal medicine, Aeromonas hydrophila, Inhibition zone, Minimum inhibitory concentration (MIC), Minimum bactericidal concentration (MBC).

1 Introduction

Rapid growing aquaculture industries and high-density cultures often lead to the deterioration of water quality, which is one of the factors that could lead to a wide range of disease outbreaks. In aquatic animals. Using of antibiotics and synthetic drugs excessively has led to drug resistance in pathogens, which is becoming a very

[*] This work was supported by Key Research Project of Lianyungang (No. CG0908) and The Open Foundation of Marine Resources Research Institute of Jiangsu Province(JSIMR10C04).

E. Zhu and S. Sambath (Eds.): Information Tech. and Agricultural Eng., AISC 134, pp. 233–239.
springerlink.com © Springer-Verlag Berlin Heidelberg 2012

serious concern not only to human health, but to the environment as well (Wu et al., 2001a; Wu et al., 2001b; Feng et al., 2006). It is therefore important to discover new drugs to combat the growing population of antibiotic resistant bacteria in the aquaculture production.

Chinese herbal medicine not only possesses antibacterial effects, but also has other beneficial effects as well. It can regulate the physiological functions of aquatic animals, strengthen body specific and non-specific immunity, stimulate digestion, absorption and growth (Cao et al., 2006; Wang et al., 2006). Most importantly, the population of bacteria resistant to Chinese herbal medicine remains low. Therefore, herbal medicine has become a hot research area for new drug discoveries.

Numerous studies have shown that Chinese herbal medicine has inhibitory effects against common human and animal pathogens. However, researches on the inhibitory role of herbal extracts against aquatic animal pathogens were lacking. Although there were some relevant studies published in recent years, these studies used a very limited number of herbal medicine or pathogens for testing (Cao et al., 2007; Liu et al., 2006; Li et al., 2007). Large scale screens have been done to study Chinese herbal compounds with antimicrobial effects against human and animal pathogens. However, such large scale studies for herbal compounds against aquamarine pathogens are absent (Xue et al., 2006; Li et al., 2006).

Ameromonas hydrophila is a widely distributed bacteria in water, mud and other natural environments (Cao et al., 2007; Zhang et al., 2006). *Aeromonas hydrophila* infections can lead to hemorrhage outbreaks, such as silver carp outbreak of hemorrhage, turtle septicemia, eel hemorrhage, and eel red fin disease. Illness caused by *Aeromonas hydrophila* infections is often more severe with higher mortality rate than other general illness (Zhang et al., 2006).

In this study, galls, terminalia, rhubarb, coptis and other Chinese herbal medicine were tested for their antibacterial effect against *Aeromonas hydrophila*. Extracts of individual herbs with strong antibacterial effect were mixed together for further inhibition studies. Our results provided the experimental basis for using Chinese herbal medicine to prevent and combat aquamarine diseases.

2 Materials and Methods

2.1 Preparation of Media and Chinese Herbal Medicine

Beef extract peptone media was prepared as follows (per 1000 mL): beef extract 3.0 g, peptone 10.0 g, sodium chloride 5.0 g, agar 20g .

Sixteen different types of Chinese herbal medicine were used: coptis, honeysuckle, houttuynia, forsythia, terminalia, daqingye, prunella vulgaris, dandelion, flavescens, pulsatilla, astragalus, rhubarb, araceae, corks, galls, and banlangen. All were purchased from the Institute of Traditional Chinese Medicine in City of Lianyungang.

The extraction method performed as previously described (Jiang, 2005). Briefly, Chinese herbal plants were smashed and dispensed in a jar. A total of 30g of each Chinese herbal medicine was dissolved with 400 ml water for 30 min, followed by

boiling and simmering for 30 min. The samples were then dried 3 times to obtain the crude product. The crude product was re-dissolved and filtered sterilized before being preserved at 4℃.

2.2 Preparation of Bacterial Suspension

Aeromonas hydrophila was inoculated in the liquid growth media and cultured in a shaker for 12-16 h. The bacteria cultures were then diluted to the concentration of 8×10^7 CFU/mL.

2.3 Determination of Zone of Inhibition

We first punched 3 holes of equal size (diameter 5.00 mm) on each media plate, and then evenly dispersed 100 μL of bacterial culture onto the plate. Next, the Chinese herbal medicine extracts (30 μL) were loaded into each hole on the plate. All plates were incubated in the 28 ℃ incubator for 24 h. The zone of inhibition was measured. This experiment was repeated 3 times.

2.4 Determination of Minimum Inhibitory Concentration (MIC)

Minimum inhibitory concentration (MIC) was determined by the double-tube dilution method (Zhou et al., 2007). Briefly, 2 ml of 1000 mg/mL extract of each herbal medicine was dissolved in 2 ml fresh liquid media in tube #1. Subsequently, 2 ml of culture from tube #1 was removed and added to tube #2 containing 2 ml liquid media. The series of dilutions was carried out for a total of 11 tubes. All 11 testing tubes along with 2 control tubes were each inoculated with 20 μL bacterial suspension and incubated in a 28℃ incubator for 24 h. The lowest drug concentration among tubes with no bacterial growth would be the drug's minimum inhibitory concentration (MIC). This experiment was performed in 3 replicates.

2.5 Determination of Minimum Bactericidal Concentration (MBC)

Cultures from the tubes with equal or greater MIC were coated onto the agar media plates and incubated in a 28℃ incubator for 24 h - 48 h. The concentration of the plate without bacterial growth would be the drug's minimum bactericidal concentration (MBC).

2.6 Statistical Analyses

The data of the inhibition zone analysis was analyzed using the SPSS software.

3 Results

3.1 The Zone of Inhibition of Individual Chinese Herbal Extract

The size of the zone of inhibition for each Chinese herbal extract was shown in Table 1. All 16 types of Chinese herbal medicine had varying antibacterial effect against

Aeromonas hydrophila. They were ranked from strongest to weakest based on their antibacterial effect: coptis, galls, terminalia, rhubarb, astragalus, flavescens, prunella vulgaris, pulsatilla, cork, araceae, banlangen, dandelion, forsythia, honeysuckle, daqingye, and houttuynia. Our results showed that coptis, galls, terminalia, rhubarb had strong inhibitory effect, and the size of the zone of inhibition was 24.96 ± 1.48 mm, 22.21 ± 1.47 mm, 15.56 ± 0.95 mm, 12.90 ± 1.44 mm, respectively.

3.2 The MIC, MBC Values of Individual Chinese Herbal Extract

Table 2 showed that galls, coptis, terminalia, rhubarb had relatively lower MIC and MBC values that other extracts. Galls had the strongest inhibitory and bactericidal effects against Aeromonas hydrophila, as suggested by its MIC (7.81 mg/mL), MBC (15.63 mg/mL). Coptis had the second strongest effect, and its MIC MBC values were 15.63 mg/mL and 62.50 mg/mL, respectively. Extracts from cork, flavescens, p. vulgaris, araceae, forsythia displayed bactericidal effect at 500 mg/mL, while other herbal extracts did not show bactericidal effect at 500mg/mL.

3.3 The Zone of Inhibition of Mixed Chinese Herbal Extracts

Gall extract was individually mixed with terminalia, coptis, and rhubarb. The zone of inhibition for these mixed extracts was shown in Table 3. The antibacterial effect of these mixed extracts were ranked from strongest to weakest: galls + terminalia, galls + coptis, galls + rhubarb.

3.4 The MIC, MBC of Mixed Extract against Aeromonas Hydrophila

As shown in Table 4, the antibacterial effect of Gall + Terminalia was the strongest, as its MIC and MBC were 3.906 mg/ml and 3.906 mg/ml, respectively We found that the mixed Chinese herbal extract had stronger antibacterial activities than the individual herbal extract. The MIC of all drugs tested was smaller or equal to 15.625 mg/mL (MIC ≤ 15.625 mg/mL), the MBI of all drugs tested was greater or equal to the MIC of all drugs tested (MBC ≥ MIC).

Table 1. The zone of inhibition of each Chinese herbal extract against *Aeromonas hydrophila*

Medicine	Inhibition zone (mm)	Medicine	Inhibition zone (mm)
Coptis	24.96 ± 1.48	Cork	9.38 ± 0.45
Gall	22.21 ± 1.47	Araceae	9.37 ± 0.94
Terminalia	15.56 ± 0.95	Banlangen	9.36 ± 0.64
Rhubarb	12.90 ± 1.44	Dandelion	8.76 ± 0.81
Astragalus	10.79 ± 0.81	Forsythia	8.72 ± 1.10
Flavescens	10.71 ± 0.94	Honeysuckle	8.42 ± 0.56
Prunella vulgaris	10.20 ± 0.88	Daqingye	7.80 ± 1.04
Pulsatilla	9.83 ± 0.74	Houttuynia	7.50 ± 0.63

Table 2. The MIC, MBC values of 16 Chinese herbal extracts against *Aeromonas hydrophila*

Medicine	MIC (mg/mL)	MBC (mg/mL)
Gall	7.81	15.63
Coptis	15.63	62.50
Terminalia	31.25	62.50
Rhubarb	62.50	125.00
Banlangen	62.50	>500.00
Dandelion	62.50	>500.00
Cork	125.00	500.00
Honeysuckle	125.00	>500.00
Daqingye	125.00	>500.00
Forsythia	250.00	500.00
Pulsatilla	250.00	>500.00
Araceae	250.00	500.00
Houttuynia	250.00	>500.00
Prunella vulgaris	250.00	500.00
Flavescens	250.00	500.00
Astragalus	500.00	>500.00

Table 3. The zone of inibition of mixed extract against *Aeromonas hydrophila*

Mixed Chinese herbal extract	Inhibition zone (mm)
Galls + Terminalia	30.18±2.13
Galls + Coptis	28.81±2.21
Galls+ Rhubarb	28.18±1.30

Table 4. The MIC, MBC of mixed Chinese herbal extract against *Aeromonas hydrophila*

mixed Chinese herbal extract	MIC (mg/mL)	MBC (mg/mL)
Galls + Terminalia	3.906	3.906
Galls + Coptis	7.813	7.813
Galls + Rhubarb	15.625	15.625

4 Discussion

Aeromonas hydrophila, a common pathogen in fish, was tested against 16 types of Chinese herbal medicine in an antibacterial drug screen. The results revealed that some of the Chinese herbal medicine had strong antibacterial effect against *Aeromonas hydrophila*, such as coptis, galls, terminalia, and rhubarb. The MIC and MBC values of coptis, galls, terminalia, rhubarb were very low.

Results in our study are consistent with other earlier studies. It was reported that the rhubarb extract had antibacterial effect against *Aeromonas hydrophila* and other

common pathogens in aquaculture (Zhou, 2007). Furthermore, Zhou suggested that rhubarb extract could enhance host's immunity and had a strong preventive role against bacterial infections (Zhou, 2007). In a separate study, different Chinese herbal medicine extracts were found to have specific antibacterial activity (Cao, 2007). Cao reported that *Aeromonas hydrophila* was highly sensitive to gall extract and terminalia. Another report considered galls, rhubarb and coptis to be ideal antibacterial drugs, as they had large zones of inhibition, low inhibitory concentration and sustained efficacy (Zhou, 2006).

In Chinese herbal medicine research and applications, large scale screenings were often carried out to evaluate and enhance the antibacterial effects of an array of herbal medicine. In this study, combining galls either with coptis, terminalia or rhubarb produced much stronger antibacterial and bactericidal activities than the individual extract. Ai et al. (1997) studied the inhibitory effect of compound "Baixuening" on hemorrhagic septicemia pathogens in freshwater fish. The MIC of "Baixuening" against *Aeromonas hydrophila* was 4 mg/mL. Xue et al. (2006) found that sophora alkaloids and their compounds had antibacterial and bactericidal effect against *Aeromonas hydrophila* as well, in which compound C and D had the strongest effect. The MIC of compound C and compound D were 15.6 mg/mL and 7.8 mg/mL, respectively. The MBC of compound C and compound D were 250 mg/mL and 125 mg/mL, respectively. Compound A and B were had relatively weaker antibiotic effects, while sophora alkaloids displayed no antibacterial activity against *Aeromonas hydrophila*.

The focus of the society today is towards environmental protection, including aquaculture preservation and regulation. Chinese herbal medicine has a series of advantages over other drugs, such as little side effects, low pathogen resistance, and no harmful by-products. Therefore, Chinese herbal medicine has become one of the key targets for new drug discovery.

The antibacterial mechanisms of some Chinese herbal medicine are not yet fully understood. The antibacterial effect of individual herbs *in vivo* is not uniform (Li et al., 2006). Its practical clinical application must be verified by *in vivo* comparison.

5 Summary

Our study showed that 16 different types of Chinese herbal medicine had different antibacterial effect against *Aeromonas hydrophila*. The extracts of galls, coptis, terminalia, rhubarb had stronger antibacterial and bactericidal effects than the other extracts. Combining gall extract with each of terminalia, coptis and rhubarb produced much stronger antibacterial and bactericidal effects than the effects of individual herb extract. Based on the results of this study, galls, coptis, terminalia, rhubarb and their mixture are recommended for use in aquaculture to combat bacteria diseases infected by *Aeromonas hydrophila*.

Acknowledgment. The authors thank the staff of Department of Marine Science and Technology for their technical support. Special thanks to anonymous referees for their constructive comments on this manuscript.

References

1. Ai, X., Zuo, W., He, L.: The study of medicine control on freshwater fish bacterial hemorrhagic septicemia. J. Fish. Sci. China 4(3), 54–61 (1997)
2. Cao, H., Huang, W., Song, J.: A review of the prevention and control of fish diseases by use of traditional Chinese herbal medicine. Mar. Sci. 30(4), 83–87 (2006)
3. Cao, H., Song, J., Li, G., Huang, W.: Study on bacteriostatic action of Chinese herbal m edicine on Aeromonas hydrophilia ST-3-3. Gui. J. TCM 13(5), 86–88 (2007)
4. Feng, Q., Zhou, Y., Xie, Z., Feng, Y.: Chinese herbal medicine and its application in aquaculture. Fish. Info. 33(6), 251–254 (2006)
5. Jiang, X.: The inhibition effect of traditional Chinese herbal medicine extracts on common pathhogenic bacteria of aquatic animals in vitro. Feed Indus. 26(22), 28–29 (2005)
6. Li, X., Huang, J., Cui, M.: In vitro antibacterial experiment of three kinds of Chinese herbal compound extracts. Gansu Anim. Hus. Vet. (1), 11–13 (2006)
7. Li, X., Zhang, Y., Hua, R., Hu, X., Liu, W.: Antibacterial Experiment of 23 Chinese M edicinal Herbs and Compound Prescriptions on 3 Bacteria from the Gut of Carassius auratus in Vitro. Fresh. Fish. 37(4), 8–11 (2007)
8. Liu, C., Qin, P., Zhou, W., Wang, G.: Antibacteria effects of water extract of peanut on three kinds of Aeromonas. Chinese Trad. Herb. Drug. 37(12), 1852–1853 (2006)
9. Wang, W., Wang, J., Li, A., Lin, X.: Herbal applications and aquaculture research profile. China Fish (7), 60–61 (2006)
10. Wu, R., Kang, S.: Herbal feed additive and green ecological animal husbandry. Feed Rev. (2), 19–20 (2001a)
11. Wu, R., Kang, S.: Immune function of herbal feed additives and application prospects. Liv. Poul. Indus. (9), 10–12 (2001b)
12. Xue, F., Zhou, W., Wang, Z., Xu, X.: The inhibition effect of sophora alkaloids and their compound on Aeromonas hydrophila. J. Hydro. 26(1), 89–91 (2006)
13. Zhang, H., Yang, G.: Killing ability of 12 Chinese herb medicines to bacterium Aeromonas hydrophila. Sci. Aqua. Prod. 25(1), 16–18 (2006)
14. Zhou, Q., Zheng, X., Liu, B., Xie, J., Xu, P.: The inhibitory effect of rhubarb extract on Aeromonas hydrophila. Jiangsu Agri (2), 64–66 (2007)

Isolate and Characterize ACC Deaminase-Containing Plant Growth-Promoting Rhizobacteria*

Guo Changhong, Liu Jiali, and Lv Yueping

Key Laboratory of Molecular Cytogenetics and Genetic Breeding of Heilongjiang Province
College of Life Science and Technology, Harbin Normal University
Heilongjiang Province, China
kaku2008@hotmail.com

Abstract. The petroleum has been overflowed and discharged by accident or abnormal running in the course of petroleum producing, storing, transporting, refining and using. The pollution of petroleum has become an environment problem, which has been paid wide attention in the world. Bioremediation technology of petroleum contaminated soil has become an important field in research of decontamination of petroleum contamination for its advantages of low cost, little environmental effect, simpleness and efficiency. Plant growth-promoting bacteria that contain the enzyme 1-aminocyclopropane-1-carboxylate (ACC) deaminase, which facilitates plant growth and development by decreasing plant ethylene levels, especially following a variety of environmental stresses. Experiment was conducted under axenic conditions to evaluate the rhizobacteria containing ACC deaminase from petroleum-contaminated soil. By amplification and sequence of the 16S rDNA, the two strains of PGPR L-11 and A-8 were identified as Pseudomonas. sp and Klebsiella. sp, respectively. We have investigated the ACC deaminase activity of the two strains of PGPR, and the results showed that the ACC deaminase of Pseudomonas. sp was higher than Klebsiella. sp. These bacteria could improve the tolerance of plants to petroleum, which may be used for the remediation of the environment.

Keywords: Petroleum pollution, Plant growth-promoting rhizobacteria (PGPR), ACC deaminase, Enayme activity.

1 Introduction

Plant growth-promoting rhizobacteria (PGPR) could play a significant role in the development of sustainable agriculture. These are rhizobacteria that are beneficial to plants and affect plant growth directly or indirectly through various mechanisms of action [1]. Indirect promotion occurs when PGPR improved plant by preventing growth restricting conditions [2, 3]. The direct promotion by PGPR entails either providing the plant with a compound that is synthesized by the bacterium or facilitating the uptake of certain nutrients from the environment [4, 5, 6]. They can fix atmospheric nitrogen, synthesize siderophores, phytochromes or some enzymes that modulate

* Natural Science Foundation of China (No.30970552).

E. Zhu and S. Sambath (Eds.): Information Tech. and Agricultural Eng., AISC 134, pp. 241–247.
springerlink.com © Springer-Verlag Berlin Heidelberg 2012

growth and development by influencing the levels of plant hormones [7]. Among the plant hormones, whose concentrations are most likely to be altered by the PGPR include ethylene, auxin, gibberellins and cytokinin [8, 9].

Many plant growth-promoting bacteria contain the enzyme 1-aminocyclopropane-1-carboxylate (ACC) deaminase and this enzyme can cleave the ethylene precursor ACC to α-ketobutyrate and ammonium and induce lower the level of ethylene in developing or stressed plants [10]. When ACC deaminase-containing plant growth-promoting bacteria are bound to a plant, they act as a sink for ACC ensuring that plant ethylene levels do not become elevated to the point, where root growth is impaired [11]. This activity is important during normal plant development and also protects plants from numerous environmental stresses, including flooding, phytopathogens, salt, drought and heavy metals [12, 13]. Moreover, ACC deaminase-containing plant growth-promoting bacteria up-regulate genes involved with plant growth and protein production while down-regulating plant genes involved with ethylene stress and defence signaling pathways [14]. The ACC deaminase-containing plant growth-promoting bacteria, in part, alleviate the need for the plant to actively defend itself against various environmental stresses. The crystal of ACC deaminase enzyme structure has been determined for the yeast [15] and recently for the bacterial. The biochemical and thermodynamic properties of the ACC deaminase from *Pseudomonas putida UW4* have been measured [16].

This study was conducted to evaluate the potential of microbial strains containing ACC deaminase activity.

2 Materials and Methods

2.1 Selection of Bacterial Strains That Contain ACC Deaminase

Rhizobacteria were isolated from the rhizasphere of *Avena fatua* (Bayou 1#) growing in salt and oil affected soil samples of Daqing, China. All strains were isolated within the same 2-week period.

The method of isolating PGPR entails screening soil bacteria for the ability to use ACC as a sole nitrogen source, a trait that is a consequence of the presence of the activity of the enzyme, ACC deaminase. One gram of soil – soil in close proximity to plant roots are generally enriched in ACC deaminase-containing bacteria, which is added to 50 ml sterile medium containing (per litre) 10 g proteose peptone, 10g casein hydrolysate, 1.5 g anhydrous $MgSO_4$, 1.5 g K_2HPO_4 and 10 ml glycerol (PAF medium) in a 250 ml flask. The flask and its contents are incubated in a shaking water bath (200 rpm) at a temperature between 25 and 30℃. After 24 h, a 1 ml aliquot is removed from the growing culture, transferred to 50 ml of sterile PAF medium in a 250 ml flask and incubated at 200 rpm in a shaking water bath for 24 h, at either 25℃ or 30℃, the same temperature as the first incubation. Following these two incubations, the population of bacteria is enriched and the number of fungi in the culture is reduced.

A 1 ml aliquot is removed from the second culture and transferred to a 250 ml flask containing 50 ml sterile minimal medium, DF salts (per litre): 4.0 g KH_2PO_4, 6.0 g Na_2HPO_4, 0.2 g $MgSO_4{\cdot}7H_2O$, 2.0 g glucose, 2.0 g gluconic acid and 2.0 g citric acid with trace elements: 1 mg $FeSO_4{\cdot}7H_2O$, 10 mg H_3BO_3, 11.19 mg $MnSO_4{\cdot}H_2O$, 124.6

mg $ZnSO_4 \cdot 7H_2O$, 78.22 mg $CuSO_4 \cdot 5H_2O$, 10 mg MoO_3, pH 7.2 and 2.0 g $(NH_4)_2SO_4$ as a nitrogen source. Following an incubation of 24 h in a shaking water bath at 200 rpm at either 25 or 30℃, the same temperature as the first incubation, a 1 ml aliquot is removed from this culture and transferred to 50 ml sterile DF salts minimal medium in a 250 ml flask containing 3.0 mM ACC (instead of $(NH_4)_2SO_4$) as the source of nitrogen. A 0.5 M solution of ACC, which is labile in solution, is filter-sterilized through a 0.2 mm membrane and the filtrate collected, aliquoted and frozen at -20℃. Just prior to inoculation, the ACC solution is thawed and a 300 ml aliquot is added to 50 ml sterile DF salts minimal medium; following inoculation, the culture is placed in a shaking water bath at 20 rpm and grown for 24 h at 25–30℃.

Dilutions of this final culture are plated onto solid DF salts minimal medium and incubated for 48h at either 25 or 30℃, the same temperature as the previous incubations. These plates are prepared with 1.8% Bacto-Agar, which has a very low nitrogen content, and are spread with ACC (30 mmol · $plate^{-1}$) just prior to use. Before streaking with either a loopful of bacteria or an individual colony, the ACC is allowed to dry fully. The inoculated plates are incubated at the appropriate temperature – no higher than 35℃ because all of the known ACC deaminases are inhibited above this temperature – for 3 days and the growth on the plates is checked daily.

2.2 DNA Extraction

Bacterial strains were revived from -80℃ storage and grown on ADF to confirm purity. Single colonies were subcultured to additional LB plates and grown for another 1–2 days, after which a loopful of cells was transferred to LB broth (containing per litre: Tryptone 10 g/L, Yeast extract 5 g/L, NaCl 10 g/L) and incubated overnight on a rotary shaker (200 rpm at 30 ℃). DNA was extracted using the Genomic DNA Rapid Isolation Kit For Bacterial Cell (BioDev, Beijing).

2.3 16S rDNA Sequence Analysis

The following was added to each 50 μl reaction mixture: 5.0 μl of 10× amplification buffer with Mg^{2+}; 5.0 μl of a 10 mM mix of dNTP; 1 μl of 10 pmol of each primer (F8:5'AGAGTTTGATCCTGGCTCAG3'; R1541:5'AAGGAGGTGATCCAGCCGC A3'); 0.5 μl rTaq; 5 μl template DNA. Amplification conditions were as follows: initial denaturation at 94℃ for 3 min; 30 cycles of denaturation at 94℃ for 30 s, annealing at 50℃ for 30 s, extension at 72℃ for 90 s; and a final extension at 72℃ for 10 min. PCR products were sequenced by Sangon Biotech (Shanghai) Co., Ltd. SongJiang Industrial Park. The significant alignments of the returned sequences were obtained through BLAST search of the NCBI database (http://www.ncbi.nlm.nih.gov/).

2.4 Culture Conditions for the Induction of Bacterial ACC Deaminase Activity

The assessment of bacterial ACC deaminase activity and root-growth enhancement both require bacterial growth conditions that favour the induction of ACC deaminase. The bacteria are cultured first in rich medium and then transferred to minimal medium with ACC as the sole source of nitrogen. Bacterial cells are grown to mid-up to late-log phase in 15ml rich medium, such as tryptic soybean broth (TSB) divided between two

culture tubes: each tube is inoculated with 5 ml of the appropriate strain. Cultures are incubated overnight in a shaking water bath at 200 rpm at the temperature most suitable for the bacterial strain. The accumulated biomass is harvested by centrifugation of the contents of the combined tubes at 8000 g for 10min at 4℃. The supernatant is removed and the cells are washed with 5 ml DF salts minimal medium. Following an additional centrifugation for 10 min at 8000 g at 4℃, the cells are suspended in 7.5 ml DF salts minimal medium in a fresh culture tube. Just prior to incubation, the frozen 0.5 M ACC solution (prepared as described above) is thawed, and an aliquot of 45 ml is added to the cell suspension to obtain a final ACC concentration of 3.0 mM. The bacterial cells are returned to the shaking water bath to induce the activity of ACC deaminase at 200 rpm for 24 h at the same temperature as the overnight incubation, either 25 or 30℃. The bacteria are harvested by centrifugation at 8000 g for 10 min at 4℃. The supernatant is removed, and the cells are washed by suspending the cell pellet in 5 ml either 0.1 M Tris-HCl, pH 7.6 if the cells are to be assayed for ACC deaminase activity, or 0.03 M $MgSO_4$ if they are to be used as a bacterial treatment in the gnotobiotic root elongation assay or the high-performance liquid chromatography (HPLC) protocol for measuring ACC. Following centrifugation at 8000 g at 4℃ for 10 min, the supernatant is discarded. The washing procedure is repeated twice to ensure that the pellet is free of the bacterial growth medium. The pelleted cells are stored at either -20℃ for measurement of ACC deaminase activity or at 4℃ for seed treatment in the gnotobiotic root elongation assay or HPLC measurement of ACC.

2.5 Measurement of ACC Deaminase Activity

ACC deaminase activity is assayed according to a modification of the method of Honma and Shimomura (1978) which measures the amount of a-ketobutyrate produced when the enzyme ACC deaminase cleaves ACC. The number of mmol of a-ketobutyrate produced by this reaction is determined by comparing the absorbance at 540 nm of a sample to a standard curve of a-ketobutyrate ranging between 0.1 and 1.0 mmol. A stock solution of 100 mM a-ketobutyrate is prepared in 0.1 M Tris-HCl pH 8.5 and stored at 4℃. Just prior to use, the stock solution is diluted with the same buffer to make a 10mM solution from which a standard concentration curve is generated. Each in a series of known a-ketobutyrate concentrations is prepared in a volume of 200 ml, 300 ml of the 2,4-dinitrophenylhydrazine reagent (0.2% 2,4-dinitrophenyl-hydrazine in 2 M HCl) is added, and the contents are vortexed and incubated at 30℃for 30 min, during which time the a-ketobutyrate is derivatized as a phenylhydrazone. The colour of the phenylhydazone is developed by the addition of 2.0 ml 2 M NaOH; after mixing, the absorbance of the mixture is measured at 540 nm.

ACC deaminase activity is measured in bacterial extracts prepared in the following manner. Bacterial cell pellets, prepared as described above, are each suspended in 1ml of 0.1 M Tris-HCl, pH 7.6, and transferred to a 1.5 ml microcentrifuge tube. The contents of the 1.5 ml microcentrifuge tube are centrifuged at 16 000 g for 5 min and the supernatant is removed. The pellet is suspended in 600 ml 0.1 M Tris-HCl, pH 8.5. Thirty microlitres of toluene are added to the cell suspension and vortexed at the highest setting for 30 s. At this point, a 100 ml aliquot of the ‘toluenized cells’ is set

aside and stored at 4℃ for protein assay at a later time. The remaining toluenized cell suspension is immediately assayed for ACC deaminase activity.

All sample measurements are carried out in duplicate. Two hundred microlitres of the toluenized cells are placed in a fresh 1.5 ml microcentrifuge tube; 20 ml of 0.5 M ACC are added to the suspension, briefly vortexed, and then incubated at 30℃ for 15 min. Following the addition of 1 ml of 0.56 M HCl, the mixture is vortexed and centrifuged for 5 min at 16 000 g at room temperature. One millilitre of the supernatant is vortexed together with 800 ml of 0.56 M HCl. Thereupon, 300 ml of the 2,4-dinitrophenylhydrazine reagent (0.2% 2,4- dinitrophenylhydrazine in 2 M HCl) are added to the glass tube, the contents vortexed and then incubated at 30℃ for 30 min. Following the addition and mixing of 2 ml of 2 N NaOH, the absorbance of the mixture is measured at 540 nm. The absorbance of the assay reagents including the substrate, ACC, and the bacterial extract are taken into account. After the indicated incubations, the absorbance at 540 nm of the assay reagents in the presence of ACC is used as a reference for the spectrophotometric readings; it is subtracted from the absorbance of the bacterial extract plus the assay reagents in the presence of ACC. The contribution of the extract, namely the absorbance at 540 nm of extract and the assay reagents without ACC, is determined and subtracted from the absorbance value calculated above. This value is used to calculate the amount of a-ketobutyrate generated by the activity of ACC deaminase. The range of 0–1.0 mmol of a-ketobutyrate absorbs in the range of 0–1.6 at 540 nm. The lowest amount of a-ketobutyrate that can be precisely determined is 0.1 mmol.

3 Results and Disccussion

3.1 Selection of Bacterial Strains That Contain ACC Deaminase

The soil samples for the separation of PGPR were collected from Daqing halophytic of rhizosphere soil. We have isolated two strains PGPR L-11 and A-8 containing ACC deaminase from the rhizosphere soil. The colony of L-11 was round, flat, smooth and moist (Fig. 1); the colony of A-8 was large, mucinous, colonies merged each other (Fig. 2).

PAF is a kind of culture medium which contains glycerol. Carried out the first two days in the ADF, is conducive to the enrichment of *Pseudomonas* and similar bacteria, the fungi and actinomyces are reduced. ADF medium is containing 3.0 mM ACC (instead of $(NH_4)_2SO_4$) as the source of nitrogen. Samples were targeted in these three kinds of medium to enrich and separate, greatly improving the efficiency of commonly used alternative to inefficient and time–consuming process of screening and biometrics to speed up new PGPR selection and application.

3.2 DNA Extraction and 16S rDNA Sequence Analysis

The 16S rDNA sequence were blasted against the NR database from NCBI. And the results of blast showed that these sequences were similar to prokaryotes 16S rDNA. The two strains of PGPR L-11 and A-8 were identified as *Pseudomonas sp* and *Klebsiella sp*, respectively.

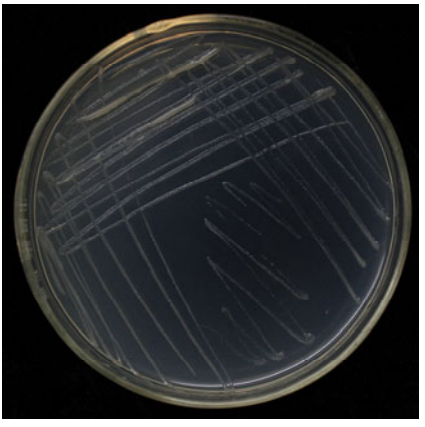

Fig. 1. The colony morphology of L-11

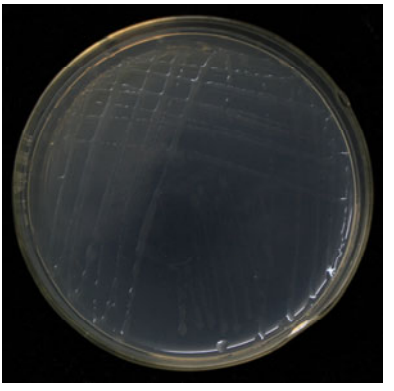

Fig. 2. The colony morphology of A-8

3.3 Measurement of ACC Deaminase Activity

The two isolated strains, which used the ACC as the sole nitrogen source, have different levels of ACC deaminase activity, and the activity is different, shown as Fig 3. The results showed that the ACC deaminase activity of L-11 is higher than A-8.

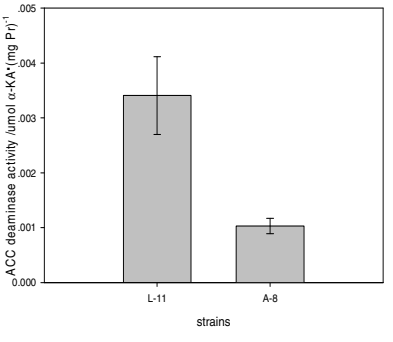

Fig. 3. The ACC deaminase activity of bacterial isolates

The procedures described here is relatively straightforward to isolate and characterize new PGPR strains. These bacteria may be used to facilitate the growth of a variety of plants, especially under stressful conditions such as flooding, heavy metals, phytopathogens, high salt, drought and so on. This activity is useful in both agricultural and horticultural settings, as well as in environmental cleanup protocols.

References

1. Mayak, S., Tsipora, T., Glick, B.R.: Plant growth-promoting bacteria confer resistance in tomato plants to salt stress. Plant Physiol. 42, 565–572 (2004)
2. Glick, B.R., Penrose, D.M., Li, J.: A model for the lowering of plant ethylene concentrations by plant growth promoting bacteria. J. Theor. Biol. 190, 63–68 (1998)

3. Belimov, A.A., Hontzeas, N., Safronova, V.I., Demchinskaya, S.V., Piluzza, G., Bullitta, S., Glick, B.R.: Cadmium-tolerant plant growth-promoting bacteria associated with the roots of Indian mustard (Brassica juncea L. Czern). Soil Biol. Biochem. 37, 241–250 (2005)
4. Shaharoona, B., Arshad, M., Zahir, Z.A.: Performance of Pseudomonas spp. Containing ACC-deaminase for improving growth and yield of maize (Zea mays L.) in the presence of nitrogenous fertilizer. Soil Biol. Biochem. 38, 2971–2975 (2006)
5. Dey, R., Pal, K.K., Bhatt, D.M., Chauhan, S.M.: Growth promotion and yield enhancement of peanut (Arachis hypogaea L.) by application of plant growth-promoting rhizobacteria. Microbiol. Res. 159, 371–394 (2004)
6. Blaha, D., Combaret, C.P., Mirza, M.S., Loccoz, Y.M.: Phylogeny of the 1-aminocyclopropane-1-carboxylic acid deaminaseencoding gene acdS in phytobeneWcial and pathogenic Proteobacteria and relation with strain biogeography. FEMS Microbiol. Ecol. 56, 455–470 (2006)
7. Glick, B.R., Hall, J.A., Peirson, D., Ghosh, S.: Root elongation in various agronomic crops by the plant growth promoting rhizobacterium Pseudomonas putida GR 12-2. Isr. J. Plant Sci. 44, 37–42 (1996)
8. Xie, H., Pasternak, J.J., Glick, B.R.: Isolation and characterization of mutants of the plant growth promoting rhizobacterium Pseudomonas putida GR 12-72 that over produce indole acetic acid. Curro Microbiol. 32, 67–71 (1996)
9. Zahir, A.Z., Asghar, H.N., Akhtar, M.J., Arshad, M.: Precursor (L-tryptophan)-Inoculum (Azotobacter) isnteraction for improving yields and nitrogen uptake of maize. J. Plant Nutr. 28, 805–817 (2005)
10. Donate, C.J., Leon, B.M., Perez, G.R.: Screening for plant growth-promoting rhizobacteria in Chamaecytisus proliferus (tagasaste), a forage tree-shrub legume endemic to the Canary Islands. Plant Soil 266, 261–272 (2005)
11. Ahmad, R., Jilani, G., Arshad, M., Zahir, Z.A., Khalid, A.: Bio-conversion of organic wastes for their recycling in agriculture: an overview of perspectives and prospects. Annals Microbiol. 4, 471–479 (2007)
12. Shaharoona, B., Jamro, G.M., Zahir, Z.A., Arshad, M., Memon, K.S.: Effectiveness of various Pseudomonas spp., and Burkholderia caryophylli containing ACC-deaminase for improving growth and yield (Triticum aestivum L.). J. Microbiol. Biotechnol. 17, 1300–1307 (2007)
13. Ahmad, R., Arshad, M., Khalid, A., Zahir, Z.A.: Effectiveness of organic-/bio-fertilizer supplemented with chemical fertilizers for improving soil water retention, aggregate stability, growth and nutrient uptake of maize (Zea mays L.). J. Sustain Agri. 4, 57–74 (2008)
14. Nadeem, S.M., Zahir, Z.A., Naveed, M., Arshad, M.: Preliminary investigations on inducing salt tolerance in maize through inoculation with rhizobacteria containing ACCdeaminase activity. Can. J. Microbiol. 53, 1141–1149 (2007)
15. Penrose, D.W., Moffat, B.A., Glick, B.R.: Determination of ACC to assess the effect of ACC-deaminase containing bacteria on roots of canola seedlings. Can. J. Microbiol. 47, 77–80 (2001)
16. Gholami, A., Shahsavani, S., Nezarat, S.: The Effect of Plant Growth Promoting Rhizobacteria (PGPR) on Germination, Seedling Growth and Yield of Maize. World Academy of Science, Engineering and Technology (2009)

Effects of *aadA* Transplastomic Tobacco on Soil Microbe Number*

Guo Changhong, Lv Yueping, Yu Jianping, Liu Jiali, and Liu Qingguo

Key Laboratory of Molecular and Cytogenetics
College of Life Science and Technology, Harbin Normal University
Heilongjiang Province, China
kaku2008@hotmail.com

Abstract. The development and use of genetic modified plants (GMPs), as well as their ecological risks have been a topic of considerable public debate since their first commercial use in 1996. Transplastomic plants as a bioreactor offers a number of unique advantages, such as high level of transgene expression, stable expression. Soil microbial communities were studied in soil, the communities of bacteria, fungi and actinomycetes were investigated between the aadA transplastomic tobacco plants (TA) and the controls (non-genetic modified tobacco). And on the impact of rhizosphere microorganisms after their stems and leaves complete decomposition. The results shown: (1) The effect of transplastomic tobacco and control tobacco to major microbial groups in amount was not significantly different; (2) No matter transplastpmic tobacco or controls, the microbial number was bacteria>actinomycete>fungi.

Keywords: Transplastpmic tobacco, Rhizosphere microbial, Stem and leaf decomposition, aadA gene.

1 Introduction

Genetically modified plants (GMPs) with a wide variety of traits have been developed via genetic engineering. In 1996, the first genetically modified seeds were planted in the Unites States for commercial agricultural production [1]. The rapid development of agricultural biotechnology and release of GMPs have provided many agronomic and economic benefits, but which have also raised concerns over the potential impact these plants might have on human health and the environment. Among the major environmental concerns are the unintended consequences of potential transgene flow to indigenous plants or organisms through pollen transfer or horizontal gene transfer [2]. Transplastomic plants as a bioreactor offers a number of unique advantages, such as high level of transgene expression, environmental safety [3]. Transplastomic plants can be avoided with the spread of pollen, and study transgenic plants on rhizosphere microorganisms [4].

Plants are known to have a profound effect on the abundance, diversity and activity of soil microorganisms living in close proximity with their roots in a soil zone defined

* Natural Science Foundation of China (No.30970552).

E. Zhu and S. Sambath (Eds.): Information Tech. and Agricultural Eng., AISC 134, pp. 249–254.
springerlink.com © Springer-Verlag Berlin Heidelberg 2012

as the rhizosphere. Bacteria are considered important bioindicators because they interact with plants during their entire life cycles and can act as precise and fast indicators of environmental changes [5], they inhabiting the rhizosphere, also referred to as rhizobacteria, are responsible for numerous functions including nutrient cycling and decomposition, which can significantly influence vegetation dynamics [6]. Rhizobacteria have been defined as good indicator organisms and have been studied to assess the general impact that GMPs might have on the soil environment.

Many factors come into play when trying to address the impact that GMPs might have on rhizobacteria. The nature of the plant genetic modification certainly represents one of the first key elements that naturally come to mind. Different transgenes, allowing the expression of novel plant proteins, can potentially alter rhizobacteria abundance and diversity in a variety of ways. These novel proteins can, for example, be directly released into the rhizosphere through root exudation or their expression trigger, through alteration of various metabolic pathways, the production and release of additional non-proteinaceous compounds [7]. Although the engineered production of some of these compounds is deliberate, targeting, for example, specific pests or pathogens [8], unintentional effects are susceptible to alter non-targeted rhizobacteria.

The persistence of some of these novel compounds in the rhizosphere, or simply an alteration in the amounts of naturally produced plant compounds due to genetic engineering can also have an impact on rhizobacteria populations [9]. Even after harvest, decomposition of plant litter can continue releasing novel gene products into environment [10], potentially altering rhizobacteria populations over long periods of time.

Soil ecosystems are complex, heterogeneous and represent a challenge when it comes to isolation, culture or identify most microorganisms inhabiting this environment. In this paper, the *aadA* transplastomic plants and control tobacco were studied as the materials. Studied under laboratory conditions, the microbial communities were studied by using selective medium.

2 Materials and Methods

2.1 Soil and Plants for the Experiment

Soil for the experiment was collected from an experimental field, situated in Heilongjiang Province, China, where no transgenic plants have ever been planted.

Two common plant species were used: *aadA* transplastpmic tobacco and wild tobacco (WT). The seeds of transgenic tobacco from our laboratory and preserved in. The seeds of wild tobacco were collected from their natural populations in the field.

2.2 Soil Sampling

Soil collected during the growth of transgenic plants
Soils in the central where plant grew were collected and combined as rhizosphere soil and subjected to various analyses. Rhizosphere soil from the field was collected during

the seeding stage, vegetative, reproductive, and senescing stages (four stages). Dig up the whole plant, shake off the soil around the roots, repeat this method for three times each plant samples. Three soil samples were then combined (about 100 g). All samples were immediately transported to the laboratory and stored at 4 ℃ [11].

Preparation of stem and seaf decomposition soil
To retrieve the soil dry naturally at room temperature, ground sieved (20 mesh), divide into pots. transplastomic tobacco and control tobacco leaf (each 30 g) was cut into yarn bags were buried after the screening soil. The samples were incubated at room temperature, training process to maintain consistent soil moisture. Sampling after 180 days, Stems and leaves have been completely degraded at this time. Remove the yarn bags, and collect the soil around the yarn bags, mixed ready for use.

2.3 Measurements

Microbial number
Soil microbial number was determined mainly following the dilution method of slab. Five gram of soil from each of the samples wassuspended in 45 ml sterile saline (0.85% w/v NaCl), using a blender for 30 min at 200 rpm. Cultivating bacteria uses beef extract peptone medium, cultivating fungi uses Rose Bengal agar, and actinomycetes uses Gauze No.1 synthetic agar [12], after 3 days, count for the number of bacterial and actinomycetes colonies, and 5 days for the fungi colonies.

2.4 Statistical Analysis

SPSS16.0 statistical software was used for statistical analysis, the difference was significant level of $p < 0.05$.

3 Results and Conclusion

The *aadA* transplastomic tobacco affect of the number of bacteria, actinomycetes, fungi in the soil.

Analyzed the number of bacteria in rhizosphere soil, there is no significant difference between the *aadA* thansplastomic and WT tobacco, and the microbial number was bacteria > actinomycete > fungi, with the growth of tobacco, the number of bacteria in the soil gradually increased, reached the maximum at maturity (Table 1). Analyzed the number of actinomycetes in rhizosphere soil, there is no significant difference between the aadA thansplastomic and WT tobacco, and the microbial number was bacteria > actinomycete > fungi, With the growth of tobacco the soil actinomycetes gradually increased, the largest number of actinomycetes in the vegetative, and the least in the flowering (Table 2). Analyzed the number of fungi in rhizosphere soil, there is no significant difference between the *aadA* thansplastomic and WT tobacco, and the microbial number was bacteria > actinomycete > fungi, with

the growth of tobacco, the number of bacteria in the soil gradually increased, reached the maximum at maturity (table 3). Data showed no significant differences in the total populations of bacteria, actinomycetes and fungi between the soils planted with transgenic tobacco and control tobacco in the rhizosphere soil after cultivation.

Effects of the transplastomic tobacco stem and leaf decomposition on microorganism populations in soil.

The effects of the transplastomic tobacco stem and leaf decomposition on the number of bacteria, actinomycetes and fungi were shown in figure 1, the impact of stem and leaves degradation on bacteria, actinomycetes and fungi were not significant. This showed that stems and leaves of transplastomic tobacco completely degraded in the soil environment does not release harmful substances to impact the number of microorganism, or the harmful substances was very little. The microbial number was bacteria > actinomycete > fungi.

Table 1. Compared the Culture Number of Bacterial in the TA and WT Tobacco Rhizosphere Soil

Culture number of bacterial ($\times 10^8$)				
	Seeding stage	Vegetative	Flowering	Senescing stages
TA	1.19±0.19a	1.43±0.21a	2.53±0.23a	1.47±0.21a
WT	0.98±0.39a	1.07±0.32a	2.72±0.20a	1.61±0.26a

Table 2. Compared the Culture Number of Actinomycete in the TA and WT Tobacco Rhizosphere Soil

Culture number of actinomycete ($\times 10^7$)				
	Seeding stage	Vegetative	Flowering	Senescing stages
TA	0.90±0.24a	1.41±0.09a	2.42±0.50a	1.47±0.15a
WT	0.82±0.10a	1.49±0.14a	2.98±0.13a	1.41±0.04a

Table 3. Compared the Culture Number of Fungi in the TA and WT Tobacco Rhizosphere Soil

Culture number of fungi ($\times 10^5$)				
	Seeding stage	Vegetative	Flowering	Senescing stages
TA	0.68±0.13a	1.10±0.21a	2.22±0.34a	1.44±0.25a
WT	0.70±0.21a	1.14±0.15a	2.04±0.58a	1.88±0.30a

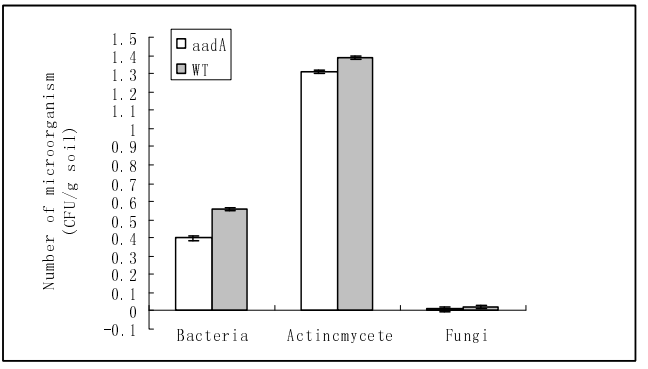

Fig. 1. Effects of the stem and leaf decomposition of transplastpmic tobacco on microorganism populations in soil. *(Note: Number of bacteria: $\times 10^6$; Number of actinomycete: $\times 10^4$; Number of fungi: $\times 10^3$.)*

Based on their key roles in plant–soil ecosystems, microbiology may play an important role in interactions between GMPs and soil ecosystems due to their biological and physiological features. Microbiology are important non-target soil microorganisms for monitoring the ecological risks of GMPs, soil microbial ecology is an important component of the system. Therefore, the evaluation of transgenic plants on soil microbes is significant. Processes that occur in the rhizosphere should be highlighted in future investigations of risk assessment of GMPs on soil ecosystems, which may enhance our understanding of the interaction between GMPs and the soil microbial community [13]. It is generally agreed with that plants could alter the population and diversity of soil microbial communities, but it is not known whether transgenic plants could affect soil nutrient cycling, and indigenous microbial populations, as inconsistent results have been obtained in terms of microbial populations between rhizospheric soil with transgenic and non-transgenic plants [14]. Yudina's studies have shown that four different Bt-transgenic cottons occurs a significant increase the number of soil bacteria and fungi. In order to eliminate other bacteria on the culture of bacteria, we using a selective medium, using the beef extract peptone medium for Bacteria, Rose Bengal medium for fungi, Gauze No.1 synthetic agar for actinomycetes. Four replicates for each strain set. In this study, no significant differences in the total populations of bacteria, actinomycetes and fungi were obtained between the soils planted with transplastomic tobacco and non-transgenic tobacco after cultivation.

The effect of transplastomic tobacco and control tobacco to major microbial groups in amount was not significantly different. No matter transplastpmic tobacco or controls, the microbial number was bacteria > actinomycete > fungi.

It was found that *aadA* transplastomic tobacco had no apparent effects on soil microbial number or the effects were very little. The conclusion and suggestions on risk assessment mentioned here should not be viewed as static or absolute. They are based on the knowledge presently available. Some key issues concerning the impact of GMPs on rhizobacteria and soil microorganisms might develop or change in light of novel findings.

References

1. Liu, W.: Do genetically modified plants impact arbuscular mycorrhizal fungi? Ecotoxicology 19, 229–238 (2010)
2. Filion, M.: Do transgenic plants affect rhizobacteria populations? Microbial Biotechnology 1, 463–475 (2008)
3. Svab, Z., Maliga, P.: High-frequency plastid transformation in tobacco by selection for a chimeric aadA gene. Waksman Institute 90, 913–917 (1993)
4. McBride, K.E., Svab, Z., Schaaf, D.J., et al.: Amplification of a chimeric Bacillus gene in chloroplasts leads to an extraordinary level of an insecticidal protein in tobacco. Biotechnol. 13, 362–365 (1995)
5. Yudina, T.G., Burtseva, L.I.: Activity of deltaendotoxins of four Bacillus thuringiensis subspecies against rokaryotes. Microbiol. 66, 25–31 (1997)
6. Kent, A.D., Triplett, E.W.: Microbial communities and their interactions in soil and rhizosphere ecosystems. Annu. Rev. Microbiol. 56, 211–236 (2002)
7. Raubuch, M., Roose, K., Warnstorff, K., Wichern, F., Joergensen, R.G.: Respiration pattern and microbial use of field-grown transgenic Bt-maize residues. Soil Biol. Biochem. 39, 2380–2389 (2007)
8. Mendelsohn, M., Kough, J., Vaituzis, Z., Matthews, K.: Are Bt crops safe? Nat. Biotechnol. 21, 1003–1009 (2003)
9. Oger, P., Mansouri, H., Dessaux, Y.: Effect of crop rotation and soil cover on alteration of the soil microflora generated by the culture of transgenic plants producing opines. Mol. Ecol. 9, 881–890 (2000)
10. Gebhard, F., Smalla, K.: Monitoring field releases of genetically modified sugar beets for persistence of transgenic plant DNA and horizontal gene transfer. FEMS. Microbiol. Ecol. 28, 261–272 (1999)
11. Huc, S.: Effects of coexisting plant species on soil microbes and soil enzymes in metal lead contaminated soils. Applied Soil Ecology 37, 240–246 (2007)
12. Snyder, T.L., Engley Jr., F.B., Penfield, R.A., Creasy, J.C.: Dilution plate counting method for certain strains of bacteriaum tularense, Publication (May 10, 1946)
13. Johansson, J.F., Paul, L.R., Finlay, R.D.: Microbial interactions in the mycorrhizosphere and their significance for sustainable agriculture. Microbiol. Ecol. 48, 1–13 (2004)
14. Wei, X.D., Zou, H.L., Chu, L.M., Liao, B., Ye, C.M., Lan, C.Y.: Field released transgenic papaya affects microbial communities and enzyme activities in soil. Plant Soil 285, 347–358 (2006)

Analysis of Crosses between CS-1E Addition Line and CS-2C Addition Line*

Guo Changhong, Liu Chunying, Xu Guohui, and Su Wenyue

Key Laboratory of Molecular Cytogenetics and Genetic Breeding of Heilongjiang Province
College of Life Science and Technology, Harbin Normal University
Heilongjiang Province, China

Abstract. Wild relatives of Triticum aestivum are important source of disease and pest resistance. Thinopyrum elongatum, one of the most important wild relatives, carries many desirable agronomic traits, including disease resistance, and several useful traits, which have been transferred into wheat by interspecific hybridization. In this study, we have used gametocidal system to induce wheat-Th. elongatum recombinant lines between CS-1E disomic addition line and CS-2C disomic addition line. Gametocidal chromosome can induce chromosome breakages and chromosome aberrations. We have observed the aberrations of chromosome behaviors in F_2 and BC_1 plants, which indicated that the gametocidal chromosome was effective during the formation of gametes. The percentage of seed setting was decreased in F_1, F_2 and BC_1 plants, which indicated that the gametocidal chromosome 2C had effect on wheat-Th. elongatum 1E chromosome addition line.

Keywords: Wheat, Thinopyrum elongatum, Gametocidal chromosome, Seed-set, Cytological characteristics.

1 Introduction

Thinopyrum elongatum, a close relative of wheat, which provides a source of novel genes for wheat improvement. *Thinopyrum elongatum* has an important source of resistance to pests and diseases [1, 2, 3]. Such as yellow dwarf virus resistance [4], leaf rust resistance [5], yellow rust resistance [6], Fusarium head blight [7], and salt stress tolerance [8]. This resource represents a large reservoir of useful traits and involves the introgression of small portions of *Th. elongatum* chromosome segments into wheat. Previous research showed that *Th. elongatum* chromosome 1E has high-molecular-weight glutenin subunits [9].

Endo [10, 11] and Endo & Gill [12] developed many alien chromosomes and these alien chromosomes have been introduced into common wheat (the genus *Triticum*) from related wildspecies (the genus *Aegilops*). Some alien chromosomes have unique genes that secure their existence in the host by causing chromosome breakage in the gametes lacking them. Such chromosomes or genes are called gametocidal (Gc)

* The Key Technology R&D Program, Heilongjiang Province of China(GA08B104) International S& T Cooperation Program of China(2009DFA32470).

E. Zhu and S. Sambath (Eds.): Information Tech. and Agricultural Eng., AISC 134, pp. 255–259.
springerlink.com © Springer-Verlag Berlin Heidelberg 2012

chromosomes or Gc genes, which is a genetic system to induce chromosome mutations in common wheat. This gametocidal system was also demonstrated to work well for rye [13], barley [14] and Haynaldia villosa [15] chromosomes added to common wheat.

In this study, the Chinese Spring-*Th. elongatum* 1E disomic addition lines and Chinese Spring-*Ae. cylindryca* gametocidal chromosome 2C disomic addition lines were hybrided, backcrossed and selfcrossed to induce wheat-*Th. elongatum* chromosome translocations. We investigated the seed-sets and cytological characteristics in F_1, F_2 and BC_1 progenies.

2 Materials and Methods

2.1 Plant Materials

Chinese Spring-*Thinopyrum elongatum* disomic addition lines 1E were obtained from the Dr Han (Institute of Genetics and Developmental Biology, Chinese Academy of Sciences). Chinese spring-Gametocidal chromosome 2C disomic addition line (2n=44 AABBDD+2C Ⅱ) was gifted by National BioResource Project, Japan (NBRP-Wheat). By crossing 1E addition lines with 2C line, we produced F_1 progeny (21 Ⅱ +1 Ⅰ 1E+1 Ⅰ 2C). By backcrossing the F_1 hybrids to the 1E addition lines to produce BC_1 plants or selfcrossed to produce F_2 plants.

2.2 Cytogenetic Analysis

Preparation of root-tip cells at mitotic metaphase: Seeds were germinated on moist filter paper in petri dishes in 4℃ for 48 h, change to 24℃ for 27.5 h. The root-tips were cut down when 1.5-2 cm long and pretreated in ice water for 24 h to accumulate metaphases, and then fixed in carnol.s fixative (95% alcohol : ice acetic acid = 3 : 1) for 1-2 d. The root-tips were squashed in 45% acetic acid, and the slides were observed under a phase-contrast microscope for chromosome number counting.

Preparation of PMC MI: Anthers at meiosis metaphase I were selected, and fixed in the carnol.s fixative, and then squashed in 45% acetic acid, then in the microscopes observed.

3 Results and Disccussion

3.1 The Seed-Set of F1, F2 and BC1 Progenies

The F_1 from two crosses of 1E × DA2C and DA2C × 1E were produced, and the seed-sets of the F_1 plants were investigated (Table 1). The average seed-set of F_1 progenies from the cross 1E × DA2C was 39.18%, higher than 19.44% from the cross DA2C × 1E, which indicated that the chromosome 2C could affect cytoplasm. When the gametocidal chromosome 2C acted as female parent, it could affect the development of zygote and reduce the seed-set of progeny.

Table 1. The Seed-set of F_1 Progeny

F_1 PROGENY	**Morphology Observation**		
	Number of florets	***Number of seed-set grains***	***Seed-set percentage (%)***
1E×2C	388	152	39.18
2C×1E	180	35	19.44

Table 2. The Seed-set of F_2 and BC_1

F_2 AND BC_1	**Morphology Observation**		
	Number of florets	***Number of seed-set grains***	***Seed-set percentage (%)***
F_2	458	136	29.69
BC_1	98	36	36.73

F_2 and BC_1 were obtained from self pollinated of F_1 or backcrossed to Chinese Spring-*Th. elongatum* 1E addition lines as male parent, and the seed-sets of F_2 and BC_1 plants were investigated (Table 2). The average seed-set of F_2 progenies was 29.69%, lower than the BC_1 progenies (36.73%). It suggested that the chromosomes pairing of PMC are more complex in F_2 than in BC_1 progenies, which would affect the seed-set of F_2 progenies.

3.2 Mitosis Analysis

We have investigated the chromosomes behavior in mitosis of F_2 and BC_1 progenies. The chromosome number in F_2 plants ranged from 39 to 45, most contained 42 and 43 chromosomes. The chromosome number of BC_1 plants ranged from 38 to 45. Mostly plants contained 43 and 44 chromosomes. Some chromosome aberrations such as ring chromosome, telosome, dicentromeric chromosome were observed in F_2 and BC_1 plants (Fig. 1).

Fig. 1. Mitosis on root tip cells of F_2 plants. Arrow shows telosome.

3.3 Meiosis Analysis

The chromosome behaviors in PMCs meiosis of F_1, F_2 and BC_1 plants were observed. The chromosome configuration of F_1 plants was mostly 21 II +2 I shown as figure. 2, equated with theoretical value. A lot of multivalents and univalents were observed in F_2 and BC_1 plants, and some abnormal phenomenons were observed in the late PMC I, PMC II such as chromosome fragment, lagging chromosome, circular chromosome and chromosome bridge (Fig. 2).

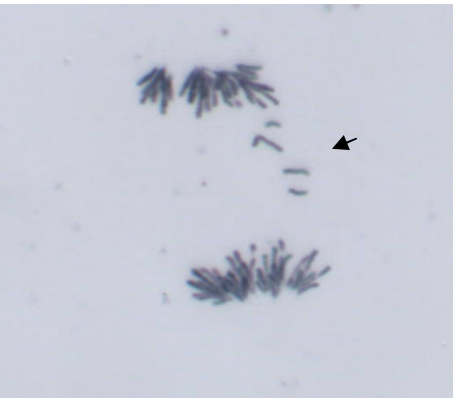

Fig. 2. Meiosis of PMC in F_2 plants. Arrow shows lagging chromosome.

There are many wild relatives exist in the cultivated wheat. A large amount of genetic variation exists in the wild relatives. The introduction of genetic variation from alien species has been a valuable method for increasing the amount of genetic diversity. Ongoing crop cultivar improvement is dependant on a continued supply of genetic variability. *Thinopyrum elongatum*, a closely related species to bread wheat, is tolerant to many biotic and abiotic stresses. *Thinopyrum elongatum* has been exploited for a wide range of traits including resistance to pests and diseases such as drought [8], waterlogging [16] and salinity [17]. The introgression of chromosome segments that carry useful genes derived from related species into cultivated wheat is an important means of improving agronomical traits. For example, the use of resistance gene(s) from *Th. elongatum* for controlling FHB is promising. Wheat-*Th. elongatum* recombinant lines that have FHB resistance, have already been developed [18]. In this study, we use gametocidal system to tranfer 1E chromosome into wheat. Gametocidal genes from several *Aegilops* species can cause random chromosome breakage and then induce chromosome aberrations [11]. We observed the aberrations of chromosome behaviors in F_2 and BC_1 plants, which indicated that the gametocidal chromosome was effective during the formation of gametes. The percentage of seed-sets was decreased in F_1 , F_2 and BC_1 plants, indicating that the gametocidal chromosome 2C had effect on wheat-*Th. elongatum* 1E chromosome addition lines. The F_2 and BC_1 seeds were good materials for breeding wheat-*Th. elongatum* 1E translocation lines and constructing chromosomal deletions of *Th. elongatum* 1E.

References

1. Jauhar, P.P.: Synthesis and cytological characterization of trigenerie hybrids involving durum wheat, Thinopyrum bessarabicum, and Lophopyrum elongatum. Theor. Appl. Genet. 84, 511–519 (1992)
2. Shukle, R., Lampe, D., Lister, R., Foster, J.: Aphid feeding behavior: relationship to barley yellow dwarf virus resistance in Agropyron species. Phytopathology 77, 725–729 (1987)
3. Friebe, B., Jiang, J., Raupp, W., McIntosh, R., Gill, B.: Characterization of wheat-alien translocations conferring resistance to diseases and pests: current status. Euphytica 91, 59–87 (1996)
4. Sharma, H.C., Ohm, H., Goulart, L., Lister, R., Appels, R., Benlhabib, O.: Introgression and characterization of barley yellow dwarf virus resistance from Thinopyrum intermedium into wheat. Genome 38, 406–413 (1995)
5. Sharma, D., Knott, D.R.: The transfer of leaf rust resistance from Agropyron to Triticum by irradiation. Can. J. Genet. Cytol. 8, 137–143 (1966)
6. Ma, J., Zhou, R., Dong, Y.: Control and inheritance of resistance to yellow rust in Triticum aestivum-Lophopyrum elongatum chromosome substitution lines. Euphytica 111, 57–60 (2000)
7. Oliver, R.E., Cai, X., Xu, S.S., Chen, X., Stack, R.: Wheat alien species derivatives: a novel source of resistance to Fusarium head blight in wheat. Crop Sci. 45, 1353–1360 (2005)
8. Roundy, B., Root, A.: Penetration and shoot elongation of tall wheatgrass and basin wildrye in relation to salinity. Can. J. Plant Sci. 65, 335–343 (1985)
9. Feng, D.S., Xia, G.M., Zhao, S.Y., Chen, F.G.: Two quality-associated HMW glutenin subunits in a somatic hybrid line between Triticum aestivum and Agropyron elongatum. Theor. Appl. Genet. 110, 136–144 (2004)
10. Endo, T.R.: Induction of chromosomal structural changes by a chromosome of Aegilops cylindrica L. in common wheat. J. Hered. 79, 366–370 (1988)
11. Endo, T.R.: Gametocidal chromosomes and their induction of chromosome mutations in wheat. Jpn. J. Genet. 65, 135–152 (1990)
12. Endo, T.R., Gill, B.S.: The deletion stocks of common wheat. J. Hered. 87, 295–307 (1996)
13. Endo, T.R., Yamamoto, M., Mukai, Y.: Structural changes of rye chromosome 1R induced by a gametocidal chromosome. Jpn. J. Genet. 69, 13–19 (1994)
14. Sakai, K., Nasuda, S., Sato, K., Endo, T.R.: Dissection of barley chromosome 3H in common wheat and a comparison of 3H physical and genetic maps. Genes Genet. Syst. 84, 25–34 (2009)
15. Chen, Q.Z., Cao, A.Z., Qi, Z.J.: Induce Haynaldia villosa 2V chromosome structural aberration by use of gametocidal chromosome 3C derived from Ae.triuncialis. Science of Chinese Agriculture 41, 362–369 (2008)
16. Taeb, M., Koebner, R.M.D., Forster, B.P.: Genetic variation for waterlogging tolerance in the Triticeae and the chromosomal location of genes conferring waterlogging tolerance in Thinopyrum elongatum. Genome 36, 825–830 (1993)
17. Omielan, J.A., Epstein, E., Dvorák, J.: Salt tolerance and ionic relations of wheat as affected by individual chromosomes of salt-tolerant Lophopyrum elongatum. Genome 34, 961–974 (1991)
18. Shen, X.R., Kong, L.R., Ohm, H.: Fusarium head blight resistance in hexaploid wheat (Triticum aestivum)-Lophopyrum genetic lines and tagging of the alien chromatin by PCR markers. Theor. Appl. Genet. 108, 808–813 (2004)

Isolation and Characteristion of Formaldehyde-Degrading Bacteria from Furniture Factory*

Guo Changhong, Song Lili, Song Ge, Yu Diansi, and Dong Rui

Key Laboratory of Molecular Cytogenetics and Genetic Breeding of Heilongjiang Province
College of Life Science and Technology, Harbin Normal University
Heilongjiang Province, China
kaku2008@hotmail.com

Abstract. Formaldehyde is a widely used and very important chemical raw material, but it is also a highly toxic substance to majority of organisms. Sources of formaldehyde include fuel combustion, industrial applications, decoration materials and various consumer goods. Formaldehyde is also one of the most common indoor air pollutants. Researchers try to separate formaldehyde resistance bacteria to biodegradation of formaldehyde. In this study, a bacterial strain, which could degrade and metabolize formaldehyde as a sole carbon source was isolated from sludge. The strain was characterized by morphological, physiological and biochemical method according to the procedures in Bergey's manual. For the more, the 16S rDNA genes were amplified and sequenced, and they were similar to Pseudomonas sp. The strain with a higher degradation ability of formaldehyde named as SG-71, which could completely degraded 20mM formaldehyde in 12 h. Our results provide a novel strategy for biodegradation of formaldehyde, and also make a greater contribution to control formaldehyde pollution.

Keywords: formaldehyde, degradation, bacteria.

1 Introduction

Formaldehyde is a flammable, colorless, and readily polymerized gas at ambient temperature. It is an important building block in the manufacture of polymers and is produced at the rate of almost 30 million tons per year. However, formaldehyde is also a ubiquitous pollutant, probably because its highly volatile nature facilitates its dispersion through air to soils and waters. Early studies of Neely revealed that formaldehyde had bacteriostatic activity at sublethal concentrations due to its ability to disrupt growth and interfere with methionine biosynthesis [1]. At higher concentrations formaldehyde is a potent biocidal agent and has thus been used to selectively inactivate *Bacillus anthracis* and *Bacillus subtilis* spores [2, 3] in soil and liquid suspensions. Formaldehyde has also been found to be efficient as a disinfectant in holding-tank sewages, particularly at alkaline pHs, and has been used to sterilize laboratory rooms and working surfaces. Formaldehyde is a reactive molecule that contains a carbonyl

* Supported by Scientific Research Foundation for Returned Scholars, Ministry of Personnel of China.

E. Zhu and S. Sambath (Eds.): Information Tech. and Agricultural Eng., AISC 134, pp. 261–267.
springerlink.com © Springer-Verlag Berlin Heidelberg 2012

group which reacts vigorously with amines (also amino groups of proteins), amides, sulphides, and purines of organic compounds [4].

In addition to its artificial production by chemical synthesis, formaldehyde is a subproduct in the metabolism of histidine, choline and a number of plant-derived methoxylated aromatic chemicals such as vanillate, veratrate and caffeate by certain microorganisms [5]. Formaldehyde has also been found as a subproduct of the metabolism of certain xenobiotic compounds such as the explosive hexahydro-1, 3, 5-trinitro-1, 3, 5-triazine (RDX), glyphosate (N-phosphonomethylglycine), atropine, and methenamine, a compound used to treat urinary track infections [6].

Because formaldehyde is produced naturally, microorganisms have evolved different mechanisms to counteract its toxicity. The mechanisms involve fixation through a number of metabolic pathways, and detoxification via oxidation to formate and CO_2. In many microorganisms formaldehyde has been shown to be assimilated via the serine pathway or the allulose pathway (ribulose phosphate cycle). *Burkholderia cepacia* growing on vanillate as a carbon source was shown to induce 3-hexulose-6-phosphate synthase and 6-phospho-3-hexuloisomerase to fix the formaldehyde produced [5]. This pathway has also been identified in the Gram-positive facultative methylotrophs *Mycobacterium gastri* MB19 [5], *Bacillus methanolicus* [7] and *Thermococcus koda* [8]. In addition, *Burkholderia fungorum* LB400 exhibits multiple pathways for formaldehyde detoxification [9].

Kummerle and his colleagues showed that *Escherichia coli* VU3695 bear a plasmid encoding a glutathione and an NAD+-dependent formaldehyde dehydrogenase that conferred a formaldehyde-degrading character to the strain. Similarly, an *fghA* mutant of *Parococcus denitrificans* defective in glutathione-dependent formaldehyde dehydrogenase was found unable to grow on methanol because of the accumulation of formaldehyde. In the *Methylobacterium extorquens* facultative methylotroph, inactivation of the H4MPT pathway led to increased sensitivity to formaldehyde [4, 9].

Formaldehyde presents as a natural product in most living systems and in the environment from manmade sources, such as indoor furniture decoration. There are few researches on formaldehyde biodegradation in sludge. We have isolated a bacterial strain from sludge, which could degrade the formaldehyde.

2 Materials and Methods

2.1 Isolation of a Formaldehyde Degrader

The sludge sample was collected from sewage outfall from a furniture factory, located in Harbin (Heilongjiang Province, China). Ten gram sludge was aseptically added to 90 mL of the sterilized distilled water in a 250-mL flask containing 90 mg glass beads, incubated on a rotary shaker (180 rpm). When the culture became obviously turbid, the culture was inoculated to LB agar plates (1%) with 4 mM formaldehyde by using a 10-time dilution method. The agar plates were incubated at 37°C, for 24 hours. Colonies with distinct morphological differences such as color, shape and size, were selected and purified by streaking at least three times on LB agar with 4 mM formaldehyde. Pure cultures were then obtained by successively re-inoculating into LB with 20 mM formaldehyde. One of the most efficient isolates, named as strain SG-71, was selected.

2.2 Physiological and Biochemical Characteristics

The temperature and pH profiles of the isolate were determined by measuring the optical density (OD) of the bacteria solution developed under aerobic conditions. The temperature profile was tested in the LB medium by incubating at 20°C, 25°C, 30°C, 35°C, 40°C and 45°C. The pH profile was tested in the LB medium at a pH range from 5 to 10. 100 mL Erlenmeyer flasks with 10 mL of LB medium inoculated with 1 ml bacteria solution, which was previously grown aerobically in 20 mL LB medium on a rotary shaker (180 rpm) at 37°C when the optical density was up to 0.2. Incubations were carried out on a rotary shaker (180 rpm) for 12 hours. Samples were measured the optical density.

All experiments were repeated three times.

2.3 Identification of Isolated Bacteria Strains

The strain was characterized by morphological, physiological and biochemical method according to the procedures in Bergey's manual [10].

Genomic DNA of the tested strains was extracted from 1.5 ml of culture at 37°C in LB by the CTAB (cetyltrimethyl ammonium bromide) method. Briefly, collected cells were suspended in 570 μl of TE (10 mM Tris, 1 mM EDTA) buffer (pH 8.0). The cells were lysed by addition of 30 μl of 10% SDS and 10 μl of proteinase K solution (10 mg/ml). Then the mixture was incubated at 37°C for 1 hour. After that, 100 μl NaCl (5M) and 80 μl CTAB/NaCl (10%, w/w) were added to the digested beads followed by a 10-min incubation at 65°C. Deproteinization was done by extraction of one volume phenol-chloroform-isoamyl alcohol (25: 24: 1) and chloroform-isoamyl alcohol (24: 1) twice. Finally, DNA was precipitated by adding 0.1 volume of 3M sodium acetate to the water phase followed by 1 volume of ice dimethyl carbinol. The DNA was collected, washed and dissolved in 25 μl sterile ultrapure water.

The 16S rDNA genes were amplified using primers F8 (AGAGTTTGATCCTGGC TCAG) and R1541 (AAGGAGGTGATCCAGCCGCA). The approximately 1500 bp sequence between these two primers corresponds to the nucleotide numbers, 8 through 1541, based on the 16S ribosomal DNA sequence of *Escherichia coli*. To further identification PCR primers based on sequences of the 16S-23S rDNA spacer region of *Pseudomonas sp*. were designed as follows: P.P1476 (GGTGAAGTCGTAACAAGG) and P.P2056 (CCACTACTAAGGGAATCTCG).

The 16S rDNA genes were amplified in a TaKaRa PCR Thermal Cycler Dice. Each sample contained 1×*Taq* buffer (TaKaRa, China), 0.2 M of each dNTP, 10 pmol of each primer, 10 ng template bacterial DNA and 1.0 U *rTaq* polymerase (TaKaRa, China). The reaction conditions were as follows: 94°C for 3 min, 94°C for 30 sec, 55°C for 30 sec, 72°C for 1.5 min, 30 cycles, and then 72°C for 10 min, 4°C forever. The 16S-23S rDNA spacer regions were amplified as previously described.

Reaction products were resolved by electrophoresis in 0.8% agarose gels and visualized by ethidium bromide staining. The interested PCR product was isolated from the agarose gel using an Agarose Gel DNA Purification Kit Ver. 2.0 (TaKaRa, China). The purified PCR fragments were used for sequencing by the corresponding sequencing primers.

DNA sequencing was performed by Sangon Biotech Co., Ltd. (Shanghai, China). The consensus sequences were obtained from two reads of 16S rDNA gene using DNAMAN software 5.2.2. The consensus sequences of the 16S rDNA gene of isolated strains, which were available in the GenBank database, were compared.

2.4 Formaldehyde Degradation Test

For testing formaldehyde degradation, 20 mM, 25 mM, 30 mM, 35 mM, 40 mM formaldehyde were added to 10 mL of autoclaved sterilized LB medium, respectively, and 1 ml bacteria solution, which was previously grown aerobically in 20 mL LB medium on a rotary shaker (180 rpm) at 37°C, when the optical density was up to 0.2, was inoculated into the medium.

After inoculation, the flasks were incubated at 30°C in a reciprocal shaker operating at 180 rpm. Samples were measured the optical density and the residual formaldehyde concentration every 2 hours. All experiments were repeated three times.

3 Results and Disccussion

3.1 Formaldehyde Degrading Bacteria

During the screening stage, one isolated bacteria strain degraded and metabolized formaldehyde as a sole carbon and energy source. The strain named as SG-71 was one of the most efficient formaldehyde-degrading bacteria. It can completely consume 20 mM formaldehyde within 12h.

3.2 Strain Identification and Phylogenetic Analysis

The isolated strain SG-71 was Gram-negative, oxidase-positive, rod-shaped, flagellated and non-motile. Colony is circular, tabular and white colored on LB agar with formaldehyde after 24h at 37°C.

To confirm the species, the nucleotide sequences of the 16S rDNA gene of the isolate was analyzed and determined by the BLAST program on NCBI. 16S rDNA gene sequences of isolate showed more than 99% similarity to *Pseudomonas sp*. Based on the analysis of 16S rDNA genes, SG-71 was accurately identified to the species level.

PCR primers based on sequences of the 16S-23S rDNA spacer region of *Pseudomonas sp*. were used for further identification. Finally, the bacterial strain SG-71 was identified as *Pseudomonas putida.*

3.3 Physiological and Biochemical Characteristics

Fig. 1 shows growth of SG-71 in different temperature in liquid culture. The temperature profile indicated that the range of optimum temperature for SG-71 was 25°C to 35°C, and the optimum temperature was 30°C, while the isolate growth was inhibited at 40°C and 45°C.

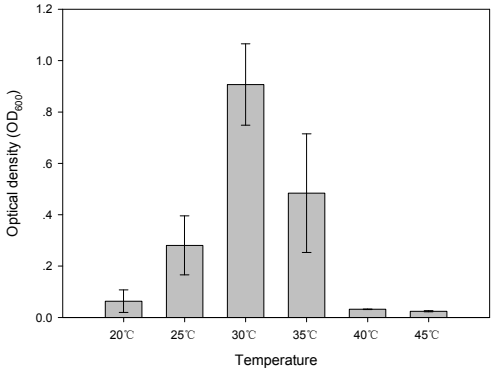

Fig. 1. Growth diagram of SG-71 in different temperature

Next we investigated the OD value changes at pH 5-10. Fig. 2 shows that the optimum pH for the isolate growth is 8. The results shows that the optimum pH range is 6 to 9.

To analyse the response of SG-71 to formaldehyde, we firstly established the strain's level of tolerance to this toxic compound. Fig. 3 shows the results of formaldehyde consumption and cell growth profiles at initial formaldehyde concentrations of 20 mM. The isolate degraded 20 mM formaldehyde within 12 h. Fig. 4 shows the degradation of formaldehyde at different initial concentrations. Formaldehyde concentrations $\geq$ 40 mM completely inhibited growth, although near 100% of the initial cells survived for more than 24 h.

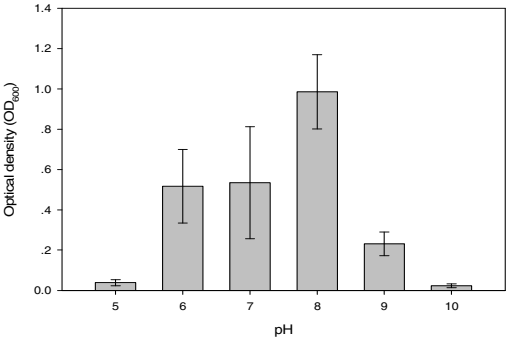

Fig. 2. Growth diagram of SG-71 in different pH value

In summary, our results shows that *Pseudomonas putida* strain SG-71 has the ability to degrade formaldehyde and used its degradation products as carbon sources. It is confirmed that this formaldehyde-degrading strain could play an important role in the depollution of formaldehyde-containing waste-waters.

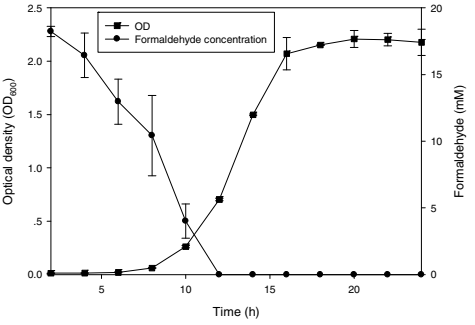

Fig. 3. Growth and degradation diagram of SG-71 in 20mM of formaldehyde

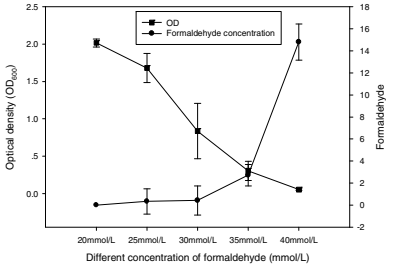

Fig. 4. Growth and degradation diagram of SG-71 in different concentration of formaldehyde

References

1. Neely, W.B.: Action of formaldehyde on microorganisms III: bactericidal action of sublethal concentrations of formaldehyde on Aerobacter aerogenes. J. Bacteriol. 86, 445–448 (1963)
2. Manchee, R.J., Broster, M.G., Stagg, A.J., Hibbs, S.E.: Formaldehyde solution effectively inactivates spores of Bacillus anthraci on the Scottish island of Gruinard. Appl. Environ. Microbiol. 60, 4167–4171 (1994)
3. Sagripanti, J.L., Bonifacino, A.: Comparative sporicidal effect of liquid chemical agents. Appl. Environ. Microbiol. 62, 545–551 (1996)
4. Vorholt, J.A., Marx, C.J., Lidstrom, M.E., Thauer, R.K.: Novel formaldehyde-activating enzyme in Methylobacterium extorquens AM1 required for growth on methanol. J. Bacteriol. 182, 6645–6650 (2002)
5. Mitsui, R., Sakai, Y., Yasueda, H., Kato, N.: A novel operon encoding formaldehyde fixation: the ribulose monophosphate pathway in the gram-positive facultative methylotrophic bacterium Mycobacterium gastri MB19. J. Bacteriol. 182, 944–948 (2000)
6. Fournier, D., Halasz, A., Spain, J., Spanggord, R.J., Bottaro, J.C., Hawari, J.: Biodegradation of the hexahydro-1,3,5-trinitro-1,3,5-triazine ring cleavage product 4-nitro-2,4-diazabutanal by Phanerochaete chrysosporium. Appl. Environ. Microbiol. 70, 1123–1128 (2004)

7. Jakobsen, Ø.M., Benichou, A., Flickinger, M.C., Valla, S., Ellingsen, T.E., Brautaset, T.: Upregulated transcription of plasmid and chromosomal ribulose monophosphate pathway genes is critical for methanol assimilation rate and methanol tolerance in the methylotrophic bacterium Bacillus methanolicus. J. Bacteriol. 188, 3063–3072 (2006)
8. Orita, I., Sato, T., Yurimoto, H., Kato, N., Atomi, H., Imanaka, T., Sakai, Y.: The ribulose monophosphate pathway substitutes for the missing pentose phosphate pathway in the archaeon Thermococcus kodakaraensis. J. Bacteriol. 188, 4698–4704 (2006)
9. Marx, C.J., Miller, J.A., Chistoserdova, L., Lidstrom, M.E.: Multiple formaldehyde oxidation/detoxification pathways in Burkholderia fungorum LB400. J. Bacteriol. 186, 2173–2178 (2004)
10. Whitman, W.B.: Bergey's Manual of Systematic Bacteriology, vol. 2 (1984)

Nucleotide Substitution Pattern in Mitochondrial Cytochrome b Pseudogenes of Ten Species in Galliformes

Jing Sun, Zeqing Feng, and Yiping Liu

College of Animal Science and Technology, Sichuan Agriculture University
Ya'an, Sichuan Province, China
liuyp578@yahoo.com

Abstract. Mitochondrial cytochrome b pseudogene sequences (numts) in ten birds of the order Galliformes were studied for the pattern of nucleotide substitutions. Our results showed that nucleotide transitions were much more common than transversion in the numts. No transversions were detected in the numts of Chrysolophus pictus and Chrysolophus amherstiae. Moreover, there was no evidence that the nucleotide substitutions could have significant neighboring biases ($P > 0.05$) in the Cyt b gene numts. The identified nucleotide deletions ranged from 0 base pair (bp) to 12 bp, while only a thymidine was inserted at the 323th site of the numt sequence of Numida meleagris. Unexpectedly, 2 bp deletions was more frequent than 3 bp deletions and 5 bp deletions, which indicated the changes of encoding amino acids. Both mitochondrial Cyt b gene and the corresponding numt were abundant in the base contents of adenine (A) and thymidine (T).

Keywords: Galliformes, cytochrome b, numts, nucleotide substitution.

1 Introduction

Mitochondrial DNA (mtDNA) has been extensively used over three decades in phylogenetic studies and evolutionary relationships of populations and species, the utilization of mtDNA relative to nuclear DNA is extensively expanded, especially for these studies of domestic species' maternal origin [1-3] and human migration [4]. The presence of translocated pieces of mtDNA in the nuclear genome of many taxa (nuclear mitochondrial insertions or numts) might be mistaken for the authentic organellar mtDNA and confuse the evolutionary studies [5], as well as medical studies [6].

Mitochondrial pseudogenes have been identified and characterized from a wide range of taxa, particularly in mammals and birds. Processed pseudogenes (or retropseudogenes) constituted the majority of pseudogenes in mammalian genomes, which were inserted into the genome by the retrotransposition of mRNA of functional genes [7]. A comprehensive database of identified pseudogenes have been described at Pseudogene site (http://www.pseudogene.org/), including 12 eukaryote and 64 prokaryote pseudogenes. We focused on the amount of pseudogenes in several important model organisms. Totally, 16946 pseudogenes in human genome and 19044 in mouse genome have been index by the end of May 17, 2010, which

E. Zhu and S. Sambath (Eds.): Information Tech. and Agricultural Eng., AISC 134, pp. 269–277.
springerlink.com © Springer-Verlag Berlin Heidelberg 2012

exceeded far the amount in chicken (over 5539 pseudogenes). In other words, the abundance of pseudogenes seems plausibly to distribute unevenly in different taxa [8]. It is likely that gene density plays an important part in the content of numts [9]. When focusing on the discovery of numts in Fungi, viridiplantae, and metazoans, Bensasson et al. [10] found that numts appeared more common in plants than in animals, and also human had a much larger proportion of numts than in Drosophila. Besides, the trend that species with a larger noncoding nuclear DNA would be expected to have more numts has become increasingly bespoke [9]. Another reason is that numts indeed conform to the nuclear mutation rate and pattern, namely, numts with the lower mutation rate will preserve longer if all other factors being equal [11].

The reported numts have increased from four to six orders of birds between 2004 and 2008 involving 244 numts [12]. The content of numts were abundant (over 85%) in birds' mitochondrial control region and Cyt b gene [12]. The chicken (Gallus gallus) mitochondrial genome consists of a circular, double-stranded DNA molecule that is up to 16775 bp in length. So far, only 15 numts in chicken have been found through alignment of sequences (NCBI-BLSTN) [12]. These numts were supposed to be independent insertions from the mitochondria into the nuclear with less repetitive elements in the chicken genome [13]. It is commonly believed that numts and their mitochondrial gene would evolve under different selective pressure once they were integrated into the nuclear genome.

In this paper, we took a particular interest in the pattern of nucleotide substitution inferred from the mitochondrial cytochrome b numts in ten birds (order Galliformes). Here, we used the Cyt b pseudogene sequences that were originated from the same regions on the functional mtDNA Cyt b gene found in the study of Qu et al. [12]. Only those sites with the same nucleotide as the consensus sequence of the functional Cyt b gene and two neoganth birds' sequences were included. When the nucleotide in Cyt b at the site is consistent with the ancestral nucleotide, we reasonably ascribe the observed nucleotide change to a substitution in Cyt b gene numts (Insertions and deletions were excluded).

2 Materials and Methods

Full-length mitochondrial Cyt b sequences of turkey (Meleagris gallopavo) were retrieved from NCBI (accession number: L08381), and the Cyt b sequence of zebra finch (Taeniopygia guttata) was retrieved from the entire mtDNA genome (accession number: DQ422742). The accession number of the Cyt b pseudogene sequences was from EU826439 to EU826448, respectively. The full-size Cyt b sequences of the corresponding ten species were obtained from NCBI. Their accession number is AB120130, AF013763, AF028793, AF028798, AF102874, L08377, L08378, L08379, L08380, L08383, respectively.

We did multiple sequence alignment using the online program Clustal (W) from the EBI (http://www.ebi.ac.uk/).When we aligned the numt with functional Cyt b gene sequence, each of the differences must be assumed to arise from a single substitution without any possibility of multiple substitutions. BioEdit [14] and MEGA4.0 [15] were used for statistic and calculator of the total nucleotide numbers, insertions, deletions, base substitutions, and base contents of Cyt b gene and their numts.

3 Results

3.1 Pattern of Nucleotide Substitutions

In order to determine the frequency of mutations from one type of nucleotide to another, we consulted the mathematical manipulation available in the studies of Zhang et al. [16]. Let Ti be the total number of type I nucleotides in a Cyt b gene and Nij be the number of base changes from the type i in a functional Cyt b gene to type j in the corresponding numt (i, j = A, T, C or G) and

$$p_{ij} = N_{ij} / T_i$$

pij represents the proportion of base changes from type i in the functional Cyt b gene to type j in the numt.

Table 1 listed some statistics about the nuclear copies of mitochondrial Cyt b gene in ten birds of the order Galliformes. Only those sites in the corresponding functional sequence that were consensus for both turkey and zebra finch were included. It is observed that, base A to G was more frequent than to base C or T, while substitutions were more frequent from C to T than to A or G. Furthermore, substitutions C: G→T: A occurred more frequently than A: G→T: C. The number of nucleotides that were missing in the numts of birds was no less than seven except for Chrysolophus pictus and Chrysolophus amherstiae. Only a thymidine was inserted at the 323th position in Numida meleagris' numt and the rests were not (shown in Figure 2).

What's more, table 1 also indicated some features of substitution rates between nucleotide pairs in Cyt b numts. On the while, the numbers are more frequent for transitions than for transversions in ten numts. In particular, the numbers for two

Table 1. Proportion of Base Mutations between Nucleotide Pairs from the Mitochondrial Cytochrome b Gene and the Numt of Ten Birds

Species	A→T T→A	A→C T→G	A→G T→C	C→A G→T	C→T G→A	C→G G→C
Gallus gallus	3/314	2/314	7/314	4/418	12/418	5/418
	2/273	0/273	5/273	1/138	4/138	2/138
Phasianus colchicus	1/314	6/314	8/314	3/393	12/393	5/393
	2/295	0/295	3/295	1/141	6/141	1/141
Pavo cristatus	3/334	4/334	9/334	4/387	9/387	5/387
	2/290	0/290	5/290	1/132	4/132	2/132
Pavo muticus	3/326	4/326	9/326	4/389	10/389	5/389
	2/290	0/290	5/290	1/138	4/138	2/138
Lophura nycthemera	3/319	5/319	5/319	2/398	11/398	3/398
	2/290	0/290	2/291	1/135	3/135	2/135
Alectoris chukar	3/319	4/319	8/319	4/400	12/400	2/400
	2/285	0/285	6/285	1/139	2/139	3/139
Coturnix coturnix	3/328	3/328	8/328	4/394	11/394	4/394
	2/290	1/290	5/290	1/131	4/131	2/131
Numida meleagris	3/323	3/323	6/323	6/401	11/401	5/401
	1/282	1/282	4/282	3/137	3/137	2/137
Chrysolophus amherstiae	0/322	0/322	2/322	0/395	2/395	0/395
	0/273	0/273	0/273	0/138	0/138	0/138
Chrysolophus pictus	0/321	0/321	2/321	0/395	4/395	0/395
	0/288	0/288	0/288	0/139	1/139	0/139

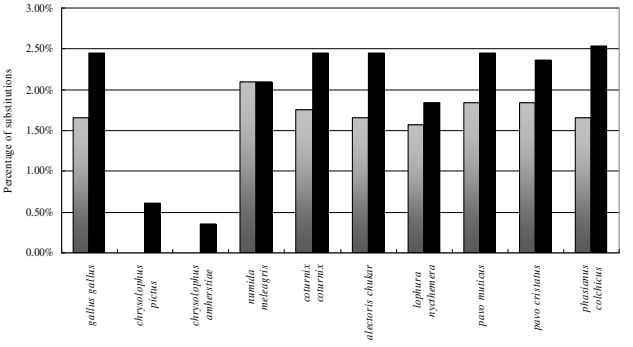

Fig. 1. The percentage of base substitutions in the mitochondrial Cytochrome b gene numts of ten birds. Grey column represents the proportion of nucleotides that have undergone transversions, whereas black one shows the percentage of nucleotides that have undergone transitions.

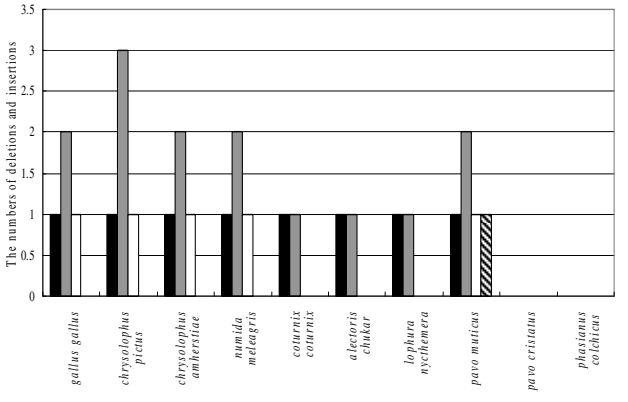

Fig. 2. The number of deletions and insertions in the Cyt b gene numt sequences of ten birds. Black column represents the number of 5 base pair (bp) nucleotide deletions that was observed; Grey column shows the number of 2 bp deletions, and the white one means the number of 3 bp deletions. The stripe column indicates the number of insertion in the numts.

transitions C→T and A→G are the largest and second largest, respectively. The percentage of transitions and transversions in numts relative to their functional Cyt b gene are showed in Figure 1. The number for transitions is equal to that for transversions in the numt of N. meleagris, account for 2.10% of the full length of Cyt b gene. No transversion was detected in the numts of C. pictus and C. amherstiae, and only seven and four transitions are identified from the two numts, respectively. The highest ratio of ts/tv (over 1.53) is observed for Phasianus colchicus.

We also calculated the relative substitution frequency that a base change had mutated to the three other types, as described in the study of Gojobori et al. [17]. Pij was defined as the proportion of substitutions,

$$P_{ij} = N_{ij} / \sum_{j \neq i} N_{ij}$$

we can note a similar result emerges in table 2, that there is a directional pattern of the substitutions. For example, substitution C: G→T: A were more frequently than A: G→T: C. Here, we also have to point out that the proportions of substitutions in C. amherstiae (57.14%) and C. pictus (63.64%) were higher than those of in other eight bird species. The proportion of base changes is generally between 46% and 64% in the Cyt b gene numts in the ten birds.

Table 2. Proportion of Substitutions from One Type to Another among the Total Number of Mutated Nucleotiides in the Cyt b Gene Numts of Ten Birds

Species	A→T T→A	A→C T→G	A→G T→C	C→A G→T	C→T G→A	C→G G→C	Total
Gallus gallus	3/18 2/21	2/18 0/21	7/18 5/21	4/41 1/12	12/41 4/12	5/41 2/12	47/92
Phasianus colchicus	1/27 2/20	6/27 0/20	8/27 3/20	3/37 1/11	12/37 6/11	5/37 1/11	48/95
Pavo cristatus	3/29 2/20	4/29 0/20	9/29 5/20	4/37 1/7	9/37 4/7	5/37 2/7	48/93
Pavo muticus	3/27 2/21	4/27 0/21	9/27 5/21	4/35 1/12	10/35 4/12	5/35 2/12	49/95
Lophura nycthemera	3/19 2/19	5/19 0/19	5/19 2/19	2/34 1/7	11/34 3/7	3/34 2/7	39/79
Alectoris chukar	3/25 2/20	4/25 0/20	8/25 6/20	4/44 1/10	12/44 2/10	2/44 3/10	49/99
Coturnix coturnix	3/29 2/28	3/29 5/28	8/29 5/28	4/36 1/10	11/36 4/10	4/36 2/10	48/103
Numida meleagris	3/19 1/27	3/19 4/27	6/19 4/27	6/38 3/13	11/38 3/13	5/38 2/13	48/97
Chrysolophus amherstiae	0/3 0	0/3 0	2/3 0	0/3 0	2/3 0	0/3 0	4/7
Chrysolophus pictus	0/4 0	0/4 0	2/4 0	0/5 0/2	4/5 1/2	0/5 0/2	7/11

3.2 Neighboring Effects on Substitutions in Ten Numts

Some studies have demonstrated that nucleotide substitutions, above all transitions, have a large neighbor bias in human's pseudogenes [16]. To study the effect of a neighboring nucleotide, it is necessary to make sure that the nucleotide has not changed after mitochondrial Cyt b sequence inserted into the nuclear genome. And it is essential to remove any site itself and those with an insertion or deletion followed immediately in the numt; additionally, we must assure that the neighboring nucleotide was consistent at the same site of functional Cyt b gene and the numt. We only considered the effect of right neighboring base effects on substitutions in the ten numts because of DNA symmetry. Table 3 listed the effect of the neighboring base on substitutions in the numts of ten birds. Different from the results of pseudogenes studies in human genome, there was no evidence that the nucleotide substitutions

could have significant neighboring biases in this study ($P > 0.05$). There was no effect of the neighboring base on the frequency of transitions or transversions. The incomplete fragments of nuclear copies in this study with a length of 400 bp might account for this pattern. Besides, only transitions have been found in the numts of C. amherstiae and C. pictus with a guanine as the first nucleotide differed to the other species with a thymidine.

Table 3. Neighboring Effects on Substitutions in the Mitochondrial Cyt b Numts of Ten Birds

Species	First nucleotide	Base in functional gene	Base on right in numt										Total bases
			Transitions				P-value	Transversions				P-value	
			A	C	G	T		A	C	G	T		
Gallus gallus	T	A	1	2	0	2	P=1.0000 χ^2=0.0850	3	0	0	0	P=0.99998 χ^2=0.4429	346
		C	3	2	3	0		0	2	1	1		
		G	0	1	0	1		0	0	1	0		
		T	1	0	0	1		0	1	0	0		
Phasianus colchicus	T	A	1	2	2	2	P=0.9997 χ^2=0.8698	2	1	0	1	P=1.0000 χ^2=0.2691	346
		C	3	3	4	1		2	2	2	1		
		G	2	1	0	1		0	1	0	1		
		T	1	1	0	0		1	0	1	0		
Pavo cristatus	T	A	1	2	3	3	P=0.9997 χ^2=0.8533	3	0	0	1	P=1.0000 χ^2=0.5133	346
		C	3	3	3	1		2	2	3	1		
		G	1	1	0	1		0	0	1	1		
		T	1	2	0	0		1	0	0	0		
Pavo muticus	T	A	1	2	3	3	P=0.9998 χ^2=0.8067	3	0	0	1	P=0.9999 χ^2=0.6021	346
		C	3	3	2	1		2	2	3	1		
		G	1	1	0	1		0	0	1	1		
		T	1	2	0	0		1	0	0	0		
Lophura nycthemera	T	A	0	1	3	1	P=0.9954 χ^2=1.6966	3	2	0	0	P=0.9998 χ^2=0.7733	351
		C	3	2	1	4		1	0	2	0		
		G	0	1	0	2		0	0	1	1		
		T	0	0	0	0		1	0	0	0		
Alectoris chukar	T	A	2	1	3	2	P=0.9995 χ^2=0.9864	4	1	0	0	P=0.9998 χ^2=0.7307	351
		C	3	3	2	0		1	2	2	2		
		G	0	1	0	1		0	0	1	2		
		T	0	3	0	0		1	0	0	0		
Coturnix coturnix	T	A	2	1	3	1	P=0.9996 χ^2=0.9181	2	1	0	1	P=0.9999 χ^2=0.5721	351
		C	3	3	1	1		1	3	2	1		
		G	0	1	0	1		0	0	1	1		
		T	0	2	0	0		2	0	0	0		
Numida meleagris	T	A	1	1	1	2	P=0.9999 χ^2=0.6205	0	1	1	2	P=0.9999 χ^2=0.6863	346
		C	3	2	2	0		2	3	2	1		
		G	0	1	1	1		1	0	1	2		
		T	0	2	0	0		2	0	0	0		
Chrysolophus amherstiae	G	A	1	1	0	0	P=0.7061 χ^2=6.3333	0	0	0	0	/	352
		C	1	1	0	1		0	0	0	0		
		G	0	1	0	0		0	0	0	0		
		T	0	0	0	0		0	0	0	0		
Chrysolophus pictus	G	A	1	1	0	0	P=0.5409 χ^2=7.9333	0	0	0	0	/	352
		C	1	1	0	1		0	0	0	0		
		G	0	0	0	0		0	0	0	0		
		T	0	0	0	0		0	0	0	0		

3.3 Base Content in Mitochondrial Cyt b Gene and Their Numts

Similarly, there was no obvious difference in the base content between the Cyt b gene and the corresponding numt (shown in table 4). However, the percent of A+T content predicted from the functional Cyt b gene was slightly higher than that of numt. In the bird's numt, the content of nucleotide C and G have a trend to increase although below the significant level.

Table 4. Base Contents in Mitochondrial Cyt b Genes and Their Corresponding Numts

Species	Cytochrome b gene						Nuclear copy of Cytochrome b gene					
	No. of base	A+T (%)	A (%)	C (%)	G (%)	T (%)	No. of base	A+T (%)	A (%)	C (%)	G (%)	T (%)
Gallus gallus	1143	51.36	27.47	36.57	12.07	23.88	346	53.47	25.43	29.77	16.76	28.03
Chrysolophus pictus	1143	53.28	28.08	34.56	12.16	25.20	352	51.70	33.24	33.24	15.06	25.28
Chrysolophus amherstiae	1143	53.37	28.17	34.56	12.07	25.20	352	51.99	26.42	32.95	15.06	25.57
Numida meleagris	1143	52.93	28.26	35.08	11.99	24.67	346	53.18	26.30	30.06	16.76	26.88
Coturnix coturnix	1143	54.07	28.70	34.47	11.46	25.37	351	52.99	26.50	31.05	15.95	26.50
Alectoris chukar	1143	52.84	27.91	35.00	12.16	24.93	351	52.71	26.50	30.77	16.24	26.21
Lophura nycthemera	1143	53.37	27.91	34.82	11.81	25.46	351	53.85	26.78	30.77	15.38	27.07
Pavo muticus	1143	53.89	28.52	34.03	12.07	25.37	346	53.47	25.43	29.77	16.76	28.03
Pavo cristatus	1143	54.59	29.22	33.86	11.55	25.37	346	53.47	25.43	29.77	16.76	28.03
Phasianus colchicus	1143	53.28	27.47	34.38	12.34	25.81	346	53.47	25.43	29.77	16.76	28.03

4 Discussion

The pattern of nucleotide substitutions in pseudogenes provides very good information for us to infer the evolutionary of numts. Recently, increasing amount of numts were discovered by the method of whole-genome sequencing technology [12]. However, the numbers of numts detected in birds was obviously less than that in human and plant [18]. The similar number of genes between chicken and human, and the loss of repetitive DNA and gene-poor chromosomal regions were believed to be the important factors to achieve the chicken's small genome size [19]. High metabolic rate was essential for the bird's flight and then led to the compact genome [20], which likely was the reason why a limited number of numts in birds.

The pattern of nucleotide substitutions in pseudogenes was similar to their functional gene, but different to the electrophoretic variants of hemoglobin in human [21]. And the most notable contrast among them was the relative frequency of C→T. In this study, the nucleotide substitutions C: G→T: A occurred more frequently than A: G→T: C in the numts of ten birds, while the rare one of C→T was found from human's pseudogenes [17]. This different pattern between bird and human could be explained by the facts that amino acid substitutions occurred primarily between those with similar biochemical characteristics in the protein evolution and free of evolutionary pressures in numts [17]. In summary, the numbers were higher for transitions than for transversions in these ten numts. Particularly, the number for transition C→T was the largest one. Our results showed a high frequency of A+T base content both in mitochondrial Cyt b genes and their corresponding numts. But on a slightly difference that was, the Cyt b genes were relatively high in A and low in T while the numts were low in A, though high in T.

We have detected the effects of the different type of immediately neighboring nucleotides on the substitution rates among the twelve possible nucleotide pairs. As opposed to the previous studies, there were no significantly correlations between them ($P > 0.05$), this result applied for both transitions and transversions. The incomplete short-sequences of numts in birds could probably be one of the most important reasons. But these numts still can be distinguished from the present of insertion, deletions, premature stop codons or frameshift mutation. The nucleotide deletions in our study stretched from 0 bp to 12 bp, while only a thymidine was inserted at the 323th site of the numt sequence of N. meleagris. Overall, it was unexpected that we found 2 nucleotide deletions were more frequent than 3 bp deletions and 5 bp deletions, which indicated the changes of encoding amino acids.

Acknowledgement. This study was supported by the National 863 Project of China (2008AA101001), the Program for New Century Excellent Talents in University (NCET-10-0889), the Science Fund for Young Scholars in Sichuan Province (Grant No: ZQ 026-017).

References

1. He, D.Q., et al.: A homogenous nature of native Chinese duck matrilineal pool. BMC Evolutionary Biology 8, 298 (2008)
2. Lai, S.J., et al.: Mitochondrial DNA sequence diversity and origin of Chinese domestic yak. Anim. Genet. 38, 77–80 (2007)
3. Liu, Y.P., et al.: Multiple maternal origins of chickens: out of the Asian jungles. Mol. Phylogenet. Evol. 38, 12–19 (2006)
4. Yao, Y.G., et al.: Phylogeographic differentiation of mitochondrial DNA in Han Chinese. Am. J. Hum. Genet. 70, 635–651 (2002)
5. Thalmann, O., et al.: Unreliable mtDNA data due to nuclear insertions: a cautionary tale from analysis of humans and other great apes. Mol. Ecol. 13, 321–335 (2004)
6. Yao, Y.G., et al.: Pseudomitochondrial genome haunts disease studies. J. Med. Genet. 45, 769–772 (2008)
7. Zhang, Z., Carriero, N., Gerstein, M.: Comparative analysis of processed pseudogenes in the mouse and human genomes. Trends Genet. 20, 62–67 (2004)
8. Benesh, D.P., et al.: Reliability of mitochondrial DNA in an acanthocephalan: the problem of pseudogenes. Int. J. Parasitol. 36, 247–254 (2006)
9. Woischnik, M., Moraes, C.T.: Pattern of organization of human mitochondrial pseudogenes in the nuclear genome. Genome. Res. 12, 885–893 (2002)
10. Bensasson, D., et al.: Mitochondrial pseudogenes: evolution's misplaced witnesses. Trends Ecol. Evol. 16, 314–321 (2001)
11. Blanchard, J.L., Lynch, M.: Organellar genes: why do they end up in the nucleus? Trends Genet. 16, 315–320 (2000)
12. Qu, H., Ma, F., Li, Q.: Comparative analysis of mitochondrial fragments transferred to the nucleus in vertebrate. J. Genet. Genomics 35, 485–490 (2008)
13. Pereira, S.L., Baker, A.J.: Low number of mitochondrial pseudogenes in the chicken (Gallus gallus) nuclear genome: implications for molecular inference of population history and phylogenetics. BMC Evol. Biol. 4, 17 (2004)

14. Hall, T.: BioEdit: a user-friendly biological sequence alignment editor and analysis program for windows 95/98/NT. Nucleic Acids Symp. Ser. 41, 95–98 (1999)
15. Tamura, K., et al.: MEGA4: Molecular Evolutionary Genetics Analysis (MEGA) software version 4.0. Mol. Biol. Evol. 24, 1596–1599 (2007)
16. Zhang, Z., Gerstein, M.: Patterns of nucleotide substitution, insertion and deletion in the human genome inferred from pseudogenes. Nucleic Acids Res. 31, 5338–5348 (2003)
17. Gojobori, T., Li, W.H., Graur, D.: Patterns of nucleotide substitution in pseudogenes and functional genes. J. Mol. Evol. 18, 360–369 (1982)
18. Richly, E., Leister, D.: NUMTs in sequenced eukaryotic genomes. Mol. Biol. Evol. 21, 1081–1084 (2004)
19. Hughes, A.L., Friedman, R.: Genome size reduction in the chicken has involved massive loss of ancestral protein-coding genes. Mol. Biol. Evol. 25, 2681–2688 (2008)
20. Gregory, T.R.: A bird's-eye view of the C-value enigma: genome size, cell size, and metabolic rate in the class aves. Evolution 56, 121–130 (2002)
21. Fitch, W.M.: Evidence suggesting a non-random character to nucleotide replacements in naturally occurring mutations. J. Mol. Biol. 26, 499–507 (1967)

Limited Genetic Diversity of Chinese Muscovy Duck (Cairina moschata) Revealed by Partial Sequences of Mitochondrial DNA Cytochrome *b* Gene

Jing Sun, Jing Huang, Xiaoling Zhao, Hang Zhong, Qing Zhu, and Yiping Liu

College of Animal Science and Technology, Sichuan Agriculture University
Ya'an, Sichuan Province, China
liuyp578@yahoo.com

Abstract. Muscovy duck is a popular domestic animal for meat in China. In this study, we tried to have an insight into the genetic diversity of Chinese Muscovy ducks (Cairina moschata). The length of 475bp of mitochondrial DNA cytochrome b (Cyt b) region from 31 individuals in two geographical populations of Chinese domestic Muscovy duck had been sequenced. Six haplotypes (S1-S6) were determined which totally contained six unique variations. In particular, Haplotype S1 was shared both geographic populations and had the highest haplotype frequency, while the other five haplotypes (S2-S6) was found exclusively from one population (Fujian population or Yuyao population). This limited genetic diversity coincided with the studies of domestic duck and the mitochondrial control region of domestic Muscovy duck in China.

Keywords: Chinese Muscovy duck, cytochrome b gene, haplotype, limited genetic diversity.

1 Introduction

Muscovy duck, likely first tamed in Mexico and central and South America, has been domesticated for 250 years in China on record [1]. Recent researches have detailed reported the multiple matrilineal components of Chinese domestic animals, such as cattle [2], chicken [3], pig [4], goat [5], and yak [6]. Recently, Chen [7] analyzed the mitochondrial DNA control region data of Muscovy duck, and found that Chinese Muscovy duck had low genetic diversity. They only determined 4 haplotypes among 70 samples, the two minor haplotypes (H3 and H4) differed from the main type (H2) only by one-mutation distance, haplotype 1 contained 3 individuals which retrieved from Genbank and had also only one mutation distance without counting the transversion variations. This pattern of low genetic variability and simple haplotype components was similar to the study of domestic duck origin in China, which found that the matrilineal pool of Chinese domestic ducks and mallards was homogeneous without clear geographic differentiation [8].

In this study, we further selected 33 samples of Muscovy duck referring to the mtDNA control region data in the study of Chen [7] for partial region of cytochrome b (Cyt b) gene to solidify the limited genetic pattern emerged in Chinese Muscovy duck.

E. Zhu and S. Sambath (Eds.): Information Tech. and Agricultural Eng., AISC 134, pp. 279–282.
springerlink.com © Springer-Verlag Berlin Heidelberg 2012

2 Materials and Methods

2.1 Samples and DNA Isolation

Total 31 blood samples of Muscovy duck (C. moschata) were collected from two indigenous populations consisting of ZM (from Yuyao County in Chekiang province) and F (from Fujian province) in this study. Genome DNA was extracted following the standard phenol-chloroform method.

2.2 PCR Amplification and Sequencing

The partial fragment of Cyt b gene (over 475 base pairs), is amplified using primer pairs (L15229: 5'-CACCCTGACCCGATTCTTC-3', and H15774: 5'-GATGCGAGTTGCCCGATGA-3') designed according to C. moschata mitochondrial complete genome (number of Genbank: NC_010965.1) in this study. The PCR reaction is as follow: denaturation at 94 ℃ for 45 s, annealing 55 ℃ for 30 s, and extension at 72 ℃ for 1 min for 35 cycles. Products of amplification reaction which produced a single and visible band are directly sequenced for both strands using Big Dye Terminator v 3.1 Cycle Sequencing Kit (Applied Biosystems, USA) on an ABI-PRISM3730 DNA sequencer according to the manufacturer's manual.

2.3 Date Analyses

Nucleotide variations were scored relative to the complete cytochrome b gene sequence of Muscovy duck (number of Genbank: L08385) [9] using the MEGA v4 [10]. An unrooted neighbor-joining tree was constructed using the Kimura 2-parameter model in MEGA v4 with 1000 bootstrap replications. Haplotype diversity and nucleotide diversity were estimated using DnaSP v5 [11].

3 Results

Six haplotypes (S1-S6) were determined at 127 variable sites among 475 bp sequences of mtDNA Cyt b gene from 31 individuals in Chinese Muscovy duck (Fig 1). These sequences totally had six unique variations, which consisting of two transitions, two transversions, and two single nucleotide deletions. Haplotype S1 were shared both geographic populations, while the other five haplotypes (S2-S6) was found exclusively from one population (Fujian population or Yuyao population) (Table 1).

The haplotype diversity and nucleotide diversity in the Yuyao population were 0.338 ± 0.128 and 0.00076 ± 0.00031; while 0.417 ± 0.191 and 0.00139 ± 0.00073 in the Fujian population, respectivley. This pattern of limited genetic diversity of the Chinese Muscovy duck was consistent with previous study [7].

In the unrooted neighbor-joining tree (Fig 1), haplotype S1 was the predominant haplotype which found in 26 individuals from two populations (Fujian and Yuyao population). The rest five haplotypes (S2-S6) were separated from S1 by only one variation. In particular, haplotype S3 and S6 were found as the result of single nucleotide base deletion.

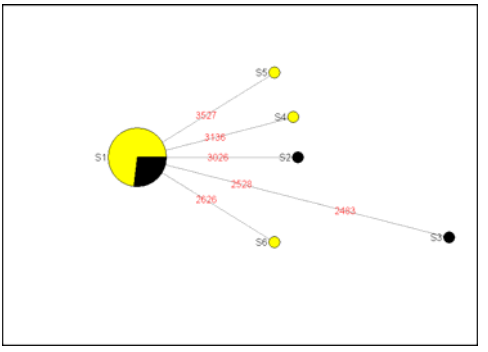

Fig. 1. Unrooted neighbor-joining tree of mtDNA cytochrome *b* gene partial sequences in 31 Chinese Muscovy ducks. Circle area is proportional to haplotype frequency. The yellow colour represents the Muscovy ducks of Yuyao population, while the black denotes those of Fujian population.

Table 1. Haplotype Distribution and Genetic Diversity of Chinese Muscovy Duck

Population	N	Geographic location	Haploytpe						Haplotype diversity (h)	Nucleotide diversity (π)
			S1	S2	S3	S4	S5	S6		
Yuyao	22	Yuyao, Zhejiang	19	-	-	1	1	1	0.338±0.128	0.00076±0.00031
Fujian	9	Fuzhou, Fujian	7	1	1	-	-	-	0.417±0.191	0.00139±0.00073
Total	31	-	26	1	1	1	1	1	0.301±0.107	0.00081±0.00033

4 Discussion

In this study, 6 haplotypes were totally found from 31 Cyt b sequences of two Chinese Muscovy duck populations. This simple haplotype components and limited genetic diversity among and within Muscovy duck populations coincided with the mtDNA control region of Muscovy ducks [7, 12]. And this pattern of low genetic diversity was also similar to the result of Chinese domestic duck, in which only contained two variable sites from 52 Cyt b sequences [8]. Therefore, we believed that our result could be served as the new evidence to support the low genetic variability pattern of Chinese Muscovy duck populations. Interestingly, the genetic variation within Muscovy duck species was relatively low in comparison to domestic duck species (Shaoxing duck and Pekin duck) [13, 14]. The high-strength breeding and bottleneck effect would be regarded as primary causes of reducing Muscovy ducks' genetic diversity to some extent.

Acknowledgment. The authors thank Shiyi Chen for sample collecting.

References

1. Chen, Y.X., Zeng, F.T.: The Chinese waterfowl. Agricultural press, Beijing (1900) (in Chinese)
2. Lai, S.J., Liu, Y.P., Liu, Y.X., Li, X.W., Yao, Y.G.: Genetic diversity and origin of Chinese cattle revealed by mtDNA D-loop sequence variation. Molecular Phylogenetics and Evolution 38(1), 146–154 (2006)

3. Liu, Y.P., Wu, G.S., Yao, Y.G., Miao, Y.W., Luikart, G., Baig, M., Beja-Pereira, A., Ding, Z.L., Palanichamy, M.G., Zhang, Y.P.: Multiple maternal origins of chickens: out of the Asian jungles. Molecular Phylogenetics and Evolution 38(1), 12–19 (2006)
4. Wu, G.S., Yao, Y.G., Qu, K.X., Ding, Z.L., Li, H., Palanichamy, M.G., Duan, Z.Y., Li, N., Chen, Y.S., Zhang, Y.P.: Population phylogenomic analysis of mitochondrial DNA in wild boars and domestic pigs revealed multiple domestication events in East Asia. Genome Biology 8(11), R245 (2007)
5. Liu, Y.P., Cao, S.X., Chen, S.Y., Yao, Y.G., Liu, T.Z.: Genetic diversity of Chinese domestic goat based on the mitochondrial DNA sequence variation. Journal of Animal Breeding and Genetics 126(1), 80–89 (2009)
6. Lai, S.J., Chen, S.Y., Liu, Y.P., Yao, Y.G.: Mitochondrial DNA sequence diversity and origin of Chinese domestic yak. Animal Genetics 38(1), 77–80 (2007)
7. Chen, S.Y., He, D.Q., Liu, Y.P.: Low genetic variability of domestic Muscovy duck (Cairina moschata) in China revealed by mitochondrial DNA control region sequences. Biochem. Genet. 47(9-10), 734–738 (2009)
8. He, D.Q., Zhu, Q., Chen, S.Y., Wang, H.Y., Liu, Y.P., Yao, Y.G.: A homogenous nature of native Chinese duck matrilineal pool. BMC Evolutionary Biology 8(298) (2008)
9. Kornegay, J.R., Kocher, T.D., Williams, L.A., Wilson, A.C.: Pathways of lysozyme evolution inferred from the sequences of cytochrome b in birds. Journal of Molecular Evolutionary 37(4), 367–379 (1993)
10. Tamura, K., Dudley, J., Nei, M., Kumar, S.: MEGA4: Molecular Evolutionary Genetics Analysis (MEGA) software version 4.0. Molecular Biology and Evolution 24(8), 1596–1599 (2007)
11. Librado, P., Rozas, J.: DnaSP v5: a software for comprehensive analysis of DNA polymorphism data. Bioinformatics 25(11), 1451–1452 (2009)
12. Khan Ahmadi, A., Rahimi, G., Vafaei, A., Sayyazadeh, H.: Microsatellite analysis of genetic diversity in Pekin (Anas platyrhynchos) and Muscovy (Cairina moschata) duck populations. International Journal of Poultry Science 6(5), 378–382 (2007)
13. Chen, Y.X., Zuo, Z.H.: Study on genetic relationship and diversity in ducks by RAPD. Journal of Xiamen University 40(1), 141–145 (2001)
14. He, D.Q., Du, J., Liu, Y.P., Wang, H.Y., Ren, Q.M., Rao, Y., Ran, Y.B.: Analysis on partial mitochondrial DNA D-loop sequences of Muscovy duck (Cairina moschata). Acta Agriculturae Shanghai 24(4), 1–4 (2008) (in Chinese)

Status and Prospect of Crop Rotation of Procambarus Clarkii and Mid-season Rice in China

Luojun Gong[1,2,3,4], Xinya Shu[2], Congyi Zhang[2], Bangxi Xiong[1,*], Lansong Yang[3], Qianhong Gu[1], and Jie Chen[1]

[1] College of Fisheries, Huazhong Agricultural University, Shizishan Road 1#, Wuchang District, Wuhan, China
[2] Hubei Provincial Fisheries Research Institute, Wuhan, China
bangxix8@mail.hzau.edu.cn
[3] Hubei Provincial Fishery Technical Extension Center, Pengliuyang Road 237#, Wuchang District, Wuhan, China
[4] Wuhan Water & Sky Biology-Environmental Engineering Co., Ltd, Luoshi South Road 519#, Hongshan District, Wuhan, China

Abstract. The paper gives an introduction to transformation of Procambarus Clarkii from being killed before to being applied and developed now, and the historical background of development of crop rotation technology of Procambarus Clarkii and mid-season rice in China. It focuses on crop rotation technology of Procambarus Clarkii and mid-season rice in China, involving environmental conditions of paddy field, engineering construction, placing mode of parent shrimps, placing mode of young shrimps, aquaculture management of adult shrimps, fishing and disease control. Besides, the paper discusses the present status and prospect of crop rotation of Procambarus Clarkii and mid-season rice in China, and the main contents include: first, the market demand is large, thus crop rotation of Procambarus Clarkii and mid-season rice will continue growing fast; second, the total yield increases each year, and sales price maintains steady and decreases gradually; third, the production cost is continuously raised each year, and the comparative benefit is reduced gradually; fourth, to improve the quality of shrimp species and guarantee supply of fingerlings; fifth, to develop high-quality baits and research bait casting technique; sixth, to pay great attention to diseases and improve aquaculture environment; seventh, to strengthen scientific research and develop aquaculture mode.

Keywords: Procambarus Clarkii, Crop Rotation, Status and Prospect, Mid-season Rice.

1 Introduction

Crop rotation of Procambarus Clarkii and mid-season rice means that after mid-season rice is reaped in September, Procambarus Clarkii will be bred in the paddy field; after Procambarus Clarkii is captured at the end of May the next year, mid-season rice will be planted there again.

* Corresponding author.

E. Zhu and S. Sambath (Eds.): Information Tech. and Agricultural Eng., AISC 134, pp. 283–291.
springerlink.com © Springer-Verlag Berlin Heidelberg 2012

Procambarus Clarkii belongs to Procambarus, Astacidae, Decapoda, Crusacea, Arthropoda. The shrimp was introduced into China from Japan in 1930s. At present, it is distributed in more than 20 China's provinces and municipalities, including Sinkiang, Gangsu, Ningxia, Inner Mongolia, Shanxi, Shanxi, Henan, Hebei, Tianjin, Beijing, Liaoning, Shandong, Jiangsu, Shanghai, Anhui, Zhejiang, Jiangxi, Hunan, Hubei, Chongqing, Sichuan, Guizhou, Yunnan, Guangxi, Guangdong, Qinghai, Fujian and Taiwan. In particular, it is widely distributed in the middle and lower reaches of Yangtze River with large population, which is also the main production area of Procambarus Clarkii in China.

2 Development of the Culture Model in China

Procambarus Clarkii had been killed before 1980s (Wang, 1999), which was applied in a rather low degree. Since 1980s, Dai Aiyun first argued that Procambarus Clarkii was a promising aquaculture target in China and thus should be effectively applied (Dai, 1983). In 1986, Hubei province established the first China's processing plant of Procambarus Clarkii in Wuhan City, and in 1988, it exported the processed products of Procambarus Clarkii to Sweden, which attracted attention from the global importing countries of crayfishes (Shu and Ye, 1989). Afterwards, the processing of Procambarus Clarkii in Hubei province gradually extended to Jiangsu Province, Shandong Province, Anhui Province, and so forth.

Large-scale processing and exporting of Procambarus Clarkii, coupled with gradual development of domestic market, greatly damages domestic natural resource of Procambarus Clarkii, and even Jiangsu Province suffered resource exhaustion and short supply of Procambarus Clarkii. To meet the demands of processing and exporting, the purchasing price of Procambarus Clarkii continues to increase, which stimulates aquaculture enthusiasm of Procambarus Clarkii. By learning from American crop rotation technology of Procambarus Clarkii and mid-season rice (Shu, 1985; Brunson and Griffin, 1988; Jover et al., 1999), we conducted a series of researches and presented crop rotation technology of Procambarus Clarkii and mid-season rice with Chinese characteristics. Hubei Province is a large agricultural province of China, possessing 2,400,000 hectares of paddy fields. Besides, it is also referred to as "province with a thousand lakes". Lots of paddy fields are waterlogged lowlands and cold waterlogged paddy fields, and the paddy fields where the paddy (mid-season rice) can only be planted for one season through the whole year cover 330,000 hectares. Applying these lands to breed Procambarus Clarkii for one season during the winter fallow period from completion of mid-season rice reaping to beginning of mid-season rice transplanting the next year is one of the effective methods to solve "three agricultural problems" in China.

3 Brief Introduction to the Technology

3.1 Cultivating Condition

Environmental conditions of paddy fields for crop rotation of Procambarus Clarkii and Mid-season Rice are very important. The paddy fields used for breeding shrimps should possess favorable ecological environment and plentiful supplies of water, with

flat sediment, strong water retaining capacity and convenient drainage and irrigation, without poisonous and harmful substances and free from flood. And the area should be preferably 6-7 hectares.

3.2 Construction of the Paddy Fields

The loop shrimp aquaculture ditches are excavated around the insides of paddy field ridges, with width of 1-1.5m, and depth of 0.8m. For the larger area, field ditches should also be dug, with width of 0.5-1m, and depth of 0.5m. The area of loop ditches and field ditches accounts for approximately 5-10% of the area of paddy field. The top of field ridge is 3m in width, which should be 0.8m above the bottom of paddy field. The water inlet and outlet are situated at ends respectively. The water outlet should be provided with fleeing-prevention facilities including filter screen, and the water inlet should be supplied with dense webs for filtering influent, to avoid entering of harmful organisms. The intake system and drainage system should be constructed according to the pattern of high-irrigation and low-drainage.

3.3 Parent Shrimps

From the end of July to the end of August each year, parent shrimps are put into loop ditches and filed ditches of paddy field, before mid-season rice is harvested. About 300-450kg of shrimps is placed for each hectare.

1) Selection of parent shrimps

The parent shrimps suited to crop rotation of Procambarus Clarkii and mid-season rice are dark red or scarlet, with luster, smooth body surface free of attachment, complete appendages, sound physique and strong motility. Female or male individuals are above 35g in weight, and the ratio of female individuals to male individuals is 2:1.

2) Aquaculture management

After parent shrimps are placed, paddy field drainage and drying and paddy reaping are performed as usual. When paddy field drainage or drying is done, parent Procambarus Clarkii may dig holes for reproducing. After mid-season rice is harvested, the straws will be returned to paddy fields which will instantly be irrigated, and compost fertilizer is applied to cultivate water quality. If many young shrimps are found, more foodstuffs should be provided for them. When paddy field drainage is carried out, water of the paddy field should be drained rapidly 10-20cm below the field level, and then drained slowly, to stimulate Procambarus Clarkii to dig holes in loop ditches and field ditches. In the end, the paddy can be reaped, when the water level of loop ditches is maintained at 5-10cm. Aquatic plants will be provided for loop ditches and field ditches where parent shrimps are placed, and the aquatic plants should cover above 40% of the area of loop ditches.

3.4 Young Shrimps

Upon completion of reaping mid-season rice, the paddy fields should be instantly irrigated, and the young shrimps will be put into the fields. The young shrimps should be cultured for a certain period of time, namely, a culture pond will be constructed around the paddy field with dense web. the yound shrimps are carried in oxygenated

nylon bags filled with water, and they are put into the water inlet with large amounts of aquatic plants in the culture pond, to avoid direct sunlight. the area of the culture pond is based on the amount of the young shrimps to be placed。 One hectare of culture pond can normally allow 3,000,000 to 4,500,000 young shrimps for each 1cm, which can be used as 10 to 30 hectares of aquaculture field. The culture pond should be provided with aquatic plants, and submerged plants and floating plants should account for 60% and 40% of the culture pond in area respectively. 1500-3000kg of compost fertilizer is applied in the culture pond for each hectare. Fresh water is injected once or twice each day during the culture period, with water level controlled at 0.3 to 0.5m and the transparency of 30-40cm. Suitable feedstuffs are provided timely. The animal feedstuffs including surimi are required 3 to 4 times a day from the first day when young shrimps are put into the culture pond. The daily feeding amount should be 5 to 8% of the shrimp in weight. After approximately 15 to 20 days of culture, the young shrimps grow to 2cm in length, and the web can be removed. The yound shrimps will climb into the paddy field, and the aquaculture of paddy field will begin.

3.5 Aquaculture Management of Adult Procambarus Clarkiis

3) Feedstuff feeding

Before the winter approaches, the aquatic plant and compost fertilizer are supplied once a month, and their respective amount is 1,500kg and 750-1500kg for each hectare. If the food organisms suffer storage, surimi, crushed snail and mussel meat, offcuts of the butchery, etc are required. The feedstuffs are not supplied when the water temperature is below 12℃. When the water temperature rises to above 16℃ the next year, more aquatic plants and compost fertilizers should be furnished. 1,500-2,250kg of aquatic plants are generally supplied once half a month for each hectare, and 750-1,500kg of compost fertilizer is provided once each month for each hectare. If possible, artificial feedstuffs, such as bean dregs and brans, should be fed once a day, and the daily feeding rate is 1-2%.

4) Water supplying

Before the winter comes, the water depth should be mainted at 30 to 40cm in the paddy field. As atmospheric temperature decreasing, water should be increased to 40-60cm in depth. After the winter leaves, the approach used to control the water depth is applied to adjust water temperature, and fresh water is supplied once every 10 days approximately.

5) Enemy expelling

Crop rotation of Procambarus Clarkii and mid-season rice has many enemies, such as frog, snake, rat, and so forth. Not only should the enemies be expelled before shrimp placing, but also enemy organisms should be eliminated at other times.

3.6 Fishing

In the process of crop rotation of Procambarus Clarkii and mid-season rice, the fishing period of Procambarus Clarkii begins from the middle ten days of April, and ends in the last ten days of May. The fishing tool is mainly ground bamboo cage. The fishing principle is long-term fishing and catching the bigger but the smaller, aiming at reducing aquaculture density and promoting rapid growth.

3.7 Disease Control

Taking prevention as main, supported by treatment. The aquaculture water should be sterilized before the shrimps are placed; water quality management should be strengthened during aquaculture period by providing fresh water termly or applying water quality regulator to regulate water quality; fresh feedstuffs are fed, and healthy aquaculture method is applied. The common diseases Procambarus Clarkiis suffer from include crusta fester disease, balantidiasis, and the like.

4 Status of the Technology in China

Hubei Provincial Fisheries Scientific Research Institute began to conduct research and application works on crop rotation technology of Procambarus Clarkii and of mid-season rice. In 2001, the rotation area was over 70 hectares in Qianjiang City, with the unit yield of 1,125kg/ha; from 2002 to 2003, the area was over 130 hectares, with the unit yield of 2,250kg/ha; from 2003 to 2004, the area was over 330 hectares, with the unit yiled of 200.1kg/ha; from 2004 to 2005, the area was over 1,670 hectares. In January, 2006, Hubei Provincial Science & Technology Bureau presided at the appraisal meeting of Crop Rotation Technology of Procambarus Clarkii and Mid-season Rice. Under active propulsion of Hubei Provincial Fishery Bureau, especially, two vice-governor of the Hubei Provincial Government presiding over agriculture and export respectively held two site meetings on popularization and application of crop rotation technology of Procambarus Clarkii and mid-season rice throughout the province, which promoted research works on crop rotation of Procambarus Clarkii and mid-season rice to the climax. In the same year, Hubei Provincial Fishery Bureau popularized crop rotation technology of Procambarus Clarkii and mid-season rice as primary productive technology throughout the province, and Hubei Provincial Fisheries Scientific Research Institute and Hubei Provincial Fisheries Technology Extension Center were engaged in popularizing the technology across the whole province and extending it to the whole country. From 2006 to 2007, the rotation area reached over 38,000 hectares, and from 2007 to 2008, the area exceeded 100,000 hectares, with average yield of 1,950kg/ha and total yield of over 195,000 tons.

In addition, many other provinces also carried out crop rotation of Procambarus Clarkii and mid-season rice, including Anhui, Zhejiang, Henan, Jiangsu, Shanghai, Jiangxi, Hunan, Chongqing and Sichuan. Of these provinces, the area of aquaculture field was much bigger in Anhui Province, Jiangsu Province and Zhejiang Province. From 2007 to 2008, Anhui Province solely developed 40,000 ha of aquaculture field for crop rotation of Procambarus Clarkii and mid-season rice. It was estimated that the crop rotation area of Procambarus Clarkii and mid-season rice reached above 160,000 ha nationwide, and the yield surpassed 240,000 tons from 2007 to 2008.

5 Prospects of the Technology in China

Taking a wide view of production and consumption of Procambarus Clarkii, and its crop rotation with mid-season rice, we consider that:

1) The market demand is large, thus crop rotation of Procambarus Clarkii and mid-season rice will continuously develop fast. There are 17 bigger-scale processing plants of Procambarus Clarkii in Hubei Province. 15 processing plants can export processed products of Procambarus Clarkii directly. From January to September, 2005, Hubei Province exported 7,580.158 tons of processed products of Procambarus Clarkii in total. However, the figure was still less than 1/5 of annual processing capacity of these plants and 1/3 of the amount in export orders. If these products are all considered as peeled shrimps, 6.0-6.5 tons of Procambarus Clarkii can produce 1 ton of peeled shrimps, 240,000 tons of Procambarus Clarkii in crop rotation with mid-season rice was produced from 2007 to 2008, and thus the amount of peeled shrimps produced from 2007 to 2008 barely met the production capacity of 17 processing plants in Hubei Province in 2005, which was slightly more than that of export orders received in 2005. Furthermore, Procambarus Clarkii possesses not only vast international market but also large domestic market of China. Therefore, in the current and the future period, the problem of supply over demand of Procambarus Clarkii will never exist. Under this circumstance, crop rotation technology of Procambarus Clarkii and mid-season rice will develop fast. The relevant departments should actively guide the farmers in carrying out the commitment, and the technology extension department should initially popularize the application of the technology.

2) The total production increases each year, and sales price maintains steady and decreases gradually. In 1970s and 1980s, rare attention was paid to Procambarus Clarkii in Wuhan; in early 1990s, its market price was 0.06$/kg (1$=8.3￥); in late 1990s, it was 0.24$/kg; in 2004, it was 1.20-1.69$/kg; in 2007 spring and summer, it was 1.87-2.4/kg(1$=7.5 ￥); and in 2008 spring and summer, it rose to 2.35-2.94$/kg(1$=6.8￥). Crop rotation area of Procambarus Clarkii and mid-season rice continuously increases, along with rise in total production yield. As a new aquaculture mode in China, crop rotation of Procambarus Clarkii and mid-season rice necessarily follows the development law of logistic curve (Gong, 1991). In recent years, popularization area and yield developed fast; however, after several years, they will be bound to enter a steady development period. Some other provinces also developed crop rotation of Procambarus Clarkii and mid-season rice in terms of their respective conditions. After the yield of Procambarus Clarkii reaches a certain amount, sales prices will decline somewhat. The turning point may be between 120 tons and 150 tons, annual yield in China. If only crop rotation area of Procambarus Clarkii and mid-season rice is considered, the aquaculture area of Procambarus Clarkii is 600-800 hectares. Certainly, the turning point is also related with production amount of other production methods of Procambarus Clarkii.

3) The production cost is raised each year, and the comparative benefit is reduced gradually. Due to demand over supply of Procambarus Clarkii in recent years, the purchasing price was on the high side, which promoted large-scale popularization and application of crop rotation of Procambarus Clarkii and mid-season rice. Judging from the production and sales situation in 2008, although the aquaculture area and total yield of Procambarus Clarkii achieved great improvement, its supply still exceeded the demand. However, the relation between supply and demand became noticeably less intense against the former years. Expect CPI growth factor and exchange difference between RM B and dollar, the purchasing price and sales price of Procambarus Clarkii maintained steady and declined somewhat. Moreover, noticeable difference of sales

price exists among different kinds of shrimps. With further enlargement of crop rotation area of Procambarus Clarkii and mid-season rice and rise of production cost, as well as increase in total yield, the market sales price will decrease under the effect of market level, and the comparative benefit of crop rotation of Procambarus Clarkii and mid-season rice will decline and tend towards social average profit. At this time, the approach to increase the profit is: first, to develop industrialization scale and reduce production cost; second, to improve commodity specification of commercial sized shrimps to increase unit sales price of commercial sized shrimps.

4) To improve the quality of shrimp species and guarantee supply of fingerlings. At present, crop rotation level of Procambarus Clarkii and mid-season rice is lower, the problem of fingerlings can be solved by placing parent shrimps and natural reproduction, and the source of shrimp species does not form bottleneck yet. However, there are still some problems: first, more links of purchasing, transporting and placing of parent shrimps readily cause their death and can not ensure the quality of parent shrimps; second, the shrimps in the paddy field can not be caught thoroughly, thus leading to inbreeding (it can also not be ensured that the newly-placed parent shrimps are not descendents through inbreeding); third, degeneration of shrimp species exists among Procambarus Clarkiis in China. In view of the above problems, it is necessary to apply relevant technology and select excellent Procambarus Clarkiis for genetic breeding, in the hope of obtaining Procambarus Clarkiis with better features. In addition, although artificial breeding of Procambarus Clarkiis has achieved success (Shu et al., 2006), its scale is still small. Thus, it is necessary to further improve the technology and establish breeding base of Procambarus Clarkiis with a certain scale, so as to provide fingerlings of Procambarus Clarkiis in large numbers and batches. The comparative tests show that the yield of the paddy field where young shrimps are put is 2,733-3,094.5kg/ha, and that of the paddy field where parent shrimps are put is 1,815-1,1845kg/ha, the former higher than the latter. If large quantities of fingerlings of Procambarus Clarkiis can be produced, the production mode of putting young shrimps into the paddy field will be one of the development directions for crop rotation of Procambarus Clarkiis and mid-season rice in the future.

5) To develop high-quality baits and research bait casting technique.In the early period of crop rotation of Procambarus Clarkiis and mid-season rice, artificial feedstuffs are not fed to the shrimps. Rice stubble, nutrients released by rice stubble submerged, or planktons cultivated by fertilized water are mainly used as the food of Procambarus Clarkiis. To help the shrimps to spend a good winter, some stable manure or plant stems or leaves are always supplied in winter. With increase in unit yield of crop rotation of Procambarus Clarkii and mid-season rice, the methods of applying fertilizer and casting baits will be developed accordingly. However, the fed feedstuffs are mainly agricultural byproducts currently. Due to various factors including aquaculture cost, the feedstuffs especially designed for Procambarus Clarkii in the market are not widely popularized and applied. As a result, it is necessary to conduct researches on nutritional physiology (Wen et al., 2003a) of Procambarus Clarkii, develop special feedstuffs, and carry out researches and application of bait-casting technology (Zhou and Zhao, 2007).

6) To pay great attention to diseases and improve aquaculture environment. Procambarus Clarkii possesses stronger antiviral ability. In the early time of crop rotation of Procambarus Clarkii and mid-season rice, Procambarus Clarkii never

suffered from major diseases. However, with the development of crop rotation of Procambarus Clarkii and mid-season rice, some fishermen greatly increase placing density, feedstuffs and fertilizer, which deteriorate the aquaculture environment and bring about some shrimp diseases. Recently, Procambarus Clarkii is found to suffer from virus diseases. Therefore, great attention should be given to disease problem of Procambarus Clarkii. Researches should be conducted on both environmental ecology of Procambarus Clarkii (Wen et al., 2003b; Luo et al., 2005; Luo et al., 2006) and disease control technology.

7) To strengthen scientific research and enhance aquaculture mode. Presently, crop rotation technology of Procambarus Clarkii and mid-season rice is still at primary stage. Therefore, it is necessary to strengthen research of application technology and basic research of application technology, to further improve the technology. The key is: first, genetic breeding research, to select and optimize Procambarus Clarkii with better aquaculture characteristic; second, reproduction physiology research, to provide technical support for industrialized artificial reproduction; third, nutritional physiology research, to research and fabricate feedstuffs for different stages; fourth, ecology research, to deeply understand living habit and behavior state of Procambarus Clarkii and provide basis for optimizing aquaculture technology; fifth, aquaculture technology research, to improve aquaculture yield, reduce production cost and increase economic income. sixth, extension of aquaculture mode of Procambarus Clarkii. Except crop rotation of Procambarus Clarkii and mid-season rice, researches should also be carried out on mixed cropping and rotation technology of cereal crop including double cropping rice, aquatic economic plant and Procambarus Clarkii, Procambarus Clarkii and other aquaculture targets including loach, and so forth.

Acknowledgment. This research is supported by the Hubei Provincial People's Government. With the concern and guidance of Tao Qiming, the deputy director of Department of Agriculture of Hubei Province, and Xu Hantao, the director of Bureau of Aquatic Products of Hubei Province. During the research process, Municipal Committee of Qianjiang city, municipal government, and Bureau of Aquatic Products of Qianjing city have given their instruction and help.

References

1. Brunson, M.W., Griffin, J.L.: Comparison of Rice-Crayfish and Grain Sorghum-Crayfish Double Cropping Systems. Aquaculture 72, 265–272 (1988)
2. Dai, A.Y.: Introduction of One Kind of Fishery Resource-Palinurus. Zoological Magazine 3, 48–50 (1983)
3. Gong, L.J.: “S” Law Analysis of Fishery Yiled in Hubei Province. Hubei Fishery 1, 46–50 (1991)
4. Jover, M., Femandez-Carmona, J., Del Rio, M.C., Soler, M.: Effect of feeding cooked-extruded diets, containing different levels of protein, lipid and carbohydrate on growth of red swamp crayfish (Procambarus clarkii). Aquaculture 78, 127–137 (1999)
5. Luo, J.B., Cao, Z.H., Wen, X.B., Cai, T.R.: Acute Toxicity Effect of Nitrite Nitrogen on Young Procambarus Clarki. Journal of Yangtze University (Natural Science Edition) 2, 64–66 (2005)

6. Luo, J.B., Cao, Z.H., Cai, T.R., Wen, X.B.: Research on Acute Toxicity of Ammonia Nitrogen in Young Procambarus Clarki. Journal of Yangtze University (Natural Science Edition) 3, 183–185 (2006)
7. Shu, X.Y., Ye, Y.Z.: Status and Prospect of Freshwater Crayfish Aquaculture. Fisheries Science & Technology Information 2, 45–46 (1989)
8. Shu, X.Y., Gong, L.J., Tao, Z.H., Pan, G., Du, J.Y., Li, J.Z., Pu, J.Y., Zhang, C.Y., Shi, Y.Y., Wei, D.Y.: Synchronous Spawning Test on Artificial Induced Procambarus Clarkii. Freshwater Fishery 36, 45–47 (2006)
9. Shu, X.Y.: New Progress in Crayfish Aquaculture. Freshwater Biology Science & Technology Information 4, 85 (1985)
10. Wang, W.M.: The Exploitation and Utilization of Red Swamp Crayfish in China. Acta Hydrobiologica Sinica 23, 375–381 (1999)
11. Wen, X.B., Ku, Y.M., Luo, J.B.: Research on Oxygen Consumption Rate and Suffocation Point of Procambarus Clarkii. Journal of Dalian Fisheries College 18, 170–174 (2003a)
12. Wen, X.B., Ku, Y.M., Luo, J.B.: Research on Physiological Ecology of Procambarus Clarkii-I Standard Metabolism. Journal of Hubei Agricultural College 23, 41–44 (2003b)
13. Zhou, W.Z., Zhao, F.G.: Research on Feeding Rhythm of Procambarus Clarkii. Fishery Science 26, 271–274 (2007)

Analysis of Codon Usage Bias in Interferon Alpha Gene of the Giant Panda (Ailuropoda Melanoleuca)

Yue Yi[1], Chengdong Wang[1,2], Zhiwen Xu[1], Desheng Li[1,2], Ling Zhu[1], Fengqin Li[1], Xinqiao Qi[1], and Wanzhu Guo[1]

[1] Animal Biotechnology Center
College of Veterinary Medicine of Sichuan Agricultural University, Ya'an, Sichuan, 625014, China
[2] China Conservation and Research Center for the Grint Panda (CCRCGP), Wolong Nature Reserve, Sichuan, 623006, China

Abstract. The analysis on codon usage bias of IFN-a gene of giant panda (Ailuropoda melanoleuca) may provide a basis for understanding the evolution relationship of giant panda and for selecting appropriate host expression systems to improve the expression of target genes. In this paper, the codon usage bias in the mature IFN-a sequence of giant panda and 15 reference species have been analyzed. The results showed that the synonymous codons with G and C at the third codon position were widely used and the ENC-GC3S plot revealed that the genetic heterogeneity in IFN-a gene was main constrained by mutational bias. Contrastive analysis revealed that there were 40 codons showing distinct usage differences between GpIFN-a and Escherichia coli, 38 codons between GpIFN-a and yeast. and only 30 between GpIFN-a and Homo sapiens. Therefore the Homo expression system may be more suitable for the expression of GpIFN-a genes.

Keywords: Ailuropoda melanoleuca, interferon alpha, codon usage bias, analysis.

1 Introduction

The genetic code uses 61 nucleotide triplets (codons) to encode 20 amino acids and three to terminate translation[1]. So the genetic code is necessarily redundant which are more than amino acids. Each amino acid is encoded by between one (Met and Trp) and six (Arg, Leu and Ser) synonymous codons[2]. Different codons that encode the same amino acid are known as synonymous codons. Changes in the DNA sequence of a protein between two synonymous codons are often assumed to have no effect and are thus called synonymous changes or even silent changes[2]. In a wide variety of organisms such as bacteria, fungi, and insects (Sharp et al. 1992), codons within synonymous groups are used with different frequencies[3-6] the phenomenon called codon usage bias.

There is continuing speculation regarding the reasons what have made these differences in codon preferences[7]. the most commonly accepted hypothesis for the unequal usage of synonymous codons stated that it was the result of mutational biases

E. Zhu and S. Sambath (Eds.): Information Tech. and Agricultural Eng., AISC 134, pp. 293–305.
springerlink.com © Springer-Verlag Berlin Heidelberg 2012

and natural selection acting at the level of translation. However, several other causes have also been reported, such as GC compositions, gene length, gene expression level, gene translation initiation signal, protein amino acid composition, protein structure, mutation frequency and patterns, and tRNA abundance [8-12]. In some other researches, it was also found that codon usage was related to gene function[13, 14] and cellular location of gene products [15-17]. Whatever the reasons for codon bias, it has become increasingly clear that codon biases can have profound impacts on the expression of heterologous proteins.

In this study, characterization of codon usage bias on interferon alpha gene without signal peptide of the giant panda had been evaluated. Giant panda is a much loved animal all over the world and is considered a symbol of China. However, it is also one of the world's most endangered species. In addition, giant pandas are considered to be particularly vulnerable to infectious disease and parasites[18]. Therefore, analysis and study on cytokine genes of the giant panda are important to facilitate the use of these cytokines in the immunotherapy of infectious diseases of the giant panda[19].

The interferons are a group of natural antiviral substances first discovered in 1957[20]. Many studies have performed on the function of IFN-a. It influences many biological processes including broad spectrum antiviral effects, inhibition of tumor cell proliferation and enhancement of immune functions. And it is considered to be a potential agents for therapy of neoplastic diseases and cancers[21].

So far, research on the giant panda genome is still rare. only a few genes with immunity function have been cloned. Recently, the interferon alpha gene of giant panda had been cloned in our laboratory called GpIFN-a. Here, we first time analyzed the codon usage data of GpIFN-a and those of other 15 species' IFN-a. Moreover, the codon usage bias in the GpIFN-a gene was also compared with Escherichia coli, yeast, and Homo sapiens. In this research, codon usage data of GpIFN-a and the comparison results might give some clues to the features of GpIFN-a gene and some evolutionary information of IFN-a gene. And also provide insights into the expression and possible function of GpIFN-a.

2 Materials and Methods

2.1 Sequence Data

The mature sequence of GpIFN-a which cloned in our laboratory had been submitted to GenBank and the accession number is HQ378189. The overall IFN-α reference sequences were download from NCBI (http://www.ncb i.nlm.nih.gov/). The signal peptide of every reference sequence had been removed to kept the statistical significance of codon usage bias. The informations such as GenBank accession No., Natural host and Length of the IFN-α gene of overall 16 reference sequence are shown in Table 1.

2.2 Analysis on Codon Usage in GpIFN-a Genes and 15 Reference Sequences

Codon bias was calculated according to methods described elsewhere. Relative synonymous codon usage (RSCU) is the observed frequency of a codon divided by the frequency expected if all synonyms for that amino acid were used equally. It is

Table 1. The Information about IFN-A Gene Used in Our Research

Species	GenBank Accession No.	Animals' IFN-α	Natural animal	Length (bp)
Mammal	AY323972	Bubalus bubalis IFN-α	Bubalus bubalis	498
	DQ520882	Canis familiaris IFN-α	Canis familiaris	495
	FJ959074	Capra hircus IFN-α	Capra hircus	501
	NM_001099441	Equus caballus IFN-α	Equus caballus	486
	NM_001009851	Felis catus IFN-α	Felis catus	516
	NM_001194384	Macaca mulatta IFN-α	Macaca mulatta	501
	EU863618	Mustela putorius furo IFN-α	Mustela putorius furo	495
	HM636502	Pteropus vampyrus IFN-α	Pteropus vampyrus	540
	AY331298	Sus scrofa IFN-α	Sus scrofa	501
	EF990625	Vulpes vulpes IFN-α	Vulpes vulpes	540
	BC074928	Homo sapiens IFN-α	Homo sapiens	501
	HQ378189	grint panda IFN-α	grint panda	495
Birds	EU029159	Anser anser rubrirostris IFN-α	Anser anser rubrirostris	492
	X84764	duck IFN-α	duck	492
	AB021154	Gallus gallus IFN-α	Gallus gallus	492
	EU022750	Shitou Goose IFN-α	Shitou Goose	492

independent of amino acid composition and is thus useful for comparing different sets of genes[22]. The effective number of codons (ENC) is a measure analogous to the effective number of alleles. Based on simulation studies, ENC appears to be low sensitive to gene length[23]. The ENC value of the IFN-a gene of each reference was computed with the EMBOSS CHIPS online service program. The degree of synonymous-codon usage bias was also measured by the codon adaptation index (CAI) which estimates the extent of bias toward codons that are known to be favored in highly expressed genes. which was calculated with the EMBOSS CAI program [24]. The peculiarity in codon usage frequency ,the G+C content of the gene sequences and the G+C content at the synonymous third position of codons (GC3S) were also calculated with the EMBOSS CUSP program[25].

2.3 Phylogenetic Analysis of the GpIFN-a Gene

The mature nucleotide sequences of the GpIFN-a gene and 15 reference IFN-a were translated into amino acid sequences by using DNASTAR software.Then, multiple sequence alignment and phylogenetic analysis by the bootstrap option were performed by using ClustalW and TREEVIEW software.

2.4 Comparison of Codon Preferences of GpIFN-a Gene with Those of E. coli, Yeast, Adenovirus, and Human

A comparison analysis was performed between the GpIFN-a, Escherichia coli, yeast, and Homo sapiens. The database of the codon usage in E. coli, yeast, and Homo sapiens was available at (http://www.kazusa.or. jp/ codon/).

3 Results

3.1 Characterization of Synonymous Codon Usage in the IFN-a Gene of Giant Panda

While the relative synonymous codon usage values (RSCU) and the related measures indicate the overall GpIFN-a codon bias, it is also important to look more closely at the patterns of codon bias. Table 2 shows the details of the codon usage patterns and codon usage data of giant panda IFN-α gene (excluding Met, Trp, and the termination codons). A high level of diversity in codon usage bias existed for coding the Ala, Leu and Ser amino acids(emphasized with underline). From the table 2 we can see that the frequencies of codons usage in coding the same amino acids are different. There are 26 codons, such as CTG(Leu), AGG (Arg), ATC(Ile), CCC(Pro), TGG(Trp), TAC(Tyr) and so on, were more frequently used. Among the preferred codons nineteen synonymous codons strong bias toward C-ended and nine toward G-ended at the third codon position. It is evident that codon usage bias in the mature polypeptide is strong bias towards the synonymous codons with G and C in the wobble.

Table 2. Codon Usage Data of Grint Panda Interferon Alpha Gene Analyzed by Cusps Program

Amino acid	codon[a]	Fract[b]	Frequency 1000[c]	Number[d]	RSCU[e]
A(Ala)	GCA	0.077	6.061	1	0.30
A	GCC[f]	0.462	36.364	6	**1.84**
A	GCG	0.154	12.121	2	0.61
A	GCT	0.308	24.242	4	**1.23**
C(Cys)	TGC	0.500	18.182	3	1.00
C	TGT	0.500	18.182	3	1.00
D(Asp)	GAC[f]	0.833	30.303	5	**1.67**
D	GAT	0.167	6.061	1	0.33
E(Glu)	GAA	0.333	24.242	4	0.67
E	GAG[f]	0.667	48.485	8	**1.33**
F(Phe)	TTC[f]	0.625	30.303	5	**1.25**
F	TTT	0.375	18.182	3	0.75
G(Gly)	GGA	0.571	24.242	4	**1.14**

Table 2. (*continued*)

G	GGC[f]	0.286	12.121	2	**1.14**
G	GGG	0.143	6.061	1	0.57
G	GGT	0.000	0.000	0	0.00
H(His)	CAC	0.250	6.061	1	0.50
H	CAT	0.750	18.182	3	**1.50**
I(Ile)	ATA	0.000	0.000	0	0.00
I	ATC[f]	1.000	30.303	5	**2.00**
I	ATT	0.000	0.000	0	0.00
K(Lys)	AAA	0.143	6.061	1	0.29
K	AAG[f]	0.857	36.364	6	**1.71**
L(Leu)	CTA	0.111	12.121	2	0.67
L	CTC[f]	0.222	24.242	4	**1.33**
L	CTG[f]	0.389	42.424	7	**2.33**
L	CTT	0.056	6.061	1	0.33
L	TTA	0.000	0.000	0	0.00
L	ATG[f]	0.222	24.242	4	**1.33**
N(Asn)	AAC[f]	0.750	18.182	3	**1.50**
N	AAT	0.250	6.061	1	0.50
P(Pro)	CCC[f]	0.667	24.242	4	**2.67**
P	CCG	0.000	0.000	0	0.00
P	CCA	0.000	0.000	0	0.00
P	CCT	0.333	12.121	2	**1.33**
Q(Gln)	CAA	0.500	36.364	6	1.00
Q	CAG	0.500	36.364	6	1.00
R(Arg)	AGA	0.444	24.242	4	**2.67**
R	AGG[f]	0.556	30.303	5	**3.33**
R	CGA	0.000	0.000	0	0.00
R	CGC	0.000	0.000	0	0.00
R	CGG	0.000	0.000	0	0.00
R	CGT	0.000	0.000	0	0.00
S(Ser)	AGC[f]	0.294	30.303	5	**1.76**
S	AGT	0.000	0.000	0	0.00
S	TCA	0.176	18.182	3	**1.06**

Table 2. (*continued*)

S	TCG	0.118	12.121	2	0.71
S	TCT	0.235	24.242	4	1.41
T(Thr)	ACA	0.250	12.121	2	1.00
T	ACC	0.125	6.061	1	0.50
T	ACGf	0.375	18.182	3	1.50
T	ACT	0.250	12.121	2	1.00
V(Val)	GTA	0.000	0.000	0	0.00
V	GTCf	0.455	30.303	5	1.82
V	GTGf	0.455	30.303	5	1.82
V	GTT	0.091	6.061	1	0.36
Y(Tyr)	TACf	1.000	24.242	4	2.00
Y	TAT	0.000	0.000	0	0.00

[a]The preferentially used codons for each amino acid are displayed in bold; [b]The ''Fract'' column shows the proportion of usage of a given codon in its redundant set (i.e., the set of codons that code for the same amino acid); [c]The ''Frequency'' column lists the number of codons present per 1000 basesin the input sequence(s); [d]The ''Number'' column lists the number of codons; [e]The ''RSCU'' column shows the proportion of relative synonymous codon usage; [f]Shows a strong bias towards the codons with A and T at the third codon position.

3.2 Codon Usage Analysis of the IFN-a Gene of Grint Panda and Reference Species

The value of CAI, ENC and GC and GC3S content analysis of grint panda IFN-α and other kinds of IFN-α genes were obtained by EMBOSS. The results are shown in Table 3. the ENC values of different IFN-α genes varied from 27.971 to 53.276, with a mean value of 41.50 and standard deviation (S.D.) of 7.86. The GC3S contents of each IFN-α gene ranged from 36.78 to 92.07% with a mean of 58.66% and S.D. of 0.097. The CAI values of different IFN-α genes varied from 0.759 to 0.85 with a mean value of 0.808 and standard deviation (S.D.) of 0.022.

It has been reported that a plot of ENC against GC_{3S} can be effectively used to explore the heterogeneity of codon usage among genes [23]. Figure 1 shows the distribution plot of the ENC and GC3S values for the IFN-α gene in the reference species. The solid line represented the curve if codon usage was only determined by GC content on the third codon position[26]. It is evident that there is only a small number of genes lying on the expect plot curve, most of the plot lay near to the solid line of this distribution (shown in Figure. 1).

Table 3. Summary Analysis of IFN-a Gene in Different Species

Species	Animals' IFN-α	CAI	ENC	Coding GC(%)	GC3S (%)
	Equus caballus IFN-α	0.809	45.690	60.20%	81.21%
	Macaca mulatta IFN-α	0.782	53.276	48.30%	59.88%
	Mustela putorius furo IFN-α	0.791	49.523	56.16%	71.52%
	Pteropus vampyrus IFN-α	0.797	47.855	54.49%	69.46%
Mammal	Vulpes vulpes IFN-α	0.813	41.025	60.61%	81.82%
	Homo sapiens IFN-α	0.791	50.840	48.50%	61.08%
	Capra hircus IFN-α	0.797	44.528	59.48%	74.85%
	Bubalus bubalis IFN-α	0.824	44.146	59.44%	77.11%
	Felis catus IFN-α	0.803	42.099	56.01%	72.67%
	Canis familiaris IFN-α	0.820	40.714	60.20%	81.21%
	grint panda IFN-α	0.759	44.692	53.94%	67.88%
	Sus scrofa IFN-α	0.850	38.773	59.08%	76.65%
Birds	Anser anser rubrirostris IFN-α	0.831	29.000	68.09%	92.07%
	Duck IFN-α	0.815	27.971	66.87%	90.24%
	Gallus gallus IFN-α	0.807	35.008	59.35%	79.88%
	Shitou Goose IFN-α	0.831	28.807	67.89%	92.07%

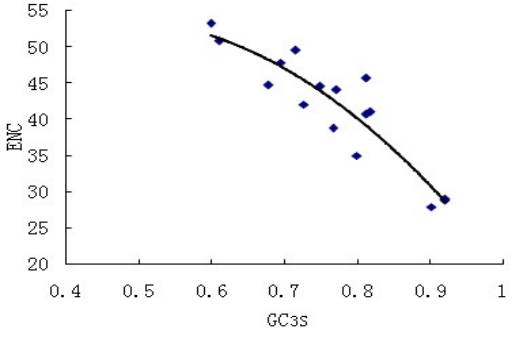

Fig. 1. The relationship between the effective number of codons (ENC) and the GC content of the third codon position (GC3) of the IFN-α gene of grint panda and 15 reference IFN-α genes

3.3 Phylogenetic Analysis on the IFN-a Gene of Grint Panda and Reference Species

A phylogenetic tree based on the amino acid sequences of the IFN-a gene of the 16 reference species was shown in Fig. 2. It shows that there are mainly two branches for the IFN-a family. GpIFN-a has been clustered in the mammal branch. And we can also see that the grint panda and mustela putorius furo clustered in a monophyletic clade, and have a closer relationship with canis famililiaris and vulpes vulpes. Multiple sequence alignment of the amino acid sequences testify to the conclusion that grint panda is evolutionarily closer to the animal mentioned above. The figure also shows that the IFN-a gene of grint panda is alienated to those whose natural host is avian on the evolution relationship.

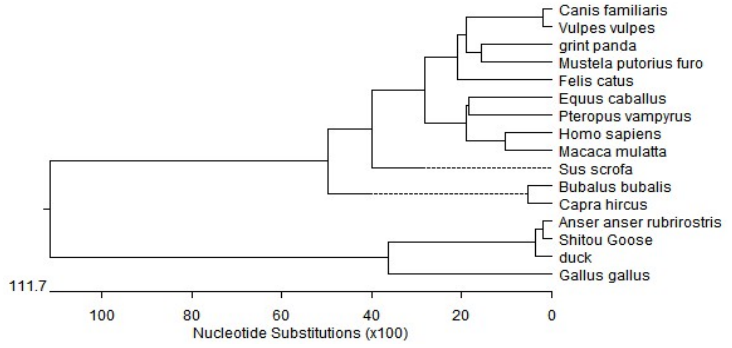

Fig. 2. Phylogenetic tree based on the amino acid sequences of the IFN-a gene of the 16 reference species (Table 1), and constructed by CLUSTAL-W and TREEVIEW software

3.4 Comparison of Codon Usage between GpIFN-a and E. coli, Yeast and H. Sapiens

The codon usage bias in genes remains at a certain level across species. We compared GpIFN-a gene with those of E.coli, yeast and H. sapiens to see which will be the suitable host for the optimal expression of GpIFN-a gene. Contrastive analysis showed that there are 40 codons showing distinct usage differences between GpIFN-a and E.coli, 38 codons between GpIFN-a and yeast, but only 30 between GpIFN-a and H. sapiens, suggesting that codon usage of GpIFN-a genes more closely resembles that of H. sapiens genes.

Table 4. Comparison of codon preferences between the GpIFN-αlpha gene and E. coli, yeast and human

		1/1000				DuIFN -α/		
Amino acid	**Codon**	***IFN-α***	***E. coli***	***Yeast***	***Human***	***E. coli***	***Yeast***	***Human***
A(Ala)	GCA	6.061	20.6	16.1	16.1	0.29	0.38	0.38
A	GCC	36.364	25.5	12.5	28.4	1.43	2.91	1.28
A	GCG	12.121	31.7	6.1	7.5	0.38	1.99	1.62
A	GCT	24.242	15.6	21.1	18.6	1.55	1.15	1.30
C(Cys)	TGC	18.182	6.9	4.7	12.2	2.64	3.87	1.49
C	TGT	18.182	5.5	8	10	3.31	2.27	1.82
D(Asp)	GAC	30.303	18.6	20.2	25.6	1.63	1.50	1.18
D	GAT	6.061	32.1	37.8	21.9	0.19	0.16	0.28
E(Glu)	GAA	24.242	38.2	48.5	29	0.63	0.50	0.84
E	GAG	48.485	17.7	19.1	39.9	2.74	2.54	1.22
F(Phe)	TTC	30.303	16.9	18.2	20.6	1.79	1.67	1.47
F	TTT	18.182	23.2	26.1	17.1	0.78	0.70	1.06
G(Gly)	GGA	24.242	9	10.9	16.4	2.69	2.22	1.48
G	GGC	12.121	27.9	9.7	22.5	0.43	1.25	0.54
G	GGG	6.061	11.3	6	16.3	0.54	1.01	0.37

Table 4. (*continued*)

G	GGT	0.000	24.4	24	10.8	0.00	0.00	0.00
H(His)	CAC	6.061	9.8	7.7	15	0.62	0.79	0.40
H	CAT	18.182	13.6	13.7	10.5	1.34	1.33	1.73
I(Ile)	ATA	0.000	5.4	17.8	7.7	0.00	0.00	0.00
I	ATC	30.303	24.2	17	21.6	1.25	1.78	1.40
I	ATT	0.000	29.8	30.4	16.1	0.00	0.00	0.00
K(Lys)	AAA	6.061	33.2	42.2	24.1	0.18	0.14	0.25
K	AAG	36.364	10.7	30.7	32.2	3.40	1.18	1.13
L(Leu)	CTA	12.121	4	13.3	7.8	3.03	0.91	1.55
L	CTC	24.242	11	5.4	19.8	2.20	4.49	1.22
L	CTG	42.424	50.9	10.4	39.8	0.83	4.08	1.07
L	CTT	6.061	11.7	12.1	13	0.52	0.50	0.47
L	TTA	0.000	13.9	26.7	7.5	0.00	0.00	0.00
L	TTG	24.242	14	27	12.6	1.73	0.90	1.92
M(Met)	ATG	24.242	27	20.9	22.2	0.90	1.16	1.09
N(Asn)	AAC	18.182	21.4	24.9	19.5	0.85	0.73	0.93
N	AAT	6.061	18.6	36.3	16.7	0.33	0.17	0.36
P(Pro)	CCA	0.000	8.5	18.2	16.7	0.00	0.00	0.00
P	CCC	24.242	5.8	6.8	20.1	4.18	3.57	1.21
P	CCG	0.000	21.8	5.3	6.9	0.00	0.00	0.00
P	CCT	12.121	7.3	13.6	17.3	1.66	0.89	0.70
Q(Gln)	CAA	36.364	15	27.5	12	2.42	1.32	3.03
Q	CAG	36.364	29.5	12.1	34.1	1.23	3.01	1.07
R(Arg)	AGA	24.242	2.9	21.3	11.5	8.36	1.14	2.11
R	AGG	30.303	1.9	9.2	11.4	15.95	3.29	2.66
R	CGA	0.000	3.9	3	6.3	0.00	0.00	0.00
R	CGC	0.000	21	2.6	10.7	0.00	0.00	0.00
R	CGG	0.000	6.3	1.7	11.6	0.00	0.00	0.00
R	CGT	0.000	20.3	6.5	4.6	0.00	0.00	0.00
S(Ser)	AGC	30.303	16	9.7	19.3	1.89	3.12	1.57
S	AGT	0.000	9.5	14.2	11.9	0.00	0.00	0.00
S	TCA	18.182	7.8	18.8	12	2.33	0.97	1.52
S	TCC	18.182	8.9	14.2	11.9	2.04	1.28	1.53
S	TCG	12.121	8.7	8.5	4.4	1.39	1.43	2.75
S	TCT	24.242	8.7	23.5	14.7	2.79	1.03	1.65
T(Thr)	ACA	12.121	8.2	17.8	15.1	1.48	0.68	0.80
T	ACC	6.061	22.8	12.6	19.4	0.27	0.48	0.31
T	ACG	18.182	14.8	7.9	6.1	1.23	2.30	2.98
T	ACT	12.121	9.1	20.3	13	1.33	0.60	0.93
V(Val)	GTA	0.000	11.1	11.8	7.2	0.00	0.00	0.00
V	GTC	30.303	15.1	11.6	14.6	2.01	2.61	2.08

Table 4. (*continued*)

V	GTG	30.303	25.5	10.6	28.4	1.19	2.86	1.07
V	GTT	6.061	18.5	22	11	0.33	0.28	0.55
W(Trp)	TGG	18.182	15.2	10.3	12.7	1.20	1.77	1.43
Y(Tyr)	TAC	24.242	12.1	14.6	15.5	2.00	1.66	1.56
Y	TAT	0.000	16.5	18.9	12.1	0.00	0.00	0.00
*	TAA	0.000	2	1	0.7	0.00	0.00	0.00
*	TAG	0.000	0.3	0.5	0.6	0.00	0.00	0.00
*	TGA	6.061	1.1	0.7	1.5	5.51	8.66	4.04

4 Discussion

Codon bias refers to the nonrandom usage of synonymous codons for encoding amino acids in organisms. As it is related to the carrier molecular of genetic information(DNA) and functional molecular (protein) of life, this phenomenon implicates important biological sense[27]. Extensive studies had shown that synonymous codon usage in various organisms. Although the codon usage pattern among different species is a complex phenomenon, it plays an important role in illuminating the underlying mechanisms of codon usage patterns in order to understand the evolution of the species.

Signal peptides consist of short stretches of amino acids which, after protein delivery to the correct subcellular compartment, are frequently removed by specialized signal peptidases[28]. Only after removal of the signal peptide sequence, the precursor protein may be allowed to entry into the secretory pathway and become a normal function of the mature protein [29]. We intend to express the GpIFN-a gene in prokaryotic expression system and test its antiviral effects in future. In order to keep the higher biological activity, we cloned the gene fragment coding for mature protein of GpIFN-a. In this study, we analyzed the codon usage data of GpIFN-a without signal peptide and those of other 15 species of IFN-a, Additionally, we investigated the correlation of codon usage between GpIFN-a gene with Escherichia coli, yeast, and Homo sapiens to find the suitable expression system.

RSCU, CAI, ENC values, GC and GC3s content of the IFN-α gene were predicted by using the EMBOSS CUSP program and CHIPS program. RSCU with direct assessment codon usage bias of different codons in each gene sample. When its value greater than 1.0 indicated that the corresponding codon was used more frequently than expected. Table 2 showed that there were 26 preferred codons, most of them were strong bias towards the synonymous codons with G and C in the wobble, coincides with high G+C content at the third codon position (the mean value was 76.85%). CAI was used as a measure to predict the level of gene expression.The value was between 0 and 1[30], a higher value means a stronger codon usage bias and a higher expression level. the CAI values for IFN-α genes were slight variation among different species and with a mean value of 0.808, so we concluded IFN-α gene was likely to be moderately expressed in giant panda genome. The ENC is a measure analogous to the effective number of alleles. It ranges from 20, where only one codon is used for each amino acid to 61 if all codons are used equally[31]. In general, if the ENC value of a gene is 35 or less, that gene is thought to possess strong codon bias[32]. Analyzing the

ENC values of all the IFN-α genes, the results showed the ENC values of mammal's IFN-α genes(mean value of 45.26) were higher than birds' IFN-α gene(mean value of 30.20), So the codon usage bias was slightly low in mammal but strong in bird.

The ENC-plot (ENC plotted against GC) is used as part of a general strategy to investigate patterns of synonymous codon usage. In fig.1, the solid line represents the curve if codon usage is only determined by GC content on the third codon position[33], There is only a small number of genes lying on the expect plot curve, most of the plot lay near to the solid line. In principle, proprietary proportion of points lay near to the solid line on this distribution. It suggested that mutational bias was the main factor determining the codon usage variation among these IFN-α genes.

Comparative analysis of IFN-α genes in giant panda and the reference species indicated that synonymous codon usage in mammal's IFN-α genes are phylogenetically conserved. Data in table 3 show that the IFN-α genes of mammal have similar CAI, ENC value and GC content. But a slight difference with birds'. Therefore we can conclude species with near homology relationship on evolution share the near codon usage frequency and preference index or the similar index. The phylogenetic tree analysis based on the IFN-α genes testify to the conclusion. So species has a centain influence to the preference of codon usage.

The expression of functional proteins in heterologous hosts is a cornerstone of modern biotechnology. In order to find the suitable host for the optimal expression of GpIFN-α genes. we compared it with those of E. coli, yeast, and H. sapiens. The ratio higher than 2 or lower than 0.050 indicated the codon usage preference differed (shown in table 4.). The rusults revealed that Homo sapiens may more efficiently to express the GpIFN-α genes. If we want to express this gene in prokaryotic expression system, maybe some strategies should be taken in the target gene so that they more closely reflect the codon usage of the host.

In summary, codon usage patterns and the phylogenetic results we proposed here were useful to understand the characteres of GpIFN-α gene and a better understanding of both the evolutionary history of these genes. And also might help in increasing the efficiency of gene delivery/expression systems.

Acknowledgment. The authors are grateful to Ya'an Research Base of Giant Panda Breeding for providing blood samples of the giant panda. Chengdong Wang contributed equally to this work and should be considered as first authors. Zhi-wen Xu, Ling Zhu are the corresponding authors. Key Laboratory of Animal Disease and Human Health of Sichuan Province & Animal Biotechnology Center, College of Veterinary Medicine of Sichuan Agricultural University, 46# Xinkang Road, Yucheng district, Ya'an 625014, Sichuan province of China. Tel.: +86 835 2885477; fax: +86 835 2885477; E-mail address: abtcxzw@126.com(Z.Xu).

References

1. Gustafsson, C., Govindarajan, S., Minshull, J.: Codon bias and heterologous protein expression. Trends in Biotechnology 22(7), 346–353 (2004)
2. Hershberg, R., Petrov, D.: Selection on codon bias. Annual Review of Genetics 42, 287–299 (2008)

3. Ikemura, T.: Codon usage and tRNA content in unicellular and multicellular organisms. Molecular Biology and Evolution 2(1), 13 (1985)
4. Sharp, P.: Codon usage in regulatory genes in Escherichia coli does not reflect selection for'rare'codons. Nucleic Acids Research 14(19), 7737 (1986)
5. Sharp, P., Li, W.: An evolutionary perspective on synonymous codon usage in unicellular organisms. Journal of Molecular Evolution 24(1), 28–38 (1986)
6. Shields, D., Sharp, P., Higgins, D., Wright, F.: " Silent" sites in Drosophila genes are not neutral: evidence of selection among synonymous codons. Molecular Biology and Evolution 5(6), 704 (1988)
7. Smith, N., Eyre-Walker, A.: Synonymous codon bias is not caused by mutation bias in G+ C-rich genes in humans. Molecular Biology and Evolution 18(6), 982 (2001)
8. Bains, W.: Codon distribution in vertebrate genes be used to predict gene length. Journal of Molecular Biology 197(3), 379–388 (1987)
9. D'Onofrio, G., Ghosh, T., Bernardi, G.: The base composition of the genes is correlated with the secondary structures of the encoded proteins. Gene 300(1-2), 179–187 (2002)
10. Bernardi, G.: Compositional constraints and genome evolution. Journal of Molecular Evolution 24(1), 1–11 (1986)
11. Gouy, M., Gautier, C.: Codon usage in bacteria: correlation with gene expressivity. Nucleic Acids Research 10(22), 7055 (1982)
12. Tao, X., Dafu, D.: The relationship between synonymous codon usage and protein structure. FEBS Letters 434(1-2), 93–96 (1998)
13. Angellotti, M., Bhuiyan, S., Chen, G., Wan, X.: CodonO: codon usage bias analysis within and across genomes. Nucleic Acids Research 35(Web Server issue), W132 (2007)
14. Epstein, R., Lin, K., Tan, T.: A functional significance for codon third bases. Gene 245(2), 291–298 (2000)
15. Ma, J., Zhou, T., Gu, W., Sun, X., Lu, Z.: Cluster analysis of the codon use frequency of MHC genes from different species. Biosystems 65(2-3), 199–207 (2002)
16. Coghlan, A., Wolfe, K.: Relationship of codon bias to mRNA concentration and protein length in Saccharomyces cerevisiae. Yeast-Chichester 16(12), 1131–1146 (2000)
17. Marais, G., Duret, L.: Synonymous codon usage, accuracy of translation, and gene length in Caenorhabditis elegans. Journal of Molecular Evolution 52(3), 275–280 (2001)
18. Tao, Y., Zeng, B., Xu, L., Yue, B., Yang, D., Zou, F.: Interferon-γ of the Giant Panda (Ailuropoda melanoleuca): Complementary DNA Cloning, Expression, and Phylogenetic Analysis. DNA and Cell Biology 29(1), 41–45
19. Xu, L., Zeng, B., Peng, R., Zou, F., Yue, B.: Molecular cloning and sequence analysis of the gene encoding interleukin-6 of the giant panda (Ailuropoda melanoleuca). Journal of Natural History 42(39), 2585–2591 (2008)
20. Isaacs, A., Lindenmann, J.: "Virus interference: I". The interferon. CA: A Cancer Journal for Clinicians 38(5), 280 (1988)
21. Bin, F., Bu-feng, L., Guang-yuan, H.: Synonymous codon usage bias and overexpression of a synthetic gene encoding Interferon α2b in yeast. Virologica Sinica 22(3), 226–232 (2007)
22. Duret, L., Mouchiroud, D.: Expression pattern and, surprisingly, gene length shape codon usage in Caenorhabditis, Drosophila, and Arabidopsis. Proceedings of the National Academy of Sciences of the United States of America 96(8), 4482 (1999)
23. Wright, F.: The effective number of codons' used in a gene. Gene 87(1), 23–29 (1990)
24. Sakai, H., Washio, T., Saito, R., Shinagawa, A., Itoh, M., Shibata, K., et al.: Correlation between sequence conservation of the 5'untranslated region and codon usage bias in Mus musculus genes. Gene 276(1-2), 101–105 (2001)

25. Lu, H., Zhao, W., Zheng, Y., Wang, H., Qi, M., Yu, X.: Analysis of synonymous codon usage bias in Chlamydia. Acta Biochimica et Biophysica Sinica 37(1), 1 (2005)
26. Gu, W., Zhou, T., Ma, J., Sun, X., Lu, Z.: Analysis of synonymous codon usage in SARS Coronavirus and other viruses in the Nidovirales. Virus Research 101(2), 155–161 (2004)
27. Wu, X., Wu, S., Ren, D., Zhu, Y., He, F.: The analysis method and progress in the study of codon bias. Yi Chuan= Hereditas/Zhongguo Yi Chuan Xue Hui Bian Ji 29(4), 420 (2007)
28. Tjalsma, H., Bolhuis, A., Jongbloed, J., Bron, S., Van Dijl: Signal peptide-dependent protein transport in Bacillus subtilis: a genome-based survey of the secretome. Microbiology and Molecular Biology Reviews 64(3), 515 (2000)
29. von Heijne, G.: The signal peptide. Journal of Membrane Biology 115(3), 195–201 (1990)
30. Zhang, S., Cheng, A., Wang, M.: Characterization of Codon Usage Bias in the Newly Identified DEV UL53 Gene, pp. 1–9. IEEE
31. Shen, F., Cheng, A., Wang, M., Huang, H., Li, C., Jiang, J., et al.: Factors affecting synonymous codon usage bias in the gC gene of DPV CHv strain. African Journal of Microbiology Research (5), 343–353
32. Xiang, J., Cheng, A., Wang, M., Zhang, S., Chang, H., Zhu, D., et al.: Analysis of Synonymous Codon Usage in the Capsid Gene UL38 of Duck Enteritis Virus, pp. 1–8. IEEE
33. Jia, R., Cheng, A., Wang, M., Xin, H., Guo, Y., Zhu, D., et al.: Analysis of synonymous codon usage in the UL24 gene of duck enteritis virus. Virus Genes 38(1), 96–103 (2009)

Effects of Amniotic Membrane Extraction on Rabbit Corneas with Herpes Simplex Keratitis*

Nan Hu**, Ling Yang, and Huaijin Guan

Department of Ophthalmology,
Affiliated Hospital of Nantong University,
Nantong, Jiangsu Province, China
hunaneye@hotmail.com

Abstract. The amniotic membrane exhibits many biological properties that may be helpful in treating ocular surface diseases. In this study, we investigated the effect of topical amniotic membrane extraction on herpes simplex keratitis (HSK) in a rabbit model. The corneas of rabbits were infected with herpes simplex type 1 virus. The rabbits were divided into 2 groups according to topical treatment methods: saline and AM extraction. The corneal lesions and angiogenesis severity were measured and graded at 0, 1, 3, 5, 7, and 14 days after treatment. Histologic examination was performed and the expression of interleukin (IL)-2, IL-10 and vascular endothelial growth factor（VEGF） were determined by enzyme-linked immunosorbent assay at 7 or 14 days after treatment. The severity of keratitis treated with AM extraction was less than saline treated eyes after 5 days of treatment ($P<0.05$). The extent of angiogenesis in the eyes of AM extraction treatment revealed greater reduction than the control ones after 3 days of treatment ($P<0.05$)**.** The amount of IL-2 and VEGF were decreased after treatment of AM extraction, whereas the amount of IL-10 was increased. The present study showed the extraction from fresh human amniotic membrane dramatically decreased the corneal inflammation and angiogenesis in experimental HSK by modulating the expression of proinflammatory cytokines and VEGF in the infected corneas.

Keywords: amniotic membrane extraction, herpes simplex virus keratitis, inflammation, angiogenesis.

1 Introduction

Herpes simplex virus keratitis (HSK) is a common eye infection that may cause permanent scarring, loss of vision, and blindness. This results mainly from a chronic inflammatory reaction in the normally transparent and avascular cornea.

The amniotic membrane (AM), consisting of a thick basement membrane and an avascular stromal matrix, is the innermost layer of the placenta. It exhibits many biological properties that may be helpful in treating ocular surface diseases, including the prevention of inflammation [1, 2], scarring [3], neovascularization [4] and

* This project is supported by a grant from the science and technology project for social development of Nantong, China (No. S2009029).

** Corresponding author.

E. Zhu and S. Sambath (Eds.): Information Tech. and Agricultural Eng., AISC 134, pp. 307–313.
springerlink.com © Springer-Verlag Berlin Heidelberg 2012

improving wound healing [5]. AM transplantation is increasingly used for the treatment of various ocular surface conditions such as chemical burns [6], persistent corneal epithelial defects [7] and corneal ulcers including HSK [8, 9]. However, clinical applications of AM grafts or patches are generally limited to severe cases of ocular surface diseases, because the treatment requires an invasive surgical procedure, which may cause a variety of complications. Therefore, the development of a topically applicable, noninvasive AM extraction would be beneficial. In addition, the biochemical effect of the AM extraction on anti-inflammatory, anti-angiogenesis, and corneal wound healing could be maintained for long periods, since it could be easily used according to the situation of the cornea.

The goal of the current experimental study was to evaluate the effects of topical AM extraction on the suppression of inflammation and angiogenesis in rabbit corneas with HSK.

2 Materials and Methods

2.1 Animals

24 New Zealand white rabbits of both sexes weighing 2.0–3.0kg were obtained from Experimental Animal Center of Nantong University (Certificate No 97024).

2.2 Virus

A laboratory strain of HSV-1 （SM44） was kindly provided by the Laboratory of Ophthalmology, School of Medicine, Suzhou University.

2.3 Preparation of AM Extracton

Human amniotic membranes were obtained from normal cesarean sections with approval of the Affiliated Hospital of Nantong University. All placentas were serologically negative for human immunodeficiency, hepatitis B and C viruses and syphilis. The AM were separated from the remaining chorion via blunt dissection and washed with normal saline containing 50 mg/ml of penicillin, 50 mg/ml of streptomycin, 100 mg/ml of neomycin, and 2.5 mg/ml of amphotericin B. The AM was sliced into small pieces and a sonicator was used to get the AM suspension. After suspension was centrifuged at 15,000r/min at 4 °C for 10 min, the supernatant was collected and designated as AM extraction.

2.4 Corneal Virus Infection and Treatment

Topical anesthesia was achieved with administration of 1 drop of 0.5% proparacaine hydrochloride to the rabbit eyes; corneas were lightly scarified with a sterile 27-G needle, and 25 μL of HSV suspension containing 5×10^5 PFU (plaque forming units) were inoculated onto each cornea. The eyelids were closed and the viral suspension rubbed gently on the corneal surface for 30 seconds. Care was taken to avoid leakage of the suspension. After inoculation, infection was allowed to proceed for 72 hours before initiation of treatment. From the 4th day after the inoculation, AM extraction was

applied topically five times per day every 2 hours starting at 8 and ending at 4 PM. The rabbits were randomly divided into 2 groups and treated with AM extraction or saline as a control. Treatment was continued for 14 consecutive days.

Slit lamp examination (SLE) was performed using fluorescein with a cobalt blue filter in the light path. The corneal lesions [10] and angiogenesis severity [11] were measured and graded using previously described scoring systems before the treatment and then at 2 days intervals. Other factors (conjunctival injection, conjunctival chemosis, blepharitis and iritis) were also observed.

2.5 Histopathology

For histopathological analysis, rabbits were sacrificed on days 14 after treatment and the corneas were fixed in 10% buffered neutral formalin. The samples were than rinsed in cacodylate buffer, dehydrated with ethanol, and embedded in paraffin. 5-mm sections were stained with hematoxylin-eosin.

2.6 Enzyme-Linked Immunosorbent Assay of Cytokines

Rabbits were sacrificed on days 7 or 14 after treatment. Infected corneas were excised and stored at −80°C until assayed. Samples were weighed, thawed, minced and placed in lysis buffer (20 mmol/L imidazole HCl, 10 mmol/L KCl, 1 mmol/L MgCl2, 1% Triton, 10 mmol/L EGTA, 10 mmol/L NaF, 1 mmol/L Na molybdate, 1 mmol/L EDTA, pH 6.8) with a protease inhibitor. After mechanical homogenization by sonication for 30 seconds, the lysate was clarified by centrifugation at 12,000r/min for 10 minutes and the supernatant was colleted. Total protein was measured using the protein assay kit and the levels of interleukin (IL)-2, IL-10 and vascular endothelial growth factor（VEGF） were determined by enzyme-linked immunosorbent assay according to the manufacturer's instructions (R&D Systems).

2.7 Statistical Analysis

Nonparametric one-way analysis of variance was used to evaluate the difference in corneal lesions and the Student's t-test was used to compare the mean number of cytokines expression. A P value of less than 0.05 was considered significant.

3 Results

3.1 AM Extraction Treated Rabbits Show Reduced Keratitis and Corneal Angiogenesis

All rabbit eyes infected with HSV exhibited dendritic or geographic corneal lesions by 3 days after virus inoculation. There was no significant difference on corneal lesion scores and angiogenesis scores of all rabbits before the treatment. The severity of keratitis in rabbits treated with AM extraction was less than saline treated eyes after 5 days of treatment ($P<0.05$). In comparison with the extent of angiogenesis following HSV infection, the eyes of AM extraction treatment revealed marked reduction of this process than the control ones after 3 days of treatment($P<0.05$)(figure 1 and Table 1).

Light microscopy showed that corneas from rabbits treated with saline for 14 days still contained many inflammatory cells (Figure 2A), whereas the number of cells had strongly decreased in corneas that were treated with AM extraction (Figure 2B).

3.2 AM Extraction Modulates Proinflammatory Cytokines and VEGF Expression in HSV-Infected Corneas

Corneas collected from rabbits after AM extraction or saline treatment for 7 and 14 days were analyzed for their content of IL-2 and IL-10. Level of VEGF was also determined. The amount of IL-2 was decreased after treatment of AM extraction, whereas the amount of IL-10 was increased. Furthermore, the VEGF content had decreased after AM extraction treatment compared with the saline group (Figure. 3).

Table 1. Corneal lesion scores and angiogenesis scores of the different treatment groups

Days after treatment	corneal lesion		angiogenesis	
	saline	AM extration	saline	AM extration
0 (n=12)	1.25±0.38	1.27±0.32	0.57±0.12	0.64±0.14
1 (n=12)	1.55±0.28	1.31±0.37	1.45±0.36	1.21±0.43
3 (n=12)	1.94±0.82	1.39±0.47	1.64±0.52	1.19±0.41*
5 (n=12)	2.06±0.92	1.30±0.35*	3.84±0.95	1.23±0.33**
7 (n=12)	2.80±0.56	1.05±0.33**	6.64±1.08	1.12±0.42**
14 (n=6)	2.69±0.65	0.85±0.50**	10.83±1.72	0.88±0.12**

*: P<0.05 compared with the results of saline group.
**: P<0.01compared with the results of saline group.

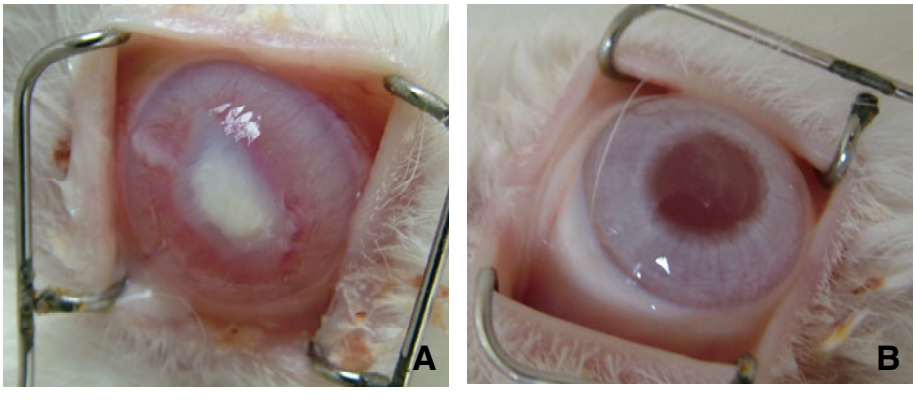

Fig. 1. Representative photographs of the infected corneas at 14 days after treatment with saline (A) and AM extraction (B)

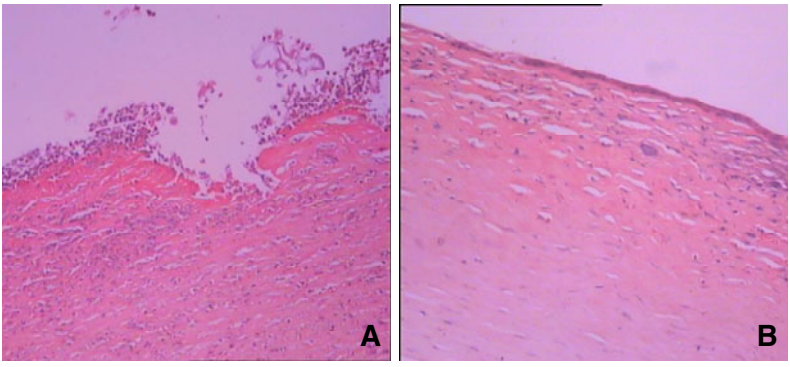

Fig. 2. HE staining of corneas 14 days after treatment. The cornea treated with saline (A) was densely infiltrated with inflammatory cells in the stroma and the infiltration was markedly reduced in the cornea treated with AM extraction(B)

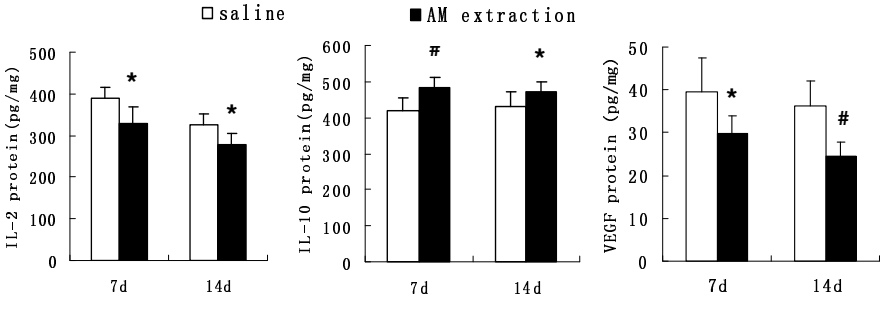

Fig. 3. Effect of AM extraction on the expression of the IL-2, IL-10 and VEGF in the infected corneas of the rabbits

* $P<0.05$ and # $P<0.01$ compared with the control group.

4 Discussion

Corneal ulceration and secondary neovascularization caused by herpes simplex virus infection are potentially vision-threatening diseases in the world. The treatment usually begins with appropriate topical antibiotic drops or ointment to prevent infection. In order to prevent scarring, suppress the immune-mediated inflammation, and maintain corneal transparency, topical corticosteroid solution is widely used after the virus proliferation has been controlled[12]. However, there exists evidence to suggest corticosteroid may increase the risk of infection and worsen stromal melting.

The present study showed the extraction from fresh human amniotic membrane dramatically decreased the corneal inflammation and angiogenesis in experimental HSK of rabbits by modulating the expression of proinflammatory cytokines and VEGF in the infected corneas.

Herpes simplex virus infection of the cornea provokes neovascularization. The mechanism of corneal neovascularization is thought to be the result of an imbalance between angiogenesis promoting factors and inhibiting factors and the predominance of promoting factors. VEGF has been demonstrated to be a key angiogenesis promoting factor in many models. In the cornea, the angiogenic process has been shown to be driven by increased secretion of VEGF [13], and anti-VEGF therapies have been demonstrated to strongly suppress corneal neovascularization[14]. In this study, we found topical application of AM extraction five times daily significantly prevented HSK-induced corneal neovascularization as confirmed by morphological observation and histochemical staining. The inhibition of corneal neovascularization is associated with a reduced expression of VEGF in the infected cornea.

Previous studies have shown that the type-1 T lymphocytes that predominantly secrete IL-2 are pathogenic in the evolution of HSK. The incidence and severity of keratitis is improved by neutralization of IL-2 [15]. In contrast, typical Th2 cytokines (IL-4, IL-10) have been detected during the healing phase of HSK and IL-10 treatment can prevent HSK from developing [16, 17]. In our study, an increased IL-10 cytokine secretion and decreased IL-2 cytokine secretion were detected in the AM extraction treated corneas of HSV infected rabbits as compared to the saline group. This suggested that AM extraction is able to cause an immmunomodulation away from Th1 cytokine to the Th2 cytokine secretion, accompanied by significantly improved clinical outcomes. The results were consistent with the previous findings.

In addition to the effects of anti-inflammation and anti-angiogenesis, it is reported that AM suspension leads to significant increases in corneal epithelial migration and proliferation, thus beneficial to corneal epithelial wound healing [5]. AM has previously been shown to evidence antibacterial properties against Pseudomonas, Streptococcus, Staphylococcus aureus, and Escherichia coli [18].

Taken together, the results of our study demonstrate the beneficial effects of topical AM extraction application on restoration of HSK with its anti-inflammatory and anti-angiogenic activity in a rabbit model. AM extraction has some advantages over AM transplantation, as the former is easy for preparation and application. Thus, topical AM extraction might be a promising and alternative strategy for the treatment of HSK.

References

1. Bauer, D., Wasmuth, S., Hennig, M., Baehler, H., Steuhl, K.P., Heiligenhaus, A.: Amniotic membrane transplantation induces apoptosis in T lymphocytes in murine corneas with experimental herpetic stromal keratitis. Invest. Ophthalmol. Vis. Sci. 50(7), 3188–3198 (2009)
2. Hori, J., Wang, M., Kamiya, K., Takahashi, H., Sakuragawa, N.: Immunological characteristics of amniotic epithelium. Cornea 25(10)(Suppl. 1), S53–S58 (2006)
3. Lee, S.B., Li, D.Q., Tan, D.T., Meller, D.C., Tseng, S.C.: Suppression of TGF-beta signaling in both normal conjunctival fibroblasts and pterygial body fibroblasts by amniotic membrane. Curr. Eye Res. 20(4), 325–334 (2000)
4. Shao, C., Sima, J., Zhang, S.X., Jin, J., Reinach, P., Wang, Z., et al.: Suppression of corneal neovascularization by PEDF release from human amniotic membranes. Invest. Ophthalmol. Vis. Sci. 45(6), 1758–1762 (2004)

5. Choi, J.A., Jin, H.J., Jung, S., Yang, E., Choi, J.S., Chung, S.H., et al.: Effects of amniotic membrane suspension in human corneal wound healing in vitro. Mol. Vis. 15(6), 2230–2238 (2009)
6. Tejwani, S., Kolari, R.S., Sangwan, V.S., Rao, G.N.: Role of amniotic membrane graft for ocular chemical and thermal injuries. Cornea 26(1), 21–26 (2007)
7. Nubile, M., Dua, H.S., Lanzini, T.E., Carpineto, P., Ciancaglini, M., Toto, L., et al.: Amniotic membrane transplantation for the management of corneal epithelial defects: an in vivo confocal microscopic study. Br. J. Ophthalmol. 92(1), 54–60 (2008)
8. Shi, W., Chen, M., Xie, L.: Amniotic membrane transplantation combined with antiviral and steroid therapy for herpes necrotizing stromal keratitis. Ophthalmology 114(8), 1476–1481 (2007)
9. Brijacak, N., Dekaris, I., Gagro, A., Gabrić, N.: Therapeutic effect of amniotic membrane in persistent epithelial defects and corneal ulcers in herpetic keratitis. Coll. Antropol. 32(Suppl. 2), 21–25 (2008)
10. Kaufman, H.E., Varnell, E.D., Toshida, H., et al.: Effects of topical unoprostone and latanoprost on acute and recurrent herpetic keratitis in the rabbit. Am. J. Ophthalmol. 131(5), 643–646 (2001)
11. Dana, M.R., Zhu, S.N., Yamada, J.: Topical modulation of interleukin-1 activity in corneal neovascularization. Cornea 17(4), 403–409 (1999)
12. Holmberg, B.J., Maggs, D.J.: The use of corticosteroids to treat ocular inflammation. Veterinary Clinics Small Animal Practice 34(3), 693–705 (2004)
13. Amano, S., Rohan, R., Kuroki, M.: Requirement for VEGF in wound- and inflammation-induced neovascularization. Invest. Ophthalmol. Vis. Sci. 39(1), 18–22 (1998)
14. Dratviman-Storobinsky, O., Lubin, B.C., Hasanreisoglu, M., Goldenberg-Cohen, N.: Effect of subconjuctival and intraocular bevacizumab injection on angiogenic gene expression levels in a mouse model of corneal neovascularization. Mol. Vis. 15(6), 2326–2338 (2009)
15. Tang, Q., Chen, W., Hendricks, R.L.: Proinflammatory functions of IL-2 in herpes simplex virus corneal infection. J. Immunol. 258(3), 11275–11283 (1997)
16. Tumpey, T.M., Cheng, H., Yan, X.T., Oakes, J.E., Lausch, R.N.: Chemokine synthesis in the HSV-1 infected cornea and its suppression by interleukin-10. J. Leukoc. Biol. 63(4), 486–492 (1998)
17. Bauer, D., Lu, M., Wasmuth, S., et al.: Immunomodulation by topical particle-mediated administration of cytokine plasmid DNA suppresses herpetic stromal keratitis without impairment of antiviral defense. Graefe's Arch Clin. Exp. Ophthalmol. 244(2), 216–225 (2006)
18. Kjaergaard, N., Hein, M., Hyttel, L., Helmig, R.B., Schønheyder, H.C., Uldbjerg, N., et al.: Antibacterial properties of human amnion and chorion in vitro. Eur. J. Obstet. Gynecol. Reprod. Biol. 94(2), 224–229 (2001)

Effects of Acetic Acid on Germination and Growth of Turions of *Potamogeton crispus* and Fragments of *Elodea nuttallii*[*]

Zuo Jin-Cheng[1,2], Liang Wei[1], Xu Dong[1], He Feng[1], Zhou Qiaohong[1], and Wu Zhen-Bin[1]

[1] StateKey Laboratory of Freshwater Ecology and Biotechnology, Institute of Hydrobiology The Chinese Academy of Sciences Wuhan, Hubei Province, China
[2] College of Life Sciences Ludong University Yantai, Shandong Porvince, China
wuzb@ihb.ac.cn, zuo2008@hotmail.com

Abstract. Anaerobic digestion of organic matters in eutrophic lake sediment produced acetic acid. Germination and growth of turions of Potamogeton crispus and fragments of Elodea nuttallii under acetic acid stresses were investigated. The propagules were exposed to acetic acid from 1 to 16mmol/l for a period of 3 or 6 days, and were subsequently cultured in absence of acetic acid. Most E. nuttallii could germinate at concentration of 1mmol/l, but the growth was significantly inhibited. No E. nuttallii could survive after exposures to 4mmol/l or over. 63.3% of P. crispus survived in the exposure to 8mmol/l for 3 days. However, the stronger stresses caused death of P. crispus. Results indicated that P. cripus was more tolerant to acetic acid than E. nuttallii, and that presence of acetic acid in sediment may cause great difficulties in reestablishing submerged macrophytes in eutrophic lakes.

Keywords: Elodea, Potamogeton, eutrophic, acetic acid.

1 Introduction

Sediment of eutrophic lakes is generally abundant in organic matter, and is usually under anaerobic conditions [1]. Anaerobic digestion of organic matters produces organic acids, in which acetic acid is dominant [2], [3]. It has been reported that acetic acid ranged 0.1-360 μmol/l in marine and freshwater sediments [4] and 2.5-8.6 mmol/l in pore water [2]. Moreover, flood may cause drastic increase of organic acids to 10-40 mmol/l, and this condition could last a few weeks [5].

Reestablishing submersed macrophytes has been proved to be one of the key measures to restore eutrophic lakes [6]-[8]. For many submersed aquatic macrophytes, vegetative propagules are the most important mechanism for their propagation and dispersal [9], [10].

[*] This work is partially supported by CNSF (50808172), Grants from the Key Science Research Project of Eleven Five-year Plan (2009ZX07106-003, 2008ZX07316-004), and Item of Scientific Research Fund For Doctor of Ludong University (LY20073301).

E. Zhu and S. Sambath (Eds.): Information Tech. and Agricultural Eng., AISC 134, pp. 315–321.
springerlink.com © Springer-Verlag Berlin Heidelberg 2012

However, few researches dealt with response of submersed macrophytes to acetic acid, except that *Hydrilla verticillata*, *Potamogeton pectinatus* and *P. gramineus* were ever reported to be significantly inhibited in germination and growth by acetic acid [1], [11], [12]. Both *Elodea nuttallii* and *P. cripus* belong to the minority of those with capacity to thrive in winter.The former is being carefully and experimentally studied in small and enclosed eutrophic lakes in China for it is exotic and the latter is a good candidate for reestablishment of submersed macrophytes [13]-[15]. Both turions of *P. cripus* and fragments of *E. nuttallii* are the most important vegetative propagules for these two species, respectively. The present study aims to understand the effects of acetic acid on germination and growth of the two kinds of propagules. This information may be useful in reestablishing submersed macrophytes in eutrophic lakes.

2 Materials and Methods

2.1 Plant Materials

Turions and fragments were collected from cultures maintained in outdoor concrete tanks in Institute of Hydrobiology, Chinese Academy of Sciences. Fragments of *E. nuttallii* without lateral shoots or apparent buds, 5cm in length, were used. Turions of *P. cripus* had been stored at 4 ^{o}C for a week to get a nearly identical and instant germination time. Only one dormant bud was reserved on one turion, and the others were removed with nipper.

2.2 Methods

Turions and fragments were treated in plastic pots (1l in cubage). Each pot was filled with 1cm layer of sediment from Lake Donghu, a typical eutrophic lake in Wuhan, China [16], then slowly irrigated with different acetic acid concentrations of 0 (the control treatment), 1, 4, 8, 16 mmol/l (prepared by dissolving acetic acid in water from Lake Donghu) to reach 0.5cm from top of the pot, avoiding disturbing the sediment. For each combination of acetic acid concentration, exposure time and plant species, 3 pots were set up and 10 fragments or turions were treated in one pot. After 3 or 6 days of cultivation, fragments or turions were taken out and rinsed softly in tap water. Their germination rate and bud length were measured. Then fragments or turions continued to be cultured in the same pot in absence of acetic acid for 13 days and 10 days, respectively. Then, total root length per plant, bud length per plant and dry weight per plant were measured. However, no dry weight data were collected for *E. nuttallii* because the sprouts were too small. Harvested plants were dried at 80 ^{o}C to constant weight to determine dry weight.

The experiment was performed in laboratory with a mean temperature of 15.6 ± 2.4 ^{o}C (mean ± S.D.) in December, 2004. The pH of acetic aced in each treatment varied little during the experiment. Average COD_{Cr} (chemical oxygen demand by potassium dichromate oxidation), TN (total nitrogen), NH_3-N and TP (total phosphor) of Lake Donghu water used in the study (mean ± S.D.) were 29.67 ± 8.29 mg/l, 2.09 ± 0.61 mg/l, 0.64 ± 0.06 mg/l and 0.18 ± 0.06 mg/l, respectively. Average TP, TN and TOC (total organic carbon) of Lake Donghu sediment used in the study (mean ± S.D.) were

0.76 ± 0.08 mg/g, 3.68 ± 0.38 mg/g and 9.55 ± 0.96 mg/g (the values were presented on basis of dry weight of sediment), respectively.

Data were statistically analyzed using ANOVA in SPSS 13.0.

3 Materials and Method

3.1 Germination Rates

No *E. nuttallii* fragments germinated when exposed to 0 and 1 mmol/l for 3 days (Fig. 1A). However, they were still alive, and in the subsequent culture in absence of acetic acid, 76.7% and 86.7% of the fragments with 0 and 1 mmol/l treatments sprouted, respectively. After 6-day exposures to 0 and 1 mmol/l, germination rate of *E. nuttallii* reached 90.0% and 80.0%, respectively. Yet no more buds germinated in the subsequent culture. Additionally, exposures to 4 mmol/l or higher for 3 days or 6 days led to death of all fragments of *E. nuttallii*.

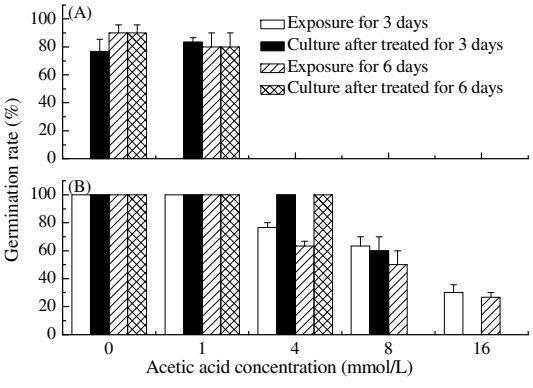

Fig. 1. Germination rates of (A) fragments of *E. nuttallii* and (B) turions of *P. cripus* in different exposures and in the subsequent cultures. Bars indicate standard errors

Fig. 1B shows increased exposure time or acetic acid concentration reduced germination rate of *P. cripus* in treatments and in the subsequent cultures. All the turions of *P. cripus* could germinate when exposed to 0 or 1 mmol for 3 or 6 days. The buds germinated white and fine roots, and none died during the subsequent culture. Germination rates of *P. cripus* were greatly ($P<0.05$) reduced when exposed to 4 mmol/l for 3 days or 6 days, but the subsequent culture led to increased germination rate to 100% for both of them. When exposed to 8 mmol/l for 3 days, over 60% of *P. cripus* turions germinated and few buds died in the subsequent culture. Some turions may germinate after exposures to 8 mmol/l for 6 days or 16 mmol/l for 3 days or 6 days, but none could survive.

3.2 Bud Length after Exposures

Average bud length of *E. nuttallii* after exposure to 1 mmol/l for 6 days was significantly lower ($P<0.05$) than that of the control plants (Fig. 2A), which indicated that growth of *E. nuttallii* was inhibited significantly by 1 mmol/l acetic acid. In contrast, for exposures to 1 mmol/l, average bud length of *P. cripus* exposed for 6 days was noticeably greater ($P<0.05$) than that of plants exposed for 3 days (Fig. 2B). Furthermore, *P. cripus* showed no significant difference ($P>0.05$) in mean bud length between the treatment of 1 mmol/l for 6 days and the control (Fig. 2B). These results indicated that acetic acid at 1 mmol/l or lower did not have any significant effects on growth of *P. cripus*. However, exposures to 4, 8 or 16 mmol/l for 3 or 6 days led to remarkably reduced mean bud length of *P. cripus* ($P<0.01$), which indicated that its growth was remarkably inhibited by 4 mmol/l of acetic acid or higher even at exposure time of 3 days.

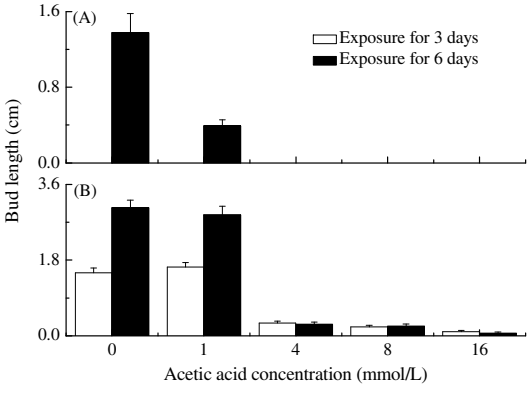

Fig. 2. Average bud length of (A) *E. nuttallii* and (B) *P. cripus* after exposures to acetic acid for 3 days or 6 days. Length of the buds that were proved to be dead in the subsequent culures (see in Fig. 2A) were still collected and presented here. Bars indicate standard errors.

3.3 Growth in the Subsequent Cultures

In the subsequent culture, growth was rapid for *E. nuttallii* which were ever exposed to 1 mmol/l for 3 days or 6 days (Fig. 3). Differences between plants ever exposed to 0 or 1mmol/l for 3 or 6 days was not significant ($P>0.05$) in total root length per plant and bud length per plant. These results indicated that *E. nuttallii* could recover quickly from exposures to 1 mmol/l acetic acid for 3 or 6 days after the stressor was removed.

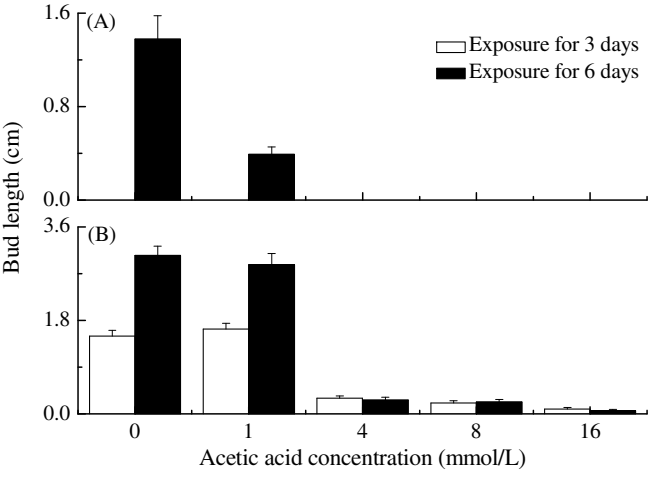

Fig. 3. Growth of *E. nuttallii* during the subsequent culture in absence of acetic acid: (A) total root length per plant and (B) bud length per plant. Information of the dead buds was excluded from the data presented here. Bars indicate standard errors.

Growth of *P. cripus* ever exposed to 0, 1 or 4 mmol/l for 3 days or 6 days were much better (P<0.05) than that of plants ever exposed to 8 mmol/l for 3 days in bud length per plant, total root length per plant and dry weight per plant (Fig. 4). Furthermore, there was no significant difference (P>0.05) among growth of *P. cripus* exposed to 0, 1 or 4 mmol for 6 days or 3 days. Therefore, it could be concluded that if the stressor was removed, *P. cripus* could recover quickly from 3 or 6 days of exposures to 4 mmol/l or lower, but slowly from exposure to 8 mmol/l for 3 days.

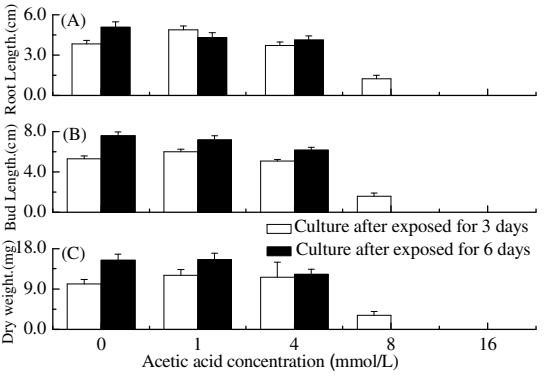

Fig. 4. Growth of *P. cripus* during the following culture in absence of acetic acid: (A) total root length per plant, (B) bud length per plant and (C) dry weight per plant. Information of the dead buds was excluded from the data presented here. Bars indicate standard errors.

4 Discussion

Exposure to 4 mmol/l acetic acid for 3 days was lethal to *E. nuttallii* while *P. cripus* still showed good survival after exposed to 8 mmol/l for 3 days and 4 mmol/l or lower for 3 days or 6 days. Moreover, *P. cripus* tended to have the higher capacity to recover from intensive exposures to acetic acid than *E. nuttallii*. Therefore, *P. cripus* seemed to be more suitable than *E. nuttallii* to act as pioneer species in reestablishing submersed macrophytes in eutrophic lakes. The high ability of tolerance to acetic acid, in addition with the strong propagation power, may help *P. cripus* grow normally in eutrophic lakes.

Response of vegetative propagules to acetic acid was ever reported in *Hydrilla verticillata*, *P. pectinatus* and *P. gramineus* [1]. Their esults showed that the response varied greatly with propagules types, and that greater damage to plants would be caused by longer exposure time, higher concentration, higher temperature or absence of sediment. Acids could damage plant tissues or organs directly, and even result in death of plants. Furthermore, what makes things worse is that leaching and activation of heavy metals in sediment would be aggravated when pH values in pore water was decreased by increased acetic acid concentration [17]. So, acetic acid in sediment may be one of the key factors that make it difficult to restore submerged macrophytes in eutrophic lakes.

Acknowledgment. We thank LUO Li-ming and ZHANG Yong-yuan for reading and editing this manuscript.

References

1. Spencer, D.F., Ksander, G.G.: Differential effects of the microbial metabolite, acetic acid, on sprouting of aquatic plant propagules. Aquatic Botany 52, 107–119 (1995)
2. Miller, D., Brown, C.M., Pearson, T.H., Stanley, S.O.: Some biologically important low molecular weight organic acids in the sediments of Loch Eil. Marine Biology 50, 375–383 (1979)
3. King, G.M., Klug, M.J.: Glucose metabolism in sediments of a eutrophic lake: tracer analysis of uptake and product formation. Applied and Environmental Microbiology 44, 1308–1317 (1982)
4. Reeburgh, W.S.: Rates of biogeochemical processes in anoxic sediments. Annual Review of Earth and Planetary Sciences 11, 269–298 (1983)
5. Ponnamperuma, F.N.: The chemistry of submerged soils. Advances in Agronomy 24, 29–96 (1972)
6. Gumbricht, T.: Nutrient removal processes in freshwater submersed macrophyte systems. Ecological Engineering 2, 1–30 (1993)
7. James, W.F., Best, E.P., Barko, J.W.: Sediment resuspension and light attenuation in Peoria Lake: can macrophytes improve water quality in this shallow system? Hydrobiologia 515, 193–201 (2004)
8. Wu, Z.B., et al.: Effects of rehabilitation of submerged macrophytes on nutrient level of a eutrophic lake. Chinese Journal of Applied Ecology 14, 1351–1353 (2003) (in Chinese with English Abstract)

9. Cho, H.J., Poirrier, M.A.: Seasonal growth and reproduction of Ruppia maritima L. s.l. in Lake Pontchartrain, Louisiana, USA. Aquatic Botany 81, 37–49 (2005)
10. Hilt, S., et al.: Restoration of submerged vegetation in shallow eutrophic lakes - A guideline and state of the art in Germany. Limnologica - Ecology and Management of Inland Waters 36, 155–171 (2006)
11. Spencer, D.F., Ksander, G.G.: Influence of dilute acetic acid treatments on survival of monoecious Hydrilla tubers in the Oregon House Canal, California. Journal of Aquatic Plant Management 37, 67–71 (1999)
12. Spencer, D.F., Elmore, C.L., Ksander, G.G., Roncoroni, J.A.: Influence of dilute acetic acid treatments on American pondweed winter buds in the Nevada irrigation district, California. Journal of Aquatic Plant Management 41, 65–68 (2003)
13. Dai, M., Ni, L.Y., Xie, P., Wang, J., Takamura, K.: Experimental studies on the effects of submersed macrophytes on the eutrophication of lake water using large-sized enclosures. Acta Hydrobiologica Sinica 23, 98–101 (1999) (in Chinese with English Abstract)
14. Huang, L., Zhai, J.P., Wang, C.Y., Nie, R., Yuan, D.H.: Removals of nitrogen and phosphorus in Taihu Lake water by four hydrophytes in winter season. Journal of Agro-Environment Science 24, 366–370 (2005) (in Chinese with English Abstract)
15. Xu, H.L., Tang, Z.Y., Zhu, D.W., Ni, L.S.: Effect of Potamogeton crispus and Elodea nuttallii on phosphorus fractionation of sediment and overlying water quality. Journal of Lake Sciences 22, 437–444 (2010) (in Chinese with English Abstract)
16. Gan, Y.Q., Guo, Y.L.: Evaluation analysis and remedy strategy for eutrophication in Wuhan Lake Donghu. Resources and Environment in the Yangtze Basin 13, 277–281 (2004) (in Chinese with English Abstract)
17. Kuang, Q.J., Xia, Y.C., Hui, Y.: Toxic effects of heavy metal on algae. Acta Hydrobiologica Sinica 20, 277–283 (1996) (in Chinese with English Abstract)

Efficacy of *Xanthium sibiricum* Fruit Extract on *Lasioderma Serricorne* (Coleoptera: Anobiidae)

Jian-Hua Lü[1] and Xin-Hong Su[2]

[1] School of Food Science and Technology, Henan University of Technology, No.140 Songshan Road, Zhengzhou 450052, Henan, China
[2] Henan Tobacco Company, Zhengzhou 450008, Henan Province, China
jianhlv@yahoo.com.cn

Abstract. The efficacy of Xanthium sibiricum fruit extract was investigated on eggs, larvae, pupae and adults of Lasioderma serricorne. X. sibiricum fruit extract had strong fumigant activity against L. serricorne, and the toxicity enhanced significantly with the increasing treatment dosage. Larvae and adults were much more susceptible to the plant extract than eggs and pupae. The corrected mortality of adults, pupae, larvae and eggs reached 89.76, 41.68, 95.13 and 32.51% at a dosage of 40μl/l air after 48 h of exposure, respectively. The declining order of susceptibility of different development stages of L. serricorne to X. sibiricum fruit extract was as follows: larvae (LD_{50}= 9.73 μl/l air), adults (LD_{50}= 10.98 μl/l air), pupae (LD_{50}= 55.32 μl/l air) and eggs (LD_{50}= 86.89 μl/l air).

Keywords: Efficacy, Xanthium sibiricum fruit extract, Lasioderma serricorne, Natural fumigant.

1 Introduction

The cigarette beetle, *Lasioderma serricorne* (Fabricius) (Coleoptera: Anobiidae) is one of the most serious pest of stored tobacco, tobacco products, cereal grains and processed foods throughout the world[1]. Currently, control of *L. serricorne* population is primarily dependent upon intensive use of phosphine[2]. However, its repeated use for decades has disrupted biological control by natural enemies and led to serious problems including insecticide resistance, environmental and human health concerns, rising cost of production, and lethal effects on non-target organisms[3, 4]. Development and implementation of alternative control strategies and integrated pest management systems have recently been considered to be the only solution to combat these increasing pesticide-resistant insect pests [1].

Plant-derived pesticides may provide potential alternatives to currently used insect-control agents because they are natural source of bioactive chemicals with complicated action mechanism, to which the insect pests are difficult to produce resistance, readily biodegradable, often less toxic to mammalian, and with less or negligible danger to the environment if used in suitable amounts. Particularly, because of the unacceptable high cost and difficulty of researching and developing new synthetic insecticides, recent research has focused on natural product alternatives for

E. Zhu and S. Sambath (Eds.): Information Tech. and Agricultural Eng., AISC 134, pp. 323–327.
springerlink.com © Springer-Verlag Berlin Heidelberg 2012

pest control in developing countries and for organic food production in industrialized countries[5-8].

Many Chinese herbal plants are potential sources of pesticides and have exhibited potent toxic bioactivity to stored-grain insects [7, 9]. In fact, as a traditional Chinese herbal plant, *Xanthium sibiricum* fruit has also for many generations been used as a traditional method by farmers to protect stored products from insect infestation in China. However, insecticidal activity of essential oil from *X. sibiricum* fruit against *L. serricorne* has not been investigated so far.

Thus, the paper describes a laboratory study to assess the potential fumigant toxicity of *X. sibiricum* fruit extract against eggs, larvae, pupae and adults of *L. serricorne*.

2 Materials and Methods

2.1 Insects

Cultures of the cigarette beetle, *L. serricorne*, were maintained in the laboratory without exposure to any insecticide at the Institute of Stored Product Insects of Henan University of Technology. They were reared on sterilized diet (wheatfeed/yeast, 95:5, w/w) at 27±2℃, 75% ±5%% r.h., and a 12:12 light:dark photoperiod. Healthy, consistent and different development stages of insects were randomly chosen for tests.

2.2 Preparation of the Extract

The *X. sibiricum* fruit was purchased from Chinese traditional drug store and finely ground to powder. Each 50 g of the powder was extracted by Soxhlet method with 250 ml anhydrous diethyl ether until the distilled liquid was colorless. The solvent was evaporated under vacuum in a rotary evaporator. The plant extract was stored in airtight fuscous glassware in a refrigerator at 4 ℃.

2.3 Fumigant Activity

1) Larvae, Pupae and Adults: Fumigant activity on *L. serricorne* adults was respectively carried out with 30 larvae (10-12 days old), pupae (1-2 days old) and unsexed adults (5-7 days old), exposed in a 250 ml flask tightly sealed with a rubber stopper. An aliquot of 0, 1.25, 2.50, 5.00 and 10 µl of the *X. sibiricum* fruit extract dissolved in 1 ml acetone (analytical purity) was evenly applied on a Whatman No.1 filter paper strip （7×9 cm） corresponding to dosages of 0 (as a control), 5, 10, 20, and 40 µl/l air, which was then dried in air for 10 min prior to being fixed on the rubber stopper by a staple at one end. The rubber stopper was tightly stuffed to keep the filter paper suspending in the top of the flask. Care was taken to avoid the filter paper contacting the flask wall. The flask was placed in the incubators at 27±2℃ and 75±5% relative humidity. Five replicates were conducted. After 48 h of exposure,

insects were moved into clean vials. The mortality of *L. serricorne* larvae and adults were determined immediately. Insects showing any movement were considered to be alive. The *L. serricorne* pupae were then kept in insect culture environment, and the number of pupae which successfully developed into adults was recorded everyday during the following 10 days. The pupae that could not reach the adult stage were considered to be dead.

2) Eggs: The eggs (0–24 h old) were exposed to *X. sibiricum* fruit extract on round cloning plates (Φ9.5 cm). Each cloning plate had 54 microwells of 6 mm diameter, and 5 mm depth, and one egg was transferred into each microwell using a moistened fine brush. Each microwell was numbered. Thirty eggs were counted for one replicate. The plates were placed in 5 l glass jars with screw-top lids. *X. sibiricum* fruit extract was applied on a Whatman No.1 filter paper strip (7×9 cm) which was attached to the lower side of the jar lid by adhesive tape. The test dosages were 0 (as a control), 5, 10, 20, and 40 μl/l air, respectively. After 48 h of exposure, plates were taken out of the jars, then kept in insect culture environment. The observation of the egg hatching condition was made with a stereomicroscope, and the number of eggs hatching into larvae was recorded everyday during the following 10 days. Unhatched eggs were counted as dead. All experiments were repeated five times.

2.4 Statistical Analysis

The percentage mortality was corrected by the Abbott formula[10]. The percentage mortality was determined and transformed to arcsine square-root values for analysis of variance (ANOVA). Treatment means were compared and separated by Scheffe's test at $P = 0.05$ [11]. The LD_{50} values were calculated using probit analysis[12].

3 Results

X. sibiricum fruit extract showed potent fumigant toxicity against *L. serricorne* and the toxicity progressively increased with increased exposure dosage ($df = 3$, $P < 0.05$). The responses also significantly varied with development stage, and larvae and adults were much more susceptible than eggs and pupae (Table 1 and Table 2). At a dosage of 40 μl/l air, the corrected mortality of larvae, adults, eggs and pupae reached 95.13, 89.76, 32.51 and 41.68%, respectively, indicating that there was similar fumigant effect on *L. serricorne* between larvae and adults, and between eggs and pupae at the same exposure concentration ($df = 1$, $P > 0.05$). The declining order of susceptibility of different development stages of *L. serricorne* to *X. sibiricum* fruit extract was as follows: larvae (LD_{50}= 9.73 μl/l air), adults (LD_{50}= 10.98 μl/l air), pupae (LD_{50}= 55.32 μl/l air) and eggs (LD_{50}= 86.89 μl/l air).

Table 1. Efficacy of *xanthium sibiricum* fruit extract on eggs, larvae, pupae and adults of *L. serricorne* after 48 h of exposure period.

Dosage (µL/L)	Egg (%)	Larva (%)	pupa (%)	Adult (%)
5	7.00±1.25d	21.30±1.51d	11.00±1.49d	23.27±2.03d
10	13.67±1.25c	59.62±2.24c	22.25±1.70c	52.43±1.66c
20	25.00±1.63b	73.39±3.13b	33.33±1.49b	65.87±2.39b
40	32.51±1.70a	95.13±0.68a	41.68±3.56a	89.76±2.62a

Each datum represents the mean corrected mortality (±SE) of five replicates (n=150). Means within a column followed by the same superscripts are not significantly different at P =0.05.

Table 2. Toxicity Parameters Calculated for Mortality of Tested Insect Stages after 48 H of Exposure to *Xanthium Sibiricum* Fruit Extract and at the Dosages of 0, 5, 10, 20 and 40 µL/L air based on the Flask Volume

Development stage	Regression line equation	LD_{50} (µl/l)	Confidence limit of LD_{50} (µl/l)	Chi-square ($\chi 2$)	Chi-square p value
Egg	Y = 1.31 X + 2.35	86.89	50.30~ 164.35	4.36	0.99
Larva	Y = 2.65 X + 3.39	9.73	7.99~ 10.82	18.98	0.39
Pupa	Y = 1.51 X + 2.12	55.32	38.78~111.31	7.90	0.98
Adult	Y = 2.67 X + 2.41	10.98	9.75~12.26	21.7	0.25

4 Discussion

X. sibiricum fruit extract showed strong efficacy on *L. serricorne* larvae and adults which depends on several factors including the treatment dosage of the plant extract and the development stage of the insect, and so on. Similarly, the extracts of *Agastache rugosa* whole plant, *Cinnamomum cassia* bark, *Illicium verum* fruit and *Foeniculum vulgare* fruit as well as cinnamon (*C. cassia*), horseradish (*Cocholeria aroracia*) and mustard (*Brassica juncea*) oils had good fumigant activity against *L. serricorne* adults [1]. Moreover, many essential oils and their constituents have been studied to possess potential as alternative compounds to currently used insect-control agents for the management of populations of stored-product insects[13-15].

Our research results demonstrates that *X. sibiricum* fruit extract is a source of biologically active vapors which may potentially prove to be effective biofumigations. Specially, provided with a proper formulation, dosage and scientific application strategy, the *X. sibiricum* fruit extract may be exploited for use to effectively control *L. serricorne*. Furthermore, the *X. sibiricum* fruit extract as a traditional pharmaceutical agent, is thus considered to be safe for human being and the environment.

Acknowledgments. This research was supported by Henan Provincial Key Science and Technology Project （No. 092102110022）, Key Science Foundation of Henan University of Technology（No. 170851）and Research and Development project of Henan Tobacco Company in 2010.

References

1. Kim, S., Park, C., Ohh, M.H., Cho, H.C., Ahn, Y.J.: Contact and fumigant activity of aromatic plant extracts and essential oils against Lasioderma serricorne (Coleoptera: Anobiidae). J. Stored Prod. Res. 39, 11–19 (2003)
2. White, N.D.G., Leesch, J.G.: Chemical control. In: Subramanyam, B., Hagstrum, D.W. (eds.) Integrated Management of Insects in Stored Products, pp. 287–330. Marcel Dekker, New York (1995)
3. Rajendran, S., Narasimhan, K.S.: Phosphine resistance in the cigarette beetle Lasioderma serricorne (Coleoptera: Anobiidae) and overcoming control failures during fumigation of stored tobacco. Int. J. Pest Manage. 40, 207–210 (1994)
4. Jovanović, Z., Kostić, M., Popović, Z.: Grain-protective properties of herbal extracts against the bean weevil Acanthoscelides obtectus Say. Ind. Crop. Prod. 26(1), 100–104 (2007)
5. Isman, M.B.: Botanical insecticides, deterrents, and repellents in modern agriculture and an increasingly regulated world. Annu. Rev. Entomol. 51, 45–66 (2006)
6. Isman, M.B.: Botanical insecticides: for richer, for poorer. Pest Manag. Sci. 64, 8–11 (2008)
7. Liu, Z.L., Goh, S.H., Ho, S.H.: Screening of Chinese medicinal herbs for bioactivity against Sitophilus zeamais Motschulsky and Tribolium castaneum (Herbst). J. Stored Prod. Res. 43, 290–296 (2007)
8. Rajendran, S., Sriranjini, V.: Plant products as fumigants for stored-product insect control. J. Stored Prod. Res. 43, 126–135 (2008)
9. Yang, R.Z., Tang, C.S.: Plants used for pest control in China: a literature review. Econ. Bot. 42, 376–406 (1988)
10. Abbott, W.S.: A method of computing the effectiveness of an insecticide. J. Econ. Entomol. 18, 265–267 (1925)
11. SAS Institute, SAS/STAT User's Guide, Version 6. SAS Institute, Cary, North Carolina (1994)
12. Finney, D.J.: Statistical Method in Biological Assay, 2nd edn. Griffin, London (1971)
13. Shaaya, E., Kostjukovski, M., Eilberg, J., Sukprakarn, C.: Plant oils as fumigants and contact insecticides for the control of stored-product insects. J. Stored Prod. Res. 33, 7–15 (1997)
14. Lee, B.H., Annis, P.C., Tumaalii, F., Choi, W.S.: Fumigant toxicity of essential oil from the Mytaceae family and 1,8-cineole against 3 major stored-grain insects. J. Stored Prod. Res. 40, 553–564 (2004)
15. Lü, J.H., He, Y.Q.: Fumigant toxicity of Ailanthus altissima Swingle, Atractylodes lancea (Thunb.) DC. and Elsholtzia stauntonii Benth extracts on three major stored-grain insects. Ind. Crop. Prod. 32, 681–683 (2010)

Study on the Meitauza Production from Okara by *Actinomucor elegans* and *Zymomonas mobilis*

Xilin Xu, Hongwei Liu, and Yanliang Zhou

College of Light Industry and Food Science South China University of Technology
Guangzhou, Guangdong Province, China
xuxilin@scut.edu.cn, hw_francis@126.com, play_plug@163.com

Abstract. In this paper, meitauza was fermented by Actinomucor elegans and Zymomonas mobilis from okara, and the changes of microbial flora, chemical and physical properties of fermentation were studied. During fermentation of meitauza, pH rose from 6.3 to 8.1, and protease activities reached 1175U/g, moisture content and crude protein decreased slowly, and free amino acids analysis of product increased from 836 to 3666 mg/100g, especially in strong-tasting and sweetening amino acids. Texture analysis method was employed to examine the growth of mucor mycelia and to assess the quality of the fermented product. Qualities improved as the fermented time and reached natural samples level in 5^{th} or 6^{th} d.

Keywords: Meitauza, Production, Okara, Texture analysis.

1 Introduction

Okara, the residue left by soy beans after extraction with water, is a byproduct of tofu and soymilk which is highly consumed in China and the neighbors. Fresh okara is easily spoiled for its high content of water and nutritive protein, and it's not a effective way to dry the okara for its low added value(O'Toole,1999). According to relative reports, China producees 20 million fresh okara per year, and most okara was used as animal feed. And in Hong Kong, it is dumped in land fills(O'Toole,1999). Many studies have focused their attention to the use of okara, especially on fermentation fields. As protein content is up to 25.0-28.4% (dry basis), therefore, okara is a good nitrogen source of fermentation of microorganism. Fermented products of okara were developed in the way as natto or tempeh(Matsumoto and Take, 1980). Meitauza, the traditional Chinese household product in the Hubei, Henan and Guangdong provinces, is produced with okara using mucor naturally from rice straw (Cao, 1994). According to traditional method, meitauza is fermented below 20°C for about 8-14days depending on the environment and the activity of microorganisms on the rice straw.

In this study, meitauza was fermented by *Actinomucor elegans and Zymomonas mobilis*, and the changes of microbial flora, chemical and physical of product were studied, and texture analysis was introduced to measure the fungal growth, and to assess the quality of meitauza products.

E. Zhu and S. Sambath (Eds.): Information Tech. and Agricultural Eng., AISC 134, pp. 329–336.
springerlink.com © Springer-Verlag Berlin Heidelberg 2012

2 Materials and Methods

2.1 Materials

Fresh okara, the soybean residue after producing soybean milk or tofu, was supplied by Shenzhen Yinmin Food Unity Co., Ltd (www.yiminfood.com). Meitauza and okara were stored at -20°C.

Actinomucor elegans and *Zymomonas mobilis*, separated from natural meitauza product, supplied by microbiology laboratory.

Natural meitauza product sampled from Hubei province.

2.2 Culture of Microorganisms

Actinomucor elegans were cultured in Rose-Bengal medium (RB) in 28°C for 7 days, *Zymomonas mobilis* were cultured in nutrition broth medium (NB) in 37°C for 2 days. All molds were incubated for 3 generations and bacteria for 5 generation, and stored in 4°C.

2.3 Meitauza Fermentation

The method of fermentation of meitauza was similar to traditional technology (Fig 1). Following the method, microorganisms isolated in 2.2 were dispersed into sterilized water about 10^7 cfu/ml (1ml to 100g okara), and added to the okara before "shaping" process. Okara was fermented in 18°C, 95%moisture degree(climate incubator, Suzhou Ltd) for 6 days.

Fresh meitauza was used as original cultural matrix in the natural meitauza fermentation.

2.4 Physical and Chemical Analysis of Meitauza Product

pH measurement: 10g samples were homogenized with 90 ml of deionized water (pH=7) and the pH of the suspension was determined with a digital pH meter. The α-amino nitrogen analysis was done by titration with formaldehyde (AOAC, 2002). Crude protein and soluble protein analysis was done by Kjeldahl nitrogen determination. Determination of protease activity was followed Y.P Zhu' method(2008).

2.5 Texture Analysis of the Product

Solid and semi-solid substrates had been in used in various ferment food such as cheese, sufu, natto, tempeh and meitauza (Kronenberg and Hang, 1984), but no direct analysis methods of the solid substrate fermentation exists presently. A texture analysis method (Texture Profile Analysis, TPA), was introduced to analyze the mycelia growth in the fermentation of meitauza. Measurement of texture were made with a texture analysis instrument (model:TA XT2i/25, SMS Ltd) equipped with P5 probe(5mm diameter cylinder stainless), Pre-speed:2.0 mm/s, test speed:1.0mm/s, post speed:5.0mm/s, distance:8.0mm, interval time: 5.00s,twice puncture. 0-6 days' samples were laid on a plate and measured fot 3 times.

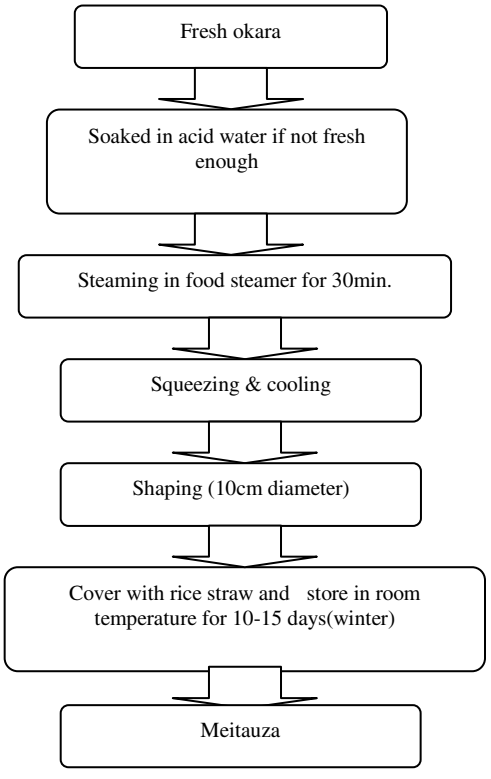
Fresh okara
Soaked in acid water if not fresh enough
Steaming in food steamer for 30min.
Squeezing & cooling
Shaping (10cm diameter)
Cover with rice straw and store in room temperature for 10-15 days(winter)
Meitauza

Fig. 1. Traditional process of meitauza fermentation

3 Results

3.1 The Changes of Microbial Flora of Meitauza Fermentation

The changes in the microbial flora of meitauza fermentation are shown in Fig. 2. During the the first 2days, *Z.mobilis* numbers easily reached 10.4 log, and stayed above 10 log in the later days. *A. elegans* cfu number was measured, showing spore mature and released during the 3rd day of the fermentation. No necessarily relation to the mucor's growth condition were suggested. Separate cultures of okara were examined simultaneously, the result showed that the two microbe did not inhibit nor promote each others' growth.

3.2 General Chemical and Physical Analysis

Fig 3 shows the changes of pH changes, moisture content and protease activities. The pH rose from 6.3 to 8.1 during the first 4d of fermentation and changed in a narrow level around 7.9. The moisture content dropped steadily from 85.8% to 74.5% resulted

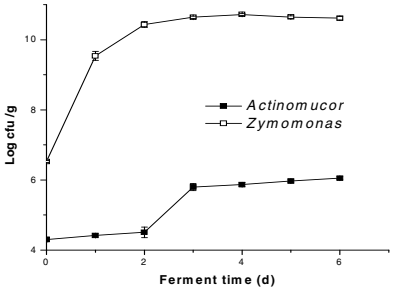

Fig. 2. Microbial flora during the fermentation Values represent the means + standard deviation (SD) of n = 3 replicate assays

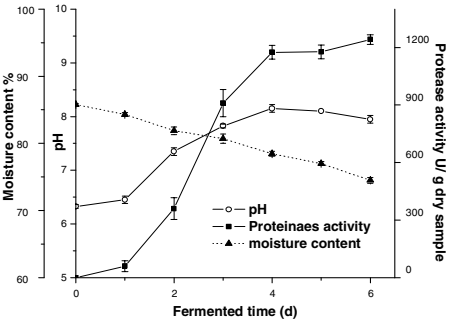

Fig. 3. pH, protease activities, moisture change during the fermentation. Values represent the means + standard deviation (SD) of n = 3 replicate assays

from the open fermentation. The protease activities was low in the first 36h as the absence of protease in *Z.mobilis*, and then rose rapidly to1175 U/g during 2^{nd} to 4^{th} d while the okara was covered with luxuriant hypha, and remained high until to the end of fermentation.

Fig 4 shows the changes of α-amino nitrogen (AAN) and crude protein. The main production of α-amino nitrogen content took place after 2^{nd} d, and then rose to 6.52 mg/g in 5^{th} d, and reached maximum to 6.78 mg/g in the 6^{th} d, and the curve was similar to the protease activities (Fig.6).As a result of metabolism of the microbe, the ANN production and consumption gradually reached a balance in the last days of fermentation. The soluble protein had a steep change in the 3^{rd} d, and remained a stable level at 6.78%. Under the interaction between microbes and open fermentation, the crude protein dropped rapidly from 23.1% to 17.15% in the form of ammonia.

Significant increase in total free amino acids were observed during the meitauza fermentation (Tab.1). Compared with fresh okara, the strong-tasting amino acids, such as Glu and Gly had greatly increased over 10 fold, Asp, Ala and Arg also increased

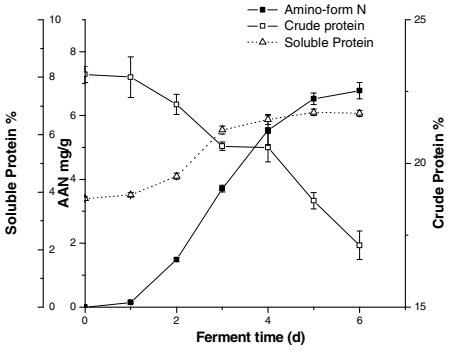

Fig. 4. α-amino nitrogen, crude protein and soluble protein change during the fermentation. Values represent the means + standard deviation (SD) of n = 2 replicate assays

Table 1. Changes in free amino acids (mg/100g) in meitauza fermentation

Time/d	0	3	6
Asp	75.6	77.4	290.22
Glu	69.22	436.11	1048.41
Ser	33.62	153.97	182
Gly	18.56	42.23	164.17
His	59.18	148.3	85.04
Arg	72.81	46.93	125
Thr	124.13	49.94	167.62
Ala	71.22	148.52	450.29
Pro	29.06	156.51	141.07
Tyr	35.11	55.69	117.54
Val	36.03	57.44	199.63
Met	4.08	18.67	42.68
Cys	/	2.45	5.70
Ile	25.87	29.71	132.70
Leu	68.16	44.05	223.33
Phe	38.01	48.59	123.28
Lys	102.67	124.76	167.88
Total	836. 29	1641.3	3666.55

several-fold; the sweetening amino acids, such as Leu, Val, Ser, Met also increased folds. Those total free amino acids spell abundant fresh sweet flavor, greatly increased the taste and nutrition of meitauza.

3.3 Texure Analysis of Meitauza Fermentation

Fig. 5 shows the 0-6 day fermented okara texure analysis graph on Texture Expert. Fig.6 shows three of the analysis result using the Texture Expert software: the hardness

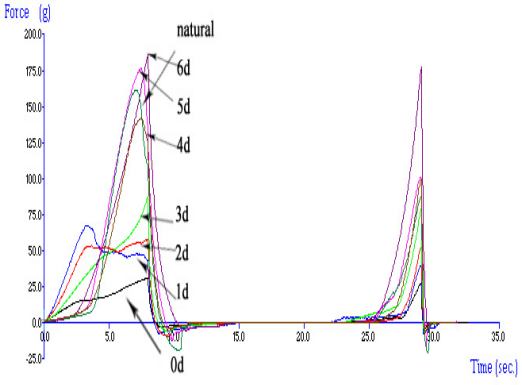

Fig. 5. 0-6d TPA curves of meitauza in Texture Expert analysis

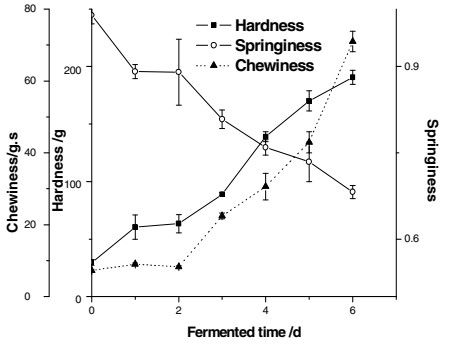

Fig. 6. Hardness, springiness and chewiness change during the fermentation. Values represent the means + standard deviation (SD) of n = 2 replicate assays

increased significantly in the 4th d and reached maximum at 186.253 g in the 6th d while the natural samples have an average of 160g. Chewiness increased quickly in 3rd to 4th d, changing from 7.269 to 68.594g.s and the natural samples were about 40g.s. The springiness dropped steadily from 0.979 to 0.700 in the fermentation, natural samples were only around 0.500. Fracturability, adhesiveness, cohesiveness, and resilience did not show any regular patterns (data not shown). The hardness and chewiness data shows the mycelia of *A.elegans* began to grow rapidly inside the okara in the 3rd to 4th d, combining the small particles of okara to integrity meitauza. Decrease in crude protein and moisture (Fig.3 and Fig.4) content have a relation to the drop of springiness.

4 Discussion

Various microbes are always involved in fungi fermented soy bean products: lactic acid bacteria(LAB), entero-bacteriaceae, other filamentous fungi or yeast were found in

commercial tempeh and sufu(Xin Mei Feng, 2005). LAB and Bacillus are common in rice straw in a natural environment but barely found in the final product meitauza in the condition of low fermented temperature (below 18℃) and long time fermentation (over 10d). And the product fermented by *Bacillus subtilis* B2 in Zhu' studies (2007) was more than a natto-like product but not meitauza.(O'Toole, 1999; Matsumoto and Take,1980).

Kronenberg & Hang (1984) isolated a strain of *Actinomucor elegans* from meitauza and tested the first pure culture in okara under 15°C for 80h, they found that an acid protease was produced as well as ammonia and non-protein nitrogen increased significantly. A texture analysis was used to monitor the degree of mycelia growth during meitauza fermentation, the studies showed that mycelia growth increased the firmness during fermentation. Zhu et al,(2007) applied *Bacillus subtilis* B2 isolated from meitauza to a pure fermentation of okara at 40°C for 24h. This product was similar to the "okara-natto"(Matsuo, 1980) and shown an increase of protease activity and antioxidant activity during, fermentation.

Generally, the finished fermentation of natural meitauza is decided by experience, expert producers(Li runsheng, 1985) make a judgment that whether meitauza product is mature with the changes of its texture and smell. As a result of chemical and physical analysis, the termination of pure cultured meitauza fermentation was set at 6d when most parameters are equal or higher than the natural samples (10-14d fermentation). Together with the data of texture analysis,

As description of the literature reported by Kronenberg and Hang(1984), with only *A. elegans* incubation for 70h, pH raised from 5.48 to 7.50, 8-fold increase in non-protein nitrogen and an acid protease was produced while in this co-cultivation studies, pH changed from 6.50 to 7.95, 4.5-fold increase inα-amino nitrogen and double in soluble nitrogen.

Meitauza has been used as a model for studying solid-state fermentation with an Instron universal testing machine and a Chatillon hand operated force gauge (Kronenberg and Hang, 1985). In their previous study, hardness increased in the 30h and 70h reached a maximum force about 1.2N(peak value, about 122g), while the meitauza fermented by our lab has a hardness about 87.960g at 72h, and about doubled in the next 48h. Texture characteristics show the mycelial growth without crust formation significantly caused increase in hardness and chewiness and decrease in springiness. Also, the force measurements could be used to monitor the degree of meitauza fermentation.

Acknowledgment. I am most grateful to Professor Mouming Zhao and Professor Jian Chen for their supporting this project. Thanks for Ms. Wenjuan Wu and Qin Chen for their works to project.

References

1. Toole, O., Desmond, K.: Characteristics and Use of Okara, the Soybean Residue from Soy Milk Production-A Review. Journal of Agricultural and Food Chemistry 47(2), 363–371 (1999)
2. Matsumoto, H., Take, T.: Studies on the utilization of tofukasu (okara). II. Selection of Bacillus natto strain. Mem. Fac.Educ., Niigata Univ., Nat. Sci. (22), 53–63 (1980)
3. Cao, S.: High cellulose healthy food—preparation of meidauza. Liangshi yu Youzhi(Chn) (01), 22–24 (1994)
4. Zhu, Y., Fan, J., Cheng, Y., Li, L.: Improvement of the antioxidant activity of Chinese traditional fermented okara (Meitauza) using Bacillus subtilis B2. Food Control 19(7), 654–661 (2008)
5. Kronenberg, H., Hang, J.: Biochemical changes in oakra during meitauza fermentation. Nutrition Reports Internetional 30, 439 (1985)
6. Xin, M., Anders, R., Eriksson, B., Schnürer, J.: Growth of lactic acid bacteria and Rhizopus oligosporus during barley tempeh fermentation. International Journal of Food Microbiology (249), 249–256 (2005)
7. Matsuo, M.: Preparation and components of okara-ontjom, a traditional Indonesian fermented food. Nippon Shokuhin Kagaku Kogaku Kaishi 44, 632–639 (1997)
8. Li, R.: Research report of technology of meidauza. Shipin Kexue(Chn) (09), 43–46 (1982)
9. Matsuo, M.: Morphological, compositional and physicochemical properties of “okara” fermented by Aspergillus oryzae. J. Agric. Chem. Soc. Jpn. 63, 1765–1770 (1989)
10. Khare, S., Jha, K., Gandhi, A.: Physicochemical and functional properties of okara protein isolate. Dairying, Foods Home Sci. 12, 132–136 (1993)

An Evaluation Method of Marine Water Quality Based on Cloud-Model Chart Representation Theory and Its Role in Tourism of Coastal Cities

Wang Lu[1], Wang Yueru[2], and Li Xin[2]

[1] Department of Tourism, College of Economics Management University of Yanshan Qinhuangdao, Hebei Province 066004, China
[2] Department of Biomedical Engineering, University of Yanshan Qinhuangdao, Hebei 066004, China
{lwang,yddylixin}@ysu.edu.cn, yvonne827@yahoo.cn

Abstract. The quality of marine water is an important factor of developing the tourism in coastal cities. The existing marine water quality evaluation methodologies are simple quantitative assessment or qualitative evaluation, which didn't fully reflect the substance of fuzziness and randomness. In this paper, we proposed a method that mixes the chart representation theory and the cloud model theory, by the use of visualization of chart representation theory and qualitative/quantitative information conversion of Cloud Model theory, to solve the key problem in marine water quality: how to obtain the comprehensive evaluation result. It was also applied in evaluating the marine water quality around Qinhuangdao as an example and the results show that comprehensive evaluation results are more in line with the distribution of actual data, and it is believed that this effective method will provide useful data and theoretical support in the development of tourism in coastal cities.

Keywords: Quantitative/Qualitative information transform, Multi-used radar chart, Cloud-model, Quality assessment.

1 Introduction

Tourism is economic lifeline of the coastal cities, however, with the development and utilization of marine resources, in particular sewage, industrial and agricultural wastewater and expanding aquaculture wastewater, Coastal marine ecological environment is worsening. The marine area around Qinhuangdao has become one of the most polluted area of China's off-shore [1-2]. So how to protect marine resources, and to promote the sustainable development of marine economy has become one of the most concern issues in economic development.

Evaluation of water quality is a special problem, which makes an overall evaluation for a complex system with multiple indicators, that is, making a global and holistic assessment for the object system with multiple attributes architecture description. The results using existing marine water quality evaluation methods are always simple quantitative assessment or qualitative evaluation, which didn't fully reflect the substance of fuzziness and randomness. It has always been a hot issue on how to obtain

E. Zhu and S. Sambath (Eds.): Information Tech. and Agricultural Eng., AISC 134, pp. 337–344.
springerlink.com © Springer-Verlag Berlin Heidelberg 2012

the comprehensive evaluation result combined qualitative and quantitative evaluation, which gets in line with the human's thinking mode [3-4].

To solve the above questions, this paper proposed a method that mixes the visual chart representation principle and the cloud-model. The powerful function of quantitative and qualitative information transformation of cloud-model and the visualization of chart representation theory were used richly.

Cloud-model is an uncertainty convert model with qualitative and quantitative conversion, which is gradually improved after academician Li Deyi proposed "the discovery state space theory" and "the cloud and language atomic model". The theory of the traditional membership functions was expanded, and a series of cloud technologies with the core of cloud-model were formed [5].

Chart, as a means of analysis and evaluation, is deeply enjoyed by many people because it can vividly and visually reflect the quantitative relation among different things and facilitate the search for the law and nature of things.

2 The Cloud Model Evaluation Method Based on the Multiple Graphics Features

2.1 Chart Representation Theory

Chart representation and analysis of multivariate data are very important ways in multivariate statistical analysis. This method could use not only graphics but also the mathematical expression and graphic shapes of geometrical graph to express the useful information [4]. It is a brand-new way that uses the chart representation method, which is based on the multi-dimensional data, to study the quantitative and qualitative information transformation in the engineering field.

Multiplex radar chart was used in comprehensive evaluation. It means that in an evaluation system, we can map the multiple evaluation indicators onto a 2D figure. Thus it was convenient to study the relationship among sample points .And by calculating some statistic, we can find out the main characteristic and graphically mixes each characteristic quantity together. In this way, we can make comments on the objects.

Multiplex radar chart's basic ideas are: (1) Make a circle and divide the circumference into P equal parts; (2) Link the center to each equinox. These P bar radius are defined as coordinates of each variables in turn, and marked with appropriate scale; (3) For a given observed value, position the P variable values respectively in the corresponding coordinates. Then link them into a p edge form; (4) According to the n times' observed values, we can draw n P edge shape. The typical Multiplex radar chart is shown in Fig 1.

2.2 Visualization Quantitative Evaluation Method Based on Chart Representation Theory Simulation and Analysis

First of all, normalize each basic index, as in (1). Transform each index to values whose mean value is 0, variance of 1.

$$x_{ij}^{'} = \left(x_{ij} - \overline{x_j}\right) \Big/ \sigma_j \tag{1}$$

x_{ij}: x_{ij} is the measured value of i, which belongs to index j of a specific sea area;

$\overline{x_j}$: $\overline{x_j}$ is the mean of index j.

σ_j: σ_j is the standard deviation of index j.

x_{ij}': x_{ij}' is the value after standardization.

After normalization, make the basic index $x_{ij}^{'}$ nonlinear transformation as follows

$$y_{ij} = \frac{2}{\pi} ty^{-1}(x_{ij}^{'}) + 1 \tag{2}$$

This transformation makes the transformation, which is near the mean value, have a better linear transformation, and the farther the mean deviates, the stronger the compressibility of the transformation was [6]. Infinite interval were transformed to limited interval [0, 2], mean value were from 0 to 1.

We could use the sea area around Beidaihe in Qinhuangdao as an example to evaluate the Radar Chart, as it shows in Fig 2. In the figure, the part that surrounded by the first broken line shows the marine area in good environment, the part that between the first broken line and the second belongs to the area in mild pollution. Ordinal analogy respectively, moderate pollution area, severe pollution area, gross pollution area. The dotted curve means the pollution level of the area.

From Fig 2, we could get the situation of marine water quality parameters vividly. In general, the sea water in this area is in mild pollution.

Chart Representation theory complete the quantitative evaluation of visualization intuitively. Combined cloud theory with the qualitative information and quantitative information, it can show the comment of the point index, and offer evaluation results correspond with the person's thinking mode.

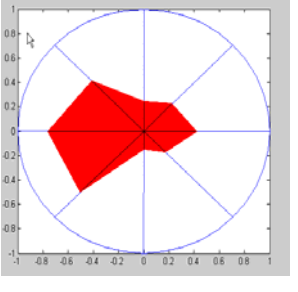

Fig. 1. Radar chart

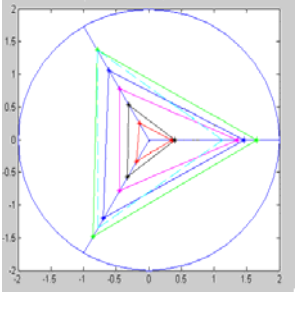

Fig. 2. Radar chart of pollution level

2.3 Natural Language Expression Based on Cloud Model

2.3.1 The Basic Concept of the Cloud

The cloud is a kind of uncertainty transformation model which is described by the linguistic value between some qualitative concept and its numerical representation. The cloud are composed of cloud droplet, the overall shape reflect important characteristics of qualitative concept. Cloud droplet is a quantitative description of qualitative concept, the generating process of cloud droplet shows the uncertainty mapping between qualitative concept and quantitative value.

The shape of membership cloud reflects the overall characteristic and regularity when largely uses membership value [3], it has been testified that:

(1) The expectation curve of the membership cloud, which reflects the fuzziness of fuzzy concept, shall obey normal distribution;
(2) Points on the membership cloud, which reflects the randomness of membership, obey the normal distribution which takes the corresponding points on membership cloud expectation curve as expectation;
(3) Variance that reflects the regularity of thickness variation of membership cloud obeys the two and a half normal distribution.

2.3.2 The Digital Features of Cloud

The digital characteristics of the cloud are represented by three values: the expected value Ex, entropy En, hyper entropy He.

A cloud model is based on Gaussian function and express the fuzziness of the concept of numerical range by entropy, and embody the magin of the fuzziness of qualitative concept; Hyper entropy represents the discrete degree of cloud droplet.

The figure feature of cloud-model completely gathers the fuzziness and randomness to constitute a mapping between qualitative and quantitative which reflects the quantitative characteristics of qualitative knowledge, as shown in Fig 3.

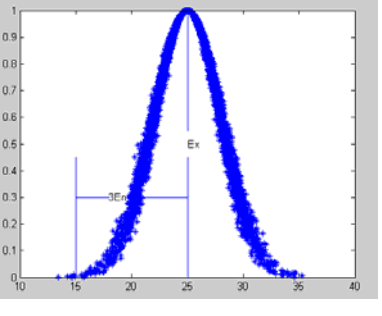

Fig. 3. Membership cloud and numeric characteristics

2.4 The Cloud Model Theory Based on the Multi-variable Graph

The cloud model theory based on the multivariate graph characteristic is shown in Fig.4:

First, extract the graphical features, and then mix the multivariate data and reduce dimensions. Take the extracted characteristics as basic variables, and build the

linguistic values which were used to describe system evaluation. Adopt positive cloud system to make the fuzzy evaluation and use reverse cloud to analyse the basic indexes, thereby obtain evaluation results which conform to the human thinking mode.

2.4.1 The Conversion Process of Qualitative and Quantitative Based on Cloud Model

We can use different directions and different kinds of cloud models to process the evaluation of qualitative variables and quantitative variables with different characteristics [7].

(1) Cloud transform of variable

The essential of the variable cloud-based is the normalized process of qualitative variables and quantitative variables, and it is the prerequisite for the qualitative and quantitative conversion.

① If the quantitative variables have the lower and upper bounds, just like $[B_{min},B_{max}]$, it becomes the forward direction cloud model. We can use the mid-value of the constraints as the expected value and use the cloud whose major region has bilateral constraints to approximate this quantitative variable. The calculation formulas of the cloud parameter are (3):

$$\begin{cases} Ex=(B_{min}+B_{max})/2 \\ En=(B_{max}-B_{min})/6 \cdot \\ He=k \end{cases} \tag{3}$$

K is a constant, which can adjust itself according to the degree of the fuzzy threshold of variables.

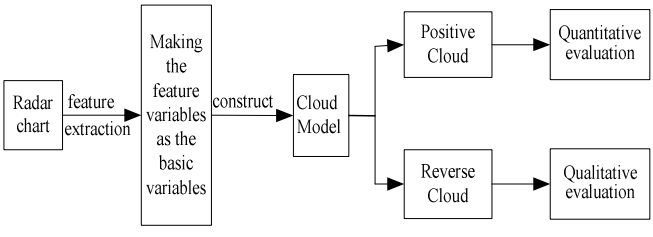

Fig. 4. Cloud model theory based on the multi-variable graph

For the quantitative variables with one bounded, such as $[B_{min}, \infty]$ or $[-\infty, B_{max}]$, we can determine its default boundary parameters or expectations depending on the upper or lower maximum of the test data, and then calculate the cloud parameter according to (3).

② Cloud transform of qualitative variable

Qualitative variable were often assigned with natural language described comments by experts. Each expert can set the experience numerical characteristics for each qualitative variable according to their own understanding to form comments cloud-model, the qualitative variable of N experts with N cloud models can be characterized by an integrated cloud, and the calculation of its numeric characteristics as in (4):

$$\begin{aligned} E_x &= \left(E_{x1} * E_{n1} + E_{x2} * E_{n2} + ... + E_{xn} * E_{nn}\right) / \left(E_{n1} + E_{n2} + ... E_{nn}\right) \\ E_n &= E_{n1} + E_{n2} + ... E_{nn} \\ He &= \left(He_1 * E_{n1} + H_{e2} * E_{n2} + ... + H_{en} * Enn\right) / \left(E_{n1} + E_{n2} + ... + E_{nn}\right) \end{aligned} \tag{4}$$

(2) Construct the cloud ruler

Put the results of the quantitative and qualitative cloud transformation in unified coordinate system and make it the cloud ruler. The cloud cluster of the cloud ruler constitute qualitative or quantitative activation interval. On any time T, qualitative or quantitative inputs select conversion cloud-model by activating the corresponding section of the cloud model.

As for a specific qualitative or quantitative variable input, cloud ruler may have two activation ways: (a) when the degree of the activation in one section is much higher than other sections (When the absolute value of the difference is greater than a given thresholdγ), the cloud model in this interval may be selected out. (b) when activating clouds in two intervals, and the difference is not very big (When the absolute value of the difference is smaller than a given thresholdθ), we can use the principle of integrated cloud theory to integrate the approximate cloud and construct a available cloud model.

(3) Construct the rules generator

We can construct the qualitative rules generator for qualitative input process according to the different X conditions structure. When the entered particular input value X= x_{ij} stimulates the single-rule generator, each generator generates a random value Y_j. These values reflect the activation of the single-rule generator inputs x_{ij} to the qualitative rules (membership). It can be interpreted as the activation intension of the corresponding interval in the cloud ruler. Choose the maximum $Y_{\max}$ of Y_j, which indicates that this qualitative rule has the highest rate of support, and it can be chosen as the precedence rules. $Y_{\max}$ control CGY_j which corresponds with the output plane to generated the cloud droplets.

The process of quantitative input is a procedure of constructing a reverse cloud generator to generate a cloud model, and form a visual description to general characteristics of large amounts of data and feedback to the experts.

2.4.2 The Cloud Model Theory Based on Multiple Graphics Features

The data are derived from the monitoring data of off-shore area in Hebei province [8]. We use the sea area around Beidaihe in Qinhuangdao as the evaluation object. The main water quality monitoring projects are$\rho(COD_{Cr})$, ρ(DIN), $\rho(PO4^{3-}\text{-}2P)$, ρ(Pb), ρ(petroleum) and so on. According to the second standard in《The water quality standard of the People's Republic of China》 [9], we make an evaluation to the status quo of Hebei off-shore marine environment. On the basis of comprehensive evaluation, the classes of marine water quality are described as follows: fine (<1), mild pollution (1~2), moderate pollution (2~5), severe pollution (5~10) and gross pollution area (>10). We utilize the principle of cloud model chart expression to make an evaluation for current comprehensive environmental quality. First, according to basic items of different pollution degree, we draw radar map, then extract features. And select the area

as the characteristic parameter entirely, which can be used as the basis variable of tectonic cloud yardstick. Use qualitative and quantitative cloud model transformation ideas for conversion, according to the criterion of quantitative variable cloud, we make a quantitative variable cloud transformation, and located it into a coordinate system with the area for coordinate axis, then form the quantitative comment cloud ruler. It shows in Fig 5.

In the figure, from left to right, it shows the cloud model in fine (<1), mild pollution (1~2), moderate pollution (2~5), severe pollution (5~10) and gross pollution area (>10).

To evaluate the water quality around Beidaihe, we can get the area $x = 0.374$ by chart expression principle. By using the x conditional cloud simulating generator, we got three randomly generated value 'y', which represents the activated strength in corresponding interval to the cloud ruler, select the maximum value of 'y', we can determine the corresponding fine area. Then using reverse cloud we can obtain that the whole area around Beidaihe is between fine area and mild pollution area. (cloud in grass green.) As shown in Fig 6:

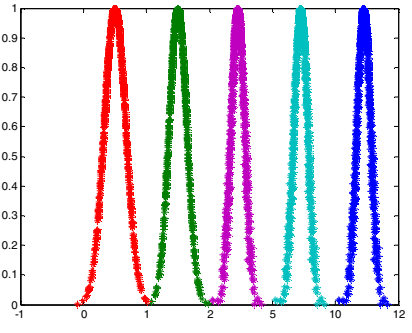

Fig. 5. Cloud rule of Marine water quality

The simulation results show that there is condensability on the expected value points described by the concept in the cloud model which used to evaluate. It is consistent with the basic principle when using vague language to evaluate directly and it is able to clearly reflect the degree of coverage of each language value. As for the same area, its membership has randomness and can reflect the diversity of the fuzzy evaluation.

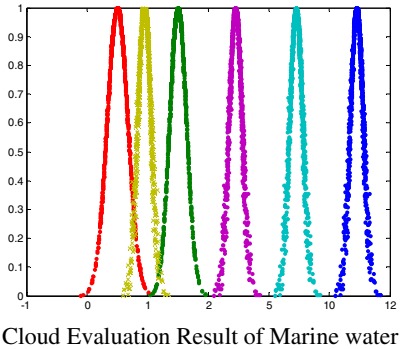

Fig. 6. Cloud Evaluation Result of Marine water quality

3 Conclusion

The main feature of the chart expression is intuitive. It maps the indexes to the 2D graphics. So we will get the image of the object vividly, and judge that the problems exist in which indexes. Cloud-model is an uncertain transformation model between a qualitative concept which was described with linguistic and its numerical representation. In this way, the assessment results not only keep the advantages of the traditional qualitative division, but also more conform to the actual data distribution and human's thinking mode. Combing the two methods together is an innovative, effective, quantitative and qualitative information transformation, which provides a valid path for the study of marine water quality evaluation and also offers reference to the development of tourism of costal cities.

References

1. Song, S.-Q., Huang, M.: The Environmental Problems and Countermeasures of Ocean Economy Sustainable Development in Hebei. Marine Development and Management (5), 7–11 (2007)
2. Wang, Y.-S.: Ocean Environment Situation and Fishery Resources Development Countermeasure in Hebei. Hebei Fisheries (9),1–3 (2006)
3. Hui, P.-S., Wong, L.-T., Mui, K.-W.: Evaluation of Professional Choice of Sampling Locations for Indoor Air Quality Assessment. Building and Environment 42(8), 2900–2907 (2007)
4. João, E.: A Research Agenda for Data and Scale Issues in Strategic Environmental Assessment (SEA). Environ Impact Asses Rev. (2007), doi: 10.1016/j.eiar, 02.009
5. Li, D.-E., Meng, H.-J., Shi, X.M.: Membership Cloud and Membership Cloud Generator. Computer Research and Development 32(6), 16–21 (1995)
6. Zheng, H.-L., Zhai, C.-L.D.: Comprehensive Evaluation Method Based on Radar Chart. Nanjing Postal College Journals 21(2) (2001)
7. Song, Y.-J., Li, D.-Y., Yang, X.-Z., Cui, D.-H.: Cloud Model Evaluation Method in Electronic Product Reliability. Journal of Electronics 12(12), 74–76 (2002)
8. Li, Z.-W., Cui, L.-T., Lin, Z.-J.: Marine Environment Quality Evaluation of Off-shore in Hebei. Research in Environment Science 21(6), 143–147 (2008)
9. State Environmental Protection Administration. GB3097—97 the Water Quality Standards, pp. 654–658. China Environmental Science Press, Beijing (1997)

The Qualitative Analysis of Generalized Kolmogorov Biological Population Model with Harvesting Rate

Zhang Jian

Department of science
University of Qiqihaer
Qiqihaer, Heilongjiang Province, China
zjqqhr@163.com

Abstract. The generalized Kolmogorov biological population model with harvesting rate is studied in this paper. It restrains the model by restricting the hypothetical conditions. By constructing Lyapunov function, the globally asymptotic stability of positive equilibrium of the model is obtained. This paper popularizes the conclusions of Kolmogorov biological population model and the distinguishing method in this paper is more succinct.

Keywords: generalized Kolmogorov model, biological population model, Lyapunov function, positive equilibrium, globally asymptotic stability.

1 Introduction

In the reality, many ecological phenomena may be expressed by Kolmogorov biological population model. To fully understanding the properties of Kolmogorov model has a practical significance in the research of population ecology. Much early work was only concerned with the way in which the properties of some predator-prey system under constant-rate harvesting and stocking. Even today, most simulation models developed for applications assume that the Kolmogorov biological population model with variable harvesting rate.

It is known that only stable equilibrium coexistence of predators and preys or extinction of predators is possible in the framework of the Kolmogorov biological population model with harvesting rate. Note that such models cannot describe the experimental observations that, with given values of system parameters, so a symptotic behavior of a singular transport equation modeling cell division is stuied.

Several authors have examined specific mathematical properties of the model, they use neural networks to analyse global asymptotic stability of delayed cellular. But a complete qualitative analysis of the generalized Kolmogorov biological population model with harvesting rate had not been achieved until now. This will be the purpose of this paper.

This paper studies the generalized Kolmogorov biological population model with harvesting rate. On the basis of existing results, it does the further expansion.

E. Zhu and S. Sambath (Eds.): Information Tech. and Agricultural Eng., AISC 134, pp. 345–352.
springerlink.com © Springer-Verlag Berlin Heidelberg 2012

2 The Kolmogorov Model

The Kolmogorov model has long been and will continue to be one of the dominant themes in both ecology and mathematical ecology due to its universal existence and importance. To the following model

$$\begin{cases} \dot{x} = xf(x,y) \\ \dot{y} = yg(x,y) \end{cases} \tag{1}$$

Many articles have deep research on this model, and obtain a lot of conclusions. Firstly, we'll study the following general Kolmogorov biological population model with variable harvesting rate.

$$\begin{cases} \dot{x} = xf(x,y) - xF(x) \\ \dot{y} = yg(x,y) - yG(y) \end{cases} \tag{2}$$

where x, y stands for prey and predator density at t moment, respectively. $F(x), G(y)$ stand for the variable harvesting rate to two populations.

According to the ecological significance of the model (2), we study the problem in the region $R = \{(x,y) | x > 0, y > 0\}$.

2.1 The Hypothesis of Model

(1) $f(x,y), g(x,y), F(x), G(y)$ all has first order continuous partial derivative.

(2) For functions $F(x), G(y)$,where $F(0) \neq 0, G(0) \neq 0$.

$F'(x) \geq 0$ as $x \geq 0$. $G'(y) \geq 0$ as $y \geq 0$.

(3) $f_y(x,y) < 0$ stands that the prey is restrained by the predator.

(4) $g_x(x,y) > 0$ stands that the predator is supplied by the prey.

(5) $f_x(x,y) < 0$ stands that the prey is density restriction.

(6) $g_y(x,y) < 0$ stands that the predator is density restriction.

(7) model exists constant $A > 0$ such that $f(0,A) = F(0)$

(8) model exists constant $B > 0$ such that $f(B,0) = F(B)$

(9) model exists constant $C > 0$ such that $g(C,0) = G(0)$

(10) Assumed that the growth of predator only dependent on the prey, so

$$yg(x,y) - yG(y) \leq \alpha[xf(x,0) - xf(x,y)] - \mu y$$

Where α, μ are positive constants. In the sign[ ], which stands the predator captures the quantity of prey in unit time. α stands the maximum digesting coefficient of the predator. μ stands the minimum death rate of predator.

2.2 Main Conclusion

Theorem 1. For model (2), the unique positive equilibrium (x_0, y_0) is asymptotic stability under the hypothetical conditions.

Proof. The model (2) has three equilibria, especially are $(0,0)$, $(B,0)$ and unique positive equilibrium (x_0, y_0).

According to the condition(2)—(9), every equilibrium corresponds to the different coefficient matrix.

$$\left|M_{(x_0,y_0)}\right| = x_0[f_x(x_0,y_0) - F'(x_0)]y_0[g_y(x_0,y_0) - G'(y_0)] - x_0y_0f_y(x_0,y_0)g_x(x_0,y_0) > 0$$

$$\left|M_{(0,0)}\right| = [f(0,0) - F(0)][g(0,0) - G(0)] < 0 \quad \left|M_{(B,0)}\right| = B[f_x(B,0) - F'(B)][g(B,0) - G(0)] < 0$$

However, the unique positive equilibrium corresponds to the trace of matrix is $trM_{(x_0,y_0)} = x_0[f_x(x_0,y_0) - F'(x_0)] + y_0[g_y(x_0,y_0) - G'(y_0)] < 0$

So the equilibria $(0,0)$, $(B,0)$ are not stable, so the positive equilibrium (x_0, y_0) is locally asymptotic stability.

Theorem 2. For model (2), the solutions which start from the first quadrant are all bounded under the conditions of the theorem.

Proof. By constructing a region in which all the path in the boundary do not cross the region, and out of the region the model does not exist the equilibrium. According to the convex and concave, we draw two isoclinallines.

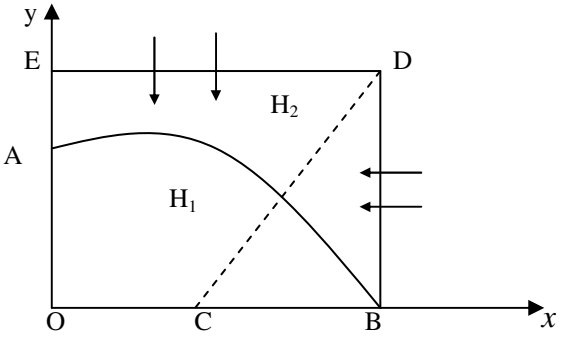

Fig. 1. Path Curve's Region of Model (2) Case 1

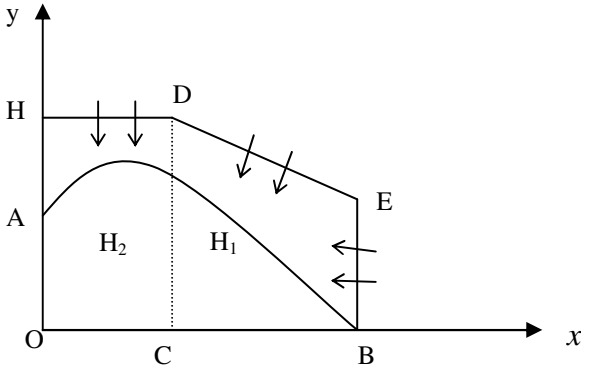

Fig. 2. Path Curve's Region of Model (2) Case 2

So the solutions which start from the first quadrant are all bounded.

Theorem 3. In the first quadrant, model (2) has no closed path curve.

Proof. Assumed Dulac function $B(x, y) = x^{-1} y^{-1}$,

$$\frac{\partial(BP)}{\partial x} = \frac{\partial}{\partial x}\{\frac{1}{y}[f(x, y) - F(x)]\} = \frac{1}{y}[f_x'(x, y) - F'(x)] < 0$$
$$\frac{\partial(BQ)}{\partial y} = \frac{\partial}{\partial y}\{\frac{1}{x}[g(x, y) - G(y)]\} = \frac{1}{x}[g_y'(x, y) - G'(y)] < 0$$
$$\frac{\partial(BP)}{\partial x} + \frac{\partial(BQ)}{\partial y} < 0$$

So by Dulac criterion, we known that the model (2) has no closed path curve in the first quadrant.

Theorem 4. In the first quadrant, the positive equilibrium (x_0, y_0) of model (2) is globally asymptotic stability.

Proof. According to the theorem 2, the solutions of model (2) which start from the first quadrant are all bounded. So any path curve which starts from the initial point does not run out of the rectangular region OBDE and OBEDHO. And in the first quadrant, the model (2) has unique positive equilibrium (x_0, y_0). Due to theorem 3, the model (2) has no closed path curve in the first quadrant. So the positive equilibrium (x_0, y_0) of model (2) is globally asymptotic stability.

3 The Generalized Kolmogorov Model

Next we'll study the following generalized Kolmogorov biological population model with harvesting rate

$$\begin{pmatrix} \dot{x} \\ \dot{y} \end{pmatrix} = \begin{pmatrix} X(x) & 0 \\ 0 & Y(y) \end{pmatrix} \begin{pmatrix} F(x, y) \\ G(x, y) \end{pmatrix} - \begin{pmatrix} \varphi(x) \\ \psi(y) \end{pmatrix} \tag{3}$$

where x, y stands for prey and predator density at t moment, respectively. $\varphi(x), \psi(y)$ stand for the harvesting rate to two populations. The model (3) is the popularization of model (1). According to the ecological significance of the model (3), we study the problem in the region $R = \{(x, y) | x > 0, y > 0\}$.

We can simplify the model (3) into the next form

$$\begin{pmatrix} \dot{x} \\ \dot{y} \end{pmatrix} = \begin{pmatrix} X(x) & 0 \\ 0 & Y(y) \end{pmatrix} \begin{pmatrix} F(x, y) - f(x) \\ G(x, y) - g(y) \end{pmatrix} \tag{4}$$

Where

$$f(x)X(x) = \varphi(x), g(y)Y(y) = \psi(y)$$

Hence, we study the stability of model (4).

3.1 The Hypothesis of Model

(C1) $X(x), Y(y), F(x,y), G(x,y), f(x), g(y) \in C'$ or it satisfies Lipschitz condition, at most has finite removable discontinuous points.

(C2) $f'(x) > 0, g'(y) > 0$.

(C3 $F'_x(x,y) < 0, G'_y(x,y) < 0$ i.e. two populations all are density restriction. $F'_y(x,y) < 0$ stands that the prey is restrained by the predator; $G'_x(x,y) > 0$ stands that the predator is supplied by the prey.

(C4) model (4) has unique positive equilibrium (x_0, y_0).

(C5) $X(x), Y(y)$ are always positive.

3.2 Local Stability Analysis of Positive Equilibrium

Theorem 5. For model (4), the unique positive equilibrium (x_0, y_0) is locally asymptotic stability under the hypothetical conditions.

Proof. According to the hypothetical condition (4), the unique positive equilibrium satisfies

$$\begin{cases} F(x_0, y_0) = f(x_0) \\ G(x_0, y_0) = g(y_0) \end{cases}$$

So at the positive equilibrium (x_0, y_0), the model (4) corresponding to the coefficient matrix of linear system takes the form of

$$A_{(x_0,y_0)} = \begin{pmatrix} X(x_0)[F_x(x_0,y_0) - f'(x_0)] & X(x_0)F_y(x_0,y_0) \\ Y(y_0)G_x(x_0,y_0) & Y(y_0)[G_y(x_0,y_0) - g'(y_0)] \end{pmatrix}$$

According to the hypothetical condition (C2), (C3) and (C5), it is easy to see that the trace and determinant of matrix is

$$trA = X(x_0)[F_x(x_0,y_0) - f'(x_0)] + Y(y_0)[G_y(x_0,y_0) - g'(y_0)] < 0$$

$$\begin{aligned} |A| &= X(x_0)[F_x(x_0,y_0) - f'(x_0)]Y(y_0)[G_y(x_0,y_0) - g'(y_0)] \\ &\quad - X(x_0)F_y(x_0,y_0)Y(y_0)G_x(x_0,y_0) > 0 \end{aligned}$$

This shows that the positive equilibrium (x_0, y_0) is locally asymptotic stability.

3.3 Globally Asymptotic Stability Analysis of Positive Equilibrium

According to the hypothetical condition (C1), we can simplify the model (4) into the next equivalent form

$$\begin{pmatrix} \dot{x} \\ \dot{y} \end{pmatrix} = \begin{pmatrix} X(x) & 0 \\ 0 & Y(y) \end{pmatrix} \begin{pmatrix} \tilde{F}_x(x,y) & \tilde{F}_y(x_0,y) \\ \tilde{G}_x(x,y_0) & \tilde{G}_y(x,y) \end{pmatrix} \begin{pmatrix} x - x_0 \\ y - y_0 \end{pmatrix}$$

Where

$$\tilde{F}_x(x,y)=\frac{\int_{x_0}^{x}[F_x(x,y)-f'(x)]dx}{x-x_0}\equiv f(x,y)\le 0$$

$$\tilde{F}_y(x_0,y)=\frac{\int_{y_0}^{y}F_y(x_0,y)dy}{y-y_0}\equiv -f_2(y)<0$$

$$\tilde{G}_x(x,y_0)=\frac{\int_{x_0}^{x}G_x(x,y_0)dx}{x-x_0}\equiv g_1(x)>0$$

$$\tilde{G}_y(x,y)=\frac{\int_{y_0}^{y}[G_y(x,y)-g'(y)]dy}{y-y_0}\equiv g(x,y)\le 0$$

So the equivalent form is

$$\begin{pmatrix}\dot{x}\\ \dot{y}\end{pmatrix}=\begin{pmatrix}X(x) & 0\\ 0 & Y(y)\end{pmatrix}\begin{pmatrix}f(x,y) & -f_2(y)\\ g_1(x) & g(x,y)\end{pmatrix}\begin{pmatrix}x-x_0\\ y-y_0\end{pmatrix}$$

Where $f(x,y), g(x,y), g_1(x), f_2(y)$ are defined as mentioned above.

Under the hypothetical condition, model satisfies the next condition

(C1') $X(x), Y(y), f(x,y), g(x,y), g_1(x), f_2(y)\in C$, or at most has finite removable discontinuous points.

(C2') $f_2(y)g_1(x)\neq 0$

(C3') $[\frac{X(x)}{g_1(x)}][\frac{Y(y)}{f_2(y)}]\ge 0$.

(C4') $X(x)f(x,y)+Y(y)g(x,y)\le 0$.

(C5') $X(x)f(x,y)Y(y)g(x,y)\ge 0$.

where $X(x)f(x,y), Y(y)g(x,y)$ are not equal to zero at the same time.

Theorem 6. If model (6) satisfies the following conditions:

(1) The condition(C1')—(C5') as mentioned above.
(2) The model ensures the existence and uniqueness of solution to the initial value.
(3) The set $E=\{(x(t),y(t))\,|\,g_1(x)f(x,y)=0\cap f_2(y)g(x,y)=0\}$
has no else path curves exclusive containing the positive equilibrium (x_0,y_0).
(4) Function

$$V(x,y)=\int_{x_0}^{x}\left|\frac{g_1(x)}{X(x)}\right|(x-x_0)dx+\int_{y_0}^{y}\left|\frac{f_2(y)}{Y(y)}\right|(y-y_0)dy$$

Under the condition of $\forall x>0, \forall y>0$, it possesses infinitely great property with respect to.

So the positive equilibrium (x_0,y_0) is positively globally asymptotic stability in the first quadrant.

Proof. In the region $R = \{(x, y) | x > 0, y > 0\}$, constructing Lyapunov function

$$V(x, y) = \int_{x_0}^{x} \left| \frac{g_1(x)}{X(x)} \right| (x - x_0)dx + \int_{y_0}^{y} \left| \frac{f_2(y)}{Y(y)} \right| (y - y_0)dy$$

Due to the condition (1) and (4), we know that function V is a positive definite function, and has the property of infinitely great.

The derivative of function V with respect to t is

$$\frac{dV}{dt} = f(x, y)|g_1(x)|(x - x_0)^2 + g(x, y)|f_2(y)|(y - y_0)^2$$

According to the condition (1) and (3), so

$$\frac{dV}{dt} \leq 0$$

And the set

$$E = \left\{ (x(t), y(t)) \left| \frac{dV}{dt} = 0 \right. \right\}$$

has no else path curves exclusive containing the positive equilibrium (x_0, y_0).

So the positive equilibrium (x_0, y_0) is globally asymptotic stability in the first quadrant.

4 Conclusion

In this paper, the method of discussing the globally asymptotic stability of the equilibrium deduces the judging condition of Kolmogorov model, and has more general practicality. The model (2) is the particular form of model (3). If we study model (3) using qualitative analysis, it is more trouble which needs constructing closed region to judges the trend of path curve and needs more restrictive condition. If we study model (3) using constructing Lyapunov function, we only need to restrict the function and the conditions are weaker. So the research method is improved. At the same time, by means of the study of Kolmogorov model, in the condition of theorems, we can see by controlling the harvesting rate of the populations, not only retaining the ecological balance but also satisfying the need of people to capture the biological population.

References

1. Brauer, F., Soudack, A.C.: Coexistence Properties of some Predator-prey System under Constant-rate Harvesting and Stocking. J. Math. Biol. 12, 101–114 (1981)
2. Annik, M., Ruan, S.: Predator-prey Models with Delay and Prey Harvesting. J. Math. Biol. 43, 247–267 (2001)
3. Kuznetsov, A., Rinaldi, S.: Remarks on Food Chain Dynamics. Math. Biosci. 134, 1–33 (1996)

4. Adimy, M.: A symptotic behavior of a singular transport equation modeling cell division. Discrete Continuous Dynamical Systems 3, 439–456 (2003)
5. Castillo-Chavez, C.: Mathematical Approaches for Engineering and Reemerging Infectious Diseases, Models, Methods, and Theory, pp. 183–201. Springer, New York (2002)
6. Arik, S.: An analysis of global asymptotic stability of delayed cellular neural networks. IEEE Trans. Neural Networks 13, 1239–1242 (2002)
7. Guan, Z., Chen, G.: On the equilibria, stability, and instability of Hopfield neural networks. IEEE Trans. on Neural Networks 11, 534–540 (2000)
8. Zhao, H.: Global asymptotic stability of Hopfield neural networks involving distributed delays. Neural Networks 17, 47–53 (2004)
9. Zhang, Y.: Absolute periodicity and absolute stability of delayed neural networks. IEEE Trans. Sys. I. 49, 639–651 (2002)
10. Wood, S.N.: Instability in mortality estimation schemes related to stage-structure population models. IMA J. Math. Appl. in Medical and Biology 6, 47–68 (2006)

Adaptive Ideal Image Reconstruction for Bacteria Colony Detection*

Anan Liu[1,**], Zheren Liu[2], Limin Song[2], and Dong Han[1]

[1] Department of Electronic Information Engineering, Tianjin University, Tianjin 300072, China
[2] Qiqihar Environmental Monitoring Center Station, Heilongjiang Province, 161005, China
anan0422@gmail.com

Abstract. This paper proposes am adaptive ideal image reconstruction method for bacteria colony detection. The philosophy of the proposed method lies in converting the problem of bacteria colony detection into image segmentation. Different from the traditional ways of image segmentation that the key point is threshold selection, this method focuses on reconstructing ideal bacteria colony image by eliminating the bias of illumination. Especially, in the reconstructed ideal image bacteria regions correspond to high intensity parts and the backgrounds lie in relatively low intensity parts. Therefore the reconstructed image can be conveniently binaried with Ostu's method and bacteria colony can be easily detected. Large-scale experiments show the accuracy and efficiency of the proposed method.

Keywords: Image reconstruction, segmentation, morphology, bacteria, colony.

1 Introduction

With the development of computer science, computing technology has penetrated into multiple fields of other subjects, especially biomedical domain. It can provide high capability of digital signal acquisition, processing, transmission, and storage due to its high capability of computation and storage. Therefore, the interdisciplinary between these two hot fields can greatly facilitate the biomedical knowledge discovery and research methodology improvement. Plate-based bacteria colony detection method has been widely used for bacteria counting under multiple circumstances, like colony counting for environmental monitoring, food test and so on. However, the current human-based method is extremely time-consuming. Moreover, this highly subjective method always leads to low robustness depending on age, experience and so on. Till now, there are only a few publications specified on automatic colony detection. We can classify them in two classes depending on the philosophy of the algorithms: 1) considering the colony detection as object recognition [1-4]. This kind of methods usually extracts colony features, like color, texture, and shape, and then learns a

* This work is partially supported by the Tianjin Research Program of Application Foundation and Advanced Technology (10JCYBJC25500), Doctoral Fund of Ministry of Education of China (20090032110028), National Natural Science Foundation of China (60976001), Qiqihar Science and technology projects, and Innovation Foundation of Tianjin University.
** Corresponding author.

E. Zhu and S. Sambath (Eds.): Information Tech. and Agricultural Eng., AISC 134, pp. 353–360.
springerlink.com © Springer-Verlag Berlin Heidelberg 2012

classifier to identify the interested region as colony or not. However, researchers usually need to spend lots of time to prepare a large amount of samples for model training and moreover the drastic changes of colony color, texture, and shape will bring much difficulty for model learning; 2) considering the colony detection as image segmentation[5-9]. The current methods usually select the global thresholds, block-based local thresholds or domain knowledge based thresholds. Therefore this kind of methods usually has limitation in large scale application due to the difficulty in optimal threshold selection. In conclusion, the state-of-art methods face two difficulties: 1) reducing the burden of the sample annotation by human; 2) reducing the dependency on threshold selection. Then we can extent the generalization of the algorithm for practical application.

To solve the problems above, we propose an adaptive bacteria colony detection method based on ideal image reconstruction. The philosophy of the proposed method is to convert the input image into ideal one by eliminating the bias of the illumination when the images are captured under different conditions. In the reconstructed image, colony regions correspond to the high intensity regions while the intensity of backgrounds approximates zero. Consequently, the intensity difference between the two clusters of pixels is so high that we can simply use the global thresholding method, Otsu's algorithm [10], to binarize the image. The superiority of the proposed method has three aspects: 1) The proposed method can recover the uniform illumination distribution and therefore can reconstruct ideal image for convenient segmentation; 2) Different from the learning-based frameworks, this method depends on the intrinsic image attributes but not huge amounts of annotated samples; 3) The method does not depend on ad-hoc threshold or prior knowledge and has high generalization. Large scale experiments demonstrated the accuracy and robustness of the propose method.

The remainder of the paper is organized as follows. In Section 2, we introduce the ideal image reconstruction in detail. Then, the bacteria colony detection framework is presented. Moreover, experimental results are illustrated in Section 4. At last, the conclusions and future work are stated.

2 Adaptive IDEAL Image Reconstruction

Fig1 (a) shows the original colony image. Although it seems that the colony region, say foreground, can be easily discriminated from background by human, we can obviously find that the illumination distribution of the background is unbalanced due to the imaging system and multiple external factors in Fig.1 (b). Take the grayscale of the blue line in Fig.1 (a) as an example. Fig.1 (c) shows the grayscale of the pixels along the line. It is perceptive that we can not simply segment colony region from background with global or local thresholding method because of the unbalanced illumination.

To facilitate image segmentation, we proposed to reconstruct the ideal image in which the background gray is even and approximates to zero while the contrast between foreground and background is as high as possible. Considering the computational complexity, we implemented the morphology-based method, *H-dome* [11] to simulate the unbalanced background. Them we can get the reconstructed image by subtracting the simulated background from the original image. The *H-dome* method will be introduced as follows.

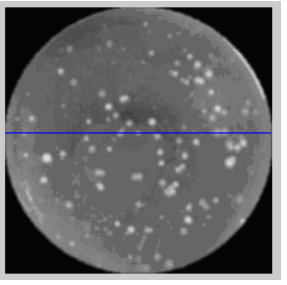

(a) Orignal Image

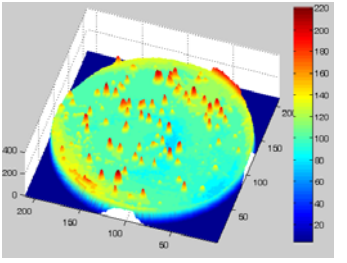

(b) 3D show of the original Image

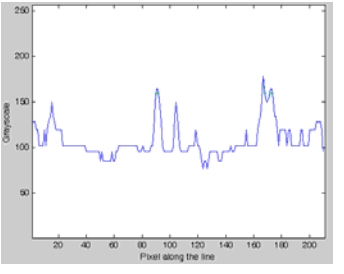

(c) Grayscale along the blue line in (a)

Fig. 1. Display of the grayscale of the colony image

H-dome

Assume I , J are two grayscale images. If $\forall p \in J, J(p) \le I(p)$, $J \le I$ is defined and in the context of grayscale reconstruction, we call image J , the marker image and image I , the mask image.

Another notion for reconstruction is geodesic distance. Geodesic distance was introduced in the framework of image analysis [12] and is at the basis of several morphological operators [13].

Given a set X (the mask), the geodesic distance between two pixels p and q is the length of the shortest paths joining p and q which are included in X.

In order to get a better understanding of grayscale geodesic dilation, we first introduce binary geodesic dilation.

Let $X \subseteq \mathbb{Z}^2$,X be a discrete set of $\mathbb{Z}^2$ and $Y \subseteq X$. The geodesic dilation of size $n > 0$ of Y within X is a set of pixels of X whose geodesic distance to Y is smaller or equal to n :

$$\delta_X^n(Y) = \{ p \in X \mid d_X(p, Y) \le n \} \tag{1}$$

Here $Y \subseteq X$ is defined as: assume two binary image I , J , if

$$\forall p \in J, J(p) = 1 \Rightarrow I(p) = 1 \tag{2}$$

Y is included in X, denote as $Y \subseteq X$.

Grayscale geodesic dilation is the arithmetic operation on pixel values, while the binary geodesic dilation is the operation on sets of points. Grayscale geodesic dilation of a given size n can be obtained by iterating n elementary geodesic dilations

$$\delta_I^n(J) = \underbrace{\delta_I^1(J) \circ \delta_I^1(J) \circ \cdots \circ \delta_I^1(J)} \tag{3}$$

where $\delta_I^1(J)$ is the elementary geodesic dilation. The elementary geodesic dilation can itself be obtained via a standard dilation of size one followed by an intersection

$$\delta_I^1(J) = (J \oplus B) \wedge I \tag{4}$$

Where $\wedge$ denotes the point-wise minimum and $J \oplus B$ is the dilation of J by flat structuring element B. The grayscale reconstruction $\rho_I(J)$ of I from J is obtained by iterating grayscale geodesic dilation of J within I till stability arrives,

$$\rho_I(J) = \bigvee_{n \geq 1} \delta_I^{(n)}(J) \tag{5}$$

where $\vee$ stands for point-wise maximum.

3 The Framework of Bacteria Colony Detection

The proposed framework of bacteria colony detection is shown in Fig.1 below. The following sections will illustrate each step.

3.1 Pre-processing

Image preprocessing includes two parts, noise elimination and histogram Equalization.

The image energy is usually concentrated in the low frequency band and noise is mainly in the high frequency band. Therefore noise can be simply filtered by image smooth process. In our algorithm, Gaussian filter is adopted to eliminate noises in the high frequency band.

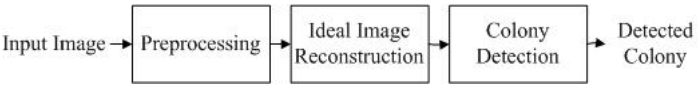

Fig. 2. The proposed framework

Histogram equalization can scatter the gray values evenly in the histogram. This operation can enhance the contrast especially when the image is captured under low illumination.

3.2 Ideal Image Reconstruction

With the *H-dome* method introduced in Section II, we can reconstruct the ideal image and rectify the unbalanced illumination distribution. The reconstructed image is shown in Fig.3 (b).

From Fig.3 (b), we can see that it is very convenient to extract regional maxima in the reconstructed image. A regional maximum M of a grayscale image I is a connected components of pixels with a given threshold h such that every pixel in the neighborhood of M has a strictly lower limit. Therefore, the regional maxima image $D_h(I)$ is computed as follows:

$$D_h(I) = I - \rho_I(I - h) \tag{6}$$

3.3 Colony Detection

This step consists of three parts, image segmentation, connected component extraction, and watershed-based post-processing.

The reconstruction image $D_h(I)$ can be considered as an ideal image with balanced illumination distribution shown in Fig.3 (b). Therefore, Otsu algorithm [10] can be implemented for adaptive image binarization. The result is shown in Fig. 3 (c).

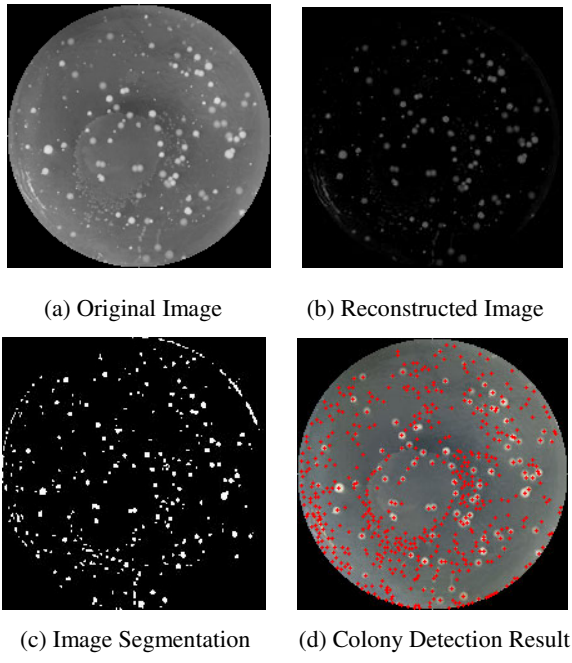

(a) Original Image (b) Reconstructed Image

(c) Image Segmentation (d) Colony Detection Result

Fig. 3. The key step of colony detection

The segmentation result in Fig.3 (c) can be scanned for connected components extraction. Ideally, each connected component denotes one colony. In reality, it may correspond to adherent colonies because it is common that several colonies may cluster together. Therefore, to increase the accuracy, we need to split them in fine level. To separate the connected colonies, we consider the intensity gradient image as

a topological surface. The watershed algorithm [14] can be applied to divide clustered colonies in the image just as water flood in a topographical surface.

With the process above, we can conveniently count the total number of visible colonies by adding up the number of the objects that have been identified as colonies. The colonies are marked with red dots in the image as shown in Fig. 3 (d).

4 Experimental Results

4.1 Dataset

To evaluate the robustness and effectiveness of the algorithm, we applied our algorithm on the prepared colony image dataset imaged with the samples of surface water. The surface water was from Nenjiang River in the northeast of China and the bacteria were cultured for 18-24 hours to ensure enough colonies in each petri dish. The data is divided into 3 groups according to the dilution factor, including 0.01, 0.1 and 1. The resolution of the images is 240*180. The intensity of the part surrounding the petri dish in each image can be automatically set to zero with a fixed size mask as shown the surrounding dart region in Fig.3 (a). Therefore the colony detection method can only implemented on the region of interest as shown in Fig.3 (a).

4.2 Evaluation

In the experiments, we evaluate the accuracy and efficiency of the proposed algorithm. For test, we randomly selected 5 images for each dilution, totally 15 images. Considering the challenge of the unbalanced illumination and high density, this dataset is enough for test.

For comparison, we get the ground truth by manual annotation by the well-trained technicians who have been working in this area for many years.

4.3 Accuracy

With the detection results in term of different dilution which denotes the colony density, the comparison between the automatic method and manual annotation shown in Table I demonstrate that the proposed method can achieve high average accuracy, 94.97%. This accuracy satisfies the real application in environmental monitoring.

4.4 Efficiency

From Table 2 we can get two important conclusions: 1) the speed of the proposed method is steady and colony-independent, about 34 ms/ image. The main reason is that the proposed method is implemented on the entire image and therefore its speed is related to the resolution but not the number of colonies; 2) the proposed method significantly improve the efficiency compared to manual annoation. The average ratio between manual counting and proposed method is 11770 and can increase drastically when the density get higher. The maximum time ratio can reach 54177 in our experiment as shown in TABLE 2.

Table 1. Accuracy

Dilution	NO	Detected	Ground truth	Error
0.01	1	19	19	0.00%
	2	16	17	5.88%
	3	25	26	3.85%
	4	11	12	8.33%
	5	21	22	4.55%
0.1	1	258	249	3.61%
	2	239	218	9.63%
	3	207	190	8.95%
	4	264	250	5.60%
	5	198	181	9.39%
1	1	1143	1123	1.80%
	2	1663	1566	6.19%
	3	1146	1133	1.08%
	4	1085	1135	4.35%
	5	2179	2131	2.25%

Table 2. Efficiency

Dilution	NO	Proposed method(**ms**)	Manually Counting(**s**)	Ratio(M/O)
0.01	1	37.91	20	527.57
	2	32.17	15	466.27
	3	37.15	30	807.54
	4	31.48	15	476.49
	5	35.51	25	704.03
0.1	1	30.88	270	8743.52
	2	29.34	225	7668.71
	3	35.51	220	6195.44
	4	35.44	260	7336.34
	5	32.49	230	7079.10
1	1	33.50	850	25373.13
	2	32.85	980	29832.57
	3	38.64	820	21221.53
	4	39.75	1070	26918.24
	5	31.92	1060	33208.02

5 Conclusion and Future Work

In this paper we propose am adaptive ideal image reconstruction method for bacteria colony detection. With this method, we can reconstruct the ideal colony image to rectify the illumination distribution of the captured images under different conditions. Especially, in the reconstructed ideal image bacteria regions correspond to high intensity parts and the backgrounds lie in relatively low intensity parts. Therefore the reconstructed image can be conveniently binaried with global thresholding method and bacteria colony can be easily detected. Large-scale experiments show the efficiency and robustness of the proposed method.

Although the proposed method has great superiority over previous methods, the parameter *h* plays an important role on ideal image reconstruction. The current adaptive strategy for *h* calculation could not perform perfectly when the contrast is not obvious enough or the illumination distribution is extremely uneven. For the future work we will formulate cost function and develop optimization algorithm to optimize the image reconstruction. Therefore the optimal reconstructed image will be obtained by setting iteration rules.

References

1. Jin, S.: Comparison between the Determination Results of Total Bacteria in Food of Machine Vision and Culture. Packaging and Food Machinery 27(4), 33–37 (2009)
2. Jin, S., Li, Y., Yin, Y.: Rapid detection of total number of bacteria in food using digital micro-image identification technique. Transactions of the Chinese Society of Agricultural Engineering 24(4), 177–180 (2008)
3. Yang, Y., Yao, C.: Study on Method of Automatic Identification and Aouncting of Bacteria Colonies on Plate. Chinese Journal of Disnfection 18(3), 141–144 (2001)
4. Ates, H., Gerek, O.N.: An Image-processing Based Automated Bacteria Colony Counter. In: 24th International Symposium on Computer and Information Sciences (2009)
5. Zhou, Y., Zeng, L.: A Method for Automatic Colony Counting Based on Image Processing and Its Realization. Journal of Data Acquistion & Processing 18(4), 460–464 (2003)
6. Wang, G., Zhang, C., Fang, J., et al.: Experimental study for automatic colony counting system based on image processing. China Dairy Industry 34(2), 40–42 (2006)
7. Men, H., Wu, Y., Wang, C., et al.: Study on Heterotrophic Bacteria Colony Counting Based on Image Processing Method. Study on Heterotrophic Bacteria Colony Counting Based on Image Processing Method 35(3), 38–41,45 (2008)
8. Chang, B.: Research on the Development of Colony Analysis System Based on Image Processing. Hebei Industry University (2008)
9. Reyna, M.-P.R., Josue, A.-B.: Color Correlation for the Recognition Vibrio Cholerae O1 in Seawater. In: Proceedings of SPIE, vol. 3749, pp. 586–587 (1999)
10. Ostu, N.: A threshold selection method from gray-level histograms. IEEE Transactions on System, Man and Cybemetics 6(3), 62–66 (1979)
11. Vincent, L.: Morphological Grayscale Reconstruction in Imgae Analysis: Applicatins and Efficient Algorithms. IEEE Transactions on Image Processing 2(2), 176–185 (1993)
12. Lantukjoul, C., Beucher, S.: On the use of geodesic metric in image analysis. Journal of Microscopy 121, 39–49 (1981)
13. Lantukjoul, C., Maisonneuve, F.: Geodesic methods in imageanalysis. Patt. Recognition 17, 117–187 (1984)
14. Luc, V., Pierre, S.: Watersheds in Digital Spaces: An Efficient Algorithm Based on Immersion Simulations. IEEE Trans. Pattern Anal. Mach. Intell. 13, 583–598 (1991)

Predicting SOC Concentrations in a Subtropical Mixed Secondary Forest Using Hemispherical Photography

Zhi-yao Su, Yu-duan Ou, and Dan-dan Xie

College of Forestry
South China Agricultural University
Guangzhou 510642, Guangdong Province, China
zysu@scau.edu.cn

Abstract. In order to detect the relations of canopy structure to surface soil organic carbon (SOC) concentrations, we carried out plant census, acquisition of hemispherical photographs and soil sampling in a secondary broadleaved forest in Deqing Sanchading Nature Reserve, Guangdong, China. SOC concentrations did not exhibit significant difference among the 5 plot groupings, though stand structure represented by mean tree height and mean diameter at breast height (DBH) had significant difference. Regression analysis indicated that a significant positive correlation existed between SOC concentration and leaf area index (LAI), while a significant negative correlation was found between SOC concentration and canopy openness (CO), direct transmitted gap light (TransDir), and diffuse transmitted gap light (TransDif), respectively. Findings from this study have implications for enhancing carbon sequestration by better management of forest and the results suggest that hemispherical photography can serve as a good means for predicting surface SOC concentrations under a forest canopy.

Keywords: SOC concentration, canopy openness, LAI, hemispherical photography.

1 Introduction

Soils represent the largest carbon reservoir of the terrestrial ecosystem and thus play a key role in the global carbon cycle. Soils store 1395 to 2200 Pg (1 Pg = 10^{15} g) carbon, approximately 2 to 3 times more carbon than the atmospheric carbon pool[1] and 2.5 to 3 times as much as that stored in vegetation[2]. Soils are also potential carbon source, with a flux estimated at 68~77 Pg C/yr by global soil respiration[3], more than 10 times the carbon emitted from fossil fuel combustion [4-5]. Therefore, a small change in the soil carbon pool will have a major impact on the atmospheric carbon dynamics.

Therefore enhancing carbon sequestration by forest soils through better forest management practices is widely recognized. Soil organic carbon (SOC) dynamics are affected by a variety of factors, including climate, topography, soil attributes, hydrology, and land use patterns[6]. Past studies indicated that, at small scales, SOC stock increases with precipitation and decreases with temperature[7]. Other studies

E. Zhu and S. Sambath (Eds.): Information Tech. and Agricultural Eng., AISC 134, pp. 361–369.
springerlink.com © Springer-Verlag Berlin Heidelberg 2012

yielded controversial results. Garten et al. observed that temperature is a primary controller of SOC dynamics at regional and global scales[8].

Forest forms a microclimate, in which the soil temperature is not only controlled by the ambient atmospheric temperature, but is also heavily influenced by canopy structural parameters and understory light regimes[9]. However, measuring understory light regimes and canopy parameters was once a formidable task using conventional methods. The emergence of hemispherical photography, a time-saving and cost-effective method that can make synchronized understory light monitoring, has made possible large-scale measurements of understory gap light[10].

In South China's Guangdong Province, deforestation in history due to rapid economic growth and population surge has left remnants of secondary forests in fragmented habitats. To stop this trend and to ameliorate the environment, vast ecological restoration projects have been carried out across the land in the past decades, including the setting up of protected areas, afforestation and reforestation, and withdrawal of tree felling for natural regeneration. Attention has been directed to ecosystem services provided by forest, including carbon sequestration for alleviating global warming[11-12]. In view of this, the forest sector seeks to increase carbon stock in both the forest soils and the forest itself through improved silvicultural techniques and forest management. Canopy structure and gap light regimes are possible modulators of forest understory biodiversity, soil temperature and other factors of the forest environment[13-14], which may affect soil respiration and the formation of organic matter. Therefore, to reveal the relations of forest soil carbon contents to canopy structure and understory will facilitate adjustment of forest canopy through reforestation, tending and tree species selection, which will possibly increase carbon sequestration.

The purpose of this study is to reveal the relations of forest soil carbon contents to canopy structure and understory gap light regimes, which will provide insights for adjustment of forest canopy through reforestation, tending, and tree species selection that will possibly increase carbon sequestration. To this end, we conducted field and laboratory research to acquire hemispherical photographs of the forest canopy and to collect plant and soil data using quadrat sampling method, in order to determine the relationships of understory surface SOC concentrations to canopy structure and gap light parameters, and to assess the spatial variability of understory soil SOC concentrations in response to the change of these parameters.

2 Methods

2.1 Site Description

Sampling plots were set up in Guangdong Zhaoqing Forest Monitoring Station (112°01′E, 23°26′N; average elevation: 500 m a.s.l.), which is located at Deqing Sanchading Nature Reserve, a municipal protected area for the conservation of forest ecosystem and wildlife in west Guangdong, covering a total area of 2044.2 hm^2. This area features a southern subtropical monsoon climate, with a mean annual temperature of 21.5℃ and a mean annual precipitation of 1502.4 mm, which falls mainly during April to September. The zonal soil is latosolic red soil developed from granite and sandstones. Major vegetation in the nature reserve is subtropical

broadleaved and coniferous mixed forest dominated by masson pine (*Pinus massoniana*) and Chinese fir (*Cuninghamia lanceolata*), and by broadleaved species of Theaceae, Lauraceae, Magnoliaceae, and Aquifoliaceae, which is secondary in nature due to felling events in 1950s and 1960s when the area was managed by a local tree farm[15].

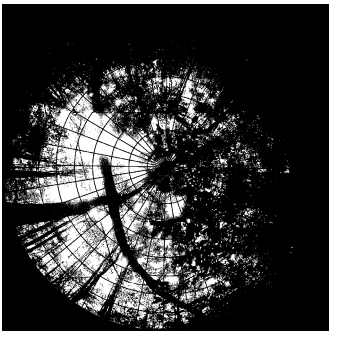

Fig. 1. A sample hemispherical photo taken from Plot 33, pre-processed with sky region grid overlay

2.2 Plant Census

We sampled each contiguous sub-plot in August 2006. All the trees≥3 cm diameter at breast height (DBH) in the plot were identified and measured for DBH and total tree height (H). Total tree height was first measured experimentally on 10 sample trees using a clinometer, whose measurement was based on the Pythagorean theorem, and then it was determined for all the other trees≥3 cm by visual estimation. DBH was measured to the nearest 0.1 cm using a stainless steel tape, while total tree height to the nearest 0.1 m. Stumps and snags were excluded from this analysis.

2.3 Soil Sampling and Laboratory Analyses

For each 400-m^2 subplot, 8 mineral soil samples were collected from the upper 25-cm surface soil. These samples were thoroughly mixed to produce a composite sample of about 1 kg. A total of 50 composite soil samples were thus collected and each was stored in a sturdy, tightly-sealed plastic bag and transported back to the laboratory for chemical determination. Samples were air-dried under room temperature, mechanically ground into fine particles with a pestle and mortar to ensure homogeneity of the material and passed through a 0.2-mm soil sieve for subsequent determination of various chemical properties, of which SOC concentration will be used in the analyses of this paper. Total SOC was determined using dichromate oxidation (with external heat applied) method [16].

2.4 Hemispherical Photography

A single hemispherical photograph was taken at the center of each 400-m^2 subplot, using a Nikon 4500 Coolpix® digital camera fitted with a Nikkor FC-E8 fisheye

converter (183°field of view, orthographic projection). The camera was mounted on a tripod 1.65 m above the ground, carefully leveled and oriented to the magnetic north as indicated by a compass, looking upwards to the sky. The hemispherical photographs were taken with the built-in "Fisheye1" mode of the camera. All the photographic images were acquired at high resolution (2272×1704 pixels) and saved as fine quality JPEG format (1:4 compression)[17]. To ensure uniform light conditions and minimize glare from direct sunlight, photographs were taken in the afternoon under overcast conditions and still air.

All the photographic images were directly downloaded from the camera to a desktop computer and analyzed with the Gap Light Analyzer (GLA), version 2.0, image processing software [18]. Since the choice of the threshold level would be less critical with a high resolution camera in producing a binary image [10], and the hemispherical photographs we acquired had relatively uniform brightness and high contrast, we used an intermediate threshold level from the intensity threshold range (0-255) set as a default in GLA [18] to separate pixels into "sky" and "canopy" for all the photographs. Intensities at or below the threshold (128) are considered to be foliage (black), while those above are classified as sky (white) [18].

The following output parameters from GLA were calculated and used in the study: %Canopy Openness (CO), LAI 4 Ring (LAI), which is the effective leaf area index integrated over the zenith angle 0 to 75°(Stenberg, et al., 1994), Direct Transmitted Gap Light (TransDir), and Diffuse Transmitted Gap Light (TransDif).

2.5 Statistical Data Analyses

Relations of surface soil organic carbon (SOC) concentrations to canopy openness (CO), effective leaf area index (LAI), direct (TransDir) and diffuse transmitted gap light (TransDif) parameters were fitted using a general linear model (GLM). Variability in SOC concentrations and stand structure between the 5 stand groupings that were delimited by cluster analysis using tree abundance data were assessed using Analysis of Variance (ANOVA), followed by a *post hoc* Fisher LSD test. ANOVA and regression analysis were performed using Statistica Version 5.5 software package, while Cluster Analysis was carried out on PC-ORD Version 4.20.

3 Results

3.1 Stand Structure in Relation to SOC Concentrations

102 tree species representing 3027 stems ≥ 3 cm DBH occurred in the stands. These stands could be further aggregated into 5 stand groupings based on Cluster Analysis (Fig. 2) using an abundance dataset with basal area data. An analysis of variance followed by Fisher LSD Test indicated that the five stand groupings exhibited significant difference in terms of tree height and DBH, however, no significant variations were found in SOC concentrations among the 5 stand groupings (Table 1). This result suggested that stand structure as expressed by tree abundance could not segregate the means and it could not serve as a good predictor for SOC concentration.

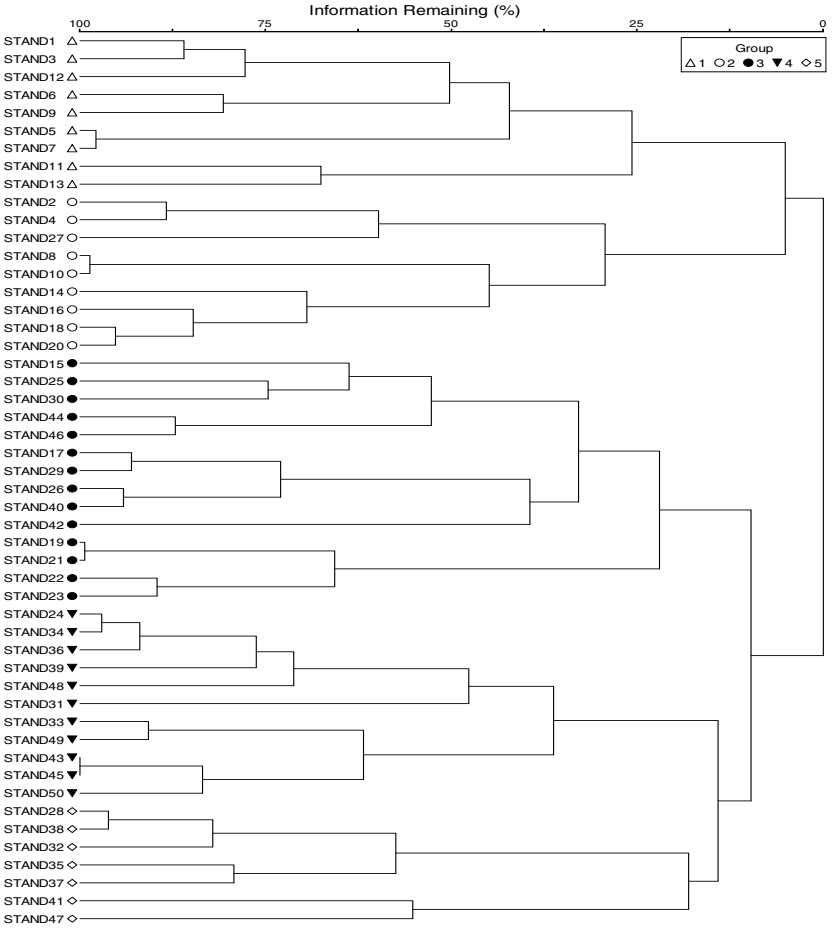

Fig. 2. Dendrogram from cluster analysis showing stand groupings

Table 1. Comparison of species composition, stand structure and SOC concentrations across stand groupings (stand groupings are defined by Cluster Analysis in Fig.2)[1)]

Stand grouping	No. of stems	No. of species	tree height/m	tree height range/m	DBH/cm	DBH range/cm	SOC concentration /g kg^{-1}
1 (n=9)	582	59	10.33±0.21a	1.7~25.0	9.52±0.23a	3.0~38.3	23.32 ± 2.35 a
2 (n=9)	655	53	10.05±0.19a	1.5~28.0	9.28±0.23a	3.0~36.2	23.59 ± 1.02 a
3 (n=14)	871	71	10.48±0.17a	1.0~28.0	10.54±0.23b	3.0~44.0	22.24 ± 1.10 a
4 (n=11)	611	52	12.57±0.23b	1.0~30.0	12.48±0.29c	3.0~38.3	18.86 ± 1.70 a
5 (n=7)	308	43	11.86±0.33b	2.0~28.0	12.40±0.44c	3.0~44.0	23.01 ± 1.41 a
The whole plot (n=50)	3027	102	10.92±0.10	1.0~30.0	10.65±0.12	3.0~44.0	22.04 ± 0.71

[1)] Values are given as mean ± 1 SE. Values followed by the same letter in a column are not significantly different (p>0.05), while values followed by different letters are significantly different at p<0.001 by Fisher LSD test.

3.2 SOC Concentrations in Relation to Canopy Structure Parameters

Canopy openness, LAI, direct transmitted gap light and diffuse transmitted gap light of the forest stands were highly variable (Table 2), indicating that the surface spots under the canopy had heterogeneous forest meteorological environment. Regression analysis showed that SOC concentration was negatively correlated with CO (r^2 = 0.3176; r = -0.5636, p = 0.00002)(Fig. 3) and positively correlated with LAI (r^2 = 0.1937; r = 0.4402, p = 0.0014)(Fig. 4), which indicated that a high canopy closure will enhance the SOC concentration in the surface soil under the canopy.

Table 2. Statistics of canopy structure and transmitted gap light variables (n=50)

Variable	Description	Mean	Range	SD	CV/%
CO	canopy openness/%	39.521	16.290~74.90	10.325	26.125
LAI	Effective leaf area index	0.955	0.215~2.023	0.349	36.545
TransDir	Amount of direct solar radiation transmitted by the canopy /mol m^{-2} d^{-1}	11.011	4.77~17.70	2.523	22.913
TransDif	Amount of diffuse radiation transmitted by the canopy /mol m^{-2} d^{-1}	9.602	4.53~16.0	2.172	22.620

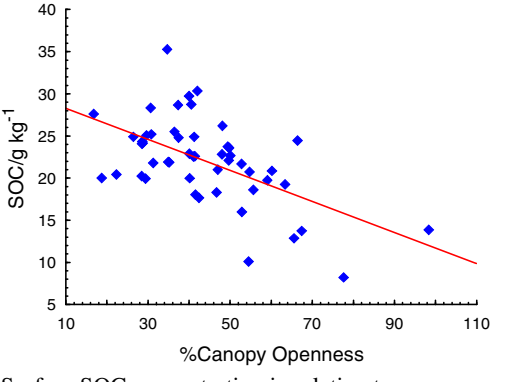

Fig. 3. Surface SOC concentration in relation to canopy openness

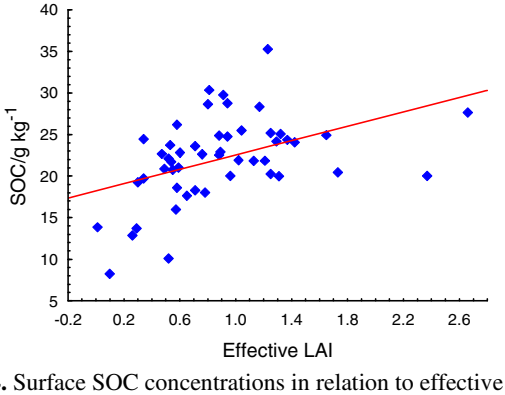

Fig. 4. Surface SOC concentrations in relation to effective LAI

3.3 Surface SOC Concentration in Relation to Transmitted Gap Light

SOC concentration was negatively correlated with both direct transmitted gap light (r^2 = 0.2798; r = -0.5290, $p < 0.0001$)(Fig. 5) and diffuse transmitted gap light (r^2 = 0.2883; r = -0.5370, $p < 0.0001$)(Fig. 6), which indicated that a low light understory environment will enhance the SOC concentration in the surface soil.

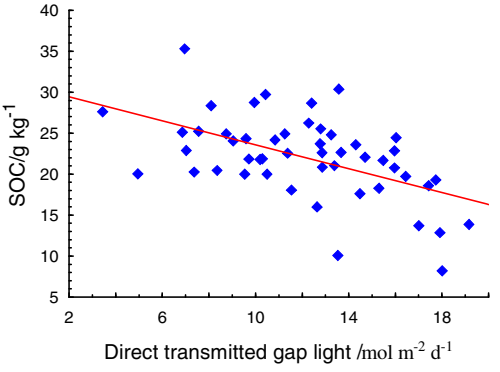

Fig. 5. Surface SOC concentrations in relation to direct transmitted gap light

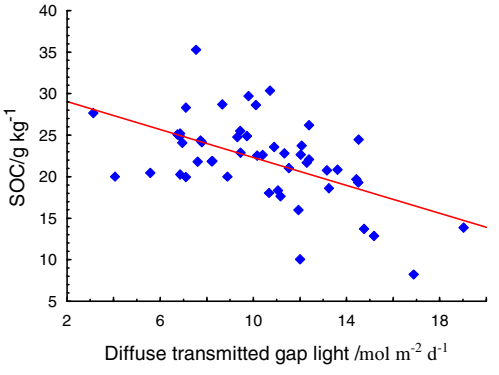

Fig. 6. Surface SOC concentrations in relation to diffuse transmitted gap light

4 Discussion

The close relation between soil organic carbon concentrations and forest gap light regimes found in the forest stands of Deqing needs further verification in other forest community types. Since past studies have yielded controversial findings on the relationship between SOC concentration and light or temperature[3, 7, 12]. Findings from this study need further verification using larger plots and in more forest types. However, our preliminary results are complied with previous studies, that is, SOC pool is negatively correlated with temperature. This study has some implications for carbon sequestration using plantation forest. For the purpose of sequestering more

carbon, fast growing trees with a wide and dense crown should be selected and planted using appropriately high density.

Acknowledgment. This work is supported by Grant #2008-10 and a special grant (Forest Ecological Research and Extension) from Guangdong Forestry Administration to Z. Su. We thank Zhenkui Li for assistance in field plant census and the staff from the Sanchading Nature Reserve for logistics support.

References

1. Aanderud, Z.T., Richards, J.H., Svejcar, T., James, J.J.: A Shift in Seasonal Rainfall Reduces Soil Organic Carbon Storage in a Cold Desert. Ecosystems 13(5), 673–682 (2010)
2. Post, W.M., Peng, T.H., Emanuel, W.R., King, A.W., Dale, V.H., DeAngelis, D.L.: The global carbon cycle. American Scientist 78, 310–326 (1990)
3. Xie, X.L., Sun, B., Zhou, H.Z., Li, Z.P.: Soil carbon stocks and their influencing factors under native vegetations in China. Acta Pedologica Sinica 41(5), 687–699 (2004) (in Chinese)
4. Raich, J.W.: Global patterns of carbon dioxide emissions from soils. Global Biogeochemical Cycles 9(1), 23–36 (1995)
5. Su, Z.Y., Xiong, Y.M., Zhu, J.Y., Ye, Y.C., Ye, M.: Soil organic carbon content and distribution in a small landscape of Dongguan, South China. Pedosphere 16(1), 10–17 (2006)
6. Oba, G., Weladji, R.B., Msangameno, D.J., Kaitira, L.M., Stave, J.: Scaling effects of proximate desertification drivers on soil nutrients in northeastern Tanzania. Journal of Arid Environments 72(10), 1820–1829 (2008)
7. Zhou, Y.R., Yu, Z.L., Zhao, S.D.: Carbon storage and budget of major Chinese forest types. Acta Phytoecologica Sinica 24(5), 518–522 (2000) (in Chinese)
8. Garten, C.T., Post, W.M., Hanson, P.J., Cooper, L.W.: Forest soil carbon inventories and dynamics along an elevation gradient in the southern Appalachian Mountains. Biogeochemistry 45, 115–145 (1999)
9. Kang, S., Kim, S., Oh, S., Lee, D.: Predicting spatial and temporal patterns of soil temperature based on topography, surface cover and air temperature. Forest Ecologe and Management 136, 173–184 (2000)
10. Jonckheere, I., Fleck, S., Nackaerts, K., Muys, B., Coppin, P., Weiss, M., Baret, F.: Review of methods for in situ leaf area index determination: Part I. Theories, sensors and hemispherical photography. Agricultural and Forest Meteorology 121, 19–35 (2004)
11. Feng, R.F., Yang, W.Q., Zhang, J.: Artificial forest management for global change mitigation. Acta Ecologica Sinica 26(11), 3870–3877 (2006) (in Chinese)
12. Hu, H.F., Liu, G.H.: Roles of forest management in global carbon dioxide mitigation. Chinese Journal of Applied Ecology 17(4), 709–714 (2006) (in Chinese)
13. Carvalho, L.M.T., Fontes, M.A.L., Oliveira-Filho, A.T.: Tree species distribution in canopy gaps and mature forest in an area of cloud forest of the Ibitipoca Range, south-eastern Brazil. Plant Ecology 149, 9–22 (2000)
14. Kincaid, J.A., Parker, A.J.: Structural characteristics and canopy dynamics of Tsuga Canadensis in forests of the southern Appalachian Mountains. Plant Ecology 199, 265–280 (2008)

15. Xie, D.D., Zhang, G.Q., Zhou, Y., Su, Z.Y.: Spatial analysis of soil moisture in Eucalyptus Plantations in West Guangdong. Journal of Central South University of Forestry & Technology 29(6), 45–50 (2009) (in Chinese)
16. Bao, S.D.: Soil and Agricultural Chemistry Analysis. China Agricultural Science and Technology Press, Beijing (2000) (in Chinese)
17. Beaudet, M., Messier, C.: Variation in canopy openness and light transmission following selection cutting in northern hardwood stands: an assessment based on hemispherical photographs. Agricultural and Forest Meteorology 110, 217–228 (2002)
18. Frazer, G.W., Canham, C.D., Lertzman, K.P.: Gap Light Analyzer(GLA), Version 2.0: Imaging software to extract canopy structure and gap light transmission indices from true-colour fisheye photographs, users manual and program documentation, pp. 1–40. Simon Fraser University, the Institute of Ecosystem Studies, Burnaby, Millbrook (1999)

Regulation of Resveratrol Prodution by Precursors and Elicitors in Cell Culture of 'Pinot Noir'

Zhen Zhang, Sheng Li*, Shaoying Ma, Wei Li, Delong Yang, and Yuan Liu

College of Life Science and Technology
Gansu Agricultural University
Lanzhou, Gansu province, China
lish@gsau.edu.cn

Abstract. Two precursors (L-phenylalanine and cinnamic acid), two abiotic elicitors (colchicine and β-cyclodextrin), and one signal elicitor (salicylic acid) were added to solid cultures of Vitis vinifera L. to study their effect on production of resveratrol. 30 mg/L was the optimum concentration of the two precursors for its production in the calli; 30 mg/L, 40 mg/L, 20 mg/L were the most suitable concentrations of salicylic acid, β-cyclodextrin and colchicines for that, respectively.

Keywords: resveratrol, precursor, elicitor, grapevine, multiplication.

Resveratrol (trans-3,5,4'-trihydroxystilbene) is a low molecular weight, constitutive and inducible phytoalexin belonging to the stilbene family [1]. It synthesized from p-coumaroyl CoA and malonyl CoA by an enzyme called stilbene synthase. Its biosynthsis is stimulated by stress, including injury, infection or UV irradiation. Stilbenes play an important role in protection plants against fungal infections [2,3] and constitute the main group of phytoalexins within the *Vitaceae*[4]. Resveratrol has been reported to have numerous health benefits, including cardiovascular protective, anti-cancer and anti-inflammatory properties [5-13].

In the present study, we used two precursors (phenylalanine and cinnamic acid), two abiotic elicitors (colchicine and β-cyclodextrin), and a signal compound (salicylic acid) to assess the response of the cultured grapevine Pinot Noir cells about the multiplication and resveratrol production for the first time, in order to facilitate the scale-up manufacture of the cell lines containing high resveratrol.

1 Materials and Methods

1.1 Establishment of Cell Cultures

In September 2006, young, actively growing grapevine shoots were obtained from plants of 'Pinot Noir' collected from vineyard of Gansu Agricultural University, China.

* Corresponding author.

E. Zhu and S. Sambath (Eds.): Information Tech. and Agricultural Eng., AISC 134, pp. 371–376.
springerlink.com © Springer-Verlag Berlin Heidelberg 2012

Stem segments, 4-5 cm long, were washed under running water for 1 h followed by a treatment with 75% ethanol for 1min, 0.1% $HgCl_2$ for 10min and then rinsed with sterile distilled water for three to four times. The disinfected stem segments were aseptically cut into single bud sections and then inoculated on GS medium with 0.2 mg/L IAA. After three-week culture, the new and young leaves were collected, and cut into small pieces of about 0.5×0.5 cm for further experiment. The B5 supplement with 3% sucrose was used as a basal medium. The medium was solidified with 0.6% (w/v) agar. Plant growth regulators (6-Benzyladenine and 2,4-Dichlorophenoxyacetic acid) at the ratio of 0.5 mg/L:1.0 mg/L were added and pH was adjusted to 5.8 before autoclaving at 121℃ for 20 min. The fragments cultures were incubated in flasks (50 mL) containing 20 mL medium and maintained at 25±2℃ under the conditions of dark. Callus was induced from the leaf pieces after 12-15 days and transferred onto B5 fresh solidified (0.6% agar) medium for both subculture and multiplication containing 0.5 mg/L Kinetin, 250 mg/L casein hydrolysate and 3% sucrose. The callus was maintained at 25±2℃ under 16 h white light from white florescent tubes at a unit of irradiance of 45 μmol/m^2·s and 8 h dark photoperiod.

1.2 Precursors Feeding and Elicitor Treatment

L-phenylalanine, salicylic acid, β-cyclodextrin and colchicines were dissolved and Cinnamic acid dissolved in small amount of ethanol, and they serially diluted in water, respectively. Their final media concentrations in the media were showed in Table1, with amino acid and other extro-compounds free medium as control. 5 lumps of the callus were inoculated in each medium equirotally, and each treatment was prepared 20 flasks as replication, and all cultures were further cultivated for 45 days under multiplication conditions before being harvested.

Table 1. Concentration of the Supplements in the Media

Concentration/mg/L Supplements	control	I	II	III	IV	V	VI
Phenylalanine	0	5	10	20	30	40	50
Cinnamic acid	0	5	10	20	30	40	50
Salicylic acid	0	5	10	20	30	40	-
β-Cyclodextrin	0	5	10	20	30	40	-
Colchicine	0	5	10	20	30	40	-

1.3 Determination of Cell Growth

The inoculation amount(IA) = post-inoculation − pre-inoculation
the harvest amount(HA) = pre-harvest − post-harvest

$$\text{Multiplication} = \frac{HA}{IA}$$

1.4 HPLC-Quantification of Resveratrol

Resveratrol was analysed by reverse-phase HPLC. The extracts were syringed and 20 μL was injected onto a 5 μm C_{18}, 150 mm×4.6 mm internal diameter column. Resveratrol was eluted by a mobile phase of CH_3CN-H_2O (15%:85%) at a flow rate of 0.8 mL/min. The column temperature was 30℃. Detection was at 306 nm.

1.5 Statistical Analysis

For the bioassay data and resveratrol quantitation data, differences were determined using the SPSS 11.5 program (SPSS Inc., Chicago) applying the LSD multiple range test to establish significant differences at $P<0.05$.

2 Results and Discussion

2.1 Establishment of Standard Curve and Calculation

A regression equation was given by the measurement of these standard samples of different concentration: y=158930x-499.93, R^2=0.9979 (y was the peak areas and x was the concentrations of the standard samples). A standard curve was established (Fig.1).

$$\text{Resveratrol content (mg/g dw)} = \frac{V * \left(\frac{y + 499.93}{158930} \right)}{m}$$

V: constant volumn of the samples, i.e. 5 mL;
m: the dry weight (DW) of the samples, i.e. 1.0 g.

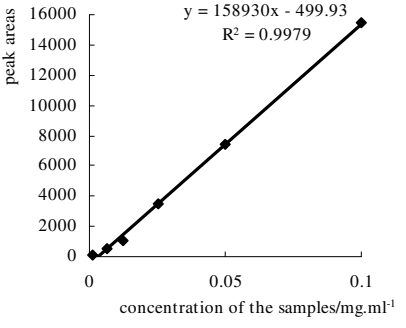

Fig. 1. Standard curve of resveratrol

2.2 Effect of the Precursor-Feeding on Cell Growth, Resveratrol Production of 'Pinot Noir' Cell Cultures

Within the concentration range of our investigation, neither low nor high concentrations were suitable for the both calli biomass and resveratrol production.

It showed obvious dose-effects. The amount of resveratrol increased significantly with the addition of L-phenylalanine (30 mg/L) and cinnamic acid (30 mg/L) to the medium (Fig.2). Contents increased 56–fold and 96-fold, respectively, compared with the control (4.920 μg/g DW). However, higher concentration lowered the positive effect, and the effect of cinnamic acid was superior to that of phenylalanine. In contrast, higher concentration of phenylalanine and cinnamic acid with any concentrations did cause a significant decrease in the callus multiplication (Fig.3), while resveratrol increased. Biomass production increased significantly in the calli when phenylalanine and cinnamic acid were added to the medium, and 30mg/L was the optimum concentration for both of them, 10.1-fold and 11.8–fold more than the control (14.89 μg/flask) (Fig.4). Generally speaking, the promotion effect on resveratrol production of phenylalanine was inferior to that of cinnamic acid. It is possible that cinnamic acid is obtained form phenylalanine ammonia-lyase (PAL), but the activity of PAL which is a key enzyme in the pathway of resveratrol biosynthesis is subjected to the influences of several factors, so the direct addition of cinnamic acid could lessen its dependence on phenylalanine.

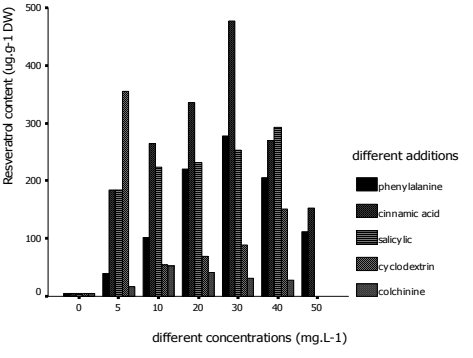

Fig. 2. Effects of different additions on resveratrol content in 'Pinot Noir' callus culture

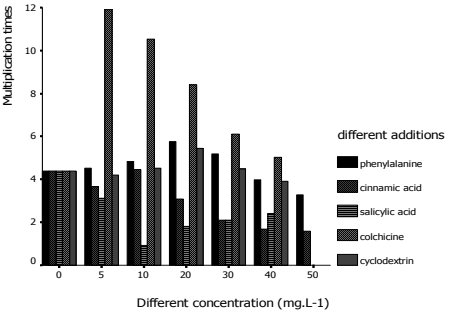

Fig. 3. Effects of different additions on 'Pinot Noir' callus multiplication

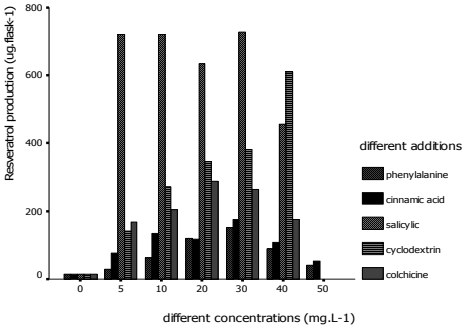

Fig. 4. Effects of different additions on resveratrol production in 'Pinot Noir' callus culture

2.3 Effect of the Elicitors on Cell Growth, Resveratrol Production of 'Pinot Noir' Cell Cultures

It can be seen that SA suppressed the callus multiplication severely (Fig.3), even at the concentration of 10 mg/L, it decreased to 0.9259, less than the initial inoculation quantity, resulting from the growth retardation and water lose. However, the addition of this elicitor to cell cultures of *Vitis vinifera* L. gave rise to an increase in resveratrol accumulation and production (Fig.4, Fig.5). Resveratrol content gradually enhanced from 4.9620 μg/g DW (control) to 292.882 μg/g DW (SA 40 mg/L) in the callus. In general, SA enhanced resveratrol production indeed. At the concentrations of 5, 10, 30 mg/L, the production reached 721.6, 720.3, 728.4 μg/flask, respectively, and the differences between them were not significant, nearly 49-fold more than the control (14.886 μg/flask).

By the presence of β-cyclodextrin at the concentrations (5 to 40 mg/L) it involved, both resveratrol content and production were heightened, though it did not show any stimulating effect on the callus growth, and they reached 151.6 μg/g DW and 610.0 μg/flask, respectively, while adding 40 mg/L β-cyclodextrin, 30.5-fold and 4.1-fold more than the control. This approved our hypothesis that cyclodextrin would prevent resveratrol from decomposition since resveratrol possesses the characteristic of light instability.

It is reasonable to add cochicine to culture medium to accelerate the callus growth so as to promote resveratrol production. Surprisingly, it can not only increase the multiplication, but enhance resveratrol content. The lowest concentration (5 mg/L) of cochicine highly stimulated the callus growth (11.9), while the higher concentration had an opposite effect. Similar tendency presented in the accumulation of resveratrol in the calli, and 10 mg/L was the most suitable concentration, 10.8-fold higher than the control (5.0 μg/g DW). However, 20 mg/L was superior to the other concentrations for resveratrol production, leading which to 289.4 μg/flask, much more than the control (14.9 μg/flask).

As for the mechanism to increase the secondary metabolite, it deserves deep research.

References

1. Langcake, P., Pryce, R.J.: A new class of phytoalexins from grapevine. Experientia 33, 151–152 (1977)
2. Dixon, R.A., Harrison, M.: Activation, structure and organization of genes involved in microbial defence in plants. Advances in Genetics 28, 165–234 (1990)
3. Hain, R., Bieseler, B., Kindl, H., Schroder, G., Stodker, R.: Expression of a stilbene synthase gene in Nicotiana tabacum results in synthesis of phytoalexin resveratrol. Plant Molecular Biology 15, 325–335 (1990)
4. Jeandet, P., Douillet-Breuil, A.C., Bessis, R., Debord, S., Sbaghi, M., Adrian, M.: Phytoalexins from the Vitaceae: biosynthesis, phytoalexin gene expression in transgenic plants, antifungal activity and metabolism. Journal of Agricultural and Food Chemistry 50, 2731–2741 (2002)
5. Arichi, H., Kimura, Y., Okuda, H., Baba, K., Kozawa, M., Arichi, S.: Effects of stilbene components of the roots of Polygonum cuspidatum Sieb. et Zucc. on lipid metabolism. Chem. Pharm. Bul. 30, 1766–1770 (1982)
6. Kinsella, J., Frankel, E., German, B., Kanner, J.: Possible mechanisms for the protective role of antioxidants in wine and plant foods. Food Technology 47, 58–89 (1993)
7. Jang, M., Lining, C., Udeani, G., Slowing, K., Thomas, C., Beecher, C., et al.: Cancer chemopreventative activity of resveratrol, a natural product derived from grapes. Science 275, 218–220 (1997)
8. Lu, R., Serrero, G.: Resveratrol, a natural product derived from grape, exhibits antiestrogenic activity and inhibits the growth of human breast cancer cells. Cellular Physiology 179, 297–304 (1999)
9. De Santi, C., Pietrabissa, A., Spisni, R., Mosca, F., Pacifici, G.: Sulphation of resveratrol, a natural compound present in wine, and its inhibition by natural flavonoids. Xenobiotica 30, 857–866 (2000a)
10. De Santi, C., Pietrabissa, A., Spisni, R., Mosca, F., Pacifici, G.: Glucuronidation of resveratrol, a natural product present in grape and wine, in the human liver. Xenobiotica 30, 1047–1054 (2000b)
11. Brakenhielm, E., Cao, R., Cao, Y.: Suppression of angiogenesis, tumor growth and wound healing by resveratrol a natural compound in red wine and grapes. FASEB J. 15, 1798–1800 (2001)
12. Kimura, Y., Okuda, H.: Resveratrol isolated from Polygonum cuspidatum roots prevents tumor growth and metastasis to lung and tumor-induced neovascularization in Lewis lung carcinoma-bearing mice. Journal of Nutrition 131, 1844–1849 (2001)
13. El-Mowafy, A.: Resveratrol activates membrane-bound guanylyl cyclase in coronary arterial smooth muscle: A novel signaling mechanism in support of coronary protection. Biochem. and Biophysical. Res. Commun. 291, 1218–1222 (2002)

Salinization Resistance Transgenic Soybean Reduced Bacterial Diversity in Rhizosphere*

Zheng Wang**, Zhihua Liu**, and Hongyan Wang***

Resources and Environment Sciences College
Northeast Agricultural University
Harbin, Heilongjiang Province, China
hongyanwang@neau.edu.cn

Abstract. In order to deeply understand the effect of Salinization Resistance Transgenic Soybean (SRTS) on diversity of rhizospheric bacteria in saline soils in Songnen Plain, Heilongjiang Province, DGGE- cloning and traditional culture-depending methods were used. DGGE fingerprint analysis results indicated that the bacterial diversity index and evenness index in rhizospheric soil of SRTS were lower than other soybean's based on analysis to the number of bands of bacterial 16SrDNA. DGGE-cloning sequencing results showed that SRTS has a certain inhibition effect on rhizospheric soil bacteria phylum Firmicutes and decreased the priority of phylum Proteobacteria, yet had no effect on rhizosphere soil bacteria phylum Acidobacteria. The study revealed that the release of SRTS in saline soil decreased the amount and the diversity of bacteria in rhizospheric soil to some extent, and phylum Alphaproteobacteria genus Sphingomonas was promoted in rhizospheric soil.

Keywords: Salinization Resistance Transgenic Soybean, saline soils, rhizospheric soil, bacterial diversity, PCR-DGGE.

1 Introduction

As the rapid development of Genetically Modified Organism, the cultivated area of Genetically Modified (GM) crops had exceeded 1.34 Million hectares in 25 countries in the world by 2009[1]. GM crops brought enormous economic benefits to mankind, which yet intensified people anxious about the ecological potential risk of GM crops [2, 3, 4]. So it is significance to appraise the ecological potential risk of GM crops on studying and researching the influence of GM crops on the rhizosphere soil microorganism [5, 6, 7, 8]. Studies have shown that transgenic crops on soil microbial

* This work is partially supported by Genetically Modified Breeding Projects 2009ZX08011-025B-02 to Honhyan Wang; NEAU Scientific Foundation and NEAU Innovation Team Foundation (CXT003-3-2) to Zhihua Liu.
** The first two authors had equal contribution to the article.
*** Corresponding author.

E. Zhu and S. Sambath (Eds.): Information Tech. and Agricultural Eng., AISC 134, pp. 377–384.
springerlink.com © Springer-Verlag Berlin Heidelberg 2012

flora had no significant effect [9], and yet, some studies showed an impact of transgenic crops on soil [10, 11].

Salinization Resistence Transgenic Soybeans (SRTS) were cultivated by technique for gene engineering in Heilongjiang Agricultural Academy of Sciences, which transformed the betaine aldehyde dehydrogenase (BADH) into cultivation soybean of Heinong 35(HN35). Few research have been conducted to know whether the soybeans can interact with microorganisms in soil as well as gene drift and the influence of abundance and diversity of rhizospheric soil microorganism, with the cultivation of SRTS. DGGE-cloning method was used to study the SRTS's effects on bacterial quantity and diversity in rhizosphere soil, and to supply some basic information on researching the bio-safety of GM soybeans.

2 Materials and Methods

2.1 Experimental Field Description

Study sites located in Anda City in Heilongjiang Province, which longitude is 124° 53' to 125° 55' and latitude is 46° 01' to 47° 01'. Anda city is semi-arid north temperate continental monsoon climate, and it is the typical arid area in the Western of Heilongjiang Province. The soil in this research is Saline-alkaline soil and its physical and chemical properties are as follows: available P is 26.683 mg/kg, TN is 1.675g/kg, Sodium Absorption Ratio is 0.382, Bicarbonate content of the soil water-soluble is 0.002 cmol/kg, Basicity is 0.040, pH is 8.439, Cation exchange capacity is 13.938 cmol/kg, Exchangeable sodium is 0.552 cmol/kg and available K is 149.949 mg/kg.

2.2 Soybean Material

The soybeans and soybean lines used in this research are Salinization Resistance Transgenic Soybean (SRTS), SRTS' parent HN-35, Wild soybean(Y-21), cultivated variety HeFeng-50(HF-50) and anti-nematode (K).

2.3 Experimental Design and Sampling

Rows were 3 m long and 0.7 m wide, with an inter-plant spacing of 6 cm; six-row plots were used in a randomized complete design. Rhizospheric soil was collected at the stage of flowering on June 29, 2010. Five-point method was used to sample the rhizospheric soil and 10 plants were used for one sample by shaking methods.

2.4 PCR Strategy for Amplification of 16S rDNA Fragments

The extraction method is CTAB-SDS [12]. According to the instruction of Promega's Wizard DNA Clean-up System, number is A7280, to purify raw DNA.

2.5 DGGE Analysis

All DGGE analysis was run in DCode system (Bio-Rad Laboratories, USA). Gels contained 8% (w/v) polyacrylamide and 1×TAE. A linear gradient from 30% to 60% denaturant were used for all analysis. Ten micro-liters of PCR product with 6×loadding buffer were used for DGGE analysis at a constant temperature of 60°C at 100V for 12h. Then, that was stained with $AgNO_3$. Pictures were captured with Tanon Gis.

2.6 Recycling and Sequence Analysis of DGGE Bands

13 prominent DGGE bands were excised from the UV illuminated acrylamide gels with sterile scalpel. There were 6 different bands and 7 bands for the common. DNA eluted from the excised gel by incubation in 30μL ddH_2O at 4°C overnight. Eluted DNA was used for PCR amplification using the primer F338 and R518 (without GC clamp). The PCR products were handed over to Boshi Biotechnology Co., Ltd for sequence analysis. All sequences from this work was submitted to GenBank and given the accessions.

2.7 Data Analysis

Analysis of dates was performed in Excel (2003). The digital processing of the bands on the DGGE profiles of the position and brightness is using Tanon Gis. Dsh and Jsh represent the bacterial diversity and uniformity, separately. The formula is as follows:

$$Dsh = -\sum Pi \ln Pi = -\sum (Ni/N) \ln (Ni/N)$$

$$Jsh = Dsh / \ln S$$

The calculation of Dsh is based on the location and intensity of DGGE bands and the peak area of the band represent the intensity. Pi means the ratio between the intensity of a sample and total intensity, Ni is peak area and N is the total area of all peaks. MEGA 4.0 software was applicator to establish the phylogenetic tree.

3 Results and Analysis

DGGE fingerprint as Fig.1 shows that different soybean varieties electrophoresis isolates number, strength and migration position were different. DGGE fingerprint bands of HN35, Y-21, HF-50 and K in terms of the number, location and the brightness has a very strong similarity. Moreover, their quantity of the DGGE bands was much more than SRTS'. Most bands were common bands. This may be related to the effects of SRTS on rhizospheric soil bacterial diversity.

The band quantity, as well as diversity index, of SRTS' rhizospheric soil was lower than that of others' (Table 1), the evenness index just in contrast. This shows that the SRTS reduced the diversity of bacteria in the rhizosphere soil, but increased evenness of bacteria in the rhizosphere soil. After the 13 bands connection, transformation,

sequenced, and similarity searches were performed in the GenBank database using the BLAST search algorithm (Table 2). Bands that produced usable sequences are listed in Table 2 along with the identity of their closest related sequence from GenBank. The sequences retrieved from clones were unique and contained more information than those in.excised DGGE bands.

Project searching, 13 sequences matched in the GenBank were identified as bacteria (Table 2). SRTS weakened the dominant bacteria belonged to *Proteobacteria* (such as 4, 6 and 16) and reduced several bands (such as 1, 18, 20 and 23).

Table 1. The number of dgge bands, diversicity index (dsh) and homogeneous degree index (jsh) of bacteria

Treatment	Band number	Dsh	Jsh
SRTS	11a*	2.29±0.09a	0.93±0.01a
HN-35	17b	2.64±0.09b	0.94±0.01a
Y-21	18b	2.67±0.17b	0.94±0.01a
HF-50	14ab	2.41±0.24ab	0.93±0.02a
K	15ab	2.57±0.14b	0.95±0.01a

*Data in the table are Mean±SE; Different letters represent the significant difference at $p < 0.05$

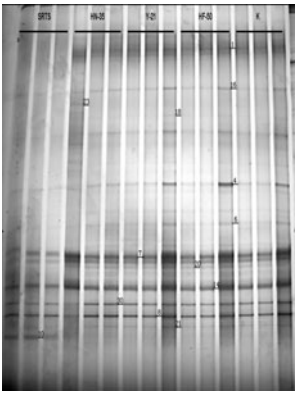

Fig. 1. DGGE fingerprinting of bacteria in rhizospheric soil. The labels were the cutting gel serial number. According to the results of digital processing, we preferred cut 13 bands which contains the SRTS rhizospheric soil bacteria missing bands (such as band 1 and band 20, etc.), SRTS-specific bands (such as band 10), the dominant bands of HN35, Y-21, HF-50 and K which were also the faint bands of SRTS and common dominant bands. DNA eluted from the excised gel by incubation in 30μL ddH2O at 4°C overnight. Eluted DNA was used for PCR amplification using the primer F338 and R518 (without GC clamp). The PCR products were handed over to Boshi Biotechnology Co., Ltd for sequence analysis. All sequences from this work was submitted to GenBank and given the accessions.

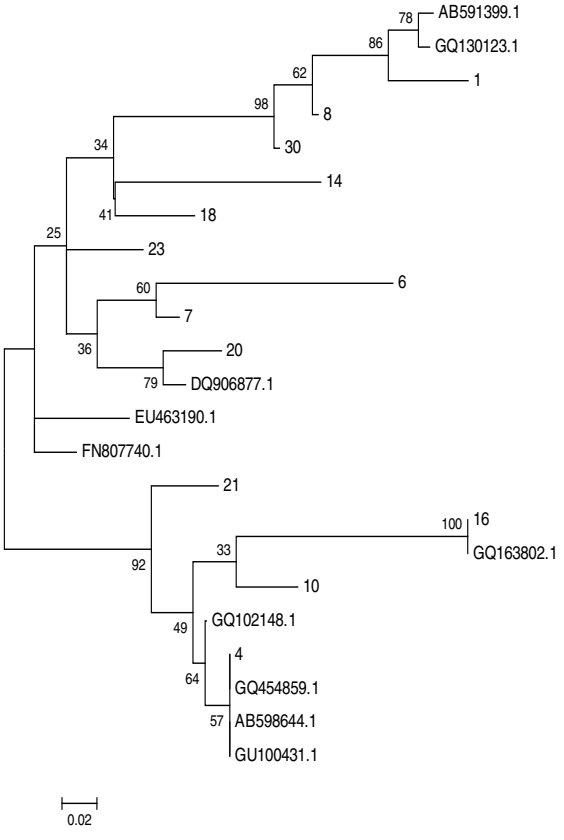

Fig. 2. Phylogenetic tree based on partial 16SrDNA sequences

Table 2. Identification of Dgge Bands and Deduced Bacteria That Dgge Band Represented Based on Dna Sequecing

Sepuences designation	Closest match strain or clone from GenBank	Identity	GenBank accession no.
1	Uncultured bacterium	98%	FJ167312.1 GI:219384663
	Uncultured firmicutes bacterium	98%	EF651740.1 GI:151506410
4	Sphinqomonas	100%	HQ331138.1 GI:311115821
	Uncultured bacterium	100%	GU100431.1 GI:310835903
6	Uncultured Bacteroidetes bacterium	98%	HM105493.1 GI:302139864
7	Uncultured bacterium	98%	GU227555.1 GI:281429941
8	Uncultured Acidobacteria bacterium	97%	HQ114024.1 GI:307940477
	Uncultured bacterium	97%	AB591399.1 GI:307777943
10	Sphingomonadaceae bacterium	100%	GQ454859.1 GI:306478670
	Uncultured soil bacterium	100%	GU366002.1 GI:285027157
14	Uncultured Acidobacteria bacterium	100%	HM062075.1 GI:299891962
16	Sphinqomonas	100%	HM240936.1
	Uncultured prokaryote	100%	GU208483.1 GI:283463334
	Uncultured sponge bacterium	100%	GQ163802.1 GI:290575712
18	Uncultured bacterium	98%	HM346770.1 GI:298104468
	Uncultured bacterium	97%	FN807740.1 GI:295005454
20	Uncultured bacterium	97%	HM185915.1 GI:300383856
	Uncultured bacterium	96%	DQ906877.1 GI:117580798
21	Sphinqomonas	97%	GU117227.1 GI:264666383
	Sphinqomonas	97%	GQ102148.1 GI:238338325
23	Uncultured bacterium	97%	GU105356.1 GI:310840828
	Uncultured bacterium	97%	EU463190.1 GI:169278665
30	Uncultured Acidobacteria bacterium	97%	HM224501.1 GI:308549727
	Uncultured bacterium	96%	GQ130123.1 GI:238915107

4 Discussions

DGGE method, as fingerprinting technique, provides detailed information about the species composition of whole communities [14, 15]. But the bands of DGGE fingerprint are very complex, there are many bands can not be observed by naked eye, human the subjective judgment and limitation of analysis software, resulting in inaccuracy of difference comparison of different treatments. Excising DGGE bands for cloning and sequencing combined with DGGE fingerprint jointly analyse soil microorganism can solve above problem. In this study a combination of DGGE and cloning was used to rapidly and accurately characterize bacterial diversity in saline soil samples based on 16S rDNA fragments. The high throughput of DGGE combined with selected cloning makes this approach suitable for tracking bacteria communities in ecological studies.

Transgenic crops effects on rhizosphere soil community structure and function has drawn wide attention by domestic and foreign scholars due to its complexity[16], some scholars have made some researches into bio-safety of transgenic crops and its potential eco-environmental problems[4,17]. Kozdroj *et al.* research showed that transgenic crops altered its root exudates and chemical constituents [18]. Donegan et al. research two kinds of American Bt insect-resistant cotton showed that there was significant difference in microbe quantity, species and composition[19]. Andreote *et al*. Research showed that transgenic tobacco could change community structure of soil microorganism, but after planting soil microorganism can recover original state[22]. Savka and Farrand studied the effects the root exudates of transgenic opine tobacco on two kinds of using pseudomonas, showed change of root exudates influenced species richness[20]. Xu et al. showed that glyphosate-resistant soybean decreased rhizosphere soil bacteria quantity and its diversity significantly by Using of routine culture and PCR-DGGE Technique[10]. This study showed that cultured by plate dilution method the number of rhizospheric soil bacteria of SRTS was no significant difference in other varieties planted soybean. DGGE-cloning sequencing results showed that SRTS showed a certain inhibition effect on rhizosphere bacteria phylum firmicutes, decreased pollution advantage of rhizosphere soil bacteria proteobacteria, had no effect on rhizospheric soil bacteria acidobacteria. This may be induced by differences root exudates between SRTS and other varieties soybean.

References

1. Fang, X.: Genetically modified crops. Guangming Daily (March 23, 2010)
2. Wang, J., et al.: Effects of transgenic crops on soil ecosystem. Chinese Journal of Applied Ecology 13(4), 491–494 (2002)
3. Wang, Z., Zhao, T., Liu, X., Deng, X.: Advances in research on the impacts of transgenic crops on soil microbes. Plant Protection 33(4), 15–20 (2007)
4. Qian, Y., Tian, Y., Wei, W.: Ecological risk assessment of transgenic plants. Acta Phytoecol Sin. 22(4), 289–299 (1998)
5. Qian, Y., Ma, K.: Progress in the studies on genetically modified organisms, and the impact of its release on environment. Acta Ecological Sinica 18(1), 1–9 (1998)

6. Douville, M., et al.: Occurrence and persistence of Bacillus thuringiensis (Bt) and transgenic Bt corn cry1Ab gene from an aquatic environment. Ecotoxicol. Environ. Saf. (66), 195–203 (2007)
7. Dunfield, K., Germida, J.: Impact of genetically modified crops on soil- and plant-associated microbial communities. J. Environ. Qual. (33), 806–815 (2004)
8. Snow, A., Palma, P.: Commercialization of transgenic plants: Potential ecological risks. Bioscience 47(2), 86–96 (1997)
9. Lai, X., Zhang, Y.S., Zhao, S., Li, G., Yang, D.: Effect of transgenic soybean on the diversity of nitrogen fixing bacteria in rhizosphere soil. Chinese Journal of Ecology 29(9), 1736–1742 (2010)
10. Xu, G., Wang, H., Liu, J.: Effects of RRS on the amount and diversity of bacteria in rhizospheric soil. Acta Ecological Sinica 29(8), 4535–4541 (2009)
11. Zhang, W., Feng, Y.: Physico-chemical properties and ecological recovery of saline-akaline soil in Songnen plain. Acta Pedologica Sinica 46(1), 169–171 (2009)
12. Yang, Z., et al.: DNA Extraction Methods from Compost for Molecular Ecology Analysis. Environmental Science 17(8), 1613–1618 (2006) (in Chinese)
13. Muyzer, G., et al.: Denaturing gradient gel electrophoresis (DGGE) in microbial ecology. Molecular Microbial Ecology Manual 34(4), 1–27 (1998)
14. Muyzer, G., Smalla, K.: Application of denaturing gradient gel electrophoresis (DGGE) and temperature gradient gel electrophoresis (TGGE) in microbial ecology. Antonie van Leeuwenhoek 73, 127–141 (1998)
15. Jia, Z., Conrad, R.: Bacteria rather than Archaea dominate microbial ammonia oxidation in an agricultural soil. Environ. Microbiol. (2), 197–205 (2009)
16. Li, C., Zhang, X., Wu, J., Liu, H.: Effect of transgenic cotton on microbial community diversity in rhizosphere soil. Journal of Agro-Environment Science 27(5), 1857–1859 (2008)
17. Kozdroj, J., Van Elsas, J.: Response of the bacterial community to root exudates in soil polluted with heavy metals assessed by molecular and cultural approaches. Soil Biol. Biochem. 32, 1405–1417 (2000)
18. Donegan, K., et al.: Decomposition of genetically engineered tobacco under field conditions: persistence of the proteinase inhibitor I product and effects on soil microbial respiration and protozoa, nematode and microarthropod populations. Journal of Applied Ecology 34(3), 767–777 (1997)
19. Andreote, E., Vogel, T., Bertolla, F., Nalin, R., Simonet, P.: In situ transfer of antibiotic resistance genes from transgenic (Transplastomic) tobacco plants to bacteria. Applied and Environmental Microbiology (8), 3345–3351 (2002)
20. Savka, M., Farrand, S.: Modification of rhizobacterial populations by engineering bacterium utilization of a novel plant-produced resource. Nature Biotechnol. 15, 363–368 (1997)

Analysis on Quality Characters Diversity of Wheat Landraces from Yangtze River Valley

Wei Zheng[1,2], Dongfa Sun[1], and Feng Pan[2]

[1] College of Plant Science and Technology, Huazhong Agricultural University, Wuhan, Hubei Province 430070, China
[2] Institute of Agricultural Quality Standards and Test Technology, Hubei Academy of Agricultural Science Wuhan, Hubei Province 430070, China
{nkyzhengwei,sundongfa,nkyzhengwei,njgwgg}@163.com

Abstract. The quality characters of 477 Wheat landraces from Yangtze River valley were evaluated by analysis of variance, correlation, and principle component in order to discover helpful traits and provide helpful information for the genetic improvement of wheat. The results showed that Wheat landraces from the Yangtze River valley was rich in middle-strength-gluten wheat, and had some high-strength-gluten and low-strength- gluten wheat. Wheat landraces of protein content up to high-strength-gluten, middle-strength-gluten, low-strength- gluten wheat index was 14.14%, 77.85%, 8.01%, respectively. Wheat landraces of wet gluten content up to high-strength-gluten, middle-strength-gluten, low-strength- gluten wheat index was 0.21%, 99.58%, 0.21%, respectively. Wheat landraces of zeleny up to high-strength-gluten, middle-strength-gluten, low-strength- gluten wheat index was 10.97%, 88.82%, 0.21%, respectively. The results of correlation analysis indicated that correlation between starch content and protein content, wet gluten content, zeleny was very significant. Correlation between protein content and wet gluten content was significant. This study provides a scientific basis for high quality wheat breeding, high-quality wheat production and using of the variety.

Keywords: wheat, landrace, quality, diversity.

1 Introduction

China is the one of the biggest wheat production and consumption countries in the world, occupying an important position. Since reform and opening-up, China's wheat production has made unprecedented achievements. Particularly over the last decade, due to the abundant wheat yield, the import quantity of wheat was significantly reduced . However, there is a clear disparity in the overall level of wheat quality compared with the developed countries because of China's vast areas , natural and social differences in various area and late studies which just begun in recent years [1].In the 1970, China's wheat quality research had only been started [2] . People need better wheat products with China's economic development and people's improving living standards. The wheat quality was directly related to the development of flour and food industry, becoming the key issue to meet the needs of people [3]. At present, China's agriculture is changing from subsistence agriculture to commodity agriculture, from traditional agriculture to modern agriculture, from extensive

E. Zhu and S. Sambath (Eds.): Information Tech. and Agricultural Eng., AISC 134, pp. 385–396.
springerlink.com © Springer-Verlag Berlin Heidelberg 2012

agriculture to intensive agriculture. The improving agricultural production capacity, the per capita increasing in the number of agricultural products, the acceleration of urbanization progress and the restructuring of urban and rural consumption provide the basis to promote the improvement of the wheat quality. The wheat quality has been greatly improved with the work promoting wheat quality and the quality regionalization deepened [3]. Although there were a number of high-quality of special high-strength-gluten and low-strength- gluten wheat varieties, but the proportion of wheat in China is still too small. In the future, we should continue to focus on wheat quality breeding, promoting the proportion of special high-quality wheat varieties in China [5]. Enhancing wheat quality breeding has great significance for China's wheat production and food processing.

Wheat landraces, also known as farm species, resulting from millennia of natural and artificial selection, are highly adapted to specific habitats. China has vast, complex topography, varied climate, a long history of agriculture and various farming systems, which has formed a highly adaptive, genetic diversity of wheat landraces. Compared with most countries in the world, Wheat landraces in China show not only some advantages: early maturity, multiple grains, great adaptability, high endophilicity and other characteristics, but also some disadvantages, for example : small kernel and grain , not conductive to high yield ; high plant height and soft stem, lodging and shattering easily, unsuited for mechanical harvesting ; poor baking quality [6]. However, as important resources, more and more researches from the agronomic traits, quality traits, resistance to preharvest sprouting characteristics, genetic variation, biochemical markers and molecular markers, and other aspects of local varieties of wheat were studied, obtaining some good genetic resources [7-13].

Tremendous crop improvement has been succeeded in agricultural production depending on the studying of agronomic and quality traits. It is significant to fully grasp the material, evaluate agronomic and quality traits performance scientificly for the rational utilization of germplasm resources, matching the parents even in today's rapid development of molecular markers. Vast territory, complicated terrain and diverse climates formed numerous wheat landraces in Yangtze River Valley of China [14,15]. So far, there were only a few reports about the diversity of wheat quality traits from some local areas of China [16-22].The systematic Analysis on wheat landraces quality traits in Yangtze-River Valley of China has not been done. Therefore, we analyzed the wheat landraces quality traits in Yangtze-River Valley of China, identifying the positive traits of wheat for Hubei and excellent genetic resources for wheat breeding in Hubei.

It is therefore necessary to determine the quality traits diversity of the landraces in Yangtze-River Valley of China, identify the positive traits of wheat for Hubei and excellent genetic resources for wheat breeding in Hubei , which could be used in researches in wheat genetic diversity, germplasm resources, wheat quality breeding, high quality wheat production.

2 Materials and Methods

2.1 Plant Material

A total of 477 accessions of bread wheat (*Triticum aestivum* L.) landraces were analyzed in our study, including 390 landraces from the Hubei province of China and

87 landraces from the Tibet Autonomous Region of China. According to the collection site data from the Hubei province, 375 out of these 390 accessions are divided into 6 populations corresponding to 6 different agroecological regions of wheat cultivation (Jianghan plain, North-west of Hubei ， North of Hubei ， West of Hubei，East of Hubei, South-east of Hubei), whereas the collection sites of the other15 accessions were not accurately recorded. All accessions were kindly provided by professor Sun, College of Plant Science and Technology, Huazhong Agricultural University, China.

2.2 Testing Methods

The landraces were planted in the experimental farm of Huazhong Agricultural University in October 31, 2007 in Wuhan, China. Field experiments were carried out with three replications arranged in order within the year. Each landrace various was sown in one row with 100 cm, with a distance of 10 cm between plants within a row, and 20 cm between rows. The field management was consistent with the field production with the heading stage recorded. The 20 plants selected random in the middle of the three rows of each landrace were harvested individually to score the following traits: plant height, Length of main head, spikelets of main head, head number per plant, the yield per plant, and the 1,000-grain weight (g) as the yield per plant divided by the number of grains multiplied by 1,000.

2.3 Quality Analysis

The quality characters (protein content, wet gluten content, starch content and zeleny) of 477 wheat varieties(3 wheat varieties not fully mature, measured 474 wheat varieties)from Yangtze River valley were analyzed by Foss1241 near infrared grain quality analyzer. the criterion of control quality was based on national " Wheat varieties for specific end-uses " (GB/T17891,17892-1999).

2.4 Statistical Analysis

The computer program DPS was used to analyze the data.

3 Results and Analysis

3.1 Quality Traits Analysis of Yangtze River Valley Wheat Landraces

The quality traits analysis of common landraces of bread wheat from Yangtze River region were given in Table 1. Table 2 showed that the average quality indexes of protein content(ranging from 8.89% ~ 17.21%), the starch content (ranging from 50.27% ~ 58.40%),the wet gluten content(ranging from19.95% ~ 32.76%,) and the subsidence value(ranging from 29.79% ~ 52.66%) were 12.87%, 54.69%, 26.05% and 40.78mL, respectively。 The content of protein and starch accounted for 67.56%. The quality traits in zeleny and starch content occupied the maximum coefficient of variation (8.28%) and the minimum (2.13%), respectively.

Table 1. Quality traits analysis of yangtze river valley wheat landrace

Quality traits	Average	Range	SD	CV/%
Protein content/%	12.87	8.89～17.21	1.04	8.11
Starch content/%	54.69	50.27～58.40	1.16	2.13
Wet gluten content/%	26.05	19.95～32.76	1.42	5.46
Zeleny/mL	40.78	29.79～52.66	3.38	8.28

1) Protein content analysis of Yangtze River valley wheat landraces: According to protein solubility in different solvents, Osborne divided the total proteins into four different categories: albumin, Globulin, gliadin, gluten in 1924. As the ability to forming wheat gluten, the 4 proteins can be divided into wheat gluten proteins (gliadin and glutenin) and non-gluten proteins (albumin and globulin). Non-gluten proteins accounted for about 10% to 20% within total proteins with little effect on wheat quality; while gluten proteins accounted for 80% to 90% within total proteins, which is the main factor to determine flour quality. The glutenins conferred visco-elasticity to the dough, while the prolamins conferred elasticity forming the dough[23,24].Protein content in wheat is an important quality-related indicator with nutritional quality and processing quality. Table 1 showed that the average protein content inYangtze River landraces is 12.87% (ranging from 8.89% ~ 17.21%), reaching the state of wheat gluten protein content quality index(14.00% ~ 11.50%), , with a small range. 67 of 474 wheat landraces met the national Wheat protein content of the high-strength-gluten quality index(≥14.00%), accounting for 14.14%; 369 reached the state of wheat gluten protein content middle-strength-gluten quality index(14.00% ~ 11.50%), accounting for 77.85%;and 38 reaching the national wheat protein content of the low-strength-gluten quality index(≤11.50%). The Specific distribution was given in Table 2 and Figure1.

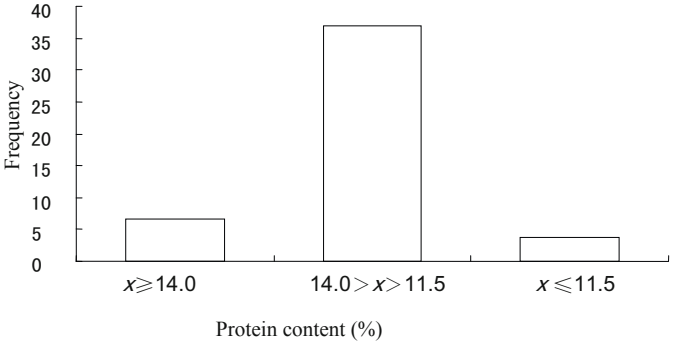

Fig. 1. Frequency distribution of protein content of Yangtze river valley wheat landrace

2) Starch content analysis of Yangtze river valley wheat landrace: Starch which makes up about 56% of wheat flour, mainly composed by the amylose and amylopectin. The proportion of amylose in the total wheat starch is 20% to 30%, amylopectin about 70% to 80%. Wheat starch content, composition and condition of

grain flour effect the flour yield, whiteness, α-amylase activity and ash et al[25], having important implications in processing quality on wheat food, especially noodle, bread and other traditional Oriental foods [26,27]. Table 1 showed that the landraces from Yangtze River contained a average protein content of 54.69%, ranging from 50.27% ~ 58.40%%. Specific distribution was given in Table 3 and Figure 2.

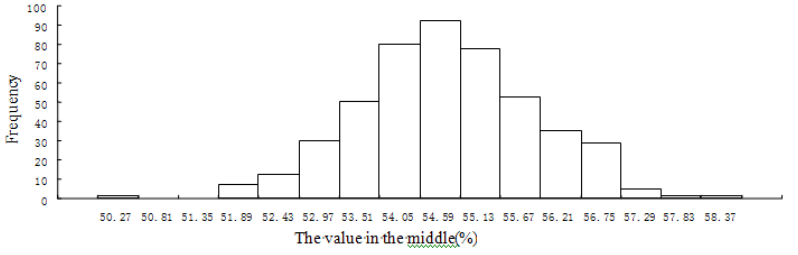

Fig. 2. Starch content distribution column of Yangtze river valley wheat landrace

Table 3. Starch content distribution of Yangtze River valley wheat landrace

Starch content(%)	The value in the middle(%)	Frequency
50.00～50.54	50.27	1
50.54～51.08	50.81	0
51.08～51.62	51.35	0
51.62～52.16	51.89	7
52.16～52.70	52.43	12
52.70～53.24	52.97	30
53.24～53.78	53.51	50
53.78～54.32	54.05	80
54.32～54.86	54.59	92
54.86～55.40	55.13	78
55.40～55.94	55.67	53
55.94～56.48	56.21	35
56.48～57.02	56.75	29
57.02～57.56	57.29	5
57.56～58.10	57.83	1
58.10～58.64	58.37	1

3) Wet gluten content analysis of Yangtze River valley wheat landraces: Gluten was a protein complex found by Italian scientist Beccari in 1745. The ability to form gluten is the main difference between Wheat proteins and other cereal crops, the gluten is mainly composed of gliadin and glutenin. The texture of gluten is different among wheat varieties due to different protein content and structure of gliadin and glutenin.

Dough strength depend mainly on the flour gluten content, structure and function [28], which depend on the amount of protein contained, the size of the peptide chain and peptide chains and the ability forming visco-elasticity glutenin macropolymer[29]. Table 1 showed that the Yangtze River landraces contained a average Wet gluten content of 26.05% (ranging from 19.95%～32.76%), reaching the state of wheat middle-strength-gluten quality index (14.00% ~ 11.50%). 472 landraces attained the state of wheat middle-strength-gluten quality index (32.00% ~ 22.00%) , with another two reaching the state of wheat high- or low-strength-gluten quality index （≥32.00%), (≤22.00%） ,respectively. Specific distribution was given in Table 4 and Figure3.

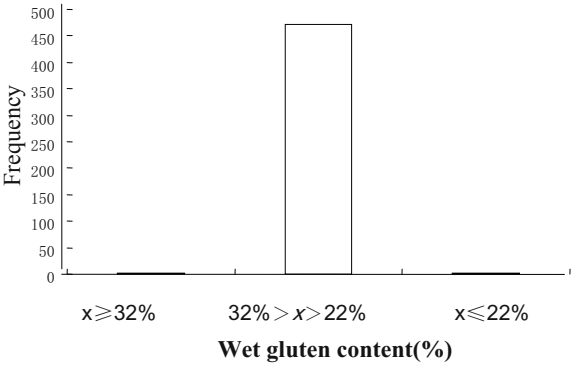

Fig. 3. Frequency distribution of wet gluten content of Yangtze river valley wheat landrace

Table 4. Wet Gluten Content Analysis of Yangtze River Valley Wheat Landrace

Wet gluten content	Frequency	Proportional/%
≥32.00%	1	0.21
32.00%～22.00%	472	99.58
≤22.00%	1	0.21
Total	474	100

4) Zeleny analysis of Yangtze River valley wheat landraces: Zeleny, a comprehensive indicator to evaluate the protein quantity and quality, is simple and quick method to analyze wheat gluten intensity, the greater zeleny is, the higher the gluten intensity is. Table 1 showed that the landraces from Yangtze River contained a average zeleny of 40.78mL (ranging from 29.79～52.66mL), reaching the state of wheat middle-strength-gluten quality index (30.00～45.00mL). 421 of 477 wheat landraces met the national high middle -strength-gluten quality index, with 52 reaching the state high-strength-gluten quality index （≥45.00mL） , only one reaching the national low-strength- gluten quality index （≤30.00mL） . Specific distribution was given in Table 5 and Figure 4.

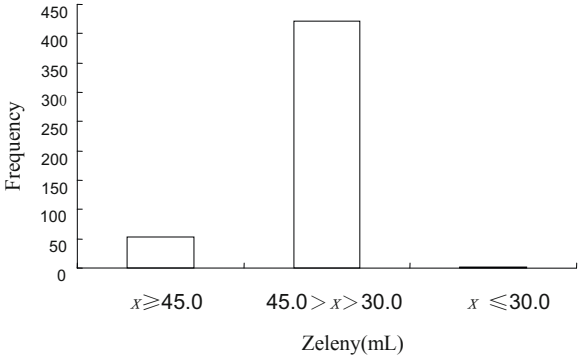

Fig. 4. Frequency distribution of zeleny analysis of Yangtze river valley wheat landrace

Table 5. Zeleny Analysis of Yangtze River Valley Wheat Landrace

Zeleny(mL)	Frequency	Proportional(%)
≥45.00	52	10.97
45.00～30.00	421	88.82
≤30.00	1	0.21
Total	474	100

3.2 The Correlation Analysis of Yangtze River Valley Wheat Landraces Quality Traits

Analyzing the quality traits correlations among wheat landraces from Yangtze River Valley, we could find whether these wheat landraces have consistency between these traits and select the key target traits easily. As seen in Table 6, the protein content, starch content, wet gluten and zeleny were significantly correlated with each other, suggesting that these traits have a good coherence. Starch content was negatively related to protein content, wet gluten content and zeleny in an extremely significant level, indicating that the starch content raised with the drop of protein content, wet gluten content and zeleny .The correlation analysis indicated that the protein content was significantly positively correlated with wet gluten content and zeleny, which indicate that the protein content is an important index of wheat quality.

Table 6. The correlation analysis of Yangtze river valley wheat landrace quality traits

Correlation coefficient	Protein content	Starch content	Wet gluten content	Zeleny
Protein content				
Starch content	-0.78**			
Wet gluten content	0.93**	-0.63**		
Zeleny	0.83**	-0.63**	0.82**	

Note: "*" was significant in 5% level, "**" was significant in 1% level.

3.3 Quality Traits Analysis of Yangtze River Valley Wheat Landraces in Different Ecological Area

Yangtze river valley wheat landraces can be divided into seven ecotypes, 76 landraces from South-east of Hubei, 30 landraces from East of Hubei, 37 landraces from Jianghan plain, 28 landraces from West of Hubei,30 landraces from North of Hubei and 158 landraces from North-west of Hubei plain, 87 landraces from Qingzang plateau. The quality traits analyzing of wheat landraces from different ecological zones of Yangtze River valley was showed in Table 7. Table 7 indicated that the average value of protein content in North-west of Hubei was the lowest(12.48%), while average value in the Qingzang plateau is the highest(13.96%). The latter reached the state of middle-strength-gluten quality index(14.00% ~ 11.50%).The results showed that the average level of starch content of Qingzang plateau(53.89%) was the lowest, while North-west of Hubei was the highest(54.99%). wheat landraces from Jianghan Plain were the most variable (2.44%), the smallest variation was in East of Hubei (1.55%). Table 7 showed the average of wet gluten content in northwest of Hubei is the he lowest（25.44%）,while Qingzang plateau is the highest（27.52%）. wheat landraces from South-east of Hubei were the most variable (5.49%), the smallest variation was in East of Hubei (3.44%).

The results showed that the mean of zeleny in northwest of Hubei the lowest (39.66%), Qingzang plateau was the highest（43.18%）. As for zeleny different ecological zones of the Yangtze River valley, wheat landraces from Jianghan Plain were the most variable (11.14%), the Qingzang plateau had the smallest coefficient of variation (6.61%).

The results also showed that the minimum coefficient of variation among different ecotypes was starch content in Fig.5, with an average of 2.00%, and the maximum coefficient of variation was zeleny, with an average of 7.97%.The average coefficient of variation of protein content and wet gluten content were 6.95% and 4.66%,respectively. The results indicated that zeleny was greatly influenced by environmental factor.

Table 7. Quality Traits Analysis of Yangtze River Valley Wheat Landrace in Different Ecological Area

Quality traits	Statistical parameters	Jianghan plain	North-west of Hubei	North of Hubei	West of Hubei	East of Hubei	South-east of Hubei	Qingzang plateau
Protein content	Average/%	12.69	12.48	12.61	12.67	12.70	12.93	13.96
	SD	1.05	0.94	0.86	0.90	0.65	0.94	0.92
	CV/%	8.25	7.50	6.79	7.08	5.13	7.30	6.61
Starch content	Average/%	54.90	54.99	54.87	54.81	54.90	54.66	53.89
	SD	1.34	1.16	1.22	1.00	0.85	1.06	1.03
	CV/%	2.44	2.11	2.23	1.83	1.55	1.95	1.91
Wet gluten content	Average/%	25.89	25.44	25.80	25.80	25.84	26.13	27.52
	SD	1.35	1.25	1.16	1.23	0.89	1.44	1.19
	CV/%	5.21	4.91	4.51	4.78	3.44	5.49	4.31
Zeleny	Average/%	40.79	39.66	40.43	40.25	40.30	41.05	43.18
	SD	4.54	3.42	2.99	3.13	2.79	3.02	2.85
	CV/%	11.14	8.63	7.38	7.77	6.91	7.37	6.61

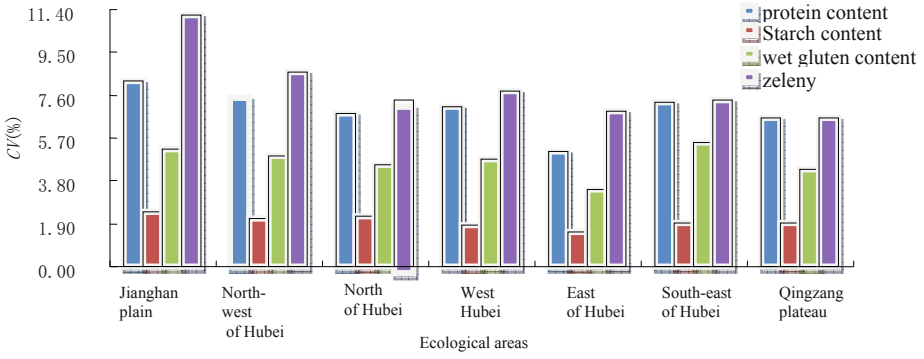

Fig. 5. *CV* of quality traits analysis of Yangtze river valley wheat landrace in different ecological area

3.4 Significant Differences of Quality Traits of Wheat Landraces in Different Ecological Areas of Yangtze river Valley

As seen in table 8, the protein content, wet gluten content and zeleny of wheat landrace from Qingzang plateau were highest and significantly different with other ecological regions. And the protein content of wheat landrace from South-east of Hubei, East of Hubei, Jianghan plain, West of Hubei, North of Hubei and North-west of Hubei had no significant difference with each other.

The Starch content of wheat landrace from Qingzang plateau was lowest and significantly different with other ecological regions. And the Starch content of wheat landrace from South-east of Hubei, East of Hubei, jianghan plain, West of Hubei, North of Hubei and North-west of Hubei had no significant difference with each other. Table 8 suggested that the protein content, wet gluten content and zeleny of

Table 8. Significant Differences of Quality Traits of Wheat Landrace in Different Ecological Areas of Yangtze River Valley

Protein content			Starch content			Wet gluten content			Zeleny		
Ecological areas	5%	1%	Ecological areas	5%	1%	Ecological areas	5%	1%	Ecological areas	5%	1%
Qingzang plateau	a	A	North-west of Hubei	a	A	Qingzang plateau	a	A	Qingzang plateau	a	A
South-east of Hubei	b	B	Jianghan plain	a	A	South-east of Hubei	b	B	South-east of Hubei	b	B
East of Hubei	b	B	North of Hubei	a	A	East of Hubei	b	B	Jianghan plain	b	B
Jianghan plain	b	B	East of Hubei	a	A	Jianghan plain	b	B	East of Hubei	b	B
West of Hubei	b	B	West of Hubei	a	A	West of Hubei	b	B	North of Hubei	b	B
North of Hubei	b	B	South-east of Hubei	a	A	North of Hubei	b	B	West of Hubei	b	B
North-west of Hubei	b	B	Qingzang plateau	b	B	North-west of Hubei	b	B	North-west of Hubei	b	B

wheat landrace from Qingzang plateau were better than the landrace from Hubei, and most varieties can be normally mature and fruit in hubei for winter wheat planting. Therefore, the wheat landrace from Qingzang plateau can be used as germplasm for improving quality.

4 Conclusions and Discuss

1) Li et al. (1990) studied the heredity of wheat quality character. They suggested that screening the high quality material in the massive germplasm resources was instructive in the quality breeding[30]. The result indicated that the Yangtze River valley wheat landraces were rich in medium-gluten wheat germplasm resources, with little strong gluten and weak gluten wheat germplasm resources, which was consistent with the requirements in " Special-purpose Wheat Regional Development Plan (2003 ~ 2007)". Wheat landraces of protein content reaching high-strength-gluten index (≥14.00%), middle-strength-gluten index(14.00%～11.50%), low-strength- gluten index (≤11.50%) made up 14.14%, 77.85%, 8.01%, respectively. Wheat landraces of wet gluten content reaching high-strength-gluten index (≥32%), middle-strength-gluten index (32.00% ～ 22.00%), low-strength- gluten index (≤22.00%) accouted for 0.21%, 99.58%, 0.21%, respectively. The percentage of local varieties of zeleny reaching high-strength-gluten index (≥45.00mL), middle-strength-gluten index (45.00～30.0mL), low-strength- gluten index (≤30.0mL) was 10.97%, 88.82%, 0.21%, respectively. Therefore, landraces in Yangtze River region of China are valuable resources in wheat breeding. It is worth using and studying the landraces.

2) The results of correlation analysis indicated that correlation between starch content and protein content, wet gluten content, zeleny was significantly negative. Starch content can be used as an important quality index on account of its tremendous impact on wheat quality. Starch quality was closely associated with protein quality, wet gluten content, zeleny,these four indicator together impact on wheat processing quality. We should have a comprehensive consideration when we evaluate wheat quality, wheat processing quality when a trait changed or improve wheat quality for different purpose. The wet gluten content showed a high positive correlation with the protein content, and the correlation coefficient was 0. 93, indicating the wet gluten content and protein content were in harmony. It was consistent with the previous report (Payne et al. 1979). The wet gluten content can be used as a quality index to evaluate wheat quality.

3) The protein content, wet gluten content, zeleny of Tibetan local varieties of wheat were maximum, reaching a very significant level compared with other ecological areas. The protein content analyzed in landraces from South-east of Hubei, East of Hubei, Jianghan plain, West of Hubei, North of Hubei, North-west of Hubei did not indicate significant difference.

The starch content of Tibetan local varieties was lowest, reaching a very significant level compared with other ecological areas. The starch content of local varieties from South-east of Hubei, East of Hubei, Jianghan plain, West of Hubei, North of Hubei, North-west of Hubei had not significant difference. The results demonstrated that

protein content, wet gluten content, zeleny of landraces from Qingzang plateau was superior to local varieties from Hubei Province. Most of the landraces from Qingzang plateau planted in winter in Hubei could normally mature and yield. Therefore they are useful germplasm resources to improve the wheat quality. According to requirements of wheat quality indicators, a full analysis and use of local germplasm, establishment of germplasm resources can be applied in the wheat quality breeding in future to improve the wheat quality breeding. And it is necessary to establish a quality evaluation system for high-quality wheat varieties, achieving a integration of high-quality wheat breeding, reproduction, production and the evaluation criteria of purchase and sale to speed up the development of high quality wheat industry.

References

1. Zhang, Y.F., Wang, T.S., Li, Z.S.: China's wheat quality analysis and development. Bulletin of the Chinese Academy of Sciences 14(2), 117–119 (1999) (in Chinese)
2. Wang, G.R.: Chinese wheat quality status and situation analysis. In: Chen, S.D. (ed.) Chinese Wheat Breeding and Industrial Progress, pp. 152–161. Chinese Agriculture Press, Beijing (2002)
3. Wan, F.S., Wang, G.S., Li, Z.Z.: A preliminary approach on present situation and objectives of improvement of wheat quality in China. Scientia Agricultura Sinica 22(3), 14–21 (1989) (in Chinese)
4. Zan, X.C., Zhou, G.Y., Wu, L.N.: Present status of wheat quality in China. Journal of Triticeae Crops 26(6), 46–49 (2006) (in Chinese)
5. Yi, L., Li, B.F.: Analysis on quality of wheat varieties (lines) in northwest Sichuan. Seed Industry in China (8), 37–40 (2008) (in Chinese)
6. Dong, Y.C., Zheng, D.S.: Chinese Wheat Genetic Resources, pp. 58–98. Chinese Agriculture Press, Beijing (2000)
7. Dong, Y.C., Cao, Y.S., Zhang, X.Y., Liu, S.C., Wang, L.F., You, G.X., Pang, B.S., Li, L.H., Jia, J.Z.: Establishment of candidate core collections in Chinese common wheat germplasm. Journal of Plant Genetic Resources 4(1), 1–8 (2003) (in Chinese)
8. Zheng, D.S., Liu, S.C., Song, C.H., Li, L.H., Li, X.Q., Yang, X.M., Chen, M.Y.: A survey of characterization on agronomic characters, cataloguing, seed multiplication and conservation of wheat genetic resources in China. Journal of Plant Genetic Resources 1(1), 1–13 (2000) (in Chinese)
9. Delacy, I.H., Skovmand, B., Huerta, J.: Characterization of Mexican wheat landraces using agronomically useful attributes. Genetic Resources and Crop Evolution 47(6), 591–602 (2000)
10. Dotlacil, L., Hermuth, J., Stehno, Z., Manev, M.: Diversity in European winter wheat landraces and obsolete cultivars. Czech Journal of Genetics & Plant Breeding 36(2), 29–36 (2000)
11. Moghaddam, M., Ehdaie, B., Waineas, J.G.: Genetic variation and interrelationships of agronomic characters in landraces of bread wheat from southeastern Iranv. Euphytica 95, 361–369 (1997)
12. Poiarkova, H., Blum, A.: Landraces of wheat from the northern region in Israel. Euphytica 32, 257–271 (1983)
13. Reif, J.C., Zhang, P., Dreisigacker, S., et al.: Wheat genetic diversity trends during domestication and breeding. Theor. Appl. Genet. 110, 859–864 (2005)

14. Nan, H.Y.: Genetic diversity of Chinese wheat landraces (degree thesis). Chinese Academy of Agricultural Sciences, Beijing (2002)
15. Liu, S.C., Zheng, D.S., Cao, Y.S., Song, C.H., Chen, M.Y.: Genetic diversity of landrace and bred varieties of wheat in China. Scientia Agricultura Sinica 33(4), 20–24 (2000) (in Chinese)
16. Ma, Y.M., Fan, Y.D., Li, S.S., Li, R.J., Zhao, Y.: Diversity of quality traits using wheat varieties of the huang-huai winter wheat area. Journal of Plant Genetic Resource 5(2), 133–138 (2004) (in Chinese)
17. Chen, H.P., Deng, T., Gou, L.L., Wei, Y.M., Zheng, Y.L.: Diversity analysis of agronomic and quality characters of wheat landraces in Sichuan. Journal of Triticeae Crops 28(6), 960–964 (2008) (in Chinese)
18. Chen, H.P., Wei, Y.M., Zheng, Y.L.: Nutritional quality analysis of wheat landraces from Sichuan. Journal of the Chinese Cereals and Oils Association 21(5), 36–40 (2006) (in Chinese)
19. Li, W.H., Li, Y.F., Zhang, H., Dong, J., Yang, W.X., Zhang, G.H.: Comparison analysis of quality characters between wheat cultivars bred and wheat landraces in Gansu. Journal of Triticeae Crops 28(6), 977–982 (2008) (in Chinese)
20. Chen, X.J., Wang, Y.J., Shen, L., Ji, W.Q.: HMW-GS diversity of wheat landraces in northwest spring wheat production area. Journal of Plant Genetic Resource 10(1), 42–45 (2009) (in Chinese)
21. Zhu, Y.H., Ji, W.Q., Wang, Y.J., Chen, X.Y.: Genetic diversity of HMW-GS composition in wheat landraces from southwest winter wheat region. Journal of Plant Genetic Resource 8(4), 401–405 (2007) (in Chinese)
22. Cong, H., Ikeda, T., Wang, H.F., Kanenori, T., Zhang, Y.F., Mikiko, Y., Tsukasa, N., Hiroshi, F.: Genetic diversity of high molecular weight glutenin subunit(HMW—GS) composition in common wheat landraces from Xinjiang China. Journal of Agricultural Biotechnology 17(6), 1070–1074 (2009) (in Chinese)
23. Kasarda, D.D., Bernardin, J.E., Nimmo, C.C.: Wheat proteins. Adv. Cereal Sci. Technol. 1, 158–236 (1976)
24. Payne, P.I., Corfield, K.G.: Subunit composition of wheat glutenin proteins, isolated by gel filtration in a dissociating medium. Planta 145, 83–88 (1979)
25. McCormick, K.M., Panozzo, J.F., Hong, S.H.: A swelling power test for selecting potential noodle quality wheats. Australian Journal of Agricultural Research 42, 317–323 (1991)
26. Endo, S., Karibe, S., Okada, K., Nagao, S.: Factors affecting gelatinization properties of wheat starch. Nippon Shokuhin Kogyo Gakkaishi 35, 7–14 (1988)
27. Du, C., Yang, X.J., Liu, G.R.: Studies on the ralations between starch properties of wheat flour and baking quality. Journal of Agricultural University of Hebei 25(4), 29–34 (2002) (in Chinese)
28. Horvatić, M., Grüner, M., Mulalić, N.: Relationship between protein nutritive quality and technological property parameters of wheat flour. Nahrung 33(9), 901–903 (1989)
29. Weegels, P.L., Hamer, R.J., Schofield, J.D.: Depolymerization and re-polymerization of wheat glutenin during dough processing I. Relationships between glutenin macropolymer content and quality parameters. Journal of Cereal Science 23, 103–111 (1996)
30. Li, Z.Z., Sun, F.T., Zhang, C.Y., Jin, Y.C.: Quality traits of different varieties and correlations among them in whea. Scientia Agricultura Sinica 23(6), 35–41 (1990) (in Chinese)

Effects of Cold Stress on Porcine Fibroblasts HSP90 mRNA Expression

Zhongqiu Li[1,3], Jianzhang Ma[1,*], Chunlong Liu[2,*], Hong Ma[3], Zhenhua Guo[3], Bo Fu[3], Liang Wang[3], Jinyan Sun[3], Fugang Peng[3], and Di Liu[3,*]

[1] College of Wildlife Resource University of Northeast Forestry Harbin, Heilongjiang Province, China
[2] Animal Husbandry Research Centre Heilongjiang Academy of Agricultural Sciences Harbin, Heilongjiang Province, China
[3] Northeast Institute of Geography and Agricultural Ecology Chinese Academy of Sciences Harbin, Heilongjiang Province, China
{lizhongqiu1974,jianzhangma,liudi1963,Liuchunlong1976}@163.com

Abstract. The stress response is a complex program of gene expression and biochemical adaptive. These cell stress response are of great interest both to basic biology and to medicine. Study of cold stress on cells and related gene expression contribute to understand the effects of cold stress on the biological mechanisms of the body. HSP90 is an important molecular chaperone，it has to maintain the protein conformation, promoting the wrong protein degradation. Stress can induce a significant increase in HSP90 expression，its expression are induced by cold exposure do not increase during the period of thermal stress itself but during the cell stress response that ensues after rewarming. We use real-time PCR detection expression of HSP90 mRNA of procine fibroblasts. We showed that preincubation of cells at 4 and 15℃ induced the expression of HSP90 mRNA upon recovery at 38.5℃, and the degree of this induction was directly related to the time that the cells spend at 4 and 15℃(data not shown).We observation that 25 and 32℃(data not shown)were the temperature of the recovery incubation period, below which litter or no induction of stress response was observed, is consistent with a role of active cell metabolism in those induction.

Keywords: Cell, cold stress, HSP90 mRNA, real-time PCR, poreine.

1 Introduction

Biologically, the ability to survive and adapt to thermal stress appears to be a fundamental requirement of cellular life[1]. Studies of in vitro cultured mammalian cells have shown that cells generally respond to cold stress by reduction rates of enzymatic reaction, diffusion, and membrane transport[2][3]; as lowed of progression through the cell cycle, whit phase G1 typically being the most sensitive[4]; inhibition of transcription and translation, lending to a generalized

* Corresponding author.

E. Zhu and S. Sambath (Eds.): Information Tech. and Agricultural Eng., AISC 134, pp. 397–403.
springerlink.com © Springer-Verlag Berlin Heidelberg 2012

reduction in protein synthesis[5]. HSP90 is an important molecular chaperone, it has to maintain the protein conformation, promoting the wrong protein degradation[6]. Stress can induce a significant increase in HSP90 expression, its expression are induced by cold exposure do not increase during the period of thermal stress itself but during the cell stress response that ensues after rewarming [7][8][9]. The stress response is a complex program of gene expression and biochemical adaptive. These cell stress response are of great interest both to basic biology and to medicine. Study of cold stress on cells and related gene expression contribute to understand the effects of cold stress on the biological mechanisms of the body.

2 Materials and Methods

2.1 Materials

Fresh Procine ear tissue was obtained from a Yorkshire(6 months).

2.2 Chemicals and Culture Medium

Dulbecco's modified Eagle's medium (DMEM) was purchased from Gibco Co. Trypsin was purchased from Sigma Co. Trizol Reagent and Fetal bovine serum(FBS) was purchased from Invitrogen Co. High-Capacity cDNA Reverse Transcription Kits and SYBR® Green PCR Master Mix Kits was purchased from ABI Co.

2.3 Cold Stress of Cultured Cells

For cold stress, cells were placed in a 4℃,15,25,32 incubator for specified time period followed by incubation at 38.5℃.In experiments where the effects of different temperatures of preincubation were compared, cells were place in incubators set at 4,15,25and32℃ for specified time periods followed by incubation 38.5℃ for time periods as indicated. To determine the effects of a transient where cold stress followed by recovery and incubation at 38.5℃on cellular HSP90 mRNA expression.

2.4 Total RNA Extraction

Total RNA was extracted with Trizol reagent according to the manufacture's nstructions. Detection of total RNA integrity by agarose gel electrophoresis. After elution with 20μL nuclease-free ouble-distilled H2O, RNA samples were stored at -80℃ until required.

2.5 Reverse Transcription

Reverse transcription to cDNA from RNA extracted form cells was carried out using the high capacity cDNA reverse transcription kit according to the manufacture, s instruction. RT reaction was carried out in a 20μL final reaction volume containing

2μL 10×Buffer, 0.8μl 25×dNTP Mi（100mM）, 2μL 10×RT Random Primer, 1μL MultiScribeTM Reverse Transcriptase, 1μl RNase Inhibitor, 3.2μl Nuclease-free H2O, 10μL RNA Sample. The thermal cycle conditions: 25℃ 10min, 37℃ 120min, 85℃ 5min, 4℃ ∞。

2.6 Design of Primers

The specific primer was designed using the Premier 5.0 software and published genomic sequences according to ABI recommentations. The sequences of specific primers were as follows: 5′GAG GAA ACC CAG ACC CAA-3′ and 5′- AGA AGC CGA CAC CGA ACT -3′ for HSP70, procine HSP90 gene was retrieved from GenBank (NM_213973.1); 5′- GGT GAA GGT CGG AGT GAA CG -3′ and 5′- CTC GCT CCT GGA AGA TGG TG-3′ for glyceraldehyde phosphate dehydrogenase (GAPDH), procine GAPDH gene was retrieved from GenBank (XM_003126534.1) HSP90 and GAPDH primers were purchased from Shanghai Sangon Biological Engineering Technology & Services Co., Ltd. (Shanghai, China).

2.7 Real-Time PCR

The optimized reaction was carried out in a 20μL final reaction volume containing 0.8μL(100nmol/L) concentration of each forward and reverse primer, 0.8μl cDNA, 7.6 μL distilled water, 10 μLMaster Mix (SYBR® Green PCR Master Mix Kits). The thermal profile for the real-time PCR was 95 °C for 10 min, followed by 40 cycles of 95 °C for 30 s, 60 °C for 1min, then 95℃ 1min, 55℃ 30s, 95℃ 30s.The control group was cells of cDNA at 38.5 ℃cultured. The expression of different temperature treatments in each group trials conducted in the same group, each sample testing three parallel tests.

2.8 Statistical Analysis

Using $2^{-\Delta\Delta^{ct}}$ analysis methodologie for relative quantitation of gene expression. All data were subjected to one-way ANOVA by using SPSS(version 17.0 for windows). A probability value of $P<0.05$ was considered to be statistically significant.

3 Results

3.1 Cell Culture

There are few cells appeared around small tissue pieces until the 3th day. More adherent cells appeared and grew surrounding most of tissue pieces on the 5th day (Figure.1). On the 7th day, cells continued to grow strongly with the mixed-phase of epithelial-like cells and fibroblast-like cells， fibroblast cells and epithelial cells can be separated based on the different sensitivity to the enzymatic digestion. After 3 passages of selected subculture, purified fibroblast cells were obtained (Figure.2).

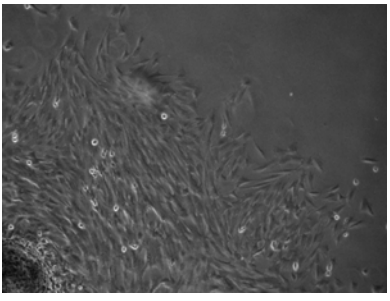

Fig. 1. The growth and emigration of fibroblasts（50×）

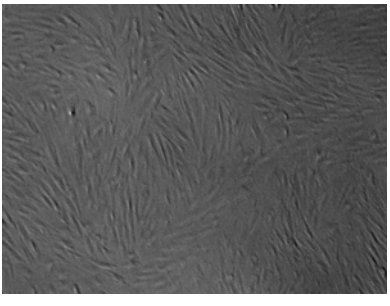

Fig. 2. Fibroblasts in isolated and purified culture （50×）

3.2 Melting Curve Analysis

Melting curve analysis was performed to measure the specificity of PCR product. The results showed that HSP90 and GAPDH genes of PCR product showed a relatively sharp single peak, no increase in fluorescence signal from primer-dimers or other non-specific amplification products (Fig.3). HSP90 and GAPDH genes melting temperatures were 84.58 ℃ and 84.60 ℃.

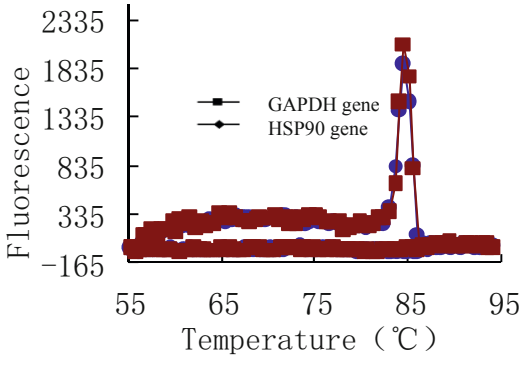

Fig. 3. Melting curve of HSP90 and GAPDH gene

3.3 Effect of Different Temperatures and Times at Cold Stress on Expression of HSP90 mRNA

The temperature dependence of this cold stress induction of expression of HSP90 mRNA is shown in Fig.4. In this experiment ,cells were preincubated at 4,15,25℃ and 32℃ for 4h followed by recovery and incubation at 38.5℃ for 4h.We showed that preincubated of cells at 4and15℃ gave a singnificantly promoted expression of HSP90 mRNA compared with the control group (P<0.05), at 25 and 32℃group had the tendency to promoted expression of HSP90 mRNA compared with the control group, but did not reach significant level (P> 0.05). Preincubation of cells at 4℃ for 4h followed by recovery and incubation at 38.5℃ for 2,4,6 and 8h. We observed that a peak increase was abserved between 4 and 6h of recovery at 38.5℃(Fig.5). Fig.6 illustrates the pattern of expression of HSP90 mRNA of cells preincubated at 25℃for 4h followed by recovery and incubation at 38.5℃ for 2,4h,6 and 8h. The results showed expression of HSP90 mRNA compared with the control group no significant difference (P> 0.05). Preincubation of cells at 4℃ for 2,4,6 and 8h followed by recovery and incubation at 38.5℃ for 4h. Our result showed the relative abundance of HSP90 mRNA was propprtional to the time of preincubation at 4℃.(Fig.7). Preincubation of cells at 25℃ for 2,4,6 and 8h followed by recovery and incubation at 38.5℃ for 4h. The results showed expression of HSP90 mRNA compared with the control group no significant difference (P> 0.05) (Fig.8).

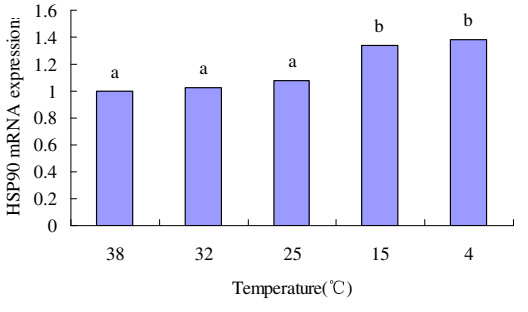

The different lowercase indicate significant difference(P <0.05),The same as below

Fig. 4. HSP90 mRNA expressions under Different temperatures

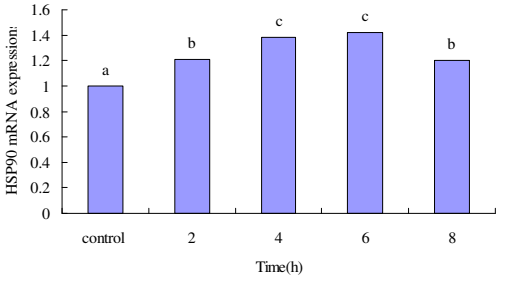

Fig. 5. HSP90 mRNA expressions under 4℃for 4h

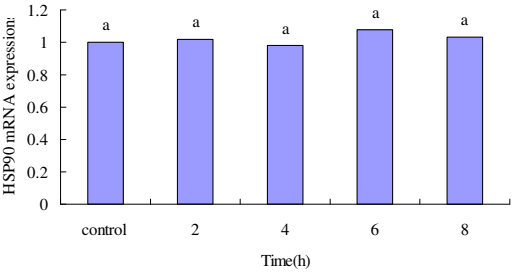

Fig. 6. HSP90 mRNA expressions under 25℃ for 4h

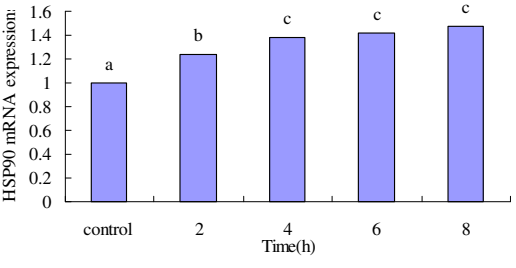

Fig. 7. HSP90 mRNA expressions under 4℃ for 2,4,6 and 8h

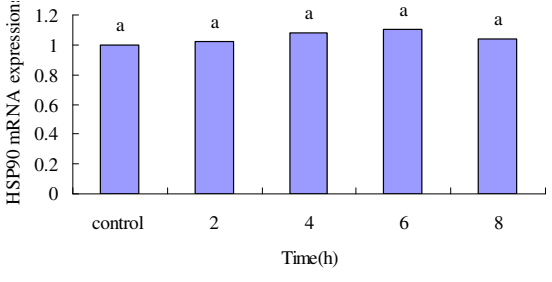

Fig. 8. HSP90 mRNA expressions under 25℃ for 2,4,6 and 8h

4 Discusion

One of the primary function of HSPs in cellular physiology is to serve as molecular chaperones. This functional role of HSPs is consistent with the observation that many of the conditions and reagents that induce the stress reponse have the ability of either damaging proteins directly or causing cells to synthesize or accumulate aberrant proteins. Most of mammalian cells gene expression is turned off under stress, transcriptional activity mainly in the HSPs gene[10]. Stress can induce a significant increase in the synthesis of HSP90, HSP90 in preventing stress-induced cell damage

and to restore damaged cells play an important role[11] . In this study, we use real-time PCR detection expression of HSP90 mRNA of procine fibroblasts that were preincubated at low temperature for specified time period and then incubated at at 38.5℃ for specified time period. We showed that preincubation of cells at 4 and 15℃ induced the expression of HSP90 mRNA upon recovery at 38.5℃, and the degree of this induction was directly related to the time that the cells spend at 4 and 15℃(data not shown). We observation that 25 and 32℃(data not shown)were the temperature of the recovery incubation period, below which litter or no induction of stress response was observed, is consistent with a role of active cell metabolism in those induction.

Acknowledgment. This work was supported by the Important Direction Foundation of National Natural Science Foundation of China(31072020).We are grateful for all the people who help us in the experimentation process.

Jianzhang Ma, Di Liu and Chunlong Liu are corresponding authors.

References

1. Sonna, L.A., Fujita, J., Gaffin, S., et al.: Molecular Biology of Thermoregulation Invited Review Effeets of heat and cold stress on mammalian gene expression. J. App. Physiol. 92, 1725–1742 (2002)
2. Carey, V., Hannah, V., Matthew, T., et al.: Mammalian Hibernation:Cellular and Molecular Responses to Depressed Metabolism and Low Temperature. J. Physiol. Rev. 83, 1153–1181 (2003)
3. Mohamed, B., Fageeh, A.L., Smales, M.: Control and regulation of the cellular responses to cold shock: the responses in yeast and mammalian systems. J. Biochem. 379, 247–259 (2006)
4. Underhill, M.F., Birch, J.R., Smales, C.M., Naylor, L.H.: eIF2α phosphory lation stress perception and the shutdown of global protein synthesis in cultured CHO cells. J. Biotechnol. Bioeng. 89, 805–814 (2005)
5. Chang, Y.S., Lo, C.W., Sun, F.C.: Diferential expression of Hsp90 isoforms in geldanamycin-treated 9L cells. J. Biechem. Biophys. Res. Communi. 344(18), 37–44 (2006)
6. Holland, D.B., Roberts, S.G., Wood, E.J., Cunliffe, W.J.: Cold shock induces the synthesis of stress proteins in human keratinocytes. J. Invest. Dermatol 101, 196–199 (1993)
7. Liu, A.Y., Bian, H., Huang, L.E., Lee, Y.K.: Transient cold shock induces the heat shock response upon recovery at 37 degrees C in human cells. J. Biol. Chem. 269, 14768–14775 (1994)
8. Filipovic, D., Gavrilovi, L., Dronjak, S.M., et al.: Liver Glucocorticoid Receptor and Heat Shock Protein 70 Levels in Rats Exposed to Different Stress Models. J. Physiol. Res. 57, 205–213 (2008)
9. Mosser, D.D., Theodorakis, J.D., Morimoto, R.I.: Coordinate changes in heat shock element-binding activity and HSP70 gene transcription rates in human cell. J. Biology 8(11), 4736–4744 (1988)
10. Iogiso, H., Kagi, N., Matsumoto, E., et al.: PhosPhorylation analysis of 90kDa heat shock Protein with in the cytosolic arylhydroearbon receptor complex. J. Biochemistry 43(49), 15510–15519 (2004)
11. Wang, X.J., Bao, E.D.: The expression of heat shock proteins. J. Husbandry and Veteinary Medicine 36(1), 41–43 (2004) (in Chinese)

Experimental Study on Acidic Fibroblast Growth Factor Composited by Partially Deproteinised Bone in Repair of Early-Stage Avascular Necrosis of the Femoral Head in Rabbits

Zhu Xiao-qi[1], Guo Hao[1], Ge Bao-feng[1,*], and Zhu Xiao-qi[2]

[1] Post-doctoral Workstation General Hospital of Lanzhou Military Area Command of Chinese PLA Lanzhou, Gansu Province, China, 730050
[2] Department of Orthopeadics Baoan Hospital, Southen Medical University Shenzhen, China, 518101
lzzyjw@sina.com, hobartzhu@hotmail.com

Abstract. Objective To evaluate the repairing effects of early-stage ANFH by Acidic fibroblast growth factor with partially deproteinised bone(aFGF/PDPB) on in rabbits Model. **Methods** Ribs from healthy, adult, New Zealand rabbits were prepared into Partially deproteinized bone(PDPB) .Acidic fibroblast growth factor (aFGF)diluted with sterile distilled water was composited by PDPB particles to prepare aFGF/PDPB bone. A bone window was made at the juncture of femoral head and femoral neck bilaterally in 24 healthy, adult, New Zealand rabbits. Rabbit models of bilateral ANFH were established by removing approximately 50% of cancellous bone and perfusion with 95% ethanol for 30 minutes. rabbit models were randomly divided into a blank group, a simple PDPB group, and aFGF/PDPB group. PDPB and aFGF/PDPB bone were implanted into the PDPB and aFGF/PDPB group accordingly, The blank group did not receive any implantation. At 2nd, 4th, and 8th weeks after surgery, ink-injected specimens were prepared for microvessel count and microvessel area analysis, X-ray examination and for histological examination on 24 animals model. **Results** Microvessel number and microvessel area were least in the blank group, followed by simple PDPB group, and lastly the aFGF/PDPB group. There was significant difference in microvessel number and microvessel area between aFGF/PDPB group and blank, simple PDPB groups (P<0.05).X-ray evaluation results demonstrated that aFGF/PDPB group yielded better effects than blank group (P < 0.05), and there was no significant difference between PDPB and aFGF/PDPB groups (P > 0.05). histological examination indicate that defects filled with granulation tissue and fibrous connective tissue, only a little osteoid tissue formed at the borderline in the blank group at the end of the 8th weeks. In PDPB group a little new bone and cavitas medullaris formed, At the 8th week, lots of graft was absorbed and cavitas medullaris formed with more osteoplast and myeloid cell in it. aFGF/PDPB group, better than that of PDPB group in each time group , At the 8th week, the graft was displaced by bone tissue, cavitas medullaris were formed with lots of bone marrow cells in it, at the borderline of the bone trabecula there were lots of

* Corresponding author.

E. Zhu and S. Sambath (Eds.): Information Tech. and Agricultural Eng., AISC 134, pp. 405–417.
springerlink.com © Springer-Verlag Berlin Heidelberg 2012

osteoplast and a little osteoclasts that play a role of bone remodeling, bone lacuna with mature bone cells in it can been seen. **Conclusion** aFGF/PDPB bone constructed by aFGF compound with PDPB scaffold material has good effect on repair femoral head avascular necrosis in rabbit model.

Keywords: Acidic fibroblast growth factor, Partially deproteinized bone, avascular necrosis of the femoral head, rabbit, vascularization.

1 Introduction

Acidic fibroblast growth factor (aFGF) possesses good effects on vascularization and osteogenesis[1-6]. Partially deproteinized bone (PDPB) prepared by allogenic bone exhibits satisfactory osteoinductivity[7-10]. Avascular necrosis of the femoral head (ANFH) is one of intractable problems in the field of orthopedics. If effective treatments can not be given timely, it often develops into femoral head collapse, and hip joint replacement is needed[11]. It is statistically analyzed that ANFH frequently occurs in people between 30- 50 years old, with a mean age of 38 years, and 25% of cases are aged < 25 years[12,13]. As for young and middle-aged patients who have more activities and expect to live long, effective methods are needed to prevent disease progression as far as possible to delay the time for joint replacement. Tissue engineering provides new means for treatment of ANFH. Can aFGF/PDPB heal early-stage avascular necrosis of the femoral head? It needs to be studied.

2 Materials and Methods

Design
A randomized, controlled, animal experiment.

Time and setting
Experiments were performed in the laboratory of the College of Life Science, Nanhua University between January 2008 and January 2009.

Materials
A total of 25 healthy, adult, New Zealand rabbits of either gender, 3 months old, weighing 2.4-3.0 kg, were provided by Laboratory Animal Center, Nanhua University. Experimental protocol was in strict accordance with the *Guidance Suggestions for the Care and Use of Laboratory Animals*, formulated by the Ministry of Science and Technology of China[14].

Table 1. Reagent and sources

Reagent	sources
aFGF	Beijing Biosynthesis Biotechnology Co.,Ltd.,China
30% hydrogen peroxide, acetone, sulfidization, 95%ethanol,formaldehyde	Tianjin Basifu Chemica Industry Co., Ltd., China
Ink	Beijing Yidege Ink Industry Co., Ltd., China
Heparin	Jiangsu Wanbang Biochemistry& Medcine Limited Company, China
Sumianxin II solution	Military veterinary Research Institute, Academy of Military Medical Sciences in Changchun, China

Preparation of PDPB [5]
One rabbit, weighing 2.8 kg, was sacrificed by injection of 15 mL air through the ear marginal vein. After thorough removal of soft tissue, the rib was cut into approximately 10 mm in length and rinsed repeatedly with distilled water to prepare PDPB according to the methods listed in Table 2.

Table 2. Preparation of partially deproteinized bone

Reagent	Treatment period	Temperature
30%H_2O_2	72h(every 24h change)	38℃
ddH_2O	30min	Room temperature
Alcohol	24h	Room temperature
ddH_2O	30min	Room temperature
Acetone	24h	Room temperature
ddH_2O	30min	Room temperature
Drying	8h	Room temperature

Preparation of artificial composite bone using aFGF and PDPB
One ampoule of aFGF (0.5 mg) was diluted into 10 μg/L with distilled water[4,5]. After addition of PDPB small blocks, the mixture was shaken in type MM-1 microoscillator to make liquid thoroughly immersing into PDPB blocks and then sub-packaged into 30 ampoules for centrifugation, 1 mL for each. Subsequently, aFGF/PDPB composite bones obtained by freeze-drying in a LGJ-10 D lyophilizer were sub-packaged with polyethylene thin film, fumigated with ethylene oxide, and preserved at 4 ℃ prior to use.

Preparation of compound ink injection[15]
150 mL of ink, 50 mL of formaldehyde, and 300 mL of physiological saline were prepared into 500 mL compound ink at a proportion of 3: 1: 6 and preserved in a closed container at room temperature.

Preparation of decalcification solution
5% formaldehyde 85ml, concentrated nitric acid 10ml and concentrated hydrochloric acid 10ml mixed.

Establishment of ANFH models [16~19]
Following anesthesia by intramuscular injection of 0.3-0.4 mL/kg sumianxin II injection, the rabbits were placed in a prone position and the skin in the surgical region was sterilized using 0.5% complex iodine.

A posterolateral incision was made at hip joint to expose greater trochanter and hip joint. Articular capsule was cut open through the intermuscular space posterior to greater trochanter of femur to expose femoral head and femoral neck, with round ligament not dissected to avoid dislocation of hip joint.

A hole, approximately 0.5 cm in depth and 2 mm lower than cartilage, was drilled using a trephine with a diameter of 3 mm, starting from juncture of femoral head and femoral neck towards femoral head. Approximately 50% of cancellous bone was removed from femoral head to induce femoral head defect. Surrounding soft tissue was protected using bandage. The cavity of bone defect was treated with 95% ethanol for 30 minutes and rinsed with sterile physiological saline for several

times. 24 successful rabbit models of ANFH were randomly divided into a blank group, a simple PDPB group, and aFGF/PDPB group, with 8 rabbits in each group. PDPB and aFGF/PDPB were implanted into the PDPB and aFGF/PDPB group accordingly. The blank group did not receive any implantation.

Following layer-by-layer suture, the incision was closed. Postoperatively, the animals were raised in separate cages. Food intake and activities as well as incision healing were observed. Within first 3 days, penicillin was daily injected into the forearms at 400,000 units per animal.

Perfusion of compound ink injection[1,20,21]

A median incision, approximately 8 cm in length, was made on the stomach. The abdominal aorta and inferior caval vein were dissociated, 2.0-3.0 cm for each. A segment of 4-cm abdominal aorta was dissected. The proximal and distal ends were separately inserted with a piece of suture line. The proximal abdominal aorta was ligated. An indewelling needle containing heparin anticoagulant was inserted towards the distal end. When needle head entered into the vessels, a part of needle core was withdrawn, subsequently the needle was advanced slowly along the vessel, and finally the whole indewelling needle was fixed and the needle core was completely withdrawn.

5 mL of heparin/physiological saline was infused through a 5 mL syringe which was connected to the indewelling needle. Following stripping of inferior caval vein, the proximal and distal ends were inserted with suture line separately. The proximal end was ligated, and the indewelling needle was inserted as above. The syringe connected to the indewelling needle in abdominal aorta was removed.

The tubing of physiological saline containing heparin was connected to the indewelling needle. The physiological saline containing heparin was allowed to slowly flow into the aorta, and the indewelling needle connected to the inferior caval vein was switched on. At this time, fresh blood first flowed out from the inferior caval vein, and perfusion was ended until blood color became clear.

The tubing for compound ink infusion was connected to the indwelling needle in the abdominal aorta. The compound ink was allowed to slowly flow into the abdominal aorta. Once ink appeared at the end of indwelling needle in the inferior caval vein, the tubing was occluded. Perfusion could be terminated when double lower limbs and finger nails became from dark to black.

Main outcome measures

Gross observation

In each group, 2 rabbits were sacrificed at 2 weeks after surgery, 3 at 4 weeks, and 3 at 8 weeks after Perfusion of compound ink injection for gross observation.

Vascularization observation

The specimen in each group after X-ray observation, take them for *Vascularization observation*. Three visual fields were randomly selected from bone grafting region or bone defect region in each section for microvessel counts and the mean value was obtained. PIPS2010 pathological analysis system was employed for microvessel count and microvessel area analysis.

X-ray observation[16]
In each group, 2 rabbits were sacrificed at 2 weeks after surgery, 3 at 4 weeks, and 3 at 8 weeks after gross observation take the specimen for X-ray observation bilateral femur was taken, adjacent soft tissue was removed, and X-ray films were taken under the conditions of 60 kV, 50 mA, and 0.12 second. Based on previous evaluation standard, precise scoring was shown in Table 2. Four physicians from radiology department who were blinded to experiments evaluated the defect repair of femoral head, as shown by X-ray examination. The X-ray examination criteria is as follows in table 5

Histological examination
At each time point, other 2 rabbits in each group sacrifice for histological examination , bilateral femur was taken, numbering femur head specime then decalcificate with decalcification solution for 48 hours, repleace decalcification solution in 24 hours. Rinse with running water for 4~8 hours. Setting with 4% paraformaldehyde then dehydration with grading alcohol paraffin embedding at last. Cut into slices by 5μm,HE staining and examine under microscope.

Statistical analysis
All data were statistically processed by the first author using SPSS 13.0 software and were expressed as Mean ± SD. One-way analysis of variance was employed.

3 Results

Gross observation
At 2 weeks after surgery
Blank group: bone window made at the juncture of femoral head and femoral neck could be clearly visible, with fibrous tissue in-growth and clearly distinguished defect edge.

Simple PDPB group: there was a blurry borderline between grafts and adjacent normal bone tissue, and joint surface was smooth.

aFGF/PDPB group: the borderline between grafts and defect edge was clear, and joint surface was smooth.

At 4 weeks after surgery
Blank group: bone window could be still visible, presenting with fibrous tissue in-growth, as well as rough joint surface in 3 rabbits.

Simple PDPB group: the borderline between grafts and defect edge was more blurry, rough joint surface could be found in 1 rabbit, and the remaining joint surface was smooth.

aFGF/PDPB group: the borderline between grafts and defect edge could be seen but very blurry, and joint surface was smooth in all rabbits.

At 8 weeks after surgery
Blank group: bone window became small, osteoid tissue and fibrous tissue grew into defect region, femoral neck fracture occurred in 1 rabbit, cough femoral head surface was observed in all rabbits (Fig.1a), and collapse of femoral head appeared in 2 rabbits.

Simple PDPB group: there was unclear borderline between grafts and defect region, cough joint surface was observed only in 2 rabbits, and no collapse of femoral head was observed.

aFGF/PDPB group: the borderline between grafts and defect region could be hardly seen, femoral head surface was smooth, and there was no collapse of femoral head (Fig. 1b).

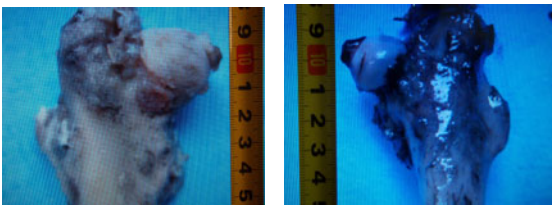

a: Blank group b: aFGF/PDPB group

Fig. 1. Gross observation at 8 weeks after surgery

Vascularization observation

At 2, 4, and 8 weeks after surgery, there were less microvessels and smaller microvessel area in the blank group than in the simple PDPB group. Compared with the simple PDPB group, abundant microvessels anastomosed together and formed net (Fig.2-4) in the artificial composite bone group. There was significant difference in microvessel count and microvessel area between artificial composite bone and the other two groups ($P < 0.05$). These findings demonstrate that aFGF exhibits the role of revascularization (Tables 2, 3).

X-ray observation[16]

The X-ray examination results in table 6

At 2 weeks after surgery

Blank group: Defect regions of ANFH models exhibited low-density shadow (Fig. 5a), presenting with no sclerotin formation, and defect region was similar to defect model in size.

PDPB group: Defect regions exhibited high-density presentations, the borderline between grafts and adjacent normal bone tissue was clear, and grafts could be clearly distinguished (Fig. 5b).

aFGF/PDPB group: All animal models of ANFH showed graft filling. The borderline was clear. A narrow euphotic zone could be observed (Fig. 5c).

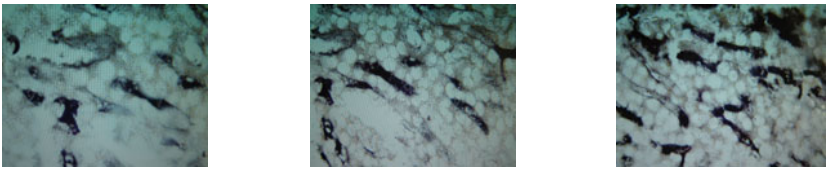

a: Blank group deproteinized bone group b: Simple partially group c: Artificial composite bone

Fig. 2. Transparent vascular specimens at 2 weeks after surgery (×100)

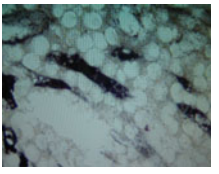
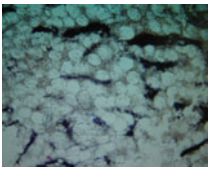
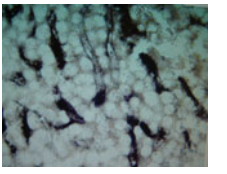

a: Blank group deproteinized bone group b: Simple partially group c: Artificial composite bone

Fig. 3. Transparent vascular specimens at 4 weeks after surgery(×100)

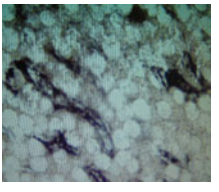
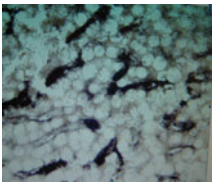
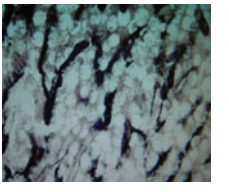

a: Blank group deproteinized bone group b: Simple partially group c: Artificial composite bone

Fig. 4. Transparent vascular specimens at 8 weeks after surgery(×100)

Table 3. Microvessel counts in each group ($\bar{x}\pm s$)

Group	2 wk (n = 2)	4 wk(n = 3)	8 wk (n = 3)
Blank	6.50±0.97	7.75±1.18	8.35±1.21
Simple PDPB	16.75±1.65	21.50±1.65	25.00±1.03
aFGF/PDPB	31.25±1.84[a]	34.50±2.21[a]	35.75±2.37[a]

PDPB: partially deproteinized bone; [a]$P < 0.05$, *vs*. simple PDPB and blank groups

Table 4. Microvessel area analysis results in each group ($\bar{x}\pm s$)

Group	2 wk (n = 2)	4 wk (n = 3)	8 wk(n = 3)
Blank	2.54±0.29	4.38±0.51	4.47±0.50
Simple PDPB	9.37±0.95	12.95±1.03	14.18±1.28
aFGF/PDPB	16.92±1.25[a]	18.22±1.11[a]	20.22±1.18[a]

[a]$P < 0.05$, *vs*. simple PDPB and blank groups

Table 5. Evaluation criteria regarding bone defect repair of the femoral head [24]

X-ray presentation	Grading	Score
Newly formed bone filling less than 25%, almost being composed of inconsecutive low-density bone	Worse	1
Newly formed bone filling 25%-75%, most being composed of normal bone density bone	Fair	2
Newly formed bone filling 76%-95%, being composed of normal bone density bone	Good	3
Normal density bone filled more than 95% of bone defect	Excellent	4

Table 6. X-ray scores in each group at each time point

Group	2 weeks	4 weeks	8 weeks
Bank	1.25±0.45	1.25±0.44	1.25±0.44
PDPB	1.50±0.73	2.25±0.53	3.25±0.44
aFGF/PDPB	1.75±0.58	3.25±0.60[a]	3.75±0.44[a]

[a]$P < 0.05$, *vs*. blank group

At 4 weeks after surgery

Blank group: Defect regions of ANFH models exhibited low-density shadow, presenting with no sclerotin formation, and defect region area was reduced compared with 2 weeks after surgery (Fig. 6a).

PDPB group: Defect regions exhibited high-density shadow, the borderline between grafts and adjacent normal bone tissue was clear, and grafts could be clearly distinguished (Fig. 6b). *aFGF/PDPB group:* Defect regions exhibited filling presentation, the borderline became unclear and could be distinguished after careful discrimination, and there was no evident difference in bone density between bone defect region and adjacent normal bone tissue (Fig. 6c).

At 8 weeks after surgery

Blank group: Defect regions of ANFH models exhibited low-density shadow (Fig. 7a). Collapse of the femoral head appeared in 2 rabbits. Representations in the defect region were reduced compared with 4 weeks after surgery.

PDPB group: Normal femoral head was observed in 1 rabbit. Bone defects could be distinguished from adjacent normal bone tissue by careful discrimination (Fig. 7b), but grafts were hardly distinguished, in 2 rabbits.

aFGF/PDPB group: Bone defect regions of all femoral head fused with adjacent normal tissue. There was no apparent difference in bone density between bone defects and adjacent normal bone tissue (Fig. 7c).

Histological examination

2 weeks after operation

Capsule cavity can been seen a lots of granulation tissue and fibrillar connective tissue growing into in Blank group. In PDPB group, A little fibrillar tissue growing into cavity of transplant,a little micrangium can been seen,lots of fibroblast and inflammatory cells can been seen, little mesenchymal cell and osteoblast seen. In aFGF/PDPB group: little fibrillar tissue growing into cavity of transplant, more micrangium and mesenchymal cells osteoblasts and less inflammatory cells can seen. (fig. 8).

a: Blank group deproteinized bone group b: Simple partially group c: Artificial composite bone

Fig. 5. X-ray presentations in each group at 2 weeks after

a: Blank group deproteinized bone group b: Simple partially group c: Artificial composite bone

Fig. 6. X-ray presentations in each group at 4 weeks after surgery

a: Blank group deproteinized bone group b: Simple partially group c: Artificial composite bone

Fig. 7. X-ray presentations in each group at 8 weeks after surgery

4 weeks after operation

Capsule cavity decrease in blank group,the cavity fill up with granulation tissue and fibrillar connective tissue a lot of fibroblast and inflammatory cellscan been seen,little osteoid tissue and chondrocyte island distribute isolatedly among fibrillar connective tissue. I n PDPB group, transplant begin to be absorbed ,a little neoplastic bone formation observed and many osteoblasts can been seen, more micrangium observed than that of 2 weeks,no inflammatory cells can seen.I n aFGF/PDPB group: the

transplant cavity fill up with osteoid tissue,a lot of osteogenic precursor cells and osteoblasts can seen , a lot of micrangium observed , osteoid tissue began o rebuild osteoblasts row up along bone trabecula and some osteoclast can seen, bone lacuna and mature osteoblasts can seen(fig. 9).

8 weeks after operation

In blank group:the cavity fill up with fibrillar connective tissue, the major cells are fibroblast and inflammatory cells, sparsely distributed blood vessels, neoplastic osteoid tissue can seen in the borderline. In PDPB group, most of the transplant has been absorbed, more osteoblasts,more new blood vessels han that of 4 weeks , some osteoclast can seen. In aFGF/PDPB group: the transplant replaced by osseous tissue, woven bone and lamellar bone exist at the same time, rich in intramedullary blood vessels , a lot of osteoblasts row up along bone trabecula and a little osteoclasts can seen, bone lacuna and mature osteoblasts can seen(fig.10).

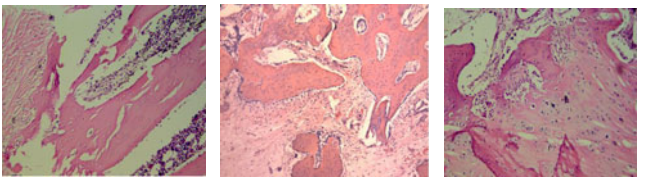

a: blank group b: PDPB group c: aFGF/PDPB group

Fig. 8. Histological observation at 2 weeks after operation

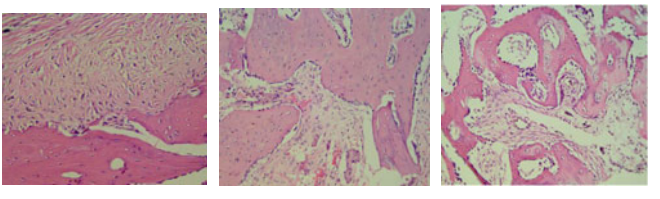

a: blank group b: PDPB group c: aFGF/PDPB group

Fig. 9. Histological observation at 4 weeks after operation

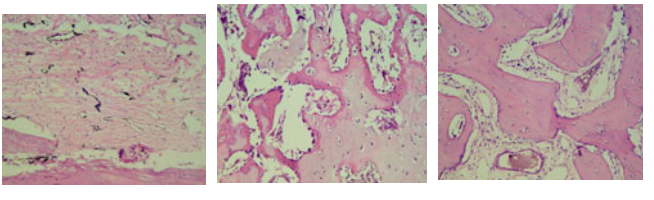

a: blank group b: PDPB group c: aFGF/PDPB group

Fig. 10. Histological observation at 8 weeks after operation

4 Discussion

In recent 30 years, there have been many studies regarding establishment of ANFH animal models[22~26]. Up to date, however, ideal models that can simulate the natural pathological process of adult ANFH and characterize the collapse of subchondral bone in human ANFH have not be established. An ideal animal model should provide several characteristics: easy and convenient establishment with high success rate, as well as able to produce different stages of osteonecrosis within short term.

Mont et al[17] established a canine femoral head defect model by making a bone window at the juncture of femoral head and femoral neck to study the therapeutic effects of bone growth factors on femoral head necrosis and acquired satisfactory effects. A study reports a canine femoral head defect model, in which 50% of sclerotin in the head was removed through a bone window made at the subchondral edge. Results showed that collapse of femoral head was observed in 3 out of 8 femoral heads and the subchondral strength was 72% of intact side[1]. Based on this, Xu et al[26] soaked canine femoral head defect model with 95% ethanol for 30 minutes. Thus, the established femoral head defect model is close to cystic degeneration in femoral head necrosis and can be used to study the effects of grafting on femoral head necrosis.

In the present study, approximately 50% of cancellous bone was removed from femoral head through a hole made at the juncture of femoral head and femoral neck, and femoral head was soaked with 95% ethanol for 30 minutes. At 8 weeks, the blank group exhibited X-ray low-density shadow of defect region and presented collapse of femoral head in 2 rabbits. The bone defect regions exhibited a reduced tendency with time, but obvious bone defects exist at 8 weeks. This indicates the feasibility of ANFH.

Established using the composite constructed by aFGF and PDPB

aFGF, one of members from fibroblast growth factor family found earliest, is expressed in most tissues and cells and can combine with corresponding receptors to exhibit promoting effects on division and differentiation of various cells from mesoderm and neuroectoderm, in particular on promoting the proliferation of vascular endothelial cells and smooth muscle cells and inducing angiogenesis. There is evidence demonstrating that aFGF has been shown to be one of primary vascular growth-promoting factors and exhibit promoting effects on vascularization through no matter local arterial administration or intramuscular injection[3~6].

The present PDPB is similar to human body bone tissue in terms of reticulated pore system, porosity, pore transportation, and aperture size of osseous tissue and reserves some inorganic salt components and protein components. Therefore, it offers some biomechanical property and exhibits weak antigenicity. Strong evidence demonstrates that the structure and composition of PDPB used in the present study correspond to physiological requirements, exhibit good cellular compatibility and histocompatibility, provide sufficient internal space and surface area for osteoblast proliferation and vascular ingrowth, and thereby exhibit good osteogenesis[7~9]. Taken together, PDPB can be considered an ideal scaffold material in the study of bone tissue engineering.

The tissue-engineered bone constructed by aFGF composited with PDPB was implanted into femoral head necrosis region. Microvessel counts and microvessel area

analysis demonstrated that aFGF/PDPB group yielded better outcomes in terms of no matter new bone formation or angiogenesis than simple PDPB and blank groups. The X-ray results showed that aFGF/PDPB yielded better effects than that of PDPB group, but there was no significant difference between these two groups. This is likely to be related to non-refined X-ray scoring criteria[27]. The present results demonstrated that aFGF/PDPB produced some satisfactory effects on promoting angiogenesis and accelerating bone formation in animal models of ANFH, which provides a potential therapeutic means for treatment of femoral head necrosis using tissue engineering method.

However, osteogenesis in vivo and angiogenesis are a process in which many factors intercoordinate. The regulation of mutual effects of aFGF and other growth factors on promoting osteoanagenesis is under investigation. In addition, repair of ANFH is a complex process and it is influenced by many factors. The present study only investigated the pathological changes in some a stage, and further studies should be needed.

References

1. Zhu, X.-Q., Guo, H.: Vascularization of acid fibroblast growth factor/partially deproteinised bone in repair of early-stage avascular necrosis of the femoral head in rabbits. Journal of Clinical Rehabilitative Tissue Engineering Research 13(38), 7469–7473 (2009)
2. Cuevas, P., de Paz, V., Cuevas, B., Marin-Martinez, J., Picon-Molina, M., Fernandez-Pereira, A., et al.: Osteopromotion for cranioplasty:an experimental study in rats using acidic fibroblast growth factor. Surg. Neurol. 47, 242–246 (1997)
3. Yu, Y., Cai, S., Xia, Y., Weririch, H.G.: Advances in acid fibroblast growth factor Research. Chinese Pharmacological Bulletin 18, 125–128 (2002)
4. Chen, J.N., Tu, C.Q., Gong, Q.: Experimental study on promote guided bone regeneration by acidic fibroblast growth factor. Zhongguo Xiufu Chongjian Waike Zazhi 13(5), 301–314 (1999)
5. Tu, C.Q., Yu, S.F., Wang, Y.P., Chen, X.O., Gong, Q., Pei, F.X.: Effect on human osteoplast growth of Recombination Human acidic fibroblast growth factor. Zhonghua Guke Zazhi 21(8), 489–492 (2001)
6. Kelpke, S.S., Zinn, K.R., Rue, L.W., Thompson, J.A.: Site-specific delivery of acidic fibroblast growth factor stimulates angiogenic and osteogenic responses in vivo. J. Biomed. Mater. Res. A 71(2), 316–325 (2004)
7. Kang, F.W., Tang, X.F., Wen, Y.M.: Experimental Research on Preparation of Natural Derived Material from Human Bone. Tongji Daxue Xuebao: Yixue Ban 26(6), 4–7 (2005)
8. Li, Y.L., Yang, H., Han, R.: Experimental Study on repairing bone segmental defect by three kinds of bio-derived materials. Zhongguo Xiufu Chongjian Waike Zazhi 19(2), 118–123 (2005)
9. Peng, K., Xiang, Z., Yang, Z., Xie, H., Wu, X., Huang, F., et al.: Clinical application of bio-derived bone transplantation with tissue engineering technique: 7 year follow-up. Zhongguo Xiu Fu Chong Jian Wai Ke Za Zhi 22(5), 606–609 (2008)
10. Li, Y.L., Yang, Z.M., Xie, H.Q., Qin, T.W., Huang, F.G.: Experimental studies on procedures and properties of natural derived scaffold materials of tissue engineered bone. J. Biomed. Eng. 19, 10–12 (2002)

11. Gangji, V., Hauzeur, J.P., Matos, C., De Maertelaer, V., Toungouz, M., Lambermont, M.: Treatment of osteonecrosis of the femoral head with implantation of autologous bone-marrow cells: A pilot study. J. Bone Joint Surg. Am. 86-A(6), 1153–1160 (2004)
12. Yoon, T.R., Song, E.K., Rowe, S.M., Park, C.H.: Failure after core decompression in osteonecrosis of the femoral head. Int. Orthop. 24(6), 316–318 (2001)
13. Gebhard, K.L., Maibach, H.I.: Relationship between systemic corticosteroids and osteonecrosis. Am. J. Clin. Dermatol. 2(6), 377–388 (2001)
14. The Ministry of Science and Technology of the People's Republic of China. Guidance Suggestions for the Care and Use of Laboratory Animals (September 30, 2006)
15. Chen, J., Huang, G.F., Qi, C.: Vascularization in transplantation of bio-derived bone compounded with marrow stromal stem cells in repair of goat tibial shaft defect. Zhongguo Xiu Fu Chong Jian Wai Ke Za Zhi 18(4), 309–313 (2004)
16. Mont, M.A., Hugeorfrd, D.S., Maryland, B.: Non-traumatic avascular necorsis of the femoral head. J. Bone Joint Surg. 77-A(3), 459–474 (1995)
17. Mont, M.A., Einhorn, T.A., Sponseller, P.D., Hungerford, D.: The trapdoor procedure using autogenous cortical and cancellous bone grafts for osteonecrosis of the femoral head. J. Bone Joint Surg. Br. 80(1), 56–62 (1998)
18. Wang, W.M., Zhao, D.W.: An experimental research of refrigeration with liquid nitrogen to ONFH. Gu yu Guanjie Shunshang Zazhi 16(6), 444–445 (2001)
19. Kun, G., Xun, P.W., He, L.: Animal model constructions of vascular necrosis of the femoral heads. Academic Journal of Kunming Medical College (2), 106–109 (2004)
20. Qi, C., Yang, Z.M., Huang, F.G., Qin, T., Li, X., Luo, J., et al.: Experimental study on repair of goat tibia defect with marrow stromal cell and bio-derived bone. Zhongguo Xiufu Chongjian waike Zazhi 19(2), 90–94 (2005)
21. Wang, X.M., Pei, G.X., Jin, D., Wei, K.H., Jiang, S., Tang, G.H.: Detecting the Vascularization of tissue engineer bone in vivo rhesus. Zhongguo Zuzhi Gongcheng Yanjiu yu Linchuang Kangfu 10(2), 87–90 (2006)
22. Wen, Q., Ma, L., Chen, Y.P., Yang, L., Luo, W., Wang, X.N.: A rabbit model of hormone-induced early avascular necrosis of the femoral head. Biomed. Enviiron. Sci. 21(5), 398–403 (2008)
23. Ma, H., Zeng, B., Li, X., Chai, Y.: Experimental study on avascular necrosis of femoral head induced by methylprednisolone combined with lipopolysaccharide in rabbits. Zhongguo Xiu Fu Chong Jian Wai Ke Za Zhi 22(3), 265–270 (2008)
24. Xu, J., Zhang, C., Sun, J., Zhang, A.: Cryosurgery for osteonecrosis of the femoral head in three-leg canine model. Zhongguo Xiu Fu Chong Jian Wai Ke Za Zhi 22(10), 1165–1168 (2008)
25. Manggold, J., Sergi, C., Becker, K., Lukoschek, M., Simank, H.G.: A new animal model of femoral head necrosis induced by intraosseous injection of ethanol. Lab. Anim. 36(2), 173–180 (2002)
26. Xu, X.L., Tong, Z.Q., Wang, K.Z., et al.: Experimental study of bBMP/collagen/coral composited bone substitute in repairing of bone defect of femoral head. Gu yu Guanjie Shunshang Zazhi 15(3), 209–211 (2000)
27. Zhu, X.-Q., Guo, H.: Acidic fibroblast growth factor composited by partially deproteinised bone in repair of early-stage avascular necrosis of the femoral head in rabbits. Journal of Clinical Rehabilitative Tissue Engineering Research 13(42), 8260–8264 (2009)

Insecticidal Activity of Extract from *Cynanchi Auriculati* against Agricultural Pests

Minli Yang*, Xiaomei Ma, and Fengxia Hao

Key Laboratory of Energy Sources & Chemical Engineering,
University of Ningxia
Yinchuan, Ningxia Hui Autonomous Region, China
yml@nxu.edu.cn

Abstract. In order to examine the insecticidal activity of Cynanchi Auriculati, dropping method was used for the testing of the activiyies of ethanol extract against the five kinds of pests (Plutella xylostella, Mythimna separata, Pieris rapae, Aphis and Homona coffearia) The results showed that 95% ethanol extract of Cynanchi Auriculati exhibited strong impact on Plutella xylostella, Aphis and Homona coffearia, but weak effect on Pieris rapae and almost no activity on Mythimna separata. The corrected mortality against five species of pests under the concentration of 50.0mg/mL were in the order of Aphis (97.70%) > Homona coffearia (88.91%) > Plutella xylostella (83.33%) > Pieris rapae (30.00%) after 48 h. Five different polar extracts were also investigated of the activities against Plutella xylostella ,the mortalities on 3th larvae of Plutella xylostella were in the order of petroleum ether (97.95%) > chloroform (42.17%) > ethyl acetate (28.57%) > distilled water (18.37%) > n-Butanol (11.53%).

Keywords: Cynanchi Auriculati, Agricultural Pests, Insecticidal Activity.

1 Introduction

Over the past half century, control of the agricultural pest prevention is primarily dependent upon the applications of chemical nsecticides. Although chemical pesticides have played a great part in the control of agricultural pests, long-term use of chemical insecticide have induced many problems, such as pest resistance, negative impact on natural enemies, environmental and health harm [1, 2]. All of these potential dangers have aroused scientists to find a new pattern of botanical pesticides.

Extensive surveys and reports on plants used as insecticides can be found in the literature[3]. Over 2000 species of plants are known to possess some insecticidal properties [4]. Recently some of the researchers have reported the bioactivity of extracts from various plants against important agricultural insect pests [5-8]. *Cynanchi Auriculati* aboundently distributes in Jiang Su, Shan Dong and Ning Xia of China. Some surveys and reports indicated it has varieties of pharmacological actions,

* This research was supported by a grant from the Natural Science Foundation of China (grant no. 20565003) and Science Fund of NingXia (NZ1013).

E. Zhu and S. Sambath (Eds.): Information Tech. and Agricultural Eng., AISC 134, pp. 419–424.
springerlink.com © Springer-Verlag Berlin Heidelberg 2012

including antitumor [9], clearing away free radicals [10], enhancing immunity [11] and reducing high serum cholesterols [12]. However, studies on its pesticidal activity are scanty and no quantitative report is available.

The objective of this study was to examine the insecticidal activity *o*f the *Cynanchi Auriculati*. Five species of agricultural pests were selected as testing pests for the study. The results showed that ethanol extract exhibited strong activity on *Plutella xylostella*, *Aphis* and *Homona coffearia*, the effect on *Pieris rapae* is quite low and almost no activity on *Mythimna separata*. Five polar-solvent extracts were obtained by extracting with different polar-solvents. The activity test of the polar-solvent extracts indicated that petroleum ether extract exhibited strongest activity, which was followed by the extract of chloroform, ethyl acetate, distilled water and *n*-butanol, which give the information that the insecticidal components may belong to a kind of weak –polar substances.

2 Materials and Methods

2.1 Plant Material

Cynanchi Auriculati was collected from the south area of Ningxia province, China. Make it dried in open air under the shade. Crushed it into a fine powder and stored in a paper bag in dark.

2.2 Test Pests

Plutella xylostella, Mythimna separata and Pieris rapae was reared and maintained in the laboratory at 23±1℃, 80±3% RH and a photoperiod of 16:8 (L:D). *Aphis* and *Homona coffearia* were collected from the crops which never sprayed any insecticide. The pests′ natural diet and stage used were displayed in Table 1.

Table 1. Agricultural Pests for Test

No	Name	Natural Diet	Stage used for bioassay
1	*Plutella xylostella*	Cabbage[a]	3nd instar larvae
2	Pieris rapae	Cabbage[a]	2nd instar larvae
3	*Homona coffearia*	Peach[b]	Adults
4	*Aphis*	Medlar[b]	Adults
5	Mythimna separate	Wheat[b]	2nd instar larvae

a. the cabbage was bought from the market.
b. the crop that never sprayed insecticide.

2.3 Preparation of the Test Samples

Ethanol extract was prepared as following: Weighting dried powder of the *Cynanchi Auriculati* 5.0g and putting into a 100mL triangle vial. Adding 95% ethanol 80mL and keeping the vial in shade for 24h. Extracting with supersonic (40khz) for 30 minutes at the temperature of 45℃. Filtrating and collecting the mother liquid. The residues were extracted with the same procedure for two times. All the mother liquids were

incorporated and concentrated by removing solvent under vacuum until dryness. Weighing up the extract (0.5g) and adding 80% acetone (10mL) to make the concentration of solution 50mg/mL. This solution was used for the screening bioassay.

Different polar-solvent extracts were prepared by extracting the ethanol extract with solvents of variation polarity. About 10.0g ethanol extract was suspended in distilled water (150mL) and then was diverted into 250mL separate funnel. The solution was extracted with 50mL petroleum ether for three times, followed by chloroform, ethyl acetate and n-Butanol. These five kinds of extract were concentrated respectively by removing solvent under vacuum until dryness and the sub-fractions were obtained, extraction yields of these different extracts were as following, distilled water (42.77%) > petroleum ether (32.90%) > n-Butanol (14.98%) > chloroform (7.86%) > ethyl acetate (1.39%). 5.0mg/mL solution of these extracts (80% acetone as the solvent) were used for the screening bioassay.

2.4 Screening Bioassay

A topical application method [13] was used to evaluate the activity of the test samples prepared above.

The selected pests were given the test samples 1.0μl on its body (chest and back). The control treatment was conducted with 80% acetone. All the tested pests were reared with their natural diet in a Petri dish (diameter = 9 cm) and maintained at 23±1℃, 80±3% RH and a photoperiod of 16:8 (L:D) in laboratory. Mortality of *Homona coffearia* and *Aphis* was determined in 24h and 48h after treatment, while *Plutella xylostella, Mythimna separate and Pieris rapae* were determined in 24h, 48h and 72h, respectively. Mortality was defined as no movement while pest body was probed with soft brush. In this experiment, 10 larvae of *Mythimna separate* and *Pieris rapae* were used in each test, while 30 larvae for *Homona coffearia, Aphis* and *Plutella xylostella.* Every experiment was carried out in triplicate.

2.5 Date Analysis

Date from all bioassays were corrected for control mortality by using [14, 15] formula.

(1) Rate of mortality = $\frac{N_1}{N} \times 100\%$

N_1: the number of death insects

N: the number of total insects

(2) Rate of corrected mortality = $\frac{M_2}{1-M_1} \times 100\%$

M_1: the rate of mortality in control group

M_2: the rate of mortality in treatment group

3 Results

3.1 The Insecticidal Activity of Ethanol Extract

The toxicity of ethanol extract against the five species of pests at the dosage (50mg/ml) is presented in Table 2.

Table 2. Corrected Mortality of Ethanol Extract to Different Pests

pests	Corrected mortality (%) ± S.D.		
	24h	48h	72h
Plutella xylostella	80.00 ± 0.0	83.33 ± 0.19	89.79 ± 0.0
Pieris rapae	20.00 ± 0.0	30.00 ± 0.0	43.33 ± 0.19
Homona coffearia	85.52 ± 1.1	88.91± 1.1	/
Aphis	96.69 ± 1.1	97.70 ± 1.1	/
Mythimna separate	0	0	0

From Table 2 it can been seen that ethanol extract exhibited obvious effects on *Plutella xylostella, Homona coffearia and Aphis,* but weak effect on *Pieris rapae and* no effect on *Mythimna separate*. The corrected mortality after 48h were in the order of *Aphis* (97.70%) > *Homona coffearia* (88.91%) > *Plutell xylostella* (83.33%) > *Pieris rapae* (30.00%). The 72h corrected mortality, *Plutella xylostella* (89.79%) > *Pieris rapae* (48.36%).

3.2 The Insecticidal Activities of Different Polar-Solvent Extracts

The activity of different polar-solvent extracts against *Plutella xylostella* were presented in the Table 3.

Table 3. Corrected Mortality of Different Extracts to *Plutella Xylostella*

Extract	Corrected mortality (%) ± S.D.		
	24h	48h	72h
Petroleum ether	86.67 ± 0.19	90.00 ± 0.0	97.95 ± 0.0
Chloroform	30.00 ± 0.0	36.67 ± 0.34	42.17 ± 0.32
Ethyl acetate	23.33 ± 0.2	26.67 ± 0.19	28.57 ± 0.36
n-Butanol	6.67 ± 0.19	10.00 ± 0.0	11.53 ± 0.68
Distilled water	10.00 ± 0.0	16.67 ± 0.19	18.37 ± 0.0
Control	0	0	2.00

The results showed that petroleum ether extract give an obvious effect on 3rd larvae of *Plutella xylostella*, and other extracts were weaker on the activity against 3rd larvae of *Plutella xylostella* 72h mortalities on 3rd larvae of *Plutella xylostella* were petroleum ether (97.95%) > chloroform (42.17%) > ethyl acetate (28.57%) > distilled water (18.37%) > n-Butanol (11.53%).

Extraction yields of different extracts were as following, distilled water (42.77%) > petroleum ether (32.90%) > n-Butanol (14.98%) > chloroform (7.86%) > ethyl acetate (1.39%). According to activity and extraction yield, petroleum ether extract was selected for further investigation.

3.3 Dose-Response Experiment

The results of dose-response experiment of petroleum ether extract against *Plutella xylostella* were listed in Table 4.

Table 4. Dose – Response of Petrolum Ether Extract to 3rd *Larvae Plutella Xylostella*

Dose of samples (mg/ml)	72h Corrected mortality (%)	Linear equation	LC_{50}
50.0	97.95		
25.0	82.99		
12.5	62.58	Y=1.0552 x +	
6.25	57.58	4.3386	4.22 mg/ml
3.125	42.17	r=0.9615	
1.56	35.38		
Control	2.00		

It was obvious that the Corrected mortality increased with the increasing of the dosage. Under the concentration of 50mg/mL the corrected mortality in 72 h was 97.95% and the LC_{50} value was 4.22mg/ml.

4 Conclusion

Activity testing of ethanol extract against different pests showed that *Cynanchi Auriculati* has an impact on *Plutella xylostella*, *Aphis* and *Homona coffearia*. Activity testing of different polar- extracts on larvae of 3rd *Plutella xylostella* showed that petroleum ether extract exhibited the strongest activity which indicated the bioactivity ingredient may belong to a sort of weak-polar substances.

According to results of this study, *Cynanchi Auriculati* could be developed into products suitable for pest management.

References

1. Roush, R.T.: Insecticide resistance management in diamondback kck moth: quo vadis. In: Proceedings of the Third International Workshop, Kuala Lumpar, Malaysia, October 1996, pp. 21–25 (1996)
2. Isman, M.B.: Plant essential oils for pest and disease management. Ind. Crop. Prod. 19, 603–608 (2000)
3. Jacobson, M.: Plants, insects and man – their interrelationships. Econ. Bot. 3, 346–354 (1982)
4. Klocke, J.A.: Plant compounds as source and models of insectcontrol agents. In: Hostettmann, K. (ed.) Economic and Medicinal Plant Research, pp. 103–144. Academic Press, London (1989)
5. Morimoto, M., Tanimoto, K., Sakatani, A., Komai, K.: Antifeedant activity of an anthraquinone aldehyde in Galium aparine L. against Spodoptera litura F. Phytochemistry 60, 163–166 (2002)
6. Park, B.S., Lee, S.E., Choi, W.S., Jeong, C.Y., Song, C., Cho, K.Y.: Insecticidal and acaricidal activity of piperonaline and piperoctadecalidine derived from dried fruits of Piper longum L. Crop Protect. 21, 249–251 (2002)
7. Koul, O., Daniewski, W.M., Multani, J.S., Gumulka, M., Singh, G.: Antifeedants effects of the Limonoids from Entandrophragma candolei (Meliaceae) on the gram pod borer, Helicoverpa armigera (Lepidoptera: Noctuidae). J. Agricult. Food Chem. 51, 7271–7275 (2003)

8. Suliman, R., Saker, I., Namora, D.: Importance of plant extracts in managing Aphis fabae. In: Khateeb, N.A. (ed.) Arab Scientist. Org. The Eighth Arab Congress of Plant Protection, October 12-16, Omar Al-Mukhtar University, El-beida City (2003)
9. Shan, L., Zhang, W.D., Zhang, C., Liu, R.H., Su, J., Zhou, Y.: Antitumor activity of crude extract and fractions from root tuber of Cynanchum auriculatum Royle ex Wight. Phytotherapy Research 19, 259–261 (2005)
10. Song, J.M., Ding, X.L.: Study on the scavenging effect of Baishouwu on superoxide free radicals. Chinese Wild Plant Resources 17, 1–4 (1997)
11. Gu, L.G., Gong, S.S., Tao, J.D., Liu, C.H., Zhou, Y.: Studies on the regulation effect of Baishouwu on the immunity of mouse. Chinese Journal of Integrative Medicine 7, 37–41 (1987)
12. Niu, J.Z., Ye, B.K., Wang, D.F.: Observation of the protection effect of Baishouwu towards the liver of the high serum cholesterol mouse. Acta Medica Sinica 3, 266–268 (1988)
13. Kim, S.I., Park, C., Ohh, M.H., Cho, H.C., Ann, Y.J.: Contact and fumigant activities of aromatic plant extracts and essential oils against Lasioderma serricorne (Coleoptera: Anobiidae). Journal of Stored Products Research 39, 11–19 (2003)
14. Xie, H.Y., Jiang, H.Y., Wang, G.P., et al.: Insecticidal activities of extracts from Acorus graminues Rhizome against Mythimna separate Walker. Chinese Joumal of Pesiticides 43(8), 367–369 (2004)
15. Xue, C.W., Wang, H.Y., Sun, Q.: Bioactivity of five insecticides against Diamond Back Moth (Plutella xylostella L.). Agrochemicals Research & Application 10(5), 25–28 (2006)

Insecticidal, Antifeedant and Growth-Inhibition Activities of Different Extracts from *Pedicularis Spicata* against *Plutella Xylostella*[*]

Minli Yang, Rui Liang, and Fengxia Hao

Key Laboratory of Energy Sources & Chemical Engineering,
University of Ningxia
Yinchuan, Ningxia, China
yml@nxu.edu.cn

Abstract. Insecticidal, antifeedant and growth-inhibition activities of five different extracts (petroleum ether, chloroform, ethyl acetate, n-butanol and water) from Pedicularis spicata against 3th instar larvae of Plutella xylostella were measured by the methods of dipping, leaf dish and feeding. The results showed the extracts of petroleum ether and chloroform have strong activity on 3th instar larvae of Plutella xylostella. Under the concentration of 4.00 mg/mL, the corrected mortalities of insecticidal activity after 72 h treatment were 100% and 93.1%, respectively, the antifeedant rates were 69.9% and 72.7% after 48 h, growth inhibition rate were 74.2% and 72.6% after 48 h, pupation rates were 53.3% and 57.8%, adult emerging rates were 40.0% and 33.3 %. Compared to the two extracts, the extracts of ethyl acetate, n-butanol and water displayed less potent or no activity on the 3th instar larvae of Plutella xylostella.

Keywords: Pedicularis spicata, Plutella xylostella, Insecticidal activity, Antifeedant activity, Growth-inhibition activity

1 Introduction

The search for new strategies or natural products to control destructive insects is desirable due to the prevalent occurrence of insecticide resistance and the problem of toxic non-biodegradable residues contaminating the environment and undesirable effects on nontarget organisms [1, 2]. Extensive surveys and reports on plants used as insecticides can be found in the literature. Over 2000 species of plants are known to possess some insecticidal properties [3]. Recently some of the researchers have reported the bioactivity of extracts from various plants against important agricultural insect pests [4-6]. *Pedicularis spicata* belongs to the family of genera *Scrophularicacac*. It is widely distributed in Northwest region and Southwest region of China. The researches on its chemical constituents and pharmacology have been reported [7, 8]. In our programme of screening of naturally occurring insecticides from the northwestern part of China, *Pedicularis spicata* was found to possess marked

* This research was supported by a grant from the Natural Science Foundation of China (grant no. 20565003) and Science Fund of NingXia (NZ1013).

E. Zhu and S. Sambath (Eds.): Information Tech. and Agricultural Eng., AISC 134, pp. 425–431.
springerlink.com © Springer-Verlag Berlin Heidelberg 2012

activity on *Plutella xylostella* [9, 10]. This work aimed to evaluate the activity of different extracts from *Pedicularis spicata* against *Plutella xylostella*, which may be helpful for the better use of this plant as an insecticidal plant.

2 Materials and Methods

2.1 Plant

Pedicularis spicata was collected from Liu-pan Mountain located in Ningxia province (altitude 3000 m). Plants were dried under shaded condition for a few days followed by drying in oven at 40 ℃ for 24 h, then crushed into a fine powder and stored in a paper bag in dark.

2.2 Insect

Plutella xylostella was reared and maintained in the laboratory at 23±1℃, 80±3% RH and a photoperiod of 16:8 (L:D). The third-instar larvae were selected for test.

2.3 Preparation of Test Samples

Weighting dried powder of plant material 500 g and putting into a 2500mL triangle vial. Adding 95% ethanol and keeping in shade for 48h. Extracting with supersonic (40khz) for 40 minutes at the temperature of 30℃. Filtrating and collecting the mother liquid. The procedure was repeated three times. All mother liquids were incorporated and concentrated by removing solvent under vacuum until dryness. The crude extract was then suspended in distilled water which was sequentially extracted with polar-varying solvents: petroleum ether, chloroform, ethyl acetate and n-butanol. The extraction rates with different solvents were 14.84% for petroleum ether, 2.17% for chloroform, 17.81% for ethyl acetate, 58.39% for n-butanol, and 6.80% for water. All extracts obtained were lyophilized and kept in the dark at +4℃prior to use. The test samples were prepared by solving the extract with 50% acetone and diluted to the required concentration.

2.4 Insecticidal Activity

The insecticidal activity of different extracts against the 3th instar larvae of *Plutella xylostella* was tested by the dipping method [11, 12].

Ten larvae were immersed in the test extract solution of 4.0mg/mL for 10s, and then taken out and removed the excrescent solution on the body. The treated larvae were transferred to the Petri dishe (9.0 cm in diameter) with a piece of wet filter paper and supplied with fresh cabbage leaves. The control experiment was carried out by immersing the larvae in 50% acetone. Triplicate was made for each test. Larvae were considered dead when a reaction to a mechanical stimulus with soft brush could no longer be observed. The mortality and corrected mortality rate were figured out according to the following formula (1) and (2)

(1) Rate of mortality = $\frac{N_1}{N} \times 100\%$

N_1: the number of death insects
N: the number of total insects

(2) Rate of corrected mortality = $\frac{M_2}{1 - M_1} \times 100\%$

M_1: the rate of mortality in control group
M_2: the rate of mortality in treated group

2.5 Antifeedant Activity

The antifeedant activity of different extract solutions against the 3th instar larvae of *Plutella xylostella* was measured by using a non-choice leaf disc method [13].

Leaf discs (1.6cm in diameter) of fresh cabbage leaf were immersed in test solutions for 5 s and left for dry. The treated disc was transferred into Petri dish with a third instar larvae starved for 6h. 10 larvae were used as a group and three replicates were arranged for each group. Leaf discs treated with 50% acetone were used as the control group. The eaten areas in the control and treated discs were measured after 24h and 48, respectively. Antifeedant rate was figured out according to the following formula (3).

(3) Rate of antifeedant = $\frac{A_1 - A_2}{A_1} \times 100\%$

A_1: the eaten area of leaves in control group
A_2: the eaten area of leaves in treated group

2.6 Growth Inhibition Activity

The Growth inhibition activity of different extracts against *Plutella xylostella* was measured with the method described by Qin, et.al [14]. Leaf discs (1.6cm in diameter) of fresh cabbage leaf were immersed in the test solutions for 5s and then taken out to dry. The treated disc was transferred into Petri dish with a third instar larvae starved for 6h, 24h later it was replaced with untreated fresh leaf which was renewed every 24h. Leaves treated with 50% acetone were used as control. Five replicates were set up for each treated and control group (30 larvae for each group). The weight of each larvae and larval mortalities were assessed every 24h after treatment. In addition, growth parameters of surviving larvae were measured and recorded every 24h up to adulthood (duration of the larval period until pupation stage and emergence of adult).

The rate of growth inhibition, rate of pupation and the adult emerging rate were figured out, respectively, according to the following formula (4), (5) and (6).

(4) Rate of growth inhibition = $\frac{W_1 - W_2}{W_1} \times 100\%$

W_1: the supernumerary of larva weight in control group
W_2: the supernumerary of larva weight in treated group

(5) Rate of pupation = $\frac{N_2}{N} \times 100\%$

N_2: the number of insects to become pupas
N: the number of total insects

(6) Rate of adult emerge = $\frac{N_3}{N} \times 100\%$

N_3: the number of eclosion insects
N: the number of total insects

2.7 Date Analysis

*Duncan's SSR Tes*ts were performed to identify if the fractions separated were statistically different in their activities.

3 Results

3.1 Insecticidal Activity of Different Extracts on Plutella xylostella

Table 1 shows the corrected mortality rates of insecticidal activity of five extracts against 3th instar larvae of *Plutella xylostella.* The difference of the insecticidal activity among the five extracts is obvious. The strong activity was exhibited by the extractS of petroleum ether and chloroform, with the corrected mortality of 98.88% and 91.01% after 48h of treatment, which was followed by the extracts of n-butanol (42.69%), ethyl acetate (19.10%) and water (3.37%). For all extracts the corrected mortality rates increased with the prolonging of treated time.

Table 1. Insectical Activity of Different Extracts Against 3th Instar Larvae of Plutella Xylostella

Extract	Corrected mortality (%)		
4.0 mg/mL	24 h	48 h	72 h
Petroleum ether	90.00	98.88	100.0
Chloroform	82.22	91.01	93.10
Ethyl acetate	12.22	19.10	22.30
n-Butanol	27.78	42.69	50.57
Water	2.22	3.37	5.75

Note: Values in a column followed by the same letters are not significantly different at <5% (one way DMRT).

3.2 Antifeedant Activity of Different Extracts on 3th Instar Larvae of Plutella Xylostella

The antifeedant rates of five extracts against 3th instar laevae of *Plutella xylostella* were presented in. Table 2. The extracts of petroleum ether and chloroform displayed strong antifeedant activity with the anttfeedant rates of 80.43% and 83.61%, respectively, at 24h. The anttfeedant rate of ethyl acetate extract was 55.18%, which was lower than that of the former two. But for the extracts of n-butanol and water, the anttfeedant rates were negative values of -142.64% and -103.01%, this may be there are some substances in the two extracts that stimulate the appetite of the 3th instars larvae and make them eat more, which need further study.

Table 2. Antifeedant Activity of Different Extracts on *Plutella Xylostella**

Extract 4.0 mg/mL	24 h		48 h	
	The eaten area of leaf disc (mm^2)	Antifeedant rate (%)	The eaten area of leaf disc (mm^2)	Antifeedant rate (%)
Petroleum ether	11.7±6.22 e	80.43	39.5±12.63e	69.91
Chloroform	9.8±6.75 e	83.61	35.8±18.49e	72.73
Ethyl acetate	26.8±8.20 d	55.18	66.5±19.03 d	49.35
n-Butanol	145.1±15.31a	-142.64	173.2±18.30a	-31.91
Water	121.4±11.87b	-103.01	148.7±24.58b	-13.25
Control	59.8±10.16c	—	131.3±13.12c	—

* Note: Date is expressed as mean ± SD. Values in a column followed by the same letters are not significantly different at <5% (one way DMRT).

3.3 Growth Inhibition Activity of Different Extracts on Plutella Xylostella

The growth inhibition effect of five extracts against *Plutella xylostella* was presented in Table 3 and Table 4 .

3.3.1 Effect on Larval Weight

At the beginning of the experiment, larvae in each treated group and control group were weighted respectively. After 2 days of post-treatment, the weight of control increased of 3.88mg (from 2.50 to 6.38mg) (Table 3). All treated groups with different extracts gained less weight than the control group. The inhibition rates were petroleum ether74.23% > chloroform of 72.68%> ethyl acetate 55.67% > water 32.22% > n-butanol 31.86%

3.3.2 Effect on Larval Mortality

Mortality rate of control group after 7 days of treatment was 14.44%. All treatments with various extracts had an increase in mortality rate compared to the control. Extracts of petroleum ether and chloroform were the most toxic with the mortality rates of 46.67% and 42.22%, respectively. Other three extracts showed low mortality, ethyl acetate (26.67%), n-butanol (21.11%) and water (23.33%).

Table 3. Effect of Different Extracts on the Weight of Larvae*

Eextract 4 mg/mL	Larvae weight (mg) (means ± SD)		Growth inhibition rate (%)	
	24h	48	24h	48h
Petroleum ether	2.88±0.29 c	3.44±0.21 d	81.12	74.23
Chloroform	2.89±0.60 c	3.41±0.69 d	76.82	72.68
Ethyl acetate	3.11±0.23 c	4.01±0.35 c	64.81	55.67
n-butanol	4.09±0.29 b	5.14±0.28 b	32.19	32.22
Water	4.10±0.53 b	5.22±0.30 b	33.48	31.86
Control	4.83±0.32 a	6.38±0.28 a	—	—

Table 4. Effect of Extracts on the Development of Larvae *

Extracts 4m g/mL	Larvae mortality (%)	Pupation rate (%)	Adult emergence (%)
Petroleum ether	46.67 a	53.33 e	40.00 d
Chloroform	42.22 b	57.78 d	33.33 e
Ethyl acetate	26.67 c	73.33 c	32.22 e
n-butanol	21.11 d	78.89 b	71.11 b
Water	23.33 d	76.67 b c	63.33 c
Control	14.44 e	85.56 a	82.22 a

*Note: Date is expressed as mean ± SD. Values in a column followed by the same letters are not significantly different at <5% (one way DMRT).

3.3.3 Effect on Pupation Rate and Emergence Rate

The pupation rate and emergence rate in all treatments were lower than that in control (85.56% and 82.22). Petroleum ether extract showed the lowest pupation rate of 53.33%, which was followed by chloroform (57.78%), ethyl acetate (73.33%), water (76.67%) and n-butanol (78.89%). For emergence rate, the lowest of 32.22% was exhibited by ethyl acetate extract, which was followed by chloroform(33.33%), petroleum ether (40.0%), water (63.33%) and n-butanol (71.11%).

4 Conclusion

It was clear from above that the stronger activities were always exhibited by the extracts of petroleum ether and chloroform, which give us a knowledge that the insecticidal active substances in *Pedicularis spicata* may belong to a kind of weak-polar compounds. The apparent symptoms caused by the two kinds extract were contacting, antifeedant, delaying of pupation and unsuccessful molting, which may be due to the inhibiting larvae's feeding, or disturbing their nutrients or hormone balance, which needs further study.

The results obtained in this work indicate the remarkable insecticidal and antifeedant properties of the plant of *Pedicularis spicata*. The need for new natural pesticides with the strong insecticidal and antifeedant potentiality may encourage further studies on its using as biode-gradable and mammalian and environmentally safe insect control agents.

References

1. Jantan, I., Yalvema, M.F., Ahmad, N.W., Jamal, J.A.: Insecticidal activities of the leaf oils of eight Cinnamomum species against Aedes aegypti and Aedes albopictus. Pharmaceutical Biol. 43, 526–532 (2005)
2. Li, S.N., Kole, R.K.: Investigation on antifeeding and ovipositing-repelling activity of the plant Corydalis sheareri against two Lepidoptera insects. Chinese Journal of Pesticide Science 3(2), 55–59 (2001)
3. Klocke, J.A.: Plant compounds as source and models of insectcontrol agents. In: Hostettmann, K. (ed.) Economic and Medicinal Plant Research, pp. 103–144. Academic Press, London (1989)

4. Morimoto, M., Tanimoto, K., Sakatani, A., Komai, K.: Antifeedant activity of an anthraquinone aldehyde in Galium aparine L. against Spodoptera litura F. Phytochemistry 60, 163–166 (2002)
5. Koul, O., Daniewski, W.M., Multani, J.S., Gumulka, M., Singh, G.: Antifeedants effects of the Limonoids from Entandrophragma candolei (Meliaceae) on the gram pod borer, Helicoverpa armigera (Lepidoptera: Noctuidae). J. Agricult. Food Chem. 51, 7271–7275 (2003)
6. Suliman, R., Saker, I., Namora, D.: Importance of plant extracts in managing Aphis fabae. Omar Al-Mukhtar University, El-beida City, Libya. In: Khateeb, N.A. (ed.) Arab Scientist. Org. The Eighth Arab Congress of Plant Protection, October 12-16 (2003)
7. Guan, F., Yu, L., Yang, Y.: Research progress on the Pedicularis spicata plants. Northwest Pharmaceutical Journal 21(3), 142–144 (2006)
8. Wang, C.Z., Jia, Z.J., Shen, X.M., et al.: Phenylpioanoid, neolignan and iridoid glycosides from pedicularis semitorta. Indian Joumal of Chemistry 36B, 150–153 (1997)
9. Liang, R., Yang, M.L.: Insecticidal Activity of Pedicularis spicata Pall against Plutella xylostella. Agrochemicals 47(3), 228–230 (2008)
10. Liang, R., Yang, M.L.: Study on the Insecticidal Activity ofPedicularis spicataPall on Wolfberry Aphis. Journal of Anhui. Agri. Sci. 36(3), 1112–1113 (2008)
11. Xie, H.Y., Jiang, H.Y., Wang, G.P., et al.: Insecticidal activities of extracts from Acorus graminues Rhizome against Mythimna separate Walker. Chinese Joumal of Pesiticides 43(8), 367–369 (2004)
12. Xue, C.W., Wang, H.Y., Sun, Q., et al.: Bioactivity of five insecticides against Diamond Back Moth (Plutella xylostella L.). Agrochemicals Research & Application 10(5), 25–28 (2006)
13. Moustafa, A.A., Samir, A.M.A., Abdel-Salam, H.B., Mona, A.A.A.: Insecticidal, antifeedant and antifungal activities of two glucosides isolated from the seeds of Simmondsia chinensis. Industrial Crops and Products 26, 345–350 (2007)
14. Qin, X.P., Zhao, H.Y., Yang, M.L.: Effect of Extracts from Dodonaea viscosa Seed on Feeding and Growth and Development of Pieris rapae L. Agrochemicals 46(7), 494–499 (2007)

Cloning, Characterization and Expression Analysis of a Cytosolic Ascorbate Peroxidase Gene from *Grimmia Pilifera*[*]

Xiao Hong Song[1], Wei Sha[2], Zhong Min Jin[2], and Yan Fu Zhang[2]

[1] College of Life Sciences Northeast Forestry University 150040 Harbin, Heilongjiang Province, China
[2] College of Life Sciences and Agroforestry University of Qiqihar 161006 Qiqihar, Heilongjiang Province, China
sxh829@126.com, shw1129@263.net

Abstract. Ascorbate peroxidase(APX) is a class I peroxidase that catalyzed the conversion of H_2O_2 to H_2O and O_2 using ascorbate as the specific electron donor. This enzyme has a key function in scavenging reactive oxygen species (ROS) and the protection against toxic effects of ROS in plants. Here we reported the identification of an APX gene from a cDNA library of Grimmia pilifera. The full-length of the gene was cloned by 3′-RACE approach, and named as GpAPX. The predicted proteins of GpAPX consisted of 256 amino acid residues with a calculated molecular mass of 28.2 kDa, and displayed high similarity to other plant proteins. It also contains three conserved domains and two signatures. QRT-PCR analysis suggested that the expression of GpAPX gene was induced in both dehydration and rehydration. Its expression level increased under drought stress, inhibited at the begining of re-watering, and peaked on 12h after re-watering. The results demonstrated that the expression of GpAPX gene closely related to dehydration and rehydration, and its isolation established a good foundation for further study on the resistance of Grimmia pilifera to drought stress.

Keywords: Grimmia pilifera, Ascorbate peroxidase(APX), GpAPX, Gene expression.

1 Introduction

Reactive oxygen species (ROS) are considered to be important damaging factors in plants exposed to stressful environmental conditions [1]. Higher plants have active oxygen-scavenging systems consisting of several antioxidant enzymes, such as superoxide dismutase (SOD), ascorbate peroxidase (APX), glutathione reductase (GR) and catalase (CAT) [2]. These systems protect membranes from the deleterious

[*] This work is supported by The National Natural Science Foundation of China (31070180), Overseas scholars cooperation project of Heilongjiang Education Department(1151HZ022), The Agriculture research project of Heilongjiang Science and Technology Department (GC06J101) .

E. Zhu and S. Sambath (Eds.): Information Tech. and Agricultural Eng., AISC 134, pp. 433–440.
springerlink.com © Springer-Verlag Berlin Heidelberg 2012

effects of reactive oxygen species(ROS), like superoxide radicals, hydrogen peroxide(H_2O_2), hydroxyl radicals and singlet oxygen, which are produced at elevated rates when plants are exposed to abiotic stress conditions [3].

Peroxidases have a prominent position in antioxidant defenses, removing peroxides. APX belongs to the class I heme-dependent peroxidases of the plant superfamily, and distribute in distinct cellular compartments such as the chloroplasts, cytosol, mitochondria and peroxisomes, each cellular compartment possessing one or several APX isoforms. APX is believed to be exhibiting both peroxidase and catalase activities, and the function of all forms of APX is thought to scavenge the hydrogen peroxide that is continuously generated in cells [4]. Furthermore, APX activity has been shown to increase in response to drought, air pollution, chilling, iron, salt, and other abiotic stress [5], and has been reported in different plant species, such as rice [6]; spinach [7] and wheat [8].

APX cDNAs are isolated and characterized from several plant species, like barley [9], Porphyra yezoensis [10], and so forth. It has been reported that the expression of APX could be used in plants to enhance the tolerance to environmental stresses. For example, the expression of APX in tobacco could protect leaves from oxidative stress damage caused by salt stress [11]; the expression of APX in arabidopsis thaliana plants indicated that the transgenic plants shown an increased resistance to salt stress [12] and water-deficit [13].

The bryophytes, in fact, are a taxonomic group consisting of species more or less tolerant to abiotic stresses widespread in different environmental conditions. Drought-tolerant moss, as resurrection plants, can remain dried in an anabiotic state for several years and, upon rehydration, are able to resume normal growth and metabolism within 24 h. The rate of recovery depend upon the rate of prior desiccation occurred. Generally, if the rate of water loss is slow (in days to weeks), rehydration is almost instantaneous (30 to 90 sec) and recovery rates are also generally very rapid with most drought-tolerant moss reaching full recovery within a few hours [14]. *Grimmia pilifera*, as a common drought tolerant moss, grows in habitats of rocky outcrops. Apart from study of physiology, ecology and systematics, however, little is known about the drought tolerance of *Grimmia pilifera* in molecular level. It seems worthwhile, therefore, to explore the mechanisms of drought response in *Grimmia pilifera*. One approach to address this question is cloning and expression analysis of drought-resistance gene. Here we cloned a full length cDNA of cytosolic APX gene by 3′-RACE method, and its expression profile during dehydration and rehydration was analyzed.

2 Materials and Methods

2.1 Isolation of Total RNA

Total RNA was extracted by SDS method. The quality of RNA was verified by the demonstration of intact 28s and 18s rRNA through agarose gel electrophoresis as well as the absorbance ratios(A260/A280)of 1.9 to 2.0. Contaminating genomic DNA was removed with the RQ1 RNase-Free DNase.

2.2 Rapid Amplification of cDNA Ends (RACE)

The first-strand cDNA was synthesized according to the manufacture's guidelines of SMART Scribe™ Reverse Transcriptase (Clontech). Then, based on the sequence of the *GpAPX* fragment, we designed primers and nested primers for 3′-RACE by Primer 5.0 software. 3′-RACE primers (GSP:5′-GCAGAGAAGAACTGTGCCCCGATCAT-3′;NGSP:5′-ATGCTGACTTCTACACGCTCGCTGG-3′).

3′-RACE was performed using SMARTer™ RACE cDNA Amplification Kit and Advantage 2 PCR Kit (Clontech). Amplified products were cloned into the pMD18-T vector (TaKaRa), and transformed into *E.coli* DH5α. Based on the color reaction using Xgal-IPTG System and PCR identification, the positive clones were picked out and sequenced.

After assembling the sequence of the 3′-RACE product and original sequence by Bioedit software, the full-length cDNA sequence *GpAPX* was deduced, and subsequently amplified via PCR using a pair of primers(F: 5′-ACGCATAT CTAGTTCGTGTCG-3′; R: 5′-CATCCACCTAATCTGTAC GTCTG-T 3′) designed according to the full-length sequence with 3'-RACE-Ready cDNA as template. The PCR products were purified and cloned into the pMD-18T vector followed by sequencing.

2.3 Bioinformatics Analysis

ORF finder program at NCBI was used to find an open reading frame; The computation of various physical and chemical parameters of protein was performed by ProtParam tool(http://www.expasy.ch/tools/protparam.html); Potential protein families was analyzed with the SEARCH function of Pfam 24.0 (http://pfam. sanger.ac. uk/) software; Conserved domains in protein was identified in Conserved Domain database(http://www.ncbi .nlm.nih.gov/structure/cdd/ cdd.shtml) ; Functional sites were predicted using ScanProsite (http://www.expasy.org/tools/scanprosite/); Sequences alignment and phylogenetic analysis were conducted based on amino acid sequences using ClustalW2(http://www.ebi.ac.uk/Tools/clustalw2/).

2.4 Materials and Treatments for Expression Analysis

Grimmia pilifera was collected from Wudalianchi city in the Heilongjiang Province, which was cultured for 7 to 10 days with sufficient water content as matched control, and then materials were collected separately 1d, 2d, 3d, 4d, 5d after dehydration and 0h, 0.5h, 1h, 6h, 12h, 24h, 36h, 48h after rehydration, and immediately frozen in liquid N_2, stored at -80°C for RNA extraction.

2.5 Expression Analysis of GpAPX

In order to investigate the expression pattern of *GpAPX* during dehydration and rehydration, fluorescent quantitative PCR was performed in chromo 4 Quantitative PCR Instrument, and using SYBR *Premix EX Taq*™ II Perfect Real Time Kit. 18S rRNA gene was performed as an internal control to normalize the mRNA fraction. Primer sequences were as follow: ascorbate peroxidase , F 5′-TGTTGGAGGGTGAG

AA GGATG-3′, R 5′-TCAGGTGCGATTCAGCGTAG-3′; 18s, F 5′-TTGACGGAAG GGCACCA-3′, R 5′-ACCACCACCCATA GAATC AAGAA-3′, and the annealing temperature of all primers were 57°C.

The specificity of the primers to the genes for which they were designed was tested by using melting curve analysis of the PCR reaction. The primer efficiency was calculated by plotting a standard curve using enfold serial dilutions ranging from 10^1 to 10^5 copies per reaction, and each dilution points was measured in triplicate. PCR efficiency (E) is the slope of the straight line that fit best to the included data points in the amplification curve, and was calculated according to the formula $E=10^{-slope}-1$.

The reaction was performed using SYBR *Premix EX Taq*™ II , and the result was analyzed by OpticonMonitor3 software, and the relative expression of target genes were determined by using comparative threshold method ($2^{-\Delta\Delta Ct}$, $\Delta Ct=(Ct._{Target}-Ct._{18s})_{Timex}-(Ct._{Target}-Ct._{18s})_{Time0}$, Time x:treatment, Time 0:control).

3 Results

3.1 Full-Length Sequence Analysis

Based on the cDNA sequence from *Grimmia pilifera*, two nested primers were designed for the amplification of 3′-end of ascorbate peroxidase gene. The PCR product of 722bp was obtained and sequenced. Blast N search confirmed that it was the sequence of 3′-end fragment. The full-length cDNA sequence composed of 1115bp including 116bp in 5′UTR, 771bp being predicted as open reading frame (ORF), and 228bp in 3′UTR (Fig.1). The predicted ORF encoded an 256 amino acid polypeptide, and the predicted protein product was calculated to have a molecular mass of 28.2 kDa with an isoelectric point of 5.79. The cDNA sequence of ascorbate peroxidase gene from *Grimmia pilifera* was named *GpAPX*, and deposited in GenBank under accession number GU989311.

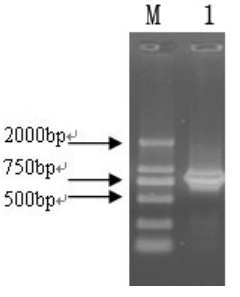

Fig. 1. Electrophoresis 3′-RACE product of GpAPX
Note: M, DL2000 Marker; lane 1, product of 3′-RACE

Multiple sequence alignment of *GpAPX* from *Grimmia pilifera* with other known APX from a variety of plant species revealed that they were highly conserved. At the aa level, sequence comparisons between *GpAPX* and other plant APX with Blast revealed that *GpAPX* shared 89.7% identity with *Physcomitrella patens*

(XP_001772538.1), 74.0% with *Picea sitchensi* (ABK26677.1), 73.6% with *Solanum lycopersicum* (AAZ77770.1), 73.1% with *Sorghum bicolour* (XP_002463451.1), 72.7% with *Nicotiana tabacum* (BAA12918.1), *Zea mays* (ACG41151.1) and *Populus trichocarpa* (XP_002322851.1), 72.3% with *Arabidopsis thaliana* (NP_172267.1), *Suaeda salsa* (AAK58449.1) and *Tamarix hispida* (ACN60159.1), 71.9% with *Hordeum vulgare* (AAL08496.1), 71.5% with *Gossypium hirsutum* (ABR18607.1), 71.1% with *Triticum aestivum* (ACO90193.1), 70.7% with *Oryza sativa* (NP_001049769.1), 70.2% with *Glycine max* (BAC92740.1).

To investigate the molecular evolution and phylogenetic relationships among ascorbate peroxidases in plants, APX protein sequences were aligned by ClustalW2 and analyzed using the Bioedit software, and the results were shown in Fig.2. The alignment of 16 APX protein sequences retrieved from the NCBI database (nonredundant list)revealed that these proteins were divided into three groups.

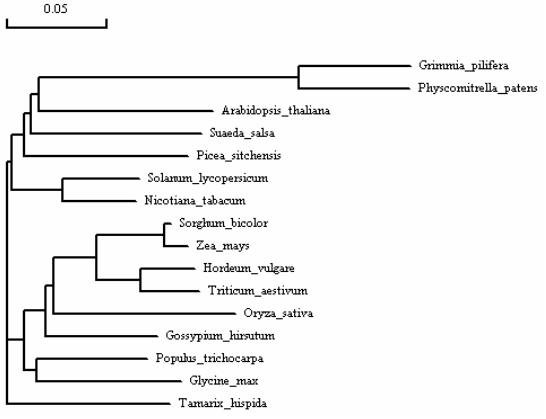

Fig. 2. Phylogenetic tree showing the relationships between the amino acids sequences of GpAPX and other plant APXs

Three highly conserved domains of ascorbate peroxidase, the binding site of substrate, potassium and heme, were also found in *GpAPX*. Signatures of peroxidases active site and peroxidases proximal heme-ligand were observed in amino acid residue 33 to 44 (ApiiLRLaWHAS) and 155 to 165 (DIVTLSGAHTL), respectively. Ascorbate peroxidase was one of the intracellular peroxidases, and was the main enzyme responsible for hydrogen peroxide removal in chloroplasts and cytosol of higher plants. The *GpAPX* obtained from *Grimmia pilifera* in this study belongs to the peroxidase protein families.

3.2 Expression during Dehydration and Rehydration

The standard curve equation obtained for the *GpAPX* was y=-0.3138x+6.70, and R^2 (Coefficient of Determination) was 0.993 with a calculated efficiency of 1.06. Concomitantly, the equation obtained for the housekeeping gene 18S was y=-0.3043x+6.97, and R^2 was 0.998 with a calculated efficiency of 1.01. Melting curve analysis results shown that there was no amplification of genomic DNA template and primer dimer. In short, the specificity and efficiency of primers designed for fluorescent quantitative PCR were good enough for experiment.

QRT-PCR was employed to analyze its expression pattern, and the results showed altered expression levels in response to dehydration and rehydration treatments (Fig.3). Reactive oxygen scavenging system was activated during the process of dehydration. The expression of *GpAPX* was up-regulated, and increased 2.4-fold after 5d of drought stress, suggesting a role of *GpAPX* in response to the drought stress and in controlling the H_2O_2 concentration in the cytosol. During the process of rehydration, the expression of *GpAPX* suppressed in the initial period, and significantly up-regulated from 6h to 12h after re-watering. The highest levels of expression appeared at 12 h of re-watering treatment.

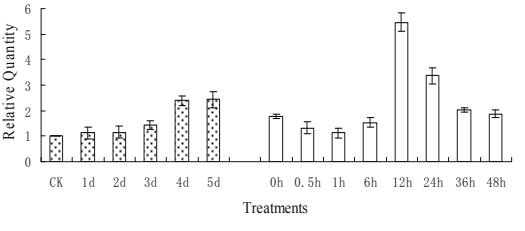

Fig. 3. Relative quantification of the expression of GpAPX during dehydration and rehydration

4 Discussion

APX in higher plants is encoded by small multigene families and the different isoforms are classified according to their subcellular location. In *Arabidopsis*, nine genes were suggested as APX genes [15]. In rice, the APX gene family is comprised of eight members. A comparison of the rice APX isoforms with those of other species revealed a high degree of conservation among these proteins [16]. In comparison with the genome-sequenced plants, *Arabidopsis* and rice, the existing knowledge of the APX gene family in other plant species such as, for example, spinach and cowpea,

seems to be only partial. In bryophytes, there is still little information about ascorbate peroxidase of mosses exists and evenless on *Grimmia pilifera*.

In the last decade, several efforts have been made to isolate and characterize genes belonging to APX isoenzyme family, to allow a better understanding of their involvement and relevance in plant physiological processes under oxidative stress conditions. Park *et al*. [17] reported that the cytosolic APX (*swAPX1*) from sweetpotato was strongly induced in the leaves following inoculation with a bacterial pathogen, and indicated that *swAPX1* may be involved in hydrogen peroxide-detoxification and thus help to overcome the oxidative stress induced by abiotic and biotic stresses. This work reports the cloning of a novel cytosolic APX gene in *Grimmia pilifera*. It was found containing a peroxidase domain, suggesting its peroxidase activity. The full-length cDNA was 1115 bp in length containing a 771 bp ORF encoding a polypeptide of 256 amino acids. Bioinformatics analysis revealed that *GpAPX* had homology to that of other organisms.

To understand the mechanism of expression and regulation of *GpAPX* gene, QRT-PCR was employed to analyze its expression pattern, and the results demonstrated that *GpAPX* was expressed continuously, and the average expression amount of *GpAPX* during rehydration was higher than dehydration, suggesting that *GpAPX* plays an important role both in the dehydration and rehydration. The up-regulation of *GpAPX* during dehydration, might be related to the role of this gene in protection against drought-dependent oxidative stress in *Grimmia pilifera*.

Taken together, these results revealed that *Grimmia pilifera* may utilize a tentative tolerance strategy that combines a constitutive protection system and a rehydration-inducible recovery mechanism [18], and provided a foundation on understanding the molecular mechanism of drought tolerance in *Grimmia pilifera*.

Acknowledgements. The research was supported by The National Natural Science Foundation of China (31070180), Overseas scholars cooperation project of Heilongjiang Education Department (1151HZ022), The Agriculture research project of Heilongjiang Science and Technology Department (GC06J101) .

References

1. Badawi, G.H., Yamauchi, Y., Shimada, E., Sasaki, G.R., Kawano, N., Tanaka, K., Tanaka, K.: Enhanced tolerance to salt stress and water deficit by overexpressing superoxide dismutase in tobacco (Nicotiana tabacum) chloroplasts. Plant Science 166, 919–928 (2004)
2. Bowler, C., Van, M.M., Inze, D.: Superoxide dismutase and stress tolerance. Annual Review of Plant Biology 43, 83–116 (1992)
3. Guo, Z., Ou, W., Lu, S., Zhong, Q.: Differential responses of antioxidative system to chilling and drought in four rice cultivars differing in sensitivity. Plant Physiology and Biochemistry 44, 828–836 (2006)
4. Asada, K.: Ascorbate-peroxidase;scavenging system of hydrogen peroxide in chloroplasts. Tanpakushitsu Kakusan Koso 33, 2957–2964 (1988)
5. Teixeira, F.K., Menezes-Benavente, L., Galva, V.C., Margis, R., Margis-Pinheiro, M.: Rice ascorbate peroxidase gene family encodes functionally diverse isoforms localized in different subcellular compartments. Planta 224, 300–314 (2006)

6. Sharma, P., Dubey, R.S.: Drought induces oxidative stress and enhances the activities of antioxidant enzymes in growing rice seedlings. Plant Growth Regulation 46, 209–211 (2005)
7. Yoshimura, K., Yabuta, Y., Ishikawa, T., Shigeoka, S.: Expression of spinach ascorbate peroxidase isoenzymes in response to oxidative stresses. Plant Physiology 123, 223–234 (2000)
8. Sgherri, C.L.M., Maffei, M., Navari-lzzo, F.: Antioxidative enzymes in wheat subjected to increasing water deficit and rewatering. Journal of Plant Physiology 157, 273–279 (2000)
9. Shi, W.M., Muramoto, Y., Ueda, A., Takabe, T.: Cloning of peroxisomal ascorbate peroxidase gene from barley and enhanced thermotolerance by overexpressing in Arabidopsis thaliana. Gene. 273, 23–27 (2001)
10. Ma, L.B., Zhang, F.Y., Ma, C.Y., Wang, S.J.: cDNA cloning and sequence characterization of an ascorbate eroxidase from marine red alga Porphyra yezoensis. Journal of Fishery Sciences of China 12, 281–287 (2005)
11. Lee, Y.P., Kim, S.H., Bang, J.W., Lee, H.S., Kwak, S.S., Kwon, S.Y.: Enhanced tolerance to oxidative stress in transgenic tobacco plants expressing three antioxidant enzymes in chloroplasts. Plant Cell Reports 26, 591–598 (2007)
12. Lu, Z.Q., Liu, D.L., Liu, S.K.: Two rice cytosolic ascorbate peroxidases differentially improve salt tolerance in transgenic Arabidopsis. Plant Cell Reports 26, 1909–1917 (2007)
13. Yan, J., Wang, J., Tissue, D., Holaday, A.S., Allen, R.: Photosynthesis and seed production under water-deficit conditions in transgenic tobacco plants that overexpression an Arabidopsis ascorbate peroxidase gene. Crop Science 43, 1477–1483 (2003)
14. Oliver, M.J., Bewley, J.D.: Desiccation tolerance of plant tissues: A mechanistic overview. Horticulture Reviews 18, 171–214 (1997)
15. Narendra, S., Venkataramani, S., Shen, G.X., Wang, J., Pasapula, V., Lin, Y., Kornyeyev, D., Holaday, A.S., Zhang, H.: The Arabidopsis ascorbate peroxidase 3 is a peroxisomal membrane-bound antioxidant enzyme and is dispensable for Arabidopsis growth and development. Journal of Experimental Botany 57, 3033–3042 (2006)
16. Henrissat, B., Saloheimo, M., Lavaitte, S., Knowles, J.K.: Structural homology among the peroxidase enzyme family revealed by hydrophobic cluster analysis. Proteins 8, 215–217 (1990)
17. Park, S.Y., Ryu, S.H., Jang, I.C., Kwon, S.Y., Kim, J.G., Kwak, S.S.: Molecular cloning of a cytosolic ascorbate peroxidase cDNA from cell cultures of sweet potato and its expression in response to stress. Molecular Genetics and Genomics 271, 339–346 (2004)
18. Oliver, M.J.: Desiccation tolerance in vegetative plant cells. Physiologia Plantarum 97, 779–787 (1996)

Isolation and Characterization of Sunflower Protein Isolates and Sunflower Globulins

Jian Ren[1,2,3], Xiao-Hong Sun[1,2,3], Guo-Ping Lin [1,3], Xi-Qun Zheng[1,2,3], and Xiao-Lan Liu[1,2,3]

[1] Food and Bioengineering College
[2] Key Laboratory of Processing Agricultural Products of Heilongjiang Province
[3] Qiqihar University Qiqihar, Heilongjiang Province, China
super_renjian1970@163.com

Abstract. Sunflower protein isolates and sunflower globulins were prepared from sunflower meals which were defatted by the method of aqueous enzymatic extraction and analyzed by gel filtration. The proximate composition, amino acid contents, functional properties of the proteins were investigated in present study. In addition, the proteins were also characterized by gel electrophoresis. The results showed that sunflower protein isolates contained less lysine than the FAO pattern of essential amino acid requirements while other amino acid levels were comparable. Functional properties of sunflower protein isolates were better or close to those of soybean protein isolates. Sunflower protein isolates showed three major fractions having molecular mass of 380×103, 100×103 and 27×103. 11S globulins were the major fraction of sunflower protein isolates. Chlorogenic acid was shown to be more associated with all proteins. It was found that there were 10 major bands in sunflower globulins with molecular mass ranging from 13000 to 53500, while sunflower protein isolates had more bands.

Keywords: sunflower protein isolates, sunflower globulins, properties, gel filtration, gel electrophoresis.

1 Introduction

Sunflower seed is one of five major oil plants in the world. The defatted sunflower meals have a relatively high content of protein, and have great economic value as food additive. Sunflower production and utilization have increased in many countries, and many investigations had been carried out on the processing, nutrition, and functional properties of sunflower [1-8]. Up to now, to the best of our knowledge, all of sunflower proteins were obtained directly from sunflower seed. Thus, the objective of this study was to obtain sunflower proteins by isolating the globulins, and the protein isolates from sunflower meals which were defatted by the method of aqueous enzymatic extraction were fractionated and characterized by gel filtration and gel electrophoresis. Their functional properties were also investigated in this study.

E. Zhu and S. Sambath (Eds.): Information Tech. and Agricultural Eng., AISC 134, pp. 441–449.
springerlink.com © Springer-Verlag Berlin Heidelberg 2012

2 Materials and Methods

2.1 Materials and Chemicals

Sunflower (Variety of High Linoleic Acid, grown in HeiLongJiang Province, China) was obtained from Qiqihar local market. All chemicals used in the experiments were of analytical grade and purchased from Sigma Chemical Co. (St. Louis, USA).

2.2 Sunflower Meal Preparation

Sunflower seeds were defatted by the method of aqueous enzymatic extraction. Sunflower seeds were mechanically dehulled, and the kernels were milled in a laboratory grinder for 3 min, and the resulting flour was sieved through a 1 mm sieve. Sunflower flour was dispersed in citric acid/cotric acid sodium buffer (1:8, w/v), then 1.5% cellulase and pectase were used degraded for 8 hours at 35℃, and the supernatant oil was removed by centrifugation and discarded. Defatted sunflower meal was obtained by concentrating and freeze-dried.

2.3 Sunflower Protein Isolates Preparation

Sunflower protein isolates were separated from sunflower meal. Sunflower meal was further defatted by petroleum ether extraction at 50℃. The meal was extracted for 3h for four times using a meal-to-solvent ratio of 1:5 (w/v). The resulting concentrate was air dried overnight at 40℃ [4-5, 9]. The protein concentrate was then extracted twice with 95% ethanol (pH=4.5, 1:10, w/v, concentrate:solvent) by mechanical stirring for 2h at 50℃, the solvent decanted off, and the concentrate air-dried at 40℃ [9-10]. The sunflower protein concentrate was extracted with 10% NaCl, 0.25% Na_2SO_3 (pH=7.0, 1:10, w/v, meal:solvent), by mechanical stirring for 2h. The precipitate was removed by centrifugation and discarded. 1M HCl was added to supernatant to pH=4.0, then the protein fraction was reprecipitated and recovered by centrifugation. It was dialyzed against double distilled water and freeze-dried [4, 11].

2.4 Globulins Fraction Preparation

Sunflower globulins were purified from sunflower meal. The sunflower meal was extracted in 10% NaCl solution by using a meal to solvent ratio of 1:10 (w/v). The suspension was stirred for 1 h at room temperature (about 25℃)and centrifuged at 4000rpm for 20min. The supernatant was added solid $(NH_4)_2SO_4$ to 6.5% saturation, stirred the solution well, and kept it at 4℃ for 30 min. The precipitate was removed by centrifugation and discarded. Ammonium sulfate was added to supernatant to increase the concentration to 13% saturation, and the suspension was kept at 4℃ for 30min again. The precipitate was separated by centrifugation and dissolved in 1M NaCl solution. Then the protein fraction was reprecipitated with 13% $(NH_4)_2SO_4$ saturation and recovered by centrifugation. It was dissolved in 1M NaCl solution and dialyzed against 0.025M Tris-glycine buffer of pH=8.3 and freeze-dried [3, 12-13].

2.5 Gel Filtration

Protein (20mg/mL) dissolved in Tris-HCl buffer (pH=8.3) was applied (4mL) onto a column (2.5×85cm) packed with Sephacryl S-200 (Pharmacia Fine Chemicals) equilibrated with the same buffer. The void volume (V_0) of the column was determined with blue dextran 2000 (Pharmacia Fine Chemicals). The protein was eluted with the same buffer at 18 mL/h at 20℃ in 3-mL fractions. The elution pattern of the protein was determined by measuring absorbance at 280nm with a spectrophotometer. The elution pattern of chlorogenic acid was determined by measuring absorbance at 328nm. To determine the molecular mass of the protein fractions, the column was calibrated by proteins with known molecular mass (ferritin, 438000Da; catalase, 240000Da; adolase, 158000Da; albumin, 67400Da; ovlalbumin, 49100Da; chymotrypsinogen A, 25000Da; ribonuclease A, 15600Da; all were obtained from Amersham Biosciences). [1, 4].

2.6 Composition Analysis

Moisture, ash and protein contents of the sunflower protein isolates were determined according to the methods of AOAC [14]. Chlorogenic acid was measured following the method of Dorrell [15]. The levels of amino acids were determined by hydrolyzing the protein with 6M HCl at 110℃ for 24h, filtering, evaporating to dryness, and analyzing the residue, redissolved in citrate butter (pH=2.2), on an amino acid analyzer (Spinco 120C, Beckman) [4].

2.7 Functional Properties

1) Nitrogen Solubility: Nitrogen solubility was determined according to the method of Mattil [16], and nitrogen content was estimated according to mico-Kjeldahl method, using a conversion factor of 6.25 [16]. The soluble nitrogen content was expressed as percent of the total nitrogen in the samples (sunflower protein isolates or globulins).

2) Water absoption capacity and fat absorption capacity: Water absoption capacity was determined according to the method of Sosulski [17] and was expressed as the amount of water absorbed by 100 g of the samples. Fat absorption capacity of the protein was measured according to the method of Sosulski et al. [18] and was expressed as the amount of oil (milliliters) bound by 100 g of the samples.

3) Foaming capacity and foaming stability: One hundred milliliters of distilled water were added to 3g of the samples and the mixture was homogenized at 3000rpm for 5min in a Virtis homogenizer at room temperature (about 25℃) and immediately transferred to a graduated cylinder. The total volume after 30s was calculated, and the increased volume was expressed as percent foam capacity. The foaming stability was dertermined by measuring the decrease in volume of foam as a function of time up to a period of 30min. Foaming density was the volume of foam devided by weight [5].

2.8 Electrophoresis

Sodium dodecyl sulfate polyacrylamide gel electrophoresis (SDS-PAGE) was performed according to the method of Laemmli [19]. SDS-PAGE was performed in 10% acrylamide with 0.4% bis-(acrylamide) as the cross-linking agent. Protein (1-2mg/mL)

dissolved in 0.025M Tris-Gly buffer (pH=8.3) was applied (20uL) on the gel slab. Electrophoresis was performed in an apparatus (DYY1-10C, BeiJing LiuYi Instruction Factory) at 100V for 3-4h. The protein was fixed with 30% methanol plus 12.5% w/v trichloroacetic acid and stained by Coomassie blue (0.1%) and destained with methanol-acetic acid–water (1:1:8). Protein bands were read in a densitometer (ATAGO). To determine the molecular mass of the bands, proteins with known molecular mass were electrophoresis along with sunflower protein. Low molecular markers ranged from 14400 Da to 66200Da (ShangHai Institute of Biochemistry, China): hen egg white lysozyme (14400Da), trypsin inhibitor 20100Da), bovine carbonic anhydrase (31000Da), rabbit actin (43000Da), bovine serum albumin (66200Da).

3 Results and Discussion

3.1 Gel Filtration

Sunflower protein isolates were separated into five fractions with three major fractions by gel filtration with Sephacryl S-200 (Fig. 1). Gel filtration of sunflower globulins with Sephacryl S-200 gave a single symmetrical peak with an elution volume corresponding to that of the first major fraction of the protein isolates (Fig. 2).

A regression equation was derived between the reduced elution volume (Ve/V_0) and the logarithm of the MW (MW is the molecular mass) of the standard proteins. The regression equation was expressed as:

$$Ve/V_0=6.6247-0.9578\log MW \quad (1)$$

which was used to draw a selective curve for the determination of MW in the sunflower protein fractions.

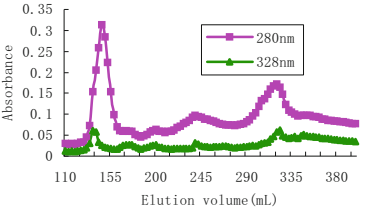

Fig. 1. Sephacryl S-200 gel filtration chromatogram of sunflower protein isolates

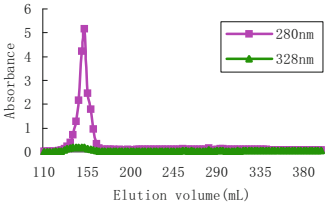

Fig. 2. Sephacryl S-200 gel filtration chromatogram of sunflower globulins

The first, second and third major fractions had molecular mass of 380,000Da, 100,000Da and 27,000Da, respectively. Kabirullah and Wills [4] reported that sunflower protein isolates showed six to seven protein fractions. Amongst the total protein fractions, three major fractions had molecular mass of 400×103Da, 125×103Da and 10×103Da. Sabir et al. [1] reported the MW of three major fractions of sunflower protein isolates were estimated to be 320,000-340,000Da, 90,000Da, and 20,000Da. As the reported of Kabirullah and Wills [4], the first major fraction should be 11S globulins, the second major fraction should be 7S globulins, the third major fraction should be 2S albumins. It was obvious that 11S globulins were the major fraction of sunflower protein isolates.

Gel filtration of sunflower globulins with Sephacryl S-200 gave a single symmetrical peak with an elution volume corresponding to that of the first major fraction of the sunflower protein isolates. The absorbance at 328nm showed that chlorogenic acid was distributed in all fractions. Sabir et al. [1] reported that chlorogenic acid was bound with the low molecular proteins, while the Fig.1 showed that chlorogenic acid not only associated with the 2S albumins, but the 11S globulins. The proximate composition analysis also showed that chlorogenic acid existed in the 11S globulins.

3.2 Proximate Composition

The average moisture, protein, ash, and chlorogenic acid contents of sunflower protein isolates were on dry basis 3.5, 87.2, 3.8, and 0.35g/100g, respectively. Those of sunflower globulins were on dry basis 2.2, 92.2, 2.0, and 0.31g/100g, respectively. Composition analysis indicated chlorogenic acid was distributed in sunflower globulins fractions.

3.3 Amino Acid Content

Sunflower protein isolates contained less lysine than the FAO (1957) pattern of essential amino acid requirements while other amino acid levels were comparable (Table 1). It indicated that sunflower protein isolates had good nutritive value as food additive.

3.4 Functional Properties

1) Protein solubility: Sunflower globulins showed a small range of minimum solubility at pH=4-5 while sunflower protein isolates showed a range of minimum solubility at pH=5-6 (Fig.3). Kabirullah and wills [4] have reported sunflower protein isolates had a small range of minimum solubility at pH=4-6. The pIs of sunflower protein isolates were higher than those of sunflower globulins due to some albumins existing in the sunflower protein isolates, while the pIs of albumins were in the region of pH=9-10 [20].

2) Water absoption capacity and fat absorption capacity: The water absorption capacity of sunflower protein isolates was lower than that of soybean protein isolates while the water absorption capacity of sunflower globulins could not be measured due to their high protein solubility. The fat absorption capacities of sunflower protein isolates and sunflower globulins were both higher than that of soybean protein isolates (Table 2).

Table 1. Amino acid content of proteins (g/100g of protein)

Amino acid content	FAO standard	Soybean protein isolates	Sunflower protein isolates	Sunflower globulins
Lysine	5.5	6.1	2.9	3.2
Threonine	4.0	3.7	3.7	3.4
Methionine	3.5	2.1	2.0	2.3
Valine	5.0	4.8	4.5	4.2
Isoleucine	4.0	4.9	3.8	5.0
Leucine	7.5	7.7	6.9	5.9
Phenylalanine	3.0	5.4	5.6	4.9

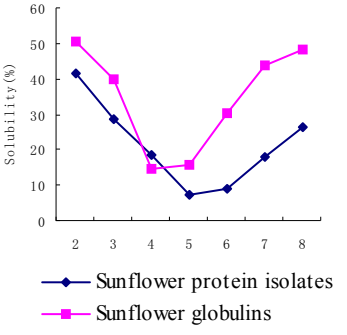

Fig. 3. Protein solubility of sunflower protein isolates and sunflower globulins at various pH

3) Foaming capacity and foaming stability: The foaming capacity and foaming stability of sunflower protein isolates and sunflower globulins were both higher than those of soybean protein isolates (Table 2). Anisimova et al. [21] reported sunflower 2S albumins were consisted of a single polypeptide chain, which may be responsible for the failure to initiate or support foaming stability. Dalgalarrondo et al. [22] reported that sunflower 11S globulins were consisted of a hexamer of subunit pairs, which comprised of an α-polypeptide and a smaller β-polypeptide linked by disulfide bonds. The structure of sunflower 11S globulins was more relaxed than 2S albumins. The data would therefore indicate that the foaming capacity of sunflower protein isolates was due to sunflower globulins. There were more globulins in sunflower protein isolates than soybean protein isolates, therefore, sunflower protein isolates had higher foaming capacity and foaming stability.

Table 2. Functional properties of proteins

Functional properties	Soybean protein isolates	Sunflower protein isolates	Sunflower globulins
Water absorption capacity(g/100g)	347	318	ND
Fat absorption capacity(g/100g)	216	395	339
Percent foaming capacity(%)	110	160	165
Foaming stability(%)	43.3	56.8	55.7

*ND means not analysis.

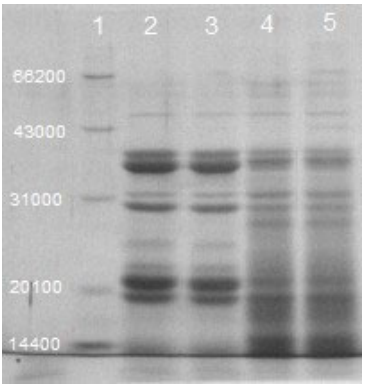

Fig. 4. SDS-PAGE pattern of sunflower globulins and sunflower protein isolates

Lane 1 is markers, lane 2 and 3 were globulins, lane 4 and 5 were sunflower protein isolates.

3.5 Electrophoresis

$NaDodSO_4$-polyacrylamide gel electrophoresis of sunflower 11S globulins was performed to determine the number and molecular mass of the subunits. It was consisted of 10 major bands. The molecular mass of the major bands were 53500Da, 42600Da, 39500Da, 33200Da, 30800Da, 24500Da, 21500Da, 19300Da, 17700Da and 13000Da. Rahma and Rao [3] reported sunflower 11S globulins was consisted of 10 major bands and 2 minor bands. Therefore, there were two minor bands existing in the bands of sunflower 11S globulins. SDS-PAGE of sunflower protein isolates found more bands than those of 11S globulins. It indicated that the sunflower protein isolates had other proteins except sunflower 11S globulins (Fig. 4). In fact, as can be seen in Fig.1, apart from the 11S globulins, there were some 7S globulins and 2S albumins present in sunflower protein isolates.

4 Conclusions

Results from this study indicated that sunflower protein isolates contained less lysine than the FAO pattern of essential amino acid requirements while other amino acid levels were comparable. Functional properties of sunflower protein isolates were better or close to those of soybean protein isolates. Sunflower protein isolates showed three major fractions having molecular mass of 380×103, 100×103 and 27×103. 11S globulins were the major fraction of sunflower protein isolates. Chlorogenic acid was shown to be more associated with all proteins. It was found that there were 10 major bands in sunflower globulins with molecular mass ranging from 13000 to 53500, while sunflower protein isolates had more bands.

Acknowledgment. This work was supported by Heilongjiang province science foundation for youths, PR China (QC08C89).

References

1. Sabir, M.A., Sosulski, F.W., MacKenzie, S.L.: Gel Chromatograghy of Sunflower Proteins. J. Agric. Food Chem. 21, 988–993 (1973)
2. Rahma, E.H., Narasinga Rao, M.S.: Characterisation of sunflower proteins. J. Food Sci. 44, 579–582 (1979)
3. Rahma, E.H., Narasinga Rao, M.S.: Isolation and Characterization of the Major Fraction of sunflower Seeds. J. Agric. Food Chem. 29, 518–521 (1981)
4. Kabirullah, M., Wills, R.B.H.: Characterization of Sunflower Protein. J. Agric. Food Chem. 31, 953–956 (1983)
5. Venktesh, A., Prakash, V.: Functional Properties of the Total Proteins of Sunflower (Helianthus annuus L.) Seed—Effect of Physical and Chemical Treatments. J. Agric. Food Chem. 41, 18–23 (1993)
6. Gueguen, J., Popineau, Y., Anisimova, I.N., Fido, R.J., Shewry, P.R., Tatham, A.S.: Functionality of the 2S Albumin Seed Storage Proteins from Sunflower (Helianthus annuus L.). J. Agric. Food Chem. 44, 1184–1189 (1996)
7. Burnett, G.R., Rigby, N.M., Clare Mills, E.N., Belton, P.S.: Characterization of the Emulsification Properties of 2S Albumins from Sunflower Seed. Journal of Colloid and Interface Science 247, 177–185 (2002)
8. Economides, S.: The nutritive value of sunflower meal and its effect on replacing cereal straw in the diets of lactating ewes and goats. Livestock Production Science 55, 89–97 (1998)
9. Gonzalez Perez, S., Merck, K.B., Vereijken, J.M.: Isolation and Characterization of Undenatured Chlorogenic Acid Free Sunflower (Helianthus annuus) Proteins. J. Agric. Food Chem. 50, 1713–1719 (2002)
10. Sripad, G., Narasinga Rao, M.S.: Effect of Methods To Remove Polyphenols from Sunflower Meal on the Physicochemical Properties of the Proteins. J. Agric. Food Chem. 35, 962–967 (1987)
11. Ordonez, C., Asenjo, M.G., Benitez, C., Gonzalez, J.L.: Obtaining a protein concentrate from intergral defatted sunflower flour. Bioresource Technology 78, 187–190 (2001)
12. Sastry, M.C.S., Narasinga Rao, M.S.: Effect of Chemical Modification of sunflower 11S Protein on the Binding of Chlorogenic Acid. J. Agric. Food Chem. 39, 63–66 (1991)
13. Sastry, M.C.S., Narasinga Rao, M.S.: Binding of Chlorogenic Acid by the Isolated Polyphenol-Free 11S Protein of Sunflower (Helianthus annuus) Seed. J. Agric. Food Chem. 38, 2103–2110 (1990)
14. AOAC "Official Metheds of Analysis", 13th edn. Association of official and Analytical Chemists, Washington, DC (1980)
15. Dorrell, D.G.: Chlorogenic acid content of meal from cultivated and wild sunflower. Crop Sci. 16, 422–424 (1976)
16. Mattil, K.F.: The functional requirements of proteins for foods. J. Am. Oil Chem. Soc. 48, 477–480 (1971)
17. Sosulski, F.W.: The centrifuge method for determining flour absorption in hard red spring wheat. Cereal Chem. 39, 344–350 (1962)
18. Sosulski, F.W., Humbert, F.S., Buil, K., Jones, J.D.: Functional properties of rapesees flours, concentrates and isolates. J. Food Sci. 41, 1349–1352 (1976)

19. Laemmli, U.K.: Cleavage of structural proteins during the assembly of the head of bacteriophage T4. Nature 227, 681–685 (1970)
20. Youle, R.J., Huang, A.H.C.: Occurrence of low molecular mass and high cysteine containing albumin storage proteins in oilseeds of diverse species. Amer. J. Bot. 68, 44–48 (1981)
21. Anisimova, I.N., Fido, R.J., Tatham, A.S., Shewry, P.R.: Genotypic variation and polymorphism of 2S albumins of sunflower. Euphytica 83, 15–23 (1995)
22. Dalgalarrondo, M., Raymond, J., Azanza, J.L.: Sunflower seed proteins: characterization and subunit composition of globulin fraction. J. Exp. Bot. 35, 1618–1628 (1984)

The Inhibitory Effects of Bamboo Vinegar against Bacteria and Fungi*

Ting Jin, Yuxue Wu, and Qiang Wang

College of Biochemical Engineering, Ningbo Institute of Technology
University of Zhejiang
Ningbo, Zhejiang Province, China
jint@nit.zju.edu.cn

Abstract. We investigated the inhibitory effects of bamboo vinegar against bacteria and fungi by a laboratory-based assay. We chose the microorganisms for test such as Micrococcus Luleus, Bacillus Subtilis, Saccharomyces Cerevisiae, Aspergillus Niger, Mucor Racemosus and Rhizopus SP. We evaluated the inhibitory effects of bamboo vinegar on the growth of the microorganisms by the determination of inhibition zone diameters and the minimum inhibitory concentrations. The results show that bamboo vinegar has inhibitory effect on the growth of bacteria and fungi and the degree of growth inhibition shows a dose-dependant response. The inhibitory effect of bamboo vinegar on the growth of the bacteria is found better than that of the fungi, based on the extent of inhibition zone at the same concentration of bamboo vinegar and the minimum inhibitory concentrations experiment.

Keywords: bamboo vinegar, bacteria, fungi, inhibitory effects.

1 Introduction

Bamboo vinegar was widely used in medicine, agriculture, chemical industry and environment protection in China, Japan and Korea [1-4]. Recently, Bamboo vinegar had attracted more and more attention as an effective disinfector used in healthcare [5-6] and a natural product. Moreover, Bamboo vinegar also had potential commercial interest.

Bamboo vinegar was a co-product during the production of bamboo charcoal [1]. The production of bamboo charcoal was divided into four stages: dryness, pre-charring, charring, calcination. Bamboo vinegar was obtained by condensation of vapour produced in the pre-charring and charring stages. Normally, bamboo vinegar was collected when the temperature was below 450℃ [7].

Bamboo vinegar was mixture comprising water, organic acids, phenols, ketones, alcohols, esters and other ingredients. The ingredients of bamboo vinegar varied with the varieties of bamboo, processing techniques, and store periods etc [8-9]. It was reported that two hundred kinds of compound were found in bamboo vinegar [1]. Thereinto, water was the main constituent whose content was 80-90% by volume. The composition of organic acids was 7-11% and acetic acid was the main component of

* This work is partially supported by NSTB Grant #2009C50032 to T. Jin.

E. Zhu and S. Sambath (Eds.): Information Tech. and Agricultural Eng., AISC 134, pp. 451–457.
springerlink.com © Springer-Verlag Berlin Heidelberg 2012

organic acids. The content of phenols was 6-8% including phenol and homologous compounds. Bamboo vinegar had the antimicrobial properties, because it contained the ingredients, such as acetic acid, formic acid, phenols and other homologous compounds [6].

However, there were few studies on the antimicrobial properties of bamboo vinegar. Thus, the aim of this work was to evaluate the antimicrobial properties of bamboo vinegar against bacteria and fungi. Bamboo vinegar has potential value as disinfectant or preservative and this work provides experimental evidence for the wide use of bamboo vinegar.

2 Materials and Methods

2.1 Bamboo Vinegar, Microorganisms and Medium

The beef extract and peptone medium for the bacterial growth assay consisted of the following components (g/L): peptone 10, beef extract 3, sodium chloride 5, and agar 20. The pH of the medium was adjusted to 7.0-7.2 before sterilization. The PDA medium for the yeast growth assay consisted of the following components (g/L): peeled potato 200, glucose 20, and agar 20. The czapek agar medium for the mold growth assay was prepared with components (g/L) including sugar 30, nitrate of sodium 2, dipotassium hydrogen phosphate 1, potassium chloride 0.5, magnesium sulfate 0.5, ferrous sulfate 0.01 and agar 20. All the media were sterilized with autoclave at 121℃ for 20 min and decanted into Petri dishes at 50℃ to solidify. After the sterile test, the Petri dishes were used to cultivate the microorganisms. *Micrococcus Luleus, Bacillus Subtilis, Saccharomyces Cerevisiae, Aspergillus Niger, Mucor Racemosus* and *Rhizopus SP* were chosen as the microorganisms for test and were kept by Institute of Biological Engineering in Ningbo Institute of Technology, Zhejiang University. Bamboo vinegar was obtained as a co-product during the production of bamboo charcoal from Lishui, Zhejiang, China. Bamboo vinegar in its original form without sterilization was diluted with sterile distilled water to different concentrations for the experiments.

2.2 Preparation of the Cell Suspension

Micrococcus Luleus and *Bacillus Subtilis* were inoculated and incubated in the beef extract and peptone medium at 37℃ for 24h. *Saccharomyces Cerevisiae* was inoculated and incubated in the PDA medium at 28℃ for 48h. *Aspergillus Niger, Mucor Racemosus* and *Rhizopus SP* were inoculated and incubated in the czapek agar medium at 28℃ for 72h.. After the lawns of microorganisms were picked up, the cell suspensions were prepared respectively by the dilution of the lawns with sterile distilled water and the concentration of the cell suspensions was 10^9 cfu/mL.

2.3 Determination of Inhibition Zone

The cell suspension of 0.1mL was added into the Petri dish and was spread evenly with a glass rod. The Petri dish was perforated with a 9mm perforator and 0.1mL bamboo vinegar of different dilution ratio was added into the holes for test of growth inhibition of the microorganisms; sterile distilled water was also added into other

holes as control. The inoculated Petri dishes were incubated at 37℃(bacteria) for 24h, 28℃(yeast) for 48h or 28℃(mold) for 72h. The diameters of inhibition zone were determined with slide caliper after the cultivation had been finished. Three times repetition of each experiment was conducted and the mean values were reported.

2.4 Determination of Minimum Inhibitory Concentrations (MIC)

For each kind of the microorganisms for test, ten tubes were marked in turn from No.1 to No.10 and 9mL liquid medium was added into No.1 tube, 5mL liquid medium was added into other tubes respectively. The liquid media were the above media excluding agar. 1mL original Bamboo vinegar was added into No.1 tube and mixed evenly. 5mL liquid was taken out of No.1 tube and was added into No.2 tube; the rest might be deduced by analogy. 10mL liquid medium was added into the control tube. 0.01mL cell suspension of each kind of the microorganisms for test was added into the tubes respectively and the tubes were incubated under the same conditions as above. The bamboo vinegar of minimum dilution ratio in the tube where the growth of microorganism could not be observed was the minimum inhibitory concentrations (MIC).

3 Results and Discussion

3.1 Inhibitory Effect of Bamboo Vinegar against Bacteria

Fig.1 shows the results of bamboo vinegar on the growth of *Micrococcus Luleus* and *Bacillus Subtilis*. Bamboo vinegar of different dilution ratios from 10% to 100% (percent of original bamboo vinegar) all had inhibitory effect on the growth of *Micrococcus Luleus* and *Bacillus Subtilis*. The inhibitory effect of bamboo vinegar on the growth of *Micrococcus Luleus* was better than that of *Bacillus Subtilis*. The inhibition zone diameters increased with the decrease of dilution ratio of bamboo vinegar and the degree of growth inhibition showed a dose-dependant response based on the extent of the inhibition zone. It was consistent with the literature report [10]. Fig.2 shows an inhibition zone of *Micrococcus Luleus* growth on the Petri dish where original bamboo vinegar was added into the hole. Fig.3 shows the inhibition zones of *Bacillus Subtili* growing on the Petri dishes where diluted bamboo vinegar was added into the holes and the dilution ratio of original bamboo vinegar was 30% and 20% (percent of original bamboo vinegar), respectively. No inhibition zone was observed on the control Petri dishes and the two microorganisms normally grew on the Petri dishes.

Bamboo vinegar was a solution and its ingredients would diffuse into agar medium at some extent. The ingredients could inhibit growth of the bacteria, thus the inhibition zones were formed. The ingredients contained some organic acids, such as acetic acid and formic acid, which resulted in low pH of bamboo vinegar. The optimal pH for bacteria growth was about 7.0. However, the pH of bamboo vinegar was 2.20-3.01 [7] and the value was much lower than the optimal value of the growth of bacteria. Thus, the acetic acid and other organic acids gave less favorable conditions for bacterial growth. Moreover, bamboo vinegar also contained other ingredients, such as phenols, 2-methylphenol and aldehydes and the cooperation of these ingredients would greatly enhance the inhibitory effect of bamboo vinegar [6].

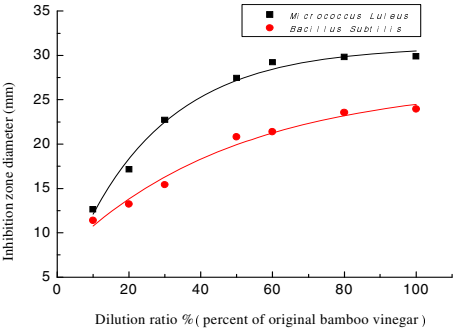

Fig. 1. Effect of bamboo vinegar on the growth of *Micrococcus Luleus* and *Bacillus Subtilis*

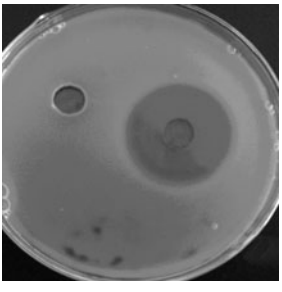

Fig. 2. Growth of *Micrococcus Luleus* on the Petri dish where original bamboo vinegar was added into the hole

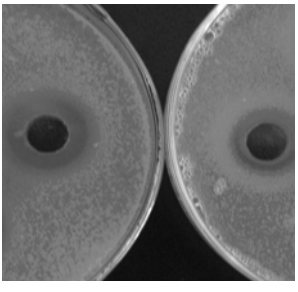

Fig. 3. Growth of *Bacillus Subtilis* on the Petri dishes where diluted bamboo vinegar was added into the holes and the dilution ratio of original bamboo vinegar was 30% (left) and 20%(right) (percent of original bamboo vinegar), respectively

3.2 Inhibitory Effect of Bamboo Vinegar against Fungi

Fig.4 shows the results of bamboo vinegar against the growth of Saccharomyces Cerevisiae, Aspergillus Niger, Mucor Racemosus and Rhizopus SP. The inhibitory effects of bamboo vinegar against fungi were obviously observed on the Petri dishes and the dilution ratios of bamboo vinegar were from 20% to 100% (percent of original bamboo vinegar). Likewise, the increase of inhibition zone diameters was related to the dilution ratio of bamboo vinegar and the degree of growth inhibition showed a dose-dependant response. The lower dilution ratio of bamboo vinegar had, the more extensive inhibition zones were formed. For the three molds, the inhibitory effect of bamboo vinegar against the growth of *Rhizopus SP* was better than that of *Aspergillus Niger* and *Mucor Racemosus*. Fig.5, 6, 7, 8 shows the inhibition zones of *Saccharomyces Cerevisiae, Aspergillus Niger*, *Mucor Racemosus* and *Rhizopus SP* growth on the Petri dishes where bamboo vinegar was in its original form without dilution. No inhibition zone was observed on the control Petri dishes, either.

It was found that the inhibitory effect of bamboo vinegar on the bacteria was better than that of the fungi based on the extent of inhibition zone at the same dilute ratio of

bamboo vinegar. Compared with the bacteria, the yeast and mold had more adaptation ability of growing under the acidic medium. Thus, only the organic acids couldn't inhibit growth of the yeast and the mold completely. Besides the organic acids, other ingredients such as benzoquinone, phenols, ketones, alcohols and aldehydes were responsible for growth inhibition of the yeast and the mold [10].

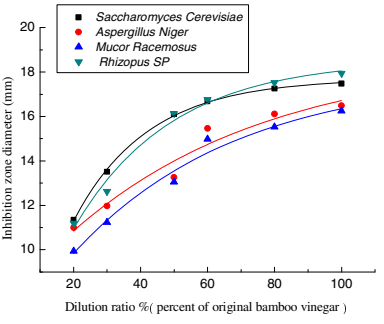

Fig. 4. Effect of bamboo vinegar on the growth of *Saccharomyces Cerevisiae*, *Aspergillus Niger*, *Mucor Racemosus* and *Rhizopus SP*

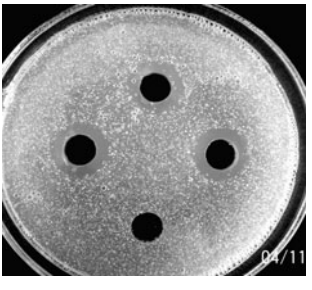

Fig. 5. Growth of *Saccharomyces Cerevisiae* on the Petri dish where original bamboo vinegar was added into the holes

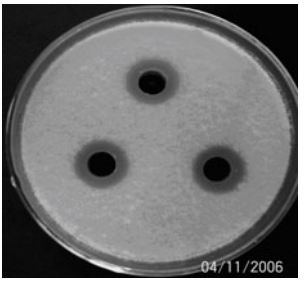

Fig. 6. Growth of *Aspergillus Niger* on the Petri dish where original bamboo vinegar was added into the holes

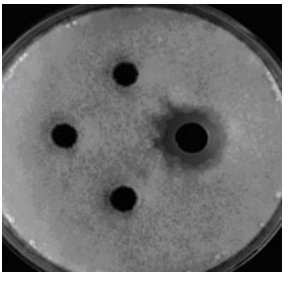

Fig. 7. Growth of *Mucor Racemosus* on the Petri dish where original bamboo vinegar was added into the holes

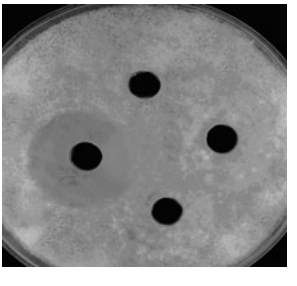

Fig. 8. Growth of *Rhizopus SP* on the Petri dish where original bamboo vinegar was added into the hole

3.3 The Minimum Inhibitory Concentrations (MIC) of Bamboo Vinegar against Bacteria and Fungi

Tab.1 shows the results of the minimum inhibitory concentrations of bamboo vinegar on the growth of the bacteria and the fungi. The growth of microorganisms for test was observed normally in the control tubes. It was well known that bamboo vinegar consisted of 80-90% water, 7-11% organic acids and other active ingredients, such as benzoquinone, phenols, ketones, alcohols and aldehydes, which were present at relatively low concentration. With the dilution of bamboo vinegar, the effective concentrations of organic acids and other active ingredients which were responsible for inhibitory effect decreased gradually. When the dilution ratio of bamboo vinegar was up to a certain value, the diluted bamboo vinegar couldn't inhibit the growth of the microorganisms in the tubes. The MIC of the bacteria was lower than the fungi's and it was consistent with the results of inhibitory effect of bamboo vinegar against bacteria and fungi on the Petri dishes.

Table 1. The MIC of bamboo vinegar against bacteria and fungi

Microorganisms	MIC (percent of original bamboo vinegar)
Micrococcus Luleus	0.313%
Bacillus Subtilis	0.625%
Saccharomyces Cerevisiae	1.25%
Aspergillus Niger	2.50%
Mucor Racemosus	2.50%
Rhizopus SP	1.25%

4 Conclusions

The inhibitory effects of bamboo vinegar against bacteria and fungi were investigated by determination of inhibition zone diameters and minimum inhibitory concentrations. It was found that bamboo vinegar had inhibitory effect on the growth of the bacteria and fungi. The degree of growth inhibition showed a dose-dependant response. The inhibitory effect of bamboo vinegar against bacteria was better than that of fungi based on the extent of inhibition zone at the same dilution ratio of bamboo vinegar and the minimum inhibitory concentrations experiment. Bamboo vinegar had inhibitory effects against bacteria and fungi and could be used as preservative or disinfectant in the area of healthcare, food production, environment protection, etc.

Acknowledgment. The authors acknowledge Ningbo Science and Technology Bureau of China for financial supports (No. 2009C50032).

References

1. Jiang, X.-L.: The production and applications of bamboo vinegar. Journal of Bamboo Research 23(3), 34–37 (2004)
2. Mu, J., Yu, Z.-M., Wu, W.-Q., Wu, Q.-L.: Preliminary study of application effect of bamboo vinegar on vegetable growth. Forestry Studies in China 8(3), 43–47 (2006)

3. Wei, Q., Huang, J.-Q., Chen, X.-N., Du, X.-G.: Study on the bamboo vinegar in agriculture production. Chinese Agriculture Science Bulletin 20(4), 51–53 (2004)
4. Mu, J., Uehara, T., Furuno, T.: Effect of bamboo vinegar on regulation of germination and radicle growth of seed plants. Journal of Wood Science 49(3), 262–270 (2003)
5. Li, Z.-Q., Ou, M.-R., Xu, X.-P., Guo, Y.-H.: Antimicrobial actions of distillated bamboo acid. Food Science and Technology (7), 78–80 (2003)
6. Jiang, X.-L.: An experiment on the sterilization effects of bamboo vinegar. Journal of Bamboo Research 24(1), 50–53 (2005)
7. Hu, Y.-H.: Progress on production technology and applications of bamboo carbon and bamboo distillate. Chemistry and Industry of Forest Products 22(3), 79–83 (2002)
8. Mu, J., Uehara, T., Furuno, T.: Effect of bamboo vinegar on regulation of germination and radicle growth of seed plants II: composition of moso bamboo vinegar at different collection temperature and its effects. Journal of Wood Science 50(5), 470–476 (2004)
9. Bai, M.-E., Chen, S.-W., Zhuang, X.-W.: Comparison of ingredients and contents between fresh and stored bamboo vinegar. Journal of Bamboo Research 24(3), 36–40 (2004)
10. Sulaiman, O., Murphy, R.-J., Hashim, R., Gritsch, C.-S.: The inhibition of microbial growth by bamboo vinegar. Journal of Bamboo Rattan 4(1), 71–80 (2005)

Cloning and Sequence Analysis of Donkey Growth Hormone Gene*

Zhu Wen-jin[1], Su Yong-mei[1], Guan Xue-min[1], Wu Jian-hua[1], and Zhao Yuan-yuan[2]

[1] College of Animal Science and Technology, Hebei Normal University of Science and Technology, Qinhuangdao, China
[2] College of Animal Science and Technology, Shanxi Agriculture University, Taigu, China
chinahbzwj@126.com, 84840293@163.com

Abstract. The PCR primers were designed online according to result of gene homology comparison. Donkey GH gene DNA and cDNA sequence were cloned from liver tissue and blood, and compared with GH gene sequences of different species by bioinformatics method. The donkey GH gene sequence was 1928bp, including the 706bp cDNA sequence with the complete CDS. By comparison for DNA and cDNA sequences, It suggested that the GH gene sequence included 5 exons and 4 introns, encoding 216AA, including signal protein of 26AA and matured protein of 190AA. Based on the analysis of the similarity of GH genes in different species on the level of cDNA, DNA and the deduced amino acid, there was the most homology to the horse. The GH gene of donkey was conservative in the process of evolution and its promotor was not specific TATA box, but was CATA box. The mutation of C→G in 1267 may affect the growth and development of donkeys and horses. All researches made an essential foundation for GH regulation of gene expression, evolution, polymorphism analysis in the future.

Keywords: Donkey, Growth hormone gene, Cloning, Sequence analysis.

1 Introduction

Growth hormone (GH) is a single-chain polypeptide hormone and secreted by anterior pituitary. GH gene is the major gene that regulates the level of GH secretion, growth, development and other important physiological activities of animals [1]. So cloning and studying GH gene of donkey function have significant for the exploitation and utilization of donkey breed resources.

GH gene sequence of horse was published in 1994 [2], the researches for it's sequence and diversity have been done in china [3-6]. However, the researches in donkey haven't published. So designed specific PCR primers online, cloned donkey GH gene DNA and cDNA sequence and analysed it. All researches made an essential

* This work is partially supported by the Natural Science Fund of Hebei Province Grant # C2007000739, Hebei Normal University of Science and Technology doctoral Start Fund Grant # 2006D006, Science and technology research and development projects of the Qinhuangdao City Grant # 201001A 155 and Department of Education project of Hebei Province Grant # Z2010137.

E. Zhu and S. Sambath (Eds.): Information Tech. and Agricultural Eng., AISC 134, pp. 459–464.
springerlink.com © Springer-Verlag Berlin Heidelberg 2012

foundation for GH regulation of gene expression, evolution, polymorphism and interaction between polymorphism and production capacity in the future.

2 Materials and Methods

2.1 Experimental Material

1)Test samples: Liver tissue and vein blood, taken from Guangling donkey in Guangling county of Shanxi Province.

2) Plasmid and strain: pGEMR-T plasmid, E.coli.JM109 strain.

3)Reagents: TRIzolR Reagent, DEPC, RNAultra total RNA extraction kit, a small mention of high purity plasmid kit, RT-PCR Kit Ver.3.0, Taq DNA polymerase, AMP, IPTG, X-gal, DNA rapid purification and extraction kit.

2.2 Experimental Methods

1) Cloning of donkey GH gene cDNA

a) PCR primer design According to the result of GH gene cDNA Homology alignmented among human, horse and pig, the primers of donkey GH gene cDNA sequences was designed by Primer3 online. Forward primer: 5'-tgtggacagctcacccaac-3; Reverse primer: 5'-gcactgaggaggggtaacag -3'.

b) Extraction of Total RNA The extraction of donkey liver total RNA based on the instructions of total RNA extracted ultra light kit, The total RNA was directly used for reverse transcription or stored at -70℃ for use after detected through electrophoresis.

c) RT-PCR test RT-PCR based on RT-PCR Kit Ver.3.0 instructions. To the total RNA extracted from liver tissue as template, with Oligo dT primer for reverse transcription and PCR amplification, the 3μL reaction solution was obtained after reaction used for Electrophoresis in 1% agarose. After the reaction products confirmed, RT-PCR products were recovered and purified by PCR products of rapid gel extraction kit to further cloning.

d) Cloning and sequencing of the target gene RT-PCR products were connected with vector pGEMR-T after recovered, and then transformed into E.coli JM109. Apply with AMP, IPTG and X-gal cultured on nutrient agar plate overnight, positive colonies were picked, shake bacteria, extracted plasmid, and sequencing after identification of colony PCR.

2) Cloning of donkey GH gene DNA

a) PCR primer design The method is the same with designed the primers of donkey GH gene cDNA, the primers of donkey GH gene DNA was designed, the detail sequence show table1.

b) Genomic DNA extraction It is according to molecular clone experiment manual which was a little modified.

c) PCR amplification The system of PCR was 25ul, annealing Temperature is in table1. Purifing and sequencing of PCR products were done by Shanghai biology engineering technology Lid.

Table 1. PCR primer of donkey GH gene

Name	Primer sequence (5′→3′)	The length of amplification	Annealing Temperature
GH1	L:atgacgagcctgggggacatg R:gtgcttacctgcagccatc	267bp	68℃
GH2	L:caagagaggagcgggtacag R:atggtctcggagaagcagaa	940bp	69℃
GH3	L:ttctgcttctccgagaccat R:gcactgaggaggggtaacag	926bp	65℃
GH4	L:gggcagatcctcaagcaaac R:tttattaggaaagatgggtaggc	240bp	65℃

3 Result and Analysis

3.1 DNA and cDNA Sequence of Donkey GH Gene

The four pair designed primers were used to amplify, 1928bp donkey GH gene DNA sequence was obtained (Fig1). A pair PCR primer was used to amplify, the 706bp of cDNA sequence was obtained (shadow part in Fig1)

ATGACGAGCCTGGGGGACATGACCCAAGAGAGGAGCGGGTACAGGATGAGTGGGAGGAGGTTCTAAATTATCCATC
AGCAGAGGCCCGTCAGTGGCCCCATGCATAAATGTATAGAGAAAATAGGTGGGGGCCGAGGGGAGAGAGAAGGAGC
CTGGGCATAAAAAGGGCCCGCAGGCGACCGATTCCAGGTTCCTAGGACCCAGCTCCCCAAACTGCTCAGGGACCTGT
GGACAGCTCACCCAACTGCG*ATG*GCTGCAGGTAAGCACCTCTAAAATCCCCCTGGGCTTGGAATCTACTGAGGGGTG
GCAGGGGGCCCTGCAGATGGATGACAGCACTAACCCTGGGCTTTGGGGCTCCTGAATGTGAGCACAGACATTTGGTC
AAGTTTAGAATGCTCTCAGTCCCTGTGGGAAGGAGGGGGAGGAAAGAAGTTTCCCTGAGGGAGGGAGAGGTCTGGC
AGGAGACCCAGGCCTCCTGCTCTCTGCCCGCCACCCTCCATGTGTTTCTCT*GCCCTCGGACCTCCGTGCTCCTGGCT*
TTCGCCCTGCTCTGCCTGCCCTGGCCTCAGGATGTGGGCGCCTTCCCCGCCATGCCGTTGTCTAGCCTGTTTGCCAACGCTG
*TGCTCCGGGCCCAGCACCTGCACCAACTGGCTGCTGACACCTACAAAGAGTTT*GTAAGCTTCCCAGGGATGGGTGCTCAT
GGAGGGTGGCAGGAAGGGGTGAATTCCCCACCGAGGGACATAATGAGAAGAAACTGACAAGTTCAGGGTTATTTTA
TCCAAGCGAAGATGCTCTCTGGAGAGCATAAACTGAGGAGGGGTTCCAAAGAATCTCGGTGATGAGAACCGTGCACC
AGCTTAGACCCCCGGGGGGCGTTCTTTCTCCC*AG*GAGCGCGCCTACATCCCCGAGGGACAGAGATACTCGATCCAGAAC
*GCCCAGGCTGCCTTCTGCTTCTCCGAGACCATCCCGGCCCCCACGGGCAAGGATGAGGCCCAGCAGAGATCT*GTGAGTGG
CCCTGCCCAGGAAGAGGGGCCTCCCTCTTTCTAAGAAGGCCGCCCTTTCGCTCCCCGGGCCCTGGGCGGCCTTGTCCC
CTAGGTGGTGGAGCAGGGCAGAGGGTGTAGGGTGACGGGGTAAGGCCCTCGGGCAGAGCGGGGCCTAGAGCGGCTG
CCCTGCGCCTGCGCACCCACTGCGCCCCTCCCCGC*AG*GACATGGAGCTGCTCCGCTTCTCGCTGCTGCTCATCCAGTCGT
GGCTCGGGCCCGTGCAGTTCCTCAGCAGGGTCTTCACCAACAGCCTGGTGTTTGGCACCTCGGACCGCGTCTATGAGAAGC
*TGAGGGACCTAGAGGAAGGCATCCAGGCCCTGATGCGG*GTGGGGATGGCGTTGCGGGTCCCCCTCTCCTGGGTCTGGAG
GCCCCTCTGGCTTAGCTGAGGGGTGGGGGCTTACATAGGCTGGGGAAGACAGATCTCGCCGCCCTCTTTGTAGCTGTC
CAGCCCTGACCTAGGAAAGATCTGACTCTTCATTTCCCCTTTTGAATCCCCCCTGTCTTTCTCTAAGCCCGGGAAGGGA
AGGTGGAAATGGAGGGGGAGGGGAGGGAGCAGCTTGCAAGTTCTCGGCCTCTCTTTTCTCCTTCTCTTCTGC*AG*GAGC
TGGAAGACGGCAGCCCCCGGGCTGGGCAGATCCTCAAGCAAACCTACGACAAGTTTGACACAAACTTGCGCAGTGATGACG
CACTGCTCAAGAACTACGGGCTACTCTCCTGCTTCAAGAAGGACCTGCACAAGGCTGAGACGTACCTGCGGGTCATGAAGTG
*TCGCCGCTTCGTGGAAAGCAGCTGTGCCTTCTAG*TGCTGGGCTTCTCTGTTACCCCTCCTCAGTGCCTCCCTTGATCCTG
GAGAGTGCCCCTCTAGTGCCTACCCATCTTTCCT**AATAAA**AGG

Fig. 1. The sequence of donkey GH gene

The cloned sequence, 1928bp DNA and 706bp cDNA of donkey GH gene, were compared with other animals in the NCBI database by BLAST, it was proved that it is true, and it included full-length of 5 exons and 4 introns. The 4 introns which lie between GT and AG, and are 253bp, 214bp, 199bp and 272bp respectively.

The 5 exons which are showed in italic type (Fig1), and are 10bp, 161bp, 117bp, 162bp and 201bp respectively.

3.2 The Protein of Donkey GH Gene

According to Fig1, the open reading frame of donkey GH gene is 651bp (23~673 bp), and encoding 216 amino acid precursor protein. Precursor protein of donkey GH gene was analyzed online, it showed that the molecular weight was 24471.1, isoelectric point PI was 6.83, the molecular formula was $C_{1098}H_{1717}N_{297}O_{317}S_{10}$. Signal peptide site was analyzed by SignalP online too, the most possible shearing site lies between 26AA and 27AA. The probability of signal peptide predicting is 1.0, and the probability of shearing site predicting is 0.917. Membrane-spanning region of the protein was analyzed by TMPRED online. It has two strong membrane-spanning region, and lie 1~22AA and 100~118AA residues respectively. Majority signal peptide sequences are included in 1~22AA residues, the membrane-spanning region mainly lies in N-terminal through to be analyzed by TMHMM online.

3.3 The Homology of Donkey and Other Animals in DNA, cDNA and the Deduced Amino Acid Sequence

Using DNA man analysed the homology of DNA, cDNA and the deduced amino acid sequence of donkeys and other animals.

Comparing the amino acid sequences of donkey with other animals, it suggests that precursor protein includes a signal peptide of 26AA and a mature peptide of 190AA, the result is the same as DeBao horse which were published by Jiang Qin-yang et al [5, 7]. While precursor protein of even-toed ungulate, such as cattle, sheep and goat, includes signal peptide of 27AA and a mature peptide of 190AA, and primate includes a signal peptide of 26AA and a mature peptide of 190AA. The homology of the signal peptide sequence is distinctly lower than the mature peptide sequence.

Table 2. The homologous comparison of DNA cDNA and amono acid of GH gene in donkey and different species

Species	DNA	cDNA	AA
Debao horse 67	98.8	99.5	99.5
Debao horse 46	98.3	98.9	98.6
Chinese dwarf horse	98.5	99.2	98.1
Braise horse	98.6	99.4	99.1
Thoroughbred	98.4	99.1	98.6
Mongolian horse	98.2	99.2	98.6
Cat	-	92.8	98.1
Dog	-	92.8	97.7
Pig	79.4	94.9	97.2
Cattle	68.3	91.1	89.8
Sheep	70.9	90.9	88.9
Goat	-	90.6	88.9
Human	68. 3	79.6	68.4

Based on table 2, the homology between donkey and horse is the highest according to DNA, cDNA or AA sequence. Compared donkey GH gene cDNA sequence with other animals, the homology successively is pig, cat, dog, cattle, sheep and goat. While the homology of AA successively is cat, dog, pig, sheep, goat and cattlt. The homology of donkey betwen primate is the lowest.

The further analysis of the homology of equine GH gene shows that the highest homology of AA sequence is DeBao and BaiSe horse, then is Thoroughbred, Mongolian horse, and it is the same trend in DNA sequence of GH gene. So the variation in DNA level is coincident to the substantial alteration of the deduced amino acid of it. In the function region of equine AA sequence, the 117st location is Phe in donkey, while it is Leu in all horse.

4 Discussion

4.1 Structure of Donkey GH Gene

The length of donkey GH gene DNA is 1928bp, including 5 exons and 4 introns. The cDNA sequence is 706bp, which is the same as 5 exons in DNA sequence. The two initiation nucleotide of 5'terminal is GT and the two end nucleotide of 3'terminal is AG in 4 introns. That is the signal of RNA splicing, and accords with GT-AG rule. But the two initiation nucleotide of 5'terminal is GC in pig, it don't accord with the rule [8]. Quantity of exons in donkey GH gene is the same as majority mammals. The five exons are 10bp, 161bp, 117bp, 162bp and 201bp respectively. But the first exon is 13bp in cattle and sheep, the third, fourth and fifth exon in human are 120bp, 165bp and 198bp respectively. Length of donkey intron is equal to horse, while it is largely different with other mammals. The open reading frame of donkey GH gene is 651bp, and initiation codon is ATG, stop codon is TAG. Two flanking regions of coding region are 5′UTR and 3′UTR. Three sites before poly (A) is AATAAAA, which is the signal of synthetic polyadenylate.

The sequence of donkey GH gene DNA, cDNA and the deduced amino acid, were compared with other animals in the NCBI database by BLAST, it was proved that the homology of them is higher, especially in cDNA and amino acid sequence. So the cloned donkey GH gene is true.

4.2 Homology Analysis of Donkey GH Gene

Comparing DNA, cDNA and the deduced amino acid sequence of GH gene of donkey with other mammals shows that the homology between donkey and horse is the highest. This conclusion is consistent with morphological classification, which prove that conservation of donkey GH gene is high.

In equine, the sequence of GH gene AA is only 1~4 different in between donkey and horse, and the AA diffrence in 117st site are the same between donkey and horse. The AA in 117st site is Phe in donkey, while it is Leu in horse. This result is caused by the diversity of GH gene DNA sequence in 1267st site. Base of GH gene DNA sequence in 1267st site change C for G in equine, which results in that AA change Leu for Phe in 117st site. This may be the reason causes the growth and development difference between donkeys and horses.

4.3 Promoter of Donkey GH Gene

Promoter is a specific DNA sequence which combines RNA polymerae and start to transcription. Various promoters have the same or similar sequence called consensus sequence which determines the transcription activity of promoter. TATA box is a location found when researched transcription mechanism in prokaryote. In subsequent researchs, the location was discovered in majority advanced animals [9].

The 5'UTR promoter sequence of donkey GH gene is predict by NNPP soft. Promoter sequence begin at the 149st and end at 199st of DNA sequence，and it's length is 50bp (agcctgggcataaaaagggcccgcaggcgaccgattccaggttcctagga). The site of predicted transcription beginning of the promoter is at 189st, and it's accuracy is 1.00. In predicted sequence, TATA frame is CATAAA (CATA box) rather than TATAAA (TATA box) in majority mammals. This suggests that transcription mechanism in donkey is different with other animals, the combination mechanism of RNA polymerae to template is different too. If want to express a certain gene of donkey in other mammals'cells or individuals, the transcription initiation factor of donor must be removed.

References

1. Sun, X., Zhu, S.-Q.: The structure and function of growth hormone. Foreign Medical Sciences Section of Pathophysiology and Clinical Medicine 19(1), 6–9 (1999) (in Chinese)
2. Jorge, A.A.M., Hugo, A.B.S.: Sequence of cDNA encoding horse growth hormone. Gene 143(2), 299–300 (1994)
3. Gluckman, P.D., Breier, B.H., Davis, S.R.: Physiology of the somatotropic axis with particular reference to the ruminant. Journal of Dairy Science 70(2), 442–466 (1987)
4. Zhang, T., Lu, H.-Z., Chen, R., Zhou, J.-J.: Genetic Variation of Growth Hormone Gene on Ningqiang Pony. Scientia Agricultura Sinica 42(12), 4435–4440 (2009) (in Chinese)
5. Jiang, Q.-Y., Wei, Y.-M., Huang, Y.-N., et al.: Cloning and Sequencing of Growth Hormone (GH) Gene from Debao Dwarf Horses. Journal of Southwest University (Natural Science Edition) 31(12), 35–38 (2009) (in Chinese)
6. Zhang, Y.-R., Mang, L.: Polymorphism Analysis of the Horse GH Gene by PCR-SSCP. Acta Veteri Nariaet Zootechnica Sinica 38(3), 209–213 (2007) (in Chinese)
7. Zhang, Y.-R., Wunerhu, Mang, L.: Cloning and Sequences Analysis of Growth Hormone Gene from Mongolian Horse. Chinese Journal of Animal Science 42(9), 10–12 (2006) (in Chinese)
8. Vize, P.D., Wells, J.R.: Isolation and characterization of the porcine growth hormone gene. Gene 55, 339–344 (1987)
9. Sun, N.N., Sun, D.X., Zhu, D.X.: Molecular genetics. University of nanjing Press, Nanjing (1990) (in Chinese)

The Roles of Timosaponin in Inhibiting Adherence of Fungus and Enhancing Function of Phagocyte*

Lianlan Ma**, Zhichun Liu, Xiaoyun Wu, and Wenping Zhang

The Department of Pathogenic Biology
Gannan Medical University
Ganzhuo Jiangxi, 341000, China
malianlan@163.com

Abstract. To understand the mechanisms of antifungal role and immunoloregulation about timosaponin, we adopt adhesion experiment that After pretreating the standard strains（ATCC14053, CMCCClc）of candida albicans with medicine of different concentration, added the human buccal epithelium cells and cultured, then calculated fungal count on each buccal epithelium which 100 cells were counted randomly in optical microscope. we adopted in vivo phagocytic experimentation on BALB/c mice that calculated phagocytic percentage and phagocytic index of phagocyte on Candida albicans. Results showed that there were the significant difference which value was $P<0.001$ compared experimental group with control group, the strength of inhibition was positively correlated with drug concentration. The mean of phagocytic percentage of phagocyte on ATCC14053 and CMCCC1c was 75.1% and 67.9%, which P value was $P<0.01$ and $P<0.01$, the mean of phagocytic index phagocyte on ATCC14053 and CMCCC1c was 2.03 and 1.53, which P value was $P<0.01$ and $P<0.01$. These results prompt that timosaponin can apparently inhibit the adherence of Candida allbicans to the human buccal epithelium cell and enhance phagocytosis of mice phagocyte on candida albicans.

Keywords: Timosaponin, Candida albicans, Buccal epithelium cell, Adherence, Phagocytic percentage.

1 Introduction

Monilia albicans, termed Candida albicans too, is the most common deep infection fungus, heads the list in clinic pathogenic fungu[1], and also is the common pathogen of complication in AIDS, Tuberculosis and tumor patient[2-4]. The medications curing fungus deep infection most are deleterious, so there are limitations in clinical application. While the bulk antifungal agent have been applied in clinic, the fungus

* This work is supported by Natural Science Foundation of Jiangxi Province (2008GZY0071) and the Department of Education of Jiangxi Province(NO:(2005)227).
** Corresponding author.

E. Zhu and S. Sambath (Eds.): Information Tech. and Agricultural Eng., AISC 134, pp. 465–470.
springerlink.com © Springer-Verlag Berlin Heidelberg 2012

resistance to these agents have appeared and is tend to be serious[5]. It is very essential to exploit new antifungal agents with high performs while low deleteriousness and slow development of the resistance to antifungal agent. Most fungus infection occurred in immunity compromised patients, besides antifungal treatment, increasing patients immunity therapy also should be adopted. Therefore there are great meanings in exploiting Chinese medical herbs with antifungal and moderating immune functions. Non specific immunity plays a important role in preventing fungus infection[6]. There is a report that neutrophils play key roles in anti infection by candida albicans[7]. Most studies focus on function of antifungal agents, while less study considers in exploiting and moderating immunity function.

Author screened several kinds Chinese medical herbs such as anemarrhenae, coptidis rhizome which are of antifungal activity to candidas albicans, coccidioides immitis and multi species of monilia in our earlier studies[8-10]. We observe effect of timosaponin act on adherence of candida albicans and phagocytosis function of mice neutrophils, aim to explore antifungal activity in avoiding invasion and enhancing nonspecity immunity level. Now report as follow.

2 Materials and Methods

2.1 Materials

Common anemarrhenae rhizome saponin was provided by Liaoning Bio-medical Technology limited company, and its solution was prepared in proportion before applying.

International standard strain ATCC 14053, a standard sensitive wild stain, was provided by fungus strain preserve center of beida hospital(Beijing). Chinese standard strain CMCC1c was bought in fungus strain preserve center of Chinese academy sciences(Nanjing).

BALB/c mice, half in female, was weighed 18~22g, average 20.0±1.2g, and provided by animal experimental center of Zhongshan University (license number: SCXK(Yue) 2004-0011Yuejianzhengzi2005A053). Animal groups: Each strain set up control group (physiologic saline) and experimental group(timosaponin) , there are 6 mice in every group.

Main reagent: Hanks solution, Wright's stain,sbouraud's dextrose agar, RPMI 1640 culture solution(bought in shanghai biosun co.ltd.,prepared according to intruction),potato dextrose agar.

2.2 Adherence Test

timosaponin solution prepare: timosaponin was prepared in proportion to 10mg/ml,5mg/ml,2.5mg/ml.

Candida albicans spore cultivation and collection: ATCC14053 and CMCCC1c were inoculated in SDA respectively and incubated for 24 hours at 37℃, activated 2 times, then transferred to PDA, vibration incubated for 20 hours at 26℃. Spores were collected by centrifugation at 300g for 3 minutes , washed by Hanks solution

three times, supernatant was discarded. Spore solution was adjusted to a concentration of 10^8/ml with RPMI 1640 containing 10% calf serum.

Buccal epithelial cells(BEC) suspension preparation: Scrape buccal mucosa of healthy volunteers without oral diseases by sterile spoon.(volunteer 20 cases, every test was from same crowd, rinse oral cavity with clear water before scraping). BEC were transferred to sterile tube with Hanks solution, centrifuged at 300g for 10minutes, washed three times, suspended by RPMI 1640, adjusted concentration to 1×10^6/ml for use.

Adherence test: every concentration timosaponin solution 0.25ml was mixed with spores solution 0.25ml respectively in experimental group, while in control group PBS replaced timosaponin solution. After incubating for 1hour at 37℃, BEC suspension 0.25ml was added, then incubated for 1hour at 37℃, centrifuged at 300g for 10minutes, washed by Hanks solution, then supernatant was discarded, sediments were made into slice, after air drying and heat fixation, was dyed by Wright's stain. Randomly count 100 BECs, then count the spores number which have adhered to the BECs and average.

2.3 Phagocytosis Test

Double MIC timosaponin solution 0.2ml each mouse was intraperitoneal injected into experimental groups mice, while in control groups physiologic saline was injected. Next day all groups mice were injected with 0.5ml candida albicans solution(concentration was 1×10^8 CFU /ml) . After 30minutes, dissect mice, take peritoneal fluid to make slice. 3 slices were made every mice. After Wright's stain, count 200 neutriphils under high power and immersion objective,count the number of neutriphils with phagocytized candida albicans and the number of phagocytized candida albicans. Then calculate the phagocytosis proportion of neutriphils and phagocytosis index in every mouse in all groups.

2.4 Statistical Analysis of Data

Data were treated by software SPSS 14.0. adherence test analyzed in ANOVA methods, and phagocytosis test in t-test.

3 Results

3.1 Adherence Test

Repeat three times experiment according to two factors factorial design. Interaction between two factors is no statistical significance. There is no statistical significance between two strains($P>0.05$); There is statistical significance in the roles of Timosaponin concentration inhibiting adherence of ATCC14053、CMCCC1c two strains($p<0.01$), and inhibiting role is positive correlation to timosaponin concentration (see table 1) .

Table 1. Timosaponin affect cells number adhering to ATCC14053、CCCMClc($\bar{x}$ ±s)

groups	Adhering cells number			
	10mg/ml	5mg/ml	2.5mg/ml	control group
ATCC14053	6.5±1.3	9.7±2.2	17.1±4.1	25.4±3.6
CMCCClc	7.3±2.0	11.5±3.2	16.6±3.9	26.7±5.0

Compare with two strains: F=22.667, $P > 0.05$; compare with different concentration F=138.404 , $P<0.01$

3.2 Phagocytosis Test

Phagocytized percentage and phagocytosis index were statistic significance between experimental group and control group, P<0.01(see table 2), phagocytic ability of phagocyte was significantly enhanced, the number of fungi which was Swallowed by each phagocyte up to 5(see figure1).

Table 2. The effects of timosaponin acting on function of mice phagocyte（x±s）

groups	Phagocytosis percentage	Phagocytosis index
Control group	0.352±0.186	0.850±0.199
ATCC14053	0.751±0.241	2.030±0.250
CMCCC1c	0.679±0.137	1.530±0.437

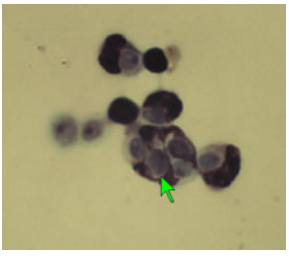

Fig. 1. The number of fungi which was Swallowed by each phagocyte

4 Discussion

The mechanisms of current antifungal agents include inhibiting cell wall composition, affecting the sterol synthesis in the cell membrane, interfering fungal nucleic acid synthesis. Due to karyon of fungal and human cells is similar, accordingly the antifungal agents interfering nucleic acid synthesis have great adverse effect on human. There is no cell wall in human cells, so the agents against cell wall have small adverse effect to human, with high selectivity as well. Essential component of fungal

cell wall are chitin, β-glucan and mannan, which plays a key role in maintaining cell develop and physiologic function. The key enzymes participating in cell wall composition are ideal target of medicine. The studies of antifungal agents that target on polysaccharide of cell walls have received more and more attention[11]. Current studies majorly focus on synthase inhibitors of glucan, chitin and mannan as well. These agents have great potential development, and are tendancy to become new generation antifungal drugs[12].

Candida albicans is a species of dimorphic fungus, has yeast and pseudohyphae phase two morphous. Adhering to tissue cell is the prerequisite to invade and colonize[13], while adherence to tissue cell has close correlation with germinal tube forming(14). Author discovered that anemarrhenae compounds have inhibition on germinal tube forming in her early studies[15]. Anemarrhenae exhibited satisfactory antifungal function in vitro, while if it can inhibit fungus adherence is unknown. Author selected BEC as adherence object, and then observed the effects of timosaponin affecting candida albicans adhering to BEC. Results indicated candida albicans was easier to adhering to epithelia cell in vitro and timosaponin evidently inhibited candida albicans adhering to epithelial cells, and following the drug concentration increased, the inhibition enhanced. Phagocytosis test results also indicated timosaponin can let phagocytosis percentage and phagocytosis index increase significantly. These findings suggest timosaponin can both inhibit fungus adherence and enhance phagocytosis function of neutrophil which means that timosaponin can prevent from fungus invasion and reinforce nonspecial immunity function to educe antifungal function.Therefore it possesses satisfactory perspective of study and exploitation, while need further study to approach the mechanism of against adhering and promote phagocytosis.

Acknowledgment. The statistical analysis of experimental data was dealed with by Yanbin Hao who work in the Department of Preventive Medicine,Gannan Medical University.

References

1. Xu, X.L., Yang, P.H., Sun, Y.Q., Fan, X.: Deep fungi infection: flora distribution and drug resistance. Chin. J. Nosocomiol. 17(3), 349–351 (2007)
2. Hernández-Hernández, F., Córdova-Martínez, E., Manzano-Gayosso, P., López-Alvarez, R., Bazán-Mora, E., et al.: Frequency of mycosis in immunosuppressed patients at a regional hospital of Mexico City. Salud Publica Mex. 45(6), 455–460 (2003)
3. Liu, Z.Y., Sheng, R.Y., Li, X.L., Li, T.S., Wang, A.X., et al.: Nosocomial fungal infections, analysis of 149 cases. Zhonghua Yi Xue Za Zhi 83(5), 399–402 (2003)
4. Chen, S.Y., Wang, C.X., Chen, L.Z., Fei, J.G., Deng, S.X., et al.: Tuberculosis in southern Chinese renal-transplant recipients. Clin. Transplant 22(6), 780–784 (2008)
5. Qiu, F.H., Cui, Y.P., Chen, Q.G.: The distribution and drug resistance analysis of 651 strains of deep infected fungi. Chinese Journal of Microecology 19(2), 211–212 (2007)
6. Chen, W.F.: Medical Immunology. People's Medical Publishing House, Beijing (2002)
7. Zhang, H.L.: Effect of granulocyte-macrophage colony-stimulating factor against Candida albicans infections. Central China Medical Journal 27(6), 342–343 (2003)

8. Ma, L.L., Zhang, W.P., Zeng, X.F., Zhang, R.Q.: Baeteriostatic test of 116 Sorfs of Chinese drugs and herbal medicine on Candida albicans. Journal of Gannan Midical College 18(3), 189–192 (1998)
9. Ma, L.L., Zhong, Y.T., Xie, S.X., Liu, Q.Y.: Bacteriostatic test of twenty sorts of Chinese drugs and herbal medicine on Cryptococcus neoformans. Modern Journal of Integrated Chinese Traditional and Western Medicine 9(18), 189–192 (2000)
10. Ma, L.L., Li, F.Z., Wang, X.L., Liu, Z.C.: Bacterilstatic efficacy about external test of coptis chinensis franch and anemarrhema asphodelodes bge on 7 kinds of Candida. U.S. Chinese Journal of Clinical Pharmacy 3(10), 18–20 (2002)
11. Xiao, Y.Z., Li, G.M.: Antifungal agents that inhibit fungal cell wall development. Dermatology and Venereology 23(2), 13–15 (2001)
12. Fang, J.R., Xie, X.M., Zhang, H.H.: Research advance in antifungal agents acting at fungal cell wall. Modern Diagnosis and Treatment 15(6), 364–366 (2004)
13. Guo, N.R., Wu, S.X.: Deep fungal pathogenesis and immunotherapy progress. Chin. J. Mycol. 1(2), 69–71 (2006)
14. Rodrigues, A.G., Mårdh, P.A., Pina-Vaz, C., Martinez-de-Oliveira, J., Fonseca, A.F.: Germ tube formation changes surface hudrophobicity of Candida cells. Infect. Dis. Obstet. Gynecol. 7(5), 222–226 (1999)
15. Liu, Z.C., Ma, L.L., Wu, X.Y., Huang, C., Luo, C.Y.: Effects of KZY-2 compound on bud formation in Candida albicans. Journal of Gannan Midical College 28(4), 471–473 (2008)

Genetic Polymorphisms of the Second Intron of GH Genes in Chinese Donkeys*

Xuemin Guan, Yanfang Liu, Yongmei Shu, and Wenjin Zhu**

Department of Life Science, Hebei Normal University of Science and Technology, Hebei, China
guanxueming109@163.com

Abstract. To reveal the genetical diversity of different donkey breeds at molecular level and provid some bases for the breed resource evaluation and utilization of donkeys in China. seven donkey breeds (Linxian, Guanzhong, Xingjiang, Cuangling, Huaibei, Dezhou, Jinnan) were used as experimental population; the genetic variations of GH genes were researched by PCR-SSCP method. The results were as follows:The polymorphic PCR-SSCP sites in the 2rd intron. Three haplotypes with the percentage of 1.7% in 174 animals were obtained.The haplotype diversity was high as 0.678 and 0.542 for the Linxian donkeys and Huaibei donkeys, and low as 0.077 for Xingjiang donkeys, with that of 0.409 and 0.462 for Cuangling donkeys and Guanzhong donkeys respectively, with that of 0.355 and 0.304 for Dezhou donkeys and Jinnan donkeys respectively. The amplified fragments of AA and BB of the fragment were cloned and sequenced. The result showed that in 214 bp BB genotype had one substitution mutation at 735 site(G→C), AA genotype had one substitution mutation at 869 site(G→T). The result above mentioned first confirmed that there are polymorphisms in intron 2 (214 bp) region of GH gene.

Keywords: GH gene, pcr-sscp, genetics diversity.

1 Introduction

PCR - SSCP technology is a combination of PCR and SSCP. After the denaturatin of PCR product, SSCP (Single Conformation Polymorphism) can be used in the separation of different spatial configuration of Single DNA PCR product through neutral polyacrylamide gel electrophoresis. Therefore, The SSCP of the PCR product can well reflect the coagulase gene differences, thus reveal the gene polymorphism.

The growth hormone (Growth Hormone GH) is a kind of single stranded multi-peptide hormone Secreted by the prehypophysis secretion, it has the influential role of adjusting the metabolism of carbohydrate, the fats and protein [1,2]. The research indicated that the growth hormone raised the growth speed obviously and

* This work is partially supported by Science and technology research and development projects of the Qinhuangdao City(201001A155) and Department of Education project of Hebei Province (Z2010137) and Natural science fund 0f Hebei Province (C2007000739).
** Corresponding author.

E. Zhu and S. Sambath (Eds.): Information Tech. and Agricultural Eng., AISC 134, pp. 471–477.
springerlink.com © Springer-Verlag Berlin Heidelberg 2012

promoted the production efficiency. In order to raise the animal growth speed and promote their performance traits, more and more scientists began to focus on the study of GH. Current studies on the GH of chicken, horses and cattle found that GH gene has rich polymorphism. And such polymorphism is related to many quantitative traits (such as growth rate, milk production rate, milk fat, egg production, etc.)of livestock [3,4]. While the report of the GH gene and its polymorphism of donkey at home and abroad is yet revealed.

The growth hormone gene is constituted by the non-code area by both sides 5 ' ,3 ' the non-code area and among the complete code area - - 5 Exon and 4 Intron. The Exons of mammal's GH gene are highly homologous, but the sequence and the length of Introns are actually various. Many Cis-acting elements participate in the duplication regulation, of which the Splice site and the branching point take the very vital effect to the precursor film editing, thus has important effect in the regulation of the gene expression [5]. Nucleotide's flaw or the sudden change may cause the mRNA film editing to be unusual, affecting the protein normal synthesis. Many human diseases are caused by unusual film editing of Introns. such as Mediterranean Sea anemia.

To reveal the molecular level of genetic diversity in local chinese Donkey breeds, GH gene sequences of the second intron in the 174 individuals of seven Chinese local Donkey breeds were analysied by PCR-SSCP in this study. Thus provide reference for the protection of local Donkey breeds germplasm.

2 Material and Method

2.1 Sample's Gathering

The research has gathered 174 donkey's blood samples of 7 breeds throughout China. Sample quantity and the sampling site can be seen in the Table 1. 15 mL blood sample is picked by the neck vein, mixed with ACD anticoagulants to prevent clotting (6:l), and preserved in the non-power source portable type refrigerator , bought back to the laboratory, loaded 3 mL preserved at - 4 ℃ , the rest were saved at - 70 ℃

2.2 Extraction of Total DNA and PCR Amplification

Total DNA was extracted by conventional phenol - chloroform extraction method,the second intron primers of GH gene are used as specific primers, they are designed by Primer3.0 GH software based on homologous sequence of horse GH. the upstream primer is 5'-CTGGCTGCTGACACCTACAA-3 'and the downstream primer is 5'-CGCTCCTGGGAGAAAGAAC-3', they are synthesized by Beijing Parkson biotechnology companies. PCR reaction system was 25 μL (10 × buffer 2.5 μL, dNTP2 μL, primer 2 μL, Taq E 0.2 μL, DNA template 2 μL, ddH_2O14.8 μL). PCR reaction conditions: Primer 94 ℃ denaturation for 2.5 min →30 ×(94 ℃ 40 s, 58 ℃ 40 s, 72 ℃ 1 min) → 72 ℃ extension 7 min.

Table 1. The number、 collection location and origin of samples of donkey breeds

Breeds and abbreviations	NO.of individuals	Collection Location	Localities
Linxian LX	8	Linxian Shanxi	Linxian west of Shanxi
Guanzhong GZ	32	Yangling Shanxi	Guanzhong plain of shanxi
Xinjiang XJ	26	市Yining city Xinjiang	Kashi region,xinjiangAutonomous Region
Guangling GL	26	Guangling	Guangling and lingqiu of shanxi
Huaibei HB	18	Mengcheng Anhui	市 Huaibei city,Anhui Province
Dezhou DZ	36	Lucheng Shanxi	The towns along bohai sea at lubei plain in shandong
Jinnan JN	28	Wenxi Shanxi	Yuncheng and linfen of shanxi

2.3 The PCR-SSCP Examination

The SSCP analysis of the PCR products in 174 samples of the 7 donkey breeds is performed through the non-denatured polyacrylamide gel electrophoresis and the silver nitrate dyeing, the mother liquor is 39:1, 10%.

2.4 The Recycling and Sequencing of PCR Product

Recycle the effective and sufficient amplified product (with the density of approximately 100 ng) and have the purification and the sequence carried on by Shanghai biological technology service Limited company.

2.5 Data Analysis Method

The number of Haplotype frequency and the diversity of Haplotype were analysed and mapped by Microsoft Excel analysis. The diversity of Haplotype was calculated by the formula as follows:

$$H = n\left(1 - \sum x_i^2\right)/(n-1)$$

Where: H is haplotype diversity; as X_i means the haplotype ranks i.

3 Results and Analysis

3.1 Haplotype Distribution and Frequency

The amplified products of the GH gene's second intron On 7 breeds (lines) were analysed by the SSCP polymorphism (Figure 1). As is seen from the Figure 1, the second intron of 214bp of the GH gene fragments appeared polymorphisms, there are three kinds of haplotypes in seven varieties, which were expressed by the English letters A, B, C.

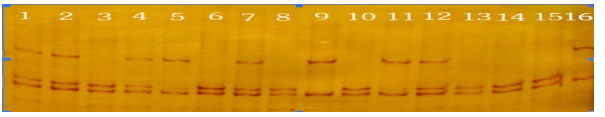

Fig. 1. Detection of a two-allele SSCP in the second intron of the donkey GH gene
Note： 3、6、8、10、13、14、15：A； 5、9、11、16：B； 1、2、4、7、12：C

Table 2 showed the detected haplotype and frequency of the breeds, and from the table we can see that three haplotypes were detected from the seven breeds. A haplotype was detected in all the breeds, totally 131, was the most, and its frequencies were quite high in each breeds. That showed haplotype A was the shared haplotype. Haplotype B was only detected in Guanzhong donkey, the Linxian donkey, the Xinjiang donkey and in the Huaibei donkey, which is the particular haplotype of the four breeds. But the quantity is quite small, with only one individual detected in each breed. Haplotype C was detected in all the donkey breeds except Xinjiang donkey, and the detected frequency in each breed was between 0.179~0.5.

3.2 Haplotype Diversity

Table 3 showed the Genetic diversity indices in the GH gene's second intron of the 174 individuals. All varieties of haplotype diversity H sizes, of which Linxian donkey up to 0.678 , showing their genetic diversity were the most abundant, followed by Huaibei donkey as 0.542, while the Xinjiang donkey is the lowest, only 0.077, indicating its relative lack of diversity; While the H size in Shanxi local Guangling donkey breeds is closer to that in the guanzhong donkey, 0.409 and 0.462 respectively.

3.3 Sequence Analysis and Comparison

Purify and sequence the PCR amplification products , using Clustal W (1.82) software on the analysis of homologous sequences of the measurement sequence. Compare the results , G → C mutation takes place in the BB-type at base 735 ; G → T mutation takes place in AA-type at base 869, both the mutations are transversions, with homology up to 99%.

Table 2. Haplotype and frequency in the second intron of the 7 donkey GH gene

Haplotype	Breeds							Total
	Dezhou	Guanzhong	Guangling	Linxian	Jinnan	Xinjiang	Huaibei	
A	28/0.778	22/0.688	19/0.731	3/0.375	23/0.821	25/0.961	11/0.611	131/0.74
B		1/0.031		1/0.125		1/0.038	1/0.056	4/0.022
C	8/0.222	9/0.281	7/0.269	4/0.5	5/0.179		6/0.333	39/0.224
Total	36/1.000	32/1.000	26/1.000	8/1.000	28/1.000	26/1.000	18/1.000	174/1.000

Table 3. Genetic diversity indices in the second intron of the 7 donkey GH gene

Breeds	Samples	No.of haplotype	Haplotype proportion	Haplotype diversity
DZ	36	2	0.056	0.355
GZ	32	3	0.093	0.462
GL	26	2	0.077	0.409
LX	8	3	0.375	0.678
JN	28	2	0.071	0.304
XJ	26	3	0.115	0.077
HB	18	3	0.167	0.542

4 Discussion

4.1 GH Gene Polymorphism of the Second Intron

The sub-fragments of the mammal's GH gene contains rich multiplicity[6]. Gao Xue et al. Analysed nanyang bovine GH by PCR-SSCP and demonstrated that the third, fourth intron of the GH gene contain polymorphism[7]. Li Meiyu et al. analysed goat GH gene and demonstrated that the first, second intron contain polymorphism. At present, research on donkey's GH gene polymorphism at home and abroad is rarer.The current research first find the second intron of donkey's growth hormone gene contains polymorphism, however, the polymorphism differences among large, medium and small kind of donkey is not significantly, whether its polymorphism is related to donkey's production traits still needs further study. In order to seek for the heredity chain-like mark with important economic characters in the poultry , the candidate gene law is very effective, it may be used to directly study the relationship between gene polymorphism and the individual economy characters. Therefore, analyse the second intron polymorphism of the GH gene and its mutation means a lot for improving donkey's production traits and donkey's industry in both theory and realistic.

4.2 The Genetic Diversity of Donkey

In this study, the second intron of growth hormone gene haplotype of seven Donkey breeds were analysed. The results shows that different breeds share haplotypes. Haplotype diversity (H) means the frequencies of two different haplotype in random samples(Nei, 1987). the greater the H is,the higher the degree of population diversity, the more abundant the genetic diversity is; in contrast, the lower the level of population diversity, the poorer the genetic diversity is . The study found that the guanzhong donkey has the relevant higher diversity, which is Consistent with Zhu Jin's analysis(2005) [8] on microsatellite as well as Chu-Zhao Lei (2002,2005) [9], Sun Weili, etc. (2007) [10] mtDNA sequence analysis. Texas donkey has relatively low diversity, haplotype diversity is only 0.355, which is Consistent with Zhaozhao Xia et al (2008) [11] The conclusions from the same mitochondria. Zhu Jin et al (2005) found [8] that southern Shanxi donkey has the highest polymorphic information content, while further expanding the number of samples in this experiment by the second intron of GH gene discovery, Jinnan donkey haplotype diversity degree is not high, only

0.304. The Guanzhong donkey, Guangling donkey's Shan Bei diverse is quite close, approximately in 0.4. Which is consistent with the record that Shanxi's large-scale donkey class group was formed after the Guanzhong donkey distributes to these areas and forms local variety [12]. Linxian donkey's haplotype diverse is biggest, is 0.678, explained that its heredity multiplicity is rich, the community hereditary change degree is high, the breeding potential is big. Xinjiang donkey's haplotype diverse is smallest, is the pure synthesis, explained that its community heredity diverse is low, preserves seed the potential to be big, but (2008) [13] uses the conclusion a little difference which with Yang Hu the micro satellite analysis obtains, this possible and the sampling different as well as sample quantity concerned. This article proved: The PCR-SSCP technology carries on the heredity multiplicity analysis is also the science reasonable and convenient feasible. Therefore inspects the community heredity structure with the growth is feasible.

4.3 Donkey Protection of Genetic Resources

Donkey has a very rich genetic resources no matter in foreign or domestic, it's valuable human gene pool, but there are still some donkey species are threatened with extinction. Such as Shanxi Guangling donkey test results are not very high, indicating its relative lack of diversity, Linxian donkey despite higher test results, but be found that the quantity in the sampling has been limited, the sampling is very difficult. Xinjiang donkeys are homozygous genotype, but since 1970, producing many of Xinjiang donkey off in the introduction of improved hybrid local donkey, leading to real Xinjiang donkey this fine dramatic reduction of local varieties, therefore, We should step up protection of these resources, otherwise it will lead to the extinction of some species.

5 Conclusion

Detected by PCR-SSCP in 7 Chinese loocal donkeys GH gene variations in the second intron, the test first confirmed that donkey GH gene intron 2 (214 bp) region polymorphism, however, the polymorphism differences among large, medium and small kind of donkey is not significant, the relation between polymorphism and the growth of donkeys still need further study. The results also show that: PCR-SSCP analysis of genetic diversity technology is reasonable, convenient and practical science. Therefore, it is possible to examine population genetic structure of diversity with the growth hormone gene loci . This study can also provide basic data for donkey breeds resources assessment, conservation and utilization in our country .

References

1. Zhang, Y.-R., Unerhu, M.: Cloning and PCR-SSCP analysis of growth hormone gene in Mongolian Horse. Chinese Journal of Veterinary Medicine 42(9), 10–12 (2006)
2. Jiang, Z.H., Rottmann, O.J., Pirchner, F.: Sequence characterization of genetic polymorphisms at the 2nd exon of procine growth hormone gene. Journal of Nanjing Agricultural University 20(2), 67–71 (1997)

3. Norio, K., Asako, N., Hisato, O.: DNA polymorphism in the chicken growth hormone gene: association with egg production. Anim. Sci. 74, 243–244 (2003)
4. Nielsen, V.H., Larsen, N.J., Agergard, N.: Association of DNA polymorphism in the growth hormone gene with basalplasma growth hormone concentration and production traits in pigs. Anim. Bred. Genet. 112, 205–212 (1995)
5. Ascacio-Martínez, J.A., Barrera-Saldaña, H.A.: Sequence of a cDNA encoding horse growth hormone. Gene 143(2), 299–300 (1994)
6. Gao, X., Xu, X.R., Ren, H.Y., Zhang, Y.H., Xu, S.Z.: The effects of the GH, IGF-I and IGF-IBP 3 Gene on growth and development traits of nanyang cattle in different growth period. Hereditas 28(8), 927–932 (2006)
7. Li, M.Y., Min, L.J., Pan, Q.J., Pan, Y.C., Wang, T.J.: PCR-SSCP analysis of growth hormone gene partial sequence in goats. Chinese Journal of Veterinary Medicine 40(10), 9–11 (2004)
8. Zhu, W.J., Zhang, M.J., Ge, M.X., Guan, X.M., Guo, C.J.: Microsatellite analysis of genetic diversity and phylogenetic relationship of eight donkey breeds. Scientia Agricultura Sinica 39(2), 398–405 (2006) (in China)
9. Lei, C.C.: Research on mtDNA genetic diversity of four domestic animal species(Cattle,Water Buffalo,Vak and Donkey). PhD dissertation, College of Animal Science and Technology Northwest Sci-Tech University of Agriculture and Forestry,Yangling (2002) (in China)
10. Sun, W.L., Yang, B.H., Chao, X.L., Sun, Y.F., Liang, C.N., Liu, J.B.: Phylogenetic relationship and genetic diversity of chinese four domestic donkeys using mtDNA D-Loop. China Herbivores 27(2), 7–9 (2007)
11. Zhao, C.X., Liu, W.Z., Zhu, W.J., Wu, J.L., Wu, Y.Q.: Analysis on the genetic diversity of partial sequences in mtDNA D-loop of six donkey breeds. China Herbivores 28(4), 3–6 (2008)
12. Zhang, Z.G., Zhu, X.H.: Historical Matericals of Chinese animal husbandry. Science Press, Beijing (1986)
13. Yang, H.A.J., Wang, J.F., Liu, M.J.: Genetic diversity in three chinese domestic donkey breeds based on microsatellite analysis. Chinese Journal of Veterinary Medicine 01, 8–10 (2008)

Degradation of Soybean Stalk Lignin with White-Rot Fungus and SEM Characterization of Surface Structure

Xu Wei

Food Engineering School
Harbin University of Commerce
Harbin, Heilongjiang Province, China 150076
xuwei20070808@yahoo.com.cn

Abstract. Conditions for degradation of soybean stalk lignin with Phanerochaete Chrysosporium Burdsall are studied in this paper. The measured degradation rates for lignin, cellulose and hemicellulose are 49.91%, 32.04% and 49.06% respectively when 12 mL of synthetic culture solution and 0.8 mL of seed liquid (concentration at 8.6×10^6 counts/mL) are added to 5.0 g of stalk when its initial pH value of culture medium is 4.5. A scanning electron microscope (SEM) is used to observe the apparent structure of soybean stalks before and after degradation and it is found that the number of holes on surface of stalk and on the inside walls of vascular bundles is increased and the surface roughness and degree of fragmentation is strengthened.

Keywords: Soybean stalks, Lignin, Phanerochaete Chrysosporium Burdsall, SEM.

1 Introduction

China is a big agricultural country in the world with the highest yield of crop stalks and straws. Such resources have not been well developed and utilized for a long time. They are mostly abandoned or burned in the field. Such practice is a tremendous waste of natural resources, and it also causes severe pollution to environment. Lignin, as the main element of cell wall of stalks, forms 15% to 30% of lignified cellulose cell walls. The higher the degree of lignification, the lower the rate of digestion[1]. So, the key measure to improve rate of digestion of stalks is to degrade lignin.

White-rot fungus is a major strain found up to now that can decompose botanical polymer and degrade lignin[2,3]. It is possible to use lignin peroxidase (LiP), manganese-dependent peroxidease (MnP), laccase and oxidases that can produce hydrogen peroxide, to degrade lignin and cellulose in stalks[4]. To use white-rot fungi for biological degradation of stalks is of practical significance for efficient utilization and conversion of stalk and straw resources, development of source of feed, increase of green energy and reduction of environmental pollution.

E. Zhu and S. Sambath (Eds.): Information Tech. and Agricultural Eng., AISC 134, pp. 479–484.
springerlink.com © Springer-Verlag Berlin Heidelberg 2012

2 Materials and Methods

2.1 Experimental Materials and Instruments

The soybean stalks come from Morin Dawa Autonomous Banner of Inner Mongolia. The phanerochaete chrysosporium, which belongs to white-rot fungi, is bought from China Center of Industrial Culture Collection (CICC) .

Instruments: Portable electro-thermal pressure steam sterilizer, multi-function juice extractor, mixer, SEM, electro-thermal constant-temperature blast drying oven, constant-temperature incubator, analytical balance, muffle furnace, filter funnel.

2.2 Experimental Methods

1) Seed Culture Medium

Glucose 2, corn syrup 0.05, $(NH_4)_2SO_4$ 0.1, KH_2PO_4 0.5, $MgSO_4{\cdot}7H_2O$ 0.5, VB_1 0.0005;

2) Synthetic Culture Solution (g/L)

$(NH_4)_2SO_4$ 15, KH_2PO_4 4.0, $MgSO_4{\cdot}7H_2O$ 0.2, $CaCl_2$ 0.2, VB_1 0.001, $FeSO_4{\cdot}7H_2O$ 0.1, $CoCl_2{\cdot}6H_2O$ 0.1, $ZnSO_4{\cdot}7H_2O$ 0.1,$CuSO_4{\cdot}5H_2O$0.02,$AlK(SO_4)_2{\cdot}12H_2O$ 0.02, $Na_2B_4O_7{\cdot}10H_2O$ 0.05, $(NH_4)_2MoO_4{\cdot}4H_2O$ 0.02, Tween-80 0.003;

3) Fermentation Culture Medium

Weigh and take 5.0 g of smashed soybean stalk. Put it into a 250 mL flask. Add synthetic culture solution. The culture solution is sterilized with high pressure steam at 121℃ for 20-30 min. Then it is taken out and made ready for future use.

4) Method for Measurement of Lignin, Cellulose and Hemicellulose Contents

Differential weight method is used in our experiment .

$$\text{Rate of degradation} = \left(1 - \frac{\text{total mass of lignin after degradation}}{\text{total mass of lignin before degradation}}\right) \times 100\%$$

3 Results and Analysis

3.1 Influence of Quantity of Added Synthetic Culture Solution on Rate of Degradation of Lignin

Take 5.0 g of sterilized soybean stalk. Inoculate 0.8mL seed liquid to fermentation culture media that contain 6mL,8 mL, 10mL, 12mL, 14mL and 16mL of synthetic culture solution respectively. The initial pH value is 4.5. Incubation is carried out in an incubator at temperature 30℃ and relative humidity 86%. The changes of rates of degradation of cellulose, hemicellulose and lignin in soybean stalk over a period of 30 days are measured and the results are shown in Fig. 1.

It can be seen from Fig. 1 that if addition of synthetic culture solution is either too high or too low in quantity, the rate of degradation for cellulose, hemicellulose and lignin will decrease. When the addition level is 10mL, the rate of degradation for hemicellulose can reach its maximum 48.09%. When the addition level is 12mL, the rates of degradation for lignin and cellulose can reach their maximum values, 49.91%, and 32.04% respectively.

3.2 Influence of Quantity of Inoculation on Rate of Degradation of Lignin

Take 5 g of sterilized soybean stalk. On condition of addition of 12mL of synthetic culture solution, inoculate 0.5 mL, 0.8 mL, 1.1mL, 1.4mL and 1.7mL of seed liquid respectively to the fermentation culture medium. The initial pH value is 4.5. Incubation is carried out in an incubator at temperature 30℃ and relative humidity 86%. The changes of rates of degradation of cellulose, hemicellulose and lignin in soybean stalk over a period of 30 days are measured and the results are shown in Fig. 2.

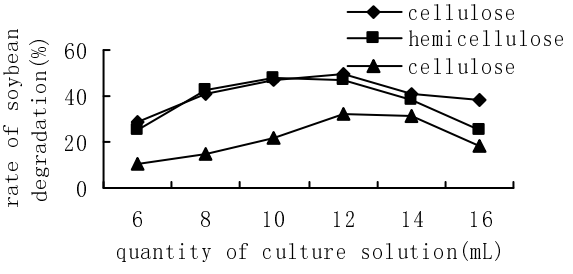

Fig. 1. Result of influence of quantity of culture solution on rate of degradation of lignin in soybean stalk

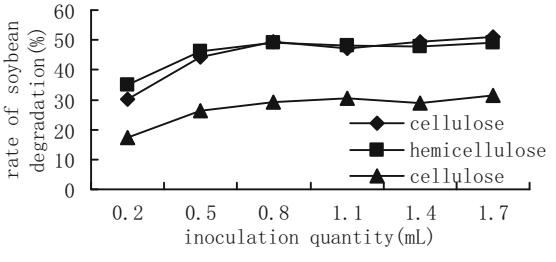

Fig. 2. Result of influence of inoculation quantityon rate of degradation of lignin in soybean stalk

It can be seen from Fig. 2 that the rate of degradation of lignin varies with inoculation quantity. When seed liquid at bacteria concentration of 8.6×10^6 counts/mL and is used and inoculation quantity reaches 0.8 mL, the rates of degradation of cellulose, hemicellulose and lignin are about their maximum values: 29.15%, 49.06% and 49.35% respectively.

3.3 Influence of Initial pH Value of Culture Medium on Rate of Degradation Lignin

Take 5g of sterilized soybean stalk. Inoculate 0.8mL of seed liquid to the fermentation media that contains 12mL of synthetic culture liquid with initial pH values at 3.5, 4.0, 4.5, 5.0, 5.5 and 6.0 respectively. Incubation is carried out in an incubator at relative humidity 86%. The rates of degradation of cellulose, hemicellulose and lignin in soybean stalk over a period of 30days are measured and the results are shown in Fig. 3.

It can be seen from Fig. 3 that pH value has significant impact on rate of degradation of lignin. This is mainly because if acid substance or alkaline substance enters the cells, it can weaken or damage the microbiological regulatory ability, so as to affect the reduction potential of environment and further affect the enzyme activity inside the microbiological cells. pH value can also affect cell respiration. Lignin is most sensitive to changes in pH value. When pH value is set at 4.5, the rates of degradation of cellulose, hemicellulose and lignin degradation can reach their maximum values: 27.1%, 44.8% and 48.0% respectively.

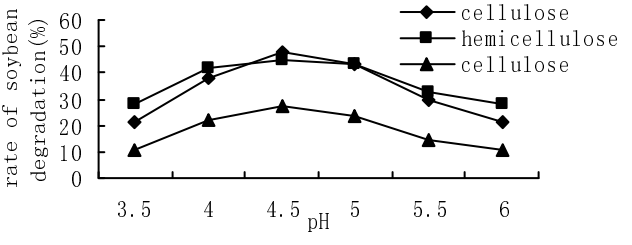

Fig. 3. Influence of initial pH value of culture medium on rate of degradation of lignin in soybean stalk

3.4 Characterization Analysis (with SEM) during Degradation of Stalks

When soybean stalks are degraded by white-rot fungi, lignin peroxidases, manganese-dependent peroxidases, laccase and catalase will be secreted to make damage to the surface of soybean stalk and its vascular bundles. To study the change of apparent structure of stalk during fermentation is very important for study on the law of degradation of lignified cellulose by white-rot fungi. The result of electron microscope scanning is shown in Fig. 4.

On its cross section is relatively compact. The stalk is smooth in surface, which is covered with a thin layer of wax, without any holes.

On the 30th day, the structure of soybean stalk is severely damaged. It can be seen from the cross section picture that large portion of vascular bundles are destroyed and no complete vascular bundles have survived. SEM pictures show that the stalk no longer has complete fiber structure, but there are more and larger holes. The stalk is severely damaged.

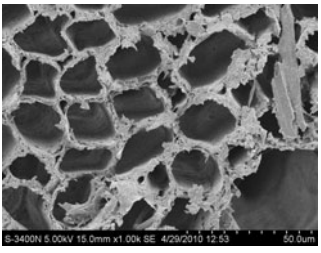

(a) Cross section of the original stalk

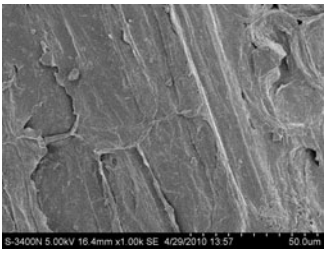

(b) Outer surface of the original stalk

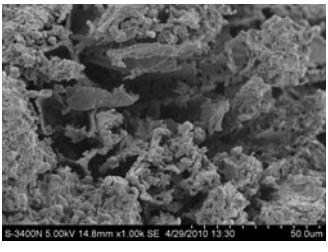

(c) Cross-section of stalk after 30 days of degradation

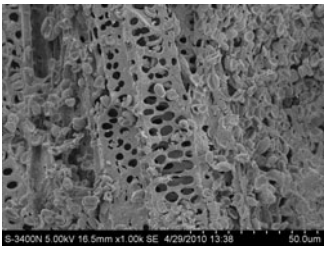

(d) Outer surface of stalk after 30 days of degradation

Fig. 4. Comparison of SEM in degradation of soybean stalk by white-rot fungi

4 Conclusions

White-rot fungi have strong ability for degradation of soybean stalks. The vascular bundles of soybean stalk are significantly damaged after degradation by white-rot fungi for 30days. There are more and larger holes on the surface. Some holes become interconnected. The degradation effect is significant. When soybean stalk is degraded by white-rot fungi, the lignin on stalk surface is the first to be degraded and holes are generated during the process. Then, hyphae extend through the holes into inside of stalk and enzymes are secreted for further degradation of internal components of the stalk. It is indicated through measurement on contents of cellulose and hemicellulose that white-rot fungi also have strong ability for degradation of cellulose and hemicellulose.

References

1. Li, X.-P.: Brief Analysis of the Comprehensive Utilization of Crop Straw. Journal of Luoyang Institute of Science and Technology 20(3), 8–11 (2010)
2. Zhang, J., Huang, M., Xu, Y.: Research and Application Advances of Ligninases from White Rot Fungi. Water Purification Technology 23(1), 19–22 (2004)

3. Vane, C.H.: The molecular composition of lignin in spruce decayed by white-rot fungi (Phanerochaete chrysosporium and Trametes versicolor) using pyrolysis-GC-MS and hermochemolysis with tetramethylammonium hydroxide. International Biodeterioration & Biodegradation 51, 67–75 (2003)
4. Ikehata, K., Buchanan, I.D., Smith, D.W.: Recent developments in the production of extracellular fungal peroxidases and laccases for waste treatment. Journal of Environmental Engineering and Science 3(1), 1–19 (2004)

Response Surface Methodology Used for Statistical Optimization of Fermentation Media of *Cordyceps Militaris*

Dongxue Liang[1], Na Zhang[1], Yaowen Zhang[1], Tinglan Zhang[1], Li Lü[1], Zhenzuo Wang[1,*], and Lirong Teng[1,2,*]

[1] College of Life Science, Jilin University, Changchun, China
[2] Zhuhai college, Jilin University, Zhuhai, China
{zhangna2003,tenglr543}@gmail.com
wzz@jlu.edu.cn

Abstract. Response surface methodology (RSM) was used for statistical optimization of fermentation medium that influenced the yield of endo-polysaccharide from cultivated mycelia of Cordyceps militaris N102. The Plackett-Burman design was used in the first step to evaluate the effects of five factors, including five fermentation medium components. Among the variables screened, sucrose, peptone and $MgSO_4 \cdot 7H_2O$ in the fermentation medium had significant effects on yields of endo-polysaccharide. In the second step, the concentrations of sucrose, peptone and $MgSO_4 \cdot 7H_2O$ were further optimized using Box-Behnken design and response surface analysis. The optimized concentration of sucrose, peptone and $MgSO_4 \cdot 7H_2O$ was 17.23 g/L, 13.80 g/L and 2.54 g/L, respectively, which increased the production of endo-polysaccharide in mycelia of Cordyceps militaris N102 by 6.33 % relative to normal medium.

Keywords: Cordyceps militaris, Fermentation, Response surface methodology (RSM), Endo-polysaccharide, Medium optimization.

1 Introduction

The fungi of Cordyceps belong to the family Clavicipitaceae of the order Hypocreales. There are more than 350 species all over the world described as Cordyceps, out of which about 120 species have been reported from China [1-2]. Cordyceps millitaris is one of the traditional Chinese medicinanl fungi which has been widely used in traditional Chinese medicine [3–4]. Because of the importance of its biological properties, a large quantity of pure materials is urgently needed for further studies [5–6]. Moreover, as a result of the immoderate exploitation, the resource of Cordyceps is in severe danger. Recent studies have revealed that the Cordyceps and its anamorph possess a variety of biologically active substances, such as polysaccharides, cordycepin, ergosterol, with extensive pharmacological effects [7]. The article deals with the recent advances in the polysaccharide production from the mycelia and fruiting bodies of Cordyceps cultured in the artificial medium.

* Corresponding authors.

E. Zhu and S. Sambath (Eds.): Information Tech. and Agricultural Eng., AISC 134, pp. 485–491.
springerlink.com © Springer-Verlag Berlin Heidelberg 2012

Recently, response surface methodology (RSM) has been used to optimize the composition of the medium for both submerged fermentation [8] and solid-state fermentation [9]. RSM, a collection of mathematical and statistical techniques for building empirical models, is gaining recognition as a powerful approach for optimizing conditions for the production of industrially important products such as chemicals and enzymes [10-11]. RSM is a useful statistical technique for investigating complex multivariate optimization process processes, especially for optimizaition of medium componets [12-14].

In this paper, the Plackett-Burman design and Box-Behnken design were applied to optimize the fermentation medium that influenced the yield of endo-polysaccharide from cultivated mycelia of *Cordyceps militaris* N102.

2 Materials and Methods

2.1 Materials

Strain: Cordyceps militaris N102 is a mutant of the original *Cordyceps militaris* CICC 14013

Seed medium: glucose 20 g/L, peptone 20 g/L, $MgSO_4$ 3 g/L, KH_2PO_4 3 g/L.

2.2 Methods

2.2.1 Culture Conditions

To prepare the inoculum, *Cordyceps militaris* N102 was cultured in seed medium. Seed culture were incubated at 26 ℃ on a rotary shaker at 150 rpm for 4 days. Each flask (250 ml) contained 100 ml of fermentation medium and was inoculated with 2 % (v/v) seed culture. The flasks fermentation were incubated at 26℃ on a rotary shaker at 150 rpm for 4 days.

2.2.2 Analytical Methods

Cordyceps militaris N102 fermentation culture were centrifuged at 4500 g for 8 min. The precipitates were recovered, washed thoroughly with distilled water, and centrifuged at 4500 g for 8 min again. The precipitate was recovered and freeze-dried to constant weight, then recorded the dry weight of mycelia and homogenized to powders (60 mesh). Dried mycelia powders were extracted with distilled water for 3 h in 60 ℃ water-bath (mycelia/distilled water ratio: 1:30), and then centrifuged at 7000 g for 5 min. The amount of polysaccharides was determined by a anthrone-sulfuric acid method [16].

2.2.3 Experimental Design

A Plackett-Burman (P-B) experimental design was used to screen the significant variables in fermentation medium that influenced the yield of endo-polysaccharide from cultivated mycelia of *Cordyceps militaris* N102. There were eight variables, including five fermentation medium components (sucrose, peptone, KH_2PO_4, $MgSO_4 \cdot 7H_2O$ and VB_1) and three dummy variables, screened in 12 experiments. Levels of factors chosen for Plackett–Burman design are given in Table 1 while the design of experiments is not shown here.

A Box-Behnken experimental design with three coded levels (-1, 0 and +1) was used to describe the nature of the response surface in the optimum region. The values of the response (yield of endo-polysaccharide) were analyzed by a polynomial equations model. Sucrose, peptone and $MgSO_4 \cdot 7H_2O$ were designated as X_1, X_2 and X_3, respectively. Table 2 shows the actual levels of the coded factors while the design of experiments is not shown here. SAS Version 9.0 TS (SAS Institute Inc., Cary, nc, USA) was used for designing and analyzing the experiments.

Table 1. Levels of Factors Chosen for Plackett–Burman Design

Factors (g/L)	Symbols	levels	
		-1	0
sucrose（g/L）	X_1	10	30
peptone（g/L）	X_2	10	30
KH2SO4（g/L）	X_3	2	4
$MgSO_4 \cdot 7H_2O$(g/L)	X_4	2	4
VB_1（g/L）	X_5	0.05	0.15
dummy variables	X_6	--	--
dummy variables	X_7	--	--
dummy variables	X_8	--	--

Table 2. Levels of Factors Chosen for Box-Behnken Design

Factors (g/L)	Symbols	-1	0	1
sucrose	X_1	10	15	20
Peptone	X_2	10	15	20
$MgSO_4 \cdot 7H_2O$	X_3	2	3	4

3 Results and Discussion

3.1 Screening of Significant Variables Using P-B Design

A Plackett-Burman design was used to screen the significant components in fermentation media. The yields of endo-polysaccharide was used as the responsive values. The experimental yields of endo-polysaccharide are not shown here. The application of SAS RSREG program was used for analyzing the experiments. A polynomial model was derived representing endo-polysaccharide production as a function of the independent variables:

$$Y=0.5221+0.0265X_1+0.0319X_2+0.0167X_3+0.0217X_4+0.0107X_5+0.0166X_6+0.0125X_7-0.0039X_8 \quad (1)$$

The analysis of variance (ANOVA) for the P-B experiment was calculated, and the effect of each variable on the yield of endo-polysaccharide was determined by Student's *t*-test (Table 3). The goodness of fit of the regression equations was tested by examining the adjusted determination coefficient, R^2. High value of correlation coefficients, R^2 (0.9636), indicates the suitability of models to predict responses. The value of *Prob>F* (0.0427) which was less than 0.05, indicating that the model for response was significant.. The effects of peptone (X_2), sucrose (X_1) and $MgSO_4 \cdot 7H_2O$ (X_4) had confidence levels >95 % and were considered to influence the yield of endo-polysaccharide significantly. The remaining variables, including KH_2PO_4 (X_3) and VB_1 (X_5), had confidence levels <95 % and were considered not significant. According to the absolute value of *t*, the effects of the five variables were in the order: peptone >sucrose >$MgSO_4 \cdot 7H_2O$ >KH_2PO_4 >VB_1. Thus, sucrose, peptone and $MgSO_4 \cdot 7H_2O$ were selected for further optimization.

Table 3. Analysis of Variance for Plackett–Burman Design

Source	Estimate	StdErr	*t*	*Pr* > |*t*|
X_1	0.0530	0.0124	4.2861	0.0233
X_2	0.0638	0.0124	5.1654	0.0141
X_3	0.0333	0.0124	2.6946	0.0741
X_4	0.0434	0.0124	3.5146	0.0391
X_5	0.0215	0.0124	1.7371	0.1808
X_6	0.0332	0.0124	2.6866	0.0746
X_7	0.0249	0.0124	2.0176	0.1370
X_8	-0.0078	0.0124	-0.6285	0.5743

3.2 Optimization of Medium Components Using RSM

A Box-Behnken experimental design was used for further optimization of fermentation medium that influenced the yields of endo-polysaccharide from cultivated mycelia of *Cordyceps militaris* N102. The levels of variables for the Box-Behnken experimental design were based on the preliminary results (Table 1).

The application of SAS RSREG program yielded the following quadratic regression equations for optimization of fermentation medium (Equation 2). The second order polynomial equations fitted to the experimental data of the Box-Behnken experimental design for predicting yield of endo-polysaccharide was shown in Equations 2:

$$Y=0.6095+0.0502X_1-0.0061X_2-0.0162X_3-0.0561X_1X_1-0.0260X_1X_2+0.0142X_1X_3-0.1099X_2X_2+0.0764X_2X_3-0.0308X_3X_3 \quad (2)$$

A summary of statistical testing for the model was conducted in the form of analysis of variance (ANOVA) (Table 4), which is required to assess the significance and adequacy of the model. The calculated *F*-value (30.5221) demonstrated that the regression model was highly significant and the value of *Prob>F* (0.0008) which was less than 0.01, indicating that the model for response was highly significant. In addition, high value of correlation coefficients, R^2 (0.9821), indicated the suitability of models to predict responses in terms of independent variables (Table 4). The linear (*P*=0.0033) and quadratic (*P*=0.0004) and interaction (*P*=0.0022) for response shown in Table 4 were all highly significant. Regression analysis results of the Box-Behnken design experiments were shown in Table 5. The significant variables in the model were X_1X_2, X_3X_3 with a *P*-values less than 0.05. X_1, X_1X_1, X_2X_2, X_2X_3 were determined to have highly significant effects.

Table 4. Regression Analysis of Box-Behnken Design

Source	DF	SS	MS	*F* values	*Pr* > *F*
X_1	1	0.0201	0.0201	53.3140	0.0008
X_2	1	0.0003	0.0003	0.7880	0.4154
X_3	1	0.0021	0.0021	5.5577	0.0650
X_1X_1	1	0.0116	0.0116	30.7153	0.0026
X_1X_2	1	0.0027	0.0027	7.1304	0.0443
X_1X_3	1	0.0008	0.0008	2.1201	0.2052
X_2X_2	1	0.0446	0.0446	118.1764	0.0001
X_2X_3	1	0.0233	0.0233	61.8050	0.0005
X_3X_3	1	0.0035	0.0035	9.2470	0.0287

Table 5. Analysis of Variance for Box-Behnken Design

Source	Estimate	StdErr	*t*	*Pr* > |*t*|
X_1	0.0530	0.0124	4.2861	0.0233
X_2	0.0638	0.0124	5.1654	0.0141
X_3	0.0333	0.0124	2.6946	0.0741
X_4	0.0434	0.0124	3.5146	0.0391
X_5	0.0215	0.0124	1.7371	0.1808
X_6	0.0332	0.0124	2.6866	0.0746
X_7	0.0249	0.0124	2.0176	0.1370
X_8	-0.0078	0.0124	-0.6285	0.5743

The mutual effect of the three independent variables on the yield of endo-polysaccharide of *Cordyceps militaris* N102 was shown in Fig. 1. The elliptical nature of the contour plots indicated that there were significant interactions between

sucrose and peptone (Fig. 1.A, P=0.0443). The highly degree of curl of the response surface plots likewise indicated that there were highly significant interactions between peptone and $MgSO_4 \cdot 7H_2O$ (Fig. 1.B, P=0.0005).

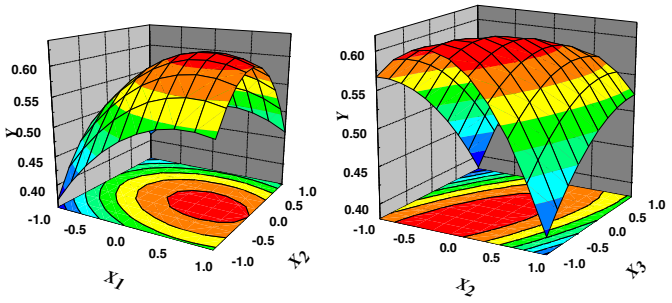

Fig. 1. Response surfaces and contour plots showing the mutual effect of sucrose and peptone (A), peptone and $MgSO_4 \cdot 7H_2O$ (B)

From the response surface and contour plots, the concentration of spores was found to present a maximum in the tested range. Based on the equation 1 and the response surface plots, the optimum adding ingredients concentration were as follows: sucrose 17.23 g/L, peptone 13.80 g/L and $MgSO_4 \cdot 7H_2O$ 2.54 g/L. The maximum yield of endo-polysaccharide, which could be obtained by the model, was 0.6251 g/L. Experiments were done in triplicate using the optimized conditions representing the maximum point of the yield of endo-polysaccharide to verify the modelling results. The average concentration found by experiment was 0.6318 g/L. The good correlation between predicted and experimental values after optimization justified the validity of the response model and the existence of an optimum point.

4 Conclusions

The statistical approach with rapid identification of important factors and development of a polynomial model showed significant results for optimizing fermentation medium that influenced the yields of endo-polysaccharide from cultivated mycelia of *Cordyceps militaris* N102. The present study identified the effect of individual variables on endo-polysaccharide production, which was found to be influenced significantly by the concentration of sucrose, peptone and $MgSO_4 \cdot 7H_2O$ in the medium. The optimum concentration was sucrose 17.23 g/L, peptone 13.80 g/L and $MgSO_4 \cdot 7H_2O$ 2.54 g/L. The yields of endo-polysaccharide from cultivated mycelia of *Cordyceps militaris* N102 using the optimized medium was 0.6251 g/L which increased the production of endo-polysaccharide by 6.33 % relative to normal medium. Therefore, RSM combined with software analysis is suitable for optimizing the medium components to increase yields of endo-polysaccharide.

Acknowledgment. We sincerely acknowledge the Central Lab of General Biology in JiLin University for their financial support and directions to carry out this research work.

References

1. Sung, J.-M., Lee, H.-K., Yang, K.-J.: Classification of Cordyceps spp. by morphological characteristics and protein banding pattern. Kor. J. Mycol. 23, 92–104 (1995)
2. Jiang, Y., Yao, Y.-J.: Current understanding of molecular systematics of Cordyceps. J. Fung. Res. 2, 58–67 (2004) (in Chinese)
3. Chang, W., et al.: Cordycepin inhibits vascular smooth muscle cell proliferation. Eur. J. Pharm. 21(4), 53–56 (2005)
4. Yoshikawa, N., Nakamura, K., Yamaguchi, Y., Kagota, S., Shinozuka, K., Kunitomo, M.: Antitumour activity of cordycepin in mice. Clin. Exp. Pharmacol. Physiol. 31, 51–53 (2004)
5. Chen, S.-Z.: Study on improved ultillization of deoxynucleoside on Cordyceps sinensis with supercritical CO2 extraction. CN Patent 1339440 (2002)
6. Chen, W., Wu, W., Gao, X.-H., Tang, L.-S., Shen, M., Zhang, H.-X.: Isolation and preparation of cordycepin by reverse-phase HPLC. Acta. Agr. Shanghai 23(1), 59–61 (2007)
7. Buenz, E.-J., Bauer, B.-A., Osmundson, T.-W., Motley, T.-J.: The traditional Chinese medicine Cordyceps sinensis and its effects on apoptotic homeostasis. J. Ethnopharmacol. 96, 19–29 (2005)
8. Gu, X.-B., Zheng, Z.-M., Yu, H.-Q., Wang, J., Liang, F.-L., Liu, R.-L.: Optimization of medium constituents for a novel lipopeptide production by Bacillus subtilis MO-01 by a Response Surface Method. Process Biochem. 40(10), 3196–3201 (2005)
9. Shih, I.-L., Kuo, C.-Y., Hsieh, F.-C., Kao, S.-S., Hsieh, C.-Y.: Use of surface response methodology to optimize culture conditions for iturin A production by Bacillus subtilis in solid-state fermentation. J. Chin. Inst. Chem. Eng. 39(6), 635–643 (2008)
10. Senanayeka, S.-P.-J.-N., Shahidi, F.: Lipase-catalyzed incorporation of docosahexaenoic acid (DHA) into borage oil: optimization using response surface methodology. Food Chem., 115–123 (2002)
11. Meyers, R.-H., Montgomery, D.-C.: Response Surface Methodology, Process and Product Optimization Using Designed Experiments. John Willey & Sons, Inc., New York (2002)
12. Öztürk, T., Ustun, G., Aksoy, H.-A.: Production of medium-chain triacylglycerols from corn oil: Optimization by response surface methodology. Bioresource Technol. 101, 7456–7461 (2010)
13. He, J., Zhen, Q.-W., Qiu, N., Liu, Z.-D., Wang, B.-J., Shao, Z.-Z., Yu, Z.-N.: Medium optimization for the production of a novel bioflocculant from Halomonas sp. V3a′ using response surface methodology. Bioresource Technol. 100, 5922–5927 (2009)
14. Jia, H.-S., Azlina, H.-K., Wei, S.-L.: Biocatalytic conversion of CO to acetic acid by Clostridium aceticum—Medium optimization using response surface methodology (RSM). Biochem. Eng. J. 40, 337–347 (2008)
15. Wang, L.-M., Xia, W.-S.: Determination of TPS by Improvement of Anthrone-sulfuric Acid Method. Food Sic. 26(7), 185–188 (2005)

Detection Class I Integron of Multidrug Resistace Pathogenic *Salmonella* from Chicken*

Qiuyue Wang[1], Yanying Zhang[1], Qiumei Shi[1], Wei Yao[2], Cuizhen Chen[1], Guangping Gao[1], Donglin Zhang[1], and Hai Fang[1,**]

[1] Key Laboratory of Preventive Veterinary Medicine of Hebei Province, Hebei Normal University of Science and Technology, Qinhuangdao, 066600, China
[2] Heibei Qinglong County Pingfangzi Junior Middle School, Qinhuangdao, 066503, China
{wangqiuyue1980,fanghaihb}@163.com

Abstract. Antimicrobial resistance test of 59 Samonella isolated from chicken was done by K-B method. The drug-resistance rate of oxacillin, tetracycline, erythromycin, penicillin G, gentamicin was 74.6%, 64.4%, 52.5%, 47.5% and 37.3% respectively. Most of the isolates were multidrug resistance and the rate was 81.36% (48/59). Among the total of the multidrug resistance isolates, the rate of resistance to three, four and five drugs was 45.76% (27/59), 23.73% (14/59) and 11.86% (7/59). PCR and DNA sequencing were used for screening and characterization of class I integrons. As a result, the detection rate of class I integron was 40.68% (24/59), and among these 48 isolates which had been proven multidrug-resistant, the detection rate of class I integron was 50% (24/48). Class I integron PCR positive isolates rate of multidrug-resistance was 100% (24/24). Results show that the class I integron has the relationship with multidrug resistance.

Keywords: Samonella, class I integron, multidrug resistance, detection.

1 Introduction

Avian Salmonellosis is a major bacteriosis in henneries, causing deaths of chickens in great numbers, hampering the growth and development of chickens, increasing the possibility of contamination of eggs [1]. Currently the control strategies of avian salmonellosis besides vaccines, antibiotics are mainly applied for disease treatment and prevention. However, due to the continual clinical using of antibiotics in large amount, antimicrobial drug resistance is an increasing problem in *Salmonella*, with strains more and more commonly being isolated exhibiting multidrug resistance (MDR). Consequently the detection of *Salmonella* drug resistance is very important to prevent avian salmonellosis.

In the study of the mechanism of bacterial multidrug resistance, the presence of genes within integrons coding for antibiotic resistance and the association of antibiotic

* This work is partially supported by Hebei Science and Technology Support Program (09220402D).
** Corresponding author.

E. Zhu and S. Sambath (Eds.): Information Tech. and Agricultural Eng., AISC 134, pp. 493–499.
springerlink.com © Springer-Verlag Berlin Heidelberg 2012

resistance phenotypes with the presence of integrons have been well documented [2,3]. Integrons are gene expression elements that play an important role in the recruitment of antimicrobial drug resistance determinants via site-specific recombination events catalyzed by the integron-encoded integrase [4]. Based on the sequence of the integrase genes, several classes of integrons have been described [5, 6].

Currently the detection of class I integron consist mainly in the amplification of its resistance gene cassette. Therefore, the aim of this study was to investigate the prevalence and characterize class I integron among *Salmonella* strains separated from chickens, and to monitor the spread of the multidrug-resistant *Salmonella* strains. Analyze the relation between class I integron and multiple drug resistance (MDR) in molecular level.

2 Materials and Methods

Bacterial strains

A total of 59 *Salmonella* strains were isolated from chicken in hebei province. The identification of each isolate as *Salmonella* was confirmed by performing PCR for the *invA* gene as described previously [7, 8] and serotyped by standard procedures. At last, all the *Salmonella* we have identified were further identified and confirmed in the professional laboratory of *Salmonella,* Chengdu Institute of Biological Products. Samples were kept in -20℃ for further study.

DNA extraction and amplification

DNA was extracted from the *Salmonella* isolates using the bacterial genomic DNA extraction kit (Takara, Dalian, China) and used as the template for the detection of integrons by PCR with primers. Three pairs of primers, shown in Table 1, were designed according to the structure of class I integron.

Amplification was performed using the following temperature profile: an initial denaturation step at 94°C for 5 min, 35 cycles each at 94°C for 40s, primer annealing at different temperature for 40s shown in Table 1 and an extension step at 72°C for 1 min. The final extension time was 10 min at 72°C. The amplified DNA products were analyzed by conventional 0.8% agarose gel electrophoresis in 1*TAE (Tris-acetate-EDTA) buffer at 120 V. Purified integron DNA samples were sequenced using primers above-mentioned in Shanghai Sangon co.ltd and blast using the BLAST program available at the NCBI BLAST homepage (http://blast.ncbi.nlm.nih.gov/Blast.cgi).

Table 1. Primers designed for this work

Region or gene	name	Sequence (5' to 3')	Temp (°C)
integrase Ⅱ	Int-F	TGCGTGTAAATCATCATCGTCGTAGAG	56℃
	Int-R	ACAGCTTACGAACCGAACAGGC	56℃
variable segment	Var-F	CGATGTTTGATGTTATGGAGCAG	53℃
	Var-F	ACTTGACCTGATAGTTTGGCTGTG	53℃
5'-3' conserved segment	3'-F	CGCAATAGTTGGCGAAGTAATC	56℃
	3'-R	GAAGAACCGCACAATCTCGTC	56℃

Drug sensitive test

Antibiotic susceptibility testing of *Salmonella* isolates was carried out by the K-B method employing a replicator. Antimicrobial breakpoints were selected according to the National Committee for Clinical Laboratory Standards (NCCLS) [9]. Quality controls strains were *Escherichia coli* ATCC 25922, *Staphylococcus aureus* ATCC 29923 and *Pseudomonas aeruginosa* ATCC 27853. All plates were incubated for 18h at 37°C.

The antibiotics selected and breakpoints for resistance were as follows: ampicillin, amoxicillin, ceftriaxone, cefoperazone, cephalothin, cefazolin, cefepime, ceftazidime, ciprofloxacin, chloramphenicol, ciprofloxacin, gentamicin, tetracycline, oxacillin, ofloxacin, erythromycin, kanamycin, sulfisoxazole/trimethoprim, levofloxacin, cefuroxime sodium, chloramphenicol, piperacillin. These antibiotics slips were purchased from Beijin temple of heaven biotechnology technical development company.

3 Result

Drug sensitive test

The drug resistance patterns of 59 strains *Salmonella* from chicken are shown in Table 2. High resistance rates in 59 strains of *Salmonella* were observed for oxacillin 74.6% (44/59), tetracycline 64.4% (38/59) and erythromycin 52.5% (31/59) respectively. The resistance rates to penicillins (oxacillin, ampicillin, piperacillin, amoxicillin, penicillin G) ranged from 0.0%~74.6% in those isolates. Except for penicillins and tetracyclines, high resistance rates (37.3%~52.5%) were observed for the other macrolides and aminoglycosides. 59 strains *Salmonella* from chicken have the high susceptibility to cephalosporins (resistance rate 0.0%) and quinolones (0.0%).

Some isolates in the 59 strains from chicken were resistant to 8 species antibiotics at most. There were only 11 strains resistant to 2 species antibiotics, and the others were multidrug resistance. Most of the isolates had the multidrug resistance pattern and the rate was 81.36% (48/59). Among the total of the multidrug resistance isolates, the rate of resistance to three, four and five drugs was 45.76% (27/59), 23.73% (14/59) and 11.86% (7/59).

Amplification of integrase Ⅱ *and 5'-3' conserved segments*

PCR and DNA sequencing were used for screening and characterization of class I integrons. A fragment of approximately 856 bp of integrase Ⅱ gene was resulted by PCR amplification using primers Int-F and Int-R (Fig.1). The PCR product were purified and used directly as templates for sequencing. Among these 59 isolates, integrase Ⅱ segment had been detected from 24 strains. On the basis of the results of integrase Ⅱ segment, the 5'-3' conserved segment were amplification using primers 3'-F and 3'-R. All the strains containing integrase Ⅱ segment proved positive. The segment of 774bp was detected which corresponds to the expected size of the 5'-3' conserved gene (Fig.2).

Table 2. 59 strains *Salmonella* isolates resistance rate

Typing	Antibacterials	Drug resistant strain	Resistance rate (%)
penicillins	oxacillin	44/59	74.6
	ampicillin	15	25.4
	piperacillin	0	0
	amoxicillin	0	0
	penicillin G	28/59	47.5
cephalosporins	cefoperazone	0	0
	cephalothin	0	0
	cefazolin	0	0
	cefepime	0	0
	ceftazidime	0	0
	cefuroxime sodium	0	0
	ceftriaxone	0	0
Aminoglycosides	kanamycin	0	0
	gentamicin	22/59	37.3
Tetracyclines	tetracycline	38/59	64.4
Amphenicols	chloramphenicol	7/59	11.9
Macrolides	erythromycin	31/59	52.5
Sulfonamides	Sulfisoxazole /trimethoprim	11/59	18.6
Quinolones	ofloxacin	0	0
	levofloxacin	0	0
	ciprofloxacin	0	0

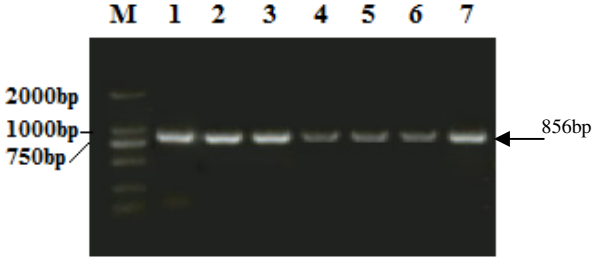

Fig. 1. PCR detection of integrase Ⅱ gene from *Salmonella* isolates M. DNA Marker DL2000; 1~7. Experiment strain

Amplification of variable segment

We detected the variable segment in the integrase-positive strains using PCR amplification. Variable segments were found in 70.8% (17/24) of integrase-positive strains. With the variable region of the resistance genes carrying different type and different number, the amplified fragment size is also different. The segments different from 300bp to 2000bp were observed (Fig.3).

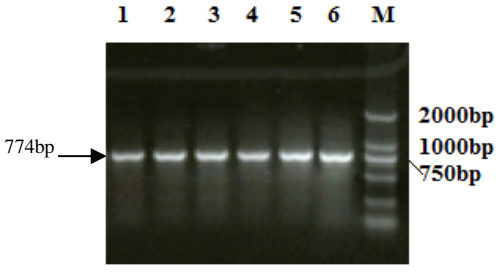

Fig. 2. PCR detection of 5'-3' conserved segments gene from *Salmonella* isolates M. DNA Marker DL2000; 1~6. Experiment strain

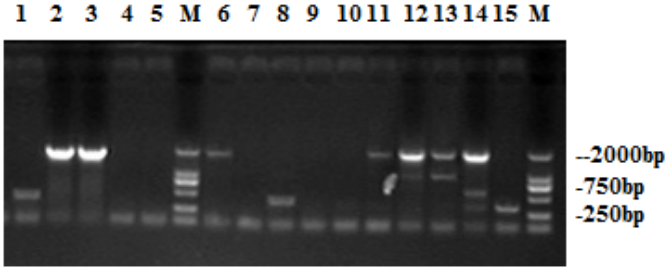

Fig. 3. PCR detection of variable segment in integrase-positive strains. M. DNA Marker DL2000; 1~15. The fragment of gene cassette ranged from 300bp to 2000bp.

Integron carriage and the association of resistance to antimicrobials

As a result, the detection rate of class I integron was 40.68% (24/59), and among these 48 isolates which had been proven multidrug-resistant, the detection rate of class I integron was 50% (24/48). Class I integron PCR positive isolates rate of multidrug-resistance was 100% (24/24). Results show that the class I integron has the relationship with multidrug resistance. However, some isolates without integrons were also had the multidrug resistance pattern, most commonly resistance to tetracycline, oxacillin, ampicillin, gentamicin.

4 Disscussion

Many gene cassettes of integrons encoding antimicrobial resistance genes are found in Gram-negative bacteria. The horizontal transfer of integrons among bacteria plays an important role in the dissemination of antimicrobial resistance gene, resulting in the development of multidrug resistance [10]. So far, 6 types of integrons are defined based on thire homology to the integrase proteins [11]. Among those integrons, class I integrons are commonly observed in bacteria. Class I integrons are most commonly found in clinical isolates of Gram-negative bacteria, and more than 100 gene cassettes that confer resistance are known.

Among the total of 59 *Salmonella* strains from chicken in our study, the rate of class I integron PCR positive isolates was 40.68% (24/59), consistent with the reported (59~70%). The results suggest that the presence of class I integron has significant effect on the rate of multidrug resistant isolates of *Salmonella*. In our study, Class I integron positive isolates rate of multidrug-resistance was 100% (24/24), while the negative strains 68.57 % (24/35). Multidrug-resistance rate of positive strains was significantly higher than the negative multidrug resistant strains. Results show that the class I integron has the obvious relationship with multidrug resistance.

In this experiment, variable segments were found in 70.8% (17/24) of integrase-positive strains. But the amplification of variable region from the other 7 strains which containing integrase Ⅱ and 5'-3' conserved segments was negative. Possible reason is carrying empty gene cassette with the strains. Once the appropriate conditions or antibiotic selection pressure appeared, the empty gene cassette can be integrated, showing drug resistance. Amplification results from the variable region above, the fragment of gene cassette ranged from 300bp to 2000bp. Previously reported in the literature to design conserved primers to amplify the variable region, as the method of detection integron positive strains [12,13], amplification results from this study explained this method is not conducive to the detection of non typical class I integron.

The aggravating resistance of bacteria against antibiotics and increasing cases of MDR pose a fatal threat to the health of humans and animals. Theory of integron system offers a new direction for researching the mechanism of bacterial resistance [14]. At present, every class of antibiotic resistance gene cassettes has been found and all the resistance gene cassettes have been associated with antibiotics. Integration of integrons, resistance genes can be exchanged and with the transformation, transduction and conjugation of plasmids, drug resistance can spread widely among creatures. Since bacterial resistance is a very complex process with many mechanisms, integron's effect on MDR is only one of them, the structure and function of integron-gene cassette system should be conducted on for further study. We need to use our current drugs better and use the best and most affordable drugs available in order to prevent further resistance.

References

1. Hall, A.J., Saito, E.K.: Avian wildlife mortality events due to salmonellosis in the united states,1985–2004. Journal of Wildlife Diseases 44(3), 585–593 (2008)
2. Maguire, A.J., Brown, D.F.J., Gray, J.J., Desselberger, U.: Rapid screening technique for class I integrons in Enterobacteriaceae and nonfermenting gram-negative bacteria and its use in molecular epidemiology. Antimicrob. Agents Chemother. 45, 1022–1029 (2001)
3. Vo, A.T.T., van Duijkeren, E., Fluit, A.C., Wannet, W.J.B., Verbruggen, A.J., Maas, H.M.E., Gaastra, W.: Antibiotic resistance, integrons and Salmonella genomic island 1 among non-typhoidal Salmonella serovars in The Netherlands. Int. J. Antimicrob. 28, 172–179 (2006)
4. Guerra, B., Soto, S., Cal, S., Mendoza, M.C.: Antimicrobial resistance and spread of class I integrons among Salmonella serotypes. Antimicrob. Agents Chemother. 44, 2166–2169 (2000)

5. Nogrady, N., Gado, I., Toth, A., Paszti, J.: Antibiotic resistance and class I integron patterns of non-typhoidal human Salmonella serotypes isolated in Hungary in 2002 and 2003. Int. J. Antimicrob. 26, 126–132 (2005)
6. Gebreyes, W.A., Thakur, S., Davies, P.R., Funk, J.A., Altier, C.: Trends in antimicrobial resistance, phage types and integrons among Salmonella serotypes from pigs, 1997–2000. J. Antimicrob. Chemother. 53, 997–1003 (2004)
7. Rao, S., Maddox, C.W., Hoien-Dalen, P.: Diagnostic Accuracy of Class I Integron PCR Method in Detection of Antibiotic Resistance in Salmonella Isolates from Swine Production Systems. Journal of Clinical Microbiology 46(3), 916–920 (2008)
8. Chiu, C.H., Ou, J.T.: Rapid identification of Salmonella serovars in feces by specific detection of virulence genes invA and spvC by an enrichment broth culture-multiplex PCR combination assay. J. Clin. Microbiol. 34, 2619–2622 (1996)
9. Wayne, P.A.: NCCLS. Performance standards for antimicrobial susceptibility testing. Eleventh International Supplement. Veterinary Antimicrobial Susceptibility Testing Document M31-A2, 21(1) (2001)
10. Yang, C.-M., Lin, M.-F., Lin, C.-H.: Characterization of antimicrobial resistance patterns and integrons in human fecal Escherichia coli in Taiwan. Jpn. J. Infect. Dis. 62, 177–181 (2009)
11. Hall, R.M., Collis, C.M.: Mobile gene cassettes and integrons: capture and spread of genes by site-specific recombination. Mol. Microbiol. 15, 593–600 (1995)
12. Rao, S., Maddox, C.W., Hoien-Dalen, P., Lanka, S., Weigel, R.M.: Diagnostic Accuracy of Class I Integron PCR Method in Detection of Antibiotic Resistance in Salmonella Isolates from Swine Production Systems. Journal of Clinical Microbiology 3, 916–920 (2008)
13. Daly, M., Fanning, S.: Characterization and chromosomal mapping of antimicrobial resistance genes in Salmonella enterica serotype Typhimurium. Appl. Environ. Microbiol. 66, 4842–4848 (2000)
14. Guerra, B., Soto, S., Cal, S., Mendoza, M.C.: Antimicrobial resistance and spread of class I integrons among *Salmonella* serotypes. Antimicrob. Agents Chemother. 44, 2166–2169 (2000)
15. Guerra, B., Soto, S.M., Arguelles, J.M., Carmen Mendoza, M.: Multidrug Resistance Is Mediated by Large Plasmids Carrying a Class I Integron in the Emergent Salmonella enterica Serotype [4,5,12:i:2]. Antimicrobial Agents and Chemotherapy 45(4), 1305–1308 (2001)

Ecological Genetics of Himalayan Snowcock (*Tetaogallus himalayensis*)*

Luzhang Ruan**, Huaxing Luo, Naifa Liu**, Lixun Zhang, and Longying Wen

School of Life Science, Nanchang University, Nanchang, 330031, China
School of Life Science, Lanzhou University, Lanzhou, 730000, China
ruanluzhang@sina.com, naifaliu@sohu.com

Abstract. The part of mtDNA cytb gene sequences were analyzed in 11 Himalayan snowcock local populations sampled across their distributions to detect the correlations between genetic diversities and environmental factors. The genetic variables including percentages of variable nucleotide sites/length of sequence, mean pairwise differences and nucleotide diversity significantly correlated only to annual average sunshine duration and variation coefficients of annual average sunshine duration. The longer the sunshine duration, the less variation of annual sunshine duration and the lower genetic diversities observed. The shorter sunshine duration and higher annual sunshine duration variation could provide a broader and better habitation to Himalayan snowcock, which lead to the higher genetic diversities. In summary, only sunshine duration was the determinant climatic factor in all populations.

Keywords: *Tetraogallus himalayensis*, environmental factor, cytochrome b gene, haplotype, genetic variable.

1 Introduction

The interplay between a genetically variable population and its ever-changing environment is the focus of attention in ecological genetics (Merrell, 1981). Climate differs in importance to different types of organism and/or different region (Huang *et al*., 2005). However, the effects of environment on population genetic diversity usually vary among different birds (Huang *et al*., 2007; Randi 1994).

Himalayan snowcock mainly inhabits in fluvial rocky hills, alpine meadow, hilly pasture and barren shrubby grassland (Cheng 1978). During warm periods the ranges of these birds shorten and restrict only in high mountains, and complete population isolation appeared again (Potapov 1992). This species is relatively sedentary, has restrictive low-temperature and high-altitude habitat requirements (Cheng 1978), and hence may act as an exemplar for faunal elements associated with alpine and cold environment. So, in this paper, the part of mtDNA cytb gene sequences and environmental factors including latitude, longitude, altitude, temperature, rainfall and sunshine duration were analyzed sampled across their distributions, and we mainly aim to: (1) describe the genetic variation within and among local populations and (2) reveal the correlations between genetic variables and the environmental factors.

* This work was supported by NFSC (30170138 and 30530130).
** Corresponding author.

E. Zhu and S. Sambath (Eds.): Information Tech. and Agricultural Eng., AISC 134, pp. 501–505.
springerlink.com © Springer-Verlag Berlin Heidelberg 2012

2 Materials and Methods

2.1 Sample Collection and DNA Extraction

A total of 102 samples of 11 local populations in Himalayan snowcock were collected from the following localities: Yili, Akesu, Urumqi, Qitai, Kashi and Hetian in Xinjiang; Akesai, Subei, Anxi and Zhangye in Gansu; and only Delingha in Qinghai. DNA was extracted from tissue with the ethanol sedimentation procedure as described by Randi and Lucchini (1998).

2.2 PCR Amplification and Sequence Analysis

Two oligonucleotide primers, A1(5'-ggc tcc tac ctg tat aaa gag -3') and A2(5'-agg atg agt act gag gct gcc-3'), were used to PCR amplify and sequenced 559bp mitochondrial DNA cytochrome b genes (cytb) segment. The sequences of Himalayan snowcock haplotypes from H1 to H26 had been deposited in GenBank with accession numbers from EU581870 to EU581895, respectively.

Consensus sequences for all individuals were aligned using the CLUSTAL X program and checked by visual inspection. Pairwise genetic distance was computed using MEGA3.1 with Kimura-2-parameter. The program Arlequin 2.0 (Schneider *et al*. 2002) and DnaSP4.0 (Rozas *et al*., 2003) were used to estimate the number of individuals and haplotypes, the private haplotypes (Pri), the percent of positions that vary, mean number of pairwise differences (k), haplotype diversity (*h*), and nucleotide diversity (π) found in the local populations. The materials were dealt with SPSS13.0.

2.3 Factor Selection

Latitude, longitude, altitude, annual average temperature (AAT), annual average rainfall (AAR), annual average sunshine duration (AAS), variation coefficients of annual average temperature (VCT), rainfall (VCR) and sunshine duration (VCS) were selected as environmental factors (Table 1).

Table 1. Environmental factors at eleven populations of *Tetraogallus himalayensis*

Population	Latitude (°)	Longitude (°)	Altitude (m)	AAT(°C)	VCT	AAR (mm)	VCR	AAS (hr)	VCS
Yili	43.92	81.33	2250	-0.670	-1.504	276.12	0.285	2845.88	0.054
Akesu	41.10	80.20	3250	-2.602	-0.279	70.60	0.466	2846.39	0.050
Urumqi	43.77	87.68	2840	-4.640	-0.254	267.21	0.274	2656.10	0.078
Qitai	44.02	89.52	2950	-7.946	-0.113	187.47	0.268	2976.67	0.052
Kashi	39.40	75.90	3000	1.631	0.503	65.14	0.496	2778.51	0.068
Hetian	37.10	79.90	4000	-3.194	-0.237	38.09	0.589	2636.40	0.081
Akesai	39.60	93.50	3750	-	-	85.80	0.185	3168.50	0.047
Subei	39.50	94.80	3350	-	-	175.35	0.410	3081.20	0.049
Anxi	40.52	95.77	3030	-2.238	-0.264	48.63	0.408	3189.55	0.044
Zhangye	39.01	100.50	2930	-1.436	-0.489	129.56	0.266	3087.98	0.040
Delingha	37.50	98.00	4500	-5.336	-0.169	166.62	0.349	3087.27	0.034

3 Results

3.1 Haplotype Description and Variability

A total of 559 nucleotides of the mtDNA cytochrome b genes (cytb) were sequenced of all the samples. The cytb sequence alignment showed 26 different haplotypes (25.49% of the all samples), defined by 28 polymorphic sites. Within populations, the number of observed haplotypes ranged from two in Anxi or Delingha to six in Zhangye (Table 2). The percentages of private haplotypes were calculated by dividing the number of unique haplotypes (Pri) by the number of samples (S, Table 2) or of the number of haplotypes (R). Within each population, S was the lowest in Yili or Delingha (0.00%), but the highest only in Zhangye (40.00%), and R was the lowest in Yili or Delingha (0.00%), but the highest in Akesu or Zhangye (66.67%). For the percentage of variable nucleotide sites (V, Table 2), the minimum was 0.18% in Delingha and the maximum was 1.25% in Kashi or Hetian. The most common haplotype was H12 (GenBank accession no. EU581881) with 34 individuals from all sampling sites except three Xinjiang populations including Akesu, Qitai and Hetian. Statistically significant differences in haplotype frequencies were observed among all populations (χ^2=44.77, p<0.001).

Table 2. Sample size(n), Haplotype no.(N), number of haplotype and private haplotypes (Pri) found within each population, percentages of variable nucleotide sites/length of sequence (V), percentages of number of unique haplotypes/ number of individuals (S) and of number of the private haplotypes/ number of haplotype (R), mean pairwise differences (K) and nucleotide diversity (π) and haplotype diversity (h) of the eleven populations in T*etraogallus himalayensis*

	n	N	Pri	V	S	R	K	$\pi\times10^3$	h
Yili	5	3	0	0.89	0.00	0.00	2.01	3.6	0.70
Akesu	6	3	2	0.36	33.33	66.67	0.67	1.2	0.60
Urumqi	7	4	2	1.07	28.57	50.00	2.69	4.8	0.71
Qitai	11	3	1	0.54	9.09	33.33	1.20	2.1	0.71
Kashi	15	5	1	1.25	6.67	20.00	1.57	2.8	0.65
Hetian	11	5	3	1.25	27.27	60.00	2.53	4.5	0.79
Akesai	9	5	3	0.72	33.33	60.00	1.06	1.9	0.72
Subei	15	4	2	0.54	13.33	50.00	1.15	2.0	0.67
Anxi	6	2	1	0.36	16.67	50.00	0.67	1.2	0.33
Zhangye	10	6	4	0.89	40.00	66.67	1.16	2.1	0.78
Delingha	7	2	0	0.18	0.00	0.00	0.48	0.9	0.48

3.2 Relationship between Genetic Variables and Environmental Factors

The genetic variables including V, K, π and h showed negative correlation with increasing longitude, altitude and AAS; contrarily, indicated positive correlation with latitude, AAT, AAR and VCS (Table 3). Significant relationships were observed between three genetic variables (including V, K and π) and AAS or VCS, all of which but the relationship between V and AAS (r=-0.689, p=0.019) were significant at the 0.01 level. The other relationships between genetic variables and environmental factors were not significant at the 0.05 level.

Table 3. The relationship coefficients between genetic variables and environmental factors in T*etraogallus himalayensis*

	Latitude	Longitude	Altitude	AAT	VCT	AAR	VCR	AAS	VCS
V	0.003	-0.544	-0.082	0.458	0.069	0.004	0.250	-0.689*	0.804**
K	0.261	-0.506	-0.260	0.097	-0.181	0.342	0.074	-0.811**	0.888 **
π	0.257	-0.503	-0.258	0.103	-0.186	0.343	0.071	-0.811**	0.885**
h	0.089	-0.266	-0.135	0.011	-0.157	0.233	-0.082	-0.459	0.461

Note: *: $0.01<p<0.05$; **: $p<0.01$

4 Discussion

Climate differs in importance to different types of organism and / or different region (Huang *et al*., 2005). We found that the genetic variables including V, K and π significantly correlated only to AAS and VCS (all $p<0.05$; Table 3), while the genetic variables including V, K, π and h of Himalayan snowcock did not apparently correlate to altitude, AAT, VCT, AAR or VCR (all $p>0.05$; Table 3). When sampling in various time or locus, the altitude sometimes falls more than 2000m in a local population, which apparently exceeds the most differences among various populations. So altitude could not be thought as a valid environmental factor in Himalayan snowcock. Himalayan snowcock is relatively sedentary, has restrictive low-temperature and high-altitude habitat requirements (Cheng 1978). So snowcock could get rid of the adverse influence of the local climate factors including temperature and rainfall by adjusting their habitation altitudes in various periods. But annual sunshine duration showed no difference in a local sampling site in spite of the different altitudes for Himalayan snowcock.

Negative relationships were observed between longitude and genetic variables including V ($r=-0.544$, $p=0.084$), K ($r=-0.506$, $p=0.113$), π ($r=-0.503$, $p=0.114$) and h ($r=-0.266$, $p=0.430$), which were relation to Himalayan snowcock's origin in Kalakunlunshan and western Kunlunshan. So the eastern populations owned lower genetic diversities in Himalayan snowcock (TABLE II). In the other hand, the genetic variables including V, k, π and h decreased with increasing of AAS (all $r<0$; Table 3) in various populations, but they increased with increasing of VCS (all $r>0$; Table 3). The sunshine duration and intensity can influence the development of sex gland in snowcock (Wu *et al*. 2008). The shorter sunshine duration and higher annual sunshine duration variation could provide a broader and better habitation to Himalayan snowcock, which lead to the higher genetic diversities.

Environment is the directing force that influences the populations in the nature (Vanhala *et al*., 2004), and natural selection will tend to adapt a population to local environmental conditions (Huang *et al*., 2007). The snowcock can drop to shrubby zones and spruce forests in winter, but climb up to the higher in the next spring (Cheng, 1978). It can survive only around the snow line or in low-temperature surroundings (Ruan *et al*., 2005), so contrary to the most other pheasants such as *Alectoris chukar* (Huang *et al*., 2005) and *Alectoris magna* (Huang *et al*., 2007), the temperature and rainfall could not decide the genetic diversities, but only sunshine duration is the determinant climatic factor in local populations of Himalayan snowcock.

References

1. Cheng, T.H.: Fauna Sinica: Aves, vol. 4, pp. 51–58. Science Press, Beijing (1978)
2. Huang, Z.H., Liu, N.F., Zhou, T.L., Ju, B.: Effects of environmental factors on population genetic structure in chukar partridge (Alectoris chukar). Journal of Arid Environments 62, 427–434 (2005)
3. Huang, Z.H., Liu, N.F., Luo, S.X., Long, J., Xiao, Y.A.: Ecological genetics of Rusty-necklaced partridge (Alectoris magna): Environmental factors and population genetic variability correlations. Korean Journal of Genetics 29(2), 115–120 (2007)
4. Merrell, D.J.: Ecological Genetics. Longman, London (1981)
5. Potapov, R.: Adaptation to mountain conditions and evolution in snowcocks (Tetraogallus sp.). Gibier Faune sauvage 9, 647–660 (1992)
6. Randi, E., Alkon, P.U.: Genetic structure of chukar (Aletoris chukar), population in Israel. The Auk 111, 216–226 (1994)
7. Randi, E., Lucchini, V.: Organization and evolution of the mitochondrial DNA control region in the avian genus Alectoris. Journal of Molecular Evolution 47, 449–462 (1998)
8. Rozas, J., Sánchez-DelBarrio, J.C., Messeguer, X., Rozas, R.: DnaSP DNA polymorphism analyses by the coalescent and other methods. Bioinformatics 19, 2496–2497 (2003)
9. Ruan, L.Z., Zhang, L.X., Wen, L.Y., Sun, Q.W., Liu, N.F.: Phylogeny and Molecular Evolution of Tetraogallus in China. Biochemical Genetics 43(9/10), 507–518 (2005)
10. Vanhala van, T.K., Rijn, C.P.E., Buntjer, J., Stam, P., Nevo, E., Poorter, H., van Eeuwijk, F.A.: Environmental, phenotypic and genetic variation of wild barley (Hordeum spontaneum) from Israel. Euphytica 137, 297–309 (2004)
11. Wu, R.L.H.Z., Ba, H.T., Mi, L., Hai, R.L.: Research on reproduction capability and breeding success improvement of Himalayan snowcock. China Poultry 30, 43–44 (2008) (in Chinese)

Isolation, Identification and Significance of Cryptococcus Neoformans and Candida Albicans from Faecal Specimen of Pigeon*

Zhichun Liu, Lianlan Ma**, Youtian Zhong, Xiaoli Wang, and Shuixiang Xie

The Department of Pathogenic Biology
Gannan Medical University
Gangzhuo Jiangxi, 341000, China
malianlan@163.com

Abstract. To understand the distribution of the deep fungal from faecal specimen of pigeon and further explore the importance of bird species as source of infection of the deep mycosis,We collected 58 faecal specimen of pigeon from different places (16 provinces and cities). These specimen were inoculated in medium to isolate Cryptococcus neoformans and Candida albicans which were identified by gram staining, budding development, chlamydospore formation, sugar fermented test, sugar assimilated test, urea testes and capsule staining. Then three purified strains of Cryptococcus neoformans and Candida albicans were dispensinged the suspension which were respectively injected into mice and rabbits. Results showed Cryptococcus neoformans alone was isolated from 29.3%（17/58） of the samples, Candida albicans alone from 20.7%（12/58）and both fungi were found together in 10.3% (6/58). These strains can cause rabbits and mice infection,disease and death and which can be re-isolated from infected animals. These results indicate there are Cryptococcus neoformans and Candida albicans in faecal specimen of pigeon and these strains have certain pathogenicity to animal.

Keywords: Cryptococcus neoformans, Candida albicans, faecal specimen, pigeon, pathogenicity.

1 Introduction

In the pigeon feces,there are many kinds of pathogens which can cause disease in the pigeon, as well as be associated with crytococcosis, hypersensitivity pneumonitis, psittacosis and so on in the human[1-3].Pigeon feces is the main sources of *Cryptococcus neoformans* while few reports about Candida albicans existing in pigeon feces[1]. *Candida albicans* and *Cryptococcus neoformans* are the common deep infectious fungi. The former is the first among all tested pathogenic fungi[4], the latter mainly spreads by respiratory and is apt to infect Central nervous system which

*This work is supported by the Department of Education of Jiangxi Province(NO:GJJ10573).
** Corresponding author.

E. Zhu and S. Sambath (Eds.): Information Tech. and Agricultural Eng., AISC 134, pp. 507–512.
springerlink.com © Springer-Verlag Berlin Heidelberg 2012

lead to the high mortality rate[5]. Therefore, it is very important to prevent disease by controlling source of infection and cutting transmitting. In order to understand the distribution of the deep fungal from faecal specimen of pigeon and further explore the importance of bird species as source of infection of the deep mycosis, we isolated and identified *Cryptococcus neoformans* and *Candida albicans* from faecal specimen of pigeon and made pathogenicity test. Now report as follows.

2 Materials and Methods

Specimen

The faecal specimen of pigeon were collected in the dovecote of park or resident of different provinces and cities such as Jiangxi, Hunan,Fujian, Guangdong, Shangdong, Yunnan, Jilin, Sichuan, Zhengjiang and so on by the students of clinical medicine of Gannan Medical University. They were taught to collect 3-4 pieces of fresh pigeon feces which weigh about 4 grams in each place with moist sterile cotton swab adopting aseptic technique and put them into sterile penicillin bottles on the day before they returned to school. 58 specimen were collected.

Medium and Experimental Animals

Sabouraud medium contain 1% peptone, 4% glucose, 1.8% agar. Cornmaeal tween sagar was prepared according to the method described by reference[6].The phenol oxidase urease agar and the caffeic acid cornmaeal agar was prepared according to the method described by reference[7,8]. Healthy adult New Zealand rabbits, weighing 1.8 kg～2.0kg each, were supplied by Ganzhou Institute of Animal Science (Animal license number: SCXK GAN2008-0002). BALB/c mice were provided by animal experimental center of Zhongshan University (Animal license number: SCXK(Yue) 2004-0011Yuejianzhengzi2005A053))

Isolation and Identification

Identificated procedure of yeast worked by reference[9] ,while the standard strains of CCCM D2a (*Cryptococcus neoformans*) and ATCC 32354 (*Candida albicans)* as controls.Each specimen which weigh 2.0g was mixed with 10ml sterile saline and miscebened by the full shock, quiescence after 15min, the supernatant which volume was 1ml was inoculated in liquid sabouraud medium. Cultured 48h by shaken at 37℃, the 100μl liquid was inoculated in SDA plate, then a single colony was inoculated in SDA slant and the culture was identified by gram staining, budding development, chlamydospore formation, sugar fermented test, sugar assimilated test, urease and oxidase tests, caffeic acid test, Hiss capsule staining, lactic acid phenol Medan staining.

Pathogenicity Test

After respectively cultured 48h and 96h, three purified strains of *Candida albicans* and *Cryptococcus neoformans* were dispensinged the bacterial suspension which concentration was 108CFU/ml. Each strain of Candida albicans was injected into 3

healthy New Zealand rabbits by me as of ear-intravenous inject on and the injected volume of each rabbit was 1ml.Each strain of *Cryptococcus neoformans* was injected into 12 BALB/c mice by me as of intracellular inoculation and the injected volume of each mice was 0.2ml. we observed daily and dissected animals when they were ill, then observed infectious tissue and took suspicious tissue of rabbit's kidney and mouse's brain) to isolate and identify *Candida albicans* and *Cryptococcus neoformans.*

3 Results

Isolation and Identification

After preliminary cultured sabouraud liquid medium, 53 specimen grew bacteria, 47 of which were suspected yeast on Sabouraud medium plate, 3 of which were not yeast by the smear and staining, 12 of which were *Candida albicans* based characteristics of morphology, culture and biochemical reaction, the positive rate was 20.7%, 17 of which were *Cryptococcus neoformans* based characteristics of morphology, culture and biochemical reaction, the positive rate was 29.3%.Both fungi were found together in 10.3%. 1 species of fungi was at least isolated in each of 15 provinces and cities.

The characteristics of cultural and biochemical reaction of isolated positive strains saw table1. 12 isolated strains could form pseudohypha and chlamydospore (figure 1 and figure 2),17 isolated strains could be oberved yeast-like budding cells and the capule(figure 3).

Table 1. The characteristics of cultural and biochemical reactions of isolated positive strains

	sugar fermented test			
	glucose	lactose	cane sugar	maltose
Cryptococcus neoformans	—	—	—	—
Candida albicans	⊕	—	—	⊕
	sugar assimilated test			
	glucose	lactose	cane sugar	maltose
Cryptococcus neoformans	+	—		+
Candida albicans	+	—	+	+
	gurease and oxidase test	budding development	chlamydospore formation	pseudo-hypha
Cryptococcus neoformans	+	—	—	—
Candida albicans	—	+	+	+

⊕means producing acid and gas, + means only producing acid or positive, —means Negative.

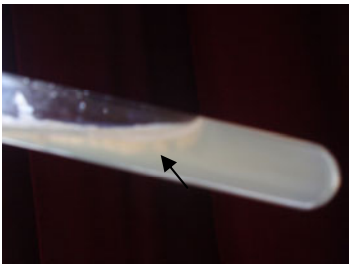

Fig. 1. C.albicans cultured in sabouraud agar (The arrow point pseudohypha)

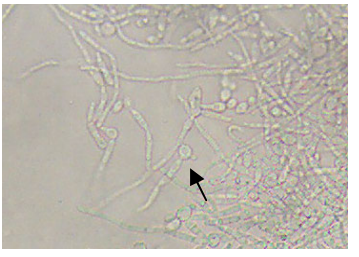

Fig. 2. C.albicans cultured in medium corn agar on glass(×400) (The arrow point chlamydospore)

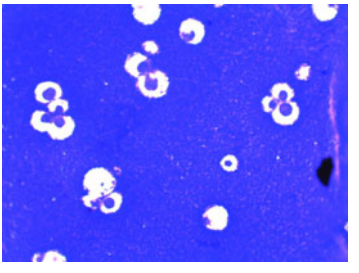

Fig. 3. Hiss capsule staining of Cryptococcus neoformans

Pathogenicity Test

After injected into animals, the isolated strains could lead to animal death, the mortality of mice was 47.2% and rabbit was 33.3%(Table 2).

Table 2. The results of animal test

strain	Cryptococcus neoformans	Candida albicans
animal	mice	rabbit
start time of disease (day)	6~9	3~5
the death time (day)	11~18	4~7
the dead animal	17	3
Mortality (%)	47.2	33.3
the survival animal	19	6
the total number of animal	36	9

4 Discussion

This study is belong to investigation which aim to get the message about the distribution of commom deep fungi. Rsults showed that the pigeon carried *Cryptococcus neoformans* and/or *Candida albicans* and the positive rate was respectively 29.3% and 20.7%, these fungi had a certain pathogenicity. Although the positive rate of isolated *Cryptococcus neoformans* was less than these reports that 52%～76% of pigeon feces and 100% of pigeon feces from pigeonhole[10-11].This may be related to collected place, sample volume, region, climate and isolated methods. The positive rate of *Cryptococcus neoformans* isolated from city pigeon feces of different latitudes had significant differences[8]. Animal experiments have confirmed that isolated *Candida albicans* and *Cryptococcus neoformans* are pathogenic, so the importance of pigeon as the source of infection of deep mycosis can not be ignored.

Because the source of specimen was disperse, the number of sample was few in each place, the positive rate of strain affect.In addition, some region was far away and it need a long time to take the collected specimens back to the lab which effected the survival rate of fungi. The situation of the pathogenic fungi in pigeon feces need to be further explored.17 strains of isolated *Cryptococcus neoformans* didn't make serological identification yet, study reported that it can grow at 37℃ that can be used as characteristics to dentify *Cryptococcus neoformans*[12],so the serotype of the isolated strains need to be further investigated.

References

1. Rosario, I., Acosta, B., Colom, M.F.: Pigeons and other birds as a reservoir for Cryptococcus spp. Rev. Iberoam Micol. 18, S13–S18 (2008)
2. Dickx, V., Beeckman, D.S., Dossche, L., Tavernier, P., Vanrompay, D.: Chlamydophila psittaci in homing and feral pigeons and zoonotic transmission. J. Med. Microbiol. 59(11), 1348–1353 (2010)
3. León, D.E., Retana, V.N., Hernández-Pando, R.: Pigeon hypersensitivity pneumonitis: immunohistochemical demonstration of the causative antigen in the lung. Prim. Care Respir. J. 16(4), 252–256 (2007)
4. Wu, S.X., Guo, N.R., Liao, W.Q., Zhang, Q.Q., Li, C.Y., et al.: Dynamic epidemiological survey of pathogenic Candiada in china during 1986,1996 and 2006. Chin. J. Infect. Chemother. 7(6), 462–465 (2009)
5. Li, S.S., Mody, C.H.: Cryptococcus. Proc. Am. Thorac. Soc. 7(3), 186–196 (2010)
6. Wu, A.W.: Experiment guidance of clinical microbiology and inspection. People's Medical Publishing House, Peking (2008)
7. Li, A.S., Wu, S.X.: The phenoloxidase test and its application to identiy Cryptococcus neoformans with various biological characteristics. Microbiology China 35(5), 97–102 (2001)
8. Li, A.S., Wu, S.X., Guo, N.R., Sheng, Y.N., LV, G.X., et al.: Ecological studies on varieties of Cryptococcus neoformans in China. J. Clin. Dermato. 37(1), 3–6 (2008)
9. Wu, S.X.: Inspection manual of modern medicine fungi. Peking Union Medical College Press, Peking (2005)

10. Wu, S.X.: 21st century medical mycology. Chinese Journal of Dermatology 28(6), 358–360 (1995)
11. Li, L., Wang, J.C., Zhang, Q.Q., Wang, J.J.: Isolation and identification Crytococcus neoformans from pigeon dropping. J. Clin. Deratol. 29(4), 198–200 (2000)
12. Lin, N., Ou, Q.S.: Virulence factors of Cryptococcus neoformans and its research progress. Int. J. LabMed. 29(4), 341–342 (2008)

Indole Alkaloids from South China Sea Marine Sponge *Callyspongia* sp.*

Bin Wang[1], Riming Huang[2], and Yonghong Liu[3]

[1] Shenzhen Shajing Affiliated Hospital of Guangzhou Medical University, Shenzhen 518104, China
[2] South China Botanical Garden, Chinese Academy of Science, Guangzhou 510650, China
[3] Key Laboratory of Marine Bio-resources Sustainable Utilization, South China Sea Institute of Oceanology, Chinese Academy of Science, Guangzhou 510301, China
yonghongliu@scsio.ac.cn

Abstract. Three known indole alkaloids were first isolated from South China Sea marine sponge Callyspongia sp.. Their structures were confirmed by detailed NMR data comparison with those in the literatures.

Keywords: Marine Sponge, Callyspongia sp., Indole Alkaloids.

1 Introduction

The genus *Callyspongia* (order *Haplosclerida*, family *Callyspongiidae*) is widely distributed and contains various bioactive secondary metabolites such as polacetylenes, peptides, terpenoids, alkaloids, fatty acids, polyketides, sterols, peroxides, and butenolides. Some of these compounds possessed antifouling, cytotoxic, anticancer, and antimicrobial properties [1−2].

Indole alkaloids have been isolated from a variety of marine invertebrates, including sponges, coelenterates, tunicates, and bryozoans. Some of these metabolites showed a wide spectrum of pharmacological activities such as antiviral, cytotoxic, anti-inflammatory, and antifungal activities [3].

In our study of bioactive compounds from marine sponge *Callyspongia* sp. colleted off the coast of Hainan, three known indole alkaloids were first isolated from marine sponge *Callyspongia* sp.. Compounds 1−3 were identified as 1,2,3,4-tetrahydro-1-methyl-β-carboline-3-carboxylic acid (1) [4], 1-methyl-1,2,3,4-teranhydro-β-carboline (2) [5], 1,2,3,4-teranhydro-β-carboline (3) [6], respectively, by comparison of their spectroscopic data with those reported in the literature [4-6].

2 Helpful Hints

The aqueous EtOH extract of the marine sponge *Callyspongia* sp. was suspended in water, and partitioned with petroleum ether, EtOAc and n-butanol, successively.

* This work is supported by grants from the National Natural Science Foundation of China (NO. 40706046), Knowledge Innovation Program of Chinese Academy of Sciences (LYQY 200703), and Guangdong Key Laboratory of Marine Materia Medica Foundation.

E. Zhu and S. Sambath (Eds.): Information Tech. and Agricultural Eng., AISC 134, pp. 513–516.
springerlink.com © Springer-Verlag Berlin Heidelberg 2012

The n-butanol fraction was subjected to silica column, Sephadex LH-20, and ODS-HPLC, to yield compounds 1−3 (Fig. 1).

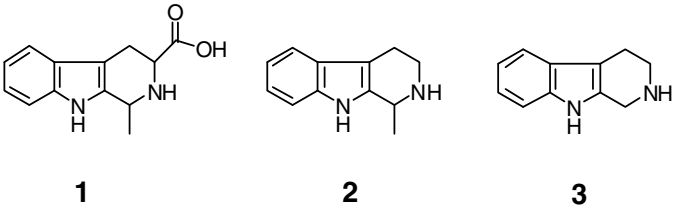

Fig 1. Structures of compounds 1−3

Compound 1 was isolated as yellowish oil, its molecular formula was determined to be $C_{13}H_{14}N_2O_2$ based on the ESI-MS spectrum (m/z 229 $[M-H]^-$, 231 $[M+H]^+$) and NMR data. The indole system was indicated by characteristic ^1H NMR signal patterns. Analysis of the NMR data of 1 indicated that 1 is identical to 1,2,3,4-tetrahydro-1-methyl-β-carboline-3-carboxylic acid.

Compound 2 was obtained as white solid and had the molecular formula $C_{12}H_{14}N_2$ as deduced from the ESI-MS spectrum (m/z 185 $[M-H]^-$, 187 $[M+H]^+$) and NMR data. An indole nucleus was indicated by the characteristic ^1H NMR and ^{13}C NMR data. 2 was identified as 1-methyl-1,2,3,4-teranhydro-β-carboline by comparison of its detail NMR data with those reported in the literature.

Compound 3 was obtained as white solid and had a molecular formula $C_{11}H_{12}N_2$ on the basis of the ESI-MS data (m/z 171 $[M-H]^-$, 173 $[M+H]^+$) and NMR data. An indole nucleus was indicated by the characteristic ^1H NMR and ^{13}C NMR data. 3 was identified as 1,2,3,4-teranhydro-β-carboline by comparison of its detail NMR data with those reported in the literature.

Compounds 1−3 are well-known 1,2,3,4-tetrahydro-β-carboline derivatives in beverages and foods. To our best knowledge, although compound 1 has been isolated from *Amanita muscaria* [7], this is the first report of its occurrence in marine sponges. Compound 1 was reported to possess antitumor [8], and antioxidant [9] activities. Although the natural origin of compound 2 was from plants of the family *Elaeagnaceae* [5], it is reported for the first time from marine resources. Compound 2 was reported to show inhibition on MAO enzymes [10], antimicrobial [11] and antioxidant [12] properties. Compound 3 was reported for the first time from marine resources. Compound 3 was reported to possess cytotoxicity [13], and antioxidant activities [9].

3 Experimental Section

General experimental procedures

NMR spectra were recorded on a Bruker AC 500 NMR spectrometer with TMS as an internal standard. ESI-MS data were measured on a Agilent 1200 LC-MS spectrometer. The silica gel GF_{254} used for TLC were supplied by the Qingdao Marine Chemical Factory, Qingdao, China. Semi-preparative HPLC was performed on a Hitachi L-2400 HPLC system, using a YMC ODS-H_{80} column (250 × 10 mm i.d.,

4 μm) coupled to a Alltech ELSD 800 detector with flow-splitter valve (Parker: NS) set at a split ratio of 20:1 (collector: detector). Spots were detected on TLC under UV light or by heating after spraying with 5% H_2SO_4 in EtOH (v/v).

Animal material

The sponge *Callyspongia* sp. was collected off the coast of Hainan Island, South China Sea, in January, 2007. The specimen was identified by Dr. Kyung Jin Lee. A voucher specimen (NO. 20070101) was deposited in Natural History Museum, Hannam University, Daejon, Korea and Guangdong Key Laboratory of Marine Materia Medica, South China Sea Institute of Oceanology, Chinese Academy of Sciences, China.

Extration and isolation

The wet sponges (10 kg) were extracted with EtOH/H_2O (90:10) for three times. The aqueous EtOH extract of the marine sponge *Callyspongia* sp. was suspended in water, and partitioned with petroleum ether, EtOAc and n-butanol, successively. The n-butanol soluble portion (80g) was chromatographed on ODS column eluted with MeOH/H_2O (0:100, 10:90, 20:80, 40:60, 60:40, 100:0) to give six fractions (I, J, K, L, M, N). The fraction J (MeOH/H_2O, 10:90, 2000 mL, 20 g) was subjected to CC with gradient $CHCl_3$/MeOH (100:0, 90:10, 80:20, 60:40, 40:60, 0:100) to give six fractions (J_1–J_6). Fraction J_2 was further purified by reverse-phase HPLC (ODS, MeOH/H_2O, 5:95) to yield 2 (3.3 mg). The fraction K (MeOH/H_2O, 20:80, 2000 mL, 12 g) was subjected to CC with gradient $CHCl_3$/MeOH (100:0, 95:5, 90:10, 80:20, 40:60, 0:100) to give six fractions (K_1–K_6). Fraction K_2 was further purified by reverse-phase HPLC (ODS, MeOH/H_2O, 5:95) to yield 1 (3.1 mg) and 3 (5.2mg).

1,2,3,4-tetrahydro-1-methyl-β-carboline-3-carboxylic acid (1): Yellowish oil. ^{1}H-NMR (500 MHz, MeOD) δ_H: 7.49 (1H, d, J = 7.9 Hz, H-8), 7.47 (1H, d, J = 8.2 Hz, H-5), 7.14 (1H, t, J = 7.9 Hz, H-7), 7.05 (1H, t, J = 7.8 Hz, H-6), 4.64 (1H, m, H-1), 3.92 (1H, dd, J = 12.0, 4.9 Hz, H-3), 3.42 (1H, dd, J = 14.7, 3.8 Hz, H-4b), 2.98 (1H, m, H-4c), 1.74 (1H, d, J = 6.8 Hz, H-1′); ^{13}C NMR (125 MHz, MeOD) δ_C: 174.9 (C-3′), 138.6 (C-9a), 132.4 (C-8a), 127.7 (C-5a), 123.1 (C-8), 120.5 (C-5), 119.1(C-7), 112.3 (C-6), 108.0 (C-4a), 59.9 (C-3), 51.1 (C-1), 24.8 (C-4), 17.7 (C-1′). ESI-MS: m/z: 229 $[M-H]^-$, 231 $[M+H]^+$.

1-methyl-1,2,3,4-teranhydro-β-carboline (2): White solid. ^{1}H-NMR (500 MHz, DMSO-d6) δ_H: 11.05 (1H, s, 9-NH), 7.42 (1H, d, J = 7.5, H-8), 7.32 (1H, d, J = 8.0 Hz, H-5), 7.07 (1H, t, J = 8.0 Hz, H-7), 6.98 (1H, t, J = 7.5 Hz, H-6), 4.45 (1H, m, H-1), 3.58 (2H, m, H-3), 3.13 (1H, dd, J = 135, 4.0 Hz, H-4b), 2.74 (1H, t, J = 13.5 Hz, H-4c), 1.59 (3H, d, J = 6.5 Hz, H-1′); ^{13}C NMR (125 MHz, DMSO-d6) δ_C: 136.2 (C-9a), 126.2 (C-8a), 121.1 (C-5a), 118.6 (C-8), 118.1 (C-5), 117.8 (C-7), 111.1 (C-6), 106.7 (C-4a), 57.7 (C-3), 48.9 (C-1), 23.5 (C-4), 17.4 (C-1′). ESI-MS: m/z: 185 $[M-H]^-$, 187 $[M+H]^+$.

1,2,3,4-teranhydro-β-carboline (3): White solid. 1H-NMR (500 MHz, DMSO-d6) δ_H: 11.87 (1H, s, 9-NH), 7.43 (1H, d, J = 7.5, H-8), 7.31 (1H, d, J = 8.0 Hz, H-5), 7.06 (1H, t, J = 7.5 Hz, H-7), 6.96 (1H, t, J = 7.5 Hz, H-6), 4.16 (2H, s, H-1), 3.16 (2H, m, H-3), 3.08 (1H, dd, J = 135, 4.0 Hz, H-4b), 2.63 (1H, t, J = 13.5 Hz, H-4c); ^{13}C NMR (125 MHz, DMSO-d6) δ_C: 136.7 (C-9a), 127.0 (C-8a), 121.5 (C-5a), 119.1 (C-8), 118.1 (C-5), 116.2 (C-7), 111.1 (C-6), 107.5 (C-4a), 54.5 (C-3), 45.5 (C-1), 24.8 (C-4). ESI-MS: m/z: 171 $[M-H]^-$, 173 $[M+H]^+$.

Acknowledgment. The authors gratefully acknowledge the support of National Natural Science Foundation of China (NO. 40706046), Knowledge Innovation Program of Chinese Academy of Sciences (LYQY 200703), and Guangdong Key Laboratory of Marine Materia Medica Foundation. Our thanks are due to colleagues of National Expriment Station of Tropical Marine Biology for their assistance in collecting of the marine sponges.

References

1. Liu, Y.H., Yang, B., Dong, J.D.: Secondary metabolites and their bioactivities of marine sponge Callyspongia. Journal of Tropical Oceanography 27(6), 73–80 (2008)
2. Yang, B., Dong, J., Zhou, X.F., Lee, K.J., Wang, L., Zhang, S., Liu, Y.: Proline-containing dipeptides from the marine sponge a Callyspongia species. Helvetica Chimica Acta 92, 1112–1117 (2009)
3. Liu, Y., Jung, J.H., Zhang, S.: Indole alkaloids from a sponge Sarcotragus species. Biochemical Systematics and Ecology 34, 453–456 (2006)
4. Kuo, F.M., Tseng, M.C., Yen, Y.H., Chu, Y.H.: Microwave accelerated pictete-spengler reactions of tryptophan with ketones directed toward the preparation of 1,1-disubstituted indole alkaloids. Tetrahedron 60, 12075–12084 (2004)
5. Massagetov, P.S.: Alkaloids of plants of the family Elaeagnaceae. Zhurnal Obshcei Khimii 16, 139–140 (1946)
6. Espada, A., Jimenez, C., Debitus, C., Riguera, R., Villagorgin, A.B.: New type of indole alkaloids with acetylcholine antagonist activity from the gorgonian Villagorgia rubra. Tetrahedron Letters 34(48), 7773–7776 (1993)
7. Matsumoto, T., Trueb, W., Gwinner, R., Eugster, C.H.: Components of Amanita muscaria. XXXI. Isolation of (-)-(R)-4-hydroxy-2-pyrrolidinone and other compounds from Amanita muscaria. Helvetica Chimica Acta 52(3), 716–720 (1969)
8. Ren, H., Gu, Q., Cui, C., Zhu, W.: The cytotoxic constituents from marine-derived Streptomyces 3320#. Journal of Ocean University of China 5(1), 75–81 (2006)
9. Herraiz, T., Galisteo, J.: Tetrahydro-β-carboline alkaloids that occur in foods and biological systems act as radical scavengers and antioxidants in the ABTS assay. Free Radical Research 36(8), 923–928 (2002)
10. Herraiz, T., Chaparro, C.: Analysis of monoamine oxidase enzymatic activity by reversed-phase high performance liquid chromatography and inhibition by β-carboline alkaloids occurring in foods and plants. Journal of Chromatography A 1120(1-2), 237–243 (2006)
11. Idowu, T.O., Onawunmi, G.O., Ogundaini, A.O., Adesanya, S.A.: Antimicrobial constituents of Chrysophyllum albidum seed cotyledons. Nigerian Journal of Natural Products and Medicine 7, 33–36 (2003)
12. Herraiz, T., Galisteo, J.: Tetrahydro-β-carboline alkaloids occur in fruits and fruit juices. Activity as antioxidants and radical scavengers 51(24), 7156–7161 (2003)
13. Storch, A., Hwang, Y.I., Bringmann, G., Feineis, D., Ott, S., Brueckner, R., Schwarz, J.: Cytotoxicity of chloral-derived-β-carbolines is not specific towards neuronal nor dopaminergic cells. Journal of Neural Transmission 113(12), 1895–1901 (2006)

Development of IgY-Based Sandwich Enzyme-Linked Immunosorbent Assay for the Detection of *Vibrio parahaemolyticus*

Qingping Zhong, Yuqing Dong, Li Wang, and Binbin He

College of Food Science, South China Agricultural University, Guangzhou 510642, China
zhongqp@scau.edu.cn

Abstract. Vibrio parahaemolyticus is one of the most important food-borne pathogen which can cause serious infection in human. One kind of sandwich ELISA method was developed in this paper to detect V. parahaemolyticus rapidly and economically, using anti- V. parahaemolyticus IgY as capture antibody and rabbit anti- V. parahaemolyticus IgG as detection antibody. The specific IgY was harvested from egg yolk of immunized hens, then was purified by ammonium sulfate precipitation, Sephadex G-25 gel chromatography and DEAE-Sehparose FF ion exchange chromatography. The established assay had a limit of detection of 2.5×10^4 cfu/ml. The cross reactivity testing showed a high specificity for V. parahaemolyticus detection and other observed bacteria were found to be non-reactive. The IgY coated microtiter plate had high stability. Results suggest that IgY-based sandwich ELISA in this study provides a simple and convenient preparation for the development of immunoassay-kit and rapid detection.

Keywords: Vibrio parahaemolyticus, Immunoglobulin Y, sandwich ELISA, detection.

1 Introduction

Vibrio parahaemolyticus is a gram-negative, halophilic bacterium and important food-borne pathogen which can cause potentially serious even fatal infections in human. If infected, there will be symptoms of diarrhea, headache, vomiting, nausea, abdominal cramps and low grade fever after incubation period of 4 to 96 h [1]. Since the first outbreak in Japan in 1950 [2], *V. parahaemolyticus*-causing food poisoning has spread to Asia, America, Europe [3], and Africa [4]. As *V. parahaemolyticus*-causing food poisoning is highly related to human health and safety, it is essential to develop rapid and reliable methods for detecting *V. parahaemolyticus* in food industry, clinical diagnosis and environmental control.

The conventional methods that involve enrichment broth and isolation on selective plating media are cumbersome and time-consuming (4-5 d to obtain outcomes). Although new enrichment broth has improved the isolation of pathogenic *V. parahaemolyticus* [5], the operation processes make it insufficient for a rapid detection. Numerous new techniques for *V. parahaemolyticus* detection are emerging. PCR [6], real-time PCR [7] and ELC-PCR [8] are being widely used and they show

E. Zhu and S. Sambath (Eds.): Information Tech. and Agricultural Eng., AISC 134, pp. 517–524.
springerlink.com © Springer-Verlag Berlin Heidelberg 2012

rapid and specific detection of pathogenic bacteria with the use of specific amplification and specially designed and labeled fluorescent probes. Although these methods have high sensitivity, their expensive equipments, materials, and strict operating procedures restrain them only in laboratories use. ELISA is also applied to *V. parahaemolyticus* detection [9,10]. Immunoassay is cheaper and simpler compared to the PCR-based technique. What's more, the commercial immunoassay-kit for the outdoor and large throughput sample detection can be expediently developed.

IgY is the major antibody produced by hens. It is a promising antibody for immunodiagnosis and immunotherapy [11]. In a therapeutic experiment for mastitis caused by *Staphylococcus aureus*, higher cure rates were observed in the use of IgY compared to that of the penicillin [12]. Chicken egg yolks have been proved to be better and more cost-effective than antivenom. Apart from the lower cost of feeding and handling, hens can produce large amounts of homogeneous IgY per month, over 100 mg of purified IgY can be obtained from a single egg [13], such yield can only be obtained from large mammals. Hens can be immunized through different routes and the production of antibody involves very simple and inexpensive steps [14].Therefore, the use of hens for the production of antibody can not only refine painful blood collection in laboratory animals but also lower the clinical or research costs.

The key idea of this study is to develop a rapid and sensitive sandwich ELISA for the detection of *V. parahaemolyticus* using IgY as capture antibody and rabbit IgG as detection antibody.

2 Materials and Methods

2.1 Reagents and Instruments

All reagents were of analytical grade unless specified otherwise. BSA, HRP labelled rabbit anti-IgY IgG, HRP labelled goat anti-rabbit IgG, complete and incomplete Freund's adjuvant as well as Sephadex G-25 were all obtained from Sigma (USA). DEAE-Sepharose FF was purchased from Pharmacia (USA). TMB were obtained from Amresco (USA). Both the ELISA washer (BIO-RAD 1575) and reader (Model 680) were from BIO-RAD (USA). The 96-well polystyrene microtiter plates were purchased from JET Biochemicals (Canada).

2.2 Buffers and Solution

PBS, 10 mmol/L sodium phosphate buffer (pH 7.4) containing 140 mmol/L NaCl; coating buffer (pH 9.6), 50 mmol/L carbonate buffer; blocking solution, PBS containing 5% (w/v) skimmed milk; dilution buffer, PBST; citrate buffer, 40 mmol /L solution of sodium citrate (pH 5.4); substrate solution, 0.01% TMB and 0.0004% H_2O_2 in citrate buffer.

2.3 Bacteria and Animals

V. parahaemolyticus, Shigella dysenteria, Escherichia coli O157:H7*, Salmonella* spp*, Staphylococcus aureus, Bacillus cereus, Alccaligenes faecalis, Bacillus subtilis, Pseudomonas* sp were all supplied by CGMCC (China). Healthy New Zealand white rabbits were purchased from GDMLAC (China). Chickens were supplied by WENS

(China). Immunization and animal housing were performed according to the routine standard.

2.4 Preparation of Immunogen

After pre-culturing for 18 h at 30 ℃, *V. parahaemolyticus* was cultured for another 18 h in 2216 E liquid medium containing 1% NaCl. Bacteria turbid liquid was obtained by centrifugation at 4500 rpm for 15 min at 4 ℃. The concentration was standardized to10^9 cfu/ml and 0.1% formaldehyde was added. The inactivation of bacteria was performed for 24 h at 30 ℃. After centrifugation at 4500 rpm for 30 min, followed by 7 times washing, the bacteria was stored at 4 ℃.

2.5 Immunization of Hens and Preparation of IgY

Five hens were raised for production of specific antibodies. For the first immunization, 1 ml immunogen at the concentration of 5×10^8 cfu/ml was emulsified with equal volume of FCA and injected into hens subcutaneously and intramuscularly at multiple sites. Subsequent (booster) injections were administered at the interval of 3 weeks using FIA. IgY was isolated from egg by the method of Bhanushali et al. [15] with modification. Then IgY was purified by ammonium sulfate precipitation, followed by Sephadex G-25 gel chromatography and DEAE-Sehparose FF ion exchange chromatography.

2.6 Immunization of Rabbits and Preparation of IgG

Healthy New Zealand white rabbits with average weight of 2-2.5 kg were observed for two weeks to ensure the health. Blood (pre-immune serum) was collected from ear vein before the day of immunization, tube agglutination test was carried out to eliminate rabbit that showed positive. The rabbits were immunized with *V. parahaemolyticus* according to the following procedure. Immunogen was emulsified with equal volume of FCA and injected into ear vein. First booster was given in FIA intramuscularly, after two weeks of primer dose, subsequent injection (booster) were administered via intra muscular route using FIA at an interval of 2 weeks. The antisera were tested by indirect ELISA. Whole blood of the rabbit was collected by cardiocentesis 7 d after the last injection. The antisera were collected by storage overnight at 4 ℃ and centrifugation at 3000 rpm for 10 min. The prepared antisera were stored at -20 ℃. Then IgG was purified by ammonium sulfate precipitation, followed by DEAE-Sepharose FF ion exchange chromatography.

2.7 Titiation of Antibodies by ic ELISA

The titration of IgY and IgG was administered by ic ELISA. All incubations were carried out at 37 ℃ and after each step the plates were washed for four times with PBST. IgY titration was administered by adding 100 µl of HRP labelled rabbit anti-IgY IgG which was diluted to a ratio of 1:5000. IgG titration was carried out by adding HRP labelled goat anti-rabbit IgG which was diluted to a ratio of 1:2500 with 0.01 mol/L PBS. Both incubation lasted for 1 h and 100 µl of TMB substrate was added afterward. The reaction was stopped 10 min later by adding 50 µl of 2 mol/L H_2SO_4. The OD_{450} was measured with an ELISA reader. All measurements were performed in triplicates.

2.8 Sandwich ELISA for Detection of V. parahaemolyticus

The assay was carried out with IgY as capture antibody and rabbit IgG as detection antibody. All incubations were carried out at 37 ℃ and after each step the plates were washed for four times with PBST. A microtiter plate was coated with 100 μl of purified IgY in 0.05 mol/L carbonate buffer (pH 9.6). Incubation was carried out for 2 h at 37 ℃ and overnight at 4 ℃, respectively. Nonspecific binding sites were respectively treated without blocking and blocking with 100 μl of PBS containing 5% (w/v) skimmed milk at 37 ℃ for 2 h. 200 μl of *V. parahaemolyticus* was added to each well, then the plate was incubated for 2 h. After washing, 100 μl of the rabbit anti- *V. parahaemolyticus* IgG was added to each well and incubated for 1 h. Then, 100 μl of the HRP labelled goat anti- rabbit IgG was added to each well and incubated for 1 h. After incubation, 100 μl of TMB substrate was added. Finally, the enzyme reaction was stopped 10 min later by adding 50 μl of 2 mol/L H_2SO_4 to each well. The OD_{450} was measured with an ELISA reader. Orthogonal experiment was applied to the optimization of sandwich ELISA. All measurements were performed in triplicates. The positive and negative were judged by the P/N values, if P/N >2.1, the result was considered to be positive. P and N were calculated as follows:

$$P = OD_{450}s - OD_{450}b \quad (1)$$

$$N = OD_{450}c - OD_{450}b \quad (2)$$

Where $OD_{450}s$ represents the mean value of samples, $OD_{450}b$ is the mean value of blank well and $OD_{450}c$ is the mean value of negative control groups.

The working concentration of IgY was optimized as follows: 40 μg/ml, 80 μg/ml, 160 μg/ml, and 320 μg/ml of diluted IgY was coated with microtiter plate, respectively, then 100 μl of HRP-labeled rabbit anti-chicken IgG at the ratio of 1:5000 was added to each well. The following steps were the same as ic ELISA procedure. The working concentration of IgG was optimized as follows: 10^5 cfu/ml of *V. parahaemolyticus* was added to the microtiter plate which was coated with IgY, incubation lasted for 2 h. Purified IgG (10 mg/ml) was serially diluted to 1600, 3200, 12 800, 25 600, and 51 200 fold and added to each well. Negative control groups were performed by adding the same concentration of negative sera while blank wells were added without sera. After incubation for 2 h, 100 μl of HRP-labeled goat anti-rabbit IgG (1:10, 000) was added. The following steps were the same as ic ELISA procedure. All concentrations were administered in triplicates.

2.9 Sensitivity of Sandwich ELISA

The *V. parahaemolyticus* standard solution was diluted to 5×10^3 cfu/ml, 10^4 cfu/ml, 5×10^4 cfu/ml, 10^5 cfu/ml, 5×10^5 cfu/ml, 10^6 cfu/ml, 5×10^6 cfu/ml, and 10^7 cfu/ml, and tested by the established sandwich ELISA. The results were expressed as the P/N values.

2.10 Cross-Reactivity Studies

V. parahaemolyticus, Shigella dysenteria , Escherichia coli O157:H7*, Salmonella* spp, *Staphylococcus aureus, Bacillus cereus, Alccaligenes faecalis, Bacillus subtilis*, *Pseudomonas* sp (CGMCC, China) were respectively detected at the concentration of 10^6 cfu/ml by the established sandwich ELISA method to study the cross-reactivity. P/N > 2.1 was considered to be the criterion of cross-reactivity.

2.11 Statistical Analysis

The student t-test (one-tailed t- test) was used to analyze the significant difference ($p < 0.5$) between the control group (zero antigen) and samples. Statistical analysis software (SPSS for windows, SPSS inc., USA) was used to carry out the one-way analysis of variance and Duncan's multiple range tests on the mean value with standard deviation.

3 Results and Discussion

3.1 Optimization of Sandwich ELISA

Variance analysis (data omitted) showed that the concentration of capture antibody and detection antibody had great influence on the results. Multiple comparisons (Tab. 1) showed that P/N values reached the highest at the IgY concentration of 320 μg/ml. Except for the concentrations of 10 μg/ml and 20 μg/ml, there was no significant difference between concentrations of 40 μg/ml, 80 μg/ml, 160 μg/ml, and 320 μg/ml. To develop an economical detecting model, the concentration of 40 μg/ml was chosen. As to the optimal IgG concentration (Tab. 2), the dilution of 3200 fold with initial concentration at 10 mg/ml got the optimal results. The dilution of 1600 fold showed significant difference with other dilution. Hence, detection antibody IgG was employed with the dilution of 3200 fold (3 μg/ml).

Table 1. Multiple Comparisons of Different Concentrations of Capture Antibody

IgY (μg/ml)	P/N value[d]
10	4.496±0.176[c]
20	4.746±0.128[bc]
40	5.420±0.154[ab]
80	5.530±0.162[a]
160	5.198±0.132[ac]
320	5.650±0.267[a]

[a], [b] and [c] in the same column indicate significant differences between different concentrations of capture antibody ($p < 0.05$).
[d] mean (±) standard deviation from triplicate determinations.

Table 2. Multiple Comparisons of Different Concentrations of Detection Antibody

Dilution of IgG (10 mg/ml)	P/N value[g]
1600	7.619±0.149[a]
3200	7.880±0.153[a]
6400	5.888±0.102[b]
12800	4.878±0.205[d]
25600	2.796±0.136[e]
51200	1.980±0.177[f]

[a], [b], [c], [d], [e], and [f] in the same column indicate significant differences between different concentrations of capture antibody ($p < 0.05$).
[g] mean (±) standard deviation from triplicate determinations.

The detecting conditions of the sandwich ELISA were optimized by orthogonal test. The orthogonal test showed that no significant difference was found between incubation overnight at 4 ℃ and at 37 ℃ for 2 h. Besides, whether the binding sites were treated with blocking or not, satisfying effect can be achieved as long as the high activity of HRP-labelled conjugates and thorough washing were ensured. Therefore, the parameters of detection system were set as follows: coating at 37 ℃ for 2 h without blocking, the binding time of capture antibody and detection antibody with antigen were 2 h and 1 h, respectively. The total detection time was about 4 h (except coating time).

3.2 Quality of the Developed Sandwich ELISA

The sensitivity of sandwich ELISA was expressed as the LOD and studied by using serially diluted *V. parahaemolyticus*. The LOD of this IgY-based sandwich ELISA was 2.5×10^4 cfu/ml, showing that this assay was suitable for the reliable detection of *V. parahaemolyticus*. Chi et al. [10] developed sandwich ELISA using monoclonal antibody and rabbit anti-mouse polyclonal antibody and reached the LOD of 5×10^4 cfu/ml. Another researcher gained LOD of 7.4×10^4 cfu/ml using disposal amperometric enzyme immunosensor [17].

Various bacteria, *V. parahaemolyticus*, *Shigella dysenteria*, *Escherichia coli* O157:H7, *Salmonella* spp, *Staphylococcus aureus*, *Bacillus cereus*, *Alccaligenes faecalis*, *Bacillus subtilis*, and *Pseudomonas* sp were applied for cross-reactivity testing. *V. parahaemolyticus* showed P/N value more than 7.0, but all other bacteria showed P/N values less than 1.5, indicating that the specificity of antibody was high enough, and the sandwich ELISA could detect *V. parahaemolyticus* without causing cross-reactivity.

A representative standard curve is shown in Fig.1, with a regression curve $Y=0.21x-0.8189$ ($R^2=0.9941$). The validity of the ELISA for *V. parahaemolyticus* was examined further by precision test. The intra-assay coefficient of variation detected by replicated measurements (n=12) of 5×10^4 cfu/ml *V. parahaemolyticus* ranged from 1.01% to 2.11%. Inter-assay coefficient of variation, determined by 4 independent measurements of *V. parahaemolyticus* ranged from 3.73% to 5.22%.

3.3 Stability of IgY Coated Microtiter Plate

To further ensure the practical application of sandwich ELISA, the IgY coated microtite plates were sealed up and stored at 4 ℃ and 25 ℃, respectively. The stability of the plates are shown in Fig.2. The OD_{450} of microtiter plate stored at 4 ℃ remained almost unchanged after 150 d while that of the 25 ℃ showed obvious decrease with the change of time. IgY can be easily made into egg yolk antibody powder, which can maintain its activity after 5 years' storage at 4 ℃ and 6 months' storage at room temperature [18]. We suggest that large amounts of egg yolk antibody powder or IgY coated microtiter plates can be produced and stored for expedient detection.

The IgY–based sandwich ELISA was developed in this study. The simple immunization procedure and high titer after purification suggested that IgY was a good polyclonal antibody for the detection of *V. parahaemolyticus*. Overall, the sandwich

ELISA had shorten the detection time and had satisfying specificity, reproducibility, stability and accuracy, indicating that it met the requirement of practical sample detection. The stability of IgY coated microtiter plates also lay a foundation for the development of immunoassay-kit and rapid detection.

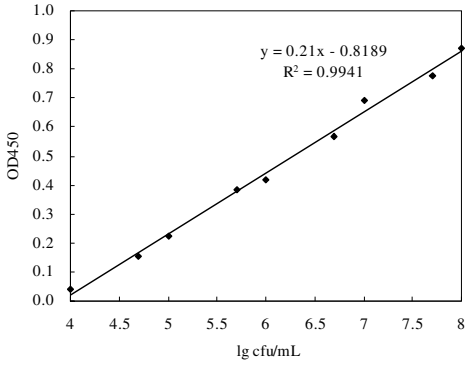

Fig. 1. Standard curve of the sandwich ELISA

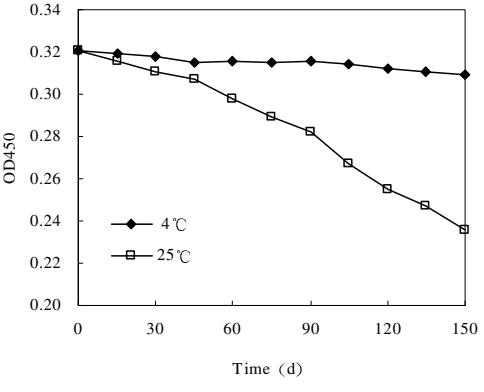

Fig. 2. Stability of IgY coated microtiter plates

Acknowledgment. The authors would like to express their gratitude to the Key Laboratory of Food Quality and Safety of Guangdong Province for equipment support and guides.

References

1. Joseph, S.W., Colwell, R.R., Kaper, J.B.: Vibrio parahaemolyticus and related halophilic Vibrios. Critical Reviews in Microbiology 10, 77–124 (1982)
2. Nishibuchi, M., Kaper, J.B.: Thermostable direct hemolysin gene of Vibrio parahaemolyticus: a virulence gene acquired by a marine bacterium. Infection and Immunity 63, 2093–2099 (1995)

3. Lozano, L.A., Torres, J., Osorio, C.R., Martinez, U.J.: Identification of tdh-positive Vibrio parahaemolyticus from an outbreak associated with raw oyster consumption in Spain. FEMS Microbiology Letters 226, 281–284 (1993)
4. Nair, G.B., Ramamurthy, T., Bhattacharya, S.K., Dutta, B., Takeda, Y., Sack, D.A.: Global dissemination of Vibrio parahaemolyticus serotype O3:K6 and its serovariants. Clinical Microbiology Reviews 20, 39–48 (2007)
5. Raghunat, P., Karunasagar, I.: Improved isolation and detection of pathogenic Vibrio parahaemolyticus from seafood using a new enrichment broth. International Journal of Food Microbiology 129, 200–203 (2009)
6. Rosec, J.P., Simon, M., Causse, V., Boudjemaa, M.: Detection of total and pathogenic Vibrio parahaemolyticus in shellfish: Comparison of PCR protocols using pR72H or toxR targets with a culture method. International Journal of Food Microbiology 129, 136–145 (2009)
7. Tyagi, A., Saravanan, V., Karunasagar, I.: Detection of Vibrio parahaemolyticus in tropical shellfish by SYBR green real-time PCR and evaluation of three enrichment media. International Journal of Food Microbiology 129, 124–130 (2009)
8. Wei, J., Chou, X.M., Xing, D., Wu, B.Y.: Rapid and sensitive detection of Vibrio parahaemolyticus in sea foods by electrochemiluminescence polymerase chain reaction method. Food Chemistry 123, 852–858 (2010)
9. Wong, J., Yan, Q.P., Su, Y.Q., Ma, L., Shao, X.: Study on indirect ELISA method for detecting Vibrio parahaemolyticus in cultured Pseudosciaena crocea. Journal of Oceanography in Taiwan Strait 20, 346–350 (2001)
10. Chi, X.C., Wong, J., Yan, Q.P., Su, Y.Q.: Preparation and applications of monoclonal antibody against the pathogenic Vibrio parahaemolyticus from Pseudosciaena crocea. Marine Science 31, 1–5 (2007)
11. Diasda, S.W., Tambourgi, D.V.: IgY: A promising antibody for use in immunodiagnostic and in immunotherapy. Veterinary Immunology and Immunopathology 135, 173–180 (2010)
12. Zhen, Y.H., Jin, L.J., Li, X.Y., Guo, J., Li, Z., Zhang, B.J., Fang, R., Xu, Y.P.: Efficacy of specific egg yolk immunoglobulin (IgY) to bovine mastitis caused by Staphylococcus aureus. Veterinary Microbiology 133, 317–322 (2009)
13. Tressler, R.L., Roth, T.F.: IgG receptors on the embryonic chick yolk sac. Journal of Biological Chemistry 262, 15406–15412 (1987)
14. Wooley, J.A., Landon, J.: Comparison of antibody production to human interleukine-6 (I-L6) by sheep and chickens. Journal of Immunology Methods 178, 253–265 (1995)
15. Bhanushali, J.K., Gilbert, J.M., McDougald, L.R.: Simple method to purify chicken immunoglobulin G. Poultry Science 73, 1158–1161 (1994)
16. Chalghoumi, R., Beckers, Y., Portetelle, D., Théwis, A.: Hen egg yolk antibodies (IgY), production and use for passive immunization against bacterial enteric infections in chicken. Biotechnology, Agronomy, Society and Environment 13, 295–308 (2009)
17. Zhao, G.Y., Xing, F.F., Deng, S.P.: A disposable amperometric enzyme immunosensor for rapid detection of Vibrio parahaemolyticus in food based on agarose/Nano-Au membrane and screen-printed electrode. Electrochemistry Communications 9, 1263–1268 (2007)
18. Larsson, A., Lindahl, T.: Chicken anti-protein G for the detection of small amount of protein G. Hybridoma 12, 143 (1993)

Subcellular Localization of Melon (*Cucumis melo* L.) Glutamine Synthetases*

Deng Yang-wu[1], Yu Shui-jing[1], Zhang Ping[1],
Zhang Yi-dong[2], and Huang Dan-feng[2]

[1] School of Materials and Chemical Engineering, Jiangxi
University of Science and Technology Ganzhou, Jiangxi, China
[2] School of Agriculture and Biology Shanghai Jiao Tong University Shanghai, China
Tosang@foxmail.com, Zhangsar@hotmail.com

Abstract. To physically characterize the subcellular localizations of M-GS1 (GenBank accession number: DQ851867) and M-GS2 (GenBank accession: AY773090), the first two glutamine synthetase (GS) genes isolated from melon, we constructed two recombinant plant expression vectors, in which the coding sequence of either M-GS1 or M-GS2 was fused with that of the yellow fluorescence protein YFP, using CamV 35S as the promoter. The recombinant plant expression vectors were then transformed into the onion epidermal cells via gene gun bombardments. After transient expression, fluorescence emission from the expressed products in cells was visualized and analyzed using laser-scanning confocal microscope techniques. The results indicated that M-GS2 was localized in the chloroplast while M-GS1 in the cytosol. It is the first report to precisely characterize the subcellular localization of melon GS, which added to the foundation for further analyses on the roles of melon GS genes in enhancing plant N use efficiency.

Keywords: GS, subcellular localization, YFP, laser-scanning confocal microscope techniques, onion epidermal cell.

1 Introduction

Glutamine synthetase (GS; EC 6.3.1.2) -glutamate oxoglutarate amino transferase (GOGAT; EC 1.4.7.1 or EC 1.4.1.14)) cycle is the primary route of plant nitrogen (N) assimilation and GS, as the first enzyme in this cycle, plays critical roles[1]. GS catalyses the ATP-dependant condensation of ammonium with glutamate (Glu) to produce glutamine (Gln), which is used as the nitrogen (N) donor in the biosynthesis of most down stream N-containing compounds. Inorganic N is effectively integrated into its organic forms through this cycle and GS is renowned as the rate-limiting step of the reactions involved in the cycle[2]. Therefore, GS has been regarded as the key factor impacting plant N use efficiency (NUE) and become the target of intensive research in the endeavor towards the enhancement of plant NUE. Low NUE of plant

* This work was supported by Key Projects of Science and Technology Research (108141, Ministry of Education of the People's Republic of China) and a startup fund for new researchers of Jiangxi University of Science and Technology.

E. Zhu and S. Sambath (Eds.): Information Tech. and Agricultural Eng., AISC 134, pp. 525–534.
springerlink.com © Springer-Verlag Berlin Heidelberg 2012

is highly relevant to plant malnutrition and reduced crop yields, which, however, is often the cause of N-fertilizer overuse in modern agriculture that inevitably results in N-pollution related human health hazards and environmental issues, such as carcinogenic effects of ingested inorganic N species, especially of nitrites, and eutrophication of waters that causes algae blooms endangering lives in water through depletion of dissolved oxygen and generation of toxins.

According to their localizations within the cell, GS in plants can exist as distinct isoforms, including GS1 isoforms in cytosol and GS2 isoforms in chloroplasts[3]. GS1 isoforms function in the cytosol and are responsible for the assimilation of ammonium that directly picked up from soil by root and that released in metabolic processes such as phenylpropanoids synthesis and degeneration of proteins and chloroplasts, to produce Gln for N transport and remobilization between cells, tissues and organs[4]. GS2 isoforms, however, function in chloroplasts to assimilate ammonium generated by photorespiration and nitrate reduction[5], ameliorating the potential toxic effect of excessive ammonium on the leaves[6].

Although catalyzing the same biochemical reaction, the primary structures of *GS1* and *GS2* gene expression products are significantly different. On the *N*-terminus of a GS2 precursor, a sequence designated *chloroplastic transit peptide* (cTP) is usually present functioned to mediate the localization of GS2 to chloroplasts [4, 7]. The cTP sequence of a GS2 precursor is cleaved off by stromal processing peptidase, upon completion of localization, to produce a mature GS2 isoenzyme that catalyzes the primary N assimilation within the chloroplast[8]. Whereas, *GS1* gene expression product lack a cTP-like structure on its *N*-terminus because it works in the cytosol where it is synthesized.

For any newly cloned *GS* genes, characterization of the subcellular localizations of their expression products is a crucial step towards a better understanding of their functions at physiological level and, most importantly, of their potentials to be used as candidates in improving plant NUE. For this purpose, in the present study we first used bioinformatics tools including TargetP[9-10] and ChloroP[7] programs to predict the subcellular localization of deduced protein of *M-GS1*(GenBank accession No.: DQ851867) and *M-GS2*(GenBank accession No.: AY773090) [4], two *GS* genes recently cloned from melon (*Cucumis melo* L.) by us. And to further physically confirm the results predicted with bioinformatics tools, we constructed recombinant plant expression vectors, in which the Open Reading Frame (ORF) of either *GS* cDNA were tagged with that of Yellow Fluorescent Protein (YFP)[11-13], to express fusion proteins GS-YFP in plant cell via gene gun bombardment transformation, which then allowed the subsequent comparative analyses of the subcellular localizations of M-GS1 and M-GS2 with laser-scanning confocal microscope techniques.

2 Materials and Methods

2.1 Bioinformatics Tools

TargetP and *ChloroP* programs, accessible at http:// www.cbs.dtu.dk/services/ TargetP/ and http://www.cbs.dtu.dk/services/ChloroP/, respectively, are used as described in [7, 9-10] to predict the subcellular localizations of the deduced proteins of *M-GS1* and *M-GS2* genes. Multiple sequence alignment was performed with Clustal W and Genedoc software.

2.2 Instruments and Chemical Reagents

Polymerase chain reactions (PCR) were performed on PTC-200 (Bio-Rad, the United States) for DNA amplifications. Gene gun typed PDS-1000/He (Bio-Rad, the United States) was used for gene transformations of plant cells. Laser-scanning confocal microscope typed Leica TCS SP5 (Leica Microsystems, Germany) was used for fluorescence recording and localization visualization. Primer synthesis and DNA sequencing services were purchased from Sangon Biotech (Shanghai) Co., Ltd. DNA polymerase, cloning vectors, restriction enzymes, ligase and other chemical reagents were all purchased from Promega or Takara Bio incorporation. QIAGEN Plasmid Plus Kits (QIAGEN, Germany) was used for recombinant plant expression plasmids extraction and purification.

2.3 Plasmids, Strains and Primers

Plant expression vector pA7-X-YFP (Fig. 1) was a gift from Prof. Yang Hong-quan (Department of Plant Science, Shanghai Jiao Tong University). Plasmid pGEM-*M-GS*1 and pGEM-*M-GS*2, hosting *M-GS*1 and *M-GS*2 ORF, respectively, are available in our lab refrigerator stock. *E. coli* strain DH5*α* was used as the host for plasmid amplification. Primer pairs listed in Table 1 were used for amplification of *M-GS* ORF that was sandwiched with restriction sites X*ho*I (sense strand) and S*pe*I (anti-sense strand).

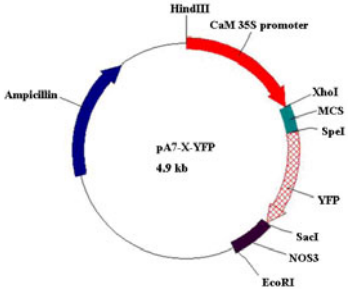

Fig. 1. Physical map of the plant expression vector 'pA7-X-YFP'. MCS means multiple cloning sites, which include *Xho*I, *Sal*I, *Sma*I, *Bam*HI and *Spe*I. Herein, *Xho*I and *Spe*I were selected to avoid cutting within the coding regions of *M-GS*1 or *M-GS*2.

Table 1. Primer pairs, designed with restriction site added, for amplification of the coding region of *M-GS*1and *M-GS*2 which can form fusion proteins with that of *YFP*

Gene name	Primer name	Primer sequences
*M-GS*1	GS1-*Xho*I-F[a]	5'-ccgctcgagcgg**atgtctctgctc tccgatctcatcaacctcaacc**-3'
	GS1-*Spe*I-R[a]	5'-cggactagtccg**tggtttccacaa gatggtggtttcagcgaccatgg**-3'
*M-GS*2	GS2-*Xho*I-F[a]	5'-ccgctcgagcgg**atggctcaga ttttagctccatccactcaatggc**-3'
	GS2-*Spe*I-R[a]	5'-cggactagtccg**aaccttcaatg acagtttctgagcagccagtgc**-3'

[a] sequences underlined are restriction sites.

2.4 Recombinant Plant Expression Vector Construction

Plasmid pGEM-*M-GS*1 and pGEM-*M-GS*2 were used as templates, with corresponding primer pairs GS1-*Xho*I-F/GS1-*Spe*I-R and GS2-*Xho*I-F/GS2-*Spe*I-R (Table 1), to amplify, respectively, the ORF of *M-GS*1 and *M-GS*2 through PCR. The amplified PCR products were purified in agarose gel, digested with DNA restriction enzymes *Xho*I and *Spe*I, purified again and recovered. The recovered products (*Xho*I-GS1 ORF-*Spe*I and *Xho*I-GS2 ORF-*Spe*I) were then used to ligate with plant expression vector pA7-X-YFP, which was also double digested with DNA restriction enzymes *Xho*I and *Spe*I, to get recombinant plant expression vectors pA7-GS1-YFP and pA7-GS2-YFP（Fig. 2）, respectively.

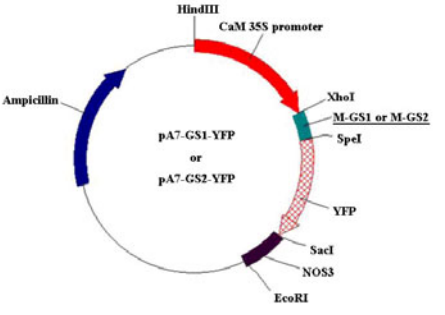

Fig. 2. The construct details of the recombinant plant expression vectors, pA7-GS1-YFP and pA7-GS2-YFP. pA7-GS1-YFP, the recombinant plant expression vector carrying *M-GS*1 fused with *YFP*; pA7-GS1-YFP, the recombinant plant expression vector carrying *M-GS*2 fused with *YFP*.

2.5 Amplification, Extraction and Purification of Recombinant Plant Expression Vectors

E. coli strain DH5*α* was used as the host for amplification of recombinant plant expression vectors pA7-GS1-YFP and pA7-GS2-YFP. DH5*α* transformed with pA7-GS1-YFP or pA7-GS2-YFP was inoculated to 50 mL LB liquid medium (Amp+), respectively, and shaken (250 rpm) at 37℃ for 18 h. Thirty mL was then taken and used for plasmid extraction and purification with QIAGEN Plasmid Plus Kits (Qiagen, Germany) according to the specifications of the manual. Plasmid concentration and purity was checked with ultraviolet spectrophotometer Evolution60 (Thermo scientific, the United States), and for efficient transformation, only those of concentration above 1 μg μL^{-1} were used subsequently in onion epidermis cell transformation via gene gun bombardment.

2.6 Transformation of Onion Epidermis Cells with Plant Expression Vectors via Gene Gun Bombardment and Subcellular Localization

Onion bulb selection and revitalization followed the descriptions in[14]. On a clean bench, Square pieces (4 cm^2) of inner-layer fleshy leaves (the 3rd or 4th layer from the

outside) were sliced from onion bulbs that showed vigorous root growth, placed with epidermis-side up in a Petri dish of 1/2 MS solid medium(1× Murashige & Skoog basal nutrients, sucrose 30 gL^{-1}, 2% agar, and pH 5.7). The Petri dishes were then covered, wrapped up with aluminum foil, and kept in dark at 22-26℃ overnight before being used in gene gun bombardment transformation. Recombinant plant expression vectors pA7-GS1-YFP and pA7-GS2-YFP and control vectors pA7-X-YFP were, respectively, wrapped onto gold micro-particles, and then bombarded to the onion epidermis in prepared Petri dishes using a gene gun PDS-1000 /He (Bio-Rad, the United States) according to the procedures as described in [15]. Bombarded Petri dishes of onion epidermis were kept again in dark at 22-26℃ for 8 h to allow transient expression of transgenes in onion epidermis cells. After transient expression, onion epidermis was gently peeled off from the fleshy leaves, rinsed in a PIPES buffer(0.12 M, pH 7)[16], and then placed on a slide, covered with a coverslip, and observed under light, fluorescence, and laser-scanning confocal microscopes, respectively.

3 Results and Discussion

3.1 Subcellular Localization Predicted by Bioinformatics Analysis

TargetP[9-10] and *ChloroP*[7] are two bioinformatics programs developed by scientists with Danmark University of Technology, designed specially for predicting subcellular-localization of cellular proteins based on their primary structures. As indicated by the results (Fig. 3 and Fig. 4) predicted with TargetP and ChloroP programs: M-GS1 did not contain a cTP-like signal peptide on the *N*-terminus of its primary structure and was, therefore, localized in cytosol where it was synthesized; M-GS2, however, like most plant proteins localizing to chloroplast[8, 17], contained an obvious cTP sequence of 53 amino acid residues on the *N*-terminus of its primary structure and was localized to chloroplast. The differences in primary structures between M-GS1 and M-GS2 were observed as outlined by sequence alignment（Fig. 5）, and it was obvious that in addition to having a cTP sequence, M-GS2 also had a conserved sequence of 16 amino acid residues on the *C*-terminus of its primary structure, which was a typical feature of GS2 proteins [18].

The predicted cTP sequence of M-GS2 contained a high proportion of positively charged residues (seven Arg and two Lys), but was completely devoid of negatively charged residues (Asp and Glu), and this was a typical feature of cTP sequences[19]. Upon localization to chloroplast and with the subsequent removal of cTP sequences, the calculated molecular mass of mature M-GS2 was around 43 kDa, which was similar to the apparent molecular mass of the GS proteins characterized as localizing to the chloroplast in other plants by protein gel blot analysis [20].

```
### targetp v1.1 prediction results ###################################
Number of query sequences:  2
Cleavage site predictions included.
Using PLANT networks.

Name                  Len     cTP    mTP     SP  other  Loc  RC  TPlen
--------------------------------------------------------------------
M-GS1                 356   0.121  0.056  0.154  0.835    _   2      -
M-GS2                 432   0.880  0.287  0.003  0.029    C   3     53
--------------------------------------------------------------------
cutoff                      0.000  0.000  0.000  0.000
```

Fig. 3. Subcellular localization results as predicted by TargetP program. Name, protein sequence name; Len, protein sequence length; cTP, probability of sequence containing a chloroplast transit peptide and localizing to chloroplast; mTP, probability of sequence containing a mitochondrial transit peptide and localizing to mitochondria; SP, probability of sequence containing a signal peptide; Loc, predicted localization site; RC, reliability class; TPlen, predicted transit peptide length; the Loc value 'C' indicates localizing to chloroplast, and '—' indicates re-localization not valid.

```
### chlorop v1.1 prediction results ##############################
Number of query sequences: 2

Name                    Length       Score  cTP       CS-     cTP-
                                                      score  length
-----------------------------------------------------------------
M-GS1                      356       0.433   -       0.719      36
M-GS2                      432       0.554   Y       1.749      53
-----------------------------------------------------------------
```

Fig. 4. Results as predicted by ChloroP program, with regards to whether protein sequence is predicted to contain a chloroplastic transit peptide or not. 'Y' indicates 'yes', '—' 'no'.

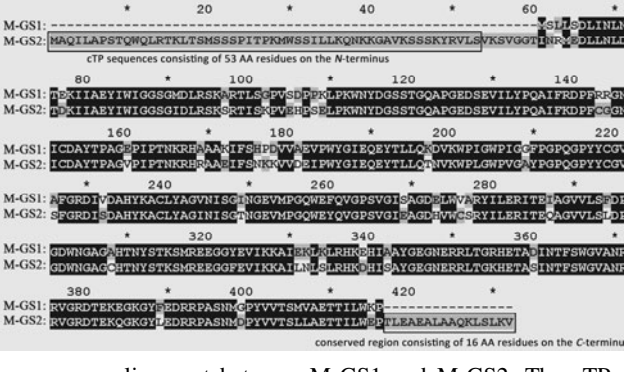
M-GS1:
M-GS2:
cTP sequences consisting of 53 AA residues on the N-terminus
conserved region consisting of 16 AA residues on the C-terminu

Fig. 5. Protein sequences alignment between M-GS1 and M-GS2. The cTP sequence of 53 amino acid residues on the *N*-terminus and the conserved sequence of 16 amino acid residues on the *C*-terminus of M-GS2 were, respectively, highlighted in a box.

Therefore, based on these results of bioinformatics analysis, we were able to preliminarily conclude that M-GS1 and M-GS2 were localized in the cytosol and chloroplast, respectively.

3.2 Subcellular Localization by Yellow Fluorescence Protein (YFP) Techniques

Yellow Fluorescence Protein (YFP) is a derivative of Green Fluorescence Protein (YFP), availability of which has thoroughly redefined fluorescence microscopy and the

way it is used in cell biology and other biological disciplines[21]. While most small fluorescent molecules such as FITC (fluorescein isothiocyanate) are strongly phototoxic when used in living cells, fluorescent proteins such as GFP and its derivatives are usually much less harmful when illuminated in living cells. This has triggered the development of highly automated living cell fluorescence microscopy systems which can be used to observe cells over time expressing one or more proteins tagged with fluorescent proteins. In comparison with conventional immunolabelling techniques, YFP techniques offered a rang of advantages including simplicity of manipulation, ease of use and the capability to carry out experiments with regular fluorescence or confocal laser scanning microscopes. These characteristics of it have made YFP a powerful tool for characterizing the real time transport and precise localization of cloned gene proteins within living cells.

M-GS1 and *M-GS2* were the first two GS genes recently isolated from melon (*Cucumis melo* L.) by us, and as indicated by the results of bioinformatics analyses, M-GS1 and M-GS2 were predicted to be localized in cytosol and chloroplastid, respectively. The successful cloning of these two *GS* genes allowed us to employ YFP technique to physically verify the localization results predicted with bioinformatics tools. The ORF of *M-GS1* and M-*GS2* were, respectively, recombined with plant expression vectors pA7-X-YFP to construct recombinant plant expression vectors pA7-GS1-YFP and pA7-GS2-YFP (Fig. 2), which expressed fusion proteins M-GS1-YFP and M-GS2-YFP, respectively. The recombinant plant expression vectors and the control vector pA7-X-YFP were, respectively, transformed into onion epidermis cells via gene gun bombardment. After transient expression, the subcellular localization of expressed products was observed under microscope (Fig. 6).

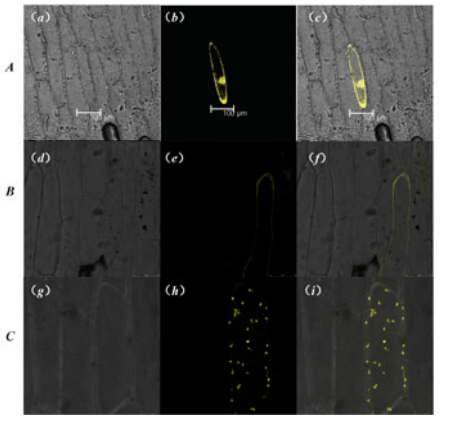

Fig. 6. Subcellular localization of M-GS1 or M-GS2. YFP, M-GS1-YFP and M-GS2-YFP fusion proteins were expressed transiently in onion epidermis cells 8 h after bombardment using a gene gun and visualized with a laser-scanning confocal microscope. Images of YFP (control) (***A***), M-GS1-YFP (***B***) and M-GS2-YFP (***C***) in onion epidermal cells, respectively. *a*, *d* and *g* were bright-field images; *b*, *e* and *h* were images of yellow fluorescence distribution in cells under the confocal microscope; *c*, *f* and *i*, were overlaid images of corresponding bright-field image with fluorescence image. Scale bar 100 μm.

For the control as shown in Fig. 6 *A*, yellow fluorescence was detected emitting from throughout the cells transformed with pA7-X-YFP (control), indicating that YFP, the expression product, was distributed throughout the cell and localized, as expected, without subcellular specificity. For M-GS1 as shown in Fig. 6 *B*, yellow fluorescence emitted from the fusion protein M-GS1-YFP was detected only in cytosol, suggesting that M-GS1 was localized where it was synthesized. This result was in agreement with that predicted by bioinformatics tools. Large vacuoles usually exist in onion epidermis cells in varying number, and sometimes an extra large vacuole could form, pressing the rest of a protoplast such as nucleus, cytoplasm and chloroplast to the cell wall (Fig. 7). For M-GS2 as shown in Fig. 6 *C,* strong yellow fluorescence was observed emitting sparkly from chloroplasts dispersed within the cell, a view evidently different from that observed in YFP or M-GS1 （Fig. 6 *A* and *B* ）, suggesting that M-GS2 was specifically localized in chloroplast. This result also agreed with that predicted by bioinformatics tools.

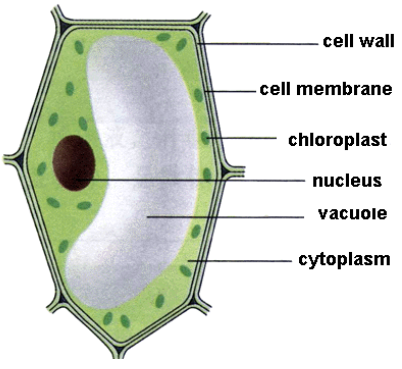

Fig. 7. The subcellular structure diagram of onion epidermis cell

The subcellular localization of proteins has been a hot topic in both cell and molecular biology, and has been intensively studied. It could provide valuable information that can be used to explore protein biological function. A variety of techniques could be used for the subcellualr localization analysis of proteins, such as immunollabeling, GFP (and its derivatives) fusion protein, density gradient centrifugation and etc. However, immunolabeling and GFP techniques were used most often. For genes that were not yet cloned, immunollabelling techniques can be convenient options if the corresponding proteins to be characterized could be efficiently separated and purified. For cloned genes, however, GFP techniques are superior because they are not only simpler but more precise, and can leave out the tedious procedures such as protein separation&purification and antibody preparation. In the present study, we employed YFP techniques and successfully characterized the precise subcellular localization of the first two *GS* genes cloned from melon. The results confirmed the prediction made by bioinformatics tools that while M-GS1 was localized in cytosol, M-GS2 was in chloroplast.

This work added to the foundation for further investigations concerning the potential roles of melon *GS* genes in improving plant NUE through transgenic strategies in the future.

References

1. Tingey, S.V., Tsai, F.Y., Edwards, J.W., Walker, E.L., Coruzzi, G.M.: Chloroplast and cytosolic glutamine synthetase are encoded by homologous nuclear genes which are differentially expressed in vivo. J. Biol. Chem. 263(20), 9651–9657 (1988)
2. Guan, S.-Q., Zhang, Y.-D., Yang, D.-D., Huang, D.-F.: Expression Analysis of Glutamine Synthetase Gene Under Different Nitrogen Sources in Melon (Cucmis Melo L.). Journal of Shanghai Jiao Tong University(Agricultural Science Edition) 25(1), 24–29 (2007)
3. Chen, Q., Silflow, C.D.: Isolation and characterization of glutamine synthetase genes in Chlamydomonas reinhardtii. Plant Physiol. 112(3), 987–996 (1996)
4. Deng, Y.-W., Zhang, Y.-D., Chen, Y., Wang, S., Tang, D.-M., Huang, D.-F.: Isolation and Characterization of a GS2 Gene in Melon (Cucumis melo L.) and its Expression Patterns under the Fertilization of Different Forms of N. Molecular Biotechnology 44(1), 51–60 (2010)
5. Wallsgrove, R.M., Turner, J.C., Hall, N.P., Kendall, A.C., Bright, S.W.: Barley Mutants Lacking Chloroplast Glutamine Synthetase-Biochemical and Genetic Analysis. Plant Physiol. 83(1), 155–158 (1987)
6. Peterman, T.K., Goodman, H.M.: The glutamine synthetase gene family of Arabidopsis thaliana: light-regulation and differential expression in leaves, roots and seeds. Mol. Gen. Genet. 230(1-2), 145–154 (1991)
7. Emanuelsson, O., Nielsen, H., von Heijne, G.: ChloroP, a neural network-based method for predicting chloroplast transit peptides and their cleavage sites. Protein Sci. 8(5), 978–984 (1999)
8. Keegstra, K., Cline, K.: Protein Import and Routing Systems of Chloroplasts. Plant Cell 11(4), 557–570 (1999)
9. Emanuelsson, O., Nielsen, H., Brunak, S., von Heijne, G.: Predicting subcellular localization of proteins based on their N-terminal amino acid sequence. Journal of Molecular Biology 300(4), 1005–1016 (2000)
10. Nielsen, H., Engelbrecht, J., Brunak, S., von Heijne, G.: Identification of prokaryotic and eukaryotic signal peptides and prediction of their cleavage sites. Protein Engineering 10(1), 1–6 (1997)
11. Phillips, G.J.: Green fluorescent protein - a bright idea for the study of bacterial protein localization. FEMS Microbiology Letters 204(1), 9–18 (2001)
12. Heim, R., Cubitt, A.B., Tsien, R.Y.: Improved green fluorescence. Nature 373(6516), 663–664 (1995)
13. Chen, B.-J., Jing, R.-L., Mao, X.-G., Chang, X.-P., Wang, S.-M.: A Response of PvP5CS2 Gene to Abiotic Stresses in Common Bean. Acta Agronomica Sinica 34(7), 1121–1127 (2008)
14. Gong, H.-M.: A method for quick regeneration of roots on onion bulb. Bulletin of Biology 41(3), 6 (2006)
15. Qi, G.-Y.: Study of subcellular localization of rice OsWrky gene. Journal of Shandong Agricultural University (Natural Science Edition) 33(4), 506–508 (2002)
16. Mo, B.-X.: Possible subcellular localization of mannosidase. Journal of Shenzhen University 23(4), 358–361 (2006)

17. Jarvis, P., Robinson, C.: Mechanisms of protein import and routing in chloroplasts. Curr. Biol. 14(24), R1064–R1077 (2004)
18. Foyer, C., Noctor, G.: Photosynthetic nitrogen assimilation and associated carbon and respiratory metabolism. In: Hirel, B., Lea, P.J. (eds.) The Biochemistry, Molecular Biology, Genetic Manipulation of Primary Ammonia Assimilation, vol. 12, pp. 71–92. Kluwer (2002)
19. Karlin-Neumann, G.A., Brusslan, J.A., Tobin, E.M.: Phytochrome control of the tms2 gene in transgenic Arabidopsis: a strategy for selecting mutants in the signal transduction pathway. Plant Cell 3(6), 573–582 (1991)
20. Ochs, G., Schock, G., Trischler, M., Kosemund, K., Wild, A.: Complexity and expression of the glutamine synthetase multigene family in the amphidiploid crop Brassica napus. Plant Mol. Biol. 39(3), 395–405 (1999)
21. Yuste, R.: Fluorescence microscopy today. Nat. Methods 2(12), 902–904 (2005)

Magnolia Ethanol Extract on Growth of Tumor in Tumor Mice S180

Lin Yuan, Xianju Huang, and Jiaqiang Sun

College of Pharmacy
South-Central University for Nationalities
Wuhan, China
yuanlinjx@126.com

Abstract. This paper carries on anti-tumor activities research of the ethanol extract of Magnolia officinalis (MEE). Our results showed that MEE has obvious anti-tumor activities to transplanted tumor model of the mouse S180 sarcoma in vivo. The inhibitory rates of tumor in both MEE 1.0 g/kg and 2.0 g/kg were more than 50 %, however it has not showed a dose-dependent manner. Although it has less damage than cisplatin, MEE can inhibit the immune system by obviously suppressed the spleen index and thymus index. These results indicated the anti-tumor mechanism of MEE might be related to the depressing of immune organs.

Keywords: Magnolia ethanol-extract, sarcoma S180, anti-tumor.

1 Introduction

Cortex Magnoliae Officinalis (*M. officinalis*), one of the most popular traditional Chinese medicine (TCM), is the dry trunk bark, branch bark, root bark of *Magnoliaceae Magnolia officinalis Rehd. et Wils.* or *Magnolia officinalis Rehd. et Wils. var. biloba Rehd. et Wils*. It has also been widely used in many countries for thousands of years. This herb has been used to treat a wide variety of clinical diseases such as neurosis, anxiety, stroke, fever and headache [1]. It has been known to have various pharmacological activities such as antivirus, antitumour, antibiotic, preventing caries, antiabscess, action of nervous system, easing pain and diminishing inflammation and some other new effect of medicine [2]. We also recently found that *M. officinalis* has the analgesic effects that might related to the peripheral nerve system but not to the central nervous system [3].

The present study was to observe the anti-tumor and immunomodulatory activities of ethanol extract of M. officinalis (MEE) in vivo using the transplanted tumor model of the mouse S180 sarcoma on mice.

2 Materials and Methods

2.1 Animals and Cells

Male and female Kuming mice aged 4 weeks and weighing 18-22 g were purchased from the Animal Research Center, Center for Disease Control and Prevention of Hubei

E. Zhu and S. Sambath (Eds.): Information Tech. and Agricultural Eng., AISC 134, pp. 535–538.
springerlink.com © Springer-Verlag Berlin Heidelberg 2012

Province, PRC. The mice were housed in plastic cages with wood-chip bedding in an animal room with a 12-hour light-dark cycle at room temperature (22 ± 1 °C), and allowed free access to food and water. Animal handling was conducted in accordance with the regulation for the use of laboratory animals, and the study protocol was approved by the ethics committee of the university.

Mouse sarcoma 180 cells (S180) were provided by the China Center for Type Culture Collection, Wuhan, PRC. The ascitic form of S-180 was maintained in mice by intraperitoneal inoculation.

2.2 Plant Materials and the Preparation of Plant Extract

Sliced and stripped *Magnolia* bark was purchased from a local wholesaler (The 3rd Market of traditional Chinese medicinal materials of Yulin, Guangxi, PRC). The *Magnolia* bark was confirmed to be the trunk bark, branch bark, root bark of *Magnolia biloba* (*Rehd. et Wils.*) by Prof. Dingrong Wan, College of Pharmacy, South-central University for Nationalities, Wuhan, China.

The bark was air-dried and milled into powder. About 400 grammes of the M. officinalis were immersed and extracted with 3 volumes of cold industrial alcohol for 1 day for three times. The ethanol extract of *Magnolia* (MEE) was concentrated in a rotating evaporator under reduced pressure until dry yielding 10.9 % (43.6 g) residue.

2.3 Tumour Inoculation and MEE Treatment

The inhibitory experiment was used internal anti-carcinoma method [4]. Transplant and grafting of animal were with S180 sarcoma. Mice with 5-7 days old of sarcoma were used as source. Extracting peritoneal fluid that contains sarcoma and diluting cells with sterilized normal saline to concentration of 5×10^6 cells / ml, inoculated 0.2 ml at right arm pits of each mouse.

One day after inoculation, the mice were randomly assigned into 4 groups: oral normal saline group (blank control group), oral MEE 1.0 g/kg · d or 2.0 g/kg · d, and intraperitoneal injection cisplatin (CDDP, provided by Qilu Pharmaceutical Co., Ltd., Shandong, PRC) 3.0 mg/kg · d (positive control group). Drugs were given the day after inoculation once daily for 10 days. After 12 hours of the last administration, the animals were weighted and perished by breaking vertebra, and subcutaneous sarcoma was separated and weighted. The formula below was applied to calculate the sarcoma inhibitory rate. At the same time, thymus and spleen was dissected and weighted. Thymus index and spleen index were calculated.

Inhibitory ratio (%) = (average sarcoma's weight in control group minus average sarcoma's weight in treatment group) divided by average sarcoma's weight in control group × 100 %.

Spleen index (thymus index) = Spleen (thymus) weight divided by body weight (gram).

2.4 Statistical Method

Data obtained were analyzed statistically by ANOVA method. Significance of any differences between groups was evaluated using Student t-test. All values were expressed as mean ± S.D.

3 Results

3.1 Effects of MEE on Tumor Growth of Sarcoma S180 Tumor-Bearing Mice

Tumor's inhibitory rate in MEE 1.0 g/kg · d group and MEE 2.0 g/kg · d group was 57.24 % and 52.38 %, respectively. Compared to the blank control group, the 2 groups had significant elevated tumor inhibitory rate ($P < 0.05$, Tab 1).

Table 1. Inhibitory rate of MEE on s180 sarcoma to the tumor-bearing mice

Group	n	Tumor Weight (g)	Rate (%)
Blank Control	10	0.99 ± 0.27	—
CDDP 3.0 mg/kg	9	0.18 ± 0.12 **	82.27
MEE 1.0 g/kg	8	0.42 ± 0.19 *	57.24
MEE 2.0 g/kg	8	0.47 ± 0. 22 *	52.38

Significant differences from blank control Group: **P < 0.01, *P < 0.05.

3.2 Effects of MEE on Immune Organ of Sarcoma S180 Tumor-Bearing Mice

The spleen index and thymus index of 1.0 g/kg · d group and 2.0 g/kg · d group significantly decreased compared to the blank control group. But the positive control group had significant difference compared to the blank control group ($P < 0.01$, Tab 2).

Table 2. Inhibitory rate of MEE on S180 sarcoma to the tumor-bearing mice

Group	n	Spleen Index	Thymus Index
Blank Control	10	10.27 ± 2.87	2.59 ± 0.67
CDDP 3.0 mg/kg	9	4.39 ± 1.70 **	0.96 ± 0.64 **
MEE 1.0 g/kg	8	6.73 ± 1.94 *	1.78 ± 0.43 *
MEE 2.0 g/kg	8	7.30 ± 1.79 *	1.52 ± 0.36 **

Significant differences from blank control Group: **P < 0.01, *P < 0.05.

4 Discussion

Carcinoma is one of the common fetal diseases detrimental to human health. Anti-tumor therapies contain surgery, radiotherapy and chemotherapy, and it depends on synthetic agents to a great extent in chemotherapy. Most chemotherapy drugs, such as 5-Fu and CDDP, are immunosuppressive because they kill many human body-friendly cells during killing tumor cells and have strong side-effects [5, 6]. TCM have been widely used in many countries for thousands of years. Some of them have been used clinically to treat cancer or as adjuvant therapy, because of its low risk for toxicity in normal tissue, and immunomodulatory properties [7, 8].

The in vivo transplanted tumor model of the mouse S180 sarcoma was established. In the MEE groups at dosage of 1.0 and 2.0 g/kg, the inhibitory rate was 57.24 % and 52.38 %, respectively. There were significant differences between the groups of MEE and the control group ($P < 0.05$). These results indicated that MEE could inhibit

growth of solid tumor of S180 mice. However it has not shown a dose-dependent manner.

The anti-tumor effect of TCM is related to some pathways and targets. Most studies on anti-tumor mechanisms of TCM showed that TCM could inhibit tumors through supporting the healthy energy and strengthening the body resistance [9, 10]. In our study, although it has less damage than CDDP, MEE showed an obvious inhibition of the immune system but not reinforce immunity of organism, according to the thymus index and spleen index. These results indicated the anti-tumor mechanism of MEE might be related to the depressing of immune organs.

Acknowledgment. The project is supported by the Natural Science Foundation of South-Central University for Nationalities (No. YZQ04001).

References

1. Song, W.Z., Cui, J.F., Zhang, G.D.: Studies on the medicinal plants of Magnoliaceae tu-hou-po of Manglietia. Yao Xue Xue Bao 24, 295–299 (1989)
2. Chen, J., Wang, B.C.: Advances in Pharmacological Studies of Cortex Magnoliae Officinalis. Journal of Chongqing University (Natural Science Edition) 28, 136–139 (2005)
3. Yuan, L., Sun, D.P.: Study on active constituents of cortex magnoliae officinalis for the analgesic effects. Journal of South-central University for Nationalities (Nat. Sci. Edition) 3, 40–42 (2010)
4. Shirai, M., Izumi, H., Yamagami, T.: Experimental transplantation models of mouse Sarcoma 180 mice for evaluation of antitumour drugs. Journal of Veterinarian Medical Sciences 53, 707–713 (1991)
5. Takiguchi, N., Saito, N., Nunomura, M., Kouda, K., Oda, K., Furuyama, N., et al.: Use of 5-FU plus hyperbaric oxygen for treating malignant tumors: evaluation of antitumor effect and measurement of 5-FU in individual organs. Cancer Chemother. Pharmacol. 47, 11–14 (2001)
6. Kouchi, Y., Maeda, Y., Ohuchida, A., Ohsawa, M.: Immunotoxic effect of low dose cisplatin in mice. J. Toxicol. Sci. 21, 227–233 (1996)
7. Hsiao, W., Liu, L.: The role of traditional Chinese herbal medicines in cancer therapy-from TCM theory to mechanistic insights. Planta Med. 76, 1118–1131 (2010)
8. Feng, Y., Wang, N., Zhu, M., Feng, Y., Li, H., Tsao, S.: Recent Progress on Anticancer Candidates in Patents of Herbal Medicinal Products. Recent Pat. Food Nutr. Agric. 29 (November 2010)
9. Zhao, F., Liu, P.: Progress of study on action mechanisms of TCM in anti-tumor and preventing metastasis of tumor. Zhongguo Zhong xi yi Jie he Za zhi 27, 178–181 (2007)
10. He, Y.H.: General survey of traditional Chinese medicine and Western medicine researches on tumor metastasis. Chin. J. Integr. Med. 12, 75–80 (2006)

Stability of Anthocyanin in Wild Blueberry Fruit and Its Degradation Kinetics

Na Zhang[1], Qingqi Guo[2], and Yongqiang Ma[1,*]

[1] College of Food Engineering, Harbin University of Commerce, Harbin, Heilongjiang Province, China
[2] College of Forestry, Northeast Forestry University, Harbin, Heilongjiang Province, China
{zhangna,mayq}@hrbcu.edu.cn, qingqiguo@126.com

Abstract. The effect of temperature on anthocyanin in wild blueberry fruit and chromatism were mensurated, and degradation kinetics of anthocyanin in wild blueberry fruit was studied. The results show that the anthocyanin in wild blueberry fruit is instable to heat, the degradation of anthocyanin in wild blueberry fruit is followed first-order reaction kinetics, and the thermal degradation activation energy of anthocyanin in wild blueberry fruit is 27.52 kJ/mol, the k_0 is 1886.35. The theoretical value and experimental value are propinquity, which indicate that the model is appropriate.

Keywords: wild blueberry fruit, anthocyanin, stability, degradation kinetics.

1 Introduction

Wild blueberry fruit have drawn special attention because of their high antioxidant capacity and high concentration of anthocyanins and other phenolic compounds, which labels the fruit as one of the most desirable and nutritious among fresh fruits and vegetables[1-5]. The seductive color of wild blueberry fruit is most decided by anthocyanin.

Colour is an important attribute related to the visual appeal and the quality of food products [6-7]. Due to increasing concerns about the safety of synthetic colorants, the use of natural sources of colorants has been considered [8-9]. Anthocyanins, a group of phenolic compounds widely found in the plant kingdom, are responsible for the orange, red, violet and blue colours observed in nature[10]. Whereas, anthocyanin is unstable material, it can facile occur chemical changes during produce and store, accordingly degradation or polumerization. The color of wild blueberry fruit alcohol and beverage are lighten during machining and store, and effect the quality of products. It is improtant to study the stability and the rule of change of anthocyanin which is extracted from wild blueberry fruit. The maths model has been established for the relation between the change of color and store life according to the dynamics theory of chemistry reaction [11-12]. It can forecast the store life and shelf life in point of temperature.

The thermal degradation of the anthocyanins has been studied for strawberry [13], black raspberry [14], raspberry [15], concord grape [16], plum [17] and sour cherry [18].

* Corresponding author.

E. Zhu and S. Sambath (Eds.): Information Tech. and Agricultural Eng., AISC 134, pp. 539–546.
springerlink.com © Springer-Verlag Berlin Heidelberg 2012

The objectives of this study was the stability of anthocyanin which had been extracted from wild blueberry fruit, deducted the dynamics equation of thermal degradation, established the dynamics model of thermal degradation of anthocyanin. It was provide theroy foundation of control the degradation of anthocyanin and prolong the store life.

2 Theory of Dynamics

The quality of food could described by the speed of change of quality factor (Q), such as color, hardness, solid content and so on. The Q can be described using the following equations:

$$-d[Q]/dt = k[Q]n \tag{1}$$

where [Q]is the concentration of quality factor after t hours. n is reaction series. k is the constant of change speed. t is the store life.

The relation between quality of most food and time were present zero-order or one level reaction, namely n＝0 or n＝1. The dynamics equations expression are:

Zero-order reaction:

$$[Q] = -k_0t + [Q_0] \tag{2}$$

First-order reaction:

$$\ln[Q] = -kt + \ln[Q_0] \tag{3}$$

where $[Q_0]$is the initial concentration of of quality factor during store or machining. k is the constant of change speed. t is the store life.

Arrhenius prove that the equation of k and T is:

$$k=k_0 \cdot \exp(-Ea/RT) \tag{4}$$

where k0· is the constant of equation. Ea is the activational energy (kJ/mol). reaction series. R is the constant of gas, 8.314 J/(mol·K). T is the absolute temperature.

K is given as follows:

$$d[Q]/dt = k[Q]n = k_0 \cdot \exp(-Ea/RT) \cdot [Q]n \tag{5}$$

In order to obtain the dynamic equation, quadrature of equation (5) , system (5) becomes:

$$[Q] = k_0 \cdot \exp(-Ea/RT) \cdot t \tag{6}$$

A model which can predict the changes of food quality during store life. The left of equation is the function of quality, and the right of equation is time or temperature of store.

The objective of this paper was to study the effect of temperature on the stability of aqueous anthocyanin extracts from wild blueberry fruit.

3 Materials and Mehtods

3.1 Materials

Wild blueberry fruit was collected from Jiagedaqi in Heilongjiang province in summer 2010 year. The fruiteries were achieved the normal collect maturity. The surface of wild blueberry fruit was clean, and the juice was extracted by juicing extractor. The wild blueberry fruit juice was got the supernatant and filtrated after clarified for 24h in 4℃. Other chemicals and reagents were analytical grade.

3.2 Pretreatment of Wild Blueberry Fruit Juice

Anthocyanins was extracted from the whole fruit of wild blueberry fruit samples by water in 25, 50, 60, 70, 80℃constant temperature water bath. About 5 g of fresh blueberry samples and 30 ml of water solution were added to a tube with a screw cap and grounded by polytron. Nitrogen was used to flush the air out of the tube. The mixture (total volume of 30 ml) was placed in the dark for 10 h. After sonication for 15 min, the samples were centrifuged at 2000 r/min for 10 min. The supernatants were again centrifuged at 5000 r/min for 20 min. [19]

3.3 Anthocyanins Assay

Anthocyanins was analysed according to the method of Giusti and Wrolstad [17].

3.4 D. kinetic of Anthocyanin Degradation

The degradation kinetics of most biological materials and color of food system follow the zero-order equation (2) or first-order equation (3) reaction [20]. Furthermore, half-life value $t_{1/2}$ of total anthocyanin content was calculated as $t_{1/2} = \ln 2/k$; D-value (the time required for the degradation of 90% anthocyanin) was also calculated as $D = 1/k$ [21].

3.5 Statistical Analysis

All data were expressed as means ± standard deviation (SD) from at least three independent experiments.

4 Results and Discussions

4.1 Kinetics of Anthocyanin Degradation During Heating

The contents of wild blueberry fruit extracts showed significantly low stabilities at 50, 60, 70, 80℃ ($P < 0.05$) (Fig. 1). The stabilities at higher temperature were lower than lower extracts. Nevertheless, there was insignificantly decrease at 25℃ (data not shown).

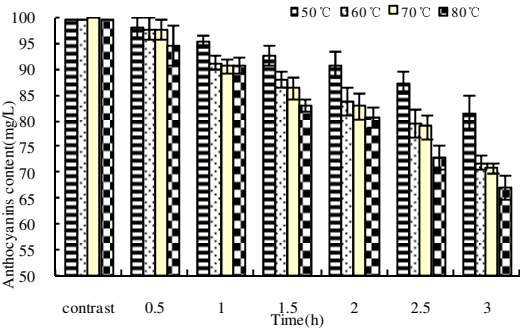

Fig. 1. Effect of heating on anthocynin in wild blueberry fruit at 50, 60, 70, 80℃. Vertical lines represent the SD (n = 3).

For eliminate the error which produce from hot conduction, the time of 0.5 h was the initial time, calculate the -ln(*C*/*C*0) (where the Co is the initial content of anthocyanins at 0.5h, and the *C* is the content of anthocyanins at 1, 1.5, 2, 2.5 and 3 h, respectively). Line regression was carried out at different temperature. The equation and R^2 were shown in Table 1. The R^2 of different equation were 0.9999, 0.9955, 0.9995 and 0.9974 at 50, 60, 70, 80℃, respectively. It were well line relation between calefaction time and -ln(*C*/*C*0).the thermal degradation of the anthocyanins corresponded to first-order kinetics.

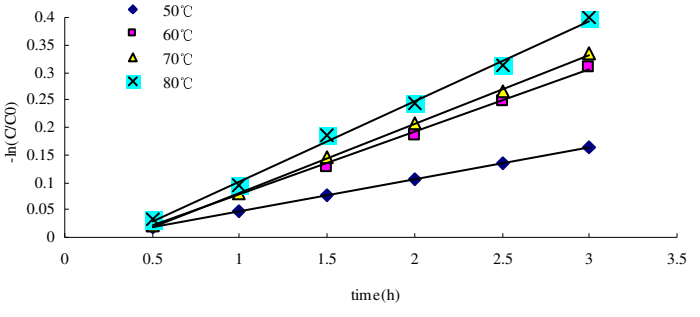

Fig. 2. Retention rates of anthocyanins in wild blueberry fruit at different temperatures

Table 1. Line regression and R^2 of Wild blueberry fruit anthocyanins at different temperture

Time	Line regression	R^2
50℃	y=0.0577x-0.0011	0.9999
60℃	y=0.11297x-0.0347	0.9955
70℃	y=0.12537x-0.0434	0.9995
80℃	y=0.14527x-0.0425	0.9974

The k values, k_0 value and E_a obtained for extract followed an Arrhenius relationship with temperature. It could been calculated from equ. 3 and equ.4. The E_a was 27.52 kJ/mol of wild blueberry fruit anthocyanins at different temperature. Higher E_a is associated to increased temperature dependence of the wild blueberry fruit anthocyanins degradation rate. K_0 values were much lower (lower k values) indicating that the wild blueberry fruit anthocyanins extracts were more stable. Therefore, the stabilities were decreased at 80℃ than 50℃.

Thermal degradation of wild blueberry fruit anthocyanins leads to colour loss and appearance of brown coloured compounds[22] but the precise mechanism is still unclear. However, possible events include chalcone formation as first step in the process[13], loss of glycosyl moieties and a-diketone formation[23]. In addition, formation of end products including coumarin derivatives [24-25], benzoic acid derivatives[26] and trihydrobenzaldehyde Furtado, Figueiredo *et al* has been reported[27]. In the present study, wild blueberry fruit anthocyanins degradation involves in part polymerization and brown pigment formation.

The kinetic parameters of anthocyanins degradation at selected temperatures are shown in Table 2 The rate constant increased at higher temperatures. This could be explained by the assumption that high temperature accelerated the anthocyanin degradation[28]. As found by Kırca *et al*[29], temperature had a strong influence on the degradation of anthocyanins in wild blueberry fruit anthocyanins. Increasing temperature from 50 to 80 ℃ increased the degradation rates of anthocyanins. Also, Wang and Xu [30]indicated that degradation of blackberry anthocyanins follows first-order reaction kinetics and variation of degradation rate constants with temperature obeyed the Arrhenius relationship.

Table 2. Kinetic parameters for the thermal degradation of wild blueberry fruit anthocyanins during storage at 50, 60, 70 and 80 °C

Time	k	$t_{1/2}$	D-value
50℃	0.0577	12	17.33
60℃	0.11297	6.14	8.852
70℃	0.12537	5.53	7.96
80℃	0.14527	4.77	6.88

4.2 The Forecast Model of Wild Blueberry Fruit Anthocyanins during Store Life

According to the change of content of wild blueberry fruit anthocyanins, the equ 3 could becomes:

$$[Q]=k0\bullet\exp(-Ea/RT)\bullet t=kt=\ln[Q0]-Ln[Q] \tag{7}$$

$$t=\frac{\ln C_0-\ln C}{k_o\bullet\exp(-Ea/RT)} \tag{8}$$

When Ea=27.52kJ/mol, k_0=1886.35, R=8.314J/(mol/K), the eqution 8 was becames:

$$t = \frac{\ln C_0 - \ln C}{1886.35 \bullet \exp(-2752/T)} \tag{9}$$

Where was the forecast model of wild blueberry fruit anthocyanins during store life.

Applicated the equation 9 to forecast the half life of wild blueberry fruit anthocyanins at 4, 20, 30, 40℃. It were 41.43,27.61, 19.16, 11.35 d. Store the 102 mg/mL wild blueberry fruit anthocyanins in 4, 20, 30, 40℃, respectively, after 41d, 27d, 19d and 11d, the content of wild blueberry fruit anthocyanins were 55.90, 55.21, 54.67 and 53.05 mg/mL, The results were approach to the half of the initial value. It was indicated that the dunamics degradation equation accord with actual result.

5 Conclusions

The results from the present study provide detailed information regarding the changes in kinetic stability of aqueous anthocyanins extracts from wild blueberry fruit as affected by temperature during manufacturing. In this study we determined first-order thermal degradation parameters, such as, k-values, k_0-values and activation energy. The degradation of wild blueberry fruit anthocyanins at different tempernature were studied. The results from this study provide additional key information characterizing the stability and the changes in visual colour of aqueous anthocyanins from wild blueberry fruit, to predict their stability during storage. These results strengthen the potential use of wild blueberry fruit as natural colouring agents with added functional value for the food industry.

References

1. Koca, I., Karadeniz, B.: Antioxidant properties of blackberry and blueberry fruits grown in the Black Sea Region of Turkey. Scientia Horticulturae 121, 447–450 (2009)
2. Barnes, J.S., Nguyen, H.P., Shen, S., Schug, K.A.: General method for extraction of blueberry anthocyanins and identification using high performance liquid chromatography–electrospray ionization-ion trap-time of flight-mass spectrometry. Journal of Chromatography A 1216, 4728–4735 (2009)
3. Lohachoompol, V., Mulholland, M., Srzednicki, G., Craske, J.: Determination of anthocyanins in various cultivars of highbush and rabbiteye blueberries. Food Chemistry 111, 249–254 (2008)
4. Wang, W.D., Xu, S.Y.: Degradation kinetics of anthocyanins in blackberry juice and concentrate. Journal of Food Engineering 82, 271–275 (2007)
5. Du, Q., Zheng, J., Xu, Y.: Composition of anthocyanins in mulberry and their antioxidant activity. Journal of Food Composition and Analysis 21, 390–395 (2008)
6. Bridle, P., Timberlake, C.F.: Anthocyanins as natural food colours –Selected aspects. Food Chemistry 58, 103–109 (1997)
7. Markakis, P.: Stability of anthocyanins in foods. In: Markakis, P. (ed.) Anthocyanins as food colors, p. 163. Academic Press, New York (1982)
8. Francis, F.J.: Food colorants: anthocyanins. Critical Reviews in Food Science and Nutrition 28, 273–314 (1989)

9. Jackman, R.L., Yada, R.Y., Tung, M.A.: A review: separation and chemical properties of anthocyanins used for their qualitative and quantitative analysis. Journal of Food Biochemistry 11, 279–308 (1987)
10. Kader, F., Irmouli, Mazza, G., Miniati, E.: Anthocyanins in fruits, vegetables and grains, p. 362. CRC Press, Boca Raton (1993)
11. Maskan, M.: Production of pomegranate (Punica granatum L.) juice concentrate by various heating methods: colour degradation and kinetics. Journal of Food Engineering 72, 218–224 (2006)
12. Goula, A.M., Adamopoulos, K.G., Chatzitakis, P.C., et al.: Prediction of lycopene degradation during a drying process of tomato pulp. Journal of Food Engineering 74, 37–46 (2006)
13. Markakis, P., Livingstone, G.E., Fillers, G.R.: Quantitative aspects of strawberry pigment degradation. Food Research 22, 117–130 (1957)
14. Daravingas, G., Cain, R.F.: Thermal degradation of black raspberry anthocyanin pigments in model systems. Journal of Food Science 33, 138–142 (1968)
15. Tanchev, S.S.: Kinetics of the thermal degradation of anthocyanins of the raspberry. Zeitschrift für Lebensmittel Untersuchung und Forschung 150, 28–30 (1972)
16. Calvi, J.P., Francis, F.J.: Stability of Concord grape (V. Labrusca) anthocyanins in model systems. Journal of Food Science 43, 1448–1456 (1978)
17. Raynal, J., Moutounet, M.: Intervention of phenolic compounds in plum technology. 2. Mechanisms of anthocyanin degradation. Journal of Agriculture and Food Chemistry 37, 1051–1053 (1989)
18. Cemeroğlu, B., Velioğlu, S., Isik, S.: Degradation kinetics of anthocyanins in sour cherry juice and concentrate. Journal of Food Science 59, 1216–1217 (1994)
19. Huang, Z., Wang, B., Williams, P.A., Pace, R.D.: Identification of anthocyanins in muscadine grapes with HPLC-ESI-MS. LWT -Food Science and Technology, 1–6 (2008)
20. Maskan, M.: Production of pomegranate (Punica granatum L.) juice concentrate by various heating methods: color degradation and kinetics. Journal of Food Engineering 72, 218–224 (2006)
21. Zhang, Y., Hu, X.S., Chen, F., Wu, J.H., Liao, X.J., Wang, Z.F.: Stability and color characteristics of PEF-treated cyanidin-3-glucoside during storage. Food Chemistry 106, 669–676 (2008)
22. Starr, M.S., Francis, F.J.: Oxygen and ascorbic acid effect on the relative stability of four anthocyanin pigment in cranberry juice. Food Technology 22, 1293–1295 (1968)
23. Markakis, P., Livingston, G.E., Fellers, C.R.: Quantitative aspects of strawberry pigment degradation. Journal of Food Science 22, 117–130 (1957)
24. Adams, J.B.: Thermal degradation of anthocyanin with particular reference on 3 glucosides of cyanidin. In acidified aqueous solution at 100°C. Journal of the Science of Food and Agriculture 24, 747–762 (1973)
25. Hrazdina, G.: Reactions of anthocyanidin-3,5-diglucosides: Formation of 3,5-di-(O-b-D-glucosyl)-7-hydroxy coumarin. Phytochemistry 10, 1125–1130 (1971)
26. Jackman, R.L., Smith, J.L.: Anthocyanin and betalains. In: Hendry, G.A.F., Houghton, J.D. (eds.) Natural Food Colorants, pp. 249–309 (1996)
27. Seeram, N.P., Bourquin, L.D., Nair, M.G.: Degradation products of cyanidin glycosides from tart cherries and their bioactivities. Journal of Agricultural and Food Chemistry 49, 4924–4929 (2001)

28. Furtado, P., Figueiredo, P., Chaves, H., Chaves das Neves, H., Pina, F.: Photochemical and thermal degradation of anthocyanidins. Journal of Photochemistry and Photobiology, A: Chemistry 75, 113–118 (1993)
29. Kırca, A., Özkan, M., Cemeroĝlu, B.: Effects of temperature, solid content and pH on the stability of black carrot anthocyanins. Food Chemistry 101, 212–218 (2007)
30. Wang, W.D., Xu, S.Y.: Degradation kinetics of anthocyanins in blackberry juice and concentrate. Journal of Food Engineering 82, 271–275 (2007)

A Preliminary Study on Activity Mechanism and Identification of an Extract of Pharbitis Purpurea Seeds against Tetranychus Cinnabarinus

Juan Du[1], Lei Zhao[1], Lan-qing Ma[1], Yu-bo Liu[1], Guang-lu Shi[1], You-nian Wang[1,*], and Bao-sheng Tong[2]

[1] Key Laboratory of Urban Agriculture (North) of Ministry of Agriculture, P.R. China
Beijing University of Agriculture, Beijing, China
[2] Inn Mongolia Yongye Biotechnology Co., Ltd.
Neimenggu, China
glshi@126.com

Abstract. The isolation fraction 8 of petroleum ether extract of Pharbitis purpurea (P. purpurea) seeds was identified and its action mechanism against Tetranychus cinnabarinus (T. cinnabarinus) was initially investigated. Thin-layer chromatography (TLC) was used to measure purity of the isolation fraction 8. Ultraviolet (UV) and infra-red (IR) spectrum, nuclear magnetic resonance (NMR), gas chromatography and mass spectrum (GC-MS) were used to identify the main component of the isolation fraction 8. The influence of several kinds of enzyme activity such as glutathione-S-transferase (GSTs), acetylcholine esterase (AChE), mono-amine oxidase (MAO) and ATPase in body of T. cinnabarinus was tested with the biochemical method. Results showed that the isolation fraction 8 was the methyl linoleate. The methyl linoleate could activate GSTs in T. cinnabarinus. The isolation fraction 8 had strong toxic effect on T. cinnabarinus because it could inhibit in various degrees AChE, MAO and ATPase related to nervous system, which might lead to blocking neurotransmission and the death of mites. So, P. purpurea seeds have better development prospects that the methyl linoleate is regarded as new pesticide.

Keywords: Pharbitis purpurea, Tetranychus cinnabarinu, Methyl linoleate, Glutathione-S-transferase, Acetylcholine esterase, Mono-amine oxidase, Ca2+-ATPase, Na+, K+-ATPase.

1 Introduction

T. cinnabarinus is recognized world-wide as the most difficult prevention biotic community, because of its character such as small in size, breeding fast, numerous ages, adaptable, serious harm and etc [1, 2]. It can damage over one hundred kinds of crops and fruit trees, seriously affecting their yields and qualities [3]. Repeatedly using

* Corresponding author.

E. Zhu and S. Sambath (Eds.): Information Tech. and Agricultural Eng., AISC 134, pp. 547–556.
springerlink.com © Springer-Verlag Berlin Heidelberg 2012

non-specificity chemical acaricide in a large amount has made a lot of mites produce drug resistance and presented the mutual resisting to acaricides [4, 5]. In the meantime, when chemical acaricides were used to kill mite, the natural enemies and other beneficial organisms were destructed simultaneously. Thus, it destroys the ecological balance, causing mite rampant and resulting in a vicious cycle in using chemical pesticide. So, it already becomes an important subject to find new, high-efficient and safe acaricide. Identification and investigation of natural acaricide is one of them. According to the literature of *Ahmed* in 1985 [6], more than 1,600 kinds of higher plant had already been reported for controlling the harmful organism in the whole world. 1,005 kinds among them had the activity killing worm. 39 kinds among them had the activity of acaricide that mainly included the alkaloid, citrin, flavone compound, plant essential oil and etc. Because natural acaricides have little environmental pollution, difficult to form drug resistance, safe to beneficial organisms and etc., natural acaricides is becoming a research focus [7-12].

In this study, thin-layer chromatography (TLC) was used to measure the purity of activity substance against *T. cinnabarinus* in the isolation fraction 8 of *P. purpurea* seeds. The structure of the substance was analyzed and identified with UV, IR, NMR, GC-MS and etc. The main component of the isolation fraction 8 was initially identified as methyl linoleate. Further, biochemical method was adopted to research the effects of the main component on several kinds of enzyme activity such as GSTs, AChE, MAO and ATPase in *T. cinnabarinus.* The preliminary study about action mechanism of methyl linoleate could offer the theoretical basis for developing new safe, effective and environmentally acaricides.

2 Materials and Methods

2.1 Materials

The *T. cinnabarinus* were susceptible strain by indoor breeding at the conditions of temperature (25±1) ℃, Relative humidity (RH =50±10) % and Light (L: D=18h: 6h).

The silica gel GF254 was purchased from the Marine Chemical Plant of Qingdao. Methyl linoleate, 1-chloro-2, 4-dinitrobenzene (CDNB), 2-nitro benzoic acid (DTNB) and physostigmine were purchased from Shanghai Branch of Sigma Company. Coomassie Brilliant Blue G-250, Glutathione (GSH), Acetylcholinesterase (AChE), Benzyl amine, Ca^{2+}-ATPase and Na^{+}, K^{+}-ATPase were purchased from Science and Technology Co., Ltd. Nanjing Jiancheng. Phosphate-buffered saline (Na_2HPO_4=1.74 g, KH_2PO_4=0.68 g, pH=6.5) were prepared in 100 ml water.

Spectrophotometer was purchased from General Analysis of Beijing General Instrument Co., Ltd. the model number was TU-1800. NMR was purchased from Japan Electronics Co., Ltd. and the model number was JNMECA600. GC-MS was purchased from Agilent United States and the model number was 5975B.

2.2 Methods

Preliminary Identification of the Isolation Fraction 8 Purity

The purity of the isolation fraction 8 was identified by TLC. The isolation fraction 8 was added on silica gel GF254 thin-layer plate using 0.05 mm capillary. Chloroform was used as spreading agent. When spreading distance reached 5 cm, the plate was

taken out and dried in shade. The sample was colored in saturated iodine vapor and the spots were counted. Finally along the perpendicular direction, the sample was spread again and the spots were counted again. If the chromatography plate showed multiple spots, they were regarded as mixtures. If single spots were shown, they were regarded as pure product.

The whole spectral analysis of wave band was carried with UV spectrophotometer. The isolation fraction 8 was diluted with chloroform and measured the greatest absorption peak with UV spectrophotometer. Chloroform was used as blank control.

Special group was detected with IR spectrum. Sample and KBr were mixed and pushed on slice. The liquid sample directly spread on slice. The absorbing peak of IR was measured with the range 400 cm^{-1} – 4,000 cm^{-1}, limit 85 cm^{-1} and precision ± 2 cm^{-1}. According to the IR absorbing peak judge what special group the compound contained.

NMR spectrum ^{1}H NMR and ^{13}C NMR were determined with JNMECA600 NMR instrument. Deuterated chloroform ($CDCl_3$) and tetramethylsilane (TMS) were used as internal standards. Data of spectrum were recorded in 600.17 MHz and 150.91 MHz.

Gas chromatography conditions: Quartz capillary column HP2FFAP (30 m × 0.25 mm, 0.25 μm). Temperature of the procedure rose from 150 ℃ and then kept 3 min. it was raised to 250 ℃ at 6 ℃/min and then kept 5 min. Loading gas was He. The flux of column was 1.0 ml/min. The temperature of injection port was 250 ℃. The split ratio was 50: 1.

Mass spectrum condition: EI source. Voltage of ionization was 70 eV. Temperature of ion source was 230 ℃. Scan range was 10 amu - 500 amu. Injection volume was 1.0 μl.

Analysis of Action Mechanism Killing Mites about the Isolation Fraction 8

Preparation of Enzyme Solution

The 500 tested female grown mites were taken at 4, 8, 12, 16, 20, 24 h, respectively, after treated with the isolation fraction 8. The normal saline 0.25 ml was added into the sample. The sample was homogenized on ice and then centrifuged at 10,000 r/min at 4 ℃ for 15 min. The supernatant was taken for future test.

Measure of Protein Content

Coomassie Brilliant Blue G-250 was used for determining the protein content [13]. Enzyme solution 0.05 ml was added into measuring tube. Distilled water 0.05 ml was added into control tube and standard sample 0.05 ml into standard tube. Coomassie Brilliant Blue G-250 reagent 3ml was added into three tubes, respectively. Mixed well and kept standing for 10min. *OD* value was determined at 595 nm. The experiments were repeated 3 times and the protein content was calculated.

Measure of GSTs

2.5 ml 66 mmol phosphate buffer, 0.2 ml 50 mmol GSH and 0.05 ml 30 mmol CDNB were mixed rapidly as control. 0.1 ml enzyme solution was added into the above solution as sample. The concentration of substrate GSH was used to reflect GSTs activity. *OD* value was determined at 340 nm at 27 ℃. The experiments were repeated 3 times.

Measure of AChE
According to He Yu Xian's method [14], AChE was used as substrate. DTNB was used as chromogenic agent. Physostigmine was used as inhibitor. They were kept at 27 ℃ for 15 min. 0.3 ml 1 mmol physostigmine was added into terminate the reaction. *OD* value was determined at 412 nm and repeated 3 times.

Measure of MAO
Benzylamine, the specific substrate of MAO, was used as reaction substrate to determine the producing amount of benzyl aldehyde. The optical absorbance after enzyme reaction was determined using the principle that benzyl aldehyde has absorbing peak at 242 nm of ultraviolet region. The experiments were repeated 3 times and the enzyme activity of MAO was determined. The enzyme activity was determined as amount of generating MAO.

Measure of Ca^{2+}-ATP Enzyme
According to Liu Su Yuan's method [15], *OD* value was determined at 636 nm. The experiments were repeated 3 times. The enzyme activity was expressed as the content of inorganic phosphorus generated by ATP enzyme to decompose ATP in tissue per mg protein per hour.

3 Results

3.1 Identification of the Isolation Fraction 8

The result of TLC showed that along the diagonal of two-dimensional chromatography plate only showed one yellow spot. The isolation fraction 8 was initially determined as high purity.

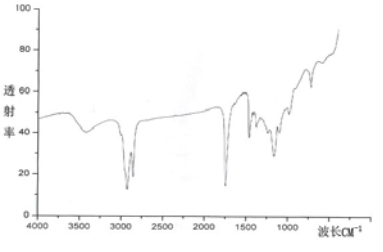

Fig. 1. IR of fraction 8

Whole spectrum analysis result of UV showed that the isolation fraction 8 existed the most absorb peak at 224 nm. The result of IR spectrum was shown in Fig. 1. There was absorption at 1,731 cm^{-1} of visible light, which indicated the vibration of carbonyl ν(C=O). The absorption at 1,053 cm^{-1} showed that C_n (n≥4) had 7 carbons at least on the straight chain alkane. The stronger absorption at 2,912 cm^{-1} showed that it contained -CH_2 long chain.

The analyzing data of hydrogen and carbon spectrum from GC-MS and NMR were shown in Fig. 2, 3, 4. ^{1}H NMR ($CDCl_3$, 600 MHz) δ: 5.37 (1H, dd, J_1=15.7, H-9'), 5.344 (1H, dd, J_1=15.7, H-10'), was a pair of bonds in reverse. A lot of protons among 4.24 (3H, m, H-1), 2.76 (2H, t, J=7.5, H-8', H-11'), 2.33 (2H, t, J=7.5, H-2'), 1.6 (2H, t, J=7.2 Hz, H-3'), 1.3-1.2 were the signal of H in saturated CH_2. 0.88 (3H, t, J=6.3 Hz, H-18'); ^{13}C NMR (150 MHz, CDCl3) δ: 173.4 (C-1'), 34.3 (C-2'), 29.6 (C-3'), 31.2 (C-4'), 27.4 (C-5'), 127.7 (C-6'), 128.3 (C-7'), 33.1 (C-8'), 130.2 (C-9'), 128.2 (C-10'), 62.3 (C-11'), 29.6 (C-12'), 29.3 (C-13'), 27.8 (C-14'), 31.3 (C-15'), 29.5 (C-16') , 22.7 (C-17'), 14.3 (C-18'), 31.8 (C-19'), 32.1 - 29.3 were the signal of many C in saturated CH_2.

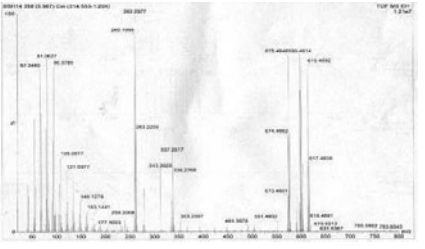

Fig. 2. GC-MS of Fraction 8

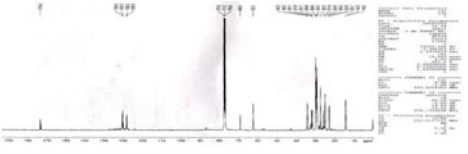

Fig. 3. ^{13}C NMR of Fraction 8

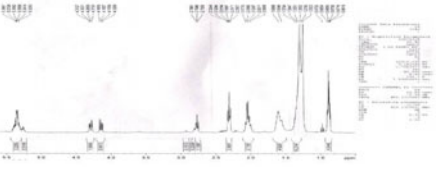

Fig. 4. ^{1}H NMR of Fraction 8

To sum up, according to spectral analysis of UV, IR, GC-MS, ^{1}H NMR, ^{13}C NMR, the isolation fraction 8 was initially identified as methyl linoleate and the molecular formula was $C_{19}H_{34}O_2$.

3.2 Effects of Methyl Linoleate on Several Kinds of Enzyme Activity in T. Cinnabarinus

In order to study whether methyl linoleate activated the enzyme related to protein synthesis. The effect of the methyl linoleate on protein contents in *T. cinnabarinus* was analyzed. The result was shown in Fig.5. The protein contents in *T. cinnabarinus* treated by the isolation fraction 8 were higher than that of control. During of treating for 4 h – 8 h, the treatment group showed an upward trend in protein contents. During of 8 h – 12 h, control began to drop, while treatment group still kept an upward trend in protein contents and till 12 h it slightly decreased followed by sharp rise after 20 h. Generally, protein contents of treatment group were higher than that of control. Methyl linoleate might have activated enzyme related to protein synthesis.

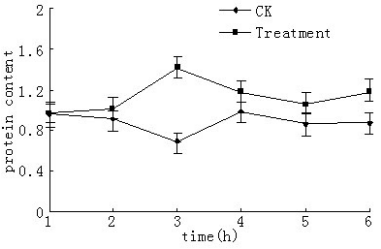

Fig. 5. Effect of methyl linoleate to protein content of *T. cinnabarinus*

The effect of the methyl linoleate on GSTs activity was shown in Fig. 6. After the isolation fraction 8 treatment 4 h, the activity of GSTs in *T. cinnabarinus* increased first, then decreased followed by increase. The treated group activity was far greater than the control group. Especially treatment for 8 h, the control group activity was less than 60% of the treated group. After 20 h, GSTs' activity increased again. GSTs was an important detoxification enzyme in organisms. It was a primary metabolize and secondary metabolize enzyme in insect. The methyl linoleate might cause accumulation of something in *T. cinnabarinus* and the detoxification metabolize was inhibited. So, the activity of GSTs decreased.

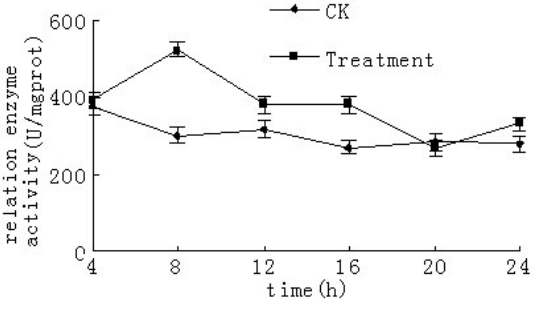

Fig. 6. Effect of methyl linoleate to GSTs of *T. cinnabarinus*

The effects of the methyl linoleate on AChE activity was shown in Fig. 7. After the isolation fraction 8 treatments, the AChE activity showed went up first, and then decreased in the overall. The activity in the treatment group was higher than that in the control in a short time at the beginning, and the activity was lower than that in the control at the other time. There existed the most significantly difference between treatment group and control group on 16h, and the treated group activity was only 23% of the control group. This showed that the AChE activity was obviously inhibited by the isolation fraction 8. So, AChE might be one of important target of the methyl linoleate in *T. cinnabarinus.*

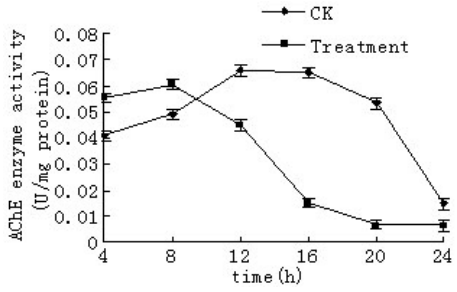

Fig. 7. Effect of methyl linoleate to AChE of *T. cinnabarinus*

The effects of the methyl linoleate on MAO activity was shown in Fig. 8. The MAO activity trends all declined in the overall within 24 h of the isolation fraction 8 treatments. From 4 h to 12 h, it was not obvious that the isolation fraction 8 affected MAO. However, there was obviously declined after 12 h. It indicated that the methyl linoleate caused a certain degree of inhibition on MAO.

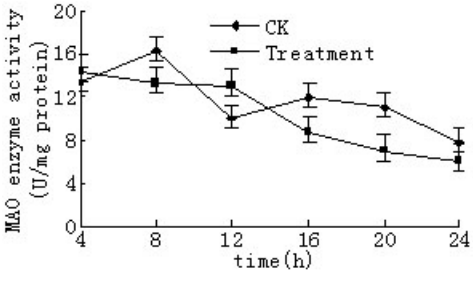

Fig. 8. Effect of methyl linoleate to MAO of *T. cinnabarinus*

The effects of the methyl linoleate on Ca^{2+}-ATPase activity was shown in Fig. 9. From 4 h to 8 h, the trends of the treatment group always increased, while the control group always decreased. The treatment group decreased sharply after 8 h, while the control group increased slowly after 16h. Generally, it was obvious that the methyl linoleate inhibited the Ca^{2+}-ATPase activity in *T. cinnabarinu*s.

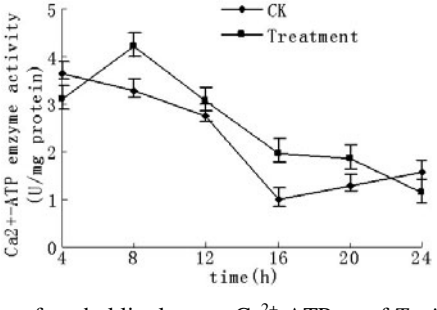

Fig. 9. Effect of methyl linoleate to Ca^{2+}-ATPase of *T. cinnabarinus*

The effects of the methyl linoleate on Na^+, K^+-ATPase activity was shown in Fig.10. The basically trends of the treatment group and control group were similar. The treatment group showed obvious fluctuation, while the tendency of the control group always flat. This trend continued till 24 h and two enzymes arrived to their tiptop. Overall compared with the control, the Na^+, K^+-ATPase activity was inhibited in various degrees by the isolation fraction 8.

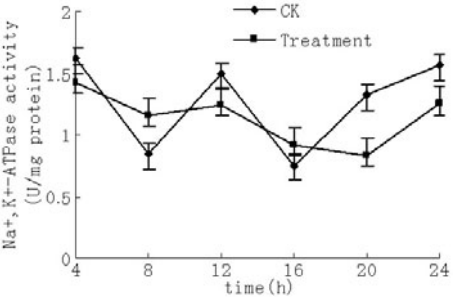

Fig. 10. Effect of methyl linoleate to Na+, K+-ATPase of *T. cinnabarinus*

4 Discussion

The isolation fraction 8 from extract of *P. purpurea* seeds was the methyl linoleate and it may affect GSTs activity in *T. cinnabarinus.* GSTs is an important conjugate enzyme to metabolize toxic substances from exogenous organisms. It can catalyze conjugation of pro-electron-donating groups between endogenous GSH and substrate. Specially, GST plays an important role in detoxification metabolize of many organophosphorous pesticides. When external sources of toxic substances go into the organisms, GSTs participates in detoxification metabolize by two ways of hydrolyzed and conjugated proteins to decompose the external sources of toxic substances. According to test results, the methyl linoleate can stimulate GSTs activity in *T. cinnabarinus* and plays detoxification function. It indicates that the methyl linoleate may specifically combine with something in *T. cinnabarinus* and change its activity structure, which can reduce detoxification metabolize and cause toxicities and death.

The methyl linoleate plays a lethal role through interfering nerve function. Research shows that most acaricides play a lethal role through interfering nerve function [16]. Analyzing the effects results of several enzymes related to nervous system, the methyl linoleate obviously inhibits AChE and MAO activity. For example, AChE is a kind of hydrolytic enzyme related to nervous system. AChE acts on nervous system to hydrolyze acetyl choline and makes it form acetic acid and choline. As neurotransmitter, acetyl choline enters into synaptic cleft, which needs to be eliminated after finishing physiological function for keeping neurotransmission continuance. Conversely, accumulation of acetyl choline may cause over-exciting of postsynaptic membrane blocking normal neurotransmission, causing abnormal reaction of nerve conduction, till eventually blocking the synaptic transmission. Once the enzyme is inhibited to some extent, the insects will die because of over-exciting. So, the methyl

linoleate has evident role on several enzymes related to nervous system in *T. cinnabarinus*, which may block the synaptic transmission and cause death of mites. It needs further research whether the methyl linoleate is nerve poison and on deep research to its toxicity.

P. purpurea seeds have already got very extensive study and application in the medical field and display great potentiality to be exploited. In recent years, some researches indicate that the petroleum ether extract of *P. purpurea* seeds has the function of killing worm and bacteriostatic. It is obvious that *P. purpurea* seeds has value of developing very much too in agriculture. Therefore, from angle of long-term development, this study has utilized fully existing plant resources to develop biological, environmentally and botanical acaricide, which offers the theoretical foundation and technical support for the investigation of new acaricide and discovery of guide compound.

Acknowledgements. The work was financially supported by the National Natural Science Foundation of China (30872029), the Key Natural Science Foundation of Beijing Municipality (6071001), the Natural Science Foundation of Beijing Municipality (6092007), the Key Foundation of Beijing Municipal Education Committee (KZ201010020016), and Funding Project for Academic Human Resources Development in Institutions of Higher Learning Under the Jurisdiction of Beijing Municipality (PHR20090516, PHR200906134).

References

1. Hazan, A., Gerson, U., Tahori, A.S.: Spider mite webbing I. The production of webbing under various environmental conditions. Acarologia 16, 68–84 (1974)
2. He, L., Yang, Y., Fu, J.Z., et al.: Resistance selection and relative fitness of Tetranychus cinnabarinus (Boisduval)to abamectin. Acta Phytophylacica Sinica 31, 395–400 (2004)
3. Ho, C.C., Lo, C.C., Chen, W.H.: Spider mite (Acari:Tetranychidae) on various crops in Taiwan. J. Agr. Res. China 46, 333–346 (1997)
4. Tang, C.C., Li, Y.X., Chen, B., et al.: Pesticide chemistry, vol. 3, p. 225. Nankai University Press (1998)
5. Wang, X., Gao, X.W., Zheng, B.Z.: Investigation on insecticide resistance of diamondback moth. World Agriculture 223, 27–29 (1997)
6. Zhao, S.H.: Chemoproection of plant, vol. 1, p. 303. China Agriculture Press (2001)
7. Wang, Y.N., Miao, P.F., Cao, H., et al.: Effect of Extracts of Leaves of Juglans regia to Several Enzyme Systems in Tetranychus cinnabarinus. Acta Horticulturae Sinica 34, 1297–1300 (2007)
8. Cao, H., Wang, Y.N., Liu, S.Q., et al.: Effect of Extracts of Kochia scoparia to Several Enzyme Systems in Tetranychus viennensis. Scientia Silvae Sinicae 43, 68–72 (2007)
9. Shi, G.L., Wang, Y.N., Wang, H.L., et al.: Effect of Tagetes erecta on glutathiong-S-transferase and protease activities and protein content in Tetranychus viennensis. Chinese Journal of Applied Ecology 183, 400–404 (2007)
10. Wang, H.X., Shen, Z.J., Du, J., et al.: Insecticidal Activity of Juglans regia Extracts against Tetranychus cinnabarinus. Scientia Silvae Sinicae 44, 16–20 (2008)
11. Dong, Y.X., Wu, W.J.: Research progress of plant insecticide toxicology. Entomological Knowledge 34, 112–116 (1997)

12. Ren, X.X., Han, Z.J., Wang, Y.C.: Cloning and sequence analysis of a DNA fragment encoding acetylcholinesterase in cotton bollworm. Acta Zoologica Sinica 48, 121–124 (2002)
13. Mu, L.Y.: Plant chemical protection. China Agriculture Press (1991)
14. He, Y.X., Wang, C.F., Chen, F., et al.: Effect of insecticides on esterase activity in beet armyworm. Acta Agriculture Universitis Jiangxiensis 25, 896–899 (2003)
15. Liu, S.Y., Sun, L.G., Xing, W., et al.: The effect of chronic lead exposure on hippocampal intraneuronal Ca^{2+} and activity of Ca^{2+}-ATPase in rats. Journal of Health Toxicology 13, 16–17 (1999)
16. Mark, A., Dekeyser, R.G.H.: Downer Biochemical and Physiological Targets for Miticides Pestic. Sci. 40, 85–101 (1994)
17. Wang, M.C.: Entomological Physiology, pp. 202–203. China Agriculture Press (2004)

The Effects of Lupeol from the Petroleum Ether Extract of Inula Britanica on the Biological and Enzyme Activity of Tetranychus Cinnabarinus

Lan-qing Ma, Dan-dan Duan, You-nian Wang, Jun Cheng, Yu-bo Liu, and Guang-lu Shi*

Key Laboratory of Urban Agriculture (North) of Ministry of Agriculture P.R. China
Beijing University of Agriculture Beijing, China
glshi@126.com

Abstract. The acaricidal and relative enzyme activity in Tetranychus cinnabarinus treated with petroleum ether extract of Inula britanica were studied. Our results indicated that petroleum ether extract of Inula britanica had acaricidal activities against Tetranychus cinnabarinus, and its mortality to Tetranychus cinnabarinus had reached 92.05 % at the concentration of 2mg•mL-1. After liquid chromatography and thin layer chromatography, there were 38 fractions gained in which fraction 7 had stronger toxicity than others, and its mortality to Tetranychus cinnabarinus was 92.05 %. Fraction 7 was identified as Lupeol by CG/MS, and the mortality of Lupeol to Tetranychus cinnabarinus was 66.46%. The activities of glutathione-S-transferase, Ca2+ -ATPase, SOD and protein content were assayed by colorimetric method after treatment with Lupeol. Our results showed that the activity of SOD was strongly induced whereas the activities of glutathione-S-transferase and Ca2+-ATPase were restrained, but there was little change in total protein content. These results suggested Lupeol from the petroleum ether extract of Inula britanica had acaricidal activities against Tetranychus cinnabarinus. These data provided useful information for the use of Inula britanica as a novel resource of botanical acaricide.

Keywords: Inula britanica, Petroleum, Tetranychus cinnabarinus, enzyme activity.

1 Introduction

Due to their small size, rapid reproduction, large population density, and severe damage, phytophagous mites have been recognized as harmful bio community hard to control (Zhao *et al*. 2005). *Tetranychus cinnabarinus,* attached to the Arachnida*,* Acariformes, Tetranychidae, are harmful to fruit trees, vegetables and greenhouse plants (Wang *et al*. 2008, Shen *et al.* 2008). At present, application of synthetic chemicals leads to pollution of environment. These mites are also difficult to control due to their resistance to many synthetic pesticides. So it is a very important research topic to find new effective acaricides. Some plants such as Juglans regia (Wang *et al*. 2009), *Stellera chamaejasme*

* Corresponding author.

E. Zhu and S. Sambath (Eds.): Information Tech. and Agricultural Eng., AISC 134, pp. 557–564.
springerlink.com © Springer-Verlag Berlin Heidelberg 2012

(Shi *et al*. 2004) and *Kochia scoparia* (Shi *et al*. 2006) contain acaricides, indicating that plants may be one of important sources of drugs to kill mites.

Inula britanica which is recorded in "Shen Nong Ben Cao Jing" plays an important role in the treatment of exogenous fever, difficulty in micturition, carbuncle swollen sores, eczema, *etc.* Numerous sesquiterpene compounds from *Inula britanica*, due to their cytotoxic activity, are considered as high value potential Traditional Chinese medicine. In recent years, attention has been paid to its antimicrobial activity, but there have been no reports on its acaricidal activities.

Lupeol belongs to three terpenoids, with a wide range of biological activity. Specifically, it exhibits important effects of anti-inflammatory (Geetha *et al*. 2001), anti-oxidant (Sudhahar *et al*. 2007), promoting skin healing (Naaimi *et al*. 2008) and other pharmacological activities in animal studies. However, its effect on the biological activity of *Tetranychus cinnabarinus* is not clear.

The purpose of this study was to examine the potential acaricidal activity of extracts of *Inula britanica* and to explore the mechanism of its acaricidal activity. Our results showed that Lupeol from petroleum ether extract of *Inula britanica* had strong toxicity to *Tetranychus cinnabarinus*. We also studied the effects of Lupeol on the activities of some enzymes in *Tetranychus cinnabarinus* in order to understand the specific acaricidal mechanisms of Lupeol. Our results indicated that *Inula britanica* can be exploited as new resources for developing potential acaricides.

2 Materials and Methods

2.1 Material Collections

The plants of *Inula britanica* were grounded to power, and oven-dried at 25 ℃ indoors. After passing a 60-mesh, the power was placed in the refrigerator for storage. *Tetranychus cinnabarinus*, the indoor reared susceptible strain, were feeding at room temperature of 24 ± 1 ℃, and a relative humidity of 50 ± 10 % and an ambient photoperiod of 18: 6 (L: D) h.

2.2 Preparation of Crude Extraction

The protocol for preparation of crude extraction was described previously. Briefly, the plant powder was immersed in a flask with petroleum ether for 3 - 5 d at room temperature of 25 ± 2 ℃, and the ratio of solid to liquid was 1: 5. The extracts were gained after filtering and evaporating.

2.3 Separation of the Concentrated Extracts

6 g of concentrated extract was separated into different components by using chromatography column. Based on band appearance in TLC, The extract eluted was amalgamated into 38 groups. Each group was evaporated to obtain concentrated isolate for use.

2.4 Bioassays

Acaricidal activity was measured using a slide dip technique. Mortality was determined at 24 h after treatment (FAO 1980, Shi *et al*. 2006). All the bioassays were repeated

three times. Distilled water with 1 % Tween 80 was used as a control. Mortality rates were corrected for control mortality by using Abbott formula (Abbott 1925).

2.5 Preparation of Enzyme Solution

150 mites were treated for 4, 8, 12, 16, 20 and 24 h, respectively and put into a different solution, according to the different enzymes measured and homogenized in an ice bath. The supernatant was collected by centrifugation at 10,00 r/min for 10 min at 4 ℃ (Cao H, *et al*,2003).The mites which are used to measure total protein content were put into 0.125 mL saline, while the mites which are used to determine activity of the glutathione-S-transferase were placed in the 60 mmol • L^{-1} phosphate buffer (pH 7.0).

2.6 Bradford Assay for Protein Quantification

Protein concentrations were determined using Coomassie brilliant blue (Li J *et al*. 2000). A 0.1ml enzyme solution was dropped into the tube and a 0.1ml phosphate buffer into the control tube. Solution in each tube is mixed with 5mL Coomassie brilliant blue G-250 reagent and heated in a water bath at 25 ℃ for 2min. After that, the *OD* values of them were determined at the 595 nm wavelength by the spectrophotometer. The protein content was calculated according to the standard curve.

2.7 Enzyme Activity Assay

Glutathione-S-transferase activity was determined using the method of Mu, *et al* (Mu, *et al*. 2000). One unit of enzyme activity was defined as GST concentration decreasing 1 μmol •L^{-1} in the reaction system, 1 mg tissue protein reacts one minute at 37 ℃ excluding non-enzymatic reaction.

Ca^{2+}-ATPase activity was determined using the method of Liu, *et al* (Liu, *et al*. 1999).The content of inorganic phosphorus produced by per mg tissue protein decomposed per minute presents enzyme activity.

SOD activity was determined as follows. Superoxide anions (O^{2-}) are generated by a Xanthine / Xanthine Oxidase (XOD) system. Superoxide anions can oxidize Hydroxylamine to nitrite. Nitrite appears prognoses in the chromogenic agent. The optical density (*OD*) value is determined using spectrophotometer. If SOD is in test sample, SOD can specifically inhibit Superoxide anions to reduce the product of nitrite. In colorimetric assay, *OD* value of experimental tube is below of control tube. SOD activity of test sample can be measured by formula.

3 Results

3.1 The Petroleum Ether Extract of Inula Britanica, Fraction 7, and Lupeol Affected the Biological Activities of Tetranychus Cinnabarinus

First, Bioassays were used to test the biological activities of Tetranychus cinnabarinus treated with the petroleum ether extract of *Inula britanica,* 38 fractions gained from extract and Lupeol. The petroleum ether extract of *Inula britanica*, fraction 7, and Lupeol had strong toxicity to *Tetranychus cinnabarinus* and their mortalities were 92.05 % , 85.53 % ,62.64 % , respectively (Tab. 1).

Table 1. The mortality of extracts from Inula britanica against Tetranychus cinnabarinus

Extracts(2 mg·mL^{-1})	Extraction rate/%	Mortality/%
Petroleum ether extract	1.56±0.09	92.05±1.4250
Fraction 7	0.98±0.03	85.53±1.0596
Lupeol	0.81±0.03	62.64±0.28

Values are mean ±SE of three determinations

3.2 The GC/MS Analysis of Optimal Fraction

The fraction 7 which has stronger acaricidal activities was identified by GC/MS. The results indicated that the main component of fraction 7 was Lupeol, and the matching score reached more than 90 % (Fig. 1, 2). We then choose fraction 7 for further study because of its high purity.

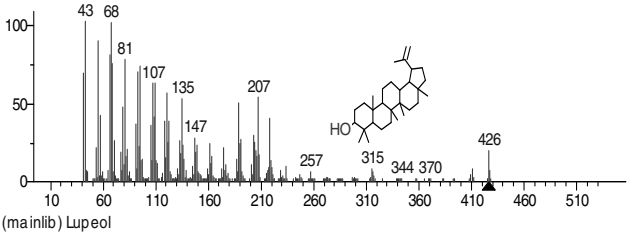

Fig. 1. GC/MS analysis of G_7

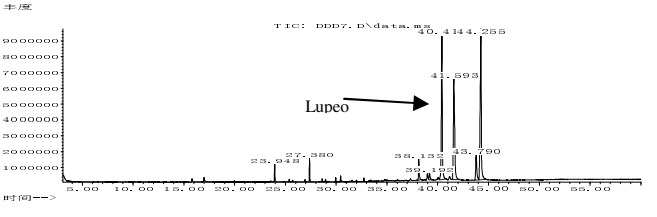

Fig. 2. Total ion current analysis of $_{G7}$

3.3 Effect of Glutathione-S-Transferase Activity of the Lupeol against Tetranychus Cinnabarinus

Glutathione-S-transferase (GSTs), an important detoxification enzyme *in vivo*, plays a regulatory role in metabolizing the exogenous toxic substances in *Tetranychus cinnabarinus*. So we detected if lupeol had significant effect on the GSTs activity of *Tetranychus cinnabarinus.* As shown in Fig. 3, The GSTs activity of *Tetranychus cinnabarinus* treated with Lupeol rose firstly and then decreased as time goes by. The GSTs activity in treatment group was higher than that in the control group at 4 or 12 h after treatment, furthermore, the activity of the control group accounted for 82 % of treatment group at 12 h after treatment. However, the GSTs activity in treatment group was lower than that in the control group at other times. Overall, these results suggest that Lupeol is able to restrain the GSTs activity in *Tetranychus cinnabarinus*.

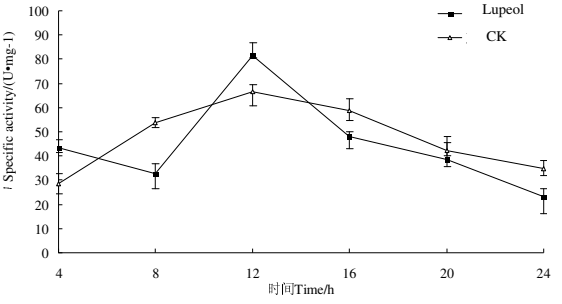

Fig. 3. Effect of GSTs activity of the Lupeol against Tetranychus cinnabarinus

3.4 Effect of Ca^{2+}-ATPase Activity of the Lupeol against Tetranychus Cinnabarinus

Most of acaricides exhibit toxicity to mites by interfering with their nervous system. Ca^{2+}-ATP enzyme plays an important role in the regulation of the excitement and conduction in nerve cells. We want to know whether Lupeol exhibits toxicity to mites by mediating their Ca^{2+}-ATPase activity. We found that Ca^{2+}-ATPase activity in *Tetranychus cinnabarinus* treated with Lupeol was lower than that in the control group. Ca^{2+}-ATPase activity in treatment group increased by 2.1 folds compared with the control group at 4 h after treatment (Fig.4). These results suggest that Lupeol plays an important role in suppressing the Ca^{2+}-ATPase activity in *Tetranychus cinnabarinus*.

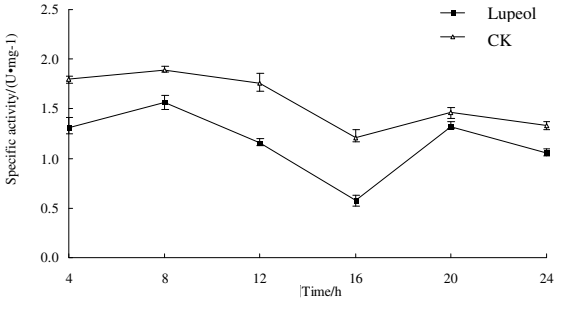

Fig. 4. Effect of Ca^{2+} -ATPase activity of the Lupeol against Tetranychus cinnabarinus

3.5 Effect of SOD Activity of the Lupeol against Tetranychus Cinnabarinus

Superoxide dismutase (SOD) plays a vital role in the balance between oxidation and anti-oxidation. SOD activity assay was used to evaluate the effects of Lupeol on SOD activity in *Tetranychus cinnabarinus.* As shown in Fig. 5, The SOD activity of *Tetranychus cinnabarinus* treated with Lupeol rose firstly and then decreased as time goes by. The SOD activity in the treatment group was higher than that in the control group, especially at 4 - 12 h after the treatment. Moreover, at 8 h after treatment, the SOD activity in the treatment group increased by 1.5 folds compared with the control

group. Generally, the changes of the SOD activity in treatment group and control group had the identical trend, but The SOD activity in the treatment group was always higher than the control group, indicating that Lupeol plays an important role in activating SOD in *Tetranychus cinnabarinus.*

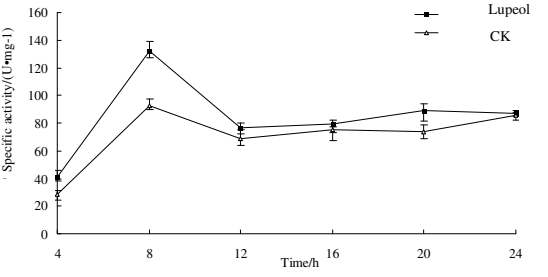

Fig. 5. Effect of SOD activity of the Lupeol against Tetranychus cinnabarinus

3.6 Effect of Total Protein Content of the Lupeol against Tetranychus Cinnabarinus

Then we studied whether total protein content of *Tetranychus cinnabarinus* was affected by Lupeol. The total protein content in treatment group was higher than that in the control group in the first 12 hours after treatment and especially at 4 h after treatment, the total protein content in the treatment group increased by 1.5 folds compared with the control group. However, after 12 h, the total protein content of the treatment group was lower than the control group. The total protein content was declined from 12 h to 16 h and raised from 16 h to 20 h, and declined again from 20 h to 24 h. Generally, the changes of total protein content in treatment group and control group exhibited the identical trend.

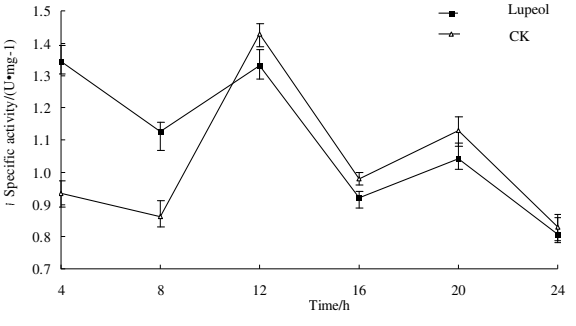

Fig. 6. Effect of protein content of the Lupeol against *Tetranychus cinnabarinus*

4 Discussion

Although the acaricides are widespread in many plants, it still needs a long term efforts to develop applicable acaricides from plants, and there are only a few reports about the

discovery of acaricides from plants and about identification of their components. We discovered in this study that petroleum ether extract of *Inula britanica* had acaricidal activities against *Tetranychus cinnabarinus*. Then our further work on extraction, column chromatographic fractionation and detection of the bioactivities of petroleum ether extract of *Inula britanica*, demonstrated that fraction 7 has strong acaricidal activities, which had been identified to be Lupeol. The extraction and identification of Lupeol provides a very important theoretic basis for the development of acaricides from plant.

Glutathione-S-transferase, Ca^{2+}-ATP enzyme and superoxide dismutase (SOD) are important enzymes *in vivo*, playing important regulatory roles in maintaining the normal life activities of the *Tetranychus cinnabarinus.* Lupeol showed a higher mortality rate against the *Tetranychus cinnabarinus,* so we wanted to study whether Lupeol had a significant impact on these enzymes in the *Tetranychus cinnabarinus*. Glutathione-S-transferase is an important detoxification enzyme *in vivo*. When the exogenous toxic substances enter the organism, it promotes the metabolic activity and helps decompose them to ensure the organism's normal physiological activities. Our results showed that the activity of glutathione-S-transferase in *Tetranychus cinnabarinus* was strongly inhibited after treatment with lupeol. The suppression of activities of glutathione-S-transferase eventually led to the death of harmful mites due to their deficiency in detoxification. Ca^{2+}-ATP enzyme was also inhibited after treatment with lupeol in our study. The main function of Ca^{2+}-ATP enzyme is to regulate the extracellular concentrations of Ca^{2+}, which is important to the neural signal transduction. Out results indicated that the activity of Ca^{2+}-ATP enzyme in *Tetranychus cinnabarinus* was inhibited after treating with the lupeol. The suppression of Ca^{2+}-ATP enzyme activity over-excited the mites and finally caused the dead. Superoxide dismutase (SOD) plays a vital role in regulating the balance between oxidation and anti-oxidation, it can remove superoxide anion radical (O^{2-}) to protect cells from damage. In this experiment, after treating with lupeol, the activity of superoxide dismutase in the treatment group was always higher than that in the control group, indicating that Lupeol could result in oxidation in *Tetranychus cinnabarinus* cells. Overall, our studies suggest that Lupeol is able to kill *Tetranychus cinnabarinus* by activating or inhibiting the significant activity of the enzymes in vivo, indicating that Lupeol may be used as a novel resource of botanical acaricide.

In this study, we not only discovered the strong toxicity of Lupeol to the mites, but also studied the effects of Lupeol on the enzyme activities of *Tetranychus cinnabarinus.* However, the specific acaricidal mechanisms of Lupeol were not clearly clarified in this paper, further studies will be needed.

Acknowledgements. The work was financially supported by the National Natural Science Foundation of China (30872029), the Key Natural Science Foundation of Beijing Municipality (6071001), the Natural Science Foundation of Beijing Municipality (6092007), the Key Foundation of Beijing Municipal Education Committee (KZ201010020016), and Funding Project for Academic Human Resources Development in Institutions of Higher Learning Under the Jurisdiction of Beijing Municipality (PHR20090516, PHR200906134).

References

1. Abbott, W.S.: A method of computing the effectiveness of an insecticide. J. Econ. Entomol. 3, 302–303 (1987)
2. Cao, H., Liu, S.Q., Shi, G.L., et al.: The effects of the extracts from stellera chamaejasmel on the biological and enzyme activity of tetranychus viennensis zacher. Science Silvae Sinicae 39(1), 98–102 (1957)
3. Dalale, N., Baudouin, C., et al.: Lupeol stimulates the production of high-quality type I collagen in human skin through HSP47 induction. Journal of the American Academy of Dermatology 58(2), AB62 (2008)
4. [FAO] Food and Agriculture Organization. Revised method for spider mites and their eggs (Tetranychus spp. and Panonychus ulmi Koch). FAO Plant Prod. Prot. 21, 49–54 (1980)
5. Geetha, T., Varalakshmi, P.: Anti - inflammatory activity of lupeol and lupeol linoleate in rats. Journal of Ethnopharmacology 76(1), 77 (2001)
6. Guo, Q.L., Yang, J.S., et al.: Sesquiterpenes in Inula L. Plants and Their Pharmacological Activities 17(6), 804–809 (2005)
7. Li, J., Zhang, Y.T., Zheng, W., et al.: Commasie brilliant blue staining was used to study the total protein content. Chinese Journal of Biologicals 13(2), 118–120 (2000)
8. Liu, S.Y., Sun, L.G., Xing, W., et al.: The effect of chronic lead exposure on hippocampal intraneuronal [Ca^{2+}] and activity of Ca^{2+}-ATPase in rats. Journal of Health Toxicology 13(1), 102–103 (1999)
9. Saleem, M.: Lupeol, a novel anti-inflammatory and anti-cancer dietary triterpene. Cancer Lett. 2009 (2000) (Epub ahead of print)
10. Shen, Z.J., Wang, H.X., Shi, G.L., et al.: Biological Activities of Extracts from 3 Species of Plants Against Tetranychus cinnabarinus. Journal of Beijing Agricultural College 23(1), 22–24 (2008)
11. Shi, G.L., Liu, S.Q., Cao, H., et al.: Acaricidal Activities of Extracts of Stellera chamaejasme against Tetranychus viennensis (Acari: Tetranychidae). Journal of Economic Entomology 97(6), 1912–1916 (2004)
12. Shi, G.L., Zhao, L.L., Liu, S.Q., et al.: Acaricidal Activities of Extracts of Kochia scoparia against Tetranychus urticae, Tetranychus cinnabarinus and Tetranychus viennensis (Acari: Tetranychidae). Journal of Economic Entomology 99(3), 858–863 (2006)
13. Sudhahar, V., Kumar, S.A., et al.: Remedial effect of lupeol and its ester derivative on hypercholesterolemia - induced oxidative and inflammatory stresses. Nutrition Research 27(12), 778 (2007)
14. Wang, Y., Shi, G.L., Wang, Y.N., et al.: Acaricidic Activity of Herbal Extracts Against Tetranychus cinnabarinus 24(5), 323–326 (2008)
15. Wang, Y.N., Shi, G.L., Zhao, L.L., et al.: Sun Extracts of Juglans regia Leaves against Tetranychus viennensis and Tetranychus cinnabarinus (Acari: Tetranychidae). Journal of Economic Entomology 100(4), 1298–1303 (2007)
16. Zhao, L.L., Liu, S.Q., Cao, H., et al.: Primary Studies of Acarocidal Activity of Wikstroemia chamedaphne against Tetranychus viennensis. Scientia Silvae Sinicae 41(6), 65–70 (2005)

The Isolation and Identification of the Acaricidal Principal Extracted from Mentha Piperita

Jian-ju Ren, Lan-qing Ma, Yu-bo Liu, Guang-lu Shi, and You-nian Wang*

Key Laboratory of Urban Agriculture (North) of Ministry of Agriculture, P.R. China
Beijing University of Agriculture, Beijing, China
glshi@126.com

Abstract. The objective of this study is to measure the toxicity of acaricidal of Mentha piperita extracts, and to isolate and identify the chemical compounds of the extracts. This experiment uses three kinds of solvents - petroleum ether, chloroform, and methanol in extraction with the. Liquid-liquid partition technique. The acaricidal substance was isolated and purified by silica gel column, chromatography, and thin layer chromatography (TLC) together with iodine chromo test; it is traced with the slide retting method. Finally the experiment employs UV photo spectrum, HPLC, RI, and MS, and other techniques in identifying the active substance. The study finds that part of the crude petroleum ether extract from the Mentha piperita land shows significant acaricidal effect to Tetranychus cinnabarinus-when its density reaches 1 mg/ml, lethal rate of mature mites is 87.05 % within 24 hours, and mites' eggs 93.16 %. According to Duncan's inspection, three kinds of solvents of crude extracts display great differences in the lethal rate of mature mites and mite eggs ($P < 0.05$). The study also finds that chloroform extract and methanol extract from the upper menthe lands has relatively weak acaricidal effect - their lethal rates to mature mites comes at 28.51% in 24 hours, and mites eggs 10.73 %. Based on a liquid-liquid extraction of petroleum ether by methanol, the crucial components of the acaricidal substance appear to exist in petroleum ether of lower polar whose lethal rate of mature mites reaches 93.75 % within 24 hours. The study gains eight fractions from the isolation of the petroleum ether extracts. With bioactive tracing, one of them provides a sample compound V which possesses higher acaricidal effect. Its lethal concentration (LC50) reaches 0.5464 mg/mL. Its credible interval is 0.3268 - 0.9134 mg/mL. The purity of the sample compound was 89.16 % based on HPLC. MS shows its molecular ion peak being 414 which reveals its sterol ring structure according to the corresponding data base. IR reflects that the substance shows notable characteristic peaks at 1160 cm-1, 1450 cm-1, 1380 cm-1 and 1700 cm-1. It is thus determined that the substance isolated from Mentha piperita in this study is a β-sitosterol.

Keywords: Mentha piperita, Isolation and identification, Acaricidal active substance, Tetranychus cinnabarinus, β-sitosterol.

* Corresponding author.

E. Zhu and S. Sambath (Eds.): Information Tech. and Agricultural Eng., AISC 134, pp. 565–576.
springerlink.com © Springer-Verlag Berlin Heidelberg 2012

1 Introduction

Tetranychus cinnabarinus is one of the most widely distributed and seriously occurring harmful mites in the fields and forests of China. It's also one of the harmful species that can't be easily prevented and controlled because of its small size, rapid reproduction, strong adaptability and frequent occurrence of its annual generations, which present extremely serious hazard (Zhang and Meng 2003, He *et al*. 2004). Currently, these harmful mites are mainly controlled by spraying such chemical reagents as organic phosphorous compounds and pyrethroids (Kim *et al*. 2003). The long-term application of them not only led to the drug resistance of mites (Wilkin 1979, Stables 1984), but also exerted disadvantageous effects on non-target organisms (Hays and Laws 1991). With their merits of unique functional mechanism, little interference with predators, no obvious toxic effects on vertebrates and rapid degradation in environment, the resourceful and renewable broad-spectrum plant-originated agricultural chemicals are ideal choices for the prevention and control of harmful mites. In addition, the active acaricidal substances are widely contained in many kinds of plants in nature. The comprehensive advantages of the secondary materials of such plants can be utterly applied, serving as compensations for the existing drawbacks of acaricides. Therefore, seeking structural materials from plant-originated natural products became one of the hot points for the research and development of new type acaricides (Luo 1997). In 1986, Mansour *et al.* once reported the toxic effects of the extracts from 14 species of Labiatae on *Tetranychus cinnabarinus* (Mansour et al. 1986). It was also reported by Grange *et al* (1988)that about 2400 kinds of plant hold the activities of controlling harmful organisms, and 40-plus of them possess the activities of mite killing. Pamo *et al* (2004) found that the extracts from the flowers of *Ageratum houstonianum* had poison effects on mites. Chiasson *et al* (2001) extracted crude materials from *Artemisia absinthium* through adopting such three extraction methods as microwave extraction, water distillation and steam distillation respectively. In the toxic experiments on *Tetranychus urticae Koch*, they found that *β*-thujone was the main mite killing substance in *Artemisia absinthium*. Wang *et al* (2007) applied different approaches to extract active materials from walnut green husk, finding that the petroleum ether-extracted materials possess strong contact poison effects on *Tetranychus cinnabarinus*. Tak *et al* (2006) reported the relatively strong poison effects of phenol and benzoic acid on *Tetranychus urticae Koch*. Both substances were extracted from the velamen of *Paeonia lactiflora*, and their values of LC_{50} amounted to 5.29 mg/L and 4.80 mg/L respectively. The poison effects were more significant in closed environment. Shi *et al* (2006) implemented toxic experiments on *Tetranychus urticae Koch* with the utilization of crude materials extracted from *Kochia scoparia* by applying such three solvents as methanol, chloroform and petroleum ether, respectively, finding a relatively high fatality rate of crude chloroform-extracted materials, which amounts to 78.86 %. At present, there are huge amounts of researches concerning the efficacies of *Mentha piperita*, whose dry above-ground parts can be applied to the treatment of such symptoms as wind-heat cold, acute febrile diseases at the initial stage, headache, swelling and pain of eye, inflammation of throat, apotheosis, rubella, measles and distension and fullness in

chest due to their coldness, pungent flavors and efficacies in dissipating wind-heat, clearing away heat from head and eyes and promoting eruption (Zheng and Cai 2003). Moreover, the significant pharmaceutical effects of *Mentha piperita* on digestive, central, reproductive, and respiratory systems were also reported (Liang *et al*. 2003). However, its noticeable killing efficacy on harmful mites has not yet been found and researched. In this paper, the mite killing activity of *Mentha piperita* was investigated and its contained active substances were preliminarily isolated and identified so as to reveal the natural configuration of these substances and provide active leading compounds for the research and development of new agricultural chemicals, thus synthesizing new type products of agricultural chemicals with brand-new structures, unique mechanisms, security and high efficacies through further modification and imitation of these substances.

2 Materials and Methods

2.1 Tested Materials

The tested peppermint (*Mentha piperita*) materials were collected from Qiliqu, Changping District, Beijing. The above-ground parts of these materials were cleansed and put to ventilation place for cooling and drying with temperatures of 25 ± 3 ℃. Then, these parts were pulverized using Pulverizer-6202 manufactured by Beijing Huanyatianyuan Co. Ltd with a particle size of 60 mesh. Finally, the pulverized parts were stored in a refrigerator (Electrolux BCD-281EA) at 4 ℃ for further use.

The tested pests were adult *Tetranychus cinnabarinus* fed by the seedlings of *Vigna unguiculata* in labs for 2 years with multiple-generation reproduction. The parameters for breeding were: temperature: 26 ± 1 ℃, relative humidity: 50 % ± 10 %, and illumination: L: D=18: 6h (Hou and Zhao 2004). Four weeks after their breeding, the uniformly-bred adults with high motilities were selected for experiments.

2.2 Extraction and Isolation

Extraction of crude botanical materials. The 6,000g pulverized plant parts were collected and equally-partitioned into 3 testing groups soaked for 3d by methanol, chloroform and petroleum ether (analytically pure: manufactured by Beijing Chemical Plant), respectively and filtered. The filter residues were continually soaked for 3d with 3 repetitions. The leaching solution were integrated and placed in a concentrator (Buchi Rotavapor R-220) for concentration and the rates of extraction were calculated. 1mg extract was applied to prepare 1mg/mL emulsion with the addition of 0.05mg Tweenum-80 and distilled water. This emulsion was adopted for the determination of mite killing activities.

Liquid-liquid extraction was implemented in the most significantly effective mite-killing portions of these 3 different solvent extracts, and the active compositions were traced through determining their biological activities. 8g effective extracts were collected as sample loading material. 200-300mesh silica gels for column chromatography (manufactured by Qingdao Haiyang Biological Reagent Plant) were applied for isolation and purification (Buchi,C-615) with an activation temperature of

120 ℃, an inner column diameter of 100mm, and a substrates height of 400 mm. Gradient elution was carried out through the application of methanol, chloroform and petroleum ether. If no flow was created under a single elution system, the mixture ratio of elution system was replaced. The flow was collected step by step at a speed of 10mL/min, 50mL per bottle. Then, thin-layer detection of collected flow was conducted (according to the methods of Qingdao Haiyang Chemical Plant) and activation was implemented under 110 ℃. If chromogenic reactions took place in iodine-cylinder, the identical compositions were integrated for toxicity determination.

Ultraviolet analysis. The samples were dissolved in chloroform using 1.0 × 1.0cm colorimetric plates and ultraviolet map scanning was conducted with a range of 200-1,100 nm (through the application of TU-1810 manufactured by Beijing Purkinje General Instrument Co., Ltd.). Analysis of HPLC samples (Using Agilent 1200) was executed under such circumstances: mobile phase: methanol: water solution (70: 30, V: V), flow speed: 1 mL/min, column temperature: 25 ℃, sampling concentration: 0.050 mg/mL, sampling amount: 10 μl and the utilization of Eclipse XDB-C18 column (4.6mm × 150 mm, 5 μm USA) and photodiode array detector (G1315B, DAD) with a wavelength range of 190 – 800 nm and a collecting time of 50min.

Infrared analysis. 2.0 mg sample powers mixed with 150.0 mg KBr were uniformly pulverized under Infrared light and preformed. The KBr tablets of samples were placed under fixed positions of the determining window of Fourier Transform Infrared Spectrometer (Bruker TENSOR 27, Germany) and scanned within the wave-number range of 4,000 - 400 cm^{-1} according to set instrumental conditions.

Mass spectrometric analysis. Gas chromatograph-mass spectrometer (VARIAN 2200, USA) was adopted for determination.

2.3 Determination of Mite Killing Activity

One end of each slide (produced by Yancheng Hengtai Glass Instrument Factory) was stuck by a 3 cm-long double-sided adhesive tape. The adult mites with strong motilities were dipped by No.0 brush and their backs were stuck to the tape, 30 or so per line, 1 line per slide. The tested mites were placed into environments with a temperature of 26 ± 1 ℃ and a relative humidity of 60 % - 80 % and detected utilizing stereoscope (SZM-45B3 manufactured by Sunny Optical Technology (Group) Company Limited, Zhejiang Province, PRC) under an amplification factor of 200. The dead and inactive mites were depleted and number of the live ones was recorded. The mite-stuck ends of slides were immersed into the prepared chemical liquid for 5s and after the slides' being taken out, the redundant liquid was quickly absorbed through using absorbent paper. Then, the mites were continually cultured under same conditions and the result was checked after 24 h. The bodies of the cultured mites were slightly contacted using brush. If there was no movement in the feet of a certain mite, it was considered dead. The test was repeated for 3 times with the addition of 0.050 mg/mL Tweenum-80 solution in the control group (Zhou *et al*. 2007).

Determination of the contact poison effects of cowpea on the eggs of *Tetranychus cinnabarinus*: the fresh leaves of cowpea (*Vigna unguiculata*) were selected, cleansed and dried. An approximate area of 3 cm^2 was marked in each leaf dorsal side, which was upwardly placed into a culture plate (d = 5 cm) padded by a layer of wet cotton

covering both sides of the marked area, and the leaves were closely stuck to the cotton layer. 15 5-day-old adult female mites were placed into the marked area, which was put into an insectary for them to lay eggs for 12 h, and then these females were removed. The chemical liquid was sprayed to leaf dorsal sides with 3-5 set concentrations; each had 3 repetitions applying 0.050 mg/mL as control group. After being dried, the leaves were re-placed into the culture plate according to the above-mentioned method, and the number of remained eggs was checked and recorded. The culture plates were maintained wet with the daily addition of water, and the situation of egg hatching was observed once per 24 h under a temperature of 26 ℃ and a relative humidity of 60 % - 80 %. 4 d after observation, if all the eggs in the control group hatched and the treated eggs still didn't hatch, these eggs were considered dead.

2.4 Data Analysis

Approach for data analysis: all the acquired data was rectified using Abbot Formula (Abbott 1925). The results were analyzed by ANOVA, and the effect differences among different treatments were compared applying Duncan Method. The linear regressions were calculated utilizing the method of probit analysis. The ANOVA and Duncan test of research data were completed through using the special version of DPS v3.01.

Mortality Rate= Number of dead mites×100%/ Total mites number

Corrected Mortality Rate= (Number of dead mites in treatment-Number of dead mites in control) × 100%/100%- Number of dead mites in control)

3 Results

3.1 Mite Killing Activities of Different Extract Liquids of Peppermint

The results showed that when the crude materials of peppermint (*Mentha piperita*) extracted by methanol, chloroform and petroleum ether, respectively, were prepared into emulsions with a concentration of 1mg/mL, their rates of contact killing to adult mites in 24 h attained 28.51 ± 4.39 %, 10.73 ± 6.19 % and 87.05 ± 6.39 %, respectively, and their rates of contact killing to eggs in 96h reached 38.91 ± 2.15 %, 16.11 ± 3.76 %, and 93.16 ± 2.11 %, respectively (See Table. 1). There existed significant differences among the contact killing effects of these three solvents on adult mites and eggs ($P < 0.05$). It can be seen from Table. 1 that compared with methanol and chloroform-extracted crude materials, petroleum ether-extracted crude materials held relatively higher mite killing effects on both adults and eggs, which was possibly because that these toxic materials can penetrate the waxy layers of mite epidermis and permeate into mite bodies more easily with their relatively low polarity. The results in table.1 showed that the extraction rates of methanol, chloroform and petroleum ether amounted to 82.73 %, 14.96 %, and 2.31 %, respectively, displaying a relatively small extraction rate of petroleum ether, which demonstrated that peppermint (*Mentha piperita*) possesses relatively low contents of low-polarity substances and relatively high contents of high-polarity substances.

Table 1. Percentages of yield of concentrated extracts of M.piperita by using three different solvents and percentages of contact toxicity of *T.cinnabarinus* at 1mg/mL of the extracts

Solvent	Extraction rate%	Contact toxicity to adult mites % (24h Mean± SE)	Contact toxicity to eggs %(96h Mean± SE)
CK	-	6.66±0.00 [d]	3.57±1.25 [d]
Methanol	17.73	28.51±4.39 [b]	38.91±2.15 [b]
Chloroform	14.96	10.73±6.19 [c]	16.11±3.76 [c]
Petroleum either	2.31	87.05±6.39 [a]	93.16±2.11[a]

The values followed by same letters in a column are not significantly different ($p<0.05$,Duncan's test). Means in columns of mortality rate were corrected by Abbott (1925).

3.2 Results of Extraction and Isolation

The petroleum ether-extracted crude materials were extracted by methanol and mite killing activities of both extracted materials were traced. The observation results of every 4 h were listed in Fig.1. From Fig.1, it can be seen that the mite killing activity of petroleum ether extracts were significantly higher than that of methanol extracts. 12 - 16 h after treatment, petroleum ether extracts witnessed their period of peak effects on mites, during which the mortality rate of mites increased obviously. 24 h after treatment, the rate of petroleum ether extracts' contact killing effects on adults amounted to more than 90 %, while such rate of methanol extracts was less than 40 %.

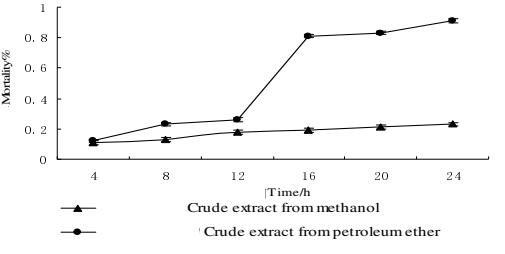

Fig. 1. The contact toxicity against *T. cinnarinus* of different partitions

3.3 Results of Column Chromatography Isolation

From Table. 2, it can be seen that among the ultimately isolated 8 compositions, composition V held the highest activity for mite killing, and its LC_{50} value reached 0.5464% in 24h with a 95 % confidence interval range of 0.3268-0.9134 mg/mL. Composition I had the second highest activity for mite killing with a LC_{50} value of 0.8718 mg/mL in 24h and a 95% confidence interval range of 0.4727 - 1.6077 mg/mL. And the LC_{50} values for mite killing of compositions II, III, IV, and VI were 1.2681 mg/mL, 1.7453 mg/mL, 1.8899 mg/mL, and 1.8149 mg/mL, respectively. It was shown in Table. 2 that among the isolated 8 compositions, composition VIII held the worst effect of mite killing with a LC_{50} value of 12.505mg/mL and a confidence

interval range of 8.4393-18.5293 mg/mL. Therefore, the active substances of mite killing in peppermint (*Mentha piperita*) were mainly contained in chloroform elution system. Meanwhile, flow I in petroleum ether elution system also displayed relatively good effects. So, it was preliminarily inferred that there occurred 2 kinds of active mite killing substances in peppermint (*Mentha piperita*) and flow I played a coordinative role in the contact killing of mites. Compared with activities of petroleum ether-extracted crude materials, activity of composition V improved apparently, indicating that this composition possessed relatively good contact killing effects on *Tetranychus cinnabarinus*. The biological detection results further confirmed that peppermint (*Mentha piperita*)'s active mite killing substances mainly presented in the petroleum ether extracts of its stalks and leaves, and there possibly occurred 2 different kinds of mite killing substances with high efficacies in these extracts.

Table 2. The toxicity regression equations of the liquid chromatography fractions against *T. cinnabarinus* adults (24h)

Code	eluted system(V:V)	Toxicity regression equation	Correlation coefficient R^2	LC_{50} and 95%confidence limit (mg/mL)
I	Petroleum ether	y = 2.3561x + 5.1403	0.9998	0.8718 (0.4727~ 1.6077)
II	8:2[a]	y = 1.6109x + 4.8338	0.9939	1.2681 (0.6667 ~2.4118)
III	5:5[a]	y = 2.7111x + 4.3442	0.9711	1.7453 (1.0134 ~3.005)
IV	2:8[a]	y = 2.5014x + 4.3085	0.9976	1.8899 (1.0864 ~3.2875)
V	Chloroform	y = 3.0796x + 5.8082	0.9784	0.5464 (0.3268 ~0.9134)
VI	7:3[b]	y = 2.0497x + 4.4694	0.9956	1.8149 (1.007 ~3.2708)
VII	6:4[b]	y = 2.0081x + 4.1458	0.9998	2.6630 (1.5589 ~4.5488)
VIII	Methanol	y = 1.2484x + 3.6304	0.9951	12.505 (8.4393 ~18.5293)

[a] petroleum ether：chloroform (V:V), [b] chloroform： methanol(V:V); letter y stands for the probability value of mortality, letter x stands for the logarithm value of different concentrates.

3.4 Purity Detection Utilizing Hplc Method

The purity of composition V with best effect of mite killing was detected adopting the method of HPLC. It was found in HPLC map that at an ultraviolet absorbance wavelength of 255 nm there appeared 4 absorption peaks within the range of T=2 min – 6 min. The heights and the integral area percentage of these peaks were listed as following: Peak No.1 (*RT*=2.303 min): 1.3467 %, peak height: 2.18171 mAU; Peak No.2 (RT=2.470): 8.4454 %, peak height: 4.94827 mAU; Peak No.3 (RT=3.019): 89.1621 %, peak height: 213.51598 mAU; Peak No.4 (RT=5.535): 1.0457 %, peak height: 1.22508 mAU. Therefore, Peak No.3 held the largest value of integral area percentage, which reached 90 % or so, showing an extremely high purity of this sample. The remaining 3 peaks (peaks No.1, No.2 and No.4) probably represented the products of a previous and a next elution system in flow V, and such products possibly shared similar polarities with the active compositions.

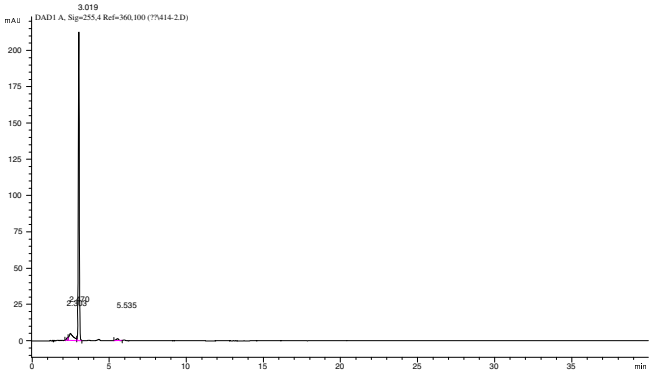

Fig. 2. HTLC analysis of the fifth fraction of *M.piperita* extract

3.5 Mass Spectrometric Detection

As shown in Fig.3, MS (EI-MS) m/z = 414(M^+), namely the detected molecular ion peak of composition V was 414, showing its molecular mass was 414. According to mass spectrometric database, it can be concluded that such substance contained sterol ring structures.

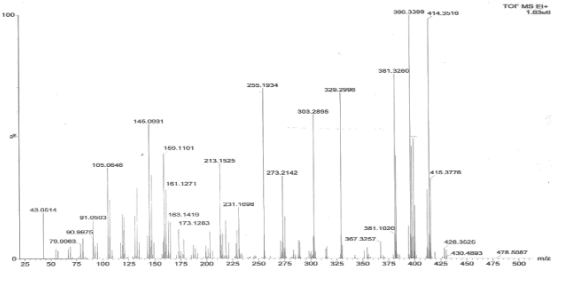

Fig. 3. MS analysis of the fifth fraction of *M.piperita* extract

3.6 Infrared Detection

In order to further determine the characteristics of this substance, infrared detection was implemented. It can be seen from the intra-red spectrogram (Fig.3) that the spectrum displayed several characteristic peaks, representing several important functional groups. The wide peak at 3440cm^{-1} showed the stretching vibration of O-H bond ($\nu_{O\text{-}H}$) of this compound. Meanwhile, the peak at 1160cm^{-1} attributed to the stretching vibration of C-O bond ($\nu_{C\text{-}O}$) of cyclic alkyl tertiary alcohols or secondary alcohols. The range of 3000-2700cm^{-1} represented the stretching vibration region of saturated C-H bond ($\nu_{C\text{-}H}$), which generally belonged to methyl or methylene. The corresponding peaks at 450cm^{-1}(δas) and 1380cm^{-1}(δs) showed the asymmetric and symmetric deformation vibrations of methyl, respectively. And the peak at 1700cm^{-1} exhibited the stretching vibration of C=C bond ($\nu_{C=C}$). According to references and MS

and IR maps, the material was determined to be β-sitosterol (Fig.4), because there appeared no decreased melting point when it mixed with standard β-sitosterol sample, and when it was implemented thin layer chromatography along with standard β-sitosterol sample, they shared identical R_f values.

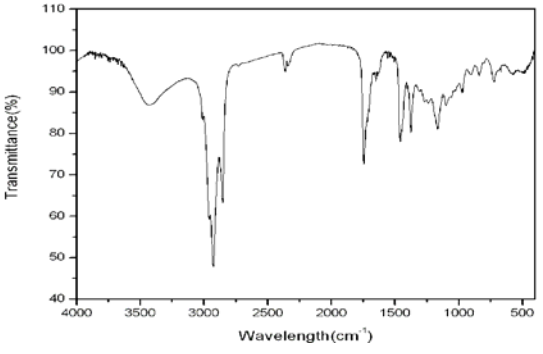

Fig. 4. IR analysis of the fifth fraction of the *M. piperita* extract

4 Discussion

Researchers showed that peppermint (*Mentha piperita*) mainly contained such organic compounds as volatile oil, flavonoids, organic acids and amino acids and so on. The volatile oil content in the fresh stalks and leaves of peppermint was approximately 1%, while such content amounted to approximately 1.3%-2% in its dry stalks and leaves. The volatile oil in peppermint consisted of approximately 77 % -87 % *L*- menthol, 8 % -12 % *L*- menthone, and approximately 3% methyl acetate (Mucciarelli *et al*. 2007). Peppermint oil has a long history of both external and internal pharmaceutical applications, and it is also widely utilized in such aspects as food, spices, and candy (Grigoleit and Grigoleit 2005). There exist a relatively huge amount of reaches regarding the inhibitive and toxic effects of menthols and menthones contained in peppermint oil on fungi and viruses. Edris *et al* (2003) found that the coexistence of peppermint oil and menthones with *Sclerotinia sclerotiorum, Rhizopus stolonifera* and *Mucor* in a closed system caused certain inhibitive effects on the growth and reproduction of these fungi. Schuhmacher *et al* (2003) found that peppermint oil exhibited relatively strong inhibitive effects on both sub-types of Herpes Simplex Virus (HSV_{21} and HSV_{22}). Among hepatotoxic researches, relatively more were related with the toxic mechanisms of peppermint oil, considering that *D*- pulegone contented in peppermint oil was possibly the main ingredient leading to the cause of liver toxicity in rodents, while *L*-pulegone did not possess such effects (Clanahan *et al*. 1989, Moorthy *et al*. 1989, Thomassen *et al*. 1992, Engel 2003). In liver, pulegone could also be oxidized into other products, thus participating into the process of liver damage (Madyastha and Raj 1993). Therefore, the bacteriostatic and toxic substances of peppermint were mostly contained in peppermint oil. In the process of extraction and isolation, this research also found that active mite killing substances mainly existed in petroleum ether with an extremely-low polarity. There were also some reports relating

to the poison killing and aversion effects of peppermint on other pests. 96 h after treating wheat seedling through adopting 2 % dry powder of peppermint leaves, Yao Kang (1981) found a 100 % mortality rate of adult rice weevil (*Sitophilus oryzae*), exhibiting strong poison killing effects. It was also found that peppermint oil had extremely strong fumigation killing effects on bean weevil (*Acanthoscelides obtectus*) (Ahmed and Eapen 1986, Raja *et al*. 2001). Masatoshi *et al* (1997) reported that 1, 8-cineole is the main active repellent ingredient in peppermint oil. However, no further discussion on the contact killing effects of peppermint oil can be found in previous researches. In this research, it was found that the active mite killing ingredient contained in peppermint had strong poison killing effects on *Tetranychus cinnabarinus* and such ingredient was determined to beβ-sitosterol, which was in accordance with the finding of β-sitosterol in peppermint conducted by Zeng *et al* (2006). In addition, the inhibitive effects of β-sitosterol on intestinal esterase were also reported in cabbage butterflies (*Pieris brassicae*), whose intestinal esterase were treated by peppermint (Wang et al. 2000), which also confirmed the toxic effects of peppermint on insects.

In this research, the active mite killing substance was first isolated from peppermint and identified to beβ-sitosterol through adopting the methods of biological detection and tracking and relevant analyses. The acquirement of the monomers of such effective mite killing substance can provide foundations for the research of mite killing mechanisms and the development of new agricultural chemicals.

Acknowledgements. The work was financially supported by the National Natural Science Foundation of China (30872029), the Key Natural Science Foundation of Beijing Municipality (6071001), the Natural Science Foundation of Beijing Municipality (6092007), the Key Foundation of Beijing Municipal Education Committee (KZ201010020016), and Funding Project for Academic Human Resources Development in Institutions of Higher Learning Under the Jurisdiction of Beijing Municipality (PHR20090516, PHR200906134).

References

1. Abbott, W.S.: A method for computing the effectiveness of an insecticide. Economic Entomology 18, 265–267 (1925)
2. Ahmed, S.M., Eapen, M.: Vapour toxicity and repellency of some essential oils to insect pests. Indian Perfumer 30, 273–278 (1986)
3. Chiasson, H.L.N., Langer, A.B., Bostanian, N.: Acaricidal Properties of Artemisia absinthium and Tanacetum vulgare(Asteraceae) Essential Oils Obtained by Three Methods of Extraction. Journal of Economic Entomology 94, 167–171 (2001)
4. Clanahan, R.H., Thomassen, D., Slattery, J.T.: Metabolic activation of (R)2(+)2pulegone to are activeen on althatcova 2 lentlybinds to mouse liver proteins. Chemical Research Toxicology 2, 349–355 (1989)
5. Edris, A.E., Farrag, E.S.: Antifungal activity of peppermint an sweet basil essential oils and their majority constituents of some plant pathogenic fungi from the vaporphase. Nahrung 47, 117–121 (2003)

6. Engel, W.: In vivo studies on the metabolism of the monoterpene pulegone in humans using the metabolism of ingestion correlated amounts(MICA) approach:explanation for the toxicity differences between (S)-(2)- and (R)2(+)-pulegone. Journal of Agriculture Food Chemcal 51, 6589–6597 (2003)
7. Grange, M., Ahmed, S.: Handbook of plants with pest control properties, pp. 202–203. Wiley Interscience (1988)
8. Grigoleit, H.G., Grigoleit, P.: Pharmacology and preclinical pharmacokinetics of peppermint oil. Phytomedicine 12, 612–616 (2005)
9. Hays, J.B., Laws, E.R.: Handbook of Pesticide Toxicology, p. 496. Academic Press, San Diego (1991)
10. He, L., Yang, Y., Fu, J.Z.: Resistance selection and relative fitness of Tetranychus cinnabarinus(Boisduval)to abamectin. Acta Phytophylacica Sinica 31, 395–400 (2004)
11. Hou, H., Zhao, L.L.: Studies on the acaricidic activity of the extracts of Kochia scoparia. Planrt Protection 30, 42–45 (2004)
12. Kim, E.H., Kim, H.K., Choi, D.H., Ahn, Y.J.: Acaricidal activity of clove bud oil compounds against Tyrophagus putrescentiae (Acari: Acaridae). Applied Entomology Zoolology 38, 261–266 (2003)
13. Liang, C.Y., Li, W.L., Zhang, H.Q., Ren, B.R.: The advance on the reseach of chemical constituants and pharmacological activities of Mentha haplocalyx. Chinese Wild Plant Resources 22, 9–12 (2003)
14. Luo, W.C.: Research in the Bioactivity of Botanical Alkaloids against Insects. Pesticides 36, 11–15 (1997)
15. Madyastha, K.M., Raj, C.P.: Studies on the metabolism of amonoterpeneketone, R2(+) 2pulegoneahepa to toxin in rat: isolation and characterization of new metabolites. Xenobiotica 23, 509–518 (1993)
16. Mansour, F., Ravid, U., Putievsky, E.: Studies on the effects of essential oils isolated from 14 species of Labiatae on the carmine spider mite Tetranychus cinnabarinus. Phytoparasitica 14, 137–142 (1986)
17. Masatoshi, H., Hiroaki, K.: Repellency of rosemary oil and its components against the onion, aphid Neotoxoptera formosana (Takahashi) (Homoptera: Aphididae). Applied Entomology Zoolology 32, 303–310 (1997)
18. Moorthy, B., Madyastha, P., Madyastha, K.M.: Hepatotoxicity of pulegoneinrats: its effects on microsomalenzymes, invivo. Toxicology 55, 327–337 (1989)
19. Mucciarelli, M., Camusso, W., Maffei, M.: Volatile terpenoids of endophyte-free and infected peppermint (Mentha piperita L.): Chemical partitioning of a symbiosis. Microbial Ecology 54, 685–696 (2007)
20. Pamo, T.E., Tendonkeng, T.: The acaricidal effect of the essential oil of Ageratum houstonianum Mill. flowers on ticks (Rhipicephalus lunulatus) in Cameroon South Africa. Journal of Animal Science 34, 244–247 (2004)
21. Raja, N., Albert, S., Ignacimuthu, S.: Effect of plant volatile oils in protecting stored cowpea Vigna unguiculata (L.) Walpers against Callosobruchus maculates (F.) (Coleoptera: Bruchidae) infestation. Journal of Stored Products Research 37, 127–132 (2001)
22. Schuhmacher, A., Reichling, J., Schnitzler, P.: Virucidal effect of peppermint oil on the developed viruses herpess implex virus type and type in vitro. Phytomedicine 10, 504–510 (2003)
23. Shi, G.L., Zhao, L.L., Liu, S.Q.: Acaricidal Activities of Extracts of Kochia scoparia against Tetranychus urticae, Tetranychus cinnabarinus, and Tetranychus viennensis (Acari: Tetranychidae). Journal of Economic Entomology 99, 858–863 (2006)

24. Stables, L.M.: Effect of pesticides on three species of Tyrophagus, and detection of resistance to pirimiphosmethyl. In: Palmarum, T., Putrescentiae, T. (eds.) Acarology, pp. 1026–1033. Ellis Horwood, Chichester (1984)
25. Tak, J.H., Kim, H.K., Lee, S.H.: Acaricidal activities of paeonol and benzoic acid from Paeonia suffruticosa root bark and monoterpenoids against Tyrophagus putrescentiae (Acari: Acaridae). Pest Management Science 62, 551–557 (2006)
26. Thomassen, D., Knebel, N., Slattery, J.T.: Reactive intermediates in the oxidation of menthofuranby cytochromes. Chemical Research Toxicology 5, 123–130 (1992)
27. Wang, Y.N., Shi, G.L.: Acaricidal activity of Juglans regia leaf extracts on Teranychus viennensis and Tetranychus cinnabarinus (Acari:Tetranychidae). Journal of Economic Entomology 100, 1298–1303 (2007)
28. Wang, Y.W., Zhang, G.Z., Xu, H.H.: The effect of compounds such as β-sitosterol on gut esterase activity of insects. Journal of Qinghai University (Natural Science) 18, 1–2 (2000)
29. Wilkin, D.R.: The control of mites in cheese stores. In: Recent Advances in Acarology, New York, pp. 221–229 (1979)
30. Yao, K.: Research profile of foreign plant grain protectants The second national grain storage professional academic exchange yindong literature, pp. 28–38 (1981)
31. Zeng, J.W., Qian, S.H., Wu, J.Z.: Studies on antiviral constituents in stems and leaves of Pithecellibium clypearia. China Journal of Chinese Materia Medical 31, 400–402 (2006)
32. Zhang, H., Meng, L.: Current status of application, development and prospect of agricultural acaricides. Pesticides 42, 14–17 (2003)
33. Zheng, H.C., Cai, S.Q.: Pharmaceutical Botany and Pharmacognosy, p. 383. People's medical publishing house, Beijing (2003)
34. Zhou, S.Y., Li, Q., Yang, Q.F.: Effect of Paris Polyphylla Smith-synergistic Substances Mixtures on Panoychus Citri (Mc Gregor). Journal of Anhui. Agri. Sci. 35, 458–459 (2007)

Effects of Mentha Piperita Extracts on Activities of Several Enzymes of Tetranychus Cinnabarinus

Jian-ju Ren, Guang-lu Shi, Lan-qing Ma, Yu-bo Liu, and You-nian Wang*

Key Laboratory of Urban Agriculture (North) of Ministry of Agriculture, P.R. China
Beijing University of Agriculture, Beijing, China
glshi@126.com

Abstract. The specific acaricidal mechanisms of Mentha piperita extracts were studied. The acaricidal and relative enzyme activity in Tetranychus cinnabarinus after treatment with Mentha piperita extracts at the concentration of 2mg·ml- 1 was studied by using the slide dip technique and colorimetric method, respectively. The effects of Mentha piperita extracts on the poisonous symptom and ultrastructure of the treated mites were also observed. Our results showed that fraction V from Mentha piperita extracts had stronger toxicity than others. The mites had experienced four phases namely quiescence, excitement, spasm and death after treatment, indicating that the Mentha piperita extracts were able to cause the poisonous symptom of the treated mites. Enzyme activity assay showed that the activities of glutathione-S-transferase (GSTs) and monoamine oxidase (MAO) were strongly induced whereas the activities of acetylcholine esterase (AChE) and protease were restrained after treatment. The changes of these enzymes led to the death of mites due to the destruction in the nervous transmission and digestive system. The transmission electron microscopic observations revealed that the treated mites suffered from the rupture of ultrastructure such as endoplasmic reticulum, mitochondria and nuclear membrane. These data provided useful information for the use of Mentha piperita as a novel resource of botanical acaricide.

Keywords: Mentha piperita, Tetranychus cinnabarinus, activity of enzyme, ultrastructure.

1 Introduction

In the 21st century, environmental protection is a current topic [1]. The hazardous influence of synthetic pesticides on health and the environment has aroused extensive attention. Hence, the search for the new types of pesticide which were safe and effective, harmless to the ecological environment has become a hot research spot. Since the end of the last century, researchers have done a great deal of research on extracts of aromatic plants to find the alternatives to conventional pesticides [2]. They found that aromatic plants exhibited important effects of toxicity, aversion and antifeeding to agricultural pests. Due to their rich resource, environment-friendly and

* Corresponding author.

E. Zhu and S. Sambath (Eds.): Information Tech. and Agricultural Eng., AISC 134, pp. 577–588.
springerlink.com © Springer-Verlag Berlin Heidelberg 2012

no toxicity to natural enemies of pest [3-6], aromatic plants have been recognized as a new resource for developing potential botanical pesticides [7-8].

Mentha piperita, belonging to Labiatae, is widely grown as a common aromatic plant. *Mentha piperita* is cool and spicy. Due to its property of dispelling wind-heat, refreshing oneself, and promoting eruption [9], *Mentha piperita* was used to cure cold, headache, conjunctive congestion, pharyngitis, rubella, measles, *etc*. *Mentha piperita* contains many chemical components such as naphtha, flavone, organic acids, amino acids and has important pharmacological effects on central nervous, digestive, respiratory, and reproductive systems [10]. Peppermint oil mainly contains *L*-menthol (menthol) and *L*-menthol, accounting for about 7 7% - 87 %, 8 % - 12 % respectively. Few mint esters also exist in Peppermint oil [11]. *Mentha piperita* not only plays an important role in inhibiting or killing the fungi and viruses [12-13], but also has toxicity to bean weevil [14-15]. However the specific insecticidal mechanisms of *Mentha piperita* against bean weevil have not been clearly clarified.

The petroleum ether extract of Mentha piperita was shown to have strong toxicity to Tetranychus cinnabarinus in our previous study. The purpose of this study was to isolate active components from the Mentha piperita extracts and to explore the mechanisms of their acaricidal activities. We also studied the effects of Mentha piperita extracts on the activities of some enzymes in Tetranychus cinnabarinus in order to understand the specific acaricidal mechanisms. Our results indicated that Mentha piperita can be exploited as a new resource for developing potential acaricides.

2 Materials and Methods

2.1 Material Collections

The plants of *Mentha piperita* were collected from growing base of aromatic plants at Beijing University of Agriculture. The plants of *Mentha piperita* were oven-dried at 25 ± 3 ℃ and grounded into power. After passing a 60 mesh, the power was placed in the refrigerator (Electrolux BCD-281EA) for storage. *Tetranychus cinnabarinus* were obtained by feeding on *Vigna unguicul* at room temperature of 25 ± 1 ℃, and a relative humidity of 60 ± 10 % and an ambient photoperiod of 18: 6 (L: D) h[16].

2.2 Reagents and Apparatus

UV-VIS spectrophotometer (Tu-1800, Purkinje General Inc., Beijing, China), High-Speed Refrigerated Centrifuge (HITACHI RX), Electronic balance (Saiduokeen Inc., Beijing, China), Stereo microscope (OLYMPUS SZ51, Olympus Inc., Japan), Ultramicrotome (Leica EM FC6, Leica Inc., Germany), Transmission electron microscope (Shimadzu Inc., Japan), 1000μL Pipette (Eppendorf Inc., Germany).

2.3 Preparation and Separation of Crude Extraction

The protocol for preparation of crude extraction was described previously. Briefly, the plant powder was immersed in a flask for 3 d at room temperature of 25 ± 3 ℃, and the ratio of solid to liquid was 1: 6. The extracts were gained after filtering and evaporating.

A 100 by 400 mm chromatography column and a 200 -300 mesh silica gel were used to isolate active components from *Mentha piperita*. 8 g of concentrated extract was added into the column, and then a combination of chloroform, ethyl acetate and methyl alcohol (1: 1: 1) was slowly added to the column at the rate of 10 ml per second. This mobile phase was continuously added to the column until all the concentrated extract eluted from the silica gel and was collected at the bottom of the column at 50 ml per collection bottle. Based on band appearance in TLC, these fractions were amalgamated into 8 groups. Each group was evaporated to obtain concentrated isolate for use.

2.4 Bioassays

Acaricidal activity was measured using the method of Wang, *et al*[26].The crude extracts of *Mentha piperita* were mixed with Tween 80 (1: 1) and diluted with distilled water at a concentration of $2mg \cdot ml^{-1}$. Acaricidal activity of *Mentha piperita* against *Tetranychus cinnabarinus* was measured using a slide dip technique [28]. The slide dip was conducted as follows. The mites were stuck onto one side of double-sided adhesive tape fixed on one end of a glass slide. The end of the slide with mites was dipped into the extract dilution or the control for 5 s. The slide was taken out, and the extra solution was removed with filter paper. Mortality was checked 24 h after treatment. Mites were considered dead if they did not respond to a gentle probe with a fine brush.

2.5 Observation of the Poisonous Symptoms of Tetranychus Cinnabarinus

Thirty female adults were placed on a clean *Vigna unguicul* leaf in a Petri dish (10 cm in diameter) containing a wet filter paper used to prevent the leaf from drying. The *Vigna unguicul* leaf with mites was dipped into the extract dilution or the control for 5 s. A circular barrier of moistened cotton was placed around the leaf to prevent mites from escaping. The poisonous symptoms of mites were observed every two hours within 24h.

Sample preparation for transmission electron microscopic analysis. 3 mites which had been observed for the poisonous symptoms in the treated and control groups were selected at random, respectively. The mites were fixed overnight in 3 % glutaraldehyde, and washed in 0.1 mol phosphate buffer at pH 7.2 for 3 h. Subsequently, the mites were post fixed in 1 % osmic acid for 1 hour at 4 ℃, and washed again in 0.1 mol phosphate buffer for 0.5 h, and then dehydrated through increasing concentrations of ethanol for 10 min each time. After embedding and polymerization with epoxy resin, thin sections were obtained by using ultramicrotome. The ultrathin sections are stained with uranyl acetate followed by lead citrate. Sections were investigated with a transmission electron microscope.

2.6 Preparation of Enzyme Solution

150 mites were treated for 4, 8, 12, 16, 20 and 24 h, respectively, and put into a different solution, according to the different enzymes measured and homogenized in an

ice bath. The supernatant was collected by centrifugation at 10,000 r/min for 15 min at 4 ℃ [17]. The mites which are used to measure MAO and protease activities were put into 0.125 ml saline, while the mites which are used to determine activity of the GSTs or AChE were placed in the 60mmol • L^{-1} phosphate buffer (pH 7.5) and the 0.1 mmol•L^{-1} phosphate buffer (pH7.5), respectively.

2.7 Enzyme Activity Assay

Glutathione-S-transferase (GST) activity was determined using the method of Mu, *et al*[18]. A 0.1ml enzyme solution was dropped into the tube and a combination of 2.5 ml phosphate buffer, 0.2 ml GSH, and 0.05 ml CDNB (0.03 mol·L^{-1}) into the control tube. Solution in each tube is mixed and reacted at 37 ℃. After that, the *OD* values of them were determined at the 340 nm wavelength by the spectrophotometer.

AChE activity was determined as follows. AChE, TNB and physostigmine was used as substrate, chromogenic agent, the inhibitor, respectively. After reaction at 27 ℃ for 15 min, a 0.3 ml of 1 mmol·L^{-1} physostigmine was added to terminate reaction. The *OD* values of them were measured at 412 nm wavelength by the spectrophotometer. The experiments were repeated 3 times.

MAO activity was determined as follows. Benzylamine is used as substrate, after the enzyme reaction, the content of benzyl was measured through its UV absorption peak at 273 nm, the content of benzyl produced by benzylamine presents enzyme activity. The experiments were repeated 3 times.

Protease activity was determined as follows. A 0.1 ml enzyme solution was dropped into the tube, and heated in a water bath at 37 ℃ for 3 - 5min. A 0.1 ml casein solution which was preheated at 37 ℃ was added, and mixed and heated at 37 ℃ for 15 min. 3 ml of 10 % trichloroacetic acid was added to the solution. The supernatant was collected by centrifugation. 1 ml Supernatant, 5 ml of 0.5 M sodium carbonate, and 1ml of Follin-phenol reagent were mixed and reacted in a water bath at 37 ℃for 15 min. The *OD* values of them were measured at 680 nm wavelength by the spectrophotometer. The experiments were repeated 3 times.

2.8 Statistical Analysis

Mortality data from the above-mentioned bioassays were corrected for control mortality by using Abbott's formula. The corrected mortality was normalized by an arcsine-square-root transformation before being subjected to a one-way analysis of variance (ANOVA). The corrected mortality data were subjected to probit analysis POLO-PC (LeOra Software 1994) to estimate the LC_{50} (the concentration at which 50% of the mites died) and 95% confidence limit. All data are processed using Excel and the DPS (v3.01).

3 Results

3.1 The Acaricidal Activities of Active Components from Mentha Piperita Extract against Tetranychus Cinnabarinus

Bioassays were used to test the biological activities of *Tetranychus cinnabarinus* treated with 8 fractions obtained from *Mentha piperita* extracts. The results showed

that the fraction V had the strongest toxicity to the mites in all the fractions (Table. 1). The mean half lethal concentration (LC_{50}) was 0.5464 mg/ml and 95 % confidence limit was 0.3268 -0.9134 mg/ml at 24 h after treatment. The fraction I was in the second place with the LC50 value of 0.5464 mg/ml and 95 %confidence limit of (0.4727 - 1.6077) mg/ml. The fraction II, fraction III, fraction IV and fraction VI showed lethal effects on the mites with the LC_{50} value of 1.2681, 1.7453, 1.8899, 1.8149 mg/ml, respectively. Fraction VIII had the lowest toxicity with LC_{50} value of 12.505mg / ml and 95 % confidence limit of (8.4393 - 18.5293) mg/ml. The results indicated that the acaricidal substance mainly existed in fraction V. In addition, the fraction I also showed a strong acaricidal activity, implying that there may be two acaricidal substances in *Mentha piperita*, or fraction I appeared to cooperate with fraction V to kill the mites. Overall, Fraction V had strong toxicity to *Tetranychus cinnabarinus*.

Table 1. The toxicity regression equations of the liquid chromatography fractions against *T. cinnabarinus* adults (24h)

Code	eluted system(V:V)	Toxicity regression equation	Correlation coefficient R^2	LC_{50} and 95%confidence limit(mg/ml)
I	Petroleum ether	y = 2.3561x + 5.1403	0.9998	0.8718 (0.4727~ 1.6077)
II	8:2[a]	y = 1.6109x + 4.8338	0.9939	1.2681 (0.6667 ~2.4118)
III	5:5[a]	y = 2.7111x + 4.3442	0.9711	1.7453 (1.0134 ~3.005)
IV	2:8[a]	y = 2.5014x + 4.3085	0.9976	1.8899 (1.0864 ~3.2875)
V	Chloroform	y = 3.0796x + 5.8082	0.9784	0.5464 (0.3268 ~0.9134)
VI	7:3[b]	y = 2.0497x + 4.4694	0.9956	1.8149 (1.007 ~3.2708)
VII	6:4[b]	y = 2.0081x + 4.1458	0.9998	2.6630 (1.5589 ~4.5488)
VIII	Methanol	y = 1.2484x + 3.6304	0.9951	12.505 (8.4393 ~18.5293)

[a] petroleum ether：chloroform (V:V), [b] chloroform： methanol(V:V); letter y stands for the probability value of mortality, letter x stands for the logarithm value of different concentrates.

3.2 Effect of Monoamine Oxidase Activity of the Fraction V against Tetranychus Cinnabarinus

Most of acaricides exhibit toxicity to mites by interfering with their nervous system. Monoamine oxidase (MAO) enzyme plays an important role in the regulation of the nervous transduction by reducing accumulation of sphingosine in nerve cells. So we detected whether fraction V had significant effect on the MAO activity of *Tetranychus*

cinnabarinus. As shown in Fig. 1, the MAO activity of *Tetranychus cinnabarinus* in the treated and control groups increased initially and then decreased at 4 h - 12h after treatment. The enzyme activity reached a peak at 8h after treatment, and the MAO activity in the treatment group increased by 1.9 folds compared with the control group. The MAO activity in the treatment group decreased from 12h to 20 h, while the MAO activity in the control group increased initially and then decreased. However, there was no difference between the treatment and the control groups in the MAO activity at 16 h and 20 h after treatment. Then the MAO activity of *Tetranychus cinnabarinus* in the treated and control groups was increased from 20 h to 24 h, and the MAO activity in the treated group increased more significantly than that in the control group. Generally, the changes of the MAO activity in treated and control groups had the identical trend, but the MAO activity in the treatment group was always higher than the control group, indicating that fraction V was able to activate MAO in *Tetranychus cinnabarinus*.

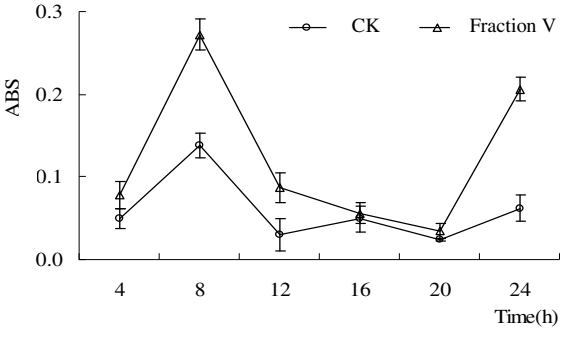

Fig. 1. Effect of monoamine oxidase activity of the fraction V against *Tetranychus cinnabarinus*

3.3 Effect of Glutathione-S-Transferase Activity of the Fraction V against Tetranychus Cinnabarinus

Glutathione-S-transferase (GSTs), an important detoxification enzyme *in vivo*, was recognized as resistance-related primary or secondary metabolic enzyme. GSTs plays a regulatory role in metabolizing the exogenous toxic substances in *Tetranychus cinnabarinus*. So we detected if fraction V had significant effect on the GSTs activity of *Tetranychus cinnabarinus*. As shown in Fig. 2, the GSTs activity in the treatment group increased initially and then decreased as time goes by, while the GSTs activity in the control group decreased initially and increased from 4 h to 12 h, and deceased again after 12 h. Generally, the GSTs activity in the treatment group was always higher than the control group, especially at 8h and 24 h after treatment. These results suggested that fraction V played an important role in activating GSTs in *Tetranychus cinnabarinus*.

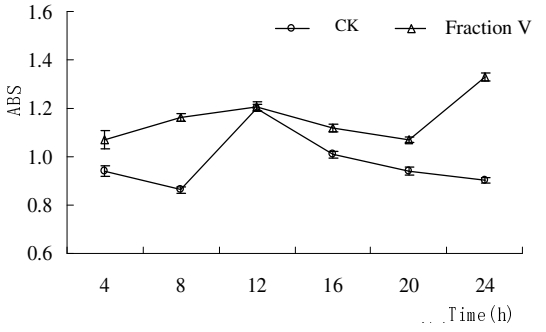

Fig. 2. Effect of glutathione-S-transferase activity of the fraction V against *Tetranychus cinnabarinus*

3.4 Effect of Acetylcholine Esterase Activity of the Fraction V against Tetranychus Cinnabarinus

Acetylcholinesterase (AChE), a key enzyme *in vivo*, plays an important role in the regulation of the nervous excitement and conduction in nerve cells. We wanted to know whether fraction V exhibited toxicity to mites by mediating AChE activity. As shown in Fig. 3, the changes of the AChE activity in treated and control groups had the identical trend from 4 h to 12 h, but the AChE activity in the treatment group was always lower than the control group, especially at 12 h after treatment, the AChE activity in the treatment group reduced to a minimum. The decrease of AChE activity in the treatment group was more obvious than that in the control group, though the AChE activity in treated and control groups declined from 4 h to 12 h. At 12 h – 16 h after treatment, the AChE activity in treatment group increased initially and then decreased as time goes by. The AChE activity in control group increased from 12 h to 20 h, and then declined again from 20 h to 24 h. The results indicated that fraction V played an important role in suppressing AChE activity in *Tetranychus cinnabarinus*.

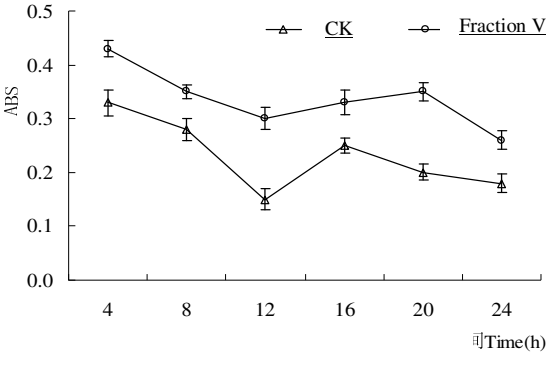

Fig. 3. Effect of acetylcholine esterase activity of the fraction V against *Tetranychus cinnabarinus*

3.5 Effect of Protease Activity of the Fraction V against Tetranychus Cinnabarinus

Protease, an important digestive enzyme in vivo, decomposes the protein into polypeptide or amino acid for absorption. The change of protease activity exhibits regulatory effects to protein metabolism. We studied whether the protease activity was mediated by fraction V. As shown in Fig. 4, the protease activity in treatment group was always lower than the control group except that at 4h and 24 h after treatment. Generally, the protease activity was restrained by fraction V.

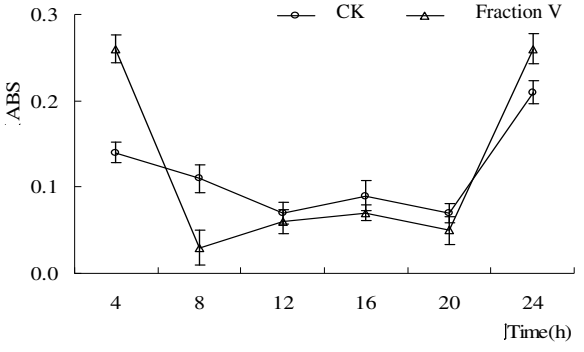

Fig. 4. Effect of protease activity of the fraction V against *Tetranychus cinnabarinus*

3.6 Observation of the Poisonous Symptoms of Tetranychus Cinnabarinus

In order to study the acaricidal activities of fraction V, we observed the poisonous symptoms of *Tetranychus cinnabarinus* after treatment, and we found that the mite underwent four stages, *i.e.*, stationary phase, excitement phase, spasm phase, and death phase. Specially, in stationary phase, most adult mites kept stock-still with their feet in a contraction in the first 4 hours after treatment. At 4 h - 12 h after treatment, the excitement phase mites crawled everywhere and were active. Subsequently, the mites exhibited spasm symptoms including over-excitement, lack of coordination, foot shaking frequently, ovulation, and the increase of red blood streaks in skin from 10h to 18h. After a brief spasm, the mites entered death phase accompany with the appearance of black granular waste (Fig.5). These results indicated that fraction V exhibits important impacts in production of stomach toxin, suppression of growth and reproduction by affecting the nervous and digestive systems.

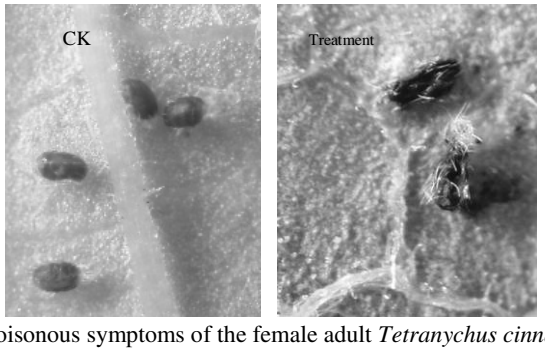

Fig. 5. Poisonous symptoms of the female adult *Tetranychus cinnabarinus*

The ultrastructure of the mites was also observed by using transmission electron microscopy at 24 h after treatment. There was obvious difference in ultrastructure of the mites in the treated and control groups. As shown in Fig. 6, the subcellular structures within inner membrane (IM) such as endoplasmic reticulum (Er), mitochondria (Mt), nucleus membrane system were not damaged in the control group (Ck a-b), while the subcellular structures were severely damaged and dissolved completely (T a-b), leading to cavity formation and production of dissolved or semi-dissolved residuals. Meanwhile, we also found that the skins of mites were severely damaged and arranged irregularly in the treatment group, on the contrary, the structure of the epidermis (ED) of mites was dense with regular apophasis in the control group. These results indicated that fraction V was able to kill *Tetranychus cinnabarinus* by destroying the ultrastructure of the mites.

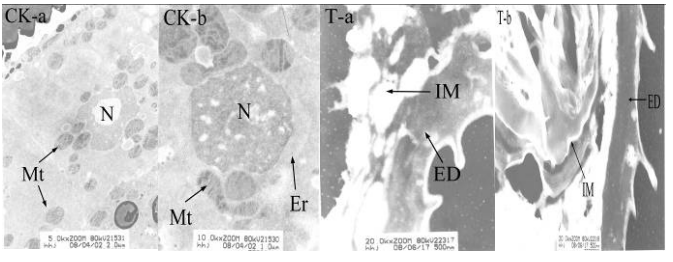

Fig. 6. Observation of the subcellural sturcture of *Tetranychus cinnabarinus*

4 Discussion

In recent years, many researchers have found that aromatic plants have toxicity to agricultural pests, but there are few reports on their acaricidal activities. We discovered in this study that the extracts of *Mentha piperita* had acaricidal activities against *Tetranychus cinnabarinus*. Our further work on the extraction, column chromatographic fractionation and detection of the bioactivities of active components from *Mentha piperita* extracts, demonstrated that fraction V had strong acaricidal activities, The discovery of acaricidal activities of *Mentha piperita* extracts provides a very important theoretic basis for the development of acaricides from *Mentha piperita*.

Glutathione-S-transferase, monoamine oxidase, acetylcholine esterase and protease are important enzymes in vivo, playing important regulatory roles in maintaining the normal life activities of the *Tetranychus cinnabarinus*. Glutathione-S-transferase, an important metabolic enzyme, exists in various tissues of organisms. Glutathione-S-transferase reduces the cytotoxicity by catalyzing the reaction between glutathione and compounds, which has an affinity for electrophilic group. So the GST plays an important role in elimination of free radicals and detoxification. It is reported that glutathione-S-transferase plays an important role in detoxifying insecticides in pests. Our results showed that the GST was activated by fraction V for detoxification, indicating that the mites were poisoned after treatment. Nervous system is one of the most targets of pesticides, Acetyl cholinesterase and monoamine oxidase are the two key enzymes to mediate nervous system. AChE terminates the transmission of nerve

impulses by hydrolyzing acetylcholine in nervous cells. Our results showed that the activity of AChE was suppressed after treatment with Fraction V, leading to the destruction of nervous transmission due to the abnormal metabolism of acetylcholine. MAO, another nerve-related enzyme, ensures the nervous transmission by reducing the accumulation of ceramide. We showed that the MAO activity in the treatment group was always higher than the control group except that at 16 and 20 h after treatment, indicating that fraction V was not able to block the nervous transmission mediated by MAO in *Tetranychus cinnabarinus*. Protease, an important digestive enzyme in vivo, plays an important role in regulating protein metabolism. We found that the protease was inhibited after treatment with Fraction V. These results suggested that suppression of AChE and protease activities might cause the death of mites by affecting the nervous transmission and protein metabolism.

In this study, we also found that acaricidal effects of fraction V resulted from nervous transmission block and protein metabolism disorder by the observation of the poisonous symptoms of *Tetranychus cinnabarinus*. This conclusion was consistent with changes of enzymes activities. Specifically, the activities of acetylcholine esterase (AchE) and protease were restrained after treatment whereas the activity of glutathione-S-transferase (GSTs) was strongly induced from 4 h to10 h, leading to the disorders of nervous and digestive systems. So the mites exhibited the over-excited symptoms. At 10 h - 18 h after treatment, the continuous inhibition of acetylcholine esterase and protease resulted in deep damage to nervous and digestive systems. Meanwhile, the activation of GSTs maintained the detoxification. The mites exhibited the spasms symptoms at this period. Then we found that the activity of AchE was strongly inhibited from 18 h to 24 h, though GSTs and MAO was still activated. The suppression of AChE led to the block of central and synaptic nervous transmission. We also found that the activity of protease increased and tissue protein started to decompose, meanwhile, the protein structures of organelle was degraded accompany with appearance of cavity by using transmission electron microscopy. Overall, our studies suggested that *Mentha piperita* was able to kill *Tetranychus cinnabarinus* by affecting the significant activity of the enzymes in vivo and destroying the ultrastructure of the mites, indicating that *Mentha piperita* may be used as a novel resource of botanical acaricide.

In conclusion, we not only discovered the strong toxicity of fraction V from *Mentha piperita* extracts to the mites, but also studied the effects of fraction V on the enzyme activities and ultrastructure of *Tetranychus cinnabarinus*. The results showed that the activities of AChE and protease were greatly restrained after treatment with fraction V. Furthermore, the transmission electron microscopic observations revealed that the treated mites suffered from the rupture of ultrastructures such as endoplasmic reticulum, mitochondria and nuclear membrane. However, the specific acaricidal mechanisms of *Mentha piperita* were not clearly clarified in this paper, and further studies will be needed.

Acknowledgements. The work was financially supported by the National Natural Science Foundation of China (30872029), the Key Natural Science Foundation of Beijing Municipality (6071001), the Natural Science Foundation of Beijing Municipality (6092007), the Key Foundation of Beijing Municipal Education Committee (KZ201010020016), and Funding Project for Academic Human Resources

Development in Institutions of Higher Learning Under the Jurisdiction of Beijing Municipality (PHR20090516, PHR200906134).

References

1. Antonious, G.F., Dahlman, D.L., Hawkins, L.M.: Insecticidal and Acaricidal Performance of Methyl Ketones in Wild Tomato Leaves Bull. Environ. Contam. Toxicol 71, 400–407 (2003)
2. Irfan, A., Hikmet, O., Onder, C., Fikrettin, S.: Toxicity of essential oil vapours to two greenhouse pests, Tetranychus urticae Koch and Bemisia tabaci. Genn. Industrial Crops and Products 19, 167–173 (2004)
3. Mansour, F., Ravid, U., Putievsky, E.: Studies on the effects of essential oils isolated from 14 species of Labiatae on the carmine spider mite, Tetranychus cinnabarinus. Phytoparasitica 14, 137–142 (1986)
4. Shaaya, F., Ravid, U., Paster, N., Juven, B., Zisman, U., Pissarev, V.: Fumigant toxicity of essential oils against four major stored product insects. J. Chem. Ecol 17, 499–504 (1991)
5. Ho, S.H., Ma, Y., Huang, Y.: Anethole apotential insecticide from Illicium verum Hook F against two stored-product insects. Int. Pest Control 39, 50–51 (1997)
6. Landolt, P.J., Hofstetter, R.W., Biddick, L.L.: Plant essential oils as arrestants and repellents for neonate larvae of the codling moth (Lepidoptera: Totricidae). Environ. Entomol. 28(6), 954–960 (1999)
7. Liu, J.H.: environmental-friendly botanical pesticide. Journal of Biology 37(6), 30–31 (2002)
8. Ardeshir, A., Rahim, E., Gholamhosein, T.: Laboratory evaluation of some plant essences to control Varroa destructor (Acari: Varroidae). Experimental and Applied Acarology 27, 319–327 (2002)
9. Committee of National Codex. Codex of People's Republic of China, Beijing: People' sanitation publishing company, 310 (2000)
10. Liang, C.Y., Li, W.L., Zhang, H.Q., et al.: The advance on the research of chemical constituents and pharmacological activities of *Mentha haplocalyx*. Chinese Wild Plant Resources 22(3), 91 (2003)
11. Chen, G.L., Yu, Y.B., Li, D.M.: Primary study of the effective constitudes and pharmacologic on peppermint oil. Chinese Journal of Infermation on TCM 7(2), 33–34 (2000)
12. Edris, A.E., Farrag, E.S.: Antifungal activity of peppermint an sweet basil essential oils and their majority constituents of some plant pathogenic fungi from the vaporphase. Nahrung 47(2), 117–121 (2003)
13. Schuhmacher, A., Reichling, J., Schnitzler, P.: Virucidal effect of peppermint oil on the developed viruses herpess implex virus type and type in vitro. Phytomedicine 10(6-7), 504–510 (2003)
14. Ahmed, S.M., Eapen, M.: Vapour toxicity and repellency of some essential oils to insect pests. Indian Perfumer 30(1), 273–278 (1986)
15. Raja, N., Albert, S., Ignacimuthu, S.: Effect of plant volatile oils in protecting stored cowpea Vigna unguiculata (L.) Walpers against Callosobruchus maculates (F.) (Coleoptera: Bruchidae) infestation. Journal of Stored Products Research 37, 127–132 (2001)

16. Jeremy, A., Rudd: Effects of pesticides on spin down and webbing production by the two-spotted spider mite, Tetranychus urticae Koch (Acari: Tetranychidae). Experimental & Applied Acarology 21, 615–628 (1997)
17. Cao, H., Liu, S.Q., Wang, H.L., et al.: The effects of extracts of Tateges eracta on activities of several enzyme of Tetranychus viennensis zacher. Scientia Silvae Sinicae 39(2), 114–115 (2003)
18. Mu, L.Y.: Methodology of plant chemical protection, pp. 160–161. China Agriculture publishing company, Beijing (1994)
19. Qu, J.H., Chen, J.C., Hu, G.D., et al.: Dynamic changes of catalase and glutathione-s-transferase in the different tissues of tilapia exposed to phenol. Ecology and Environment 15(4), 687–692 (2006)
20. Chen, F.J., Gao, X.W., Lei, M.Q., et al.: Effects of tannic acid on glutathione S-transferases in Helicoverpa armigera(Hűbner). Acta Entomologica Sinica 46(6), 684–690 (2003)
21. Ku, C.C., Chiang, F.M., Hsin, C.Y., YaoY, E., Sun, C.N.: Glutathion transferases isozymes involved in insecticide resistance of diamond bacmoth larvae. Pestic. Biochem. Physiol 50, 191–197 (1994)
22. Prapanthadara, L., Promter, N., Koottathep, S., Somboon, P., Ketterman, A.J.: Isoenzymes of glutathione-S-transferasess from the mosquito Anopheles dirus species B: the purification, partial characterization and interaction with various insecticides. Insect Biochem. Mol. Biol 30, 395–403 (2000)
23. Wang, D., Tang, Z.H., Shang, J.Y., et al.: Advances in the studies of acetylcholinesterase genes from insects. Acta Entomologica Sinica 49(3), 497–503 (2006) (in Chinese)
24. Chen, J.C., Wu, W., Qu, J.H., et al.: Activities of catalase and monoamine oxidase in different tissues of tilipia under stress of deltamethrin. Journal of Agro-Environment Science 25(6), 1441–1445 (2006)
25. Cao, H., Wang, Y.N., Liu, S.Q., et al.: Effects of the Chloroform Extracts of Kochia scoparia to Several Enzyme Systems in Tetranychus viennensis. Scientia Silvae Sinicae 42(2), 68–72 (2007)
26. Wang, Y.N., Shi, G.L., Zhao, L.L., et al.: Acaricidal activity of Juglans regia leaf extracts on Tetranychus viennensis and Tetranychus cinnabarinus (Acari: Teranychidae). Journal of Economic Entomology 100(4), 1298–1303 (2007)
27. Abbott, W.S.: A method for computing the effectiveness of an insecticide. Econ. Entomol. 18, 265–267 (1925)
28. FAO. Revised method for spidermites and their eggs(Tetranychus spp.and Panonychus ulmi Koch). FAO Plant Production 21, 49–54 (1980)

Analysis of Acaricidal Activities and Enzymatic Activities of Polygonum Aviculare Extracts against Tetranychus Cinnabarinus

Jun Cheng, You-nian Wang, Lan-qing Ma, Yu-bo Liu, and Guang-lu Shi*

Key Laboratory of Urban Agriculture (North) of Ministry of Agriculture, P.R. China
Beijing University of Agriculture, Beijing, China
glshi@126.com

Abstract. The toxicity and relative enzyme activities of different extracts of Polygonum aviculare against Tetranychus cinnabarinus were studied. It was found that the acaricidal activity of the chloroform extract of Polygonum aviculare was significantly higher than the petroleum ether and the methanol ones in the concentration of 2 mg·mL-1 ($P < 0.05$). At 48 h after treatment, the corrected mortality of female adults of Tetranychus cinnabarinus was 89.95 % and the LC50 was 0.7153 ± 0.1253 mg·mL-1. After parted and purified by extracting and chromatograph, there were 19 parts gained finally, in which the sec, 7th, 8th, 15th, 16th, 17th and 18th parts had higher acaricidal activities than others, their mortalities had been all above 70 %. The 16th part's mortality reached 87.12 % and its effect on AchE, Na+, K+-ATPase and GSH-S-transferase was detected by colorimetric method, which showed that these enzyme activities were affected differently.

Keywords: Tetranychus cinnabarinus, Polygonum aviculare, AChE, Na+, K+ -ATPase, GSH-S-transferase.

1 Introduction

Tetranychus cinnabarinus is a kind of worldwide important economical insect (Hazan et al, 1974; Ho et al., 1997).It is characterized by small size, quick breed, high population density and serious damage (Shi guanglu et al, 1994; Li lianchang et al, 1992), which is more easily resistant to insecticides than other injurious mites. The cost of prevention increases with its insecticide resistance increasing annually. So it is inevitable and necessary to find more safer and efficient acaricides. The characteristics of the botanical acaricide are selective drug action, low toxicity and easy degradation and the injurious mites are not easily resistant to it. It has small hazard to the Cactoblastis cactorum of the targeted injurious mites. In recent years, the high activity materials have been screened out from plant to develop new botanical acaricides directly or take them as the forerunners to synthetize new, safe and efficient pesticides, which has been a focus in research and development fields of pesticides at home and abroad.

* Corresponding author.

E. Zhu and S. Sambath (Eds.): Information Tech. and Agricultural Eng., AISC 134, pp. 589–598.
springerlink.com © Springer-Verlag Berlin Heidelberg 2012

The alternate name of Polygonum aviculare is Stolonifera polygonum aviculare, which belongs to polygonaceae and it is annual or perennial herb. Polygonum aviculare is distributed throughout the country. There is high yield in Henan, Sichuan, Zhejiang, Shandong, Jilin and Hebei Province. It grows in the field, beside the road, in water side and in wetland. There are many studies about polygonum aviculare used in medicine, but there are few reports about its acaricidal active ingredients. In this paper, combined with the present productive practice tightly, we carried out systematic study on acaricidal active ingredients and their mechanisms of action, which offered the scientific theoretical foundation for developing botanical insecticides.

2 Materials and Methods

2.1 Materials

Polygonum aviculare was crushed by high speed disintegrator (Type: 6202, Beijing Huanya Tianyuan mechanical technology co.), filtrated by 40-eyes sifter and stored in the refrigerator preparation for use. Tetranychus cinnabarinus originates from the sensitive strain bred in the room where the temperature is (25 ± 1) ℃, the relative humidity is 50 ± 10 percent and the illumination condition is L: D=18h: 6h. All reagents are all analytical ones (Beijing Chemical Factory).

2.2 Methods

Extraction and Separation of Active Ingredients in Polygonum Aviculare. A certain amount of dry powder was weighed accurately and bottled into the jar. Then a fivefold amount of organic solvents were added to the jar. At room temperature the materials were extracted for 3 times, every time for 3 to5 days. Then three kinds of extract was combined, decompressed, concentrated to paste and the weight was determined. 15 gram of Polygonum aviculare extract was weighed dissolved with tenfold amount of petroleum ether and the separating funnel was loaded with it. Then it was extracted for three times with methanol. Finally extract was combined, decompressed, concentrated to thick paste and its weight was determined. 100 times amount of silica gel was weighed, mixed with the right amount of eluent and poured into chromatographic column quickly. The column wall was tapped with the rubber hammer. At the same time, the plug cock at the bottom was opened to make the solution move down slowly and ludox be deposited tightly at the bottom of column. Seven gram of extract was dissolved with small quantity of initial eluent and poured into chromatographic column by the inner layer of it when the distance from the surface of solution to one of silica gel was about one centimeter. When materials to be separated shifted below the surface of silica gel, it was covered with a layer of quartz sand. Then it was eluted with the petroleum ether, chloroform and methanol solvents system with the flow of 10ml/min. 50 ml of every part was collected, which was detected in iodine stream and marked after thin layer chromatography (TLC).The identical components were combined, decompressed and concentrated. Then the biological activities were detected.

Acaricidal Activities. Biological activities were detected by method of slide impregnation (FAO, 1980).Thirty lively, healthy and same size female adults of

Tetranychus cinnabarinus were stuck to one end of object slides with two-faced GLUE TAPE. After they were soaked in liquid medicine for five seconds, they were taken out and the extra liquid medicine around the mite soma was sopped up with filter paper. Then the Tetranychus cinnabarinus was placed at room temperature and the deaths were observed after 48h. When they are touched, the moving ones are living and the stationary ones are dead. Finally the corrected mortalities were calculated according to the Abbott formula (Abbort, 1987).

Symptoms Observing. Symptoms were observed by method of leaf disc impregnation (Zhu limei, et al. 2002). Clean and flat soybean leaves were placed on the water culture platform. More than thirty adults of Tetranychus cinnabarinus were placed on every leaf. When they were steady, the leaves were nipped and soaked in liquid medicine for five seconds. The water treated group served as control. The edges of the leaves were surrounded with wet cotton slivers to prevent Tetranychus cinnabarinus from escaping. The activities of adults and their response were observed once every twelve hours for four times totally.

Enzyme Solution Preparation. The tested mites were treated by contact method. 0.25mL of physiological saline was added to 150 female adults of Tetranychus cinnabarinus after treatment for 8h, 16h, 24h, 32h, 40h and 48h respectively, which were homogenate with ice-bath and centrifuged at 4℃ at the speed of 10 000r·min^{-1}. Finally, the supernatant was acquired preparation for use.

Protein Content Detection. Protein content was detected by Coomassie brilliant blue G-250 method (Mu liyi, 1991). After 0.1 ml of enzyme solution was added to 5 ml of Coomassie brilliant blue G-250, they were mixed to become homogeneous and heated at 25℃ constant temperature in water bath for two minutes. The OD value was detected using colorimetry at 590nm wavelength. Then protein content was calculated according to the standard curve.

Enzymatic Activity Detection. Enzymatic activities of acetylcholinesterase (AChE), Na^+, K^+-ATPase and GSH-S transferase were all detected according to the related methods in Prevention Research Method of Photochemistry (Mu liyi, 1991).

3 Results and Analysis

3.1 Acaricidal Activities of Extracts against Tetranychus Cinnabarinus

The rates of extraction from polygonum aviculare of three kinds of solvents were (11.86 ± 0.56) % of methanol and (2.65 ± 0.38) % of chloroform greater than (1.56 ± 0.08) % of petroleum ether. The methanol extract, chloroform extract and petroleum ether extract were used respectively to dispense 2 mg·mL^{-1} medicine. Toxicity of harmful mites detection results (Table 1) demonstrated that acaricidal activities of chloroform extract after 48 h were significantly higher than ones of two other organic solvent extracts($P < 0.05$). Its mortality to Tetranychus cinnabarinus reached 89.95 %. Therefore the chloroform extract is further extracted and purified.

Table 1. Extract rate and mortality of different extracts from *Polygonum aviculare* against *Tetranychus cinnabarinus*

Extracts(2 mg·mL^{-1})	Extraction rate/%	Mortality/%
Petroleum ether extract	1.56±0.09	49.51±2.97 ^{b}
Chloroform extract	2.65±0.32	89.26±3.93 ^{a}
Methanol extract	11.86±1.05	13.61±7.35 ^{c}

Values are mean ±SE of three determinations the averages within the same column not followed by the same letter are significantly different at 5% level of confidence the same below.

3.2 Acaricidal Activities of Extracts against Tetranychus Cinnabarinus

Chloroform extract having good acaricidal activities was extracted and separated with methanol and petroleum ether (Table 2). The extraction rates were (58.42 ± 1.40) % of petroleum ether and (32.88 ± 2.32) % of methanol greater than (8.70 ± 0.68) % of the middle undisclosed substance. Biological assay results of extracts showed that the mortality of the middle undisclosed substance was (84.00 ± 5.32) %, which was significantly higher than methanol (40.74 ± 2.64) % and petroleum ether ones (32.69 ± 1.32) % ($P < 0.05$). Thereby, it can be determined that the active substances of *Polygonum aviculare* killing *Tetranychus cinnabarinus* mainly reside in the middle undisclosed substances.

Table 2. Extract rate and mortality of chloroform extracts from *Polygonum aviculare* against *T.cinnabarinus*

Extracts(2 mg·mL^{-1})	Extraction rate/%	Mortality/%
Petroleum ether extract	58.42±1.40	32.69±1.32c
indiscerptible substance	8.70±0.68	84.00±5.32a
Methanol extract	32.88±2.32	40.74±2.64b

3.3 The Best Isolation Fraction and Its Biological Activity Assay

Nineteen isolation fractions acquired after chromatography extract and TLC detection were bioassayed (Table 3). The result demonstrated that the sec, 7th, 8th, 15th, 16th, 17th and 18th isolation fractions had strong acaricidal activities and their mortalities had been all above 70 %. The 16th part had the best acaricidal activity in the concentration of 2mg·/mL and its mortality had reached 87.12 %. Moreover, because of its higher yield, it was selected to carry out toxicology studies. Five different concentrations of liquid medicine (0.5, 1, 2, 4, 8 mg·mL^{-1}) was made up using the 16th part and the biological activities were detected. The toxicity regression equation was y=5.2702+1.0038x and the median lethal concentration LC_{50} was 0.988 mg·mL^{-1}, which showed that it had better biological activities. When the concentration of liquid medicine was 2 mg·mL^{-1}, the mortality of harmful mites reached 87.12 % after treatment for 48 h, which was suitable for further investigation of the following enzymatic activities. Therefore, symptoms observing and enzymatic activities assay were carried out in the concentration of 2 mg·mL^{-1}.

Table 3. Extract rate and mortality of fractions of chromatography extract of *P. aviculare* against *T.viennensis*

Isolation fraction	Isolation rate/%	Mortality /%
1	2.77	69.52 ± 7.36^{b}
2	1.68	76.61 ± 7.26^{a}
3	2.04	38.55 ± 14.03^{abc}
4	0.68	38.49 ± 3.77^{abc}
5	1.02	36.86 ± 6.25^{abc}
6	0.42	47.08 ± 3.30^{ab}
7	0.26	73.68 ± 3.07^{b}
8	3.23	76.94 ± 13.27^{a}
9	2.12	58.5 ± 7.18^{abc}
10	0.45	15.46 ± 9.21^{abc}
11	0.67	11.29 ± 15.73^{ab}
12	0.49	4.72 ± 0.21^{ab}
13	1.14	27.83 ± 0.19^{ab}
14	0.98	67.45 ± 7.08^{bc}
15	2.28	71.87 ± 7.36^{b}
16	22.32	87.12 ± 0.04^{ab}
17	2.90	83.20 ± 6.32^{abc}
18	5.48	75.68 ± 4.12^{bc}
19	14.23	61.99 ± 6.22^{a}

3.4 Symptoms Observing

After female adults of *Tetranychus cinnabarinus* were treated with the 16th part (2 mg·mL^{-1}) and water, their symptoms were observed. It was found that from 0 to 12 h the harmful mites in the treatment group were very excited, moved about and laid eggs rapidly. However, ones in the control group moved slowly and fed on leaves normally. From 12 to 24 h, humor began to exude from the back of ones in the treatment group, they pattered about and egg laying amount decreased to some extent. However, ones in the control group acted normally and began to lay eggs. From 24 to 36h, ones in the treatment group were still in a state of extravasation. Its body began to contract. However, ones in the control group crawled normally and no abnormality was seen. From 36 to 48 h, the bodies of ones in the treatment group contracted gradually until they died. However, ones in the control group were bulging in the body and acted normally. After the 16th part treatment, Tetranychus cinnabarinus showed symptoms similar to ones resulting from the nerve poison such as excitation and spasm *et al*. Therefore it was speculated that the active substance may have effect on the nervous system.

3.5 Activities Assay of Acetylcholinesterase

The 16th part (2 mg·mL^{-1}) and water were sprayed to the body surface of the *Tetranychus cinnabarinus* and served as the treatment group and control group respectively. Specific activity changes of acetylcholinesterase in two groups were shown in Fig. 1. At 8h after treatment specific activity in the **t**reatment group was

0.0098 U·mg-1prot, which was significantly lower than control ($P < 0.01$). Specific activity in the control group was 4.75 times as treatment. From 16 to 48 h, specific activity in the control group was 2.83 times, 1.75 times, 1.94 times, 2.47 times and 0.707 times as treatment respectively. On the whole, specific activities in the treatment group were lower than control. Therefore the 16th part had definite inhibiting effect on acetylcholinesterase of *Tetranychus cinnabarinus*.

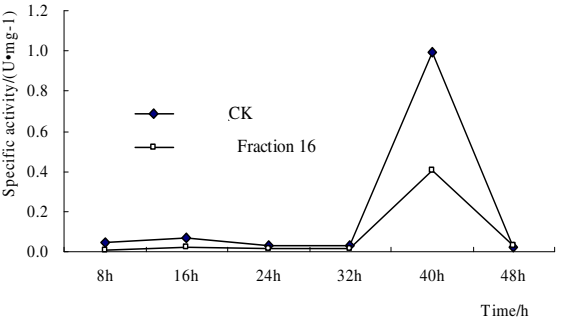

Fig. 1. Effect on the activity of Ache of the extracts of *P. aviculare* against *T.cinnabarinu*

3.6 Activities Assay of Na^+, K^+-ATPase

It can be seen from Fig. 2 that after the 16th part treatment of harmful mites, variation trend of specific activity of Na^+, K^+-ATPase was different from control (water). Changes at 8 h, 16 h, 32 h and 40 h after treatment were nominal. While changes at 24 h and 48 h were evident and specific activities in the control group were 3.18 times and 18 times as treatment, which showed that the 16th part had evident inhibitory effects.

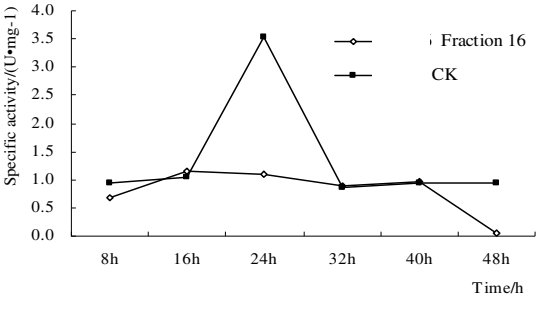

Fig. 2. Effect on the Na^+, K^+-ATPase activity of the extracts of P. aviculare against T.cinnabarinus

3.7 Effect on Glutathione-S-Transfease Activities

Glutathione-s-transferase is one of the most active detoxification enzyme systems in mites, which can catalyze the conjugation reaction between poisonous electrophilic compounds and endogenous reduced glutathione leading to detoxifying metabolism of

poisons. It could be known from figure 3 that the inhibitory effects were evident at 8 h, 24 h, 32 h and 40 h, at which specific activities in the control group were 1.29 times, 1.26 times, 1.29 times and 1.32 times as treatment, while at 48h it was 0.52 times. So on the whole, glutathione-s-transferase was inhibited.

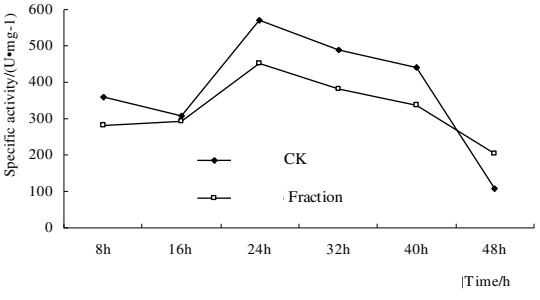

Fig. 3. Effect on the GSTs activity of the extracts of P. aviculare against T.cinnabarinus

4 Discussion

We separated and purified acaricidal active components of *Polygonum aviculare* by extraction, chromatography, spectral technology and chromatography technology for the very first time. It was found that the active components had different effects on acetylcholinesterase(AChE), Na^+, K^+-ATPase and glutathione-s-transferase activities. Most acaricides cause the lethal effects by interfering with the nervous system. The characteristics of poisons are shiver, spasm, paralysis or other behavior changes. Intercellular chemical information transfer of neurons mainly depends on synthesis and decomposition of neurotransmitter. Many recognized neurotransmitters have been reported such as acetylcholine, gamma-amino butyric acid (GABA) and nitramine *et al*, some of which have been proven to be targets of acaricides (Market al, 1994). In this paper, symptoms of harmful mites after drugs treatment observed by authors were similar to ones caused by the previous nerve agents. So two important enzymes of the nervous system namely acetylcholinesterase and Na^+, K^+-ATPase were selected for enzyme activities assay. Acetylcholine lies in gap of synapses and can be decomposed by acetylcholinesterase leading to termination of neural excitement transmission. Once the enzyme is inhibited to some extent, the insects will die of hyper excitability (Lin xinglian *et al*, 2001). This result demonstrated that the 16th part of the polygonum aviculare extracts had inhibitory effect on acetylcholinesterase activities. The evident inhibitory effects could be seen after16h and 40h.

Ion compositions of neural cells are different from peripheral medium, which depend on cellular membrane penetration for different ions, concentrations of these ions and the ion pumps activities on the cellular membrane (Lin xinglian *et al*, 2001). Na^+, K^+-ATPase distributes extensively in cellular membrane and membranous components of endoplasmic reticulum, which is related to Na^+ and K^+ transfer. When the Na^+, K^+-ATPase is inhibited, membrane penetration for ions decreases and the flow of Na^+ is inhibited leading to increase of Na^+ concentration within the membrane and

causing nervous system dysfunction to be in an excitement state continuously. Thus nervous system dysfunction was caused and insects died finally (Zhang zongbing, 1982). The results showed that variation trend of Na^+, K^+-ATPase activities of harmful mites with pesticide treatment was different from control. From 40h to 48h, changes of Na^+, K^+-ATPase activity were evident. The period was identical with one when the stronger inhibition point of the acetylcholinesterase happened and identical with one when the corresponding symptoms were observed. Therefore, it could be speculated that active substances might cause interruption of neurotransmission which led to death of mite soma by affecting this two kinds of enzyme activities. Glutathione-s-transferase can catalyze the conjugation between the reduced glutathione (GSH) in vivo and electrophilic radical of exogenous compounds, which finally formed mercapturic acid and eliminated from the body. Increase of mercapturic acid activities may be the sensitive index for animal tissue damage (Shen tong *et al*, 1990; Shenjian Shunyi, 1994).The efficient detoxification metabolism system may play important roles in the adapted process of organism and bad environmental factors. Based on this research result, inhibition of enzyme activities in the treatment group may have effect on normal detoxifying metabolism of *Tetranychus cinnabarinus*, which caused accumulation of toxic substances in vivo and led to death.

In recent years, reports about *Polygonum aviculare* are almost limited to clinical medicine. It was also reported that *Polygonum aviculare* had insecticidal activities against cotton bollworm, diamondback moth and *Pieris rapae*. However, there were almost no reports about the acaricidal activities of *Polygonum aviculare* against *Tetranychus cinnabarinus*. In this study, the acaricidal active substances were isolated from *Polygonum aviculare* on the basis of the principle that the similar substance is more likely to be dissolved by each other and their effects on bioactivity of *Tetranychus cinnabarinus* and several important enzymes were determined, which laid a good foundation for its structure identification, further studies on toxicity and new botanical pesticide development. The following research results will be reported one by one.

Acknowledgment. The work was financially supported by the National Natural Science Foundation of China (30872029), the Key Natural Science Foundation of Beijing Municipality (6071001), the Natural Science Foundation of Beijing Municipality (6092007), the Key Foundation of Beijing Municipal Education Committee (KZ201010020016), and Funding Project for Academic Human Resources Development in Institutions of Higher Learning Under the Jurisdiction of Beijing Municipality (PHR20090516, PHR200906134).

References

1. Wang, Y.N., Shi, G.L., Zhao, L.L., et al.: Sun Extracts of Juglans regia Leaves against Tetranychus viennensis and Tetranychus cinnabarinus (Acari: Tetranychidae). Journal of Economic Entomology 100(4), 1298–1303 (2007)
2. Shi, G.L., Liu, S.Q., Cao, H., et al.: Acaricidal Activities of Extracts of Stellera chamaejasme against Tetranychus viennensis (Acari: Tetranychidae). Journal of Economic Entomology 97(6), 1912–1916 (2004)

3. Shi, G.L., Zhao, L.L., Liu, S.Q., et al.: Acaricidal Activities of Extracts of Kochia scoparia against Tetranychus urticae, Tetranychus cinnabarinus and Tetranychus viennensis (Acari: Tetranychidae). Journal of Economic Entomology 99(3), 858–863 (2006)
4. Abbort, W.S.: A method of computing the effectiveness of an insecticide. J. Am. Mosq. Control Assoc. 3, 302–303 (1987)
5. FAO. Revised method for spider mites and their eggs (Tetranychusspp. And Panonychus ulmi Koch). FAO Plant Production 21, 49–54 (1980)
6. Hazan, A., Gerson, U., Tahori, A.S.: Spider mite webbingI. the production of webbing under various enviromental conditions. Acarologia 16, 68–84 (1974)
7. Ho, C., Maggi, V.: Spider mite (Acari: Tetranychidae) on various crops in Taiwan. J. Agr. Res. China 46, 333–346 (1997)
8. Mahoney, N., Molyneux, R.J., Mckenna, J., et al.: Resistance of'Tulare'Walnut (Juglans regia cv. Tulare) to aflatoxigenesis. J. Fo. Sci. 68(2), 619–621 (2003)
9. Mark, A., Roger, G.: Downer biochemical and physiological targets for miticides. Pestic. Sci. 40, 85–101 (1994)
10. Sachiko, K., Youko, K., Hamitsu, K.: A novel miticide. Norio O and Tadakazu WAKD-2023: Biological activity and mode of action IUPAC Congress (1999)
11. Yi, M., et al.: Plant chemical protection methods. China Agriculture Press, Beijing (1991)
12. Cao, H., Liu, S.Q., Wang, H.L., et al.: The effects of extracts of Tateges eracta on activities of several enzyme of Tetranychus viennensis zacher. Scientia Silvae Sinicae 39(2), 114–115 (2003)
13. Shi, G.L., Wang, Y.N., Wang, H.L., Zhao, L.L., Liu, S.Q., Cao, H., Yu, T.Q., Lu, P.: Effect of Tagetes erecta on glutathiong-S-transferase and protease activities and protein content in Tetranychus viennensis. Chinese Journal of Applied Ecology 183, 400–404 (2007)
14. Cao, H., Wang, Y.N., Liu, S.Q., et al.: Effect of Extracts of Kochia scoparia to Several Enzyme Systems in Tetranychus viennensis. Scientia Silvae Sinicae 43, 68–72 (2007)
15. Wang, H.X., Shen, Z.J., Du, J., et al.: Insecticidal Activity of Juglans regia Extracts against Tetranychus cinnabarinus. Scientia Silvae Sinicae 44, 16–20 (2008)
16. Li, L., Zhen, L., Fan, Y., et al.: Chinese jujube tree pests. China Agriculture Press, Beijing (1992)
17. Shi, G.-L., Zheng, W.-Y., Dang, Z.-P., Li, L.-C.: Fruit pests. China Agriculture Press, Beijing (1994)
18. Jingcheng: Walnut leaf constituents of biological activity. Northwest A & F University, a master's degree thesis (2003)
19. Zhang, X.: Botanical pesticides in the biological control of the position and role. World Agriculture 2(1), 31–32 (2003)
20. Zhai, M., Li, X., Lin, Q., et al.: Extract of Inhibiting Composition and Inhibitory Activity from Walnut Leaves. Journal of Northwest Forestry University 18(4), 89–91 (2003)
21. Zhai, M., Yang, X., Lin, Q., et al.: A Study on the Bioactivity of Walnut Leaves Against Stilpnotia candida. Journal of Northwest Forestry University 18(2), 65–67 (2003)
22. Zhang, Z.: Progress in insect toxicology. Beijing University Press, Beijing (1982)
23. Zhu, L., Ni, Y., Huang, C., et al.: Multiple Bioassy Method to Tetranychus cinnabarinus. Journal of Nanjing Agricultural Technology College 17(1), 13–17 (2002)
24. Yu, Z.H., Sun, K.: The chemical constituents of Polygonum aviculare. Herbal Medicine 33(6), 495–499 (2002)

25. Zhao, A.-H., Zhao, Q.F., Lin, Z., et al.: The chemical constituents of *Polygonum aviculare*. Natural Product Research and Development 14(5), 29 (2002)
26. Xiaohu: Pharmaceutical Disciplines, The chemical constituents of Polygonum aviculare. Chinese Materia Medica. 29 (9): 918–919 (2004)
27. Zheng, X.-D., Hu, H.-B., Zheng, S., et al.: Qingyang Wu to volatile oil constituents. Northwest Normal University (Natural Science) 35(3), 68–70 (1999)

Acaricidal Activity of Stigmasterol from Inula Britannica against Tetranychus cinnabarinus

Jun Cheng, Dan-dan Duan, You-nian Wang, Lan-qing Ma,
Yu-bo Liu, and Guang-lu Shi*

Key Laboratory of Urban Agriculture (North) of Ministry of Agriculture, P.R. China
Beijing University of Agriculture, Beijing, China
glshi@126.com

Abstract. The activity of fraction 12 identified as stigmasterol by GC/MS from the petroleum ether extract of Inula britannica was evaluated against Tetranychus cinnabarinus in laboratory. The bioactivities and mechanism of stigmasterol against Tetranychus cinnabarinus was further investigated. Superoxide dismutase, peroxidase and catalase in T. cinnabarinus treated with stigmasterol were examined through biochemical methods. The ultrastructure of the treated mites was observed by using transmission electron microscope (TEM). The stigmasterol showed lethal effects on the mite adults, and corrected mortality was over 50% with the concentration of 2 mg/ml. Superoxide dismutase (SOD), peroxidase (POD) and catalase (CAT) in treated mites were enhanced in activity. The results showed that stigmasterol can destroy the balance between oxidation and anti-oxidation. Glutathione-S-transferase (GSTs) activity was strongly induced after treatment. The results indicated that stigmasterol was perhaps attributing to over excitation and dead of treated mites. TEM observations revealed that the treated mites suffered from the ruptures of cuticle, muscular filament, nuclear membrane, mitochondria and endoplasmic reticulum. Thus, stigmasterol appears a strong acaricidal activity against Tetranychus cinnabarinus, can be exploited as new resources for developing potential botanical acaricides.

Keywords: Stigmasterol, Tetranychus cinnabarinus, glutathione-S-transferase, superoxide dismutase, peroxidese, catalase, transmission electron microscopy.

1 Introduction

Due to the advantages of low toxic and residue levels, easy to decompose, and harmony with the environment, botanical acaricides are attracting more and more attentions. In contrast, the chemical acaricides kill the natural enemies of mites and other beneficial organisms during preventing and treating mites; it also destroy the ecological balance, cause mite resurgence and chemical resistance (Shi *et al*. 1994), and vicious circle (Hou *et al*. 2004). New sources of acaricidal substance are urgently needed. A carmine spider mite, *Tetranychus cinnabarinus,* which is classified to the

* Corresponding author.

E. Zhu and S. Sambath (Eds.): Information Tech. and Agricultural Eng., AISC 134, pp. 599–609.
springerlink.com © Springer-Verlag Berlin Heidelberg 2012

Arachnida class, Acariformes order, and Tetranychidae family, is a worldwide economical pest that is harmful to fruits, vegetables, greenhouse plants, etc (Hazan *et al.* 1974; Ho et al. 1997; Wang *et al*. 2008; Shen *et al*. 2008) They can damage grain, cotton, oil, trees, fruit trees and other plants of 43 families including 146 species (Chu *et al.* 2002). Many domestic and international researches have reported that there are substances with acaricidal activities in many plants, such as *Juglans regia* leaf (Wang *et al*. 2007), *Stellera chamaejasme* (Shi *et al*. 2004), *Kochia scoparia* (Shi *et al*. 2006) etc. However, researches about the acaricidal activity of *Inula britannica* and stigmasterol are yet to be conducted; its mechanism is not clear yet.

Stigmasterol is a major component of natural plant sterols, which can inhibit the absorption of cholesterol of rat (Ikeda 1988), lower the level of cholesterol (David 2005), inhibit tumor growth (Awad 2005), and prevent hyperplasia of prostate gland (Kassen 2000). Stigmasterol has obtained wide awareness among medical staff and drugs distributors. As time goes on, there are growing interests among worldwide researchers in this area.

In the present study, it was found that stigmasterol from petroleum ether extract of *Inula britannica* had better acaricidal activity by using *Tetranychus cinnabarinus*. The biological activity of stigmasterol against *Tetranychus cinnabarinus* was determined and the mechanism of mite killing was discussed. Results revealed that stigmasterol, the extract of *Inula Britannica*, were mainly through the influence on activity of several important enzymes involved in metabolic process to kill the mites, and had significant destructive effect on ultrastructure of *Tetranychus cinnabarinus* cells. The results of this study showed that *Inula britannica* and stigmasterol are potentially new resources for developing potential botanical acaricides.

2 Materials and Methods

2.1 Materials

From March to December 2009, the experiment was completed in key laboratory of urban agriculture (north) ministry of agriculture and key laboratory of new technology of agricultural application of Beijing. The materials were ground to a fine powder by using high speed grinder, packed after fileted through a 40-mesh filter (pore size 40 μm), and stored in fridge for further analysis. The sensitive mites were cultured in laboratory at 24 ± 1 ℃, 60 % ± 10 % relative humidity and a photoperiod of 18: 6 hours (L: D).

2.2 Isolation of Extracts from Inula Britanica

Certain amount of *Inula britannica* powder was placed in a flask with 5 fold volumes of petroleum ether and maintained for 3 - 5 days. This process was replicated three times. The extracts were concentrated, combined together and weighed, followed by dissolving with 10 folds volumes of petroleum ether and then loading into a separator funnel. Then some methanol as a partitioning solvent was added to the funnel. The partition was replicated three times. The extracts were concentrated and then weighed. Petroleum ether, a combination of petroleum ether and chloroform (9: 1, 8: 2, 7: 3, 6: 4, 5: 5, 3: 7, 2: 8, 1: 9), chloroform A medium-pressure chromatography column was

used to isolate components from the concentrated *Inula britannica* extract. Thin layer chromatography (TLC) was used to compare constituents. In total, 38 fractions were collected.

2.3 Determination of Toxicity in Laboratory

The crude extract was diluted with distilled water into five different concentrations and evaluated for its acaricidal activity against *Tetranychus cinnabarinus* by using a slide dip technique based on the method outlined in Liu et al. (2004) with slight modification. The crude extracts were diluted with distilled water into five different concentrations and tested for bioactivities on *Tetranychus cinnabarinus*. The corrected mortality rates were obtained. Distilled water with 1.0 % Tween 80 was used as the control. Each treatment was replicated three times.

2.4 Identification of Fraction 12 by GC/MS

GC/MS was used to identify the structure of fraction 12 and carried out using Agilent 6890/5973N. The column temperature was programmed from 150 ℃ to 180 ℃ at 2 ℃/min and then raised to 200 ℃ at 2 ℃/min and finally raised to 250 ℃ at 8 ℃/min. Other settings included 250 ℃ interface temperature, 230℃ ion source temperature. The NIST (National Institute of Standards and Technology) was used for database searching.

2.5 Preparation of Enzymes

The enzymes were prepared based on the method of Liu *et al*. (2004). The stigmasterol was made into 2 mg/ml and used to treat the adult mites. After treating for 4, 8, 12, 16, 20 and 24 h, 200 adult mites were made into homogenate with 0.25 ml normal saline on ice, followed by centrifuging for 15 min at 10,000 r/min at 4 ℃. The supernatants were collected.

2.6 Determination of Enzyme Activity

The enzymatic activity of glutathione-S-transferase (GSTs) was evaluated based on the method of Mu (1994). One milligram tissue protein reacted for 1 min at 37 ℃ to deduct non-enzymatic reaction, setting the GSTs decreasing for 1μmol/L as a unit of enzyme activity. Determination of superoxide dismutase (SOD) activity: Methane reacts with hydroxyl to produce formaldehyde by xanthine reacts with xanthine oxidase to produce superoxide anion which can oxidize carboxylic amine into nitrites. The nitrite appeared magenta in chromogenic agent and absorbance was measured with visible light spectrophotometer. SOD had specific inhibition on the superoxide anion to reduce the formation of nitrite, so the absorbance value of sample with SOD should be lower than of the control. The absorbance was determined at 550 nm and the activity of SOD in the measured sample was obtained through formula. Determination of catalase (CAT) activity: The decomposition of H_2O_2 catalyzed by CAT could be suspended rapidly by adding ammonium molybdate, and the remaining H_2O_2 reacted with ammonium molybdate to produce a light yellow complex. The absorbance was

determined at 405 nm, and then the CAT activity was calculated. Determination of peroxidase (POD): The principle of catalyzed reaction of POD catalysis of hydrogen peroxide (H_2O_2) was applied to determine the absorbance at 420 nm, and the enzyme activity of the measured sample was calculated through the formula.

2.8 Transmission Electron Microscopy

Preparing the stigmasterol into 2 mg/ml concentration liquid, spray the liquid under test over harmful mites with a throat spray, and the excess liquid was removed with absorbent paper 5 s latter. The mites were put into fixative solution after 20 h treatment with stigmasterol. The mites treated by distilled water plus 1.0% Tween 80 was used as the control. Preparation of sample: Samples were rinsed with 0.1 % PBS for 4 times, each time for 2 h. They were then postfixed in 1% osmium tetroxide for 2 h with gently vortex once and then washed with 0.1% PBS for 4 times, each time for 15 min. The samples were then dehydrated with a graded ethanol series (30 %, 50 %, 70 %, 80 %, 90 %, 95 % and 100 %) once and with 100% acetone for three times, each time for 2 min. Dehydrated samples were then infiltrated, embedded, polymerized, sectioned, stained and photographed.

3 Results

3.1 Identification of Content from Fraction 12 by GC/MS

After the database searching using NIST, the main content of fraction 12 was identified as stigmasterol with the matching score over 90%.

3.2 Activity of Stigmasterol from Inula Britanica on Tetranychus cinnabarinus

Table 1 was the mortality of stigmasterol against adult mites at different concentrations. The corrected mortality was over 50% with the concentration of 2 mg/ml. The results indicated that stigmasterol appeared to have a strong acaricidal activity against *Tetranychus cinnabarinus*.

Table 1. The mortality of stigmasterol from *inula britanica* against *tetranychus cinnabarinus**

Stigmasterol ($mg \cdot mL^{-1}$)	Corrected mortality (%)	Mortality/%
10	82.45±0.55	81.13[a]
8	76.41±0.41	75.63[b]
4	67.33±0.16	66.52[c]
2	55.46±0.39	54.69[d]
1	4.11±1.43	3.62[e]
CK	2.09±0.55	-

***:** Values are mean ±SE of three determinations the averages within the same column not followed by the same letter are significantly different at 5% level of confidence the same below.

3.3 Effect of GSTs Activity of the Stigmasterol against Tetranychus cinnabarinus

Glutathione-S-transferase (GSTs) has been considered to be a very important enzyme with detoxication function in many organisms, especially in the detoxification of dimethyl methylphosphonate (DMMP) and dimethyl hydrogen dithiophosphate. GSTs is one of most activated antitoxic enzymes. As shown in Fig 1, the GSTs activity of the treated group and the control had the same change. The activity was increased at first and then declined as time goes on. However the enzyme activity of the treated group was higher than that of the control throughout the treatment, especially after 8 hours, it's about 2.5-fold higher than that of control. The results showed that stigmasterol could strongly induce the activity of glutathione-S-transferase (GSTs) activity after treatment.

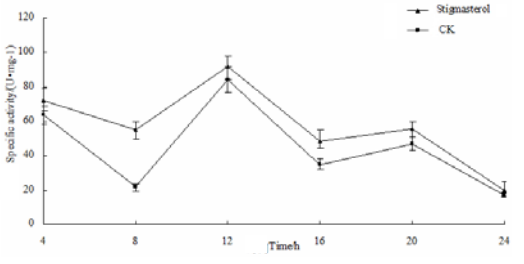

Fig. 1. Effect of GST activity of the Stigmasterol against Tetranychus cinnabarinus

3.4 Effect of SOD Activity of the Stigmasterol against Tetranychus cinnabarinus

The level of superoxide dismutase (SOD) can be used as a direct indication of death and SOD also can remove toxic traces in organisms. In the present study, the activity of SOD had the same change between treated group and control (Fig. 2).The specific activity went up initially and then declined after 20 hours of treatment, but the enzyme activity of the treated group was higher than that of control all the time, especially the activity values of stigmasterol-treated mites were 1.5 and 1.3 times higher at 16 and 20 h, respectively. In light of general trends, SOD in treated mites was enhanced in activity compared to the control.

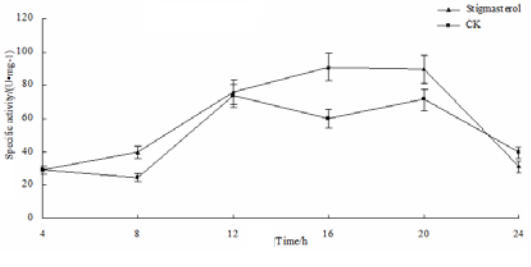

Fig. 2. Effect of SOD activity of the Stigmasterol against Tetranychus cinnabarinus

3.5 Effect of CAT Activity of the Stigmasterol against Tetranychus cinnabarinus

Catalase (CAT) as one of the key enzymes of defense system can clear away the hydrogen peroxide (H_2O_2) in the body, anti-oxidation. As shown in Fig. 3, the activity of CAT had the same change between the treated group and control and the values of activity were always higher in the treated group. After 16 h treatment, the CAT activity of the treated group was increased significantly and it was 2.1 and 2.6 times higher at 20 h and 24 h, respectively. In light of general trends, CAT in mites treated with stigmasterol was enhanced in activity compared with the control.

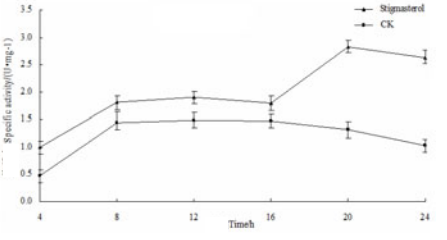

Fig. 3. Effect of CAT activity of the Stigmasterol against Tetranychus cinnabarinus

3.6 Effect of POD Activity of the Stigmasterol against Tetranychus cinnabarins

Peroxidase (POD) has the function of clearing away the poisonous substance such as hydrogen peroxide, phenolic compounds, amine and so on. They could catalyze many reactions and most of them are in the peroxisomes of cell. As shown in Fig. 4, the activity of CAT had the same change between the treated group and the control. However, the values of activity were always higher in the treated group. There were two big fluctuations in enzyme activity of the treated group, especially at 12 h and 20 h the values of activity were 1.8 and 1.7 times higher than those of the control. In light of general trends, CAT in mites treated with stigmasterol was enhanced in activity compared with the control.

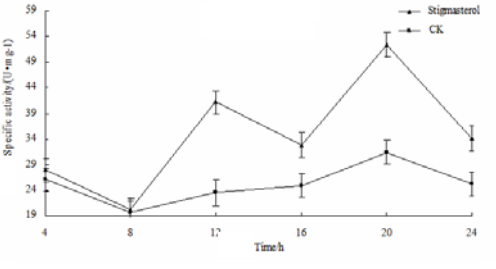

Fig. 4. Effect of POD activity of the Stigmasterol against Tetranychus cinnabarinus

3.7 Observation of Ultrastructure of Tetranychus cinnabarinus Treated by Stigmasterol

The ultrastructure changes of the treated female adults of *Tetranychus cinnabarinus* were obtained by transmission electron microscope (TEM) (Fig. 5). The cuticle of mite adults was changed after treating by stigmasterol. The cuticle of the control had even texture and regular waved protuberances (Fig. 5-A, top), whereas the cuticle of mites was ruptured and the protuberances were almost disappeared (Fig. 5-A, bottom). The ultrastructure of muscular filament of *Tetranychus cinnabarinus* was also changed after stigmasterol treatment. The muscular filament of control was smooth and even. There was an alternation of bright and dark stripe in the muscular filament (Fig. 5-B, top). In contrast, the muscular filament of the treated group was expanded, loosens and ruptured (Fig. 5-B, bottom). The structures of nucleus and nuclear membranes were different between the treated group and the control. Nuclear membranes of the control had a complete structure and regular ellipse. Furthermore, nucleolus, nuclear membranes and cytoplasmic matrix could be observed very clearly (Fig. 5-C, top). But the nucleus of the treated mites had irregular structure with ruptured and dissolved nuclear membranes and spillage of inner substance. The structure of nucleolus was disappeared, dissolved and broken (Fig. 5-C, bottom). There were some noticeable changes observed in mitochondria of the treated group. The mitochondria structure of the control was intact, even and appeared regular ellipse (Fig. 5-D, top). But the mitochondria structure of the treated group was damaged, and the ridges were not well aligned and even disappeared in seriously damaged mitochondria (Fig. 5-D, bottom). The endoplasmic reticulum (ER) structure was also changed in mites after treatment. The structure of ER was completely, orderly and densely covered by many ribosomes (Fig. 5-E, top). However, the ER of the treated group was dissolved, ruptured and randomly arranged and the ribosome was disappeared (Fig. 5-E, bottom).

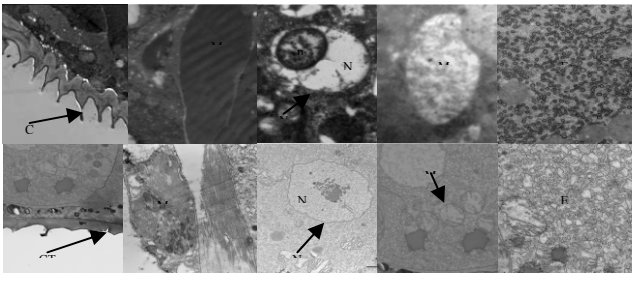

Fig. 5. The ultrastructure difference of Tetranychus cinnabarinus between treated group and control

The top images were from control and the bottoms from treated group. (A) CT, Cuticle ×40,000; (B) MF, Muscular filament ×10,000; (C) NM, Nuclear membrane ×25,000; N, Nuclear; n: Nucleolus; (D) MT, Mitochondria ×20,000; (E) ER, Endoplasmic reticulum ×50,000.

4 Discussion

Inula britanica is a commonly used traditional Chinese medicine. Pharmacopoeia of the People's Republic of China (Volume one) records, “ShenNongBenCaoJing” mentioned that *Inula britanica* is “warm-natured”, bitter in taste, pungent and salty, can be used to sending down abnormally ascending, dissolving phlegm, promoting circulation of “Qi” and antiemetic. As a traditional Chinese medicine with a great potential medicinal value, *Inula britanica* can be used for the treatment of chills and cough, phlegm, stuffiness in chest and abdomen, coughing and phlegm, vomiting and eructation, epigastria fullness and rigidity. Stigmasterol has a wide range of applications in the areas of biotechnology and pharmaceutical (Moreau 2002). Adrenal cortical hormone and luteinizing hormone drugs are synthesized by stigmasterol. Stigmasterol has a wide range of biological activity. For example, it can lower blood cholesterol levels and inhibit absorption in rat intestinal (Batta 2006). Stigmasterol had inhibitory effect on hepatoma cells of SMMC-7721 and BEL-7402 in vitro, and in vivo inhibition of H22. In addition, stigmasterol also can inhibit cell proliferation cycle, and promote apoptosis of hepatoma cells. Researchers around the world are exploring the biological activity of stigmasterol. The antibacterial activity of *Inula britanica* has been reported previously. However, for the first time, we studied and reported the acarcidal activity of *Inula britannica* and stigmasterol, and the influence on enzymes activity and ultrastructure.

Tripeptide glutathione (GSH) can be involved in several cellular functions, for example cell transportation, protection and exogenous compounds metabolism etc. Glutathione-S-transferase (GSTs) is one of the important conjugated enzymes involved in the metabolism of insects to insecticides. GSTs enzymes catalyze the conjugation of toxic and carcinogenic electrophilic molecules with glutathione and thereby protect cellular macromolecules from damage, such as protein and DNA (Shi et al 2007). When external sources of toxic substances were invaded into the organism, it leads to an increased enzyme activity to enhance metabolism and to warrant the normal physiological activities of organisms. In the present study, the enzymes activity of the treated group was higher than those of the control all the time, especially at 8 h of treatment, being 2.5 times higher. The results indicated that stigmasterol could activate glutathione-S-transferase in *Tetranychus cinnabarinus* significantly. The detoxification metabolism and the activation of the glutathione-S-transferase may be caused by the strong toxicity of stigmasterol against *Tetranychus cinnabarinus*.

Superoxide dismutase, catalase, peroxidase are ubiquitous and they play an important role in regulating the vital processes in living organisms. The level of superoxide dismutase in vivo can be used as direct indicator of death. SOD can fight and block the cell damage caused by oxyradicals, and repair injured cells in time. Therefore, SOD becomes more and more important in the biological mechanisms of antioxidant, and has hence evolved into an important area of biology, medicine and life science. In this study, the three important enzymes were activated to some extent. This indicated that stigmasterol functions as an oxidative catalyst or inhibitor of anti-oxidation to cells in *Tetranychus cinnabarinus*. These effects could result in imbalance between oxidative and antioxidant in *Tetranychus cinnabarinus* thus leads to the death of pest mites ultimately.

By observing the ultrastructure of *Tetranychus cinnabarinus* by transmission electron microscopy (TEM), it was found that cuticle, muscular filament, nuclear and organelles, such as mitochondria, endoplasmic reticulum etc, had significant changes. The cuticle appeared lysis or even the humps disappeared, which might be resulted from the structure damages of cuticle and cells caused by stigmasterol; Stigmasterol could lead to the fracture behavior between adjacent smooth muscular filament and interruption of chemical information transportation and nervous excitement in treated mites, perhaps attributing to non-synchronized contraction of muscular filament (Caulfield 1993). Stigmasterol destroyed structure of nuclear membrane, and this might result in blocking of the signal transmission and interrupting of nervous excitement conduction. The damages of mitochondrial in *Tetranychus cinnabarinus* caused by stigmasterol might lead to obstruction of oxidative phosphorylation in cell, reduction of ATP activity, energy deficiency and death of mites finally (Kazuhiko *et al*. 1992; Zizka *et al*. 1997).

Through the studies of effects of stigmasterol against *Tetranychus cinnabarinus* in two aspects including activities of important enzymes and the damage of ultrastructure of cells, it was concluded that stigmasterol had a significant influence over oxidoreductase system within a certain time. TEM observations revealed that the treated mites suffered from the ruptures of cuticle, muscular filament, nuclear membrane, mitochondria and endoplasmic reticulum. However, the specific mechanism still needs further research to determine, and we will further conduct in-depth study of its toxicity.

Acknowledgment. The work was financially supported by the National Natural Science Foundation of China (30872029), the Key Natural Science Foundation of Beijing Municipality (6071001), the Natural Science Foundation of Beijing Municipality (6092007), the Key Foundation of Beijing Municipal Education Committee (KZ201010020016), and Funding Project for Academic Human Resources Development in Institutions of Higher Learning Under the Jurisdiction of Beijing Municipality (PHR20090516, PHR200906134).

References

1. Batta, A.K., Xu, G.R., Honda, A., Miyazaki, T., Salen, G.: Stigmasterol reduces plasma cholesterol levels and inhibits hepatic synthesis and intestinal absorption in the rat. Metabolism 55, 292–299 (2006)
2. Caulfield, M.P.: Muscarinic receptor characterization, coupling and function. Pharmacol. Ther. 58, 319–379 (1993)
3. Chu, J.X., Yuan, G.H., Shi, S.S.: Agricultural Entomolog. China Agriculture Press, Beijing (2002) (in Chinese)
4. Fang, Y.X., Zhang, Y.C., Chen, M.M., Zheng, S.H., Zhang, K.: Anticancer Drug Hedyotis diffusa willd and active components. Chinese Traditional Patent Medicine 26, 577–579 (2004) (in Chinese)
5. Hazan, A., Gerson, U., Tahori, A.S.: Spider mite webbing I. The production of webbing under various enviromental conditions. Acarologia 16, 68–84 (1974)
6. Ho, C.C., Lo, C.C., Chen, W.H.: Spider mite (Acari: Tetranychidae) on various crops in Taiwan. J. Agr. Res. China 46, 333–346 (1997)

7. Hou, H., Zhao, L.L., Shi, G.L., Li, Z.H.: Studies on the acaricidic activity of the extracts of Kochia scoparia. Plant Protection 30, 42–45 (2004) (in Chinese)
8. Ikeda, I., Tanaka, K., Sugano, M., Vahouny, G.V., Gallo, L.L.: Inhibition of cholesterol absorption in rats by plant sterols. J. Lipid Res. 29, 1573–1582 (1988) (Journal of lipid research)
9. Kassen, A., Berges, R., Senge, T.: Effect of Beta-Sitosterol on Transforming Growth Factor-Beta-1 Expression and Translocation Protein Kinase C Alpha in Human Prostate Stromal Cells in vitro. Eur. Urol. 37, 735–741 (2000) (European Urology)
10. Kazuhiko, M., Takashi, S., Matazaemon, U.: Effect of a New, fenpyroximate, on energy Metabolism and mitochondrial morphlolgy in adult female Tetranychus urticae (Two-Spotted Mite). Pestic. Biochemi. Physiol. 43, 37–44 (1992)
11. Liu, Y.P.: Biological activities evaluation of principal acaricidal components of Eupatorium adenophorum. Sichun University, Chengdu (2004) (in Chinese)
12. Moreau, R.A., Whitaker, B.D., Hicks, K.B.: Phytosterols, phytostanols and their conjugates in foods: structural diversity, quantitative analysis and health promoting uses. Prog. Lipid Res. 41, 457–500 (2002)
13. Mu, L.Y.: Research technique of chemical protection of plants, pp. 160–161. China Agriculture Press, Beijng (1994) (in Chinese)
14. Shen, Z.J., Wang, H.X., Shi, G.L., Wang, Y.N.: Biological activities of extracts from 3 Species of plants against Tetranychus cinnabarinus. Journal of Beijing Agricultural College 23, 22–24 (2008) (in Chinese)
15. Shi, G.L., Wang, Y.N., Wang, H.L., Zhao, L.L., Liu, S.Q., Cao, H., Yu, T.Q., Lu, P.: Efects of Tagetes erecta extracts on glutathione S-transferase and protease activities and protein content in Tetranychus viennensis. Chin. J. Appl. Ecol. 18, 400–404 (2007) (in Chinese)
16. Shi, G.L., Liu, S.Q., Cao, H., Zhao, L.L., Li, J., Li, S.Y.: Acaricidal Activities of Extracts of Stellera chamaejasme against Tetranychus viennensis (Acari: Tetranychidae). J. Econ. Entomol. 97, 1912–1916 (2004)
17. Shi, G.L., Zhao, L.L., Liu, S.Q., Cao, H., Clarke, S.R., Sun, J.H.: Acaricidal Activities of Extracts of Kochia scoparia against Tetranychus urticae, Tetranychus cinnabarinus and Tetranychus viennensis (Acari: Tetranychidae). J. Econ. Entomol. 99, 858–863 (2006)
18. State Pharmacopeia Committee of China. Pharmacopoeia of the People's Republic of China, vol. 1, p. 260. Chemical Industry press, Beijing (2000) (in Chinese)
19. Wang, Y., Shi, G.L., Wang, Y.N., Wu, Z.Y.: Acaricidic Activity of Herbal Extracts Against Tetranychus cinnabarinu. Chinese Agricultural Science Bulletin 24, 323–326 (2008) (in Chinese)
20. Wang, Y.N., Shi, G.L., Zhao, L.L., Liu, S.Q., Yu, T.Q., Clarke, S.R., Sun, J.H.: Acaridical activity of Juglans regia leaf extracts on Teranychus viennensis and Tetranychus cinnabarinus (Acari: Tetranychidae). J. Econ. Entomol. 100, 1298–1303 (2007)
21. Zizka, Z., Pelc, R., Jizba, J., Kandybin, N.V., Sergeeva, M.V.: In Situ assessment at subcellar level of the effects of macrotetrolide insecticides on mites by electron microscopy and X-Ray Microanalysis. Pestic. Biochemi. Physiol. 58, 165–172 (1997)
22. Zhang, S.: Experimental research of anti-cancer effects and related mechanism of compound Traditional Chinese Medicine of Qian Kun Ning. Chengdu University of Tradtional Chinese Medicine (2005) (in Chinese)
23. Zhang, S., Yue, W., Wang, L., Song, Y.Q., Yang, Z.H.: Inhibitive effect of Stigmasterol from Hedyotis diffusa willd. on hepatoma cells in vitro & vivo and its influence on transplanted H22 tumor cell's multiplication cycle, apoptosis. Progress in Modern Biomedicine 8(11), 2016–2017 (2008)

24. David, K., Chen, S.C.: Phytosterols - Health Benefits and Potential Concerns:A Review. Nutrition Reasearch (25), 413–428 (2005)
25. Awad, A.B., Williams, H., Fink, C.S., Phyto David, K., Chen, S.C.: Phytosterols - Health Benefits and Potential Concerns: A Review. Nutrition Reasearch (25), 413–428 (2005)
26. Shi, G.L., Zheng, W.Y., Dang, Z.P., Li, L.C.: Fruit pests. China Agricultural Press, Beijing (1994)

Insecticidal Activity of *Juglans regia* Extracts against *Tetranychus cinnabarinus* and Their Effects on Relative Enzymes Activity in *Tetranychus cinnabarinus*

You-nian Wang, Hai-xiang Wang, Yu-bo Liu, and Guang-lu Shi*

Key Laboratory of Urban Agriculture (North) of Ministry of Agriculture, P.R. China
Beijing University of Agriculture
Beijing, China
glshi@126.com

Abstract. The experiment was conducted to determine the insecticidal activity of three different extracts from walnut green husk against Tetranychus cinnabarinus. The results showed that the female insect mortality was 83.44 % at 24 h after exposed in the petroleum ether extract(1 mg·mL-1) from walnut green husk, which was significantly higher than that in the chloroform and methanol extracts ($P < 0.05$) . After parted and purified by extracting and chromatography, it was found that the acaricidal activity of petroleum ether part from crude extracts was significantly more than the methanol part in the concentration of 1 mg·mL-1, and the female insect mortality reached 84.39 % at 24 h after exposed in the petroleum ether part. There were 19 parts gained from petroleum ether part by chromatography, and the insecticidal activity of 4 parts (6th, 7th, 13th, 17th parts) was higher than other parts, which mortality to female insects was more than 60 %. And the purity of 6th part has been above 90 % by HPLC. After detailed gradient detection, it was found that the extraction rate of 6th part from crude extracts was 6.34% in the concentration of 10mg·mL-1, and the female insect mortality was 98.45 %. On the other hand, the effect of 6th part on relative enzymes activity in Tetranychus cinnabarinus was also researched by colorimetric method. The results showed that the activity of AchE and Na+, K+-ATPase in Tetranychus cinnabarinus were 0.47 and 0.62 times as the control after the exposure in the concentration of 10 mg·mL-1 at 8 hours.

Keywords: Tetranychus cinnabarinus, Juglans regia, acetylcholine esterase, Na+, K+-ATPase.

1 Introduction

Plants-phytophagous acarid is the major pest biome in the agriculture because of the small individual, fast reproduction, high population density and serious harm (Shi guanglu *et al*., 1994; Li lianchang *et al*., 1992). Every year, there was mint expense used to buy chemic acaricide and prevent the pest acarid in orange, pear, apple, peach trees in China(Cao Hui *et al*, 2007). But the natural enemies of pest acarid can also die

* Corresponding author.

E. Zhu and S. Sambath (Eds.): Information Tech. and Agricultural Eng., AISC 134, pp. 611–620.
springerlink.com © Springer-Verlag Berlin Heidelberg 2012

largely, and the resistive population of this acaricide maybe produced after the frequent application of simplex acaricide (Sachiko *et al.*,1999). At present, the extraction of insecticidal and antibacterial component from plants is an important pesticide research area in the world (Zhang xing, 2003). After application of botanical pesticide, the environment pollution and pesticide-resistant pest can be decreased, while there was no harm effect on the beneficent pest (He yanbiao *et al*., 2004; Zhang xing *et al*., 2003; Wang *et al.*, 2007). Therefore, the study and develop of effective botanical pesticide was advanced by modern sciences and technologies in the world.

In China, there is abundance resource of *Juglans regia*, which belongs to walnut genus of walnut family. At the same time, *Juglans regia* has been planted in long history because it's remarkable economic benefit and medicine value. And the insecticidal and antimicrobial active effect of *Juglans regia* leaves and green rind extract have been reported in many researches (Zhai meizhi *et al*., 2003a; Zhai meizhi *et al*., 2003b). But there were few reports about the insecticidal activity of the *Juglans regia* extract and its possible mechanism. *Tetranychus cinnabarinus* is the major pest biome in the forestry and agriculture, which can harm the tree, fruit and crop more than one hundred species (Hazan *et al*., 1974; Ho *et al*., 1997). This research was conducted to determine the insecticidal activity of three different extracts from walnut green husk against *Tetranychus cinnabarinus,* and explain its possible mechanism, which can support the effective method to control *Tetranychus cinnabarinus* and reduce the environmental pollution from normal pesticide.

2 Materials and Methods

2.1 Sampling

Walnut green husk samples were taken from Suziyu village, Pinggu district, Beijing. Each sample was carefully washed, air-dried and ground. The susceptible strain of Tetranychus cinnabarinus were collected from Peach Garden in University of Science & Technology Beijing. The plants used for rearing were glycine max seedlings. The infested glycine max was held at (25 ± 1) ℃, 50 ± 5 RH, and the photoperiod was 16: 8 (L: D).

2.2 Extraction and Separation of Active Components from Walnut

The Method of Extraction. Dry material were accurately weighed into jars, add 5× organic solvents (petroleum-ether, chloroform, methanol), then incubate at room temperature (25 ± 2) ℃, with three replicates per solvent; each times 3 - 5d. The merger of three extracts was evaporated to paste and then weighing.

Separation by Liquid - Liquid Partition Method. Bioassay results showed that petroleum ether extract from Walnut have strong biological activity, therefore, it need further purification. Weighed 6g Walnut extract, then dissolved into 10 × petroleum ether, the mixture was loaded into a separator funnel, extracted three times with methanol, combined extract and evaporated to thick paste, then weighed.

Separation by Column Chromatography. A 5 × 80cm glass chromatography column was prepared. A mixture of 100 × (100 - 200 mesh) silica gel and extract was placed in the column quickly. Then tapped the wall with a rubber hammer to remove air bubbles in solution. At the same time, open the cocks at the bottom of the chromatography column, so the solutions sink down slowly with silica particles and finally accumulate closely in the bottom of the column. A mixture of 5 g extraction and a small amount of the initial elute were injected into the column when the solution was about 1cm away from the surface of silica. While the extraction was under the surface of silica, covered a layer of quartz sand, and then added petroleum ether, chloroform, methanol to the column in turn. The flow rate was 3 - 4 drops·S^{-1}. Eluents from the silica gel was collected at the bottom of the column into a 60-ml collection bottle. The mixture was separated into different components based on polarities.

There were 299 fractions (bottles) collected from the extracts. Thin layer chromatography (TLC) was used to compare constituents in each of the 299 fractions. Each fraction sample was partitioned into separate bands from the bottom to the top of the plate in TLC. Based on band appearance under daylight and UV light the 299 fractions were pooled into 19 groups. Each group was then evaporated to obtain concentrated isolates of green walnut husks. Then the Biological effects of green walnut husks would be measured in the laboratory.

2.3 Contact Toxicity

Slide impregnation (FAO, 1980) was used to measure biological activity. Stacked 30 healthy female adults to one end of the slide with double-sided tape, immersed in the liquid for 5s, and dried the excess liquid around worms with a filter paper, treated at room temperature (25 ± 1) ℃, observed mortality after 24h, access to actors as a living, fixed as the death, calculated according to Abbott corrected mortality (Abbort, 1987).

2.4 Symptoms Observation

Leaf disc dip method (Li-Mei Zhu, 2002), the clean flat leaves of soybean were put on the water table. More than 30 adult mites were choose into each leaf, then immersed in the liquid (10mg·mL^{-1}) for 5s. The action and response of mites were observed every 6 hours.

2.5 Enzyme Preparation

The insects treated by contact toxicity test approach, and 150 adult mites would be taken to plus 0.25mL saline homogenate in an ice bath after 4, 8, 12, 16, 20, 24 h treatment. Then centrifuged 15min by 10,000 r/min, 4 ℃, and the supernatant spare would be collected to measure the enzymes activity.

2.6 Determination of Protein Content

Coomassie Brilliant Blue G-250 method (Muli Yi, 1991) was used to determine the protein content. Added 0.1mL of enzyme solution in 5 mL Coomassie Brilliant Blue G-250 reagent, then incubated at 25 ℃ for 2 min, measure the protein content at 595 nm wavelength colorimetric determination of *OD* values.

2.7 Determination of Activity

Acetylcholine esterase and Na^+, K^+-ATPase activity measured using the AChE test kit and ultra capacity Na^+, K^+-ATPase kit, which were made by Nanjing Jiancheng Institute of Biology.

3 Results

3.1 Contact Toxicity of Walnut Extraction against Tetranychus cinnabarinus

Extraction rate of the Walnut extraction decreased in the order: methanol (3.77 ± 0.39) % > chloroform (1.13 ± 0.05) % > petroleum ether (1.05 ± 0.30) %. Treated the *Tetranychus cinnabarinus* with three diluted extraction (1 mg·mL^{-1} of methanol, chloroform and petroleum ether) for 24h, the result showed that (Table 1), the acaricidal activity of the petroleum ether extract was significantly higher than the chloroform and methanol ones in the concentration of 1 mg·mL^{-1} (P < 0105). The mortality from petroleum ether extract of walnut green husk was 80.61 %. So we choose the petroleum ether extract as the one for next Extraction and purification.

Table 1. Extract rate and mortality of different extracts from *Juglans regia* against *Tetranychus cinnabarinus*

Extracts(1mg•mL^{-1})	Extraction rate (%)	Mortality (%)
Petroleum ether extract	1.05±0.30	83.44±3.55^a
Chloroform extract	1.13±0.05	32.16±6.78^b
Methanol extract	3.77±0.39	35.07±1.37^b

Note: values are mean ± SE of 3 determinations, the averages within the same column not followed by the same letter are significantly different at 5% level of confidence.

Extract Rate and Mortality of Petroleum Ether Extracts from Juglans regia against Tetranychus cinnabarinus

For effective effect on the contact toxicity of petroleum ether extract was extracted with methanol (see Table 2). Two kinds of solvent extraction rate were: methanol (52.08 ± 2.37) % > petroleum ether (47.92 ± 6.54) %; two solvent extracts bioassay results showed that: petroleum ether extract of the mortality rate was 84.89 %, significantly higher than methanol extracts (36.11 %) (P < 0.05), can ascertain the acaricidal active substance Walnut mainly in the petroleum ether extract.

Table 2. Extract rate and mortality of petroleum ether extracts from *Juglans regia* against *Tetranychus cinnabarinus*

Extracts (1mg•mL^{-1})	Extraction rate (%)	Mortality (%)
Petroleum ether extract	47.92±6.54	84.89±2.68^a
Methanol extract	52.08±2.37	36.11±2.02^b

Note: values are mean ± SE of 3 determinations, the averages within the same column not followed by the same letter are significantly different at 5% level of confidence.

3.2 The Best Flow of Petroleum Ether Extract and Their Biological Activity Measurement

All the 19 fractions were detected by the column chromatography and TLC methods (see Table 3). The bioassay results showed that the insecticidal activity of 4 parts (6^{th}, 7^{th}, 13^{th}, 17^{th} part) was higher than other parts, which mortality to female insects was more than 60%. And the extraction flow rate of 6, 7 were better, which was 6.34 %, 6.74 % respectively. TLC results showed that the purity of flow in 6 was effective than other materials, by HTLC figure of the sixth fraction of *Juglans regia* (Fig. 1) confirmed that its purity reached to more than 90%. The substance was the first material for Toxicology research.

Table 3. Extract rate and mortality of fractions of chromatography extract of *Juglans regia* against *Tetranychus viennensis*

Isolation fraction	Isolation rate (%)	Mortality(%)
1	0.17	27.70 ± 7.36^{bc}
2	0.14	26.18 ± 7.08^{bc}
3	0.11	32.88 ± 6.25^{abc}
4	0.20	50.89 ± 3.30^{abc}
5	27.57	25.97 ± 3.07^{bc}
6	6.34	64.98 ± 15.73^{ab}
7	6.74	71.34 ± 7.26^{a}
8	25.61	54.32 ± 0.21^{abc}
9	1.82	48.58 ± 0.19^{abc}
10	1.60	43.22 ± 0.04^{abc}
11	1.05	43.84 ± 14.03^{abc}
12	1.60	49.58 ± 3.77^{abc}
13	0.76	72.31 ± 13.27^{a}
14	1.49	42.42 ± 7.18^{abc}
15	0.45	55.36 ± 9.21^{abc}
16	0.72	46.19 ± 6.32^{abc}
17	0.50	26.98 ± 4.12^{bc}
18	0.37	71.40 ± 6.22^{a}
19	1.70	22.06 ± 1.09^{c}
CK		16.04 ± 4.70^{c}

Note: values are mean ± SE of 3 determinations,the averages within the same column not followed by the same letter are significantly different at 5% level of confidence.

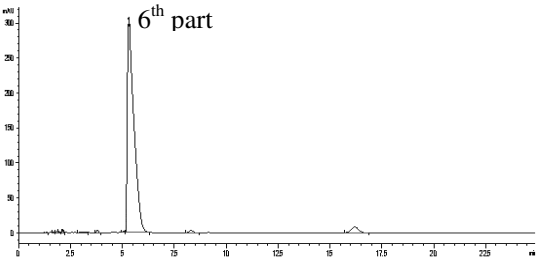

Fig. 1. HTLC figure of the sixth fraction of *Juglans regia* extract

After detailed gradient detection (1, 2, 4, 5, 8, 10 mg·mL^{-1}) of 6th part, it was found that the 6th part had a better biological activity, and the toxicity regression equation was calculated by y=4.402 + 2.170x. The lethal dose LC_{50} was 1.886 mg·mL^{-1}. When the extracts concentration up to 10 mg·mL^{-1}, the mortality of mites was 98.45 % after 24 h treatment, which was greater than 95 %. Therefore, the treatment concentration to determine the symptoms and acetylcholine esterase and Na^+, K^+-ATPase activity was 10mg·mL^{-1}.

3.3 Symptoms Observe

During 0 – 6 h, the pest mites in treatment group were very excited, crawling around, and rapidly spawning, but the pest mites in control group did not have these performances.

During 6 – 12 h, fluid extravasation was found from tested insects back, and the mites pest express the phenomenon of convulsions, or around a rocky ledge. The fecundity was decreased. But the control pests have the normal behavior.

During 12 – 18 h, the insects in the treatment group remained fluid leakage in the stage. And the action was the excitement alternating with rest, but the body starts to contract. There was no abnormality action in control group.

During 18 – 24 h, the body of treatment group insects gradually contracted to death, while both the body condition and the action of control group insects were still normal.

There was a similar phenomenon between 6th part and nerve agents to pests, such as excitement and convulsions, which indicated that 6th part had a function on the nervous system to pest mites.

3.4 Activity of Acetylcholine Esterase

The 6th part, which concentration was 10 mg·mL^{-1}, was sprayed on the body surface of *Tetranychus viennensis* in the treatment group when the acetylcholine esterase activity was measured in the research, while the water was used in control group. From Fig. 2,

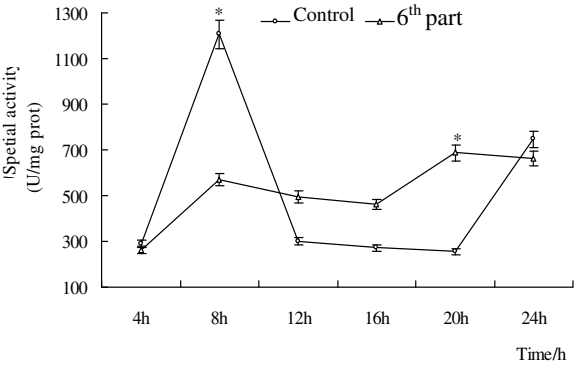

Fig. 2. Effect on the activity of Ache of the extracts of Juglans regia against Tetranychus cinnabarinus

Note: *is significantly different at 1% level of confidence.

it was found that the specific activity of acetylcholine esterase in the treatment group was 570.90 U/mg prot at 8 h, which was 0.47 times and significantly higher than that in the control group ($P < 0.01$). During 12 - 20h, the specific activity of acetylcholine esterase in the treatment group was 494.81, 461.73, 686.98 U/mg prot, while that in control group was 299.45, 271.99, 255.41 mg prot respectively. However, the specific activity of acetylcholine esterase in the treatment group was significantly lower than that in the control group, which was 0.89 times as the control group. In a word, it could be concluded that the 6th part could restrain the acetylcholine esterase activity in *Tetranychus viennensis.*

3.5 Activity of Na^+, K^+-ATPase

In the determination of Na^+, K^+-ATPase activity, the treatment and control group was same as the above experiment. And the change trend of Na^+, K^+-ATPase activity in the treatment group was similar with that in the control group. During 4 - 8h, the specific activity of Na^+, K^+-ATPase in the treatment group was from 125.46 down to 41.68 U/mg prot, which was 0.62 times and significantly lower than that in the control group ($P < 0.01$). The specific activity in the treatment group was 0.67 times, 0.78 times as that in the control group at 12 h, 16 h. At the 24 h, the specific activity in the treatment group was 112.54 U/mg prot, which was 0.67 times with the control.

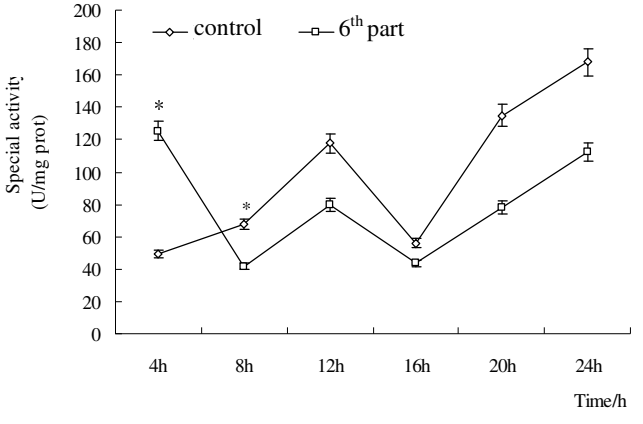

Fig. 3. Effect on the Na^+, K^+-ATPase activity of the extracts of Juglans regia against Tetranychus cinnabarinus

Note: * is significantly different at 1% level of confidence.

4 Discussion

Most miticides displayed their lethal effects by disturbing the nervous system, and the toxic character was shudder, tic, anesthesia or other behavior change. The chemistry

information transfer between neuron mainly depended on the synthesis and decomposability of neurotransmitters. The reported putative neurotransmitters were as following, such as acetylcholine, gamma-amino butyric acid, octopamine, and so on. And some were proved as the drone of miticide (Mark *et al.*, 1994). The symptoms of pest acarid after treated with miticide in this research was similar to those above-mentioned neurotoxins, Therefore, the acetylcholine esterase and Na^+, K^+-ATPase, which were the important enzymes of nervous system, were chosen to measure in the research. Acetylcholine, which consists in synapse clearance, can be decomposed by acetylcholine esterase to end the conduction of nerve excitement. Therefore, the insects would die because of excess excitement when the acetylcholine esterase activity was restrained (Lin Zhonglian *et al*, 2001). In this research, it was concluded that 6^{th} part from extracts of walnut green husk could restrain the activity of acetylcholine esterase in *Tetranychus viennensis,* which function was most significant at 8h during the 24 hour treatment.

The ion composition in neurocyte is different from that in ambient medium, which was decided by osmosis of cell membrane for different ions, ion concentration among ambient medium and ion pump activity of cell membrane (Lin Zhonglian *et al*, 2001). Na^+, K^+-ATPase widely distribute in the cell membrane and endoplasmic reticulum, which is related with the transfer of Na^+, K^+. When the enzyme activity is restrained, osmosis of cell membrane for ion is decreased, and the Na^+ in the neurilemma was increased, which continue to lead dysfunction of nervous system, which can induce the death of insects at last (Zhang Zhongbin, 1982). In this research, the change trend of Na^+, K^+-ATPase activity in the treatment group was similar with that in the control group, and the best effects were found at 8 hour within 24 hour treatment, which was same as the obvious change time of acetylcholine esterase. On the other hand, the relative symptom was also found at 8h within the 24h treatment. Therefore, it could be concluded that the effect of 6^{th} part from extracts of walnut green husk on the acetylcholine esterase and Na^+, K^+-ATPase activity may lead to the interdiction of nerve transfer, which made the pest die.

China is one of the origins of walnut, and the plant history of walnut was more than 2000 years in China. The resource of walnut was very rich. From Sui and Tang period, the walnut had been widely used, and the medicinal value of walnut had been sure (Tang Jingcheng, 2003). It was reported that the walnut leaves extract had anti-feeding effect and stomach poisoning action to *Mythimna separate* and *Plutella xylostella*, and the extracts from walnut leaves had more powerful contact effect on aphid than that on *Stilpnotia candida* (Zhai meizhi et al., 2001, Zhai meizhi et al., 2003). In this research, the insecticidal activity of walnut green husk (which purity was more than 90%) against *Tetranychus cinnabarinus* was determined, and the effect of 6^{th} part from extracts of walnut green husk on the acetylcholine esterase and Na^+, K^+-ATPase activity in *Tetranychus cinnabarinus* was also measured. All this work can support the continue research of walnut green husk, such as the structural identification of activity materials, advanced toxicology research of walnut green husk, development of botanical pesticides, and so on. Therefore, the next experiment will be conducted to research the eco-toxicology of walnut green husk and explain its structural identification, which can help to develop the new type botanical pesticides.

Acknowledgements. The work was financially supported by the National Natural Science Foundation of China (30872029), the Key Natural Science Foundation of Beijing Municipality (6071001), the Natural Science Foundation of Beijing Municipality (6092007), the Key Foundation of Beijing Municipal Education Committee (KZ201010020016), and Funding Project for Academic Human Resources Development in Institutions of Higher Learning Under the Jurisdiction of Beijing Municipality (PHR20090516, PHR200906134).

References

1. Cao, H., Wang, Y., Shi, G., et al.: Effects of the Chloroform Extracts of Kochia scoparia to Several Enzyme Systems in Tetranychus viennensis. Scientia Silvae Sinicae 43(2), 68–72 (2007) (in Chinese)
2. He, Y., Zhan, R., Zhao, Y.: Advances in Research and Application of Botanical Pesticides. Chinese Journal of Tropical Agriculture 24(3), 58–62 (2004) (in Chinese)
3. Lin, Z., Zhang, L.: The Effecy of Phophine on Acetylcholine esterase in Adults of Rhyzopertha Dominica(Fabricius) and Sitophilus Zeamais(Motschulsky) in Vivo. Journal of Zhengzhou Institute of Technology 22(4), 35–41 (2001) (in Chinese)
4. Li, L., Li, L., Fan, Y., et al.: Insect Pests of Chinese Jujube. China Agriculture Press, Beijing (1992) (in Chinese)
5. Shi, G., Zheng, W., Dang, Z., et al.: Insect Pests of Fruit Trees. China Agriculture Press, Beijing (1994) (in Chinese)
6. Tang, J.: Study of the Bioactive Constituents from the Leaves of Juglans Regia. Master Thesis in Northwest Agriculture&Forestry University (2003) (in Chinese)
7. Zhang, X.: Function and Niche of Botanical Pesticide. World Agriculture 2(1), 31–32 (2003) (in Chinese)
8. Zhai, M., Li, X., Lin, Q., et al.: Extract of Inhibiting Composition and Inhibitory Activity from Walnut Leaves. Journal of Northwest Forestry University 18(4), 89–91 (2003) (in Chinese)
9. Zhai, M., Yang, X., Lin, Q., et al.: A Study on the Bioactivity of Walnut Leaves Against Stilpnotia candida. Journal of Northwest Forestry University 18(2), 65–67 (2003) (in Chinese)
10. Zhang, Z.: New Developments of Insect Toxicology. Peking University Press, Beijing (1982) (in Chinese)
11. Zhai, M., Yang, X., Liu, L.: The Contact Effect of Extracts from Walnut Leaves on Aphid. Journal of Northwest Forestry University 16(4), 55–56 (2001) (in Chinese)
12. Zhu, L., Ni, Y., Huang, C., et al.: Multiple Bioassy Method to Tetranychus cinnabarinus. Journal of Nanjing Agricultural Technology College 17(1), 13–17 (2002)
13. Abbort, W.S.: A method of computing the effectiveness of an insecticide. J. Am. Mosq. Control Assoc. 3, 302–303 (1987)
14. FAO. Revised method for spider mites and their eggs (Tetranychus spp. and Panonychus ulmi Koch). FAO Plant Production 21, 49–54 (1980)
15. Hazan, A., Gerson, U., Tahori, A.S.: Spider mite webbing I. the production of webbing under various enviromental conditions. Acarologia 16, 68–84 (1974)
16. Ho, C., Maggi, V., et al.: Spider mite (Acari: Tetranychidae) on various crops in Taiwan. J. Agr. Res. China. 46, 333–346 (1997)

17. Mahoney, N., Molyneux, R.J., Mckenna, J., Leslie, C., Mcgranahan, G.: Resistance of 'Tulare' Walnut (Juglans regia cv. Tulare) to aflatoxigenesis. J. Fo. Sci. 68(2), 619–621 (2003)
18. Dekeyser, M.A., Downer, R.G.H.: Biochemical and Physiological Targets for Miticides. Pestic. Sci. 40, 85–101 (1994)
19. Sachiko, K., Youko, K., Hamitsu, K.: A novel miticide. Norio O and Tadakazu WAKD-2023: Biological activity and mode of action IUPAC Congress (1999)
20. Wang, Y., Shi, G., Zhao, L., et al.: Acaridical activity of Juglans regia leaf extracts on Teranychus viennensis and Tetranychus cinnabarinus (Acari: Tetranychidae). J. Econ. Entomo. 100, 1298–1303 (2007)

Acaricidal Activity of the Oleic Acid Methyl Ester from Pharbitis purpurea Seeds against Tetranychus Cinnabarinus

Juan Du[1], Lei Zhao[1], Lan-qing Ma[1], Yu-bo Liu[1], Guang-lu Shi[1], You-nian Wang[1,*], and Bao-sheng Tong[2]

[1] Key Laboratory of Urban Agriculture (North) of Ministry of Agriculture, P.R. China
Beijing University of Agriculture, Beijing, China
glshi@126.com
[2] Inn Mongolia Yongye Biotechnology Co., Ltd., Neimenggu, China

Abstract. Acaricidal activities of the extraction of Pharbitis purpurea seeds against Tetranychus cinnabarinus were determined and fraction 8 was confirmed to be the active components. GC-MS analysis showed that fraction 8 was mainly composed of methyl oleate. Effects of the methyl oleate against Tetranychus cinnabarinus were investigated by slide-dip method and leaf-dip method. Effects of methyl oleate on the organization of Tetranychus cinnabarinus were observed by transmission electron microscope (TEM). The results revealed that the methyl oleate showed killing effects on Tetranychus cinnabarinus and inhibitory effects on the growth of the eggs. After treated with 5 mg/mL methyl oleate for 24 h, the corrected mortalities of Tetranychus cinnabarinus and eggs were 73.68% and 76.16 %, respectively, and the LC50 values were 1.1671 mg/mL and 0.9533 mg/mL, respectively. The inhibitory rates of eggs of Tetranychus cinnabarinus were 78.46%. TEM observation showed that the skin structure, muscle fiber, nuclear membrane, mitochondria, and endoplasmic reticulum of mites were damaged to varying degrees by the methyl oleate. Thus, the methyl oleate from the extraction of Pharbitis purpurea seeds showed a high acaricidal activity, and provided a theoretical basis for the development of botanical acaricides.

Keywords: Tetranychus cinnabarinus, Methyl oleate, Biological activities, Scanning electron microscope.

1 Introduction

Tetranychus cinnabarinus has been accepted to be one of the most difficult to be treated biological communities in the world [1, 2]. They can cause serious harm to hundreds of kinds of crops and fruit trees due to their small size, rapid reproduction rates, large number of populations and strong adaptabilities to the environment as well as the rigid damages they caused [3]. However, large and repeatable employments of unspecific chemical acaricides have unavoidably led to the resistant of mites to the chemical agents [4], and resulted in the cross-resistant to the acaricides [5]. At the same time, the

* Corresponding author.

E. Zhu and S. Sambath (Eds.): Information Tech. and Agricultural Eng., AISC 134, pp. 621–628.
springerlink.com © Springer-Verlag Berlin Heidelberg 2012

employment of chemical acaricides to kill mite has simultaneously led to the damage of the natural enemies and other beneficial organisms, and destroyed the ecological balance. This has caused the resurgence of mites and resulted in a vicious cycle. Therefore, the developments of novel, efficient and safe acaricide have been an important topic.

It has been reported that there are more than 1600 kinds of higher plants with bio control activities on the harmful organisms, which includes 1005 kinds of plants with insecticidal activity and 39 kinds of plants with acaricidal activities [6]. These include alkaloids, citrin, flavonoids, and plant essential oils, etc. Many researchers focus on the investigations of natural acaricides. Currently, there have been many reports which are related to effects of plant extracts on mites [7-12]. During the process of screening for the acaricides from plant extracts, we have found that fraction 8 from the petroleum ether extracts showed good acaricidal activities on *Tetranychus cinnabarinus*. GC-MS analysis of fraction 8 showed that it was mainly composed of oleic acid methyl ester, linoleic acid methyl ester, palmitic acid methyl ester and palmitoleic methyl ester. In the present study, the primary acaricidal activities of oleic acid methyl ester were investigated against *Tetranychus cinnabarinus*, which offer theoretical basis for the developments of safe, effective, environmental, and novel acaricides.

2 Materials and Methods

2.1 Materials

The *P. purpurea* seeds were purchased from Beijing Tong Ren Tang Chinese Dispensary (Beijing, China). The dry seeds were pulverized by a mechanical grinder and passed through a 40 mesh sieve, and the resultant fine powder was kept in refrigerator at 4 ℃. 100 g of the dried powder was extracted by 500 mL petroleum ether, chloroform, and methanol, respectively, for 3-5 days. Each fraction was subjected to the acaricidal screening, and the petroleum ether extract was found to have the best acaricidal activity. Then the petroleum ether extract was selected for further isolation and purification. The extract was diluted by petroleum ether (1: 10, *w*/*v*) and subjected to a liquid-liquid partitioning extraction by using methanol. The extraction was performed 3 times, and the petroleum ether phase was combined together followed by a rotary evaporation. 10 g petroleum ether extract was further applied on a medium-pressure column chromatography (BUCH Switzerland) with a silica gel column. The column was washed successively by petroleum ether, petroleum ether: chloroform (9: 1, 8: 2, 7.5: 2.5, 6: 4, 5: 5, and 3: 7) with a flow rate of 10 mL/min. Each fraction was collected at an interval of 10 min and 616 fractions were obtained in total. Each fraction was detected by thin layer chromatography (TLC) with petroleum, petroleum: chloroform (9: 1, 7: 3, 5: 5), and chloroform. The same fraction was combined according to the equal R_f value. Fraction 8 which was eluted by petroleum ether: chloroform (9: 1) was the best acaricidal fraction.

T. cinnabarinus was selected from the susceptible species by indoor breeding at 25 ± 1 ℃, RH = 50 ± 10% and 18 h: 6 h light/dark cycle.

2.2 GC-MS Analysis of Fraction 8

Fraction 8 was analyzed by GC/MS on a Shimadzu QP5050A (Shimadzu Corporation, Kyoto, Japan) system equipped with a AOC-20i auto sampler under the following conditions: J&W Scientific DB-5MS fused silica capillary column (30 cm × 0.25 mm, 0.25 μm) operating in electron impact mode at 70 eV. The oven temperature was programmed from 60 ℃ (isothermal for 3 min), with an increase of 10 ℃/min to 180℃ and maintaining at 180℃ for 3 min, then 6 ℃/min to 250 ℃, ending with a 5 min isothermal at 250 ℃. Helium (99.999 %) at a constant flow of 1.2 mL/ min was used as the carrier gas. The injector temperature was 250 ℃ and the inject volume was 1.0 μl (split ratio of 50: 1). Mass spectra were taken at 70 eV with a scan interval of 0.5 s and fragments from 10 to 500 aum. The sampling detention time was 5 min.

2.3 Acaricidal Assay

Adulticide bioassay. The slide-dip method which is recommended by the FAO [13] was used to evaluate the toxicity of the compounds against T. urticae adult females (susceptible strain). Miticide compound concentrations were made in distilled water containing Tween 80, and distilled water containing Tween 80 alone was used as a control treatment. With the aid of a binocular microscope and a fine paintbrush 40-50 adult female mites who were attached to the slide by double-stick tape were introduced on the surface of the glass slide. The glass slide with mites was immersed in the miticide test solutions for 5 s. The drug solution around mites was blotted up and mites were placed in the room at 24 ± 2 ℃. The survivors were counted after 24 h and the mean mortality rates were calculated according to the values from three separate experiments.

Ovicidal Test. The leaf-dip method was recommended by the FAO. Briefly, 20 adult females TSSM were allowed to oviposit for 24 h on bean leaf resting on wet cotton wool in a petri dish. Then the adult females were removed and the eggs were counted and placed in a 25 ℃ incubator. When the egg ages were reached to 36 - 48 h, the leaf was dipped into the drug solution for 5 s and then dried on the bibulous paper. They were placed on wet cotton wool in a petri dish. The eggs which were not oviposited at the fifty day were considered as the signs of mortality. Hatching ratio and larvael mortality was assessed for five days after treatment. Three replicates were used in every treatment and control. Oviposition index = (control laying - treated laying) / (control laying + treated laying); Inhibitory rate (%) = (control laying - treated laying)/control laying×100%

2.4 Transmission Electron Microscopy

For transmission electron microscopy (TEM) mites were fixed at room tem-perature for 1 hr. in 4 % glutaraldehyde in 0.1M cacodylate buffer. It was necessary to pierce the cuticle with a fine needle to permit entry of the fixative. The animals were post-fixed in 1 % OsO_4 in phosphate buffer, dehydrated through an ethanol series, and embedded in Spurr's (1969) low viscosity epoxy resin. Sections were cut with a Porter-Blum MT-1 ultramicrotome on diamond knives and viewed in a Hitachi HU 11E electron microscope.

2.5 Statistical Analysis

The data are expressed as the mean ± S.D. Groups were compared using two-way ANOVA for repeated measurements and, where necessary, Bonferroni's test was used for post hoc analysis. A value of $P < 0.05$ was considered significant.

3 Results

3.1 Identification of the Fraction with Best Acaricidal Activity

Acaricidal activity evaluation of the methanol, chloroform, and petroleum ether extracts of dried powder *P. purpurea* seeds showed that the petroleum ether extract had the highest acaricidal activity up to 81.7 %. Therefore, the petroleum extract was selected for further isolation and purification. Two fractions were obtained by extraction of petroleum extracts with methanol, and the petroleum extract showed an acaricidal activity up to 83.2 %. The petroleum ether was then subjected to the medium-pressure column chromatography, which led to the obtainment of 12 fractions. Acaricidal assay for the 12 fractions showed that fraction 8 was the best acaricidal fraction whose inhibitory rate is 85.6 %.

3.2 Components of Fraction 8

Chemical analysis of fraction 8 was performed by GC-MS. It showed that faction 8 was composed of 16 compounds, which were mainly composed of oleic acid methyl ester, linoleic acid methyl ester, palmitic acid methyl ester and palmitoleic methyl ester (Table 1). Among these, oleic acid methyl ester was the main component and was selected for further evaluation of the acaricidal activity.

Table 1. GC-MS of Fraction 8

No	Rt(min)	Name	Match degree (‰)	Relative mass fraction (%)
1	5.24	11- hexadecenoic acid ethyl ester	623	0.02
2	5.69	2-methyl-1- Hexadecanol	584	0.009
3	6.25	oleic acid methyl ester	876	19.03
4	7.63	N- (2- Methylbutyl) - (2E,4E) – undecadienoic - 8, 10 - diyne lactam	701	0.12
5	9.32	Methyl linoleate	908	12.23
6	8.17	14-methyl-15-phenylpentadecanoate	721	0.33
7	15.39	Tridecane	562	0.005
8	17.46	Tert-hexadecyl mercaptan	795	3.21
9	23.56	Methyl hexadecanoate	827	11.81
10	15.36	Heptacosane	770	3.61
11	12.78	Nonadecanoic Acid Ethyl Ester	745	0.184
12	19.61	Ethyl linoleate	588	1.25
13	18.34	Docosanoic acid ethyl ester	682	0.054
14	18.21	1- heptatriacontanol	725	1.87
15	19.54	10,13-Eicosadienoic acid methyl ester	652	2.13
16	21.41	Methyl palmitate	725	13.24

3.3 Acaricidal Activity of Methyl Oleate against Adult Mites and Eggs

The results from the acaricidal assay of methyl oleate were shown in Table 2. After treated with 5 mg/mL methyl oleate for 24 h, the corrected mortalities of *Tetranychus cinnabarinus* and eggs were 73.68% and 76.16 %, respectively. Acaricidal assay for five different concentrations of methyl oleate showed that the LC_{50} values were 1.1671 mg/mL and 0.9533 mg/mL, respectively.

Table 2. Acaricidal activities of methyl oleateagainst *T. cinnabarinus*

Concentration (mg/mL)	Action against adult		Action against egg	
	Mortality (%)	*Corrected mortality(%)*	*Mortality (%)*	*Corrected mortality (%)*
0.5	36.73 ± 2.42^{e}	34.74 ± 2.41^{e}	45.12 ± 1.52^{e}	39.32 ± 0.27^{e}
1.0	43.75 ± 0.84^{d}	41.97 ± 0.62^{d}	54.29 ± 1.82^{d}	49.47 ± 0.02^{d}
1.5	60.61 ± 1.35^{c}	59.36 ± 1.23^{c}	62.14 ± 2.45^{c}	58.15 ± 2.14^{c}
2.5	67.37 ± 2.12^{b}	66.34 ± 2.12^{b}	70.48 ± 1.08^{b}	67.37 ± 1.15^{b}
5.0	74.49 ± 0.92^{a}	73.68 ± 0.63^{a}	78.43 ± 1.15^{a}	76.16 ± 0.72^{d}

1 Replicated three times.

2 Mean values in each column with the same letter are not significantly different at theα= 0.05 level(small letter).

Table 3. Contact toxicities of methyl oleate from petroleum ether extract on *T. cinnabarinus*

Treatment	Regressive equation	LC_{50}(mg/ml)	Correlation coefficient	95%confidence limit (mg/ml)
Adult	Y=4.9265+1.0956X	1.1671±0.1536	0.9741	0.9017~1.5107
Egg	Y=5.0209+1.0071X	0.9533±0.1473	0.9981	0.7043~1.2906

3.4 Inhibitory Activity of Methyl Oleate on the Ovipositing Activity of T. cinnabarinus

It showed from Table III that the inhibitory effects of methyl oleate were significantly different when treated for 24 h, 48 h and 72 h ($P < 0.05$). The inhibitory rates were 78.46 %, 90.09 %, 93.33 %, respectively.

3.5 Effects of Methyl Oleate on the Ultrastructure of T. cinnabarinus

TEM observation was performed to detect the effects of methyl oleate on the ultrastructure of *T. cinnabarinus*. It showed that ultrastructure of muscle fibers of mites were morphologically changed when treated with methyl oleate (Fig. 1). The cuticle structure in the control group was uniform, and muscle fibers showed regular shape with wave structure. In the treated group, the cuticle structure was damaged and muscle fibers were relax and ruptured. Morphologies of endoplasmic reticulum were also changed (Fig. 2). In the control group, the structure of endoplasmic reticulum of pest mites were unchanged, ribosome-line were covered densely, while in the treated group, the endoplasmic reticulum of mites was changed and appeared in an irregular arrangement. Changes in mitochondrial surrounding the membrane were more obvious

(Fig. 3). In the control group, pest mites mitochondria cristae was arranged regularly around the membrane which was visible, while in the treated group, arrangement of mitochondrial cristae was irregular, and some even disappeared. Membranes around the mitochondrial cristae were also dissolved.

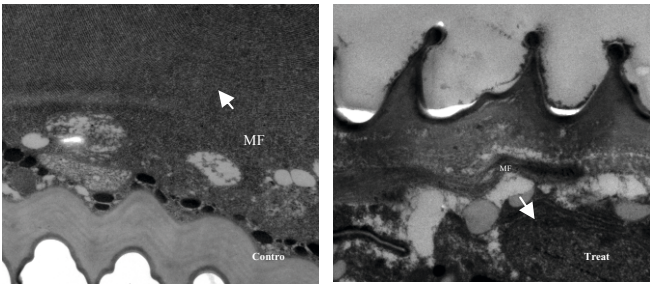

Fig. 1. Muscular filament of methyl oleate against *T.cinnababarinus*

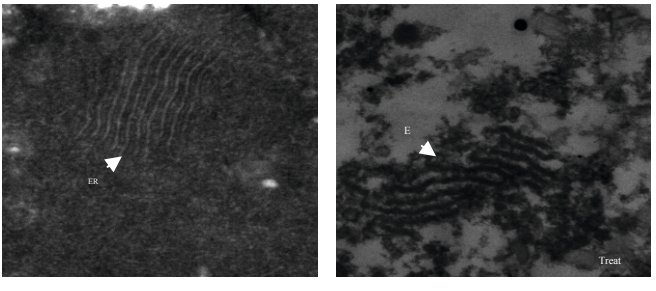

Fig. 2. Endoplasmic reticulum of methyl oleate against *T.cinnababarinus*

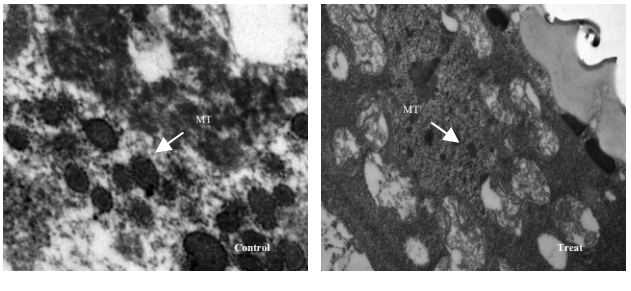

Fig. 3. Mitochondria of methyl oleate against *T.cinnababarinus*

4 Discussions

The present study showed that methyl oleate showed good acaricidal activity. After treated with 5 mg/mL methyl oleate for 24 h, the corrected mortalities of *T. cinnabarinus* and

eggs were 73.68% and 76.16 %, respectively, and the LC_{50} values were 1.1671 mg/mL and 0.9533 mg/mL, respectively. The inhibitory rates of eggs of *T. cinnabarinus* were 78.46%. TEM observation showed that the skin structure, muscle fiber, nuclear membrane, mitochondria, and endoplasmic reticulum of mites were damaged to varying degrees by the methyl oleate. The epidermis holes were appeared which may be due to that methyl oleate with good permeability activities can enter the body through the skin, thereby undermining the structure of the epidermis and in vivo cell structure. Methyl oleate also destroyed adjacent gap junctions between smooth muscle fibers, thus blocking nerve impulses of chemical information and communication, so that muscle contraction cannot be formed and shrieked [14]. The damage of the membrane structure can lead to the blockage of signal transmission and the transmission interruption of nerve excitability. Mitochondrial damage will result in the obstacle of oxidative phosphorylation in cells, the decrease of ATP activity of the cells and inadequate energy of the cells, which will finally lead to the death of *T. cinnabarinus* [15, 16].

Currently, studies on chemical constituents of the *P. purpurea* seeds have been more specific. For example, the *P. purpurea* seeds contain many kinds of alkaloids, which have similar structures and function to the strong hallucinogens lysergic acid diethylamide [17]. Moreover, they also contain emodin, coffee acid and fatty acid [18, 19]. Xu *et al*. have employed six different organic solvents to extract different parts of the *P. purpurea* (seeds, calyces and vine), and the methanol extract was found to be the best active fraction which had inhibitory activity against *Plutella xylostella* according to the bioassay. Contact toxicity experiments showed that the activity of petroleum ether extract was weak than that of the methanol extract [20]. Although many chemical constituents of the *P. purpurea* seeds have been reported, acarcidal effects of the active ingredient have not been reported. The present study demonstrated the acaricidal activity of methyl oleate and organization of mites were suffered to different degrees of damage. We concluded that the methyl oleate may act as a nerve agent; however, further investigations were needed to elucidate its specific mechanism and toxicology.

Acknowledgment. The work was financially supported by the National Natural Science Foundation of China (30872029), the Key Natural Science Foundation of Beijing Municipality (6071001), the Natural Science Foundation of Beijing Municipality (6092007), the Key Foundation of Beijing Municipal Education Committee (KZ201010020016), and Funding Project for Academic Human Resources Development in Institutions of Higher Learning Under the Jurisdiction of Beijing Municipality (PHR20090516, PHR200906134). Correspondence: You-nian WANG, e-mail: glshi@126.com.

References

1. Hazan, A., Gerson, U., Tahori, A.S.: Spider mite webbing I. The production of webbing under various environmental conditions. Acarologia 16, 68–84 (1974)
2. He, L., Yang, Y., Fu, J., et al.: Resistance selection and relative fitness of Tetranychus cinnabarinus(Boisduval) to abamectin. Acta Phytophylacica Sinica 31(4), 395–400 (2004)
3. Ho, C.C., et al.: Spider mite (Acari:Tetranychidae) on various crops in Taiwan. J. Agr. Res. China 46, 333–346 (1997)

4. Tang, C., Li, Y., Chen, B., et al.: Pesticide Chemistry, vol. 3, p. 225. Nankai University Press (1998)
5. Wang, X., Gao, X., Zheng, B.: Investigation on insecticide resistance of diamondback moth. World Agariculture 223(11), 27–29 (1997)
6. Zhao, S.: Plant Protection, 1st edn., p. 303. China Agriculture Press (2001)
7. Wang, Y., Miao, P., Cao, H., et al.: Effects of extracts of leaves of Juglans regia to several enzyme systems in Tetranychus cinnabarinus. Acta Horticulturae Sinica 34(5), 1297–1300 (2007)
8. Cao, H., Wang, Y.N., Liu, S., et al.: Effects of the chloroform extracts of Kochia scoparia to several enzyme systems in Tetranychus viennensis. Scientia Silvae Sinicae 43(2), 68–72 (2007)
9. Shi, G., Wang, Y., Wang, H., et al.: Effects of Tagetes erecta extracts on glutathione S-transferase and protease activities and protein content in Tetranychus viennensis. Chinese Journal of Applied Ecology 183(2), 400–404 (2007)
10. Wang, H., Shen, Z., Du, J., et al.: Insecticidal activity of Juglans regia extracts against Tetranychus cinnabarinus. Scientia Silvae Sinicae 44(5), 16–20 (2008)
11. Dong, Y., Wu, W.: New progress on the toxicological mechanism of plant Insecticides. Entomological Knowledge 34(2), 112–116 (1997)
12. Ren, X., Han, Z., Wang, Y.: Clong and sequence analysis of a cDNA fragment encoding acetylcholinesterase in cotton bollworm (Helicoverpa armigera). Acta Zoologica Sinica 48(1), 121–124 (2002)
13. FAO. Plant production and protection 21, recommended methods for measurement of resistance to pesticides. Rome, Italy, pp. 49–54 (1980)
14. Caulfield, M.P.: Muscarinic receptors-characterization, coupling and function. Pharmac. Ther. 58, 319–379 (1993)
15. Kazuhiko, M., Takashi, S., Matazaemon, U.: Effect of a New, Fenpyroximate, on Energy Metabolism and Mitochondrial Morphlolgy in Adult Female Tetranychus urticae (Two-Spotted Mite). Pesticide Biochemistry and Physiology 43, 37–44 (1992)
16. Zizka, Z., Pelc, R., Jizba, J., Kandybin, N.V., Sergeeva, M.V.: In Situ Assessment at Subcellar Level of the Effects of Macrotetrolide Insecticides on Mites by Electron Microscopy and X-Ray Microanalysis. Pesticide Biochemistry and Physiology 58, 165–172 (1997)
17. Ao, D., Luo, J., Wu, H., Yin, J., Yin, Y., Wei, Q.: Effect of calcineurin activator extracted from Pharbitis nil on learning and memory impairment induced by scopolamine. Journal of Beijing Normal University(Natural Science) 39(6), 803–806 (2003)
18. Chen, L., Li, P., Zhang, Z., Jing, R.: Fatty oil components analysis of Semen Pharbitidis. Chinese Traditional and Herbal Drugs 34(11), 983–984 (2003)
19. Li, P., Chen, Z.: GC-MS Analysis and CO_2 supercritical fluid extraction of fatty oil of Semen Pharbtidis. China Pharmacy 14(7), 431–432 (2003)
20. Xu, X.: Trace Insecticidal active constituents from Pharbitis purpurea and study on its application [Master thesis]. Chinese Academy of Agarical Sciences (2005)

Studies on Action Mechanism of Acrocidal Activity of Extracts of Pharbitis purpurea Seeds against Tetranychus cinnabarinus

Yan-Wang, Guang-lu Shi, Lan-qin Ma, Yu-bo Liu, and You-nian Wang*

Key Laboratory of Urban Agriculture (North) of Ministry of Agriculture, P.R. China
Beijing University of Agriculture, Beijing, China
glshi@126.com

Abstract. Action mechanism of isolation fraction 8 of petroleum ether extract of Pharbitis purpurea seeds against Tetranychus cinnabarinus was investigated. The acaricidal activities of isolation fraction 8 were measured by Slide-dip and Leaf-residue, and several kinds of important enzymes in T. cinnabarinus treated with isolation fraction 8 were tested. The ultrastructure of T. cinnabarinus treated by isolation fraction 8 was observed through transmission electron microscope (TEM). The isolation fraction 8 had strongly acaricidal activities against adult and egg of T. cinnabarinus, the LC50 value were 0.4686 mg/ml and 1.2212 mg/ml, the LC90 value were 2.5935 mg/ml and 3.1234 mg/ml. The activities of glutathione-S-transferase in T. cinnabarinus were strongly induced, but the activities of acetylcholinease, monoamine oxidase and Ca2+-ATPase were restrained after treating with isolation fraction 8. The result suggested that isolation fraction 8 of P. purpurea seeds was effective against T. cinnabarinus, which may be the cause the transmit block of nerve in mites. Observation under TEM revealed that cuticle, muscular filament, nuclear membrane, mitochondria and endoplasmic reticulum were ruptured. The result from the experiment indicated that the discovery had some exploiter value for making full use of P. purpurea seeds as new resources of botanical acaricide.

Keywords: Pharbitis purpurea, Tetranychus cinnabarinus, glutathione-S-transferase, acetylcholinease, monoamine oxidase, Ca2+-ATPase, transmission electron microscope.

1 Introduction

Phytophagous mite, an important class of biological taxa, is harmful to Chinese agricultural production. It is small in size, breeding fast, adaptable and easy to produce drug resistance. It is recognized as the most difficult taxa to prevent the damage to plants and to control its spreading. *T. cinnabarinus*, therefore, is one of the major economic pest mites (Li *et al.* 1992, Kieiewiez 1996), which can damage more than 100 kinds of crops and fruit trees (Hazan *et al.* 1974, Ho et al. 1997), seriously affecting their yields and qualities. However, in the meantime when chemical acaricides were used to kill mite, the natural enemies and other beneficial organisms

* Corresponding author.

E. Zhu and S. Sambath (Eds.): Information Tech. and Agricultural Eng., AISC 134, pp. 629–641.
springerlink.com © Springer-Verlag Berlin Heidelberg 2012

were destructed simultaneously. Thus, it destroyed the ecological balance, causing mite rampant and resulting in a vicious cycle (Hou *et al.* 2004). So, it is imperative to find efficient and safe acaricide.

In recent years, many studies have been carried out by using plant extracts as acaricide. There were reports that several enzyme activities of *T. cinnabarinus* and *Tetranychus viennensis* were activated or inhibited by using *Juglans regia*'s leaf extract (Wang *et al.* 2007b), using *Kochia scoparia*'s extract (Cao *et al.* 2007) and using *Tagetes patula*'s root extracts (Shi *et al.* 2007). Glutathione-S-transferase is one of the most active metabolic detoxification enzymes. It participated in metabolic detoxification of the endogenous and heterogonous toxic substance (Dong and Wu 1997). Studies have shown that the major target of a variety of acaricide is to inhibit the enzymatic activity in the nervous system, causing neurotransmission blocked and excitement leading to death (Ren *et al.* 2002). An effective method of studying the mechanism of killing mites is to observe the diseased cells of organism using TEM. The impact of new chemical substances on tissues and organs of organisms is the basis of experimental toxicology. By observing the impact of chemicals on tissues, organs and cells of organisms, the mode of action and site of action can be determined on cells in diseased organs (Wu 2006). By screening extracts of various plants active on killing mites, the authors found that petroleum ether extract of *Pharbitis purpurea* seeds has strong biological activity on *T. cinnabarinus* (Wang et al. 2007a). It was also reported that the methanol extract of *P. purpurea* seeds have a high insecticidal activity on diamondback moth (Xu 2005). So it can be seen that *P. purpurea* seeds has great potential as insecticidal plant.

There is no report of *P. purpurea* seeds' effects on *T. cinnarinus* enzymatic activities in vivo and its damage effects on *T. cinnarinus* cell ultrastructure. The mechanism remains unknown.

Through biological activity tracking, it is clear that isolation fraction 8 of petroleum ether extract of *P. purpurea* seeds has best effect on killing mites. By study the effects of the isolation fraction 8 on several enzymes activities of *T. cinnabarinus* and by observing the changes of its organs, tissues and cells using TEM, it is anticipated that the action mechanisms of the isolation fraction 8 on *T. cinnabarinus* could be determined, and therefore, provide theoretical basis for developing new safe, effective and environmentally friendly plant-derived acaricides.

2 Materials and Methods

2.1 Materials

The experiments were carried on in the spring of 2008 in Beijing Key Laboratory of New Technology in Agricultural Application of Beijing, Beijing University of Agriculture. The *P. purpurea* seeds were purchased from Beijing Tong Ren Tang Dispensary. The dry seeds were crushed into powder by high-speed grinder. After screening by 40 mesh sieve, the fine powder was kept in fridge. The *T. cinnabarinus* were susceptible strain by indoor breeding at the conditions of 25 ± 1 ℃, RH = 50 ± 10 % and L: D=18 h: 6 h.

2.2 The Isolation of Active Ingredients of P. Purpurea Seeds

A certain amount of dry powder was put in wide-mouth bottle and petroleum ether five times in dry powder amount was also added in the bottle for 3-5 days solvent extraction accompanied with vacuum concentration. The procedure was repeated 3 times and the extracts were mixed together. The extracts were dissolved in petroleum ether in 10 times in amount and dropped into separator funnel. Liquid-liquid partitioning extraction was carried out 3 times using methanol. The extracts were combined together followed by decompression concentration. 10g petroleum ether extract was accurately weighed. Pure petroleum ether, petroleum ether: chloroform (9: 1, 8: 2, 7.5: 2.5, 6: 4, 5: 5, and 3: 7) and pure chloroform elution in sequence was followed by column chromatography separation using medium-pressure chromatography. 12 isolation fractions were obtained. Through biological activity tracking, the isolation fraction 8 was tested pharmacy. The isolation fraction 8 was eluted and collected by petroleum ether: chloroform (9: 1).

2.3 In-door Toxicity Test

The experiment was carried out according to the FAO recommended slide dipping method to kill mature mites and leaf residue method to kill eggs with a little improvement (FAO 1980). To test the biological activities, the isolation fraction 8 was diluted into 5 different concentrations. 1 % (*v*/*v*) Tween-80 in distilled water was used as control. The experiments were repeated 3 times. The regression equation of virulence, LC_{50} and LC_{90} was therefore obtained.

Slide dipping method: The double-sided tape was attached to the one side of the slide and the top of the paper was thrown off. The same size, lively female adult mites were picked by using a zero size brush pen. The back of the mites was glued to the tape. The mites cannot be stick to feet, mouse and limbs to ensure their freedom of movement. Each slide stuck 30 mites and was check under microscope. Inactive, injuries mites were excluded. The test mites were immersed in the isolation fraction 8 solutions for 5 s, then shake gently to remove excess solution around the body of mites. The treated mites were feed on the same culture conditions. After 24 hours, the tested mites were checked under microscope. By using brush to touch the mite bodies, they were regarded to death if the mite feet did not move.

Leaf residue method (FAO 1980): Fresh cowpea leaves were collected and 0.5 cm petiole was cut. The rest petiole was put in wet cotton ball and put in Petri dish which was covered with wet cotton. The leaf was also surrounded by wet cotton. 20 mites were put on each leaf to allow the spawn for 24 hours at 25 ± 1 ℃. Then the mature mites were discarded, and the eggs were counted and put in 25 °C constant temperature incubator till the eggs reach age of 36-48 h. The leaf containing eggs was then immersed in the liquid agents for 5 s. And then placed on absorbent paper and dried in the shade. Put back in Petri dish which was covered a layer of wet cotton. When the control eggs hatched and reached the stage of nymph (120 h), counted the test eggs and the eggs not hatched were regarded as death. Calculate the mortality rate by statistical methods.

2.4 Preliminary Identification of the Isolation Fraction 8 Purity

The purity of the isolation fraction 8 was identified by thin-layer chromatography (TLC). The isolation fraction 8 was added on silica gel GF254 thin-layer plate by using 0.05 mm capillary. Chloroform is used as spreading agent. When spreading distance reached 5 cm, the plate was taken out and dried in shade. The sample was colored in saturated iodine vapor and the spots were counted. Finally along the perpendicular direction, the sample was spread again and the spots were counted again. If the chromatography plate showed multiple spots, they were regarded as mixtures. If single spots were shown, they were regarded as pure product.

2.5 Preparation of Enzyme Solution

The enzyme solution was prepared according slide immersion method (FAO 1980). The isolation fraction 8 was made up to solution at the concentration of 2.59 mg/ml (LC_{90}) to test the mites. The 200 tested mites were taken at 4, 8, 12, 16, 20, 24 h respectively after treated with the isolation fraction 8. The normal saline was added to the sample. The sample was homogenized on ice and then centrifuged at 10,000 r/min at 4 ℃ for 15 min. The supernatant was taken for future test.

2.6 Measure of Protein Content

Coomassie Brilliant Blue G-250 was used for determining the protein content (Mu 1991). 0.05 ml enzyme solution was added in measuring tube, 0.05ml distilled water in control tube and 0.05 ml standard sample in standard tube. 3 ml Coomassie Brilliant Blue G-250 reagent was added into three tubes respectively. Mixed well and kept standing for 10 min. The *OD* value was determined at the 595 nm. The experiments were repeated 3 times and the protein content was calculated.

2.7 Measure of GSTs

2.5 ml 66 mM phosphate buffer, 0.2 ml 50 mM GSH and 0.05 ml 0.03 M CDNB were mixed rapidly as control. 0.1 ml enzyme solution was added into the above solution as sample. The concentration of substrate GSH was used to reflect GST activity. The *OD* value was determined at 340 nm at 27 ℃. The experiments were repeated 3 times.

2.8 Measure of EChE

According to He Yu Xian's method (He *et al*. 2003), Asch was used as substrate, DTNB as chromogenic agent and physostigmine as inhibitor and were kept at 27 ℃ for 15 min. 0.3 ml 1 mM physostigmine was added to terminate the reaction. *OD* value was determined at 412 nm and repeated 3 times.

2.9 Measure of MAO

According to MAO kit (Jiang-Cheng, Nanjing), benzylamine, the specific substrate of MAO, was used as reaction substrate to determine the producing amount of benzyl aldehyde. The optical absorbance after enzyme reaction was determined using the

principle that benzyl aldehyde has absorbing peak at 242 nm of ultraviolet region. The experiments were repeated 3 times and the enzyme activity of MAO was determined. The enzyme activity was determined as amount of generating MAO.

2.10 Measure of Ca^{2+}-ATP Enzyme

According to the method of Ca^{2+}-ATP enzyme kit, the *OD* value was determined at 636 nm. The experiments were repeated 3 times. The enzyme activity was expressed as the content of inorganic phosphorus generated by ATP enzyme to decompose ATP in tissue per mg protein per hour.

2.11 TEM Observation

Fresh cowpea leaves were collected and 0.5cm petiole was cut. The rest petiole was put in wet cotton ball and put in Petri dish which was covered with wet cotton. The leaf was also surrounded by wet cotton. 20 mites were put on each leaf. The isolation fraction 8 was made up to the solution at the concentration of 2.59 mg/ml (LC_{90}) and throat sprayer was used to treat mites. The excess solution was dried by absorbent paper after 5s. After 16 h, the treated mites were put in fixation solution. 1% (*v*/*v*) Tween-80 in distilled water was used as control.

Before fixation, the sample was rinsed (0.1 % PBS rinse 4 times, 2 h every time), post fixed (the sample was put in 1% osmic acid with gentle shake to fix the sample fully for 2 h. during the fixation, the sample was shaken one time), then 0.1% PBS was rinsed 4 times (15 min every time), then dehydrated (30 %, 50 %, 70 %, 80 %, 90 %, 95 % and 100 % ethanol one time respectively, 100% acetone three times, 2 min every time), and then by soak, embedding, polymerization, slices, dyeing and photography (Yan 2006).

2.12 Data Processing

The data obtained was used SPSS13.0 Finney probit analysis to get virulence regression equation. The formula was then to do chi-square test. When the regression was in line with the actual situation, LC_{50} and LC_{90} were calculated. The analysis of variance and corrected mortality were according to Duncan's method and Abbott formula.

3 Results

3.1 Measure of the Isolation Fraction 8 on Biological Activity of T. cinnbarinus

From Table 1 and 2, the isolation fraction 8 has strong biological activity on adult *T. cinnabarinus* and their eggs. When the concentration of the isolation fraction 8 was 3 mg/ml, the corrected mortality of adult mites reached 94.90 %. When the concentration was 5 mg/ml, the corrected mortality of eggs was up to 98.98 %. The LC_{50} of adults and eggs by the isolation fraction 8 were 0.4686 mg/ml and 1.2212 mg/ml, LC_{90} were

2.5935 mg/ml and 3.1234 mg/ml respectively. Thus the isolation fraction 8 of petroleum ether extracts of *P. purpurea* seeds contains the active ingredients in killing adult *T. cinnabarinus* mites and their eggs.

Table 1. Acarocidal activity of *Pharbitis purpurea* seed isolation fraction against *T. cinnabarinus*

Action against adult		Action against egg	
Concentration (mg/ml)	***Corrected mortality(%)***	***Concentration (mg/ml)***	***Corrected mortality(%)***
3.0	94.90±2.469[a]	5.0	98.98±1.880[a]
1.5	79.78±1.250[b]	2.5	84.00±2.622[b]
0.9	66.33±0.943[c]	1.5	57.47±1.234[c]
0.6	64.13±3.743[c]	1.0	38.33±3.639[d]
0.3	38.25±2.443[d]	0.5	14.92±4.554[e]

Mean values in each column with the different letter are significantly different at the P= 0.05 level.

Table 2. Regressive equation of *Pharbitis purpurea* seed isolation fraction against *T. cinnabarinus*

Treatment	Regressive equation	LC_{50} (mg/ml)	LC_{50}95% confidence limit(mg/ml)	LC_{90} (mg/ml)	LC_{90}95% confidence limit(mg/ml)
Adult	Y=0.5680+1.7329x	0.4683	0.3585~0.5703	2.5935	1.9590~3.9875
Egg	Y=-0.2727+3.1422x	1.2212	1.0994~1.3487	3.1234	2.6836~3.8140

3.2 Preliminary Analysis of Purity Test

The two-dimensional thin-layer chromatography is taken to detect the purity of the isolation fraction 8. The result showed that along the diagonal of two-dimensional chromatography plate the isolation fraction 8 only showed one yellow spot, R_f=0.57. It was initially determined that it is active substance with high purity.

3.3 Effects of the Isolation Fraction 8 on Protein Contents in T.cinnabarinus

It showed from Fig. 1 that the protein contents in *T. cinnabarinus* treated by the isolation fraction 8 were higher than that of control. After treated for 4 h, the treatment group showed an upward trend in protein contents. Till 12 h, it slightly decreased followed by sharp rise after 20 h. Protein content of the control group showed an overall downward trend. 8 h reached the lowest. Afterwards it had a slight recovery, but still lower than the contents in 4 h. There existed significant difference between the treatment and the control except that of 4 h.

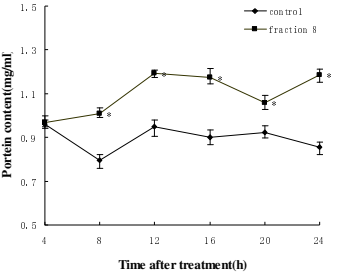

Fig. 1. Effect of isolation fraction 8 to protein content of *Tetranychus cinnabarinus*
Note:* mean significantly different at the *P*= 0.05 level.

3.4 The Effects of the Isolation Fraction 8 on GSTs Activity in T. cinnabarinus

As showed in Fig. 2, after the isolation fraction 8 treatment 4 h, the activity of GSTs in T. cinnabarinus increased first, then decreased followed by increase. Its activity was far greater than the control group and there existed significant difference, especially treatment for 8 h. At this point, the enzyme activity (505.202 U/mg prot) induced by the isolation fraction 8 was 1.730 times higher than that of control (292.705 U/mg prot). Afterwards it declined, but increased after 20 h. This showed that the isolation fraction 8 had strong activating function on GSTs in mites.

3.5 The Effects of the Isolation Fraction 8 on TChE Activity in T. cinnabarinus

As showed in Fig 2, after the isolation fraction 8 treatments, the AChE activity showed a downward trend in the overall as time goes by. However, the activity in the control group showed went up first, and then decreased. The activity in the treatment group was higher than that in the control in a short time at the beginning, and the activity was lower than that in the control at the other time. There existed significantly difference between treatment group and control group from12 h to 20 h of treatment. The AChE activity of the treatment group (0.019 U/mg prot) at 12 h was only 0.275 times of that control group (0.069 U/mg prot). This showed that the AChE activity was obviously inhibited after the isolation fraction 8 treatments for 12 h.

3.6 The Effects of the Isolation Fraction 8 on MAO in T. cinnabarinus

Fig. 2 showed that the MAO activity trends broadly were in line with the control group and all declined within 24 hours of the isolation fraction 8 treatments. At early stage of treatment, it was not obvious that the isolation fraction 8 affected MAO and there was no significant difference compared with the control. However, it was subject to a certain degree of inhibition at the mid-term. The inhibitions were significant at 16 h and 20 h, whereas it was not obvious at 24 h.

3.7 The Effects of the Isolation Fraction 8 on Ca2+-ATP Enzyme Activity in T. cinnabarinus

From Fig. 2, the basically trends of the treatment group and control group were similar. They started with upward trends, then decreased sharply after 8 h, and rise again after

12 h. At 4 h, the treatment group was significantly lower than that the control group. This trend continued till 20 h. the enzyme activity in treatment group increased after 20 hours and it showed higher than that the control group at 24 h. At this point, there was no significant difference. Overall compared with the control, the Ca^{2+}-ATP enzyme activity was to some extent inhibited after the mites were treated by the isolation fraction 8.

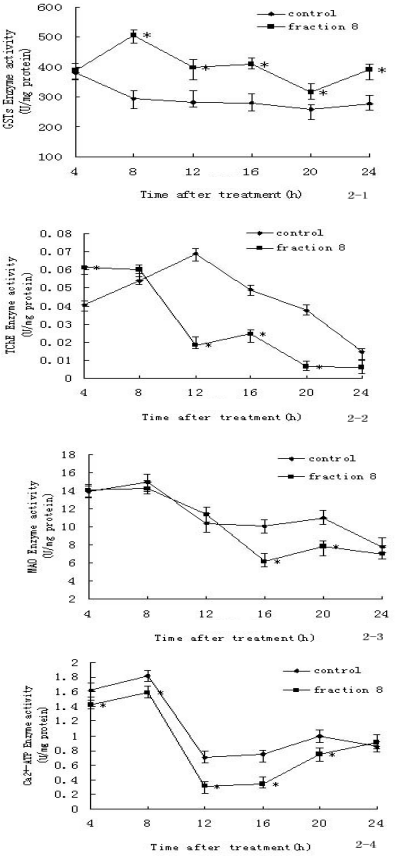

Fig. 2. Effect of isolation fraction 8 to Enzyme activity of Tetranychus cinnabarinus

Note: 2-1, 2-2, 2-3, 2-4 are effect of isolation fraction 8 to GSTs, AChE, MAO, Ca^{2+}-ATPase of T. cinnabarinus.
* mean significantly different at the P= 0.05 level.

3.8 The Cell Ultrastructure Changes of T. Cinnabarinus under the Isolation Fraction Treatment

Fig. 3 showed that cell ultrastructure changes of adult female *T. cinnabarinus* were observed using transmission electron after treated with the isolation fraction 8.

The results indicated that the cuticle structure of teleonymph showed morphological changes. In control group (3-1), the mite cuticle structure was uniform, showing regular shape with wave structure. In treatment group (3-2), the cuticle structure was damaged accompanying with holes appearing. There was evidence that the reagent went into the body through cuticles (3-6). After treatment, the cell ultrastructure structure of muscle fibers was changed apparently. In the control group (3-3), the mite muscle fibers were arranged closely and uniformly in parallel and had light and shade with a white, whereas in treated group (3-4), the mite muscle fibers were not arranged in close parallel, swelling, loose, and there was the phenomenon of fractures. The changes in nuclear membranes were obvious after treatment. In control group (3-5), the mite nuclear membrane was intact, and clearly visible. However, in treated group, (3-6) the nuclear membrane structure was not clear, some parts were dissolved resulting in some substances spilled from the nuclear. The change on mitochondrial was more obvious. In control group (3-7), the mitochondrial cristae were arranged regularly. In treated group (3-8), the arrangement of mitochondrial cristae was irregular, disorder, and the inner cristae of severely damaged mitochondrial was disappeared. The endoplasmic reticulum morphology has also changed after treatment. In control group (3-9), the endoplasmic reticulum was integrated, parallel arranged with ribosomal clouding on it. In the treated group (3-10), the mite endoplasmic reticulum was deformed and distorted. And the fracture and irregular arrangement can be seen.

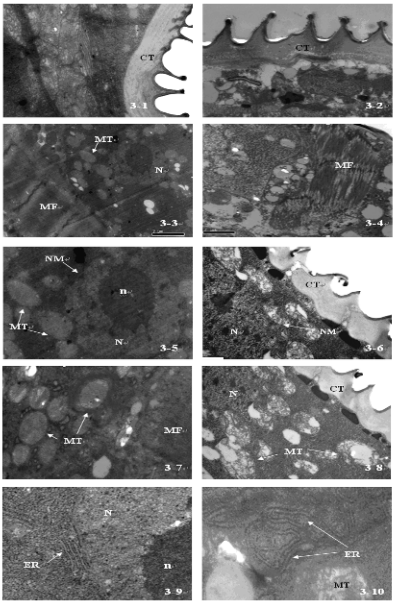

Fig. 3. Cuticle of control (3-1) and isolation fraction 8 (3-2) against Tetranychus cinnabarinus; Muscular filament of control (3-3) and isolation fraction 8 (3-4) against T. cinnabarinus; Nuclear membrane of control (3-5) and isolation fraction 8 (3-6) against T.cinnabarinus; Mitochondria of control (3-7) and isolation fraction 8 (3-8) against T. cinnabarinus; Endoplasmic reticulum of control (3-9) and isolation fraction 8 (3-10)against T. innabarinus.

Note: Abbreviations used: CT, Cuticle; MF, muscular filament; N, nuclear; MT, mitochondria; NM, nuclear membrane; n, nucleolus; ER, endoplasmic reticulum. Fig. 3(3-1) (3-2) Original magnification was 40,000; (3-3) (3-4) Original magnification was 10,000; (3-5) (3-6) Original magnification was 25,000; (3-7) (3-8) Original magnification was 20,000; (3-9) (3-10) Original magnification was 50,000;

4 Discussion

For a long time, the control of mites was majorly dependent on agrochemicals. If chemical pesticides were used over-frequently, it is escalated inevitably that the mites produce resistance. At the same time, a large number of natural enemies of insect were killed, resulting in ecological balance destroyed and 3R problem. The key for comprehensive management of mites is to choose environmentally friendly, naturally degraded acaricides (Hou *et al*. 2004) The author extracted the active substances from Chinese herbal medicine *P. purpurea* seeds. The result showed that the isolation fraction 8 of petroleum ether extract of *P. purpurea* seeds has strong toxic effect on *T. cinnabarinus*. It has some value for development.

Glutathione-S-transferase is an important detoxification enzyme in organisms and an important method to metabolize toxic substances from exogenous organisms. It can catalyze conjugation of pro-electron-donating groups between reduced glutathione and exogenous compounds in organisms, finally forming sulfide acid and excreted from the body, reducing their cytotoxicity (Leng *et al*. 1996). When external sources of toxic substances go into the organisms, it caused the increased metabolic enzyme activity to enhance the metabolism and ensure the normal physiological activities of organisms. In this experiment, treating with the isolation fraction 8 of petroleum ether extract of *P. purpurea* seeds, the activity of GSTs in mites significantly increased. Thus it can be used as sensitive indicator of detoxication metabolism on test mites.

Most acaricides play a lethal role through interfering nerve function (Mark *et al*. 1994). Accumulation of AChE may cause neurotransmission repeatedly post-releasing, causing abnormal reaction of nerve conduction, till eventually blocking the synaptic transmission. Once the enzyme was inhibited to some extent, the insects died because of over-exciting (Lin and Zhang 2001). Some interfaces of neural synaptic transmission use nerve-amine as transmission substance. When MAO was suppressed, it will lead to neural amine accumulating, blocking nerve transmission and causing the death of organisms. ATP enzyme exists on the membrane of tissue cells and organelles. It has role in material transportation, energy conversion and information transmission (Shen and Wang 1999). Ca^{2+}-ATP enzyme is one of the ATP enzymes. It plays a very important role in maintaining the stability of intracellular Ca^{2+}, maintaining balance of intracellular and extracellular Ca^{2+} and nerve cell excitability and conduction (Liu *et al*. 1999). In this assay, acetylcholinesterase was not inhibited at 4 - 8 h. Inhibition of Monoamine oxidase was not significant. At this time, the activities of mites were not obvious, most time having rest, having feet relaxed and stretching. At 12 - 20 h, acetylcholine and Ca^{2+}-ATP enzymes were subject to a strong suppression. At 16 - 20h, the monoamine oxidase was in strong inhibition. During this period, the feet of most mites move strenuously and the mites were in the state of extreme exciting. At 20 - 24 h, the activity inhibition of three enzymes decreased gradually. The mites went into the period of large number mites deaths. By analyzing

the changes of several enzymes in nerve system under the isolation fraction 8 treatment, the inhibitory action of the agent on AChE, MAO and Ca^{2+}-ATP enzyme were obvious in a certain time, probably blocking the neurotransmission and resulting in the death of mites.

Using transmission electron microscope we observed the mites cell ultrastructure of cuticle, muscle fibers, the nucleus and various organelles such as mitochondria, endoplasmic reticulum, etc, and found that they had significant changes. The holes appeared on the cuticle maybe explained that the permeability of the isolation fraction 8 is strong. It can go through the cuticle and enter into the body, resulting in destroying cuticle structure and cell structure of the body. The isolation fraction 8 destroyed the connection between adjacent smooth muscle fibers, blocking the communication between the chemical information and nerve impulses and causing that muscle fibers could not contract simultaneously (Caulfield 1993). The destruction of membrane structure may block signal transduction, interrupting the conduction of nerve excitability. Destroy of mitochondria may lead to disorder of intracellular oxidative phosphorylation and decrease ATP enzyme activity. The cell energy supply was in shortage and the mites died finally (Kazuhiko *et al*. 1992,, Zizka *et al*. 1997). This is consistent with the inhibition of activities of several enzymes mention above.

This assay only conducted a preliminary study of the mechanism from the aspects of effects of several important enzymes activities and the destruction of cell ultrastructure of *T. cinnabarinus* under the isolation fraction 8 treatment. It can be seen that the isolation fraction 8 of petroleum ether extract of *Pharbitis purpurea* seeds significantly affects the enzyme activities of *T. cinnabarinus* in a certain period. After the isolation fraction 8 treatment, the obvious changes of muscle fibers, cell membranes, cell organelles such as mitochondria, endoplasmic reticulum, and cuticle were observed using TME. However, a clear mechanism would be determined by the further studies. In addition, we will identify the structure of the isolation fraction 8 and deeply study its toxicity.

5 Conclusion

Through the measure biological activity, it can be concluded that the isolation fraction 8 of petroleum ether extract of Pharbitis purpurea seeds has a strong toxic effect on T. cinnabarinus. LC_{50} of isolation fraction 8 against the adult and egg of T. cinnabarinus were 0.4686 mg/ml and 1.2212 mg/ml respectively, and LC_{90} were 2.5935 mg/ml and 234 mg/ml respectively. The isolation fraction 8 could activate the glutathione-S-transferase activity of *T. cinnabarinus*, and inhibited significantly the enzyme activity of acetylcholinesterase, monoamine oxidase, Ca^{2+}-ATP in nervous system of *T. cinnabarinus* in a certain period. In addition, the isolation fraction 8 significantly destructed cell ultrastructure of *T. cinnabarinus* such as the cuticle structure, muscle fibers, cell membranes, and cell organelles mitochondria and endoplasmic reticulum etc. The cuticle structure was damaged accompanying with holes appearing; the muscle fibers were swelling, loose, and fracture; the nuclear membrane structure were dissolved resulting in some substances spilled from the nuclear; the endoplasmic reticulum was deformed, distorted, and irregular of arrangement; the mitochondrial inner cristae was irregular and disorder, and the inner cristae of severely damaged mitochondrial was disappeared.

Acknowledgements. The work was financially supported by the National Natural Science Foundation of China (30872029), the Key Natural Science Foundation of Beijing Municipality (6071001), the Natural Science Foundation of Beijing Municipality (6092007), the Key Foundation of Beijing Municipal Education Committee (KZ201010020016), and Funding Project for Academic Human Resources Development in Institutions of Higher Learning Under the Jurisdiction of Beijing Municipality (PHR20090516, PHR200906134). Correspondence: You-nian WANG, e-mail: glshi@126.com.

References

1. Cao, H., Wang, Y.N., Liu, S.Q., Zhao, L.L., Lu, P., Yu, T.Q., Shi, G.L.: Effect of Extracts of Kochia scoparia to Several Enzyme Systems in Tetranychus viennensis. Scientia Silvae Sinicae 43, 68–72 (2007)
2. Caulfield, M.P.: Muscarinic receptors–characterization, coupling and function. Pharmac. Ther. 58, 319–379 (1993)
3. Dong, Y.X., Wu, W.J.: Research progress of plant insecticide toxicology. Entomological Knowledge 34, 112–116 (1997)
4. FAO. Plant production and protection 21, recommended methods for measurement of resistance to pesticides. Rome, Italy, 49–54 (1980)
5. Hazan, A., Gerson, U., Tahori, A.S.: Spider mite webbing I. The production of webbing under various enviromental conditions. Acarologia 16, 68–84 (1974)
6. He, Y.X., Wang, C.F., Chen, F., Yang, X.J., Weng, Q.Y.: Effect of insecticides on esterase activity in beet armyworm. Acta Agriculture Universitis Jiangxiensis 25, 896–899 (2003)
7. Ho, C.C., Lo, C.C., Chen, W.H.: Spider mite (Acari:Tetranychidae) on various crops in Taiwan. J. Agr. Res. China 46, 333–346 (1997)
8. Hou, H., Zhao, L.L., Shi, G.L., Li, Z.H.: Studies on the acaricidic activity of the extracts of Kochia scoparia. Plant Protection 30, 42–45 (2004)
9. Kazuhiko, M., Takashi, S., Matazaemon, U.: Effect of a New, Fenpyroximate, on Energy Metabolism and Mitochondrial Morphlolgy in Adult Female Tetranychus urticae (Two-Spotted Mite). Pesticide Biochemistry and Physiology 43, 37–44 (1992)
10. Kieiewiez, M.: Dispersal of Tetranychus cinnabarinus on various tomato cultivars. Entomological Experimentalis Applicata 80, 254–257 (1996)
11. Leng, X.F., Tang, Z.H., Wang, Y.C.: Molecule Poisonology and Insect Antipesticide of Insecticides, pp. 18–21. China Agriculture Press, Beijing (1996)
12. Li, L.C., Li, L.Z., Fan, Y.L., Shi, G.L.: Chinese jujube pests. China Agricultural Press, Beijing (1992)
13. Lin, Z.L., Zhang, L.L.: The effect of phosphine on acetylchloinesterase in adults of Rhyzopertha dominica and Sitophilus zeamais in vivo. Journal of Zhengzhou Grain College 22, 35–41 (2001)
14. Liu, S.Y., Sun, L.G., Xing, W., Wai, B.J.: The effect of chronic lead exposure on hippocampal intraneuronal Ca^{2+} and activity of Ca^{2+}-ATPase in rats. Journal of Health Toxicology 13, 16–17 (1999)
15. Mark, A., Dekeyser, Roger, G.H.: Downer Biochemical and Physiological Targets for Miticides Pestic. Sci. 40, 85–101 (1994)
16. Mu, L.Y.: Plant chemical protection. China Agriculture Press, Beijing (1991)

17. Ren, X.X., Han, Z.J., Wang, Y.C.: Cloning and sequence analysis of a DNA fragment encoding acetylcholinesterase in cotton bollworm. Acta Zoologica Sinica 48, 121–124 (2002)
18. Shen, T., Wang, J.Y.: Biochemistry, pp. 32–34. Higher Education Press, Beijing (1999)
19. Shi, G.L., Wang, Y.N., Wang, H.L., Zhao, L.L., Liu, S.Q., Cao, H., Yu, T.Q., Lu, P.: Effect of Tagetes erecta on glutathiong-S-transferase and protease activities and protein content in Tetranychus viennensis. Chinese Journal of Applied Ecology 183, 400–404 (2007)
20. Wang, Y., Shi, G.L., Wang, Y.N., Wu, Z.Y.: Acaricidic Activity of Herbal Extracts Against Tetranychus cinnabarinus. Chinese Agricultural Scinece Bulletion 24, 323–326 (2007a)
21. Wang, Y.N., Mia, P.F., Cao, H., Liu, S.Q., Shi, G.L.: Effect of Extracts of Leaves of Juglans regia to Several Enzyme Systems in Tetranychus cinnabarinus. Acta Horticulturae Sinica 34, 1297–1300 (2007b)
22. Wu, W.J.: From crude production to create of new pesticide–principle*means. Chemistry industry press, Beijing (2006)
23. Xu, X.R.: Trace Insecticidal Active Constituents from Pharbitis purpurea and Study on its Application [degree thesis]. The Chinese Academy of Agricultural Sciedces, Beijing (2005)
24. Yan, R.L.: Effects of Deoxypodophyllo toxin on endocrine systems in Mythimna Separate. Northwest Sci-Ttech Univeisity of Agriculture and Forestry (2006)
25. Zizka, Z., Pelc, R., Jizba, J., Kandybin, N.V., Sergeeva, M.V.: In Situ Assessment at Subcellar Level of the Effects of Macrotetrolide Insecticides on Mites by Electron Microscopy and X-Ray Microanalysis. Pesticide Biochemistry and Physiology 58, 165–172 (1997)

Componential Analysis and Acaricidal Activities of Stellera chamaejasme Extracts by Supercritical Fluid Extraction

Wei Liang, Jun Cheng, Lan-qing Ma, Yu-bo Liu, Guang-lu Shi, and You-nian Wang*

Key Laboratory of Urban Agriculture (North) of Ministry of Agriculture, P.R. China
Beijing University of Agriculture, Beijing, China
glshi@126.com

Abstract. Extracts of Stellera chamaejasme by supercritical fluid extraction (SFE) were shown to have acaricidal activities against Tetranychus cinnabarinus. In these experiments, we extracted the components of Stellera chamaejasme through optimizing the supercritical parameters of CO2 in SFE by uniform experimental design, and analyzed the extracts of Stellera chamaejasme, which were isolated under the optimal supercritical condition, by GC/MS analysis. Our results showed that the optimal condition of supercritical CO2 extraction was extracting pressure 49 MPa, extracting temperature 15 ℃, resolution pressure 43 MPa, and resolution temperature 6.25℃. Under the optimal condition, the theoretical extract rate was 3.7731%, and actual measurement extract rate was 3.7534 %. Extracts of Stellera chamaejasme from the optimal SFE condition had contacting and systemic toxicity against Tetranychus cinnabarinus, which were more active than extracts by cold-soaked extraction method, with LC50 value of 2.407 mg/mL and 2.990 mg/mL, respectively. There were 13 compounds detected in the extracts from Stellera chamaejasme by supercritical fluid extraction, 99.99% of all components. The major compounds were Squalene, 9,12-Octadecadienoic acid (Z,Z)-, n-Hexadecanoic acid, Quinoline, and Campesterol. Squalene was the first time found from Stellera chamaejasme. Here, we also showed that Squalene had contacting and systemic toxicity against Tetranychus cinnabarinus, with LC50 value of 9.918 mg/mL and 12.918 mg/mL, respectively.

Keywords: Stellera chamaejasme, supercritical fluid extraction (SFE), GC/MS, Tetranychus cinnabarinus, acaricidal activities, Squalene.

1 Introduction

Stellera chamaejasme is one of the major poisonous plant species to meadow, and causes severe degradation of grassland, distributing wildly in Northeast, Northwest, Southeast and West of China. The roots of *Stellera chamaejasme* can be used to make pesticides with desensitization, muscacide and larvicide activities, therefore, they can be used as botanical pest control agents to control pests in crops and fodder grasses [1].

* Corresponding author.

E. Zhu and S. Sambath (Eds.): Information Tech. and Agricultural Eng., AISC 134, pp. 643–652.
springerlink.com © Springer-Verlag Berlin Heidelberg 2012

In recent years, the acaricide resistance in agricultural pest mites became more serious in China; meanwhile, the natural enemies of pest mites have also been harmed during the acaricidal process. Therefore, the damage caused by mite resurgence seriously affects the yield and quality of crops and economic forest [1-2]. There are numbers of studies showing that extracts of *Stellera chamaejasme* have acaricidal activities against agricultural pest mites [2-7]. Shi *et al.* [2] and Cao *et al.* [3] found that chloroform extracts from roots of *Stellera chamaejasme* had contacting and systemic toxicity against *Tetranychus viennensis*, LC_{50} of 8.3972 mg / mL and 5.5888 mg / mL, respectively. Han *et al.*[4] reported that the contact rate of petroleum ether extracts from *Stellera chamaejasme* against *Panonychus citri* was 100%, and the ovicidal rate was nearly 100%, at 24 hours in the concentration of 0.01 g / mL. Pan *et al.* [5] showed that the acaricidal activity of *Stellera chamaejasme* roots extracts by n-hexane and petroleum ether Soxhlet extracts against *Panonychus citri* were 12.8 and 11.5 times of Omethoate, respectively. Chen *et al.*[6] reported that the extract rate of *Stellera chamaejasme* root oil was 2.68% by supercritical CO_2 extraction, and they showed that extracts of *Stellera chamaejasme* had contacting toxicity against *Tetranychus cinnabarinus*, with a LC_{50} value of 2.4366 mg / mL. Peng *et al.*[7] extracted daphnoretin, 7-methoxy-daphnoretin and 1,5-diphenyl-1-pentanone from the roots of *Stellera chamaejasme* by using supercritical CO_2 extraction, additionally, they optimized the experiment conditions. However, there is no evidence shown that extracts of *Stellera chamaejasme* by supercritical fluid extraction had systemic toxicity against *Tetranychus cinnabarinus*; moreover, the chemical components of supercritical extraction of *Stellera chamaejasme* have not been studied. Also, in the current reports, the extract rate of supercritical fluid extraction is relatively low.

In this study, we adopted uniform design in our experiments and optimized conditions of supercritical CO_2 extraction process for extracting oil from *Stellera chamaejasme* roots. In addition, the volatile chemical components of *Stellera chamaejasme* roots extractions were analyzed by gas chromatography - mass spectrometry (GC / MS) technology. Meanwhile, the contact and systemic toxicity against *Tetranychus cinnabarinus* have been investigated and compared with the cold-soaked extraction, wherein, the extractions were from the optimal supercritical CO_2 extraction condition. Thereby, we presented a clue for developing a novel acaricide.

2 Materials and Methods

2.1 Material

The roots of *Stellera chamaejasme* were from the Jinshatan of Datong, Shanxi Province. The roots of *Stellera chamaejasme* were dried in a shady and airy place, then crushed with an electric grinder, and screened over 60 mesh.

The mites used in our studies were female adult *Tetranychus cinnabarinus*, which were the indoor breeding sensitive strain. After indoor cultivated (25 ± 1 ℃, relative humidity 60 ± 10%, L: D = 18 h: 6 h), the healthy and lively mites were selected by the same sizes and age in days. The mites were fed with the seedlings of French beans.

2.2 Supercritical CO_2 Extraction

The supercritical CO_2 extraction equipment (HA221-50-06) was from Huaan Supercritical Fluid Extraction Ltd. in Nantong, Jiangsu Province. CO_2 was provided by Beijing AP Beifen Gases Industry Co., Ltd., purity ≥ 99.5%. The powder of *Stellera chamaejasme* (100 g) was applied to the extractor (1 L), under the selected temperature and pressure, and then extracted with 21 L / h extraction flow rate for 2 hours, and anhydrous ethanol was used as entrained. Under experimental conditions, four factors (the extracting pressure, extracting temperature, and resolution pressure and resolution temperature) were divided into seven levels (Table 1), triplicate. The ranges of these four factors were as following: extraction pressure 31 ~ 49 MPa, extraction temperature 15 ~ 33 ℃, resolution pressure 25 ~ 43 MPa, and resolution temperature 6 ~ 12 ℃.

Table 1. Uniform design U_7 (7^4) factors levels

No.	Extracting pressure /MPa	Extracting temperature/ ℃	Resolution pressure/ MPa	Resolution temperature/ ℃
1	3	2	6	7
2	2	7	5	2
3	5	5	7	4
4	6	6	2	6
5	4	3	1	1
6	1	4	3	5
7	7	1	4	3

2.3 Cold-Soaked Extraction

The powder of *Stellera chamaejasme* (100 g) was added into a beaker, then applied petroleum ether and chloroform as extraction solvent[3], which volumes were 5 times of *Stellera chamaejasme* powder, and kept at room temperature to extract up to 5 days. After filtration, the residue was additionally soaked for 3 more days, then repeated this process three more times. Extracts were combined and concentrated under vacuum.

2.4 The Biological Activity of the Extracts from Stellera chamaejasme by SFE against Tetranychus cinnabarinus

Contacting Toxicity. For contacting toxicity assay, we adopted and modified Busvine [8] slide-dip method. The slides were taped with double-sided adhesive tapes at one end of slides, and then the paper of double-sided adhesive tapes was thrown off. The healthy and lively adult female mites, which were selected by the same sizes and same age in days, were picked with brush and stuck their backs onto the double-sided tape, about 30 mites per slide. The mites can not be stuck on legs, mouthparts and limbs to ensure their full freedom of movement. The slides were dissected under an anatomical microscope, and the inactive, injuries, and unqualified mites were removed. The slides were immersed into different liquids, containing different

extracts, then gently shake about 5 seconds, and absorbed the excess liquid by using absorbent paper carefully around the mites' body. All of treatments were triplicated. For the control, we used distilled water plus 1% Tween -80. After 24 hours cultured at the same conditions, mites were dissected and exanimated under an anatomical microscope by using a brush to touch mite bodies, and the mite, whose legs could not move, was considered as death.

Systemic Toxicity. The petioles of fresh French bean leaves were amputated about 0.5 cm, and inserted into individual extract liquids, then placed in Petri dishes after 72 hours. The healthy female adult mites were fed with treated French bean leaves, about 30 mites per leaf, and then observed mortality after 24 hours. Each extract was titrated by the concentration (5 levels) and triplicated. Distilled water plus 1% Tween-80 was used as the control treatment.

2.5 Analysis of Supercritical Fluid Extraction Components

For analyzing the chemical components of *Stellera chamaejasme* roots SFE extractions, gas chromatography - mass spectrometry (GC / MS) technology were applied, herein, we used Agilent 6890 gas chromatograph-5973N mass spectrometer. The HP-5MS column was a Ultra-2, crossed linked silica capillary column with a length 30 mm, 0.25 mm, and 0.25μm film thickness.

The injector temperature was 300 ℃, and the oven temperature programming was set from an initial temperature of 150 ℃ (2 min) to 180 ℃ (2 min) at a step rate of 2 ℃/min, then increased to 200 ℃ (3 min) at a step rate of 5 ℃/min, then to a final temperature of 250℃ (10 min) at a step rate of 8 ℃/min. With split less injection, the injection volume was 2 μl.

MS conditions: The temperature of the ion source and the transfer line were 230 ℃ and 280 ℃, respectively. The quadrupole temperature was 150 ℃, Ionization mode was by using EI ionization source 70 eV, and electron multiplier voltage was 1718 eV. Herein, the solvent was delayed for 8 min. By detecting with SIM, ions were scanned with 63, 79 and 210 m / z.

2.6 Verification of aCaricidal Activities of the Active Ingredients

According to GC/MS analysis, we compared the contacting and systemic toxicity against *Tetranychus cinnabarinus* of extracts to the standard component (Sigma-Aldrich).

Data Analysis

Our data were analyzed by using SPSS 17. Uniform experiments were fitted by using partial least squares regression, and toxicity regression equation were established and fitted by using mortality rate. By multiple comparisons, our data were analyzed by Duncan's new multiple range method test.

3 Results

3.1 The Optimal Parameters of Stellera chamaejasme Supercritical Co_2 Extraction

The extract rate of *Stellera chamaejasme* by supercritical CO_2 extraction at different conditions was shown in Table 2. By using least squares regression on the extract rates, which were extracted under different extraction conditions, we obtained the quadratic regression equation:

$$y = 4.9627 + 0.1230x_1 - 0.2185x_2 - 0.2709x_3 + 0.4488x_4 - 0.0011x_1^2 + 0.0036x_2^2 + 0.0045x_3^2 - 0.0359x_4^2$$

$$(R^2 = 0.9301,\ d_f = 6,\ F = 10.154).$$

Based on the regression equation and the ranges of extraction equipment, our optimum supercritical CO_2 extraction condition was extraction pressure 49 MPa, extraction temperature 15 ℃, resolution pressure 43 MPa, and resolution temperature 6.25 ℃. The theoretical extract rate by equation calculation was 3.7731%, and the actual measurement extract rate was 3.7534%, then the relative error was 0.52%.

Table 2. Extract rate of SFE fraction with *S. chamaejasme*

No.	Extracting Pressure / MPa (x_1)	Extracting temperature /℃ (x_2)	Resolution pressure /MPa (x_3)	Resolution temperature /℃ (x_4)	Extract rate/ % (y)
1	37	18	40	12	1.6990
2	34	33	37	7	1.9714
3	43	27	43	9	2.5846
4	46	30	28	11	1.3576
5	40	21	25	6	2.4566
6	31	24	31	10	1.2758
7	49	15	34	8	3.0143

3.2 The Biological Activity of the Extracts From Stellera chamaejasme by SFE against Tetranychus Cinnabarinus

In order to test the biological activities of the extracts from *Stellera chamaejasme*, the petroleum ether, chloroform and SFE extracts were prepared into emulsifiable solution with a concentration of 4 mg / mL, 1% Tween-80 as the control. The results of biological activities were shown in Table 3. Our results displayed that SFE extracts of *Stellera chamaejasme* contained contacting and systemic toxicity against *Tetranychus cinnabarinus*, which were more active than petroleum ether and chloroform methane extracts. The contacting toxicity was 1.15 times and 1.54 times of petroleum ether and

chloroform methane extracts, respectively. The systemic toxicity was 1.24 times and 0.98 times of petroleum ether and chloroform methane extracts, respectively.

Table 3. The contacting and systemic toxicity of different extracts from *S. chamaejasme* (24 h)

Extract	Contacting toxicity		Systemic toxicity	
	Mortality/%	*Corrected Mortality/%*	*Mortality/%*	*Corrected Mortality/%*
Petroleum ether	68.89 b	67.42 b	54.44 c	53.26 b
Chloroform	51.11 c	50.00 c	68.89 a	67.38 a
SFE extract	78.89 a	77.20 a	66.67 b	65.95 a

* Each extract concentration was 4 mg/mL. Mean values in each column with the same letter were not significantly different（α=0.05）(Duncan's test)．The same as below.

Furthermore, based on the logarithm value of concentrations and the corrected mortality of *T. cinnabarinus*, we calculated the toxicity regression equation, shown in Table 4. There were three kinds of *S. chamaejasme* extracts had efficiently contacting and systemic toxicity on female adult *T. cinnabarinus* mites, with LC_{50} of 2.407 mg/mL and 2.990 mg/mL, respectively, and LC_{90} of 5.239 mg/mL and 8.079 mg / mL, respectively.

Table 4. The contact and systemic toxicity of different extracts of *S. chamaejasme* with *T. cinnabarinus* (24 h)

Extract		Regressive equation	LC50 /(mg·mL^{-1})	LC50 95% confidence limit /(mg·ml^{-1})	LC90 /(mg·mL^{-1})	LC50 95% confidence limit /(mg·ml^{-1})
Contact toxicity	Petroleum ether	y = 2.713 x – 1.234	2.849	2.520 ~ 3.238	8.452	6.939 ~ 10.919
	Chloroform	y = 2.428 x – 1.521	4.231	3.677 ~ 4.965	14.268	10.983 ~ 20.455
	SFE extract	y = 3.794 x – 1.447	2.407	2.176 ~ 2.665	5.239	4.544 ~ 6.279
Systemic toxicity	Petroleum ether	y = 2.719 x – 1.511	3.596	3.173 ~ 4.117	10.646	8.592 ~ 14.169
	Chloroform	y = 3.137 x – 1.410	2.816	2.517 ~ 3.159	7.215	6.093 ~ 8.963
	SFE extract	y = 2.990 x – 1.412	2.990	2.661 ~ 3.372	8.079	6.740 ~10.215

3.3 Analysis of Supercritical Fluid Extraction Components

We analyzed the components of *S. chamaejasme* SFE extracts under the optimal condition by using GC / MS, and the relative contents in fraction of components were calculated by using area normalization method. The results were shown in Table 5. There were 13 compounds detected in the SFE extracts of *S. chamaejasme*, 99.99% of all components. The main compounds of *S. chamaejasme* SFE extracts were Squalene,

9, 12-Octadecadienoic acid (Z, Z), n-Hexadecanoic acid, Quinoline and Campesterol. Squalene was more than 1 / 3 of all of components. Therefore, the standard Squalene from Sigma-Aldrich was further used in our studies.

Table 5. Components of SFE fraction of *S. chamaejasme*

No.	Components	Content in fraction /%	Content in *S. chamaejassme* /%
1	Squalene	37.24	1.40
2	9,12-Octadecadienoic acid (Z,Z)-	26.61	1.00
3	n-Hexadecanoic acid	8.72	0.33
4	Quinoline	5.11	0.19
5	Campesterol	4.31	0.16
6	2R-Acetoxymethyl-1,3,3-trimethyl-4-(3-methyl-2-buten-1-yl)-1-cyclohexanol	4.05	0.15
7	Ergost-5-en-3-ol, (3.beta.)-Campesterol	2.89	0.11
8	1,2-Benzenedicarboxylic acid	2.58	0.10
9	1-Formyl-2,2,6-trimethyl-3-trans-(3-methyl-but-2-enyl)-5-cyclohexene	2.26	0.08
10	cis-Vaccenic acid	2.24	0.08
11	Octadecane	1.91	0.07
12	1-Methylene-2b-hydroxymethyl-3,3-dimethyl-4b-(3-methylbut-2-enyl)-cyclohexane	1.25	0.05
13	Sulfurous acid	0.82	0.03

3.4 The Biological Activity of Squalene on T. cinnabarinus

The biological activity of Squalene on *T. cinnabarinus* in the different concentrations was shown in Table 6. The regression equation of squalene contacting toxicity was y = 1.96 x -1.953, then LC_{50} was 9.918 mg / mL (95% confidence limit 8.505 ~ 11.653 mg / mL), and LC_{90} was 44.707 mg / mL (95% confidence limit 33.763 ~ 65.5900 mg / mL). The toxicity regression equation of systemic toxicity was y = 1.976x - 2.195, then LC_{50} was 12.918 mg / mL (95% confidence limit 11.052 ~ 15.365 mg / mL), and LC_{90} was 57.534 mg / mL (95% confidence limit 42.499 ~ 87.510 mg / mL). Our results showed that Squalene contained contacting and systemic toxicity against *T. cinnabarinus*, wherein the contacting toxicity was more active.

Table 6. The toxicity of squalene in different concentrations (24 h)

Concentration/ $mg \cdot mL^{-1}$	Contacting toxicity		Systemic toxicity	
	Mortality/%	*Corrected Mortality/%*	*Mortality/%*	*Corrected Mortality/%*
2	5.56 e	5.49 e	2.22 e	2.20 e
4	28.89 d	28.57 d	21.11 d	20.88 d
8	41.11 c	40.66 c	34.44 c	30.07 c
16	62.22 b	61.11 b	55.56 b	54.95 b
32	85.56 a	84.62 a	77.78 a	76.92 a

4 Discussion

In this study, we showed that the optimum supercritical CO_2 extraction condition of SFE was as follows: extraction pressure 49 MPa, extraction temperature 15 ℃, resolution pressure 43 MPa, resolution temperature 6.25 ℃. Under this condition, the theoretical extract rate was 3.7731%, and the actual measurement extract rate was 3.7534%, therefore, the relative error was 0.52%. Extracts of *Stellera chamaejasme* from the optimal SFE condition had contacting and systemic toxicity against *T. cinnabarinus,* which were more active than extracts by cold-soaked extraction method, with LC_{50} of 2.407 mg/mL and 2.990 mg/mL, respectively. There were 13 compounds detected in the extracts of *Stellera chamaejasme* by SFE, 99.99% of all components. The major components were Squalene, 9, 12-Octadecadienoic acid (Z,Z)-, n-Hexadecanoic acid, Quinoline and Campesterol. Squalene was the first time found in *S. chamaejasme* extracts. Then we showed that Squalene had contacting and systemic toxicity against *T. cinnabarinus,* with LC_{50} value of 9.918 mg/mL and 12.918 mg/mL, respectively.

The studies of the chemical components of *S. chamaejasme* were mainly focused on the isolation of medicinal ingredients from *S. chamaejasme*. For example, Feng *et al.* [9] had isolated 6 kinds of two-flavonoid compounds with anti-diabetic activity and anti-diabetic retinopathy from *S. chamaejasme*. Yang *et al.* [10] showed that isosikokianin A from *S. chamaejasme* had antiviral effect on hepatitis B virus. For the control of pest, it has been demonstrated that umbelliferone [11, 12], Daphnoritin [11, 12], Chamechromone [11, 12] and β-sitosterol [12] had antifeeding activity on *Pieris rapae L.*. Tang *et al.*[13] and Lu *et al.*[14] reported that 1, 5 - Diphenyl-1 - pentanone from *S. chamaejasme* had contact toxicity on *Aphis craccivora* and *Culex pipiens pallens*. Additionally, Liu *et al.* [15] reported that S-(+)-1, 5-diphenly-3-hydroxy-1-pentanone from *S. chamaejasme* could be used to control *Peries rapae*. Moreover, there were displayed that extracts of *S. chamaejasme* had acaricidal activity [2-6]. However, the chemical components of the crude extracts of *S. chamaejasme* have not been reported. Squalene was the first time detected from *S. chamaejasme,* and its contacting and systemic toxicity against *T. cinnabarinus* has also been demonstrated in our studies. In addition, previous studies found that Quinoline, 1, 2-Benzenedicarboxylic acid and other ingredients had strong teratogenicity and carcinogenicity [16, 17], which maybe contributed to the acaricidal activity on *T. cinnabarinus*, however, limited in the application of acaricides.

Squalene is mainly existing in marine fish and plant oils, and widely used in pharmaceuticals and cosmetics. It has been proved that Squalene had anti-tumor [16], anti-cholesterol [18] and detoxification activities [19]. Meanwhile, the studies showed that Squalene can be used as anti-bacterial agents [20] and pesticides, in particular, good to use in controlling the fire ants and mosquitoes [21]. Furthermore, Squalene is beneficial and harmless to human, and there is no residual damage been reported. Therefore, our studies provide a potential property of Squalene as a novel acaricide agent by modifying the molecular structure or using other methods to enhance its acaricidal activity. However, the mechanism of Squalene acaricidal activity against mites is still not clear and needs to be further investigated. Also, the other compounds of SFE extracts from *S. chamaejasme* were rarely reported, therefore, their biological activity need to be studied further.

Acknowledgment. The work was financially supported by the National Natural Science Foundation of China (30872029), the Key Natural Science Foundation of Beijing Municipality (6071001), the Natural Science Foundation of Beijing Municipality (6092007), the Key Foundation of Beijing Municipal Education Committee (KZ201010020016), and Funding Project for Academic Human Resources Development in Institutions of Higher Learning Under the Jurisdiction of Beijing Municipality (PHR20090516, PHR200906134). Correspondence: You-nian WANG, e-mail: glshi@126.com.

References

1. Kalaisekar, A., Naidu, V.G., Rao, N.V.: Efficacy of some pesticides against citrus rust mite, Phyllocoptruta oleivora. Indian Journal of Entomology 65(3), 308–310 (2003)
2. Shi, G.L., Liu, S.Q., Cao, H., Zhao, L.L., Li, J., Li, S.Y.: Acaricidal activities of extracts of Stellera chamaejasme against Tetranychus viennensis (Acari: Tetraanychidae). Journal of Economic Entomology 97(6), 1912–1916 (2004)
3. Cao, H., Liu, S.Q., Zhao, L.L., Shi, G.L., Zeng, X.N.: The effects of the extracts from Stellera chamaejasme L. on the biological and enzyme activity of Tetranychus viennensis zache. Scientia Silvae Sinicae 39(1), 98–102 (2003)
4. Han, J.Y., Zeng, X.N., Du, L.X., Chen, X., Liu, Y.: Progress on studying the activities of some plants for controlling mites. Guangdong Agricultural Sciences (2), 43–46 (2003)
5. Pan, W.G., Gao, P., Liu, Y.P., Luo, P., Huang, J.H., Li, Y., Liu, S.G.: The Toxicity of Components Extracted from the Root of Stellera chamaejasme L.to Panonychus citri and the Interaction between Components. Journal of Sichuan University (Natural Science Edition) 41(1), 208–211 (2004)
6. Chen, M., Shi, G.L., Li, Z.H.: The Supercritical CO2 extraction of Stellera chamaejasme L. and the analysis of extracts acaricidal activities. Journal of Beijing Agricultural College 23(3), 40–42 (2008)
7. Peng, J.Y., Dong, F.Q., Xu, Q.W., Xu, Y.W., Qi, Y., Han, X., Xu, L.N., Fan, G.R., Liu, K.X.: Orthogonal test design for optimization of supercritical fluid extraction of daphnoretin, 7-methoxy-daphnoretin and 1,5-diphenyl-1-pentanone from *Stellera chamaejasme* L. and subsequent isolation by high-speed counter-current chromatography. Journal of Chromatography A 1135(2), 151–157 (2006)
8. Busvine, J.R.: Recommended methods for measurement of resistance to pesticides, FAO. Plant Production and Protection 21, 77–90 (1980)
9. Feng, B.M., Wang, T., Zhang, Y., Hua, H.M., Jia, J.M., Zhang, H.L., Pei, Y.H., Shi, L.Y., Wang, Y.Q.: Aldose reductase inhibitors from Stellera chamaejasme. Pharmaceutical Biology 43(1), 12–14 (2005)
10. Yang, G.H., Chen, D.F.: Billavanones, flavonoids, and coumarins from the roots of Stellera chamaejasme and their antiviral effect on hepatitis B virus. Chemistry & Biodiversity 5(7), 1612–1872 (2008)
11. Wang, Y.W., Zhang, G.Z., Xiu, H.H., Chiu, S.F.: Isolation of Extraction of Stellera chamaeja sme. Journal of Anhui Agricultural Sciences 32(4), 671–672 (2004)
12. Zhang, G.Z., Zhao, H.H., Chiu, S.F., Wang, Y.W.: Isolation and Identification of Extraction of Stellera chamaeja sme. Journal of Hubei Agricultural College 20(1), 19–22 (2000)

13. Tang, X.R., Hou, T.P.: Separation and identification of botanical insecticide 7-hydroxycoumarin and its biological activity against Aphis craccivora and Culex pipiens pallens. Natural Product Research 22(4), 365–370 (2008)
14. Lu, T., Chen, L., Hou, T.P.: Synthesis and structure-activity study of botanical aphicides 1,5-diphenyl-1-pentanone analogues. Pesticide Biochemistry and Physiology 89(1), 60–64 (2007)
15. Liu, Q., Jia, H., Xiao, B., Chen, L., Zhou, B., Hou, T.P.: A new compound against Peries rapae from Stellera chamaejasme. Natural Product Research 22(4), 248–252 (2008)
16. Zhang, X.X., Wu, W.L., Shan, B.L., Fang, M.M., Zhao, C.C.: Kinetics of Quinoline degradation by innobilized bacteria Q5. Acta Petrolei Sinica(Petroleum Processing Section) 25(3), 442–446 (2009)
17. Tan, J., Lin, Z.G.: GC-EI-MS Internal Standard Analysis of Phthalic Acid Esters in Fish. Acta Chimica Sinica 65(24), 2875–2882 (2007)
18. Huang, Z.R., Lin, Y.K., Fang, J.Y.: Biological and Pharmacological Activities of Squalene and Related Compounds: Potential Uses in Cosmetic Dermatology. Molecules 14(1), 540–554 (2009)
19. Seiki, S., Frishman, W.H.: Pharmacologic Inhibition of Squalene Synthase and Other Downstream Enzymes of the Cholesterol Synthesis Pathway A New Therapeutic Approach to Treatment of Hypercholesterolemia. Cardiology in Review 17(2), 70–76 (2009)
20. Zieglfr, H.: Detoxification of humans and animals with squalane and squalene. DE Patent: 4 017 172 (December 20, 1990)
21. Masuda, A., Akiyama, S., Kuwano, M., Ikekawa, N.: Potentiation of antifungal effect of amphotericin B by squalene, an inter-mediate for sterol biosynthesis. Journal of Antibiotics 35(2), 230–234 (1982)
22. Yoder JA, Pollack RJ, Spielman A. Insecticides comprising farnesol. US Patent: 5 484 599 (January 16, 1996)

Antifungal Activity of Extracts by Supercritical Carbon Dioxide Extraction from Roots of Stellera chamaejasme L. and Analysis of Their Constituents Using GC-MS

Xue-na Bai, Jun Cheng, Wei Liang, Lan-qing Ma, Yu-bo Liu, Guang-lu Shi, and You-nian Wang*

Key Laboratory of Urban Agriculture (North) of Ministry of Agriculture, P.R. China
Beijing University of Agriculture, Beijing, China
glshi@126.com

Abstract. In this work the supercritical fluid extraction with carbon dioxide was applied to obtain the extracts from roots of Stellera chamaejasme L. The extracts were evaluated through the antifungal activity against Monilinia fructicola. Furthermore, the active compounds from the extracts were separated by macro porous resin and analyzed using gas chromatography-mass spectrometry (GC-MS). The results showing that the extracts, obtained using supercritical carbon dioxide (SC-CO2) extraction technique, had strong antifungal activity against M. fructicola with inhibition ratio of 88.71% at 2000 μg/mL, minimum inhibitory concentration (MIC) of 250 μg/mL, and minimum fungicidal concentration (MFC) of 2000 μg/mL. After separation with macro porous resin chromatography, fourteen fractions were collected from the SC-CO2 extracts. At concentration of 2000 μg/mL, fraction 4, 7, and 12 presented highly antifungal activity against M. fructicola, with inhibition ratio of 83.97 %, 80.23 %, and 75.69 %, respectively. Followed by the GC-MS analysis, the main active compounds from fraction 4, 7, and 12 included hexanedioic acid, bis (2-ethylhexyl) ester, πsitosterol, 7-methyl-Z-tetradecen-1-ol acetate9, 9-hexadecenoic acid-hexadecyl ester (Z), 1, 2-benzenedicarboxylic acid-diisooctyl ester, (3π24Z) stigmasta-5, 24(28)-dien-3-ol, stigmastan-3, 5-diene, and squalene.

Keywords: Antifungal Activity, GC-MS, SC–CO2 extraction, Stellera chamaejasme L.

1 Introduction

Stellera chamaejasme L. is a perennial herb in family Thymelaeaceae, and distributed chiefly in Northwest and North of China (Liu *et al*., 2004). Together with the roots of *Euphorbia fischeriana* Steud. and *E. ebracteolata* Hayata. (family Euphorbiaceae), the root of *S. chamaejasme* is widely used as the drug "Euphorbiae Radix" in traditional Chinese herbal medicine. The drug can be used for the treatment of psoriasis, chronic bronchitis, trichomonas vaginalis; as the antituberculotic, insecticide, and antipruritic; external use for carbuncles and sores (Zhang *et al*., 2006).

* Corresponding author.

E. Zhu and S. Sambath (Eds.): Information Tech. and Agricultural Eng., AISC 134, pp. 653–662.
springerlink.com © Springer-Verlag Berlin Heidelberg 2012

The medical and pharmacological activities of the medicinal plant against inflammation, cancer and other ailments have been well studied (Wang *et al*., 2003; Wang *et al*., 2004). In recent years, based on researches in agricultural production, *S. chamaejasme* was also identified as an appropriate target to develop into the plant-originated pesticides. Generally, the extracts of *S. chamaejasme* using chloroform, petroleum ether, and methanol as solvents, had strongly pesticidal activities against *Tetranychus viennensis* (Cao *et al*., 2003); the ethanol extracts possessed strong activity against *Pieris rapae* , *Myzus persicae*, and *Ostrina furnacalis* (Zhang *et al*., 2002); daphnoritin and chamechromone from *S. chamaejasme* had insecticidal activity against *P. rapae* by effects of antifeeding and stomach poison (Zhang *et al*., 2001); the ethyl acetate extracts had significant inhibitory action against many kinds of fungi, such as *Trichophyton gypsum*, *Monilinia fructicola*, *Physalospora piricola*, *Fusarium graminearum*, *F. oxysporum* f. sp. *cucumberinu* (Gong *et al*., 2006; Wen *et al*., 2008).

Organic solvent extraction has been applied for more than decades in the researches of natural products. Although organic solvents, for example, ethyl acetate, chloroform, methanol and acetone, are effective, these extraction methods have many disadvantages such as time consuming and labor intensive. Moreover, when the methods are applied, large amounts of solvent and sample are usually required. And the used solvents may represent a potential hazard to human health and environment. The supercritical fluid extraction (SFE) is a relatively recent technique which presents various advantages over traditional methods, like the use of low temperatures and reduced energy consumption and high product quality due to the absence of solvent in solute phase (Chester *et al*., 1996). Supercritical carbon dioxide (SC-CO_2) is the most used solvent for SFE due to its particular characteristics such as moderate critical conditions (31.1 ℃ and 73.8 MPa) and of easy availability. It is also non-toxic, inflammable and chemically stable. The applications of SFE are multiple in the areas of cosmetics, essences, foods, and environmental protection (Brunner, 2005). Related to the root of *S. chamaejasme*, only few studies were performed about the use of SC-CO_2 extraction to obtain bioactive substances (Peng *et al*., 2006; Cheng *et al*., 2008), which might provide another effective method looking for the active components from the medicinal plant.

To investigate the potential for roots of *S. chamaejasme* to develop into a botanical fungicide, in the present work, the supercritical CO_2 extraction was applied to obtain the extracts from roots of *S. chamaejasme*. Then the extracts were evaluated through the antifungal activity against *Monilinia fructicola*. Furthermore, the active compounds from the extracts were separated by macro porous resin and analyzed using gas chromatography-mass spectrometry (GC-MS).

2 Materials and Methods

2.1 Materials

S. chamaejasme L. was collected at Jinshatan, Shuozhou, Shanxi Province of China, in September 2008, by Beijing key laboratory of new technology of agricultural application, Beijing University of Agriculture. Fungal strain *Monilinia fructicola* was obtained from the laboratory of plant pathology, Beijing University of Agriculture.

2.2 Instruments and Chemicals

HA221-50-06 type of SC-CO_2 extraction instrument (Huaan Supercritical Fluid Extraction Instrument Co. Ltd., Nantong, Jiangsu Province, China); CO_2 with purity ≧99.5% was provided by Beijing Hepubeifen Gas Industry Co. Ltd., Beijing, China; HYP-150 type of disintegrator (Beijing Huanyatianyuan Mechanical Technologies Co. Ltd., Beijing, China); Agilent 6890 gas chromatography-5973N mass spectrometry (Agilent Technologies Inc., USA); Milli-Q water purification system (Millipore Inc., USA). All reagents were of chromatographic reagent grade (Beijing Chemical Reagents Co. Ltd., Beijing, China).

2.3 Sample Preparation and Sc-Co_2 Extraction

After being cleaned, the dried roots of *S. chamaejasme* were crushed by the disintegrator and passed through 60 mesh sieve. The obtained sample powder was stored in the desiccator until the extraction was performed. The sample powder (1,000 g) was placed inside the SC-CO_2 extraction cell and submitted to the extraction. The operating conditions were set as: CO_2 flow rate 21 L/h, extraction pressure 30 MPa, extraction temperature 46 ℃, separation temperature 45 ℃, separation pressure 5.5 MPa, total extracting time 100 min. Through the SC-CO_2 extraction, fat soluble extracts were collected into flasks.

2.4 Antifungal Activity Assay

The assay was manipulated by the means of plate-based fungal growth inhibition method (Wu *et al*., 2009) with certain revision. The procedure was as follows: (1) Fungal strain *Monilinia fructicola* was cultured on potato-dextrose-agar (PDA) medium plates at 25 ℃ for five days, then its hyphae discs with 6 mm in diameter were cut off from petri dishes; (2) acetone solution of the SC-CO_2 extracts and 0.5 ml Tween-80 were added to 20 ml PDA medium to produce the PDA plates with final concentration of 2000, 1000, 500, 250, and 125 μg/mL, respectively; the same volume of acetone was similarly treated as negative control; (3) each of the hyphae disc above was inoculated on the PDA plates with different concentration of the extracts; (4) inhibition of the fungal growth was determined by the diameter of hyphal growth at 25℃ until the hyphal growth of the negative control was full of the plates. Inhibition ratio was calculated using the following formulation:

Inhibition ratio (%) = [(diameter of negative control – diameter of experimental hyphae)/diameter of negative control] × 100 %.

Calibration curves were constructed by plotting the inhibition ratio (Y) against the concentrations (X), to calculate linear regressive equation, median effective concentration (EC_{50}) and 90% effective concentration (EC_{90}) against *M. fructicola*. For each concentration, the antifungal activity was evaluated with three replicates. Software SPSS13.0 was used for Duncan's Multiple Range Test.

2.5 Value of Minimum Inhibitory Concentration (MIC) and Minimum Fungicidal Concentration (MFC) against M. Fructicola

According to the fungal growth inhibition method mentioned above, the PDA plates containing the SC-CO_2 extracts with final concentration of 4000, 2000, 1000, 500, 250,

125, 62.5 and 31.25 μg/mL were prepared, respectively. The same volume of acetone was similarly treated as negative control. Then, 100-μl suspension of the spores (5×10^4 spores/ml) was added into the PDA plates and co-incubated at 25 ℃ for 48 h. Minimum inhibitory concentration (MIC) was defined as the minimum concentration that totally inhibited fungal growth at this moment. Based on the MIC, the further co-incubation was continued for 7 days to determine the minimum fungicidal concentration (MFC) that totally inhibited fungal growth.

2.6 Macroporous Resin Chromatography

To further investigate the bioactive compounds of *S. chamaejasme* roots, macro porous resin HP-20 was employed to separate the antifungal components from the SC-CO_2 extracts. Prior to the separation experiments, HP-20 resin was washed with ethanol and loaded into a column (4×150 cm). Then HP-20 resin was extensively washed with plenty of distilled water to remove ethanol. Sample solution (30 mg/ml) of SC-CO_2 extracts was loaded into the resin column, followed by elution with distilled water, gradient solution of water-acetone (9: 1, 7: 3, 5: 5, 3: 7, 1: 9, *v*/*v*), and acetone at a flow rate of 1.5 mL/min, respectively. The elute was received in an auto-partial collector (10 min per test tube). After analysis by thin layer chromatography, the eluted fractions with the same mobility were mixed together, and concentrated by rotary evaporation and freeze-dried. Antifungal activity of the eluted fractions was evaluated using the method described above (section Antifungal activity assay).

2.7 Gc-Ms Analysis

The GC-MS analysis was conducted with an Agilent 6890-5973N GC/MS network system, equipped with a split less injector, and a network mass selective detector. A HP-5MS capillary column was used (30 m × 0.25 mm ID, 0.25 μm film thickness). The carrier gas was ultra-pure helium at constant flow of 1.0 mL/min. The injector temperature was set at 300 ℃. The initial oven temperature of 150 ℃ was held for 2 min; the temperature was increased by 2 ℃/min to 180 ℃ and held for 2 min; the temperature was increased by 5 ℃/min to 200 ℃ and held for 3 min; and the temperature was increased by 8 ℃/min to final 250 ℃ and held for 10 min. Injections of 1 μl were made in split less mode.

The Agilent 5973N mass spectrometer was operated in the electron ionization (EI) mode at 70 eV and electron multiplier voltage at 1718 eV. The MS transfer line temperature was set at 280℃, the source temperature 230 ℃, and the quadrupole temperature 150 ℃. Detection was accomplished in selected ion monitoring (SIM) mode, scanned m/z 63, 79, 210. Compounds were identified by comparing their spectra with those in the Wiley (v.138) library and those of authentic standards.

3 Results

3.1 Antifungal Activity of the Sc-Co_2 Extracts

To evaluate the antifungal activity of the SC-CO_2 extracts from roots of *S. chamaejasme* against fungal pathogen *M. fructicola*, the plate-based assay was used.

The result showed that negative controls (acetone) haven no inhibitory activities against the fungal growth. Whereas on the PDA plate with the SC-CO_2 extracts, the growth of the fungal was inhibited, showing a decreased diameter of hyphae disc. There is a dose-effect relationship between concentration of the SC-CO_2 extracts and inhibition ratio, and significant difference ($P < 0.05$) between the inhibition ratios at different concentrations (Table 1). The SC-CO_2 extracts could inhibit the fungal growth with EC_{50} and EC_{90} values of 295 μg/mL and 2,713 μg/mL (Table 1), MIC and MFC values of 250 μg/mL and 2,000 μg/mL (Table 2), respectively.

Table 1. Inhibitory effects of different concentrations of the SC-CO_2 extracts against *M. fructicola*

Test fungus	concentrations (μg/mL)	Colony growth diameter (mm)	Inhibitory ratio (%)	Regressive equation	EC_{50} (μg/mL)	EC_{90} (μg/mL)	Correlation coefficient
M. fructicola	2000	8.2	88.71a	y =1.72 +0.58x	295	2713	0.9771
	1000	17.2	76.31b				
	500	32.8	54.82c				
	250	41.5	42.84d				
	125	46.0	36.64e				
	CK	72.6	0.00f				

Colony growth diameter was the mean value of three experiments. Different letters are significant different at $P<0.05$ based on Duncan's Multiple Range Test.

Table 2. The results of MIC and MFC

zTest fungus	Inhibitory effects	concentrations (μg/mL)							
		31.25	*62.5*	*125*	*250*	*500*	*1000*	*2000*	*4000*
M. fructicola	MIC	+	+	+	—	—	—	—	—
	MFC	+	+	+	+	+	+	—	—

"+"to show *M. fructicola* growth; "—" to show no *M. fructicola* growth.

3.2 Antifungal Activity of Fractions Separated via Macroporous Resin Chromatography

Via macro porous resin HP-20, total of 87 fractions was separated from the SC-CO_2 extracts. Preliminary analyzed by thin layer chromatography, those fractions with the same mobility were mixed together. And finally 14 fractions were collected and evaluated through the antifungal activity against *M. fructicola* (Table 3). There is a significant difference ($P < 0.05$) between the inhibition ratios of the fractions. Fractions 2, 4, 7, 12 and 14 showed stronger activity against *M. fructicola*, with inhibition ratios of 65.51 %, 83.97 %, 80.23 %, 75.69 % and 62.21 %, respectively (Table 3).

Table 3. Inhibitory action of fractions via macroporous resin against *M. fructicola*

Isolation fraction	Appearance properties	Isolation ratio (%)	Colony growth diameter (mm)	Inhibitory ratio (%)
1	white powder	0.12	24.52	59.80f
2	white powder	0.33	21.04	65.51d
3	white powder	1.26	32.68	46.43h
4	yellow oily	2.45	9.78	83.97a
5	light yellow powder	3.84	41.90	31.31k
6	light yellow woolly	1.72	45.21	25.89l
7	milky powder	11.72	12.06	80.23b
8	light yellow solid	1.08	39.62	35.05i
9	yellow-brown solid	2.42	32.15	47.30 g
10	yellow woolly	8.42	39.67	34.97i
11	yellow woolly	38.26	41.83	31.43j
12	yellow-brown oily	23.67	14.83	75.69c
13	yellow solid	4.43	54.71	10.31m
14	yellow solid	0.28	23.05	62.21e

Negative control's diameter was 61mm. Colony growth diameter was the mean value of three experiments at solvent concentration of 2000 μg/mL. Different letters are significant different at $P<0.05$ based on Duncan's Multiple Range Test.

3.3 Chemical Constituents Analyzed by GC-MS

Based on the antifungal activity assay, the fractions 4, 7 and 12 with the inhibition ratios >75% were selected for GC-MS analysis (Fig. 1, 2 and 3). Mass spectrometer identification showed that fraction 4 consisted of hexanedioic acid, bis(2-ethylhexyl) ester, πsitosterol, 7-methyl-Z-tetradecen-1-ol acetate9, 9-hexadecenoic acid-hexadecyl ester (Z), 1,2-benzenedicarboxylic acid-diisooctyl ester, and (3π24Z) stigmasta-5,24(28)-dien-3-ol, and fractions 7 and 12 contained plenty of stigmastan-3,5-diene and squalene, respectively (Table 4).

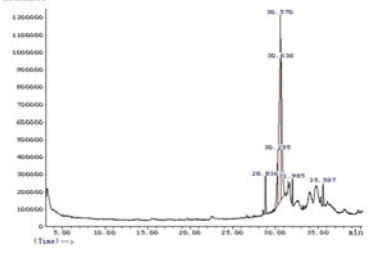

Fig. 1. Total ioncurrent chromatogram of fraction 4

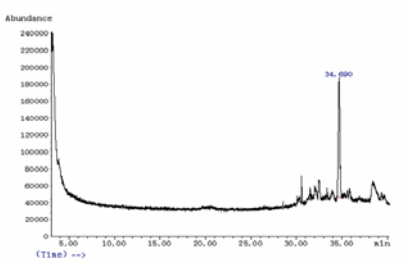

Fig. 2. Total ioncurrent chromatogram of fraction 7

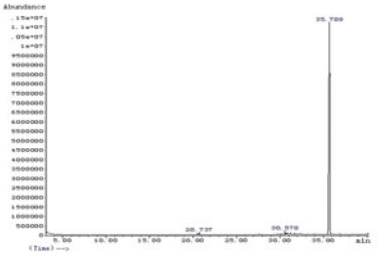

Fig. 3. Total ioncurrent chromatogram of fraction 12

Table 4. Compounds of fractions 4, 7 and 12 from *S. chamaejasme* roots

Isolation fraction	Peak No	Retention time/min	Compounds	Molecular formula	Molecular mass
4	1	28.836	Hexanedioic acid, bis(2-ethylhexyl) ester	$C_{22}H_{42}O_4$	370
	2	30.295	πSitosterol	$C_{29}H_{50}O$	414
	3	30.570	7-Methyl-Z-tetradecen-1-ol acetate9	$C_{17}H_{32}O_2$	268
	4	30.636	9-Hexadecenoic acid, hexadecyl ester, (Z)	$C_{32}H_{62}O_2$	508
	5	31.985	1,2-Benzenedicarboxylic acid, di isooctyl ester	$C_{24}H_{38}O_4$	390
	6	35.597	Stigmasta-5,24(28)-dien-3-ol, (3π24Z)-	$C_{29}H_{48}O$	412
7	1	34.690	Stigmastan-3,5-diene	$C_{29}H_{48}$	396
12	3	35.708	Squalene	$C_{30}H_{50}$	410

4 Discussion

Supercritical carbon dioxide (SC-CO_2) extraction is a highly effective technique for the researches of natural products. There is an increasing interest in employing SC-CO_2 to extract active components in practices (Ling *et al*., 2006). In present work, the antifungal components were extracted from roots of *S. chamaejasme* using the SC-CO_2

technique. The SC-CO_2 extracts had high antifungal activity against *M. fructicola* with EC_{50} and EC_{90} values of 295 μg/mL and 2713 μg/mL (Table I), MIC and MFC values of 250 μg/mL and 2000 μg/mL (Table II), respectively. Further via macro porous resin chromatography, 14 fractions with different antifungal activity against *M. fructicola* were separated from the extracts. *M. fructicola* has been known as a fungal pathogen, which can cause fruits such as peach, plum and apricot to be quickly rotten and serious loss in store, transport and sale (Wang, 2000). Unfortunately, there are no effective and safe treatments to control the fungal disease (Li *et al*., 2000). Although chemical fungicides can protect the fruits from the fungal disease at certain degree, pesticide residues would pollute environment and endanger consumers (Holmes *et al*., 1999). Existence of antifungal components against *M. fructicola*, indicated the potential for roots of *S. chamaejasme* to develop into a botanical fungicide.

To further investigate the bioactive compounds of *S. chamaejasme*, macro porous resin HP-20 was employed to separate the antifungal components from the SC-CO_2 extracts. Separation method by macro porous resin has been widely used in the separation and enrichment of bioactive compounds from many natural products (Zhang *et al*., 2008). Macro porous resin produces good recovery because of their unique adsorption properties and other advantages, including its simple procedure, high efficiency and easy regeneration. Therefore, the separation method is suitable for large-scale industrial production. In the present work, the antifungal components were separated by macro porous resin chromatography, which indicating that the separation method may be applied to the large-scale separation and purification of bioactive components from roots of *S. chamaejasme* for their practical use.

Many chemical constituents with bioactivities have been found in roots of *S. chamaejasme*, including flavonoids, coumarins, diterpenoid, lignans and phenylproene (Zhang *et al*., 2006; Yu *et al*., 2008). The medical and pharmacological activities of constituents against inflammation, cancer and other ailments have been well studied (Wang *et al*., 2003; Wang *et al*., 2004). In present work, many kinds of chemical constituents, such as hexanedioic acid, bis(2-ethylhexyl) ester, πsitosterol, 7-methyl-Z-tetradecen-1-ol acetate9, 9-hexadecenoic acid-hexadecyl ester (Z), 1,2-benzenedicarboxylic acid-diisooctyl ester, and (3π24Z) stigmasta-5,24(28)-dien-3-ol, stigmastan-3,5-diene and squalene, were identified from the antifungal fractions (Table 4). Squalene has been used in medical and cosmetic areas for its bioactivity (Zhao *et al*., 2004). Stigmastan-3,5-diene is a botanical steroids, which has fibrinolytic and anti-inflammation activities (Zhang, 2008), and found in key fruit oil and ethyl acetate extracts of *Medicago sativa* L. (An *et al*., 2006; Zhang, 2008). It is the first time that stigmastan-3,5-diene was reported in *S. chamaejasme*. π sitosterol and (3π24Z) stigmasta-5,24(28)-dien-3-ol are of important steroids (Xiao, 2006). They have been widely used in chemical industries and medical production for their anti-oxidative activities (Blair, 2000; Kevin *et al*., 2001). Summarily, the chemical constituents in roots of *S. chamaejasme* may provide a material basis against fungal pathogen *M. fructicola*.

Acknowledgment. This work was supported by the National Natural Science Foundation of China (NO. 30872029), the Natural Science Foundation of Beijing (NO. 6071001and 6092007), the Grand Project Foundation of Beijing Education Committee (NO. KZ201010020016), the Basal Construction Foundation of Beijing

Education Committee, and the Deepen Talents Scheme of Beijing Municipal Education Colleges and Universities (PHR20090516 and 200906134).

References

1. An, Y., Shi, J., Yan, W.: Separation and analysis of phytosterols in key fruit oil. Journal of Chinese Institute of Food Science and Technology 6(1), 235–237 (2006)
2. Blair, S.: Incremental reduction of serum total cholesterol and low-density lipoprotein cholesterol with the addition of plant stanol ester-containing spread to statin therapy. American Journal of Cardiology 86, 46–52 (2000)
3. Brunner, G.: Supercritical fluids: technology and application to food processing. Journal of Food Engineering 67, 21–33 (2005)
4. Cao, H., Liu, S., Zhao, L., et al.: The effects of the extracts from *Stellera chamaejasme* L. on the biological and enzyme activity of *Tetranychus viennensis*. Scientia Silvae Sinicae 39(1), 98–102 (2003)
5. Chen, M., Shi, G., Li, Z.: Extractive technique from *Stellera chamaejasme* by supercritical fluid extraction and its biological activities against *Tetranychus cinnabarinus*. Journal of Beijing University of Agriculture 23(3), 40–42 (2008)
6. Chester, T., Pinkston, J., Raynie, D.: Supercritical fluid chromatography and extraction. Analytical Chemistry 68, R487–R514 (1996)
7. Gong, X., Li, W., Ouyang, Q., et al.: The research on antifungal constituents from the root of *Stellera chamaejasme* L. Journal of Sichuan University (Natural Science Edition), 43(3), 697–704 (2006)
8. Holmes, G.J., Eckert, J.W.: Sensitivity of *Penicillium digitatum* and *P. italicum* to postharvest citrus fungicides in Dalifornia. Phytopathol. 89, 716–721 (1999)
9. Kevin, B., Hicks, R.A.: Phytosterols and phytostanols: functional food cholesterol busters. Food Technology 55(1), 63–67 (2001)
10. Li, H., Chen, L.: Practicable techniques to keep fruits and vegetable fresh. Science and Technology Reference Press, Beijing (2000)
11. Ling, J., Dai, L., Ding, X., et al.: GC-MS analysis of supercritical carbon dioxide extraction from the stroma of *Cordyceps sinensis*. Mycosystema 25(1), 138–141 (2006)
12. Liu, X., Ye, W., Che, Z., et al.: Chemical components of *Stellera chamaejasme* L. Chinese Traditional and Herbal Drugs 35(4), 379–381 (2004)
13. Peng, J., Dong, F., Xu, Q., et al.: Orthogonal test design for optimization of supercritical fluid extraction of daphnoretin, 7-methoxy-daphnoretin and 1,5-diphenyl-1-pentanone from *Stellera chamaejasme* and subsequent isolation by high-speed counter-current chromatography. Journal of Chromatography A 1135, 151–157 (2006)
14. Wang, B., Wang, R., Jia, Z., et al.: In vitro antitumor activities of the fractions of the petroleum ether extract primarily separated from*Stellera chamaejasme* L. by column chromatography on silica gel. Medicinal Journal of National Defense of Northwest of China 25(3), 167–169 (2004)
15. Wang, L.: Horticultural plant pathology. Chinese Agriculture Press, Beijing (2000)
16. Wang, R., Zhang, K., Tong, H., et al.: Study on the anti-tumor mechanisms of the methanol extract of *Stellera chamaejasme* L. Chinese Journal of Microbiology and Immunology 23(9), 734–737 (2003)
17. Wen, Z., Shi, G., Su, X., et al.: Biological activityof extract from the root of*Stellera chamaejasme* L. on fungi and enzyme of peach fruits. Journal of Beijing University of Agriculture 23(1), 25–27 (2008)

18. Wu, Z., Wang, Y., Ai, Q., et al.: Inhibitory effect and antimicrobial mechanism of pyrolin on *Monilinia fructicola* in peach. Scientia Agricultura Sinica 42(8), 2784–2792 (2009)
19. Xiao, Y.: Investigation and prospect of bioactive components in vegetable oil. Cereal and Food Industry 13(4), 1–5 (2006)
20. Yu, B., Xu, W.: Advances Chemical constituents and activity studies on *Stellera chamaejasme* L. Agrochemicals 47(12), 863–865 (2008)
21. Zhang, G., Wang, Y., Xu, H.: Studies on insecticidal activity of extract of *Stellera chamaejasme*. Journa of Changde Teachers University 14(3), 60–64 (2002)
22. Zhang, G., Xu, H., Wang, Y., et al.: Effects of antifeedant and stomach poison of daphnoritin and chamechromone to the insect. Journal of Qinghai University 19(6), 1–3 (2001)
23. Zhang, H., Ju, A., Zhou, X.: Advances chemical constituents and bioactivity on *Stellera chamaejasme* L. Chinese Traditional and Herbal Drugs 29(11), 1256–1259 (2006)
24. Zhang, Y.: Study on extract method and medical efficiency of the total flavoniod of Medicago sativa L. and secondary metabolites of several legumes grass. Doctoral Dissertation of Gansu Agricultural University (2008)
25. Zhang, Y., Jiao, J., Liu, C., et al.: Isolation and purification of four flavone C-glycosides from antioxidant of bamboo leaves by macroporous resin column chromatography and preparative high-performance liquid chromatography. Food Chemistry 107, 1326–1336 (2008)
26. Zhao, Z., Sun, Z.: Research progress on natural resources and application of the bioactivity substance squalene. Chemistry and Industry of Forest Products 24(3), 107–112 (2004)

Isolation and Identification of the Acaricidal Components Extracted from Stellera chamaejasme

Wei Liang, Jun Cheng, Chun-ya Bu, Yong-sheng Jin, Lan-qing Ma, Yu-bo Liu, Guang-lu Shi, and You-nian Wang*

Key Laboratory of Urban Agriculture (North) of Ministry of Agriculture, P.R. China
Beijing University of Agriculture, Beijing, China
glshi@126.com

Abstract. The research of Botanical acaricide is an important aspect of integrated agricultural mite management. Eight kinds of different organic solvents were used for cold-soak extraction from Stellera chamaejasme. Combined with tracking activity, the fraction E7-4 was isolated from ethyl acetate extract using medium-pressure liquid chromatography (MPLC) and preparative HPLC. Using nuclear magnetic resonance, it was determined that fraction E7-4 was Scopoletin. The results showed that the scopoletin in Stellera chamaejasme was the important acaricidal activity ingredient which exhibited contact and systemic activity against Tetranychus cinnabarinus. The Lethal concentrations (LC50) to Tetranychus cinnabarinus were 1.267 mg/mL and 7.388 mg/mL respectively.

Keywords: Stellera chamaejasme, Tetranychus cinnabarinus, Contact toxicity, Systemic toxicity, Scopoletin.

1 Introduction

Tetranychus cinnabarinus, common name red spider, is one of the worldwide pests which could cause economic harm. It is the most widely distributed and most serious agricultural mite in China. It has a grave effect on production and quality of crops and economic forests [1-2]. The use of chemical acaricides not only harms the mite's natural enemy and leads to pesticide residues but also causes insecticides resistance and mite rampant, which in true causes vicious circle [3-5]. Therefore, it is imperative to find the new, efficient and safe acaricides. Botanical acaricides maybe an important source for novel acaricides.

Previous results showed that extracts of *Stellera chamaejasme* exhibited some toxic activities against agricultural mites. Cao Hui *et al* [6] reported that chloroform extract of *Stellera chamaejasme* had contact toxicity and systemic toxicity against *Tetranychus viennensis*, with LC_{50} of 8.3972 mg/mL and 5.5888 mg/mL respectively. Shi *et al* [7] obtained fraction 26 from chloroform extract of *Stellera chamaejasme*. At the concentration of 0.5 mg/mL, the contact toxicity to the *Tetranychus viennensis* can

* Corresponding author.

E. Zhu and S. Sambath (Eds.): Information Tech. and Agricultural Eng., AISC 134, pp. 663–671.
springerlink.com © Springer-Verlag Berlin Heidelberg 2012

achieve 96.8 % within 24h. Additionally, several components of *Stellera chamaejasme*, including umbelliferone, daphnoritin, chamechromone and *β*- sitosterol have been reported on the previous study on Disease and Pest Control [8, 9]. Compared with other plants which have insecticidal and acaricidal activities, *Stellera chamaejasme* is a poisonous weed and has a large population and wide distribution. It has clear resource advantages and is a good example of how to change waste into a beneficial product.

In order to reveal the molecular structure of the acaricidal activity substance from *Stellera chamaejasme,* and to define a lead compound for the research and development of a new type acaricide, *Tetranychus cinnabarinus* was used in this study to isolate and identify the acaricidal activity substance of *Stellera chamaejasme.*

2 Materials and Methods

2.1 Materials

Root of *Stellera chamaejasme* came from the Golden Beach in Datong of Shanxi Province. Root was naturally air dried and grinded with electric mill and then filtered in 60 mesh sieves.

Took the female adults *Tetranychus cinnabarinus* as experimental mites, which were susceptible strain through multiple-generation reproductive in the indoor culture (25 ± 1 ℃, 60 ± 10 % RH, L: D=18 h: 6 h.) Chose the healthy and activity experimental mites in the same instar and size, breeding with kidney bean seedlings.

Extraction solvents were petroleum ether, cyclohexane, dichloromethane, n-butyl alcohol, acetic ester, trichloro- methyl alcohol, methyl alcohol and absolute alcohol (all were analytically pure).

2.2 The Cold-Soaked Extraction

Put the *Tetranychus cinnabarinus* dry powder into wild-mouth bottle and added 5 times amount of dissolvent. Extracted at room temperature for 5 days, the filtered residues were kept soaking for 3 days, repeated 3 times, combined the extraction and then concentrated by vacuum.

2.3 Column Chromatographic

Chose the sections which had better acaricidal effect from 8 kinds of different dissolvent extraction. Then isolated them by medium-pressure liquid chromatography (MPLC), tracking activity composition along with biological activity. Used Biotage SNAP 100 g. pillar in the medium-pressure liquid chromatography. Used the dry method upper sample: dissolved adequately with the effective extracted. Added 1.5 times amount silica gel (200 - 300 mesh, Qingdao marine organism reagent company) stirred uniformly and concentrated by vacuum. The velocity was 40 mL/min, 9 mL per tube. The clipping silica gel plate (TianJin TianHe medical instruments co. Ltd.) was used as the thin detection tool. Saturated iodine vapor was used as color developing tool. Then combined the same components and detected the toxicity.

2.4 High Performance Liquid Chromatography (HPLC) Detection

Detected the fraction purity with HPLC method. The detection conditions were HPLC-Agilent 1200 type, SUPELC0 chromatographic column(15 cm × 4.6 mm × 5 μm)with the column temperature 25 ℃, velocity 1.0 mL/min and injection volume 20 μl. The procedure of detection was: 0 - 10 min (CH_3OH 10% + H_2O 90%); 10 - 100 min CH_3OH gradient elution from 10% to 100%, increasing 1% per minute. 90 - 120 min CH_3OH 100% elution.

2.5 HPLC Preparative

According to the HPLC results, the Varian Prostar 210 type HPLC was used to prepare the main fraction. Set the elution gradient on the basis of the detection result.

2.6 Structure Elucidation of Active Component

Bruker-300 type nuclear magnetic resonance was used to collect the ^{1}H NMR spectrum and ^{13}C NMR spectrum data of compound. Identify the compound structure with documents.

2.7 Bioactivity Assay

Contact toxicity. Modified slide dip method invented by Busvine [10]. Stacked the double-sided tape to the one side of the slide, and then tore off the upper slip. Chose the active female adults with the same size and vivid color. Stacked their backside to double-sided tape to avoid sticking the feet, mouthparts and pedipalp and be sure the feet can run freely. 30 adults' mites can be glued in each slide. Put the slide under binocular dissecting microscope and take out the inertia, injured and unqualified mites. Shaking lightly the mites around 5 seconds in each different medical solution required to be examined. Took the mites out and absorbed the solution over the mites with absorbent paper. Repeated 3 times for each treatment. Distilled water added 1% (Volume) TWEEN-80 was used as control groups. Mites were cultured 24h in the same conditions as before, observed the mites under binocular dissecting microscope. Mites without response by lightly touch with writing brush being considered as dead.

Systematic toxicity test. Flesh kidney bean leaf was truncated 0.5 cm in petiole and then inserted into medical solutions. Put them into the culture dishes after 72 h. Check the mortality rate after the mites were fed with leaves after 24 h. 30 larvaes were inoculated on each leaf. 5 different concentrations for each extraction. Three replicates were performed for each concentration. Distilled water added 1 % (Volume) TWEEN-80 was used as control groups.

2.8 Data Processing

The data obtained was analyzed with SPSS 17.0 by the method of multi-comparison of Duncan's new-multiple significant ranges. The Abbot formula was used to calculate the toxic regression equation.

3 Results and Analysis

3.1 The Toxicity Test Result of Cold-Soak Extractions

According to the concentration logarithm values of 8 kinds extraction and the corrected mortality probit values of Tetranychus cinnabarinus we obtained the toxic regression equation respectively). The results are shown in table 1 and 2.

Table 1. The contact toxicity of *S. chamaejasme* extraction against *T. cinnabarinus* (24 h)

	Regressive equation	**LC_{50} /(mg·mL^{-1})**	**LC_{50} 95% confidence limit/(mg·ml^{-1})**	**LC_{90} /(mg·mL^{-1})**	**LC_{50} 95% confidence limit/(mg·ml^{-1})**
Petroleum ether	y = 2.713 x - 1.234	2.849	2.520 ~ 3.238	8.452	6.939 ~ 10.919
Cyclohexane	y = 2.554 x – 1.594	4.208	3.676 ~ 4.900	13.359	10.453 ~ 18.667
Dichloromethane	y = 3.154 x – 2.467	6.059	5.328 ~ 7.089	15.444	12.100 ~ 22.148
n-butanol	y = 2.370 x - 1.509	4.333	3.751 ~ 5.114	15.050	11.470 ~ 21.911
Anhydrous alcohol	y = 2.891 x – 2.432	6.938	5.979 ~ 8.436	19.255	14.333 ~ 30.334
Ethyl acetate	y = 3.095 x - 1.924	4.186	3.721 ~ 4.762	10.864	8.906 ~ 14.192
Chloroform	y = 2.428 x - 1.521	4.231	3.677 ~ 4.965	14.268	10.983 ~ 20.455
Methanol	y = 2.576 x – 2.279	7.673	6.437 ~ 9.780	24.128	16.933 ~ 42.110

Table 2. The systemic toxicity of *S. chamaejasme* extraction against *T. cinnabarinus* (24 h)

	Regressive equation	**LC_{50} (mg·mL^{-1})**	**LC_{50} 95% confidence limit/ (mg·ml^{-1})**	**LC_{90} /(mg·mL^{-1})**	**LC_{50} 95% confidence limit/ (mg·ml^{-1})**
Petroleum ether	y = 2.719 x – 1.511	3.596	3.173 ~ 4.117	10.646	8.592 ~ 14.169
Cyclohexane	y = 2.374 x – 1.654	4.975	4.280 ~ 5.952	17.247	12.902 ~ 25.963
Dichloromethane	y = 2.721 x – 1.548	3.722	3.281 ~ 4.269	11.048	8.884 ~ 14.799
n-butanol	y = 2.763 x - 1.408	3.232	2.860 ~ 3.678	9.405	7.688 ~ 12.260
Anhydrous alcohol	y = 2.598 x – 2.209	7.080	6.004 ~ 8.818	22.044	15.849 ~ 36.542
Ethyl acetate	y = 3.549 x - 1.432	2.533	2.282 ~ 2.816	5.818	5.006 ~ 7.046
Chloroform	y = 3.137 x - 1.410	2.816	2.517 ~ 3.159	7.215	6.093 ~ 8.963
methanol	y = 2.738 x – 2.559	8.602	7.559 ~9.952	25.267	20.031 ~ 34.709

Different solvent extractions of *Stellera chamaejasme* had a contact toxicity and systemic toxicity on the female adults of *Tetranychus cinnabarinus.* Petroleum ether extract's contact toxicity effect was the strongest followed by Ethyl acetate extract with LC_{50}s were 2.849 mg/mL and 4.186 mg/mL respectively; Ethyl acetate extract's systemic toxicity was the strongest followed by chloroform that the LC_{50}s were 2.533 mg/Ml and 2.816 mg/mL respectively. Therefore, the Ethyl acetate extract of *Stellera chamaejasme* showed good contact toxicity and systemic toxicity. The ethyl acetate extract was further investigated by column chromatography.

3.2 Column Chromatography Results

15 kinds of fractions were obtained in ethyl acetate extract by silica gel column Chromatography and combined with the bioactivity assay and linear gradient elution for ethyl acetate extract: Methanol and thin plate determination. E7 showed the best contact toxicity and systemic toxicity against *Tetranychus cinnabarinus.* The results are shown in table 3. Toxic regression equation of the contact toxicity effect was y = 3.363 x – 0.464, LC_{50} was 1.374 mg/mL; 95% confidence interval was 1.255 - 1.529 mg/mL. Toxic regression equation of systemic toxicity was y = 1.482 x – 1.449, LC_{50} was 9.501 mg/mL; 95% confidence interval was 7.940 - 11.682 mg/mL. The contact toxicity of fraction E7 against *Tetranychus cinnabarinus* was increased but the systemic toxicity was decreased.

Table 3. The toxicity of fraction E7 in different concentrations (24 h)

Contact toxicity			**Systemic toxicity**		
Concentration/ mg·mL^{-1}	***Mortality/ %***	***Corrected Mortality/%***	***Concentration/ mg·mL^{-1}***	***Mortality/ %***	***Corrected Mortality/%***
0.50	10.11 ^{e}	10.00 ^{e}	2.00	16.85 ^{e}	16.67 ^{e}
0.75	15.73 ^{d}	15.56 ^{d}	4.00	33.71 ^{d}	33.33 ^{d}
1.00	29.21 ^{c}	28.89 ^{c}	8.00	44.94 ^{c}	44.44 ^{c}
1.50	57.30 ^{b}	56.67 ^{b}	16.00	60.67 ^{b}	60.00 ^{b}
2.00	73.03 ^{a}	72.22 ^{a}	24.00	74.16 ^{a}	73.33 ^{a}

Mean values in each column with the same letter are not significantly different at α=0.05 level (Duncan's test). The same as below.

E7 was detected by Agilent 1200 type HPLC. 55 peaks were observed under a 230 nm wavelength; 51 peaks under wavelength 210nm, 18 peaks under wavelength 254 nm and 7 peaks were appeared under wavelength 280 nm. Therefore, most peaks occurred under a wavelength of 230 nm. (Shown in Fig. 1). The area of peak number 2 (RT = 20.569 min) took up 20.9027 %, the number 4 (RT = 27.487) was 47.3670 %. According to the results of HPLC, E7-4 could be obtained by collecting the number 4 peaks at 230 nm with a preparative HPLC method. Preparative conditions were CH_3OH 20% + H_2O 80% and 10 mL/min velocity.

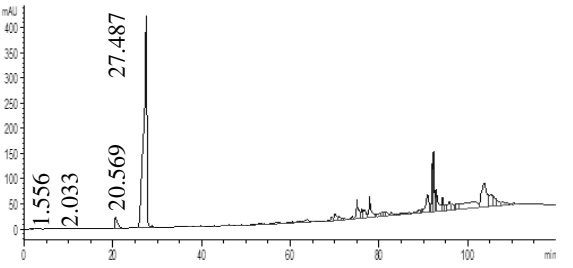

Fig. 1. HPLC analysis of fraction E7 (230 nm)

3.3 Nuclear Magnetic Resonance Detection of E7-4

We measured the nuclear magnetic resonance spectrum of E7-4. The 1H NMR spectrum is shown in Fig. 2; the 13C NMR spectrum is shown in Fig. 3. Table 4 shows the E7-4 data compared with nuclear magnetism date on reference 11. At last, Scopoletin was determined as the E7-4.

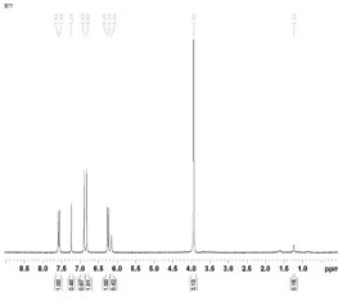

Fig. 2. ^{1}H NMR of E7-4 fraction

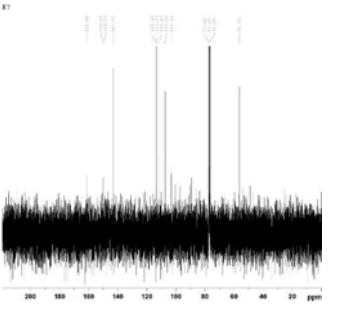

Fig. 3. ^{13}C NMR of E7-4 fraction

Table 4. Comparison of NMR data of E7-4 and reference

^{1}H NMR		**^{13}C NMR**			
Reference Value	***measured value***	***Reference Value***	***measured value***	***Reference Value***	***measured value***
6.25	6.26	161.5	161.4	103.2	103.1
7.60	7.59	107.6	107.5	149.8	149.5
6.92	6.89	143.4	143.3	111.5	111.5
6.85	6.82	113.4	113.4	56.5	56.4
6.16	6.16	144.1	114.2	—	—
3.95	3.93	150.3	150.3	—	—

NMR solvent is CDCl3

3.4 Verification of Active Component

We verified the acaricidal activity using a standard compound of scopoletin produced by Sigma-Aldrich. The results of contact toxicity and systemic toxicity were shown in table 5. The toxic regression equation on the basis of concentration logarithm value and corrected mortality probit value of *Tetranychus cinnabarinus* can be calculated. Contact toxicity effect was y = 3.519 x – 0.362, LC_{50} was 1.267 mg/mL and the 95% confidence interval was 1.164~1.393 mg/mL. Toxic regression equation of Systemic toxicity was y = 1.599 x – 1.389, LC_{50} was 7.388 mg/mL, with a 95% confidence interval of 6.304~8.814 mg/mL. The scopoletin standard compound showed both higher contact toxicity and systemic toxicity against *Tetranychus cinnabarinus* than fraction E-7 did, but showed much lower systemic toxicity against *Tetranychus cinnabarinus* than ethyl acetate extract did.

Table 5. The toxicity of scopoletin in different concentrations (24 h)

Contact toxicity			Systemic toxicity		
Concentration/ mg·mL^{-1}	***Mortality/ %***	***Corrected Mortality/%***	***Concentration/ mg·mL^{-1}***	***Mortality/ %***	***Corrected Mortality/%***
0.50	11.11 e	10.00 e	2.00	6.67 e	18.89 e
0.75	17.78 d	16.67 d	4.00	12.59 d	36.67 d
1.00	32.22 c	31.11 c	8.00	16.67 c	48.89 c
1.50	61.11 b	60.00 b	16.00	22.22 b	65.56 b
2.00	77.78 a	76.67 a	24.00	27.04 a	80.00 a

4 Discussion

Eight kinds of organic solvents were used in cold-soaked extraction for *Stellera chamaejasme.* Of these eight, ethyl acetate extract has better contact toxicity and systemic toxicity. Through medium-pressure liquid chromatography (MPLC), fraction E7 was isolated from ethyl acetate extract. The LC_{50} of contact toxicity and systemic toxicity achieved 1.374 mg/mL and 9.501 mg/mL respectively. Furthermore, we obtained the fraction E7-4 from fraction E7 by preparative HPLC. By nuclear magnetic resonance, it was determined that fraction E7-4 was scopoletin. The Lethal concentrations (LC_{50}) against *Tetranychus cinnabarinus* was 1.267 mg/mL and 7.388 mg/mL respectively.

Previous results had shown that the main chemical components of *Stellera chamaejasme* were flavonoid [12], coumarin [13], diterpenoids [14] and lignans [15]. They had prominent medicinal activity and pesticidal activity [16]. Wang Yawei *et al* [17] and Zhang Guozhou *et al* [18] isolated umbelliferone, daphnoritin, chamechromone and β- sitosterol from *Stellera chamaejasme* and they proved that these 4 components had antifeeding activity to *Pieris rapae* L. Liu *et al* [19] proved that S-(+)-1,5-diphenly-3-hydroxy-1-pentanone could prevent *Peries rapae* from eating. Feng Baoming *et al* [20] isolated scopoletin from *Stellera chamaejasme.* Liang ran *et al* [21] reported that scopoletin isolated from *Stellera chamaejasme* had pesticidal activity. Using a recrystallization method, Zhang Yongqiang [22] isolated scopoletin from *Artemisia annua* and studied the acaricidal activity. In contrast with

the previous research, preparative HPLC was used to isolate the scopoletin from *Stellera chamaejasme* fraction with high purity and in a short time, facilitating ease for mass manufacture; meanwhile, scopoletin was shown to be an important acaricidal component of *Stellera chamaejasme* and exhibited contact toxicity and systemic toxicity against *Tetranychus cinnabarinus.*

Scopoletin, belonging to coumarins compounds, has the effects of analgesia, anti-inflammation, decreasing blood pressure and relieving muscle spasm [23]. Compared with ethyl acetate extract, the systemic toxicity of scopoletin was decreased; possibly due to other components in the crude extracts have synergistic actions. Therefore, other components of crude extracts should be purified and isolated and the acaricidal activity of scopoletin-complex pesticides should be researched in the future. Additionally, in order to provide theoretical basis for processing new, efficient and safe acaricides, the mechanisms of acaricidal activity should be defined.

Acknowledgment. The work was financially supported by the National Natural Science Foundation of China (30872029), the Key Natural Science Foundation of Beijing Municipality (6071001), the Natural Science Foundation of Beijing Municipality (6092007), the Key Foundation of Beijing Municipal Education Committee (KZ201010020016), and Funding Project for Academic Human Resources Development in Institutions of Higher Learning Under the Jurisdiction of Beijing Municipality (PHR20090516, PHR200906134).

References

1. Mo, T.L., Liu, T.: Biology, life table and predation of Feltiella acarisuga (Diptera: Cecidomyiidae) feeding on Tetranychus cinnabarinus eggs (Acari: Tetranychidae). Biological Control 39(3), 418–426 (2006)
2. Wang, Y.N., Shi, G.L., Zhao, L.L., et al.: Acaricidal activity of Juglans regia leaf extracts on Tetranychus viennensis and Tetranychus cinnabarinus (Acari: Tetranychidae). Journal of Economic Entomology 100(4), 1298–1303 (2007)
3. He, L., Zhao, Z.M., Deng, X.P., et al.: Resistance selection of Tetranychus cinnabarinus to three acaricides and its management strategy. Scientia Agricultura Sinica 36(4), 403–408 (2003)
4. He, L., Gao, X.W., Wang, J.J., et al.: Genetic analysis of abamectin resistance in Tetranychus cinnabarinus. Pesticide Biochemistry and Physiology 95(3), 147–151 (2009)
5. Wang, Y.N., Wang, H.X., Shen, Z.J., et al.: Methyl Palmitate, an Acaricidal Compound Occurring in Green Walnut Husks. Journal of Economic Entomology 102(1), 196–202 (2009)
6. Cao, H., Liu, S.Q., Zhao, L.L., et al.: The effects of the extracts from Stellera chamaejasme L. on the biological and enzyme activity of Tetranychus viennensis Zacher. Scientia Silvae Sinicae 39(1), 98–102 (2003)
7. Shi, G.L., Liu, S.Q., Cao, H., et al.: Acaricidal activities of extracts of Stellera chamaejasme against Tetranychus viennensis (Acari: Tetraanychidae). Journal of Economic Entomology 97(6), 1912–1916 (2004)
8. Wang, Y.W., Zhang, G.Z., Xu, H.H., Zhao, S.H.: Separation and identification of extraction of Stellera chamaejasme. Journal of Anhui Agricultural Sciences 32(4), 671–672 (2004)

9. Zhao, G.Z., Xu, H.H., Zhao, S.H., Wang, Y.W.: Separation and identification of insecticidal extracts of Stellera chameajasme. Journal of Hubei Agricultural College 20(1), 19–22 (2000)
10. Busvine, J.R.: Recommended methods for measurement of resistance to pesticides. FAO. Plant Production and Protection 21, 77–90. FAO, Rome (1980)
11. Zhang, J., Lin, Y.Y., Kong, L.Y.: Study on chemical constituents of Artemisia selengensis Turcz. Chinese Traditional and Herbal Drugs 35(9), 979–980 (2004)
12. Niwa, M., Liu, G.Q., Tatematsu, H., Hirata, Y.: Chamaechromone, a Novel Rearranged Biflavonoid from Stellera chamaejasme L. Tetrahedron Letters 25(34), 3735–3738 (1984)
13. Modonova, L.D., Zhapova, T., Bulatova, N.V., Semenov, A.A.: Coumarins from Stellera chamaejasme. Chemistry of Natural Compounds 21(5), 666–667 (1985)
14. Feng, W.J., Fujimoto, Y., Ohkawa, M., Teragawa, T., Xu, J.Y., Yoshida, M., Ikekawa, T.: Piscicidal Constituents of Stellera chamaejasme L. Chinese Journal of Cancer Research 9(2), 89–95 (1997)
15. Jin, C.D., Ronald, G., Micetich, D., Mohsen, D.: Phenylpropanoid glycosides from Stellera chamaejasme. Phytochemistry 50(4), 677–679 (1999)
16. Yu, B.Q., Xu, W.C.: Advances chemical constituents and activity studies on Stellera chamaejasmme L. Agrochemicals 47(12), 863–866 (2008)
17. Liu, Q., Jia, H., Xiao, B., Chen, L., Zhou, B., Hou, T.P.: A new compound against Peries rapae from Stellera chamaejasme. Natural Product Research 22(4), 248–252 (2008)
18. Feng, B.M., Pei, Y.H., Hua, H.M.: Chemical constituents of Stellera chamaejasme L. Journal of Chinese Pharmaceutical Sciences 10(2), 65–66 (2001)
19. Liang, R.: Study on Coumarin Constituents from Stellera Chamaejasme L. Northwest Sci-Tech University of Agriculture and Forestry, Shanxi (2005)
20. Zhang, Y.Q.: Studies on acaricidal action mechanism and bio-guided isolation of bioactive substance from Artemisia Annua L. Southwest University, Chongqing (2008)
21. Wei, L.J., Zhou, J.P., Dai, Y.: Progress in the study of natural product scopoletin. Strait Pharmaceutical Journal 21(4), 10–13 (2009)

Effects of Inula britannica Extracts on Biological Activities against Tetranychus cinnabarinus and Several Enzyme Systems in Tetranychus cinnabarinus

Lan-qing Ma, Dan-dan Duan, You-nian Wang,
Yu-bo Liu, and Guang-lu Shi*

Key Laboratory of Urban Agriculture (North) of Ministry of Agriculture, P.R. China
Beijing University of Agriculture, Beijing, China
glshi@126.com

Abstract. Acaricidal activities of the extracts from Inula britannica (I. britannica) against Tetranychus cinnabarinus (T. cinnabarinus) and several enzyme systems in T. cinnabarinus treated with I. Britannica extracts were evaluated under laboratory conditions. It was found that crude extracts from I. britannica with petroleum ether exhibited high acaricidal activities against T. cinnabarinus, and the corrected mortality after treatment for 24 h was 92.05 % at the concentration of 2 mg ml-1. After a liquid-liquid partition from petroleum ether crude extracts with methanol, the resulting petroleum ether extracts were separated into 38 fractions by column chromatography, and further tests for their acaricidal activities were conducted. Fraction 33, the most major component of the resulting extracts, was found to possess the strongest acaricidal activity against T. cinnabarinus in all 38 fractions, and its corrected mortality against T. cinnabarinus was 90.12 % after 24 h. Moreover, GC-MS analysis results determined that chemical composition of fraction 33 was ethyl palmitate. Laboratory bioassay results indicated that the corrected mortality of ethyl palmitate against T. cinnabarinus after treatment for 24 h was 90.61 %, and the mean lethal concentration (LC50) was 1.255 ± 0.167 mg ml-1. In order to determine the mechanism of the toxic effect of ethyl palmitate on T. cinnabarinus, several kinds of important enzyme systems including glutathione S-transferase (GSTs), acetylcholinesterase (AChE) and Na+-adenosine triphosphatase (Na+-ATPase) as well as total protein content in T. cinnabarinus were tested by the colorimetric method. The experimental results showed that after treatment with ethyl palmitate, total protein content in T. cinnabarinus obviously increased, and the activities of GSTs and AChE in T. cinnabarinus were strongly induced, while the activities of Na+-ATPase in T. cinnabarinus were restrained. Been restrained of Na+-ATPase could cause the transmit block of nerve, and eventually result in the death of the mite. These results indicated that Inula britannica extracts possessed significantly high acaricidal activity.

Ketwords: Ethyl palmitate, Tetranychus cinnabarinus, glutathione S-transferase, acetylcholinesterase, Na+ -adenosine triphosphatase, total protein content.

* Corresponding author.

E. Zhu and S. Sambath (Eds.): Information Tech. and Agricultural Eng., AISC 134, pp. 673–682.
springerlink.com © Springer-Verlag Berlin Heidelberg 2012

1 Introduction

The phytophagous mite is an important pest species that is badly endangering the agricultural production. The prevent and control cost of miticide application in a variety of crops and plants such as citrus, apples, pears, peaches, cotton and vegetables, as well as wheat and teas, is more than 9 billion yuan per year in China (Wang Younian *et al*., 2007). *T. cinnabarinus* population is especially major pest that may attack 146 species within 43 families of plants (grains, cottons, oils, forests, fruit trees, *etc*) (Li Lianchang *et al*., 1992, Wu Junxiang *et al*., 2002). Control of this mite relies overwhelmingly on sprays of chemical pesticides for many years. However, the frequent applications of pesticides may not only kill their natural enemies and other beneficial organisms but also result in high resistance in the mite population. In order to reduce harmful side-effects of chemical pesticides on public health and the environment, effective and safe agents for the mite control are needed. Plants extracts or their constituents have been suggested as an alternative source to currently mite-control agents because some are selective to control mite species, often biodegrade to non-toxic products and have relatively harmful effects on non-target organisms and the environment (Kim *et al*., 2007). Therefore, the development of new botanical miticides based on certain active ingredients of plant extracts against the phytophagous mite is a frontier research area in the world. Sertkaya *et al*. evaluated the acaricidal activities of essential oils obtained from medicinal plants such as oregano, thyme, lavender and mint against the adults of *T. cinnabarinus* (Sertkaya *et al*., 2010). Wang *et al*. found that petroleum ether extracts from leaves of *Juglans regia* had strongly acaricidal activities against *T. cinnabarinus* (Wang *et al*., 2007). Shi *et al*. studied acaricidal activities of crude extracts with three solvents (petroleum ether, chloroform, and methanol) from *Kochia scoparia* against *Tetranychus urticae* Koch, and found that extracts with chloroform resulted in the highest mite mortality (78.86%) (Shi *et al*., 2006). These results indicated that active ingredients with significant acaricidal activity against the pest mites might be obtained from plants extracts, and could lead to the development of safe and high effective botanical a miticides.

In the course of screening natural products extracts for the mite control, we found that petroleum ether extracts from *I. britannica* flowers showed significant acaricidal activity against *T. cinnabarinus*. *I. britannica*, a well known traditional herbal medicine, is widely distributed in China, Korea and Japan. The flowers of *I. britannica* have been used for the treatment of digestive disorders, bronchitis, and inflammation (Kim *et al*., 2002). It has been reported that crude extracts from *I. britannica* with petroleum ether exhibit high acaricidal activity against *T. cinnabarinus* (Duan *et al*., 2009). However, the effective components of the crude extracts have not been identified, and their effects on the biological activity of *T. cinnabarinus* have not been studied. The aim of this study was to determine acaricidal activity of *I. britannica* extracts and their active components against *T. cinnabarinus* in a bioassay under laboratory conditions, specifically, to examine their effects on several enzyme systems in *T. cinnabarinus* and try to elucidate the mechanism of the toxic effect. It would be beneficial to develop new classes of safe and effective botanical miticides.

2 Materials and Methods

2.1 Materials

The dried flowers of *I. britannica* were crushed with a high-speed disintegrator, filtered through a 40 mesh sieve and then stored in the refrigerator for use.

T. cinnabarinus breeding indoor under artificial climate was considered relatively susceptible strain. Indoor breeding conditions: temperature of 25 ± 1℃, relative humidity (RH) of 50 ± 10 %, 18 h of light, 6 h in darkness. An experimental *T. cinnabarinus* colony was maintained on small (with six leaves) seedlings of bean (*Vigna unguiculata*) plants in the nutritive bowl (10 cm tall and 10 cm diameter) at 27 ± 2℃, 60 % RH, and a 16: 8 h L: D photoperiod.

2.2 Methods

Extraction and Isolation of Active Components of I. Britannica. An accurately weighed amount of I. britannicaa powder (15 kg) was transferred to a wide-necked bottle, soaked and extracted with five times volume of petroleum ether for three times (each for 3 - 5 days) at room temperature. All leaching solution after vacuum concentration were combined and weighed.

The dried crude extract was suspended in ten times amount of petroleum ether and then further extracted with methanol for three times in the separating funnel. After concentration of the combined petroleum ether extracts under reduced pressure, the resulting extract was accurately weighed amount of 7 g, and then chromatographed on a medium-pressure column, eluting with a petroleum ether-chloroform (10: 0, 9: 1, 8: 2, 7: 3, 6: 4, 5: 5, 4: 6, 3: 7, 2: 8, 1: 9, 0: 10) gradient solvent system. After that, the elution fractions were separated by thin layer chromatography, and the resulting fractions were combined according to the same component and then stored for test.

The analysis of acaricidal activity component was performed using GC-MS according to Zha Jianpeng's method (Zha Jianpeng *et al.*, 2005).

Toxicity tests. The standardized FAO slide-dip method (FAO, 1980) with a little modification, the direct-dip method, was used to test the acaricidal activity of petroleum ether extracts from I. britannica against T. cinnabarinus. The distilled water containing 1 % (v/v) Tween-80 was used as the control group. All treatments were replicated three times. The corrected mortality would be determined by Abbort's formula (Abbort, 1987).

2.3 Determination of Enzyme Activity

Preparation of Enzyme Solution. The adult mites were treated with ethyl palmitate (2 mg ml^{-1}) by applying FAO slide-dip method (FAO, 1980). After treatment for a period of time (4, 8, 12, 16, 20 and 24 h), 200 adult mites were homogenized in 0.25 ml physiological saline on ice, followed by centrifugation at 10000 r/min for 15 min at 4 ℃. The supernatant was place on ice for testing.

Determination of GSTs Activity. GSTs activity was measured according to GSTs test kit method (Nanjing Jiancheng). Enzyme activity is expressed as μmol min^{-1} per mg protein, namely, one unit of GSTs activity is the amount of enzyme catalyzing the

conjugation of 1 μmol substrate (glutathione) per min at 37 ℃. The absorbance was recorded at 412 nm. The experiments were replicated three times, and the OD average value was obtained from the three repeated data.

Determination of AChE Activity. AChE activity was measured according to He Yuxian's method (He Yuxian et al., 2003), using acetylthiocholine (Asch) iodide as the substrate, 5, 5'-dithiobis-(2-nitrobenzoic acid (DTNB) as the color developing agent, as well as eserine as the inhibitor in a standard assay. The reaction was incubated at 27 ℃ for 15 min, and then terminated by addition of 0.3 ml of 1 mmol l^{-1} eserine. One unit of enzyme activity is defined as the amount of the AChE that catalyzes the hydrolysis of 1μmol Asch/min per mg protein under standard conditions. The absorbance was recorded at 412 nm. The experiments were replicated three times, and the OD average value was obtained from the three repeated data.

Determination of Na^+-ATPase Activity. Na^+-ATPase activity was measured according to Na^+-ATPase test kit method (Nanjing Jiancheng). One unit of enzyme activity is the amount of inorganic phosphate (P_i) liberated by the hydrolysis of ATP, and is expressed as μmol P_i per mg protein per hour. The absorbance was recorded at 636 nm. The experiments were replicated three times, and the OD average value was obtained from the three repeated data.

3 Results

3.1 Aacaricidal Activity of Crude Extracts from I. Britannica against T. cinnabarinus

Mortality for *T. cinnabarinus* treated with petroleum ether crude extracts from *I.britannica* was shown in Table 1. As seen in Table 1, the extraction rate of crude extracts (1.56%) was comparatively low, however, the crude extracts exhibited high acaricidal activities against *T. cinnabarinus*, and the corrected mortality after treatment for 24 h was 92.05% at the concentration of 2 mg ml^{-1}.

3.2 Isolation of Effective Active Components and Their Acaricidal Activity against T. cinnabarinus

The resulting extracts were separated by column chromatography and thin layer chromatography, to give 38 fractions, and further tests for acaricidal activities of these fractions were conducted. As shown in Table 1, fraction 33, the most major component of the resulting extracts, was found to possess the strongest acaricidal activity against *T. cinnabarinus* in all 38 fractions, and its corrected mortality was 90.12 % after 24 h, but the extraction rate of fraction 33 is merely 2.65 %.

The chemical composition of fraction 33 was further identified by GC-MS. The results of total ion current analysis of fraction 33 were shown in Fig.1. Based on GS-MS analysis results, the major component of fraction 33 was identified as ethyl palmitate, which had high match (> 90%) with its standard mass spectral data. Further bioassay results showed that the corrected mortality of ethyl palmitate against T. cinnabarinus after treatment for 24 h was 90.61 %, but its extraction rate (1.67 %) was also very low (Table 1).

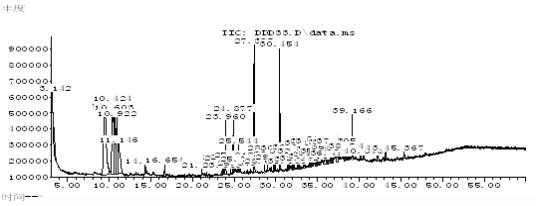

Fig. 1. Total ion current analysis of fraction 33

Table 1. Acaricidal activities of different components separated from *I. britannicaa* extracts against *T. cinnabarinus*

***Inula britannicaa* extracts (2 mg ml^{-1})**	**Extraction percent (%) [a]**	**Mortality (%) [a]**
Petroleum ether extracts	1.56 ± 0.09	92.05 ± 1.4250
Fraction 33	2.65 ± 0.32	90.12 ± 3.934
Ethyl palmitate	1.67 ± 0.03	90.61 ± 2.23

[a] Values are mean ± S.E. for three repeated data.

In addition, in order to further determine the acaricidal activity of ethyl palmitate, the contract acaricidal virulence regression analysis was performed in this study (Table 2). As shown in Table 1, at the concentration of 2 mg ml^{-1}, the mean lethal 2 concentration (LC_{50}) of ethyl palmitate against female adult mite was 1.255 ± 0.167 mg ml^{-1}, and its 95 % confidence limit was (1.468 - 2.204) mg ml^{-1}. These results further confirmed that the effective active component of petroleum ether extracts from *I. britannica* was ethyl palmitate, which possessed significantly strong acaricidal activity against *T. cinnabarinus* adult mites.

Table 2. Toxicity analysis of ethyl palmitate against female adult mites

T. cinnabarinus	**Toxicity regression equation**	**Correlation coefficient**	**LC_{50} (mg ml^{-1})**	**95% confidence interval (mg ml^{-1})**
Female adult mites	Y=4.507 + 1.934x	0.912	1.255 ± 0.167	1.468

3.3 Effect of Ethyl Palmitate on Total Protein Content in T. cinnabarinus

In order to elaborate the effect of ethyl palmitate on total protein content in *T. cinnabarinus*, specific activity in ethyl palmitate-treated group and control group was compared (Fig. 2). The plots in Fig. 2 showed that total protein content in *T. cinnabarinus* for the treated group and the control group varied with time with a similar overall tendency, firstly increasing after treatment from 4 h to 8 h and then decreasing. As a whole, specific activity in the treated group was higher than that in the control group. However, it should be noted that specific activity of *T. cinnabarinus* treated for 24 h was lower than that in the control group. A possible explanation for the lower content was based on the death of treated group, which might result in the acute decrease of total protein content.

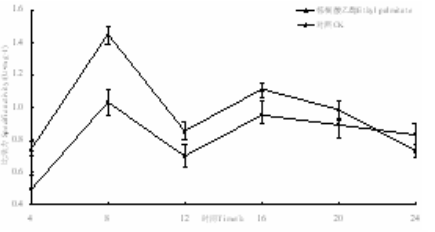

Fig. 2. Effect of ethyl palmitate on total protein content in *T. cinnabarinus*

3.4 Effect of Ethyl Palmitate on GSTs Activity in T. cinnabarinus

In order to elaborate the effect of ethyl palmitate on GSTs activity in *T. cinnabarinus*, specific activity in ethyl palmitate-treated group and control group was compared (Fig. 3). As seen in Fig. 3, GSTs activity for the treated group and the control group varied with time with a similar overall tendency. GSTs activity at first slightly decreased after treatment from 4 h to 8 h, and then rapidly increased until 16 h. After treatment for 20 h, specific activity was found to be basically steady in the treated group, as well as slightly increase in the control group. GSTs activity in both treated group and the control group exhibited a peal vale after treatment for 16 h, and specific activity in the treated group and in the control group was 87.03 U mg^{-1} and 71.14 U mg^{-1}, respectively. As a whole, specific activity in the treated group was much higher than that in the control group, especially, GSTs activity in *T. cinnabarinus* treated for 4 h and 20 h was 1.8 and 1.9 times higher than that in the control group. Hence, it was apparent that GSTs activity in *T. cinnabarinus* was significantly promoted by induction of ethyl palmitate.

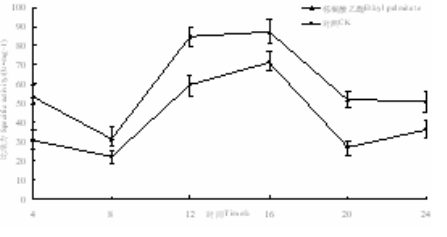

Fig. 3. Effect of ethyl palmitate on GSTs activity in *T. cinnabarinus*

3.5 Effect of Ethyl Palmitate on AChE Activity in T. cinnabarinus

In order to elaborate the effect of ethyl palmitate on AChE activity in *T. cinnabarinus*, specific activity in ethyl palmitate-treated group and control group was compared (Fig. 4). As shown in Fig. 4, AChE activity for the treated group and the control group varied with time with a similar overall tendency, significantly decreasing after treatment from 4 h to 8 h and slightly increasing after 16 h. As a whole, specific activity in the treated group was higher than that in the control group, especially after

treatment from 4 h to 8 h. It should be noted that AChE activity in the ethyl palmitate-treated group after treatment for 4 h was 5.7 times higher than that in the control group. Therefore, AChE activity in *T. cinnabarinus* was markedly promoted by induction of ethyl palmitate after treatment from 4 h to 8 h.

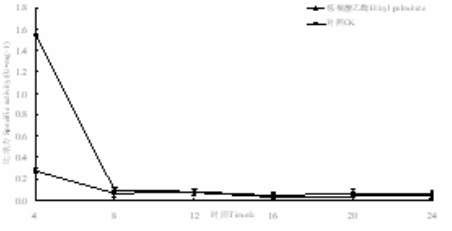

Fig. 4. Effect of ethyl palmitate on AChE activity in *T. cinnabarinus*

3.6 Effect of Ethyl Palmitate on Na+-atpase Activity in T. cinnabarinus

In order to elaborate the effect of ethyl palmitate on Na^+-ATPase activity in *T. cinnabarinus*, specific activity in ethyl palmitate-treated group and control group was compared (Fig. 5). As seen in Fig. 5, Na^+-ATPase activity for the treated group and the control group varied with time with a similar overall tendency, acutely decreasing after treatment from 4 h to 8 h. However, Na^+-ATPase activity in the control group exhibited a peal vale after treatment for 16 h, and specific activity in the control group (3.14 U mg^{-1}) was 1.9 times higher than that in the treated group. Besides, it should be noted that specific activity in the treated group was obviously lower than that in the control group. These results indicated that Na^+-ATPase activity in ethyl palmitate-treated group was markedly inhibited.

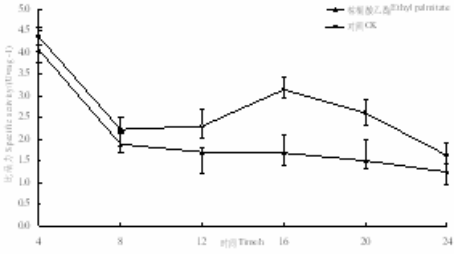

Fig. 5. Effect of ethyl palmitate on Na^+-ATPase activity in *T. cinnabarinus*

4 Discussion

I. britannica is a traditional Chinese medicinal herb that contains a variety of sesquiterpenes, flavonoids and steroids (Bai *et al*., 2005, 2006; Park *et al*., 2000; Kim *et al*., 2002). The pharmacological studies on *I. britannica* extracts mostly focused on

their diversified effects, such as bactericidal, autioxidative and cytotoxic in recent years (Ding *et al*., 2005; Bai *et al*., 2005; Park *et al*., 1998). However, the effects of effective components of *I. britannica* extracts on the biological activities of *T. cinnabarinus* have not been studied before.

The present study for the first time found that ethyl palmitate possessed the strongest acaricidal activities against *T. cinnabarinus* in all 38 fractions of petroleum ether extracts from *I. britannica*, and its extraction rate was 1.67%. Ethyl palmitate as an agent has gained some applications in the domains of biology and medicine. Rothwell *et al*. reported that reticuloendothelial system in the rabbits was inhibited by the intravenous administration of ethyl palmitate for the survival and efficacy of human platelets in a rabbit model (Rothwell *et al*., 1998, 2000). Pillai *et al*. revealed that ethyl palmitate could be used as a macrophage cytotoxin, and which was found to have toxic effect on *Plasmodium berghei* in macrophage of mice in a certain range of concentration (Pillai *et al*., 1997). At present, there is no reference available to evaluate the acaricidal activity of ethyl palmitate against *T. cinnabarinus* and its effect on several enzyme systems in *T. cinnabarinus*.

Laboratory bioassay results indicated that, at the concentration of 2 mg ml^{-1}, the corrected mortality of ethyl palmitate against *T. cinnabarinus* after treatment for 24 h was 90.61 %, and the mean lethal concentration (LC_{50}) was 1.255 ± 0.167 mg ml^{-1}. It was apparent that ethyl palmitate possessed significantly strong acaricidal activity against *T. cinnabarinus* adult mites. Further studies on the effects of ethyl palmitate on several enzyme systems in *T. cinnabarinus* were performed to try to elucidate the mechanism of the toxic effect.

GSTs, a family of detoxification enzymes in mites, may detoxify xenobiotics by catalyzing the conjugation of xenobiotic compounds having electrophilic centers with endogenous reduced glutathione. The conjugation products are rendered less toxic and become more water soluble so that they can be easily excreted from cells after further metabolism (Olsen *et al*., 2001). Thus, the enhancement of GSTs activity may serve as a sensitive biomarker of the detoxification and metabolism functions for the test mites. AChE has a major role in hydrolyzing the synaptic acetylcholine to maintain normal nerve function. Inhibition of AChE may lead to an accumulation of acetylcholine to disrupt synaptic neurotransmission, and an excessive stimulation at the nerve synapses eventually result in death of the insect. At present, the acute toxic effects of most miticides are based on interfering with neurotransmission (Mark *et al*., 1994). ATPase is an important protease present in the plasma membrane of histiocyte and organelle in organism, and plays an important role in substance transport, energy transformation and message transmission (Wang Jingyan *et al*., 1999). Na^+-ATPase as a ubiquitous crucial transport membrane enzyme, is responsible for maintaining cellular homeostasis of the sodium ion, the sodium ion gradient across the cell membrane, as well as the excitement and conduction of nerve cells (Liu Suyuan *et al*., 1999).

The experimental results showed that GSTs activity in *T. cinnabarinus* treated with ethyl palmitate was significantly promoted, and AChE activity in *T. cinnabarinus* was markedly promoted by induction of ethyl palmitate after treatment from 4 h to 8 h. It may be due to GSTs is a family of detoxification enzymes in mites. After ethyl palmitate entering into the organism, GSTs activity was promoted, and consequently metabolism function was enhanced to ensure normal physiological activities in

organism. However, Na^+-ATPase activity was markedly inhibited by ethyl palmitate, and it might destroy the balance of Na^+ which existed both in and out of the cell, influence the transmit and excitement of neuron, cause the transmit block of nerve, and eventually result in the death of the mite.

Acknowledgements. The work was financially supported by the National Natural Science Foundation of China (30872029), the Key Natural Science Foundation of Beijing Municipality (6071001), the Natural Science Foundation of Beijing Municipality (6092007), the Key Foundation of Beijing Municipal Education Committee (KZ201010020016), and Funding Project for Academic Human Resources Development in Institutions of Higher Learning Under the Jurisdiction of Beijing Municipality (PHR20090516, PHR200906134).

References

1. Shi, G.-L., Zheng, W.-Y., Dang, Z.-P., Li, L.-C.: Fruit pests. China Agriculture Press, Beijing (1994)
2. Li, L., Li, L., Fan, Y., et al.: Chinese jujube tree pests. China Agriculture Press, Beijing (1992)
3. Wu, J.-X., Yuan, G.-H., Shi, S.-S.: Agricultural Entomology. China Agriculture Press, Beijing (2002)
4. Duan, D.-D., Wang, Y.-N., Yang, A.-Z., et al.: Herbal extracts on Tetranychus cinnabarinus biological activity. Chinese Agricultural Science Bulletin 25(21), 285–288 (2009)
5. Zha, J., Fu, Y., Wu, Y., et al.: Essential oil from *Inula britannica* L. GC / MS analysis. Chinese Herbal Medicines 28(6), 466–468 (2005)
6. Liu, Y.-P.: Acaricidal active substances of Eupatorium. Sichuan University, Chengdu (2004)
7. Wang, Y.-S., Feng, C., et al.: Insecticide-treated sugar beet *armyworm larvae* on enzyme activity. Jiangxi Agricultural University 25(6), 896–899 (2003)
8. Ding, H., Li, G., Feng, J.-T., et al.: *Inula britannica* sterilization Isolation and identification of active ingredients. Northwest A & F University (Natural Science) 33(3), 90–94 (2005)
9. Wang, J., Zhu, S., Xu, C.: Biochemistry, pp. 32–34. Higher Education Press, Beijing (1999)
10. Liu, S.Y., Sun, L.G., Xing, W., et al.: The effect of chronic lead exposure on hippocampal intraneuronal Ca^{2+} and activity of Ca^{2+}-ATPase in rats. Journal of Health Toxicology 13, 16–17 (1999)
11. Kim, S.I., Na, Y.E., Yi, J.H., et al.: Contact and fumigant toxicity of oriental medicinal plant extracts against Dermanyssus gallinae (Acari: Dermanyssidae). Veterinary Parasitology 145(3-4), 377–382 (2007)
12. Sertkaya, E., Kaya, K., Soner, S.: Acaricidal activities of the essential oils from several medicinal plants against the carmine spider mite (*Tetranychus cinnabarinus* Boisd.) (Acarina: Tetranychidae). Industrial Crops and Products 31, 107–112 (2010)
13. Wang, Y., Shi, G., Zhao, L., et al.: Acaricidal activity of *juglans regia* leaf extracts on *Tetranychus viennensis* and *Tetranychus cinnabarinus* (Acari: Tetranychidae). Journal of Economic Entomology 100(4), 1298–1303 (2007)

14. Shi, G., Zhao, L., Liu, S., et al.: Acaricidal Activities of Extracts of *Kochia scoparia* against *Tetranychus urticae*, *Tetranychus cinnabarinus*, and *Tetranychus viennensis* (Acari: Tetranychidae). Journal of Economic Entomology 99(3), 858–863 (2006)
15. Kim, S.R., Park, M.J., Lee, M.K., et al.: Flavonoids of Inula britannica protect cultured cortical cells from necrotic cell death induced by glutamate. Free Radical Biology & Medicine 32(7), 596–604 (2002)
16. Abbort, W.S.: A method of computing the effectiveness of an insecticide. J. Am. Mosq. Control Assoc. 3, 302–303 (1987)
17. Bai, N.S., Lai, C.S., He, K., Zhou, Z., et al.: Sesquiterpene lactones from Inula britannica and their cytotoxic and apoptotic effects on human cancer cell lines. J. Nat. Prod. 69(4), 531–535 (2006)
18. Park, E.J., Kim, Y., Kim, J.: Acylated flavonol glycosides from the flower of Inula Britannica. J. Nat. Prod. 63(1), 34–36 (2000)
19. Bai, N.S., Zhou, Z., Zhu, N.Q., Zhang, L., et al.: Antioxidative flavonoids from the flower of *Inula britannica*. Journal of Food Lipids 12, 141–149 (2005)
20. Park, E.J., Kim, J.: Cytotoxic sesquiterpene lactones from Inula britannica. Planta Medica 64, 752–754 (1998)
21. Rothwell, S.W., Maglasang, P., Krishnamurti, C.: Survival of fresh human platelets in a rabbit model as traced by flow cytometry. Transfusion 38, 550–556 (1998)
22. Rothwell, S.W., Maglasang, P., Reid, T.J., et al.: Correlation of in vivo and in vitro functions of fresh and stored human platelets. Transfusion 40, 988–993 (2000)
23. Pillai, C.R., Devi, C.U.: CAB Abstracts. Journal of Communicable Diseases 29(4), 355–359 (1997)
24. Olsen, T., Ellerbeck, L., Fisher, T., et al.: et al. Crane M. Environmental Toxicology and Chemistry 20(8), 1725–1732 (2001)
25. Dekeyser, M.A., Downer, R.G.H.: Biochemical and physiological targets for miticides. Pesticide Science (40), 85–101 (1994)

Antifungal Activity of Extracts of *Stellera chamaejasme* against *Botrytis cinerea*

Lei Zhao, You-nian Wang, Juan Du, Chun-ya Bu, Lan-qing Ma, Yu-bo Liu, and Guang-lu Shi*

Key Laboratory of Urban Agriculture (North) of Ministry of Agriculture, P.R. China
Beijing University of Agriculture, Beijing, China
glshi@126.com

Abstract. The antifungal activity of the extracts from Stellera chamaejasme against Botrytis cinerea was investigated in our work. The active components of Stellera chamaejasme extraction were primary analyzed by bioactive tracking method followed by separation of the highly active components by column chromatography, and then the structure of the final extract was identified by liquid chromatography-mass spectrometry (LC-MS) and nuclear magnetic resonance (NMR). The results showed that the main antifungal bioactive compound in the eluotropic component 3 was umbelliferone. And a positive correlation between umbelliferone concentration and antifungal activity was observed. The minimal inhibitory concentration (MIC) of umbelliferone was 1.52 mg ml-1. Depending on the analysis of ultrastructure by scanning electron microscope (SEM), it was found that the morphology of Botrytis cinerea spore and mycelium were obviously destroyed by umbelliferone existing in eluotropic component 3.

Keywords: Stellera chamaejasme, Umbelliferone, LC-MS, Botrytis cinerea, Antifungal activity.

1 Introduction

Plant pathogenic fungi bring on major economic damages in agriculture in China and other areas of the world (Gilbert *et al*, 2006; Partida-Martinez and Hertweck, 2005). Chemical pesticides play a very important role in preventing and controlling crop diseases and pests as well as maintaining high yield in agriculture and forestry, and the fungicides market has been generally dominated since the 1970s by several chemical classes of amides, methoxyacrylates, pyrimidinamines, triazoles and so on (Russell, 2005). However, long term illegitimate application of pesticides has elicited a series of severe problems such as high pesticide residues, notably environmental contamination and the development of multi resistant strains which are insidious dangers to people's health (McGrath, 2001). Thus, developing new bio pesticides which are highly active against resistant strains, safe to non-target organisms, and environmentally compatible has become a tendency in pesticide industry in the future (Liu *et al*. 2005).

* Corresponding author.

E. Zhu and S. Sambath (Eds.): Information Tech. and Agricultural Eng., AISC 134, pp. 683–692.
springerlink.com © Springer-Verlag Berlin Heidelberg 2012

Botanical fungicides are already known to play an important role in control plant pathogenic fungi (Abbassy *et al*, 2007; Cho *et al*, 2006 and 2007). Compared with traditional synthetic pesticides, botanical fungicides are generally considered broad-spectrum and safe for the environment because the array of compounds they contain quickly biodegrade in the soil (Lu et al, 2007).

Stellera chamaejasme L., also named *Chamaejasmine gelsemium* belongs to *Stellera* L. Thymelaeaceae. is widely distributed in mountains and subalpine grasslands in northern and western China, which are characterized by high topography, inclement climate and complicated environment. *Stellera chamaejasme* is a kind of perennate herb, which can regenerate, endure drought and cold, yield bountiful seeds and grow luxuriantly. It is medicinally moderate and bitter in taste and has a wide range of applications as a famous ancient medicine literature such as sterilization, insecticidal, removing obstruction and water retention, and alleviating pain. To date, many bio pesticides with high pesticidal activities, had been found from *Stellera chamaejasme* and some of them displayed promising antifungal activity against bacilli, cocci and fungi *in vitro* (Liu 1997:Zhang *et al*. 2000). Whereas, there is little research has been reported on its antifungal activity against plant pathogens. Therefore, it is necessary to carry out systemic research on this work.

In the present study, firstly, the efficacy of different *Stellera chamaejasme* extract against mycelium growth of *Botrytis cinerea* was tested, subsequently, the structure of the bioactive composition in the methanol extract was identify by LC-MS and NMR. Finally, the ultrastructure of *Botrytis cinerea* spore and mycelium were observed by SEM after treated by methanol *Stellera chamaejasme* extract. In this work, we found the ways of the action of *Stellera chamaejasme* extract against *Botrytis cinerea*. This work will provide new evidence for the development of botanical fungicides.

2 Materials and Methods

2.1 Materials

Strain of *Botrytis cinerea* was supplied by the Lab for Plant Protection of Beijing University of Agriculture. *Stellera chamaejasme* was collected from Golden sands, Shuozhou, Shanxi Province, China.

2.2 Extraction and Isolation

The roots of *Stellera chamaejasme* were washed by tap water, ventilated for cooling and drying at 25 ℃ followed by baking in a drier at 40 – 45 ℃. The dried roots of *Stellera chamaejasme* were ground and screened through 0.3 mm sieve for further use. One milligram powder was soaked by 5 mg methanol, petroleum ether, chloroform and dichloromethane, respectively, for 3 – 5 days at room temperature and filtered. The filtrate was condensed to solid by reduced pressure and pooled after 3 repetitions.

The extracts were dissolved by corresponding solvents, and then were prepared to emulsions at the concentration of 2 mg ml- by distilled water containing 2 - 3 drops of

Tweenum-80. These emulsions were used for the determination of antifungal activity as described below. The results showed that the *Stellera chamaejasme* methanol extract displayed the strongest biological activity. Thereby, we did further isolation and purification analysis on the methanol extract. The crude extraction was separated by liquid-liquid distribution method. Ten gram methanol extract was dissolved by 100 g methanol and the crude extract was extracted by petroleum ether for 3 times. The resultant filtrates were pooled together followed by condensing to solid by reduced pressure and weighed.

Five gram effective fraction as described above was collected as sample loading material. Middle pressure column chromatography was performed for isolation and purification. Totally, 453 eluotropic components were obtained, relaying on gradient elution with methanol, methanol-chloroform mixture (9: 1, 8: 2, 7.5: 2.5, 6: 4, 5: 5 and 3: 7) and chloroform, respectively. Then, the collected flows were dealt with thin-layer chromatography (TLC) followed by the chromogenic reactions took place in iodine-cylinder, and then the identical components obtained were pooled. Finally, 10 eluotropic components were collected, condensed by reduced pressure, and their biological activity was determined.

2.3 Determination of Antifungal Activity of the Extracts

According to the methods of Wu (2002), potato dextrose agar (PDA) culture medium containing the 10 eluotropic components at the concentration of 2 m ml^{-1}, respectively, was used as treatment, while PDA culture medium with only equimolar solvent was used as control treatment. A 5 mm diameter fungus disk, collected from the edge of the active colony was inoculated on the center of the PDA plate. All the treatments were propagated in the thermostat at 28 ℃ in triplicates. The colony morphology was inspected regularly and the colony diameter was measured by crossing method to calculate the inhibitory rate:

Inhibitory rate = [(net increment of CK diameter - net increment of Treatment diameter)/net increment of CK diameter] × 100%

2.4 Analysis of the Structure of the Most Active Eluotropic Component

The structure of the most bioactive component was analyzed by liquid chromatography-mass spectrometry (VARIAN 2200, USA). Chromatographic column: C18 column (50 × 4.65um), mobile phase: methanol: water solution (70: 30, *V*: *V*), flow speed: 10 ul s^{-1}, sampling concentration: 2 μg, column temperature: 20 ℃. JNM ECA 600 NMR was employed for further determination. Solvent: CDC_{l3}, internal standard: TMS.

2.5 Determination MIC of the Extract

PDA mediums containing umbelliferone with five different concentrations (8, 4, 2, 1 and 0.5 mg ml^{-1}) were prepared using double dilution methods. Each of them was used to test the inhibitory effect on *Botrytis cinerea* mycelium. Toxicity regression equation and MIC were calculated accordingly.

2.6 SEM Observation

Fresh dishes of *Botrytis cinerea* from PDA medium including control and umbelliferone treatment were taken out 96 h after growth, and these dishes were disposed as follows: fixed by 2 % glutaraldehyde for 2 - 4 h, washed by 0.1 mol l^{-1} PBS saline, fixed by 1 % osmium tetroxide for 1.5 h, washed free of osmium tetroxide by redistilled water, gradient dehydration using ethanol at different concentrations (30, 50, 70, 80 90, 95 and 100 %) for 5-10 min for each gradient, and replaced by isoamyl acetate, dried at the critical point and glued onto the sample holders with conductive adhesive in order for gold spraying using IB-3 arc ion plating. Finally, the samples were observed and photographed using SEM (Xie *et al*. 2005, Li et al. 2004).

2.7 Data Analysis

Statistical analysis was performed using SPSS 13.0 software. Finney probability analysis method was used to calculate toxicity regression equation and MIC. Analysis of variance and correction of the mortality rate were done using the Duncan's test ($P < 0.05$).

3 Results

3.1 Antifungal Activity of the Extracts of Stellera chamaejasme against Botrytis cinerea

The results (Table. 1) showed that the order of extraction rates of four different solvents of Stellera chamaejasme was methanol (3.15 ± 0.23) % > chloroform (1.65 ± 0.05) % > dichloromethane (1.03 ± 0.33) % > petroleum ether (1.17 ± 0.13) %. Antifungal activity of extracts on *Botrytis cinerea* were always significantly affected by their extraction rates and the inhibitory rate was increased as a consequence of high extraction rate. As described in table 1, methanol extract which shown the highest extraction rate, significantly improved the inhibitory rate up to 61.78 % on *Botrytis cinerea* compared with other 3 extraction methods.

Table 1. Extraction rate of different extracts from *Stellera chamaejasme* and inhibitory rate against *Botrytis cinerea*

Extracts(2mg/mL)	Extraction rate±SE(%)	Inhibitory rate±SE (%)
Methanol	3.15±0.23	61.78±2.46[a]
Chloroform	1.65±0.05	48.33±5.34[b]
Petroleum ether	1.03±0.33	30.12±1.36[c]
Dichloromethane	1.17±0.13	37.84±4.81[c]

Values presented are means at a concentration of 2 mg/ml. Values followed by the same letter are not significant different, $P < 0.05$ (Duncan, SPSS 13.0). The same below.

3.2 Antifungal Activity of Fractions of Stellera chamaejasme against Botrytis cinerea

Since methanol extract exhibited the best inhibitory effect on *Botrytis cinerea*, further isolation and purification was performed using petroleum ether (Table. 2). Methanol displayed the better extract ability (53.16 %) than petroleum ether (46.84 %). Meanwhile, the mortality of methanol extract (57.31 %) was stronger than petroleum ether extract (31.25 %). Evidently, the dominant bioactive components of *Stellera chamaejasme* against *Botrytis cinerea* were existed in methanol extract.

Table 2. Extraction rate of different fractions from *S. chamaejasme* and inhibitory rate against *B. cinerea*

Extracts(mg/mL)	Extraction rate±SE (%)	Inhibitory rate±SE (%)
Methanol	53.16±2.17	57.31±2.03
Petroleumether	46.84±6.56	31.25±2.48

3.3 Column Chromatography Fractions Isolation and Bioactivity Measurement

Ten eluotropic components were obtained depending on the isolation of column chromatography isolation and detection of TLC detection (Table 3). Bioactivity detection of the collected flow of *Stellera chamaejasme* extracts was conducted and the results showed that the third fraction had the strongest antifungal activity against *Botrytis cinerea* with an inhibitory rate up to 69 %.

Table 3. Inhibitory rate of column chromatography isolation fractions against *B. cinerea*

Isolation fraction	Inhibitory rate±SE (%)	Isolation fraction	Inhibitory rate±SE (%)
1	32.31 ± 1.92^{d}	6	23.31 ± 0.91^{ef}
2	25.62 ± 3.64^{e}	7	53.07 ± 1.15^{b}
3	69.53 ± 0.88^{a}	8	31.79 ± 0.68^{d}
4	32.04 ± 0.57^{d}	9	21.02 ± 0.88^{f}
5	45.37 ± 2.07^{c}	10	33.03 ± 0.86^{d}

3.4 Analysis of the Chemical Structure of the Third Fraction

The third fraction of Stellera chamaejasme extracts was detected by TLC and it emitted strong fluorescence when scanned by ultraviolet map. The results suggested that the compound belonged to coumarin. According to the analysis of LC-MS (Fig. 1, 2), MS(m/z): 163, the molecular formula estimated by elemental analysis was C9H6O3, 1H NMR (CDCl3) δ: 10.14(1H, s, OH), 6.19(1H, d, J=9 Hz, H-3), 7.71(1H, d, J=8.8 Hz, H-4), 7.23(1H, d, J=8.3Hz, H-5), 6.96(1H, dd, J=8.5Hz, 2.7Hz, H-6), 6.73(1H, d, J=2.4 Hz, H-8); 13C NMR (CDCl3)δ: 160.2(C-2), 144.8(C-4), 131.1(C-5), 113.2(C-6), 162.7(C-7), 101.9(C-8), 155.9(C-9), 111.8(C-3, C-10). The data above was in accordance with literature (Yu and Yang 1989), thereby the third fraction was preliminarily determined as umbelliferone.

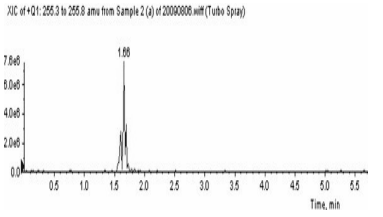

Fig. 1. LC-MS analysis of the third fraction of *S.chamaejasme* extract

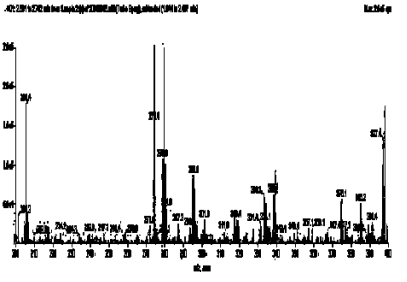

Fig. 2. MS analysis of the third fraction of *S. chamaejasme* extract

3.5 Determination of Antifungal Activity of Umbelliferone

PDA medium with umbelliferone at 5 different concentrations were prepared and their different inhibitory effects against *Botrytis cinerea* were checked (Fig. 3). The colony of control was even, flat and the mycelia were close and many of them yielded spores. Whereas the colony treated with umbelliferone grew slowly and sparsely and the mycelium was short because the growth of peripheral mycelium was inhibited. A positive correlation between umbelliferone concentration and antifungal activity (dose-effect relationship) was observed, and the maximum inhibitory rate 84.79 % was obtained at the highest umbelliferone dosage 8 mg ml^{-1}. A linear fit yielding the equation y = 4.7401+1.4217 x (y, inhibitory rate; x, log of concentration) was observed between the log of fraction concentration and the inhibitory rate, and the MIC was 1.523 mg ml^{-1}.

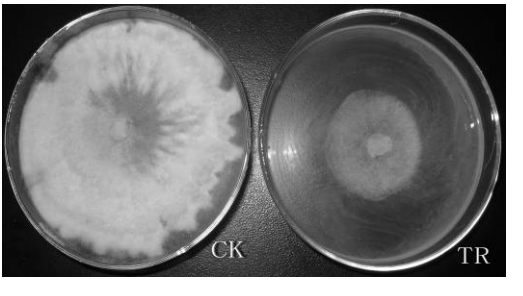

Fig. 3. Inhibitory rate and inhibitory effect of umbelliferone against *B. cinerea*

3.6 SEM Observation of the Effect of Umbelliferone on Botrytis cinerea Ultrastructure

The morphology of Botrytis cinerea treated with umbelliferone changed compared with the control by SEM analysis (Fig. 4). The spores growing on PDA culture medium were transparently lustrous, and the size was consistent, whereas the shape of the spore changed and protuberances occurred if being treated with umbelliferone. In addition, the mycelium on CK culture medium was complete, smooth, plump and exhibited a good state of growth. On the contrary, the mycelium treated with umbelliferone showed rough surface, its content spilled over, and many of the mycelia broke and decomposed.

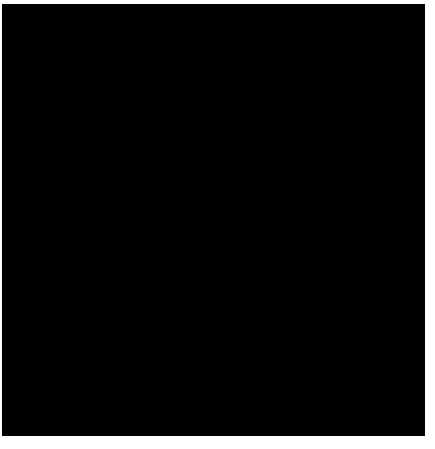

Fig. 4. SEM analysis

4 Discussion

The use of chemical pesticides such as benzimidazole fungicides, dicarboximides fungicides and N-phenylcarbamates, is one of the most effective methods in preventing and controlling gray mold and reducing the loss. But long-term and large-scale application of the pesticides has led to the emergence of new Botrytis cinerea strains with pesticide-resistant ability (Zhang *et al*. 2004, Liu *et al*. 1992). Since 1971 Bollen and Scholten reported that strain of *Botrytis cinerea* infected *Cycalmen persicum* became resistant to benzimidazole fungicides in greenhouse in Holland, others pesticide-resistant strains of *Botrytis cinerea* incited grape, strawberry and tomato were also found in other countries such as America and Italy (He *et al*. 2004). *Botrytis cinerea* strains resistant to fungicides including benzimidazoles were also reported many times in China (Zhou and Ye 1987, Ding *et al*. 2002). Therefore, it is necessary to develop new type drugs to prevent and control *Botrytis cinerea*.

Stellera chamaejasme, as a traditional Chinese medicine was widely used for treatment of various diseases (Ligaa and Tsembel, 2003; Tian *et al*, 2005). The extraction of *Stellera chamaejasme* and the synthesized novel class of fungicides as

extraction of *Stellera chamaejasme* as a lead structure, exhibited satisfied disease control ability in vitro against *Phytophthora capsici*, *Botrytis cinereu*, *Rhizoctonia solan*i and so on (Jin *et al*, 2009). However, some of the compounds with antifungal activity in the extraction were still unknown.

In this study, the antifungal activity of four different solvents-derived extracts of *Stellera chamaejasme* against *Botrytis cinerea* was measured. The results demonstrated that methanol extract displayed the strongest antifungal activity in comparison to petroleum ether, chloroform and dichloromethane. Relying on the separating by liquid-liquid distribution method and detection by TLC, the component in third fraction in methanol extract showed the best disease suppression ability.

In recent years, diterpenoids, coumarin, lignans, flavonoids and others constituents were isolated and purified from the extracts of *Stellera chamaejasme*, and considered to be the interesting antifungal components (Jiang *et al*, 2002; Jin *et al*, 1999; Xu *et al*, 2001). Umbelliferone, a widespread natural product of the coumarin family, was shown to suppress *Penicillium digitatum*, *Penicillium italicum*, *Phytophthora citrophthora*, *Botrytis cinerea* and *Alternaria alternate* in vitro (Afek *et al*, 1999). Depending on the analysis of LC-MS and NMR, our results elucidated the predominant antifungal constituent in the third fraction was umbelliferone which exhibited satisfied disease inhibitory activity on *Botrytis cinerea* in vitro.

Interesting but not surprising, a positive correlation between umbelliferone concentration and antifungal activity was observed. The maximum inhibitory rate 84.5% was obtained at the highest application dosage of umbelliferone at the concentration of 8 mg ml-. The minimal inhibitory concentration (MIC) of umbelliferone was 1.52 mg ml-. Botrytis cinerea mycelium treated with umbelliferone was twisted and deformed, and adhered to each other, the cell wall ruptured and floccule appeared on the surface via the detection of SEM. Those phenomenon demonstrated that umbelliferone spoiled the integrity of the fungus and disturbed the physiology metabolism of *Botrytis cinerea* thus producing the inhibitory effect.

In summary, we have demonstrated that the methanol extract of the *Stellera chamaejasme* displayed the best antifungal activity on *Botrytis cinerea*. The antifungal effect of the methanol extract was associated with their dosage, and a positive correlation was observed between antifungal effect and extract dosage. Umbelliferone was considered to be the key constituent for suppress the growth of *Botrytis cinerea*.

Stellera chamaejasme is a kind of botanical fungicide with great potential exploiting value and wide marketing prospect. The identification of new biological compounds from this plant and exploration of specific pathways of their actions against diseases are the future targets of our research.

Acknowledgements. The work was financially supported by the National Natural Science Foundation of China (30872029), the Key Natural Science Foundation of Beijing Municipality (6071001), the Natural Science Foundation of Beijing Municipality (6092007), the Key Foundation of Beijing Municipal Education Committee (KZ201010020016), and Funding Project for Academic Human Resources Development in Institutions of Higher Learning Under the Jurisdiction of Beijing Municipality (PHR20090516, PHR200906134).

References

1. Abbassy, M.A., Abdelgaleil, S.A.M., Belal, A.S.H., Rasoul, M.A.A.A.: Insecticidal, antifeedantand antifungal activities of wo glucosides isolated from the seeds of Simmondsia chinensis. Indian Crop Prod. 26, 345–350 (2007)
2. Afek, U., Orenstein, J., Carmeli, S., Rodov, V., Joseph, M.B.: Umbelliferone, a phytoalexin associated with resistance of immature Marsh grapefruit to Penicillium digitatum. Phytochemistry 50, 1129–1132 (1999)
3. Cho, J.Y., Choi, G.J., Son, S.W., Jang, K.S., Lim, H.K., Lee, S.O., Sung, S.N., Cho, K.Y., Kim, J.: Isolation and antifungal activity of lignans from Myristica fragrans against various plant pathogenic fungi, Pest. Manag. Sci. 63, 935–940 (2007)
4. Cho, J.Y., Kim, H.Y., Choi, G.J., Jang, K.S., Lim, H.K., Lim, C.H., Cho, K.Y., Kim, J.C.: Dehydro-a-lapachone isolated from Catalpa ovata stems: activity against plant pathogenic fungi, Pest. Manag. Sci. 62, 414–418 (2006)
5. Ding, Z., Liu, F., Mu, L.: Study on Susceptibility of Different Resistance Type of Botrytis Cinerea to Fungicides with Different Mechanism. Chinese Journal of Pesticide Science 3(4), 59–63 (2002)
6. Gilbert, M.J., Thornton, C.R., Gavin, E., Wakley, G.E., Talbot, N.J.: A P-type ATPase required for rice blast disease and induction of host resistance. Nature 440, 535–539 (2006)
7. He, Y.B., Feng, Y.B., Tao, H.: Filtration of Chemic Prevention Medicament of Cucumber Grizzle Mildew. Agriculture & Technology 24(6), 139–141 (2004)
8. Jiang, Z.H., Tanaka, T., Sakamoto, T., Kouno, I., Duan, J.A., Zhou, R.H.: Chem. Pharm. Bull. 50, 137 (2002)
9. Jin, C., Michetich, R.G., Daneshtalab, M.: Phytochemistry 50, 505 (1999)
10. Jin, H., Geng, Y., Yu, Z., Tao, K., Hou, T.: Lead optimization and anti-plant pathogenic fungi activities of daphneolone anaogues from Stellera chamaejasme L. Pesticide Biochemistry and Physiology 93, 133–137 (2009)
11. Ligaa, U., Tsembel, D.: Medicinal plants of Mongolia and their use in traditional medicine. In: Badarch, D., Zilinskas, R.A., Balint, P.J. (eds.) Mongolia Today: Science, Culture, Environment and Development, Routledge Curzon, London, pp. 116–119 (2003)
12. Li, Z.X., Wang, X.H., Shi, D.Y., et al.: Observation of in Vitro Antibacterial Activity of Galla Chinensis Ethanol Extractant Against Staphylococcus Epidermidis and the Examination under SEM and TEM. Chinese Journal of Information on Tratitional Chinese Medicine 11(10), 867–869 (2004)
13. Liu, B., Ye, Z.Y., Liu, J.F.: Study on the Character of Procymidone against Botrytis Cinerea. Acta Phytophylacica Sinica 19(4), 297–301 (1992)
14. Liu, H.Y., Gao, W.W., Fan, Y.: Advances in Research and Development of the Botanical Fungicide. Chinese Agricultural Science Bulletin 21(4), 254–257 (2005)
15. Liu, S.S.: Abstract of Research Article on Traditional Chinese Medicine (1820–1961), p. 552. Science Press, Beijing (1997)
16. Liu, S.S.: Abstract of Research Article on Traditional Chinese Medicine (1820–1961), p. 622. Science Press, Beijing (1997)
17. Lu, T., Chen, L., Hou, T.: Synthesis and structure-actiity study of botanical aphicides 1,5-diphenyl-1-pentanone analogues. Pesticide Biochemistry and Physiology 89, 60–64 (2007)
18. McGrath, M.T.: Fungicide resistance in cucurbit powdery mildew: experiences and challenges. Plant Dis 85, 236–245 (2001)
19. Partida-Martinez, L.P., Hertweck, C.: Pathogenic fungus harbours endosymbiotic bacteria for toxin production. Nature 437, 884–888 (2005)

20. Russell, P.E.: A century of fungicide evolution. J. Agric. Sci. 143, 11–25 (2005)
21. Tian, Q., Li, J., Xie, X., Sun, M., Sang, H., Zhou, C., An, T., Hu, L., Ye, R.D., Wang, M.W.: Stereospecific induction of nuclear factor-kB activation by Isochamaejasmin. Mol. Pharmacol. 68, 1534–1542 (2005)
22. Wu, X.A.: Antibacterial Activity of Extracts of Chinese Herbs against Animal Pathogens Anhui Agricultural University, pp. 18–19 (2002)
23. Xie, J.Y., Dong, G.J., Liu, Z.: Microbial samples of Scanning Electron Microscope Preparation Methods. Journal of Chinese Electron Microscopy Society 437, 975–980 (2005)
24. Xu, Z.H., Qin, G.W., Li, X.Y., Xu, R.S.: Acta Pharm. Sin. 36, 668 (2001)
25. Yu, D.Q., Yang, J.S.: Analytical Chemistry Handbook 5. Chemical Industry Press, Beijing (1989)
26. Zhang, C.Y., Huang, J.P., Wang, R.: Resistance Detection of Botrytis Cinerea Isolate to Procymidone. Journal of Anhui Agricultural Sciences 32(3), 310–311 (2004)
27. Zhang, G.Z., Wang, Y.W., Xu, H.H.: Bioactivities of Extraction of Stellera chamaejasme Against Insects. Journal of Hunan Agricultural University 26(5), 366–367 (2000)
28. Zhang, G.Z., Wang, Y.W., Xu, H.H.: Separation and Identification of Extraction of Stellera chamaejasme. Journal of Anhui Agricultural Sciences 28(5), 623–628 (2000)
29. Zhou, M.G., Ye, Z.Y.: Detection on the Field Resistance of Botrytis Cinerea against Benzimidazole Fungicides in Nanjing SuburbS. Journal of Nanjing Agricultural University 6(2), 53–57 (1987)

Inhibitory Effect and Antifunal Mechanism of Umbelliferone on Plant Pathogenic Fungi

Xue-na Bai[1], Wei Liang[1], Jun Cheng[1], Lan-qing Ma[1], Yu-bo Liu[1], Guang-lu Shi[1], You-nian Wang[1,*], and Ji-cheng Gu[2]

[1] Key Laboratory of Urban Agriculture (North) of Ministry of Agriculture, P.R. China
Beijing University of Agriculture, Beijing, China
[2] Beijing Forestry University, Beijing, China
glshi@126.com

Abstract. Low concentrations of 7-hydroxycoumarin (umbelliferone) were found of antifungal activity towards plant pathogenic fungi using growth rate method. Umbelliferone inhibited mycelia growth in Monilia fructigena, Fusarium moniliforme, Botrytis cinerea and Colletotrichum capsici with the minimal inhibitory concentration (MIC) values of 250, 500, 1000, and 2000 μg mL-1, respectively. The results also showed its minimal fungicide concentration (MFC) values of M. fructigena and F moniliforme were both 1000 μg mL-1. But no MFC values towards B. cinerea and C. capsici were obtained in this study. It is noteworthy that umbelliferone was very active against the spore germination of the four fungi. 100% inhibition of spore germination of M. fructigen and F. moniliforme were observed, when the umbelliferone concentrations were up to 1000 μg mL-1 and 2000 μg mL-1, respectively. The antifungal mechanism of umbelliferone was further investigated using scanning electron microscope (SEM) and transmission electron microscope (TEM). After umbelliferone treatment, the fungal mycelia appeared to deform or adhere. The cell structure of fungal mycelium was destroyed, and the cell contents were spilled. Antifungal mechanism of umbelliferone is probably based on its destruction activity towards pathogenic fungal cellular organs. According to our investigation, umbelliferone has the potential to be useful as a phytogenous pesticide.

Keywords: Umbelliferone, Plant pathogenic fungi, Antifungal activity, Ultrastructure.

1 Introduction

Chemical pesticides play a very important position in modern agricultural fields. They are an effective method for diseases and insect pests controlling. During their use for more than half a century, we have found that chemical pesticides can provide high production, rich production and huge profit in agricultural production. They also showed their bad influences after the long period use and abuse. Resistance,

* Corresponding author.

E. Zhu and S. Sambath (Eds.): Information Tech. and Agricultural Eng., AISC 134, pp. 693–702.
springerlink.com © Springer-Verlag Berlin Heidelberg 2012

resurgence and residue (three R phenomenons) are now great trouble to the food safety of the human beings. Nowadays, the specialists in agricultural pesticides have paid much more attention and emphasis on deficiency of chemical pesticides and devote themselves to green and safe substitutes of them. Biosynthetic pesticides, which have the benefits of high bioactivity, safety to the untargeted organisms, and good compatibility with environment, have become the new trend of the development of the pesticides. Phytogenous pesticides, as an important part of biosynthetic pesticides, have their own developing opportunity due to their unique predominance such as low poisonous, high selective and easily degradable properties (Liu *et al*. 2005).

Umbelliferone (UM), a kind of simple natural phenol compound named 7-hydroxycoumarin, is extracted from several plants, such as Rutaceae and Umbelliferae (Zhang *et al*. 2000; Liu *et al*. 2005; Liu *et al*. 2008)). Previous study demonstrate UM is widely exists in Chinese herbal medicine such as *Stellera chamaejasme* L., *Heracleum*, *Saussurea involucrate*, *Aegle marmelos*, and so on (Zhang *et al*. 2000; Yang *et al*. 1996; DaWa *et al*. 2008; Wang *et al*. 1996). Phenolics were reported to relate with the anti-disease activities of the plants and had strong antibacterial functions (Abram *et al*. 1999; Otake *et al*. 1991; Cambier *et al*. 2001; Tombola *et al*. 2003; Mohamalawar *et al*. 2002). Zhang *et al* (2000) found that UM had a strong insecticide activity to fifth instar larva of *Pieris rapae* Linne. Yang *et al* (2007) reported that UM had a strong inhibitory activity on the proliferation of the human bladder carcinoma E-J cell lines and also showed effective correlation to its concentration. Weber et al carried out a study on the metabolites in vivo of the coumarin and UM (metabolites of coumarin *in vivo*) with antitumor activity. They found that both compounds can inhibit the proliferation of the gastric carcinoma cell, Colon cancer cells (Caco-2), Hepatoma ($HepG^{+}$) and precursor lymphoblastic lymphoma (CCRF CEM). There were some relations between the inhibition and the concentration of the compounds (Weber *et al*. 1998). Some data also showed that UM has lowering blood pressure, antibacterial and antitumor activity (Jiangsu new medical college. 1977; The national medicine administration bureau Chinese Medicine information central station. 1986; Sha. 1984).

At present, the reports of UM were majored on the existence and isolation of UM from the variety of Chinese herbal medicines and inhibitory activities towards insects and antitumor activity. Few reports were on the antifungal activities and their mechanism towards the plant pathogenic fungi. In this study, we take the common plant pathogenic fungi as the test strains, and research the inhibition of UM towards the mycelia growth and the spore germination of plant pathogenic fungi. Further research was to find out the changes of the ultrastructure of the UM-treated pathogenic fungi through the electron microscopes.

2 Materials and Methods

2.1 Materials

Four plant pathogenic fungi *Monilia fructigena*, *Fusarium moniliforme, Botrytis cinerea* and *Colletotrichum capsici* were identified and collected by the Key

Laboratory of Urban Agriculture (North) of Ministry of Agriculture P.R, Beijing University of Agriculture. Umbelliferone was purchased from Sigma-Aldrich. All other chemicals were of reagent grade.

2.2 Preparation for Spore Suspension

Mycelia disks (6 mm in diameter) of the test plant pathogenic fungi were placed in the center of sterile petri dishes (100 mm × 15 mm) containing 20 mL potato dextrose agar (PDA) and incubated in darkness at 28 ℃ for 5-7 d. Spores were collected using distilled water with 0.05 % Tween-80 (*v*/*v*). Cell numbers of spore suspension were adjusted to about 1.0×10^6 - 1.0×10^7 cell/mL using blood cell counting chambers.

2.3 Assay for Antifungal Activity

In the assay for antifungal activity, growth rate method was used. Umbelliferone was dissolved in acetone. Mycelial disks (6 mm in diameter) of the test plant pathogenic fungi were placed in the center of sterile petri dishes (100 mm × 15 mm) containing 20 ml potato dextrose agar with 125, 250, 500, 1000, and 2000 μg mL^{-1} umbelliferone. PDA containing the same volume of distilled water and acetone were used as control 1 (CK) and control 2, respectively. Mycelia growth was determined by measuring the colony diameter using decussating method when the mycelia colonies of control 1 groups were just full in the petri dishes. Each treatment was replicated 3 times and the experiment was repeated twice. The antifungal activity was calculated as % Growth Inhibition = (C − T)/C × 100 %, where C was the mycelia growth of control 1 group and T was the mycelia growth of umbelliferone-treated group. Toxicity regression equations were calculated using Logarithm of umbelliferone concentration - Growth inhibition plot. The half maximal effective concentration (EC_{50}), as a key index for inhibitory activity, was calculated through the toxicity regression equations. All the data were analyzed by analysis of variance followed by Duncan's multiple range tests using SPSS13.0.

2.4 Assay for Measurements of MIC and MFC

10 μl spore suspension of the test plant pathogenic fungi were added into the sterile test tube containing potato dextrose with 31.25, 62.5, 125, 250, 500, 1000, and 2000 μg mL^{-1} umbelliferone and incubated at 28 ± 2 ℃ for 2-7 d. PD containing the same volume of distilled water was used as a control. The minimal inhibitory concentration (MIC) was defined as the lowest concentration inhibited the visible mycelia growth. The media were continued incubating for another 7 d when the MIC values were got. The minimal fungicide concentration was defined as the lowest concentration that no mycelia growth was observed (Wu *et al*. 2009).

2.5 Assay for Inhibition of Spore Germination

In the assay for inhibition of spore germination, each spore suspension was mixed with 31.25, 62.5, 125, 250, 500, 1000, 2000, and 4000 μg mL^{-1} umbelliferone. The mixtures were incubated on the glass slides at 28 °C in wet room. After 4 h of incubation, germination rates were subsequently recorded under the light microscope using the Lacto phenol Cotton Blue Stain Droppers. The spore germination with acetone was used as a control. Each treatment was replicated 3 times and the experiment was repeated twice (Bajpai *et al*. 2009).

2.6 Ultrastructure Analysis by Scanning Electron Microscope

Scanning electron microscope (SEM) was performed to observe the effect of umbelliferone on mycelia ultrastructure. The cultured colonies of *M. fructigena* and *F. moniliforme* were cut into 1 mm^3 in sterile conditions. Fungal colonies were subsequently added into umbelliferone solutions with the concentrations at MIC and MFC values. After 8 h of incubation, the test samples were fixed in glutaraldehyde (2 %) for another 2 - 4 h. Then the glutaraldehyde was washed off using 0.1 M phosphate buffered saline (PBS). The samples were subsequently fixed in osmium tetroxide for 2 h, and washed off using double distilled water till no osmium tetroxide was totally cleared. The samples were put into the iso-Amyl acetate solution for 30 min, after dehydration through a 30, 50, 70, 80, 90, and 100% ethanol series (5-10 min in each series). Following conventional critical point drying, adhesion, metal spraying, the samples were observed under scanning electron microscope (Xie *et al*. 2005).

2.7 Ultrastructure Analysis by Transmission Electron Microscopy

Transmission electron microscope (TEM) was performed to observe the effect of umbelliferone on cell ultrastructure. A same procedure was used in sample treatments till ethanol dehydration. Following the impregnation and embedment at 37 ℃ for 12 h, 45 ℃ for 12 h, and 60 ℃ for 18 h, respectively, extra-thin slices were dyed using uranium-lead method and subsequently observed under H-7500 transmission electron microscope (Zhang *et al*. 2008).

3 Results

3.1 Antifungal Activity of Umbelliferone

Umbelliferone had high inhibitory activity toward the test plant pathogenic fungi *M. fructigena*, *F. moniliforme, B. cinerea* and *C. capsici* with EC_{50} of 244, 358, 596, and 1772 μg mL^{-1}, respectively (Table 1). Inhibitory activities towards *M.*

fructigena and *F. moniliforme* were higher than those towards *B. cinerea* and *C. capsici*. When umbelliferone concentration reached to 200 μg ml^{-1}, the inhibition percentages towards *M. fructigena*, *F. moniliforme, B. cinerea* and *C. capsici* were 96.70 %, 83.38 %, 68.14 %, and 49.87 %, respectively. Umbelliferone also showed dose-dependent inhibitory activity when the dose increased. Results indicate statistically significant difference in each treatment ($P < 0.05$). Logarithm of umbelliferone concentration - Growth inhibition plot showed linear correlation with significant correlation coefficients.

Table 1. Inhibitory effects of different concentrations of umbelliferone on plant pathogenic fungi

Test strains	Concentrations (μg ml-1)	Colony diameter (mm)	Inhibitory rate (%)	Toxicity regression equation	EC_{50} (μg ml^{-1})	Correlation coefficient (r)
M. fructigena	2000	2.2	96.70_a	Y=0.7545x+0.8526	244	0.96
	1000	11.2	83.18_b			
	500	26.8	59.76_c			
	250	35.5	46.70_d			
	125	40	39.94_e			
	CK	66.6	0.00_f			
F. moniliforme	2000	11.6	83.38_a	Y=0.5816x+1.5795	358	0.9242
	1000	22.5	67.77_b			
	500	27.8	60.17_c			
	250	29.5	57.74_d			
	125	57.2	18.05_e			
	CK	69.8	0.00_f			
B. cinerea	2000	25.3	68.14_a	Y=0.3586x+2.7079	596	0.9709
	1000	35.6	55.16_b			
	500	46.5	41.44_c			
	250	48.3	39.17_d			
	125	55.5	30.10_e			
	CK	79.4	0.00_f			
C. capsici	2000	40.3	49.87_a	Y=0.4002x+2.0066	1772	0.9809
	1000	48.5	39.68_b			
	500	51.7	35.70_b			
	250	62.4	22.39_d			
	125	70.2	12.69_e			
	CK	80.4	0.00_f			

Note: Different letters (a-f) were significant different at P<0.05 based on Duncan's Multiple Range Test.

3.2 Measurements of MIC and MFC

The MIC and MFC values of umbelliferone towards each fungus were listed in Table 2. Umbelliferone showed high inhibitory activity towards *M. fructigena* and *F.*

moniliforme with MIC values of 250 μg mL^{-1} and 500 μg mL^{-1}, respectively. Their MFC values were both 1000 μg mL^{-1}. MIC values towards *B. cinerea* and *C. capsici* were 1000 μg $mL^{-1}$and 2000 μg mL^{-1}, respectively. Their MFC values were not obtained in this experimental range. We also found that acetone did not inhibit the mycelia growth (data not shown).

Table 2. The results of the MIC and MFC

Inhibitory effect (μg ml-1)	**Test strains**			
	M. fructigena	***F. moniliforme***	***B. cinerea***	***C. capsici***
MIC	250	500	1000	2000
MFC	1000	1000	—	—

3.3 Inhibition of Spore Germination

It is noteworthy that umbelliferone was very active against the spore germination of the four fungi in different concentrations of 31.25-4,000 μg mL^{-1} (Fig. 1). 100% inhibition of spore germination of *M. fructigen* and *F. moniliforme* were observed, when the umbelliferone concentrations were up to 1,000 μg mL^{-1} and 2,000 μg mL^{-1}, respectively. While the umbelliferone concentrations were up to 4,000 μg mL^{-1}, the spore germination of *B. cinerea* and *C. capsici* were inhibited for about 70-90 %.

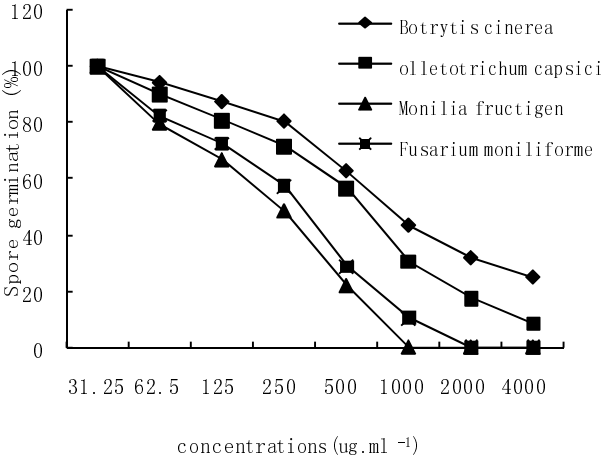

Fig. 1. The influence of unbelliferone on spore germination

3.4 Ultrastructure Analysis by SEM

Observation with scanning electron microscope, the mycelia ultrastructure of *M. fructigen* and *F. moniliforme* were showed in Fig. 2. In the no-umbelliferone

treatments, the mycelia of *M. fructigen* and *F. moniliforme* kept their normal growth condition containing mellow and smooth mycelia (Fig. 2 T-1, T-4, M-1, and M-4). After umbelliferone treatments of MIC concentration, the mycelia of *M. fructigen* and *F. moniliforme* both occurred to be nodal and adhesive. Local depression and anomalistic rupture emerged on the mycelia surface, and overflow of cell contents were also observed in small amounts (Fig.2 T-2, T-5, M-2, and M-5). When the umbelliferone concentration was up to MFC values, the depression and rupture of mycelia surface and overflow of cell contents became very serious (Fig.2 T-3, T-6, M-3, and M-6).

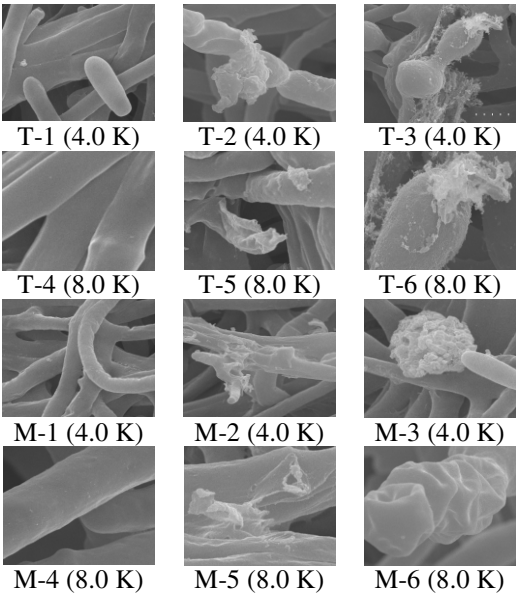

Fig. 2. The untreated and treated mycelia morpha of M. fructigena and F. moniliforme under SEM (T for M. fructigena, M for F. Moniliforme; 1 and 4 for control, 2 and 5 for unbelliferone concentration of MIC values, 3 and 6 for unbelliferone concentration of MFC values)

3.5 Ultrastructure Analysis by Tem

Observation with transmission electron microscope, the cell ultrastructure of *M. fructigen* and *F. moniliforme* were showed in Fig. 3. In the TEM photographs, the mycelia of *M. fructigen* and *F. moniliforme* kept their normal cell condition in the no-umbelliferone treatment groups (Fig.3 T-1, T-2, M-1, and M-2). After umbelliferone treatments of MIC concentration, degradation of cellular organs, cell cavity, cytoplasm agglutination, and plasmolysis occurred in the cells of *M. fructigen* and *F. moniliforme* (Fig.3 T-3, T-4, M-3, and M-4). When the umbelliferone concentration was up to MFC values, all the phenomena became more serious (Fig.3 T-5, T-6, M-5, and M-6).

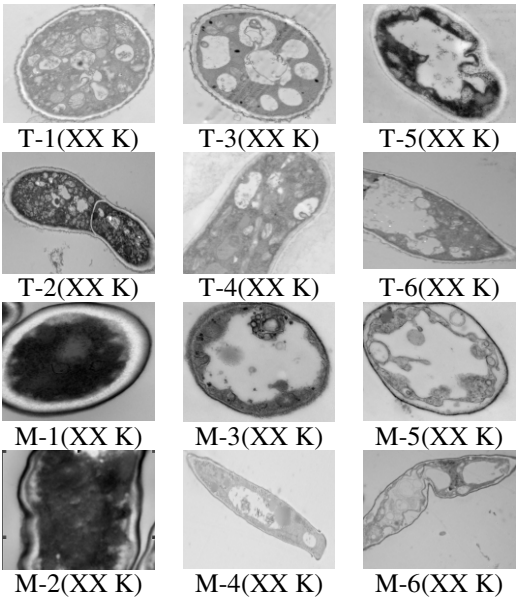

Fig. 3. The untreated and treated mycelia morpha of M. fructigena and F. moniliforme under TEM (T for M. fructigena, M for F. Moniliforme; 1 and 2 for control, 3 and 4 for unbelliferone concentration of MIC values, 5 and 6 for unbelliferone concentration of MFC values; 1-3 for cross section, 4-6 for longitudinal section)

4 Discussion

Phytogenous pesticides, coming from nature with low harm to the environment, are now a new research focus on plant diseases and insect pests. Researchers in Bionic center of Qingdao Agricultural University synthesized an artificial fungicide, named Lu Di, using bioactive fraction B from *Ginkgo biloba* Linn as the chemical template. It showed significant inhibitory activities towards many plant pathogenic fungi (Meng and Yuan. 2001). Li *et al* (2008) reported that "fungicide 402" was successfully synthesized from allicin. Syngenta (Sweden) synthesized a new fungicide named amistar from an edible mushroom of rain forests. Research and development of bionic pesticides synthesization have been an inevitable trend of pesticides in 21th century. Umbelliferone, as a simple compound of coumarin, has great potential in its high anti-insect and antifungal activities. It might have a wide application prospect in biosynthetic pesticides.

After the umbelliferone treatments, the mycelia of *M. fructigen* and *F. moniliforme* occurred to be nodal and adhesive and cellular organs degraded. These many because umbelliferone made some functional enzymes inactive and repressed the metabolism and transportation of nutrients. Through TEM, we can observe that the cell membranes of the test fungi were not destroyed. It might because umbelliferone transports into the cells by osmosis. After umbelliferone treatments, mitochondria totally vanished, many cellular organs degraded, and lots of cell cavity emerged.

We can conclude that umbelliferone degraded the mitochondria and made the cells lost their metabolism function. That might be the reason why the fungal mycelia were killed. Further researches are needed for mechanisms of umbelliferones' degradation activities towards cellular organs. In the experimental range, umbelliferone cannot effectively kill *B. cinerea* and *C. capsici*, researches of their MFC values and the differences of the four fungi are also needed.

In conclusion, umbelliferone has effective antifungal activity towards plant pathogenic fungi and high inhibitory activity towards spore germination. Antifungal mechanism of umbelliferone is probably based on its destruction activity towards pathogenic fungal cellular organs. Since umbelliferone is a natural phytogenous pesticide of a simple coumarin compound, it has great potential to be widely used in food fresh-keeping, plant protection, biosynthetic pesticides fields.

Acknowledgements. The work was financially supported by the National Natural Science Foundation of China (30872029), the Key Natural Science Foundation of Beijing Municipality (6071001), the Natural Science Foundation of Beijing Municipality (6092007), the Key Foundation of Beijing Municipal Education Committee (KZ201010020016), and Funding Project for Academic Human Resources Development in Institutions of Higher Learning Under the Jurisdiction of Beijing Municipality (PHR20090516, PHR200906134).

References

1. Abram, V., Donko, M.: Tentative identification of polyphenols in *Sempervivum tectorum* and assessment of the antimicrobial activity of *Sempervivum* L. Journal of Agricultural and Food Chemistry 47, 485–489 (1999)
2. Bajpai, V.K., Yoon, J.I., Kang, S.C.: Antifungal potential of essential oil and various organic extracts of *Nandina domestica* Thunb. against skin infectious fungal pathogens. Applied Microbiology Biotechnology 83, 1127–1133 (2009)
3. Cambier, V., Hance, T., Hoffmann, E.D.: Effects of 1,4-Benzoxazin-3-One derivatives from maize on survival and fecundity of *Metopolophium dirhodum* (Walker) on artificial diet. Journal of Chemical Ecology 27, 359–370 (2001)
4. DaWa, Z.M., Zhou, Y., Bai, Y., GeSang, S.L., Xie, P., Ding, L.S.: Studies on chemical constituents of *Saussurea laniceps*. China Journal of Chinese Materia Medica 33, 1032–1035 (2008) (in Chinese)
5. Li, L.Z., Lu, Y.X., Wang, L., Liu, H.: Research review and prospect of botanical pesticide. Henan Chemical Industry 25(8) (2008) (in Chinese)
6. Liu, G.L., Ni, Y.N.: Fluorescence spectrometric study on the interaction between umbelliferone and bovine serum album in with the use of MCR-ALS. Chemical Journal of Chinese Universities 29, 1339–1343 (2008) (in Chinese)
7. Liu, H.Y., Gao, W.W., Fan, Y.: Advances in research and development of the botanical fungicide. Chinese Agheultural Seienee Bulletin 21, 254 (2005) (in Chinese)
8. Liu, X.F., Xia, Y.M., Fang, Y., Zou, L., Liu, L.L.: Interaction between bovine serum albumin and umbelliferone with/without metal ions of Cu^{2+} or Zn^{2+}. Spectroscopy and Spectral Analysis 25, 1301–1302 (2005) (in Chinese)
9. Jiangsu new medical college, The great Chinese Medicine dictionary, p.1703. People's Publishing House, Shanghai (1977) (in Chinese)

10. Meng, Z.L., Yuan, Z.L.: Preparation & application of Lü Di–an artificial synthetic fungicide. Scientia Agricultura Sinica 34, 168 (2001) (in Chinese)
11. Mohamalawar, D., Sharma, N.C., Cristae, P., Sahi, S.V.: Transformation of maize by 2,4-dihydroxy-7-methoxy-2H-1,4-benzoxazin-3(4H)-one resistant *Agrobacterium* strains. Biotechnology Letters 24, 197–203 (2002)
12. Otake, S., Makimura, M., Kuroki, T., Nishihara, Y., Hirasawa, M.: Anticaries effects of polyphenolic compounds from Japanese green tea. Caries Research 25, 438–443 (1991)
13. Sha, S.Y.: The analysis method on plant resistance effective compostion, p. 212. People's Health Publishing House, Beijing (1984) (in Chinese)
14. The national medicine administration bureau Chinese Medicine information central station, Plant resistance effective compostion resistance manual, p. 943, 1098. People's Health Publishing House, Beijing (1986) (in Chinese)
15. Tombola, F., Campello, S., Luca, L.D., Ruggicro, P., Giudice, G.D., Papini, E., Zoratti, M.: Plant polyphenols inhibit VacA, a toxin secreted by the gastric pathogen *Helicobacter pylori*. Federation of European Biochemical Societies 543, 184–189 (2003)
16. Wang, T.Y., Yang, W.Y.: Simultaneous determination of scopoletin and umbelllferone in *Angelica pubescens* by RP-HPLC. Chinese Journal of Analysis Laboratory 15, 17 (1996) (in Chinese)
17. Weber, U.S., Steffen, B., Siegers, C.P.: Antitumor-activities of coumarin, 7-hydroxy-coumarin and its glucuronide in several human tumor cell lines. Research communications in molecular pathology and pharmacology 99, 193–206 (1998)
18. Wu, Z.Y., Wang, Y., Ai, Q.J.: Inhibitory effect and antimicrobial mechanism of pyrolin on *Monilinia fructicola* in peach. Scientia Agricultura Sinica 42, 2784–2792 (2009) (in Chinese)
19. Xie, J.Y., Dong, G.J., Liu, Z.Y.: Method of preparing specimens of microorganism for SEM. Journal of Chinese Electron Microscopy Society 437, 975–980 (2005) (in Chinese)
20. Yang, X.W., Masao, H., Tsuneo, N.: Two new coumarins from the roots of *Aegle marmelos*. Journal of Chonese Pharmaceutical Sciences 5, 66–68 (1996) (in Chinese)
21. Yang, X.W., Xu, B., Shen, F.X.: Inhibitory effects of 11 coumarin compounds against growth of human bladder carcinoma cell line E-J in vitro. Journal of Chinese Interative Medicine 5, 56 (2007) (in Chinese)
22. Zhang, G.Z., Wang, Y.W., Xu, H.H., Wu, G.Q.: Isolation and identification of extraction of *Stellera chamaejasme* (I). Journal of Anhui Agricultural University 27, 340–344 (2000) (in Chinese)
23. Zhang, W., Ai, Q.J., Wu, Z.Y., Wei, Y.Q.: Inhibitory effect of pyrolin on *Alternaria alternata* causing occurrence of black spot in postharvest pear. Journal of Fruit Science 25, 755–759 (2008) (in Chinese)

Acaricidal Activity of Ethyl Palmitate against Tetranychus cinnabarinus

Chun-ya Bu, Dan-dan Duan, You-nian Wang, Lan-qing Ma, Yu-bo Liu, and Guang-lu Shi*

Key Laboratory of Urban Agriculture (North) of Ministry of Agriculture, P.R. China
Beijing University of Agriculture, Beijing, China
glshi@126.com

Abstract. Isolation and identification of bioactive compounds from medicinal plant of Inula flower is a potential approach for the development of new pesticides against the mite of Tetranychus cinnabarinus. Dry Inula Flower was used as the starting material to obtain active substances with acaricidal activity by organic solvent extraction and bioactivity assay verification. The main component of the active substances in fraction 33 was further identified by GC/MS and proven to be ethyl palmitate. In order to clarify the roles of ethyl palmitate playing against mites of Tetranychus cinnabarinus, the enzymatic activities were assayed regarding to four essential enzymes in the process of either nerve conduction or anti-oxidation reaction of the mites, including assays for Ca2+-ATPase, superoxide dismutase (SOD), catalase (CAT) and peroxidase (POD). In addition, the substructures of the ethyl palmitate treated adult female mite of T. cinnabarinus were observed by transmission electron microscopy. In the bioassay, ethyl palmitae showed strong activities against the mites with the corrected mortality rates of more than 90% for samples at 2mg/ml concentration. The activity increases of antioxidant enzymes indicate a certain degree of stimulation of the anti-oxidant mechanisms to response for the ethyl palmitate treatment in vivo. The Ca2+-ATPase plays essential role in the maintenance of nerve cell excitability and conduction. Its enzymatic activity was subject to a certain degree of declination, which might cause the death of the mites due to suppression in nerve conduction. The toxicity effect of the mites by ethyl palmitate was further confirmed by TEM observation. The significant destruction of the skin structures and cellular substructures can directly affect the normal function of the cells, and ultimately lead to the death of the mites. Based on the strong acaricidal activity of ethyl palmitate has against the carmine spider mite, it is valuable to be further investigated for a new type of botanical pesticides development.

Keywords: Inula Flower, ethyl palmitate, acaricidal activity, Tetranychus cinnabarinus, Ca2+-ATPase, superoxide dismutase, catalase, peroxidase (POD), TEM.

1 Introduction

Phytophagous mites are populations of pests that are very harmful for the agricultural production. It's not easy to control them due to the facts that they are small sized

* Corresponding author.

E. Zhu and S. Sambath (Eds.): Information Tech. and Agricultural Eng., AISC 134, pp. 703–712.
springerlink.com © Springer-Verlag Berlin Heidelberg 2012

insects, can be rapidly reproduced and quick pesticide resistance development. It's a huge expense for a lot of countries including China to prevent the loss by mites in the agricultural field. Synthetic pesticides are widely used for the mites control with the compromise of a few side effects involved, including the damage to the environment, poisonous to the natural enemy of the mites and etc.

More and more attention has now been paid to the research and development of pesticides of new generation from botanical resources. There're many reports that have been published recently about different approaches, including the extraction of active compounds from *Fructus kochiae* to poison the hawthorn leave mite (Chao *et al*., 2007), toxicity effect of extraction from walnut leaf to *T. cinnabarinus* (Wang *et al*., 2007), and active components from *Tagetes erecta* root was a killer of hawthorn leaf mite (Shi *et al*., 2007).

The carmine spider mite, *Tetranychus cinnabarinus* (Boisduval) (Acari: Tetranychidae), is an economically important pest worldwide (Kieiewiez, 1994). They are widely distributed in China, attacking a variety of vegetable crops and fruit trees. To date, there is no report about the acaricidal effect of ethyl palmitate on essential enzymes of the mites of *Tetranychus cinnabarinus*, and little is known about the mechanism of its function as an acaricide.

In this study, we extracted active fractions from *Inula* flower and identified ethyl palmitate as the main active component by its toxicological effects against the mites of *Tetranychus cinnabarinus*. Through the observation of electron microscope, the significant destruction of the substructures of mites treated by ethyl palmitate indicated an obvious acaricidal effect of the compound. Finally, the activities of several essential enzymes were performed after ethyl palmitate treatments, which indicate the demonstrated influences of the compound on the metabolism process of the mites. The results of this study will be very valuable in the development of new botanical compounds with higher activity, selectivity, and more environmental friendly.

2 Materials and Methods

2.1 Plant Materials

Inula flower sample were purchased from Beijing TongRenTang Pharmacy of China. The dried flowers were grounded into fine powder by a crusher, filtered, and then stored in the refrigerator for the later usage.

2.2 Mites Preparation

A sensitive species of *T. cinnabarinus* was established at the Beijing University of Agriculture by collecting naturally occurring mites from flowering peach and transferring them to cowpeas (*Vigna unguiculata*) that were sown in plastic pots (10 × 10 cm) and grown in a greenhouse with a temperature of 25 ± 1 ℃, 50 ± 10% relative humidity and 16: 8(L: D) h light illumination.

2.3 Preparation of the Crude Extraction

The grounded power of *Inula* flower was mixed with petroleum-ether of 5 times volumes and kept for 3-5 days. After three times of extraction, the crude extracts were

concentrated, combined and weighted. (All the reagents used were analytical grade solvents, including petroleum-ether, chloroform, and methanol, from Beijing Chemical Reagents Co., Beijing, China).

2.4 Preparation of Re-extraction of Crude Extraction

For the re-extraction, the crude extraction powder was resolved by petroleum-ether of 10 times volumes and put into a separating funnel (Beijing Glass Factory, Beijing, China), the partitioning agent of methanol was added to the funnel, mixed well and extracted for three times. The extractions were combined, concentrated using a rotary evaporator and weighed.

2.5 Preparation of Isolation of Concentrated Extracts

7 g of the extract powder was weighed precisely and separated by chromatography at medium pressure, eluted by petroleum-ether, petroleum-ether: chloroform mixture (ratio of 9: 1, 8: 2, 7: 3, 6: 4, 5: 5, 3: 7, 2: 8, 1: 9) and pure chloroform respectively. A total of 38 fractions were collected finally.

2.6 Bioassays

Acaricidal activity assay against *T. cinnabarinus* was performed for the crude extractions of *Inula* flower powder, re-extractions from petroleum-ether and methanol preparation, and eluted fractions by medium pressure chromatography. Bioassays were conducted using a improved slide dip technique (Liu *et al*. 2004). Thirty one-day old adult female *T. cinnabarinus* were picked up with a fine brush and affixed on double-sided adhesive tape attached to one end of a 10 × 2 cm glass slide. The mites were dipped into an extract solution or distilled water (control) for 5 s, respectively. Once the slide was removed away, the extra solution was absorbed with filter paper. Mortality was determined at 24 h after the treatment by observing mites under an Olympus SZ51 solid microscope (Olympus Ltd., Japan), where they were considered dead if they did not respond to a gentle probe with a fine brush. Each bioassay was repeated three times for each solvent extract.

To compare the mortality of fraction 33 and pure ethyl palmitate, the extracts power or pure compound was diluted with Tween 80 and distilled water at a final concentration of 2 mg powder/ml. Distilled water with 1% Tween 80 was used as a control. The experiments were replicated for three times and the mortality rates were corrected for control mortality by using Abbott's formula (Abbott 1925). All statistical analyses were performed in SPSS 13.0 (SPSS Institute. 2004).

2.7 GC/MS Identification for Fraction 33

GC/MS experiment was performed on a Agilent 6890/5973N for fraction 33, which showed demonstrated bioactivity against the mite tested. The temperature was raised from 150 to 180 at 2 ℃/min rate, 200 ℃ at 5 ℃/min rates and 250 ℃ at 8 ℃/min rate, respectively. The temperature for the sample injection port was set at 250 ℃, and 230℃

for the ion-source. The result was used for searching in NIST (National Institute of Standards and Technology) to identify the molecular structure of fraction 33.

2.8 Enzymatic Preparation

The enzyme solution used in the Slip-dip method was prepared with the mite treated with 2mg/ml ethyl palmitate. 200 mites were collected at every 4 hours intervals after the drug treatment. The mites were mixed with 0.25ml physiological saline and homogenized on a ice booth, the supernatant containing the enzymes was transferred to a new tube after centrifugation for 15min at 10000 rpm at 4℃. The protein quantization of the crude enzyme lysates were performed later.

2.9 Calcium ATPase Activity Assay

Calcium ATPase activity assay kit was purchased from Nanjing Jiancheng. *OD* value were measured at 636nm and assayed for three times. The enzyme activity was defined as the amount of phosphor generated from ATP in one hour by 1 mg protein enzyme.

2.10 Superoxidase Dismutase (SOD) Activity Assay

The xanthine/xanthine oxidase assay was used for SOD activity determination. Xanthine oxidase catalyzes the oxidation of xanthine to generates O^{2-}, leading to the oxidation of hydroxylamine to nitrite that can be detected by adding color development reagent. The nitrite formation can be reduced by the O^{2-} quenching activity of SOD, resulting in a lower OD value at 550nm on the spectrometer. One unit (U) of SOD activity was defined as the amount that reduced the absorbance at 550 nm by 50%. The enzyme activity was expressed as U/mg protein.

2.11 Catalase (CAT) Activity Assay

Catalase (CAT) activity was detected using ammonium molybdate method by measuring the intensity of a yellow complex formed by molybdate and H_2O_2 at 405 nm, after ammonium molybdate was added to terminate the H_2O_2 degradation reaction catalyzed by CAT. An enzyme activity unit was defined as the degradation of 1 mmol H_2O_2 per second per mg tissue protein and the enzyme activity was expressed as U/mg protein.

2.12 Peroxidase (POD) Activity Assay

According to the reaction principle of POD catalysis hydrogen peroxide, we detected the changes of absorbance at 420 nm and calculated the POD activity. The POD enzyme activities were expressed as the average change in absorbance per minute per mg of protein, and the enzyme activity was expressed as U/mg protein.

2.13 Transmission Electron Microscopy (TEM) Observation

The fresh cowpea leaves were truncated about 0.5cm from the petiole end. The petioles were wrapped up with wet cotton sliver and put on the pad with a layer of wet filter

paper in the dishes. 20 adult female mites were put on the leaves which were surrounded by the wet sliver. The ethyl palmitate was prepared as a liquid at a concentration of 2 mg/ml and spayed on the mites' body using a throat spray. Excess liquid on the leaves was removed with absorbent paper after 5 s treatment. The mites were put into the fix solution after 20 hours of the treatment. Distilled water with 1 % Tween -80 was set as a blank control.

The mites' samples were prefixed and washed with 0.1 % PBS for four times at a 2 hour interval. In the post fixation, the sample was merged into 1 % osmium tetroxide and gently vibrated to make sure the sample was completely merged, and shook the sample once during the 2 h fixation. After washing the sample for four times with 0.1 % PBS and 15 min for each wash, the samples were dehydrated by a series of ethanol solutions at concentrations of 30 %, 50 %, 70 %, 80 %, 90 %, 95 % and 100 %, respectively, and followed by 100 % acetone three times at a 2 min interval. The samples were further soaked, embedded, polymerized, sliced, and they were stained and imaged finally.

3 Results

3.1 GC/MS Identification of Fraction 33

Through searching in NIST (National Institute of Standards and Technology), the result indicates Ethyl Palmitate is the main component of fraction 33 with a matching parameter of more than 90%.

3.2 Acarcidal Activity Comparison of Fraction 33 and Ethyl Palmitate

As seen in Tab. 1, both fraction 33 and pure Ethyl palmitate showed strong activities against the mites. The corrected mortality rates were more than 90% for both samples at 2mg/ml concentration.

Table 1. The mortality of extracts from *Inula britanica* against *Tetranychus cinnabarinus*

Extracts(2 mg·mL^{-1})	Extraction rate/%	Mortality/%
Fraction 33	2.65±0.32	90.12±3.934
Ethyl palmitate	1.67±0.03	90.61±2.23

Values are mean ±SE of three determinations

3.3 Ca^{2+}-ATPase Enzymatic Activity of T. cinnabarinus after Ethyl Palmitate Treatment

As seen in Fig. 1, Ca^{2+}-ATPase activities for both the treatment group and the control showed similar tendencies, with significant fluctuation within 24 hours. The activities declined within 8h and went up during 8 h – 12 h and reached the peak at 12 h. There're several fluctuations in 12 – 24 h period. In general, after the treatment of carmine spider mites by ethyl palmitate, the Ca^{2+}-ATPase activities of treatment group were suppressed compared with the control.

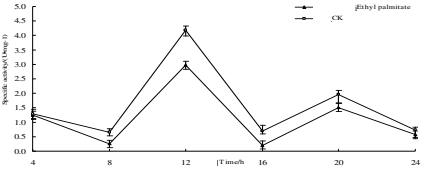

Fig. 1. Time course of Ca^{2+}-ATPase activities of the ethyl palmitate against *T. cinnabarinus*

3.4 Superoxide Dismutase (SOD) Activity of T. Cinnabarinus after Ethyl Palmitate Treatment

As seen in Fig. 2, SOD activities for both the treatment group and the control showed similar tendencies. The activities went upward and reached a peak at 12 h point, slowly declined afterwards. Meanwhile, the treatment group always showed higher SOD activities during the 24 h period. The significant increases of the activities for the treatment group were observed at the 4 h and 12 h points with 2.7 times and 1.3 times activities of the control, respectively. In general, after the treatment of carmine spider mites by ethyl palmitate, the SOD activities of treatment group were activated somehow compared with the control.

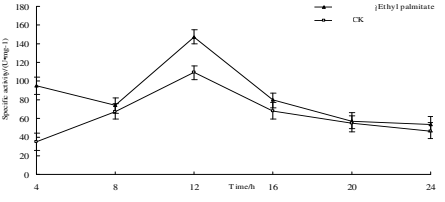

Fig. 2. SOD activities after the ethyl palmitate treatment against *T. cinnabarinus*

3.5 Catalase (CAT) Activity of T. cinnabarinus after Ethyl Palmitate Treatment

Fig. 3 indicates significant fluctuations of the CAT activities for both the two groups during the 24h observation. After the ethyl palmitate treatment, CAT activity reached a peak at the 4h, which showed a 1.9 times higher activity than the control. In general, the CAT activity of treatment group is subject to a certain degree of activation during the ethyl palmitate treatment.

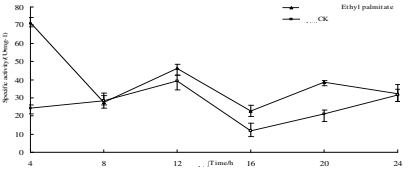

Fig. 3. CAT activities of the ethyl palmitate against *T. cinnabarinus*

3.6 Peroxidase (POD) Activity of T. cinnabarinus after Ethyl Palmitate Treatment

As seen in Fig. 4, carmine spider mite treated by ethyl palmitate treatment showed similar tendency of POD activity compared with the control with the maximum enzymatic activity at 4h, undergone a process of dramatically declination between 4 - 8 h and a flat lower stage afterwards. The activity of the treatment group is always higher than the control within the 24 h. Especially at 12 h and 16 h, the differences between two groups of enzyme activity were significant, with values of 2.1 times and 1.8 times of the control, respectively. Similar to SOD and CAT, carmine spider mite treated by ethyl palmitate, is subject to a certain degree of activation of the POD.

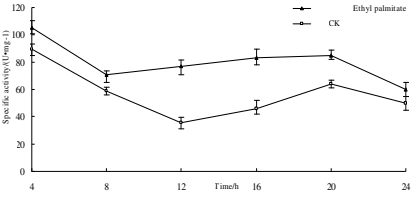

Fig. 4. POD activities of the ethyl palmitate against *T. cinnabarinus*

3.7 Substructure Observation of T. cinnabarinus by TEM

The substructures of the ethyl palmitate treated adult female mite of *T. cinnabarinus* were observed by transmission electron microscopy, the result was summarized in Fig. 5.

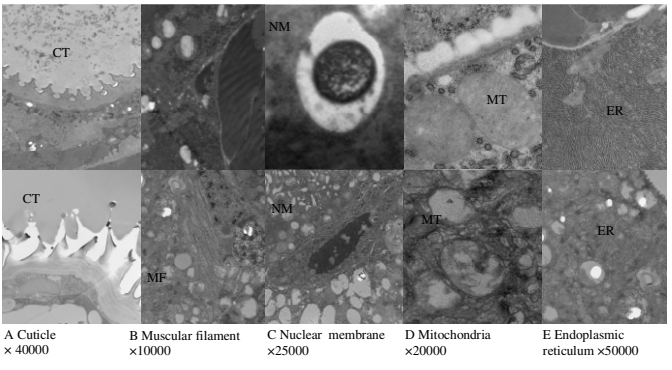

Fig. 5. Comparison of the ultrastructure of *T. cinnabarinus* with or without Ethyl palmitate treatment under TEM observation (top: Control, bottom: Treatment).CT: Cuticle; MF: Muscular filament; N: Nuclear; MT: Mitochondria; NM: Nuclear membrane; n: Nucleolus; ER: Endoplasmic reticulum)

After the ethyl palmitate treatment, a significant change of the morphology of the skin were observed (5-A, below). The skin structure was severely damaged and its wave shape was severely distorted. On the contrary, the skin structure of the control were still homogeneous and orderly widely shaped (5-A, above).

The muscle fibers structures of the treated mites were also changed dramatically (5-B, below), with the muscle fibers not in close parallel arrangement, as well as swelling, loose and fragmentation occurrence. However, the uniform muscle fibers of control group were well arranged, showing light and dark stripes (5-B, above).

The nuclear membrane and the nucleolus changed significantly after the treatment (5-C, below). The nuclear membrane was vague and broken, and the nucleus was out of integrity with material dissolution and rupture. However, the nuclear membrane in the control group was intact, clear and smooth, presenting the perfectly oval-shaped nucleolus with a structural integrity (5-C, above).

The destruction of mitochondrial structure was observed after treatment (5-D, below). The well ordered internal cristae was replaced by an irregular, disordered, severely damaged structure. On the contrary, the structural integrity of the mitochondria was well presented (5-D, above).

As to the endoplasmic reticulum, the deformation, distortion, dissolution, fracture and irregular arrangement represents a big loss of the structural integrity (5-E, below) compared with the well maintained, orderly arranged endoplasmic reticulum structure of the control (5-E, above).

4 Discussion

In the process of pesticide development, safer pesticides with low toxicity are now gradually replacing the usage of the traditional pesticide with high toxicity. To date, more and more attention has been paid to the development of botanical pesticides, which has abundant resources without damaging the ecological environment, less residue, no side effect for the natural enemy of the pest (Zhang, 2002; Chai Seung-woo, *etc*. 2002; Liu Junhua, 2002). In this report, dry *Inula* flower was used as the starting material to obtain active substances with acaricidal activity by organic solvent extraction and bioactivity assay verification. The main component of the active substances was further determined by chromatography and MS and proven to be ethyl palmitate, which showed strong activities in the bioactivity assay against the mites, indicates a potential in botanical pesticides development.

In order to clarify the roles of ethyl palmitate playing against mites of *Tetranychus cinnabarinus*, the enzymatic activities were assayed regarding to four enzymes which play essential roles in the process of either nerve conduction or anti-oxidation reaction of the mites.

Most of acaricides function through the interference with normal operation of the nerve system. The Ca^{2+} ATPase is a transport protein in the plasma membrane of cells that serves to remove calcium (Ca^{2+}) from the cell. It is vital for regulating the amount of Ca^{2+} within cells, which play essential roles in the maintenance of nerve cell excitability and conduction (Liu, 1999). In this experiment, although the treatment group and control group is basically the same trend, however, has been higher than the control group, treatment group. Its enzymatic activity was subject to a certain degree of declination, which might cause the death of the mites due to suppression in nerve conduction.

Superoxide dismutase (SOD), which catalyzes the dismutation of the superoxide anion into hydrogen peroxide and molecular oxygen, is one of the most important anti-oxidative enzymes for the organism to get rid of free radicals and other harmful

substances. It can block the damage by oxygen free radicals and repairing damaged cells in a timely manner. Catalase, another oxidoreductase that catalyzes the conversion of hydrogen peroxide to water and oxygen, is one of the key enzymes in bio-defense system, representing 40% of the peroxisomes and existing in almost all organisms. It can protect cells from damage induced by hydrogen peroxide, H_2O_2. Peroxidase, also existing in the peroxisomes, catalyzes oxidation of substrates using hydrogen peroxide as an electron acceptor. It can catalyze a lot of reactions to prevent the damage produced by hydrogen peroxide, phenolic and amine type substances. In the study, activation of the all the three enzymes occurred after ethyl palmitate treatment of the mites. For the SOD, the strongest activation occurred at 4, 20 hours, CAT at 4 hours, and POD at 12-16 hours. The activity increases of antioxidant enzymes suggest a certain degree of stimulation of the anti-oxidant mechanisms to response for the ethyl palmitate of *T. cinnabarinus* in vivo.

The toxicity effect of the mites by ethyl palmitate was further confirmed by TEM observation. Significant changes in various substructures of the mites were indicated, including changes in the skin, muscle fibers, the nucleus and organelles such as mitochondria and endoplasmic reticulum and etc.. The damaged adjacent muscle fiber connectivity can result in the holdback of the chemical and nerve impulse conduction, as well as incorrect message communication, leading to the function loss of the muscle fiber contraction (Caulfield, 2002). The damaged membrane may block the signal transmission, interrupt the conduction of nerve excitability; the destruction of mitochondria within cells may lead to impaired oxidative phosphorylation, a decreased ATPase activity, and supply shortage of the cell energy, eventually leading to the death of the mites of *T. cinnabarinus* (Kazuhiko, 1992; Zizka, 1997). The destruction of the skin structure and cellular structures can directly affect the normal function of the cells, and ultimately lead to the death of the mites.

In summary, to investigate the mechanism of acaricidal activity of ethyl palmitate to *T. cinnabarinus*, we not only tested the activities of several essential enzymes after the compound treatment, but also observed the destructed submicroscopic structures of the mites. The results indicate a significant influence of the compound treatment on both the anti-oxidative system and normal function of the cells. However, a clear mechanism for its function needs to be further demonstrated.

In addition, research and development of pesticides with high activity and low toxicity also depends on the application of advanced biology methods to clarify the mechanism of active compounds to function in the mites. After the active compounds treatment, significant changes at the molecular level in terms of gene transcription and protein expression may occur in some key cellular processes such as proliferation, apoptosis, and etc., as well as changes in a variety of signal transduction pathways, including the oxidative stress response pathway mentioned above. Gene chips, qRT-PCR, RNAi or proteomics analysis technique will be very effective means to identify the molecular changes in a specific pathway or a process, and further identify target proteins for the compound to function. On this basis, gene cloning and expression of specific target proteins can be very helpful to facilitate the functional study in terms of activity and selectivity of active compounds both in vitro and in vivo. Moreover, structure-based modification of the compounds can also be used as an efficient approach. All the efforts will in turn come together to promote the research and development of pesticides with high acaricidal activity and selectivity against mites of *T. cinnabarinus*.

Acknowledgements. The work was financially supported by the National Natural Science Foundation of China (30872029), the Key Natural Science Foundation of Beijing Municipality (6071001), the Natural Science Foundation of Beijing Municipality (6092007), the Key Foundation of Beijing Municipal Education Committee (KZ201010020016), and Funding Project for Academic Human Resources Development in Institutions of Higher Learning Under the Jurisdiction of Beijing Municipality (PHR20090516, PHR200906134).

References

1. Kieiewiez, M.: Dispersal of *Tetranychus cinnabarinus* on various tomato cultivars. Entomological Experimentalis Applicata 80, 254–257 (1996)
2. Abbort, W.S.: A method of computing the effectiveness of an insecticide. J. Am. Mosq. Control Assoc. 3, 302–303 (1987)
3. Caulfield, M.P.: Muscarinic receptors—characterization, coupling and function. Pharmacology & Therapeutics 14, 319–329 (2002)
4. Kazuhiko, M., Takashi, S., Matazaemon, U.: Effect of a New, fenpyroximate, on energy Metabolism and mitochondrial morphlolgy in adult female *Tetranychus urticae* (Two-Spotted Mite). Pesticide Biochemistry and Physiology 43, 37–44 (1992)
5. Zizka, Z., Pelc, R., Jizba, J., Kandybin, N.V., Sergeeva, M.V.: In Situ assessment at subcellar level of the effects of macrotetrolide insecticides on mites by electron microscopy and X-Ray Microanalysis. Pesticide Biochemistry and Physiology 58, 165–172 (1997)
6. Shi, G.-L., Zheng, W.-Y., Dang, Z.-P., Li, L.-C.: Fruit pests. China Agriculture Press, Beijing (1994)
7. Hou, H., Zhao, L.L., Shi, G.L., Li, Z.H.: Studies on the acaricidic activity of the extracts of Kochia scoparia. Plant Protection 30, 42–45 (2004)
8. Cao, H., Wang, Y., Shi, G., et al.: Effects of the Chloroform Extracts of Kochia scoparia to Several Enzyme Systems in Tetranychus viennensis. Scientia Silvae Sinicae 43(2), 68–72 (2007)
9. Wang, Y.N., Shi, G.L.: Acaricidal activity of Juglans regia leaf extracts on *Teranychus viennensis* and *Tetranychus cinnabarinus* (Acari: *Tetranychidae*). Journal of Economic Entomology 100, 1298–1303 (2007)
10. Shi, G.L., Wang, Y.N., Wang, H.L., et al.: Effect of Tagetes erecta on glutathiong-S-transferase and protease activities and protein content in Tetranychus viennensis. Chinese Journal of Applied Ecology 183, 400–404 (2007)
11. Liu, Y.-P.: Eupatorium acaricidal active substance of. Sichuan University, Chengdu (2004)
12. Yan, R.: Deoxypodophyllotoxin on Armyworm endocrine system. Northwest Agriculture and Forestry University, Yangling (2006)
13. Liu, S.Y., Sun, L.G., Xing, W., et al.: The effect of chronic lead exposure on hippocampal intraneuronal (Ca^{2+}) and activity of Ca^{2+}-ATPase in rats. Jounal of Health Toxicology 13(1), 102–103 (1999)
14. You, C., Zhang, J.: Anhui pesticide types of woody plants. Anhui Agricultural Sciences 30(1), 65–68 (2002)
15. Liu, J.H.: environmental-friendly botanical pesticide. Journal of Biology 37(6), 30–31 (2002)
16. Zhang, B.: Dynamic Summary botanical insecticide. Jiangxi Agricultural Science and Technology (6), 29–31 (2002)

Acaricidal Activity of Lupeol from Inula britanica against Tetranychus cinnabarinus (Acari: Tetranychidae)

You-nian Wang[1], Dan-dan Duan[1], Jun Cheng[1], Yu-bo Liu[1], Guang-lu SHI[1,*], and Bao-sheng Tong[2]

[1] Key Laboratory of Urban Agriculture (North) of Ministry of Agriculture, P.R. China
Beijing University of Agriculture, Beijing, China
[2] Inn Mongolia Yongye Biotechnology Co., Ltd., Neimenggu, China
glshi@126.com

Abstract. Extracts of Inula britanica were bioassayed to determine their acaricidal activities against Tetranychus cinnabarinus in the laboratory. The results showed lupeol from I. britanica is toxic to these mites, which showed high mite mortality. The present paper reports lupeol changed the balance of acetylcholinesterase (AChE), Na+-ATPase, POD, and catalase to damage the cuticle, muscular filament, nuclear membrane, mitochondria, and endoplasmic reticulum of treated mite, then ultimately killed T. cinnabarinus. This study is the first to report the acaricidal property of I. britanica and its potential as a botanical pest control agent.

Keywords: Inula britanica, lupeol, Tetranychus cinnabarinus, enzyme activity, Transmission electron microscope.

1 Introduction

Many mites are serious pests in agriculture and forestry in China and many parts of the world. They attack agricultural crops, orchard trees such as apple, pear, and peach. Acaricides used to minimize the impact caused by mites often are more toxic to their natural enemies, and their application may actually aggravate the problem. Furthermore, control of mites has become increasingly difficult due to their resistance to many common synthetic pesticides. Given the imposed quality restrictions on fresh market fruit, new pesticides that are effective against phytophagous mites and nontoxic to their natural enemies are urgently needed to combat these mites in China.

In recent years, much attention has been focused on the acaricidal activity of plants. So many species have been studied by research groups and several acaricidal plants were found, for example Kochia (Shiguanglu, 2006), *Stellera chamaejasme* (Shiguanglu, 2004), *Pharbitis purpurea* (Wang Yan, etc., 2008), Shuo Rao flowers (Cao, 2007), and walnut leaves (WangYounian, 2007). As far as we know, this study is

* Corresponding author.

E. Zhu and S. Sambath (Eds.): Information Tech. and Agricultural Eng., AISC 134, pp. 713–719.
springerlink.com © Springer-Verlag Berlin Heidelberg 2012

the first to report the acaricidal property of *I. britanica* and its potential as a botanical pest control agent.

Lupeol from *I. britanica* was bioassayed to determine its acaricidal activity against *T. cinnabarinus* in the laboratory. The result showed that lupeol from I. britanica is toxic to these mites, which showed high mite mortality. In this article, we investigated the effects of acetylcholinesterase (AChE), Na^+-ATPase, peroxidase, catalase on acaricidal mechanism.

2 Materials and Methods

2.1 Material Collections

The air-dried plants of *I. britanica* were powdered, which (40 mesh) were placed in the refrigerator. Adult females of *T. cinnabarinus* were obtained from laboratory rearing stock, which held at an ambient photoperiod of 18:6 (L: D) h, room temperature (24 ± 1°C) and a relative humidity of 60 ± 10 %.

2.2 Methods

Extraction, Isolation and Identification, Extraction: The air-dried *I. britanica* (15.0 kg) were powdered, placed in a flask, and then extracted (7 days × 3) with petroleum ether. Evaporation of the solvent in vacuo afforded a residue, which was suspended in petroleum ether, and then partitioned with methanol.

Isolation: The petroleum ether fraction (7.0 g) was chromatographed on a normal-phase preparative MPLC column eluted with a petroleum ether-CHCl3 (10: 0, 9: 1, 8: 2, 7: 3, 6: 4, 5: 5, 3: 7, 2: 8, 1: 9, and 0: 10) to give 38 fractions on the basis of TLC analysis.

Identification: All fractions were dissolved and then subjected to GC-MS analysis under the following conditions: electron-impact (EI) mode, temperature programming from 150 ℃ to 180 ℃ at 2 ℃/ min, them to 200 ℃ at 5 ℃/ min, carrier N2 gas.

Bioassay: Every fraction was diluted in distilled water to form a series of concentrations and evaluated for its acaricidal activity against T. cinnabarinus by using the slide dip method recommended by FAO. Thirty female adults were stuck onto one side of double-sided adhesive tape fixed on one end of a glass slide. The end of the slide with mites was dipped into the extract dilution or the control for 5 s. The slide was taken out, and the extra solution was removed with filter paper. Mites were considered dead if they did not respond to a gentle probe with a fine brush. Mortality was checked 24 h after treatment. Distilled water was used as the control. Mite mortality rates were corrected for control mortality by using Abbott's formula.

2.3 Determination of Enzyme Activity

Preparation of enzyme solution: Every fraction was diluted with distilled water to final concentration 2mg/ml, and tested acaricidal activity against T. cinnabarinus.

Mortality was checked at 4, 8, 12, 16, 20, and 24 h. Every time, 200 female adults and 0.25ml physiological saline were stirred in an ice bath (10000r/min, 4 ℃). The supernatant was used for acaricidal activity against T. cinnabarinus assay.

Determination of AChE: The acaricidal activity against T. cinnabarinus was determined using standard acetylcholinesterase light kit method (purchased from Nanjing Jiancheng). The optical densities were read on an enzyme-labeled detector (Denley MK-2) at wave length of 412 nm. Results are expressed as an average of three independent determinations.

Determination of Na^+-ATP Enzyme: Refer to Na^+-ATP enzyme kit method, the acaricidal activity was tested against T. cinnabarinus. The optical densities were read on an enzyme-labeled detector (Denley MK-2) at wave length of 636 nm. Results are expressed as an average of three independent determinations. The content of inorganic phosphorus from the decomposition of ATP showed the change of Na^+-ATP enzyme. According to the standard curve, the content of Na^+-ATP enzyme was calculated.

Determination of Catalase (CAT): Decomposition reaction of H_2O_2 was rapidly finished by adding ammonium suspension. Reaction of the remaining H_2O_2 with ammonium molybdate produced a pale yellow complex, which was measured at 405 nm.

2.4 Transmitting Electronic Microscopy

Mites are sprayed with 2 mg/ml of lupeol dilution for 5 s, and the extra solution was removed with filter paper. Pre-treatment condition: Firstly, mites are fixed with 2.5 % glutaraldehyde, and then rinsed with 0.1% PBS 4 times (4 × 2 h). Secondly, they are fixed with 1% osmium tetroxide, then with 0.1 % PBS rinsing four times (4 × 15 minters); and then mites are dehydrated by 30 %, 50 %, 70 %, 80 %, 90 %, 95 % and 100 % ethanol. At last the treated mites were embedded by Epon812. Cell ultra-structural changes were studied by transmission electron microscopy (JEM21200EX type).

3 Results and Analysis

3.1 Identification

The main component of fraction **7** was identified as lupeol by comparison of GC-MS data.

3.2 Acaricidal Activity

The corrected mortality (2 mg/ml) and the mean lethal concentrations (LC_{50} = 1.370 ± 0.303) of lupeol to the mites were given (see Tables 1 and 2)

Table 1. The mortality of Lupeol from Inula britanica against Tetranychus cinnabarinus

Lupeol (mg·mL-1)	Corrected mortality (%)	Mortality/%
10	91.32±1.33	90.91[a]
8	84.23±0.98	83.67[b]
4	79.63±0.81	78.95[c]
2	66.64±0.28	66.87[cd]
1	11.11±1.23	10.89[e]
CK	7.45±0.21	

Values are mean ±SE of three determinations, the averages within the same column not followed by the same letter are significantly different at 5% level of confidence, the same below.

Table 2. Toxicity regression equation of Lupeol against *Tetranychus cinnabarinus* female adults

Mite	Toxicity regression equation	Correlation coefficient	LC_{50}/(mg mL^{-1})	95% confidence limit / (mg mL^{-1})	
Female adult	Y=4.159+ 2.268x	0.939	1.370±0.303	2.011	2.739

3.3 Acetylcholinesterase (AChE) Activity

Acetylcholinesterase played a very important role to maintain normal nerve function. We can see AChE activity showed an overall downward trend (Fig.1). The specific activity values of test group are higher than those of control group16 h after treatment.

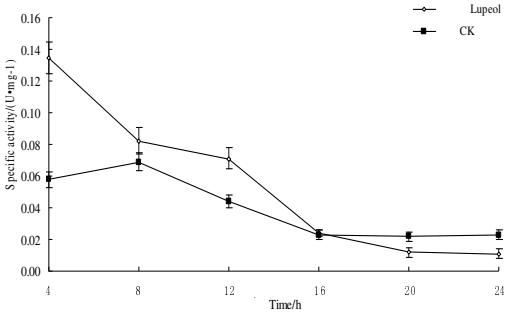

Fig. 1. Effect of TChE activity of the Lupeol against *Tetranychus cinnabarinus*

3.4 Na^+-ATP Enzyme Activity

Na^+-ATP enzyme can regulate the intracellular concentration of sodium ions to maintain the cell resting potential. The lupeol from *Inula britanica* can effectively

affect the activity of Na^+-ATP enzyme. From 4 h to 8 h, the test group and control group have the same trend, which increase quickly. However, the Na^+-ATPase activities of these two groups decrease quickly from 8 h to 12 h, and then they increase slowly 12 h after treatment (Fig. 2).

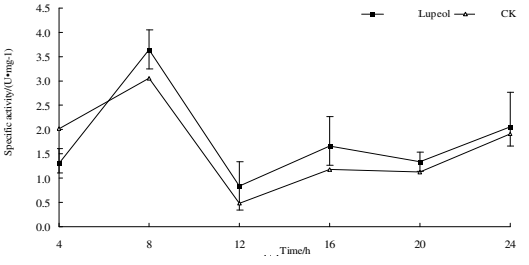

Fig. 2. Effect of Na^+-ATPase activity of the Lupeol against *Tetranychus cinnabarinus*

3.5 Catalase

Catalase is found in many organisms, which is the key enzyme of biological activities of life. It played the important role of antioxidant. Bioassay results indicated that the specific activity values of test group is consistently higher than those of control group (Fig. 3).

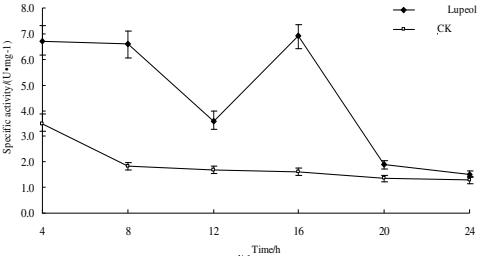

Fig. 3. Effect of CAT activity of the Lupeol against *Tetranychus cinnabarinus*

3.6 Peroxidase

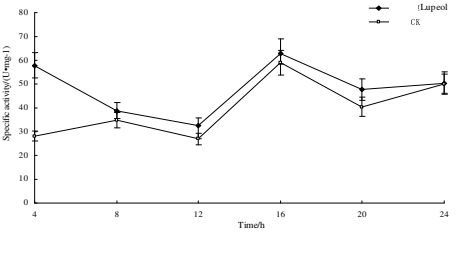

Fig. 4. Effect of POD activity of the Lupeol against *Tetranychus cinnabarinus*

3.6 Ultrastructure

Under transmission electron microscope, the cuticle, muscular filament, nuclear membrane, mitochondria, and endoplasmic reticulum of treated mites were severely damaged or changed by lupeol solution. Variety of lupeol on the ultrastructure of *T. cinnabarinus* was given in fig. 5 (top: Control, bottom: Treatment)

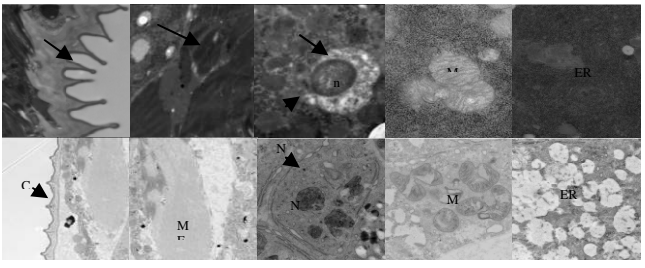

Fig. 5. Variety of Lupeol on the ultrastructure of *Tetranychus cinnabarinus* (top: Control, bottom: Treatment)
CT: Cuticle; MF: Muscular filament; N: Nuclear; MT: Mitochondria; NM: Nuclear membrane; n: Nucleolus; ER: Endoplasmic reticulum
Cuticle×40,000; Muscular filament ×10,000; Nuclear membrane ×25,000; Mitochondria ×20,000; Endoplasmic reticulum ×50,000

4 Discussion

Acaricides from plants damaged or changed the balance of a serious of enzyme in treated mites to kill them, however, which are nontoxic to their natural enemies and environment. A large number of studies showed acaricidal mechanism of substances from plants is different from that of conventional synthetic pesticides.

Currently, the nervous system is an important target in acaricidal bioassay, especially acetylcholinesterase, which plays an important role in neuronal development and nerve regeneration. Biochemical and chemical research suggests that there are important relationships between neural cell proliferation and acetylcholinesterase. The release of acetylcholine is necessary for synaptic transmission in organism, but it must be quickly broken down and removed, because the accumulation of it will cause the abnormal reaction of nerve conduction, until the final block synaptic transmission (Cao Fai *e.t. al*, 2007). Therefore, the activity of acetylcholinesterase was tested in acaricidal activity against *T. cinnabarinus*. We found the AChE activity of test group is higher than the control group within 16h after treatment. These results suggest that lupeol from *Inula britanica* may be a potential nerve agent of *T. cinnabarinus*.

ATP enzyme can catalyze and hydrolyze adenosine triphosphate (ATP) to obtain adenosine diphosphate (ADP) releasing energy. This process is widely used in all known forms of life, which could input many of the required for cell metabolism, at the same time, also could output toxic substances, metabolic waste, and other substances hindering cellular processes. Na^+-ATP enzyme can regulate the intracellular concentration of sodium ions, thereby maintaining the cells resting potential. These

results prove that lupeol from *I. britanica* can effectively regulate Na^+-ATP enzyme in *T. cinnabarinus* to kill mites.

Biological activity proved lupeol from *I. britanica* changed the balance of acetylcholinesterase (AChE), Na^+-ATPase, POD, and catalase to damage the cuticle, muscular filament, nuclear membrane, mitochondria, and endoplasmic reticulum of treated mite, and ultimately kill *T. cinnabarinus*. Therefore control of mites has become increasingly easy due to without resistance of mites to lupeol from *I. britanica*, which is a potential botanical acaricidal agent.

Acknowledgment. The work was financially supported by the National Natural Science Foundation of China (30872029), the Key Natural Science Foundation of Beijing Municipality (6071001), the Natural Science Foundation of Beijing Municipality (6092007), the Key Foundation of Beijing Municipal Education Committee (KZ201010020016), and Funding Project for Academic Human Resources Development in Institutions of Higher Learning Under the Jurisdiction of Beijing Municipality (PHR20090516, PHR200906134).

References

1. Xu, H.H., Zhang, Z.X., Cha, Y.G.: Development prospects of China's pesticide plant. Pesticide 43(3), 1–10 (2003)
2. Shi, G.L., Zhao, L.L., Liu, S.Q., Cao, H.R., Clarke, Sun, J.H.: Acaricidal Activities of Extracts of *Kochia scoparia* against *Tetranychus urticae*, *Tetranychus cinnabarinus*, and *Tetranychus viennensis* (Acari: Tetranychidae). Journal of Economic Entomology 99(3), 858–863 (2006)
3. Shi, G.L., Liu, S.Q., Cao, H., Zhao, L.L., Li, J., Li, S.Y.: Acaricidal Activities of Extracts of *Stellera chamaejasme* against *Tetranychus viennensis* (Acari: Tetranychidae). Journal of Economic Entomology 97(6), 1912–1916 (2004)
4. Wang, Y., Shi, G.L., Wang, Y.N., Wu, Z.Y.: Acaricidic activity of herbal extracts against *Tetranychus cinnabarinus*. *Chinese Agricultural*. Science Bulletion 24(5), 323–326 (2008) (in Chinese)
5. Cao, H., Wang, Y.N., Zhang, T.Q., Zhao, L.L., Li, S.Y., Shi, G.L.: Acaricidal Actions of *Wikstroemiae chamedaphne* against *Tetranychus viennensis.*. Scientia Silvae Sinicae 43(8), 65–70 (2007)
6. Wang, Y.N., Shi, G.L., Zhao, L.L., Clarke, S.J.H.: Acaricidal activity of Juglans Regia leaf extracts on Tetranychus viennensis and Tetranychus cinnabarinus (Acari: Tetranychidae). Journal of Economic Entomology 100(4), 1298–1303 (2007)
7. Effects of Tagetes erecta extracts on glutathione-S-transferase and protease activities and protein content in Tetranychus viennensis. Chinese Journal of Applied Ecology 18(2), 400–404 (February 2007)
8. FAO. Recommended methods for measurement of pest resistance to pesticides. FAO 21, 49–53 (1980)
9. Abbort, W.S.: . A method of computing the effectiveness of an insecticide. J. Am. Mosq. Control Assoc. 3, 302–303 (1987)
10. Caulfield, M.P.: Muscarinic receptors—characterization, coupling and function. Pharmacology & Therapeutics 14, 319–329 (2002)

Effects of Stigmasterol to Activities of Several Enzymes of Tetranychus cinnabarinus

Dan-dan Duan, Chun-ya Bu, Jun Cheng, Lan-qing Ma, Yu-bo Liu, You-nian Wang, and Guang-lu Shi*

Key Laboratory of Urban Agriculture (North) of Ministry of Agriculture, P.R. China
Beijing University of Agriculture
Beijing, China
glshi@126.com

Abstract. The acaricidal activity of stigmasterol was carried out on the Tetranychus cinnabarinus, using the slide dip technique. Here the female adult mites were treated by the Stigmasterol extracted from Inula japonica. Bioassay-guided purification of the 12th fraction had higher activity against the T. cinnabarinus, Gas chromatography-mass spectrometry (GC/MS) demonstrated that the chemical composition of the active fraction 12th sample was mainly composed of Stigmasterol. That had not been reported before. And the acaricidal mechanism of Stigmasterol to T. cinnabarinus is unknown. Our results showed that the nervous symptoms of the T. cinnabarinus in response to the Stigmasterol. The protein content, the acetylcholine esterase (AChE) activity, the Calcium enzyme ATP (Ca2+-ATPase) activity and Sodium enzyme ATP (Na+-ATPase) activity of the mites treated with Stigmasterol were assayed. The results showed that the protein content and the activity of AchE in the T. cinnabarinus treated with the Stigmasterol were increased. The activity of Ca2+-ATPase and Na+-ATPase were induced by the Stigmasterol. The effects of the T. cinnabarinus indicated that the central nervous system was the main target of Stigmasterol. The long time over excitation caused the treated mites to die.

Keywords: Stigmasterol, Tetranychus cinnabarinus, activity of enzyme.

1 Introduction

Tetranychus cinnabarinus is an important agricultural animal. For many years, these mites were sufficiently controlled using synthetic chemical acaricides. Recently, however, people have experienced increased resistance by mites to chemical pesticides, which are also known to leave residues in agricultural products such as vegetables and fruits. Thus there has been increased emphasis on nonchemical integrated pest management control tactics for *T. cinnabarinus*. The high effective and low residue pesticides will instead the high toxic pesticides in the 21th century. Today

* Corresponding author.

E. Zhu and S. Sambath (Eds.): Information Tech. and Agricultural Eng., AISC 134, pp. 721–729.
springerlink.com © Springer-Verlag Berlin Heidelberg 2012

the plant source pesticides are highly regarded for the plentiful natural source, environment-friendly, low toxic residue, high selective, no harm to the natural enemies of pests and environment. However, more botanical bioactive compound need to be identified and more toxicological effects of botanicals need investigation. Some compounds from plants with the antifeeding effects and insecticide activities have been found. For example, the acaricidal activities of extracts were found in *Kochia scoparia*, *Stellera chamaejasme* and *Juglans regia* leaf against *Tetranychus urticae*, *Tetranychus cinnabarinus* and *Tetranychus viennensis* (Shi, G. L., 2006; Shi, G. L., 2004; Wang, Y. N., 2007).

There is a growing interest in natural triterpenoids, also known as phytosterols, due to their wide spectrum of biological activities (P.G. Bradford, 2007). Triterpenes are natural components of human diets and are largely derived from cereals, fruits, vegetables, and plant-derived oils (P.G. Bradford, 2007). One such triterpene which has gained wide attention of medical professionals, pharmaceutical marketers, and researchers all around the world is Stigmasterol.

The purpose of this study was to examine the potential miticidal activity of Stigmasterol to the *T. cinnabarinus*. Then revealed the acaricidal mechanism of the Stigmasterol against the *T. cinnabarinus*. The results of this study could be useful for the development of new botanical agents for the control of this serious mite.

2 Materials and Methods

2.1 Isolation of the Inula japonica

The *I. japonica* was bought from Beijing Tong Ren Tang drugstore. The dried *I. japonica* was ground to fine powder. Then the powder was sieved with a sieved (the bore diameter 0.38 mm). The adult female *T. cinnabarinus* were reared at an ambient photoperiod of 18: 6h (L: D), a room temperature of 27 ± 2 ℃, and a relative humidity of 60 % at the Key Laboratory of Agricultural Technology in Beijing University of Agriculture.

The cold-soaked extracting method was used to get the extraction of Stigmasterol. 10 kg of the fine powder were put into flask and was immersed with petroleum ether at room temperature. The volume of the solvents was five times that of the powder. The powder was extracted for 3 days and was extracted three times. Afterwards, the mixture was combined and passed through filter papers, and then was concentrated using a rotary evaporator (R-220, Büchi Labortechnik AG, Switzerland). Twenty grams of extracts diluted in petroleum-ether were mixed with 250 ml methanol in a 500-ml separating funnel (Beijing Glass Factory, Beijing, China), and stayed at room temperature for 24 h. This step was repeated for three times. Afterwards, the methanol parts and the petroleum-ether parts were respectively concentrated using a rotary evaporator and weighed.

The silica gel column chromatography was used to further isolate the acaricidal components from the petroleum-ether extract of *I. japonica*. After the column was balanced using the solvent petroleum-ether, seven grams of extract was loaded into the column. This was followed by eluting the column step by step using 11 solvents with ratio of petroleum-ether to dichloromethane: 10: 0, 9: 1, 8: 2, 7: 3, 6: 4, 5: 5, 4: 6, 3: 7,

2: 8, 1: 9 and 0: 10 respectively. A flow velocity of 6 ml per minute was used to elute the column, and a total of 750 fractions were collected. Thin-layer chromatography (TLC) (model GF 254, silica gel 60 precoated commercial plates, 20 × 10 cm, 0.2 - 0.25cm in thickness, Tian-He Medical Instrument Company, Tianjin, China) was used to compare constituents in each of the 750 fractions. Each fraction sample was partitioned into separate bands from the bottom to the top of the plate in TLC. Based on band appearance under daylight and UV light the 750 fractions were pooled into 38 groups. Each group was then concentrated and kept at 4 ℃ for later study.

2.2 GC/MS Analysis

The chemical components of the fractions with high acaricidal activities isolated from I. japonica was further analyzed by GC/MS (Agilent 6890/5973N), using chromatography equipped with a fused silica capillary column. The temperature was programmed from 150 ℃ to 180 ℃ at 2 ℃/min, followed by 5 ℃/min to 200 ℃, and then 8 ℃/min to 250 ℃. Injector temperatures were set at 250 ℃. The GC/MS analysis had a quadrupole MS system, operating at 70 eV, and the ion source kept at 230 ℃. Helium was used as the carrier gas at the rate of 1 ml/min. The compounds were identified by comparing the means of their retention times with mass spectral data (MS) from reference NIST library (National Institute of Standards and Technology).

2.3 Bioassay

The contact toxicity of the extracts of the Stigmasterol against *T. cinnabarinus* was identified with the slide dip technique according to (FAO, 1980). The extracts were diluted into different concentration with Water-Tween 80 solvent 20: 1 *V/V*, and 10 % Tween 80 was used as a control. The healthy female adults of *T. viennensis* were selected with a #0 brush pen. 40-50 female adults were stuck on each glass slide with double-sided adhesive. The glass slides with mites on were dipped into the extraction of *I. japonica* for 5 seconds. The superfluous solution around the mites was removed. 24 hours later, the number of living mites and dead mites was checked and the mortality was calculated. The experiment was repeated for three times and the average mortality was got. The mortality was adjusted according to Abbott's formula (Abbott, 1925) and calculated with SPSS13.0 (SPSS, 2004) for Windows.

2.4 Sample Preparation for the Enzyme Activities Assay

The sample 150 mites were collected at 4 h, 8 h, 12 h, 16 h, 20 h and 24 h hours after treatment to determine the enzyme activities. Then they were immediately ground in different buffer solution according to different enzyme under ice bath. The supernatant was collected by centrifugation (10,000 × G, 15 min) at 4 ℃ for the further research.

2.5 Determination of the Protein Content

Protein concentration mensuration: Coomassie brilliant blue G-250 method was employed in our test to determine the protein concentration. 0.1 ml the prepared enzyme liquid or 0.1 ml phosphate buffer (as control) was mixed into 5 ml Coomassie brilliant blue G-250 solvent. The mixture was heated in the 25 ℃ water bath for 2

minutes. Then OD_{595} was measured and the concentration of protein was obtained according to the standard curve.

2.6 Acetylcholinesterase Activity Determination

The activities of acetylcholinesterase of the *T. cinnabarinus* was determined with the acetylcholinesterase (AChE) detection Kit produced by Nanjing Jiancheng Bioengineering Institute, China. The acetylcholinesterase activity was determined according to the method described by. The Ache was used as the substrate to measure the acetylcholinesterase activity of the treated female mites. The enzyme liquid was mixed and reacted with the Ache solution for 15 minutes at 27 ℃. Then 0.3 ml physostigmine (1 mmol.L^{-1}) was added to the mixture to end the reaction. The OD_{412} were detected with the DTNB as color developing reagent.

2.7 Determine the Atp Enzyme Activity

The activities of ATPase of the *T. cinnabarinus* was determine with the Na^{+}-ATPase and Ca^{2+}-ATPase detection Kit produced by Nanjing Jiancheng Bioengineering Institute, China.

3 Results

3.1 Identification of the Fraction with High Acaricidal Activity

The petroleum ether re-extract of the I. japonica was separated into 38 fractions (G_1, G_2, G_3-G_{38}) by the column chromatography and silica gel thin layer chromatography. The contact toxicities of these 38 fractions to *T. cinnabarinus* were further determined using glass slide-dipping method. Our results showed that at a concentration of 4 mg/ml, mite mortality rate of fraction 12 was higher than 50 %. The result of GC/MS showed that it is Stigmasterol, and matching degree higher than 90%. So G_{12} was researched deeply.

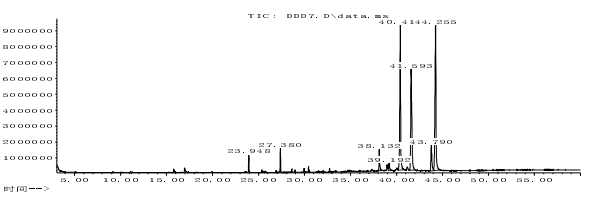

Fig. 1. Identification of the G_{12} fraction

3.2 Contact Toxicity of Extracts on Tetranychus cinnabarinus

In our study, the *I. japonica* extracts exhibited high toxicity to *T. cinnabarinus* (Table 1). From table 1, we can also see that the 12 fractions and Stigmasterol caused significantly higher mite mortality rates. Our results showed that at a concentration of 4 mg/ml, mite mortality rates of 12 fractions was higher than 50 %, and Stigmasterol was higher than 60 %.

Table 1. The mortality of extracts from Inula britanica against Tetranychus cinnabarinus

Extracts(4 mg•mL-1)	Extraction rate/%	Mortality/%
Fraction 12	1.38 ± 0.12	58.48 ± 0.2142
Stigmasterol	0.92 ± 0.05	67.33 ± 0.16
CK		4.09 ± 0.13

3.3 Effect of the 12th Fraction on the Protein Content of the Treated Mites

The protein contents of the mites were detected at the 4th, 8th, 12th, 16th, 20th and 24th hour after the mites were treated (Fig. 2). The results showed that the change of the protein content after treatment was similar to the control group. However, the protein content of the treated mites was significant higher than that of the control group.

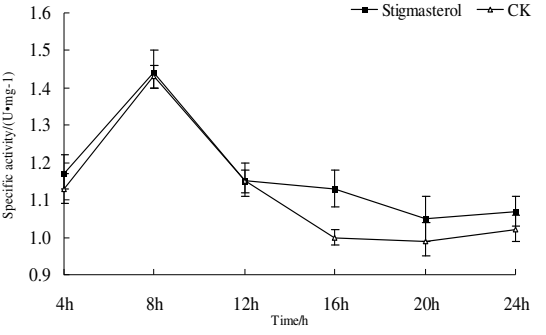

Fig. 2. Effect of protein content of the Stigmasterol against *Tetranychus cinnabarinus*

3.4 Effect of the 12th Fraction against the Nervous System of Tetranychus cinnabarinus

The enzymes of the mites were detected at the 4 h, 8 h, 12 h, 16 h, 20 h and 24 h hour after the mites were treated. The activity changes of the acetylcholinesterase, the Na^{+}-ATPase and Ca^{2+}-ATPase of the treated mites were detected respectively.

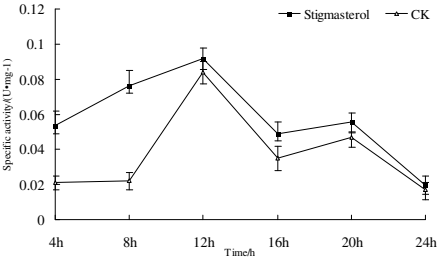

Fig. 3. Effect of TChE activity of the Stigmasterol against *Tetranychus cinnabarinus*

As Fig. 3 indicated, the change trend of the acetylcholinesterase of the treated mites was similar to that of the control mites, but the specific activity of the treated mites was higher than that of the control mites. The result indicated that the activity of the acetylcholinesterase was activated significantly by the 12^{th} fraction. The specific activities of the acetylcholinesterase of the treated mites at the 4^{th}, 8^{th}, 12^{th} after treatment were 2.5, 3.4 and 1.1 times of that of the control mites respectively.

As Fig. 4, 5 showed that the change trends of the specific activities of the Na^+-ATPase and Ca^{2+}-ATPase of the treated mites were similar to that of the control group mites, but the activities of the treated mites were all lower than that of the control mites. The activities of the control mites at the 4^{th}, 8^{th}, 12^{th}, 16^{th}, 20^{th} and 24^{th} after treatment were 1.9, 1.4, 2.1, 1.5, 1.9 and 2.6 times of that of Na^+-ATPase of the treated mites respectively, and the activities of the control mites at the 4^{th}, 8^{th}, 12^{th}, 16^{th}, 20^{th} and 24^{th} after treatment were 2.3, 5.7, 2.5, 2.1, 1.4 and 1.1 times of that of the Ca^{2+}-ATPase of the treated mites respectively. That was to say the activities of the Na^+-ATPase and Ca^{2+}-ATPase was inhibited significantly by the 12^{th} fraction.

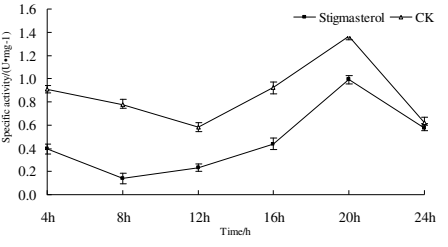

Fig. 4. Effect of Ca^{2+}-ATPase activity of the Stigmasterol against *Tetranychus cinnabarinus*

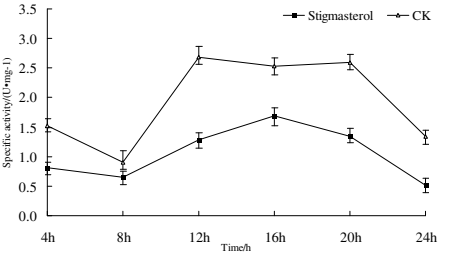

Fig. 5. Effect of Na^+-ATPase activity of the Stigmasterol against *Tetranychus cinnabarinus*

4 Discussion

There is a growing interest in natural plant sterols. The plant sterols can inhibit the cholesterol absorption in rats (Ikeda I, 1988), and has the abilities of cholesterol lowering (David K, 2005), tumor inhibition (Awad A B, 2001), prevention the hypertrophy of prostate (Kassen A, 2000). One such plant sterols which has gained

wide attention of medical professionals, pharmaceutical marketers, and researchers all around the world is Stigmasterol.

Stigmasterol has a wide range of biological activity. Such as, it reduces plasma cholesterol levels and inhibits hepatic synthesis and intestinal absorption in the rat (Batta AK, 2006). The hepatoma cell SMMC-7721, BEL-7402 were inhibited in vitro and the hepatoma cell H22 was inhibited in vivo by Stigmasterol. The proliferation cycle the hepatoma cell was inhibited by Stigmasterol. The apoptosis of the hepatoma cell was promoted (Zhang S *et al*., 2008; Fang Yan Xiong, 2004; Zhang Shuo, 2005). Adrenal cortical hormone and luteinizing hormone pharmaceuticals were synthesized through Stigmasterol. Stigmasterol has a very wide range of applications of biotechnology and pharmaceutical sectors (Moreau R A, 2002). It was found that plasma incorporation of stigmasterol was significantly lower than that of campesterol and sitosterol in agreement with earlier studies in the rabbit where it was shown that stigmasterol was not absorbed (R. Schonheimer, 1930), whereas the lymphatic absorption of Stigmasterol has been shown to be similar to that of sitosterol when administered intragastrically to rat (G.V. Vahouny, 1983).Thus, we considered that stigmasterol was discriminated against more strongly for intestinal absorption and hepatic secretion than sitosterol and might competitively inhibit cholesterol and plant sterol absorption while simultaneously suppressing hepatic cholesterol synthesis. Although there are several reports on the intestinal absorption and metabolism of campesterol and sitosterol (G. Salen, 1970; A.M. Lees, 1977; S.M. Grundy, 1969), little is known about the fate of stigmasterol in humans and animals (*T. Heinemann*, 1993), even the activity of Stigmasterol to the *T. cinnabarinus*.

Our results showed that at a concentration of 4 mg/ml, mite mortality rates of 12 fractions was higher than 50%, and stigmasterol was higher than 60%. Through observing the toxicities symptoms of the *T. cinnabarinus* in the active stigmasterol, may affect the nervous system. The further research showed that the activities of several important enzymes of the treated mites *T. cinnabarinus* were changed.

According to the results, we supposed that the target of stigmasterol worked on might be the nervous system of the mites. The acetylcholinesterase is an important enzyme of the nervous system of creatures. The acetylcholinesterase which improves the acetylcholine to hydrolyze is mainly in the nervus centralis and the sympathetic nervous system (Wang, Y. C. 2004.). The acetylcholinesterase can keep the nerve conduction in correct condition by hydrolyzing the acetylcholine of the neurotransmitter, so it is the important target of the organophosphorous and N-Methyl carbonates pesticides (Kondo M, 1995). The change trend of the acetylcholinesterase of the treated mites was similar to that of the control mites, but the specific activity of the treated mites was higher than that of the control mites.

The results showed that the activities of the Na^+-ATPase and Ca^{2+}-ATPase of the treated female mites were inhibited significantly by the stigmasterol. The extracellular concentrations of Ca^{2+} were regulated by the Ca^{2+}-ATP enzyme. Our results indicated that the activities of the Ca^{2+}-ATP enzyme were inhibited. The neurotransmitters threshold potential was declined. In particular, Ca^{2+} is an important material in the process of neural signal transduction. Maybe the nervous system of the *T. cinnabarinus* is the target of the Stigmasterol.

Acknowledgements. The work was financially supported by the National Natural Science Foundation of China (30872029), the Key Natural Science Foundation of Beijing Municipality (6071001), the Natural Science Foundation of Beijing Municipality (6092007), the Key Foundation of Beijing Municipal Education Committee (KZ201010020016), and Funding Project for Academic Human Resources Development in Institutions of Higher Learning Under the Jurisdiction of Beijing Municipality (PHR20090516, PHR200906134).

References

1. Batta, A.K., Xu, G., Honda, A., Miyazaki, T., Salen, G.: Stigmasterol reduces plasma cholesterol levels and inhibits hepatic synthesis and intestinal absorption in the rat. Metabolism 55(3), 292–299 (2006)
2. Wang, Y.C.: Insect physiology, pp. 202–203.China Agriculture Publishment Company (2004)
3. Kondo, M., Hada, T., Fukui, T.: Enzyme-linked immunosorbent assay(ELISA) for Aleuria aurantia lectinreactive serum cholinesterase to differentiate liver cirrhosis and chronic hepatitis. Clin. Chim. Acta 243, 1–9 (1995)
4. Ikeda, I., Tanaka, K., Sugano, M., Vahouny, G.V., Gallo, L.L.: Inhibition of cholesterol absorption in rats by plant sterols. J. Lipid Res. 29(12), 1573–1582 (1988)
5. Salen, G., Arhens, E.H., Grundy, S.M.: Metabolism of β-sitosterol in man. J. Clin. Invest. 49, 952–967 (1970)
6. Lees, A.M., Mok, H.Y.I., McCluskey, M.A., et al.: Plant sterols as cholesterol-lowering agents: clinical trial in patients with hypercholesterolemia and studies of sterol balance. Atherosclerosis 28, 325–338 (1977)
7. Grundy, S.M., Arhens, E.H., Davignon, J.: The interaction of cholesterol absorption and cholesterol synthesis in man. J. Lipid Res. 10, 304–315 (1969)
8. Heinemann, T., Aztmann, G., von Bergmann, K.: Comparison of intestinal absorption of cholesterol with different plant sterols in man. Eur. J. Clin. Invest. 23, 827–831 (1993)
9. Schonheimer, R., Behring, H., Hummel, R.H.: Uber die spezifitat der resorption von sterin, abhanging von ihren konstitution. Hoppe-Seyler Z Physiol. Chem. 192, 117–124 (1930)
10. Vahouny, G.V., Connor, W.E., Subramaniam, S., et al.: Comparative lymphatic absorption of sitosterol, stigmasterol, and fucosterol and differential inhibition of cholesterol absorption. Am. J. Clin. Nutr. 37, 805–809 (1983)
11. Shuo, Z., Wang, Y., Lei, W., et al.: Inhibitive effect of Stigmasterol from Hedyotis diffusa willd on hepatoma cells in vitro & vivo and its influence on transplanted H22 tumor cell's multiplication cycle, apoptosis. Progress in Modern Biomedicine 8(11), 2016–2017 (2008)
12. Fang, Y., Zhang, Y., Chen, M., et al.: An anti-tumor traditional Chinese herb: Hedyotis diffusa willd and its active ingredients. Chinese Patent Medicine 26(7), 577–579 (2004) (in Chinese)
13. Zhang, S.: Experimental research of anti-cancer effects and related mechanism of compound Traditional Chinese Medicine of Qian Kun Ning.Chengdu University of Tradtional Chinese Medicine (2005) (in Chinese)
14. Moreau, R.A., Whitaker, B.D., Hicks, K.B., et al.: Hicks, Phytosterols, phytosterols, and their conjugates in foods: structural diversity, quantitative analysis, and health-promoting uses. Progress in Lipid Research 41, 457–500 (2002)
15. David, K., Chen, S.C.: Phytosterols - Health Benefits and Potential Concerns: A Review. Nutrition Reasearch (25), 413–428 (2005)

16. Awad, A.B., Williams, H., Fink, C.S.: Phytosterols Reduce in Vitro Metastatic Ability of MDA-MB- 231 Human Breast Cancer Cells. Nutrition and Cancer 40(2), 157–164 (2001)
17. Kassen, A., Berges, R., Senge, T.: Effect of Beta- Sitosterol on Transforming Growth Factor - Beta - 1 Expression and Translocation Protein Kinase C Alpha in Human Prostate Stromal Cells in Vitro. European Urology 37(6), 735–741 (2000)
18. Bradford, P.G., Awad, A.B.: Phytosterols as anticancer compounds. Mol. Nutr. Food Res. 51, 161–170 (2007)
19. Shi, G., Liu, S.Q., Cao, H., Zhao, L.L., Li, S.Y.: Acaricidal activities of extracts of Stellera chamaejasme against Tetranychus viennensis (Acari: Tetranychidae). J. Econ. Entomol. 97, 1912–1916 (2004)
20. Shi, G., Zhao, L.L., Liu, S.Q., Cao, H., Clarke, R., Sun, J.H.: Acaricidal Activities of Extracts of Kochia scoparia against Tetranychus urticae, Tetranychus cinnabarinus and Tetranychus viennensis (Acari: Tetranychidae). J. Econ. Entomol. 99, 858–863 (2006)
21. Wang, Y.-N., Shi, G.L., Zhao, L.L., Liu, S.Q., Yu, T.Q., Clarke, S.R., Sun, J.H.: Acaridical activity of Juglans regia leaf extracts on Teranychus viennensis and Tetranychus cinnabarinus (Acari: Tetranychidae). J. Econ. Entomol. 100, 1298–1303 (2007)
22. Abbott, W.S.: A method of computing the effectiveness of an insecticide. J. Econ. Entomol. 18, 265–267 (1925)
23. FAO. Food and Agriculture Organization. Revised method for spider mites and their eggs (Tetranychus spp. and Panonychus ulmi Koch). FAO Plant Prod. Prot. 21, 49–54 (1980)
24. SPSS, Inc., SPSS base 11.5 user's guide. SPSS Inc., Chicago, IL (2004)
25. Wang, M.T., Xie, P.S., Wang, Z.D., et al.: The Extraction Isolation and Structural Identification of Natural organic compounds. Chemical Industry Press, Beijing (2004)
26. Mu, L.: Methodology of plant chemical protection, pp. 160–161. China Agriculture Publishing Company, Beijing (1994)
27. He, Y.X., Wang, C.F., Chen, F.: Effect of Insecticides on Esterase Activity in Beet Armyworm (Spodoptera exigua). Acta Agriculturae Universitatis Jiangxiensis 25(6), 896–899 (2003)

Acaricidal Activities of the Polygonum Aviculare Extracts against Tetranychus cinnabarinus and Its Affection to the Enzyme Activities

Yong-sheng Jin, Qing Li, Jun Cheng, Lan-qing Ma, Yu-bo Liu, You-nian Wang, and Guang-lu Shi*

Key Laboratory of Urban Agriculture (North) of Ministry of Agriculture, P.R. China
Beijing University of Agriculture, Beijing, China
glshi@126.com

Abstract. This paper showed a study on acaricidal activities of the plant extracts from Polygonum aviculare against Tetranychus cinnabarinus and its affection to the activity among several relative enzymes. The plant extracts were prepared using different solvents such as chloroform, petroleum ether and methanol. It was found that the corrected mortality of female adults could reach 89.95 % (2 mg·mL-1) and the main lethal concentrations (LC50) was 0.7153 ± 0.1253 mg·mL-1 when using chloroform as the solvent, which exhibited best acaricidal activities among three solvents ($P < 0.05$). Through further extraction and column chromatography, we obtained 19 components from the chloroform extracts, and the number 2, 7, 8, 15, 16, 17 and 18 components had acaricidal activities higher than 70%, among them, number 16 had highest motality (87.12 %). Furthermore, colorimetry assay showed that the component number 16 could affect the activity of acetylcholinesterase (AChE), Na+, K+-ATPase, GSH-S-transferase (GSTs) of T. cinnabarinus.

Keywords: Tetranychus cinnabarinus, Polygonum aviculare, acetylcholinesterase (AChE), Na+, K+-ATPase, GSH-S-transferase.

1 Introduction

The carmine spider mite *Tetranychus cinnabarinus* is one of the most important pest worldwide (Hazan *et al*., 1974; Ho *et al*., 1997). Because of the characters such as small body size, high fertility, high population density, usually making serious damage (Shi *et al*., 1994; Li *et al*., 1992), and higher ability in developing acaricide-resistance than other mites, costs of controlling *T. cinnabarinus* are increasing steadily by years. It is imperative to find new acaricide with high efficiency and environmental friendly. Botanical acaricide has good selectivity, low toxicity to non-target organisms, high degradable rate, low ability in forming resistance by mites and safety to natural enemies. Therefore, using plant extracts with high bio-activity in developing new biogenic acaricide or producing new pesticides had already been one of the hot spots of pesticide research and developing science.

* Corresponding author.

E. Zhu and S. Sambath (Eds.): Information Tech. and Agricultural Eng., AISC 134, pp. 731–738.
springerlink.com © Springer-Verlag Berlin Heidelberg 2012

Polygonum aviculare, annual or perennial herb in Polygonaceae, distributes in Henan, Sichuan, Zhejiang, Shandong, Jilin and Hebei provinces. Most of studies of *P. aviculare* were about the medical use its extractions, and little knowledge was known about using *P. aviculare* extractions in acaricide development. In this paper, we studied the acaricidal activities of *P. Aviculare* extracts against *T. cinnabarinus*; the potential action mechanism of the extractions was discussed.

2 Materials and Methods

2.1 Materials

The plants used in this study were ground by Rotor Speed Mill (6202, Beijing Huaya Tianyuan Machine Technology Co., LTD) and then sieved by 40 meshes. The powder was stored in the fridge (BCD-278WNN, QINGDAO HAIER Co., LTD) until used. The susceptible strain of *T. cinnabarinus* was reared indoor without pesticide exposure (25 ± 1 ℃, 50 ± 10% RH and 18: 6 h L: D photoperiod). All the chemicals used in this study were AR grade (Beijing Chemical Works).

2.2 Methods

Immersion Extraction: Plant powder was put into a wide-neck bottle, immersed in organic solvents with 5 × volume of powder for 3 day - 5 day, and replicated 3 times at room temperature (25 ± 2 ℃). Then, same extract liquids was pooled and followed by vacuum concentration to paste shape and weigh.

Extraction: 15 g immersion extraction was dissolved with 10 × volume petroleum ether and extract three times by methanol in separating funnel. Pool same extract liquids and followed by vacuum concentration to paste shape and weigh.

Column Chromatography: The silica gel (100 × weight than extracts, 100 - 200 mesh) was mixed with appropriate amount of eluent and injection into chromatography columns immediately, open the cap of the end of the column and shake the column with a rubber hammer, the silica particles would precipitate in the bottom of the column while the solution flowing down slowly. Dissolved 7 g extracts in a small amount of the initial eluent, and then inject it into the column when the liquid surface in the column was about 1 cm away from the surface of precipitated silica. After the extracts moved into silica in the column, covered it with a layer of quartz sand, and then eluted the column with petroleum ether, chloroform, methanol elution solvent system, respectively. The flow rate is 10 ml/min and components are collected every 50 ml. Components were separated by thin layer chromatography (TLC), and detected it in iodine vapor, respectively. Pooled same components and concentrated under vacuum.

Bioassay: Slide dipping was conducted in bioassay according to FAO (1980). Thirty female healthy adults in same age were stick onto a glass slide, soaked in solution of extracts for 5 s, and then air dry. Treated mites were put at room temperature (25 ± 1 ℃) for 24 h, individuals with no activity while being touched were considered as dead. Corrected mortality is then calculated according to Abbort (1987). Poison

symptom was observed according to Zhu et al. (2002). Clean bean leaves were put on water culture plate, then thirty adults were transferred onto each piece of leaf. Leaf with mites were co-soaked in solution of extracts (2 mg·mL^{-1}) for 5 s, using water only as CK. Blade edge was surrounded by wet cotton to prevent mites from escaping. The adults' activity and touching-reaction were observed every 12 h in 48 h duration.

Enzyme Preparation: Mites were treated according to contact toxicity method. Totally 150 treated female mite adults were used to homogenate in 0.25 ml 0.9 % NaCl solution on ice. Homogenate mix was then centrifuged at 10,000 r/min, 4 ℃ for 15 min and supernatant was collected. Protein concentration was tested via Coomassie Brilliant Blue G-250 method (Mu, 1991). Activities of AchE, Na^+, K^+-ATPase and GSH-S-transferase were detected according to Mu (1991).

3 Results

3.1 Contact Toxicity of P. aviculare Extracts to T. cinnabarinus

The extraction rate of three solvents were methanol (11.86 ± 0.56) % > chloroform (2.65 ± 0.38) % > petroleum ether (1.56 ± 0.08) %. After 48 h exposure, chloroform extracts (CE) exhibited highest mortality (89.95 %) among three solvents at the concentration of 2 mg·mL^{-1} ($P < 0.05$, Table 1), therefore, we further extracted and purified CE.

Table 1. Extract rate and mortality of different extracts from *P. aviculare* against *Tetranychus cinnabarinus*

Extracts(2 mg•mL^{-1})	Extraction rate/%	Mortality/%
Petroleum ether extract	1.56 ± 0.09	49.51 ± 2.97^b
Chloroform extract	2.65 ± 0.32	89.26 ± 3.93^a
Methanol extract	11.86 ± 1.05	13.61 ± 7.35^c

Values are mean ±SE of three determinations; the averages within the same column not followed by the same letter are significantly different at 5% level of confidence, the same below.

3.2 Contact Toxicity of further Extracted CE to T. cinnabarinus

After a second extraction on CE, the extraction rate was petroleum ether extracted CE (58.42 ± 1.40) % > methanol extracted CE (32.88 ± 2.32) % > insoluble substance (8.70 ± 0.68) %, respectively. Bioassay results showed that the highest mortality was caused by insoluble substance, and followed by methanol extracted CE and petroleum ether extracted CE ($p<0.05$, Table 2), which indicated that the acaricidal active ingredient was in the insoluble substance.

Table 2. Extract rate and mortality of chloroform extracts from *P. aviculare* against *T.cinnabarinus*

Extracts(2 mg•mL^{-1})	Extraction rate/%	Mortality/%
Petroleum ether extract	58.42 ± 1.40	32.69 ± 1.32^{c}
indiscerptible substance	8.70 ± 0.68	84.00 ± 5.32^{a}
Methanol extract	32.88 ± 2.32	40.74 ± 2.64^{b}

3.3 Contact Toxicity of TLC Separated Components

Bioassay was based on nineteen components separated by column chromatography and TLC detection (Table 3). Results showed that the No. 2, 7, 8, 15, 16, 17 and 18 components had acaricidal activities higher than 70 %, among them; number 16 had highest motality (87.12 %).

Table 3. Extract rate and mortality of fractions of chromatography extract of *P. aviculare* against *T.viennensis*

Component (2 mg•mL^{-1})	Isolation rate/%	Mortality/%
1	2.77	69.52 ± 7.36^{c}
2	1.68	76.61 ± 7.26^{b}
3	2.04	38.55 ± 14.03^{f}
4	0.68	38.49 ± 3.77^{f}
5	1.02	36.86 ± 6.25^{f}
6	0.42	47.08 ± 3.30^{e}
7	0.26	73.68 ± 3.07^{bc}
8	3.23	76.94 ± 13.27^{b}
9	2.12	58.5 ± 7.18d
10	0.45	15.46 ± 9.21^{h}
11	0.67	11.29 ± 15.73^{h}
12	0.49	4.72 ± 0.21^{i}
13	1.14	27.83 ± 0.19^{g}
14	0.98	67.45 ± 7.08^{c}
15	2.28	71.87 ± 7.36^{c}
16	22.32	87.12 ± 0.04^{a}
17	2.90	83.20 ± 6.32^{a}
18	5.48	75.68 ± 4.12^{bc}
19	14.23	61.99 ± 6.22^{d}

The component number 16 was then diluted into five concentrations (0.5, 1, 2, 4, 8 mg·mL^{-1}) for bioassay. The toxicity regression equations (y=5.2702 + 1.0038x) and LC_{50} (0.988 mg·mL^{-1}) were calculated according to the bioassay results.

3.4 Poison Symptom Observation

The concentration of 2 mg·mL^{-1} was used in poison symptom observation experiments. In poison symptom observation experiment, component number 16 and water were used as treatment and control, respectively. During the first 12 hours after treatment, the mites of treated group exhibited hyperactivity symposium and moved around in excitement and laid a lot of eggs, while mites of control group did not.

During 12 h - 24 h after treatment, the treated group mites were still hyperactive, and body fluid began to extravasate, while control group moved normally and began to lay eggs. In the duration 24 h - 36 h after treatment, the mites in treated group kept extravasating and began to shrink, while the control group moved normally. During the last 36 h - 48 h after treatment, the mites in treated group was shrinking to death, while mites in the control group lived well. These poison symptoms are similar with neurotoxic agent, which indicated that the active ingredient of *P. Aviculare* extracts may act on insect nervous system.

3.5 Activity Assay of AchE

Component number 16 (2 mg·mL^{-1}) and water were used as treatment and control to spray on mites used in this experiment, respectively. The specific activity of treated group (0.0098 U·mg^{-1} prot) was significantly lower than that of control group ($P < 0.01$), which was 4.75 fold higher than that of treated group at 8 h after treatment. During 16 h - 48 h after treatment, the specific activity ration of control group/treated group were 2.83, 1.75, 1.94, 2.47, respectively (Fig. 1), which indicated the inhibition activity of component number 16 on AchE in *T. cinnabarinus*.

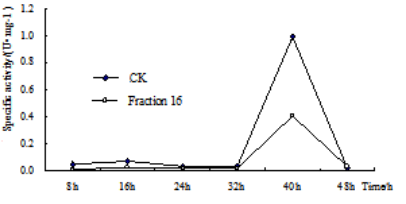

Fig. 1. Effect on the activity of AChE of the extracts of *P. aviculare* against *T.cinnabarinus*

3.6 Activity Assay of Na^+, K^+-ATPase

Component number 16 (2 mg·mL^{-1}) and water were used as treatment and control to spray on mites used in this experiment, respectively. The activities of Na^+, K^+-ATPase were similar between treated group and control group at 8 h, 16 h, 32 h and 40 h after treatment, but significantly different at 24 h and 48 h after treatment, and the specific activity of control group was as 3.18 and 18 folds higher than that of treated group, respectively (Fig. 2).

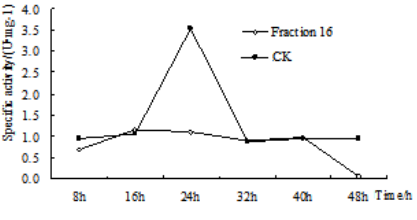

Fig. 2. Effect on the Na^+, K^+-ATPase activity of the extracts of *P. aviculare* against *T.cinnabarinus*

3.7 Effect on Activity of GSTs

GSTs are one of the most important detoxification enzymes in mites, the detoxification function could be achieved through catalyzing the conjugation reaction between the electrophilic toxic compounds and endogenous glutathione. Component number 16 (2 mg·mL^{-1}) and water were used as treatment and control to spray on mites used in this experiment, respectively. The component number 16 could inhibit the activity of GSTs at 8 h, 24 h, 32 h and 40 h after treatment, and the specific activity of control group was as 1.29, 1.26, 1.29 and 1.32 folds as that of treated group, respectively. But the specific activity of control group was as 0.52 folds as that of treated group (Fig. 3).

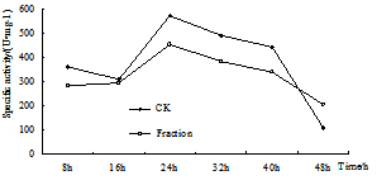

Fig. 3. Effect on the GSTs activity of the extracts of *P. aviculare* against *T.cinnabarinus*

4 Discussion

We analyzed the acaricidal activity substances from *P. aviculare* by extraction, column chromatography and Spectroscopy, and found that the active ingredient could affect the activity of AchE, Na^+, K^+-ATPase and GSTs *in vitro*. Most of the acaricides kill mites by disturbing the mite nervous system, and the poisonous symptoms are usually exhibited as shivering, spasticity, paralysis or other behavior disorder. The pulse transmission among nerve cells is mainly based on the balance of synthesis and degradation of neurotransmitter, it has been reported that many neurotransmitters, such as acetylcholine, gamma amino butyric acid and ammonium nitrate, have been proven to be the target of acaricide. The poison symptom observed in this study was similar with the nerve poison agent mentioned before; therefore, we detected the activity of AchE and Na^+, K^+-ATPase, two of the most important enzymes in mite nervous system, after treatment with component number 16. Acetylcholine is expressed in the synaptic cleft of nerve system and can be decomposed by AchE, thereby terminating pulse transmission, once the enzyme is inhibited, it will lead to insect death by causing hyperactivity (Lin *et al*., 2001). Na^+, K^+-ATPase distributed in the cell membrane and endoplasmic reticulum membrane, and is related with Na^+, K^+ transferring. Once the enzyme is inhibited, the permeability of membrane to ions decreased, then Na^+ concentration will increase because of the inhibition of Na^+ current, resulting in a constant state of excitement in nerve membrane, then triggering the nervous system dysfunction, ultimately leading to insect death. The results in this paper showed that the Na^+, K^+-ATPase activity of the mites treated by component number 16 shared similar dynamics change with control group along time, and during 40 h - 48 h after treatment, both Na^+, K^+-ATPase and AChE activity from mites of

treated group were inhibited significantly, which corresponding with the expressed period of poison symptoms. We could deduce that the active ingredient may act on the two enzymes to cause interruption of nerve transmission, and resulting in mite death. GSTs catalyzes the conjugation of glutathione (GSH) and electrophilic group of exogenous toxins *in vivo*, and the final product is excreted. The increasing of GSTs' activity can be used as sensitive indicator of the injury of animal tissue (Shen *et al*., 1990). This highly efficient detoxification system plays an important role in the adaptation of the organism to the unsuitable environmental factors. From this point of view, the results that GSTs activity in treated group is inhibited indicated that the active ingredient of *P. Aviculare* extracts might affect the normal detoxification of *T. cinnabarinus*, which leading to accumulation of toxic substances in the mites and resulting in death.

Most of reports about utilization of *P. aviculare* extract limited in clinical field. Hyoung Ja Kim *et al*. (1994) isolated *Astragalus saponins*, *Polygonum aviculare* glycosides, oak leather glycosides, bayberry bark saponins from *P. aviculare*. Zheng *et al*. (1999) isolated five flavonoids from *P. aviculare*. Vysochina (1998) isolated uglanin, kaempferol, myricetin, myricetin-3-O-(Gal) 2 and two unknown flavonoids from the aerial parts of *P. aviculare*. Yu *et al*. (2002) isolated eight materials from *P. aviculare*. Zhao *et al*. (2002) isolated ten compounds from the acetone extracts of *P. aviculare*. Chen *et al*. (2004) isolated 13 compounds from the ethyl acetate extracts of *P. aviculare*. Zheng *et al*. (1999) isolated ketone a-camphene, linalool, key press oil enolase and camphene from the volatile oil of *P. aviculare*. Al-Hazimi *et al*. (2002) isolated 6-methoxyplumbagin from the acetone extracts of *P. aviculare*. It had been reported that *P. aviculare* extract has insecticidal activity on *Helicoverpa armigera*, *Plutella xylostella* and *Pieris rapae*, but the acaricidal activities of *P. aviculare* extract has not been reported before. In this study, we separated *P. aviculare* extract into 19 components and component number 16 showed highest acaricidal activities, the poison symposium of it indicated that the active ingredient from *P. aviculare* might act on nerve system of *T. cinnabarinus*. These results provided fundamental data for further determining the structure of the active ingredient, toxicology study and development of new botanical pesticides.

Acknowledgements. The work was financially supported by the National Natural Science Foundation of China (30872029), the Key Natural Science Foundation of Beijing Municipality (6071001), the Natural Science Foundation of Beijing Municipality (6092007), the Key Foundation of Beijing Municipal Education Committee (KZ201010020016), and Funding Project for Academic Human Resources Development in Institutions of Higher Learning Under the Jurisdiction of Beijing Municipality (PHR20090516, PHR200906134).

References

1. Abbort, W.S.: Amethod of computing the effectiveness of an insecticide. J. Am. Mosq. Control Assoc. 3, 302–303 (1987)
2. Al-Hazimi, H.M., Haque, S.N.: A new naphthoquinone from Polygonum aviculare. Nat. Prod. Lett. 16, 115–118 (2002)

3. FAO. Revised method for spider mites and their eggs (Tetranychusspp. and *Panonychus ulmi* Koch). FAO Plant Production, 21, 49–54 (1980)
4. Hazan, A., Gerson, U., Tahori, A.S.: Spider mite webbing I, the production of webbing under various enviromental conditions. Acarologia 16, 68–84 (1974)
5. Ho, C., Maggi, V.: Spider mite (Acari: Tetranychidae) on various crops in Taiwan. J. Agr. Res. China 46, 333–346 (1997)
6. Kim, H.J., Woo, E.-R., Park, H.: A novel lignan and flavonoids from Polygonum aviculare. J. Nat. Prod. 57(5), 581–586 (1994)
7. Mark, A., Roger, G.H.: Downer biochemical and physiological targets for miticides. Pestic Sci. 40, 85–101 (1994)
8. Vysochina, G.I.: Total and individual contents of several of the principal flavonoids found in aerial parts of *Polygonum aviculare* grown in Siberia. Rastitel. Resursy 34(4), 47–55 (1998)
9. Chen, X.: Pharmaceutical Disciplines, The chemical constituents of Polygonum aviculare. Chinese Materia Medica 29(9), 918–919 (2004)
10. Li, L., Li, L., Fan, Y., et al.: Chinese jujube tree pests. China Agriculture Press, Beijing (1992)
11. Lin, Z., Zhang, L.: Phosphine on the impact of acetylcholinesterase. Zhengzhou Institute of Technology 22(4), 35–41 (2001)
12. Mu, L.: Plant chemical protection methods. China Agriculture Press, Beijing (1991)
13. Fukami, J., Uesugi, Y., Hao, S., et al.: Pesticide Experiments - Fungicides article. Agricultural Publishing House, Beijing (1991); Translation: Plum, A., Cheng, T.
14. Shen, T., Wang, J.-Y.: Biochemistry. Higher Education Press, Beijing
15. Shi, G.-L., Zheng, W.-Y., Dang, Z.-P., Li, L.-C.: Fruit pests. China Agriculture Press, Beijing (1994)
16. Yu, Z.-H., Sun, J.: The chemical constituents of *Polygonum aviculare*. Herbal Medicine, 33 (6), 495–499
17. Zhang, Z.: Insect toxicology of new development. Beijing University Press, Beijing (1982)
18. Zhao, A.-H., Fact, Z.Q., Lin, Z., et al.: The chemical constituents of Polygonum aviculare. Natural Product Research and Development 14(5), 29–32 (2002)
19. Zheng, X.-D., Hu, H.-B., Zheng, S., et al.: Qingyang Wu Polygonum volatile oil constituents. Northwest Normal University (Natural Science) 35(3), 68–70 (1999)
20. Zheng, X.-D., Tiao, S.: Qingyang Wu Polygonum study of flavonoids. Northwest Normal University (Natural Science) 35(2), 47–49 (1999)
21. Zhu, L.-M., Ni, Y.-P., Huang, C.-X., et al.: Mites Comprehensive Test Methods. Nanjing Agricultural College 17(1), 13–17 (2002)

Identification of Acarcidal Compounds in Inula japonica Extracts against Tetranychus cinnabarinus

Dan-dan Duan, Chun-ya Bu, Lan-qing Ma, Yu-bo Liu,
You-nian Wang, and Guang-lu Shi*

Key Laboratory of Urban Agriculture (North) of Ministry of Agriculture, P.R. China
Beijing University of Agriculture, Beijing, China
glshi@126.com

Abstract. In this study, we aimed to identify acaricidal compounds in Inula japonica against Tetranychus cinnabarinus. Here, I. japonica petroleum-ether extracts were found toxic to T. cinnabarinus with a LC50 value of 1.18 mg/ml. Silica gel column chromatography was used to further separate acaricidal components from I. japonica petroleum-ether extracts. Contact toxicity data showed that 17 out of 38 fractions groups had mite mortality rates above 50%, 9 fraction groups above 60 %, and fractions groups G5, G7 and G15 even above 80 % at a concentration of 2 mg/ml. The major vital compounds in the bioactive fraction groups were identified by GC/MS, and four compounds, namely β-Sitosterol (1), Stigmasterol (2), Lupeol (3), and α-Amyrin (4) were determined to have acaricidal activity to Tetranychus cinnabarinus.

Ketwords: Inula japonica, acaricidal activity, Tetranychus cinnabarinus.

1 Introduction

Tetranychus cinnabarinus, also called spider mites or boisduval, are serious pests for many vegetables including beans, eggplants, peppers, tomatoes and cucurbits (Zhang *et al*. 2007; Cakmak *et al*. 2005; Zhang J P *et al*. 2004; He *et al*. 2005). *Tetranychus cinnabarinus* can also cause serious damage to orchard trees such as apple (*Malus pumila*), pear (*Pyrus bretschneideri*) and peach (*Pruns persica*) (Kielkiewicz. 1996; Pande *et al*. 1996; Shi *et al*. 1996). *Tetranychus cinnabarinus* can produce 10 - 20 generations per year in China, and develop from eggs to adults in about one week (Shi *et al*. 1996). Although normally they do not kill their host plants directly, *T. cinnabarinus* can significantly weaken their host plant vigor. The heavily infected trees may even lose their leaves and fruits, resulting in yield reduction and leaf loss (Shi et al. 1996; Gotoh. 1984). Recently, *T. cinnabarinus* have developed serious resistance to many chemical pesticides such as fenpyromimate, pyridaben, tebufenpyrad and pyrimidifen (Granham *et al*. 1985; Grosscurt *et al*. 1988; Gu *et al*. 2000; Sagawa *et al*. 1972; Shen 1999). Since *T. cinnabarinus* are highly reproductive mites and have short generation time, they can build up their population very fast. Outbreak of *T. cinnabarinus* is sudden. It is urgent to develop alternative acaricides which have low frequency to

* Corresponding author.

E. Zhu and S. Sambath (Eds.): Information Tech. and Agricultural Eng., AISC 134, pp. 739–746.
springerlink.com © Springer-Verlag Berlin Heidelberg 2012

cause *T. Cinnabarinus* resistance. Plant insecticides are desirable in pest control as they are often environmentally benign and with low frequency to cause pest resistance. Botanical compounds may be alternative acaricides to control *T. cinnabarinus*.

Inula japonica is a traditional Chinese herbal medicine with antibetchic, anti-microbial and anti-tumor effects. Recently, *I. japonica* extracts were reported to have antifungal activity against *Sphaerotheca fuliginea*, *Pseudoperonospora cubensis*, *Colletotrichum orbiculare*, *Botrytis cinerea*, *Alternaria solani* and *Fulvia fulva* (Wang Hong-gang *et al*. 2007). So far, three active anti-fungi compounds have been identified in *Inula britannica*. One was sesquiterpene compound, 1-O-Acetylbritannilactone, and the other two were triterpenes compounds, Taraxasteryl palmitate and Taraxasterol acetate (Ding *et al*. 2005). In our previous research, we found that the extract of *I. japonica* had high acaricidal activity against *T. cinnabarinus*. Isolation and identification of bioactive compounds in *I. japonica* could provide a potential approach in developing new pesticides to control *T. cinnabarinus*. In this study, we identified potential acaricidal compounds in *I. japonica*. against *T. cinnabarinus.*

2 Materials and Methods

2.1 Materials

Inula japonica were purchased from Beijing Tong Ren Tang drugstore. Dried *I. japonica* were then ground into fine powder using a HYP-150 Crusher (Huan-ya-tian-yuan Machinery Ltd., Beijing, China) followed by filtering through a Φ 200 × 50mm screen. Subsequently, *I. japonica* powder was collected and sealed in black plastic bags at room temperature (27 ± 3 ℃, 40 % relative humidity) for later study. *Tetranychus cinnabarinus* were raised and maintained in Key Laboratory of New technology of Agricultural Application of Beijing at a temperature of (27 ±2) ℃, 60 % RH and a photoperiod of 16: 8 h (L: D). The mites were fed on leaves of *Vigna unguiculata,* which were grew in greenhouse and had six true leaves.

2.2 Preparation of the Crude Extract of I. Japonica

The petroleum-ether was used as solvent in the preparation of *I. japonica* extracts. Ten kilograms of *I. japonica* powder were mixed with 50 L petroleum-ether (Analytical grade, Beijing Chemical Reagents Company, Beijing, China) in a 50L bottle and kept at room temperature (27 ± 2 ℃) for 3 d. This step was repeated for three times. Then, the mixtures were combined, passed through filter papers, and concentrated in a rotary evaporator (R-220, Büchi Labortechnik AG, Switzerland). Twenty grams of above extracts were diluted in petroleum-ether and then mixed with 250 ml methanol in a 500-ml funnel (Beijing Glass Factory, Beijing, China). The mixture stayed at room temperature for 24 h. Once the methanol and petroleum-ether were separated, the two parts were concentrated individually in a rotary evaporator and weighed. This step was repeated for three times. Their extraction rates were calculated by the ratio of extract weight (kg) to the total *I. japonica* powder weight.

2.3 Chromatography Analysis of the Concentrated Extracts

A silica gel column chromatography was used for further isolation of the acaricidal components from the petroleum-ether extract of *I. japonica*. After the column was

balanced by petroleum ether, seven grams of extract was loaded into the column. Subsequently, the column was eluted orderly by 11 solvents with their petroleum-ether/dichloromethane ratios 10: 0, 9: 1, 8: 2, 7: 3, 6: 4, 5: 5, 4: 6, 3: 7, 2: 8, 1: 9 and 0: 10, respectively. A flow velocity of 6 ml per minute was used to elute the column. Total 750 fractions were collected. Thin-layer chromatography (TLC) (model GF 254, Tina-He Medical Instrument Company, Tannin, China) was used to compare the constituents of 750 fractions. Based on their TLC patterns, the 750 fractions were pooled into 38 groups. Each group was further concentrated and kept at 4 ℃ for later study.

2.4 Toxicity Test

Acaricidal activities of various samples against *T. cinnabarinus* were determined by glass slide-dipping method. Various extracts, fraction groups or compounds (β-Sitosterol, Stigmasterol, Lupeol and *α*-Amyrin bought from sigma) were diluted with 10 % Tween 80 at a concentration of 2 mg/ml respectively. The 10 % Tween 80 was used as control. Female adult mites were affixed on double-sided adhesive tape, which was pre-attached to one end of a 10 × 2 cm glass slide. Afterwards, the mites were individually dipped into various sample solution or control for 5 s. Once the slide was removed, any extra solution was absorbed with filter papers. Total 30 females were used in each dosage assay. All treated mites were maintained at a temperature of (27 ± 2) ℃, 60 % RH and a photoperiod of 16: 8h (L: D). the mite mortality rates were determined 24 h after each treatment (FAO 1980). The tested mites were considered dead if mites did not move when touched gently with a camel hair brush. All treatments were replicated for three times.

2.5 GC/MS Analysis

The chemical components of the high bioactive fractions isolated from *I. japonica* was further analyzed by GC/MS (Agilent 6890/5973N), using chromatography equipped with a fused silica capillary column. The temperature was programmed from 150 to 180 ℃ at 2 ℃ /min, followed by 5 ℃/min to 200 ℃, and 8 ℃/min to 250 ℃. Injector temperature was set at 250 ℃. The GC/MS analysis had a quadruple MS system operated at 70 eV. The ion source was kept at 230 ℃. Helium was used as the carrier gas with a flow rate of 1 ml/min. The compounds were identified by comparing the means of their retention times with mass spectral data (MS) from reference NIST library (National Institute of Standards and Technology).

2.6 Statistical Analyses

The mite mortality rates of various treatments were corrected according to the mortality rate of the control group using Abbott's formula (Abbott 1925). The corrected mortality rates were further normalized by an arcsine square-root transformation and subjected to one-way analysis of variance. Independent-Samples-T-Test and One-Way ANOVA with Duncan were used to compare the differences of the mortality rates between different groups. All statistical analyses were performed using SPSS 13.0 (SPSS Institute. 2004).

3 Results

3.1 Contact Toxicity of Various Extracts, Fraction Groups on T. cinnabarinus

In our study, the *I. japonica* extracts exhibited high toxicity to *T. cinnabarinus*. As showed in Table 1, the *I. japonica* petroleum-ether extracts caused significantly higher mite mortality rates than methanol extracts ($P < 0.05$). The *I. japonica* petroleum-ether extracts had a LC_{50} value of approximately 1.18mg/ml, while the LC_{50} value of methanol extracts was 3.46 mg/ml. Thus, petroleum-ether was chosen as the solvent to prepare crude extracts for further concentration and partition.

Table 1. Contact toxicity of Inula japonica extracts against Tetranychus cinnabarinus

Extract solvent	Regressive equation	Correlation coefficient (r)	LC_{50} / (mg·mL^{-1})	95% confidence limit
Petroleum ether	Y=4.79+2.83x	0.93	1.18±0.09	1.02~1.37
Methanol	Y=4.02+1.82x	0.37	3.46±0.62	1.74~4.28

The *I. japonica* petroleum-ether extracts were further partitioned using silica gel column chromatography. Total 750 fractions were collected and divided into 38 groups based on their thin layer chromatography patterns. The contact toxicities of 38 groups against *T. cinnabarinus* were further tested by glass slide-dipping method. Our results showed that at the concentration of 2 mg/ml, 17 fractions groups had mite mortality rates higher than 50%, nine higher than 60%, G_5, G_7 and G_{15} fractions even higher than 80 % (Table 2).

Table 2. Contact toxicity of various fractions groups obtained by column chromatography against *Tetranychus cinnabarinus*

Fraction groups	Mortality ± SE (%)	Fraction	Mortality± SE (%)
*G_1(100-105)	78.48±0.79	*G_{20}(1326-1619)	76.02±0.70
*G_2(106-126)	57.38±0.19	G_{21}(1620-1735)	22.41±0.76
*G_3(127-200)	75.56±0.69	*G_{22}(1835-1935)	55.19±0.13
*G_4(201-208)	51.83±0.04	G_{23}(2000-2135)	46.59±0.08
*G_5(209-219)	90.86±1.33	G_{24}(2200-2317)	25.95±3.07
*G_6(220-230)	67.12±0.44	G_{25}(2318-2323)	46.15±0.10
*G_7(231-235)	85.53±1.06	G_{26}(2324-2326)	31.31±0.31
G_8(300-310)	32.14±0.46	G_{27}(2327-2330)	41.53±0.21
*G_9(311-335)	53.42±0.08	G_{28}(2401-2435)	15.12±1.03
G_{10}(400-435)	30.43±0.51	G_{29}(2500-2520)	44.16±0.15
G_{11}(535-612)	33.33±0.43	G_{30}(2611-2630)	34.78±0.39
*G_{12}(613-635)	58.48±0.21	G_{31}(2631-2635)	31.03±1.99
G_{13}(701-724)	31.33±0.49	G_{32}(2700-2705)	23.31±0.76
G_{14}(803-928)	59.06±0.23	G_{33}(2706-2735)	45.57±0.11
*G_{15}(929-1009)	84.40±1.01	G_{34}(2800-2807)	38.82±0.28
*G_{16}(1010-1025)	59.26±0.23	G_{35}(2808-2815)	23.43±0.72
*G_{17}(1026-1119)	64.05±0.36	G_{36}(2816-2825)	15.74±0.85
*G_{18}(1120-1230)	75.00±0.67	G_{37}(2826-2835)	43.24±0.17
*G_{19}(1231-1325)	54.03±0.10	G_{38}(2900-2935)	37.43±0.32
CK	9.03±0.65	-	-

3.2 Identify Acarcidal Compounds in High Bioactive Fraction Groups

Since most petroleum-ether extracts are volatile, GC/MS was used to identify the acaricidal compounds in the active fractions with their mite mortality rates above 50%. The identified volatile compounds from the *I. japonica* fractions were listed in Table 3. From the study results, we can see that the majority of volatile compounds in the bioactive fractions of *I. japonica* are monoterpenes or triterpenes. For example, major volatile compounds in G_5 are 4, 4, 6a, 6b, 8a, 11, 11, 14b -Octamethyl-1, 4, 4a, 5, 6, 6a, 6b, 7, 8, 8a, 9, 10, 11, 12, 12a, 14, 14a, 14b-octadecahydro-2H-picen-3-one and Lup-20(29)-en-3-one, á-Amyrin and Lupeol found in G_7, and dibutyl phthalate detected in G_{15}. The other compounds, such as Octacosane, 9, 19-Cyclolanost-24-en-3-ol, acetate, and Lup-20(29)-en-3-ol, acetate, were also found in the high bioactive fractions.

Table 3. Identification volatile chemical components from the bioactive fractions groups by GC/MS

Compound	Fraction No.	Relative amounts in its Fraction (%)	Relative amounts in extracts(%)
Octacosane	G_1	25.9	
9,19-Cyclolanost-24-en-3-ol, acetate	G_1	34.5	
Lup-20(29)-en-3-ol, acetate	G_{3-4}	100	2.17
4, 4, 6a, 6b, 8a, 11, 11, 14b -Octamethyl - 1, 4, 4a, 5, 6, 6a, 6b, 7, 8, 8a, 9, 10, 11, 12, 12a, 14, 14a, 14b – octadecahydro - 2H - picen -3-one	G_5	16.6	0.13
Lup-20(29)-en-3-one	$G_{5, 6}$	14.5/28.7	1.02
Friedelin	G_6	6.0	0.07
á-Amyrin	$G_{7, 9}$	26.9/61.3	2.07
Lupeol	$G_{7, 9}$	58.7/13.4	2.76
Octadecanal	G_9	3.2	0.05
á-Amyrin	G_9	61.3	0.89
Stigmasterol	G_{12}	54.4	4.19
β-Sitosterol	G_{12}	38.9	2.99
Dibutyl phthalate	$G_{15, 16-20}$	100.0 / 63.0	1.93

3.3 Contact Toxicity of Four Compounds Identified by GC/MS on T. cinnabarinus

The acaricidal activity of four compounds (β-Sitosterol, Stigmasterol, Lupeol and *α*-Amyrin) identified by GC/MS was determined by glass slide-dipping method. The study results showed that the mite mortality rates of all the four compounds were above 50% at a concentration of 2 mg/ml. Especially, *α*-Amyrin had a high mite mortality rate of 82.82%. LC_{50} value of the four compounds was further tested. *α*-Amyrin had a LC_{50} value of 0.511 mg/ml, while the others were all above 1 mg/ml.

Table 4. Contact toxicity of standard compounds against *Tetranychus cinnabarinus*

compounds	Regressive equation	Correlation coefficient (r)	LC_{50}/(mg·mL^{-1})	95% confidence limit
β-Sitosterol	Y=3.61+2.55x	0.89	1.55±0.49	3.12~3.95
Stigmasterol	Y=4.49+2.15x	0.93	1.72±0.17	1.42~2.08
Lupeol	Y=4.16+2.27x	0.94	1.37±0.30	2.01~2.74
α-Amyrin	Y=5.62+2.12x	0.97	0.51±0.05	0.41~0.63

4 Discussion

Inula japonica is traditional Chinese herbal medicine with antibetchic, anti-microbial and anti-tumor activity. So far one sesquiterpene, 1-O-Acetylbritannilactone, and two triterpenes, Taraxasteryl palmitate and Taraxasterol acetate, were identified as anti-fungal compounds in *I. japonica* by Ding Hai-xin *et al* (2005). Further, *I. japonica extracts* were reported to have antifungal activity against *Sphaerotheca fuliginea*, *Pseudoperonospora cubensis*, *Colletotrichum orbiculare*, *Botrytis cinerea*, *Alternaria solani* and *Fulvia fulva* (Wang Hong-gang *et al*. 2007). In this study, high acarcidal activity was detected in the petroleum-ether extracts of *Inula japonica* with a LC_{50} value of approximately 1.18 mg/ml. GC/MS analyses were used to identify the acaricidal compounds in the bioactive fractions from *Inula japonica*. The study results showed that the majority of volatile compounds in the bioactive fractions are monoterpenes or triterpenes. Triterpenes are plant secondary metabolites or allele chemicals produced by plants as defense substances against plant-feeding pests. The mixtures of these low molecular weight volatiles are called essential oils, which often have significant insect toxicity. Triterpenes were also found to have antimicrobial, hepatoprotective and anti-inflammatory effects (Laszczyk et al. 2006).

In developed countries, an average of 250 mg per day of botanic triterpenes (member of phytosterol family) is consumed by one person (Saleem M. 2009). Lupeol (also known as Fagarsterol), is a triterpene found in white cabbage, green pepper, strawberry, olive, mangoes and grapes. Lupeol was reported to be therapeutic and chemopreventive agents in anti-inflammation and anti-cancer treatments (Laszczyk e*t al*. 2006; Saleem M. 2009). Furthermore, Lupeol and Sitosterol were isolated from the petroleum ether extract of *Sapium baccatum* leaves, and both of them showed high activity in brine shrimp lethality bioassay (Yunus *et al*. 2009). Strong antimicrobial activity was detected both in Lupeol and *β*-Sitosterol isolated from *Dunalia spinosa* (Erazo *et al*. 2008). Lupeol from *Curtisia dentata* was also reported as an antibacterial and antifungal triterpenoid (Shai *et al*. 2008). From a methanol extract of dried-ground aerial parts of *Senecio lyratus*, an active anti-fungal and anti-bacterial compound was isolated and identified as *β*-sitosterol by spectroscopic analysis (Kiprono *et al*. 2000). *β*-Sitosterol was found in a variety of plants as an anti-tumor, anti-microbial, chemopreventive and immunomodulatory compound (Yuk *et al*. 2007; Ovesná *et al*. 2004). Recently, beta-sitosterol was identified in the acaricidal fractions of *Mentha piperita* (Ren Jianjun *et al*. 2009). In this study, four compounds (*β*-Sitosterol, Stigmasterol, Lupeol and α-Amyrin) identify from the *Inula japonica* were found to have acarcidal activity to *T. cinnabarinus*. Especially, á-Amyrin had a LC_{50} value of

0.511mg/ml. Based on our results and other related studies, the four terpenes (β-Sitosterol, Stigmasterol, Lupeol and α-Amyrin) that we identified from the petroleum ether extracts *of I. japonica* maybe potential botanical acaricides.

Acknowledgements. The work was financially supported by the National Natural Science Foundation of China (30872029), the Key Natural Science Foundation of Beijing Municipality (6071001), the Natural Science Foundation of Beijing Municipality (6092007), the Key Foundation of Beijing Municipal Education Committee (KZ201010020016), and Funding Project for Academic Human Resources Development in Institutions of Higher Learning Under the Jurisdiction of Beijing Municipality (PHR20090516, PHR200906134).

References

1. Abbott, W.S.: A method of computing the effectiveness of an insecticide. J. Econ. Entomol. 18, 265–267 (1925)
2. Cakmak, B.H., Madanlar, N.: Control of the carmine spider mite *Tetranychus cinnabarinus* Boisduval by the predatory mite *Phytoseiulus persimilis* (Athias-Henriot) in protected strawberries in Aydin, Turkey. Turkey Journal of Agriculture and Forest 29, 259–265 (2005)
3. Chaturvedi, P.K., Bhui, K., Shukla, Y.: Lupeol: connotations for chemoprevention. Cancer Lett. 263(1), 1–13 (2008)
4. Cranham, J.E., Helle, W.: Pesticide resistance in Tetranychides. In: Helle, W., Sabelis, M.W. (eds.) Spider Mites: their Biology, Natural Enemies and Control, vol. 1B, pp. 405–421. Elisevier, Amsterdam (1985)
5. Ding, H.-X., Li, G.-Z., Feng, J.T., Zhang, X.: Anti-fungi active compounds from Inula britannica. Journal of Northwest A&F University (Natural Science Edition) 33(3), 90–94 (2005)
6. Erazo, S., Rocco, G., Zaldivar, M., Delporte, C., Backhouse, N., Castro, C., Belmonte, E., Delle Monache, F., García, R.: Active metabolites from *Dunalia spinosa* resinous exudates. Z Naturforsch C 63(7-8), 492–496 (2008)
7. FAO. Plant production and protection 21recommended methods for measurement of resistance to pesticides, Rome, Italy, 49–54 (1980)
8. Gotoh, T.: Annual life cycle of the hawthorn spider mite, *Tetranychus viennensis* Zacher (Acarina: *Tetranychidae*) on deciduous oak. Japan. J. Appl. Entomol. Zool. 28, 254–259 (1984)
9. Grosscurt, A.C., Haar, M.T., Jongsma, B., Stoker, A.: A new acaricide and insecticide interfering with chitin deposition. Elsev. Appl. Sci. Pub. 22, 51–59 (1988)
10. Gu, Y., Zhang, Y.C., Zhao, C.D., Li, S.X.: Toxicity comparison on a few acaricides to three species spider mites. J. Laiyang Agri. Coll. 17, 203–206 (2000)
11. He, L., Zhao, Z.M., Cao, X.F., Deng, X.P., Wang, J.J.: Resistance selection of *Tetranychus cinnabarinus* to fenpropathrin and genetic analysis. Scientia Agricultura Sinica 38, 719–724 (2005) (in Chinese)
12. Kielkiewicz, M.: Dispersal of Tetranychus cinnabarinus on various tomato cultivars. Entomol. Exp. Appl. 80, 254–257 (1996)
13. Kiprono, P.C., Kaberia, F., Keriko, J.M., Karanja, J.N.: The in vitro anti-fungal and anti-bacterial activities of beta-sitosterol from *Senecio lyratus* (Asteraceae). Z Naturforsch C 55(5-6), 485–488 (2000)

14. Laszczyk, M., Jäger, S., Simon-Haarhaus, B., Scheffler, A., Schempp, C.: Physical, chemical and pharmacological characterization of a new oleogel-forming triterpene extract from the outer bark of birch (betulae cortex). Planta Med. 72(15), 1389–1395 (2006)
15. Ovesná, Z., Vachálková, A., Horváthová, K.: Taraxasterol and beta-sitosterol: new naturally compounds with chemoprotective / chemopreventive effects. Neoplasma 51(6), 407–414 (2004)
16. Pande, Y.D., Ray, D.C., Saha, H.P.: Seasonal incidence of *Tetranychus cinnabarinus* (Boisd.) (Acarina: *Tetranychidae*) and loss and yield in Okra corp. J. Advan. Zool. 17, 7–14 (1996)
17. Ren, J., Shi, G., Wang, J., Gu, J., Wang, Y.: Isolation and Identif ication of the Principal Acaricidal Components Extracted from *Mentha piperita*. Scientia Silvae Sinicae 45(6), 77–82 (2009)
18. Sagawa, T., Hirano, S., Takahashi, H., Tanaka, N., Oishi, H., Ando, K., Togashi, K.: A new miticidal antibiotic. II. miticidal and other biological properties. J. Econ. Entomol. 65, 372–375 (1972)
19. Saleem, M.: Lupeol, a novel anti-inflammatory and anti-cancer dietary triterpene. Cancer Lett. 285(2), 109–115 (2009)
20. Shai, L.J., McGaw, L.J., Aderogba, M.A., Mdee, L.K., Eloff, J.: Four pentacyclic triterpenoids with antifungal and antibacterial activity from *Curtisia dentata* (Burm.f) C.A. Sm. leaves. J. Ethnopharmacol. 119(2), 238–244 (2008)
21. Shen, H.M.: Resistance and cross-resistance of *Tetranychus viennensis* (Acari: *Tetranychidae*) to 14 insecticides and acaricides. System. Appl. Acarol. 4, 9–14 (1999)
22. Shi, G.L., Liu, X.Q.: China walnut pests. Chinese Agriculture and Sci-technology Press, Beijing (1996)
23. Wang, H.-G., Wang, W.-Q., Han, X.-Y., Zhang, X.-F., Ma, Z.-Q., Li, H.-X., Chi, G.-T.: Primary Studies on Inhibitory Effect of *Inula japonica* Extract against 6 Phytopathogenic Fungi. Acta Agriculturae Boreali-Sinica. 22 (Suppl.), 225–229 (2007)
24. Yuk, J.E., Woo, J.S., Yun, C.Y., Lee, J.S., Kim, J.H., Song, G.Y., Yang, E.J., Hur, I.K., Kim, I.S.: Effects of lactose-beta-sitosterol and beta-sitosterol on ovalbumin-induced lung inflammation in actively sensitized mice. Int. Immunopharmacol. 7(12), 1517–1527 (2007)
25. Ahmed, Y., Sohrab, M.H., Al-Reza, S.M., Tareq, F.S., Hasan, C.M., Sattar, M.A.: Antimicrobial and cytotoxic constituents from leaves of Sapium baccatum. Epub. ahead of print, November 22 (2009)
26. Zhang, Y.-Q., Ding, W., Zhao, Z.-M., Wu, J., Fan, Y.-H.: Studies on Acaricidal Bioactivities of *Artemisia annua* L. Extracts Against Tetranychus cinnabarinus Bois (Acari: Tetranychidae) Agricultural Sciences in China 7(5), 577–584 (2008)
27. Zhang, J.P., Wang, J.J., Zhao, Z.M., Dou, W., Chen, Y.: Effects of simulated acid rain on the physiology of carmine spider mite, *Tetranychus cinnabar* in us (Boisduvals) (Acari: *Tetranychidae*). Journal of Applied Entomology 128, 342–347 (2004)

Characterization of Synonymous Codon Usage in the Newly Identified Duck Plague Virus UL16 Gene

Qin He[1], Mingshu Wang[1,2], Anchun Cheng[1,2,3], Dekang Zhu[1,2], Xiaoyue Chen[1,2,3], Renyong Jia[2], Qihui Luo[2], Yi Zhou[2], and Zhengli Chen[2]

[1] Avian Disease Research Center College of Veterinary Medicine of Sichuan Agricultural University, Ya'an, Sichuan, 625014, China
[2] Key Laboratory of Animal Diseases and Human Health of Sichuan Province, Sichuan Agricultural University, Ya'an, Sichuan, 625014, China
[3] Epizootic Diseases Institute of Sichuan Agricultural University, Ya'an, Sichuan, 625014, China
chenganchun@vip.163.com

Abstract. A comparative analysis of the codon usage bias in the newly identified UL16 gene(GenBank accession no.EU195095) of DPV and the UL16 gene of 22 reference herpesviruses was performed. In this study, the synonymous codon usage bias of UL16 gene in the 23 herpesviruses have been analyzed and the results showed obvious differences by the CAI, RSCU, ENC and GC_{3s}. The results revealed that the synonymous codons with A and T at the third codon positon have widely usage in the codon of UL16 gene of DPV. The ENC-GC_{3s} plot revealed that the genetic heterogeneity in UL16 gene of herpesviruses was constrained by G+C content at the third codon position. The phylogenetic analysis suggested that DPV was evolutionarily closer to herpesviruses which further clustered into Alphaherpesvirinae. Furthermore the ORF of DPV UL16 gene has sequential rare codons. There were 21 codons showing distinct usage differences between DPV with Escherichia coli, 19 codons showing distinct usage differences between DPV with yeast, and 20 between DPV and Human. Therefore the Escherichia coli, Yeast and Human expression system were suitable for the expression of DPV UL16 gene if some codons could be optimized.

Keywords: Duck plague virus, UL16 gene, codon usage bias.

1 Introduction

Codon Usage Bias was defined as deviation from equal usage of synonymous codons[1]. Within the standard genetic codes used in a number of different ways, all amino acids except Met and Trp are coded by 2–6 synonymous codons, but the synonymous codon usage are not used equally both within and between genomes[2]. Previous research have been showed that codon usage bias may be very complicated and associated with various biological factors, such as gene expression level[3], gene length[4], gene translation initiation signal[5], protein amino acid composition[6], protein structure[7], tRNA abundance[8,9], mutation frequency and patterns[6,10], GC composition[11,12], and environmental factors[13]. For a number of different

E. Zhu and S. Sambath (Eds.): Information Tech. and Agricultural Eng., AISC 134, pp. 747–761.
springerlink.com © Springer-Verlag Berlin Heidelberg 2012

organisms, it was suggested that codon usage is best explained by selection for tRNA abundance, gene expression levels, and translational optimization[14]. Recently, it was also suggested that codon usage is related to gene function[15,16] and the the evolutionary history of an organism in metazoan genomes[17]. Codon usage bias can reveal information about the molecular evolution of individual genes and provide data to train genome-specific gene recognition algorithms which recognize protein coding regions in uncharacterized genomic DNA. Codon usage bias is also widely studied in particular organisms to achieve high expression of heterologous proteins in vitro and to vaccine design where the efficient expression of viral proteins may be required to generate immunity[18,19]. Recently, analyses of the patterns of codon usage bias of herpesviruses are primarily focused on the pseudorabies virus (PRV)[20], herpes simplex virus type 1 (HSV-1)[21], Epstein-Barr virus [22], but the codon usage bias in DPV genome was known little.

Duck plague, which is caused by duck plague virus(DPV), a member of the Herpesviridae family, is an acute, lethal and contagious disease that occurs worldwide among domestic and wild ducks, geese, swans, and other water fowl, with migratory waterfowl contributing to spread between continents[23,24]. Now most of the previous research work has focused on the epidemiology and prevention of this disease. However, the molecular biology information about the DPV genome is limited. Recently, the UL16 gene was isolated and identified from DPV CHv strain in our laboratory[25]. The UL16 gene of herpes simplex virus encodes tegument proteins, which are conserved throughout the herpesvirus family[26]. Little is known about the molecular informations and function of DPV UL16 protein at present. In this study, we first analyzed the synonymous codon usage in the UL16 gene of DPV and compared with those of 22 other species of herpesviruses. Moreover, the codon usage bias in the DPV genes was compared with those of *Escherichia coli*, Yeast and Human. In addtion, we also investigated the rare codons of UL16 gene. All these datas might provide some insights into the features of the DPV genome, the possible function of DPV UL16 gene as well as the suitable expression system in in vitro.

2 Materials and Methods

2.1 Virus Species and Gene Sequences

The DPV CHv strain, a high-virulence strain of DPV, was obtained from Key Laboratory of Animal Disease and Human Health of Sichuan Province. The UL16 gene of the DPV CHv strain was isolated and identified by our laboratory. The nucleotide sequences of the UL16 gene of 22 reference herpesviruses were obtained from the NCBI GenBank nucleotide database (table 2).

2.2 Analysis on Codon Usage in UL16 Gene of DPV and 22 Reference Herpesviruses

For each gene, codon usage was estimated by using CAI, CHIPS and CUSP program of EMBOSS. The RSCU values of UL16 gene was analyzed with the CodonW. Generally, The‘Effective Number of Codons’(ENC) was often used to quantify the codon usage bias of an ORF in an individual gene. The values range from 20 to 61.

In an extremely biased gene where only one codon is used for each amino acid, this value would be 20; in an unbiased gene, it would be 61[27]. The codon adaptation index (CAI) value was regarded as a reference set of highly expressed genes from a species to assess the relative merits of each codon. Higher CAI value expected stronger codon usage bias and higher expression level, whereas the reverse was true for lower CAI value. The relative synonymous codon usage (RSCU) value was used to examine the codon usage variation among the genes without the confounding influence of amino acid composition. It is defined as the ratio of the observed frequency of codons to the expected frequency if all the synonymous codons for those amino acids are used equally[28]. GC_{3s} is a good indicator of the extent of base composition bias, which represents the frequency of the nucleotide G + C at the synonymous 3rd codon position, excluding Met, Trp and the stop codons. The codon usage pattern across genes was examined by the ENC-plot, which is a plot of ENC versus GC_{3s}.

2.3 Molecular Characterization and Phylogenetic Analysis of the DPV UL16 Gene

The nucleotide sequences of the DPV UL16 gene and 22 reference herpesviruses were translated into amino acid sequences by using DNASTAR software. After this, multiple sequence alignment and phylogenetic analysis were performed for the UL16 genes of 23 herpesviruses with CLUSTAL-X and TREEVIEW software.

2.4 Analysis the Rare Codons of DPV UL16 Gene

The proteins in heterologous hosts are often difficult to express or at very low levels. They might contain codons that are rarely used in the desired host. Log to http://nihserver.mbi.ucla.edu/RACC/ to analyze the rare codons of the DPV UL16 gene.

2.5 Comparison of Codon Preferences of DPV UL16 Gene with those of E. coli, Yeast and Human

To examine whether different species follow with the same codon usage rule, Codon usage bias in the DPV UL16 gene was determined with the SPSS 13.0 software, and we compare the UL16 codon usage bias among DPV, *E. coli*, yeast and Human (create a codon usage table). The database of the codon usage in E. coli, yeast and Human is available at http://www.kazusa.or.jp/codon.

3 Results

3.1 Variation in DPV UL16 Codon Usage and Amino Acid Composition

While RSCU and the related measures indicate the overall DPV UL16 codon bias, it is also important to closely investigate the pattern of codon bias. Table 1 shows the codon preferences of DPV UL16 gene. Sixty-one codons (excepting Met and the termination codons) in the polypeptide, with twenty-six synonymous codons strong

bias toward A-ended and T-ended at the third codon position, were used. A high level of diversity in codon usage bias existed for coding the Ala, Gly, Leu, Pro, Arg, Ser, Thr and Val amino acids because they have a 6-fold and 4-fold coding degeneracy.

3.2 Codon Usage Analysis of the UL16 Genes of DPV and Reference Herpesviruses

The results obtained by CodonW and EMBOSS analysis of the ENC, CAI, coding G + C content (GC%) and the G + C contents at the third codon position content (GC_{3S}%) of 23 herpesviruses species are shown in table 2 . Codon usage in the UL16 gene is highly nonrandom in all the herpesviruses, and the overall base composition of the UL16 genes in these species also differs dramatically. From the table 2, the ENC values of different UL16 genes vary from 28.504 to 60.115, with a mean value of 50.519 and standard deviation (S.D.) of 8.206. The GC_{3S} contents of each UL16 gene range from 27.65 to 97.97% with a mean of 56.826% and S.D. of 18.152. The CAI values of different UL16 genes vary from 0.6 to 0.764, with a mean value of 0.681 and standard deviation (S.D.) of 0.045.

Table 1. Synonymous Codon Usage of DEV UL16 Gene Analyzed with Cusp Program

Rank	AA	Codon	Fraction[a]	Frequency[b]	Number[c]	RSCU[d]
1	A(Ala)	GCA	0.297	30.303	11	1.19
2		GCC	0.189	19.284	7	0.76
3		GCG	0.243	24.793	9	0.97
4		GCT	0.270	27.548	10	1.08
5	C(Cys)	TGC	0.385	13.774	5	0.77
6		TGT	0.615	22.039	8	1.23
7	D(Asp)	GAC	0.444	22.039	8	0.89
8		GAT	0.556	27.548	10	1.11
9	E(Glu)	GAA	0.882	41.322	15	1.76
10		GAG	0.118	5.510	2	0.24
11	F(Phe)	TTC	0.444	11.019	4	0.89
12		TTT	0.556	13.774	5	1.11
13	G(Gly)	GGA	0.438	19.284	7	1.75
14		GGC	0.125	5.510	2	0.50
15		GGG	0.188	8.264	3	0.75
16		GGT	0.250	11.019	4	1.00
17	H(His)	CAC	0.444	11.019	4	0.89
18		CAT	0.556	13.774	5	1.11

Table 1. (*continued*)

19	I(Ile)	ATA	0.423	30.303	11	1.27
20		ATC	0.231	16.529	6	0.69
21		ATT	0.346	24.793	9	1.04
22	K(Lys)	AAA	0.778	19.284	7	1.56
23		AAG	0.222	5.510	2	0.44
24	L(Leu)	CTA	0.179	19.284	7	1.08
25		CTC	0.179	19.284	7	1.08
26		CTG	0.077	8.264	3	0.46
27		CTT	0.154	16.529	6	0.92
28		TTA	0.256	27.548	10	1.54
29		TTG	0.154	16.529	6	0.92
30	M(Met)	ATG	1.000	30.303	11	1.00
31	N(Asn)	AAC	0.385	13.774	5	0.77
32		AAT	0.615	22.039	8	1.23
33	P(Pro)	CCA	0.308	22.039	8	1.23
34		CCC	0.077	5.510	2	0.31
35		CCG	0.308	22.039	8	1.23
36		CCT	0.308	22.039	8	1.23
37	Q(Gln)	CAA	0.600	8.264	3	1.20
38		CAG	0.400	5.510	2	0.80
39	R(Arg)	AGA	0.214	16.529	6	1.29
40		AGG	0.107	8.264	3	0.64
41		CGA	0.179	13.774	5	1.07
42		CGC	0.107	8.264	3	0.64
43		CGG	0.071	5.510	2	0.43
44		CGT	0.321	24.793	9	1.93
45	S(Ser)	AGC	0.031	2.755	1	0.19
46		AGT	0.125	11.019	4	0.75
47		TCA	0.312	27.548	10	1.88
48		TCC	0.062	5.510	2	0.38
49		TCG	0.156	13.774	5	0.94

Table 1. (*continued*)

50		TCT	0.312	27.548	10	1.88
51	T(Thr)	ACA	0.368	19.284	7	1.47
52		ACC	0.158	8.264	3	0.63
53		ACG	0.316	16.529	6	1.26
54		ACT	0.158	8.264	3	0.63
56	V(Val)	GTA	0.364	22.039	8	1.45
57		GTC	0.136	8.264	3	0.55
58		GTG	0.273	16.529	6	1.09
59		GTT	0.227	13.774	5	0.91
60	W(Trp)	TGG	1.000	19.284	7	1.00
61	Y(Tyr)	TAC	0.333	5.510	2	0.67
62		TAT	0.667	11.019	4	1.33
63	*	TAA	1.000	2.755	1	3.00

The strong bias towards the codons with A and T at the third codon position and the preferentially used codons for each amino acid are displayed in red.

a. The ‘‘Fract’’ shows the proportion of all synonymous codons encoding the same amino acid
b. The ‘‘Frequency’’ lists the number of codons present per 1000 bases in the input sequence(s)
c. The ‘‘Number’’ lists the number of codons
d. The ‘‘RSCU’’ shows the proportion of relative synonymous codon usage

In general speaking, the gene is thought to possess strong codon bias if the ENC value is less than 35[29]. Analyzing the ENC values of all the UL16 genes, the results showed the majority of them do not have a strong codon bias. The plot of ENC and GC_{3S} content is another effective way to explore codon usage variation among different genes[29]. In fig.1, the solid line represents the curve if codon usage is only determined by GC_{3S} content[30]. In principle, proprietary proportion of points lay near to the solid line on this distribution. It suggested that mutational bias was the main factor determining the codon usage variation among these UL16 genes. But the ENC values were mostly dispersed below the curve. Hence, other than mutational bias, there might be few additional factors driving the codon usage variation among these UL16 genes such as natural selection.

Table 2. Summary Analysis of UL16 Gene In Different Herpesvirus Species

	Virus name	GenBank	L(bp)[a]	CAI[b]	ENC[c]	GC(%)	GC_{3s}(%)[d]
Alphaherpsvirinae	Duck plague virus(DPV)	EU195095	1089	0.600	58.928	46.74	38.29
	Meleagrid herpesvirus 1 (MeHV-1)	NC_002641	1056	0.700	53.775	46.40	52.27
	Bovine herpesvirus 1 (BoHV-1)	NC_001847	1020	0.695	32.900	75.49	90.29
	Bovine herpesvirus 5(BoHV-5)	NC_005261	1032	0.732	28.504	77.91	97.97
	Equid herpesvirus 1(EHV-1)	NC_001491	1113	0.711	50.845	57.41	65.77
	Equid herpesvirus 4(EHV-4)	NC_001844	1110	0.662	54.901	50.45	50.54
	Gallid herpesvirus 2(GaHV-2)	NC_002229	1083	0.712	55.371	43.49	48.20
	Gallid herpesvirus 3(GaHV-3)	NC_002577	1056	0.675	57.994	51.04	51.14
	Human herpesvirus 1 (HHV-1)	NC_001806	1200	0.701	47.551	68.08	80.25
	Human herpesvirus 2 (HHV-2)	NC_001798	1150	0.686	56.366	71.45	59.01
	Human herpesvirus 3(HHV-3)	NC_001348	1092	0.624	56.500	47.44	42.31
	Suid herpesvirus 1(SuHV-1)	NC_006151	982	0.663	42.623	78.39	55.66
	Psittacid herpesvirus 1(PsHV-1)	NC_005264	1068	0.719	48.946	59.83	70.79
	Ceropithecine herpesvirus 2 (CerHV-2)	NC_006560	1089	0.701	42.382	76.95	72.45
	Ceropithecine herpesvirus 9(CerHV-9)	NC_002686	1083	0.605	50.657	41.83	33.52
Betaherpsvirinae	Murid herpesvirus 1(MuHV-1)	NC_004065	1080	0.764	40.985	61.02	79.72
	Human herpesvirus 7(HHV-7)	NC_001716	1020	0.627	48.404	33.14	27.65
	Human herpesvirus 6 (HHV-6)	NC_001664	1080	0.608	55.424	39.07	39.72
	Human herpesvirus 5 (HHV-5)	NC_006273	1080	0.643	60.115	57.31	46.94
Gammaherpsvirinae	Human herpesvirus 4 (HHV-4)	NC_007605	1080 1074	0.714	56.761	53.80	53.33
	Human herpesvirus 8(HHV-8)	NC_009333	1005	0.716	54.946	53.83	61.19
	Murid herpesvirus 4 (MuHV-4)	NC_001826	984	0.693	55.547	43.60	41.77
	Alcelaphine herpesvirus 1 (AlHV-1)	NC_002531	1008	0.723	51.518	47.32	48.21

a Represents the length of identified ORF
b Effective number of codons
c Codon Adaptation Index
d G + C frequency at the synonymous third position of codons

3.3 Characterization of the DPV UL16 Gene

Usinng CLUSTAL-X and TREEVIEW software, A phylogenetic tree was established from the deduced amino acids encoded by the 1089 bp ORF of the UL16 gene of DPV and the 22 reference herpesviruses (Fig. 2). It shows that there are mainly three branches for the 23 herpesvirus. The DPV, MaHV-2, GaHV-3, and MeHV-1 are clustered in a distinct subbranch in Alphaherpesvirinae. The amino acid sequence of DPV UL16 is higher similarity and has a closer evolution with MaHV-2, GaHV-3, and MeHV-1.

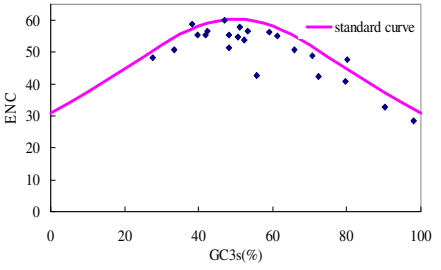

Fig. 1. The plot of ENC and guanine (G) + cytosine (C) frequency at the synonymous third position of codons (GC_{3S}) of the UL16 gene in the DEV CHv strain and those of 23 reference herpesviruses. The curve indicates the expected codon usage if GC compositional constraints alone accout for codon usage bias.

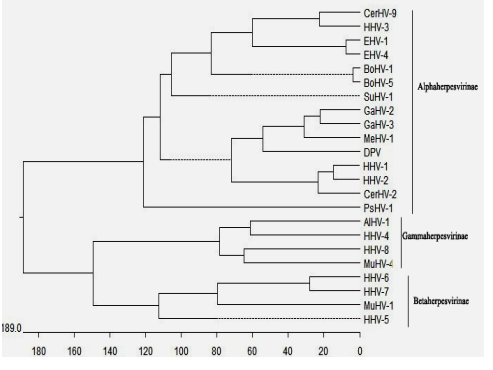

Fig. 2. Phylogenetic tree based on the UL16 amino acid sequences in 24 herpesviruses (Table 2), and constructed with CLUSTAL-X and TREEVIEW software

Rare condons analysis showed that there are 34 rare condons (9.366%) in the ORF of the DPV UL16 gene by using codon usage database on line (http://nihserver.mbi.ucla.edu/RACC/) (shown in Fig.3). The result revealed that there have sequential two rare codons in the ORF of the DPV UL16 gene.atg gct cgc agt act att aca cgt CGA tta tca tca tgt acg gaa ctc gac gat gga gaa ctg aat tcg cca ATA tta ttt tta aat gac ccg tct ctc ggt agt gtt cac CTA gct cgg gca ttg aac aca caa gtg tgt tca tgg cgc ctt att AGA tct gat tct cgt atc aag atc atg atc gca att aca gca ctc ggg gac cgt ctt tgt gct ttc gcg cct cca CTA gaa gat CGA gaa AGG gcg gca atg gtg gaa ATA ATA ttg tac tta acg cgt cct aaa gcg tta gct ctc cca tct gga act ttc cat gcc gtg ttt att gtc aac cgt tca tca atg tat gct gca ATA gca gct ATA cat atc gaa gca CTA aac caa tct gga acc ctg ttc tca tta ttg ttt tcc tca gta gaa acg acc ccg ccg cct ccg gaa gtt cct gac ccg tcg aca gaa att atg ccg cag gcc cct gct tca atc CTA aat CTA gaa gac cat acg gaa aat ATA acg ccg cca AGG gat cct cat aac tgt AGA atg gta tct gtt ggg gcg tgg tgg tct ttt CCC aaa CGA AGG ctc tac tat tta CGA atg gat aca cca ctt tta gct ATA tgc ccg gcg gga tgg aaa gca AGA acg ctt gga gac gtt CTA gcg AGA ctc gta gac cat aca cca ggt tgc gag acc tgc att agc ggc cac gat cac gtg gat tcg tat aat gcc ATA tgg aag cct ggc gaa gtc gca gag gca tgt

tta tgt aaa gga cca tgc ctg tgg ctc aaa tca aaa cag cgg gat atg ATA gta gaa ggg gat gtg agt atg tgt cgc gtt ttg ttc atg gac gct gta gat act ATA CGA ctt gta tct aac cgt aat cca cgt att tct gca aat ttg gcc gaa gta att tcc gcc ttt ggt tca gcc AGA caa gta cct gtc aat gcg gcc gga tgg cac ttg gtg gcg tta tcg gaa att gct agt tcg atc atg ATA tct ggt tgc gcg cgt ctt AGA cgt CTA tgt tat CCC aaa aca taa

Fig. 3. Rare condons analysis of the DPV UL16 gene **Red** = rare Arg codons **AGG, AGA, CGA** ; **Green** = rare Leu codon **CTA** ;**Blue** = rare Ile codon **ATA** ;**Orange** = rare Pro codon **CCC**

3.4 Comparison of Codon Usage between DPV and E. coli , Yeast and Human

The DPV UL16 gene was compared with those of *E. coli*, Yeast and Human to see which will be the suitable host for the optimal expression of DPV genes. From table 3, there are 21 codons distinct usage differences between DPV UL16 gene and E.coli (a DPV-to-E. coli ratio higher than 2 or lower than 0.50), 19 between DPV UL16 gene and yeast (a DPV -to-Yeast ratio higher than 2 or lower than 0.50), 20 between DPV UL16 gene and Human (a DPV -to- Human ratio higher than 2 or lower than 0.50) . Codons usage analysis datas (Fig.4) shows variation between DPV UL16 gene, E.coli, Yeast and Human. All these might suggest that expressing DPV genes more efficiently in Yeast systems.

Table 3. Comparison of Codon Preferences Between the DPV UL16 Gene and E. Coli, Yeast And H. Sapiens

Condon	Amino acid	E.coli (1/1000)	Yeast (1/1000)	Human (1/1000)	UL16 (1/1000)	UL16 /E.coli	UL16 /Yeast	UL16 /Human
GCA	A(Ala)	20.6	16.1	16.1	30.303	1.471	1.882	1.882
GCC	A	25.5	12.5	28.4	19.284	0.756	1.542	0.679
GCG	A	31.7	6.1	7.5	24.793	0.782	4.064	3.306
GCT	A	15.6	21.1	18.6	27.548	1.766	1.306	1.481
TGC	C(Cys)	6.9	4.7	12.2	13.774	1.996	2.931	1.129
TGT	C	5.5	8	10	22.039	4.007	2.755	2.204
GAC	D(Asp)	18.6	20.2	25.6	22.039	1.185	1.091	0.861
GAT	D	32.1	37.8	21.9	27.548	0.858	0.729	1.258
GAA	E(Glu)	38.2	48.5	29	41.322	1.082	0.852	1.425
GAG	E	17.7	19.1	39.9	5.51	0.311	0.288	0.138
TTC	F(Phe)	16.9	18.2	20.6	11.019	0.652	0.605	0.535
TTT	F	23.2	26.1	17.1	13.774	0.594	0.528	0.805
GGA	G(Gly)	9	10.9	16.4	19.284	2.143	1.769	1.176

Table 3. (*continued*)

GGC	G	27.9	9.7	22.5	5.51	0.197	0.568	0.245
GGG	G	11.3	6	16.3	8.264	0.731	1.377	0.507
GGT	G	24.4	24	10.8	11.019	0.452	0.459	1.020
CAC	H(His)	9.8	7.7	15	11.019	1.124	1.431	0.735
CAT	H	13.6	13.7	10.5	13.774	1.013	1.005	1.312
ATA	I(Ile)	5.4	17.8	7.7	30.303	5.612	1.702	3.935
ATC	I	24.2	17	21.6	16.529	0.683	0.972	0.765
ATT	I	29.8	30.4	16.1	24.793	0.832	0.816	1.540
AAA	K(Lys)	33.2	42.2	24.1	19.284	0.581	0.457	0.800
AAG	K	10.7	30.7	32.2	5.51	0.515	0.179	0.171
CTA	L(Leu)	4	13.3	7.8	19.284	4.821	1.450	2.472
CTC	L	11	5.4	19.8	19.284	1.753	3.571	0.974
CTG	L	50.9	10.4	39.8	8.264	0.162	0.795	0.208
CTT	L	11.7	12.1	13	16.529	1.413	1.366	1.271
TTA	L	13.9	26.7	7.5	27.548	1.982	1.032	3.673
TTG	L	14	27	12.6	16.529	1.181	0.612	1.312
ATG	M(Met)	27	20.9	22.2	30.303	1.122	1.450	1.365
AAC	N(Asn)	21.4	24.9	19.5	13.774	0.644	0.553	0.706
AAT	N	18.6	36.3	16.7	22.039	1.185	0.607	1.320
CCA	P(Pro)	8.5	18.2	16.7	22.039	2.593	1.211	1.320
CCC	P	5.8	6.8	20.1	5.51	0.95	0.810	0.274
CCG	P	21.8	5.3	6.9	22.039	1.011	4.158	3.194
CCT	P	7.3	13.6	17.3	22.039	3.019	1.621	1.274
CAA	Q(Gln)	15	27.5	12	8.264	0.551	0.301	0.689
CAG	Q	29.5	12.1	34.1	5.51	0.187	0.455	0.162
AGA	R(Arg)	2.9	21.3	11.5	16.529	5.700	0.776	1.437
AGG	R	1.9	9.2	11.4	8.264	4.349	0.898	0.725
CGA	R	3.9	3	6.3	13.774	3.532	4.591	2.186
CGC	R	21	2.6	10.7	8.264	0.394	3.178	0.772
CGG	R	6.3	1.7	11.6	5.51	0.875	3.241	0.475
CGT	R	20.3	6.5	4.6	24.793	1.221	3.814	5.390

Table 3. (*continued*)

AGC	S(Ser)	16	9.7	19.3	2.755	0.172	0.284	0.143
AGT	S	9.5	14.2	11.9	11.019	1.160	0.776	0.926
TCA	S	7.8	18.8	12	27.548	3.532	1.465	2.296
TCC	S	8.9	14.2	11.9	5.51	0.619	0.388	0.463
TCG	S	8.7	8.5	4.4	13.774	1.583	1.620	3.130
TCT	S	8.7	23.5	14.7	27.548	3.166	1.172	1.874
ACA	T(Thr)	8.2	17.8	15.1	19.284	2.352	1.083	1.277
ACC	T	22.8	12.6	19.4	8.264	0.362	0.656	0.426
ACG	T	14.8	7.9	6.1	16.529	1.117	2.092	2.710
ACT	T	9.1	20.3	13	8.264	0.908	0.407	0.636
GTA	V(Val)	11.1	11.8	7.2	22.039	1.985	1.868	3.061
GTC	V	15.1	11.6	14.6	8.264	0.547	0.712	0.566
GTG	V	25.5	10.6	28.4	16.529	0.648	1.559	0.582
GTT	V	18.5	22	11	13.774	0.745	0.626	1.252
TGG	W(Trp)	15.2	10.3	12.7	19.284	1.269	1.872	1.518
TAC	Y(Tyr)	12.1	14.6	15.5	5.51	0.455	0.377	0.355
TAT	Y	16.5	18.9	12.1	11.019	0.668	0.583	0.911
TAA	*	2	1	0.7	2.755	1.378	2.755	3.936
TAG	*	0.3	0.5	0.6	0	0	0	0
TGA	*	1.1	0.7	1.5	0	0	0	0

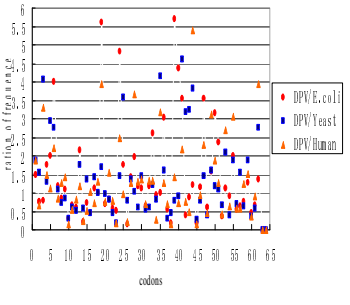

Fig. 4. The comparisons in the ratio of codon usage frequency (1/1000) of DPV to *E. coli*, yeast and H.sapiens. The ratio higher than 2 or lower 0.5 indicates that the codon usage preference differs, and vice versa.

4 Discussions

The degeneracy of the genetic code implies that multiple triplets codes for the same amino acid . The frequencies with which different codons are used vary significantly between organisms and between proteins within the same organism[31]. In this paper, a comprehensive analysis of codon usage including ENC, CAI value, GC content and the RSCU values of the DPV UL16 gene was performed by using EMBOSS programs and CodonW, and these values were subsequently compared with those of the 22 reference herpesvirus species. These datas of synonymous codon usage bias showed certain disparity of each herpesvirus from the different organisms with the result revealing that: (1) the DPV UL16 gene and its 22 reference herpesviruses adopt relatively similar codon usage patterns, although the DPV UL16 gene shows a few differences of codon usage bias with its reference herpesvirus species; and (2) the DPV UL16 gene prefers to use the codons with A and T at the 3rd codon position. From the table 1, twenty-six synonymous codons strong bias toward A- and T-ended at the third codon position were used. The DPV UL16 gene is an AT-rich gene. At the same time, random mutations increase the population of AT rather than CG as a result, undergo spontaneous deaminations[32]. So it is reasonable that codons ending in A and/or T are predominant in the gene. The ENC value and GC_{3S} content, two important codon usage indices, have been widely used to explore the codon usage variation among different genes[33-35]. Values of ENC range From 20(when only one codon is used per amino acid) to 61(when all synonyms are used with equal frequency). The ENC values of herpesvirus UL16 genes are dramatically different (from 28.504 to 60.115 shown in table 2) but mostly the codon usage bias is lower stronger. The ENC value of DPV UL16 gene is high (ENC>50), so that the codon usage bias is low stronger. If G+C compositional constraint influences the codon usage, then the GC_{3S} and ENC correlated spots would lie on the expected curve[30]. If a gene is subject to selection for translationally optimal codons, it will lie considerably below the expected curve[36]. In Fig.1, a large number of points do not follow the theoretical curve suggesting that other factors other than gene composition contribute to the codon usage pattern in the reference herpesviruses, which maybe mutational bias and natural selection, such as translational selection, the tRNA abundance, leading to the codon usage variation among genes in different organisms.

Comparative analysis of UL16 genes in DPV and the reference herpesviruses indicated that synonymous codon usage in these genes is phylogenetically conserved. Datas in table 2 show that the UL16 genes in DPV, MeHV-1, GaHV-2 and GaHV-3, whose natural host is avian, have a stronger correlation than the UL16 genes of herpesviruses with other hosts. In the table 3, the CAI value of DPV UL16 gene is 0.600, which is a little slight higher. The CAI value is much closer to 1, the codon usage is a little stronger and the gene expressing level is much higher. We can infer UL16 gene is highly expressed gene in DPV genome. Simultaneously, the phylogenetic tree analysis based on the UL16 gene products revealed that UL16 protein of the DPV CHv strain and some avian herpesviruses such as MeHV-1, GaHV-2 and GaHV-3, were clustered within a monophyletic clade and grouped within Alphaherpesvirinae. We speculate that the codon usage bias of DPV UL16 gene has a very close relation with its gene function and gene type. DPV UL16 gene is similar to the UL16 gene function of the herpesviruses. Studies on the HHV-1 have

well documented that the tegument UL16 protein is not required for viral replication in cell culture and its function may be in viral DNA packaging, virion assembly, budding, and egress by providing an interaction with the membrane-bound UL11 protein and the UL21 protein[26,37-39]. In the absence of murine Gammaherpesvirus 68 (MuHV-4) ORF33 (UL16 homologue), immature virions were restrained in a state interacting with actin and glycoproteins gB and failed release of infectious virions[40]. Furthermore, bioinformatics analysis indicated that the DPV UL16 protein has higher similarity with these homologues, and may also play a similar role to that of HHV-1 in the viral DNA packaging, virion assembly, budding, and egress. However, further studies are required to confirm this hypothesis.

The most plausible selection-based explanation for codon usage bias is the selection for efficient translation related to the relative abundance of isoaccepting tRNAs[33,34]. In order to show the codon usage variation among genes from different organisms, the codon usage bias of DPV was compared with that of E. coli, Yeast, and Human. There are 21 codons distinct usage differences between DPV UL16 gene and E.coli, 19 between DPV UL16 gene and Yeast, 20 between DPV UL16 gene and Human. Thus, we can assume that the E.coli, Yeast and Human expression system were suitable for heterologous expression of the DPV gene. In addition, we analyzed the rare condons of the DPV UL16 gene. There were 34 rare codons and sequential two rare codons in UL16 gene ORF, which may influence the expression of the UL16 gene in vitro. So if we choose the prokaryotic expression system, we should choose the host bacteria Rosseta, which should impove the expression of the exogenous genes. All of these may be of great importance for gene characterization, for gene classification and for assessing the possible role of UL16 protein in viral pathogenesis.

Acknowledgments. The research were supported by grants from Changjiang Scholars and Innovative Research Team in University (PCSIRT0848), the earmarked fund for Modern Agro-industry Technology Research System (nycytx-45-12), the Cultivation Fund of the Key Scientific and Technical Innovation Project, the Ministry of Education of China (No. 706050), the Cultivation Fund of the Key Scientific and Technical Innovation Project, Department of Education of Sichuan Province (No. 07ZZ028). The first two authors contribute equally to this work and should be considered as first author. An-chun Cheng and Ming-shu Wang are the corresponding authors. Key Laboratory of Animal Disease and Human Health of Sichuan Province & Avian Disease Research Center, College of Veterinary Medicine of Sichuan Agricultural University, 46# Xinkang Road, Yucheng district, Yaan 625014, Sichuan province of China. Tel.: +86 835 2885774; fax: +86 835 2885774. E-mail address: chenganchun@vip.163.com (A. Cheng); mshwang@163.com (M. Wang).

References

1. Jan, B.: Does codon bias have an evolutionary origin? Theor. Biol. Med. Model 5(16), 1–16 (2008)
2. Fuglsang, A.: Accounting for background nucleotide composition when measuring codon usage bias: brilliant idea, difficult in practice. Mol. Biol. Evol. 23(7), 1345–1347 (2006)

3. Nakamura, M., Sugiura, M.: Translation efficiencies of synonymous codons are not always correlated with codon usage in tobacco chloroplasts. Plant J. 49(1), 128–134 (2007)
4. Marais, G., Duret, L.: Synonymous codon usage, accuracy of translation, and gene length in Caenorhabditis elegans. J. Mol. Evol. 52(3), 275–280 (2001)
5. Ma, J., Campbell, A., Karlin, S.: Correlations between shine-dalgarno sequences and gene features such as predicted expression levels and operon structures. J. Bacteriol. 184(20), 5733–5745 (2002)
6. Noboru, S.: Two aspects of DNA base composition: G+C content and translation-coupled deviation from intra-strand rule of A = T and G = C. J. Mol. Evol. 49(1), 49–62 (1999)
7. Plotkin, J.B., Dushoff, J., Desai, M.-M., Fraser, H.-B.: Codon usage and selection on proteins. J. Mol. Evol. 63(5), 635–653 (2006)
8. Kanaya, S., Yamada, Y., Kudo, Y., Ikemura, T.: Studies of codon usage and tRNA genes of 18 unicellular organisms and quantification of Bacillus subtilis tRNAs: gene expression level and speciesspecific diversity of codon usage based on multivariate analysis. Gene 238(1), 143–155 (1999)
9. Noguchi, S., Satow, Y.: Purification of human β2-adrenergic receptor expressed in methylotrophic yeast Pichia pastoris. J. Biochem. 140(6), 799–804 (2006)
10. Sau, K., Gupta, S.-K., Sau, S., Ghosh, T.-C.: Synonymous codon usage bias in 16 Staphylococcus aureus phages: implication in phage therapy. Virus Res. 113(2), 123–231 (2005)
11. Sueoka, N., Kawanishi, Y.: DNA G+C content of the third codon position and codon usage biases of human genes. Gene 261(1), 53–62 (2000)
12. Wan, X.-F., Xu, D., Kleinhofs, A., Zhou, J.: Quantitative relationship between synonymous codon usage bias and GC composition across unicellular genomes. BMC Evol. Biol. 4(9), 19–29 (2004)
13. Lynn, D.-J., Singer, G.-A., Hicker, D.-A.: Synonymous codon usage is subject to selection in thermophilic bacteria. Nucleic Acids Res. 30(19), 4272–4277 (2002)
14. Duret, L.: tRNA gene number and codon usage in the C.elegans genome are co-adapted for optimal translation ofhighly expressed genes. Trends Genet. 16(7), 287–289 (2000)
15. Cai, M.-S., Cheng, A.-C., Wang, M.-S., Zhao, L.-C., Zhu, D.-K., Luo, Q.-H., et al.: Characterization of synonymous codon usage bias in the duck plague virus UL35 gene. Intervirology 52(5), 266–278 (2009)
16. Zhao, L.-C., Cheng, A.-C., Wang, M.-S., Yuan, G.-P., Cai, M.-S.: Characterization of codon usage bias in the dUTPase gene of duck enteritis virus. Prog. Nat. Sci. 18(9), 1069–1076 (2008)
17. Prat, Y., Fromer, M., Linial, N., Linial, M.: Codon usage is associated with the evolutionary age of genes in metazoan genomes. BMC Evol. Biol. 9(1), 285–299 (2009)
18. Hassard, S., Ward, G.: Efficient creation of sequencing libraries from blunt-ended restriction enzyme fragments. Biotechniques 18(3), 396–398 (1995)
19. Jenkins, G.-M., Holmes, E.-C.: The extent of codon usage bias in human RNA viruses and its evolutionary origin. Virus Res. 92(1), 1–7 (2003)
20. Ma, X.-R., Xiao, S.-B., Fang, L.-R., Chen, H.-C.: Bias of base composition and codon usage in pseudorabies virus genes. In: Yi Chuan Xue Bao, vol. 32(6), pp. 616–624 (June 2005)
21. Hall, J.-D., Gibbs, J.-S., Coen, D.-M., Mount, D.-W.: Structural organization and unusual codon usage in the DNA polymerase gene from herpes simplex virus type 1. DNA 5(4), 281–288 (1986)

22. Karlin, S., Blaisdell, B.-E., Schachtel, G.-A.: Contrasts in codon usage of latent versus productive genes of Epstein-Barr virus: data and hypotheses. J. Virol. 64(9), 4264–4273 (1990)
23. Davison, S., Converse, K.-A., Hamir, A.-N., Eckroade, R.-J.: Duck viral enteritis in domestic Muscovy ducks in Pennsylvania. Avian Dis. 37(4), 1142–1146 (1993)
24. Saif, Y.-M., Barnes, H.-J., Glisson, J.-R., Fadly, A.-M., McDougald, L.-R., Swayne, D.-E.: Diseases of Poultry, 11th edn., pp. 354–363. Iowa State University Press, Ames (2003)
25. Cheng, A.-C., Wang, M.-S., Wen, M.: Construction of duck enteritis virus gene libraries and discovery, cloning and identification of viral nucleocapsid protein gene. High Technolagy Letters, Institute of Scientific and Technical Information of China 16, 948–953 (2006)
26. Meckes Jr., D.-G., Wills, J.-W.: Dynamic interactions of the UL16 tegument protein with the capsid of herpes simplex virus. J. Virol., American Society For Microbiology, United States 81(23), 13028–13036 (2007)
27. Comeron, J.-M., Aguade, M.: An evaluation of measures of synonymous codon usage bias. J. Mol. Evol. 47(3), 268–274 (1998)
28. Liu, Q., Dou, S., Ji, Z., Xue, Q.: Synonymous codon usage and gene function are strongly related in Oryza sativa. Biosystems 80(2), 123–131 (2005)
29. Wright, F.: The 'effective number of codons' used in a gene. Gene 87(1), 23–29 (1990)
30. Jiang, P., Sun, X., Lu, Z.: Analysis of Synonymous codon usage in Aeropyrum pernix K1 and other Crenarchaeota Microorganisma. J. Genet. Genomics 34(3), 275–284 (2007)
31. Akashi, H.: Gene expression and molecular evolution. Curr. Opin. Genet. Dev. 11(1), 660–666 (2001)
32. Lindahl, T.: Instability and decay of the primary structure of DNA. Nature 362(6422), 709–715 (1993)
33. Sakai, H., Washio, T., Saito, R., Shinagawa, A., Itoh, M., Shibata, K., et al.: Correlation between sequence conservation of the 5' untranslated region and codon usage bias in Mus musculus genes. Gene 276(1-2), 101–105 (2001)
34. Gu, W., Zhou, T., Ma, J., Sun, X., Lu, Z.: Analysis of synonymous codon usage in SARS Coronavirus and other viruses in the Nidovirales. Virus Res. 101(2), 155–161 (2004)
35. Zhou, T., Gu, W., Ma, J., Sun, X., Lu, Z.: Analysis of synonymous codon usage in H5N1 virus and other influenza A viruses. Biosystems 81(1), 77–86 (2005)
36. Zhou, T., Sun, X., Lu, Z.: Synonymous codon usage in environmental chlamydia UWE25 reflects an evolutional divergence from pathogenic chlamydiae. Gene 368(1), 117–125 (2006)
37. Baines, J.-D., Roizman, B.: The open reading frames UL3, UL4, UL10, and UL16 are dispensable for the replication of herpes simplex virus 1 in cell culture. J. Virol. 65(2), 938–944 (1991)
38. Oshima, S., Daikoku, T., Shibata, S., Yamada, H., Goshima, F., Nishiyama, Y.: Characterization of the UL16 gene product of herpes simplex virus type 2. Arch. Virol. 143(5), 863–880 (1998)
39. Nalwanga, D., Rempel, S., Roizman, B., Baines, J.D.: The UL16 gene product of herpes simplex virus 1 is a virion protein that colocalizes with intranuclear capsid proteins. Virol. 226(2), 236–242 (1996)
40. Guo, H., Wang, L., Peng, L., Zhou, Z.-H., Deng, H.: Open Reading Frame 33 of a Gammaherpesvirus Encodes a Tegument Protein Essential for Virion Morphogenesis and Egress. Virol. 83(20), 10582–10595 (2009)

Microbe Distribution and Dynamic Characters of Oil Degradation in the Contaminated Soils*

Luqing Jiang, Xilai Zheng, and Lei Chen

College of Environmental Science and Engineering
Ocean University of China
Qingdao, Shandong Province, China
zhxilai@ouc.edu.cn

Abstract. The soil features, distribution and dynamic characters of Shen Fu irrigation area were studied by analyzing statistical data and oil degradation tests in order to further study the ralationship between microbes and oil degradation. Data collected in Shen Fu sewage irrigation area show that indigenous microbial flora addicted to oil has formed after a long-term oil sewage irrigation and the quantity and distribution of microbes varied with time and temperature. Through oil degradation tests, it was found that oil contents in soil and water decreased with time. The microbial degradation rate in soil accorded with the first class kinetic equation.

Keyword: microbes, oil, degradation, dynamic characters.

1 Introduction

Oil is a mixture with complex components, which is mainly comprised by hydrocarbon. After it enters surface water bodies, most of them float above the water, while a small amount can be dissolved in the water accompanying with volatilization. When using oil polluted water for irrigation, the components of oil will be absorbed onto soil particles very easily, which can also be degraded by microorganism in soil.

The relationship between oil and microbes was originally recognized in the 40's and researchers' interest focused on the relationship between microbes and oil causes; in the 50 and 60 years, the basic theory and application of hydrocarbon metabolism began to serve as a study field; with the sank of No. TORRY CANYON super oil tanker in 1967, many microbiologists of oil turn to research oil pollution ecology and the fate and effects of oil pollutants widely [1]. In 1977, Zobell identified 30 more kinds of microbes which could degrade hydrocarbons and exist in fresh water, salt water, soil and groundwater [2]; Atlas [3] sampled from 12 oil-contaminated aquifer and found that the content of bacteria in the water was mostly above the level of 100 per ml.

Testa and Paczkowski [4] abroad applied land farming to degrade soil by microbes for 18 months with the result that the content of alkanes in oil decreased by 80-82%.

* This work is financially supported by National Natural Science Foundation of China(No.40272108).

E. Zhu and S. Sambath (Eds.): Information Tech. and Agricultural Eng., AISC 134, pp. 763–770.
springerlink.com © Springer-Verlag Berlin Heidelberg 2012

Therefore, they believed this method could be used to dispose surface oil pollution. Shafer [5] and Jamison [6] selected three Ameriacan regions, the eastern, central and western, to apply 6 kinds oil to plant cabbage and broad bean and the concentration of each oil averagely reduced by 48-90%.

In the seventies and early eighties, Liu Qisong, Wei Kaimei, Wu Weizhong, Zheng Xilai [7-16] and others systematicly studied the microbial ecology and degradation in Shen (yang) Fu (shun) oil sewage irrigation area. They considered the reason that oil sewage irrigation area didn't remarkably accumulate much more oil mainly due to the degradation of microbial groups formed there, namely the formation of dorminant microbial groups in heavy, medium, mild oil polluted regions. Besides, they separated 135 kinds of bacteria, 78 fungus and 65 Nitrogen-fixing bacteria. During the 75 days in degradation test for Da Qing crude oil and biodiesel hydrocarbon, oil content degraded by 65.1%, including the removal of 70.7% alkanes and 41.3% aromatics. While naphthalene, anthracene, benzene, fluoranthene, benzopyrene and benzanthracene of aromatics totally disappeared in the last sample.

Shen Fu irrigation area mainly use oil sewage for irrigation and receive approximately 260 thousand tons of oil sewage from factories in Fu Shen City every day for the area of 133 km^2. The aim of the study is to reveal the soil features, microbes distribution and the dynamic characters of oil degradation of Shen Fu irrigation area in order to further study the ralationship between microbes and oil degradation.

2 The Composition and Main Characteristics of Tested Soil and Microbes

2.1 The Composition and Main Characteristics of Tested Soil

Soil samples used in the experiment were collected in Shen Fu sewage irrigation. The three sampling points, Li Shizhai, Si Fangtai and Xing Nong were selected taking into account of the history of oil pollution in this area and the structure of unsaturated soils. In addition, considering the texture and nature differences between topsoil and subsoil, each soil profile was further divided into upper and lower layers. The mechanical composition and main characteristics of both layers showed in table 1.

2.2 The Dorminant Microbial Groups of Oil Sewage Irrigation Area

According to the separation and identification results of microbes in oil sewage irrigation area, indigenous microbial flora addicted to oil has formed after a long-term oil sewage irrigation, which was dorminated by bacteria with bacillus bacteria prevailing; the following were pseudomonas, xanthomonas, plesiomonas, acinetobacter and brevibacterium; fewer were fungi and actinomycetes dorminated by penicillium and aspergillus and streptomyces respectively (Table 2) [17].

Table 1. Mechanical composition and major characters

Sampling Location	*Layer*	*Stratum Code*	*Sampling Range (cm)*	*Soil Mechanical Composition(%)*						*pH*	*Organic Matter (g/kg)*	*Bulk Density (g/cm^3)*	*Total Porosity*	*Moisture Water Content (%)*
				< 0.001 (mm)	*0.001-0.005 (mm)*	*0.005-0.01 (mm)*	*0.01-0.05 (mm)*	*0.05-0.25 (mm)*	*> 0.25 (mm)*					
Li Shizhai	Upper layer	L2-1	0-30	7.80	8.40	6.40	33.88	23.60	20.92	6.25	40.2	1.38	0.48	2.67
	Under layer	L2-2	30-130	3.24	4.06	2.23	13.17	42.33	34.9 7	6.95	4. 9	1.49	0.44	1.35
Si Fangtai	Upper layer	S1-1	0-25	11.78	13.43	9.92	50.23	9.56	5.08	5.55	74.0	1.32	0.50	3.23
	Under layer	S1-2	25-130	10.10	10.09	7.21	50.48	18.70	3.4 2	6.30	11.4	1.51	0.43	3.02
Xing Nong	Upper layer	X1-1	0-35	8.93	14.74	7.06	56.89	11.07	1.31	5.25	21.6	1.33	0.50	3.81
	Under layer	X1-2	35-130	8.95	15.81	10.19	48.69	16.07	0.2 9	6.45	7. 0	1.41	0.47	4.02

Table 2. Dominant microbe cluster in oil-contaminated area

Soil Samples		*Bacteria*	*Fungi*
Heavily Polluted Area	Topsoil	Bacillus Plesiomonas Pseudomonas Acinetobacter Kurthia Brevibacterium	Penicillium frequentans Penicillium citrinum Penicillium roqueforti Aspergillus versicolor Penicillium uticale December urophylla Neurospora
	Subsoil	Bacillus Plesiomonas Arthrobacter Xanthomonas Acinetobacter Pseudomonas	Penicillium chrysogenum Demodex Penicillium Aspergillus niger Aspergillus versicolor
Medium Polluted Area	Topsoil	Bacillus Arthrobacter Plesiomonas Staphylococcus	Penicillium chrysogenum Penicillium italicum Penicillium implication
	Subsoil	Bacillus Plesiomonas Pseudomonas Kurthia Enterobacteriaceae	Aspergillus terreus Aspergillus versicolor Penicillium chrysogenum Penicillium italicum Penicillium roqueforti Alternaria alternata
Lightly Polluted Area	Topsoil	Bacillus Pseudomonas Xanthomonas Xanthomonas Arthrobacter Enterobacteriaceae	Demodex Penicillium Penicillium funiculosum Penicillium italicum Aspergillusinuii December urophylla Neurospora
	Subsoil	Bacillus Plesiomonas Arthrobacter Xanthomonas Staphylococcus	Paecilomyces variotii Penicillium citrinum Aspergillium candidus Aspergillus wentii Aspergillus versicolor

2.3 Dynamic Change of Soil Microbes in Oil Sewage Irrigation Area

The results of plate count test for soil microbes in April, July and September in Shenfu sewage irrigation area indicated that the quantity and species of soil microbes varied with sampling time although of the same contaminated area and the same soil [18]. The bacteria amount in July (high temperature) was higher than that of April and September while the amounts of actinomycetes and fungi were higher in April than in July with rare actinomycetes in September. This was due to the largest amount sewage irrigation in paddy fields in July, which inhibited the growth of actinomycetes and fungi. When soil thawed in April, the surface microbs were still subject to impact of temperature difference between day and night, which led to a greater damage of cells. In addition, surface soil temperature were higher in July and September, therefore more bacteria exist in surface soil (Table 3).

3 Oil Degradation Test

3.1 Materials and Methods

Because the compositions of oil residues, petroleum products and soluble oil are different, the degradation tests were carried out respectively. To degrade oil residues in surface soil (L-1, S1-1 and X1-1), 20 samples of 20 g soil were directly weighed and then placed in incubator within aluminum boxes under a temperature of 20℃. Afterwards, the oil content of them were measured during certain periods (0 d, 2 d, 4 d, 8 d, 15 d, 25 d, 40 d, 60 d, 80 d, 110 d) (Table 4).

The process of degradation tests for petroleum products included the following stages. Firstly, No. 20 heavy diesel oil was dissolved in petroleum ether (30-60 ℃). Secondly, as required, tested soil samples (L2-1, L2-2, S1-1, S1-2, X1 -1, X1-2) were added into the oil to volatile under room temperature. After 24hours, they were placed into incubator (20℃). At last, oil contents were measured according to the time intervals above (Table 4).

Table 3. Dynamic change of soil microbes in the oil-contaminated region

Soil Sample		*Sampling Time*	*Soil Microbes Amount (a/g soil)*		
			Becteria	*Fungi*	*Actinomycosis*
Polluted Heavily Area	Topsoil	April	15.95×10^4	10.05×10^3	26.00×10^3
		July	42.34×10^4	31.00×10^2	0
		September	7.27×10^4	0	0
	Subsoil	April	18.63×10^4	35.00×10^2	35.00×10^2
		July	34.65×10^4	52.70×10^2	0
		September	5.65×10^4	0	0
Polluted Medium Area	Topsoil	April	30.78×10^4	28.00×10^2	7.00×10^2
		July	46.34×10^4	10.90×10^3	0
		September	35.99×10^4	0	0
	Subsoil	April	22.07×10^4	42.00×10^2	56.00×10^2
		July	42.25×10^4	31.3×10^2	0
		September	26.33×10^4	0	0

Table 3. *(continued)*

Polluted Lightly Area	Topsoil	April July September	9.07×10^4 18.62×10^4 10.62×10^4	7.00×10^3 12.70×10^2 0	26.00×10^2 0 0
	Subsoil	April July September	14.06×10^4 15.60×10^4 3.63×10^4	12.80×10^3 16.60×10^3 0	64.00×10^2 0 0

Microbial degradation test of dissolved oil was to mix 100g soil with 1 liter tap water at the C: N: P ratio of 100:10:1. After vaccinated for 30 days, this supernatant was mixed with 4.0 liters of oil saturated solution, and then put into incubator (20 ℃) At last, oil contents were measured according to the time intervals above (Table 4).

3.2 Results and Discussion

3.2.1 Oil Degradation Rate

The fallowings can be drawn from the above tests results:

3.2.1.1 Oil Residues. The degradation rate of oil residues which have been accumulated for a long time was the lowest, with olny about 10% on the day of 110.

3.2.1.2 Petroleum Products. No. 20 heavy diesel oil added to soil (L2-2, S1-2 and X1-2) had the highest degradation rate which reached over 45%. In the meanwhie, since oil content in topsoil (L2-1, S2-1 and X1-1) was high itself, the degradation of No. 20 heavy diesel oil couldn't be reflected when formed into mixture with oil in topsoil. Therefore, the degradation rate was between oil residues and No. 20 heavy diesel oil

3.2.1.3 Dissolved Oil. Dissolved oil also had a higher degradation rate with the value of 40.33%.

3.2.2 Kinetics of Microbial Degradation

According to the results in Table 4, the oil content in soil and water decreased with time and the degradation rule could be expressed as:

$$C = C_0 e^{-\lambda} \tag{1}$$

where C_0 is the initial oil concentration in soil of water; C is the instantaneous oil concentration of soil or water; λ is the microbial degradation constant.

In addition, it could be found from Eq. (1)that the microbial degradation rate in soil accorded with the first class kinetic equation, that is

$$\frac{dC}{dt} = \lambda C \tag{2}$$

Meanwhile, the half-life ($t_{1/2}$) of oil degradation in soil and water could be derived as

$$t_{\frac{1}{2}} = \frac{0.693}{\lambda} \tag{3}$$

As a result, the reaction rate was measured according to bio-degradation coefficient (λ) and half-life ($t_{1/2}$), that is, the larger λ value (the $t_{1/2}$ smaller), the faster responded.

Table 4. Degradation experimental results of remnant oil and aqueous oil

Test Samples	*Oil Content (mg/l)*	*Oil Content in Soil and Water of Different Time (mg/l)*										*Degradation ratio(%)*
		0d	*2d*	*4d*	*8d*	*15d*	*25d*	*40d*	*60d*	*80d*	*110d*	
L2-1	0	676.3	671.5	652.1	638.9	632.4	631.7	622.4	618.0	609.0	604.4	10.63
	272	931.0	911.4	876.0	841.1	838.2	822.3	199.1	764.5	731.9	716.0	23.09
S1-1	0	1404.7	1396.1	1389.2	1342.1	1326.2	1311.3	1301.4	1281.7	1269.2	1267.9	9.74
	272	1710.1	1711.2	1678.9	1644.1	1590.0	1521.1	1485.0	1445.8	1421.7	1420.9	16.91
X1-1	0	171.4	174.4	168.9	162.1	160.0	159.1	157.1	154.0	156.2	153.5	10.53
	136	313.2	302.9	284.0	262.2	240.1	230.4	210.1	197.0	189.2	192.1	38.17
S1-2	68	97.9	92.3	89.2	78.2	70.4	61.7	58.3	55.6	56.1	53.7	45.15
X1-2	68	98.1	91.4	85.1	72.4	67.3	61.4	59.0	56.4	56.7	51.3	47.71
L2-2	68	94.4	89.7	82.7	78.5	71.6	66.4	57.1	52.6	53.1	51.9	45.02
Dissolved Oil	Saturated	18.1	17.3	16.8	16.6	16.1	14.7	13.9	12.7	11.4	10.8	40.33

Table 5. Dynamic characters of oil degradation

Tested samples	*Oil Content (mg/l)*	*Dynamic equation*	*R2*	*Detant Constant(1/h)*	*Half Life(h)*
L2-1	0	$y=654.8e^{-0.00004x}$	0.7538	4×10^{-5}	17325
	272	$y=885.1e^{-0.00009x}$	0.8973	9×10^{-5}	7700
S1-1	0	$y=1369e^{-0.00007x}$	0.7715	4×10^{-5}	17325
	272	$y=1649.1e^{-0.0000x}$	0.8192	7×10^{-5}	9900
X1-1	0	$y=167.05e^{-0.00004x}$	0.6675	4×10^{-5}	17325
	136	$y=277.69e^{-0.0002x}$	0.7871	2×10^{-4}	3465
L2-2	68	$y=82.26e^{-0.0002x}$	0.8027	2×10^{-4}	3465
S1-2	68	$y=82.23e^{-0.0002x}$	0.7008	2×10^{-4}	3465
X1-2	68	$y=81.23e^{-0.0002x}$	0.7227	2×10^{-4}	3465
Dissolved Oil	Saturated	$y=17.209e^{-0.0002x}$	0.968	2×10^{-4}	3465

By numerical calculation, the dynamic equation and eigenvalue of oil degradation in soil and water were presented in table 5. On the basis of calculation results, the degradation half-life of No. 20 heavy diesel oil was 3465 h (144 d), while the half-life of oil in topsoil (L2-1, S1-1 and X1-1) was 17325 h (722 d).

4 Conclusions

- Indigenous microbial flora addicted to oil has formed after a long-term oil sewage irrigation, which was dorminated by bacteria with bacillus bacteria prevailing.
- The quantity and species of soil microbes varied with sampling time although of the same contaminated area and the same soil, which mainly due to temperature.
- The degradation rate of oil residues which have been accumulated for a long time was the lowest, with olny about 10% on the day of 110. No. 20 heavy diesel oil added to soil (L2-2, S1-2 and X1-2) had the highest degradation rate which reached over 45%. Dissolved oil also had a higher degradation rate with the value of 40.33%.
- The oil content in soil and water decreased with time. The microbial degradation rate in soil accorded with the first class kinetic equation. The reaction rate was measured according to bio-degradation coefficient (λ) and half-life ($t_{1/2}$), that is, the larger λ value (the $t_{1/2}$ smaller), the faster responded. No. 20 heavy diesel oil was 3465 h (144 d), while the half-life of oil in topsoil (L2-1, S1-1 and X1-1) was 17325 h (722 d).

Acknowledgment. The authors would like to express their thanks to NSFC (National Natural Science Foundation of China) for financial support by the foundation item No.40272108.

References

1. Huang, D.: Petroleum Microbiology. Petroleum Industry Press, Beijing (1991)
2. Alexander, M.: Introduction to Soil Microbiology. John Wiley, New York (1977)
3. Atlas, R.M.: Microbial Degradation of Petroleum Hydrocarbons. Microbio. Rev. 45, 180–209 (1981)
4. Testa, S.M., Paczkowski, M.T.: Volume Determination and Recovery of Free Hydrocarbon. Ground Water Mornitoring Review 9(1), 120–127 (1989)
5. Shafer, J.M.: Reverse Pathline Calculation of Time Related Capture Zones in Nonuniform Flow. Ground Water 25(3), 283–289 (1989)
6. Jamison, V.W.: Biodegration of High Octane Gasoline in Ground water. Developments in Industrial Microbiology 16 (1975)
7. Zheng, X., Liu, X., Qian, H.: Mechanism of Oil Water Emplacement in Soil. Acta Scientiae Circumstantiae, 218–220 (1999)
8. Zheng, X., Liu, X., Yang, X.: Study on Coupling Model of Oil Contaminant Transport in Groundwater and Its Application. Geotechnical Investigation & Surveying, 37–41 (1999)
9. Zheng, X., Qiu, H.: Numerical Modeling on Elimination of Oil-polluted Soils in Shenyang-Fushun Irrigation Area. Earth Science(Journal of China University of Geosciences), 462–466 (2000)
10. Chen, Y., Zheng, X., She, Z., Jin, C.: The Groundwater Pollution of Daqing Oilfield Light Oil Spill. Earth Science Frontiers, 421–424 (2001)

11. Zheng, X., Li, Y., Lin, G., Ma, Y., Xia, W.: Adsorption of Aqueous Oil on Soils and Its Analysis of Effective Factors. Earth Science (Journal of China University of Geosciences), 563–566 (2003)
12. Zheng, X., Qiu, H.: Numerical Analysis of Aqueous Oil Transport and Control in Soil-water Systems. Environmental Geology (6) (2001)
13. Zheng, X., Qiu, H.: Numerical Analysis on Aqueous Oil Transport and Control Strategy in a Soil-water System. In: International Symposium on Hydrogeology and the Environment, Wuhan, pp. 163–167 (2000)
14. Zheng, X., Li, Y., Lin, G.: Behaviors of Aqueous Oil Adsorption-release in Oil-contaminated Soils. In: Proceedings of the International Symposium on Water Resources, Wuhan (2003)
15. Zheng, X., Lin, G.: Behaviors of Aqueous Oil Adsorption-Release in Oil-contaminated Soils. In: Proceedings of the International Symposium on Water Resources, Wuhan (2003)
16. Zheng, X., Wang, B., Li, Y.: Studies of Degradation Kinetics of Petroleum Contaminants in Soil-water Systems. Geologica Sinica (3) (2004)
17. Gao, Z.: Study on Soil-plant System Pollution Ecology. Chinese Science and Technology Press, Beijing (1986)

Iteratively Predict Protein Functions from Protein-Protein Interactions

Xiaoxiao Chi[1] and Jingyu Hou[2]

School of Information Technology, Deakin University, Melbourne, Australia
{xchi,jingyu}@deakin.edu.au

Abstract. Current similarity-based approaches of predicting protein functions from protein-protein interaction (PPI) data usually make use of available information in the PPI network to predict functions of un-annotated proteins, and the prediction is a one-off procedure. However the interactions between proteins are more likely to be mutual rather than static and mono-directed. In other words, the un-annotated proteins, once their functions are predicted, will in turn affect the similarities between proteins. In this paper, we propose an innovative iteration algorithm that incorporates this dynamic feature of protein interaction into the protein function prediction, aiming to achieve higher prediction accuracies and get more reasonable results. With our algorithm, instead of one-off function predictions, functions are assigned to an unannotated protein iteratively until the functional similarities between proteins achieve a stable state. The experimental results show that our iterative method can provide better prediction results than one-off prediction methods with higher prediction accuracies, and is stable for large protein datasets.

Keywords: Functional Prediction, Iterative Method, Protein-Protein Interaction, Gene Ontology.

1 Introduction

One of the major challenges in post-genomics is to assign biological functions to uncharacterized proteins[1]. With the availability of various high-throughput datasets, it becomes feasible to use computational approaches to annotate functions of uncharacterized proteins. Protein-protein interaction (PPI) datasets are among the commonly used datasets for this purpose. The interaction data in a PPI dataset is usually modelled as an undirected acyclic graph. The nodes in the graph represent unique proteins and the edges represent the interactions between proteins [2]. Recent research [3] indicated that proteins interact with each other to perform their functions in various biological processes rather than working alone. Therefore it is possible to predict functions for an unannotated protein from the available functions of its neighbour proteins [4].

In addition to the protein interaction information, a protein function annotation scheme which gives a functional description/definition to each function is also necessary for function prediction. The commonly used annotation schemes are Function Catalogue (FunCat) [5] and Gene Ontology (GO) [6]. FunCat describes

E. Zhu and S. Sambath (Eds.): Information Tech. and Agricultural Eng., AISC 134, pp. 771–778.
springerlink.com © Springer-Verlag Berlin Heidelberg 2012

protein functions with a hierarchical and numerical structure. It is organism-independent, flexible and scalable. GO gives a well-defined structure which defines functional terms as well as their relationships. It is a dynamic, controlled vocabulary that can be applied to all of gene and protein roles. In this work, we use GO for function prediction.

With the available PPI datasets and function annotation schemes such as GO, a number of approaches have been proposed to predict protein functions. Our work in this paper just focuses on the approaches that are based on the similarity definition between proteins, as well as the similarity between functions. The early work by Schwikowski [17] proposed a simple but feasible Neighbour Counting approach which annotated a protein with the functions that occurred most frequently among its neighbour proteins. Hishigaki [7] improved Schwikowski's method by using the Chi-Square statistics instead of frequency as a scoring function. Other work extended the Neighbour Counting approach in different ways, such as Chua [8] that included indirect neighbors when predicting the function of a protein. Recently, more and more research focused on predicting protein functions semantically by combining the inter-relationships of function annotation terms in a scheme such as GO with the topological structure information in the PPI network. For semantically predicting protein functions, various methods have been proposed to calculate functional similarities between the annotation terms [9]. For instance, Resink [10] used the concept of information content to calculate the semantic similarity between two GO terms. Jiang and Lin [11-12] improved Resink's method by scaling the similarity to a fixed range. With the similarities between functions (i.e. functional terms) and the similarities between proteins, some methods such as k-Nearest Neighbour (kNN) based ones [16] have been developed to combine these similarities in function prediction.

Although the existing approaches can predict functions effectively to some extents, the prediction results were not satisfactory in most cases. Actually the existing approaches, whether they are semantic or not, just considered the function prediction as a one-off procedure. That is, the available functional information determines the functions of the unannotated proteins, and once the functions of the unannotated proteins are determined or predicted, the prediction procedure is then completed. In real biological processes, however, proteins have high mobility and they dynamically interplay for producing a framework which is ever-changing but overall stable[13]. These proteins exchange their biological information and share functions in a dynamic circumstance rather than a mono-directed and static process. In other words, the dynamic interactions between pair wise proteins reveal the reality of biological processes, and this dynamic feature of protein interactions should be taken into account in function prediction. Unfortunately, the existing approaches did not investigate this dynamic process and validate whether all the interactions achieved a stable state in terms of similarity after the first, which is also the last, prediction.

In this paper, we propose an innovative algorithm to predict functions iteratively by simulating the dynamic process of protein interactions in terms of protein and function similarities. Details of the algorithm are presented in the following section.

The rest of the paper is organized as follow. In section 2, we give details of our iterative algorithm. In section 3, we present the evaluation results of our algorithm, as well as comparison results with other existing methods. We conclude our work in section 4 and give some possible improvements of the iterative algorithm in the future.

2 Algorithm

Our iterative prediction algorithm is based on the weighted kNN algorithm. We denote the unannotated protein as p, the neighbour proteins of p as $N(p)$. The neighbour proteins of a protein p are those that have direct and/or indirect interactions with p in the PPI network. For simplicity of the algorithm, in this work the neighbour proteins of p are those proteins that have direct interactions with p. We also denote the set of functions of a protein p as $F(p)$, and the set of functions of all the neighbour proteins of p as $F_N(p) = \{F(p') \,|p' \in N(p)\}$. The functions in our work are represented as the GO terms.

Suppose we have already defined the similarity between two proteins p and p' as $sim(p,p')$. Then the score of the unannotated protein p being annotated by a function f is defined as:

$$score(p,f) = \sum_{p' \in N(p)} [sim(p,p') \times I_{f,p'}] \quad (1)$$

where $f \in F_N(p)$ and the $I_{f,p'}$ function is defined as follow

$$I_{f,p'} = \begin{cases} 1 & f \in F(p') \\ 0 & f \notin F(p') \end{cases}$$

The function prediction is then based on (1). In fact, each $f \in F_N(p)$ has a score with respect to p according to (1), and all functions in $F_N(p)$ can be ordered by their scores from the highest to the lowest. We then select the first k functions with the k highest scores as the predicted functions of the protein p. The value of k is determined empirically or by the prediction requirements. In this work, we select k as the average number of functions of the neighbour proteins.

It can be seen from (1) that the similarity between two proteins plays a key role in function prediction. If the protein similarity is defined by other ways rather than by protein functions, the prediction algorithm (1) is just a normal weighted kNN algorithm, and the iterative prediction does not make sense. So the prediction does not reflect the dynamic features of protein interactions, and it is just a one-off process. What makes our algorithm different from the existing algorithms is that our protein similarity $sim(p,p')$ is defined from the function similarities of these two proteins. With this similarity definition, prediction algorithm (1) has to go through an iterative process to finally predict functions when the similarities achieve a stable state. During this iterative process, the dynamic features of protein interactions are incorporated into the prediction.

Now we give the similarity definition of two proteins from their functions. Suppose the number of function in $F(p)$ is m, and the number of functions in $F(p')$ is n. The similarity between two proteins p and p' is defined as

$$sim(p,p') = \frac{1}{m \times n} \sum_{f \in F(p)} \sum_{f' \in F(p')} \delta_{f,f'} \quad (2)$$

where $\delta_{f,f'}$ is an indicator function, i.e. if f and f' are the same, its value is 1, otherwise 0.

To kick off the iterative prediction of (1) with the similarity (2), we need to assign initial functions to the unannotated protein p. The initial functions are assigned to p according to their scores calculated by (1) as well. But since the functions of p at this moment are unknown, and in turn the protein similarity $sim(p, p')$ in (1) is unknown either, we calculate the function scores by setting $sim(p, p') = 1$ for any $p' \in N(p)$, i.e.

$$score^{(0)}(p, f) = \sum_{p' \in N(p)} I_{f,p'} \text{ , for } f \in F_N(p) \quad (3)$$

We set the threshold of initial function selection as follow:

$$\varepsilon = \frac{1}{size(F_N(p))} \sum_{f \in F_N(p)} score^{(0)}(p, f) \quad (4)$$

where $size(F_N(p))$ is the number of functions in the set $F_N(p)$. Then the functions with scores calculated by (3) over the threshold (4) are selected as the initial functions of the unannotated protein p.

With the initial functions of the unannotated protein p, the prediction can be conducted iteratively by (1) until a stable state is achieved in terms of similarities. The pseudo-code of the iterative prediction algorithm is presented below.

Inputs: The unannotated protein: p
The interaction neighbours of p: $N(p)$
The function annotations of $N(p)$: $F_N(p)$
The preferred number of predicted functions: k

1. $F(p)$=[ ]; //set of predicted functions of p before the next iteration
2. $F'(p)$=[ ]; //set of predicted functions of p after the iteration
3. *Rank*($F(p)$); //the set of ranked functions of $F(p)$
4. *Rank*($F'(p)$); //the set of ranked functions of $F'(p)$
5. Initialize $F(p)$ by (3) and (4);
6. Calculate the protein similarities by (2);
7. Calculate the function scores by (1);
8. $F'(p)$ = selected k functions in $F_N(p)$ with the highest k scores
9. If ($F'(p)$=$F(p)$ and the function order in *Rank*($F'(p)$) = the function order in *Rank*($F(p)$))
10. { output the prediction results $F'(p)$; stop the iteration; }
11. Else { $F(p)$=$F'(p)$; go to step 6;}

3 Evaluations

We used the protein-protein interaction (PPI) dataset of *S. Cerevisiae* derived from the BioGrid site (http://thebiogrid.org/) to build a protein interaction network for our experiment. The GO terms [6] and GO annotation dataset [14] used in the experiment were downloaded from http://www.geneontology.org/ in April 2010. We only took the biological process ontology and the GO annotations of *S. Cerevisiae* in our experiment.

The performance of prediction algorithms was evaluated by their *precision*, *recall* and *F-value*, which are defined as follows:

$$Precision = \frac{N_P}{N_R} , \quad Recall = \frac{N_P}{N_A} ,$$

$$F - value = \frac{2 \times Precision \times Recall}{Precision + Recall} ,$$

where N_P is the number of correctly predicted functions for a given protein p, N_A is the number of known functions of protein p, N_R is the number of all predicted functions for protein p. It is hard to guarantee both precision and recall achieve a high value simultaneously, so *F-value* which combines *precision* and *recall* values was used to evaluate the overall performance of the algorithms [15] .

When using *precision*, *recall* and *F-value* to evaluate the algorithm performance, it was common that the evaluation only focused on the exact match between predicted and known functions. However, function annotations of proteins have their specific features in the context of an annotation scheme such as GO. For example, as illustrated in Figure 1, the structure of GO is hierarchical with the nodes representing the GO terms and the edges representing ancestor-child relationships. If a protein p is annotated by a node, for instance G6, it is also annotated by all ancestor nodes of G6, i.e. the nodes G4, G2 and G0 [16]. Suppose the known function annotation of protein p is G6 and the only predicted function annotation is G5, the values of both recall and precision are 0 if we just consider the exact match of the functions. However, as we can see in Figure 1, G5 should be very similar to G6 as they share the same ancestors, and we should not say they are totally different. Therefore in our evaluations, in addition to evaluating the exact match of functions, we also evaluated the performance of the algorithms (in terms of *precision*, *recall* and *F-value*) over the ancestor annotation terms in GO. This ancestor annotation evaluation does make sense in biology because although two proteins interact with each other, they are not necessarily to be with the exact same functions but might be in a more general function category (i.e. the ancestors in GO). It can be seen that this kind of ancestor prediction and evaluation is more feasible and practical in real biological applications. In this example, although the values of precision and recall are 0 for the exact function match, the values are 1 (100%) for the evaluation of ancestor prediction.

In the evaluation, we also compared our iterative algorithm with two algorithms that are also based on kNN method. One is Neighbour Counting (NC) [17] which predicted functions in the same way as the initial function assignment in our algorithm, but without iterations. Another one is the k Nearest Neighbor Classifier (kNNC) [16]. With the kNNC algorithm, the score of a function f with respect to the unannotated protein p is calculated as follow:

$$score(p,f) = \sum_{p' \in N(p)} [sim(p,p') \times \sum_{f' \in F(p')} linsim(f,f')], \quad f \in F_N(p).$$

The function similarity $linsim(f,f')$ is calculated as:

$$linsim(f,f') = \frac{2 \times [\log p_{ms}(f,f')]}{\log p(f) + \log p(f')}$$

where $p(f)$ is the appearance probability of the function term f in GO, and $p_{ms}(f,f')$ is the minimum appearance probability of the common ancestors of function terms f and

f'. To make the kNNC algorithm be comparable with our algorithm, we used our definition of $sim(p, p')$ in the above score calculation and also went through iterations in the prediction.

The experimental results of our iterative algorithm (denoted as Iteration), NC and kNNC algorithms are presented in figure 2 and figure 3 for the exact function annotations and ancestors of function annotations respectively. The evaluation was conducted over test datasets with different sizes ranging from 20 to 200. The experimental results showed that our iterative algorithm over performed other selected algorithms in terms of precision, recall and F-value, and was stable with large datasets.

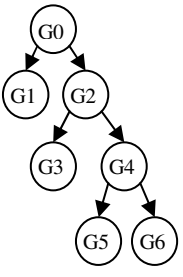

Fig. 1. A GO structure example

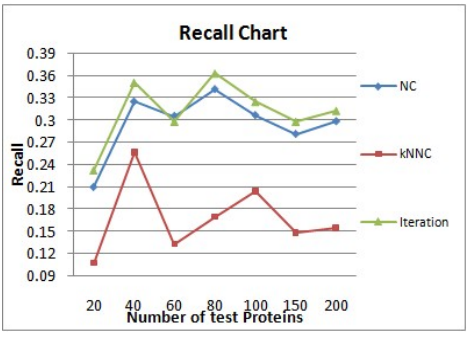

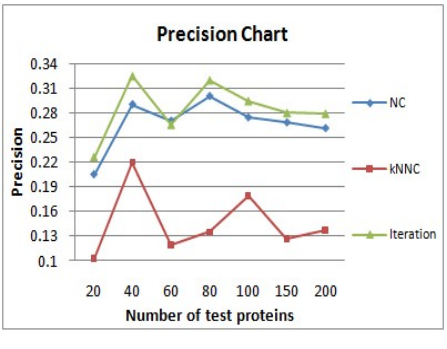

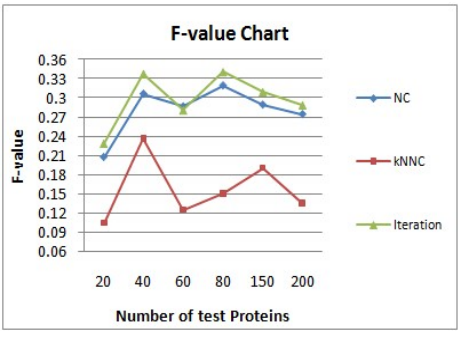

Fig. 2. Recall, precision, F-value for exact function annotations

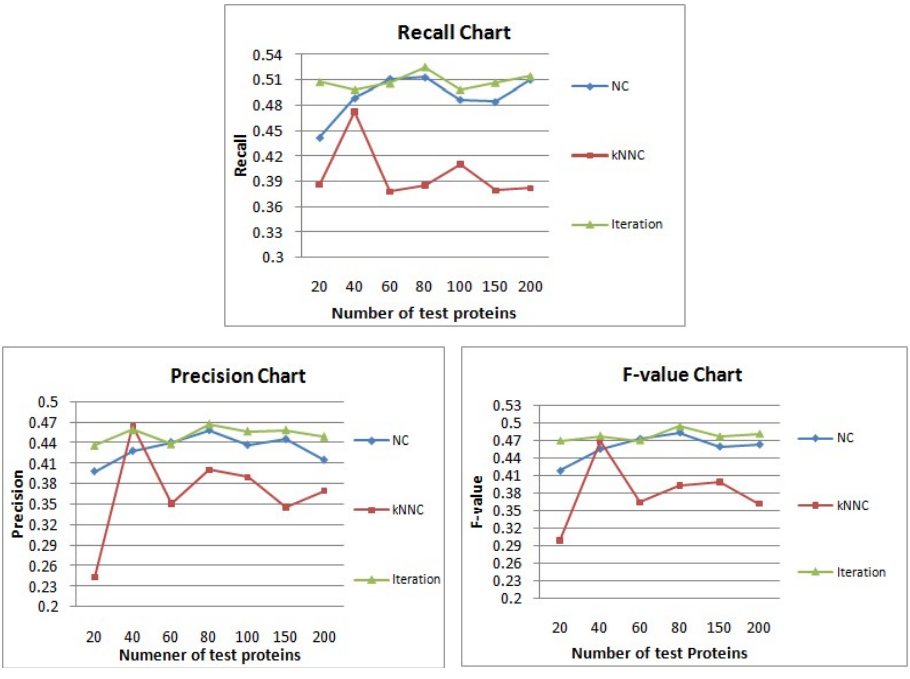

Fig. 3. Recall, precision, F-value for ancestors of function annotations

4 Conclusions

In this paper, we propose a novel iteration algorithm for predicting functions of unannotated proteins iteratively from protein-protein interaction (PPI) datasets. This approach takes into account the dynamic features of interactions between proteins, and is more likely to reflect the real biological processes between proteins. The evaluation results showed the feasibility, effectiveness and higher prediction accuracies of the proposed algorithm.

Although our iterative method performs better than other similar methods, some issues still need to be addressed in the future work. Since the definition of function or GO term similarity, and in turn the protein similarity, plays an important role in the algorithm, how to reasonably define the similarities to improve the prediction performance of the algorithm is worth investigation. As we can see, the prediction is based on the neighbour proteins as well as their available information. In this work, we just selected those proteins that directly interact with the unannotated protein as the neighbours. Further research could be done to select better neighbours to improve the prediction results while reducing the impact of noise data. Whether the way of selecting initial functions for iterations will affect the final prediction results or not also needs to be investigated. These issues will be the focuses of our future research.

References

1. Ching, W., Li, L., Chan, Y., Mamitsuka, H.: A Study of Network-based Kernel Methods on Protein-Protein Interaction for Protein Functions Prediction. In: The Third International Symposium on Optimization and System Biology, pp. 25–32 (2009)
2. Wang, M., Shang, X., Zhang, S., Li, Z.: Using Direct and Indirect Neighbours to Predict Protein Function in GO-Evaluated PPI Data Set. In: Intelligent System and Applications(ISA), pp. 1–4 (2010)
3. Chua, H., Wong, L.: Predicting Protein Functions from Protein Interaction Networks. Biological Data Mining in Protein Interaction Networks, 204–223 (2009)
4. Deng, M., Zhang, K., Mehta, S., Chen, T., Sun, F.: Prediction of protein function using protein-protein interaction data (2002)
5. Ruepp, A., Zollner, A., Maier, D., Albermann, K., Hani, J., Mokrejs, M., Tetko, I., Güldener, U., Mannhaupt, G., Münsterkötter, M.: The FunCat, a functional annotation scheme for systematic classification of proteins from whole genomes. Nucleic Acids Research 32, 5539 (2004)
6. Ashburner, M., Ball, C., Blake, J., Botstein, D., Butler, H., Cherry, J., Davis, A., Dolinski, K., Dwight, S., Eppig, J.: Gene ontology: tool for the unification of biology. Nature Genetics 25, 25–29 (2000)
7. Hishigaki, H., Nakai, K., Ono, T., Tanigami, A., Takagi, T.: Assessment of prediction accuracy of protein function from protein-protein interaction data. Yeast 18, 523–531 (2001)
8. Chua, H., Sung, W., Wong, L.: Exploiting indirect neighbours and topological weight to predict protein function from protein–protein interactions. Bioinformatics 22, 1623 (2006)
9. Chen, G., Wang, J., Li, M.: GO semantic similarity based analysis for huaman protein interactions, pp. 207–210 (2009)
10. Resnik, P.: Using information content to evaluate semantic similarity in a taxonomy. Arxiv preprint cmp-lg/9511007 (1995)
11. Jiang, J., Conrath, D.: Semantic similarity based on corpus statistics and lexical taxonomy. Arxiv preprint cmp-lg/9709008 (1997)
12. Lin, D.: An information-theoretic definition of similarity, pp. 296–304 (1998)
13. Misteli, T.: Protein dynamics: implications for nuclear architecture and gene expression. Science 291, 843 (2001)
14. Dwight, S., Harris, M., Dolinski, K., Ball, C., Binkley, G., Christie, K., Fisk, D., Issel-Tarver, L., Schroeder, M., Sherlock, G.: Saccharomyces Genome Database (SGD) provides secondary gene annotation using the Gene Ontology (GO). Nucleic Acids Research 30, 69 (2002)
15. Zhu, W., Hou, J., Phoebe Chen, Y.: Semantic and layered protein function prediction from PPI networks. Journal of Theoretical Biology (2010)
16. Pandey, G., Myers, C., Kumar, V.: Incorporating functional inter-relationships into protein function prediction algorithms. BMC Bioinformatics 10, 142 (2009)
17. Schwikowski, B., Uetz, P., Fields, S.: A network of protein–protein interactions in yeast. Nature Biotechnology 18, 1257–1261 (2000)

Integration of Multiple Methods to Identify Major Wild Bird Species around Qinghai Lake*

Li Jian[1], Zhang RuiYing[2], Wan SunHua[1], Cao WenBin[1],
Zhu ChaoDong[2], Lei FuMin[2], and Yan BaoPing[1]

[1] Computer Network Information Center, Chinese Academy of Sciences,
Beijing, China 100080
[2] Institute of Zoology, Chinese Academy of Sciences, Beijing, China 100101
{lijian,wsh,wbcao,ybp}@cnic.cn,
{zhangry,zhucd,leifm}@ioz.ac.cn

Abstract. With a view to conducting targeted monitoring, protection and study on the wild birds around Qinghai Lake, this paper attempts to propose an identification system on the major species of wild birds around Qinghai Lake via morphology (DELTA and image retrieval) and molecular data (DNA barcoding), etc. which can specify the bird species in the area of Qinghai Lake in a fast and accurate way and provide multiple interfaces for the international systems of the same kind to achieve seamless integration. It is aimed at creating an efficient academic environment for scientists, which is also of great significance in science popularization.

Keywords: Species identification, Morphological identification, DELTA, image retrieval, DNA barcoding, BLAST.

1 Overview

As the largest inland saltwater lake and internationally important wetland in China, Qinghai Lake area is one of the regions with most biodiversity on the Qinghai-Tibet Plateau and over 160,000 in more than 160 types of aquatic birds subsist around this water habitat, such as bar-headed goose, brown-headed gull. In May 2005, there was an outbreak of avian flu H5N1 in the lake area, causing death to large numbers of wild birds including over 300 bar-headed geese, which raised wide concern from the international communities.

Taking this incident very seriously, Computer Network Information Center (CNIC) of Chinese Academy of Science (CAS), in collaboration with other six academic institutions in CAS and Administration Bureau of Qinghai Lake National Natural Reserve, set up the'Joint Research Center of Chinese Academy of Sciences and Qinghai Lake National Nature Reserve'. In the past five years, many effective methods like the field data collection system based on PDA and the networked video monitoring system have been developed to monitor wild bird populations around the Qinghai Lake.

* This work is financially supported by NSFC (30925008), CAS Innovation Program (INFO-115-D02,INFO-115-C01-SDB2-02) and CNIC Grant (CNIC QN 10010).

E. Zhu and S. Sambath (Eds.): Information Tech. and Agricultural Eng., AISC 134, pp. 779–788.
springerlink.com © Springer-Verlag Berlin Heidelberg 2012

According to the collected scientific data, the spatial distribution pattern analysis based on data mining and researches on cross-host transmission ability of avian influenza virus have been carried out. In this research process, to identify a wild bird species has become a key point which is much needed for fast and accurate scientific solution,especially in fast identifying the host wild birds killed by avian influenza viruses.

Combining the current species identification methods, the paper proposes an identification system for major bird species around Qinghai Lake as an initial start of the whole wild bird identification program, which not only adopts the morphological ways including description language for taxonomy(DELTA)[1] and morphology-based retrieval of birds' image and also employs such methods as molecular biology based DNA barcoding. With these methods, species can be identified in a fast and precise manner from morphological and genetic characteristics.

2 Structure of the Identification System on the Major Wild Bird Species around Qinghai Lake

The design procedure of this system can be summarized as follows:

1) To collect gene data, sample data and other relevant data of major wild birds around Qinghai Lake and build a database as the standard data for follow-up species identification;
2) To conduct algorithm analysis and processing on the specific information about morphology and DNA of species to be identified against the above standard data in order to accurate identification and visualization on the target species morphology/DNA data information.

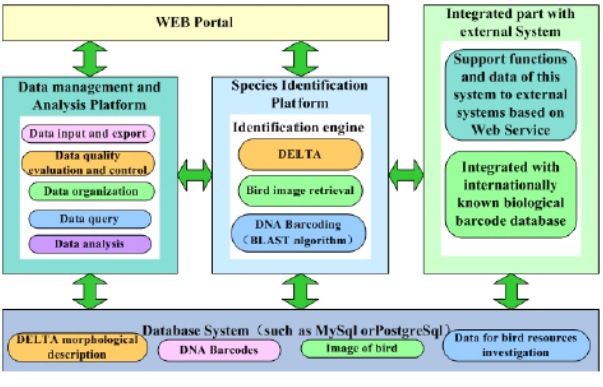
WEB Portal
Integrated part with external System
Data management and Analysis Platform
Data input and export
Data quality evaluation and control
Data organization
Data query
Data analysis
Species Identification Platform
Identification engine
DELTA
Bird image retrieval
DNA Barcoding (BLAST algorithm)
Support functions and data of this system to external systems based on Web Service
Integrated with internationally known biological barcode database
Database System (such as MySql orPostgreSql)
DELTA morphological description
DNA Barcodes
Image of bird
Data for bird resources investigation

Fig. 1. Structure of this identification system for major wild bird species around Qinghai Lake

According to the design procedure in Figure 1, the system can be divided into the following main modules:

1) data entry: various data including DNA barcodes, DELTA morphological description, birds' image and birds resources investigation data will be gathered into the database. Meanwhile, the system provides data quality evaluation and control, scientific organization and integration of data resources along with the functions of data query and analysis.
2) identification methods: Based on the above standard data, the identification platform provides methods of DELTA morphological taxonomy, birds' image retrieval and DNA barcodes comparison through BLAST[2] algorithm, which greatly facilitate users to identify the unknown species by using this platform.
3) WEB portal: WEB portal offers three users-oriented services:
   a) provide website administrators with easy access to scientific management and maintenance of the system;
   b) offer the scientific researchers with simple and usersfriendly scientific working platform;
   c) offer an integrated platform of popular science, knowledge dissemination and education for the general public;
4) The integrated part with the external system: It involves of two functions:
   On one hand, regarding the needs and demands of the scientists and based on the Web Service method, the internationally known biological barcode database (such as Barcode Of Life Data System, (short for BOLD system)[3], GenBank[2], and among others) can be integrated to obtain the latest scientific data.

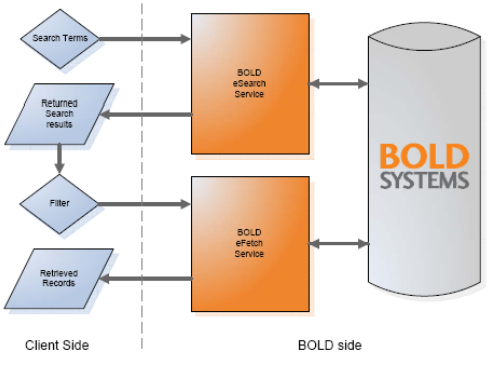

Fig. 2. Illustration of BOLD Web Service architecture [3]

The Figure 2 shows the integration between this system and BOLD system. BOLD can provide open data for users to search and acquire through the interface of Web Service, which can be interpreted as follows in Figure 2:

a) Remote calling can be conducted to the eSearch function via keywords so that relevant information, like taxid of the species, can be obtained from the feedback results.
b) After the feedback results are filtered as required, users can get access to the database again via the eFetch function, then back to the detailed data for the specific species to select what they need among gene sequence, sample information and species taxonomy, etc.

On the other hand, this system can also provide similar interfaces with web service of BOLD system to enable seamless integration with modules of spatial distribution pattern, virus transmission for wild birds and collaboration environment.

3 Species Identification by Morphology

As it has prevailed for over 250 years, the Morphologybased biological taxonomy method currently has identified about 1.7 million species and gradually evolves into many morphology-related identification methods. This system adopts two methods to identify species, which are DELTA system and birds' image retrieval.

3.1 DELTA Morphological Identification Method

Many systems have been designed for species identification using taxonomic description language. We choose two of them, DELTA and LUCID[4], which are correspondingly successful, to make a detailed introduction.

1) DELTA
DELTA is a computer information processing system for taxonomic description. It was designed, established by Dallwitz et al in Division of Entomology of CSIRO[5]. For the past 40 years, it has been gradually improved. It's mainly used to provide a standard for morphological description so that automatic description of taxonomic groups, interactive identification and management of classification information can be realized based on this standard.

Table 1. Local delta vs. delta online

items	local Delta	Delta online
usage mode	Set up in local system	access it over Internet explorer
System request	Run in windows system	No request to local system
Storage	need local storage	Need no local storage
update	difficult to update in time	only update on server
data validity	can't be ensured because users will establish data	can be guaranteed because experts will establish data

However, as a local software, DELTA inevitably has its shortcomings. Both users and developers hope to get the taxonomy description system onto the Internet. Compared with the local software, DELTA online has its advantages. The table 1 demonstrates the detailed comparison.

2) LUCID
LUCID system is established by Centre for Pest Information Technology and Transfer (CPITT) in University of Queensland. It's a multi-way expert system for identification and diagnosis based on multimedia technology. This system is widely used both at

home and abroad. For example, there are ”Grape pest identification and diagnosis” and ”Identification and control of pests in warehouse” abroad and ”The webbased entry-exit plant quarantine information management and decision assistance system” published in Journal of Zhejiang University. All of these systems take LUCID as a developing tool for recognition and diagnosis[6].

Users can judge an individual’s species based on its several morphological characteristics through LUCID, which has great taxonomic significance. However, although LUCID can be accessed on Web, it needs to start up JVM on usersside, which also brings inconvenience by affect the system’s response speed. In addition, LUCID is commercial software so users need to pay for it while DLETA system can be used free of charge although it doesn’t open its source codes.

3) Web-based Bird DELTA System

DELTA system and LUCID system are mainly used in taxonomy of plants and insects, but rarely in vertebrate. The morphological characteristics library for birds has yet to be established. Web-based Bird DELTA System proposed in this paper innovatively provides a morphological taxonomic method aimed at wild birds around Qinghai Lake. Experts build a database of birds’ Latin names and their form characteristics, such as bill color, pattern of plumage and the features of tarsometatarsus. Relation between species and its features is also added in the database.

This system draws on the powerful functions of DELTA system and LUCID system and overcomes their defects. Based on B/S architecture, this system assigns the appropriate extent of power to different users. Table 2 indicates specific functions and power for various kinds of users.

Firstly, administrators input correlative data into the database. Secondly, professionals look through the database to ensure data accuracy. Then, the verified data can be provided for users to identify the species of birds.

Table 2. Different users of internetized bird delta system

Identity	Functions and Power Limit
Administrators	They can add or delete the data of species and its features. New species added will be marked for experts’ validation. An example image will be offered for each feature in order to visualize features.
Experts	They can examine new species information and export data from the current database as local DELTA-format documents.
Users	Descriptions about species’ features are transparent to users. They can judge the species of birds based on the features of bird individual they see.

3.2 Content-Based Birds’ Image Retrieval Module

1) Rationale

As the images of birds are much easier for users to obtain, this system tries to allow users to submit images of birds to be identified for later automatic identification of species taxonomy. This module requires image features for retrieval including color,

texture and shape of the birds in the image. Among these features, the color of the birds in the image is the most important factor in identification process that this module will focus on. The advantages of using color features as a key factor are remarkable: they have low computation complexity, require less memory space, which enables color to be commonly used in the content-based image retrieval[7].The frequently used color features consist of color histograms, color moments, color coherent vector, color correlogram, color sets and so on. Color histogram is a statistical method on the proportion of each color in all pixels of an image. As it targets at the overall feature of an image, this method is quite robust in recognizing the shift, rotation, distortion and scaling of birds in the image. So, the color histogram is suitable for birds image identification.

2) System Architecture and Procedure

This paper gives out a specific way to retrieval birds' image with color histogram[8]. The figure 3 has shown that there are three major steps involved:

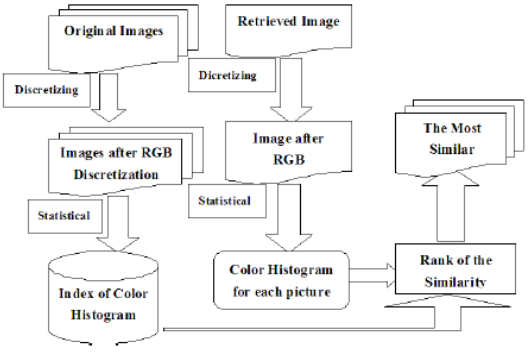

Fig. 3. Architecture of Image Retrieval System Based on Color Histogram

3.2.1 Discredited RGB Color Space

As three primary colors in RGB color space, red, green and blue are independent with each other. They can represent any other colors by mixing up in proportion. Our system use RGB as the color model. Each pixel in the image is separated into three color channels-R, G and B. And each color channel will be divided into N parts evenly. This is the discretization of RGB color space. After discretization, the number of pixels falling into each part will be counted to get the feature of color histogram of the image.

3.2.2 Image Feature Indexing

After the RGB quantization of all the birds' images in the database, an image information database will be established which requires statistical analysis to generate the index of color histogram for all the original images. The color histogram index will be represented as double array. As in practice, the representation of color histograms changes as RGB discretization standards adjust, it is proper to use file or semi-structure databases to store the color histogram index[9].

3.2.3 Retrieval of Images

After the establishment of the color histogram feature index based on the original images database, image retrieval can be conducted based on the content of the images[10]. The main steps involve as follows: similar to establishment of original color histogram, the input image will be RGB discretized first; then to generate the color histogram of the image after statistical analysis; Compare this color histogram with all the color histogram in the indexes and figure out the similarities; Rank the result of comparison and figure out the most similar image[11].

The similarity of the color feature between two images will be measured by the distance of the features. The most common ways of measuring distances are shown as follows:

a) Correlation: $d_{correl}(H_1, H_2) = \frac{\sum_i H_1'(i) \cdot H_2'(i)}{\sqrt{H_1'^2(i) \cdot H_2'^2(i)}}$, $H_k'(i) = H_k(i) - (\frac{1}{n})(\sum_j H_k(j))$

N is the number of divisions in color space discretization. In this formula, result represents total match, -1 represents total mismatch, and 0 epresents no correlation between two images.

b) Chi Square: $d_{chi-square}(H_1, H_2) = \sum_i \frac{(H_1(i) - H_2(i))^2}{H_1(i) + H_2(i)}$.

In the interaction distance, the high score represents better atch and low score represents mismatch.

c) Bhattacharyya Distance: $d_{chi-square}(H_1, H_2) = \sqrt{1 - \sum_i \frac{\sqrt{H_1(i) \cdot H_2(i)}}{\sqrt{\sum_i H_1(i) \cdot \sum_i H_2(i)}}}$.

In Bhattacharyya distance, 0 represents total match while

1 represents total mismatch.

3) Results and Improvement

The system has achieved good experimental results currently. The species of the birds in the input image can be determined correctly only in the first few results of the similarity ranking. However, as a new species identification method, the system has potential of improvement in the aspects of accuracy and efficiency.

In terms of accuracy, as the color histograms only take the whole color feature of the birds into consideration, they neglect the color differences in different parts of a bird. For example, the image of a bird which has black feather covered with white spots is similar to a bird which has a white head and a black body in the color histogram. This problem can be addressed by using color moment[9]. In addition, the image of the birds needs to be separated from the background image either by hands or automatically, in order to reduce the interference of the background image with the retrieval result.

In terms of efficiency, the system works well so far. It takes over ten seconds to retrieve in a database containing more than a thousand images. However, as the database of original images will have a higher capacity, the operational efficiency will plummet. In that case, the algorithm of retrieval should be improved to ensure that the system is efficient enough.

4 Species Identification by DNA

4.1 Overview of DNA Bar-Coding

Although morphological bio-taxonomy is the major way to identify birds, it still has defects, which is concluded in the following [12]:

a) Phenotypic plasticity and genetic variability will lead to incorrect identification;
b) The morphological method cannot identify the potential taxa, which are commonly found in many communities.
c) The morphological method has limits in identifying the gender and developmental stage of the species so that some creatures can not be identified by this method.
d) Taxonomists can only identify a limited number of species, among whom few can make accurate identification on 1000 species. In addition, the groups of taxonomists are far from sufficient.
e) The morphology-based method can not be applied in identifying the incomplete individual of the species, such as scattered feathers or bloodstain.

Considering the above reasons, the morphology-based taxonomy cannot fully meet the scientific demand for bird identification. In 2004, Canadian taxonomist Paul Hebert from Guelph University proposed the concept of DNA bar-coding, which used a small DNA fragment, 648-bp of the mitochondrial gene cytochrome c oxidase subunit I (COI) to discriminate species [13]. Later the conference"Taxonomy and DNA" was held at Cold Spring Harbor, U.S. to propose the large-scale plan of sequencing on COI gene in all the animal species around the world.

Now, the international DNA bar-coding plan for birds has been launched, i.e. ABBI, which lasts for five years and is expected to obtain DNA barcodes of 10,000 bird species with at least five notes for each species. However, ABBI stores birds' DNA barcodes in National Center for Biotechnology Information (NCBI) or BOLD instead of within itself. Along these two platforms, there are also European Molecular Biology Laboratory (EMBL)[14] and DNA Data Bank of Japan (DDBJ)[15].

4.2 Basic Local Alignment Search Tool (BLAST)

Widely used in bioinformatics, BLAST is an algorithm for comparing primary biological sequence information, such as the amino-acid sequences of different proteins or the nucleotides of DNA sequences. The BLAST program was designed by American scientists Eugene Myers, Stephen ALtschul, Warren Gish, David J. Lipman at the National Center of Biotechnology Information(NCBI) and Webb Miller at the NIH (National Institute of Health)[2]. It has main practical applications in the following aspects:

a) To enable a researcher to compare a query sequence in a library or database of sequences and identify library sequences that resemble the query sequence;
b) To enable the researcher to identify sequences in the human genome that resembles the unknown non-human gene based on similarity of sequence;
c) To identify the origin of a certain sequence of DNA;
d) To search bacterial species whose protein is related in lineage to a certain protein?

4.3 Species Identification by DNA Bar-Coding

In this module, the gene sequence of species to be identified will be compared and matched with the gene sequence in the database so that the sequences with high level of similarity will be found out and shown to the user according to their sequence, which consists of the following steps in figure 4:

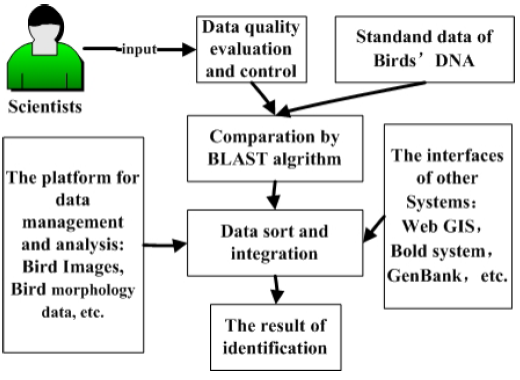
Scientists
input
Data quality evaluation and control
Standand data of Birds' DNA
Comparation by BLAST algrithm
The platform for data management and analysis: Bird Images, Bird morphology data, etc.
Data sort and integration
The interfaces of other Systems: Web GIS, Bold system, GenBank, etc.
The result of identification

Fig. 4. Species identification procedure by DNA bar-coding

First, user presents the DNA sequence data to be identified to check whether the data are consistent with certain quality criteria, such as without improper character or appropriate sequence length;

Second, the eligible DNA sequence data will be compared with the preset standard DNA data of birds using BLAST algorithm;

Third, the comparison result based on BLAST will be sequenced and then linked to the platform of data management and analysis as well as other system interfaces to get detailed information of the species and report it to the user.

Experiments prove that DNA bar-coding has unparalleled advantages over the morphology-based identification method. Due to its objective and complete DNA data of birds, this method ensures that the result of identification is accurate and comprehensive and the above module is running in a highly efficient manner, which plays a significant role in the system.

5 Conclusion

The above species identification methods can offer different users with a fast and convenient approach to identify the unknown species and do effective correlation and integration about the results so that users can not only figure out the species' taxon, but also can get access to the relevant DELTA information and data of image, DNA bar-coding and investigation on the species distribution. Practice shows that this system will create an efficient working environment for scientific researchers, but also make due contribution to the development of popular science education. In the following work, efforts will be made on improving algorithm and efficiency and ensuring

accuracy as well as expanding the study area to include more biological species like mammals and insects and viruses in addition to birds so that a more comprehensive and powerful system will be archived.

Acknowledgment. The authors would like to thank Ding Liang in the Institute of Zoology and Luo Ze, Zhou Yuanchun in CNIC for their constructive suggestions and help in building our system.

References

1. DELTA, DEscription Language for TAxonomy, http://delta-intkey.com
2. NCBI, Basic Local Alignment Search Tool, http://www.ncbi.nlm.nih.gov
3. BOLD Web Service, http://services.boldsystems.org/
4. lucid, http://lucidcentral.org
5. Zhang, M.: DELTA system-a recommendable information processing tool for taxonomic description. Journal of Plant Resources and Environment 18(1), 87–90 (2009)
6. Zheng, Y., Cheng, J., Zhang, Q.: Utilization and development of Expert System in rice protection. China Rice (2), 31–33 (2004)
7. Smith, J., Chang, S.: Tools and techniques for color image retrieval. In: Storage & Retrieval for Image and Video Databases IV, vol. 2670, pp. 426–437 (1996)
8. Smeulders, A., et al.: Content-based image retrieval at the end of the early years. IEEE Transactions on Pattern Analysis and Machine Intelligence 22, 1349–1380 (2000)
9. Swain, M., Ballard, D.: Indexing via color histograms, pp. 390–393 (1990)
10. Mehtre, B., et al.: Color matching for image retrieval. Pattern Recognition Letters 16, 325–331 (1995)
11. Bradski, G., Kaehler, A.: Learning OpenCV: Computer vision with the OpenCV library. O'Reilly Media (2008)
12. Xiao, J., Xiao, H., Huang, D.: DNA barcodingnew approach of biological taxonomy. Acta Zoologica Sinica 50(5), 852–855 (2004)
13. Hebeft, P.D.N., Stoeckle, M.Y., Zemlak, T.S., Francis, C.M.: Identification of birds through DNA barcodes. PLoS Biol. 2(10), 1657–1663 (2004)
14. EMBL, European Molecular Biology Laboratory, http://www.embl.org
15. DDBJ, DNA Data Bank of Japan, http://www.ddbj.nig.ac.jp

Downregulation of IL-15 and IL-18 in Chicken Embryo Fibroblasts in Response to Virulent or Lentogenic Newcastle Disease Virus Infection

Yuanping Wang, Wenquan Liu, Mingxing Tian, Yan Lin, Fangfang Zhao, Min Shi, Sanjie Cao, Xintian Wen, and Yong Huang*

College of Veterinary Medicine Sichuan Agricultural University Ya'an, Sichuan, 625014, China
hyong601@163.com

Abstract. Newcastle disease virus (NDV) is an important pathogen hazardous to poultry industry, and the pathogenicity of NDV strains varies with different virulence. Chicken Embryo Fibroblasts can serve as a laboratory host systems for NDV, and cytopathic effects (CPE) has some relationship to the strain's virulence. In order to explore the rhythm of cytokine expression in CEF following velogenic or lentogenic strain infection, NDV virulent strain F48E9 and vaccine strain Lasota were used to infect CEF separately, and cells were collected at 0, 4, 8, 12, 24, 36 hours post-infection (h.p.i.). The total RNA was isolated and real-time quantitative RT-PCR was used to detect the expression of interleukin (IL)-15 and IL-18 gene. The results showed that the expression of both IL-15 and IL-18 gene of F48E9 and Lasota groups were significantly lower than the control group at 4 h, 8 h, 12 h, 24 h.p.i.. But at 36 h.p.i., the expression level of both IL-15 and IL-18 gene of F48E9 group increased rapidly to the level higher than that of control group, while in the Lasota group, the picture was quite different, the expression level of both IL-15 and IL-18 are still lower than that of the control group. The expression change of other cytokines showed no clear regularity in F48E9 or Lasota group. Expression of IL-15 and IL-18 may play an important role in mediation of NDV pathogenesis in CEF.

Keywords: CEF, Newcastle disease virus, cytokine, IL-15, IL-18, Real-time PCR.

1 Introduction

Newcastle disease (ND) is an important disease hazardous to poultry industry, and ND virus (NDV) is the etiological agent. Currently, the disease has a global distribution with a wide host range [1]. It can not only cause the death of birds (the mortality can reach 100%), but also has a great negative effect on the productivity of surviving birds, such as impaired growth, poor feed conversion, reduced egg production, and decreased fertility and hatchability of eggs. Though vaccination has

* Corresponding author.

E. Zhu and S. Sambath (Eds.): Information Tech. and Agricultural Eng., AISC 134, pp. 789–800.
springerlink.com © Springer-Verlag Berlin Heidelberg 2012

successfully controlled the worldwide epidemic of ND, ND outbreaks unexpectedly is still occurring in some area. The global economic impact of virulent NDV is enormous, until the emergence of the highly pathogenic H5N1 influenza virus, this impact was unsurpassed by other poultry virus. NDV is classified as a member in the genus *avulavirus*, subfamily Paramyxovirinae, family Paramyxoviridae, order *Mononegavirales*. NDV has a negative-sense, single-stranded RNA genome of 15186 [2] or 15192 [3] or 15198 [4] nucleotides that contains six genes in the order of 3'-NP-P-M-F-HN-L-5', encoding six proteins including nucleoprotein (NP), phosphoprotein (P), matrix protein (M), fusion protein (F), hemagglutinin-neuraminidase (HN) and large protein (L). Additional proteins (designated as V and W proteins) may also be produced by an RNA-editing event that occurs during transcription of P gene [5-6].

The virulence of NDV strains varies greatly with the host, chickens and goose are highly susceptible, while ducks shows few or no clinical signs after the challenge of virulent strains. In chickens, the pathogenicity of NDV is mainly determined by the strains of virus, and NDVs were designated as velogenic or mesogenic or lentogenic based on their virulence. The cleavage site amino acid sequences of fusion (F) protein of NDVs were commonly used as a molecular character to assess the virulence of ND viruses, although HN and V may influence the virulence [7-8].

Newcastle disease virus strains can replicate in many kinds of cells including chicken embryo fibroblasts (CEF). Cytopathic effects (CPE) can be observed with subsequent cell death. The CPE has some relationship to the strain's virulence for chickens. Plaque formation in chick embryo cells is restricted to velogenic and mesogenic viruses unless Mg^{2+} ions and DEAE or trypsin are added to the overlay.

Cytokines are low molecular weight proteins that are secreted by many different cell types. Cytokines are not only involved in the modulation of major immune responses such as lymphocyte activation, proliferation, differentiation, survival, apoptosis and angiogenesis, but also able to initiate, mediate and propagate numerous cellular inflammatory responses. The cellular inflammatory response is important in protection against virus infection, and is usually characterized by distinct cytokine profiles [9].

The expression of cytokines in various organs of chickens after infection with Marek's disease virus [10], Salmonella enteritidis [18] and Eimeria maxima [11], have been reported, but the expression of cytokines after NDV infection have not been reported until now. As the result of NDV infection varies with different virulence, the elucidation of infection mechanism of different virulent NDV infection is of great interest for NDV research.

In this study, NDV velogenic strain F48E9 and lentogenic strain Lasota was chose to infect CEF separately, and cells were collected. Real-time PCR were then used to detect the expression of eight kinds of immune-related cytokine genes, and the NDV loads in the cellular supernatant were also detected. The results showed that the expression of IL-15 and IL-18 were downregulated after virulent or lentogenic NDV infection. While the expression change of other cytokines showed no clear regularity in F48E9 or Lasota group. This result may benefit to the elucidation of the infection mechanism of NDV on CEF.

Table 1. Sequence of primers used in quantitative RT-PCR

Genes	Primer Sequences (5'-3')		Product (bp)	Reference*
	Forward	*Reverse*		
β-actin	tcaccaactgggatgatatgga	ttggctttggggttcagg	118	L08165
IL-15	cgaggcttgtaccgcaatgt	gccatccccagcatcttgt	89	AF139097
IL-18	acaaggaatgttcttggccttt	cttcatcttctctcggcagtttc	80	NM_204608
NDV	tgatgacccagaagatagatggag	ctgtgagtgggagcataaaagaga	121	AY845400

* GenBank accession numbers of target cytokines.

2 Materials and Methods

2.1 Infection Virus Strain

Newcastle disease virus strain F48E9 were purchased from china institute of veterinary drug control (Beijing, China) and propagated in 10-day-old SPF chicken eggs. The allantoic fluid were harvested and stored at –70℃. Lasota was purchase from Merial Animal Health Co., Ltd (Nanchang, Jiangxi, China). The titer of virus was determined by a standard microtitration assay. Briefly, 2×10^4 cells in 200 μl medium were plated into each well of a 96-well plate (Nunc, Denmark). The virus was serially diluted 10-fold in culture medium and 40μl of each dilution were added to each of 10 wells of a 96-well plate. The cells were incubated at 37℃and evaluated microscopically for cytopathic effects (CPE). When a pronounced CPE was visible the 50% tissue culture infectivity doses (TCID50) were calculated according to Reed and Muench method.

2.2 Chicken Embryo Fibroblasts (CEF) Cell Cultures

Specific pathogen free (SPF) eggs were obtained from the Beijing experimental animal center (Merial Inc., Beijing, China) and hatched at our lab. Ten-day-old chicken embryos were used to prepare the CEF cell cultures according to the method described by Schat and Purchase. The cell was counted by haemocytometer and seeded onto six-well plate (Nunc, Denmark) at a density of 3×10^6 cells/well with 3ml DMEM, The cells were incubated in a humidified environment at 37 ℃ with 5% CO_2 throughout the experiment. At 24h the medium was replaced with fresh medium.

2.3 Experimental Design

The CEF were divided into three groups. Six-well plate containing confluent monolayers of CEF were inoculated with 100μl of virus suspension containing 100 $TCID_{50}$ of strain F48E9 or Lasota based on CEF cell titer. The control group was mock infected with DMEM. After absorption for 2h at 37℃, the inoculum was removed. Cells were then washed with DMEM and 3ml of maintenance media was added to each plate before the plate were returned to the incubator. Samples, consisting of 3ml of maintenance media, were collected at 0, 4, 8, 12, 24, 36h p.i. (hours post-infection) and total RNA was isolated immediately.

2.4 RNA Isolation and cDNA Synthesis

When all the cell samples have been harvested, total cellular RNA was isolated using the RNeasy Mini RNA isolation kit (Qiagen Inc., Shanghai, China). Purified RNA was resuspended in 20 μl RNase-free water and stored at -70℃ until further use. For the reverse transcription (RT) reaction, the Quantscript RT Kit (TIANGEN Biotech Co., LTD, Beijing, China) was used, and the total reaction volume was 40 μl, including 4μl of 10×RT buffer, 4 μl of random 6 mers (10 μM), 4μl of dNTPmix (2.5 mM each), 2μl of Quant Reverse Transcriptase, 20μl of template RNA and 6 μl Rnase-free water . The reaction mixture was incubated at 37℃ for 60min, and 94℃ for 4 min. The cDNAs were stored at -70 °C until use.

2.5 Primers Design

All real-time PCR primers used in this research specific for cytokine genes were designed by the Vector NTI™ suite version 5.5 (Invitrogen, Carlsbad, California 92008 USA). Those primers were used for the relative quantification of expression of the cytokines interleukin-15 (IL-15), IL-18 and used for the absolute quantification of NDV loaded in CEF, beta-actin (β-actin) was used as the housekeeping gene and reference gene to normalized the level of expression of cytokines. Details of the primers were given in Table 1. The primers were synthesized by Takara China Ltd. (Takara Inc., Dalian, China).

2.6 Preparation of Constructs as Standards

Quantification of cytokine gene expression was done using standard curves. In order to obtain standard DNA used for quantification of transcripts of target genes , IL-15, IL-18, β-actin and NP gene of NDV F48E9 strain were amplified by reverse transcription – polymerase chain reaction (RT-PCR) with specific primer pairs in table 1. PCR amplification was carried out using 4μl cDNA as a template in a total volume of 50 μL containing 25μl 2×PCR MixTopTaq™ master mix kit (Qiagen Inc., Shanghai, China) Taq PCR MasterMix (TIANGEN, Beijing, China), 2 μl of each of the two primers (10 μM), and 17μl ddH_2O. The optimum conditions for PCR were as follows: 94 °C for 1 min, followed by 45 cycles each consisting of 10 s at 94 °C, 25 s at 60 °C, 10 s at 72 °C and a final elongation at 72℃for 2 min. Each product was analyzed by electrophoresis on a 2% agarose gel containing 0.5 μg/ml of ethidium bromide. The target gene were isolated from agarose gels and purified using QIAquick™ Gel Extraction Kit (Qiagen Inc., Shanghai, China) and cloned into the

The groups were as follows: control: CEF that were mock infected with DMEM and sampled at 0,4,8,12,24 and 36 h.p.i.; F48: CEF that were infected with F48E9 strain and sampled at 0,4,8,12,24 and 36 h.p.i. Lasota: CEF that were infected with Lasota vaccine and sampled at 0, 4, 8, 12, 24 and 36 h.p.i. The difference in cytokine expression between groups was assessed by t-test and comparisons were considered significant at $P \leq 0.05$.pMD18-T™ (Takara Inc., Dalian, China) plasmid to yield recombinant plasmid. Confirmation of clones containing recombinant plasmid was achieved by PCR and restriction enzyme (RE) digestion. The correct clones were sequenced by Takara biotechnology (Dalian) co., Ltd. DNA plasmid concentrations

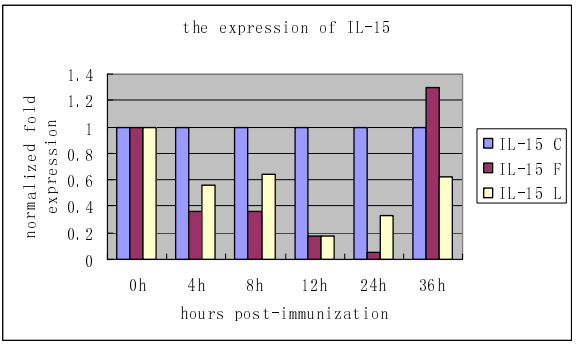

Fig. 1. IL-15 gene expression in CEF infected with different NDV strains

(C) were measured by absorbance at 260 nm, expressed in g/μl and converted to copy numbers (N) per μl of target DNA using the equation: $N = (C \times 6.02 \times 10^{23}) /$ plasmid MW (molecular weight).

2.7 Quantification of cDNA by Real-Time RT-PCR Using SyBr Green Ⅰ Method

To study the dynamics of cytokine gene transcription and NDV loading in CEF after NDV infection, each real-time RT-PCR assay was run along with a dilution series of the standard plasmid that served as the calibrator. A no template control was also included with each run. All the real-time PCR runs were conducted in a LightCycler instrument (BIO-RAD IQ5) by using the RealMasterMix (SYBR Green) Kit (TIANGEN, Beijing, China). Firstly, 125μl of 20× SYBR solution was added to 1.0ml of 2.5×RealmasterMix and mixed completely, then real-time PCR was carried out in a total volume of 20 μl which containing 9μl of solution from the above mixture, 1μl of each of the two primers (20μM each), 1μl of cDNA, 8μl of PCR grade water. The optimum thermal cycling parameters varied according to the gene detected. Annealing temperatures for each primer set were standardized and amplification of specific products was performed in keeping with the manufacturer's instructions. Briefly, the thermal cycling conditions included pre-incubation at 95℃ for 5 min, followed by 40 cycles of 95℃ for 10 s, 55.0-62.5℃ (based on specific primer annealing temperatures) for 25 s and 72℃ for 10 s. The fluorescent intensity was measured at the end of the elongation phase of each cycle. A melting curve analysis was then performed to confirm specific.

The groups were as follows: control: CEF that were mock infected with DMEM and sampled at 0,4,8,12,24 and 36 h.p.i.; F48: CEF that were infected with F48E9 strain and sampled at 0,4,8,12,24 and 36 h.p.i. Lasota: CEF that were infected with Lasota vaccine and sampled at 0,4,8,12,24 and 36 h.p.i. The difference in cytokine expression between groups was assessed by t-test and comparisons were considered significant at $P \leq 0.05$.amplification of a single product by incrementally increasing the temperature at a rate of 0.5℃/s from 65 to 95℃. Amplicon size was confirmed on a 1.5% agarose gel.

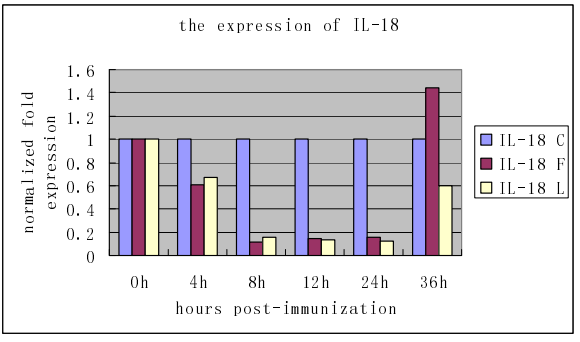

Fig. 2. IL-18 gene expression in CEF infected with different NDV strains

A standard curve for each primer sets was prepared using serial cDNA dilutions plotted against the CT (threshold cycle), which denotes the cycles at which the fluorescence of the sample rises above background levels, with the slope of the standard curve indicating primer efficiency. The absolute amount of a NDV RNA samples was calculated based on the standard curve. The expression of cytokine gens was calculated relative to the expression of β-actin gene and expressed as ratios, the ratios were normalized and then compared with each other, and the expression difference of cytokines between different infected groups was denoted as fold change.

2.8 Calculations of NDV Copies in the Peripheral Blood

NDV copies fluctuate in the CEF was determined by the formula, $\log X_0 = \log M - Ct \log (1+Ex)$. X_0 represented the original copy number, Ex represented the efficiency, $M = X_0 \times (1+Ex)^{ct}$, Ct represented the cycle number when reaching the threshold. The copy numbers of NDV were calculation by the Bio-Rad IQ5 software (Bio-Rad).

2.9 Calculations and Statistics Analysis of Cytokine Expression

Fold change was determined by the $-\Delta\Delta Ct$ method using β-actin as the reference gene to normalize the level of target gene expression. Logarithmic transformation was performed on fold change values before being analyzed by the Student's T-test (Microsoft Excel 2007). The Student's T-test was used to determine significant difference between fold change values of the transcripts of chicken cytokine of different groups. Standard error was calculated using the fold change values of three replicates for each gene measured. Data were evaluated by multifactorial variance analysis. The factors considered were group and time. Comparisons were considered significant at $P \leq 0.05$.

3 Results

3.1 Generation of Standards Curves

Standard curves for relative quantification of IL-15, IL-18 and NDV were generated. The values recorded for slope of the curve of IL-15, IL-18 and NDV were −3.422,

−3.330 and −3.506 respectively, The PCR efficiency of IL-15, IL-18 and NDV were 96%, 99.7% and 92.9% respectively. The PCR efficiency of various cytokines was calculated by the formula $E = 10^{-1/slope}$ and $E\% = (E-1) \times 100\%$. And the regression coefficients recorded for IL-18 and NDV were 1.000 and that for IL-15 was 0.999.

3.2 Expression IL-15 Gene in CEF

The expression of IL-15 was detected at all time points and across all treatment groups, and there was a statistically significant difference in the expression of IL-15 gene among the various groups. The expression of IL-15 gene of F48E9 and Lasota groups were significantly lower than the control group at 4 h, 8 h, 12 h, 24 h.p.i.. But at 36 h.p.i., IL-15 of F48E9 was in a rapid increase in higher expression than control group. Lasota group is still lower than the control group. The expression of IL-15 in F48E9 group and in Lasota group showed no remarkable difference at 12 h.p.i. There was a significant differences ($P<0.001$) in IL-15 gene expression of F48E9 ,compared to Lasota groups (Fig. 1), at 4h,8h,24h,36 h.p.i. The expression of IL-15 gene of F48E9 decreased gradually from 4 h.p.i., peaked by 36 h.p.i. and was at its lowest at 24 h.p.i. (Fig. 1). The increase of IL-15 mRNA in F48E9 group at 36 h.p.i. was significantly higher than all other time points ($p<0.05$).

3.3 Expression IL-18 Gene in CEF

The expression pattern of IL-18 was similar to IL-15 in that it was expressed in all time points in each group.

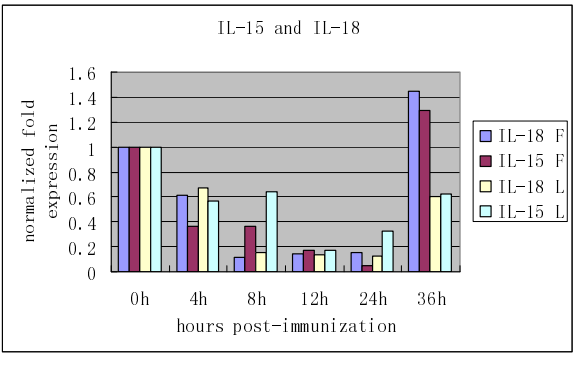

Fig. 3. IL-15 and IL-18 gene expression in CEF infected with different NDV strains

The groups were as follows: control: CEF that were mock infected with DMEM and sampled at 0,4,8,12,24 and 36 h.p.i.; F48: CEF that were infected with F48E9 strain and sampled at 0,4,8,12,24 and 36 h.p.i. Lasota: CEF that were infected with Lasota vaccine and sampled at 0,4,8,12,24 and 36 h.p.i. The difference in cytokine expression between groups was assessed by t-test and comparisons were considered significant at $P \leq 0.05$.

The expression level of IL-18 was the same in all the three groups at 0 h.p.i. But at 4 h.p.i., there was a tendency for lower expression in F48E9-infected or Lasota-infected compared to uninfected groups. This trend was maintained until 24 h.p.i. At 36 h.p.i., IL-18 of F48E9 was in a rapid increase in higher expression than control group. Lasota group is still lower than the control group. The expression of IL-18 in F48E9 group and in Lasota group showed no remarkable difference at 4 h, 8 h, 12 h, 24 h.p.i.($p>0.05$) There was a significant differences ($p<0.001$) in IL-18 gene expression of F48E9 group ,compared to Lasota groups (Fig. 2), at 36 h.p.i. The expression of IL-18 gene of F48E9 decreased gradually from 4 h.p.i., peaked by 36 h.p.i. and was at its lowest at 8 h.p.i. (Fig. 1). The increase of IL-18 mRNA in F48E9 group at 36 h.p.i. was significantly higher than all other time points ($p<0.05$).

3.4 Correlation between IL-15 and IL-18 mRNA Levels in CEF

The expression pattern of IL-15 and IL-18 between the NDV group and control group were almost the same, Its expression level in NDV group were significantly lower than those of the control group, except the expression level of IL-15 and IL-18 in F48E9 group were higher than those of the control group at 36 h.p.i.. The expression level of IL-15 and IL-18 in Lasota group were always lower than those of the control group at 4 h, 8 h, 12 h, 24 h.p.i. and 36 h.p.i.,.

3.5 Quantization of NDV-Specific RNA in CEF Cell Cultures

The relative amount of NDV-specific RNA was determined for the CEF cultures by normalization to β-actin mRNA. The amplification efficiency of β-actin cDNA and NDV virus-specific cDNA were evaluated by comparing the standard curves. The RNA of NDV in Lasota group and The F48E9 group can be detected at 8 and 12 hour post- infection respectively, and could also be detected at 24 h and 36 hour post-infection.

4 Discussion

Cytokines are essential molecules of innate and acquired immunity that initiate and coordinate cellular and humoral responses aimed at eradicating pathogens. Detecting avian cytokines is limited by the lack of specific antibodies and reliable bioassays. However, recent cloning of chicken cytokines and chemokines have enabled development of a more comprehensive array of reagents for investigating innate and acquired immune responses at cellular and molecular levels. Chicken interferon-gamma (IFN-γ), interleukin (IL)-18, interleukin (IL)-15, the proinflammatory cytokines IL-6, and the chemokines IL-13 have all been cloned and sequenced. This makes it possible to design probes and primers to quantify cytokine mRNA expression levels using quantitative real-time RT-PCR (qRT-PCR). Although measuring cytokine mRNA expression levels by qRT-PCR does not necessarily equate to the production of bioactive protein, recent publications demonstrate qRT-PCR is the most highly sensitive method available to reliably quantify a broad spectrum of avian cytokines, particularly in the absence of effective bioassays.

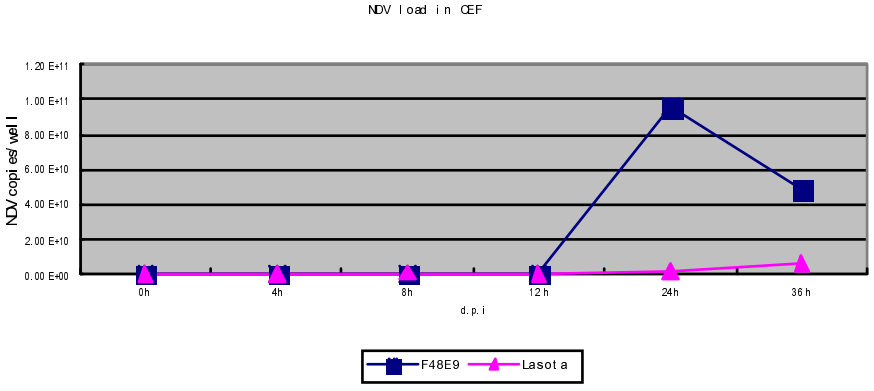

Fig. 4. Detection of NDV load in CEF following infection. Six-well plate containing confluent monolayers of CEF were inoculated with 100µl of virus suspension containing 100 $TCID_{50}$ of strain F48E9 or Lasota based on CEF cell titer. The control group was mock infected with DMEM . Cells were collected for detection of NDV load on 0, 4, 8, 12, 24 and 36 hours post-infection (h.p.i.) respectively. NDV copies fluctuate in the CEF was determined by the formula, $\log X_0 = \log M - Ct \log (1+Ex)$. X_0 represents the original copy number, Ex represents the efficiency, $M = X0 \times (1+Ex)^{ct}$, Ct represent the cycle number when reaching the threshold.

Cytokines are organized within complex networks and act as important mediators of the immune system. They influence the pathogenesis and outcome of infectious diseases and studies have been undertaken to quantitate cytokine mRNA during disease to monitor progression of diseases and pathogenesis [13]. Several methods have been developed to determined the relationship between cytokine profile and disease developments including quantitative competitive RT–PCR, Northern blot and PCR [14-15].

Currently, real-time RT-PCR has been used to quantitate virus-specific RNA and to better understand host response to infection. However, normalization of quantitative real-time RT-PCR need a suitable internal control. The β-actin gene, a gene encoding ubiquitous cytoskeleton protein, has been used as an internal control in qRT-PCR assays [16], in addition, glyceraldehyde-3-phosphate dehydrogenase (GAPDH), β-2-microglobulin, TATA box-binding protein (TBP), 28S rRNA, and 18S rRNA were also selected as internal controls. As β-actin gene was most constantly expressed, with no significant difference between normalized and non-normalized assays, So, β-actin could be a good internal control in qRT-PCR for studying gene expression and virus load in CEF cell cultures during NDV infection.

Interleukin (IL)-15 was originally discovered in culture supernatants of simian kidney epithelial cells by virtue of its T cell growth promoting activity [17]. IL-15 gene expression is regulated transcriptionally, translationally and at the level of intracellular trafficking [18-19] such that its gene product is produced primarily by activated macrophages, monocytes and epithelial cells. IL-15 shares structural and functional characteristics with IL-2, another T cell growth factor important in the regulation of cell-mediated immunity Biologically, IL-15 and IL-2 stimulate T cell growth, B cell proliferation and differentiation, chemoattraction, and resistance to apoptosis [17]. Both IL-15 and IL-2 play a pivotal role in the differentiation of natural

killer cells which exhibit a proliferative response to both cytokines [20]. Now, chicken IL-15 genes have been cloned [20-21]. But there are a few articles reported the expression of IL-15 in chickens. We examined mRNA expression of IL-15 in CEFs infected with Newcastle Disease Virus F48E9 and Lasota..

IL-18 is an inducer of cell-mediated immunity, especially in combination with IL-12, and is primarily associated in Th1 responses to intracellular pathogen infections, such as coccidiosis [22-23]. In chickens, heterophils from Salmonella-resistant chickens displayed significantly higher levels of IL-18 mRNA compared with heterophils from Salmonella susceptible animals [24]. IL-18 is considered proinflammatory cytokines and their lower expression has been shown to be associated with genetic resistance against MD in genetically defined lines. Abdul-Careem (2007) [25] discovered that expression of IL-18 genes was significantly lower in the chickens in the vaccinated protected group compared to unvaccinated controls. Abdul-Careem (2008) [26] found that the expression of IL-18 was significantly lower in those chickens that were mock immunized pre-hatch compared to those that were mock immunized post-hatch on day 4 post-immunization.

In this study, we investigated the kinetic response of immune-related cytokines in CEF following experimental infections with F48E9 or Lasota. In general, IL15 and IL-18 levels after NDV infection were highly down-regulated compared to the control group, whereas at 36h.p.i., cytokine mRNA levels were significantly higher in F48E9-infected compared to control group or Lasota-infected group.

Acknowledgment. The work was financially supported by Sichuan youth science & technology foundation (Grant number: 2007Q14-034) and Chinese national postdoctrainee fund and a postdoc fund from Sichuan Agricultural University. As well as, Program for Changjiang Scholars and Innovative Research Team in University “PCSIRT” (Grant No: IRTO848).

References

1. Alexander, D.J.: Newcastle Disease, Other Avian Paramyxoviruses, and Pneumovirus Infections, 12th edn. Blackwell Publishing Professional, 2121 State Avenue (2008)
2. Phillips, R.J., Samson, A.C., Emmerson, P.T.: Nucleotide sequence of the 5’-terminus of Newcastle disease virus and assembly of the complete genomic sequence: agreement with the “rule of six”. Arch. Virol. 143, 1998 (2002), pmid: 9856086
3. Huang, Y., Wan, H.Q., Liu, H.Q., Wu, Y.T., Liu, X.F.: Genomic sequence of an isolate of Newcastle disease virus isolated from an outbreak in geese: a novel six nucleotide insertion in the non-coding region of the nucleoprotein gene. Brief Report. Arch Virol 149, 1445–1457 (2004), pmid: 15221544
4. Czegledi, A., Ujvari, D., Somogyi, E., Wehmann, E., Werner, O., Lomniczi, B.: Third genome size category of avian paramyxovirus serotype 1 (Newcastle disease virus) and evolutionary implications. Virus Res. 120, 36–48 (2006), pmid: 16766077
5. Kolakofsky, D., Pelet, T., Garcin, D., Hausmann, S., Curran, J., Roux, L.: Paramyxovirus RNA synthesis and the requirement for hexamer genome length: the rule of six revisited. J. Virol. 72, 891–899 (1998), pmid: 9444980

6. Steward, M., Vipond, I.B., Millar, N.S., Emmerson, P.T.: RNA editing in Newcastle disease virus. J. Gen. Virol. 74(pt. 12), 2539–2547 (1993), doi:10.1099/0022-1317-74-12-2539
7. Huang, Z., Panda, A., Elankumaran, S., Govindarajan, D., Rockemann, D.D., Samal, S.K.: The hemagglutinin-neuraminidase protein of Newcastle disease virus determines tropism and virulence. J. Virol. 78, 4176–4184 (2004), doi:10.1128/JVI.78.8.4176-4184.2004.
8. Mebatsion, T., Verstegen, S., De Vaan, L.T., Romer-Oberdorfer, A., Schrier, C.C.: A recombinant newcastle disease virus with low-level V protein expression is immunogenic and lacks pathogenicity for chicken embryos. J. Virol. 75, 420–428 (2001), doi:10.1128/JVI.75.1.420-428.2001.
9. Kaiser, P., Staheli, P.: Avian cytokines and chemokines, 1st edn. Elsevier Ltd., London (2008)
10. Xing, Z., Schat, K.A.: Expression of cytokine genes in Marek's disease virus-infected chickens and chicken embryo fibroblast cultures. Immunology 100, 70–76 (2000), doi:10.1046/j.1365-2567.2000.00008.x.
11. Carvajal, B.G., Methner, U., Pieper, J., Berndt, A.: Effects of Salmonella enterica serovar Enteritidis on cellular recruitment and cytokine gene expression in caecum of vaccinated chickens. Vaccine 26, 5423–5433 (1870), pmid: 18706948
12. Hong, Y.H., Lillehoj, H.S., Lee, S.H., Dalloul, R.A., Lillehoj, E.P.: Analysis of chicken cytokine and chemokine gene expression following Eimeria acervulina and Eimeria tenella infections. Vet. Immunol. Immunopathol 114, 209–223 (2006), pmid: 16996141
13. Rottman, A.J.B.: Key role of chemokines and chemokine receptors in inflammation, immunity, neoplasia, and infectious disease. Vet. Pathol. 36, 357–367 (1999), pmid: 10490203
14. Montagne, Grepinet, O., Peloille, M., Lantier, F., Lalmanach, A.C.: Quantification of ovine cytokine gene expression by a competitive RT-PCR method. J. Immunol. Methods 253, 83–93 (2001)
15. Ryan, E.J., Nilsson, L., Kjellman, N., Gothefors, L., Mills, K.H.: Booster immunization of children with an acellular pertussis vaccine enhances Th2 cytokine production and serum IgE responses against pertussis toxin but not against common allergens. Clin. Exp. Immunol. 121, 193–200 (2000), pmid: 10931131
16. Mill, A.J., Asherson, P., Browes, C., D'Souza, U., Craig, I.: Expression of the dopamine transporter gene is regulated by the 3' UTR VNTR: Evidence from brain and lymphocytes using quantitative RT-PCR. Am. J. Med. Genet. 114, 975–979 (2002), pmid: 12457396
17. Grabstein, K.H., Eisenman, J., Shanebeck, K., Rauch, C., Srinivasan, S., Fung, V., Beers, C., Richardson, J., Schoenborn, M.A., Ahdieh, M., et al.: Cloning of a T cell growth factor that interacts with the beta chain of the interleukin-2 receptor. Science 264, 965–968 (1994), pmid: 8178155
18. Onu, Pohl, T., Krause, H., Bulfone-Paus, S.: Regulation of IL-15 secretion via the leader peptide of two IL-15 isoforms. J. Immunol. 158, 255–262 (1997), pmid: 8977197
19. Waldmann, T.A., Tagaya, Y.: The multifaceted regulation of interleukin-15 expression and the role of this cytokine in NK cell differentiation and host response to intracellular pathogens. Annu. Rev. Immunol. 17, 19–49 (1999), doi:10.1146/annurev.immunol.17.1.19
20. Carson, W.E., Giri, J.G., Lindemann, M.J., Linett, M.L., Ahdieh, M., Paxton, R., Anderson, D., Eisenmann, J., Grabstein, K., Caligiuri, M.A.: Interleukin (IL) 15 is a novel cytokine that activates human natural killer cells via components of the IL-2 receptor. J. Exp. Med. 180, 1395–1403 (1994), pmid: 7523571

21. Choi, K.D., Lillehoj, H.S., Song, K.D., Han, J.Y.: Molecular and functional characterization of chicken IL-15. Dev. Comp. Immunol. 23, 165–177 (1999), doi: S0145-305X(98)00046-9 [pii]
22. Biet, F., Kremer, L., Wolowczuk, I., Delacre, M., Locht, C.: Mycobacterium bovis BCG producing interleukin-18 increases antigen-specific gamma interferon production in mice. Infect. Immun. 70, 6549–6557 (2002), pmid: 12438324
23. Dinarello, C.A., Fantuzzi, G.: Interleukin-18 and host defense against infection. J. Infect. Dis. 187(suppl. 2), S370–S384 (2003), doi: JID21051 [pii]10.1086/374751
24. Swaggerty, C.L., Kogut, M.H., Ferro, P.J., Rothwell, L., Pevzner, I.Y., Kaiser, P.: Differential cytokine mRNA expression in heterophils isolated from Salmonella-resistant and -susceptible chickens. Immunology 113, 139–148 (2004), pmid: 1782542
25. Abdul-Careem, M.F., Hunter, B.D., Parvizi, P., Haghighi, H.R., Thanthrige-Don, N., Sharif, S.: Cytokine gene expression patterns associated with immunization against Marek's disease in chickens. Vaccine 25, 424–432 (2007), pmid: 17070626
26. Abdul-Careem, M.F., Hunter, B.D., Sarson, A.J., Parvizi, P., Haghighi, H.R., Read, L., Heidari, M., Sharif, S.: Host responses are induced in feathers of chickens infected with Marek's disease virus. Virology 370, 323–332 (2008), pmid: 17949771

Changes in Phenotypic Traits for Key Inbred Lines of Chinese Maize

Ying-Hong Liu[1], Yubi Huang[1,2], Mengliang Tian[2], and Junjie Zhang[3]

[1] Maize Research Central of Sichuan Agriculture University, Ya'an 625014, China
[2] College of Agronomy, Sichuan Agricultural University, Ya'an 625014, China
[3] College of Life Science, Sichuan Agricultural University, Ya'an 625014, China
yubihuang@sohu.com

Abstract. The phenotypic stability of plant key inbred lines among generations is one basic demand for plant breeding. In this study, we collected a set of 63 key inbred lines of Chinese maize which have been developed during the past 30 years and studied the phenotypic changes of 25 traits after having been planted at three independent ecological locations for two years. The 63 key inbred lines could be classified into four heterotic groups, namely Sipingtou, Lancaster, Luda Red Cob, and Reid. Our results showed that the plant type, maturity, and value weight were stably inherited in Sipingtou. However, in group Lancaster, the traits of Cob weight/100-kernel weight/double ear rate and no near ear rate could be stably inherited, and Kernel per row, tassel branch and kernel depth in group Luda Red Cob; but then yield traits were not obviously changed in group Reid.

Keywords: Maize, Key inbred line, Phenotypic character, Heredit.

1 Introduction

Maize production is significant to meet the basic requirement for life in developing China. During the past 30 years, there were four maize key inbred lines having played a crucial role to enlarge the maize variety. They were widely crossed with a number of wild breeds/strains and resulted in lots of valuable parents inbred lines with wide distribution. However, the limited knowledge of main formation mechanism of the key maize key inbred lines has largely hindered the development of new maize inbred lines.

In China, there are 4 key maize inbred lines, which could be classified into four heterotic groups (Sipingtou, Lancaster, Luda Red Cob, and Reid)(Li et al, 2003). Among them, the Huangzaosi, derived from open pollinated plant of Sipingtou, is one of the most important inbred lines in maize breeding and production. Since 1975, more than 42 hybrids produced by using Huangzaosi and its derived lines have been successfully developed (Li, 1997; Zeng et al, 1996). In Lancaster group, Mo17 is the most important key inbred line. Up to now, Mo17 has been employed in more than 100 hybrids, such as Zhongdan2, Nongda108, and Yandan14 with significant contribution in the maize production in China (Xu et al, 2006). Dan340, one of the key inbred lines of Luda Red Cob, has been widely used because of its high resistance

E. Zhu and S. Sambath (Eds.): Information Tech. and Agricultural Eng., AISC 134, pp. 801–809.
springerlink.com © Springer-Verlag Berlin Heidelberg 2012

to diseases, lodging resistance, high combining ability, and suitable fertility (Ning et al, 2002). Inbred line 478 was bred from two maize inbred lines 8112 and 5003. According to the statistics, 478 has been used as parent in more than 41 hybrids, which have totally covered at least 39,570,000 hectare. In addition, more than 19 hybrids were produced by its improved-lines, which have covered at least 7960000 hectare (Li, 2005).

Although a large number of widely spread valuable inbred lines have been successfully selected from key lines, the formation mechanism of key lines remained largely unknown. Averagely, the improvements in hybrids have been responsible for about 50–70% of the on-farm yield gains since their introduction (Duvick, 1992). In contrary to the yield traits, ear length, rows per ear, and 100-kernel weight without obvious difference over the past decade, the leaf orientative value and ear height/plant height have significantly changed in different years (Niu, 2004). In addition, kernel weight per plant and cob diameter of lines have been increased with little effect on other yield traits, while ear height and ear height/plant height of the lines decreased significantly (Wang et al, 2001). It was proposed that kernels per plant has a fundamental effect on yield improvement of inbred lines (Xie et al, 2007). The traits of 1000-kernel weight and kernel per ear are important to improve yield traits of inbred lines (Wang, 1997).

In this study, we planted a set of 63 key inbred lines of Chinese maize under different ecological conditions in different years and investigated the expression, delivery, and coordination mechanisms of important traits among these key inbred lines. The agronomic and yield traits were further evaluated on the basis of pedigree analysis.

2 Materials and Methods

2.1 Plant Material and Experimental Design

In 2007 and 2008 main season, a set of 63 maize inbred lines were planted in three different ecological locations, including Duoying farm of Maize Research Institute of Sichuan Agricultural University in Sichuan province, the farm of Dongbei Agricultural University in Heilongjiang province, and the farm of Shandong Agricultural University in Shandong province. The detailed information of 63 studied inbred lines is listed in Table 1. The inbred lines were classified into 4 clusters with heterotic groups determined by their pedigree information and breeders′ experiences (i.e. Sipingtou, Lancaster, Reid and Luda Red Cob) (Li et al, 2003). The first cluster was composed of related lines numbered 1 to 29, the second cluster numbered 30 to 46, the third cluster numbered 47 to 53 and cluster 4 numbered 54 to 63, with backgrounds determined by review of detailed proprietary company or unit pedigree records. In addition, some lines were classified by the experience of breeders as supplementary.

We arranged entries in a randomized complete block design with three replications each year. The rows were 5m long, 66.6cm and 50cm spacing between rows and plants with the row. Thus, the final stand was approximately 60 000 plants ha-1. Ten plants from each block were selected at random to measure traits.

We observed and recorded plant height (cm), ear height (cm), stem diameter (cm), leaf area of ear leaf (cm2), tassel length (cm), tassel branch, total leaves, ear leaf, green leaves kept, leaf orientative value (LOV), double ear rate, barren plants, and harvest index (HI) during their growth period. After ripening, all the inbred lines were harvested and shelled by hand. The data of ear length (cm), bald length (cm), ear diameter (cm), cob diameter (cm), kernel depth (cm), number of row per ear, number of kernels per row, ear weight (g), cob weight (g), yield per plant (g), 100-kernel weight (g), and value weight (g/L) were subsequently recorded. Grain yield was adjusted to 13% moisture.

2.2 Statistical Analyses

All the data was analyzed with Univariate methods in SAS V12.0 package (SAS Inst. Inc., Cary, NC, USA). Variance analysis was used to evaluate the differences of traits among the inbred lines. Following the analysis of variance, the protected LSD0.05 was calculated among the inbred lines. The error estimate and Pearson correlation were computed using variance within inbred lines. Statistically significant traits were adopted for the Principal Component Analysis (PCA). Three principal components were selected to draw Matrix plot to show the main relationships of those key inbred lines.

3 Results

By conducting PCA, the three principal components accounted for 87.79% of the variance, whose eigenvalue, variance explained, and the loading factors were showed in Table 2 and Table 3. The first component, as a measure of plant type, was dominated by high loadings for tassel branch, plant height, ear height, cob diameter, and harvest index. The second component, as a measure of yield factor 1, was comprised of ear diameter and 100-kernel weight. The third component, referred to yield factor 2, included number of kernels per row and number of row per ear. Matrix plots were drawn to show the main inherited relationships of those key inbred lines (Figs. 1-3).

There was obvious difference between cluster Sipingtou and the other three clusters in Prin1 (Fig. 1). Substantial difference in Prin1 but obvious difference in Prin2 and Prin3 in cluster Sipingtou (Figure 3). The results showed that plant type was inherited stably in cluster Sipingtou. The variance analysis of two year showed that the maturity and value weight were inherited stably (data not shown) in cluster Sipingtou. Changes of phenotypic characters were mainly caused by yield factor 1 and 2.

There was dramatic difference between cluster Lancaster and others in Prin3 (Figure 2), which indicated that yield factor 2 is inherited stably. The variance analysis showed that 100-kernel weight, cob weight, double ear rate and barren plants were inherited stably because the difference was not statistically significant in this cluster (data not shown).

Difference was observed between Luda Red Cob and Reid in Prin1 (Figure 1). Number of kernels per row was inherited stably because of no significant difference in Luda Red Cob cluster. There were obvious differences in Prin2 and Prin3 (Figure 3) between Ye478 and its derived lines. Kernel per row, 100-kernel weight, tassel branch, ear height and cob diameter were inherited stably for no significance.

Table 1. Pedigree and origin of the 63 inbred lines of maize in China

Nos	Inbred line	Pedigree or origin	Heterotic group
1	Huangzaosi	Derived from open pollinated plant of Sipingtou	Sipingtou
2	Yuanfuhuang	Derived of Huangzaosi	Sipingtou
3	Dhuang212	Derived from Huangzaosi	Sipingtou
4	8723	Derived from Huangzaosi	Sipingtou
5	Duo27	Derived from Huangzaosi	Sipingtou
6	Kanghuang4	Derived from Huangzaosi	Sipingtou
7	Huangzao4-15	Derived from Huangzaosi	Sipingtou
8	Wenqing1331	Dan340×Huangzaosi	Sipingtou
9	Huangyesi	(Huangzaosi×Yejihong)BC3	Sipingtou
10	⑦61	Aijin525×5344/santuan ×Huangzaosi	Sipingtou
11	Wenhuang 31413	Dan340×Huangzao4 /Huangzaosi	Sipingtou
12	Baiye4	Haungzao4×Haidong013 /Huangzaosi	Sipingtou
13	Ji35	Jiduo142×Huangzao4 /Huangzaosi	Sipingtou
14	Jing404	Huangzaosi×Mobai02 /Huangzaosi	Sipingtou
15	Jing7huang	Huangzaosi×Luoxi3 /Huangzaosi	Sipingtou
16	H21	Hangzaosi×H84	Sipingtou
17	Qi310	Huangzao4×Jin02	Sipingtou
18	Qi401	Huangzao4×Hengbai502	Sipingtou
19	Dan341	5003×56 - 1·332 - 2·nei·B·330 / cutuan	Sipingtou
20	Jing7	Huangzaosi×Luoxi3	Sipingtou
21	Chang7-2	Huangzaosi×Wei95	Sipingtou
22	K12	Huangzaosi×Weichun	Sipingtou
23	Tianya4	Wu109×Huangzaosi	Sipingtou
24	Ji444	A619×Huangzaosi	Sipingtou
25	Jing24	Zaoshu302×Huangzaosi	Sipingtou
26	Ji853	Huangzaosi×Zi330F2	Sipingtou
27	Ji854	Huangzaosi×Zi330F2	Sipingtou
28	Shuang105	Aijin525×Weier44 /Huangzaosi×santuan	Sipingtou
29	Shuang741	Aijin525×Weier44 /Huangzaosi×santuan	Sipingtou
30	Huotanghuang17	Huotangbai42× Hai1917/A619ht×Mo17	Lancaster
31	Mo17	187-2×C103	Lancaster

Table 1. (*continued*)

Nos	Inbred line	Pedigree or origin	Heterotic group
32	4F1	Derived from Mo17	Lancaster
33	477	Derived from Mo17	Lancaster
34	K14	Dian11×Mo17×K16	Lancaster
35	412	Derived from Mo17	Lancaster
36	Qi35	Derived from Mo17	Lancaster
37	Guan17	Derived from Mo17	Lancaster
38	Mo17-ht	A619ht×Mo17	Lancaster
39	He344	A619ht×Mo17	Lancaster
40	Xi14	Mo17×Xu503	Lancaster
41	Qi302	Mo17×Tai183	Lancaster
42	Ji842	Ji63×Mo17	Lancaster
43	Ji846	Ji63×Mo17	Lancaster
44	Nan23232	B73×Mo17	Lancaster
45	Ji1037	Mo17×Suwan	Lancaster
46	Nongda178	78599×Mo17/O2	Lancaster
47	Zao48	Ye478×249×Ye478	Reid
48	K22	K11×Ye478	Reid
49	DH4866	7922×Ye478	Reid
50	Ye478	U8112 ×Shen5003	Reid
51	Zheng58	Derived from Ye478	Reid
52	478-31	Derived from Ye478	Reid
53	478-19	Derived from Ye478	Reid
54	Cai11-8	Sister-line of Zi330	Luda Red Cob
55	Huangc	Huangxiao162× Zi330/o2/Mobai	Luda Red Cob
56	Weifeng322	W59E×Fengke1	Luda Red Cob
57	3H-2	Xianda203×Zi330×H84	Luda Red Cob
58	Dan340	Baigulv9 ×Pod corn	Luda Red Cob
59	Wa138	Dan360×Meihuang	Luda Red Cob
60	48-2	Mo17×Dan340×S37	Luda Red Cob
61	502	Huangzaosi×Dan340	Luda Red Cob
62	200B	Zi330×187-2	Luda Red Cob
63	Chang3154	Zi330×Tai183	Luda Red Cob

Table 2. Cumulative, Eigenvalue, Difference and Proportion of 3 Main Components of the Key Inbred Lines

	Cumulative	Eigenvalue	Difference	Proportion
Prin 1	5.30923378	3.30766313	0.5309	0.5309
Prin 2	2.00157065	0.53384248	0.2002	0.7311
Prin 3	1.46772817	—	0.1468	0.8779

Table 3. Rotated Component Loadings for Character Variables

Character variables	Prin1 (plant type factor)	Prin2 (yield factor 1)	Prin3 (yield factor 2)
Ear length	0.320	0.355 a	0.004
Ear diameter	0.219	0.512a	-0.329
Number of kernels per row	0.020	0.386 a	0.637a
Number of row per ear	0.176	-0.369 a	-0.472a
100-kernel weight	-0.173	-0.483a	0.409 a
Tassel branch	0.406a	-0.137	0.214
Plant height	-0.409a	0.067	-0.090
Ear height	-0.410a	0.112	-0.172
Cob diameter	0.379a	-0.206	-0.051
Harvest index	-0.381a	0.118	-0.096

Notes. Loading refers to the relative contribution ratio of an original variable to the principal component axis. The components were rotated orthogonally to maximize the correlations among variables within each component and minimize correlations between components. [a]Individual character variables were weighted most heavily in each principal component

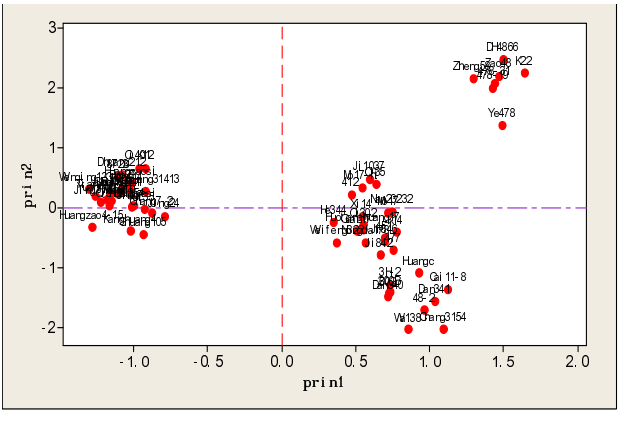

Fig. 1. Matrix plot of prin2 vs prin 1

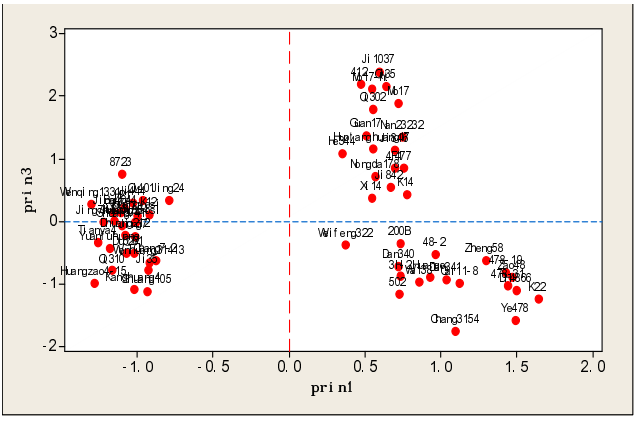

Fig. 2. Matrix plot of prin3 vs prin 1

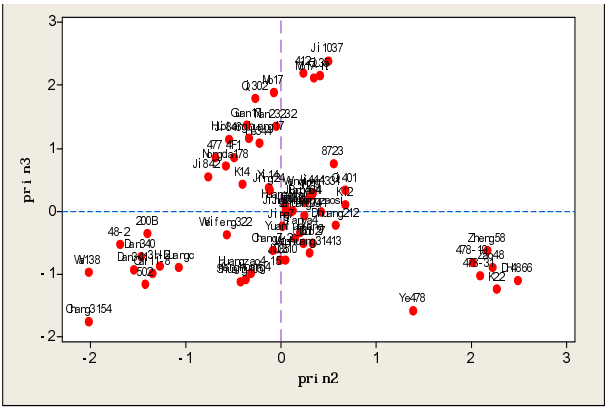

Fig. 3. Matrix plot of prin3 vs prin 2

Yield per plant was positive correlated (sig.<0.05) with cob diameter, numbers of kernel per row, ear weight, green leaves kept, HI in cluster Sipingtou, Mo17 and Dan340. Tassel branch was negative correlated with HI only in cluster Sipingtou; total leaves and ear leaf were correlated with yield per plant only in cluster Mo17; in cluster 340 value weight was correlated with yield per plant and Hi, numbers of row per ear was correlated with yield per plant (data not show).

4 Discussion

The key inbred lines have specific traits with significant contribution for the genetic improvement of their offspring. To effectively dissect and utilize these outstanding traits of key lines are very essential in maize breeding. However, the deserved traits always differed among the key inbred lines distributed in different ecological areas and heterotic groups. For example, one of the main heterotic combination is “Group

Reid × Group Tropic" in southwest China over the past decades. The combination always has the excellent traits such as resistance to barrenness, resistance to disease, resistance to drought, and good stay-green. The hybrids obtain these characters from each parent which belong to one heterotic group and derived from one key inbred line, each. So, if we can decide the main genetic characters of each heterotic group, the breeding procedure may be more efficient. In this study, we found that three components can be used to distinguish these inbred line groups. Plant type was obviously different between Sipingtou and others. Yield factor 1 was significant different between Luda Red Cob and Reid. Yield factor 2 was different between Lancaster and others.

Huangzaosi has been widely used because of its high and stable combining ability, upright-leaf plant type, and elite agronomical characters (Zeng, 1996). We have done much work to improve the disease-resistant and plant yield of Huangzaosi (Li, 2008). In addition, yield is changed in this group, but it was not stable increase in our experiment. So continued improvement the yield characters is the most important thing to improve Sipingtou group.

Few row and long ear are the topic characters of Mo17. 100-kernel weight, cob weight, yield factor 2 were not changed between Mo17 and its derived lines in our experiments. We can conclude that long ear and big kernel are main characters which are inherited from Mo17. So, modifying the number of row per ear and kernel depth are very important to improve Lancaster.

Number of kernels per row, tassel branch and kernel depth are stably inherited from Dan340 in group Luda Red Cob (data not show). Number of row per ear is very important to improve group Luda Red cob. The variance analysis shows that number of kernels per row, 100-kernel weight, tassel branch, ear height, cob diameter and other yield characters are inherited stably for no significance in group Reid. So we should enhance the resistance to improve group Reid.

Acknowledgements. We are grateful to Dr Yongjian Liu (College of Agronomy, Sichuan Agriculture University) for many useful suggestions of data analysis. Two anonymous reviewers read the manuscript and made some useful suggestions. The work was supported by the National Basic Research Program of China.

References

1. Duvick, D.N.: Genetic contribution to advances in yield of u. S. Maize. Maydica. 37, 69–79 (1992)
2. Wang, J.: Improvement of chinese maize inbred lines traits. Journal of Maize Sciences 5(4), 26–29 (1997)
3. Li, D., Mao, L., Yang, J., Liu, J., Zhang, Y.: Breeding process and utilization of excellent maize inbred line 478. Journal of Laiyang Agricultural College 22(3), 159–164 (2005)
4. Li, X., Yuan, L., Li, X., Zhang, S., Li, M., Li, W.: Heterotic grouping of 70 maize inbred lines by ssr markers. Scientia Agricultura Sinica 36(6), 622–627 (2003)
5. Lu, B., Zhao, W., Liu, R., Guan, G.: The influence and contribution of the hybrids corssed by mo17 deriving self inbred lines to the production of china. Journal of Maize Sciences 12, 127–128 (2004)

6. Ning, J., Gao, H., Qu, G., Yu, B., He, J.: Utilization of inbred lines of ludahonggu group in corn breeding and production in china. Rain Fed Crops 22(2), 63–65 (2002)
7. Niu, L.: Research in improve trends of maize inbred lines in different years. China Seed Industry 12, 37–38 (2004)
8. Li, S.: Selection and application of maize inbred line huangzaosi. Beijing Agricultural Sciences 15, 19–21 (1997)
9. Wang, Z., Wang, Y., Wang, Y., Zhang, X., Dong, J., Liu, J.: Genetic improvement of plant types and yield characteristics in corn inbred lines 1, 15–16 (2001)
10. Xie, Z., Li, M., Li, X., Zhang, S., Zhang, B.: Relativity between yields and agronomic traits of major maize inbred lines of north china. Journal of Shenyang Agricultural University 38(3), 265–268 (2007)
11. Xu, Y., Liu, X., Sun, F., Jiao, R.: The application of mo17 and derived in chinese maize breeding. Journal of Jilin Agricultural Sciences 31(3), 26–28 (2006)
12. Li, C., Cai, Z., Li, F., Lu, Y., Liu, Y.: The effect of tangsepingtou on maize breeding in jilin province. Journal of Maize Sciences 16(6), 11–14 (2008)
13. Zeng, S., Ren, R., Liu, X.: The important position of huangzaosi in maize breeding and production in china. Journal of Maize Sciences 4(1), 1–6 (1996)

Association of EphrinB2 Gene Polymorphism with Litter Size in Pigs

Yanfeng Fu*, Guiying Wang, Jinluan Fu**, and Aiguo Wang**

College of Animal Science and Technology China Agricultural University / The Key Laboratory of Animal Genetics and Breeding of Ministry of Agriculture, 100193, Beijing, China
fuyanfeng@gmail.com, fujinlian@126.com, agwang@cau.edu.cn

Abstract. EphrinB2, a transmembrane ligand for Eph receptor tyrosine kinases, was one of the potential candidate genes for reproductive traits in pigs. In the study, one single nucleotide polymorphism (SNP) locus in Exon 4 of EphrinB2 gene was analyzed to determine whether EphrinB2 influenced total number born (TNB) and number born alive (NBA) in pigs. Association of two diallelic polymorphisms with reproductive traits was assessed in Landrace, Yorkshire and Duroc populations with 1,023 litter records of 485 pigs. The results showed that C allele at EphrinB2 locus seemed to have advantageous effects on litter size. The results in this study demonstrated that EphrinB2 gene was significantly ($P < 0.05$) associated with litter size in pigs. Further studies were needed to confirm these preliminary researches.

Keywords: EphrinB2, Pig, SNP, Litter size.

1 Introduction

Litter size, as one of the most significant reproductive traits, is extremely important economically to the swine industry [1-2]. However, improvement of litter size in pigs by traditional selective breeding has proved to be difficult due to the low heritability (10-15%) [3]. The candidate gene approach, which employed in identifying the polymorphisms in genes likely to cause phenotypic variation based on physiological, immunological or endocrine evidence, could accelerate the improvement of swine reproductive traits [4]. Many major genes affecting important economic traits in pigs have been successfully identified with the development of candidate gene and comparative mapping approaches, such as the estrogen receptor (ESR) gene [4], the prolactin receptor (PRLR) gene [5], the retinol-binding protein 4 (RBP4) gene [6], the leukemia factor (LIF) gene [7] and so on.

* Author, male, pregraduated PhD, major in animal breeding and genetics research.
** Corresponding author.

E. Zhu and S. Sambath (Eds.): Information Tech. and Agricultural Eng., AISC 134, pp. 811–818.
springerlink.com © Springer-Verlag Berlin Heidelberg 2012

Blastocyst implantation is an important step in the establishment of pregnancy because the most of embryonic death take place in this time [8]. And the loss of potential piglets is predominantly the result of early embryonic (day 10-30) deaths through the gestation [9], so the major limitation for increasing litter size is embryonic loss. Recently, many studies found that Eph-Ephrin system plays an important role in embryo implantation in human [10-12] and mice [13]. The system contains at least 14 receptors and 8 ephrin ligands [14-15]. As an important member of the Eph-Ephrin system, EphrinB2 plays a crucial role in vascular development [16] and controls lymphangiogenic growth [17] in embryonic development, which will influence embryo implantation in pigs. EphrinB2 is a marker of arterial endothelial cells in the vasculature [17-21], and it functions in the early embryo as a typical instructive ligand to stimulate EphB4 receptor forward signaling during angiogenic remodeling, later in embryonic development EphrinB2 functions as a receptor to transduce reverse signals involved in cardiac valve maturation and axon pathfinding [22]. Hence, the EphrinB2 might be a positional and functional candidate gene for reproductive traits in pigs.

The objective of our study was to examine EphrinB2 as a candidate gene for swine reproductive traits. To achieve this target, we identified one SNP mutations in the EphrinB2 gene cDNA sequence, investigated allele and genotype frequencies in Landrace, Yorkshire and Duroc pigs, estimate the additive and dominance effects of the SNP on litter size in different parity, and performed statistical associations with partial reproductive traits in different pig breed.

2 Materials and Methods

2.1 Animals

All animals used in this study came from the seed stock farm of Beijing Huadu Swine Breeding Company, Ltd, (Beijing, China). A total of 485 sows, including 198 Landrace, 201 Yorkshire and 86 Duroc pigs, were used to investigate the allele and genotype frequency. Ear tissue were collected in centrifuge tubes (1.5 ml) with 70% ethanol solution, stored at -20 °C, and genomic DNA was extracted by the high-salt method according to the protocol [23], dissolved in TE solution and stored at 4 °C. Litter size records included total number born (TNB) and number born alive (NBA), which were recorded by parity.

2.2 Reagents

SDS, Bromophenol blue, Acrylamide, N, N'-methylene bisacrylamide and tetramethylethylenediamine (TEMED) were all produced by Amresco company in USA, and Taq DNA Polymerase, 1500 bp Marker and dNTPs were all produced by Yatai Hanson Bio Corporation in Beijing. In addition, NaCl and ethanol solution were both produced in the Beijing Chemical Plant. Furthermore, 1 × TAE buffer, 1 × TBE buffer, 75% ethanol solution, EDTA and ultra-pure water were all prepared by myself. Proteinase (Roche), Agarose (Spain) and other conventional reagents were purchased from Beijing Chemical Reagent Company.

Table 1. Primer pairs and PCR conditions used in the analysis of the swine EphrinB2 gene, GAPDH was as housekeeping gene

Primers	Sequences (5'→3')	Annealing temp.(°C)	Product (bp)
EphrinB2_1	TGTGGAAGTACTGCTGGGGA GGGATTGCGGACGCTACTTA	61	121
EphrinB2_2	TACCCACAGATAGGAGACAA GGTTAGGGCTGAATTCTTGG	59	211
EphrinB2_3	TCAGCATCCCATACGTTCAG TCGTGAAACAGCAGGTGGTC	61	270
EphrinB2_4	CTGTGCCGTAAAGTAATCGC TTCTGTCCTACCCTGTGATG	60	217
EphrinB2_5	GCATCATCTTCATCGTCATC TCTCCTGGACTATGTACACC	59	258
GAPDH	ACCACAGTCCATGCCATCAC TCCACCACCCTGTTGCTGTA	62	452

2.3 Determination of EphrinB2 Exons

In order to identify swine EphrinB2 exons, EphrinB2 exons of human (GenBank: NM_004093.2) and murine (GenBank: NM_010111.5) were compared with swine cDNA (NM_001114286.1) using DNAMAN software, respectively. Specific locations of EphrinB2 exons on chromosome 11 were identified by BLAST in NCBI (http:// www.ncbi.nlm.nih.gov/ blastn) website.

2.4 Primers Design

To genotype the polymorphism of EphrinB2 gene mutative locus (a T/C transition at position 510 bp of swine EphrinB2 gene cDNA sequence), five pairs of primers for PCR-SSCP were designed based on intron sequences at both ends of each exon, and with these primers, all of EphrinB2 exons were amplified. In addition, all the primers were synthesized by Invitrogen Shanghai Branch (Table 1).

2.5 PCR Amplification Conditions

PCR reactions were performed in a 15 μL reaction volume containing 50 ng genomic DNA, 1.5 μL of 10×PCR buffer containing 100 mM Tris-HCl (pH 8.0), 500 mM KCl, 10 mM of $MgCl_2$ and 0.1% Triton X-100, 200 μM of each dNTPs, 0.5 μL of each primer (10 pM) and 3U of Taq DNA polymerase (TIANGEN, China). The amplifying conditions of PCR for EphrinB2 were 94 ºC for 5 min, followed by 35 cycles of 94 ºC for 30 s, 59-62 ºC for 30 s, 72 ºC for 30 s, then 72 ºC for 7 min. PCR products was identified on 1.5% agarose gel electrophoresis and stored at 4 ºC. The sequencing results of different pig breeds were compared by using BLAST (http://www.ncbi.nlm.nih.gov).

2.6 SSCP Analysis for Genetic Variation

After 5 μl PCR products were denatured with 8 μl buffer for 10 min at 98 ºC, single-strand conformation polymorphism (SSCP) was used to identify polymorphism of

EphrinB2 by 10% polyacrylamide gel electrophoresis (110 V, 14~17 h) for 10-15h in 1×TBE buffer, and DNA band patterns were detected by silver staining method [23].

2.7 Statistical Analysis

Allele and genotype frequencies of EphrinB2 were calculated from the genotypes of the sows, respectively. Hardy-Weinberg equilibrium in the studied population was tested by comparing expected and observed genotype frequencies using a chi-square test. Genotype effects of EphrinB2 were analyzed by the established linear mode (1). Additive and dominant effects of genotypes and least squares means for litter size were also analyzed by the model (1). The data were processed using GLM procedure and Genetics program of SAS (8.1 version) for the first, second, third to eighth parity and all parities. Litter size corresponding to each genotype was expressed in the form of least square means ± standard error (LSmeans ± SE), and the linear model is as follows:

$$Y_{ijklm} = \mu + HYS_i + B_j + P_k + G_l + e_{ijklm}. \quad (1)$$

where Y is the reproductive trait (TNB or NBA), μ is the overall mean, HYS_i is the effect of herd-year-season (i = 1-31), B_j is the effect of breed(j=1, 2, 3), P_k is the effect of parity (k = 1, 2 and 3-8), G_l is the effect of genotype (l = 1, 2, 3) and e is the random residual.

Table 2. Allele and genotype frequencies of EphrinB2 in Landrace, Yorkshire and Duroc sows

Breed	EphrinB2					
	NO. of sows	Genotype distribution			Allele frequencies	
		TT	TC	CC	T	C
Landrace	198	47	85	66	0.45	0.55
Yorkshire	201	41	106	54	0.47	0.53
Duroc	86	20	35	31	0.44	0.56
Total	485	108	226	151	0.46	0.54

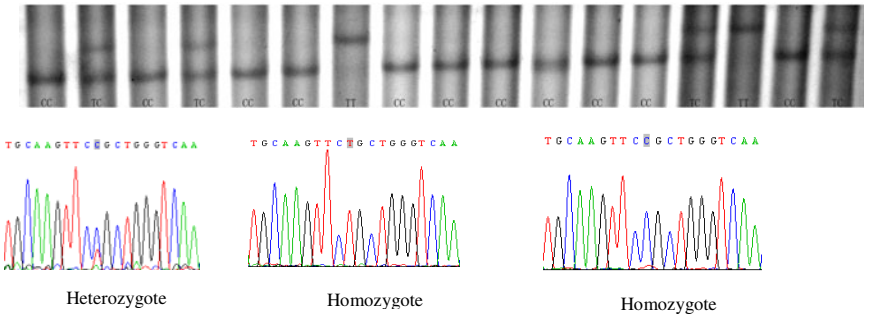

Fig. 1. The PCR-SSCP (Single-Strand Conformation Polymorphism) results for the EphrinA2 gene polymorphism

Table 3. Effects of EphrinB2 on litter size in different parities (LS means ± SE)

Item	Geno-type	First parity			Second parity		
		Litters	TNB	NBA	Litters	TNB	NBA
Ephr-inA2	TT	107	10.35 ± 0.23^{Aa}	9.88 ± 0.22^{Aa}	50	10.97 ± 0.45^{ABa}	9.99 ± 0.44^{ABa}
	TC	228	$10.84\pm0.17A^{Bb}$	10.04 ± 0.17^{Aa}	102	10.50 ± 0.37^{Aa}	9.60 ± 0.36^{Aa}
	CC	150	11.37 ± 0.20^{Bc}	10.79 ± 0.20^{Bb}	79	11.89 ± 0.40^{Bb}	10.87 ± 0.39^{Bb}
Additive effect			-0.51	-0.45		-0.46	-0.44
Dominant effect			-0.12	-0.30		-0.93	-0.84
Item	Geno-type	Third to eighth parity			All parities		
		Litters	TNB	NBA	Litters	TNB	NBA
Ephr-inA2	TT	85	11.35 ± 0.42^{Aa}	10.77 ± 0.39^{Aa}	242	10.72 ± 0.22^{Aa}	9.80 ± 0.22^{Aa}
	TC	136	11.86 ± 0.36^{Aab}	11.03 ± 0.34^{Aa}	466	11.08 ± 0.20^{Aa}	9.93 ± 0.19^{Aa}
	CC	86	12.21 ± 0.42^{Ab}	11.43 ± 0.40^{Aa}	315	11.77 ± 0.22^{Bb}	10.70 ± 0.22^{Bb}
Additive effect			-0.42	-0.33		-0.53	-0.45
Dominant effect			0.08	-0.07		-0.16	-0.32

Values with different superscripts show significant levels within columns (A,B $P\leq0.01$, a,b$P\leq0.05$)

3 Results

3.1 SNPs Identification

Five Exons of swine EphrinB2 gene, 1002-bp cDNA sequence was scanned by PCR-SSCP approach, and a T→C transversion at 510 bp was found. The EphrinB2 SNP locus was in Exon 4, and PCR products of each genotype of the SNP were random selected and sequenced by automated sequencing to validate the results (Fig. 1).

3.2 Allele and Genotype Frequencies

The data of TNB and NBA were analyzed by parity, involving the first parity, the second parity, the third to eighth parity, and all parities. All genotypes of EphrinB2 occurred in the Landrace, Yorkshire and Duroc sows, which were both found to be in Hardy-Weinberg equilibrium for the genotyped locus through chi-square test ($P > 0.05$). The allele and genotype frequencies are shown in Table 2.

3.3 Association of Polymorphism with Litter Size

Least squares means, additive effects and dominant effects for litter size were calculated using (1). The results were shown in Table 3.

At EphrinB2 locus, the homozygote CC significantly differed from either homozygous TT or heterozygous T genotypes for TNB and NBA ($P < 0.05$ or $P < 0.01$) in first, second parity, third to eighth parity and all parities, but there was no difference between the TT and TC genotypes. The sows with the CC genotype of EphrinB2 had an advantage of 1.02, 0.92, 0.86, 1.05 piglets for TNB and 0.91, 0.88, 0.66, 0.90 piglets for NBA per litter over the TT sows in first, second, third to eighth parity and all parities. The favorable allelic additive effects at EphrinB2 locus were -0.53 and -0.45, respectively, for TNB and NBA in all parities; and the favorable allelic dominance effects at EphrinB2 locus were -0.08 and -0.07, respectively, for TNB and NBA in third to eighth parity (Table 3).

4 Discussion

Genetic progress in animal breeding could be improved by marker-assisted selection (MAS), and application of MAS would increase as more associations between markers and traits were identified. This technology seems to be especially promising for reproductive traits such as litter size. To find the specific marker associated with litter size, some hormone-related genes had been chosen as candidate genes for litter size, such as ESR[4,24], follicle-stimulating hormone b (FSHb) [25], PRLR[5] and RBP4[6]. Recently, more and more studies had found that some cytokines were also important to reproduction, especially to embryo implantation, such as TGF-β1[26], RNF4 [27] and LIF[7], which were also candidate genes for litter size. And EphrinB2 is one of these cytokines.

EphrinB2, which belongs to Eph-Ephrin family, plays essential roles in vascular development during embryogenesis [28]. Targeted inactivation of EphrinB2 in mice impaired angiogenesis and caused embryonic lethality [29-31]. EphrinB2 induces angiogenesis in vivo and that the Phosphatidylinositol-3 Kinase signaling pathway contributes to angiogenic events induced by EphrinB2 [16]. EphrinB2 also controls lymphangiogenic growth in embryonic development [17]. All of the studies showed that EphrinB2 plays an important role in embryo development and implantation. Therefore, EphrinB2 gene was developed as a candidate gene influencing litter size in pigs.

This polymorphism is significantly associated with TNB, NBA in Landrace and Yorkshire breeds. The effect of EphrinB2 polymorphism on litter size in these breeds with different genetic background suggested that this EphrinB2 might be a good candidate gene for reproductive traits. Sows with CC genotypes at EphrinB2 locus had significantly more TNB or NBA than sows with any other genotype ($P < 0.05$ or 0.01) in first, second, third to eighth parity and all parities. The difference between TT and TC at EphrinB2 locus did not reach statistical significance. So it seemed that pigs carrying the C allele at EphrinB2 locus could increase TNB and NBA in first, second and all parities.

There were significant differences among TT and TC genotypes in Yorkshire, Duroc and all breeds, but no difference was found in Landrace, this showed that application of this SNP is more suitable for Yorkshire and Duroc pigs. In this study, the EphrinB2 locus in Exon 4 didn't directly alter amino acid residue, which was possible that the polymorphism indirectly affects reproductive traits by being in linkage disequilibrium with another polymorphism that directly influences the quantitative traits analyzed [27].

In conclusion, a T/C transversion in swine EphrinB2 exon was detected. Association analyses indicated that pigs carrying the C allele at EphrinB2 locus could increase TNB and NBA.

Acknowledgment. The authors greatly appreciate Beijing Huadu Swine Breeding Company, LTD for collecting samples. This study was supported by National Natural Science Foundation of China (No. 30771540) and National High-Technology Research Development Program of China (No. 2007AA10Z166).

References

1. Linville, R.C., Pomp, D., Johnson, R.K., Rothschild, M.F.: Candidate gene analysis for loci affecting litter size and ovulation rate in swine. Journal of Animal Science 79, 60–67 (2001)
2. Campbell, E.M.G., Nonneman, D., Rohrer, G.A.: Fine mapping a quantitative trait locus affecting ovulation rate in swine on chromosome 8. Journal of Animal Science 81, 1706–1714 (2003)
3. Johnson, R.K., Nielsen, M.K., Casey, D.S.: Responses in ovulation rate, embryonal survival, and litter traits in swine to 14 generations of selection to increase litter size. Journal of Animal Science 77, 541–557 (1999)
4. Rothschild, M., Jacobson, C., Vaske, D., Tuggle, C., Wang, L., Short, T., et al.: The estrogen receptor locus is associated with a major gene influencing litter size in pigs. Proceedings of the National Academy of Sciences 93, 201–205 (1996)
5. Vincent, A.L., Evans, G., Short, T.H., Southwood, O.I., Plastow, G.S., Tuggle, C.K., et al.: The prolactin receptor gene is associated with increased litter size in pigs, p. 15. University of New England (1998)
6. Rothschild, M.F., Messer, L., Day, A., Wales, R., Short, T., Southwood, O., et al.: Investigation of the retinol-binding protein 4 (RBP4) gene as a candidate gene for increased litter size in pigs. Mammalian Genome 11, 75–77 (2000)
7. Lin, H.C., Liu, G.F., Wang, A.G., Kong, L.J., Wang, X.F., Fu, J.L.: Effect of polymorphism in the leukemia inhibitory factor gene on litter size in Large White pigs. Molecular Biology Reports 36, 1833–1838 (2009)
8. Park, K.R., Inoue, T., Ueda, M., Hirano, T., Higuchi, T., Maeda, M., et al.: CD9 is expressed on human endometrial epithelial cells in association with integrins α6, α3 and β1, pp. 252–257. Oxford Univ. Press (2000)
9. Geisert, R.D., Schmitt, R.A.M.: Early embryonic survival in the pig: Can it be improved. J. Anim. Sci. 80, 54–65 (2002)
10. Frisen, J., Holmberg, J., Barbacid, M.: Ephrins and their Eph receptors: multitalented directors of embryonic development. The EMBO Journal 18, 5159–5165 (1999)
11. Fujiwara, H., Yoshioka, S., Tatsumi, K., Kosaka, K., Satoh, Y., Nishioka, Y., et al.: Human endometrial epithelial cells express ephrin A1: possible interaction between human blastocysts and endometrium via Eph-ephrin system. J. Clin. Endocrinol. Metab. 87, 5801–5807 (2002)
12. Red-Horse, K., Kapidzic, M., Zhou, Y., Feng, K.T., Singh, H., Fisher, S.J.: EPHB4 regulates chemokine-evoked trophoblast responses: a mechanism for incorporating the human placenta into the maternal circulation. Development 132, 4097–4106 (2005)
13. Fujii, H., Tatsumi, K., Kosaka, K., Yoshioka, S., Fujiwara, H., Fujii, S.: Eph-ephrin A system regulates murine blastocyst attachment and spreading. Dev. Dyn. 235, 3250–3258 (2006)

14. Flanagan, J.G., Vanderhaeghen, P.: The ephrins and Eph receptors in neural development. Annual Review of Neuroscience 21, 309–345 (1998)
15. Committee Eph Nomenclature. Unified nomenclature for Eph family receptors and their ligands, the ephrins. Cell 90, 403–404 (1997)
16. Maekawa, H., Oike, Y., Kanda, S., Ito, Y., Yamada, Y., Kurihara, H., et al.: Ephrin-B2 induces migration of endothelial cells through the phosphatidylinositol-3 kinase pathway and promotes angiogenesis in adult vasculature. Arteriosclerosis, Thrombosis, and Vascular Biology 23, 2008–2014 (2003)
17. Foo, S.S., Turner, C.J., Adams, S., Compagni, A., Aubyn, D., Kogata, N., et al.: Ephrin-B2 controls cell motility and adhesion during blood-vessel-wall assembly. Cell 124, 161–173 (2006)
18. Lawson, N.D., Weinstein, B.M.: Arteries and veins: making a difference with zebrafish. Nature Reviews Genetics 3, 674–682 (2002)
19. le Noble, F., Moyon, D., Pardanaud, L., Yuan, L., Djonov, V., Matthijsen, R., et al.: Flow regulates arterial-venous differentiation in the chick embryo yolk sac. Development 131, 361–375 (2004)
20. Lamont, R.E., Childs, S.: MAPping out arteries and veins. Science's STKE, pp. 1–3 (2006), doi:10.1109/SCIS.2007.357670
21. Adams, R.H., Alitalo, K.: Molecular regulation of angiogenesis and lymphangiogenesis. Nature Reviews Molecular Cell Biology 8, 464–478 (2007)
22. Cowan, C.A., Yokoyama, N., Saxena, A., Chumley, M.J., Silvany, R.E., Baker, L.A., et al.: Ephrin-B2 reverse signaling is required for axon pathfinding and cardiac valve formation but not early vascular development. Developmental Biology 271, 263–271 (2004)
23. Sambrook, J., Russell, D.W.: Molecular cloning: a laboratory manual. CSHL press (2001)
24. Short, T.H., Rothschild, M.F., Southwood, O.I., McLaren, D.G., De Vries, A., Van der Steen, H., et al.: Effect of the estrogen receptor locus on reproduction and production traits in four commercial pig lines. Journal of Animal Science 75, 3138–3142 (1997)
25. Li, N., Zhao, Y.F., Xiao, L., Zhang, F.J., Chen, Y.Z., Dai, R.J., et al.: Candidate gene approach for identification of genetic loci controlling litter size in swine, p. 183. University of New England (1998)
26. Wu, Y.P., Wang, A.G., Li, N., Fu, J.L., Zhao, X.B.: Association with TGF-β1 Gene Polymorphisms and Reproductive Performance of Large White Pig. Reproduction in Domestic Animals, pp. 1–5 (2009), doi:10.1111/j.1439-0531.2009.01480.x
27. Niu, B.Y., Ye, L.Z., Li, F.E., Deng, C.Y., Jiang, S.W., Lei, M.G., et al.: Identification of polymorphism and association analysis with reproductive traits in the porcine RNF4 gene. Animal Reproduction Science 110, 283–292 (2009)
28. Wang, H.U., Chen, Z.F., Anderson, D.J.: Molecular distinction and angiogenic interaction between embryonic arteries and veins revealed by ephrin-B2 and its receptor Eph-B4. Cell 93, 741–753 (1998)
29. Wang, H.U., Chen, Z.F., Anderson, D.J.: Molecular distinction and angiogenic interaction between embryonic arteries and veins revealed by ephrin-B2 and its receptor Eph-B4. Cell 93, 741–753 (1998)
30. Adams, R.H., Wilkinson, G.A., Weiss, C., Diella, F., Gale, N.W., Deutsch, U., et al.: Roles of ephrinB ligands and EphB receptors in cardiovascular development: demarcation of arterial/venous domains, vascular morphogenesis, and sprouting angiogenesis. Genes & Development 13, 295–306 (1999)
31. Gerety, S.S., Wang, H.U., Chen, Z.F., Anderson, D.J.: Symmetrical mutant phenotypes of the receptor EphB4 and its specific transmembrane ligand ephrin-B2 in cardiovascular development. Molecular Cell 4, 403–414 (1999)

Efficient Water-Saving Irrigation Solution for Direct Seeding Rice under No-Tillage after Cultivating Wheat*

Zhengguo Sun[1,2], Chengming Sun[1,2], Yizhao Chen[1], Jianlong Li[1,**], and Hongcheng Zhang[2]

[1] College of Life Science, University of Nanjing, Nanjing, Jiangsu Province, China, 210093
[2] College of Agriculture Science, University of Yangzhou,Yangzhou, Jiangsu Province, China, 225009
jlli2008@nju.edu.cn

Abstract. In order to explore the water-saving irrigation pattern of direct rice for high yield and excellent quality under no-tillage after wheat, the research was carried out on the experimental farm of Yangzhou University in the year 2005, which selected Wuxiangjing 14 and Lianjiajing 1 as the experimental cultivar. The semi-arid irrigation and general irrigation regime were employed under 3000 thousand basic seedling per hectare with Lianjiajing 1 and wuxiangjing 14. The productivity was similar between the two types of irrigation regime. There was no remarkable difference on the yield components, leaf area index, photosynthesis potential, net assimilation rate, and dry matter at different stage, milling quality and appearance quality, the cooking quality and nutrition quality. But all these aspects in the semi-arid irrigation treatment had a trend of decrease. The rice under semi-arid irrigation regime was strong; their leaves color were light, and the N content of the stem and grain were lower than those of conventional irrigation regime. Semi-arid irrigation saved the amount of water by one third, compared with the general irrigation regime. On the basis of the research, semi-arid irrigation with appropriately improved seeding pattern under no-tillage after wheat could be one of approaches to gain high yield and excellent quality, but the best combination need to be confirmed through further experiments.

Keywords: Direct seeding rice, No-tillage, Water-saving irrigation, Yield, Quality.

1 Introduction

The research of water-saving irrigation on crop has been more reported at home and abroad [1-6].The reports aimed at highlighting different possible strategies for a more efficient use of water [7-11], particularly in areas where water resources are limited. But the water-saving irrigation techniques of direct seeding rice reported less.

* This work is supported by "the key project of chinese national programs for fundamental research and development (973 program, 2010cb950702), apn project (arcp2010-14nmy-li) and the project of "dynamic monitoring the change of landuse, agricultural productivity and their drive force in zhangjignag city by 3s technology "(2007zk1098).

** Corresponding author.

E. Zhu and S. Sambath (Eds.): Information Tech. and Agricultural Eng., AISC 134, pp. 819–826.
springerlink.com © Springer-Verlag Berlin Heidelberg 2012

The direct seeding rice under no-tillage after wheat, the soils stay the natural state which has frozen and melt, the soil density decreased relatively and the porosity became larger, the root of wheat rot into the natural channel, so the water seepage has evidently increased. It helps to update soil environment, but the water-retention capacity declines. If general irrigation management pattern in all life of rice was employed, water consumption and the cost of water for rice production will increase. Moreover, the seeds of direct seeding rice under no-tillage after wheat are shallow in the soil, even exposed to air. Confronted irrigation water layer over a long period of time, the soil is soft and muddy, has a strong resistance to lodging. It is necessary to discover efficient water-saving irrigation pattern of direct seeding rice under no-tillage after wheat to achieve the unity of high yield and water-saving and resistance to lodging.

2 Materials and Methods

2.1 Experimental Site and Materials

The research was carried out on the experimental farm of Yangzhou University in the year 2004. The soil type is sandy loam soil and high fertility. The cultivar for the experiment is Wuxiangjing 14 and Lianjiajing 1.

2.2 Trial Design and Management

According to the growth and development character and water-demand trait of direct seeding rice under no-tillage after wheat, from the unity of density and water, six treatments were designed:(a)1500000 basic seedling per ha, conventional water management pattern, Lianjiajing 1;(b)3000000 basic seedling per ha, conventional water management pattern, Lianjiajing 1;(c)3000000 basic seedling per ha, the semi-irrigation regime pattern, Lianjiajing 1;(d)1500000 basic seedling per ha, conventional water management pattern, Wuxiangjing 14;(e)3000000 basic seedling per ha, conventional water management pattern, Wuxiangjing 14;(f)3000000 basic seedling per ha, the semi-irrigation regime pattern, Wuxiangjing 14.

2.3 Test Items

1) Main Growth Period
Observation records of the main growth period of each treatment and the corresponding exact date.

2) Growth Dynamics of Rice Population
Leaf process: Systematical tracking the process of rice leaf.

Tiller dynamics of rice population : Investigated tiller dynamics every six day until heading period. Concurrently general surveyed and corrected in the shooting stage and heading stage.

eaf area dynamics of groups: determination in the shooting stage, heading and maturity stage.

Group dynamics of dry matter accumulation: Tested the accumulated dry matter in the shooting stage, heading stage and maturity groups.

3) Rice Yield and Its Components
General surveyed Panicles in group and number of grain per ear in mature stage in a district.

Tested ripening rate by conventional water skip way, and corrected the standard water content by 14%.

4) Determination of Rice Quality
The milling quality, appearance quality, cooking and eating quality and nutritional quality of rice major quality indicator were measured after Three months of the grain harvested.

3 Results and Analysis

3.1 The Effects of Combination of Different Densities and Water Management on Yield and Components of Rice

1) The Effects of Combination of Different Densities and Water Management on Yield of Rice
Through multiple comparisons of yield on different combinations of density and water management with Lianjiajing 1 and Wuxiangjing 14,it can be seen from table Ⅰ that the yield of 3000000 basic seedling treatment was significantly higher than 1500000 basic seedling on the general irrigation condition. On the condition of 3000000 basic seedlings, the yield of general water management is slightly higher than semi-arid irrigation treatment, but the difference was not significant. To some extent this show that water-saving irrigation can be achieved by means of turning general water management pattern to semi-arid irrigation.

2) The Effects of Combination of Different Densities and Water Management on the Components of Yield
As can be seen from table Ⅰ ,the changes of each treatment in yield components:

(1) On the general irrigation condition, as the density of Lianjiajing 1 increases, the headings per hectare increases significantly, but which on the general irrigation condition is more than semi-arid irrigation, the difference between the two treatments were not significant. Grains per spike were not significant difference among all treatments. On the general irrigation condition, the indexes of ripening rate and thousand seed weight of 1500000 basic seedling treatment is larger than the treat of 3000000 basic seedling, but on this basic seedling condition, the index of ripening rate and thousand seed weight of general irrigation condition is larger than that of semi-arid irrigation condition.

(2) The headings of Wuxiangjing 14 per hectare of 3000000 basic seedling treatment is more than the treatment of 1500000 basic seedling on the general irrigation condition, but the index of ripening rate is reverse. On the 3000000 basic seedling conditions, the index value of headings per hectare and ripening rate of the general irrigation is larger than the treatment of semi-arid irrigation pattern, but the difference between the two treatments were not significant. Grains per spike on general irrigation and 1500000 basic seedlings per hectare condition is the most of all the treatments.

Table 1. The yield and components of different combinations of density and water management

treat	headings (10^4/ha)	grains per spike (grain)	ripening rate(%)	thousand seed weight(g)	theoretical yield (kg/ha)	actual yield (kg/ha)
a	408b	101.3a	89.9a	26.7a	9925.5b	10279.5b
b	450a	98.1a	88.8b	26.4b	10329a	10291.5a
c	450a	97.4a	88.3b	26.2b	10104 ab	10039.5ab
d	421.5b	101.8a	87.4a	26.7a	9976.5b	9921b
e	474a	95.2b	86.4b	26.5a	10333.5a	10281a
f	466.5a	96.2c	86.4b	26.4a	10201.5ab	10137ab

Note: Significant difference by Duncan's new multiple range method, significance level: 0.05.

3.2 Rice Group Dry Matter Accumulation of Different Combination of Density and Water Management

As can be seen from table 2:

1) The dry matter accumulation of the two cultivars for trial, the treatment of 3000000 basic seedling and general irrigation is most, the treatment of 3000000 basic seedling and semi-arid irrigation is more, and the treatment of 1500000 basic seedling and general irrigation at the jointing, heading and maturity stage.
2) The dry matter accumulation of the treatment of 3000000 basic seedling and general irrigation is higher than the other two treatments from jointing to heading stage and from heading stage to maturation. The proportion of the dry matter accumulation from heading to mature stage to total biomass is higher than the other treatments. The dry matter accumulation of the treatment of 3000000 basic seedling and general irrigation is almost or slightly higher than the treatment of 1500000 basic seedling and general irrigation from jointing to heading stage and from heading stage to maturation.

3.3 The Effects on Quality of Different Rice Group Density and Water Treatment Combinations

As can be seen from table 3, rate of husked rise of the treatment of 1500000 basic seedling and general irrigation is the largest on the two cultivars of Lianjiajing 1 and Wuxiangjing14, respectively84.8% and 84.9%.the treatment of 3000000 basic seedling and semi-arid irrigation is the minimum, respectively84.1% and 84.2%.On the index of milled rice rate, the treatment of 1500000 basic seedling and general irrigation is also the largest, 78.3% and 78.5%,the treatment of 3000000 basic seedling and semi-arid irrigation is the minimum, 77.8% and 77.7%. According to head milled rice rate, 1500000 basic seedling and general irrigation is the largest, respectively71.3% and 73.1%, the treatment of 3000000 basic seedling and semi-arid irrigation is the minimum, 70.0% and 72.3%. Noticeable, the difference between the above-mentioned treatments is even smaller.

Table 2. Dry matter accumulation of diferent density and water combinations treatments

treat	Jointing stage (kg/ha)	heading stage (kg/ha)	maturity stage (kg/ha)	Jointing-heading		heading－maturity	
				(kg/ha)	Percentage of total biomass	(kg/ha)	Percent-age of total biomass
a	4231.5	11464.5	17254.5	7231.5	41.9	5790	33.6
b	4474.5	11937	18528	7464	40.3	6591	35.6
c	4362	11578.5	17737.5	7216.5	40.7	6159	34.7
d	4279.5	11335.5	17407.5	7056	40.5	6072	34.9
e	4587	11907	18627	7320	39.3	6720	36.1
f	4431	11557.5	17923.5	7126.5	39.8	6366	35.5

On the appearance quality (Table 3), for the two cultivars of Lianjiajing 1 and Wuxiangjing14, Chalk rate, chalkiness size and chalkiness of the treatment of 3000000 basic seedling and semi-arid irrigation is the largest, the treatment of 3000000 basic seedling and general irrigation is lager, and the treatment of 1500000 basic seedling and general irrigation is the minimum. However, very little difference between the treatments.

In the cooking and nutritional quality (Table 4), the same trend can be taken on the two cultivars. According to the index of gel consistency and the content of protein, the treatment of 1500000 basic seedling and general irrigation is larger than the treatment of 3000000 basic seedling and general irrigation, and the treatment of 3000000 basic seedlings and semi-arid is the minimum. As for amylase content, the treatment of 3000000 basic seedling and semi-arid irrigation is the largest, the treatment of 3,000,000 basic seedling and general irrigation takes second place, and the treatment of 1500000 basic seedling and general irrigation is the minimum.

Table 3. The quality of different density and water combinations

treat	Milling quality			appearance quality			cooking nutritional quality		
	husked rise rate (%)	milled rice rate (%)	head milled rice rate (%)	chalk rate (%)	chalkin-ess size (%)	Chalk-iness (%)	gel consiste-ncy (mm)	mylase content (%)	protein content (%)
a	84.8	78.3	71.3	21.1	18.2	3.8	87.5	18.0	9. 6
b	84. 7	77.9	70.4	21.8	18.5	4.0	86.8	18. 5	9. 3
c	84.1	77.8	70.0	21.9	18.8	4.1	86.8	18. 8	9.1
d	84.9	78.5	73.1	23.4	19.7	4.6	86.3	17.1	7. 9
e	84.5	77.9	72.6	23.8	20.3	4.8	86.1	17.4	7. 8
f	84.2	77.7	72.3	24.0	20.5	4.9	86.0	17.8	7.5

4 Discussions

The experimental results show that on the condition of 3000000 basic seedlings, the yield by semi-arid irrigation pattern is nearly or slightly decreased than the general irrigation, but there are not significant differences. Semi-arid irrigation saved the amount of water by one third, above 30%. This result probably is caused by the fact that the semi-arid irrigation reduced the amount of seepage without influencing the regular water requirement of crops [12]. The experiment of Tripathi et al.[13] also indicated that the reduce of evaporation play an important role in the water-saving process, their results showed that compared with the high dairy mean evaporanspiration of general irrigation(7.2-9.2 mm/d), the statistic of intermitted irrigation is only 6.1-7.1mm/d. Further more, there was no remarkable difference on the yield components, and dry matter at different stage, milling quality and appearance quality, the cooking quality and nutrition quality. But all these aspects in the semi-arid irrigation model had a trend of decreasing With the respect of quality, the two irrigation patterns are more nearly. It showed that the re-irrigation in the ditch of 10cm deep did not created water stress on rice growth. The rice under semi-arid irrigation regime were stronger, their leave color were light, and the N content of the plant and of the grain were lower than those of conventional irrigation regime. As N is the main formational component of chlorophyll, the concentration of chlorophyll and the leave color are largely influenced by its supply. However, if the absorption of N is connected with the supply of water, is not that clear. According to the result of experiment of J. Yang et al. [14], the reduction of N supply for crop may relate to water deficient in soil. And others also reported the physiological mechanism to increase yield by fertilization (especially N fertilizer) under soil water stress, such as promoting the develop of root system, regulating C and N metabolism and leaf photosynthetic rate. On the other hand, an experiment showed that water and N have little interaction to each other on yield of rice, biomass, water use efficiency, absorption of nutrients and N using efficiency [15].

Compared the treatment of 3000000 basic seedlings with 1500000 basic seedlings, the spike number increased by 10.5%.though ripening rate and thousand grain weight decreased slightly, but the yield increased evidently. This phenomenon may be related to the breeding characteristics of direct seeding rice: 1) short vegetative growth period; 2) large amount of peak seedlings and low percentage of ear bearing rate; 3) stable ripening rate and thousand seed weight. Therefore under no-tillage after wheat by the way of appropriately improving seeding density and employing the semi-arid irrigation pattern, the high yield and water saving can be achieved, but the best combination of density (basic seedling) and semi-arid irrigation pattern need further confirm through experiment.

Experimental observations also show that semi-arid irrigation plants produce a series of effects on rice. For example, the leaf color of rice plants is light, but also stronger during whole growth stages. The effects in this regard have yet to be in-depth study.

After the seventies of twenty century, almost all the countries from America, Australia and Europe applied technology of mechanization of direct seeding in rice cultivation. The area of direct seeding rice is over 95% of their total rice cultivate area. However, in China, the largest country of rice production in the world, the area

of direct seeding rice is limited which partly caused by the fact that rural labor force is relatively redundancy. But as the change of development strategy of agriculture and the acceleration process of agriculture modernization, to improve the technique of direct seeding rice is significantly necessary. Direct seeding rice under no-tillage, which is chiefly introduced above, has been widely researched and applied all around the world. Kondo et al. [16] and Dingkuhn et al. [17] found that, compared with transplanting rice, dry matter, the number of tiller and plant N uptake of plow direct seeding rice increased in the period of vegetative growth, however, plant N uptake and production of dry matter decreased in the period of reproductive growth. Another report also showed that there are more tillers and higher LAI in direct seeding rice rather than in transplanting rice [18]. As no-till direct seeding rice not only shares the advantages of plow ones on vegetative growth and material production, but also promote the growth of tiller, it is helpful in actual production.

5 Conclusions

A. The semi-irrigation regime and general irrigation regime were employed under basic seedling was 3000 thousand per hectare with Lianjiajing 1 and wuxiangjing 14. The productivity was similar between the two types of irrigation regime.

B. There was no remarkable difference on the yield components, dry matter at different stage, milling quality and appearance quality, the cooking quality and nutrition quality. But all these aspects in the semi-arid irrigation model had a trend of decreasing.

C. The rice under semi-arid irrigation regime were strong, their leaves color were light, and the N content of the plant and of the grain were lower than those of conventional irrigation regime.

D. Semi-arid irrigation saved the amount of water by one third, above 30%, contrast with the conventional irrigation regime.

E. On the basis of the years of systematical research, Semi-arid irrigation and appropriately improved seeding pattern under no-tillage after wheat might be a high yield and excellent quality approach, but the best combination need to further confirm through experiment.

Acknowledgment. We are grateful to the chief editor and anonymous reviewers for Illuminating comments. This research was mainly supported by THE KEY PROJECT OF chinese national programs for fundamental research and development (973 program, 2010cb950702), apn project (arcp2010-14nmy-li) and the project of “dynamic monitoring the change of landuse, agricultural productivity and their drive force in zhangjignag city by 3s technology” (2007zk1098)

References

1. Allen, R.G., Pereira, L.S., Raes, D., Smith: Crop evapotranspiration: guidelines for computing crop water requirements. Irrigation and Drainage Paper, No. 56. FAQ, Rome, 300 (1998)

2. Adachi, F., Kobata, T., Arimoto, M.: Comparison of water use efficiency of paddy rice (Oryza sativa L.) among location and interannual variation in humid area.1.Reliablity of estimated canopy transpiration rate from meteorological and physiological data of the crop. Jpn. J. Crop. Sci. 64, 509–515 (1995)
3. Matsushima, S.: High-Yielding Rice Cultivation, pp. 367–372. Japan Scientific Societies Press, Tokyo (1976)
4. Grimes, D.W., Dickens, W.: Dating termination of cotton irrigation from soil water-retention characteristics. Agron. J. 66, 403–404 (1974)
5. Hanson, B.R., Schwankl, L.J., Fulton, A.E.: Scheduling irrigations: when and how much water to apply (Water management series publication no 3394). University of California Irrigation Program, Davis, Calif., USA (1999)
6. Mao, Z.: Principle and technique of water saving irrigation for rice. Wuhan University of Hydraulic and Electric Engineering, Wuhan (1993)
7. Asseng, S., Turner, N.C., Keating, B.A.: Analysis of water-and nitrogen-use efficiency of wheat in a mediterranean climate. Plant Soil 233, 127–143 (2001)
8. Anbumozhi, V., Yamaji, E., Tabuchi, T.: Rice crop growth and yield as influenced by changes in ponding water depth, water regime and fertigation level. Agric. Water Manag. 37, 241–253 (1998)
9. Uphoff, N.: The system of rice intensification: using alternative cultural practices to increase rice production and profitability from existing yield potentials. International Rice Commission Newsletter, Number 55, UN, Food and Agriculture Organization, Rome (2007)
10. Li, X.Y., Xu, X.L., Li, H.: A socioeconomic assessment of the system of rice intensification (SRI), a case study from Xinsheng Village, Jianyang County (2005)
11. Peng, S.Z., Li, S.S., Xu, G.L., Wu, Z.J.: New water consumption pattern of rice under water-saving irrigation. Irrigation and Drainage System 8, 97–108 (1994); Sichuan Province, Centre for Integrated Agricultural Development, China Agricultural University, Beijing
12. Tabbal, D.F., Lampayan, R.M., Bhuiyan, S.I.: Water efficient irrigation technique for rice. Soil and Water Engineering for Paddy Field Management. Asian Institute of Technology, Bangkok, Thailand, 146–159 (1992)
13. Tripathi, R.P., Kushwaha, H.S., Mishra, R.K.: Irrigation requirements of rice under shallow water table conditions. Agricultural Water Management 12, 127–136 (1986)
14. Yang, J., Wang, Z., Zhu, Q.: Effect of nitrogen nutrition on grain yield of rice and its physiological mechanism under different soil moisture. Sci. Agric. Sin. 294, 7–14 (1996)
15. Cabangon, R.J., Tuong, T.P., Castillo, E.G.: Effect of irrigation method and N-fertilizer management on rice yield, water productivity and nutrient-use dfficiencies in typical lowland rice conditions in China. Paddy Water Environ. 4, 195–206 (2004)
16. Kondo, M., Aragones, D.V., Pablico, P.P.: Effect of tillage intensity, water control and planting method on seeding establishment and growth of direct-seeded rice. In: Peng, S., Mardy, B. (eds.) Rice Research for Food Security and Poverty Alleviation, Manila, IRRI, pp. 521–532 (2001)
17. Dingkuhn, M., Schnier, H.F., De. Datta, S.K.: Relationship between ripening-phase productivity and crop duration, canopy photosynthesis and senescence in transplanting and direct-seeded low land rive. Field Crops Res. 26, 327–345 (1991)
18. Sam, S.Y., Mano, Y., Ookawa, T.: Comparisons of dry matter\production and related characters between transplanted and direct-sown plants in the submerged paddy field in rice cultivar, Takanari, with reference to planting pattern. In: IRRI (ed.) Proceedings of the Abstracts of Beijing International Rice Congress, Manila, IRRI, pp. 371–375 (2004)

Molecular Cloning of Arabidopsis thaliana HsfA2 Gene and Agrobacterium-Mediated Genetic Transformation of Chrysanthemum morifolium Ramat

Lingli Zhao[1], Huitang Pan[1], Ming Sun[1], and Qixiang Zhang[1,2,**]

[1] College of Landscape Architecture, Beijing Forestry University, Beijing, China
[2] National Engineering Research Center for Floriculture, Beijing, China
zqx@bjfu.edu.cn

Abstract. In this paper, the *HsfA2* gene from *Arabidopsis thaliana* ecotype Columbia was firstly isolated by RT-PCR, the PCR fragment of *HsfA2* gene was inserted into the binary vector pBI121 and got the resulted expression vector, which named pBI121-*AtHsfA2*. The vector was further transformed into the *Agrobacterium tumefaciens* LBA4404, and then the *AtHsfA2* was transmitted into *Chrysanthemum morifolium* Ramat 'Yurenmian' by *Agrobacterium*-mediated method. Finally, four positive transgenic plants were obtained successfully after antibiotic selection, PCR and PCR-Southern detection. Our results provide scientific references for transgenic breeding of *Chrysanthemum.*

Keywords: Arabidopsis thaliana L., HsfA2 gene, Genetic transformation, Chrysanthemum morifolium Ramat.

1 Introduction

During cell activity stress conditions, especially under heat shock stress, heat shock proteins as molecular chaperones play an important role in survival to promote refolding, stability, assembly, intracellular transport and degradation of proteins to repair of damaged proteins (Wang *et al.*, 2004; Weng and Hong, 2006). The expression of heat shock proteins by heat shock transcription factor (Hsfs) combined with heat shock protein in heat shock gene promoter elements (heat shock element, HSE), it raise other transcription factors to form the transcription complex, promoting heat shock protein gene expression. Plant heat shock transcription factor is more diversity than in animal systems, the formation of the long process of evolution complex and diverse types of heat shock transcription factors to adapt to rapid change and extreme environments (Wang *et al.*, 2004; Weng and Hong, 2006; Wu and Xu, 2005; Sangster and Queitsch, 2005). *HsfA2* is a upstream gene of transcription factor that can regulate the expression of downstream multiple stress tolerance related genes, it is not expressed under normal conditions, when rapid gene expression subject to stress, *HsfA2* with high potential and sustainable accumulation of activated to a very high level (Weng and Hong, 2006; Sangster and Queitsch, 2005; Charng *et al.*, 2007; Ayako *et al.*, 2006;

* Corresponding author.

E. Zhu and S. Sambath (Eds.): Information Tech. and Agricultural Eng., AISC 134, pp. 827–834.
springerlink.com © Springer-Verlag Berlin Heidelberg 2012

Banti *et al.*, 2010; Chan-Schaminet *et al.*, 2009). Ayako *et al.* (2006) and other tests prove that *HsfA2* gene is an important regulatory factor of defense system in *Arabidopsis* under many stress conditions. Li *et al.* (2005) analyzed and identified functions of *AtHsfA2* under high temperature and oxidative stress response, his research results indicated that the *AtHsfA2* can improve tolerance to heat and oxidative stress, it may be common components of heat and oxidative stress signal transduction pathway. With the adverse change of global climate, the impact of stress on plants growing significantly, the use of genetic engineering means to improve and enhance the resistance of plants is one of the most important breeding research direction in plant. Molecular breeding provides a new means and ways to improve plant varieties as it overcome the difficulties of conventional breeding hybridization, such as the limitations of long cycle, difficulties in distant hybridization. *Agrobacterium* with its easy operation, low cost, high efficiency, insert big DNA fragments, good stability, and lower transgenic copy number to become the preferred method in transgenic strategies (Wang and Fang, 2002).

In ornamental plants, *Agrobacterium*-mediated transformation of foreign genes is still the most effective way. *Chrysanthemum morifolium* Ramat. is applied currently in "Three North" areas of China, but not yet been widely introduced cultivation in the south of China because hot and humid climate. If HsfA2 gene was directed transfer to *Chrysanthemum* varieties that can better enhance its tolerance to environmental stress, and improve overall quality of plants to promote a wide range of applications on *Chrysanthemum*. In this study, we attempt to cloned HsfA2 gene of *Arabidopsis* and construct the appropriate plant expression vector, which was introduced into *Agrobacterium tumefaciens* using the freeze-thaw method, then *AtHsfA2* gene will be transferred into *Chrysanthemum morifolium* Ramat. 'Yurenmian' through *Agrobacterium*-mediated and provide stress resistance genes and potential genetic resources for breeding of ornamental plants.

2 Matrials and Methods

2.1 Plant Materials and Biochemical Reagents

Arabidopsis thaliana ecotype Columbia, *Chrysanthemum morifolium* Ramat.'Yurenmian', pBI121, *Escherichia coli* TOP10, *Agrobacterium tumefaciens* LBA4404 were conserved and provided by the laboratory of Beijing Forestry University. DIG labeling and hybridization kit was purchased from Beijing MyLab Medicine Technology Co., Ltd; EASY spin of plant RNA extraction kit was purchased from Beijing Gainingjinnuo Biotechnology Co., Ltd; pGM-T Cloning Kit and DNA fragment gel extraction kit were from Beijing Tiangen Biotechology Co., Ltd; and all enzymes were from Promega, USA.

2.2 Total RNA Extraction

Matured leaves of *Arabidopsis* at 20d growth period was collected to quickly extraction RNA by using the Plants EASY spin RNA extracted kit and extraction step was reference to instructions of the kit. After the plants placed at 37℃ for 1h and stored the

plant material frozen in liquid nitrogen, total RNA was extracted, then 1% agarose gel electrophoresis was used to check the purity and integrity of total RNA.

2.3 PCR Primers for AtHsfA2

According to sequence of *HsfA2* gene of *Arabidopsis* (GenBank accession number: NM-128173), the special primer pair was designed by Olig6.0 software and synthesized by Beijing Augct Biotechnology company. Primer1:5'-TTTCTAGACTCTCAACTCAA AACTCAACA-3'(underlined part is the *Xba* I restriction site), primer2: 5'-TCCCCCGGGTCAAAACAAACAAACAAACAA-3'(underlined part is the *Sma* I restriction site)

2.4 Gene Cloning and Sequencing of HsfA2

The first strand cDNA was first synthesized according to reverse transcription kit (Promega, USA). As the template, PCR was performed. The PCR reaction system was 50μL, of which 10× Buffer 5μL, dNTP (10mM) 1μL, forward and reverse primer 4μL, template cDNA 2μL, high-fidelity DNA polymerase 0.6μL, double distilled water 33.4μL. PCR reaction conditions were: 94℃ for denaturation 2 min; then 94℃ for 35 s, 54℃ anneal for 35 s, 72℃ extension for 2 min, 35 cycles; 72℃ extension 6 min. After the reaction, used pGM-T cloning kit added A for PCR reaction products, then it was connected with pGM-T vector through T4 ligase at 16℃ overnight. Finally, transformed the connection into *E. coli* TOP10, and positive clones were picked after blue-white screening.

2.5 Construction and Identification of Excessive Plant Expression Vector pBI121-AtHsfA2

pGM-T plasmid with *AtHsfA2* containing gene fragments and the plant expression vector pBI121 plasmids were used restriction enzymes *Sma* I (25℃, 4h) and *Xba* I (37℃, 4h) to digested respectively, The purpose of purified fragments were mixed and placed at 16℃ overnight after used T4 ligase to added, ligation products were transformed into *E. coli* TOP10 competent cells, and then coated plates with kanamycin (100mg/L), cultured at 37℃ overnight, picked a single colony placed to *kanamycin* liquid medium. Recombinant plasmid DNA was extracted and identification by enzyme digestion. Construction of recombinant plasmid was named pBI121-*AtHsfA2*, and then the recombinant plasmid was transferred into *Agrobacterium* LBA4404 by liquid nitrogen freeze-thaw.

2.6 PCR and PCR-Southern Hybrid Detection

Middle part leaves of plant after 1d pre-incubation was cut into small pieces, and than infected with *Agrobacterium* of OD_{600} about 0.6, middle part leaves of resistant rooting plants were selected to distilled genomic DNA after co-culture, later-culture and select culture. According to *Kanamycin* gene sequence, primer pair was designed as following: primer 1 (5'-ATTGCACGCAGGTTCTCCGG-3 ') and primer 2 (5'-GAGCGGCGATACCGTAAAGCAC-3'). The pBI-*AtHsfA2* plasmid was detected

as a positive control and DNA of non-transgenic plants was detected as a negative control for PCR to detect the transgenic plants. Reaction system was template DNA 1.0 μL, 2 mmol / L dNTP 2.0μL, 10 x Buffer 2.5μL, Primer l and Primer 2 each 1.0μL, Taq DNA polymerase 0.25μL, sterilization ddH_2O fill level to 25μL. PCR amplification reaction procedure was: 95℃ denaturation for 4min, 1 cycle; 95℃ denaturation for 35 S, 59℃ anneal for 45 S, 72℃ extension for 1 min, 35 cycles; and then 72℃extend for 8 min, Finally, 5 μL of PCR product was detected by 1.0% agarose gel electrophoresis.

PCR-Southern hybridization was used DIG labeling kit in accordance with instructions (MyLab) for probe labeling, DNA transfer to membrane and fix, and then wash membrane, incubate, close at room temperature, connect antibodies after the hybridization reaction for 16 h. Finally, used NBT/BCIP to develop and photograph.

3 Results and Discussion

3.1 Cloning of AtHsfA2 Gene by RT-PCR

AtHsfA2 gene was amplified by RT-PCR and the reaction product was detected by 1% agarose gel electrophoresis (Figure 1), the result showed that the amplified fragment size was the same length with designed fragment size, and is about 1300bp. Then it was built into the middle of pGM-T vector and sequenced, the sequencing result showed it is the same as the published NCBI gene sequences in *Arabidopsis HsfA2*, which also contain a complete open reading frame (ORF) and encoded 345 amino acids.

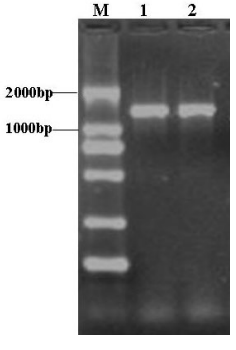

Fig. 1. PCR amplification of *AtHsfA2* gene. (M) DL2000 DNA Marker.

3.2 PCR and Enzyme Digestion of Recombinant Plasmid pBI121-AtHsfA2

After specific PCR amplification, about 1300bp target band was gain (Figure 2). And further restriction enzyme digestion also showed that recombinant plasmid pBI121-AtHsfA2 has been constructed successfully (Figure 3).

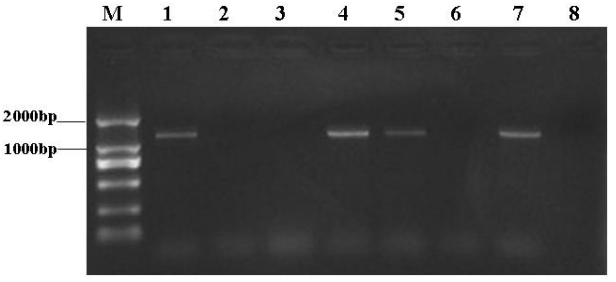

Fig. 2. PCR test of pBI121-*AtHsfA2*. (M) DL2000 DNA Marker. (1, 4, 5, 7) *AtHsfA2*.

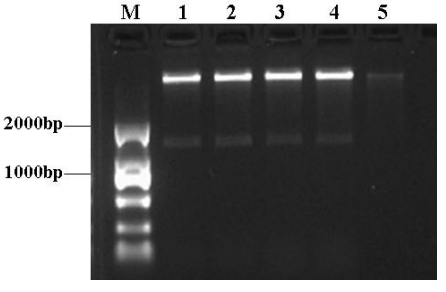

Fig. 3. Restriction enzyme test of pBI121-*AtHsfA2*. (M) DL2000 DNA Marker. (1, 2, 3, 4) pBI121-*AtHsfA2* was digested by *Sma* I and *Xba* I. (5) pBI121 was digested by *Sma* I *and Xba*

4 Construction and Identification of Plant Expression Vectors of Athsfa2

Recombinant plasmid was transferred into *Agrobacterium tumefaciens* LBA4404 by freeze-thaw method (Wang and Fang, 2009). Three single colonies were picked randomly as template to PCR amplification, then used enzyme *Sma* I and *Xba* I conducted double-enzyme digested the bacterium extracted plasmid clone DNA which was identified as positive initially. The results shown the recombinant plasmid was successfully introduced into *Agrobacterium* cells (Figure 4).

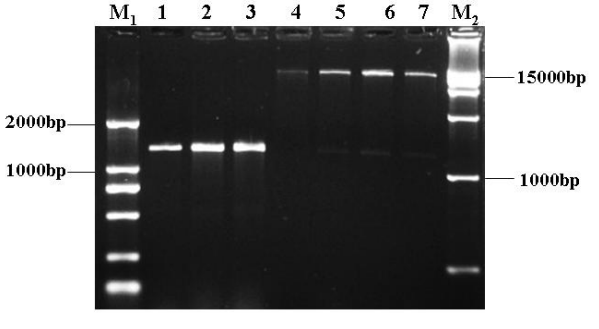

Fig. 4. PCR and restriction enzyme test of pBI121-*AtHsfA2* in *Agrobacterium*. (M_1) DL2000 DNA Marker; (M_2) DL15,000 DNA Marker. (1, 2, 3) PCR test of pBI121-*AtHsfA2*; (4) pBI121 was digested by *Sma* I *and Xba* I; (5, 6, 7) pBI121-*AtHsfA2* was digested by *Sma* I and *Xba* I.

4.1 PCR Detection of Transgenic Plants

The middle part of leaves was used to genomic DNA isolation when the resistance rooting plants grow to 5cm long, and as templates, PCR reaction was perform using specific primers of *NPTII* gene, the result shown, the positive plasmids and transgenic resistant plants were amplified out of about 750bp fragment which is consistent with sequence size of *Kan* gene (Figure 5), while non-transgenic plants is not detected target fragment. Our results also showed that *AtHsfA2* gene had been integrated into the genome of *Chrysanthemum*.

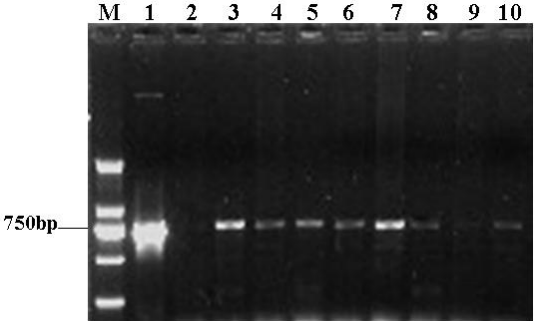

Fig. 5. PCR analysis of transgenic plants. (M) DL2000 DNA Marker. (1)pBI121-*AtHsfA2* Positive control. (2) Negative control . (3-10) Transgenic plants.

4.2 PCR-Southern Detection of Transgenic Plants

A total of four plants identified as positive transgenic plants by PCR-Southern hybridization detection (Figure 6). These results further confirmed *AtHsfA2* gene has integrated into the chrysanthemum genome, while plants with no specific hybridization were not transform successfully.

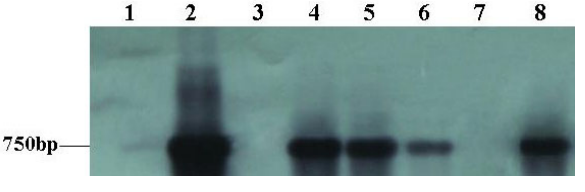

Fig. 6. PCR–Southern test of transgenic plants of *Chrysanthemum*. (1) DL2 000 Marker; (2) Positive control; (3) Negative control; (4, 5, 6, 8) Transgenic plants; (7) False positive plants.

4.3 The Acquisition of Resistant Chrysanthemum Plants

Leaves were infected with *Agrobacterium* after pre-culture, and then the transgenic plants were gained by co-culture, later culture and filter culture (Figure 7). Thick bulge edge of the explants and granular callus formation was can be seen after training 10 days, the explants generated little green bud or become albino or become brown and die after continue culture for 30 days. After cultured for 60 days, resistant differentiated

shoots plants was cut to culturing on rooting selection medium, transgenic plants was taking root while some false-positive plants were not root, and gradually died.

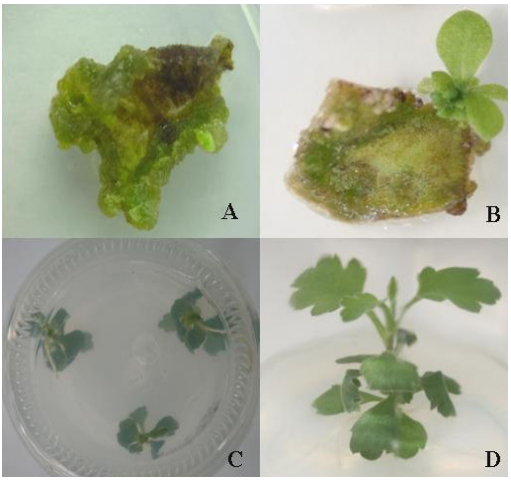

Fig. 7. Growth process of resistant plant of *Chrysanthemum*. (A) Form of G418 resistant callus after cultivating 10 days; (B) Form of G418 resistant buds after cultivating 30 days; (C) Growth conditions and rooting of G418 resistant buds after cultivating 60 days; (D) Growth conditions of resistant plants.

At present, the heat shock transcription factors in animal and plant has been in extensive studied progress (Weng and Hong, 2006; Wu and Xu, 2005). Heat shock transcription factor have been successfully carried out in transgenic experiments of some crops. Tang et al. (2009) has reported heat shock transcription factor 8 (hsf8) gene in the plant expression vector for the receptor of cotyledon node was constructed and hsf8 was transferred into soybean to got a new strain of soybean by *Agrobacterium* conductivity method. Chen et al. (2006) transferred *GmHsfA1* gene into soybean, its over-expression promote activation of downstream 3 heat shock protein gene to transcription or expression and the heat resistant capacity of transgenic soybean plants increased significantly. However, due to the complexity of plant genomes, only some studies about hsfs in some models plant currently. Hsf as a member of stress signal transduction in the regulation network, we have little known about how the regulatory mechanism worked and *AtHsfA2* genetic transformation of ornamental plants has also not been reported.

In summary, we cloned *Arabidopsis thaliana* heat shock transcription factor *HsfA2* gene and it was inserted into the plant expression vector pBI12 successfully, and then pBI-*AtHsfA2* was transferred to *Agrobacterium* LBA4404 by freeze-thaw method. *Chrysanthemum morifolium* Ramat. 'Yurenmian' was to be as the receptor material and using *Agrobaterium*-mediated genetic transformation method, four positive transgenic plants were obtained after antibiotic selection, PCR and PCR-Southern detection. Our results may provide technical references for molecular improvement and increase on the resistance capabilities of ornamental plants.

Acknowledgement. This work is part of a research project supported by the National High Technology Research and Development Program of China “863 project” (Grand No.2008AA10Z156).

References

1. Wang, W., Vinocur, B., Shoseyov, O., Altman, A.: Role of plant heat-shock proteins and molecular chaperones in the abiotic stress response. Trends Plant Sci. 9, 244–252 (2004)
2. Weng, J.Z., Hong, Y.Y.: The roles of plant heat shock transcription factors in abiotic stress. Molecular Plant Breeding 4(1), 88–94 (2006)
3. Wu, Y., Xu, X.L.: Advances in the research of heat stress transcription factors in plants. Natural Sciences Journal of Harbin Normal University 21(3), 73–78 (2005)
4. Sangster, T., Queitsch, C.: The HSP90 chaperone complex, an emerging force in plant development an phenotypic plasticity. Curt. Opin. Plant Biol. 8, 86–92 (2005)
5. Charng, Y.Y., Liu, H.C., Liu, N.Y., Chi, W.T., Wang, C.N., Chang, S.H., Wang, T.T.: A heat-inducible transcription factor, HsfA2, is required for extension of acquired thermotolerance in Arabidopsis. Plant Physiology 1(143), 251–262 (2007)
6. Ayako, N., Yukinori, Y., Eriko, Y., Takanori, M., Kazuya, Y., Shigeru, S.: Arabidopsis heat shock transcription factor A2 as a key regulator in response to several types of environmental stress. The Plant Journal 48, 535–547 (2006)
7. Banti, V., Mafessoni, F., Loreti, E., Alpi, V.A., Perata, P.: The heat-inducible transcription factor HsfA2 enhances anoxia tolerance in Arabidopsis. Plant Physiology 152(3), 147–183 (2010)
8. Chan-Schaminet, K.Y., Baniwal, S.K., Bbulak, D., Nover, L., Scharf, K.D.: Specific Interaction between Tomato HsfA1 and HsfA2 Creates Hetero-oligomeric Superactivator Complexes for Synergistic Activation of Heat Stress Gene Expression. Journal of Biological Chemistry 284(31), 20848–20857 (2009)
9. Li, C.G., Chen, Q.J., Gao, X.Q.: Arabidopsis heat stress transcription factors AtHsfA2 regulate stress genes expression and improve the properties of heat and oxidative stress. Chinese Science C 35(5), 398–407 (2005)
10. Wang, G.L., Fang, H.J.: Plant genetic engineering, pp. 395–397. Science Press, Beijing (2002)
11. Wang, G.L., Fang, H.J.: Plant Genetic Engineering, 2nd edn. Science Press, Beijing (2009)
12. Tang, X.F., Liu, L.J., Gao, M.J.: A grobacterium-mediated transformation of hsf8 into soybean. Molecular Plant Breeding 7(3), 444–450 (2009)
13. Chen, X.J., Ye, C.J., Lv, H.Y.: Cloning of GmHsfA1 gene and its over expression leading to enhancement of heat tolerance in transgenic soybean. Hereditas 28(11), 1411–1420 (2006)

Isolation, Characterization and Sequence Analysis of Resistance Gene Analogs (RGAs) in Plants Related to Huanglongbing(HLB)

Liu Tingting, Yin Youping, Lin Yayu, and Wang Zhongkang

Key Laboratory of Gene Function and Regulation at Chongqing,
College of Bioengineering at Chongqing University, Chongqing 400030, China
xintiing0627@126.com, zkwang646@sina.com

Abstract. Citrus production is seriously affected by HLB to which no resistant plant is available in the cultivated germplasm. Degenerate primers designed based on conserved NBS (nucleotide binding site) motifs contained in some plant resistance genes were used to isolate analogous sequences called resistance gene analogs (RGAs). About xx resistance gene analogs (RGAs) were cloned from several spices related to HLB using PCR method with primers above-mentioned. The BLASTN searches revealed that 43 DNA fragments showed different sequence homology with known plant R-genes or deposited RGAs and 12 sequences could be translated to polypeptides without stop codons. These RGAs and 12 deduced amino acid were analyzed by Clustalx and DNAMAN software. Sequence analysis showed these RGAs contain the conserved domains P-loop, Kinase-2a, Kinase-3a, and HD, which was conserved in NBS-LRR type disease resistance gene. These 12 RGAs shared 37.39%-43.43% identity with the resistance genes of Tobacco*N*、Flax*L6*、Arabidopsis thaliana *RPS2*、*RPS5*、*RPP8*、*RPM1*. Gene duplication followed by sequence divergence were proposed as the mode for the evolution of a large number of distantly or closely related RGA genes in plants, and this mode may play a role in the generation of new resistance specificity and cloning related resistance genes about HLB.

Keyword: Huanglongbing(HLB), Resistance gene analogs(RGAs), NBS conserved region, Degenerate primers.

1 Introduction

Plants defend themselves against pathogens in many sophisticated mechanisms, one of which is the gene-for-gene hypothesis, where resistance (R) genes perform an important role in defense-response initiation [1]. Numerous disease R genes have been cloned and characterized from plenty of plant species either by map-based cloning [2] or transposon tagging [3] since the first R gene *Hml* was cloned. Comparative analysis of these R-genes have shown some conserved amino acid including nucleotide-binding sites (NBS), leucine-rich repeat (LRR), serine/threonine protein kinase (PK) and transmembrane domains (TM) [1]. The largest known R genes so far encode a nucleotide-binding site (NBS) and leucine-rich repeats (LRR) domain. The NBS

E. Zhu and S. Sambath (Eds.): Information Tech. and Agricultural Eng., AISC 134, pp. 835–841.
springerlink.com © Springer-Verlag Berlin Heidelberg 2012

regions of R genes cloned contain several highly conserved motifs such as P-loop, kinase-2, kinase-3a, and GLPL, etc. The P-loop and kinase-2 are responsible for ATP/GTP binding and hydrolysis in defense system [4]. The Kinase-3a and GLPL are part of a putative weak hydrophobic region in R genes. Using PCR method with degenerate primers according to the conserved motifs, a large number of NBS-encoding sequences homology to R genes, so-called ''R gene analogs'' (RGAs), have been successfully obtained from many kinds of plant species such as rice[5]、tabacco[6], potato[7]. Actually, RGAs are rich in plant genome, which provides a facile system to study the evolutionary biology and genetics of NBS-encoding gene family [8].

Huanglongbing (HLB) is one of the most destructive diseases of citrus [9]. HLB affects not only all known citrus species and citrus relatives with little known resistance but other plants. Sweet oranges, mandarins and tangelos were found to be highly susceptible to HLB. Some previous research and field observations of our laboratory revealed that sour orange, grapefruits, murraya paniculata and some commercially important citrus varieties show a little different resistance to HLB [10. 11]. Most of these species are woody perennials with a long generation time and big plant canopy, which makes the classic genetic analysis more difficult and therefore lead to their genomes hardly known [12]. More and more researchers come to realize the importance of molecular genetics. It is reported that tree fruit Genome Database Resources (tfGDR), the Citrus Genome Database will house the genomics, genetics and breeding data for major citrus crops such as orange, grapefruit, mandarin, tangerine, lemon, lime and pummelo. Genome information governs important traits and so will have great potential use in plant breeding.

In this study, using PCR-based strategy with degenerate primers, 43 RGAs were isolated from several plants genome related to HLB. At the same time, we download 14 other RGAs form NCBI. A total of 59 RGAs were collected and used for evolutionary analysis. The phylogeny was comparatively analyzed both on species and genus level, suggesting that gene duplication followed by divergence may have occurred after the radiation of species or genus.

2 Materials and Methods

2.1 Primers and PCR Amplification of RGA Sequences

Five degenerate primers were used in six combinations (Table 1) for PCR amplifications. Primer F1 was based on the sequence GGVGKTT the amino-acid sequence found in the P-loop of *N*, *L6* and *RPS2*; primers R1, R2 and R3 were designed according to the sequence GLPLAL. Total genomic DNA was extracted from leaves of Citrus maxima and Murraya paniculata. PCR reaction was carried out in a volume of 25 µlµl containing 5 $U \cdot \mu L^{-1}$ Taq DNA polymerase (TAKARA, Japan), 10×PCR buffer, 25 $mM \cdot L^{-1}$ $MgCl_2$, 2.5 $mM \cdot L^{-1}$ dNTP, 10 µM of each primer and 20 $ng \cdot \mu L^{-1}$ template DNA. Touchdown-PCR amplification was performed for an initial denaturation at 94°C for 5 min, followed by 20 amplification cycles of 94°C for 30 s, at 0.5°C of 45–55°C for 30 s and 72°C for 30s, and then 30 cycles of 94°C for 30 s, 45°C for 30 s and 72°C for 30s, a final extension step at 72°C for 7 min. The PCR reaction with deionized water as template was used for a negative control.

Table 1. The primers used for the PCR amplification of RGAs

Prime name	Prime sequence 5'- 3'	Conserved amino acid
cquF1	GGDGTDGGNAARACWAC	GGVGKTT(P-loop)
cquF2	GGIGGIRTIGGNAAIACIAC	(L/I/V)LVLDDVW
cquR1	AGIGCHAGNGGNAGNC	GLPLAL
cquR2	AGNGCHAGNGGYAANCC	GLPLAL
cquR3	AANGCHAGNGGYAANCC	GLPLAL

Codes for degenerate positions: W = A/T; R = A/G; H = A/T/C; N = A/T/G/C; Y = C/T; D = A/G/T; V = G/A/C; I = inosine; F: forward orientation; R: reverse orientation.

2.2 RGA Cloning and Restriction Analysis

PCR products were separated on a 1.5% agarose gel, and DNA fragments equal or larger than the expected sizes were recovered for cloning. The purified PCR products were cloned into the plasmid pMD-19 simple vector (TaKaRa, Japan). Plasmid DNA was isolated from randomly selected positive clones and digested overnight at 37 °C with *Rsa* Ⅰ, *Hae*Ⅲ and *Msp* Ⅰ restriction enzymes (Promega, USA). Fragments were separated by electrophoresis on a 2% agarose gel. According to the restriction profiles, clones with a unique restriction profile were selected for sequencing.

2.3 Sequences Analysis

Phylogenetic analysis was executed to evaluate further relationship among these RGAs and plant R genes. Multiple alignments of nucleotide and deduced amino acid sequences were performed using ClustalX [13] and DNAMAN software, and then the output was edited by the GeneDoc software [14]. A phylogenetic tree was constructed with the MEGA4 software. The trees were visualized using the program TREEVIEW.

3 Results and Analysis

3.1 Amplification and Collection of RGA Sequences

Seventy-nine NBS sequences were collected for identification by the below methods: 14 published sequences form NCBI; and 43 sequences isolated by PCR amplifying with degenerate primers (Table 1), fragments of target sizes were amplified from Citrus maxima and Murraya paniculata. The approximately 500 bp band from each primer combination was close to the fragment size expected and therefore these bands were cloned. Restriction analyses showing different restriction patterns of insert fragments were identified and characterized further by sequencing and sequence analysis.

3.2 Sequence and Phylogenetic Analysis

A total of 43 clones which contains 15 from Citrus maxima (accession NO.: HM800469--HM800480), 28 from Murraya paniculata (accession NO.: HM769623--HM769650) were obtained. The BLASTN searches revealed that 43 DNA

fragments showed different sequence homology with known plant R-genes or deposited RGAs, which one clones were highly similar to Helianthus arqophyllus gene, some had no or only very weak similarity to resistance genes. 12 sequences could be translated to polypeptides without stop codons, and they showed strong overall similarities to several plant R-gene sequences. Multiple alignments performed with these RGAs and the three most similar R-gene peptide sequences showed that the similarity was especially high at the three NBS motifs (P-loop, kinase-2, and kinase-3a) (Fig. 1).

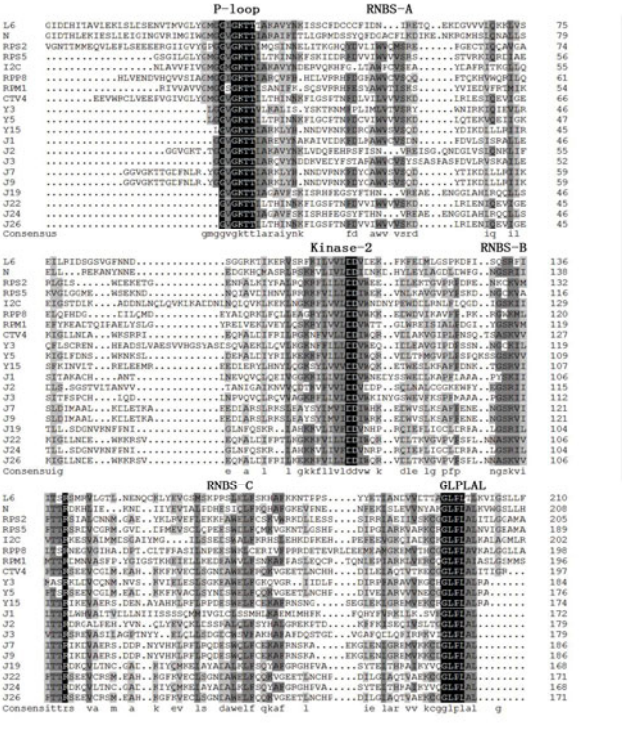

Fig. 1. Alignment of the deduced amino acids of 12 RGA sequences with the NBS domain of eight R genes from the GenBank database using DNAMAN [11]: Tobacco *N* (U15605), Flax *L6* U27081), Arabidopsis thaliana *RPS2* (U14158), *RPM1* (AAF27008), *RPP8* (AF089710), and *RPS5* (AF074916),Tomato *I2C* (AF004878),*CTV4*(AAN62348.1). Conserved amino acids such as the P-loop, Kinase - 2, GLPL motifs are highlighted.

57 sequences include 15 from Citrus maxima, 28 from Murraya paniculata and 14 from NCBI was used for phylogenetic trees construction. The deduced amino acid sequences of the 12 RGAs and 3 known NBS-LRR resistance proteins from other plant species were pooled for a protein phylogenetic analysis. Tree construction and bootstrap tests were carried out as described previously. The result of neighbor-joining phylogenetic tree was shown in Fig. 2.

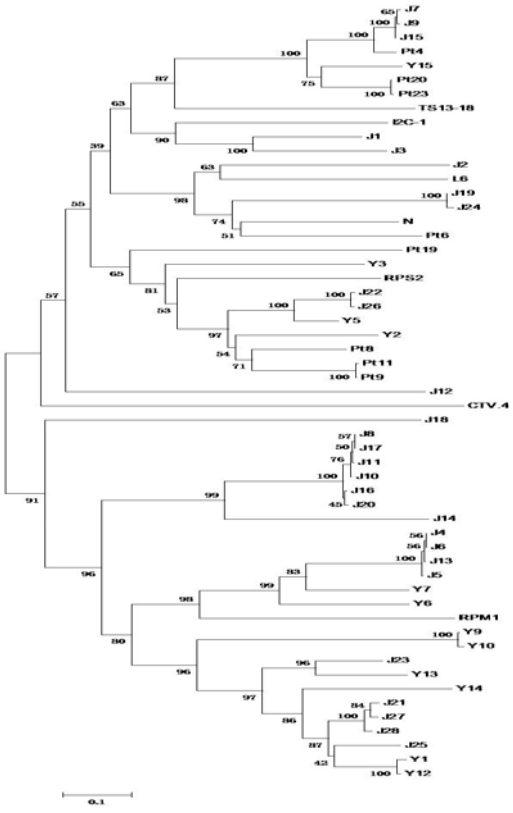

Fig. 2. Phylogenetic comparison of Citrus maxima, Murraya paniculata RGAs. Sequences were aligned using ClustalX, and the tree was generated using the neighbor-joining method. Bootstrap values (1000 replicates) with only values >50% were shown on the branches.

4 Discussion

RGAs have been successfully isolated from many plants using PCR amplification with degenerate primers based on the conserved motifs of known plant R-genes. While no molecular cloning of putative R genes from plants related to HLB has yet been reported, the objective of this study is to isolate and characterize RGAs from plants related to HLB and to evaluate their diversity and phylogenetic relationships. The relation of RGAs to plant R-genes may have three categories: (1) RGAs are actual R-genes. For example, the full-length cDNA of the soybean R-gene KR1 was cloned using an RGA fragment as a hybridization probe to screen a cDNA library [15]; (2) RGAs are linked to plant R-genes, for instance, NBS-encoding RGAs of sunflower are linked to down mildew-resistant locus P15/P18 [16], and three RGA sequences were shown to be co-segregated with wheat rust resistance gene [17]; (3) RGAs are not functionally related to R-genes. This result may be depended on our choice to the primers or the limited in number of RGAs sequenced as well.

Meyers et al. [18] analyzed the NBS domains of the plant NBS-LRR class R genes and a large number of RGAs and found that they could be classified into either TIR (Toll/Interleukin-1 receptor homology) or non-TIR groups. In their analysis, *N* and *L6* belong to the TIR group, while *RPS2*, RPM1 and I2C-2 fall into the non-TIR group. Our data indicate that J2, J19 and J14 formed a major cluster with *N* and *L6*, and they have an aspartic acid residue (D or N) at the final residue position of the kinase-2 motif that is often seen in the TIR group. Most of citrus RGAs were clustered with *RPS2* and have a tryptophan residue (W), indicating that they might belong to the non-TIR group. Attempts are being made to obtain the upstream sequence information; when this becomes available, it should assist in the classification of these citrus RGAs regarding TIR or non-TIR grouping.

Most cloned plant R-genes encode proteins with the NBS region, which is required for ATP or GTP binding. However, genes involved in development process and other signal transduction pathways not relevant to plant disease resistance also encode proteins containing a conserved NBS region [19]. Likewise, apart from their role in plant disease resistance, genes encoding kinases also function in other aspects of plant physiology. The isolation of RGAs will provide valuable resources for further clarifying the molecular mechanism of HLB resistance.

References

1. Dangl, J.L., Jones, J.D.G.: Plant pathogens and integrated defence responses to infection. Nature 411, 826–833 (2001)
2. Dixon, M.S., Hatzixanthis, K., Jones, D.A., Harrison, K., Jones, J.D.G.: The tomato Cf-5 disease resistance gene and six homologs show pronounced allelic variation in leucine-rich repeat copy number. Plant Cell 10, 1915–1925 (1998)
3. Anderson, P., Lawrence, G., Morrish, B., Aylife, M., Finnegan, E., Ellis, J.: Inactivation of the Xax rust resistance gene M associated with the loss of a repeated unit within the leucine-rich repeat coding region. Plant Cell 9, 641–651 (1997)
4. Belkhadir, Y., Subramaniam, R., Dangl, J.L.: Plant disease resistance protein signaling: NBS-LRR proteins and their partners. Curr. Opin. Plant Biol. 7, 391–399 (2004)
5. Zheng, X., Cui, W., Li, X.: NBS-LRR disease resistance analogues of Rice Varieties. Science in China 31(1), 43–51 (2001)
6. Gao, Y., Xu, Z., Jiao, F., Yu, H., Xiao, B., Li, Y., Lu, X.: Cloning, structural features, and expression analysis of resistance gene analogs in Tobacco. Mol. Biol. Rep. 37, 345–354 (2010)
7. Brugmans, B., Wouters, D., van Os, H., et al.: Genetic mapping and transcription analyses of resistance gene loci in potato using NBS profiling. Theor. Appl. Genet. 117, 1379–1388 (2008)
8. Meyers, B.C., Dickerman, A.W., Michelmore, R.W., Sivaramakrishnan, S., Sobral, B.W., Young, N.D.: Plant disease resistance genes encode members of an ancient and diverse protein family within the nucleotide-binding superfamily. Plant J. 20, 317–332 (1999)
9. Bove, J.M., Huang, L.: A destructive, newly-emerging, century-old disease of citrus. Plant Pathol. 88(1), 7–37 (2006)
10. Nariani, T.K.: Integrated approach to control citrus greening disease in India. Proc. Int. Soc. Citricult. 1, 471–472 (1981)

11. Miyakawa, T.: Experimentally-induced symptoms and host range of citrus likubin (greening disease). Annu. Phytopathol. Soc. Jpn. 46, 224–230 (1980)
12. Dirlewanger, E., Graziano, E., Joobeur, T., Garriga-Caldere, F., Cosson, P., Howad, W., Arus, P.: Comparative mapping and markerassisted selection in Rosaceae fruit crops. Proc. Natl. Acad. Sci. 101, 9891–9896 (2004)
13. Thompson, J.D., Gibson, T.J., Plewniak, F., Jeanmougin, F., Higgins, D.G.: The CLUSTAL_X windows interface: flexible strategies for multiple sequence alignment aided by quality analysis tools. Nucleic Acids Res. 25, 4876–4882 (1997)
14. Nicholas, K.B., Nicholas Jr., H.B., Deerfield II, D.W.: GeneDoc: analysis and visualization of genetic variation. EMBnet News 4, 14–17 (1997)
15. He, C.Y., Tian, A.G., Zhang, J.S., Zhang, Z.Y., Gai, J.Y., Chen, S.Y.: Isolation and characterization of a full-length resistance gene homolog from soybean. Theor. Appl. Genet. 106, 786–793 (2003)
16. Radwan, O., Bouzidi, M.F., Vear, F., Philippon, J., De Labrouhe, D.T., Nicolas, P., et al.: Identification of non-TIR-NBS-LRR markers linked to the Pl5/Pl8 locus for resistance to downy mildew in sunflower. Theor. Appl. Genet. 106, 1438–1446 (2003)
17. Yan, G.P., Chen, X.M., Line, R.: Resistance gene-analog polymorphism markers co-segregating with the Yr5 gene for resistance to wheat stripe rust. Theor. Appl. Genet. 106, 636–643 (2003)
18. Meyers, B.C., Dickerman, A.W., Michelmore, R.W., Sivaramakrishnan, S., Sobral, B.W., Young, N.D.: Plant disease resistance genes encode members of an ancient and diverse protein family within the nucleotide-binding superfamily. Plant J. 20, 317–332 (1999)
19. Shirasu, K., Schulze-Lefert, P.: Regulators of cell death in disease resistance. Plant Mol. Biol. 44, 371–385 (2003)

Quantum Yields in Photolyses of Mammalian Carboxy-Hemoglobin Studied by Pulsed Laser Pump-Probe Technique

Jin-yu Zhao[1], Min Qu[1], Jia-huang Li[2], Zheng Zhang[3], Shu-yi Zhang[1,*], Yue-tao Yang[1], and Zi-chun Hua[2]

[1] Laboratory of Modern Acoustics, Institute of Acoustics, Nanjing University, Nanjing, 210093, China
[2] Laboratory of Pharmaceutical Biotechnology, Institute of Life Science, Nanjing University, Nanjing, 210093, China
[3] Nanjing First Hospital, Attached to School of Medicine, Nanjing University, Nanjing, 210006, China
zhangsy@nju.edu.cn

Abstract. The mechanisms describing the cooperative binding of CO or other ligands to hemoglobins (Hb) has been widely studied as an important fundamental problem for a long time. In this paper, the quantum yields in photolyses of carboxy-hemoglobins (HbCO) of mammals, such as human, pig, bovine, horse and rabbit, are investigated by the optical pump-probe technique. In the technique, the HbCO of the mammals are irradiated by a pulsed laser beam, and then the HbCO is photo-dissociated. Another continuous optical beam is used as a probe beam to detect the absorbance change induced by the photo-dissociation of the HbCO. The measured results show that the photolysis quantum yields of the HbCO are different for varies mammals, among them the quantum yields for porcine, bovine and equine HbCO are very close, but for the HbCO of rabbit, which is much smaller than the others. Finally, the results are analyzed and discussed.

Keywords: carboxy-hemoglobin, photolysis, quantum yield, optical pump-probe technique.

1 Introduction

Hemoglobin (Hb) as the allosteric protein, in photo-dissociations of liganded Hbs has been studied widely [1-5]. With the development of time-resolved photoacoustic calorimetry (PAC), enthalpy and conformational volume changes in photoinduced ligand dissociations can be directly measured [6-9].

The quantum yield of photo-dissociation is the efficiency of the transfer from the reactants to the products generated by light irradiation. As a very sensitive parameter, it may easily be affected by the experimental conditions including temperature, pressure, density and pH state, etc. [10-13]. Hoshino et al. have studied carefully on the photolysis of chemical complexes, and described a theoretical model [14].

E. Zhu and S. Sambath (Eds.): Information Tech. and Agricultural Eng., AISC 134, pp. 849–856.
springerlink.com © Springer-Verlag Berlin Heidelberg 2012

In this paper, the optical pump-probe technique is used to study the photo-dissociation of five mammalian HbCO solutions, including the HbCO of human, bovine, pig, horse and rabbit. The quantum yields of the photo-dissociation of the HbCO for these mammalian species are obtained, and the differences of them are also analyzed and discussed.

2 Experimental Principle and Method

2.1 Quantum Yield Calculation

The quantum yield Φ is defined as the molecular number of photoproduct species divided by the absorbed photon number, which can be measured by the optical pump-probe technique. In the technique, the HbCO solution of the mammals is irradiated by pumping laser beam with the wavelength Λ, and another optical beam with the wavelength λ is used as a probe beam to detect the absorbance change before and after laser pulse illuminating HbCO.

Thus, the yield Φ is formulated by [14]:

$$\Phi = \Delta D^{\lambda} / (qdE\rho\varepsilon^{\Lambda}\Delta\varepsilon^{\lambda}), \tag{1}$$

where ΔD^{λ} and is the absorbance change induced by the photolysis, which is measured by before and after laser pulse illuminating HbCO at the probing light wavelength λ, q, d and E are the irradiated area, optical path length and energy of the solution by the pumping laser pulse respectively, ρ is the density of the HbCO solution, ε^{Λ} is the molar absorption coefficient by HbCO at pumping laser wavelength Λ, $\Delta\varepsilon^{\lambda}$ is the difference in the molar absorption coefficient between Hb and HbCO at the probing light wavelength λ.

In the experiments, if taking a solution with the recognized quantum yield Φ_0 as a standard, and adjust the q, d, E, ρ and ε^{Λ} of the measured solutions to be the same data as that of the standard solution, then the quantum yield Φ of the measured solution can be obtained by:

$$\Phi = (\Delta D^{\lambda}\Phi_0\Delta\varepsilon_0^{\lambda}) / (\Delta D_0^{\lambda}\Delta\varepsilon^{\lambda}), \tag{2}$$

where the subscript $_0$ represent the standard solution.

2.2 Experimental Method and Sample

1) Apparatus and method: Based on the optical spectra of the Hb and HbCO shown in Fig. 1, The pumping beam is chosen at the wavelength 532 nm, where the absorption coefficients of Hb and HbCO are the same, and the probing beam is at 432 nm, where the difference of optical densities between carboxy- and deoxy-Hb is the biggest and also sufficiently away from the wavelength of the pumping beam.

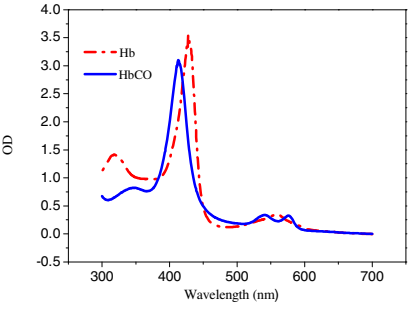

Fig. 1. Optical density spectra of Hb and HbCO in buffer at pH 7.0

Then the experimental system is shown in Fig. 2. A Nd:YAG laser operating at wavelength 532 nm, frequency 10 Hz and pulse width 8 ns is used as the excitation source. The pulsed-laser beam is divided into two beams, one is focused by a cylindrical lens onto the sample cuvette as the pump beam, the other is directed into a monitoring pulse ergometer. At the same time, a continuous laser beam as the probe beam is directed through the sample perpendicular with the pump beam. Then the probe beam is received by a photomultiplier. A digital oscilloscope records the data for further processing and analyzing by a computer. Meanwhile, $\Delta\varepsilon^{\lambda}$ and $\Delta\varepsilon^{\lambda}{}_{0}$ are obtained from the absorption differences of Hb and HbCO measured for the sample and standard solutions with the UV-3100 Spectrophotometer (Shimadzu, Japan), respectively. All the experiments are taken at 20°C.

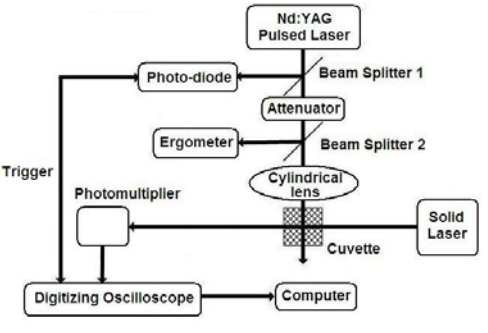

Fig. 2. Experimental setup of optical pump-probe technique

2) Samples: The samples are all lyophilized Hb powders, in which human, porcine, equine and lapine Hbs are made by Sigma Co., USA, and that of bovine is made by Sinopharm Chemical Reagent Co., Ltd, China. The powders are dissolved in 50 mM phosphate buffer at pH 7.0, and then reduced with sodium dithionate ($Na_2S_2O_4$). The HbCO samples are got by bubbling CO through the solutions for about 20 minutes.

3 Results

CO is dissociated from the HbCO when the laser pulse is irradiating on the solution, but it then rebinds to the HbCO in the dark duration. As examples, the measurement results of human and rabbit are shown in Fig. 3. Using $Aexp(-t/\tau)$ to fit the rebinding process, where A is in proportion to the absorbance change ΔD^{λ}, and τ is the ligand rebinding relaxation time.

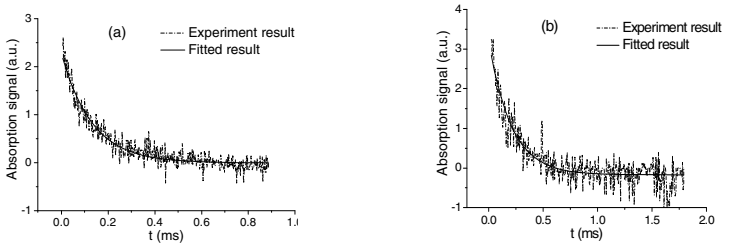

Fig. 3. Time-resolved absorption spectra obtained in HbCO at 432 nm and 20 °C: (a) human; (b) rabbit

In the experiments, changing the pumping energy E for the samples of the five species, the A VS E can be obtained as shown in Fig. 4. The slopes are proportional to the quantum yields. Taking the quantum yield of the photolysis of human HbCO of 0.52 at 20°C as the standard [15], the quantum yields of bovine, porcine, equine and lapine HbCO can be obtained and listed in Table 1.

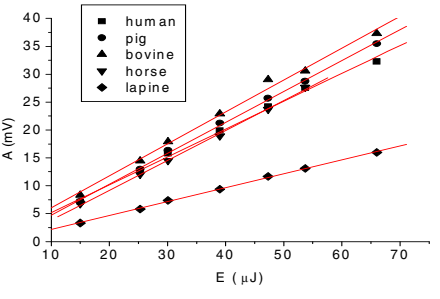

Fig. 4. A versus E of five mammals

Table 1. Quantum yield of HbCO

Sample	$\Delta D_m/\Delta D_0$	M*	$\Delta\varepsilon_m/\Delta\varepsilon_0$	Φ
Human	1	61987.16	1	0.52
Bovine	1.144 ± 1%	62015.14	0.981 ± 3%	0.61 ± 4%
Pig	1.114 ± 1%	62006.84	0.918 ± 2%	0.63 ± 3%
Horse	1.046 ± 1%	62245.14	0.918 ± 2%	0.59 ± 3%
Rabbit	0.502 ± 1%	62917.92	0.828 ± 2%	0.32 ± 3%

M*: Molecular weight

4 Discussions

From Table 1, it can be seen that the quantum yields of HbCO of bovine, pig and horse are very close, but different from that of human and rabbit. The amino acid sequences, the hydrogen bonds, salt bridges and tetramer structures of different Hbs are considered to explain the differences.

1) All of the amino acid sequences of Hbs of five species are taken from swiss-prot, and using GeneDOC program to compare them as shown in Fig. 5. It shows that the Hbs have above 80% sequence identity to each other, but still have 18 variant residues of 141 amino acid residues in α globin chains and 18 of 146 in β globin chain. Most of the different positons are on the surface of the protein and exposed to solvents, so the differences are easily to be displayed. The variant fragments of residues are 111-120 in α-chains and 115-118 in β-chain [16-19].

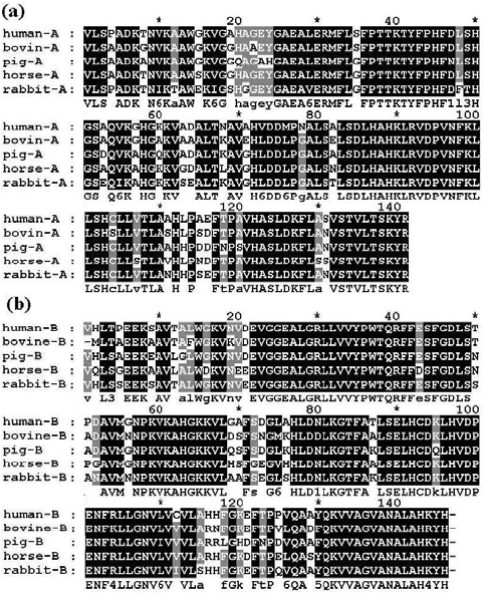

Fig. 5. The alignments of the sequences of Hb from human, bovine, horse, pig and rabbit. The amino acid identities are shown in black and the relevant amino acid similarities are indicated by gray: (a) α chains; (b) β chains.

2) As one kind of molecule forces in HbCO, the different hydrogen bonds exist in different mammals, which have important allostric effectors and considerable influences on the dynamics in photo-dissociations of liganded Hbs. Analyzing subunit interfaces of five HbCO shown in Fig. 6, It is clear that the hydrogen bonds formed at the α1-β1 and α1-β2 interfaces have differences in the different mammals. Due to the hydrogen bonds formed at the α1-β1 interfaces shown in Fig. 6(a) have been described in our former work [14], the hydrogen bonds formed at the α1-β2 interfaces shown in Fig. 6(b) are described as follows:

The hydrogen bond α1Thr41 – β2Arg40 appears in human, porcine and equine HbCO, besides α1Asp94 –β2Asn102 appears in human and bovine, α1Arg141 – β2Gln39 in porcine, α1Arg92 – β2Asp43 and α1Arg141 – β2Leu48 in equine. At these interfaces, only one hydrogen bond α1Arg141 – β2Leu48 exists in lapine, and it is far away from the heme plane shown in Fig. 6(b) and do not influence the active site directly. Therefore the hydrogen bonds exist in different mammals are obvious differences, especially in the lapine HbCO.

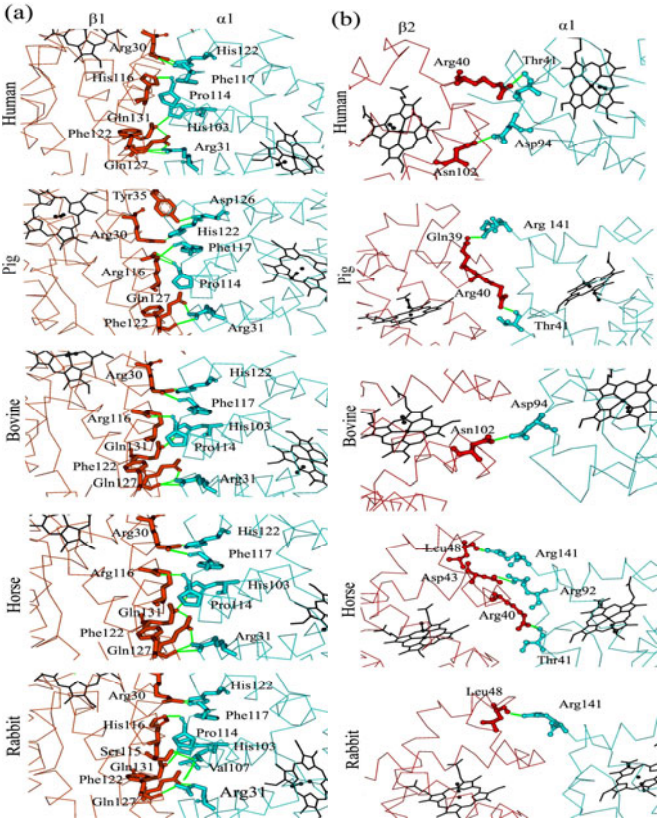

Fig. 6. Hydrogen bond (green) and haem(black) in HbCO of five species: α1(cyan)-β1(red); (b) α1(cyan)-β2(red).

3) Salt bridge is another kind of molecule force in HbCO as listed in Table 2, two salt bridges across the αβ interface appear in the lapine HbCO, and only one appears in the equine. In the bovine HbCO, there is one salt bridge across the αα interface. None salt bridge appears in the HbCO of human and pig.

4) The structures of the five mammalian HbCO are compared using X-ray crystallographic ananlyses and Insight II (Accelrys, San Diego, USA) [16-19], the superposition of the tetramer structures displays that some differences exist among them although they are mainly similar to each other. Especially in the lapine HbCO at the active sites in β-chain, the differences are obvious.

Generally, the amino acid sequences of Hb, hydrogen bonds, salt bridges formed and the tetramer structures of HbCO may be the main factors to affect the differences of the quantum yields among the five mammals.

Table 2. Salt-bridges across subunits

Bovine	Horse	Rabbit
α1Asp6-α2Arg141		
	α1Arg92- β2Asp43	α1Arg92-β2Glu43
		α1Lys99-β1Glu101

5 Conclusion

The optical pump-probe technique is used to obtain the quantum yields of the photo-dissociation of five mammalian HbCO including the HbCO of human, pig, bovine, horse and rabbit. The results show that the quantum yields among the five mammals are different from each other, although the data are very close among bovine, pig and horse, but the data of the lapine HbCO is much smaller. To explain the differences, some analyses and discussions on the differences of the amino acid sequences, the hydrogen bonds, salt bridges and the tetramer structures among the five mammals are presented. However, the mechanisms of the quantum yields differences among the mammalian HbCO are still not very clear because of the complexation of the hemoglobin structures, which need to be studied in more details.

Acknowledgement. This work is supported by National Natural Science Foundation of China, No. 11074125.

References

1. Gibson, Q.H.: An Appratus for Flash Photolysis and its application to The reactions of myoglobin with gases. The Journal of Physiology 134, 112–122 (1956)
2. Noe, L.J., Eisert, W.G., Rentzepis, P.M.: Picosecond photodissociation and subsequent recombination processes in carbon monoxide hemoglobin. Proceedings of the National Academy of Sciences, USA 75, 573–577 (1987)
3. Ghelichkhani, E., Goldbevk, R.A., Lewis, J.W., Kliger, D.S.: Nanosecond time-resolved absorption studies of human oxyhemoglobin photolysis intermediates. Biophysical Journal 71, 1596–1604 (1996)
4. Esquerra, R.M., Goldbeck, R.A., Reaney, S.H., Batchelder, A.M., Wen, Y., Lewis, J.W., et al.: Multiple geminate ligand recombination in human hemoglobin. Biophysical Journal 78, 3227–3239 (2000)
5. Kuzmin, V.V., Salmin, V.V., Salmina, A.B., Provorov, A.S.: Study of photodissociation of parameters of carboxyhemoglobin with laser flash-photolysis. Quantum Electronics 38(7), 695–701 (2008)
6. Peters, K.S., Watson, T., Logan, T.: Photoacoustic calorimetry study of human carboxy hemoglobin. Journal of the American Chemical Society 114(11), 4276–4278 (1992)

7. Chen, H., Sun, L., Li, G., Zhang, S.Y., Chen, H.L.: Laser-induced time-resolved photoacoustic calorimetery study on photo-dissociation of human and bovine oxyhemoglobin. Biochemical and Biophysical Research Communication 319, 157–162 (2004)
8. Yang, N.L., Zhang, S.Y., Sun, L., Qu, M., Shui, X.J., et al.: Photo-dissociaton of Oxy-hemoglobins by Pulsed Photoacoustic Calorimetry. Journal of Nanjing University (Natural Sciences) 43(1), 73–78 (2007) (in Chinese)
9. Qu, M., Li, J.H., Zhang, S.Y., Shui, X.J., Hua, Z.C.: Photolyses of mammalian Carboxy-hemoglobin studied by time-resolved photoacoustic calorimetry. Acta Acustica 33(5), 425–429 (2008) (in Chinese)
10. Noble, R.W., Brunori, M., Wyman, J., Antonini, E.: Studies on the Quantum yields of the photodissociation of carbon monoxide from hemoglobin and myoglobin. Biochemistry 6(4), 1216–1222 (1967)
11. Morris, R.J., Gibson, Q.H.: The apparent quantum yield of T-state human hemoglobin. Contribution of protein and heme to rates of oxygen reactions. The Journal of Biological Chemistry 259(1), 365–371 (1984)
12. Camnron, R.T., Zhu, X.R., Harris, J.M.: Evaluating rates and yields of second-order, photoinitiated reaction under condition of Gaussian-profile excitation. Journal of Physics and Chemistry 98, 8726–8733 (1994)
13. Fu, S.W., Luo, L.B., Chen, H.L., Wu, Z.S., Zhang, S.Y.: Quantum yields of photolyses of coenzyme B12 investigated by photoacoustic calorimetry. Acta Physico-chimica Sinica 13(3), 193–195 (1997) (in Chinese)
14. Hoshino, M., Ozawa, K., Seki, H., Ford, P.C.: Photochemistry of Nitric Oxide Adducts of Water-Soluble Iron(III) Porphyrin and Ferrihemoproteins Studied by Nanosecong Laser Photolysis. Journal of the American Chemical Society, vol 115, 9568–9575 (1993)
15. Saffran, W.A., Gibson, Q.H.: Photodissociation of ligands from heme and heme proteins. Effect of temperature and organic phosphate. The Journal of Biological Chemistry 252, 7955–7958 (1977)
16. Paoli, M., Liddington, R., Tame, J., Wilkinson, A., Dodson, G.: Crystal structure of T state haemoglobin with oxygen bound at all four haems. Journal of Molecular Biology 256, 775–792 (1996)
17. Safo, M.S., Abrahum, D.J.: The X-ray structure determination of bovine carbonmonoxy hemoglobin at 2.1 resoultion and its relationship to the quaternary structures of other hemoglobin crystal forms. Protein Science 10(6), 1091–1099 (2001)
18. Lu, T.H., Panneerselvam, K., Liaw, Y.C., Kan, P., Lee, C.J.: Structure determination of porcine haemoglobin. Acta Crystallogr D56, 304–312 (2000)
19. Shibayama, N., Miura, S., Tame, J.R.H., Yonetani, T., Park, S.Y.: Crystal structure of horse carbonmonoxy hemoglobin-bezafibrate complex at 1.55-A° resolution. The Journal of Biological Chemistry 277(41), 38791–38796 (2002)

Chromosomal Heterozygosity of Knob-Associated Sequences in Maize Inbred Line Zi330

Fei Yang[1] and Yanho Xu[2]

[1] Department of Molecular Biology
College of Medicine, Yangtze University
Jingzhou, 434023, China
[2] Department of Genetics and Breeding
College of Agriculture, Yangtze University
Jingzhou, 434023, China
yfwhu@163.com, xyh09@yangtzeu.edu.cn

Abstract. Two classes of knob-associated sequences, 180-bp repeat unit and TR-1 element，were located on chromosomes of maize (Zea mays) inbred line Zi330 by fluorescence in situ hybridization (FISH). In Zi330, knob-associated sequences were just present in one chromosome 1 but absent in another homologous chromosome 1. And in this line we also observed the positional change of these knob-associated sequences on homologous chromosomes 2, which revealed the inversion of these two knob-associated sequences. This genetic behavior was akin to the characteristic of retroelements. These variations of distribution and heterozygosity were discussed in this paper.

Keywords: knob-associated sequences, fluorescence in situ hybridization, chromosomal heterozygosity.

1 Introduction

Knobs were heavily stained and cytologically distinguishable heterochromatin regions located in a number of different chromosomal sites in maize, especially on the pachytene of meiosis [1]. McClintock found 10 chromosomes had 23 knob heterochromatin sites [2]. The polymorphism of distribution made the knob become an important landmark of chromosome change and reorganization, and an essential proof of maize evaluation [2]. Knob heterochromatins were related with the frequency of recombination, meiotic drive and flowering time [3].

In 1981, Peacock et al [4]. isolated a highly repeated 180-bp sequence within the maize knobs. In situ hybridization analysis showed a correlation between knob size and the 180-bp repeat content [5]. Another 350-bp tandem repeat (TR-1), which was associated with knob regions, was isolated from a maize chromosome 9 alien addition line of oat (Avena Sativa L.) [6]. Short stretches of DNA sequences between the 180-bp and TR-1 units that showed some level of homology indicated TR-1 units might have evolved from the 180-bp repeat as the result of a duplication and subsequent

E. Zhu and S. Sambath (Eds.): Information Tech. and Agricultural Eng., AISC 134, pp. 843–847.
springerlink.com © Springer-Verlag Berlin Heidelberg 2012

divergence [7-8]. Other reteroelements were also isolated from knob regions with low contents, including RE-10, Zeon, Grande PREM2 and RE-15 [7]. However, a low amount of the 180-bp repeats might exist in some euchromatic sites [8].

FISH is a powerful technique to investigate the sequence distribution on chromosome and the chromosomal rearrangement in cell. The 180-bp repeat and the TR-1 element were tandem repeated DNA sequences, which can be regarded as valuable chromosome landmarks for the identification of chromosomes and analysis of changes of chromosome structures. The previous work showed that the locations of the two repeated DNA sequences were not fully correlated with the appearance of knobs on chromosomes [9].

Sadder [10] used TR-1 repeat, 180-bp repeated sequence and centromere sequence as probes to construct karyotype and identify the chromosome. Using knob-associated sequence and much sequences as probes, Kato [11] completed the chromosome painting model in maize. So as the significant lander-marker of maize chromosome, knob-associated sequences were conducted in cytology. Knob was contributed to many retroelements and gave a hypothesis that the knob was a complex megatransposon, but the hypothesis need much more research to prove [7]. To further investigate the nature of knob DNA variability, we used TR-1 repeat and 180-bp repeating units as FISH probes to analyze chromosomal distribution of these two tandem repeat elements in the maize inbred line Zi330, which were widely used in China as the major inbred lines.

2 Materials and Methods

2.1 Plant Material

The standard maize inbred line Zi330 used in this study. Seeds were kindly provided by professor Gu Ming-guang, institute of genetics, CAS.

2.2 Chromosome Preparations and Probe Labeling

Mitotic chromosome preparation was performed using the outline protoplast technique as Li and Arumuganathan [12]. A dimmer of 180-bp repeat, ZmKR180-2 and a monomer of TR-1 repeat, ZmKR350-1 [9] were kindly provided by Dr. Rachel Wang at University of California-Berkeley. ZmKR180-2 and ZmKR350-1 were labeled respectively with digoxin and biotin using a nick translation method.

2.3 Fluorescence in Situ Hybridization and Detection

Fluorescence In situ hybridization and signial decttion were carried out using the procedure described by Li and Arumuganathan [12]. The hybridization mixture(40μl) contained 50% deionized formamide, 10% sodium dextran sulphate, 2×SSC, 1mg/ml salmon sperm DNA, 30ng probe, denatured at 75℃ for 5 min, and then chilled on ice for 5 min. Hybridization was performed overnight at 37℃.

Biotin-labled probes were detected in a three-step detection /amplification: stretavidin-Cy3 (Vector Laboratories, Burlingame, CA, USA), biotinlated anti-streptavidin

(Vector Laboratories, Burlingame, CA, USA) and strepavidin-Cy3 (Vector Laboratories, Burlingame, CA, USA). Digoxigenin-labled probes were detected with sheep-anti-digoxigenin-FITC (Roche Molecular Biochemical) and amplified with rabbit-anti-sheep-FITC (Vector Laboratories, Burlingame, CA, USA). For each step of immune reaction, slides were placed in a wet chamber at 37℃ for 1h and washed with PBS, three times, each for 5min. Chromosomes were counterstained with 1μg/ml DAPI(4', 6-diamidino-2-phenylin-dole) in Vectashield (Vector Laboratories, Burlingame, CA, USA, Burlingame, CA, USA).

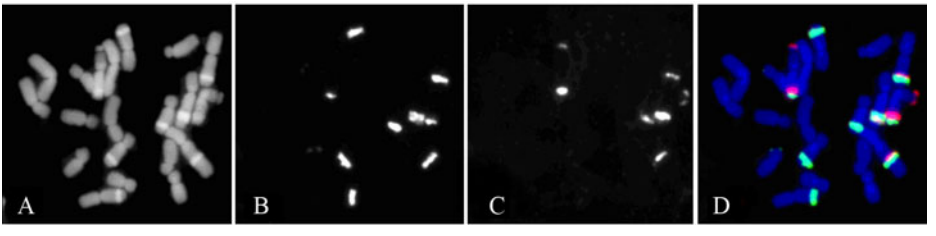

Fig. 1. FISH analyses of the 180-bp and TR-1 repeats in five maize lines. The 180-bp repeat is detected by a green color and the TR-1 by a red color. The yellow signal was due to the overlap of the red and green colors. (A) maize metaphse chromosomes, (B) signals of 180-bp repeat, (C) signals of TR-1 element, (D) combine of the chromosomes and the signals. (Scale bar, 10μm.)

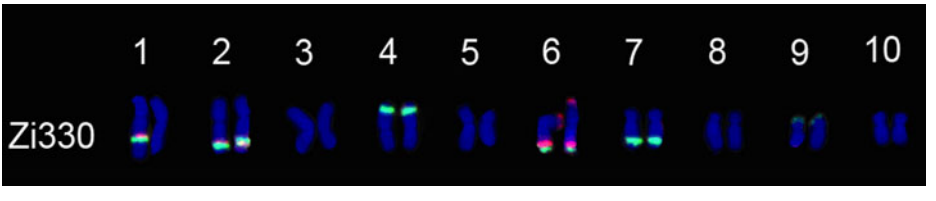

Fig. 2. The somatic karyotype of five inbred lines probed with knob-associated sequences. The chromosome was shown in blue, the 180-bp repeat is shown in green, and the TR-1 repeat is shown in red. (Scale bar, 10μm.)

Chromosomes and signals were visualized using an Olympus BX60 fluorescence microscope system (equipped with a Metamorph 4.6.3, Universal Imaging Crop.) and gray scale image were captured with a cooled CCD camera Sensys 1401E using the appropriate filter for each fluorescent channel and then processed with Photoshop 8.0.1 software.

3 Results and Discussion

The 180-bp repeat and the TR-1 element were labeled respectively with digoxin and biotin, and FISH was performed simultaneously with both labeled probes on the same microscopic slide. Hybridization signals detected from probes were reproduced in at least three independent experiments, each comprising 5-10 slides of chromosome

preparations. On each slide, 30-79 spreads of mitotic metaphase chromosomes were analyzed. Signals were observed in 80-90% of the chromosomes.

In this study, we observed heterozygosity two pairs of homologous chromosomes in Zi330. Zi330 is a stable inbred lines and one of the major commercial inbreds. However, the hybridization signals of the knob-associated sequences one homologous chromosome of the chromosome 1and 2 (Figure 2) were not pure. Considering the FISH sensitivity of somatic chromosomes, the absence of knob-associated sequences in a chromosome 1 may attribute to deletion or the low copy of tandem sequences, which the FISH cannot detect in somatic cell. Chromosome 1 is heterozygous for a large knob locus, this phenomenon reflect that in the homologous chromosome the copy of the knob-associated sequences were largely different.

And the FISH signals were not the same on two homologous chromosomes of chromosomes 2 (Figure 2). Considering Zi330 is being inbred, in the process of inbreeding, allelic heterozygosis difficultly remained from one generation to another. Although the theory of a balanced lethal system could explain this phenomenon, this almost certainly can not be the case in an inbred line that shows full fertility. So, the inversion of TR1 and 180-bp repeats on two homologous chromosomes of chromosomes 2 probably resulted from sequences moving away from their original location through chromosome breakage [13], or transposition of Knob tandem repeats [3, 7]; or transposition of retrotransposons [7]. The divergence of knob-associated sequences on homologous chromosome proved the hypothesis that maize knobs might be considered as a complex megatransposons and knob polymorphism might be explained as the result of molecular rearrangements and transpositions of entire knob regions or their parts [7].

References

1. McClintock, B.: Chromosome morphology in Zea mays. Science 69, 629 (1929)
2. McClintock, B., Kato, Y., Blumenshein, A.: Chromosome Constitution of Races of Maize. Chapingo, Mexico, Colegio de Postgraduados (1981)
3. Buckler IV, E.S., Phelps-Durr, T.L., Buckler, C.S., Dawe, R.K., Doebley, J.F., Holtsford, T.P.: Meiotic drive of chromosomal knobs reshaped the maize genome. Genetics 153, 415–426 (1999)
4. Dennis, E.S., Peacock, W.J.: Knob heterochromatin homology in maize and its relatives. J. Mol. Evol. 20, 341–350 (1984)
5. Ananiev, E.V., Phillips, R.L., Rines, H.W.: Complex structure of knob DNA on maize chromosome 9: retrotransposon invasion into heterochromatin. Genetics 149, 2025–2037 (1998)
6. Ananiev, E.V., Phillips, R.L., Rines, H.W.: A knob-associated tandem repeat in maize capable of forming fold-back DNA segments: are chromosome knobs megatransposons? Proc. Natl. Acad. Sci. U.S.A. 95, 10785–10790 (1998)
7. Hsu, F.C., Wang, C.J., Chen, C.M., Hu, H.Y., Chen, C.C.: Molecular characterization of a family of tandemly repeated DNA sequences, TR-1, in heterochromatic knobs of maize and its relatives. Genetics 164, 1087–1097 (2003)
8. Viotti, A., Privitera, E., Sala, E., Pogna, N.: Distribution and clustering of two highly repeated sequences in the A and B chromosomes of maize. Theor. Appl. Genet. 70, 234–239 (1985)

9. Chen, C.C., Chen, C.M., Hsu, F.C., Wang, C.J., Yang, J.T., Kao, Y.Y.: The pachytene chromosomes of maize as revealed by fluorescence in situ hybridization with repetitive DNA sequences. Theor. Appl. Genet 101, 30–36 (2000)
10. Sadder, M.T., Weber, G.: Karyotype of Maize (Zea mays L.) Mitotic Metaphase Chromosomes as Revealed by Fluorescence in situ Hybridization (FISH) With Cytogenetic DNA Markers. Plant Mol. Biol. Reporter 19, 117–123 (2001)
11. Kato, A., Lamb, J.C., Birchler, J.A.: Chromosome painting using repetitive DNA sequences as probes for somatic chromosome identification in maize. Proc. Natl. Acad. Sci. U.S.A. 101, 13554–13559 (2004)
12. Li, L., Arumuganathan, K.: Physical mapping of 45s and 5s rDNA on maize metaphase and sorted chromosomes by FISH. Hereditas 134, 141–145 (2001)
13. Pryor, A.J., Faulkner, K., Rhoades, M.M., Peacock, W.J.: Asynchronous replication of heterochromatin in maize. Proc. Natl. Acad. Sci. U.S.A. 77, 6705–6709 (1980)

Last Instar Larval Morphology of Three Species of Catocalinae (Lepidoptera: Noctuidae) from China

Piao Mei-hua, Fan Le-hui, and Zheng Ying-cha

College of Life Sciences, China Jiliang University, Hangzhou, Zhejiang, China
parkmeihua@163.com

Abstract. The last-instar larval external morphologies of Mocis undata (Fabricius), Dysgonia (Parallelia) stuposa (Fabricius) and Anua indiscriminata Moore of Catocalinae is described and illustrated.

Keywords: Entomology, Larvalmorphology, Catocalinae, Noctuidae, Lepidoptera.

1 Introduction

A mature larva of Catocalinae is small to medium. The head is rounded and the body usually is cylindrical and stout; eighth abdomen (A8) is angulated dorsally in lateral view in some groups. transverse ridges, middorsal humps, and/or lateral fringes may be present on abdominal segments. Cuticle is smooth or bearing granules or spinules. Body is concolorous, marked with chevrons or triangles, or longitudinally striped. The larvae may have two, three, or four pairs of abdominal prolegs in addition to a pair of caudal prolegs those bear crochets in homoideous mesoseries.

The larval color and major features of *Mocis frugalis* Fabricius,*Anua triphaenoides* Walker, *A. olista* Swinhoe, *Parallelia crameri* Moore, *P. arcuata* Moere, *P. yoviana* Stoll, *P. amygdalis* Moore, *P. algira* L. and others Noctuidae larvae have been presented by Gardner (1947). The larval brief morphology, distribution and food plant Of *Mocis disseverans* (Wlk.), *Parallelia bistriaris* Hbn. and others 100 species of Catocalinae have been studed by Crumb(1956). The larval color pattern, mandible, spiracle, labrum and body chaetotaxy of *Anua tirhaca* (Cramer), *Mocis ancilla* Walker, *Parallelis arctotacnia* (Guenée), *P. stuposa* (Fabricius) and others 9 species of Catocalinae have been described by Zhu et al.(1963). The pupa, adult, and larval morphology of *Dysgonia algira* L. of Catocalinae have been published by Sannino (1986). This paper provides detailed descri- ptions and illustrations of larvae of *Mocis undata* (Fabricius), *Dysgonia stuposa* (Fabricius) and *Anua indiscriminata* Moore.

2 Materials and Methods

The collected larvae were reared to last stage for morphological examination. About 1/3 of the last stage larvae were preser- ved in 70% alcohol, and the left were reared with host plant to obtain adults.

E. Zhu and S. Sambath (Eds.): Information Tech. and Agricultural Eng., AISC 134, pp. 857–862.
springerlink.com © Springer-Verlag Berlin Heidelberg 2012

The morphological features of the body of mature larvae in alcohol were examined. They were macerated in 10% KOH for several minutes and dissected under stereoscopic microscope (40×). The head capsule with attached mouthparts was first removed from the body by a cut made with a fine forceps around the edges of the occipital foramen. The maxillae and labium as a unit were removed from the head capsule. The head was sketched under this condition from dorsal and ventral sides. Then the mandi- bles with attached tendons were removed from the head capsule. Mouthparts and skins were mounted on microscopic slides for detailed examinations (100× or 150×).

The nomenclature of larval setae and puncture follows Hinton (1946), and the terminology of labrum, maxillary lobe, and palpi follows Heinrich (1916),and Grimes and Neunzig (1986a,b).

3 Descriptions

3.1 Mocis Undata (Fabricius) (Figs. 1-6)

General: Length 38~45mm; width 2.4~2.8mm. Body usually milk white with dark brown longitudinal stripes; head milk white with brown and blackish brown stripes, thoracic shield and anal shield indistinct, with brown stripes; thoracic legs brown; dorsal area with a dark brown ring around milk white spot on A1; spiracles cream yellow with black peritrems.

Head: The adfrontal suture not reaching epicranial notch, the distance from vertical triangle to apex of adfrontal sutures about three times the distance from apex of adfrontal sutures to apex of frons sutures, the frons extends half of the distance to the vertical triangle. Seta A2 closer to A1 than to A3.

Mouthparts: Labrum emargination about one-fourth deep, forming a normal arc; M2 lateroventral to M1; L1 slightly laterodorsal to L2. Epipharynx with small spines. Mandible with six apical teeth on cutting edge, the first to third teeth large, others small; inner surface with three internal teeth. Labium having membranous postmentum, with two conspicuous setae; spinneret bilobed apically, about 2 times as long as median breadth, and shorter than tip of seta on apical segment of labial palpi. Maxillae: cardo mostly membranous, with hook-like sclerites basally; stipes with two setae; palpus: basal segment with a maxillary lobe and one seta, median segment longer than apical segment.

Thorax: T1: D1 closer to D2 than to XD1; XD2, SD1 and SD2 forming an obtuse angle at SD1; L group bisetose; SV1 and SV2 present above leg. T2 and T3: D1, D2 and SD2 arranged a straight vertical line; SD1 anteroventral to SD2; L1, L2 and L3 present; SV group unisetose.

Abdomen: On A1-8, D1 anterodorsal to D2; SD1 anterodorsal to spiracle; L1 caudal to spiracle in A1-6, posterocaudal to spiracle in A7-8; L2 anteroventral to spiracle in A1-6 and A8, straight below from spiracle in A7; L3 posteroventral to L2 in A1-6 and A8, straight below from L2 in A7. SV group trisetose on A1-6, unisetose on A7-8. On A9, D1 anteroventral to D2; D2, SD1 and L almost forming straight line; L group

unisetose. Prolegs on A5-6 and A10, the crochets uniordinal, arranged in homoideous mesoseries.

Materials examined: Mature larvae collected from leaves of *Glycine max* (L.) at Hangzhou City, Zhejiang Province, 24-Ⅷ-2008.

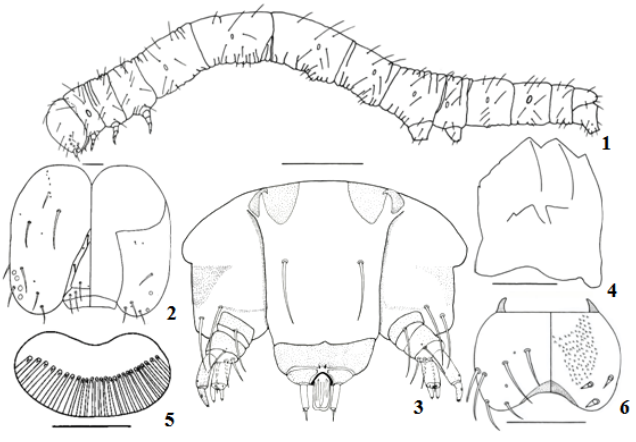

Fig. 1-6. Mocis undata (Fabricius)

1.larva; 2. head [frontal (left) and ventral (right) view]; 3. maxillae and labium; 4. mandible (ventral view);5. crochets of A3-6; 6. labrum(left) and epipharynx(right). scales : 0.5 mm

3.2 Dysgonia (Parallelia) Stuposa (Fabricius) (Figs. 7-12)

General: Length 43~50mm; width 2.8~3.0mm. Body usually yellowish brown with brown maculation, the dorsum of A8 and A9 with papillae, and end portion bearing setae D2 and D1; head grayish brown, with yellowish white maculation ; thoracic shield indistinct, anal shield yellowish brown with brown maculation; thoracic legs yellowish brown with brown claws, anal legs yellowish brown with brown stripes; pinaculum indistinct; spiracles brown with black peritrems.

Head: The adfrontal suture not reaching epicranial notch, the distance from vertical triangle to apex of adfrontal sutures about twice the distance from apex of adfrontal sutures to apex of frons sutures, the frons extends two-fifths of the distance to the vertical triangle. Seta A2 closer to A3 than to A1.

Mouthparts: Labrum emargination one-third deep, forming a normal arc; M2 slightly lateroventral to M1; L1 laterodorsal to L2. Epipharynx with small spines. Mandible with indistinct apical teeth on cutting edge, inner surface with two internal teeth. Labium having membranous postmentum, with two conspicuous setae; the spinneret apical rounded, about 5 times as long as median breadth, and shorter than tip of seta on apical segment of labial palpi. Maxillae: cardo mostly membranous, with hook-like sclerites basally; stipes with dark sclerite and two setae; palpus: basal segment with a maxillary lobe and one seta; median segment longer than apical segment.

Thorax: T1: D1 closer to D2 than to XD1; XD2, SD1 and SD2 forming an obtuse angle at SD1; L group and SV group bisetose. T2 and T3: D1, D2, SD2 and SD1 arranged a straight vertical line; L1, L2 and L3 present; SV group unisetose.

Abdomen: On A1-8, D1 anterodorsal to D2; SD1 anterodorsal to spiracle On A1-7, anteral to spiracle on A8; L1 caudal to spiracle in A8, posterocaudal to spiracle in A1-7; L2 anteroventral to spiracle in A1-2 and A7-8, straight below from spiracle in A3-6; L3 posteroventral to L2 in A1-8; SV group trisetose on A1-6, bisetose on A7, unisetose on A8. On A9, D1 anteroventral to D2; D2, SD1 and L almost forming straight line; L group unisetose. Prolegs on A3-6 and A10, A5 and A6 prolegs subqual, may decrease in size cephalad, the crochets uniordinal, arranged in homoideous mesoseries. Materials examined: Mature larvae collected from leaves of *Punicagrunatum* L. at Zaozhuang City, Shandong Province, 26-Ⅶ-2002.

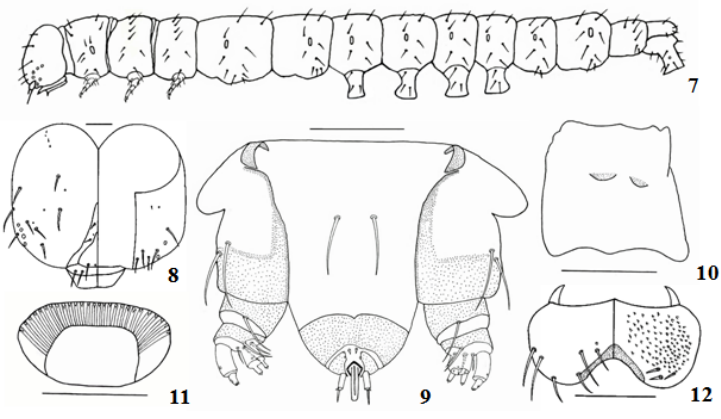

Fig. 7-12. Dysgonia stuposa (Fabricius)

7. larva; 8. head [frontal (left) and ventral (right) view]; 9. maxillae and labium; 10. mandible (ventral view);11. crochets of A3-6; 12. labrum(left) and epipharynx(right). scales: 0.5 mm

3.3 Anua Indiscriminata Moore (Figs. 13-18)

General: Length 57~80 mm; width 4.1~5.0 mm. Body usually yellowish brown, with brown to blackish brown stripes, dorsal area with black moon markings on A5, the dorsum of A8 and A9 with papillae, and end portion bearing setae D2 and D1; head yellowish brown, with brown to blackish brown stripes; thoracic shield and anal shield yellowish brown with blackish brown maculation; thoracic legs brown; pinacula indistinct; spiracles brown with black peritrems.

Head: The adfrontal suture not reaching epicranial notch, the distance from vertical triangle to apex of adfrontal sutures about twice the distance from apex of adfrontal sutures to apex of frontal sutures, the frons extends half of the distance to the vertical triangle. Seta A2 equidistant from A1 and A3.

Mouthparts: Labrum emargination about one-fifth deep, forming a normal arc; M2 lateroventral to M1; L1 dorsal to L2. Epipharynx with small spines. Mandible with six

apical teeth on cutting edge, inner surface with two internal teeth. Labium having membranous postmentum with two conspicuous setae; the spinneret apical rounded, about 8 times as long as median breadth, and longer than tip of seta on apical segment of labial palpus. Maxillae: cardo mostly membranous with hook-like sclerite basally; stipes with dark sclerite and two setae; palpifer sclerotized and one seta; palpus: basal segment with one seta and a lobe; median segment longer than apical segment.

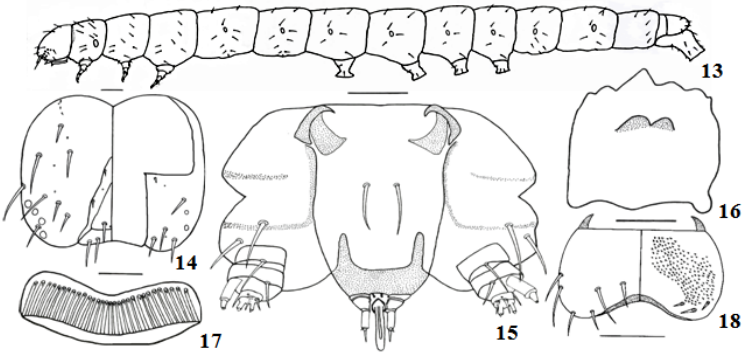

Fig. 13-18. *Anua indiscriminata* Moore
13. larva; 14. head [frontal (left) and ventral (right) view]; 15. maxillae and labium; 16. mandible (ventral view);17. crochets of A3-6; 18. labrum(left) and epipharynx(right). scales: 0.5 mm

Thorax: T1: D1 closer to D2 than to XD1; XD2, SD1 and SD2 forming an obtuse angle at SD1; L group bisetose; SV1 and SV2 present above leg. T2 and T3: D1, D2 and SD2 arranged a straight vertical line; SD1 anteroventral to SD2; L1, L2 and L3 present; SV group unisetose.

Abdomen: On A1-8, D1 anterodorsal to D2; SD1 anterodorsal to spiracle; L1 posterocaudal to spiracle in A1-8; L2 anteroventral to spiracle in A1-6 and A8, straight below from spiracle in A7; L3 posteroventral to L2 in A1-8; SV group trisetose on A1-6, unisetose on A7-8. On A9, D1 anteroventral to and D2; D2, SD1 and L almost forming straight line; L group unisetose. Prolegs on A3-6 and A10, the crochets uniordinal, arranged in homoideous mesoseries.

Materials examined: Mature larvae collected from leaves of *Eucalyptus* spp. at Jiaoling County, Guangdong Province, 20-Ⅶ-2006.

References

1. Crumb, S.E.: The larvae of the Phalaenidae, vol. 1135, pp. pp. 1-355. USDA. Washington. DC. Tech. Bull. (1956)
2. Gardner, J. C. M.: C.I.E., F.R.E.S. On larvae of the Noctuidae (Lepidoptera)-III. Trans. Roy. Ent. Soc. Lond., 98, 59–90 (1947)
3. Grimes, L.R., Neunzig, H.H.: Morphological Survey of the Maxillae in Last Stage Larvae of the Suborder Ditrysia (Lepidoptera): Palpi. Ann. Ent. Soc. Amer. 79, 489–509 (1986a)

4. Grimes, L.R., Neunzig, H.H.: Morphological Survey of the Maxillae in Last Stage Larvae of the Suborder Ditrysia (Lepidoptera): Mesal Lobes (Laciniogaleae). Ann. Ent. Soc. Amer. 79, 510–526 (1986b)
5. Heinrich, C.: On the taxonomic value of some larval characters in the Lepidoptera. Pro. Ent. Soc. 18, 154–164 (1916)
6. Hinton, H.E.: On the homology and nomenclature of the setae of Lepidoptera larvae, with some notes on the phylogeny of the Lepidoptera. Trans. Roy. Ent. Soc., Lond. 97, 1–37 (1946)
7. Sannino, L., Balbiani, A., Parenzan, P.: Dysgonia algira L (Lepidoptera: Noctuidae: Catocalinae) Harmful to pomegranate (Punica granatum L.). Entomologica 21, 127–139 (1986)
8. Zhu, H., Fang, C., Wang, L.: Economic insect fauna of China, Fasc. 7, Lepidoptera: Noctuidae (III), pp. 64–69. Science Press, Beijing (1963)

3D Observation and Preliminary Quantitative Analysis of Germinal Vesicle Oocytes in Aging and Pubertal Mice

Ning Tian[1], Lu Zhang[2], Jing-gao Zheng[1],
Die-yan Chen[1], Ying Li[2], and Wan-yun Ma[1,*]

[1] Key Laboratory for Atomic and Molecular Nanosciences of Education Ministry, Department of Physics, Tsinghua University, Beijing 100084, People's Republic of China
[2] Department of Histology and Embryology, School of Basic Medical Sciences, Peking University Health Science Center, Beijing, 100191, People's Republic of China
mawy@mail.tsinghua.edu.cn

Abstract. The method involved in this paper may bring new prospects for research of immature oocytes quality between the aging mice and the pubertal mice. By adopting the two-photon excitation laser scanning microscopy and studying nucleolus morphological parameter such as the shape, volume size and location, more abundant information were obtained about the immature oocytes of aging and pubertal mice, and may provide a broader approach to search the relationship between the oocyte quality and maternal-age effect as well as other predisposing factors.

Keywords: Aging mouse, Nucleolus, Germinal vesicle oocytes.

1 Introduction

Progressive decline in female fertility with increasing maternal age have been noticed already for many years [1]. In spite of the gradual depletion of oocytes as a major factor of this decline [2], it is also suggested that poor oocyte quality is responsible for the aging-related decline in female fertility. It has been well recognized that decreased oocyte quality accompanied by non-disjunction, chromosome misalignment and abnormal congression occurs during meiosis I [3]. Therefore it is meaningful to analyze the chromosome or chromatin formation for exploring the correlations between oocytes degradation and age.

The oocytes in the germinal vesicle can be divided into two categories in accordance with different chromatin configuration. Chromatin in growing mouse oocytes is decondensed in a configuration termed non-surrounded nucleolus (NSN), and chromatin becoming progressively condensed, forming a heterochromatin rim in close apposition with the nucleolus, is termed Surrounded nucleolus (SN) [4], [5]. In the mouse neonatal ovary, chromatin in all the oocytes was initially found decondensed namely NSN configuration, then transited into the SN configuration with the timely progression of meiotic maturation [5]. Actually GV (germinal vesicle) oocytes of both classes were capable of meiotic resumption, however oocytes possessing SN

* Corresponding author.

E. Zhu and S. Sambath (Eds.): Information Tech. and Agricultural Eng., AISC 134, pp. 863–869.
springerlink.com © Springer-Verlag Berlin Heidelberg 2012

chromatin organizations, in contrast with NSN oocytes which never developed beyond the two-cell stage, were found with higher ability to reach the blastocyst stage and develop to term [6]. The oocytes quality can be evaluated due to the diameters of oocytes, comparing aging mouse oocytes and pubertal mouse oocytes, it was found that the diameters of young GV oocytes were almost larger than 70um, nevertheless one-third of old GV oocytes had diameters smaller than 70um[7]. Otherwise young GV oocytes had NSN and SN chromatin configurations, while old GV oocytes also had chromatin configurations that could not be classified as NSN or SN [7]. Recently other differences have been described between mouse SN and NSN oocytes, such as, transcription level [8], the extent of DNA methylation, histone acetylation, and histone methylation[9] and so on.

Two-photon excitation laser scanning microscopy, relying on the simultaneous absorption of two photons by a molecule, is one of the most exciting recent developments in biomedical imaging [10]. This technique with the character of high penetration capability, high 3D spatial resolution, and minimized photodamage and photobleaching effects is convenient for observing the thick biological samples [11], such as the oocytes.

In this paper, with two-photon fluorescence imaging technique we reported the nucleolus morphology information in immature oocytes by acquiring the shape, volume size, location of nucleolus, and tried to provide a checkpoint for further research about germinal vesicle.

2 Materials and Methods

2.1 Animals

Female Kun-Ming mice purchased from Chinese Academy of Medical Sciences (CAMS, Beijing, PRC) were housed and bred under standard conditions with food and water available ad libitum according to the Chinese National Standard (GB14925-2001). All the animal experiments were approved by the Institutional Animal Welfares and Ethics Committee of Peking University (assurance No.LA2009-020).

2.2 Germinal Vesicle Oocytes Collection

Unstimulated 7-8-week (pubertal, control) and 40-47-week (aging) female mice were sacrificed by cervical dislocation, and their oocytes were isolated by puncturing the ovarian follicles with a sterile needle in HTF (human tubular fluid, Millipore). Only the denuded oocytes in diameter reached 70-80μm and displaying an intact germinal vesicle (GV) were collected for experiment. After several careful washes in HTF, the selected oocytes in the germinal vesicle were immediately fixed in 4% paraformaldehyde for 30 minutes at RT. The numbers of oocytes with SN configuration in aging mice and pubertal mice are both more than six, as well as for NSN.

2.3 Fluorescence Staining

Nuclei were stained with 5μg/ml Hoechst 33342 (Molecular Probes, Leiden, The Netherlands) for 15 min. Following three washes in 0.3% PBSA, oocytes were placed

on a glass bottom dish (MatTek Corp., Ashland, MA, USA) for observing with two-photon laser scanning microscope (TPLSM).

2.4 Two-Photon Fluorescence Imaging

The two-photon microscopy system used in this study adapts a BioRad MRC1024 scanning unit along with a Nikon TE300 microscope. A diode-pumped solid state (millennia X, Spectra-Physics, Mountain View) titanium-sapphire laser system (Tsunami, Spectra Physics, Mountain View, CA) with the output wavelength set at 730 nm, a repetition rate of 82MHz and a pulse width of 120fs was used as the excitation source. For high resolution image acquisition, a objective: 100×oil (LWD, NA 1.40; Nikon) were used. The consecutive optically sectioned images of germinal vesicle oocytes acquired by TPLSM were reconstructed to facilitate morphological description of nuclei.

3 Results and Discussion

3.1 Chromatin Conformation

In the mammalian neonatal ovary, oocytes were naturally arrested at prophase I of meiosis [12]. From the onset of ovarian follicle activation, oocytes were maintained in a protracted meiotic arrest at the diplotene or dictyate stage during postnatal development [12]. And at this stage, the nuclear in immature oocytes was called germinal vesicle (GV). After entering into the growing stage, the diameters of oocytes extended from 12um to 80um (Not including the zona pellucid).As mentioned above, the chromatin configuration of the germinal vesicle oocytes can be divided into two main types: NSN and SN, there were also two intermediate types called PNSN and PSN [5], [8]. The 2D and 3D shapes of SN and NSN configuration were shown in figure 1.

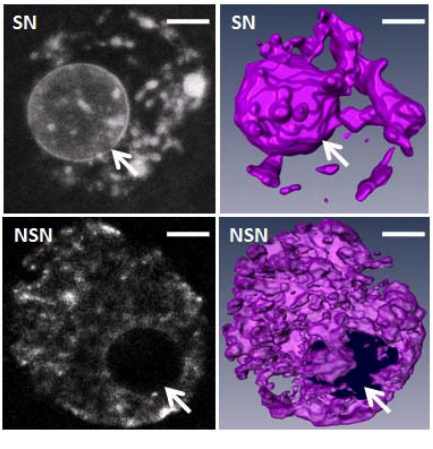

Fig. 1. The 2D and 3D shapes of GV oocytes. The first column is the 2D projection images of z direction; the second column is the 3D reconstruction images. The arrows point to the nucleolus regions. The bar is 10um.

3.2 The Shape of Nucleolus Region

There was a fluorescent light rim appeared around the nucleolus in chromatin with SN configuration loaded by Hoechst 33342. However for NSN configuration, the fluorescent dark zone corresponded to the nucleolus region. Minimum inclusive rectangle (MIR) was used to parcel the nucleolus region surrounded by a heterochromatin rim of SN configuration in the 2D projection images of z direction (Direction of stepper motor movement) illustrated in Figure 2. Therefore the shape of nucleolus can be indicated by the Parameters-MIR aspect ratio.

We found that the majority of nucleolus surrounded by heterochromatin rim was approximately a circle shape with the value of MIR aspect ratio close to 1. In aging mice, the nucleolus with ellipse shape emerged with the value of MIR aspect ratio slightly larger than 1. We also got the similar conclusion for NSN cases.

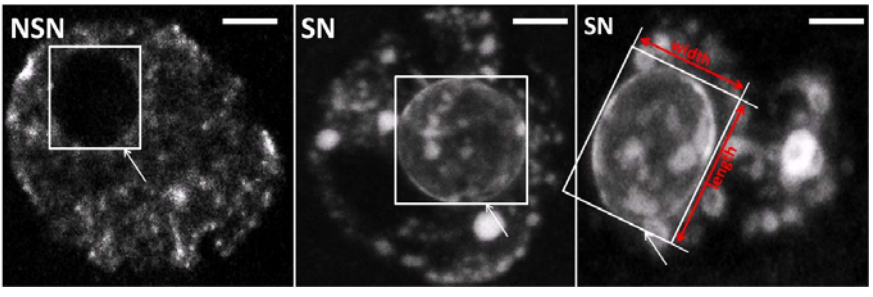

Fig. 2. Minimum inclusive rectangle of SN & NSN oocytes

White rectangles parceling the nucleolus region are the minimum ones as pointed by arrows. The shape of nucleolus can be depicted by aspect ratio of that. The average of aspect ratio regarding pubertal SN oocytes is 1.035 ±0.003, very close to 1. In contrast, the average of aging SN oocytes is 1.067 ±0.030. Although the data about aging mice is also close to 1, its standard error is larger than pubertal mice, since the nucleolus with the shape of ellipse was observed in aging mouse oocytes, and its aspect ratio is about 1.100-1.200. The bar is 10um.

3.3 The Volume Size of Nucleolus Region

The volume size of nucleolus (VSN) in the aging and pubertal mouse immature oocytes can also be taken as a parameter to descript the oocyte quality. The averages of aging mouse and pubertal mouse oocytes with SN configuration were respectively 742.05±27.13μm^3 and 742.67±40.61μm^3, and the averages of NSN configuration were 495.09±34.41μm^3 and 470.74±32.38μm^3 listed in Table 1.

Comparing the VSN of NSN configuration with that of SN configuration, the VSN of NSN configuration was a little smaller than that of SN in both aging mice and pubertal mice. During this experiment, we noticed that not all the VSNs of NSN oocytes were smaller than that of SN, part of NSN oocytes had the approximately equal size of SN. Chouinard[13] reported a heterochromatin rim emerging around nucleolus was prerequisite for germinal vesicle breakdown (GVBD). It was further confirmed that after oocytes entering into growing stage, the transition between NSN and SN configuration necessitated ovulation [14]. The transition may been achieved following nucleolus firstly extended to right size, then enveloped by condensed chromatin rings. It followed that in both aging mice and pubertal mice, the transition from NSN to SN which accompanied with the growing nucleolus volume size was not affected by increasing maternal age.

Table 1. The Average of the Volume Size of Nucleolus Region (Vsn) and Distance Between the Centers of Nucleolus and Nucleus (Dcnn)

	Aging mice		Pubertal mice	
	SN	NSN	SN	NSN
VSN/μm^3	742.05±27.13	495.09±34.41	742.67±40.61	470.74±32.38
DCNN/μm	4.73±0.46	3.18±0.45	2.51±0.20	4.21±0.54

3.4 The Location of Nucleolus Region

The center average coordinates of nucleolus region or nuclei are defined according to the following formula:

$$(x, y, z) = \left(\frac{\sum x_i}{\sum pixel}, \frac{\sum y_i}{\sum pixel}, \frac{\sum z_i}{\sum pixel} \right)$$

Where x_i is X coordinate of each pixel, the same definition to y_i and z_i, denominators are the sum of all pixels.

The location of aging mouse and pubertal mouse nucleolus was defined as the distance between the centers of nucleolus and nucleus（DCNN） as shown in Figure 3. For aging mouse oocytes with SN and NSN configuration, the averages of DCNN were respectively 4.73±0.46μm and 3.18±0.45μm. Nevertheless for pubertal mice, the averages were 2.51±0.20μm and 4.21±0.54μm as listed in Table 1.

In aging mouse oocytes, the location of nucleolus in SN configuration may be closer to the nuclear membrane compared with that of NSN. That means nucleolus may likely undergo migration from center to the membrane of nuclear with transition between NSN and SN. However for pubertal mice, the location of nucleolus in immature oocytes with SN and NSN configuration, as well as the possible migration behavior may be reverse with that of aging mice. The action of nucleolus still needed to be further study.

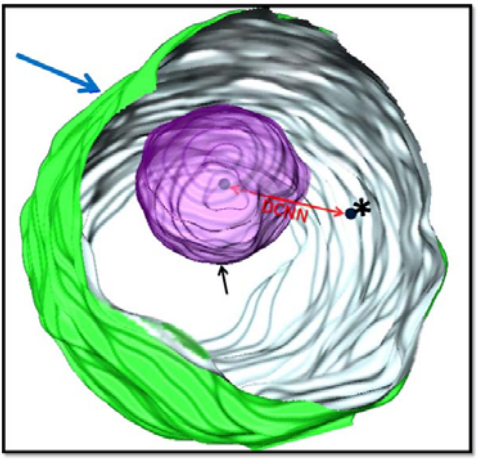

Fig. 3. The distance between the centers of nucleolus and nuclei (DCNN).The center of nucleus-the black dot is indicated by (*). The slightly transparent purple region stands for the nucleolus pointed by the small black arrow, and the big blue arrow points to the nucleus.

4 Conclusions

Oocyte maturation is a critical process in mammalian development. It is meaningful to do some research about immature oocytes. The imaging technique of two-photon excitation fluorescence with the character of high penetration capability, high 3D spatial resolution, and minimized photobleaching effects make it easy to observe the mouse immature oocytes with large size. Following the subsequent image process, three dimensional simulation restoration of chromatin was obtained, and more information about immature oocytes such as the shape, volume, location of nucleolus was acquired. These may serve as a pathway for further research concerning the germinal vesicle oocytes.

Acknowledgments. This study is supported by the grants from Chinese National Basic Research Program (also called 973 Program) (Grants 2007CB5119004), National Nature Science Foundation of China (Grants 90919012 and 10874099) and the Doctoral Program Research Fund of Chinese Ministry of Education (Grant 20090002110065).

References

1. Liu, L., Keefe, D.L.: Ageing-associated aberration in meiosis of oocytes from senescence-accelerated mice. Hum. Reprod. 17(10), 2678–2685 (2002)
2. Eichenlaub, R.U.: Genetics of oocyte ageing. Maturitas 30(2), 143–169 (1998)
3. De La Fuente, R.: Chromatin modifications in the germinal vesicle (GV) of mammalian oocytes. Devl. Biol. 292(1), 1–12 (2006)

4. Fuente, R.D.L., EPPig, J.J.: Transeriptional activity of the mouse oocyte genome: Companion granulosa cells modulate transeription and chromatin remodeling. Dev. Biol. 229, 224–236 (2001)
5. Debey, P., Szollosi, M.S., Szollosi, D., et al.: Competent mouse oocytes isolated from antral follieles exhibit different chromatin organization and follow different maturation dynamics. Mol. Reprod. Dev. 36, 59–74 (1993)
6. Inoue, A., Nakajima, R., Nagata, M., Aoki, F.: Contribution of the oocyte nucleus and cytoplasm to the determination of meiotic and developmental competence in mice. Human Reproduction 23, 1377–1384 (2008)
7. Manosalvaa, I., Gonzálezb, A.: Aging changes the chromatin configuration and histone methylation of mouse oocytes at germinal vesicle stage. Theriogenology 74, 1539–1547 (2010)
8. Bouniol-Baly, C., Hamraoui, L., Guibert, J., et al.: Differential transeriptional activity assoeiated with chromatin configuration in fully grown mouse germinal vesicle oocytes. Biol. Reprod. 60, 580–587 (1999)
9. Kageyama, S., Liu, H., Kaneko, N., Ooga, M., Nagata, M., Aoki, F.: Alterations in epigenetic modifications during oocyte growth in mice. Reproduction 133, 85–94 (2007)
10. Benninger, R.K., Hao, M., Piston, D.W.: Multi-photon excitation imaging of dynamic processes in living cells and tissues. Rev. Physiol. Biochem. Pharmacol. 160, 71–92 (2008)
11. Wang, B.-G., Onig†, K.K. Halbhuber, K.-J.: Two-photon microscopy of deep intravital tissues and its merits in clinical research. Journal ofMicroscopy 238, 1–20 (2010)
12. Hassold, T., Hunt, P.: To Err (Meiotically) Is Human: The Genesis Of Human Aneuploidy. Nature Genetics 2, 280–291 (2001)
13. Chouinard, L.A.: A light and electro-microscope study of the nucleolus during growth of the oocyte in the prepubertal mouse. J. Cell. Sci. 40, 503–508 (1971)
14. Zuccotti, M., Piccinelli, A., Rossi, P.G., Garagna, S., Redi, C.A.: Chromatin organization during mouse ooeyte growth. Mol. Reprod. Dev. 41, 479–485 (1995)

Species Sensitivity Distribution for Arsenic Toxicity on Plant Based on Soil Culture Data: Implications for Benchmarks of Soil Risk Assessments

Bai-ye Sun[1], Xiao-ru Pan[2], and Feng Zhou[3]

[1] Department of Agricultural Engineering, Weifang Vocational College, Weifang, People's Republic of China
[2] College of Chemistry and Chemical Engineering, Weifang University, Weifang, People's Republic of China
[3] College of Geographic Science, Nanjing Normal University, Nanjing, People's Republic of China
bys298@yahoo.com.cn, zhoufeng-198704@163.com

Abstract. Species sensitivity distributions (SSDs) have attracted increased interest to ecological risk assessment due to greater statistical confidence and transparent. However, it is of difficulty to apply the SSD approach to terrestrial ecological risk assessments for the scarcity of uniform terrestrial ecotoxicological data. Literature soil culture data of arsenic (As) toxicity on plant were reanalyzed. Toxicity coefficients (EC10 and EC50) were systematically calculated using S-shape dose response model. SSD of As for plant were constructed based on 161 literature-derived toxicological records of 28 species. The S-shape Boltzmann model describes the constructed SSD curves well, and the calculated soil As concentration causing 5% of plant species suffering a damage of reducing growth by about 10% (EC10-HC5) and 50% (EC50-HC5) are 7.83 and 25.27 mg·kg−1, respectively. The constructed SSD of As is important and necessary for the derivation of Ecological Soil Screening Levels for terrestrial ecological risk assessments.

Keywords: Arsenic, Plant, Soil culture, Species sensitivity distribution, Ecological risk assessment, Soil screening level.

1 Introduction

Arsenic is a major soil contaminant with significant toxicity threatening terrestrial biota and human health. In order to assess the ecological risk, species sensitivity distribution (SSD) based methods have attracted increased interest [1, 2]. With sufficient superior quality laboratory ecotoxicity data, a hazardous concentration for the ecosystem can be derived from the fitted SSD [3, 4]. If used correctly, the SSD method can offer greater statistical confidence and more transparent to ecological risk assessments than traditional assessment factor approaches [4].

To date SSD methods have been used mainly in ecological risk assessments of aquatic ecosystem[4]. However, it is of difficulty to apply SSD in terrestrial

E. Zhu and S. Sambath (Eds.): Information Tech. and Agricultural Eng., AISC 134, pp. 871–879.
springerlink.com © Springer-Verlag Berlin Heidelberg 2012

ecosystems, because of fewer data available for terrestrial species (especially for plant) than for aquatic species. In fact, numerous terrestrial ecotoxicological experiments have been conducted on plant. However, majority of these experiments were not originally designed for SSD analysis, the values of toxicity coefficients, such as effective concentrations (ECs) thus were not reported, while these toxicity coefficients are necessary to SSD analysis. Ecotoxicological data of soil culture experiments are assumed to be representative of the exposure of plants to contaminants measured in field soils [5]. Hence the present study reanalyzed literature soil culture data on As toxicity to terrestrial plants, and the SSD of As on plant was constructed based on the estimated ECs. This study is important to enrich terrestrial ecotoxicity data of As to plant, and useful to terrestrial ecological risk assessment.

2 Materials and Methods

2.1 Database Creation

Data of As to terrestrial plants were mainly obtained from published literatures, including research papers, reports, etc. Bibliographic databases included Chinese databases (CNKI, VIP and Wanfang) and English databases (SCIE and EBSCO). Selected 41 toxicological literatures were collected. A total of 161 toxicological records of 28 species were selected from the collected literatures.

2.2 Re-analysis of Ecotoxicity Data

*EC*s were estimated based on the dose-response model. Plant growth indexes including germination rate, plant height, root length, biomass, and production were used as the toxicity endpoint according to the U.S. EPA [6]. *EC*10 and *EC*50 were used as the toxicity coefficients according to the U.K. Environment Agency [7] and the U.S. EPA [8]. The inhibition rate of growth index was calculated using the method described in [9]. The dose-response curve was plotted with the logarithm of the total As concentration in soil [log(*C*)] as Y and the inhibition rate (*I*) as X. If the dose-response curve exhibited an S shape, *EC*10 and *EC*50 were estimated by curve fitting using the Boltzmann model [9]; if the curve showed a linear shape, *EC*s were calculated by linear interpolation.

2.3 SSD Curve Construction

1) Calculation of Species-specific ECs: For a given plant species, there may be several reported toxicity experiments, and for a given experiment, there may be several toxicity endpoints (e.g., plant height, biomass, etc.). Given that each endpoint can give an *EC* value, there would consequently be several *EC* data for this species. Nevertheless, the duplication of *EC* value for a same species would inevitably lead to an over-weight for this species in the cumulative frequency distribution (i.e., SSD). To overcome this bias, a weight-free approach was followed and the species-specific *EC*s were calculated.

First, for each experiment, the endpoint-weighted mean (μ') of a given *EC* (take *EC*10 as the example) was estimated by calculating the arithmetic mean of the *EC*10s derived from every growth index toxicity endpoint (e.g., plant height, biomass, and

other growth indexes). Second, for each plant species, the experiment-weighted mean of the *EC*s of a given species (μ, the species-specific *EC* used for SSD construction) was estimated by calculating the arithmetic mean of the *EC*10s derived from every experiment. In this way, each plant species appear only once in the SSD distribution; Also, this method allows the utilization of all available data. μ' and μ were calculated using (1) and (2).

$$\mu' = \frac{1}{n} \cdot \sum_{i=1}^{n} EC_i \tag{1}$$

$$\mu = \frac{1}{m} \cdot \sum_{j=1}^{m} u'_j \tag{2}$$

where n is the number of *EC*10 (if take EC10 as the example) derived from different growth indexes of a given experiment, EC_i is the *EC*10 value for a certain growth index i (e.g., root length), m is the number of experiments for a given plant species, μ_j' is the endpoint-weighted mean of *EC*10 of this species for a certain experiment j.

2) Modeling SSD Curves and HC_5 Estimation: For each toxicity coefficient (*EC*10 or *EC*50), the final weighted species-specific *EC*s (μ) were used to build up the SSD curve. The SSD curves were plotted in the coordinate system using Log concentration as x, and cumulative probability as y. The S shape SSD curves were fitted using the modified Boltzmann model (3)[10].

$$y = 100 - \frac{100}{1 + \exp\left[\left(x - x_0\right)/dx\right]} \tag{3}$$

where x_0 is the hazardous concentration for 50% of the species in an ecosystem, and dx is the slope of the SSD curve.

The hazardous concentration for 5% of the species in plant ecosystem (HC_5) was calculated by the interpolation method. Equation (3) was rearranged and solved for x to yield (4):

$$HC_5 = x_0 - 2.94 \cdot dx \tag{4}$$

where x_0 and dx are determined from (3). In addition, if x is log(concentration), then the calculated HC_5 is the logarithm of the As concentration, after which an antilog conversion will be made to obtain the actual HC_5.

2.4 Statistical Analysis

Normality was tested by the Shapiro-Wilk test using SPSS software. Data regression analysis and model fitting were performed using Origin software.

3 Results and Discussion

161 reliable toxicological records of 28 species of plant with growth index as toxicity endpoint were obtained. weighted species-specific *EC*s were estimated for each plant

species (Table 1). Normality test showed that at the 0.05 level both *EC*10s and *EC*50s of 27 species of plant were significantly drawn from a lognormal distribution with mean of log(*EC*) 1.67 and 2.15, respectively, and with standard deviation 0.52 and 0.43, respectively.

SSD curve constructed based on the data of *EC*10 and *EC*50 of 27 species showed an S shape and can be well fitted by the modified Boltzmann model (3) ($P<0.01$, Fig. 1 and Fig. 2). And the calculated HC_5 was 7.83 mg·kg^{-1} for *EC*10-SSD, indicating that the total soil arsenic concentration of 7.83 mg·kg^{-1} may cause 5% of plant species in a terrestrial ecosystem suffering a damage of reducing growth by about 10%. And the calculated HC_5 was 25.27 mg·kg^{-1} for *EC*50-SSD, indicating that the total soil arsenic concentration of 25.27 mg·kg^{-1} may cause 5% of plant species suffering a damage of reducing growth by about 50%.

Table 1. Species-specific ecs for as derived from experiments conducted in soil culture using growth index as toxicity endpoint

Plant species	***EC*10 (mg·kg^{-1})**	***EC*50 (mg·kg^{-1})**	**References**
Spring wheat	42.60	106.89	[12-15]
Soybean	37.48	74.28	[15, 16]
Tomato	28.73	76.53	[17-19]
Wild cabbage	15.17	91.49	[20]
Sweet potato	568.12	795.22	[21, 22]
Ryegrass	-	106.00	[23]
Groundnut	91.23	233.61	[15, 21, 22, 24]
Cucumber	1.95	16.30	[20]
Scutellaria	210.24	411.25	[25]
Cured tobacco	19.56	86.27	[26, 27]
Swamp cabbage	178.68	565.46	[21, 22]
Hot pepper	136.14	331.15	[21, 22]
Radish	50.85	123.60	[13, 28]
Jatropha curca	13.04	278.01	[29]
Paspalum	136.86	259.73	[21, 22]
Clover	47.93	>50	[30]
Ginger	51.84	225.74	[21, 22]
Rice	28.96	79.06	[15, 31-42]
Alternanthera philoxeroides	179.68	591.81	[21, 22]
Green bean	28.11	64.86	[43]
Lettuce	39.12	137.21	[44, 45]
Amaranth	38.26	164.11	[21, 22]
Pakchoi	42.09	63.29	[46]
Wheat	65.30	165.02	[44, 47-50]
Tobacco	169.93	394.47	[21, 22]
Cole	31.97	55.25	[51, 52]
Maize	64.15	262.12	[13-15]
Kidney bean	4.49	14.86	[20]

Currently, about a dozen of countries or regions have provided ecological soil screening levels. For arsenic, around the world the maximum allowable concentration in soil was in the range of 10~20 mg·kg^{-1} [11]. In China, soil environmental quality standards stipulated the maximum ecological allowable total As concentration in soil is 30 mg·kg^{-1} for paddy field, and 40 mg·kg^{-1} for dry field (level III) [11]. According to the results of the present study, the HC_5 of both *EC*10-SSD and *EC*50-SSD are less than the critical value of soil arsenic environmental standards of China, indicating that the present soil environmental quality standards of China may be loose for soil screening in ecological risk assessment and soil screening levels of China should be developed. However, further study is still needed due to the variety of soil types and characteristics.

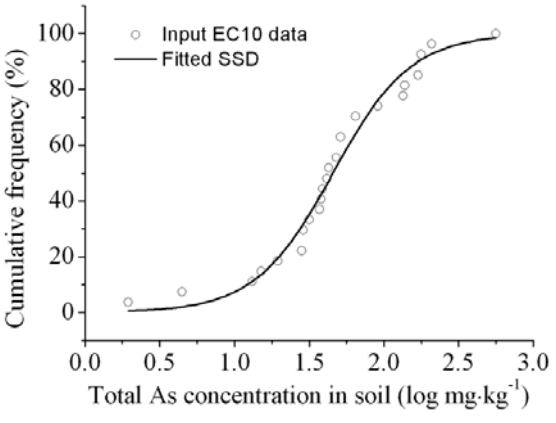

Fig. 1. Species sensitivity distribution for plants exposed to soil arsenic using growth index as toxicity endpoint and with EC10 as toxicity coefficient

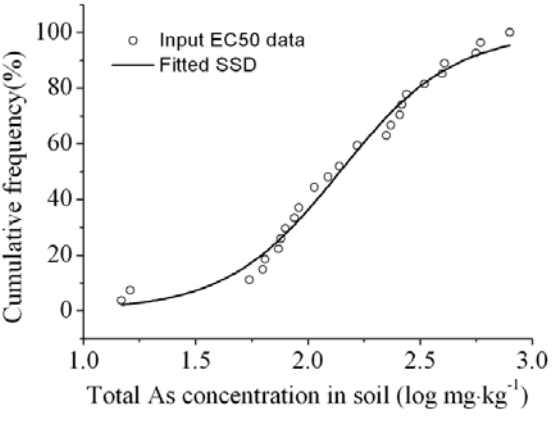

Fig. 2. Species sensitivity distribution for plants exposed to soil arsenic using growth index as toxicity endpoint and with EC50 as toxicity coefficient

Acknowledgment. This Work was supported by National Key Technology R&D Program of China (No. 2008BADC4B04), and Natural Science Theoretical Research Youth Foundation of Weifang University (No. 2008Z021).

References

1. Domene, X., Ramírez, W., Mattana, S., Alcañiz, J.M., Andrés, P.: Ecological Risk Assessment of Organic Waste Amendments Using the Species Sensitivity Distribution From a Soil Organisms Test Battery. Environmental Pollution 155, 227–236 (2008), doi:10.1016/j.envpol.2007.12.001
2. Posthuma, L., Suter, G.W., Traas, T.: Species sensitivity distributions in ecotoxicology. CRC Press, Florida (2002)
3. Aldenberg, T., Slob, W.: Confidence Limits for Hazardous Concentrations Based on Logistically Distributed NOEC Toxicity Data. Ecotoxicology and Environmental Safety 25, 48–63 (1993), doi:10.1006/eesa.1993.1006
4. Wheeler, J.R., Grist, E.P.M., Leung, K.M.Y., Morritt, D., Crane, M.: Species Sensitivity Distributions: Data and Model Choice. Marine Pollution Bulletin 45, 192–202 (2002)
5. Efroymson, R.A., Will, M.E., Suter, G.W., Wooten, A.C.: Toxicological Benchmarks for Screening Contaminants of Potential Concern for Effects on Terrestrial Plants:1997 Revision, Oak Ridge National Laboratory, US Department of Energy, Oak Ridge, Tennessee ES/ER/TM-85/R3 (1997)
6. U. S. EPA, Guidance for Developing Ecological Soil Screening Levels. Washington (2003)
7. Fishwick, S., Scientist, S., Quality, S., Land, P.A.: Soil screening values for use in UK ecological risk assessment, United Kingdom Environment Agency, Warrington Environment Agency R&D Technical Report P5-091 (2004)
8. USEPA, Guidance for developing ecological soil screening levels, Office of Solid Waste and Emergency Response, U.S. Environmental Protection Agency, Washington (2005)
9. Sun, B.Y., Kan, S.H., Zhang, Y.Z., Deng, S.H., Wu, J., Yuan, H., Qi, H., Yang, G., Li, L., Zhang, X.H., Xiao, H., Wang, Y.J., Peng, H., Li, Y.W.: Certain Antioxidant Enzymes and Lipid Peroxidation of Radish (Raphanus sativus L.) as Early Warning Biomarkers of Soil Copper Exposure. Journal of Hazardous Materials 183, 833–838 (2010), doi:10.1016/j.jhazmat.2010.07.102
10. McKarns, S.C., Hansch, C., Caldwell, W.S., Morgan, W.T., Moore, S.K., Doolittle, D.J.: Correlation Between Hydrophobicity of Short-Chain Aliphatic Alcohols and Their Ability to Alter Plasma Membrane Integrity. Toxicological Sciences 36, 62–70 (1997), doi:10.1093/toxsci/36.1.62
11. Xia, J.Q.: Detailed explanations to environmental quality standard for soils. China Environmental Science Press, Beijing (1996)
12. Xiao, L., Li, G., Zhao, Y.G.: Toxic Critical Values of Arsenic Pollution in Loess Soil. Journal of Northwest A & F University 24, 105–108 (1996)
13. Yang, J., Ge, J.: Studies on the Effects of Arsenic on Farmland Ecosystem. Acta Ecologica Sinica 4, 34–45 (1984)

14. Xu, J., Yang, J., Jing, H.: Effects of Arsenic Polluted Soils on Crops and Its Influencing Factors. Soils 2, 85–89 (1996)
15. Xia, J.Q.: Studies on the Soil-Environmental Criteria for Arsenic. Rural Eco-Environment 4, 1–4 (1993)
16. Zhang, X.X., Xiong, X.Z., Wang, Y.S., Wang, L.P., Ren, H.: Environmental Capacity of Meadow Brown Soil for Heavy Metals. Acta Scientiae Circumstantiae 8, 295–306 (1988)
17. Miteva, E.: Accumulation and Effect of Arsenic on Tomatoes. Communications in Soil Science and Plant Analysis 33, 1917–1926 (2002)
18. Liu, Y., Zhu, Y.G., Chen, B.D., Christie, P., Li, X.L.: Yield and Arsenate Uptake of Arbuscular Mycorrhizal Tomato Colonized by Glomus Mosseae BEG167 in As Spiked Soil under Glasshouse Conditions. Environment International 31, 867–873 (2005), doi:10.1016/j.envint.2005.05.041
19. Han, L.Y.: Effects of Arsenic on Tomato in Pot Culture Experiments. Journal of Heilongjiang Environment 4, 24–25 (1989), doi:CNKI:SUN:HLJO.0.1989-04-006
20. Zhao, M., Zhao, Z., Cai, K., Yu, Q., Wang, W.: Effects of As and Cr on the Vegetable Growth of Characteristics and Products Safety. Journal of Agro-Environment Science 26, 489–493 (2007)
21. Liu, G.L., Gao, S.D.: Effects of Arsenic on Crops in Red Soils. Chinese Journal of Soil Science 5, 231–233 (1987)
22. Liu, G.L., Chen, F.X., Gao, S.D., Li, M.Q.: Effect of Arsenic in Soil on Plants - Research on 'Arsenic-Toxic Field' in South China. Scientia Agricultura Sinica 4, 9–16 (1985)
23. Anderson, R.H., Basta, N.T.: Application of Ridge Regression to Quantify Marginal Effects of Collinear Soil Properties on Phytotoxicity of Arsenic, Cadmium, Lead, And Zinc. Environmental Toxicology and Chemistry 28, 1018–1027 (2009), doi:10.1897/08-062.1
24. Xu, L.F., Liu, F.Q.: Effects of Additional Arsenic in Latosol Soil on Peanut Growth and Residual. Guangdong Agricultural Sciences 1, 27–30 (1991), doi:CNKI:SUN:GDNY.0.1991-01-009
25. Cao, H.B., Jiang, Y., Chen, J.J., Zhang, H., Huang, W., Li, L., Zhang, W.: Arsenic Accumulation in Scutellaria baicalensis Georgi and Its Effects on Plant Growth and Pharmaceutical Components. Journal of Hazardous Materials 171, 508–513 (2009)
26. Chang, S., Ma, X., Zhao, X.: Effects of Arsenic on Development and Yield and Quality of Flue-Cured Tobacco. Journal of Northwest A & F University 35, 165–170 (2007)
27. Chang, S.M., Ma, X.M., Zhang, G.L., Xiong, S.P., Zhan, K.H., Liu, G.S.: Effects of Arsenic Toxicity on Carbon and Nitrogen Metabolism and the Yield and Quality of Flue-Cured Tobacco. Journal of Plant Ecology 30, 682–688 (2006)
28. Jian, F.L., Qing, C.L.: The After-Effects of Arsenate and Its Critical Value. Journal of Southwest Agricultural University 14, 74–77 (1992), doi:CNKI:SUN:XNND.0.1992-01-016
29. Juwarkar, A.A., Yadav, S.K., Kumar, P., Singh, S.K.: Effect of Biosludge and Biofertilizer Amendment on Growth of Jatropha Curcas in Heavy Metal Contaminated Soils. Environmental Monitoring and Assessment 145, 7–15 (2008)
30. Mascher, R., Lippmann, B., Holzinger, S., Bergmann, H.: Arsenate Toxicity: Effects on Oxidative Stress Response Molecules and Enzymes in Red Clover Plants. Plant Science 163, 961–969 (2002), doi:10.1016/S0168-9452(02)00245-5.

31. Zhang, Y.: Study on Pollution Critical Concentration of Arsenic and Soil Environmental Capacity in Latosolic Red Soil and Red Soil. Journal of Agro-environmental Science 11, 256–260 (1992)
32. Wang, F.M., Chen, Z.M., Zhang, L., Gao, Y.L., Sun, Y.X.: Arsenic Uptake And Accumulation in Rice (Oryza sativa L.) at Different Growth Stages Following Soil Incorporation of Roxarsone and Arsanilic Acid. Plant and Soil 285, 359–367 (2006), doi:10.1007/s11104-006-9021-7
33. Kang, L., Li, X., Liu, J., Zhang, X.: Effect of Arsenic on Growth Development of Rice and Residual Rules in the Loam Paddy Soil. Journal of Jilin Agricultural University 18, 58–61 (1996)
34. Chen, T.B., Liu, L.G.: Effect of Arsenic on Rice (Oryza sativa L.) Growth and Development and Its Mechanism. Scientia Agricultura Sinica 26, 50–58 (1993)
35. Du, D.D., Li, Y.X., Dai, B.Q., Zhou, Y.: Experimental Study on Effects of Arsenic on Rice Growth and Residual. Sinica Environmetal Science & Technology 3, 11–12 (1987)
36. Li, X.P., Li, X.G.: Effects of Arsenide and Exposure Duration on Toxicity to Rice. Soils 2, 90–93 (1996)
37. Yang, G.D., Liu, C.H., Lu, J.C., Wang, H.B., Zeng, C.M., Chen, R.S., Guo, X.K., He, H.B.: Effect of Photosynthetic Physiological of Rice Seedling under Arsenic Stress. Academic Periodical of Farm Products Processing 1, 5–7 (2009)
38. Luo, J.F., Xia, Z.L., Li, S.Z.: Chemical Behavior of As in Purple Soils and Their Effects on Crop. Acta Scientiae Circumstantiae 11(3), 269–275 (1991), doi:CNKI:SUN:HJXX.0.1991-03-002
39. Su, Y.S., Cao, Y., Xie, M.Y., Chen, S.Y., Wu, C.Y., Yang, Y.Q.: The Effects of Cu and As Added to Soil in Single or in Combination on Rice. Journal of Plant Resources and Environment 3, 23–28 (1994) doi:CNKI:SUN:ZWZY.0.1994-04-005
40. Li, X.G., Li, X.P.: Soil Adsorption of Arsenic and Toxicity of Arsenic to Rice. Soils 2, 98–100 (1996)
41. Su, L.K., Yuan, H.X.: Effect of Cu and As on Growth of Rice. Tropical and Subtropical Soil Science 6, 194–197 (1997)
42. Rahman, M.A., Hasegawa, H., Rahman, M.M., Miah, M.A.M., Tasmin, A.: Straighthead Disease of Rice (Oryza sativa L.) Induced by Arsenic Toxicity. Environmental and Experimental Botany 62, 54–59 (2008), doi:10.1016/j.envexpbot.2007.07.016
43. Li, D.L., He, F., Ma, C.Z., Tian, C.: Effects of Arsenic on Biological Activity of Soils and Its Toxicity to Selected-Vegetables. Agro-Environmental Protection 19, 148–151 (2000)
44. Cao, Q., Hu, Q.H., Baisch, C., Khan, S., Zhu, Y.G.: Arsenate Toxicity for Wheat and Lettuce in Six Chinese Soils with Different Properties. Environmental Toxicology and Chemistry 28, 1946–1950 (2009), doi:10.1897/08-660.1
45. Tu, C., Miao, J.Y.: A Preliminary Study on Toxic Critical Value of Arsenic in Soils. Journal of Agro-environmental Science 11, 80–83 (1992), doi:CNKI:SUN:NHBH.0.1992-02-007
46. Jian, F.L., Qing, C.L., Mu, S.S.: Studies on the Effect of the As on Growing of Vegetable and Its Critical Value. Chongqing Environmental Science 14, 6–9 (1992)
47. Wang, Y.B., Liu, D.Y.: Effect of Cu, As and Their Combination Pollution on Eco-Physiological Index of Wheat. Chinese Journal of Applied Ecology 12, 773–776 (2001)
48. Cao, Q., Hu, Q.H., Khan, S., Wang, Z.J., Lin, A.J., Du, X., Zhu, Y.G.: Wheat Phytotoxicity from Arsenic and Cadmium Separately and Together in Solution Culture and in a Calcareous Soil. Journal of Hazardous Materials 148, 377–382 (2007)

49. Yang, Q.: Effects of Arsenicon on Wheat Growth. Soils and Fertilizers 3, 23–25 (1992)
50. Zhu, Y.J., Wang, C.Y., Ma, Y.X., Xia, G.J., Wang, Y.H.: Effect of Arsenic Stress on the Growth and Metabolism of the Wheat Root System. Acta Ecologica Sinica 20, 707–710 (2000)
51. Cox, M.S., Kovar, J.L.: Soil Arsenic Effects on Canola Seedling Growth and Ion Uptake. Communications in Soil Science and Plant Analysis 32, 107–117 (2001)
52. Hu, L.J., Zeng, X.B., He, Y.C., Li, L.F.: Influence of Different Speciation and Added Amounts of outer Source Arsenic on Rape (Brassica campestris) Growth and Absorption of Arsenic. Journal of Agro-Environment Science 27, 2357–2361 (2008)

SA and PEG-Induced Priming for Water Stress Tolerance in Rice Seedling

Xuemei Li[1] and Lihong Zhang[2]

[1] College of Chemical and Life Science, Shenyang Normal University
Shenyang, 110034, China
[2] Environmental Science Department, Liaoning University
Shenyang, 110036, China
{lxmls132,lihongzhang132}@163.com

Abstract. An experiment was conducted to evaluate the effect of different seed priming methods to enhance the polyethylene glycol-6000 (PEG-6000) stress tolerance in rice (Oryza sativa L.). Seeds were subjected to different priming treatments such as water, PEG, and salicylic acid (SA). The primed seeds were grown for 8 days and then the seedlings were subjected to PEG (15%) stress. The different biochemical responses were studied 2 days after treatment. Under PEG stress, the root length was higher in PEG and SA-primed sets as compared to water-primed, while the shoot height had no change. SA-primed increased photosynthetic pigment content and Chla/Chlb of rice under PEG stress. Net photosynthetic rate and water use efficiency were higher in PEG and SA-primed sets as compared to water-primed under PEG stress. SA-primed enhanced the activities of superoxide dismutase and peroxidase, but decreased the activity of catalase under PEG stress. Proline content was lower in PEG-primed, but higher in SA-primed as compared to water-primed treatment. The study thus suggests the use of SA-priming as a more effective strategy to alleviate the PEG induced stress in rice.

Keywords: Rice, salicylic acid, PEG, photosynthesis, antioxidative enzyme, water stress.

1 Introduction

Water stress is one of the major factors limiting the growth of land plants. It induced stomatal closure and therefore reduces photosynthesis [1]. It also can cause lipid peroxidation, protein degradation and chlorophyll bleaching by forming reactive oxygen species (ROS) [2]. In order to tackle such problems, researches are being made to seek effective method to enhance water stress tolerance of the plants.

Salicylic acid (SA) is a common plant-produced signal molecule which plays an important role in the regulation of numerous physiological processes including photosynthesis [3]. Exogenous SA treatment could enhance stress tolerance and the effect is closely related to modulate redox balance, counteract the negative effects of reactive oxygen intermediates caused by oxidative stress by increasing the activity of antioxidant enzymes [4]. Although SA-induced water stress tolerance has been

E. Zhu and S. Sambath (Eds.): Information Tech. and Agricultural Eng., AISC 134, pp. 881–887.
springerlink.com © Springer-Verlag Berlin Heidelberg 2012

shown, the underlying mechanisms including physiological and biochemical basis under the stressed environments are poorly understood. Upon appropriate stimulation, plants can increase their resistance against future stress exposure. Primed plants display either faster and, or stronger, activation of various defence responses that are induced following attack by either biotic or abiotic stress. The efficiency of differential exogenous agents, such as SA and PEG in increasing the tolerance against water stresses has not been comparatively investigated. Therefore, the present study was aimed to examine the comparative potential of water, PEG, and SA to overcome the negative effects of PEG stress in rice.

2 Materials and Methods

Plant material and treatments. Rice (*Oryza sativa* L.) was used in this study. Three different agents viz., distilled water, 15% PEG and 1 mmol/L SA were used for the purpose of seed priming. Seeds were first surface sterilized with 30% ethanol for 3 min, washed thoroughly to remove any traces of ethanol, and were distributed in three different sets. Seeds were separately immersed in different priming solutions (ca. 150 seeds/200 ml solution) for 18 h at 25℃ under dark conditions. After the priming period, seeds were rinsed three times with distilled water and then dried to their original moisture content in shed.

The air-dried seeds were then germinated in Petri dishes with wetted filter paper at 30°C. After 48 h incubation, uniformly germinated seeds were cultivated in a 500 ml beaker containing Hoagland solution. The hydroponically cultivated seedlings were grown for 8 days in a growth chamber maintained at 27℃ day/20℃ night, 16 h/8 h light/dark, 800 $\mu molm^{-2}s^{-1}$ PPFD and 80% relative air humidity. After 8 days of germination, each set was distributed into two different sets. One set was treated with Hoagland solution containing 15% PEG for water stress; other was treated with Hoagland solution as control. After 2 days, samples from all the two sets, given seed priming treatment with PEG (PT), SA (ST), and water (WT), were harvested for the analysis of various biochemical parameters.

Measurement of chlorophyll content. Total chlorophyll contents were extracted from 0.1 g of leaf discs with 10 ml 80% acetone and absorbances at 663 and 645 nm were measured.

Measurements of photosynthetic gas exchange. Gas exchange was measured under saturated light between 10:00 and 12:00. Net photosynthetic rate (Pn), stomatal conductance (Gs) and transpiration rate (E) were measured on the second leaves using a portable photosynthesis system (LI-6400, Li-Cor, USA) with an open system and logged at CO_2 concentration of about 370 $\mu mol\ mol^{-1}$ in the leaf chamber. Water use efficiency was calculated as Pn/E.

Enzyme extraction and assay. The samples were ground with a mortar and pestle under the chilled condition in 50mM potassium phosphate buffer (pH 7.6) containing 1mM EDTA, 2% (w/v) PVP. The activities of antioxidative enzymes such as superoxide dismutase (SOD), peroxidase (POD) and catalase (CAT) were simultaneously determined.

SOD activity was measured as described by Beyer and Fridovich [5]. POD and CAT activities were determined by the method of Chance and Maehly [6].

Measurements of Proline Content. Fresh leaves were extracted in 3% sulphosalicylic acid and the homogenates were centrifuged at 10,000g for 10 min. The supernatant was reacted with acid ninhydrin reagent and glacial acetic acid for 1 h at 100℃ and the reaction terminated in an ice bath. The reaction mixture was extracted with toluene. The chromophore containing toluene was aspirated from the aqueous phase, warmed to room temperature and the absorbance measured at 520 nm.

Statistical Analysis. All data were subjected to an analysis of variance (ANOVA) and when a significant ($P < 0.05$) F ratio occurred for treatment effects, a least significant difference (LSD) was calculated.

3 Results

Under similar treatment, shoot heights of PT and ST were comparable to WT, while the shoot height of WT under control condition was significant lower than that of WT under PEG stress (Fig. 1). Under control condition and PEG stress, root lengths of PT and ST were significant higher than that of WT.

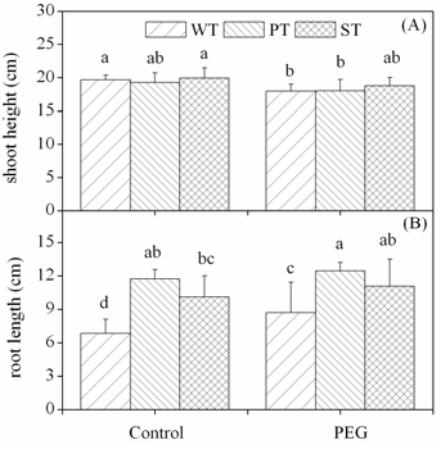

Fig. 1. Effect of water-primed (WT), PEG-primed (PT), and SA-primed (ST) on shoot height and root length of rice subjected to PEG stress

Under control condition, Chlt content and Chla/b in PT were lower, whereas in ST were almost equal to these of WT (Fig.2). Under PEG stress, in PT, Chlt content and Chla/b were almost equal to these of WT, whereas in ST, the above parameter was significantly higher than these of WT.

Under control condition, in PT and ST, net photosynthetic rate (Pn), stomatal conductance (Gs), transpiration rate (E) and water use efficiency were almost equal to these of WT (Fig.3). Under PEG stress, Pn, E and WUE were significantly higher in ST, as compared to WT, while, in PT, Pn and WUE were significantly increased.

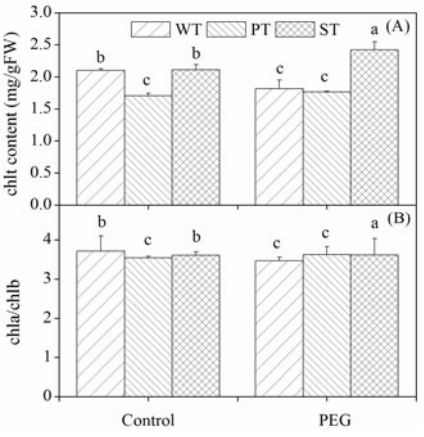

Fig. 2. Effect of water-primed (WT), PEG-primed (PT), and SA-primed (ST) on chlorophyll content of rice subjected to PEG stress

Under control condition, in PT, SOD and POD activities were lower but CAT activity was similar as compared to WT (Fig. 4). Under PEG stress, in PT, the CAT and POD activities were lower as compared to WT, whereas the SOD activity was almost equal to that of WT. However, under PEG stress, as compared to WT, SOD and POD activities were significantly higher while CAT was significantly lower in ST.

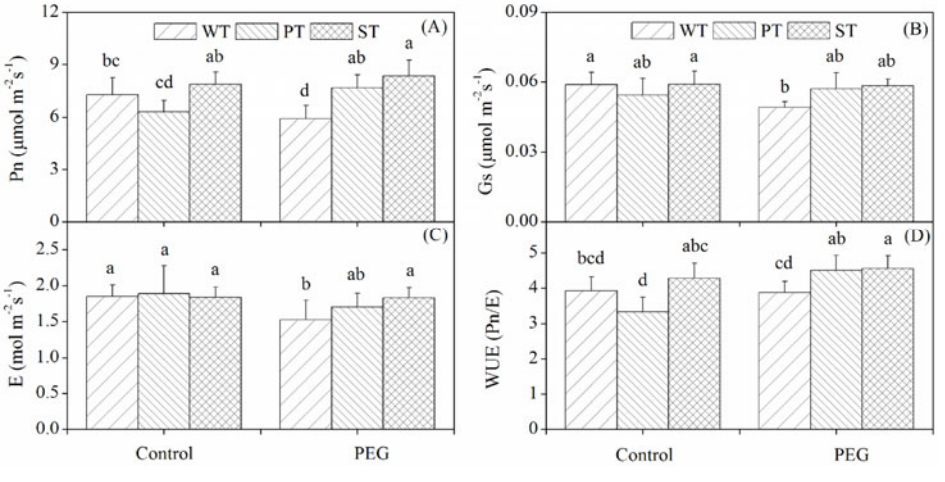

Fig. 3. Effect of water-primed (WT), PEG-primed (PT), and SA-primed (ST) on net photosynthetic rate, Pn (A), stomatal conductance, Gs (B), transpiration rate, E (C) and water use efficiency, WUE (D) of rice subjected to PEG stress

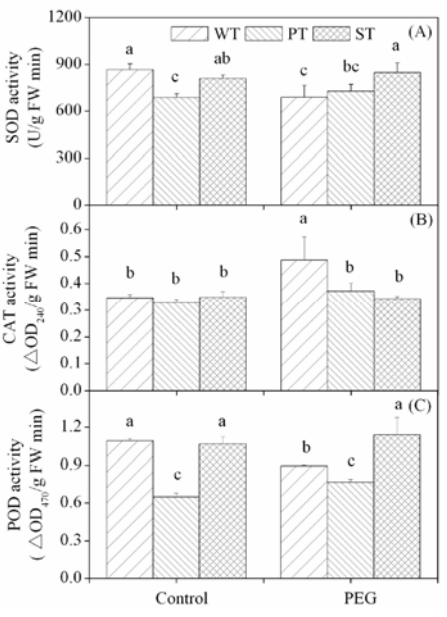

Fig. 4. Effect of water-primed (WT), PEG-primed (PT), and SA-primed (ST) on antioxidant enzymes activity of rice subjected to PEG stress

The accumulation of proline was lower under control condition; however, significant accumulation was observed in response to PEG stress. The level of proline under PEG stress was higher in ST and lower in PT as compared to WT (Fig. 5).

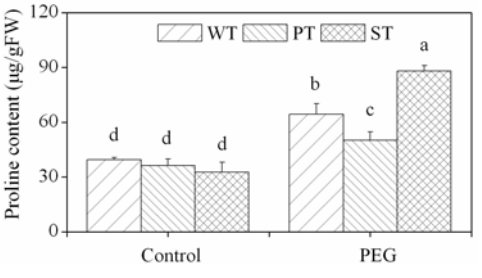

Fig. 5. Effect of water-primed (WT), PEG-primed (PT), and SA-primed (ST) on proline content of rice subjected to PEG stress

4 Discussion

Many researches have showed that SA generates an array of metabolic responses in plants and affects plant water relations [7]. Data presented in this study indicated that SA-primed and PEG-primed may help reduce adverse effects of water stress in rice. Under PEG stress, root length increased in ST and PT as compared to that of WT.

The increase in root length can maintain water balance by increasing water absorption.

Under PEG stress, total chlorophyll content, an important parameter for the measurement of growth, increased in ST as compared to WT and PT. Korkmaz et al [8] reported that the application of SA increased relative chlorophyll content. Furthermore, SA treatment was found to enhance the net photosynthetic rate, water use efficiency, stomatal conductance and transpiration rate in *Brassica juncea* [9]. Similar results were obtained in PEG-primed and SA-primed in this study. Higher chlorophyll content, water use efficiency, stomatal conductance and transpiration rate may have caused higher photosynthesis, which in turn enhanced the growth.

Antioxidant defense system plays vital roles in plant's tolerance to stressful conditions. There is data supporting that SA increases the activity of antioxidant enzymes such as CAT, POD and SOD [10], which in turn protect plants against ROS generation and membrane injury or may affect synthesis of other protective substances [11]. On the other hand, it was reported that SA treatment increased the activities of SOD and APX but inhibited CAT activity [12]. Our results showed that ST increased SOD and POD activities, while PT and ST decreased CAT activity under PEG stress.

Plants subjected to water stress accumulate molecules such as sugars and proline in their tissues. This accumulation may serve as a means of osmotic adjustment, which protect plant's tissues from damaging effects of water stress. Our results indicated that proline was accumulated to a higher level under PEG stress in ST, indicating the plant's response to maintain the osmotic homeostasis. PT showed lower accumulation of proline under PEG stress, as compared to WT, which signified the better maintenance of water balance in WP treatment that delimited the need for the synthesis of osmolytes.

Summarizing the findings, we demonstrate that seedlings given PT and ST perform better under PEG stress as compared to WT. We propose that PT and ST might cause the positive changes at the epigenetic level at an early stage of seed treatment to occur and activate set of genes to combat the stress. However, this proposed hypothesis needs further investigation.

Acknowledgment. This work was supported by the National Natural Science Foundation of China (30870205, 31070285).

References

1. Nemeth, M., Janda, T., Hovarth, E., Paldi, E., Szali, G.: Exogenous salicylic acid increases polyamine content but decrease drought tolerance in maize. Plant Sci. 162, 569–574 (2002)
2. Kang, G.Z., Wang, Z.X., Sun, G.C.: Participation of H_2O_2 in enhancement of cold chilling by salicylic acid in banana seedlings. Acta Bot. Sin. 45, 567–573 (2003)
3. Arfan, M., Athar, H.R., Ashraf, M.: Does exogenous application of salicylic acid through the rooting medium modulate growth and photosynthetic capacity in two differently adapted spring wheat cultivars under salt stress? J. Plant Physiol. 6, 685–694 (2007)

4. Yang, Y.N., Qi, M., Mei, C.S.: Endogenous salicylic acid protects rice plants from oxidative damage caused by aging as well as biotic and abiotic stress. Plant J. 40, 909–919 (2004)
5. Beyer, W.F., Fridovich, I.: Assaying for superoxide dismutase activity: some large consequences of minor changes in conditions. Anal. Biochem. 161, 559–566 (1987)
6. Chance, B., Maehly, A.C.: Assay of catalase and peroxidases. Methods Enzymol 11, 764–775 (1955)
7. Hayat, Q., Hayat, S., Irfan, M., Ahmad, A.: Effect of exogenous salicylic acid under changing environment: a review. Environ. Exp. Bot. 68, 14–25 (2010)
8. Korkmaz, A., Uzunlu, M., Demirkiran, A.R.: Treatment with acetyl salicylic acid protects muskmelon seedlings against drought stress. Acta Physiol. Plant. 29, 503–508 (2007)
9. Fariduddin, Q., Hayat, S., Ahmad, A.: Salicylic acid influences net photosynthetic rate, carboxylation efficiency, nitrate reductase activity, and seed yield in Brassica juncea. Photosynthetica 41, 281–284 (2003)
10. Hayat, S., Hasan, S.A., Fariduddin, Q., Ahmad, A.: Growth of tomato (Lycopersicon esculentum) in response to salicylic acid under water stress. J. Plant Interact. 3, 297–304 (2008)
11. Kadioglu, A., Saruhan, N., Saglam, A., Terzi, R., Acet, T.: Exogenous salicylic acid alleviates effects of long term drought stress and delays leaf rolling by inducing antioxidant system. Plant Growth Regul., doi:10.1007/s10725-010-9532-3
12. Janda, T., Szalai, G., Rios-Gonzales, K., Veisz, O., Paldi, E.: Comparative study of frost tolerance and antioxidant activity in cereals. Plant Sci. 164, 301–306 (2003)

Exogenous Treatment with Salicylic Acid Attenuates Ultraviolet-B Radiation Stress in Soybean Seedlings

Lihong Zhang[1] and Xuemei Li[2]

[1] Environmental Science Department, Liaoning University
Shenyang, 110036, China
[2] College of Chemical and Life Science, Shenyang Normal University
Shenyang, 110034, China
{lihongzhang132,lxmls132}@163.com

Abstract. Soybean (Glycine max L.) seedlings were sprayed with salicylic acid (SA) and treated with UV-B radiation of 7.1 Wm-2. Exposure of UV-B significantly reduced the shoot height, root length, shoot and root fresh weight. Exogenous application of SA moderated the reduction of growth. UV-B significantly reduced contents of chlorophyll (Chl) a and b, photosynthetic rate (Pn), stomatal conductance (gs), but increased carotenoids (Car) and flavonoids content. Exogenous application of SA mitigated the reduction of Chl, Car, Pn, gs and the increase of flavonoids in plants treated with UV-B. Exogenous application of SA did not moderate transpiration rate (E) and water use efficiency (WUE) reduction. There was no significant difference in Fv/Fm and Fv/Fo in all treatments. Foliar spray of SA counteracted the UV-B effects on soybean.

Keywords: UV-B radiation, salicylic acid, photosynthesis, chlorophyll fluorescence.

1 Introduction

The level of UV radiations in the environment is increasing day by day and the plants, which use direct sunlight for photosynthesis are unable to avoid UV radiations which imparts adverse effects on photosynthesis and other physiological processes [1]. Failure to protect from UV-B may result in a wide range of morphological, physiological and metabolic responses including altered plant growth, reduced yield, damage to photosystem II (PSII), affected chlorophyll fluorescence and decrease in chlorophyll content [2,3].

Salicylic acid (SA) acts as a signal involved in the expression of specific responses in plants to biotic and abiotic stresses. SA induced significant effects on various biological aspects in plants [4]. It has been reported that plants accumulated large amounts of SA when exposed to UV radiations [5]. Exogenous application of SA increased yield and number of pods in mung bean [6]. Ervin et al. [7] showed that the exogenous application of salicylic acid alleviated the damaging effects induced by UV-B radiation exposure in Kentuky blue grass. Further, SA stimulated photosynthetic machinery, increased the content of chlorophyll (Chl) [8,9]. Although SA has a beneficial effect against different abiotic or biotic stresses, the compound

E. Zhu and S. Sambath (Eds.): Information Tech. and Agricultural Eng., AISC 134, pp. 889–894.
springerlink.com © Springer-Verlag Berlin Heidelberg 2012

itself stressed the plants. It has been reported that SA plays different roles based on its endogenous levels in particular plant species under specific developmental and environmental conditions [10].

The aim of the present study was to investigate the effects of SA on the photosynthesis of UV-B stressed plants.

2 Materials and Methods

Plant material and growth conditions. Soybean cultivars (*Glycine max* cv.Tiefeng 29) were grown from seed in pots. Each pot was filled with vermiculite and seedlings were watered to saturation on alternate days with Hoagland solution in a greenhouse (25℃ day/20℃ night, 16 h/8 h light/dark period, 800 μmol m^{-2} s^{-1} photosynthetically active radiation and 80% relative humidity).

UV-B and SA treatment. Supplemental UV-B was provided artificially by UV-B fluorescent tubes (Beijing Electric light Source Research Institute, 40 W, China). The 30 cm distance between the top of the seedling canopy and UV-B lamps were kept constant by adjusting steel frame. The radiation was filtered through 0.127 mm cellulose diacetate to remove all incident UV-C (<280 nm). The seedlings were exposed to UV-B irradiation with a density of 7.1 Wm^{-2}.

After 15 d from sowing the seedlings were subjected to one of four treatments: (a) control, (b) SA: seedlings treated with SA (0.5 mM), (c) UV-B: seedlings that received UV-B, (d) SA+UV-B: seedlings pre-treated with SA (0.5 mM) and then exposed to UV- B.

Seedlings were irradiated with UV-B radiation (280–320 nm), 6 h d^{-1}, from 10:00-16:00. Before UV-B treatment, 0.5 mM SA solutions were sprayed once on leaves. The seedlings were treated for 6 d for harvest. All parameters were measured at 3 and 6 d after the beginning of the experiment. Each treatment was carried out in triplicate.

Biomass production and growth. Biomass production and growth parameters were determined at 6 d after treatment. At harvest, the seedlings were divided into roots and shoots. Seedling biomass was measured on fresh weight basis.

Photosynthetic pigment determination. Total chlorophyll and carotenoid contents were extracted from 0.1 g of leaf discs with 10 ml 80% acetone and absorbances at 663, 645, and 470 nm were measured.

Analysis of flavonoids. Fresh sample was immersed in an 80% ethanol 20% water solution (v/v) at a rate of 10 mg of tissue/mL of solution and incubated at 55℃ for 30min. Absorption spectra were obtained at room temperature.

Photosynthetic parameters. Gas exchange by leaves was measured with a Li-6400 portable photosynthesis system (Li-COR Company, USA). Net photosynthetic rate (Pn), stomatal conductance (gs) and transpiration rate (E) were measured under ambient CO_2 (370 μmol mol^{-1}) under saturated light between 10:00 and 12:00. Gas exchange was measured average values of three seedlings were considered as one replicate.

Chlorophyll fluorescence. Fluorescence parameters of intact leaves were measured using Li-6400-40LCF. After 30 min of dark adaptation, the fluorescence was

measured at exposure to a 1600 μmol m^{-2} s^{-1} flash of actinic red light at λmax=650 nm. The measurements were carried out in the morning. For each sample, we measured *F*o: initial fluorescence (all reaction centres of PSII open), *F*m: maximum fluorescence (all reaction centres of PSII closed), *F*v/*F*m: quantum yield of PSII, variable fluorescence: i.e. *F*v=(*F*m−*F*o), *F*v/*F*o: the potential activity of PSII.

Statistical analysis. Statistical analysis was carried out by one-way analysis using SPSS (SPSS Inc., USA, version 13.0). Differences between treatments were resulted to be statistically significant when they occurred at $P<0.05$.

3 Results

Exposure of UV-B significantly reduced the shoot height, root length, shoot and root fresh weight (Table 1). Exogenous application of SA moderated the shoot height, shoot and root fresh weight reduction but had no effect on the root length.

UV-B significant decreased Chl a and Chl b contents but increased flavonoids content compared with control on days 3 and 6, respectively (Fig. 1). Exogenous application of SA moderated Chl reduction and flavonoids increase. UV-B significant increased Car content on days 3 then decreased on days 6. Exogenous application of SA inhibited Car increase at 3 d then promoted Car reduction on days 6.

Table 1. Changes in shoot height, root length, shoot and root fresh weights of soybean seedlings in response to UV-B treatment in presence or absence of salicylic acid (SA).

Treatment	Shoot height (cm)	Root length (cm)	Shootfreshweight (g/plant)	Rootfresh weight (g/plant)
CK	23.92±1.24a	17.67±2.86a	1.39±0.14a	0.53±0.07a
SA	24.05±1.24a	17.50±2.09a	1.40±0.13a	0.55±0.06a
UV-B	17.60±1.14b	13.20±3.27b	1.02±0.10b	0.42±0.06b
SA+UV-B	19.50±2.43c	13.17±1.06b	1.27±0.17a	0.55±0.07a

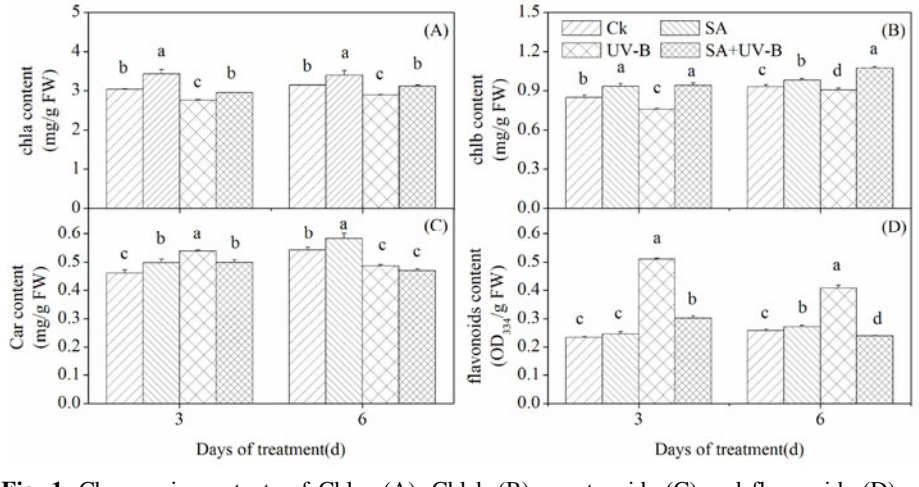

Fig. 1. Changes in contents of Chl a (A), Chl b (B), carotenoids (C) and flavonoids (D) of soybean seedlings in response to UV-B treatment in presence or absence of salicylic acid (SA)

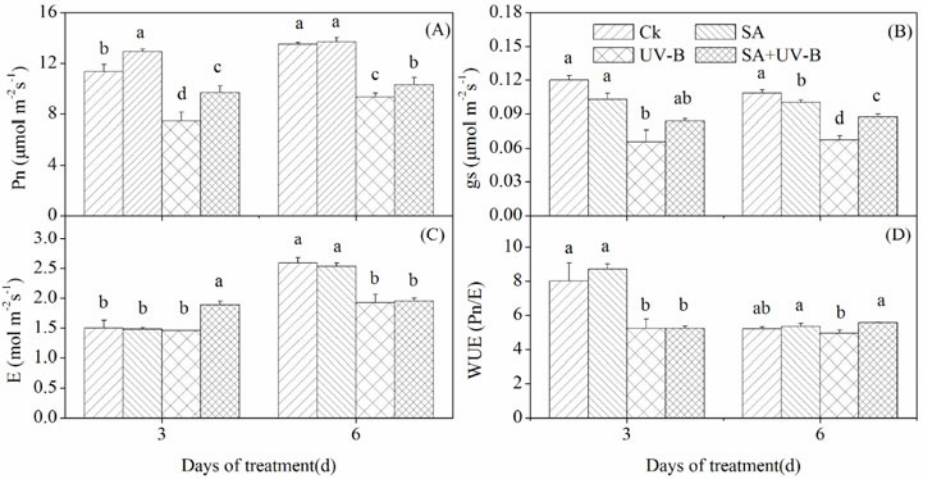

Fig. 2. Changes in net photosynthetic rate, Pn (A), stomatal conductance, gs (B), transpiration rate, E (C) and water use efficiency, WUE (D) of soybean seedlings in response to UV-B treatment in presence or absence of salicylic acid (SA).

Exposure of UV-B significantly decreased net photosynthetic rate (Pn) and stomatal conductance (gs) compared with control on days 3 and 6, respectively (Fig 2). Exogenous application of SA inhibited Pn and gs reduction. Exposure of UV-B significantly decreased transpiration rate (E) on days 6 and water use efficiency (WUE=Pn/E) on days 3. Exogenous application of SA did not moderate E and WUE reductions.

There was no significant difference in Fv/Fm and Fv/Fo in all treatments throughout the experimental period (Fig. 3).

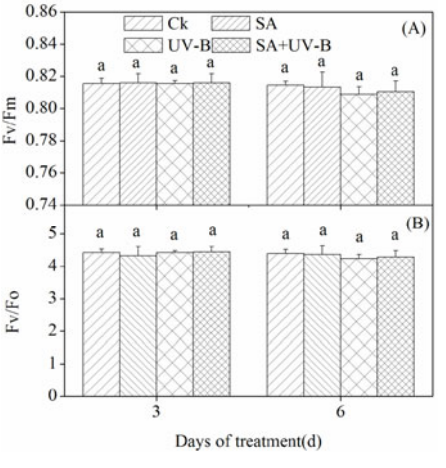

Fig. 3. Changes in Fv/Fm (A) and Fv/Fo (B) of soybean seedlings in response to UV-B treatment in presence or absence of salicylic acid (SA)

4 Discussion

In the present study, exposure of UV-B decreased the growth of soybean seedlings. The growth inhibition was found to be associated with UV-B induced decrease in net photosynthesis and water-use efficiency. Our result is similar to the other report on leguminous crops [11]. Salicylic acid-induced increase in the growth of soybean under UV-B stress can be attributed to an increase in photosynthesis.

The UV-B induced decrease in contents of photosynthetic pigments in agreement with findings of Mahdavian *et al.*[8] in pepper. UV-B significantly decreased Chl contents, primarily because UV-B destroyed the structure of chloroplast, inhibited synthesis of Chl and increased the rate of Chl degradation. We found that SA treatment counteracted pigment destruction. In soybean plants treatment with SA, pigment contents were increased [9]. Contents of flavonoids increased rapidly in response to UV-B radiation. The flavonoids play many defensive roles in plants, and interception of UV-B by epidermal flavonoids is often proposed as an adaptive mechanism preventing UV-B from reaching the mesophyll and affecting photosynthesis [12].

Photosynthesis of soybean seedlings was adversely affected by UV-B irradiation. Similar effects were noticed in other studies [13]. The decrease in net photosynthetic rate may be correlated with the decrease in contents of photosynthetic pigments (Fig. 1) as observed in the present study. It has been observed that alteration in photosynthesis with exogenous SA under environmental stresses could be due to either non-stomatal or stomatal factors [14]. In the present study, salicylic acid-induced increase in photosynthesis of soybean under UV-B stress can be attributed to an increase in gs. However, quantum yield of PSII (Fv/Fm) was not changed due to UV-B stress or SA application, which is in agreement with findings of Arfan *et al.*[15] in pepper. Thus, quantum yield of PSII cannot be considered as one of the factors to regulate Pn in soybean seedlings. Thus, the adverse effects of UV-B on growth, photosynthetic pigment and photosynthesis in soybean seedlings can be alleviated by foliar spray of SA.

Acknowledgment. This work was supported by the National Natural Science Foundation of China (31070285, 30870205).

References

1. Rajendiran, K., Ramanujam, M.P.: Alleviation of ultraviolet-B radiation induced growth inhibition of green gram by triadimefon. Biol. Plant 46, 621–624 (2003)
2. Germ, M., Kreft, I., Osvald, J.: Influence of UV-B exclusion and selenium treatment on photochemical efficiency of photosystem II, yield and respiratory potential in pumpkins (Cucurbita pepo L.). Plant Physiol. Biochem. 43, 445–448 (2005)
3. Surabhi, G.K., Reddy, K.R., Singh, S.K.: Photosynthesis, fluorescence, shoot biomass and seed weight responses of three cowpea (Vigna unguiculata (L.)Walp.) cultivars with contrasting sensitivity to UV-B radiation. Environ. Exp. Bot. 66, 160–171 (2009)
4. Hayata, Q., Hayata, S., Irfan, M., Ahmad, A.: Effect of exogenous salicylic acid under changing environment: A review. Environ. Exp. Bot. 68, 14–25 (2010)

5. Yalpani, N., Enyedi, A.J., Leon, J., Raskin, I.: Ultraviolet light and ozone stimulate accumulation of salicylic acid, pathogenesis-related proteins and virus resistance in tobacco. Planta 193, 372–376 (1994)
6. Singh, G., Kaur, M.: Effect of growth regulators on padding and yield of mung bean (Vigna radiata L.) Wilczek. Indian J. Plant Physiol. 23, 366–370 (1980)
7. Ervin, E.H., Zhang, X.Z., Fike, J.H.: Ultraviolet-B radiation damage on Kentucky Bluegrass II: hormone supplement effects. Hort Sci. 39, 1471–1474 (2004)
8. Mahdavian, K., Kalantari, K.M., Ghorbanli, M., Torkzade, M.: The effects of salicylic acid on pigment contents in ultraviolet radiation stressed pepper plants. Biol. Plant. 52(1), 170–172 (2008)
9. Zhao, H.J., Lin, X.W., Shi, H.Z., Chang, S.M.: The regulating effects of phenolic compounds on the physiological characteristics and yield of soybeans. Acta Agron. Sin. 21, 351–355 (1995)
10. Pancheva, T.V., Popova, L.P., Uzunova, A.N.: Effects of salicylic acid on growth and photosynthesis in barley plants. J. Plant. Physiol. 149, 57–63 (1996)
11. Amudha, P., Jayakumar, M., Kulandaivelu, G.: Impacts of ambient solar UV (280–400 nm) radiation on three tropical legumes. J. Plant Biol. 48, 284–291 (2005)
12. Liu, L., Gitz, D.C., McClure, J.W.: Effects of UV-B on flavonoids, ferulic acid, growth and photosynthesis in barley primary leaves. Physiol. Plant. 93, 725–733 (1995)
13. An, L.Z., Chen, T., Qiang, W.Y., Xu, S.J., Zhang, M.X., Wang, X.L., Cheng, G.D.: The effect of enhanced ultraviolet-B radiation on growth, photosynthesis and stable carbon isotope composition (δ13C) of two soybean cultivars (Glycine max) under field conditions. Environ. Exp. Bot. 49, 1–8 (2003)
14. Dubey, R.S.: Photosynthesis in plants under stressful conditions. In: Pessarakli, M. (ed.) Photosynthesis, pp. 717–737. CRC Press, Taylor and Francis Group, NY (2005)
15. Arfan, M., Athar, H.R., Ashraf, M.: Does exogenous application of salicylic acid through the rooting medium modulate growth and photosynthetic capacity in two differently adapted spring wheat cultivars under salt stress? J. Plant Physiol. 164, 685–694 (2007)

Effect of Cold-Active Protease Treatments on Bigeye Tuna (Thunnus obesus) Meat during Chilled Storage

Wang Quan-fu[1], Hou Yan-hua[2], and Yan Pei-sheng[2]

Harbin Institute of Technology, Harbin, China
Harbin Institute of Technology at Weihai, Weihai, China
{marry7718,houyanhua2006}@163.com, psyan6@hotmail.com

Abstract. The effects of cold-active protease treatments on shelf life and the taste of bigeye Tuna (Thunnus obesus) meat during chill storage were examined. The cold-active protease produced by Antarctic sea ice bacteria Pseudoalteromonas sp.NJ276 were sprayed onto the surfaces of fish samples, and then stored at 0 oC for 20 days. The control and the treated fish samples were analyzed periodically for microbiological (total viable count), chemical (pH, TBA, TVB-N and TMA-N), and the amino acids composition. The results indicated that the effect of cold-active protease on fish samples was to extend the shelf life and improve the taste, which had potential application in sea fish processing industry.

Keywords: Cold-active protease, thunnus obesus, free amino acid, taste, shelf-life.

1 Introduction

Cold-active enzymes are produced by organisms existing in permanently cold habitats. Antarctica sea ice, which characterized by strong seasonal changes in low-temperature (–50 °C in winter), high dissolved oxygen and high-salinity (150‰ salinity in sea ice saline channels), is considered as an extreme cold environment on the earth [1]. Bacteria living within Antarctic sea ice have a high potential for biotechnological applications as they produce a variety of cold-active enzymes [2]. Numerous studies have indeed shown that cold-active enzymes are generally characterized by higher turnover numbers (k_{cat}) and catalytic efficiencies (k_{cat}/K_m) at low temperatures (<10 °C) compared to their mesophilic counterparts. Cold-active proteases, constitute an important group of these enzyme, offer novel opportunities for biotechnological exploitation in cleaning detergents, leather processing, food processing and molecular biology based on their high catalytic activity at low temperature and low thermostability and novel substrate specificities [3].

Export of frozen marine fish from china is on the increasing trend, but the consumers in the international market prefer fresh fish than processed fish. Compared with frozen fish, chilled fish keeps its original colour and taste, and maintains nutritional value during the course of freezing and thawing [4]. In our provious study, the protease produced from the psychrophilic bacterium *Pseudoalteromona*s sp. NJ276, was identified as serine protease. Its optimum activity temperature was around 30 °C. Most

E. Zhu and S. Sambath (Eds.): Information Tech. and Agricultural Eng., AISC 134, pp. 895–902.
springerlink.com © Springer-Verlag Berlin Heidelberg 2012

importantly, its protease activity under 0 °C exhibited nearly 30% of the optimum activity, moreover, it had high tolerance to a wide range of NaCl concentrations (0-3M) and broad substrate specificities [5]. These properties were specific compared with other cold-active proteases, which would make this protease interesting for application food processing and bioremediation in low-temperature and high-salinity industry. This paper first reports the effects of cold-active protease treatments on shelf life and the taste of bigeye Tuna (*Thunnus obesus*) meat during chill storage, as assessed by chemical, microbiological and the amino acids composition.

2 Materials and Methods

2.1 Bacteria and Their Cultivation

P.sp. NJ276 (GenBank, accession number AY781155) producing cold-active protease was isolated from Antarctic sea ice (68°30′E, 65°00′S). Strain was inoculated in the 2216E medium (peptone 0.5%, yeast extract 0.1%, pH 7.5, made by natural sea water) with shaking at 100 rpm and 8 °C.

2.2 Proteases Preparation

Cells were removed from the culture medium by centrifugation at 12 000 rpm for 15 min at 4 °C and the supernatant fluid was extracellular proteases. The purified protease as the material were performed by a method of Wang et al.[5].

2.3 Samples Preparation and Storage of Fish

Samples were obtained from the tropical Pacific Ocean in October, 2008. Fish samples were stored in boxes with ice after catching and delivered to the laboratory in insulated containers. After delivery, whole fish were filleted (length of 12+1.8 cm and weight of 100+8.0 g). 10 ml cold-active protease (250 U/ml) and 1%(w/w) NaCl were sprayed onto the surface of the samples. The control was sprayed with the same amount of distilled water containing 1%(w/w) NaCl. After that they were surrounded by flake ice at a fish-ice ratio of 2:1 (w/w) and stored in a refrigerated boxes at 0 °C. During storage, ice was added to the boxes as required. All analyses were performed in triplicate at regular intervals.

2.4 Microbiological Analysis

Total viable counts on fish samples were estimated by the standard plate count method. The bacterial loads of the fish samples were expressed as colony forming units (log CFU/g).

2.5 Biochemical Analysis

Determination of total volatile basic nitrogen (TVB-N). TVB-N content of samples was measured according to the Antonacopoulos (1960) method with some modifications. The results were expressed as mg TVB-N per 100 g fish muscle.

2.6 1.5.2 Determination of Trimethylamine Nitrogen (TMA-N)

TMA-N content of samples was determined by means of the picrate method, as previously described [6]. This involves the preparation of a 5% (w/v) trichloroacetic acid extract of fish muscle. TMA-N concentration was expressed as mg per 100 g fish muscle.

Determination of Thiobarbituric Acid (TBA). TBA were determined spectrophotometrically according to the method of Siu[7]. TBA values were expressed in units of mg malonaldehyde/kg sample.

pH Value Measurement. The pH value was recorded using a pH meter (Metrohm 691). Fish muscle (10 g) was homogenized thoroughly with 90 ml of distilledwater and the homogenatewas used for pH determination.

2.7 Amino Acid Analysis

The amino acids composition of proteins of samples was determined by using an automatic amino acid analyzer (HITACHI, 835-50) following GB/T14965-1994 methods (National Standard of PRC) besides tryptophan.

2.8 Amino Acid Analysis

Experiments were replicated twice on different occasions with different treated samples. Triplicate samples were taken per replicate. Data were subjected to analysis of variance (ANOVA). Significant differences were defined as $P < 0.05$.

3 Results and Discussion

3.1 Chemical Analysis

TVB-N changes. TVB-N is well documented as a useful index of fish freshness an index of the quality of fresh fish, and it is commonly used to evaluate spoilage of fresh and frozen fish during the storage period. TVB-N in marine fish is mainly composed of ammonia and primary, secondary and tertiary amines. A level of 35–40 mg TVB-N/100 g of fish muscle is usually regarded as spoiled [8]. Changes in TVB-N values for fish samples during the 20 day storage period are shown in Fig. 1. At the beginning of storage, the TVB-N value was 14.8 mg/100 g, indicating that the fresh fish samples was of good quality. The TVB-N contents showed an increasing trend in all samples. The increases of TVB-N reported by other authors during storage of various fish species in ice [9]. This increase was significantly lower ($P < 0.05$) in the treated samples than in the control samples after day 8. The TVB-N value in the control samples surpassed 30 mg/100 g, while that in the treated samples increased over 25.1 mg/100 g at the end of the storage period. Low levels of TVB-N in treated samples were due to either a reduced bacterial population or decreased capacity of bacteria for oxidative deamination of non-protein nitrogen compounds or both [10].

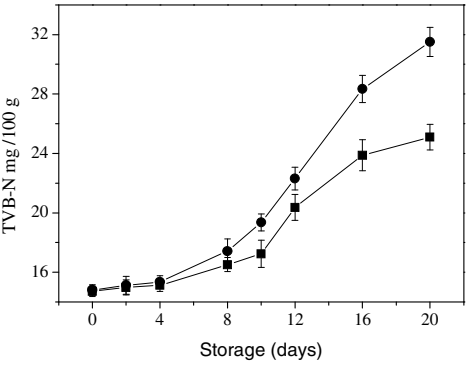

Fig. 1. Changes in TVB-N values of bigeye Tuna (*Thunnus obesus*) meat treated with cold-active protease and and untreated during storage at 0 °C. ● (Control); ■(Treated).

TMA-N changes. TMA-N is produced by the decomposition of trimethylamine oxide (TMAO) caused by bacterial action and possibly through the action of intrinsic enzymes [11],which has been used as an indicator of fish meat quality during storage. Changes in TMA-N values for fish samples during the storage are shown in Fig. 2. The initial TMA-N content of mackerel used in the study was 2.30 mg /100g. On storage, the TMA-N content increased gradually in all samples. This increase was significantly lower ($P< 0.05$) in the treated samples than in the control samples after day 8. The TMA-N value in the control samples reached 5.32 mg/100g at the end of the storage period, which exceeded the limit for acceptability of 5.0-10 mg/100g in fish [12]. While that in the treated samples increased over 4.12 mg/100 g at the end of the storage period, indicating that the treated fish were still fresh in this study.

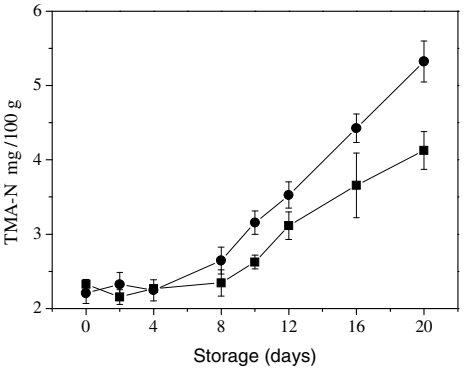

Fig. 2. Changes in TMA-N values of bigeye Tuna (Thunnus obesus) meat treated with cold-active protease and and untreated during storage at 0 °C. ● (Control); ■(Treated).

TBA changes. TBA value is a measure of oxidative rancidity of the product. Changes in TBA values for fish samples during the 20 day storage period were shown in Fig.3. The TBA contents of fish samples showed an increasing trend in all samples. The increase in TBA value during the iced storage may be attributed to the partial

dehydration of fish and to the increased oxidation of unsaturated fatty acids. Other authors have reported the similar result[13]. Treated samples produced lower ($P < 0.05$) TBA values than that of the control samples after day 8. TBA value in the range 1-2 mg malonaldehyde/kg of fish sample is usually taken as the limit of acceptability [13]. In all the samples, the TBA values were within the limit throughout the storage period.

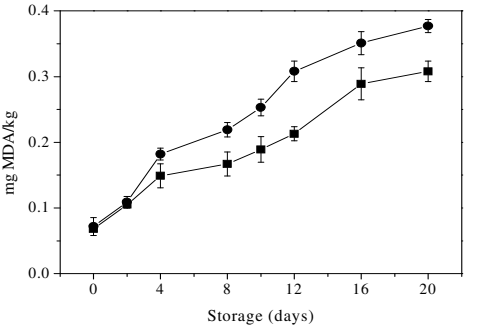

Fig. 3. Changes in TBA values of bigeye Tuna (Thunnus obesus) meat treated with cold-active protease and and untreated during storage at 0°C. ● (Control); ■(Treated) .

pH changes. Values of pH changes in fish samples were given in Fig. 3. The initial pH of fish samples was 5.62 (Fig .4). The pH values showed statistically significant ($p<0.05$) increases (5.98 and 5.89 for control and treated samples, respectively) at the end of the storage period. The increases in the pH are related to the accumulation of alkaline compounds, such as ammonia mainly derived from microbial action during fish muscle spoilage. Similar pH values were found for other fish species during storage in ice [18].

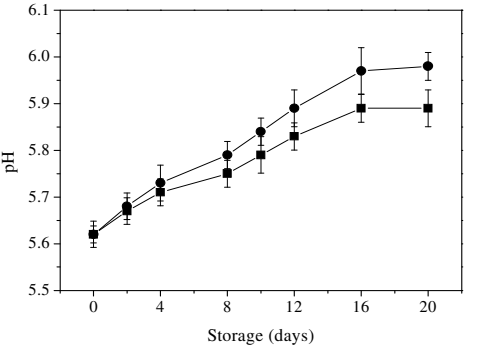

Fig. 4. Changes in pH values of bigeye Tuna (Thunnus obesus) meat treated with cold-active protease and and untreated during storage at 0 °C. ● (Control); ■(Treated) .

3.2 TVC Changes

Total viable counts (TVC) on fish samples were shown in Fig. 5. The initial quality of fish used in this study was good, as indicated by a low initial number of bacteria. There were increases in TVC over the period of storage. Treated samples showed statistically significant reduction ($p<0.05$) in bacterial counts compared to the control samples after day 4. The significant reduction in TVC observed in the treated samples could be attributed to the inhibitory effect of the spoilage bacteria.

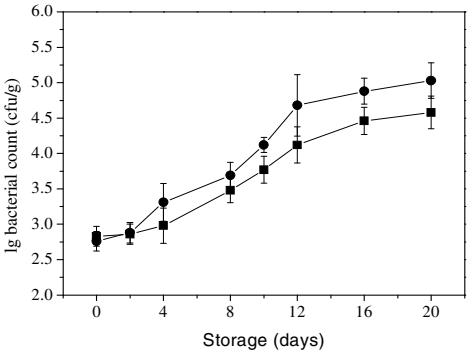

Fig. 5. Changes of Total viable count (TVC) in bigeye Tuna (Thunnus obesus) meat treated with cold-active protease and and untreated during storage at 0 °C. ● (Control); ■(Treated).

3.3 FAA Analysis

The free amino acids (FAA) present in Tuna meat are recognized as being important contributors to the flavour. Table 1 showed the FAA contents of fish sample. After treatment with cold-active protease, the amount of released free amino acids increased 1.31 times more than that from control. In the case of essential amino acids such as Thr, Lys, His and Arg, increase ($P<0.05$) compared with both in treated and in control. Eight free amino acids Glu, Asp, Met, Ser, Thr, Gly, Ala and Pro were identified to be the taste active components [14]. After treatment with cold-active protease the released Glu and Asp increased 3.99 and 1.27 times more than that from the control. Glu contributes to meat taste including 'umami' and 'brothy' descriptors, and is one of the important taste-active components of meat [15]. Therefore, treated sample with cold-active protease had better taste than the control.

The growing number of commercial refrigerated and frozen foods creates new needs for enzymes active at low temperatures for food processing and preservation. This study, in combination with current, knowledge on the potential use of cold-active protease as a ''natural'' preservative in foods was limited. Cold-active protease and might delay the growth of specific spoilage organisms by depleting metabolites required by other organisms, disrupting microbial cells, or degrading other enzymes [16]. In the present study, the significant reduction in TVC in treated samples, leading to minimal formation of chemical parameters (pH, TBA, TVB-N and TMA-N), more importantly, improving the taste, compared to the control samples. Therefore, as a new kind of taste enzyme, this cold-active protease has good potential in sea fish processing industry.

Table 1. Changes In The Free Amino Acids From Bigeye Tuna (*Thunnus Obesus*) Meat Treated With Cold-Active Protease And And Untreated At 0 ^{O}c For 16 Days

Amino acid	Control (%)	Treated (%)
Asp	0.081	0.103
Thr	0.064	0.080
Ser	0.022	0.054
Glu	0.164	0.655
Gly	0.025	0.039
Ala	0.501	0.634
Cys	⁄	⁄
Val	0.360	0.331
Met	0.336	0.309
Ile	0.208	0.180
Leu	0.353	0.326
Tyr	0.174	0.145
Phe	0.163	0.150
Lys	0.300	0.397
NH3	0.047	0.054
His	1.267	1.863
Arg	0.129	0.162
Trp	⁄	⁄
Pro	⁄	⁄
Summary	4.194	5.482

Acknowledgment. This study was supported by Program of Excellent Team in the Harbin Institute of Technology, China Postdoctoral Science Foundation (No.20090451004), the Natural Science Foundation of Shandong Province (No.ZR2009DQ023), Heilongjiang Province Postdoctoral Science Foundation (No. LRB 08-537), and Science and Technology Development Project of Weihai (No.2008087), and Natural Scientific Research Innovation Foundation in Harbin Institute of Technology (HIT-NSRIF200807).

References

1. Thomas, D.N., Dieckmann, G.S.: Antarctic sea ice - a habitat for extremophiles. Science 295, 641–644 (2002), doi:10.1126/science.1063391
2. Mock, T., Thomas, D.N.: Recent advances in sea ice microbiology. Environmental Microbiology 7, 605–619 (2005), doi:10.1111/j.1462-2920.2005.00781.x
3. Kasana, R.C.: Proteases from psychrotrophs: An overview. Critical reviews in microbiology 36, 134–145 (2010), doi:10.3109/10408410903485525
4. Ngapo, T.M., Babare, I.H., Reynolds, J., Mawson, R.F.: Freezing and thawing rate effects on drip loss from samples of pork. Meat Science 53, 149–158 (1999), doi:10.1016/S0309-1740(99)00050-9
5. Wang, Q.F., Hou, Y.H., Xu, Z., Miao, J.L., Li, G.Y.: Purification and properties of an extracellular cold-active protease from the psychrophilic bacterium Pseudoalteromonas sp. NJ276. Biochemical Engineering Journal 38, 362–368 (2008), doi:10.1016/j.bej.2007.07.025

6. Tozawa, H., Erokibara, K., Amano, K.: Poposed modification of Dyer's method for trimethylamine determination in codfish. In: Kreuzer, R. (ed.) Fish Inspection and Quality Control, pp. 187–190. Fishing News Books Ltd., London (1971)
7. Siu, G.M., Draper, H.H.: A survey of the malonaldehyde content of retail meats and fish. Journal of Food Science 43, 1147–1149 (1978), doi:10.1111/j.1365-2621.1978.tb15256.x
8. Lakshmanan, P.T.: Fish spoilage and quality assessment. In: Iyer, T.S.G., Kandoran, M.K., Mary, T., Mathew, P. (eds.) Quality Assurance in Seafood Processing, pp. 26–40. Society of Fisheries Technologists (India), Cochin (2000)
9. Huss, H.H.: Quality and quality changes in fresh fish. FAO Fisheries Technical Paper, 348 (1995)
10. Ruiz-Capillas, C., Moral, A.: Sensory and biochemical aspects of quality of whole bigeye tuna (Thunnus obesus) during bulk storage in controlled atmospheres. Food Chemistry 89, 347–354 (2005), doi:10.1016/j.foodchem.2004.02.041
11. Reddy, N.R., Roman, M.G., Villanueva, M., Solomon, H.M., Kautter, D.A., Rhodehamel, E.J.: Shelf-life and Clostridium botulinum toxin development during storage of modified atmosphere-packed fresh catfish fillets. Journal of Food Science 62, 878–884 (1997), doi:10.1111/j.1365-2621.1997.tb15478.x
12. Sikorski, Z.E., Kolakowska, A., Burt, J.R.: Post harvest biochemical and microbial changes. In: Seafood: Resources, Nutritional Composition and Preservation, pp. 55–76. CRC Press, Inc., Boca Raton (1989)
13. Erkan, N., Ozden, O.: Quality assessment of whole and gutted sardines (Sardina pilchardus) stored in ice. International Journal of Food Science & Technology 21, 1549–1559 (2008), doi:10.1111/j.1365-2621.2007.01579.x
14. Fuke, S.: Taste-active components of seafoods with special reference to umami substances. In: Shahidi, F., Botta, J.R. (eds.) Seafoods: Chemistry, Processing Technology and Quality, pp. 115–139. Blackie Academic and Professional, Glasgow (1994)
15. Yamaguchi, S.: Basic properties of umami and its effects on food flavor. Food Reviews International 14, 139–176 (1998), doi:10.1080/87559129809541156
16. Whitaker, J.R.: New and future uses of enzymes in food processing. Food Biotechnology 4, 669–697 (1990), doi:10.1080/08905439009549782

Application Efficacy of Biological Seed Coating Agent from Combination of PGPR on Cotton in the Field*

Zhansheng Wu[1,2], Lixia Yao[2], Imdad Kaleem[1], and Chun Li[1,**]

[1] School of Life Science, Beijing Institute of Technology, Beijing 100081, China
[2] School of Chemistry and Chemical Engineering, Shihezi University, Shihezi 832003, China
wuzhans@126.com, yaolixia303@163.com,
kaleemgcs@gmail.com, lichun@bit.edu.cn

Abstract. Application efficacy of the biological seed coating agent (BSCA) prepared with polyvinyl alcohol, sodium carboxymethyl celullose and Na-bentonite and having plant growth-promoting rhizobacteria (PGPR) Rs-5 and BCL-8, was investigated on cotton plants in the field. The results showed that the germination rate of cotton seeds treated with BSCA was increased by 11.3%, but the incidence rate of cotton seedlings was decreased by 10.8%, while other growth factors such as plant height, fresh weight, dry weight and leaf area of cotton seedlings were increased by 14.4%, 19.1%, 25.7% and 47.4% compared to treated with chemical seed coating agent (CSCA), respectively. Further analysis demonstrated that enzymatic activity of PAL, POD, PPO, SOD and photosynthetic pigment contents were improved to a certain extent as well, while MDA activity was declined. Moreover, the ionic uptake of Ca2+, Mg2+ and K+ in cotton was enhanced, while Na+ absorption was reduced in BSCA compared to CSCA. The yield of cotton seeds treated with BSCA was increased up to 10.5% in comparison with CSCA treatment. Hence, our results revealed that the use of BSCA could not only alleviate the adverse effects of salinity but also has a promising plant growth promoting potential in salinized soil.

Keywords: Biological seed coating agent, cotton, plant growth-promoting rhizobacteria.

1 Introduction

Cotton is an important cash crop in Xinjiang, the largest agricultural hub of China, but soil salinization has gradually become an enormous problem of this region and significantly decreased the net agricultural productivity. The major reasons for this secondary soil salinization are high rate of ground water evaporation, inappropriate water irrigation system, long-term drip irrigation and so on [1, 2]. In addition, the

* This work was financially supported by National Natural Science Foundation of China (20904033, 20976014) and Open Fund of Extremophiles Key Laboratory of Xinjiang Academy of Agricultural Science (XJYS0203-2009-01).
** Corresponding author.

E. Zhu and S. Sambath (Eds.): Information Tech. and Agricultural Eng., AISC 134, pp. 903–910.
springerlink.com © Springer-Verlag Berlin Heidelberg 2012

soil-borne pathogens, such as *Rhizoctonia solani, Pythium* spp. and *Fusarium* spp. are destructive disease causative agents of cotton plants and badly affect the cotton crop resulting in the huge economic losses to field-grow cotton in this area [3].

In recent years, a modern approach has been developed to biocontrol soil-borne pathogens and alleviate salt stress in plants by treating the crop seeds and seedlings with plant growth-promoting rhizobacteria (PGPR) for a more sustainable crop production [3-4]. PGPR are a group of root-colonizing bacteria in the rhizosphere of many plant species, and the application of PGPR may prove useful in developing strategies to facilitate plant growth in saline soils as these bacteria can facilitate rooting and growth of plants along with other beneficial effects on plants [5-7].

In our previous studies, we isolated *Klebsiella oxytoca* Rs-5 with 1-aminocyclopmpane-1-carboxylic acid deaminase activity from saline soil samples of cotton fields in Xinjiang province of China which successfully exhibited the ability to relieve salt stress and promote plant growth [1]. The bacterial combination BCL-8 (*Bacillus* sp. SL-13, *Bacillus* sp. SL-14 and *Bacillus* sp. SL-44) also showed great potential for growth-promotion and seedling protection against Rhizoctonia root rot disease-suppression on tomato [3].

For a successful practical application of the biological seed coating agent (BSCA), we used a combination of biocontrol strains BCL-8 and Rs-5 having growth-promoting and relieving-salt-stress bacteria on cotton seeds in the field. The main objectives of this study were to evaluate the application efficacy of BSCA for cotton along with other effects such as the germination rate of cotton seed, biomass of cotton, incidence of cotton seedlings, enzymatic activity of cotton seedling, photosynthetic pigment contents of cotton seedling, ionic uptake of cotton seedling and the yield of cotton in the field after their treatment with BSCA.

2 Materials and Methods

Materials. The microbial strain, *Klebsiella oxytoca* Rs-5 was isolated from the secondary salinized soil of cotton rhizosphere under the depth ranged between 5-25 cm layer in Xinjiang region of China [1]. The bacterial combination BCL-8 mixed with *Bacillus* sp. SL-13, *Bacillus* sp. SL-14 and *Bacillus* sp. SL-44 were screened from the rhizosphere of processing tomato in Xinjiang [3].The strain was cultivated at 30 °C and 200 rpm in NA broth (beef extract) consisting 10 g/l of tryptone, 5 g/l of beef extract, and 5 g/l of NaCl. The culture was collected for the preparation of BSCA at the early stationary phase.

Field-experiment design. We carried out various experiments at 121 Farms to evaluate the efficacy of BSCA on the disease control, relieving-salt-stress and promoting growth of cotton (*Gossypium hirsutum* L variety Xinluzao26) under secondary salinized soil of field, in Xinjiang, China. According to the chemical properties, the soil of the fields was termed as secondary salinized soil and the ratio of various contents was determined as: (g/kg) the total organic content 23.3, total nitrogen content 1.20, total phosphorous content 1.03, Ca 0.16, Mg 0.04, Na 1.10, K 0.10 and the total salt content 3.50. The cotton seeds were coated by biological seed coating agent (BSCA) and chemical seed coating agent (CSCA) with an equal number of microbial living cells (10^9 cfu ml^{-1}) (Wei Fu, 2.5 kg/ 100 kg) and then were placed

in the furrow at a depth of 4 cm after drying in the open air. The experiments were designed as a randomized complete block (RCB) with five replications. The germination rate of cotton seeds was recorded by counting the germinated seedlings per 100 holes after 10 days of sowing, while individual plant height, fresh weight (FW), dry weight (DW) and the incidence rate of cotton seedlings were recorded by counting the germinated seedlings, and various elemental contents such as calcium (Ca), potassium (K), magnesium (Mg) and sodium (Na) of cotton plants were determined from the dry weights by the same method as described in our previous experiment [1, 3] after 30 days of seed germination.

Determination of some defense-related enzymatic activites and MDA content. Some defense-related enzymes (MDA, SOD, POD, PAL, PPO) from cotton seedlings were extracted for the determination of their activities following the procedure described by zhao et al. [8]. The amount of MDA of cotton seedlings was measured by Thiobarbituric acid reaction as described by Rao et al. [9]. Specific absorbance at 532nm and non-specific absorbance at 600 nm were measured and expressed as μmol MDA per 1 g of fresh weight. SOD activity assay performed was based on the method of Beauchamp and Fridovich [9] which measures the inhibition rate in the photochemical reduction of nitroblue tetrazolium (NBT) spectrophotometrically at 560 nm wavelength and the specific enzyme activity was mentioned in units' mg^{-1} protein g FW. POD activity was determined as described in the literature [10] and expressed as $U \cdot g^{-1}$ $FW \cdot min^{-1}$ while PAL activity was measured by the method described by Liu et al. [11] and expressed as $0.01\Delta OD_{290} \cdot g^{-1} \cdot min^{-1}$. The activity of PPO was determined by the method termed as $0.001\Delta OD_{525} \cdot g^{-1} \cdot s^{-1}$ [11]. The above mentioned all determinations were repeated thrice for each variety.

Determination of photosynthetic pigment contents in cotton leaves. Chlorophyll a, chlorophyll b, total chlorophylls and carotenoids contents in cotton leaves were determined and calculated according to the procedure described by Wellburn [12]. Absorbance was measured by a spectrophotometer at various wavelengths of 470, 646 and 663 nm.

3 Results

Preparation and properties of BSCA. BSCA was prepared by selecting suitable coating materials, adjuvants materials and according to the compatible combination of microbial strains. The coating agent types and dosages were determined as a mixture of 2% PVA and 1% SCMC as the film-forming agent exhibited good film performance having concentration of 0.3% Na-bentonite as a tackifier, 0.8% sodium lignin sulfonate as a dispersant, 3% concentration of 1,3-propanediol as an antifreezing agent, less than 0.05% of concentration of potassium sorbate as preservative; and microbial strains Rs-5 and BCL-8 (the concentration of 10^9 cfu/ ml, volumetric ratio of 1:1) ≥ with an amount of living cells 10^9cfu/ml [4]. The living cells of the BSCA were determined as 10^9 cfu/ml and then coated for experiments. Biological seed coating demonstrated good film properties such as film formation time of 9 min, coating uniformity 98%, and off rate 0.15%; water swelling property 57.42 g/g, viscosity of 480 mPa·s, and coating volume of 10^6 cfu/seed.

Effect of the BSCA on growth-promotion of cotton plants. The germination rates of cotton seeds coated with BSCA were evaluated in different field experiments. The germination rate of BSCA treated seeds was increased up to 11.3% compared to CSCA. Moreover, plant height, dry weight, fresh weight and leaf area index in treatment of BSCA were increased by 14.4%, 19.1%, 25.7% and 47.4% compared to the CSCA respectively, while the incidence rate of cotton seedlings was significantly decreased by 10.8% in BSCA compared to CSCA treatment. These results revealed that BSCA is also beneficial in improving the germination rate of cotton seeds. It was also reported that *Achromobacter piechaudii* was capable of increasing the fresh and dry weights of tomato seedlings grown in the presence of 172 mM NaCl salt while tomato plants treated with *Bacillus subtilis* yielded the highest number of shoots as compared to the control [6]. More recently, Jalili et al. [5] reported the rate of germinating seeds inoculated with the strains of ACC deaminase-producing *Pseudomonas fluorescens* and *Pseudomonas putida*, and seedling growth were significantly higher under salinity stress. Therefore, from the results of our experiments, we can infer that the introduction of BSCA formulation into seeds could not only protect the plants against salt stress and soil-borne pathogens but also impart a positive effect on their growth promotion.

Table 1. Effect of BSCA and CSCA on the germination rate and growth promotion of cotton seedlings

Treatments	Germination rate (%)	Incidence rate(%)	Plant height (cm)	Dry weight (g)	Fresh weight (g)	Leafareaindex (dm^2)
CSCA	58.2±1.6	98.6±2.5	17.8±1.2	3.93±0.12	31.9±2.1	5.7±0.8
BSCA	69.5±2.3	87.8±2.7	21.4±1.5	4.68±0.25	40.1±2.5	8.4±0.6

Effect of BSCA on enzymatic activities and MDA content of cotton seedlings. Key enzymes involved in the disease resistance and detoxification of foreign pathogens in plant are named as PPO POD, PAL, and SOD. Therefore, these enzyme activities along with MDA content in cotton leaves in different treatments were investigated. Polyphenol oxidase (PPO) enzyme activity of cotton seedlings in treatment with BSCA, resulted in a increase of 7.9% as compared to CSCA. It was found that PPO activity was intensively induced by BSCA, which are defense-related proteins. The increase in activities of PPO and POD cause the accumulation of phenolic oxide, which could suppress the growth of pathogens, and PPO has its natural ability to oxidise either phenols or polyphenols that reflects its mechanism of action as a defensive or protective protein. The increase in cell wall resistance is also due to the defensive actions of PPO, since they are involved with melanin to form polymerised, insoluble complexes with PPO oxidised phenols generating a resistant barrier against the entry and spread of pathogens. POD activity of cotton leaves in BSCA treatment showed a sharp increase as well and it was 1.94 times higher than that of CSCA treatment. The POD activity is also positively correlated with plant resistance as during defensive response, POD is associated with the thickening of the plant cell wall that could form a stronger physical barrier against the invading

pathogens [8]. PAL activity of cotton leaves in BSCA treatment was enhanced by 7.8% compared to CSCA. The data suggested that stress stimulation could increase the PAL activity. PAL is considered to be a crucial enzyme of phenylpropanoid pathway, catalysing deamination of L-phenylalanine to trans-cinnamic acid [13] and produces many secondary metabolites, thus enhancing the ability of plant resistance against salt stress and foreign pathogens, so increase in PAL activity is positively correlated with the plants resistance against external factors. Examination of SOD activity revealed that there is no significant change in its activity in both treatments of BSCA and CSCA, while a slight non significant rise in SOD activity was observed as compared to CSCA which still shows a mild beneficial effect of BSCA over CSCA application.

The level of MDA in plant tissue is considered to be a measure of lipid peroxidation status and changes in phenylpropanoids metabolism are the major symptoms of the degree of salt stress injury. Hence, the production of MDA can be used as an indicator of membrane lipid peroxidation [14]. MDA content of cotton leaves in CSCA treatment was 1.14 times higher than BSCA treatment. So the application of BSCA could reduce the MDA content of cotton seedlings and alleviate the damage normally caused by salt stress. Salt stress exposure can alter the structure of the membranes due to lipid peroxidation. Therefore, change in MDA concentration of cells shows the structural integrity of the membranes of plants subjected to salt stress [15]. Hence, we observed that after biological seed coating, the activities of PAL, POD, PPO and SOD are increased than the control plants (CSCA). These enzymes play a vital role in defending the plant body from external stresses and pathogens [8]. So the combination of BSCA along with microbial strains contributes to enhance the ability of cotton plants against pathogens infection and salt stress conditions.

Table 2. Effect of BSCA and CSCA on enzymatic activities and MDA content of cotton seedling

Treatments	SOD U g^{-1} FW	POD$U \cdot g^{-1}$ $FW \cdot min^{-1}$	PPO$0.001\Delta OD_{525} \cdot g^{-1}$ $FW \cdot s^{-1}$	PAL$0.01\Delta OD_{290} \cdot g^{-1}$ $FW \cdot min^{-1}$	MDA$mmol \cdot g^{-1}$ FW
CSCA	272±12.4	2010±56	689±23	144.6±8.4	16.2±1.3
BSCA	295±13.2	3899±79	744±31	155.8±9.6	14.2±1.2

Effect of BSCA on ionic uptake of cotton seedlings. The ionic content of Mg, K, Ca and Na elements of cotton both treatments were measured after 30 days of germination. The Mg^{2+}, Ca^{2+} and K^{+} contents of cotton leaves in BSCA treatment were increased by 29.5%, 14.8% and 21.3% compared to CSCA, respectively. The content of Mg^{2+}, Ca^{2+} and K^{+} of cotton roots were also increased by 23.6%, 10.9% and 8.7% compared to CSCA, respectively. However, the content of Na^{+} in BSCA was decreased as compared CSCA treatment. Moreover, the treatment of BSCA resulted in an increase in the ratios of K^{+}/Na^{+} and Ca^{2+}/Na^{+} in cotton's leaves and were 3.16 times and 2.99 times higher, while in roots, these ratios were 1.54 times and 1.61 times higher than that of CSCA, respectively. So, these results suggested that

BSCA could strengthen cotton' absorbability of Ca^{2+}, Mg^{2+} and K^+, and weaken the absorbability of Na^+ under saline conditions providing an additional supply of Ca^{2+}, Mg^{2+} and K^+, which tend to replace exchangeable Na^+ on the adsorption sites.

The accumulation of Na^+ in tissues of plants growing in saline media restricts the uptake of essential nutrients (mainly K^+ and Ca^{2+}) [16]. In addition, the excessive salt amount adversely affects plant physical and chemical properties and under various biotic and abiotic stresses, plants exhibit a variety of responses to counter the effects of stresses that enable them to tolerate and evolve resistance to adverse conditions and BSCA assisted plants in this counter mechanism.

Table 3. Effect of BSCA and CSCA on ionic uptake of cotton L* leaves R*roots

Treatments	K(mg/g DW)	Na(mg/g DW)	Ca(mg/g DW)	Mg(mg/g DW)
BSCA-L	28.5±1.58	16.2±1.25	38.1±0.64	8.33±0.59
BSCA-R	43.8±2.01	37.5±1.31	14.2±0.82	7.18±0.47
CSCA-L	23.5±1.32	42.3±1.12	33.2±0.95	6.43±0.42
CSCA-R	41.2±1.97	54.3±1.51	12.8±0.52	5.81±0.45

Effect of BSCA on photosynthesis pigment contents of cotton leaves. The content of chlorophyll a, chlorophyll b, total chlorophylls and carotenoids of cotton in treatments of BCSA and CSCA were recorded after 30 days of their germination respectively. It was found that the content of chlorophyll a, chlorophyll b, total chlorophylls and carotenoids of cotton leaves in BSCA treated plants were enhanced by 6.9%, 12.2%, 8.7% and 16.5 % compared to CSCA treatment, respectively. These results revealed that BSCA could improve the photosynthesis of cotton seedlings. The increase in chlorophyll content may also be the result of increased photosynthetic leaf area of plant by inoculation of PGPR compared to uninoculated control.

This could be attributed either to an increase in synthesis and/or a decrease in degradation of chlorophyll, and to chlorophyllase activity stimulation [17]. It is considered that K^+ is involved in the photochemical reactions and high correlation was found between their utilization efficiency and photosynthetic activity [18]. Similarly for plant germination, more nutrients uptake, high enzymatic activities and photosynthetic pigment, are required and BSCA showed all such beneficial effects on cotton plants for photosynthesis.

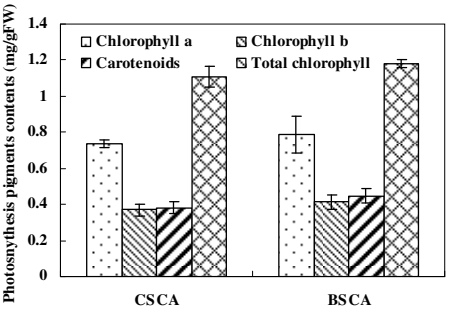

Fig. 1. Effect of BSCA and CSCA on pigment contents of cotton leaves

The effect of BSCA on the yield of cotton in field. BSCA application also increased the cotton boll number, boll weight and average yield by 8.4%, 6.4% and 10.5% compared to CSCA respectively thus increasing the yield. BSCA application with PGPR proved to be a good growth promoting and disease preventing method, and also conform to the modern developing trend of green agriculture, to avoid the target pathogens resistance to chemical fungicides. Similarly, it is concluded that inoculation with *Pseudomonas* or *Serratia* strains containing ACC-deaminase could be an effective approach for reducing/alleviating the stress-induced ethylene and consequently improving the growth and yield of wheat even in the presence of high salinity stress [7]. Such applications of BSCA can not only effectively control the cotton under salt stress, but also reduce the amount of pesticides and their residues in soil for an eco-friendly environment.

Table 4. Effect of BSCA and CSCA on yield of cotton in field

Treatments	Boll number /plant	Dry weight g /Boll	Yield (kg/666.7 m^2)
CSCA	5.35	4.84	333.9
BSCA	5.80	5.15	369.0

4 Conclusion

In the fields, the germination rate of the cotton seeds treated with BSCA increased up to 11.3%, but incidence rate of seedlings was lowered to 10.8%; total biomass (plant height, fresh weight, dry weight, leaf area) also increased. Some key enzymes PAL, POD, PPO and SOD activities improved, and MDA activity decreased, uptake of K^+, Ca^{2+}, Mg^{2+} increased, and Na^+ absorption decreased. BSCA application also increased the cotton output up to 10.5% compared to CSCA. Cotton coated with BSCA from the combination of PGPR not only proved helpful in improving the germination rate and biomass but also enhanced the resistance of cotton plants against salt stress. Therefore, these researches could provide some important theoretical basis and technical support for the development and application of biological seed coating agents to improve the yield of crops.

References

1. Yue, H., Mo, W., Zheng, Y., Li, C., Li, H.: The salt stress relief and growth promotion effect of Rs-5 on cotton. Plant Soil 297(1-2), 139–145 (2007)
2. Yao, L., Wu, Z., Zheng, Y., Imdad, K., Li, C.: Growth promotion and protection against salt stress by Pseudomonas putida Rs-198 on cotton. European Journal of Soil Biology 46(1), 49–54 (2010)
3. Tao, J., Li, H., Li, C.: Growth-promotion and disease control effect of combination BCL-8 on tomato and growth-promotion mechanism. Plant Protection 36(1), 87–90 (2010) (in Chinese)
4. Yao, L., Wu, Z., Li, C.: Film-forming properties of the blend films and effect on the inhibiting activity of biocontrol bacteria. Chinese Journa of Pesticide Science 11(3), 381–387 (2009) (in Chinese)

5. Jalili, F., Khavazi, K., Pazira, E., Nejati, A., Rahmani, H., Sadaghiani, H., et al.: Isolation and characterization of ACC deaminase-producing fluorescent pseudomonads, to alleviate salinity stress on canola (Brassica napus L.) growth. Journal of Plant Physiology 166(6), 667–674 (2009)
6. Mayak, S., Tirosh, T., Glick, B.: Plant growth-promoting bacteria confer resistance in tomato plants to salt stress. Plant Physiology and Biochemistry 42(6), 565–572 (2004)
7. Zahir, Z., Ghani, U., Naveed, M., Nadeem, S., Asghar, H.: Comparative effectiveness of Pseudomonas and Serratia sp. containing ACC-deaminase for improving growth and yield of wheat (Triticum aestivum L.) under salt-stressed conditions. Archives of Microbiology 191(5), 415–424 (2009)
8. Zhao, H., Zhao, H., Wang, B., Wang, J.: Effect of local stress induction on resistance-related enzymes in cucumber seeding. Colloids and Surfaces B-Biointerfaces 43(1), 37–42 (2005)
9. Rao, K., Sresty, T.: Antioxidative parameters in the seedlings of pigeonpea (Cajanus cajan L. Millspaugh) in response to Zn and Ni stresses. Plant Science 157(1), 113–128 (2000)
10. Wang, B., Wang, J., Zhao, H., Zhao, H.: Stress induced plant resistance and enzyme activity varying in cucumber. Colloids and Surfaces B-Biointerfaces 48(2), 138–142 (2006)
11. Liu, T.G.: Induced resistance of tobacco to TM V with non-fungicidal chemical compounds. J. Northeast Agric. Univ. 33(2), 129–133 (2002)
12. Wellburn, A.: The spectral determination of chlorophyll-a and chlorophhyll-b, as well as total carotenoids, using various solvents with spectrophotometers of different resolution. Journal of Plant Physiology 144(3), 307–313 (1994)
13. Janas, K., Cvikrová, M., Palagiewicz, A., Eder, J.: Alterations in phenylpropanoid content in soybean roots during low temperature acclimation. Plant Physiology and Biochemistry 38(7-8), 587–593 (2000)
14. Li, Q., Niu, H., Yin, J., Wang, M., Shao, H., Deng, D.: Protective role of exogenous nitric oxide against oxidative-stress induced by salt stress in barley (Hordeum vulgare). Colloids and Surfaces B: Biointerfaces 65(2), 220–225 (2008)
15. Jouve, L., Engelmann, F., Noirot, M., Charrier, A.: Evaluation of biochemical markers (sugar, proline, malondialdehhyde and ethylene) for cold sensitivity in microcuttings of two coffee species. Plant Science 91(1), 109–116 (1993)
16. Ghoulam, C., Foursy, A., Fares, K.: Effects of salt stress on growth, inorganic ions and proline accumulation in relation to osmotic adjustment in five sugar beet cultivars. Environmental and Experimental Botany 47(1), 39–50 (2002)
17. Santos, C.: Regulation of chlorophyll biosynthesis and degradation by salt stress in sunflower leaves. Scientia Horticulturae 103(1), 93–99 (2004)
18. Dos Santos, U., De Carvalho, G., Feldpausch, T.: Growth, leaf nutrient concentration and photosynthetic nutrient use efficiency in tropical tree species planted in degraded areas in central Amazonia. Forest Ecology and Management 226(1-3), 299–309 (2006)

Arsenite Exposure Induces Oxidative Stresses in the Nematode Caenorhabditis Elegans

Shunchang Wang[1], Zhizhong Geng[1], Yan Yu[1], and Jinhua Guo[2]

[1] School of Life Science Huainan Normal University Huainan, Anhui 232001, P.R. China
[2] Anhui Wenda College of Information and Technology
Hefei, Anhui 231201
scwangl@yahoo.com.cn, guojinhua08@163.com

Abstract. Arsenic is a ubiquitous environmental toxicant and is classified as the most hazards substances by ATSDR. It has been shown that arsenite exposure causes oxidative stress through the generation of ROS, and alters the expression of genes related to stress response and antioxidant activities. In the present studies, the nematode caenorhabditis elegans were exposed to graded doses of arsenite. The results presented here indicated that arsenite exposure increased the generation of ROS in a dose- and time-dependent manner. GST-4, SOD-3, HSP-4, and HSP-70 were semi-quantified using transgenetic strains carrying GFP as a reporter. The results indicate that arsenite exposure increased the expression of GST-4, HSP-4, and HSP-70, while the superoxide dismutase (SOD-3) kept steadily.

Keywords: Caenorhabditis elegans, arsenite, heat shock proteins, glutathione-S-transferase, superoxide dismutase.

1 Introduction

Inorganic arsenicals are ubiquitous environmental toxicants which represent a significant health problem for people worldwide. Arsenic has been classified as the principal and most potent hazardous substances by ATSDR. Chronic exposure to arsenic is associated with liver injury, peripheral neuropathy, and an increased incidence of cancer of the lung, skin, bladder, and liver [1,2]. Arsenic has been reported to cause multiple damages at cellular level, such as cell cycle arrest, mitotic spindle collapse, cytoskeletal injury and apoptosis. It has also been shown that arsenic exposure generates reactive oxygen species (ROS) and induces expression of stress response genes in many organism cells [3].

Arsenic has been studied in many animal models, which provide us with reliable data for a better understanding the mechanisms of arsenic toxicity. As a well-known oxidative stress inducer, arsenite exposure altered the expression of enzymes involved in free radical metabolism [4]. Heat shock proteins (HSPs) are highly conserved during evolution. The expression of HSPs functions in diverse cellular processes including stress responses [5,6]. Arsenite exposure induces HSPs expression in several cell lines and species, including the accumulation of HSP27 in C6 rat glioma cells, HSP70 in

E. Zhu and S. Sambath (Eds.): Information Tech. and Agricultural Eng., AISC 134, pp. 911–918.
springerlink.com © Springer-Verlag Berlin Heidelberg 2012

human breast MDA 231 cells and HSP30 and HSP70 in *Xenopus laevis* A6 kidney epithelial cells [7-9]. However, the antioxidant genes induced by arsenite in the in vivo animal models have not well investigated.

The nematode *Caenorhabditis elegans* has been widely used in developmental biology and genetics studies [10]. It is also a good model for stress response and aging, drug screens, genotoxic stress and environmental toxic studies [11,12]. Since Williams and Dusenbery proposed that *C. elegans* could be used as a model organism for aquatic toxicity tests, many researchers investigated its potential in various settings [13,14]. The *C. elegans* is a free-living worm that survives in terrestrial, benthic, and aquatic environments, where it can be exposed to many kinds of environmental toxicants such as heavy metals. It has a short lifespan, high fertility, easy to culture in laboratory, thereby producing many offspring in a short period of time, and reducing test costs. Moreover, the fully sequenced genome in which 60% of the genes have vertebrate counterparts, forward and reverse genetic tractability provides powerful tools to investigate the mechanisms of toxicants at organism-level. Also, there are plentiful transgenetic strains that carry GFP report genes, which provide us powerful tools to analysis the expression of many proteins in vivo.

The aims of the present study were to determine the effects of arsenite exposure on the generation ROS and the expression of GST-4, SOD-3 and HSPs in *C. elegans*.

2 Materials and Methods

Worm Strains and Reagents. Worm strains used in the present study were Wild-type N2, CL2166, CF1553, SJ4005, BC10060 and CL2070. All of the strains were provided by the Caenorhabditis Genetics Center, which is funded by the NIH National Center for Research Resources. Worms were cultured at 20 ^{o}C in Petri dishes on nematode growth medium (NGM) seeded with *Escherichia coli* strain OP50 as food. Synchronized worm cultures were obstained by lysing gravid hermaphrodites in an alkaline hypochlorite solution as described previously [15]. For the strain BC10060, only wild-type phenotype worms were maintained and picked for experiments. Sodium arsenite (NaAsO2, AsIII) was a commercial product of Sigma Chemical (St. Louis, MO), and 5',6'-chloromethyl-2',7'-dichlorodihydro-fluorescein diacetate (CM-H2DCFDA) were purchased from Molecular Probes (Eugene, OR).

Experimental Design. The procedures for animal handling and chemical exposure were conducted as described previously (30). Briefly, arsenite was dissolved in distilled water and diluted to final concentrations of 0, 1.0, 10.0, 100.0 and 500.0μM or at indicated concentrations in K-medium (52mM NaCl and 32mM KCl) containing E. coli strain OP50 as a food source. Aliquots of 1.0ml test solution were dispensed into a Costar 12-well tissue plate. For animal exposure, synchronized young adult hermaphrodites were picked and transferred into the wells. Worms were grown at 20 oC and removed for further analysis at 24h or at indicated time points after arsenic exposure.

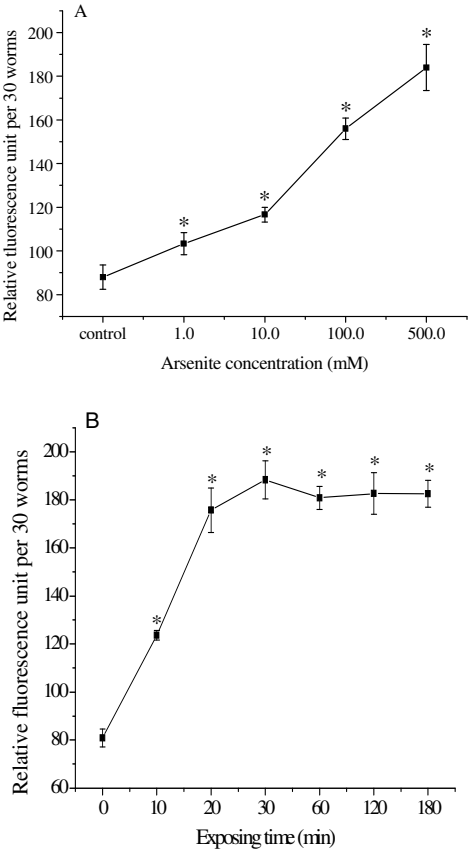

Fig. 1. Arsenite exposure causes the generation of ROS. (A) ROS production is dependent on arsenite concentration. (B) Arsenite induced ROS generation at different time point. All values are represented as means±SE. Error bar with different letters represents statistical significance (p value <0.05).

Reactive Oxygen Species Determination. For ROS determination, 40 synchronized hermaphrodites were treated with 0, 1.0, 10.0, 100.0 and 500.0μM arsenite for 2h. Worms were piped and added to 150μl PBS containing 0.1% Tween 20 and then homogenized with glass homogenizer followed by sonication on ice. Aliquotes of 100μl samples were added to 96-well plates after vortex. Aliquotes of 5μl 100μM CMH2DCFDA in PBS were added to the samples and incubated at 37 ^{o}C for 45min in a fluorescent microplate reader (Molecule Device). The arbitary fluorescence were determined at excitation 485nm and emission 640nm wavelength. To determine the kinetics of ROS production, worms were treated with 100μM arsenite for 0, 10, 20, 30, 60, 120min and 180min and assayed as described above.

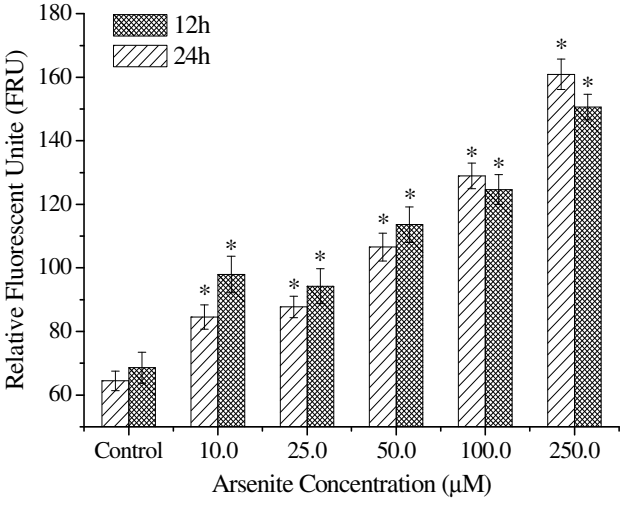

Fig. 2. Arsenite exposure cause dose-dependent increase in GST-4 expression. All values are represented as means±SE, n=15-26. Error bar with asterisk represents statistical significance (*p* value <0.05).

Semi-quantification of GFP. To determine whether arsenite exposure affected the levels of GST-4, SOD-3, HSP-4, HSP-16.48 and HSP-70 in *C. elegans*. Synchronized transgenetic worm strains were transferred to 1ml of K-medium with or without test solutions at indicated times. Animals were mounted on 2% agar pads in 60 μg/ml levamisole and examined with a Olympus IX 71 fluorescence microscope equiped with FITC exitation filter. Pictures were caught using a Olympus DP72 camera. The relative fluorescence intensities were semiquantified using the Adobe Photoshop software.

Data Analysis. All values were expressed as means ± standard error. Significant differences ($p<0.05$) between different treatments or different time points were tested using analysis of variance (ANOVA) followed by Tukey's multiple comparison test.

3 Results

Arsenite Induces Time-Dependent ROS Production. To determine whether arsenite exposure induces the generation ROS, synchronized young adult hermaphrodites were exposed to graded dose of arsenite for 2h in K-medium, the relative fluorescence unite (RFU) quantified after CM-H2DCFDA staining. As shown in Fig. 1, arsenite exposure significantly increased the generation of ROS in *C. elegans*. The RFU increased from 88.0±5.6 at untreated control to 103.3±5.0 after exposing to 1.0 μM of arsenite for 2h ($p<0.05$). With doses increase, RFU increased significantly. To test the kinetics of the ROS generation, RFU were determined at 10 to 180 min after exposing to 100μM arsenite. The generation of ROS was detectable as early as 10min and kept steadily

from 20 to 180min (Figure 1B). These results suggest that arsenite- induced ROS generation is depedent on doses and exposing time.

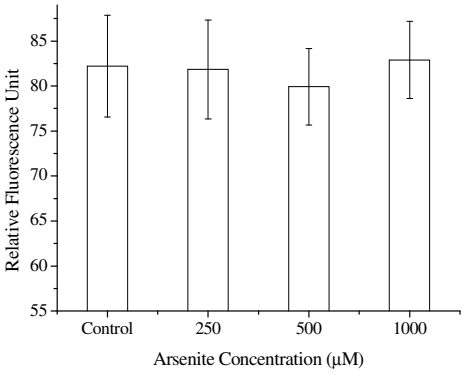

Fig. 3. Arsenite exposure does not decline the expression of SOD-3 at all concentrations. All values are represented as means±SE, n=15-26, *p* value >0.05.

Arsenite Exposure Induces. glutathione-S-transferase expression Glutathione-S-transferase is the important enzyme that functions in oxidative stress. To test the roles of GST on arsenite in *C. elegans*, the transgenetic worm strains carrying mammalian GST homolog were exposed to graded doses of arsenite for 12 and 24h, respectively. GST-4::GFP expressed mainly in the anterior of the body, mainly in the pharynx region and intestine. Arsenite exposure induces significant increase in GST-4 with the dosage increase (Fig. 2). However, the prolonged exposing time showed no effects on GST-4 expression at all doses.

SOD-3 Keeps Unchanged under Arsenite Exposure. Previous studies have shown that arsenic exposure reduced the expression of superoxide dismutase (SOD). In the present study, *C. elegans* strain carrying SOD-3::GFP reporting gene was exposed to graded concentrations of arsenite for 24h. SOD-3 expressed steadily at pharynx and intestine, and no significant SOD-3 decline were observed at all doses of exposure (Fig. 3)

Arsenite Exposure Induces the Expression of hsp-4 and hsp-70. In *C. elegans*, HSPs are stress-resistance genes, which expressed under environmental stresses such as thermal treatment, oxidative stresses and heavy metals exposure. To test whether arsenic exposure causes an increase in HSPs expression, worm transgenetic strains carrying HSP-16.48::GFP, HSP-4::GFP and HSP-70::GFP were exposed to 0.0, 250, 500 and 1000μM for 24h, GFP were semiquantified under a Olympus IX 71 fluorescence microscope. There were no HSP-16.48::GFP expression at all doses, indicating that arsenite exposure does not induces the express of HSP-16.48 (data not shown). However, the expression of HSP-4 and HSP-70 increased significantly with the increase of the doses. In *C. elegans*, HSP-4 expressed mainly in the intestinal cells. Under arsenite exposure, HSP-4::GFP increased significantly at the

doses of 500 and 1000μM (Fig. 4A). HSP-70 mainly expressed at the tail and intestine, arsenite exposure induced dose-dependent increase in HSP-70 (Fig 4B).

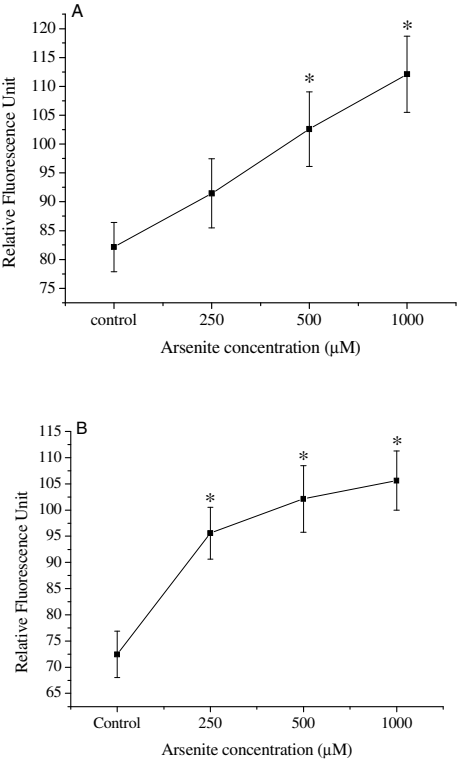

Fig. 4. Arsenite exposure induces the expression of HSP-4 and HSP-70 with the increase of dosages. (A) semiquantitive of HSP-4::GFP. (B) the expression of HSP-70 under different doses of arsenite. All values are represented as means±SE, n=15-26. Error bar with asterisk represents statistical significance (p value <0.05).

4 Discussion

C. elegans is a free-living nematode, ~1 mm in length, with relatively simple behaviors and structures. A complete life cycle takes three days, during which the worm goes through four larval stages. In recent years, there are increasing evidence indicate that this tiny animal is an attractive *in vivo* model for environmental toxicants monitoring. Unfortunately, according to Williams and Dusenbery [13], and also Liao, *C. elegans* was the most insensitive animals to inorganic arsenic using lethality as the endpoint.

It has been shown that arsenic exposure causes oxidative stress in several experimental systems. In living organisms, ROS is generated under physiological conditions and is important for normal cell signaling. However, excess ROS production affected multiple cell processes resulting oxidative damage and cell death. By exposing

C. elegans to different doses of arsenite, our data demonstrate that arsenite exposure produce ROS and thus induce the expression of stress response proteins.

In living cells, SOD and GST are important antioxidant enzyme systems that play important roles in eliminating ROS and protect lipids and proteins from peroxide [16,17]. It has been reported that arsenite exposure deplete the activities of SOD and GST in the liver of Swiss albino mice and also in several in vitro cell lines. In *C. elegans*, *gst-4* encodes a putative glutathione-requiring prostaglandin D synthase and is required for sperm to normally migrate towards a PUFA-based signal exuded by oocytes. The *C. elegans sod-3* encodes a iron/manganese superoxide dismutase, that might defend against oxidative stress and promote normal lifespan. In the present studies, we found that the expression of GST-4 increased with the dosages increase, while the SOD-3 keeps unchanged at all concentrations. The steady in GST-4 and SOD-3 may the causes of the animal that is most resistance to arsenite exposure.

As molecular chaperones, heat shock proteins (HSPs) are evolutionary conserved, and play diverse roles in transporting, folding, assembling of degraded or misfolded proteins [18]. The *C. elegans* HSP-16.2 and HSP-16.48 have been used as biochemical makers of heavy metals exposure [12]. However, our results indicate that HSP-16.2 and HSP-16.48 are not sensitive to arsenite exposure, indicating that the mechanisms of arsenite exposure to *C. elegans* are different to that of heavy metals. In *C. elegans*, *hsp-4* transcription is upregulated in response to endoplasmic reticulum stress induced by dithiothreitol (DTT) or tunicamycin as well as in response to heat shock. The *C. elegans hsp-70* encodes a heat-shock protein that is a member of the hsp70 family of molecular chaperones. The present results indicate that the HSP-4 and HSP-70 may act as biomarkers for arsenite exposure in *C. elegans*.

References

1. ATSDR: Top 20 Hazardous Substances: ATSDR/EPA Priority List for 1997, Agency for Toxic Substances and Disease Registry, Atlanta, GA, USA (1997)
2. Abernathy, C.O., Liu, Y.P., Longfellow, D., Aposhian, H.V., Beck, B., Fowler, B., Goyer, R., Menzer, R., Rossman, T., Thompson, C., Waalkes, M.: Arsenic: Health effects, mechanisms of actions, and research issues. Environ. Health. Perspect. 107(7), 593–597 (1999)
3. Hei, T.K., Liu, S.X., Waldren, C.: Mutagenicity of arsenic in mammalian cells: Role of reactive oxygen species. Proc. Natl. Acad. Sci. U.S.A. 95(14), 8103–8107 (1998)
4. Hayakawa, F., Privalsky, M.L.: Phosphorylation of PML by mitogen-activated protein kinases plays a key role in arsenic trioxide-mediated apoptosis. Cancer Cell 5(4), 389–401 (2004)
5. Lindquist, S.: The heat-shock response. Annu. Rev. Biochem. 55, 1151–1191 (1986)
6. Pirkkala, L., Nykanen, P., Sistonen, L.: Roles of the heat shock transcription factors in regulation of the heat shock response and beyond. FASEB J. 15(7), 1118–1131 (2001)
7. Kim, Y.-H., Park, E.-J., Han, S.T., Park, J.-W., Kwon, T.K.: Arsenic trioxide induces Hsp70 expression via reactive oxygen species and JNK pathway in MDA231 cells. Life Sci. 77(22), 2783–2793 (2005)
8. Gellalchew, M., Heikkila, J.J.: Intracellular localization of Xenopus small heat shock protein, hsp30, in A6 kidney epithelial cells. Cell Biol. Int. 29(3), 221–227 (2005)

9. Young, J.T.F., Gauley, J., Heikkila, J.J.: Simultaneous exposure of Xenopus A6 kidney epithelial cells to concurrent mild sodium arsenite and heat stress results in enhanced hsp30 and hsp70 gene expression and the acquisition of thermotolerance. Comp. Biochem. Physiol., Part A 153(4), 417–424 (2009)
10. Brenner, S.: The genetics of Caenorhabditis elegans. Genetics 77, 71–94 (1973)
11. Ankeny, R.A.: The natural history of Caenorhabditis elegans research. Nat. Rev. Genet. 2, 474–479 (2001)
12. Leung, M.C.K., Williams, P.L., Benedetto, A., Au, C., Helmcke, K.J., Aschner, M., Meyer, J.N.: *Caenorhabditis elegans:* An emerging model in biomedical and environmental toxicology. Toxicol. Sci. 106, 5–28 (2008)
13. Williams, P.L., Dusenbery, D.B.: Aquatic toxicity testing using the nematode Caenorhabditis elegans. Environ. Toxicol. Chem. 9, 1285–1290 (1990)
14. American Society for Testing and Materials Standard guide for conducting laboratory soil toxicity tests with the nematode Caenorhabditis elegans. In: Annual book of ASTM standards. Philadelphia, PA, 11.05, pp. 1606–1616 (2002)
15. Sulston, J., Hodgkin, J.: Methods. In: Wood, W.B. (ed.) The Nematode Caenorhabditis Elegans, pp. 587–606. Cold Spring Harbor Laboratory, New York (1988)
16. Fridovich, I.: Superoxide anion radical (O2-.), superoxide dismutases, and related matters. J. Biol. Chem. 272(30), 18515–18517 (1997)
17. Oxidative stress: animal adaptations in nature. Braz. J. Med. Biol. Res. 29(12) (December 1996)
18. Moseley, P.L.: Heat shock proteins and heat adaptation of the whole organism. J. Appl. Physiol. 83(5), 1413–1417 (1997)

RNA3 of a Cucumber Mosaic Virus Strain Infecting Musa Basjoo Based on the Molecular Characterization of Its 5' UTR

Zuodong Qin[1,2], Leilei Jin[2], Fangjiao Xu[2], Jingwei Zhang[2], Pingkai Ouyang[1], and Jishuang Chen[1,*]

[1] College of Life Science and Pharmaceutical Engineering, Nanjing University of Technology Nanjing 210009, Jiangsu, China
[2] Institute of Bioengineering, Zhejiang Sci-Tech University, Hangzhou 310018, Zhejiang, China
{qinzd,biochenjs}@njut.edu.cn

Abstract. This A strain of Cucumber mosaic virus (CMV), namely CMV-Mb, was detected from a naturally infected Musa basjoo (Mb) plant. After biological and serological tests, a full-length sequence of RNA3 was determined with products of RT-PCR. CMV-Mb RNA3 was found to be composed of 2189 nucleotides (nt). The results of sequence comparisons showed that CMV-Mb RNA3 formed an independent but highly supported clade within CMV subgroup II, revealing that CMV-Mb is derived from this subgroup but is a unique naturally homozygote strain. This strain may have evolved independently to infect Musa species, and its distribution may have been facilitated by the vegetative propagation of its host. It is considered that under vegetative propagation conditions, both host and geographical environment have impacted on evolutional types of this tripartite RNA virus.

Keywords: Cucumber mosaic virus, Musa, sequence analysis, Evolution.

1 Introduction

As one of the most widely distributed plant viruses with broad host ranges, *Cucumber mosaic virus* (CMV), the type species of the genus *Cucumovirus* (family *Bromoviridae*), is a tripartite +ssRNA plant virus [1-2]. Its RNA1 and RNA2 encode 1a and 2a proteins, respectively, both of which are associated with the replication of the viral genome. RNA3 encodes a movement protein (MP) and a coat protein (CP). The MP is thought to be involved in cell-to-cell movement of virus particles or genomic RNAs, while the CP is related to symptom determination and RNA encapsidation. Like most ssRNA viruses, CMV has a great deal of variation for fitness across different hosts and geological conditions. According to serological relationships and other molecular properties, CMV isolates have been classified into two main subgroups, Subgroup I and II [3]. A further division of Subgroup I into IA and IB was proposed based on the nucleotide sequences of 5′-untranslated regions (UTRs) of RNA3 [4].

* Corresponding author.

E. Zhu and S. Sambath (Eds.): Information Tech. and Agricultural Eng., AISC 134, pp. 919–924.
springerlink.com © Springer-Verlag Berlin Heidelberg 2012

Musa basjoo, a perennial herbaceous plant originating from the Ryukyu Islands of Japan, has been used widely as an ornamental plant or a food material for several thousands of years in China. It belongs to the genus *Musaceae*, family *Musa*, and is susceptible to a wide range of pests and diseases [5]. In previous reports, *Musa* has been found to be infected by *Banana streak virus* (BSV) [6-7], CMV [8] and several other viruses.The symptoms of these viruses including yellow streaks on leaves in a mosaic pattern, leaf yellowing and leaf mosaic. Severe mosaic with development into yellow spots has been found on a *M. basjoo* grown in Hangzhou China, and virus detection reflected the natural occurrence of CMV. Molecular determination of the virus genome has replicated the existence of a new variation of this virus for its adoption to host and environmental conditions. Our results could possibly reveal a new model of RNA virus evolution.

2 Materials and Methods

2.1 Virus Sample

Diseased leaf tissues were collected in spring from newly developed plants and tested against antibodies of Cucumber mosaic virus (CMV) with an ELISA kit (Agdia, USA) according to the manufacturer′ s instructions. Samples that had an absorbance value at A405 nm three times higher than that of healthy control leaves were evaluated as positive. A known strain of CMV, CMV-Fny, was used as a positive control. Samples collected from naturally infected M. basjoo and systemically infected N. glutinosa inoculated with CMV-Fny positive were both found to be CMV positive.

2.2 Viral RNA Analysis and RT-PCR

The Double stranded RNAs (dsRNAs) were extracted from the infected leaves of M. basjoo and leaf tissues of N. glutinosa inoculated with CMV-Fny, using a method described previously [9]. The dsRNA pattern was analyzed using 1% agarose gel electrophoresis and was purified with AxyPrep DNA Gel Extraction Kit according to the instruction manual. The above results demonstrated that the diseased leaf tissues from M. basjoo were infected with a Cucumovirus, which was named CMV-Mb. The purified dsRNA was used for RT-PCR with a single primer amplification technique as per our previous report [10], using a 3′ amino blocked adaptor (primer A: 5′-PO4-tcttcgggtgtccttcctcg-nh2-3′) for terminal ligation and a complementary primer (primer B: 5′-CGAGGAAGGACAAAAGAAGA-3′) for reverse transcription [11]. The PCR product was purified with AxyPrep DNA Gel Extraction Kit.

2.3 Cloning and Sequencing

The purified PCR product was cloned into a pMD18-T vector (TaKaRa, Dalian) and transferred into E. coli HB101 (Takara, Dalian) by standard procedures. Recombinant colonies were picked out by blue white spot and the plasmids were identified by PCR and enzyme digestion.

2.4 Sequence Analysis

Three clones of each sample were sequenced. Positive clones were sequenced by a model 3730 ABI Prism DNA analyzer (Invitrogen, USA). The sequences were assembled and analyzed with DNAStar version 6.1.3 software. Full length sequences of CMV-Mb RNA3 were submitted to the GenBank under the accession number GU002300. It was found that CMV-Mb RNA3 contains 2189 nt, encoding 3a of 280 amino acids and CP of 218 amino acids, corresponding to the nt sequences from 86 to 925 and 1211 to 1867, respectively. Compared to the nucleotides of CMV strains Fny, Nt9, and Q, CMV-Mb is more closely related to the Q strain. The nucleotide sequences of CMV-Mb RNA3, 3a and CP ORF showed over 98% sequence identities to the O strain but less than 85% sequence identities with those of Fny and Nt9. These results indicated that CMV-Mb RNA3 is derived from a CMV Subgroup II strain.

Nucleotide sequence alignments were carried out by using CLUSTAL X [12] with the ER strain of Peanut stunt virus (ER-PSV) as an outgroup. Phylogenetic analyses were conducted employing the Neighbor-Joining method. A distance matrix was calculated according to Kimura's two-parameter model with the MEGA 4.0 by 1000 bootstrap replications. All branches under 50% were judged invalid and collapsed. Some typical strains of CMV were used as references. Amongst Fny, Leg, Mf, Y and O are CMV subgroup IA strains; Nt9, Tfn, Ix, SD and IA are CMV subgroup IB strains; Q, Ly, LS, Tagetes, Kin, M2, TN, Tsh, Xb and Trk7 are Subgroup II strains. Outgroup is PSV ER strain. The GenBank accession numbers of nucleotide sequences of CMV-RNA3 used here are as follows: Fny (D10538); Leg (D16405); Mf (AJ276481); O (D00385); Nt9 (D28780); Tfn (Y16926); Ix (U20219); Sd (AB008777); IA (AB042293); Q (M21464); Ly (AF198103); S (AF063610); LS (AF4127976); Trk7 (L15336); Tagetes (EU665002); Kin (Z12818); M2 (AB006813); TN (AB176847); Tsh (EF202597); Xb (AF268598); Mb (GU002300); ER (U15730).

3 Results and Discussion

3.1 Double Stranded RNA Analysis of Diseased Plants of Musa basjoo

Four samples were used for dsRNA extraction. The products were detected by 1% agarose gel electrophoresis, using CMV-Fny as positive control. All samples obtained from tested plants revealed four dsRNA segments with molecular sizes of about 3.3, 3.0, 2.2 and 1.0 kbp, with their mobility of these dsRNAs similar to those of CMV-Fny (data not shown). The above results demonstrated that those diseased leaves tissues from *M. basjoo* were infected with a *Cucumovirus*.

3.2 Gene Structure of CMV-Mb RNA3

Full length sequences of CMV-Mb RNA3 have been submitted into GeneBank under the accession numbers of GU002300. It was found that CMV-Mb RNA3 contains 2219 nt, encoding 3a of 280 amino acids and CP of 219 amino acids, corresponding to the nt sequences from 86 to 925 and 1211 to 1867, respectively. Comparisons of the nucleotide CMV strains Fny, Nt9, and Q, CMV-Mb are more closely related to the Q strain. The nucleotide sequences of CMV-Mb RNA3, 3a and CP ORF showed over

98% sequence identities to O strain but less than 85% sequence identities with those of Fny and Nt9. These results indicated that CMV-Mb RNA3 is derived from a CMV Subgroup II strain.

3.3 Some Phylogenetic Estimation of 22 Strains of CMV Based on 3a and CP ORF and 5′ UTR of RNA3

The results of the phylogenetic analysis for 3a and CP ORFs and 5′ UTR between CMV-Mb and the other 21 CMV strains are shown in Fig. 1. For all 3a, CP and 5′ UTR, CMV-Mb appeared independently in Subgroup II strains with supporting values of 100%, 96% and 77% respectively. Thus, the sequence comparisons and phylogenetic analyses revealed that CMV-Mb RNA3 falls into Subgroup II.

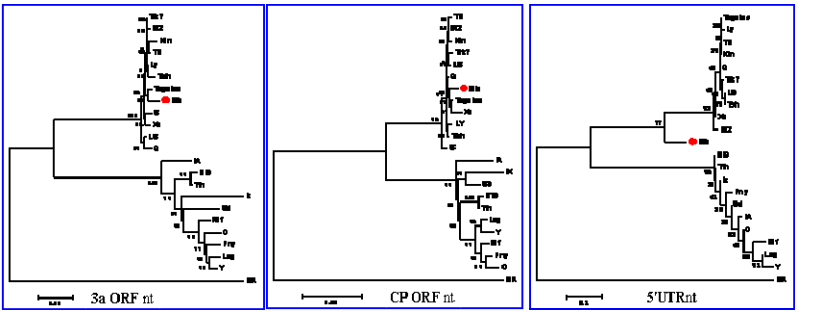

Fig. 1. Phylogenetics tree for RNA3 sequences of CMV obtained from NCBI constructed by Neighbor-Joining method based on that of 3a, CP and 5' UTR nucleotides

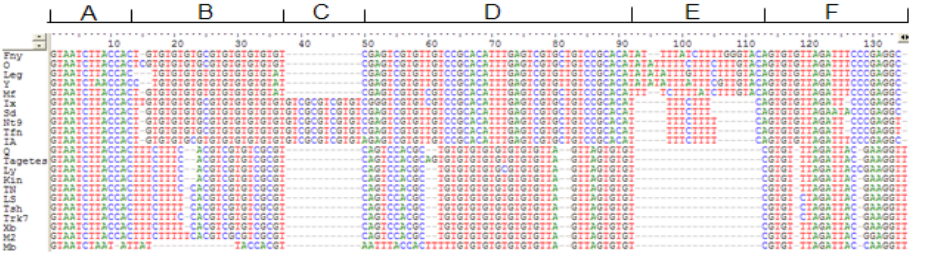

Fig. 2. Nucleotide sequence rearrangements in the 5' UTR of CMV RNA3. 21 strains were used for the alignment and bases are shown with colored highlights. *The sequences reported in this paper were submitted to the GenBank database and have been assigned the accession numbers GU00230

3.4 Variation of the 5′ UTR of RNA 3

All 22 strains of CMV RNA3 sequences herein were used for 5′ UTR analysis. As shown in Fig. 2, it was found that natural mutant areas (from 8~33 nt and 50~ 63 nt) could be distinguished in CMV-Mb RNA3, and that may have independent evolution in Subgroup II. Sequence alignment analysis revealed that the sequence of 5′ UTR

CMV-RNA3 could be assigned into six motifs according to their conserved characters. Motif A was found to be common for all the strains of CMV including IA, IB and II. The replication initiating domain was on the 3′ end of the RNA3 negative strand, but one nt deletion and two nt substitutions were found in CMV-Mb RNA3. Motif B varied clearly between subgroups I and II, but CMV-Mb RNA3 had more deletions, with 12-14 nt deleted in comparison with other strains for Subgroup I or II. Motif C is specific to IB and CMV-Mb RNA3 lacks this region of 13 nt. Similar to motif B, CMV-Mb has almost the same nt to Subgroup II against Subgroup I except two nt substitutions and two more nt than in motif D. Motif E is specific for Subgroup I but different between IA and IB, CMV-Mb lacks this region as per other Subgroup II strains. Motif F is different between subgroup I and II and is conserved among those two subgroups, and CMV-Mb has the same structure like other II strains.

In conclusion, the sequence analyses showed that CMV-Mb RNA3 is diverted from Subgroup II, but unlike previously described CMV II strains, the 5′ UTR seems to have evolved into a new branch. This may be due to the specific conditions of transmission, host interactions or environment. It could be considered that the deletion and rearrangement of nt at RNA3 5′ UTR of CMV-Mb is part of its evolution. Understanding the mechanism of evolution of CMV is helpful in calculating the emergence of new viral diseases.

Acknowledgment. We thank Dr. Peter Palukaitis for his kindly advice. This work was supported by the National Science Foundation of China (30971898) and National High-Tech Development Project (863: 2008AA 10Z129).

References

1. Palukaitis, P., Roossinck, M.J., Dietzgen, R.G., Francki, R.I.: Cucumber mosaic virus. Adv. Virus Res. 41, 281–348 (1992)
2. Roossinck, M.J.: Evolutionary history of cucumber mosaic virus deduced by phylogenetic analyse. J. Virol. 76, 3382–3387 (2002)
3. Owen, J., Palukaitis, P.: Characterization of cucumber mosaic virus. I. Molecular heterogeneity mapping of RNA 3 in eight CMV strains. Virology 166, 495–502 (1988)
4. Roossinck, M.J., Zhang, L., Hellwald, K.-H.: Rearrangements in the 59 nontranslated region and phylogenetic analyses of cucumber mosaic virus RNA 3 indicate radial evolution of three subgroups. J. Virol. 73, 6752–6758 (1999)
5. Nelson, S.C., Ploetz, R.C., Kepler, A.K.: Musa species (banana and plantain). Species Profiles for Pacific Island Agroforestry, version 2.2 (August 2006)
6. Lockhart, B.E.L.: Purification and serology of a bacilliform virus associated with banana streak disease. Phytopathology 76, 995–999 (1986)
7. Harper, G., Hull, R.: Cloning and Sequence Analysis of Banana Streak Virus DNA. Virus Genes 17, 271–278 (1998)
8. Singh, Z., Jones, R.A.C., Jones, M.G.K.: Identification of Cucumber Mosaic Virus Subgroup I Isolates from Banana Plants Affected by Infectious Chlorosis Disease Using RT-PCR. Plant Dis. 79, 713–716 (1995)

9. Morris, T.J., Dodds, J.A.: Isolation and analysis of double-stranded RNA from virus infected plant and fungal tissue. Phytopathology 69, 854–858 (1979)
10. Lambden, P.R., Cooke, S.J., Caul, E.O., Clarke, I.N.: Cloning of noncultivatable human rotavirus by single primer amplification. J. Virol. 66, 1817–1822 (1992)
11. Chen, L., Chen, J.S., Liu, L., et al.: Complete nucleotide sequences and genome characterization of double-stranded RNA1 and RNA2 in the Raphanus sativus-root CV. Yipinghong. Arch. Virol. 151, 849–859 (2006)
12. Thompson, J.D., Gibson, T.J., Plewniak, F., Jeanmougin, F., Higgins, D.G.: The CLUSTAL_X windows interface: flexible strategies for multiple sequence alignment aided by quality analysis tools. Nucleic Acids Res. 25, 4876–4882 (1997)

Analysis of Flavonoids and Phenolic Acids of Aqueous Extracts in Leaves of Apocynum venetum L.*

Xiao-ying Yin, Jian-jiang Fu, Hua-sheng Yang,
Hong-ning Liu, and Yong-ming Luo**

College of Pharmacy Jiang Xi University of Traditional Chinese Medicine Nanchang, Jiangxi Province, China
{ncyxoy,jxluoyongming}@163.com, {906954195,1040799006}@qq.com, yanghuasheng456@126.com

Abstract. In the present study a method was built based on liquid chromatography with diode array detection (HPLC/DAD) coupled to an electrospray ionization (ESI) interface for the mainly active compounds in aqueous extracts from dried leaves of Apocynum venetum L. Overall, 10 constituents were separated and identified, which belong to two classes of compounds: caffeoylquinic acids and flavonoids. Among them, the qualitative and quantitative analysis of chlorogenic acid and cryptochlorogenic acid was the first report. 5 of them were further quantitatively analyzed. The contents of chlorogenic acid, cryptochlorogenic acid, hyperoside, isoquercitrin and astragalin were detected by this method as 2.1-3.9%, 0-0.71%, 1.1-2.2%, 0.47-0.87%, 0.19-0.35%, respectively. This method has a low detection limit with results range from 0.50 μg/mL to 1.5 μg/mL. Recovery was determined with standard addition method for sample, with results ranging from 94.2% to 106.1%. The data results provided a valuable reference to explore action mechanism of the true active constituents and improve the quality control for the herd Apocynum venetum L.

Keywords: Apocynum venetum L., phenolic acids, flavonoids, HPLC-MS.

1 Introduction

The Apocynaceae plant Apocynum venetum, known as 'Luobuma' in Chinese, has three Species: Apocynum venetum L., Poacynum hendersonii and Poacynum Pictum. Among them, the former is the prescribed herbs in Chinese Pharmacopoeia. The two latter are known as the confused herbs of the former in China. Leaves of Apocynum venetum L. have also been used for the treatment of cardiac disease, hypertension, nephritis, and other diseases [1]. They have been also used as a health food in Japan [2]. Aqueous extract from the leaves of A. venetum has been reported to have a

* This work is supported by the National Science and Technology of key projects Grant# 2009ZX09310-005 to H.N. Liu, National Natural Science Foundation Grant#20962012 to X.Y. Yin, #30973959 to Q.S. Liu..

** Corresponding author. E-mail address: jxluoyongming@163.com

E. Zhu and S. Sambath (Eds.): Information Tech. and Agricultural Eng., AISC 134, pp. 925–933.
springerlink.com © Springer-Verlag Berlin Heidelberg 2012

hepatoprotective effect and antioxidant activity [3-5]. The mainly active constituents are the flavonoids and phenolic acids [6, 7]. For analysis of these constituents, previous reports more emphasis to determine them in alcohol extracts of this plant, such as methanol or ethanol [8, 9], while the true active constituents are in the water extract of this plant. The composition of the two kinds of extracts has great differences. Little attention has been devoted to the analysis for constituents in the aqueous extract of the leaves of Apocynum venetum L. But the studies to analyze these compounds should be still necessary to discovery the true active compounds and compound groups.

In this paper, we analyzed qualitatively the flavonoids and phenolic acids in the aqueous extract from the leaves of Apocynum venetum L. by HPLC–MS and HPLC–DAD. Interestingly, these active compounds of flavonoids and phenolic acids are pairs with the form of isomers in the plants. In them, the qualitative and quantitative analysis of chlorogenic acid and cryptochlorogenic acid was the first report from the leaves of Apocynum venetum L.. In this work a sensitive, dependable, and simple method for determination of flavonoids and phenolic acids in the aqueous extract from the leaves of Apocynum venetum L. was also developed by HPLC.

2 Material and Methods

2.1 Chemicals and Plants

Chlorogenic acid, hyperoside were purchased from National institute for the control of pharmaceutical and biological products (Beijing, China). Isoquercitrin and astragalin were supplied by Yonghengbiological technology Co., Ltd. (Shanghai, China). Cryptochlorogenic acid was obtained from Yuanye Biological Technology Co., Ltd. (Shanghai, China). The roasted leaves of *Apocynum venetum* L. from different regions were purchased from Huangqingren drugstore (Nanchang, China). Organic solvents such as methanol, aceticacid and acetonitrile were obtained from Tianjin Chemical Reagent Company (Tianjin, China). All chemicals and solvents were analytical or HPLC grade.

2.2 Extraction of Herbal Medicine

The roasted leaves of Apocynum venetum L. were ground into powder (passed through a 30 μm sieve), weighted 2 g into a flask and added 30 mL distilled water, then extracted by a heated reflux for 120 minutes. After filtration through a paper filter, the extraction was again filtered by a 0.22 μm filter. The filtrate was kept for HPLC–MS analysis.

2.3 HPLC-UV Analysis

The HPLC-UV analysis was performed using Agilent 1200series HPLC (Agilent, USA). Elite C18 column (250 mm × 4.6 mm i.d., 5 μm particle size, Dalian, China) was used. A mixture of acetonitril and ammonium acetate aqeous solution (PH 4.0, 10 mM) was used as the mobile phase. The LC flow rate was 1mL/min. The gradient

elution procedure was performed as following: 0 min, 10% acetonitril; 8min, 15% acetonitril; 16min, 17% acetonitril; 40min, 38% acetonitril. UV detection wavelength λ was set at 254nm and a 20μL volume was used for injection solution.

2.4 HPLC-MS Analysis Condition

The analysis was performed on a Waters 2695 ZQ4000 system (Waters, USA) using the above column by a mass spectrometer with electron spray ionization source. HPLC conditions were as the above. Flow rate was 0.8 mL/min; MS parameters were as follows: ionization mode, positive and negative; sheath gas, nitrogen; collision gas, helium; source temperature, 110℃; desolvation temperature, 350℃; capillary voltage, 3.2 kV; cone voltage, 30 V; full scan acquisition, from m/z 200 to 1,000.

3 Units Results and Discussion

3.1 Qualitative Analysis of Flavonoids and Phenolic Acids by HPLC-MS

From the Chromatograms of the aqueous extract from the leaves of Apocynum venetum L. in Fig. 1 can be seen, the majority of peaks, total 10 compounds can be separated. The 10 compounds were identified by UV and MS spectral data showed in Table 1, where the retention time, UV absorptions and electrospray ionization mass spectrometry of all the compounds detected are reported. These constituents belong to two representing classes of constituents: quinic acid derivatives and flavonoids, which are associated with the bioactive properties of hepatoprotective effect and antioxidant activity. Flavonoid glycosides and its derivatives were the main constituents of the extract.

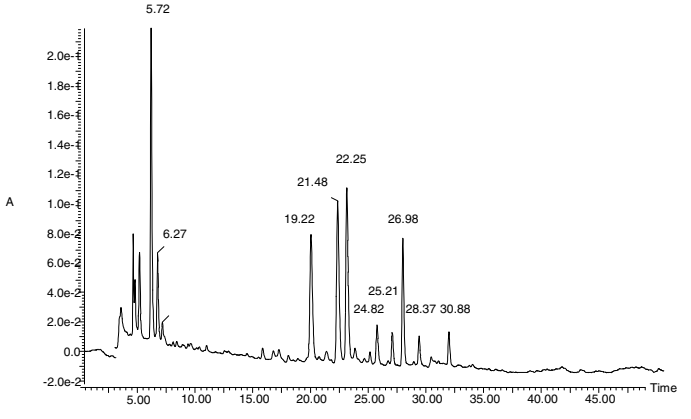

Fig. 1. Chromatograms of the aqueous extract from the leaves of Apocynum venetum L

1) Identification of caffeoylquinic acids: The first elution two peaks at 5.72, 6.27 min in chromatogram showed similar UV spectra with a characteristic absorbance curve of caffeoylquinic acid derivatives, maximum absorbance at 325 nm and a shoulder

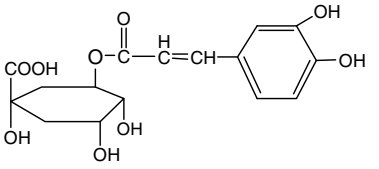

Compound 1: Chlorogenic acid(3-caffeoylquinic acid)

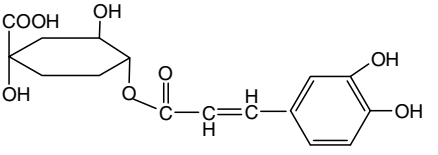

Compound 2: Cryptochlorogenic acid (4- caffeoylquinic acid)

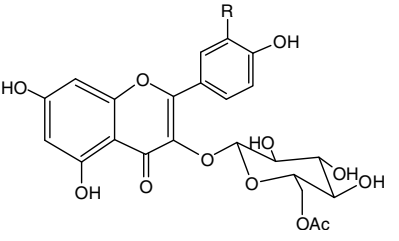

Compound 3: R=OH 6”-O-acetylated hyperoside
Compound 10: R=H 6”-O-acetylated trifolin

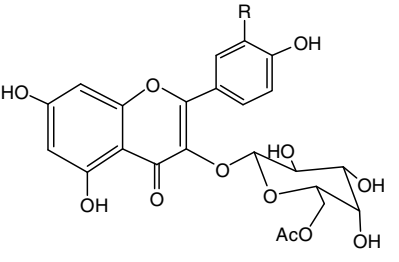

Compound 8: R=OH 6’-O- acetylated isoquercitrin

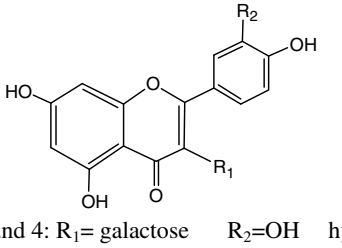

Compound 4: R_1= galactose R_2=OH hyperoside
Compound 5: R_1= glucose R_2=OH isoquercitrin
Compound 6: R_1= galactose R_2=H trifolin
Compound 7: R_1= glucose R_2=H astragalin
Compound 9: R_1= glucose R_2=OAc 3’-O- acetylated isoquercitrin

Fig. 2. Structures of 10 separated compounds

around 298 nm. The Quasimolecular fragments at 353 $[M-H]^-$ and the characteristic ion at m/z 179, 191 suggested the presence of chlorogenic acid or its isomers. 3-caffeoylquinic acid can be distinguished by base fragment peaks at m/z 191 [quinic acid$-H]^-$ accompanied by an intense (> 50% base peak) [caffeic acid$-H]^-$ fragment at m/z 179; 4-caffeoylquinic acid can be distinguished by base fragment peak at m/z 173 (due to m/z 191 losing H_2O), which is not observed for the other isomers [11]. Thus, two peaks at 5.72, 6.27 min could be determined as 3-caffeoylquinic acid and 4-caffeoylquinic acid. Complete identification of the two compounds was further proved by comparing its UV spectra and retention times with those of the reference substance. Structures of the two compounds are showed in Fig. 1. The two compounds are only a few reports in the leaves of Apocynum venetum L.

2) Identification of flavonoids: Other eight peaks in the chromatogram of Fig. 1. were detected and identified as flavonoids glycoside, which can be divided into two types: one is a class of flavonoids by quercetin as aglycone, and the other is based on kaempferol as the aglycone of flavonoid glycosides. The difference of two type flavonoids can be easily distinguished by comparing their UV spectra. As Table 1 showed, No.3, 4, 5, 8, 9 peaks (retention time at 19.22, 21.48, 22.25, 26.98, 28.37 min, respectively) belong to the front class with two maximum peaks of absorption at 256 nm and 354 nm in the UV spectrum. No.6, 7, 10 peaks (retention time at 24.82, 25.21 and 30.88 min) are classified to the latter one with two maximum peaks of absorption at 266 nm and 350 nm. No. 4, 5 peaks are the isomer with the same pseudomolecular ion at m/z 463 $[M-H]^-$ and similar fragment ions. They were identified as hyperoside and isoquercitrin by comparing fragment ions and retention times with those of the reference substance. The two compounds are the obvious characteristic components in the Leaves of Apocynum venetum L.

No.3, 8, 9 peaks, as isomers to each other, have the same pseudomolecular ion at m/z 505 $[M-H]^-$. Two maximum absorption peaks of the three compounds for UV absorption spectra are very similar, but for the 9th peak, the absorption intensity of the second maximum UV absorption peak at 354 nm was lower than that on the 8th and the 3rd component. It indicated that there is a substituent on cinnamon acid system (the band Ⅱ) of flavonoids, causing decreased absorption peak intensity. The pseudomolecular peaks at m/z 505 $[M-H]^-$, the ion $[M-CH_3CO]$ at 462.6 m/z and $[462.6-C_6H_{10}O_5]$ at 300.8 m/z, again according with the elution order, the peak at 19.22, 26.98 min (compound 3, 8 respectively) were assigned as 6”-O-acetylated hyperoside and 6”-O-acetylated isoquercitrin. Combining with the change of the band Ⅱ of UV absorption spectra and the elution order of the peak, the compound 9 at 28.37 min was assigned as 3’-O- acetylated isoquercitrin.

Two peak at 24.82, 25.21 min gave common quasi-molecular ions at m/z 283.8 $[M-C_6H_{10}O_5]$, 254.8 [283.8 –CHO] as the isomers, and were assigned as trifolin and astragalin [5]. The latter compound was further identified by comparing the retention time with those of the reference substance. Finally, a peak at 30.88 min (compound 10) having pseudomolecular ions at m/z 491 $[M-H]^-$and at m/z 449.0 [M–CH3CO], 287.0 $[449.0- C_6H_{10}O_5]$ was presumed to 6”-O-acetylated trifolin.

In sum, 10 peaks in the chromatogram of Fig. 1 were all identified and their structure list in Fig. 2.

3.2 Quantitative Analysis of Flavonoids and Phenolic Acids

1) Precision, linearity and detection limits of analytes : As part of the 10 components in the extract is difficult to be separated, the amount of separated not enough for quantitative analysis, so a sufficient number of the active phenolic and flavonoid compounds were selected to further quantitative analysis, a total of five components. These compounds were chlorogenic acid, cryptochlorogenic acid, hyperoside, isoquercitrin, astragalin.

The method was validated for precision of the peak area of the analytes. The precision is estimated by making six replicate injections of a standard mixture solution (389.9 μg/mL, 392.0 μg/mL, 72.8 μg/mL, 123.1 μg/mL, 55.4 μg/mL for chlorogenic acid, cryptochlorogenic acid, hyperoside, isoquercitrin, astragalin, respectively) under the selected optimum conditions. The relative standard derivations (RSDs) of peak areas are 0.47%, 0.34%, 0.10%, 0.20%, 0.15% for chlorogenic acid, cryptochlorogenic acid, hyperoside, isoquercitrin, astragalin, respectively. The relative standard derivations (RSDs) of retention time are 0.35%, 0.29%, 0.10%, 0.16%, 0.14% for the above 5 compounds, respectively.

To determine the linearity relationships between concentrations and the corresponding peak areas of the 5 compounds, a series of the mixed standard solution was tested at the same situations. The detection limit is evaluated on the basis of a signal-to-noise ratio of 3. The results of regression analysis on calibration curves, linear ranges and detection limits are summarized in Table 1.

Table 1. The regression equations and detection limits for 5 analytes

Compound	Regression equation	Correlation coefficient	Linear range (mg/mL)	Detection Limits (μg/mL)
Chlorogenic acid	y = 41.56x + 630.9	0.9991	0.195-1.950	1.5
cryptochlorogenic acid	y = 43.66x + 51.51	0.9993	0.018-0.1821	1.2
hyperoside	y = 27.27x - 4.13	0.9999	0.036-0.364	0.72
isoquercitrin	y =273.47x + 15.46	0.9995	0.062-0.616	0.50
astragalin	y = 9.90x - 8.36	0.9993	0.277-2.771	1.1

2) Reproducibility: The repeatability was assessed by analyzing six independently prepared samples of the extraction of herbal *Apocynum venetum* L from Jilin. The relative standard deviation of peak areas for chlorogenic acid, cryptochlorogenic acid, hyperoside, isoquercitrin, astragalin was below 2.6%, 3.2%, 1.2%, 1.8%, 2.0% respectively. And the relative standard deviation of retention time for the above five ingredients was 0.40%, 0.31%, 0.14%, 0.20%, 0.18% respectively.

3) Recovery and practical sample analysis: The recovery experiments under the same conditions were also conducted to evaluate the precision and accuracy of the method.

Recovery was determined with standard addition method in sample, with results ranging from 94.2% to 106.1%, and the results in details are listed in Table 2. The results showed that method has better accuracy and the relative standard derivations.

Three different areas of herbal medicine and a standard reference herb of the leaves of *Apocynum venetum* L. were was carried out the quantitative analysis under the conditions of the above chromatography, the results showed in Table 3. It indicated that the content of phenolic and flavonoid components in herb of the leaves of *Apocynum venetum* L from different areas has a great difference.

Table 2. The recoveries in this method with the leaves of Apocynum venetum L. (n = 5)

Ingredient	Original amount (μg /mL)	Added mount (μg /mL)	Found (μg /mL)	Recovery (%)	RSD (%)
chlorogenic acid	334.8	350.2	664.7	94.2	3.1
cryptochlorogenic acid	32.86	43.0	73.8	95.2	3.4
hyperoside	117.6	100.8	222.2	103.8	2.3
isoquercitrin	50.64	52.4	106.2	106.0	4.2
astragalin	36.4	40.5	78.6	104.2	3.7

Table 3. Assay results of flavonoids and phenolic acids of extracts in leaves from different producing area

Peak no.	Comounds	Jilin (%)	Tianjin (%)	Shanxi (%)	Standard reference herb (%)
1	Chlorogenic acid	2.9	3.3	3.9	2.1
2	cryptochlorogenic acid	0.49	0.18	0.71	0
3[a]	6″-O-acetylated hyperoside	1.0	1.7	1.8	0.65
4	hyperoside	1.1	1.5	2.2	1.8
5	isoquercitrin	0.47	0.68	0.87	0.74
6[a]	trifolin	0.24	0.19	0.35	0.25
7	astragalin	0.24	0.19	0.30	0.34
8[a]	6″-O-acetylated isoquercitrin	0.68	0.84	0.35	0.47
9[a]	3′-O-acetylated isoquercitrin	0.16	0.21	0.090	0.16
10[a]	6″-O-acetylated trifolin	0.19	0.13	0.062	0.065

[a]. For the result calculated according to hyperoside as standard sample. % (w/w)

4 Conclusions

An effective and simple method was developed and validated for the aqueous extract from the leaves of Apocynum venetum L. by HPLC-MS and HPLC-DAD. The developed analytical method provided a good separation of the different classes of constituents present in such extracts, such as caffeoylquinic acids, flvonoids. Overall 10 constituents were detected and identified and among them 5 mainly active compounds of caffeoylquinic acids and flavonoids were further quantitative analysis. This study provided a value reference to explore action mechanism for the true active constituents and improve the quality standard for the herd Apocynum venetum L..

The next step is to obtain the other five single components for quantitative analysis, while the 10 components would be further performed a series of the pharmacological experiments to explore the material basis.

Acknowledgment. This work is supported by the Natural Science Foundation, Jiangxi Province, RP China (Grant No. 2009GZY0096), the Education Research project of Science and Technology Foundation, Jiangxi Province, RP China (Grant No. GJJ10553), Jiangxi University of Traditional Chinese Medicine Experimental Zone of Creative Talents funded project.

References

1. Chinese Pharmacopeia Committee of Ministry of Public Health of the People's Republic of China Chinese pharmacopeia, vol. 1, pp. 196–196. Chemical and Technical Press, Beijing (2010)
2. Grundmann, Nakajima, J., Kamata, K., Seo, S., Butterweck, V.: Kaempferol from the leaves of Apocynum venetum possesses anxiolytic activities in the elevated plus maze test in mice. Phytomedicine 16(4), 295–302 (2009)
3. Tagawa, C., Kagawa, T., Nakazawa, Y., Onizuka, S., Nishibe, S., Kawasaki, H., Yakugaku, Z.: Studies on antihypertensive effect of Luobuma (Apocynum venetum L.) leaf extract (3). Yakugaku Zasshi. 124(11), 851–856 (2004)
4. Kwan, C.Y., Zhang, W.B., Nishibe, S., Seo, S.: A novel in vitro endothelium-dependent vascular relaxant effect of Apocynum venetum leaf extract. Clin. Exp. Pharmacol. Physiol 32(9), 789–795 (2005)
5. Grundmann, Nakajima, J., Seo, S., Butterweck, V.: Anti-anxiety effects of Apocynum venetum L. in the elevated plus maze test. J. Ethnopharmacol 110(4), 406–411 (2007)
6. Xiong, Q., Fan, W., Tezuka, Y., Adnyana, I.K., Stampoulis, P., Hattori, M., Namba, T., Kadota, S.: Hepatoprotective effect of Apocynum venetum and its active constituents. Planta. Med. 66(2), 127–133 (2000)
7. Yokozawa, T., Nakagawa, T.: Inhibitory effects of Luobuma tea and its components against glucose-mediated protein damage. Food Chem. Toxicol. 42(6), 975–981 (2004)
8. Kamata, K., Seo, S., Nakajima, J.: Constituents from leaves of Apocynum venetum L. J. Nat. Med. 62(4), 160–163 (2008)

9. Murakami, M., Kishi, A., Matsuda, H., Hattori, M., Yoshikawa, M.: Medicinal foodstuffs, XXIV, chemical constitution of the processed leaves of Apocynum venetum L: absolute stereostruc-tures of aposinoside I and II. Chem. Pharm. Bull. 49(7), 845–848 (2001)
10. Teoh, H., Leung, S.W., Man, R.Y.: Short-term exposure to physiological levels of 17 beta-estradiol enhances endothelium-independent relaxation in porcine coronary artery. Cardiovasc. Res. 42(4), 224–231 (1999)
11. Zheng, W., Clifford, M.N.: Comparison of the profiles of chlorogenic acids and their derivatives from three Chinese traditional herbs by LC-MSn. Acta Pharmaceutica Sinica 43(2), 185–190 (2008)

Effect of Glomus Mosseae Inoculation on Growth and Reproduction of Rice

Wang Li*, Ma Fang, Zhang Shujuan, and Zhang Xue

School of Municipal and Environmental Engineering, State Key Laboratory of Urban Water Resource and Environment, Harbin Institute of Technology
Harbin, China
wli@hit.edu.cn

Abstract. Effect of inoculating rice *(Oryza sativa* L.) with mycorrhizal fungi (*Glomus mosseae*) was studied using potted seedlings. Vegetative growth and reproductive traits were compared between inoculated and non-inoculated plants. Result showed that there was a high mycorrhizal dependency of the rice on *G. mosseae*. Mycorrhizal fungal inoculated rice seedlings grew significant better compared to non-mycorrhizal controlled seedlings, and had increased height (34%), shoot biomass (122%), root biomass (590%) at maximum tillering stage, and grain yield (9.7%) at harvesting stage. Plant architecture and reproductive traits were changed by mycorrhizal fungi inoculation. Rice inoculated with *G. mosseae* invested more in the root development for effective nutrient absorption, which was the fundamental to achieve the maximum grain yield. *G. mosseae* was available to form an association with rice plant. The symbiosis of mycorrhizal fungi and rice would be of benefit to crop growth and grain yield.

Keywords: Rice, Arbuscular mycorrhizal fungi, Glomus mosseae, Mycorrhizal dependency, Ecological strategy.

1 Introduction

Although the beneficial effects of inoculating crop plants with arbuscular mycorrhizal fungi (AMF) are well known, rice, the most important food crop in Asia, has received little attention in mycorrhiza research. This is because plants growing in marshy environments were rarely found to be mycorrhizal[1]. Rice fields present unique conditions for the activity of a number of microorganisms[2].*Glomus mosseae*, the most common mycorrhizal fungi ever reported to form a symbiotic relationship with wetland plant, was inoculated to observe the extent of arbuscular mycorrhizal fungi root colonization in wetland rice and to assess the effect of fungi inoculation on the growth of wetland rice[3].

AMF is directly or indirectly attributed to an improved nutrient status in land by forming association with plants. It increases the plant growth[4] and productivity in enhancing the uptake of nutrition[5], in resisting against pathogen[6], in improving tolerance to drought stress[7] and in increasing the effective absorption surface of roots[8].

Resource uptake property is a critical element in determining grain yield[9], and functional morphology for resource use competition should be included in early evaluation.

E. Zhu and S. Sambath (Eds.): Information Tech. and Agricultural Eng., AISC 134, pp. 935–942.
springerlink.com © Springer-Verlag Berlin Heidelberg 2012

It has been demonstrated that mycorrhizal inoculation may change the morphological index of plant[10], especially the ratio of above and below ground parts[11], and lead to a reallocation between vegetative and reproductive parts[12-13].

According to P'yankov and Ivanov's result[14], i.e. different contributions of organs to the total plant weight represented as different ecological strategies, we hypothesized that plant ecological strategies would be re-selected by the inoculation of mycorrhizal fungi.

The purpose of this study was to compare the biomass allocation strategy between inoculated or non-inoculated rice in order to evaluate the mycorrhizal dependency of rice, and to reveal the ecological mechanisms in the symbiosis benefit for crop growth and grain yield.

2 Material and Methods

A pot experiment was conducted in diluted soil. The soil collected from Heilongjiang Province, China, was a paddy type, pH=(7.7), total nitrogen content 6.75g/kg, and total phosphorus content 13.07g/kg[15] . It was mixed with paddy soil, sand and vermiculite in the ratio of 2:5:3), and sterilized by steaming(2 h under 0.15 Mpa and 121℃).

The diluted soil was inoculated with a stock culture of *Glomus mosseae* which was a soil containing spores, mycelium and infected root fragments. 140 grams of the inoculums was added per pot. Equal numbers of control pots were of the sterilized soil plus filtered infected root washing was added to the pot.

Seeds of wetland rice, *Oryza sativa* L. were soaked in water for 24h and then allowed to germinate in warm (30℃), moist condition. These pre-germinated seeds were used for sowing in the nursery. The plants were grown in square pots carry trays and watered daily.

At three-leaf stage the transplants were transplanted to pots under either inoculated (+AMF) or not (-AMF) soil condition.

Sampling was performed in the growth stages throughout the maximum tillering stage to value the vegetative growth pattern. And reproductive traits of rice were also measured at the end of the growth season.

Mycorrhizal dependency was evaluated using the relative mycorrhizal dependency index (MDI)[16] as follows:

$$MDI = (B_{AMF} - B_{non\text{-}AMF})/B_{AMF} \quad (1)$$

where B_{AMF} was biomass of the plants in mycorrhizal inoculation treatment and $B_{non\text{-}AMF}$ was biomass of the control plants. Moreover, MDI was further divided into shoot mycorrhizal dependency index (SMDI) and root mycorrhizal dependency index (RMDI) to tell the partial dependency between above ground and ground vegetative parts.

$$SMDI=(SB_{AMF} - SB_{non\text{-}AMF})/SB_{AMF} \quad (2)$$

$$RMDI=(RB_{AMF} - RB_{non\text{-}AMF})/RB_{AMF} \quad (3)$$

Fitting of models and statistic analysis were performed using statistical software, SPSS 10.0 (SPSS Inc., Chicago).

3 Results

3.1 Mycorrhizal Dependency

The vesicles of *G. mosseae* appeared at the 2nd week and reached a stable intensity in the 4th week after inoculation. 25% percentage of arbuscular mycorrhizal fungi root colonization was found at the 4th week stage in the inoculated rice plants. This growth process was similar to previous research from Rajeshkannan et al. (2009) [17].

After a successful inoculation with *G. mosseae*, an increasing dependency upon mycorrhizal fungi was observed in our experiments with rice growing. The mycorrhizal dependency was moderate in the beginning of inoculation but increased fast over time in a log linearly way (Fig. 1). The mycorrhizal dependency index (MDI) reached up to 76% in the experimental period, which was a clear indication of a very high mycorrhizal dependency of the wetland rice on *G. mosseae*.

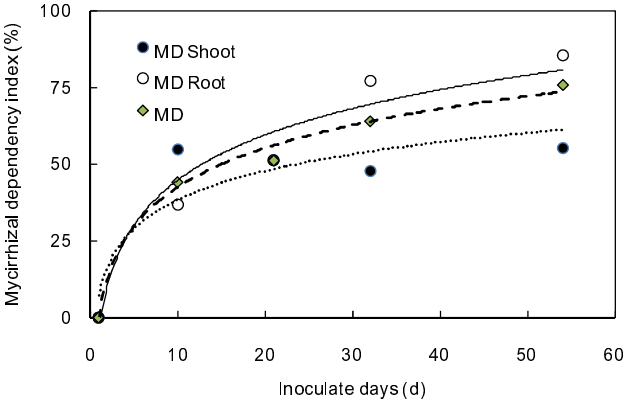

Fig. 1. Mycorrhizal dependency index (MDI) variation with inoculated rice plant growth

Rice growth dependency on the mycorrhizal fungi was further divided into shoot mycorrhizal dependency and root mycorrhizal dependency in the present paper. Results showed that the root production more depended on the mycorrhizal condition. Root mycorrhizal dependency index (RMDI) increased as plant growing and as high as 86% at the 54th day after inoculation. In contrast, shoot production moderately depended on mycorrhizal promotion at the stable level of 50% shoot mycorrhizal dependency index (SMDI). This result provided support for previous research that root production seemed to be an important factor in mycorrhizal dependency[18].

3.2 Growth Promotion

There was a positive correlation between plant production and mycorrhizal dependency. Rice growth was greatly improved by the inoculation of *G. mosseae*. Application of mycorrhizal inoculation resulted in a 34% increment in the plant height (Fig. 2), and 314% in total biomass at the tillering stage. Those extremely promotion in

plant biomass was more primarily attributed to the root production, which is 590% increment (relative to 122% increment in aboveground plant parts)(Fig. 3).

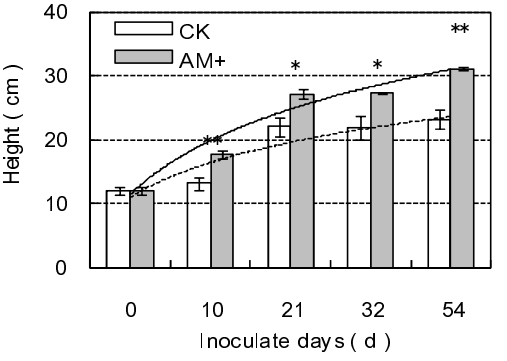

Fig. 2. Plant height variation in the tillering stage under inoculated and non-inoculated treatment,Values are means ± standard error

* Indicate significance at p<0.05 and **at p<0.01

Significant differences in plant growth were observed between plants inoculated with *G. mosseae* and non-inoculated control (P<0.05). And, this difference became more obvious as plant growing (Fig. 3).

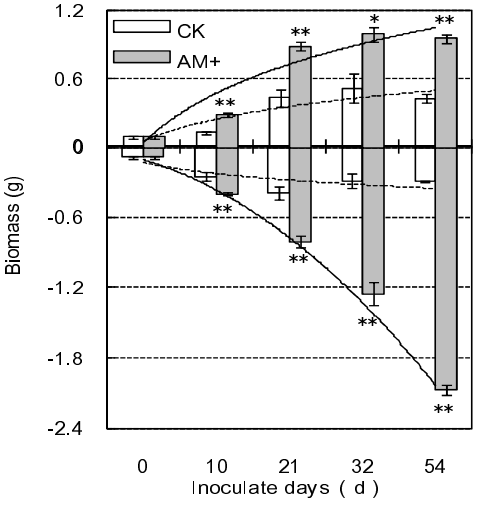

Fig. 3. Plant biomass allocation between above- and under-ground parts in the tillering stage under inoculated and non-inoculated treatment,Values are means ± standard error

* Indicate significance at p<0.05 and **at p<0.01

Aboveground parts of Plants were both growing in a logarithmic way whether it was with or without mycorrhizal inoculation. The height and biomass increment of controlled plant turned to level off around 3-4weeks growing, while plants inoculated with *G. mosseae* kept on growing at the experimental period.

Belowground parts of plants were developed extremely different between plants inoculated with *G. mosseae* or not. The root of non-inoculated plant grew to a certain length in the experimental period. In contrast, unlimited root development was found in the AMF inoculated plant.

3.3 Root-Shoot Allocation Strategy

Plant with different contributions of their organs to the total plant weight could be identified as different ecological strategies.

The differences in biomass allocation of the plants with and without mycorrhizal inoculation were more pronounced when comparing the indices calculated as ratio between the weight of root and shoot expressed in percentages (Fig.4)

In the case of plants without mycorrhizal inoculation, the root: shoot ratio decreased with plant growth. More energy was allocated to the above ground organs with plant growing. That was an adaptation to maximize the photosynthetic organs for the photosynthetic assimilation and dry matter accumulation.

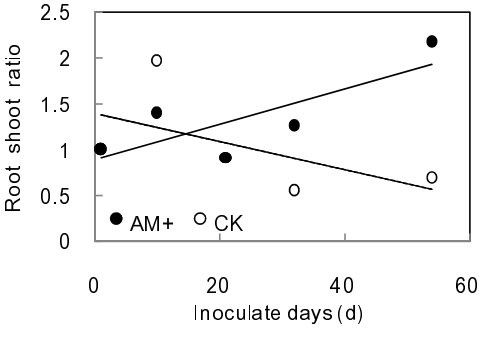

Fig. 4. Plant biomass allocation between above- and under-ground parts in the tillering stage under inoculated and non-inoculated treatment,Values are means ± standard error

For plants inoculated with *G. mosseae*, the underground biomass consisted of both root and extraradical mycelium, which is increased exponentially and spread without end. The proportion of root in the total plant weight significantly increased in the AMF inoculated plant(Fig.4). It indicated that AMF-rice symbiosis tended to distribute more energy or assimilation to the belowground part. Developing root and extraradical mycelium could benefit the water and nutrients uptake in a larger area.

3.4 Reproductive Strategy

Mycorrhizal inoculation or not was also an important factor that influenced grain size heterogeneity and grain yield within the plant. Compared to the non-inoculated rice,

mycorrhizal fungi inoculated rice has more grains in amount but smaller in size. The grain yield was increased 9.7% by mycorrhizal promotion, but the difference was not significant from non-inoculated plant (Table 1).

Table 1. Influence of mycorrhizal inoculation on reproductive traits of rice

M±SE	hundred grain weight (g)	grains of single-ear	Grain number	Yield (g)
CK	2.524±0.040	13.5±0.618	747.6±32.4	18.87±0.647
AM+	2.468±0.027	14.15±0.577	835.7±64.3	20.62±1.418
AMF Promotion (%)	-2.2%	1.4%	11.8%	9.7%

Several theories have been proposed to explain the relative investment in the reproductive compartment, and between above and below ground vegetative parts[14,19]. The allocation to reproduction was important for plant dissemination, and the vegetative part was closely related to plant competition and survival. Plants have to balance the investment between reproduction and vegetative production to achieve the best fitness under specific environment.

For agricultural crops, plants have been manipulated by human for a longtime through plant breeding and agricultural practices. The large gain in productivity among agricultural species is basically a result of a change in the carbon allocation pattern within the plant. Rice is a typical ruderals strategy plant, in contrast to competitors strategy and stress-tolerant strategies, have smaller underground organs and high seed productivity[20]. The biomass allocation strategy was changed by mycorrhizal inoculation. Rice inoculated with *G. mosseae* invested more energy in the vegetative growth, especially in the roots development, which cost more energy for plant growth and maintenance. While, the energy cost did not reduce the reproductive yield. Plant was still benefit from the root expansion for an effective nutrient uptake.

Inoculation of mycorrhizal fungi may change the plant vegetative and reproductive allocation strategies. Expansion in root colonization provided an optimal resources supply, that bring about a high yield and make plant more competitive and stress-tolerant.

4 Conclusions

(1) *G. mosseae* was a plant growth-promoting rhizobacterium, and the high mycorrhizal dependency and growth responsiveness of rice was confirmed.

(2) A positive correlation was found between plant production and mycorrhizal independency in the present paper. Root development was most strongly related to the mycorrhizal inoculation.

(3) Plant architecture and reproductive traits were changed when it was inoculated by mycorrhizal fungi. These changes of morphological index indicated the trade-offs in

ecological strategies. Investment in large below ground parts could be of benefit to inoculated rice by nutrient absorption. More small-grains was the ecological strategy of inoculated rice to achieve the maximum grain yield.

Rice productivity can be improved by the application of *G. mosseae*, and intensified inoculation will be an effective way to increase grain yield. Mycorrhizal fungi inoculation can be used for biological fertilizer to reduce the chemical agriculture pollution.

Acknowledgment. This study was supported by National Natural Science Foundation of China (50809020, 50778052), Natural Science Foundation of Hei Longjiang Province, China (QC07C11), Development Program for Outstanding Young Teachers in Harbin Institute of Technology, China (HITQNJS.2008.043), and State Key Lab of Urban Water Resource and Environment, Harbin Institute of Technology, China (HIT) (HC200816, 2008ts03).

References

1. Roger, P.A., Zimmerman, W.J., Lumpkin, T.A.: Microbiological management of wetland rice fields. In: Metting, B. (ed.) Soil Microbial Ecology: Applications in Agricultural and Environmental Management, pp. 417–455. Marcel Dekker, New York (1993)
2. Chaubal, R., Sharma, C.D., Mishra, R.R.: Vesicular arbuscular mycorrhiza in subtropical aquatic and marshy plant communities. Proc. Indian Acad. Sci (Plant Sci.) 91(1), 69–77 (1982)
3. Secilia, J., Bagyaraj, D.J.: Selection of efficient vesicular-arbuscular mycorrhizal fungi for wetland rice-a preliminary screen. Mycorrhiza 4, 265–268 (1994)
4. Chinnusamy, M., Kaushik, B.D., Prasanna, R.: Growth, nutritional, and yield parameters of wetland rice as influenced by microbial consortia under controlled conditions. Journal of Plant Nutrition 29, 857–871 (2006)
5. Carpio, L.A., Davies, F.T., Arnold, M.A.: Arbuscular mycorrhizal fungi, organic and inorganic controlled-release fertilizers: Effect on growth and leachate of container-grown Bush Morning Glory [Ipomoea carnea subsp. fistulosa] under high production temperatures. Journal of American Society for Horiticulture Sciences 130, 131–139 (2005)
6. Jeffries, P., Gianinazzi, S., Perotto, S., Turnau, K., Barea, J.M.: The contribution of arbuscular mycorrhizal fungi in sustainable maintenance of plant health and soil fertility. Biology and Fertility of Soil 37, 1–16 (2003)
7. Varma, A.: Ecophysiology and application of arbuscular mycorrhizal fungi in arid soil. In: Varma, A., Hock, B. (eds.) Mycorrhiza-Structure, Function, Molecular Biology and Biotechnology, pp. 561–592. Springer, Berlin (1995)
8. Bolan, N.S.: A critical review on the role of mycorrhizal fungi in the uptake of phosphorus by plant. Plant and Soil 134, 189–207 (1991)
9. Wang, L., Jia, W., Ma, F., Li, S., Zhang, S.J.: Perspective of mycorrhizal technology application for environmental remediation. Ecology and Environmental Sciences 19(2), 487–493 (2010)
10. Schroeder, M., Janos, D.P.: Plant growth, phosphorus nutrition, and root morphological responses to arbuscular mycorrhizas, phosphorus fertilization, and intraspecific density. Mycorrhiza 15, 203–216 (2005)

11. Crush, J.R.: Plant growth responses to vesicular-arbuscular mycorrhiza.VII. Growth and nodulation of some herbage legumes. New Phytologist (73), 743–749 (1974)
12. Secilia, J., Bagyaraj, D.J.: Selection of efficient vesicular-arbuscular mycorrhizal fungi for wetland rice - a preliminary screen. Mycorrhiza 4, 265–268 (1994)
13. Chinnusamy, M., Kaushik, B.D., Prasanna, R.: Growth, nutritional, and yield parameters of wetland rice as influenced by microbial consortia under controlled conditions. Journal of Plant Nutrition 29, 857–871 (2006)
14. P'yankov, V.I., Ivanov, L.A.: Biomass allocation in boreal plants with different ecological strategies
15. Zhang, S.J., Wang, L., Ma, F., Li, S.Y., Zhang, X., Wu, J.T.: Application of arbuscular mycorrhizal on promoting the trowth of rice and reducing the usage of chemical fertilizer. Journal of Harbin Institute of Technology 42(6), 1–5 (2010)
16. Plenchette, C.: Growth responses of several plant species to mycorrhizae in a soil of moderate P-fertility. IMycorrhizal dependency under field conditions. Plant and Soil 70, 199–209 (1983)
17. Rajeshkannan, Y., Sumathi, C.S., Manian, S.: Arbuscular mycorrhizal fungi colonization in upland rice as influenced by agrochemical application. Rice Science 16(4), 307–313 (2009)
18. Nemec, S.: Response of six citrus rootstocks to three species of Glomus, a mycorrhizal fungus. Proceeding of Florida State Horticulture Society 91, 10–14 (1978)
19. Grime, J.P.: Plant strategies and vegetation processes. Wiley, Chichester (1979)
20. Grime, J.P.: Vegetation classification by reference to strateties. Nature 250, 26–31 (1974)

Distinctness Determination of DUS Test on Some Quantitative Characteristics of Rice*

Yanfang Liu, Xiaohong Yang, Jianhua Zhang**, Junjiao Guan, Jiangmin Wang, and Hui Zhang

Kunming DUS Test Station, Ministry of Agriculture, Yunnan Academy of Agriculture Sciences, Kunming, Yunnan, China
{Liuyf528,Zhjhua6748}@163.com

Abstract. When separately using the DUS Test Guideline to determine the distinctness of some quantitative characteristics, we found even the characteristics of the same variety had different "Notes" in different environments. So, the correlation of quantitative characteristics with environment factor, with variety factor, and characteristics themselves were discussed in this paper. Results showed that, in order to improve the reliability of DUS test, all the quantitative characteristics should be grouped according to their stability or correlation coefficients with environment changes; different groups can be given corresponding weighting coefficients according to their stability; the distinctness determination could be based on the weighted measurements of characteristic groups; variety factor should be considered in DUS test and also in the selection of standard varieties used in DUS test.

Keywords: DUS test, quantitative characteristics, environment factor, variety factor.

1 Introduction

Distinctness, Uniformity and Stability, or "DUS test" is the major component of the examination of new varieties of plants(PVP), and the basis for the authority of Plant Breeder Right(PBR) [1]. In DUS test, distinctness determination is the most critical step, and it is based on the difference of characteristic expression between candidate variety (the variety applying for Plant Breeder Right, or PBR) and its similar varieties. All the characteristics listed in DUS test guidelines are generally classified as qualitative characteristics (QN), quantitative characteristics (QN) and pseudo-qualitative characteristics (PQ). "Quantitative characteristics" are those where the expression covers the full range of variation from one extreme to the other. The expression can be recorded on a one-dimensional, continuous or discrete, linear scale. Its continuity can easily be influenced by environment changes, which makes it difficult to correctly determine its expression state. Furthermore, the difference

* This work is partially supported by "Research of New Techniques on DUS Test "-Ministry of Agriculture's Special Funds for Technique Research on Public Causes 200903008-14.
** Corresponding author.

E. Zhu and S. Sambath (Eds.): Information Tech. and Agricultural Eng., AISC 134, pp. 943–951.
springerlink.com © Springer-Verlag Berlin Heidelberg 2012

between candidate variety and its similar varieties has become less and less in recent years because of the singleness of breeding purpose, the homogenization of breeding techniques, and the frequent use of certain parent lines. Some candidate varieties have no difference in QN or PQ characteristics with their similar varieties. So, it is extremely important to effectively use quantitative characteristics to determine the distinctness.

In China, only the research of how to use statistic analysis to determine the distinctness of quantitative characteristics is involved in quite few papers [2-5], and there is no report yet in other countries. So, there is little comprehensive research in this field.

In this paper, rice, the most important crop with the largest application and authorization in China, is chosen as the research object. Using the DUS Test Guideline of Rice and statistics analysis software as the tools, we analyze the correlation of some quantitative characteristics with environment, with variety's nature (variety factor), and characteristics themselves. We try to introduce the concept of "ecology fitness of characteristic expression" into DUS test, which could provide the theory basis and technique platform for the scientific use of DUS Test Guideline.

2 Material and Method

2.1 Material

The test materials are the following rice varieties: Chugeng27, Diantun502 and Yunlu29, which are identified as A_1, A_2 and A_3. Among which, A_1 is mid-matured japonica rice; A_2 is indica rice with aroma and soft quality, while A_3 is alpine rice. Such selection is mainly based on the difference of their growth periods and suitable growing environments, where A_2 has short growth period, and adapts to low attitude and high temperature condition, while A_3 is just the reverse, and A_1 is in middle condition.

2.2 Method

The test is carried out from April to October, 2009 and 2010, and is located in Yunnan Academy of Agriculture Science, where the attitude is 1920m. At the beginning of April, seeds were sown in trays for wet seedling nursing. After one month, the four-leaved seedlings were transferred to 30cm-diameter pots, with the density of 4 plants per pot [6].

1）Test Design

The three varieties were treated in three different conditions (represent three different environments), namely outdoor condition (B_1), shelter condition (B_2), and greenhouse condition (B_3), and each treatment has 3 repeats. Such treatments are based on the light decrease and temperature increase of the three environments in order. Light and temperature are two important factors, which can dramatically influence plant metabolism and its growth, and are difficult to control (see Table 1).

Table 1. Treatment

combination	outdoor (B_1)	Shelter (B_2)	Greenhouse (B_3)
Chugeng27 (A_1)	A_1B_1	A_1B_2	A_1B_3
Diantun502 (A_2)	A_2B_1	A_2B_2	A_2B_3
Yunlu29 (A_3)	A_3B_1	A_3B_2	A_3B_3

2）Distinctness Determination

We carried out the distinctness determination on some quantitative characteristics (during plants' vegetative growth stage) in strict accordance with "Guideline for the Conduct of Tests for Distinctness, Uniformity and Stability-Rice (State Standard of the People's Republic of China) " [7-8] (hereinafter referred to as "Guideline").Measurements or observations are recorded according to the expression of characteristics, and each expression state is attributed a numerical "Note"

3）Statistic Analysis

Using statistics analysis software of SPSS16.0, Analysis of Variance, Correlation Analysis, and curve estimation were applied for the data.

3 Results

3.1 Distinctness Determination Based on DUS Test Guideline

According to the "Guideline", the measurements of the following quantitative characteristics have been translated into corresponding "Notes". The difference of "Notes" is used to determine distinctness of the same variety under the above-mentioned environments (see Table 2). It is clear that, under different environments, plants of variety A_2 have different expression states in the characteristics of "length of 2^{nd} last leaf" and "length of flag leaf", so does variety A_3. Besides, all the three varieties have quite different expression state in the characteristic of "stem length", especially that the difference of plants of variety A_3 between greenhouse treatment and the other two conditions has reached 4 "Notes". So, it is obvious that, the expression difference of these characteristics has environmental basis. Taking variety A_3 for example, it is the great difference between high-temperature greenhouse and its optimal growth condition that cause the quite abnormal expression of "stem length".

3.2 Analysis of Environment Factor and Variety Factor to Characteristic Expression Based on Analysis of Variance

In order to investigate the influence of environment factor and variety factor to characteristic expression, we use SPSS16.0 statistics software to do Analysis of Variance on the data above (see Fig.1). From Fig.1, it is clear that the influence of environment factor to the characteristics of "length of 2nd last leaf" and "width of 2nd last leaf" has reached "extremely significant level". Furthermore, the environment influence has much greater impact than the variety factor on those frontal characteristics. The results fully demonstrate that, the expression difference of these characteristics has both environment

factor and variety factor. However, the most likely reason for why environmental impact is greater on those frontal characteristics is that, all these characteristics were investigated in the same time, and the latter characteristics haven't fully developed, so the environmental impact on the characteristic expression has been interfered by the variety factor.

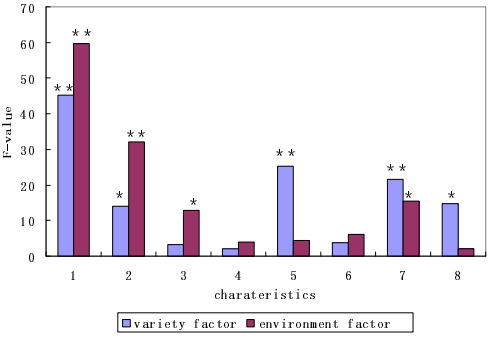

Fig. 1. Influence of variety factor and environment factor to characteristic expression

1) "*","**"indicates the influence has reached "significant level", "extremely significant level".

2) characteristics 1-characteristics 8 are "length of 2nd last leaf", "width of 2nd last leaf", "angle of 2nd last leaf", "stem length", "stem thickness", "length of flag leaf", "width of flag leaf" and "angle of flag leaf" respectively.

Table 2. Distinctness determination of quantitative characteristics based on dus test guideline

characteristic	measurements and corresponding Notes								
	A_1B_1	A_1B_2	A_1B_3	A_2B_1	A_2B_2	A_2B_3	A_3B_1	A_3B_2	A_3B_3
length of 2nd last leaf /cm	28(3)	29.5(3)	37.5(3)	35.2(3)	40.6(5)	48(5)	35.4(3)	37.1(3)	47.7(5)
width of 2nd last leaf /cm	1.1(5)	1.3(5)	1.4(5)	1.2(5)	1.3(5)	1.4(5)	1.0(5)	1.1(5)	1.3(5)
angle of 2nd last leaf /°	11(3)	16 (3)	19(3)	8(3)	13(3)	14(3)	9(3)	10(3)	18(3)
stem length /cm	52.9(3)	61.6(3)	76.6(5)	42.8(1)	45.1(1)	51.5(3)	50.3(3)	51.7(3)	103.4(7)
stem thickness/cm	0.35(5)	0.4(5)	0.4(5)	0.3(5)	0.35(5)	0.41(5)	0.48(5)	0.49(5)	0.5(5)
length of flag leaf /cm	20.8(3)	21.1(3)	23.2(3)	21(3)	23.1(3)	25.7(5)	22.4(3)	24.2(3)	32.1(5)
width of flag leaf /cm	1.1(7)	1.2(7)	1.4(7)	1.5(7)	1.7(7)	1.8(7)	1.2(7)	1.3(7)	1.7(7)
angle of flag leaf /°	18 (1)	20(1)	23(1)	5(1)	9(1)	14(1)	13(1)	13(1)	12(1)

1) In the "measurements and corresponding Notes", the figures between brackets are Notes, while figures outside brackets are measurements.

2) Those painted figures represent the difference of the characteristics of the same variety in different environments.

3.3 One-Way ANOVA of Environment Factor to the Difference of Characteristic Expression

Fixing variety factor, we use SPSS16.0 statistics software to do the one-way ANOVA of environment factor. From Table 3, we can come to the conclusion that, different environment conditions have different influence to characteristic expression. In the eight characteristics, there are around 4.5 characteristics (or 60%) have significantly or extremely significantly different expression under the treatments of different environments. When longitudinally comparing(see Fig.2), for variety A_1, the variation of characteristic expression caused by B_1B_2 and B_2B_3 is moderate and the change trend appears as a stably uprising line; for variety A_2, B_1B_2 has much greater influence, which occupies the majority of the whole variation range(B_1B_3); while for variety A_3, the condition is just opposite. After comparing the difference of B_1B_2 and B_2B_3, we find that, B_1B_2 mainly has difference in light intensity, while B_2B_3 mainly has difference in temperature, which will be easy to explain why each variety has different variation in B_1B_2 and B_2B_3. The variation trend of each variety is coincident with their growth habit. For example, variety A_2 is temperature eurytopic, and it adapts to high temperature condition, so its variation of characteristics in B_2B_3 is less than in B_1B_2. So, it is clear that, environmental impact on characteristic expression is influenced by variety factor. The horizontal comparison is also carried out to see the environmental impact on the each characteristic (see Fig.3). The difference of "stem length" and "angle of 2nd last leaf" of the three varieties has reached "significant level" or "extremely significant level" under both B_1B_2 and B_2B_3, which indicates that, the two characteristics can easily be affected by environmental changes. The difference of B_2B_3 has greater impact on "length of 2nd last leaf" and "length of flag leaf" than B_1B_2, while B_1B_2 has greater influence on "width of 2nd last leaf", "width of flag leaf", "angle of flag leaf" and "stem thickness". All of these data indicate that the difference of environments has various impact on each characteristic.

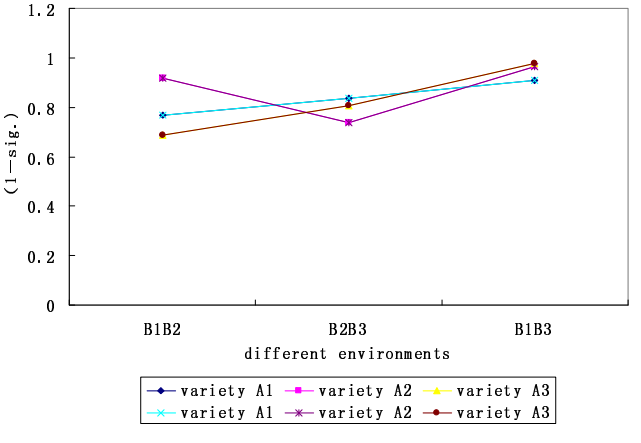

Fig. 2. Environmental impact on each variety

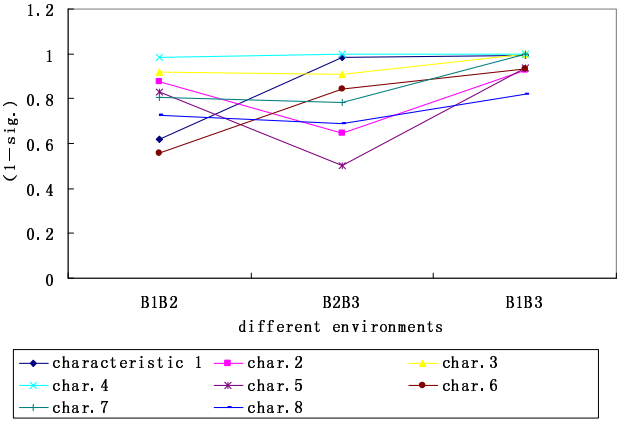

Fig. 3. Environmental impact on each characteristic

Table 3. Single Factor of Environment Influence to Characteristic Expression

characteristics	variety (A_1)			variety (A_2)			variety (A_3)		
	B_1B_2	A_1B_2	B_1B_3	B_1B_2	B_2B_3	B_1B_3	B_1B_2	B_2B_3	B_1B_3
length of 2nd last leaf /cm	.650	.031*	.013*	.057	.014*	.000**	.437	.000**	.000**
width of 2nd last leaf /cm	.033*	.056	.001**	.216	1.00	.216	.119	.001**	.000**
angle of 2nd last leaf /°	.008**	.114	.000**	.000**	.158	.000**	.230	.000**	.000**
stem length /cm	.000**	.000**	.000**	.000**	.000**	.000**	.044*	.000**	.000**
stem thickness/cm	.002**	1.00	.002**	.006**	.002**	.000**	.500	.500	.189
length of flag leaf /cm	.851	.182	.134	.371	.283	.062	.111	.000**	.000**
width of flag leaf /cm	.196	.018*	.001**	.014*	.640	.006**	.369	.000**	.000**
angle of flag leaf /°	.108	.135	.006**	.003**	.002	.000**	.703	.799	.527

1) "*","**"indicates "significant level", "extremely significant level".

3.4 The Correlation of Environment Changes and Difference of Characteristic Expression

Using SPSS16.0 statistics software to analyze the correlation of environment changes and difference of characteristic expression (see Table 4), we can find in the three varieties that, the Kendall's correlation coefficient of the difference of "stem length" and environmental changes is the highest, and "angle of 2nd last leaf" is the second highest correlated. The result is the same as the *"One-way ANOVA"* of *C*. Furthermore, the change trend of correlation coefficients (correlated to environment changes) is almost the same in the following two characteristics, namely "length of 2nd last leaf" and "length of flag leaf", and it is the same story for "width of 2nd last

leaf" and "width of flag leaf" (see Fig.4). Such results indicate the correlation exists not only in environment changes and characteristic difference, but also in characteristics themselves. From the symmetry of the change trend in these characteristics, we can infer that, characteristics need to be grouped so that repeated invalid records can be avoided, which will improve the reliability of DUS test. We can also find that, except A_3, A_1 and A_2 have the same trend of correlation coefficient to environment changes in the characteristics of "angle of 2nd last leaf" and "angle of flag leaf". The reason why A_3 is not included is maybe that the correlation has been affected by variety factor. In this case, A_3 has long growth period, and "angle of flag leaf" develops generally late than others, so the environmental impact has been interfered by variety factor. The same reason can also been explained in the characteristic of "stem thickness". Furthermore, ten curve estimations were made to analyze the correlation of "stem length" and environment changes. We found the regression equation of "Quadratic" is the most coincident, with the R square of 0.975, 0.982 and 0.999 in A_1, A_2 and A_3 respectively. The regression equation is: y=9.4158-0.2658x+0.0021x2 (see Fig.5).

Table 4. Correlation of Environment Changes and Characteristic Difference

variety / Characteristics	A_1	A_2	A_3
Char.1	0.485*	0.668**	0.691**
Char.2	0.722**	0.370	0.789**
Char.3	0.665**	0.727**	0.692**
Char.4	0.845**	0.849**	0.762**
Char.5	0.563**	0.808**	0.284
Char.6	0.283	0.512*	0.736**
Char.7	0.706**	0.579*	0.763**
Char.8	0.645**	0.824**	0.135

1) "*","**"indicates "significant level", "extremely significant level"

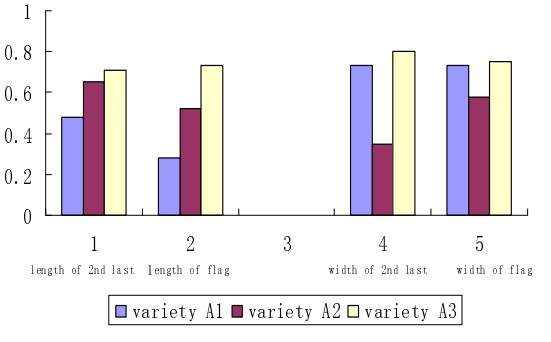

Fig. 4. The change trend of correlation coefficients

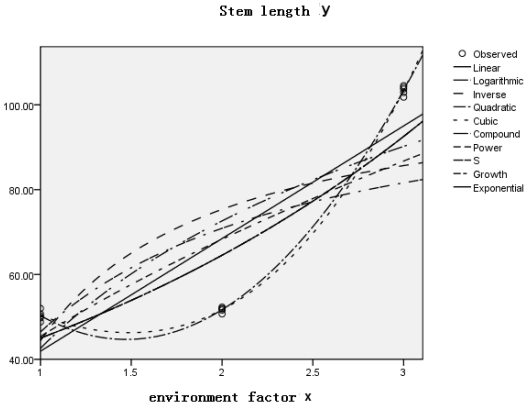

Fig. 5. Curve estimations of the correlation between "stem length" and environment changes

5 Discussion

5.1 The Consideration of Environment Factor and Variety Factor in the DUS Test

In this paper, three varieties, which are representative in growth habit and growth period, are treated in three environments, which are different in light intensity and temperature. In part "Ⅲ", it is clear that, some quantitative characteristics are more or less influenced by environment factor and variety factor.

On one hand, as the main variation of environment factor, light intensity and temperature can influence plants' metabolism and growth period, and cause the changes of characteristics to adapt to environment changes, which we can call as "ecology fitness of characteristic expression". In the field design of DUS test, it is hard to control light and temperature. So, it is essential to research the correlation of environment factor (especially light and temperature) and characteristic expression. This paper aims at introducing "ecology fitness of characteristic expression" to DUS test, paving roads for the deep research of this field and finally establishing mathematical models to make their correlation clear. Besides, it is necessary for different ecological zones to establish their own databases, which will be quite important for the effectiveness of DUS test.

On the other hand, variety factor determines characteristic expression, and it also influences the correlation of environment and variety. So, in order to ensure objectiveness and authenticity of DUS test, the test condition should meet the growth requirement of corresponding varieties, only then can characteristics fully develop. Furthermore, it should also be clear that, the selection of standard variety to be listed in DUS Test Guideline should be based not only on characteristic' s representativeness, but also on stability of its expression in different environments. Eurytropic varieties with wide ecological amplitude should be considered as standard varieties of DUS test.

5.2 Distinctness Determination of Quantitative Characteristics and the Consideration of New Aiding Methods

From the data, we find that the impact of different environment on different quantitative characteristics is various, and such impact is similar on the same kind of characteristics, such as "length of 2nd last leaf" and "length of flag leaf". So, besides the research on characteristics' stability and correlation with environment, it is also essential to make clear the correlation of different characteristics. Then characteristics can be grouped according to their correlation coefficient and different groups can be given corresponding weighting coefficients according to their stability. So, the distinctness determination could be based on the weighted measurement value of quantitative characteristics. Taking "stem length" for example, it has high correlation coefficient with environment, and it should be given small weighting coefficient. So, even there is great difference in the characteristic of "stem length", it should not always determined as distinctness. In that case, the distinctness determination could be based on the weighted measurement value of quantitative characteristics, which will definitely improve the reliability of DUS test.

Generally speaking, environmental impact on quantitative characteristics takes effect through affecting transcription and regulation of genes, but gene itself is stable. So, molecular techniques could provide a new way for DUS test.

Acknowledgment. Yanfang Liu and Jianhua Zhang, et. Thank the support of "Research of New Techniques on DUS Test "-Ministry of Agriculture's Special Funds for Technique Research on Public Causes 200903008-14.

Reference

1. Ma, S.: The Basic Knowledge of Protection of New Varieties of Plants (PVP), pp. 50–51. Lantian Press, Bejing (1999)
2. Xu, Z., Liu, H.: Study on the Statsitical Assessment of Distinctness of quantitative characteristics in DUS Testing of the New Rice Varieties. Journal of South China Agricultural University 29(1), 6–9 (2008)
3. Chen, H., Gu, X.: Discriminant Analysis on Significance of Character Difference in Testing New Rice Varieties. Acta Agriculturae Shanghai 19(4), 18–20 (2003)
4. Li, X.: Study on the Sample Size of quantitative characteristics in DUS Testing of New Varieties of Maize. Chinese Agricultural Science Bulletin 25(08), 150–153 (2009)
5. Zhang, J., Wang, J., et al.: Analysis on Difference of Character of Maize Standard Variety for DUS Testing in Yunnan. Southwest China Journal of Agricultural Sciences 17, 224–227 (2004)
6. Wei, X., Zhu, Z., et al.: DUS Test Techniques on Rice. Chinese Rice 4, 15–16 (2004)
7. Guideline for the Conduct of Tests for Distinctness, Uniformity and Stability-Rice (State Standard of the People's Republic of China), pp. 14–24 (2003)
8. Guideline for the Conduct of Tests for Distinctness, Uniformity and Stability-Rice (State Standard of the People's Republic of China), pp. 15–19 (2007)

Effect of Different Wet Oxidation Pretreatment Conditions on Ethanol Fermentation from Corn Stover

Zhang Qiang[1] and Anne Belinda Thomsen[2]

[1] School of Life Science and Technology, Changchun University of Science and Technology Changchun, Jilin Province, China
[2] Biosystems Division Risø DTU, Technical University of Denmark, Denmark
corn11@126.com

Abstract. Corn stover is an abundant raw material for fuel ethanol production. Finding out the appropriate process for ethanol production will be possible to achieve industrilization. Three different wet oxidation pretreatment conditions were adopted to produce ethanol from corn stover by simultaneous saccharification and fermentation (SSF). Recovery of cellulose and hemicellulose, enzymatic hydrolysis of cellulose and ethanol yield were studied under the three conditions. The results showed that about 90% of cellulose was remained in the solid cake and most of hemicellulose and lignin were solubilized and degraded under three pretreatment conditions. Under the best condition (195℃,15min ,Na2CO3 2g/L ,O2 12bar) , the recovery of cellulose was 95.87%. After 142 h of SSF , ethanol yield of 79.0 % of the theoretical and corresponding ethanol concentration of 25.0g/L and volumetric productivity of 0.176gL-1h-1 were obtained by baker' yeast .The values were higer than those under other pretreatment conditions. No obvious inhibition effect occurred during SSF.

Keywords: Ethanol, Corn stover, Pretreatment, Simultaneous saccharification and fermentation(SSF).

1 Introduction

Corn stover is an abundant agricultural residue and consists of cellulose、 hemicellulose and lignin. Corn stover is ubiquitous in China comprising more than 100 million tonnes every year. Only small part of corn stover is collected and used and the most part is buried in the air in our country. This causes great pollution and waste. This method of direct combustion results in low thermal efficiency ----about 10%. If direct combustion is converted into gas or liquid fuel (ethanol、 hydrogen、 diesel、 etc.) , thermal efficiency can reach up to 30% .This will not only alleviate the resource crisis ,food shortages, environmental pollution and other issues, but also provide a guarantee for the sustainable development of society[1].

Due to the close association to lignin in the plant cell wall, pretreatment is necessary to make the carbohydrates available for enzymatic hydrolysis. Wet oxidation pretreatment has been proven to be more efficient for treating some

E. Zhu and S. Sambath (Eds.): Information Tech. and Agricultural Eng., AISC 134, pp. 953–958.
springerlink.com © Springer-Verlag Berlin Heidelberg 2012

lignocellulosic materials .It has the advantage of producing fewer by products, such as furfural and hydroxymethyl furfural[2-3].

Now many experiments were not made on real fibrous substrate. In order to test the real process, the glucose and xylose should be derived from enzymatic treatment of the pretreated material as performed in simultaneous saccharification and fermentation (SSF).

Different pretreatment conditions was optimized by this work. Recovery of cellulose and hemicellulose, enzymatic hydrolysis of cellulose were studied under the three conditions. With substrate concentration of 8%, dry yeast was adopted to produce ethanol.

2 Material and Methods

2.1 Strain

Dry yeast was produced in Denmark(Danske Spritfabrikker A/S)

2.2 Raw Material

Corn stover was grown in Italy and harvested in July 2004**. T**he air-dried corn stover was milled to 1mm for the pretreatment experiments.

2.3 Pretreatment of Corn Stover

The pretreatment was performed in a 2L loop autoclave designed by Risø National Laboratory[4] .60 g milled corn stover (dry weight, DW) was mixed with 1 L water. autoclave was freed of oxygen by flushing with N_2. Experiment design (Table1) . After pretreatment the slurry was filtered and both the solid cake and hydrolysate were collected .

Table 1. Experimental design for hydrothermal pretreatment conditions

Pretreatment condition	Temperature (℃)	Time(min)	O_2(bar)	Na_2Co_3(g/L)
A	195	15		
B	195	15	12	
C	195	15	12	2

2.4 Enzymatic Hydrolysis

The enzymatic convertibility was tested as well as the untreated corn stover which was used as control. The enzymatic hydrolysis was carried out at 50 ◦C and pH 4.8. Please see[5].

2.5 Composition Analysis of Solid Cake and Raw Corn Stover

The composition of solid cake and raw corn stover was determined by two-step acid hydrolysis. The first hydrolysis step was done at 30 ℃ with 1.5ml H_2SO_4 (72%). After 60min, the second step was carried out in the autoclave at 121℃ for 1 h.

2.6 Composition of the Hydrolysate

The hydrolysate was hydrolyzed by 4% H_2SO_4 at 121℃for 10min, The sugar content was determined by HPLC.

2.7 Simultaneous Saccharification and Fermentation (SSF)

8.0g solid fraction and 100ml hydrolysate (PH adjusted to 4.8 with 0.1M H_2SO_4) were mixed .As the first step, prehydrolysis was carried out for approximately 24 h at 50 ℃ with addition of 10 FPU/g DM enzyme solution Cellubrix (Novozymes). After 24 h the temperature was32℃ and new enzyme loading (20 FPU/g DM)and 0.2 ml urea (w/v, 24%) and 0.2 g dry baker's yeast were added, the SSF was continued for approximately 6 days. The amount of ethanol was determined as weight loss caused by CO_2 release[6]. The final ethanol concentration was determined by HPLC.

2.8 Mass Balance Calculations

Recovery of cellulose (% [w/w])=[Cellulose in solid (g)] + [Cellulose in hydrolysate (g)]/Cellulose in raw corn stover (g)

Recovery of hemicellulose (% [w/w]) = [Hemicellulose in solid (g)] + [Hemicellulose in filtrate (g)/]/Hemicellulose in raw corn stover (g)

3 Results and Discussions

3.1 Effect of t Pretreatment on Corn Stover

Chemical composition of corn stover greatly changed after pretreatment. From table 2, the solid cake was all enriched in cellulose under A B C conditions. The relative cellulose content was 55.8%, 74.7% and 73.3% compared with 38.8% of cellulose in untreated corn stover, The highest cellulose recovery was 89.8% under C condition. In wet oxidation, the most part of hemicellulose and ligin was solubilized or degraded at high temperature. The high concentration of cellulose resulted from the removal of lignin and especially hemicellulose.

From fig1, the overall recovery of cellulose was 95.87% under C condition which was higher than that of hemicellulose. This relatively low recovery of hemicellulose was probably owing to hemicellulose oxidation to other products, such as carboxylic acids, CO_2 and H_2O.

Table 2. Chemical composition of treated and untreated corn stover (g/100g raw corn stove

	Raw corn stover	A	B	C
Solid cake				
DM	100	60.16	45.85	47.54
Cellulose	38.8	33.57	34.25	34.85
hemicullulose	22.4	5.72	3.25	4.94
lignin	14.7	15.18	8.0	6.48
Hydrolysate				
cellulose	-	1.80	2.43	2.28
hemicellulose	-	10.99	8.02	10.37

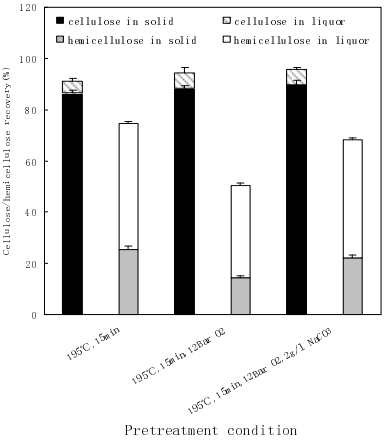

Fig. 1. Recovery of cellulose and hemicellulose

3.2 Enzymatic Hydrolysis

Enzymatic accessibility of the cellulose in the pretreated solid cake is very important for ethanol production.

Table 3 showed the percentage of enzymatic convertible cellulose of solid cake after 24 h of hydrolysis at 50°C.

The highest enzymatic conversion of pretreated cellulose in the remaining solid was 67.6% compared with 16.2% for raw corn stover under C condition which is 4.17 times of that of raw corn stover.

Table 3. Conversion of cellulose (%) of solid cake

Pretreatment condition	Conversion of cellulose (%)
Raw corn stover	16.2
A	64.8
B	65.8
C	67.6

3.3 Ethanol Production by SSF

Ethanol production was evaluated from dried solid cake by baker' yeast and the hydrolysate was employed as liquid fraction followed by SSF. Raw corn stover was also tested as control.

Table 4 showed the ethanol production expressed as the percentages of the theoretical yield compared to the raw corn stover. The highest ethanol production of 79.0% was obtained under C condition and the corresponding ethanol concentration and volumetric productivity were 25.0g/L and 0.176g/L.h respectively whereas A and B only yielded 73.1% and 75.2% ethanol.

From fig2, lag phase was observed for the fermentation within 4 hours under B and C because of furfural. In general, furfural is inhibitory to yeast metabolism at a level of 1 g /L or higher[7]. The content of furfural was almost zero under A condition whereas the content of furfural was 0.23g/L and 0.14g/L respectively under B and C. An initial lag phase (about 4hour) was used by the yeast to adjust or detoxify the substrate[8].

Table 4. Effect of different pretreatment conditions employed on ethanol production

	Ethanol (g/L)	Qp(g/L h)	Y(% of theoretical)
Untreated	4.22	0.030	27.5
A	17.2	0.121	73.1
	24.3	0.171	75.2
	25.0	0.176	79.0

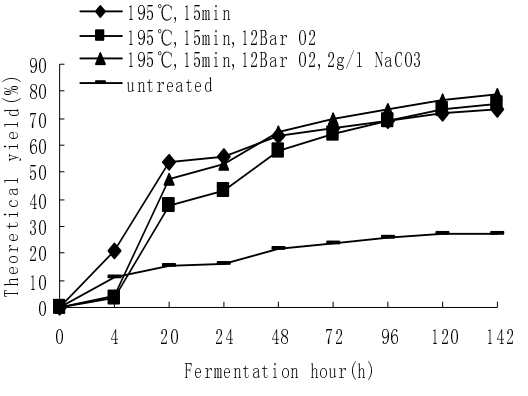

Fig. 2. Ethanol content vs time during SSF

4 Conclusions

Under three different pretreatment conditions,about 90% of cellulose was remained in the solid cake and most of hemicellulose and lignin were solubilized and degraded.

The best condition was 195℃,15min , Na_2CO_3 2g/L ,O_2 12bar.Under the best condition, the recovery of cellulose was 95.87% which was higher than that under other pretreatment conditions. After 24h hydrolysis using cellulose (Cellubrix L),the achieved conversion of cellulose to glucose was 67.6% compared with 16.2% for raw corn stover . After 142 h of SSF with substrate concentration of 8%, ethanol yield of 79.0 % of the theoretical was obtained. The corresponding ethanol concentration and volumetric productivity were 25.0g/L and 0.176g/L.h respectively. Detoxification procedures was not used in fermentation process. This will reduce production costs.

Reference

1. Guo, P., Wang, X., Zhu, W., Yang, H., Cheng, X., Cui, Z.: Degradation of corn stalk by the composite microbial system of MC1. J. Environ. Sci. 20, 109–114 (2008)
2. Lissens, G., Klinke, H., Verstraete, W., et al.: Wet oxidation of organic household waste enriched with wheat straw for simultaneous saccharification and fermentation into ethanol. Environ. Technol. 25(6), 647–655 (2004)
3. Olsson, L., Hahn-Hagerdal, B.: Fermentative performance of bacteria and yeasts in lignocellulose hydrolysates. Proc. Biochem. 28(4), 249–257 (1993)
4. Bjerre, A.B., Sørensen, E.: Thermal decomposition of dilute formic acid solutions. Ind. Eng. Chem. Res. 31(6), 574–577 (1992)
5. Varga, E., Schmidt, A.S., Réczey, K., Thomsen, A.B.: Pretreatment of corn stover usingwet oxidation to enhance enzymatic digestibility. Appl. Biochem. Biotechnol. 104, 37–50 (2003)
6. Varga, E., Helene, B., Rećzey, K.K., et al.: High Solid Simultaneous Saccharification and Fermentation of Wet Oxidized Corn Stover to Ethanol. Biotechnology and Bioengineering 88(5), 567–574 (2004)
7. VanZyl, C., Prior, B.A., Preez, J.C.: Production of ethanol from sugarcane bagasse hemicellulose hydrolysate by Pichia stipitis. Appl. Biochem. Biotechnol. 17(1), 357–369 (1988)
8. Roberto, I.C., Lacis, L.S., Barbosa, M.F.S., et al.: Utilization of sugar cane baggasse hemicellulose hydrolysate by Pichia stipitis for the production of ethanol. Proc. Biochem. 26(1), 15–21 (1991)

Polysaccharides from Acanthopanacis Senticosi: Isolation, Purification, Antioxidant and Immunological Activities In Vitro

Chen Ruizhan[1], Yang Simin[1], Dong Hang[1], and Liu Zhiqiang[2]

[1] College of Chemistry, Changchun Normal University, Changchun, China
[2] Laboratory of New Drug Research, Changchun Institute of Applied Chemistry, Chinese Academy of Sciences, Changchun, China
{ruizhanchen,yangsimin456,duang.good}@163.com, liuzq@ciac.jl.cn

Abstract. A water-soluble polysaccharide fraction, coded as ASP-2-1, were extracted from Acanthopanacis Senticosi with hot-water.They were isolated and purified by chromatography on EDAE-Sepharose Fast Flow Ion-exchange column and Sephadex G-75 gelpermeation column successively. Monosaccharide composition was determined by capillary zone electrophoresis (CZE), molecular weight and purity was determined by high-performance gel-permeation chromatography (HPGPC). The gel permeation chromatography (GPC) analysis showed that the average molecular weight (Mw) of polysaccharides were approximately 14573 Da which contained 89.47% carbohydrate, 7.45% uronic acid, 2.16% protein and six kinds of monosaccharides including glucose (Glu), arabinose (Ara), galactose (Gal), fructose (Fru), rhamnose (Rha), xylose (Xyl) in a molar ratio of 27.33:8.92:3.03:1:7.59:20.51. Furthermore, the immunobilological and antioxidant activities of ASP-2-1 were evaluated by MTT assay, ferric-reducing antioxidant power (FRAP) assay and the scavenging activities of •O2-,•OH and DPPH, respectively. The ASP-2-1 could significantly promote the Spleen lymphocyte proliferation, pronounced higher reductive power, strong •OH radical scavenging activity, moderate •O2- and DPPH• radicals scavenging activities. It should be explored as a novel and potential natural antioxidant and immunostimulating agent for use in functional foods or medicine.

Keywords: Polysaccharides, Acanthopanacis Senticosi, Mon-osaccharides composition, Antioxidant activity, Immunological activity.

1 Introduction

Acanthopanax senticosus Harms which is widely used in China can make body strong, relax the mental, and protect spleen and kindney[1]. Some studies has shown that acanthopanax polysaccharides are the main bioactive components with antitumor, immune, radiation, antioxidant and other pharmacological activities[2-3]. The polysaccharide has a multitarget, low toxicity, the clinical application prospect. This paper studies the Acanthopanax **Senticosi** Polysaccharides(ASP), structural information, antioxidant and immune activity, and provided a theoretical basis for development and utilization of functional food as well as Acanthopanax polysaccharides drug product.

E. Zhu and S. Sambath (Eds.): Information Tech. and Agricultural Eng., AISC 134, pp. 959–966.
springerlink.com © Springer-Verlag Berlin Heidelberg 2012

2 Material and Methods

2.1 Materials and Chemicals

Acanthopanax senticosus (Jilin Fusong booming town production); Sephadex G-75; DEAE fast flow Sepharose (Pharmacia Biosciences Co.,); 1,1 - diphenyl-2 - bitter base hydrazine (DPPH) ;ascorbic acid (Vc) ;dimethyl thiazole - diphenyl tetrazolium bromide (MTT) ;2,4,6 - Tris (2 - pyridyl) -1,3,5 - triazine (TPTZ) ;1 - benzene -3 - methyl -5 - pyrazolone (PMP) ; ConA (Sigma Co.,); dextran standards (Pharmacia Co.,); 1640 PRMI medium (GIBICO) ,other reagents were analytical pure reagents.

2.2 Methods

2.2.1 Extraction of Polysaccharide from Acanthopanacis

After crushed and degreased, the leaves of Acanthopananx were extracted at 90℃ for 3 h by adding wate according to 1:30 (g / mL) and repeated three times. The extract was deposited by 95% ethanol. The final ethanol concentration of 70 %. Protein was removed with Sevag method. Finally, the polysaccharide pellets were obtained by centrifugation, resuspended in appropriate volume of distilled water and dialysed for 2 days against distilled water (ASP).

2.2.2 Purification of Polysaccharide from Acanthopanacis

The crude ASP were dissolved in 0.2 mmol/L Tris-HCl. buffer. The solution was applied to a DEAE-Sepharose fast-flow column (20×460 mm) Fractions were prepared in a stepwise elution with increased concentration of NaCl (0.1, 0.3, 0.5, 0.8 M) solution at a flow rate of 1.0 ml/min, and with collection of 5 ml for each tube. The content of ASP in each fraction was detected by phenol–sulphuric acid method. The appropriate fraction of ASP-2-1 wasconcentrated, dialysed against water, and finally lyophilised.

2.2.3 Molecular Weight of Polysaccharide Determination

The sample solution was applied to Agilent 1100 HPLC system equipped with a Dhpak SB-803 HQ (8.0×300 mm, 35℃), eluted with 0.05 M Na2SO4 solution at a flow rate of 0.5 ml/min and detected by a RID-10A refractive index detector .The columns were calibrated with T-series dextran (T-200, T-70,T-40, T-20 and T-10) and glucose as standards. The molecular weight of ASP-2-1 was estimated by the calibration curve made above.

2.2.4 High-Performance Capillary Electrophoresis(HPCE) Analysis

The polysaccharide was hydrolysed with TFA and derivated by PMF. 75 mM sodium tetraborate buffer (pH 9.5) was used as solvent. Electrophoresis was performed at 15 kV using normal polarity. The samples to be analysed were injected automatically, using the low pressure injection mode (0.5 psi), in which the sample is pressurised for 5 s. The absorbance was detected at 254 nm.

2.2.5 For Aut Determination of Contents of Total Sugar, Total Uronic Acid, and Protein in the Polysaccharide

Total sugar content in the purified polysaccharide was deterned by the phenol–sulphuric acid method, using D-glucose as andard[4]. Total uronic acid content was determined by photometry with m-hydroxybiphenyl using GlcA as the standard[5]. Protein content was also determined by BSA standard curve[6].

2.2.6 Determination of Antioxidant Activities of Polysaccharide

a) Ferric-reducing antioxidant power (FRAP) assay

50 μL of sample or 5 μL of Vc (0.5 mmol/L) were added to the 50 μL of FRAP reagent. The absorbance values of standards and samples at 0min and 4min were determined and repeated six times. 0.5mmol/L of Vc was used as the standard. The formula is: FRAP=(0-4 min ΔA593nm of samples)/ (0-4 min ΔA593nm standard) ×500 (μmol/L).

b) Superoxide radical-scavenging assay

The reaction was performed in 5.0 ml of phosphate buffer (50 mM, pH 8.2) and 4.7ml of water with 0.1mL of the samples to be tested at different amounts. After adding 0.2mL of 3 mM pyrogallol solution, the reaction mixture was incubated at 25 ℃ for 20 min, and the change speed of absorbance (A/min) of the reactive solution was measured at 325 nm, against a blank (water and 50 mM phosphate buffer instead of sample). The percent scavenging activity of superoxide radical was calculated by the following formula:

$$\text{Scavenging activity } (\%)=(1-A_1/A_0) \times 100;$$

where A_0 is the change speed of absorbance of the control group in the superoxide radical generation system and A_1 is the change speed of absorbance of the test sample. Three parallel experiments for each sample.

c) Hydroxyl radical-scavenging assay Selection

The 1 mL of sodium phosphate buffer (pH 7.4), which contained FeSO4, sodium salicylate (520 μg/mL), 6% H_2O_2, and varying concentrations of polysaccharides were incubated at 40 ℃ for 1 h. The absorbance was detected at 514.9 nm, and each concentration was repeat three times. Ac is the absorbance of the control group in the hydroxyl radicals generating system (water instead of test sample solution), Ai the absorbance of the test group.Scavenging activity (SA %)= [(Ai-Aj)/(Ac-Aj)]×100

d) DPPH radical-scavenging assay

0.1 mM solution of DPPH in methanol was prepared and 1.0 ml of this solution was added to 3.0 ml of the polysaccharides of various concentrations (0.01–1.0 mg/ml) in water. The mixture was shaken and incubated at 25 ℃ for 30 min in the dark,then the absorbance was measured at 517 nm against a blank (water instead of test sample and DPPH solution). Scavenging activity (SA %)= [1-（Ai-Aj）/Ac]×100%; where Aj is the absorbance of the control (water instead of test sample solution), Ai is the absorbance of the sample. Each sample was repeat three times.

2.2.7 Immunomodulatoryl Activity of Polysaccharide on Mouse Spleen Tlymphocytes

The cells of spleen with phosphate-buffered (PBS) was adjusted to a density of 1×106 cells/ml in the RPMI 1640 complete medium. The sample was set at five different concentrations: 1,2, 5, 10, 20 μg / mL. After incubation at 37℃ in a humid atmosphere with 5% CO_2 for 48 h, 20 ℃ of MTT solution (5 mg/ml) were added to each well and incubated for another 4 h. The plate was centrifuged on 2000 rpm for 10 min, the supernate was discard. Absorbance at 570 nm was measured on an ELISA reader. Test results were used the value of (x ±s) A570 nm and the test for the difference between the groups. The p-value less than 0.05 was considered significant difference between groups.

3 Results and Discussion

3.1 Isolation of Polysaccharides Composition

The leaves of Acanthopananx were processed by water extraction, ethanol precipitation, de-proteinized by Sevag method, dialysed with water and lyophi lised in freeze–dry apparatus. The total yield of ASP was 6.98% (w/w) of the dried material.

3.2 Purification of ASP

1) DEAE-Sepharose Fast Flow column chromatography

The ASP were further purified by DEAE fast flow Sepharose anion exchange chromatography. Different fractions were selected based on total carbohydrate elution profile (Fig. 1). The results showed that ASP was mainly composed of three sub-fractions, namely ASP-1, ASP-2 and ASP-3. Each fraction was eluted as a single symmetrical peak, which indicated that 5.93% (ASP-1), 10.33% (ASP-2) and 8.83% (ASP-3) were three homogeneous polysaccharide.

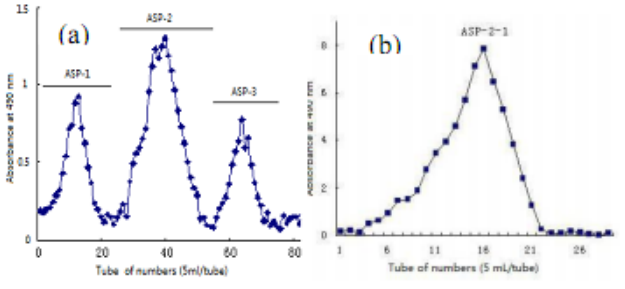

Fig. 1. (a) Profiles of ASP on DEAE-Sepharose fast flow chromatography column (20×460 mm) with 0,1–0.8 M NaCl stepwise elute.(b)Profiles of ASP-2-1 on Sephadex G-75 gelpermeation chromatography column (16 ×500 mm) with 0.1 M NaCl elute

2) Sephadex G-75 gel permeation chromatography

To obtain high-purity and homogeneity polysaccharide products for stable functional property, the main fraction of ASP-2 was further purified by Sephadex G-75 gel

permeation chromatography based on the molecular size (Fig. 1b). The profiles showed a single and symmetrical sharp peak, indicating that ASP-2-1 was a homogeneous polysaccharide. The yield of ASP-2-1 was 54.98% (relative to ASP-2).

3) Molecular weight determination of ASP-2-1

The HPGPC (Fig. 2a) profiles showed a single and symmetrical sharp peak, indicating that ASP-2-1 was a homogeneous polysaccharide with an average molecular weight of about 14,573 Da, according to the calibration curve with standard dextrans. LogMr=－0.1029TR+2.34 ((R^2=0.9726, retention time 17.425 min).

4) HPCE analysis of ASP-2-1

Monosaccharide compositions of ASP-2-1 were determined by the TFA hydrolysis and HPCE analysis method that were shown in Fig 2(b-c). The results indicated that glucose and xylose were the major monosaccharides constructing the backbones of ASP-2-1. ASP-2-1 was composed of Glu、Ara、Gal、Fru、Rha、Xyl with molar rations of 27.33： 8.92：3.03：1：7.59：20.51.

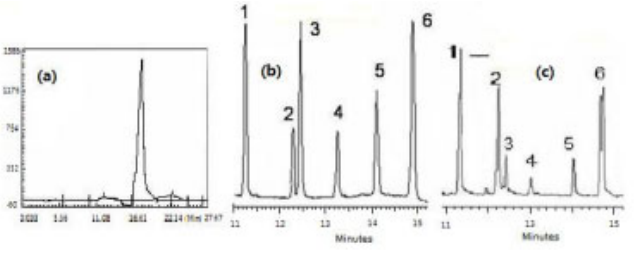

Fig. 2. (a) The profile of ASP-2-1 fraction in HPGPC. (b)HPCE electropherogram of monosaccharides tandard mixture (①Glu, ②Ara, ③Gal, ④Fru, ⑤Rha, ⑥Xyl); (c) sample (① Glu, ②Ara, ③Gal, ④Fru, ⑤Rha, ⑥Xyl).

5) Determination of contents of total sugar, total uronic acid, and protein in the ASP-2-1

The total sugar content in ASP-2-1 was determined by y = 9.8414x-0.0488 (R^2 = 0.9998) (y : absorbance at 486nm, x: the concentration of glucose μg / mL).The total uronic acid content was determined by y = 0.0017x - 0.0153 (y : absorbance at 523nm, x: the concentration of uronic acid μg / mL). The total protei content was determined by y = 1.128123x- 0.6083 (y : absorbance at 635nm, x: the concentration of protein mg/mL). The total sugar content, uronic acid, and protein content of ASP-2-1 were determined as 89.47% total sugar, uronic acid content of 7.45%, 2.16% protein content.

6) Antioxidant activities analysis of polysaccharides

e) **The total antioxidant activity of polysaccharides**

The results of antioxidant was were shown in Fig 3(a) The FRAP values of ASP-1, ASP-2-1, ASP-3, ASP and Vc were 724, 785.1, 553, 593.2, and 809 μM at the concentration of 0.2 mg/ml, respectively. Moreover, ASP-2-1 was found to have

higher antioxidant capacities than ASP-1, ASP-3 and ASP, and the antioxidant capacities of ASP-2-1 was close to that of Vc's at 0.2 mg/ml. These results clearly demonstrated that all the samples possessed antioxidant capacities, especially purified fraction of ASP-2-1showed strong antioxidant capacity.

f) **Scavenging effects on superoxide radical of polysaccharides**

The results of ASP, ASP-2-1 and Vc on • O^{2-}scavenging activity were shown in Figure 3 (b). The results indicated a concentration-dependent radical scavenging activity at all tested concentrations of all the samples. Especially in relative lower concentration range of 0–0.3 mg/ml, ASP-2-1 exhibited higher superoxide radical scavenging activity, which was close to that of Vc's. However, in the higher concentration range of 0.5–2.0 mg/ml, the radical scavenging activity ASP-2-1 was lower than that of Vc's. At the concentration of l mg/ml, the scavenging activity of the ASP-2-1 and Vc was 65.37%and 85.21%.

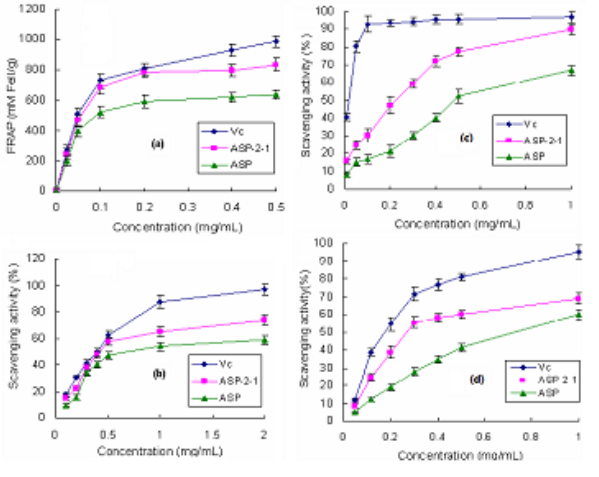

Fig. 3. Antioxidant activities of ASP, ASP-2-1 and Vc. (a) Ferric-reducing antioxidant power (FRAP);(b) Scavenging ability on •O2;(c) Scavenging ability on •OH;(d) Scavenging ability DPPH•. Each values is the mean ± SD of triplicate measurements.

g) **Scavenging effects on hydroxyl radicals of polysaccharides**

The results of hydroxyl radical scavenging activities of the ASP-1, ASP-2-1 and Vc were given in Fig. 3c. The scavenging effects of all samples increased significantly with the increase of sample concentration. At a concentration of 1.0 mg/ml, the scavenging activity was 77.91% for ASP-2-1. Therefore, ASP-2-1 had the strongest activities.

h) **Scavenging effects on DPPH radicals of polysaccharides**

As shown in Fig. 3(d), the results indicated that ASP-2-1, and ASP showed obvious scavenging activity on DPPH radical in a concentration-dependent manner. These polysaccharides are reductive agents as they can supply hydrogen, which can combine

with radical and form a stable radical to terminate the radical reaction. These results indicate that the polysaccharide might act as a natural anti-oxidants.

i) **Immunomodulatoryl activity of polysaccharide on mouse spleen Tlymphocytes**

In order to investigate a possible immunomodulatory effect of the polysaccharides, the MTT assay was used to evaluate spleen lymphocyte proliferation induced by Con A or LPS in vitro. As shown in Table 1, ASP-2-1 could significantly enhance Con A-induced lymphocyte proliferation ($P < 0.05$) as compared with those of the normal control group under the concentrations between 1 ～ 20 μg/mL. ASP-2-1 can significantly promote the proliferation of lymphocytes in vitro, and showed a dose-dependent. On lymphocyte proliferation significantly facilitating role in the concentration 10μg/mL, the facilitating role of the spleen lymphocyte proliferation reaches its maximum, compared with the control group significant difference ($P <0.001$).

Table 1. Effects of ASP-2-1 on ConA-induced proliferation activity of mouse splenocytes in vitro

C(μg/ml)	*Blank control*	*Con A control*	*1*	*5*	*10*	*20*
OD value	0.338± 0.012	0.376± 0.018	0.4045± 0.019*	0.4511± 0.016**	0.5061± 0.023***	0.4482± 0.022***

4 Conclusion

After a series of isolated, purified from a homogeneous polysaccharide ASP-2-1, which total sugar content of 89.47%, uronic acid content of 7.45%, 2.16% protein content, mainly composed of glucose, arabinose, galactose, fructose, rhamnose sugar, xylose composition, molar ratio of 27.33: 8.92:3.03:1:7.59:20.51 molecular weight of 14573 Da; ASP-2-1 has a strong reducing power of • O^{2-}, • OH and DPPH • free radical better scavenging effect, and its ability to remove a significant amount of polysaccharide concentration-effect relationship; ASP-2-1 can significantly promote the proliferation of mouse spleen lymphocytes, a higher immune activity.

Acknowledgment. The study was conducted in Jilin Province Natural Science Foundation (project number: 201 015 106) and Education Department of Jilin Province, the "Eleventh Five-Year" scientific and technological research projects (UNESCO Ji He Zi [2009] No. 209) funding for completion.

References

1. Cui, M., Sun, W.X., Song, F.R., et al.: Multi-stage mass spectrometric studies of triterpenoid saponins in crude extracts from Acanthopanax senticosus Harms. Rapid Communication in Mass Spectrometry 13, 873–879 (1999)

2. Han, S.B., Yoon, Y.D., Ahn, H.J., et al.: Toll-like receptor-mediated activation of B cells and macrophages by polysaccharide isolated from cell culture of Acanthopanax senticosus. International Immunopharmacology 3, 1301–1312 (2003)
3. Meng, Q.F., Yu, X.K., Xu, M.Y., et al.: Extraction of Acanthopanacis Senticosi Polysaccharides and Their Antioxidative Effect. Journal of Jilin University (Science Edition) 43(5), 683–686 (2005)
4. Chen, R.Z., Meng, F.L., Liu, Z.Q., et al.: Antitumor activities of different fractions of polysaccharide purified from Ornithogalum caudatum Ait. Carbohydrate Polymers 80, 845–851 (2010)
5. Blumenkrantz, N., Asboe-Hansen, G.: New method for quantitative determination of uronic acids. Analytical Biochemistry 54, 484–489 (1973)
6. Lowry, O.H., Rosebrough, N.J., Farr, A.L., et al.: Protein measurement with the folin phenol reagent. Journal of Biochemistry 193, 265–275 (1951)

Effects of Trehalose, Glycerin and NaCl on the Growth and Freeze-Drying of Lactobacillus Acidophilus

Chen He, Ji Zhe, Wang Lei, and Shu Guowei

College of Life Science and Engineering, Shaanxi University of Science and Technology, Xi'an, China

Abstract. The effects of trehalose, glycerin and NaCl on the growth and vacuum freeze-drying of Lactobacillus acidophilus were investigated by single-factor tests. Results showed there was negative correlate between cell growth and different concentration of trehalose, glycerin and NaCl; the experimental group of 6g/L trehalose or 6mL/L glycerin gave a above 80% survival rate for Lactobacillus acidophilus of the freeze-dried powder while the control group rated 42%. The results suggest that trehalose, glycerin and NaCl inhibit the growth of Lactobacillus acidophilus but contribute to improve anti-freezing capacity.

Keywords: Trehalose, Glycerin, Sodium chloride, Lactobacillus acidophilus, Freeze-drying.

1 Introduction

In recent years, awareness of the therapeutic effect on human health of consuming probiotic bacteria has increased [1]. A number of health benefits have been reported upon consumption of probiotic including reduction of gastrointestinal symptoms in lactose-intolerant individuals, relief from symptoms of constipation, treatment of infantile diarrhea, prevention of travellers' diarrhea, and activity against *Helicobacter pylori* [2-5]. *Lactobacillus acidophilus* is one of the most commonly recognized species of probiotic bacteria used as food adjuncts [6], it was first isolated from the intestinal tract and vagina of humans and animals and has been shown to play an important role in promoting and maintaining human health [7].

Freeze-drying can be used for manufacture of probiotic powders on a large-scale, but expose the cultures to extreme environmental conditions and not all strains survive the process [8-10]. The major causes are probably eutectic crystal formation, high osmolarity, macromolecule denaturation, and the removal of water [11]. Adding protective agents could enhance the stability of probiotics during freeze-drying, and adonitol, betaine, glycerol, lactose, skim milk and dimethyl sulphoxide have been reported as efficient protective agents[12]. We add trehalose, glycerin and NaCl to MRS broth intending to explore the effects of them on the growth and freeze-drying of *Lactobacillus acidophilus* and giving a reference to prepare highly active probiotic powders.

E. Zhu and S. Sambath (Eds.): Information Tech. and Agricultural Eng., AISC 134, pp. 967–971.
springerlink.com © Springer-Verlag Berlin Heidelberg 2012

2 Materials and Methods

2.1 Materials

A probiotic lactic acid bacterial strain, *lactobacillus acidophilus* obtained from College of Life Science and Engineering, Shaanxi University of Science and Technology, Xi'an was used. Stock cultures in MRS broth (Hopebio, Qingdao, China) and grown three successive times in anaerobic condition. The transfer volume was 2% (v/v), and the the incubation was at 37℃ for 18 h.

Trehalose, glycerin and NaCl were of analytical grade.

2.2 Growth Condition

The MRS broth added trehalose, glycerin and NaCl in anaerobic tube for 2, 4, 6 and 8g/L respectively. MRS broth without trehalose, glycerin and NaCl was included in this experiment as control group. MRS broth was used as a growth medium after inoculate with 5% (v/v) *lactobacillus acidophilus* in exponential phase grown three successive times in anaerobic tubes before use. The growth temperature was kept at 37℃.

Record the number of colonies and measured OD values and pH every two hours, then constructed the growth curve.

2.3 pH Evaluation

Evaluated the pH of the culture with a pH-meter (pHS-3C, Shanghai Precision Scientific Instrument Co., Ltd, Shanghai, China).

2.4 Growth Determination

Monitored the growth of the strains by measuring the optical density of the culture at 600nm (OD_{600}) through a spectrophotometer (SP-756PC, Shanghai Spectrum Instruments Co., Ltd., Shanghai, China).

2.5 Freeze-Drying

Centrifuged for 10min at 6000r/min to collect bacteria, washed twice with physiological saline, centrifuged again and collected bacteria to make suspension of 7±1×1010cfu/mL. Mix the protective agent (Skim milk powder 100g/L, NaCl 8.5g/L) and bacterial suspension for 3: 1 (v/v) into Freeze-drying tube, stood for 30min. Then pre-preezed at -35℃~ -40℃ for 24h, freeze-dried at -55℃ and 4-6pa for 24h through a vacuum freeze drier (FD-1D-50,Beijing Boyikang Instruments Co., Ltd., Beijing, China).

3 Results and Discussion

3.1 Effect of Trehalose, Glycerin and NaCl on Growth of Lactobacillus Acidophilus

The effect of different concentrations of trehalose, glycerin and NaCl on growth of *Lactobacillus acidophilus* after incubated 18h was showed in Figure 1-2.

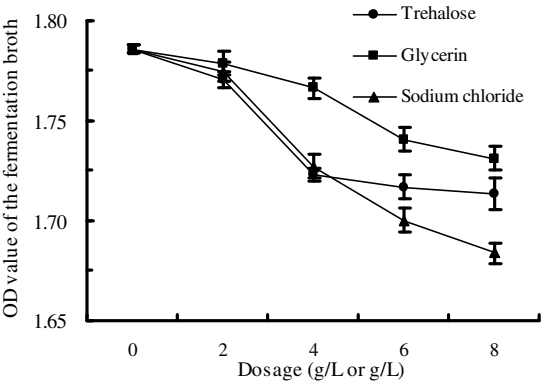

Fig. 1. Effect of trehalose, glycerin and NaCl on growth of Lactobacillus acidophilus

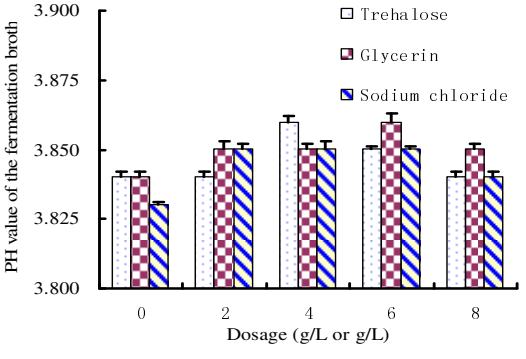

Fig. 2. Effect of trehalose, glycerin and NaCl on pH of Lactobacillus acidophilus

The growth of *Lactobacillus acidophilus* inversely with the concentration of trehalose, glycerin and NaCl, for the inhibitory effect became more significant with the increasing concentration of the solution. And the inhibitory effect of NaCl was particularly noticeable, for OD_{600} was only 1.684 at 8g/L NaCl (Fig 1).

The pH value of the medium stayed between 3.83-3.86 (Fig 2) indicated that the different concentration of trehalose, glycerin and NaCl have no significant effect on acid-producing of the strain.

3.2 Effect of Trehalose, Glycerin and NaCl on Vacuum Freeze-Drying of Lactobacillus Acidophilus

The effect of different concentrations of trehalose, glycerin and NaCl on survival of *Lactobacillus acidophilus* after freeze-drying was showed in Figure 3.

Referring to Fig 3, trehalose, glycerin and NaCl, to some extent, could improve the survival rate of *Lactobacillus acidophilus* after freeze-drying. The anti-freezing capacity of *Lactobacillus acidophilus* was positively correlated with the concentration of NaCl, while excess NaCl would significantly inhibit the cell growth. However, the

relationship between the anti-freezing capacity of the strain and the concentration of trehalose and glycerin was like a parabola.

The main causes of trehalose, glycerin and NaCl in promoting anti-freezing capacity was: trehalose could combine with protein on the membrane of the bacteria to form hydrogen bonds, while glycerin could diffuse into the cell and combine with protein in vivo to form hydrogen bonds, both of them could provide protection to protein of the cell; NaCl in vivo could protect organelles and a variety of active substances by preventing cell sap from forming eutectic crystal.

The optimum concentration of trehalose to resistance against freeze-drying was 6g/L which gave a survival rate above 82%; while the optimum concentration of glycerin was 6ml/L and the survival rate was above 80%. Meanwhile, the survival rate of the control group was just about 42%.

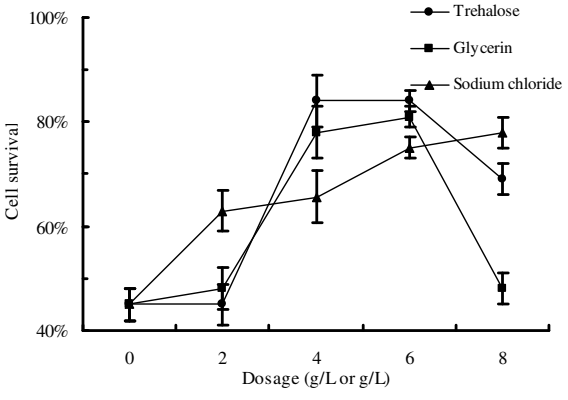

Fig. 3. Effect of trehalose, glycerin and NaCl on vacuum freeze-drying of Lactobacillus acidophilus

4 Conclusions

Presence of trehalose, glycerin or NaCl could inhibit the growth of *Lactobacillus acidophilus* and has no significant effect on pH of the *Lactobacillus acidophilus*, however they show resistance against freeze-drying.

Acknowledgment. The project was supported by key project of Shaanxi Provincial Department of Agriculture, China (No.2009-45), key project of Shaanxi Provincial Department of Education (No.2010JK437), Science and Technology Bureau of Yulin and Weiyang science and technology Plan, Xi'an (No.201002).

References

1. Gomes, A.M.P., Malcata, F.X.: Bi. dobacterium spp. and Lactobacillus acidophilus: Biological, biochemical, technological and therapeutical properties relevant for use as probiotics. Trends Food Sci. Tech. 10, 139–157 (1999)

2. Choi, S.C., Kim, B.J., Rhee, P.L., et al.: Probiotic Fermented Milk Containing Dietary Fiber Has Additive Effects in IBS with Constipation Compared to Plain Probiotic Fermented Milk. Gut Liver 5(1), 22–28 (2011)
3. Tabbers, M.M., de Milliano, I., Roseboom, M.G., et al.: Is Bifidobacterium breve effective in the treatment of childhood constipation Results from a pilot study. Nutr. J. 2(23), 10–19 (2011)
4. Rerksuppaphol, S., Rerksuppaphol, L.: Lactobacillus acidophilus and Bifidobacterium bifidum stored at ambient temperature are effective in the treatment of acute diarrhoea. Ann. Trop. Paediatr. 30(4), 299–304 (2010)
5. Jain, S., Yadav, H., Sinha, P.R., et al.: Anti-allergic effects of probiotic Dahi through modulation of the gut immune system. Turk. J. Gastroenterol. 21(3), 244–250 (2010)
6. Fung, W.Y., Woo, Y.P., Liong, M.T.: Optimization of growth of Lactobacillus acidophilus FTCC 0291 and evaluation of growth characteristics in soy whey medium: a response surface methodology approach. J. Agric. Food Chem. 56(17), 7910–7918 (2008)
7. Salminen, S., Ouwehand, A.C., Isolauri, E.: Clinical application of probiotic bacteria. Int. Dairy J. 8, 563–572 (1998)
8. Meng, X.C., Stanton, C., Fitzgerald, G.F., et al.: Anhydrobiotics: The challenges of drying probiotic cultures. Food Chemistry 106, 1406–1416 (2008)
9. Berny, J.F., Hennebert, G.L.: Viability and stability of yeast cells and filamentous fungus spores during freeze-drying: effects of protectants and cooling rates. Mycologia 83, 805–815 (1991)
10. Abadias, M., Benabarre, A., Teixido, N., et al.: Effect of freeze drying and protectants on viability of the biocontrol yeast Candida sake. Int. J. Food Microbiol. 65, 173–182 (2001)
11. Thammavongs, B., Corroler, D., Panoff, J.M., et al.: Physiological response of Enterococcus faecalis JH2-2 to cold shock: growth at low temperatures and freezing/thawing challenge. Lett. Appl. Microbiol. 23, 398–402 (1996)
12. Kearney, L., Upton, M.M., Loughlin, A.: Enhancing the viability of Lactobacillus plantarum inoculum by immobilizing the cells in calcium-alginate beads incorporating cryoprotectants. Appl. Environ. Microbiol. 56, 3112–3116 (1990)

Microbial Changes and Fresh-Keeping of Fresh Noodles under Refrigerated Condition

Shuncheng Ren, Ruiping Ma, and Ning Wang

School of Food Science and Technology, Henan University of Technology
Zhengzhou 450052, China
{scren,maruiping2008}@163.com, wangning19880808@126.com

Abstract. This research aimed to study on microbe change and fresh-keeping of wet-fresh noodles under refrigerated condition. On the basis of studying on the microbe change of wet-fresh noodles, we studied antimicrobial effect of several food preservatives on wet-fresh noodles under refrigerated condition. The optimize formulation was accquired by single-factor tests and orthogonal tests. Results indicated that the acidity and number of bacterial colony in wet-fresh noodles both showed an incresing trend under refrigerated condition. The optimal antistaling agents were ethylparabe, SDA(Sodium Diacetate) and R-polysaccharide. When 0.04% of ethylparaben, 0.05% of SDA, 0.04% of R-polysaccharide were added to wet-fresh noodles. which can be preserved for at least 14 days under refrigerated condition.

Keywords: Wet-fresh noodles, Microbe, Preservation.

1 Introduction

Noodles are very commen cooked wheaten food in people's daily life. The wet-fresh noodles are characterized in fresh, tasty and refreshing, al dente, surface fragrance thick in comparision with fine dried noodles, and are very popular in consumers. How to keep the noodles fresh and clean during its shelf life is always one of the hottest research topics. This kind of noodles have high content moisture and are suitable for the development of spoilage organisms, so it's hard to gain a long term preservation. Therefor, a thorough research is needed to achieve a long safety preservative time[1-2].

For the time being, researchers both from domestic and overseas have developed several researches on refreshing and quality improving of wet-fresh noodles, and put forward some related technics. However, the shelf life of wet-fresh noodles is still limited[3]. The key point of this article was researching the microbe change regularity of the wet-fresh noodles under refrigerated condition. After analysis of changing trend of microbe and acidity, pertinently select and formulate the preservatives, and finally achieved a long shelf life.

E. Zhu and S. Sambath (Eds.): Information Tech. and Agricultural Eng., AISC 134, pp. 973–980.
springerlink.com © Springer-Verlag Berlin Heidelberg 2012

2 Materials and Methods

2.1 Materials and Reagent

Wheat flour: JinYuan first class flour; natamycin, sodium dehydroacetate, ethylparaben, *R*-polysaccharide, sodium diacetate(SDA), sodium benzoate: food grade, Zhejiang Yin Xiang Biological Engineering Co.LTD; potassium sorbate: food grade, Tianjin Guang Fu Fine Chemical Industry Research Institute; preservative film(polyethylene film): food grade, bought from local market.

2.2 Instruments

150 AB Biochemical Incubator, Shanghai Shu Li Instruments Co.LTD; 101-FX-1 Electric Drying Oven with Forced Convection, Shanghai Shu Li instruments Co.LTD; JYC-21ES17 Induction Cooker, JiuYang Co., LTD; MT140 Press Flour Machine, Hubei Province Zaoyin City Ju Xin Machinery Co., LTD; SHA-C Bathing Constant Temperature Vibrator, Jintan City Instrument Co.LTD; FS-280M Autoclave, Zhejiang Xin Feng Medical Equipment Co.LTD; 85-2 Constant Temperature Magnetic Blender, Shanghai Sile Instrument Co.LTD.

2.3 Production Process

The process was as follows[4]:

Flour→dough making(solve the food additives into 30℃ water, then add them into the dough) →rolling→cutting noodles(noodles are wide in 5mm, thick in 1mm)→covering the preservative film→refrigerating(at 4℃).

2.4 Organoleptic Investigation[5]

At first, measure 500ml tap water and put it into small aluminum pan(20 cm in diameter). Then, measure 50g noodle sample and put them into the pan, make the water boiled. Next, fish out the noodles when there is no white fresh flour in noodles. At last, shower the noodles with flowing tap water for 10s, put them in bowl and taste. The standard for evaluation of noodles as shown in Table 1.

2.5 Acidity Test[6]

Get 20g wet noodles, add 180ml distilled water and bruise the noodles with waring blender, then make it standing. Measure 50g liquid supernatant and titrate it with 0.01mol/L standard NaOH solution, the result is just the acidity of noodles(titrate 3 drops of phenolphthalein to reddish, use the same volume distilled water to do blank test).

Table 1. The Organoleptic Investigation Standard of Wet-Fresh Noodles

Items	Full mark	Standard for evaluation
Color and luster	10	Refers to the color and brightness of noodles, 8.5～10 for high lightness ; 6～8.4 for middle lightness; 1～6 for weak lightness, like darkness, gray.
Preformence	10	Refers to the smooth and swelling degree of noodles, 8.5～10 for fine and smooth surface structure; 6.0～8.4 for middle status; 1～6 for rough surface, and high degree swelling and deformation.
Palatability	20	The power needed to bite off a piece of noodle. 17～20 for suitable power, 12～17 for a little hard or tender, 1～12 for too hard or tender.
Toughness	25	The bite strength and elasticity of noodles when chewing them, 21～25 for good bite strength and high elasticity, 15～21 for general bite strength and elasticity, 1～15 for bad bite strength and low elasticity.
Viscosity	25	Refers to sticky strength of noodles during chewing them. 21～25 for daintily and no sticking teeth; 15～21 for rather daintily and a little sticky, 10～15 for bad daintily and sticky.
Slickness	5	Refers to the smooth degree of noodles when tasting, 4.3～5 for smooth, 3～4.3 for middle degree smooth, 1～3 for little smooth.
Taste	5	Refers to the flavor during tasting, 4.3～5 for fresh scent, 3～4.3 for basically no odour, 1～3 for existing odour.
Total score	100	The total score of refined wheat flour product is no less than 85.The total score of ordinarywheat flour product is no less than 75.

$$\text{acidity (mL)} = \frac{C(NaOH)\times[V(NaOH)-V(blank)]\times 10}{m(samplequality)\times 0.1000}$$

2.6 Microbe Test

Testing of total number of bacterial colony. Refer to GB/T4789.2-2010, pour into flat method.

2.7 Test of Shelf Life[7]

Preserve the sample under refrigerated condtion(at 4℃). Observe the color, odour and moldy status at regular time, and recorde it in time. If the color changed obviously, white mold point or moldy odour emerged, it can be definated as the expiration period end.

3 Results and Discussion

3.1 Acidity Measurement of Noodles during Refrigerating Storage

From Table 2, we knew that the acidity of noodles increased with the prolongation of time. This was because the accumulation of water soluble organic acid of noodles, which developed during storage. In addition, mildewed noodles can also increase its acidity. Therefore the change of acidity is connected with water content, temperature and microbe's metabolism.

Table 2. Acidity Change of Noodles under Refrigerated Condition

Water addition/mL	Acidity/mL						
	0h	6h	12h	24h	48h	72h	96h
32	0.77	0.81	0.90	1.10	0.92	0.96	0.93
35	0.77	0.78	0.88^4	1.04	1.26	1.18	1.25
38	0.77	0.79	0.92	0.96	1.29	1.07	1.30
41	0.77	0.81	0.90	1.16	1.31	1.11	1.10

3.2 Shelf Life Measurement of Noodles under Refrigerated Condition

From Table 3, we knew that the longest shelf life was achieved with 35ml water addition, and it was followed by 32ml water addition and 38ml water addition, the noodles added with 41ml water got the shortest shelf life. This kind of noodles became soft and sticky during the late stage of preservation, and existed a certain extent of adhesion. It was perhaps because the mass propagation of yeast and bacterium. When there are different degree color change, emergement of white moldy point and odour of rancidity mildew it can be definated as the expiration period end.

Table 3. The Effect of Quantity of Added Water on Shel Life of Wet-Fresh Noodles

Water addition/mL	32	35	38	41
Shelf life/d	5	6	5	4

Table 4. Measurement of bacterial colony number

Water addition /mL	Bacterial colony number /(cfu/g)						
	0h	6h	12h	24h	48h	72h	96h
32	6.44×10^2	7.18×10^3	5.66×10^4	9.09×10^4	1.00×10^5	4.86×10^6	3.31×10^6
35	6.44×10^2	4.26×10^3	3.43×10^4	8.45×10^4	2.18×10^5	2.41×10^6	2.86×10^6
38	6.44×10^2	9.99×10^3	5.09×10^4	2.27×10^5	1.91×10^6	3.77×10^6	Too many
41	6.44×10^2	1.32×10^4	8.09×10^4	2.31×10^5	1.25×10^6	Too many	Too many

Table 5. Different preservative addition(%) and serial number

	Concentration 1	Concentration 2	Concentration 3	Concentration 4	Concentration 5
Sodium dehydroacetate	0.01 (A1)	0.02 (A2)	0.03 (A3)	0.04 (A4)	0.05 (A5)
Potassium sorbate	0.02 (B1)	0.04 (B2)	0.06 (B3)	0.08 (B4)	0.10 (B5)
Ethylparaben	0.01 (C1)	0.02 (C2)	0.03 (C3)	0.04 (C4)	0.05 (C5)
R- polysaccharide	0.06 (D1)	0.12 (D2)	0.18 (D3)	0.24 (D4)	0.30 (D5)
Sodium diacetate	0.02 (E1)	0.04 (E2)	0.06 (E3)	0.08 (E4)	0.10 (E5)
Sodium benzoate	0.01 (F1)	0.02 (F2)	0.03 (F3)	0.04 (F4)	0.05 (F5)

Table 6. Sensory evaluation of wet-fresh noodles after adding preservatives

Serial number	Sensory score			
	0h	2d	4d	6d
A1	95.1	90.5	73.2	68.8
A2	92.3	91.2	76.4	74.9
A3	92.7	88.4	72.6	69.1
A4	89.2	85.7	80.1	73.6
A5	92.9	89.1	82.8	75.3
B1	93.7	87.5	85.8	79.3
B2	92.6	88.5	86.3	79.8
B3	89.5	85.9	79.4	72.9
B4	90.8	86.5	87.0	80.5
B5	92.0	87.6	84.9	78.4
C1	91.7	88.9	84.6	78.1
C2	93.6	86.7	79.5	73.0
C3	89.1	85.7	83.1	76.4
C4	91.0	89.1	84.7	78.3
C5	89.0	87.5	82.8	76.4
D1	93.5	88.5	87.2	80.9
D2	91.7	85.9	85.5	79.1
D3	93.5	88.3	87.2	80.8
D4	94.4	91.8	88.1	81.8
D5	95.6	90.1	89.3	83.0
E1	94.8	91.2	88.5	82.1
E2	92.4	88.5	86.1	79.8
E3	92.7	89.1	86.4	80.1
E4	94.3	90.2	88.1	81.7
E5	94.4	91.6	89.1	81.7
F1	91.0	89.3	83.1	76.7
F2	90.3	86.9	82.1	75.4
F3	92.1	88.2	81.2	78.9
F4	93.0	89.4	86.1	79.0
F5	94.1	90.1	87.1	76.2

Table 7. The influence of preservatives on shelf life of wet-fresh noodles

Preservaties	Shelf life /d				
	0.01%	0.02%	0.03%	0.04%	0.05%
Sodium dehydroacetate	7	8	9	8	7
Potassium sorbate	7	8	8	8	6
Ethylparaben	9	10	8	8	9
R-polysaccharide	8	9	10	9	7
Sodium diacetate	9	8	9	7	7
Sodium benzoate	8	8	8	8	7

Table 8. Factor and level of orthogonal((L933)

Level	Factor		
	A （ethylparaben） /%	B （*R*-polysaccharide） /%	C （sodium diacetate） /%
1	0.02	0.03	0.02
2	0.03	0.04	0.03
3	0.04	0.05	0.04

Table 9. Results and Analysis of orthogonal test

Serial number	Factor and Level Evaluation index				
	A	B	C	Sensory evaluation /score	Shelf life /d
1	1	1	1	82.7	11
2	1	2	2	84.6	11
3	1	3	3	84.3	12
4	2	1	2	85.0	13
5	2	2	3	82.1	12
6	2	3	1	86.2	11
7	3	1	3	87.5	13
8	3	2	1	86.1	14
9	3	3	2	86.1	12
	K value and extreme difference R			Factor A	Factor B	Factor C
	K1			251.6	255.2	255.0
	K2			253.3	252.8	255.7
	K3			259.7	256.6	253.9
Sensory evaluation	K1			83.9	85.1	85.0
	K2			84.4	84.3	85.2
	K3			86.6	85.5	84.6
	Extreme difference		R1	2.70	1.27	0.60
	K1			34.0	37.0	36.0
	K2			36.0	37.0	36.0
	K3			39.0	35.0	37.0
Shelf life	K1			11.3	12.3	12.0
	K2			12.0	12.3	12.0
	K3			13.0	11.7	12.3
	Extreme difference		R2	1.67	0.67	0.33

Table 10. Results of verification test about total number of colonies

Experiment	Total number of colonies / (cfu/g)						
	0h	6h	12h	1d	2d	3d	4d
Contrast group	1.43×10^2	4.26×10^3	3.43×10^4	4.45×10^4	2.18×10^5	2.41×10^5	2.86×10^6
Optimum group	1.43×10^2	2.75×10^3	6.76×10^3	3.36×10^3	7.66×10^3	1.87×10^4	5.92×10^4

3.3 Change of Bacterial Colony Number of Wet-Fresh Noodles during Refrigerated Storage

From Table 6, we knew that bacterial colony number increased with the prolongation of storage time. During storage, the bacterial colony number of noodles with 32ml and 35ml water addition were less than the other two groups. This was due to that the microbe processes was weak in low water activity(Aw).

The quality of wet-fresh noodles decreased gradually under refrigerated condition. Acidity increased and microbial number increased were the specific performance. It turned out as darken color, adhesion, noodles' soften and more sticky. The organoleptic quality decreased significantly in later stage. The major microbes were mould and bacteria. Above results indicated that noodles with 35ml water were in better level and were most suitable for refrigerated storage.

3.4 Screening and Formulation of Wet-Fresh Noodles Preservatives

1) Serial number of different preservatives and additive amount

Based on the antibacterial range of preservatives we targeted seclected sodium acetate, potassium sorbate, ethylparaben, *R*-polysaccharide, SDA, sodium benzoate as fresh noodles preservatives. During the allowed range, we have the maximum addition which is provisioned by the health standards of additives application as the highest concentration. The concentration is divided into five parts evenly, then numbering them 1-5 in accordance with the order from small to large. After numbering the different groups, we operation the single-factor test, and selecte three kinds of preservatives which work better (see Table5).

2) Sensory evaluation of wet-fresh noodles after adding preservatives

Sensory evaluation of wet-fresh noodles after adding preservatives(see Table6, Table 7).

Based on the above results, we choose group C, group D, group E as orthogonal group ($L_9 3^3$) (see Table 8). According to extreme difference, we can determine the order of factors. targeting on sensory evaluation of fresh noodle, as can be seen from Table 9, ethylparaben was main factor and level 3 was optimal, followed was *R*-polysaccharide and level 3 was optimal, the last was sodium diacetate and level 3 was optimal. The optimum formulation was: ethylparaben 0.04%, sodium diacetate 0.05%, *R*-polysaccharide 0.04%. In addition, targeting on shelf life, we knew that level 1、2 of *R*-polysaccharide was optimal, level 3 of sodium diacetate was optimal. Comprehensive consideration of above two factors, the optimum combination was to add 0.04% of ethylparaben, 0.05% of SDA, 0.04% of *R*- polysaccharide into wet-fresh noodles, which can be preserved for at least 14 days under refrigerated condition.

3) Verification Test

As verification test showed(see Table 10), compound preservative can keep wet noodle fresh at least 14 days under refrigerated condition. From Table 10, we know that compound preservative get the multiply of microorganism under control effectively. Contrast optimum group with contrast group, bacterial colony number of the former is more less than the latter. This showed that synergy of preservatives can acquire better fresh-keeping effect with less dosage.

4 Conclusions

Under refrigerated conditions, acidity and total number of colonies of wet-fresh noodles keep incresing. General preservatives have certain effective on fresh-keeping, but the effect is often not satisfactory when they are used alone. Combination of several preservatives generally have well synergy. By the combination study of preservatives, The optimal antistaling agent formulation is ethylparabe, SDA(Sodium Diacetate) and *R*-polysaccharide. When 0.04% of ethylparaben, 0.05% of SDA, 0.04% of *R*-polysaccharide were added to wet-fresh noodles, which can be preserved for at least 14 days under refrigerated condition.

Acknowledgment. This research was supported by Key Scientific and Technological Project of Henan Province(102101110138) .

References

1. Lin, J., Yun, T.: Quality improver and keeping time of wet Noodle. Journal of the Chinese Cereals and Oils Association 17, 55–58 (2002) (China)
2. Yang, M., Yu, Y.: The evolvement of noodle study in China and foreign Country. Journal of the Chinese Cereals and Oils Association 18, 1–3 (2003) (China)
3. Lu, Y., Chen, H.: Development on instant wet noodles. Cereals & Oils 3, 1–4 (2006) (China)
4. Yang, M., Yu, Y.: The Study on making technique of wet noodle and the influence factor of wet noodle quality. Journal of the Chinese Cereals and Oils Association 19, 35–41 (2004) (China)
5. Li, M., Zhang, J.: Study on the evaluation indexes and methods of noodle quality. Journal of Triticeae Crops 74, 625–629 (2007) (China)
6. Ye, Y., et al.: Study on keeping fresh of the wet noodle. China Food Additives 5, 32–35 (2002) (China)
7. Xu, L., et al.: Study on different preservatives for wet corn noodle fresh-keeping. Academic Periodical of Farm Products Processing 7, 44–46 (2006) (China)

Effects of Functional Protein from Milk on Osteoclasts of Rats

Jie Sun* and Guoyou Yin

Biological Engineering Department
Henan University of Urban Construction Pingdingshan, China
{sunjie124,yinguoyou}@163.com

Abstract. To assess the effects of the functional protein from milk on osteoclast, Large quantity of high-purity osteoclasts had been cultivated successfully through the whole bone marrow. Swiss staining and Giemsa staining are used to identified the osteoclasts. The bone resorption function was detected by the number and area of the bone resorption and study the effects of functional protein from milk on osteoclasts of Rats preliminary.

Keywords: Functional Frotein, Osteoclasts, Bone Resorption.

1 Introduction

Milk contains human growth and development of the necessary nutrients. The study shows that in recent years, milk protein is with nutrition value, but also has the important physiological function. Bovine milk osteopontin(OPN) is an important functional factor in bone remodeling. OPN is a sialic acid-rich, highly phosphorylated glycoprotein. Mainly used as the collagen extracellular matrix distribution in mineral organization (such as bone and teeth bone), promote the osteoclast (OC) adhesion and the bone creatures of mineralization. Some research show that osteopontin exists in bone cells, adhere to the extracellular matrix, can be used as the bone formation and the early stages of the chemical induction[1].

OPN molecules are composed of 300 molecules amino acid residues, molecular weight is 44000Da ~ 75000Da and signal peptide is composed by 16 amino acid residues. OPN for the physiological function of osteoclasts is very important. It can promote OC and bone matrix adhesion, induce broken bone process, and may be the key step of Osteoporosis disease mechanism.OPN has chemotaxis role to OC and strengthen the migration and aggregation. Chellaiah et al shown that OPN stimulated CD44 expression on the osteoclast surface, and CD44 was shown to be required for osteoclast motility and bone resorption. Exogenous addition of OPN to $OPN^{-/-}$ osteoclasts increased the surface expression of CD44, Exogenous OPN only partially restored bone resorption because addition of OPN failed to produce OPN secretion into resorption bays as seen in wild-type osteoclasts [2]. The lack of OPN makes OPN-deficient mice resistant to ovariectomy-induced bone resorption in vivo, in an

* Corresponding author.

E. Zhu and S. Sambath (Eds.): Information Tech. and Agricultural Eng., AISC 134, pp. 981–985.
springerlink.com © Springer-Verlag Berlin Heidelberg 2012

established animal model of postmenopausal osteoporosis [3]. However, the mechanism through which OPN deficiency protects bone is not understood. Namely, whether OPN deficiency directly causes a reduction in bone resorption or not has yet been known.

2 Materials and Methods

2.1 OC Culture

Referred to in vitro OC incubation method of Zhang [4]

2.2 OC Identification

The study on the appraisal of the OC was the method of Geimsa staining and Wright's staining.

2.3 Resorption Assay

The preparation and processing of periosteum. Cow femoral slices were used in these experiments. The slices were cut with an isomet low speed saw, cleaned by sonication, and sterilized by UV for 2h on each side. They were invubated for 2h before the experiment in α-MEM supplemented with 10% heat-inactivated FBS, 50IU/mL Pen, 50IU/mL Strep, 2mM Glutamax.

The preparation of coverslip. Wash the coverslip, cut it into sheets whose size are 1cm×1cm with diamond knife and put them into the acid for one night. After taking them out, rinse them with tap water, wash them three times with distilled water and dry them in the oven. After sterilization, put them in the poly-L-lysine. Before using them, take them out, dry them in the ultra-clean bench and irradiate 1h for each side of coverslip with ultraviolet light.

Resorption assay. Wipe off non-adherent OC and add 2mL α-MEM culture medium and made OPN final concentration were 2.5μg/mL, 5.0μg/mL, 10.0μg/mL, 20.0μg/mL, 40.0μg/mL each hole. Remove 1mL culture medium for every 24 hours and use the α-MEM culture medium which contains the corresponding proportion of OPN to make up a deficiency. Take the thin bone slices out when they are cultured for 7 days and 10 days. Fix the thin bone slices at 4℃ for 7 minutes with 2.5% glutaraldehyde. Then clean them for 5 minutes with ultrasound when they are placed in 0.25mol/ml of ammonia. Then dehydrate with series of ethanol, dry under natural conditions and stain at room temperature for 4 minutes with 1% toluidine blue. After washing them with distilled water, observe absorption lacuna with light microscope at 100, detect the area of bone resorption lacunas and record the number of resorption lacunas with image analysis software which is Image proplus 5.0.

Effect of OPN on bone absorption. Take out one 24-hole cell plate and two 6-hole cell plates. Add the bone pieces in 24-hole cell plate and add coverslips in 6-hole cell plates. Add 1mL α-MEM culture medium in each hole, bone chips and coverslips which are processed in cell plates and pre-culture for 1 hour in carbon dioxide incubator. Then plus 1mL OC suspension in each hole and continue to cultivate for 24

hours in carbon dioxide incubator. Take out another 24-hole cell plate, add 1mL α-MEM culture medium which contains OPN whose concentration are 0, 2.5μg/mL, 5.0μg/mL, 10.0μg/mL, 20.0μg/mL, 40.0μg/mL in each hole. The same concentration was given four-hole. Take small bone chips and coverslips which were isolated, cultured and contain OC out, then draw medium with sharp straw to wash out the non-adherent cells on the bone chips and slides. Put them into new culture plates and continue to cultivate in carbon dioxide incubator and observe changes in size and number of absorption lacuna on the bone chips. Pick out two 6-hole cell plates, plus 1mL α-MEM culture medium which contains OPN whose concentration are 2.5μg/mL, 5.0μg/mL, 10.0μg/mL, 20.0μg/mL, 40.0μg/mL in each hole. The same concentration was given two-hole. Draw medium with sharp straw to wash out the non-adherent cells on the bone chips and slides. Put them into new culture plates and continue to foster in carbon dioxide incubator and observe changes in size and number of absorption lacuna on the bone chips and the morphology of OC on the slides.

3 Results

3.1 OC Identification

The cells was round or elliptic with purple below light microscope after Geimsa staining(Fig.1,A). Cytoplasm were full, containing many empty bubble structure, and nucleoli actin filaments are fine granula after Wright's staining(Fig.1B).

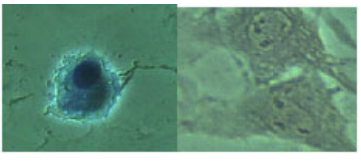

A OPN B Normal bone

Fig. 1. The identification of OC

3.2 Effect of OPN on Bone Absorption

Identification of bone lacune morphology. There were a small amount lacuna after 24h. It seemed appeared clear on the bouders. Fig.2.

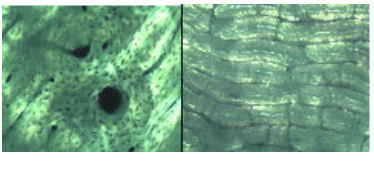

A Geimsa staining 400× B Wright's staining400×

Fig. 2. The result of bone resorptiong (7d,100 ×)

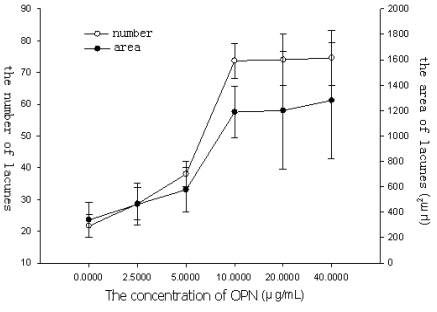

Fig. 3. The effect of different concentration of OPN on the amount and the area of lacunes

Identification of bone lacune and area. Fig.3 shown that the absorption of the lacuna number and absorb lacunes higher than other groups when OPN concentration for 10.0μg/mL. The group of 10.0μg/mL,20.0μg/mL and 40.0μg/mL were significant difference compared with control group. There was not a significant dose dependent.

4 Discussion

OPN was a highly secretion phosphorylated glycoprotein[5], mainly as the collagen of extracellular matrix in mineral tissue(bone and Cementum)[6]. Some of former research work showed that OPN exists in bone cells, adhere to the extracellular matrix, as a chemical induction content of the early stages of bone formation[7]. OPN can be secreted by the OB and OC. There was expressed high concentration OPN on the surface of bone absorption[8].

OPN is a ligand for the integrins αvβ1、αvβ3、αvβ5、α4β1. αvβ3 were missing in mice could be occured bone sclerosis. Therefore, OPN couble be regarded as a function of the markers to OC [9].

OPN could promote OC adhesion by αvβ3 in vitro. There were rich in OPN on the bone surface and the concentration of OPN were low around OC include the regions such as absorbance and cuticular ridge[10]. By the immune electron microscopy,OPN were on the bottom of the bright band of OC (there was relation between the brignt band and bone matrix). Therefore, OPN adjusted the dissolved bone controlled by OC. OPN could promote the adherenet of OC and enhance the activity of dissolved bone, but there were some concrete mechanism need to be further study.

References

1. Somerman, M.J., Prince, C.W., Butler, W.T.: Cell attachment activity of the 44 kilodalton bone phosphoprotein is not restricted to bone cells. Matrix 9, 49–54 (1989)
2. Chellaia, M.A., Kizer, N., Biswas, R., et al.: Osteopontin deficiency produces osteoclast dysfunction due to reduced CD44 surface expression. Mol. Biol. Cell 14, 173–189 (2003)
3. Ihara, H., Denhardt, D.T., Furuya, K., et al.: Parathyroid homone induced bone resorption does not occur in the absence of osteopontin. J. Biol. Chem. 276, 13065–13071 (2001)
4. Zhang, W., Yu, S., Zheng, L.: Acta Anatomica Sinica 26, 291–293 (1995)

5. McKee, M.D., Zalza, S., Nanci, A.: Extracellular matrix in tooth cement and mantled dentin:localization of osteopontin and other noncollagenous proteins, plasma proteins, and glycoconjugates by electronic mistroscopy. Anat. Rec. 245, 293–312 (1996)
6. Butler, W.T., Ridall, A.L., Mckee, M.D.: In: Bilezikian, J.P., Raisz, J.G., Rodan, G.A. (eds.) Principles of Bone Biology, pp. 167–181. Academic Press, San Diego (1996)
7. Somerman, M.J., Prince, C.W., Butler, W.T., et al.: Cell attachment activity of the 44 kilodalton bone phosphoprotein is not restricted to bone cells. Matrix 9, 49–54 (1989)
8. Alexis, M.P., Michaer, S.: Functional atomic force microscopy investigation of osteopontin affinity for silicon stabilized tricalcium phosphate bioceramic surfaces. Biomaterials 27, 3–14 (2006)
9. Denhardt, D.T., Noda, M.: OPN expression and function:role in bone remodeling. J. Cell Biochem. 72, 92–102 (1998)
10. Ek-Rylander, B., Florest, M., Wendel, M., et al.: Dephosphorylation of osteopontin and bone sialoprotein by osteoclastic tartrate-resistant acid phosphatase. Modulation of osteoclast adhesion in vitro. The Journal of Biological Chemistry 269, 14853–14856 (1994)

Author Index

Bai, Liming 107
Bai, Xue-Liang 143
Bai, Xue-na 653, 693
Bai, Yan-Ling 143
Bo, Cai 121
Bu, Chun-ya 663, 683, 703, 721, 739

Cao, Sanjie 789
Cao, WenBin 779
Cao, Zhi-min 191
Chang, Yonghong 39
Changhong, Guo 261
Chen, Cuizhen 493
Chen, Die-yan 863
Chen, He 967
Chen, Jie 283
Chen, Jishuang 919
Chen, Lei 763
Chen, Liehuan 233
Chen, Rong 183
Chen, Ruizhan 959
Chen, Xiaoyue 747
Chen, Xin 135
Chen, Yizhao 819
Chen, Zhengli 747
Chen, Zhiwei 61
Cheng, Anchun 747
Cheng, CuiLin 85
Cheng, Jun 557, 589, 599, 643, 653, 663, 693, 713, 721, 731
Cheng, Xiaosong 113
Cheng, Yingkun 135
Chia, Xiaoxiao 771

Dai, Yujie 39
Deng,Yang-wu 525
Diansi, Yu 261
Dong, Hang 959
Dong, Yuan 135
Dong, Yuqing 517
Du, Ai-ling 191
Du, Juan 547, 621, 683
Duan, Dan-dan 557, 599, 673, 703, 713, 721, 739

Fan, Le-hui 857
Fang, Hai 493
Feng, Liping 113
Feng, Zeqing 269
Fu, Bo 397
Fu, Jian-jiang 925
Fu, Jinluan 811
Fu, Yanfeng 811

Gao, Guangping 493
Ge, Bao-feng 405
Ge, Song 261
Geng, Zhizhong 911
Gong, Luojun 283
Gu, Ji-cheng 693
Gu, Qianhong 283
Guan, Huaijin 307
Guan, Junjiao 943
Guan, Xue-min 459, 471
Guo, Changhong 241, 249, 255
Guo, Hao 405
Guo, Jinhua 911
Guo, Liu Jian 121
Guo, Qingqi 539

Guo, Wanzhu 293
Guo, Zhenhua 397

Han, Dong 353
Han, Youfa 183
Han, Zhao 31
Hao, Fengxia 419, 425
Hao, Ran 31
He, Binbin 517
He, Feng 315
He, Qin 747
He, Xugang 151
Hou, Jingyu 771
Hou, Yan-hua 895
Hu, Guangfu 151
Hu, Nan 307
Hua, Zi-chun 849
Huang, Dan-feng 525
Huang, Jing 279
Huang, Riming 513
Huang, Xianju 535
Huang, Yong 789
Huang, Yubi 801

Ji, Chenfeng 7
Ji, Yubin 1, 7, 15, 23
Ji, Zhe 967
Jia, Renyong 747
Jia, Shiru 39
Jian, Zhang 345
Jiang, Luqing 763
Jiang, Yong 31
Jin, Leilei 919
Jin, Ting 451
Jin, Yong-sheng 663, 731
Jin, Zhong Min 433

Kaleem, Imdad 903

Lei, FuMin 779
Li, Chun 903
Li, Chunyan 113
Li, Desheng 293
Li, Fengqin 293
Li, Jia-huang 849
Li, Jian 779
Li, Jianlong 819
Li, Ming 49, 57
Li, Qing 731
Li, Sheng 371
Li, Wei 371
Li, Wenhao 199, 211
Li, Wenlan 1, 15, 23
Li, Xin 337
Li, Xuemei 881, 889
Li, Ying 863
Li, Zhongqiu 397
Liang, Dongxue 485
Liang, Rui 425
Liang, Wei 315, 643, 653, 663, 693
Liao, Wei 69
Lili, Song 261
Lin, Feng 135
Lin, Guo-Ping 441
Lin, Yan 789
Lin, Yayu 835
Liu, Anan 353
Liu, Chunlong 397
Liu, Chunying 255
Liu, Cong 135
Liu, Danyang 61
Liu, Di 397
Liu, Hong-ning 925
Liu, Hongwei 329
Liu, Jiali 241, 249
Liu, Jin-Gao 69
Liu, Lingyan 135
Liu, Mingyuan 183
Liu, Naifa 501
Liu, Qing 143
Liu, Qingguo 249
Liu, Sihua 77, 95
Liu, Tingting 835
Liu, Wenquan 789
Liu, Xiao-Lan 441
Liu, Yanfang 471, 943
Liu, Ying-Hong 801
Liu, Yiping 269, 279
Liu, Yonghong 513
Liu, Yuan 371
Liu, Yu-bo 547, 557, 565, 577, 589, 599, 611, 621, 629, 643, 653, 663, 673, 683, 693, 703, 713, 721, 731, 739
Liu, Zheren 353
Liu, Zhichun 465, 507
Liu, Zhihua 377
Liu, Zhiqiang 959
Lu, Guangtao 151
Lü, Jian-Hua 323
Lü, Li 485

Luo, Huaxing 501
Luo, Qihui 747
Luo, Xiaoqing 61
Luo, Xue-gang 31
Luo, Yong-ming 925
Lv, Jian-wei 49, 57
Lv, Yueping 241, 249

Ma, Fang 935
Ma, Hong 397
Ma, Jianzhang 397
Ma, Lan-qin 629
Ma, Lan-qing 547, 557, 565, 577, 589, 599, 621, 643, 653, 663, 673, 683, 693, 703, 721, 731, 739
Ma, Lianlan 465, 507
Ma, Ruiping 973
Ma, Shaoying 371
Ma, Wan-yun 863
Ma, Xiaomei 419
Ma, Yongqiang 539
Man, Chaolai 129

Nei, Hongwei 161

Ou, Yu-duan 361
Ouyang, Pingkai 919

Pan, Feng 385
Pan, Huitang 827
Pan, Junbo 113
Pan, Xiao-ru 871
Peng, Fugang 397
Piao, Mei-hua 857
Ping, Wang 121

Qi, Xinqiao 293
Qiang, Li Shu 121
Qiang, Zhang 953
Qin, Zuodong 919
Qu, Min 849
Qu, Zhongyuan 7, 15, 23

Ren, Jian 441
Ren, Jian-ju 565, 577
Ren, Shuncheng 973
Ruan, Luzhang 501
Rui, Dong 261

Sha, Wei 433
Shan, Guo-Yong 167, 175
Shao, Shu-li 49, 57
Shi, Guang-lu 547, 557, 565, 577, 589, 599, 611, 621, 629, 643, 653, 663, 673, 683, 693, 703, 713, 721, 731, 739
Shi, Hongxi 135
Shi, Min 789
Shi, Qiumei 493
Shu, Guowei 967
Shu, Xinya 283
Shu, Yongmei 471
Song, Li Dong 121
Song, Limin 353
Song, Xiao Hong 433
Su, Wenyue 255
Su, Xin-Hong 323
Su, Yong-mei 459
Su, Zhenxia 233
Su, Zhi-yao 361
Sun, Bai-ye 871
Sun, Chengming 819
Sun, Dongfa 385
Sun, Jiaqiang 535
Sun, Jie 981
Sun, Jing 269, 279
Sun, Jinyan 397
Sun, Ming 827
Sun, Xiao-Hong 441
Sun, Yingying 199, 211
Sun, Zhengguo 819

Tan, Fangyuan 183
Teng, Lirong 135, 485
Thomsen, Anne Belinda 953
Tian, Hua 31
Tian, Mengliang 801
Tian, Mingxing 789
Tian, Ning 863
Tong, Bao-sheng 547, 621, 713

Wan, SunHua 779
Wang, Aiguo 811
Wang, Bin 513
Wang, Bo 225
Wang, Changhai 199, 211
Wang, Chengdong 293
Wang, Dan 143
Wang, Guiying 811
Wang, Guoliang 39
Wang, Hai-xiang 611
Wang, Hongyan 377

Wang, Hui 61
Wang, Jiangmin 943
Wang, Lei 967
Wang, Li 517, 935
Wang, Liang 397
Wang, Ling 167
Wang, Lu 337
Wang, Mingshu 747
Wang, Nan 31
Wang, Ning 973
Wang, Qiang 451
Wang, Qiuyue 493
Wang, Quan-fu 895
Wang, Shunchang 911
Wang, Shuqi 225
Wang, Xiaoli 507
Wang, Yong 143
Wang, You-nian 547, 557, 565, 577, 589, 599, 611, 621, 629, 643, 653, 663, 673, 683, 693, 703, 713, 721, 731, 739
Wang, Yuanping 789
Wang, Yueru 337
Wang, Zheng 377
Wang, ZhenYu 85
Wang, Zhenzuo 485
Wang, Zhongkang 835
Wei, Feng 121
Wei, Xu 479
Wen, Longying 501
Wen, Xintian 789
Wu, Jian-hua 459
Wu, Xiaoyun 465
Wu, Yanmin 61
Wu, Yuxue 451
Wu, Zhansheng 903
Wu, Zhen-Bin 315

Xiao, Hui 233
Xiao, Ying 95
Xie, Dan-dan 361
Xie, Shuixiang 507
Xing, Fenglan 107
Xiong, Bangxi 283
Xiong, Minghua 113
Xu, Changru 1, 15, 23
Xu, Chun-Dong 69
Xu, Chunhong 113
Xu, Dong 315
Xu, Fangjiao 919
Xu, Guohui 255
Xu, Huiyu 61
Xu, Shenzhen 199, 211
Xu, Xilin 329
Xu, Xing-jun 49, 57
Xu, Yanho 843
Xu, Yong 161
Xu, Zhiwen 293

Yan, BaoPing 779
Yan, Pei-sheng 895
Yang, Delong 371
Yang, Fei 843
Yang, Hua-sheng 925
Yang, Lansong 283
Yang, Ling 307
Yang, Minli 419, 425
Yang, Simin 959
Yang, Xiaohong 943
Yang, Yue-tao 849
Yan-Wang, 629
Yao, Lei 85
Yao, Lixia 903
Yao, Wei 493
Yi, Yue 293
Yin, Guoyou 981
Yin, Xiao-ying 925
Yin, Youping 835
Yu, Jianping 249
Yu, Shui-jing 525
Yu, Tian-fei 49, 57
Yu, Yan 911
Yuan, Lin 535
Yun, Jun 167

Zhang, Congyi 283
Zhang, Donglin 493
Zhang, Feng 39
Zhang, Hongcheng 819
Zhang, Hui 943
Zhang, Jian-Hua 175, 943
Zhang, Jing 199, 211
Zhang, Jingwei 919
Zhang, Junjie 801
Zhang, Lihong 881, 889
Zhang, Lixun 501
Zhang, Lu 863
Zhang, Meng 61
Zhang, Na 485, 539
Zhang, Ping 525
Zhang, Qixiang 827

Zhang, RuiYing 779
Zhang, Shujuan 935
Zhang, Shu-yi 849
Zhang, Tinglan 485
Zhang, Tong-Cun 31
Zhang, Wenping 465
Zhang, Wenyi 183
Zhang, Xue 935
Zhang, Yan Fu 433
Zhang, Yanying 493
Zhang, Yaodong 161
Zhang, Yaowen 485
Zhang, Yibo 135
Zhang, Yi-dong 525
Zhang, Zhen 371
Zhang, Zheng 849
Zhao, Fangfang 789
Zhao, HaiTian 85
Zhao, Jin-yu 849
Zhao, Lei 547, 621, 683
Zhao, Lingli 827
Zhao, Ming 107
Zhao, Nan 135
Zhao, Xiaoling 279
Zhao, Yuan-yuan 459
Zhao, Yunpeng 107
Zheng, Jing-gao 863
Zheng, Wei 385
Zheng, Xilai 763
Zheng, Xi-Qun 441
Zheng, Ying-cha 857
Zhong, Hang 279
Zhong, Qingping 517
Zhong, Youtian 507
Zhou, Feng 871
Zhou, Jinyu 1
Zhou, Mu-Gui 69
Zhou, Qiaohong 315
Zhou, Yanliang 329
Zhou, Yi 747
Zhu, ChaoDong 779
Zhu, Dekang 747
Zhu, Ling 293
Zhu, Qing 279
Zhu, Wen-jin 459, 471
Zhu, Xiao-qi 405
Zhu, Xingjie 1, 15, 23
Zhu, Ye-Rong 143
Zou, Xiang 7
Zuo, Jin-Cheng 315